

# Appendix 1

## Hydrograph and High Water Mark Analysis

---

### Introduction

During Hurricane Katrina, flooding and overtopping, levee erosion, and the sequencing of levee/floodwall failures, all depended on the time variation of water level. Variation of water level during the storm was a key driving force in the response of the hurricane protection system. For such a complex and expansive system, water levels are expected to have great spatial variability. Unfortunately, measured data were not available at many locations where information was needed. Therefore, the IPET study used a combination of measured data and model-simulated data to characterize the time varying water level conditions. Both types of data complemented each other. Measured data fell into two categories, high water mark measurements that capture peak water levels (with some uncertainty) and hydrographs which capture the water level as a function of time. This chapter describes the work done to characterize water level, based on measured data, along the periphery of the hurricane protection system, outside of the areas protected by the levee system.

An extensive post-storm effort was undertaken to identify and survey high water marks following passage of the storm. While certain high water marks capture the peak water levels well, they contain no information about the temporal variation of water level. High water marks also have their own inherent issues of quality, uncertainty whether they in fact do reflect a peak condition, and whether or not water surface motions due to short wind waves or other factors are reflected in a high water mark.

Measured hydrographs are the most reliable source of data for capturing both the temporal variation and the maximum water level, and they were used to define conditions wherever possible. Water level fluctuations were measured with instrumentation during the build-up stage of the storm at a number of sites throughout the study region; however, few instruments operated throughout the storm. Most of them failed prior to the peak. Consequently, there is little measured data that captures peak conditions. In a few cases, photographs and other visual images were utilized to provide information about the temporal variation of water level to supplement the recorded hydrographs. These reconstructed hydrographs proved to be extremely valuable for characterizing conditions along the south shore of Lake Pontchartrain.

Storm surge modeling was used to complement high-quality water level measurements where they existed and provide water level information in the many locations where measurements were not available or were of questionable quality. The model computations provide hydrographs that capture the peaks and temporal variation on either side of the peak. In a complementary way, hydrograph data and the highest quality high water marks also are used to evaluate the accuracy of the storm surge model. Model-to-measurement comparisons provide valuable information for quantifying the uncertainty in model predictions, which is important because model results were used to estimate the temporal variation of water level in many locations, particularly in St. Bernard and Plaquemines Parishes.

## **High Water Mark Acquisition and Analysis - Overview**

The acquisition of high water marks (HWMs) is generally a two-step process. The first step is identification and documentation of the mark including photographs or electronic images, location (local landmarks and latitude, longitude coordinates), type of mark (e.g., mud line on interior or exterior of a building), the vertical distance above some fixed permanent object or structure such as a concrete foundation slab, and any other noteworthy characteristics, such as length. This step is performed as rapidly as possible as the marks are perishable and subject to eradication by natural causes or human activity.

The second step is termed “recovery” of the mark and refers to the vertical leveling of the mark relative to an established and accepted vertical datum such as NAVD-88 or NAVD-88 (2004.65). This second step typically is more time consuming and expensive than the first, but the HWMs would be of little value if not surveyed to a common datum.

Acquisition of HWMs following Katrina was performed by three Federal agencies, USGS, USACE, and FEMA (or a FEMA contractor), and the State of Louisiana through the Louisiana State University (LSU). All four entities shared the data. Marks identified by USACE, FEMA, and LSU were also recovered by each respective agency. Most of the marks identified by USGS were recovered by FEMA (or a FEMA contractor). A selected subset of approximately 50 marks identified by USGS was also recovered by USGS field crews to confirm elevations provided by FEMA contractors.

The passage of hurricanes often results in short-period wind waves on top of the much longer-period storm surge that creates significant entrainment of various types of debris including vegetation, seeds, dirt, man-made trash, and dislodged building material. Depending on local conditions, the entrained debris will deposit on or adhere to some surfaces once the peak stage has been reached and the stages begin to fall. The deposited debris leaves what is referred to as a high water mark (HWM) and the mark is used to quantify the magnitude of peak storm surge. The highest quality marks for estimating storm surge are those that have little or no wave effect (i.e., no influence of wave crests or wave run-up). Some HWMs are collected where significant wave effects are present but that effect is noted. In this analysis, the focus was on use of HWMs as indicators of storm surge, without the effects of wave crest and wave run-up.



All HWMs were reviewed and assigned a reliability value. The reliability of each HWM is assessed as “Excellent,” “Good,” or “Fair/Poor”. There is no standard method for determining HWM reliability. Moreover, assignment of reliability values to HWMs is not a totally objective process, but by its nature involves both objective and subjective elements. Discussion by the team assigning the reliability values led to a consensus that the mark should reflect, as closely as possible, the storm surge, stable or mean, water level. That is, the physical setting where the mark was located should approximate a tide gage stilling-well type environment. The basis for this consensus is that storm surge models do not explicitly include wave crest or runup effects, and one of the important uses of the HWM data is validation and verification of surge model simulations.

Other criteria for assigning quality or reliability values have been used (and could have been used herein), such as the degree of confidence that the surveyed HWM elevation is indicative of the actual peak water elevation, and without regard to the physical processes involved in establishing the mark.

For Hurricane Katrina, the criteria used for this report are:

**Observer notes** – The notes included in the description of HWMs by the field survey teams identifying the marks, generally contain an initial assessment of the reliability of the mark.

**Interior** (inside structures) or **exterior** (outside structures such as levee debris) HWM – For this report, only interior HWMs were classed as excellent. No exterior HWMs are classed as excellent because of the possibility the HWM includes other physical effects. This does not have to be the case, but that criterion was adopted in this study.

**Self-consistency** – Groups of similar types of marks in a small geographic area should show elevations consistent with one another. There is no objective test for consistency, but HWM values in the limited geographic area generally should not vary by more than about 10 percent from one another to be assessed as “Excellent” and not more than about 20 percent to be assessed as “Good.”

**Obvious inclusion of wind, wave, or rainfall effects** – Some HWMs, because of location and/or field observer notes, include wind, wave, or rainfall effects. These effects tend to elevate the water surface above that produced by the surge, so degrades the mark reliability.

Approximately 790 HWMs were identified and recovered by the four previously identified agencies in Louisiana and Mississippi following Katrina’s passage, excluding marks identified and recovered within the New Orleans levee system. Of these 790 marks, approximately 95 marks (about 12%) were recovered from the interior of structures and are considered to be the most reliable measures of the storm surge. The remaining 695 HWMs are debris lines (wrack lines), or on the exterior of structures where they could include wave or wind-blown water effects. It should be emphasized here that the exterior HWMs are not less valid measures of inundation, just that they are not as accurate indicators of what is generally defined as storm surge.

The area of southeast Louisiana including the New Orleans metropolitan area is known to be subsiding. To provide the best vertical datum reference for leveling marks in Louisiana, the National Geodetic Survey (NGS) was consulted. The NGS staff recommended a time-dependent datum designated NAVD88 (2004.65) be used. The use of NAVD88 (2004.65) resulted in vertical adjustment of network monumentation in this geographic area of between 0.4 ft and 0.7 ft. Adjustment of the vertical datum used for Mississippi HWMs was considered not required at this time, so all HWMs in Mississippi are referenced to NAVD88 vertical datum.

Figure 1-1 is an example image of a HWM presentation, which includes the HWM identifier, and water elevation. The shape of the HWM identifier indicates the HWM reliability. The setting in which a high water mark was collected is important in assessing the quality of a mark and those processes that might be reflected in the mark. Superposition of the mark on a photographic image aids in assessment and interpretation of HWMs in light of their geographic setting. Images 1 through 58 (two photo index images and 56 separate images with HWMs) at the end of this chapter show the HWMs in the metropolitan New Orleans vicinity and southeastern Louisiana area, which were utilized in this study. Images depict the location, elevation and reliability of all HWMs, focusing on unprotected areas.



Figure 1-1. Sample image of the 17th Street Canal Entrance showing locations of HWMs and water elevation for each mark.

Plates 1-1 through 1-3 contain spreadsheets with identification, location, and elevation of all HWMs for Louisiana and Mississippi that were acquired as part of this study, in unprotected and protected areas. There are a number of HWMs in protected areas. There are fewer HWMs in unprotected areas of eastern St. Bernard, eastern Orleans, and southern Plaquemines Parishes.

## **Hydrograph Acquisition and Analysis - Overview**

Hydrograph data, as defined herein, differ from High Water Mark (HWM) data in that time and magnitude are known for water level data whereas only magnitude is known for HWM data. The hydrograph data come from various sources including gage data, staff readings, and survey of physically identifiable objects in time-tagged digital pictures. In the usual (and strict) sense of usage, the term “hydrograph” refers to water level data from a calibrated staff or instrument recorded either manually or automatically. Because the time sequence of events is of paramount importance for the post-Katrina project performance studies, every available technique has been used to depict as accurately as possible the rise, peak, and fall of storm water levels. All hydrograph data from identified conventional gages or calibrated staffs in the affected area have been reviewed. Unfortunately, most gages malfunctioned or did not survive, therefore did not record the peak water level of Katrina. Of greatest interest, there were no gages at the entrances of the 17th Street, Orleans, and London Avenue canals, the GIWW, or the Inner Harbor Navigation Canal (IHNC) except at the IHNC Lock.

Time-tagged digital images from the Lake Pontchartrain - New Orleans lakefront were taken by several individuals who were in buildings or vessels during Katrina’s passage. Using these images (which contained physically identifiable reference marks), logs of observations, and nearby HWMs, hydrographs were constructed for the 17th Street Canal entrance, the New Orleans Lakefront Airport, and the IHNC lock. Recorded and reconstructed hydrographs are presented in the following sections. Note that all elevations are presented in the time-dependent datum NAVD88 (2004.65).

## **Observed Water Levels in Lake Pontchartrain and Along the South Shore**

This report summarizes observed water levels from gages in Lake Pontchartrain and high water marks along the south shore of Lake Pontchartrain. Figure 1-2 shows a map of various locations in Lake Pontchartrain used herein. All elevations presented herein are in the time dependent datum of NAVD88 (2004.65).

Figure 1-3 shows a plot of 5 gage hydrographs and two constructed hydrographs. Each hydrograph is labeled with a relative location in Lake Pontchartrain as either west, central, or east. The constructed hydrographs at the 17th Street Canal and the Lakefront Airport and the gage hydrographs at Southshore Marina, Little Irish Bayou, Pass Manchac, and Bayou Labranch are in NAVD88 (2004.65). The Midlake Gage was adjusted to NAVD88 (2004.65) by matching the average of the Pass Manchac and Bayou Labranch gage hydrographs before the storm.



Figure 1-2. Lake Pontchartrain gages and other locations referenced herein.

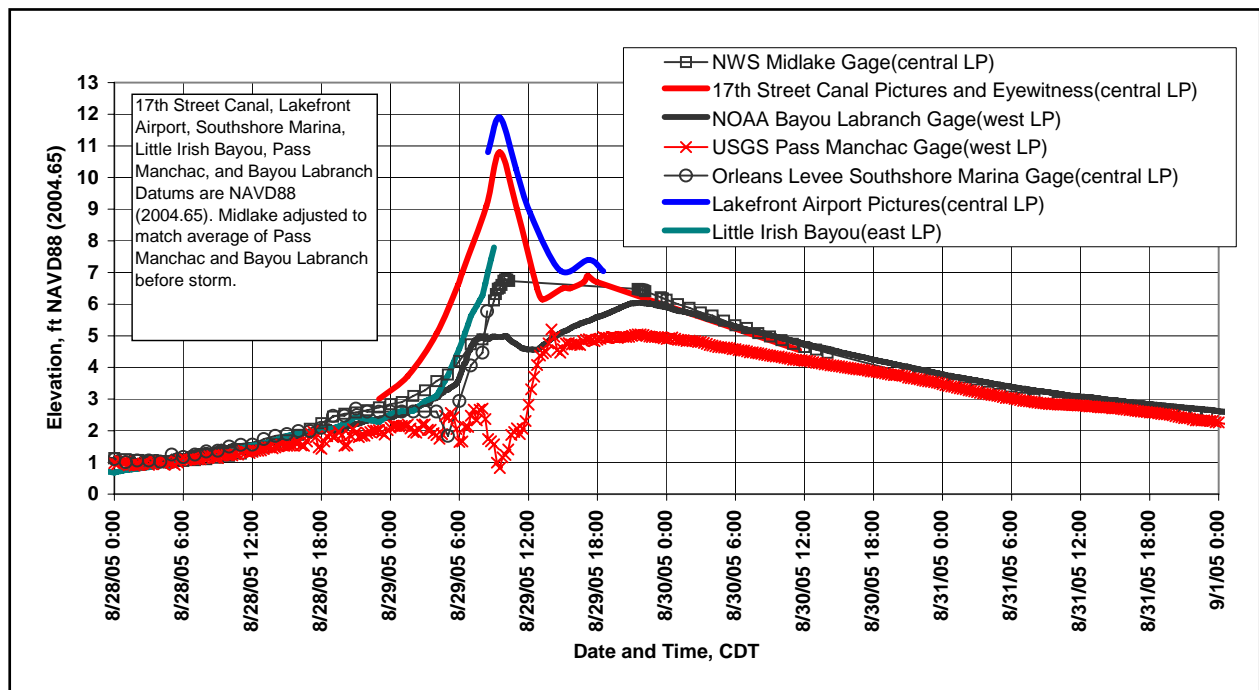


Figure 1-3. Gage hydrographs and constructed hydrographs on Lake Pontchartrain.

Figure 1-4 shows a plot of high water marks along the south shore of Lake Pontchartrain. The marks are separated into 3 categories of USACE marks inside buildings, USACE levee debris, and FEMA wrack or debris lines with the last two categories being essentially the same type of mark. The plot also shows a best estimate of peak storm water level based on the high water marks. With the exception of the Williams Boulevard location, the best estimate line is based on USACE marks inside buildings. At Williams Boulevard, there is a restroom that has all the characteristics of an excellent stilling well. The elevation of the mark (6.5 ft) in this restroom is much lower than the levee debris found by both the USACE and the FEMA teams. The 6.5 ft elevation is consistent with the elevations from Hurricane Rita. Any marks on Figure 1-4 less than about 7.5 ft and to the east of Bayou Labranch could reflect Hurricane Rita rather than Hurricane Katrina. The levee debris is accepted at this location because the foreshore slope between the levee debris and the lake is extremely flat and long that would have resulted in minor wave action at the location where the levee debris was deposited.

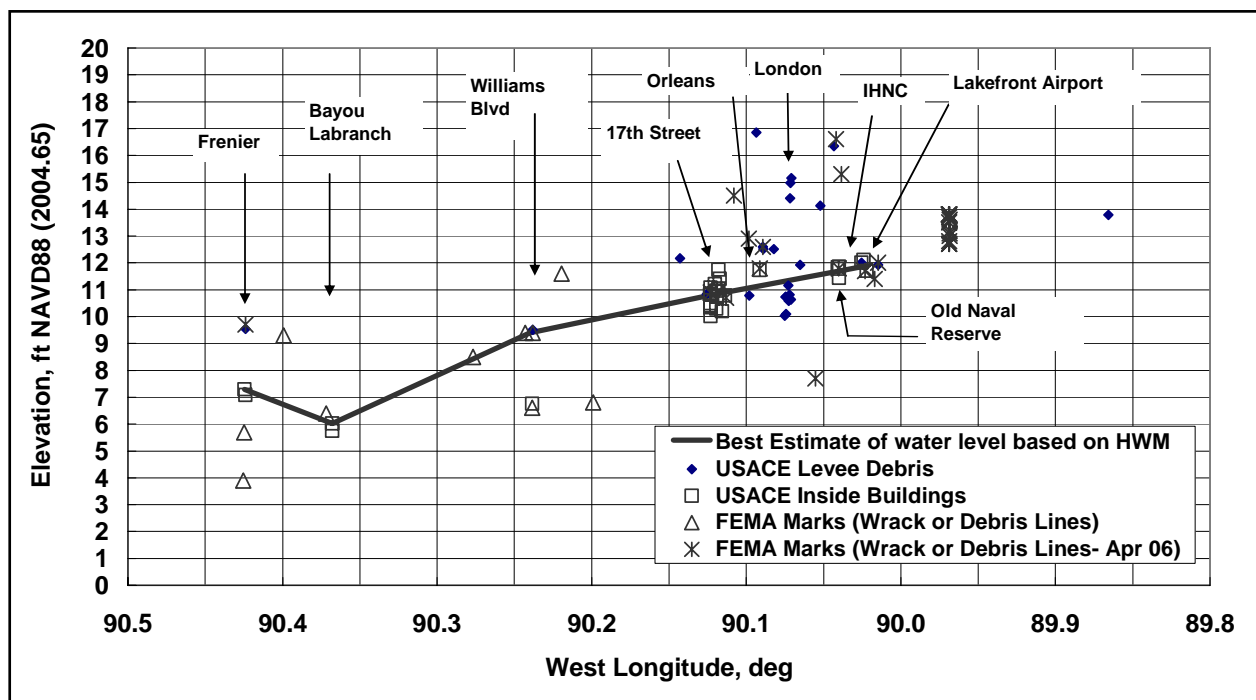


Figure 1-4. Variation of peak water level along south shore of Lake Pontchartrain based on high water marks.

Starting at Frenier on the west, the best estimate line is based on two excellent marks inside buildings. At the next point east at Bayou Labranch, the best estimate is based on two excellent marks inside buildings at 5.75 ft and 6.0 ft and the Bayou Labranch gage. Notice that the Bayou Labranch gage in Figure 1-3 peaks at an elevation of 6.0 ft. It is possible that the Bayou Labranch readings are affected by the fact that the gage and the HWMs are connected to the Lake by a channel that is about 0.5 mile long. An alternate estimate of water level along the south shore is to connect Frenier and the Williams Blvd points. The next point on the best estimate line at Williams Boulevard has already been discussed. From Williams Blvd to the next points at 17th Street Canal, the profile is assumed to be linear but water levels could have stayed high for some distance west of 17th Street before dropping to the level at Williams Blvd. The



selection of a value of 10.8 ft for the 17th Street Canal was based on 13 excellent (inside buildings) high water marks. These marks are discussed subsequently in this report. Continuing to the east, there is a high water mark LA 1012 that is an excellent mark inside Shelter No. 2 on the Lakefront in a restroom at elevation 11.7 ft. The door to this restroom was not latched but was held closed by an automatic door closer. Although this restroom was inside another room whose door was open to the storm, waves could have pushed the restroom door open allowing some wave effect of this mark. For this reason and because it is a single point, this mark was not used in the best estimate line.

The next marks to the east are the numerous levee debris marks that exhibit large variability. The marks south of the lakefront levee and inside London Avenue Canal would be expected to have a lower wave component. However, the two breaches on London Avenue Canal occurred as early as 7:00 AM that is roughly 2 hours before the peak water level. During peak water levels, a large amount of flow would be entering London Avenue Canal. Any high water marks in the canals would be affected by the entrance loss at the junction of London Canal and Lake Pontchartrain as well as the conversion of potential energy in the Lake to kinetic energy in the canal. For that reason, points inside London Canal were not used. Levee debris points along the lakefront levee were not used because of the large variability. The next inside building points to the east were at the old Naval Reserve on the west side of the IHNC. Three points LA 1050 at 11.4 ft, LA 1086 at 11.9 ft, and LA 1154 at 11.8 ft result in an average value of 11.7 ft for this location. The last inside building marks were at the Lakefront Airport east of the IHNC where three marks were found LA 1033 at 11.7 ft, LA 1063 at 12.1 ft, and LA 1253 at 11.8 ft for an average of 11.9 ft. No inside building marks could be found east of the Airport.

Using the best estimate curve, the 4 canals have the following values of peak water level: 1) 17th Street Canal at 10.8 ft, 2) Orleans Canal at 11.1 ft, 3) London Canal at 11.4 ft, and 4) IHNC at 11.8 ft. All elevations are in NAVD88 (2004.65). Using these peak water levels at the canal entrances along with the constructed hydrographs at 17th Street Canal and the Lakefront Airport (discussed in the following section), hydrographs were interpolated for Orleans, London, and the IHNC Canal entrances as shown in Figure 1-5 for a general plot and Figure 1-6 for a detailed plot.

## Constructed Hydrograph for 17th Street Canal Entrance

**General Description.** Gage data defining the time variation of water level during Hurricane Katrina were not available on the South shore of Lake Pontchartrain in the vicinity of the breaches on 17th Street and London Canals or on the Inner Harbor Navigation Canal. The time variation of water level is needed to define the water level at various events during the hurricane, such as the water level at the time of a floodwall breach. As part of the data collection task of the IPET, high water marks, intermediate water marks from photographs, and observations recorded in a log by an individual are used to construct a hydrograph for the 17th Street Canal. All elevations are in the time dependent datum of NAVD88 (2004.65).

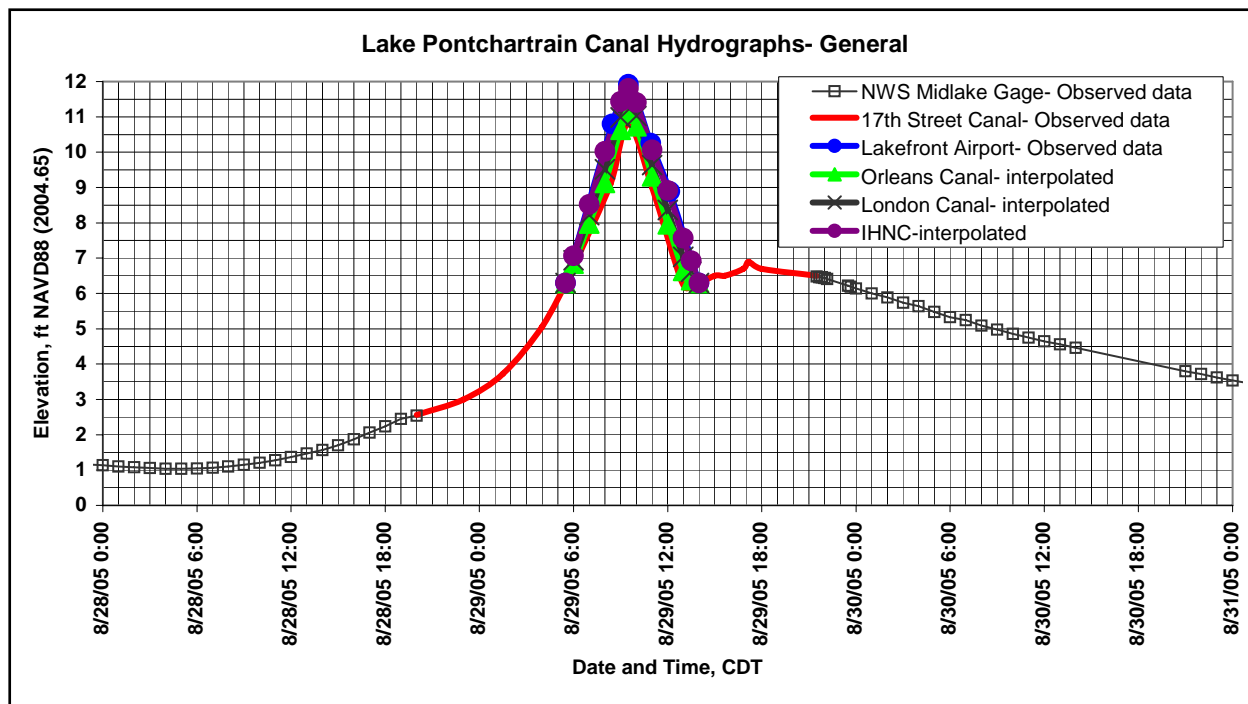


Figure 1-5. Constructed and interpolated hydrographs at canal entrances- general view.

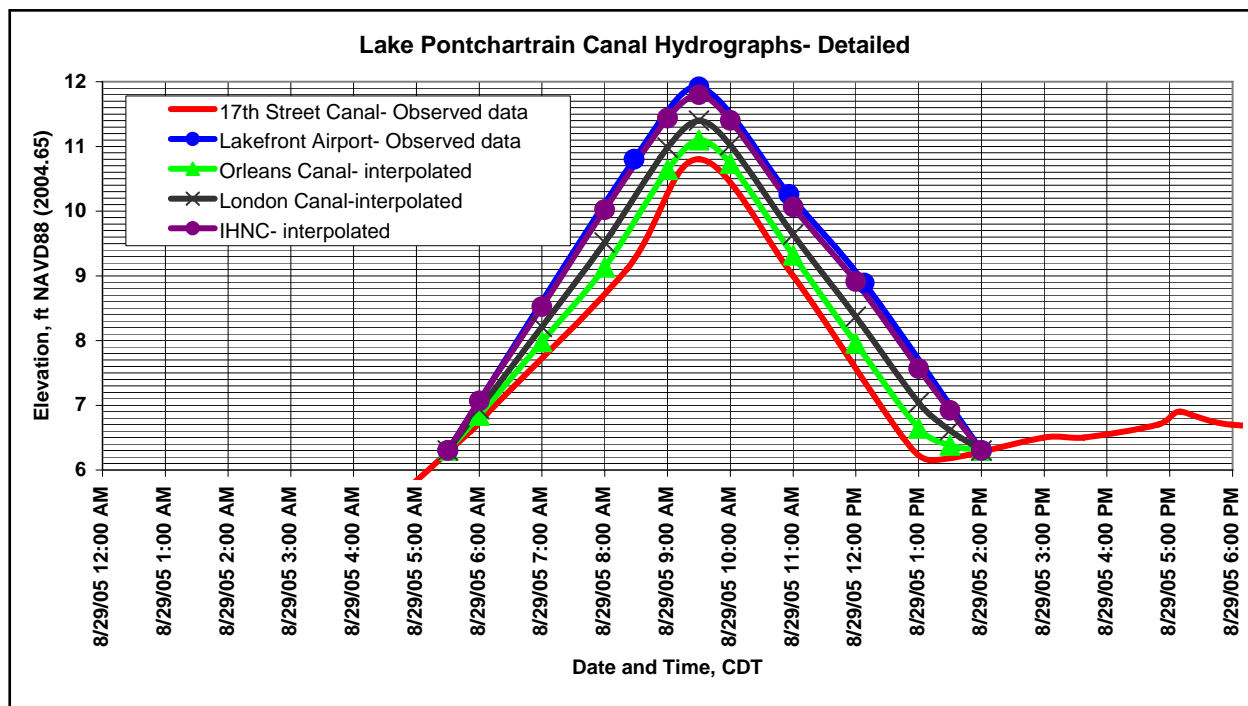


Figure 1-6. Constructed and interpolated hydrographs at canal entrances- detailed view.

**Water level data from digital pictures.** A boat owner stayed at the Municipal Yacht Harbor (MYH) on his boat during Katrina. The MYH is located immediately east of the entrance to the 17th Street Canal on Lake Pontchartrain as shown in Figure 1-7. The boat was a large steel

hulled trawler moored in the location shown on Figure 1-7. The boat was moored with multiple 2” diameter hawsers. Figure 1-8 shows a view looking south toward the MYH building that is located on the south side of the Harbor. Figure 1-8 also shows blue railing (background) and piling (foreground) that were used to define water surface elevation in the digital photographs. The blue railing has two levels above the concrete dock supporting the railing. The center of the lower rail is 1.95 ft above the concrete dock. The center of the higher rail is 3.85 ft above the concrete dock. The rails are 0.2 ft in diameter. Table 1-1 shows various surveyed elevations pertinent to determining elevations from the photographs including the average tops of pilings looking northeast from the position of the boat. These pilings are shown in subsequent pictures labeled “looking northeast” and were relatively consistent in top elevation and only visible at elevations less than about 6.9 ft. The points taken from the digital pictures were initially surveyed in November 2005. These points were resurveyed by a different company in March 2006 and found to be correct.

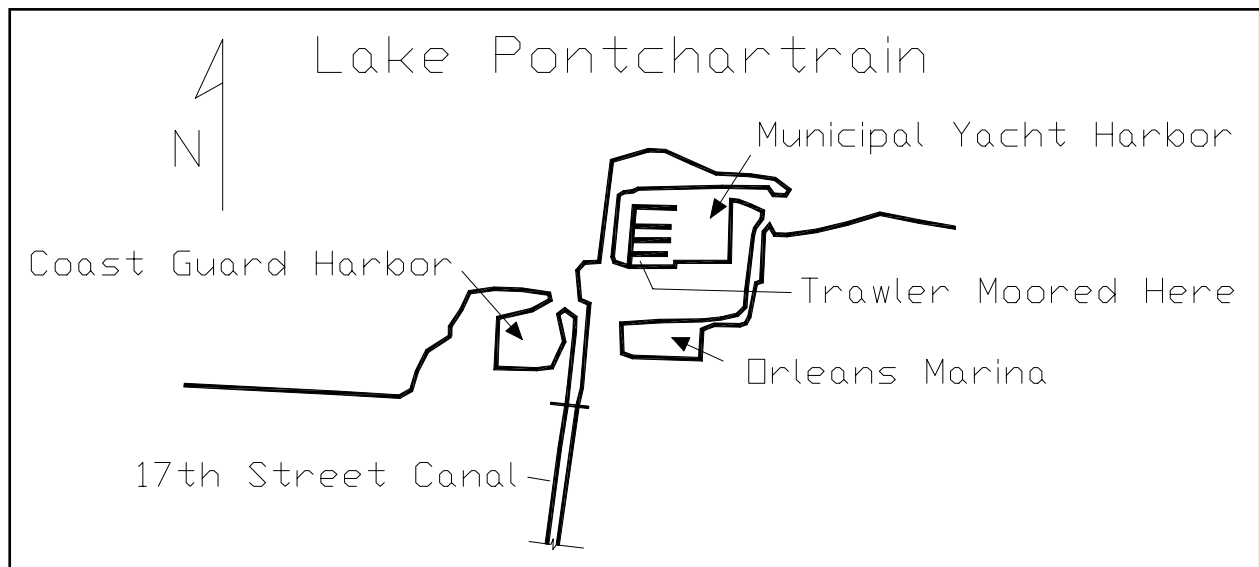


Figure 1-7. Location of Municipal Yacht Harbor and Orleans Marina at 17th Street Canal.



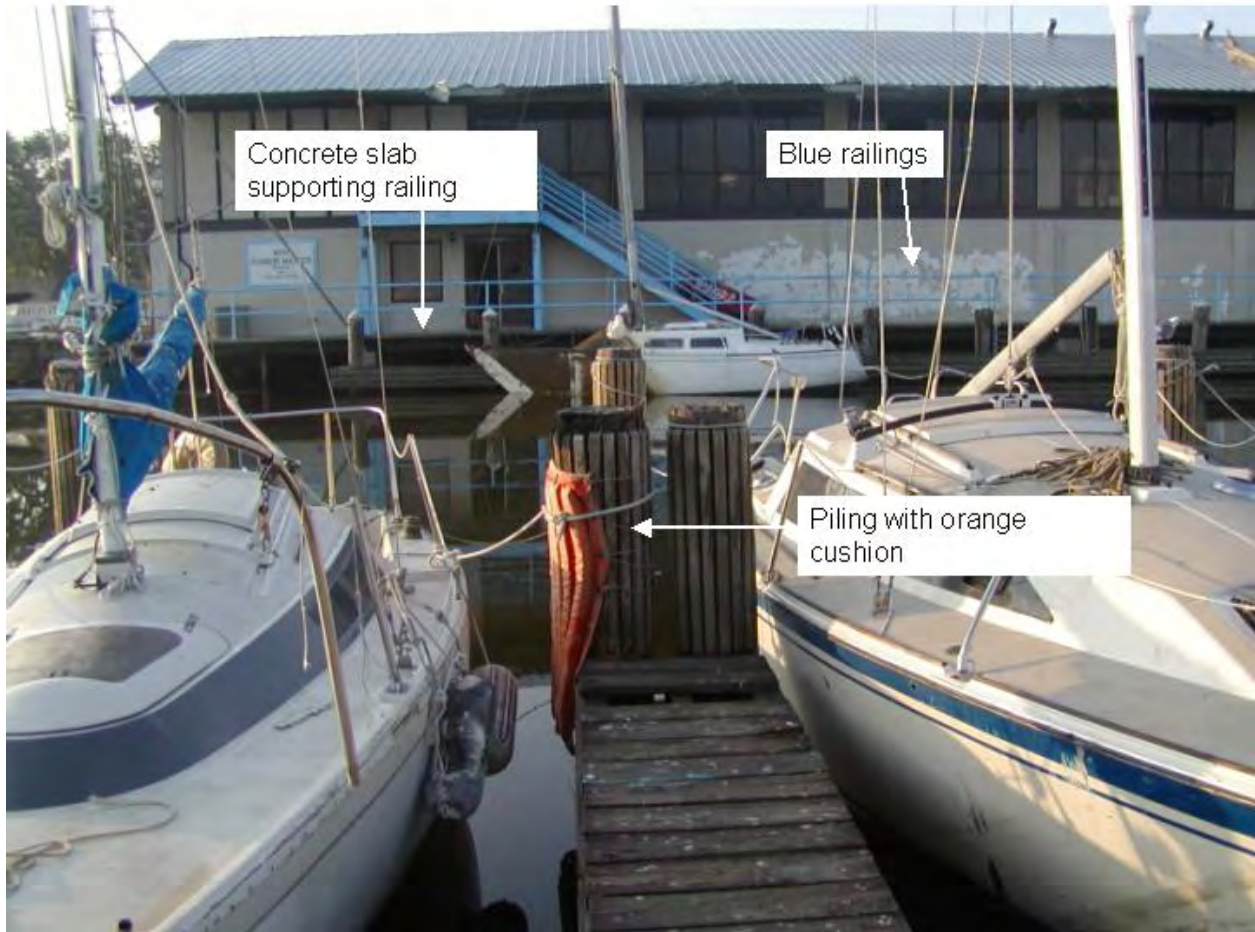


Figure 1-8. Railings, pilings, and other features near Municipal Yacht Harbor Building. Looking south

<b>Table 1-1 Elevations of Features Pertinent to Determine Water Surface Elevations from the Boat Owner Pictures</b>		
<b>Feature</b>	<b>Elevation, ft NAVD88 (2004.65)</b>	<b>Source</b>
Slab supporting blue railing	5.25	Surveyed
Center of lower railing	7.2	Slab elevation plus 1.95 ft
Center of Upper railing	9.1	Slab elevation plus 3.85 ft
Slab near chain link fence	3.9	Surveyed
Top of piling with orange cushion wrapped	6.6	Surveyed
High water mark	10.3	Surveyed
Average tops of pilings northeast of moored boat	6.9	Surveyed
Water level on electrical box showing elevation on 8/30 at 1132 (CDT)	4.55	Surveyed

A series of digital photographs were taken with a Sony DSC-F828. Some provided information for delineating water level while others did not. The pictures were tagged with time that was one hour behind Central Daylight Time (CDT). The camera owner/operator and the LSU Hurricane Center personnel confirmed that the camera file times were in Central Standard

Time. References to time in this report will use CDT by adding 1 hour to the digital picture tagged times. To convert to UTC, add 5 hours to CDT.

- a. 0552 (CDT) on 8/29/05, elevation 6.6 ft: Figures 1-9 and 1-10 show pictures taken of the blue rail at 0552 (CDT). By knowing the distance between the top and bottom rails and the elevation of both rails, the distance from the bottom rail to the water surface can be determined using the ratio of distances in the photograph. In Figure 1-9 the water level is 1.0 ft below the lower rail. In Figure 1-10, the water levels at the 3 vertical posts are 0.2, 0.6, and 0.7 ft below the lower rail. The differences in distance below the lower rail is the result of wave action that has a wave height (trough to crest) of at least 0.8 ft based on these two pictures. By averaging the distances, the wave effects are reduced but not eliminated. Averaging all 4 yields an average distance below the lower rail of 0.6 ft for a water surface elevation of  $7.2 - 0.6 = 6.6$  ft.
- b. 0814 (CDT) on 8/29/05: Pictures DSC02233-DSC02236 show the harbor with no tops of piling visible but no elevations can be determined.
- c. 0816 (CDT) – 0826 (CDT) on 8/29/05, elevation 9.1 ft: Figures 1-11 to 1-15 (pictures DSC02237-DSC02241) show the water level at the top rail in all available pictures. Figure 1-14 shows the double door in the middle of the north wall of the MYH building. The boat owner said the double door was knocked down sometime on the 8/29/05. Elevation of the top rail is 9.1 ft.
- d. 0934 (CDT) – 0935 (CDT) on 8/29/05: Pictures DSC02242-DSC02244 show intense rain but no features that provide an elevation. These pictures are in the middle of the time range that contains the peak storm surge presented subsequently.
- e. 1005 (CDT) on 8/29/05: Pictures DSC02245-DSC02250 show boats in the harbor but no tops of piling that could provide an elevation. These pictures are at the end of the time range that contains the peak storm surge presented subsequently.
- f. 1312 (CDT) – 1313 (CDT) on 8/29/05, elevation 6.3 ft: Pictures DSC02251-DSC02256 show pilings in the harbor. Figure 1-16 (DSC02255) shows a double piling with some orange visible beside the piling. At the site visit, only one double piling had an orange wrap that was loose at the bottom and would have floated up during the higher water level. A mark was placed on this piling at the water level estimated from the picture. The mark was 0.5 ft below the top of the piling. This mark was surveyed and found to be at elevation 6.2 ft. Other pilings in the picture were also about 0.5 ft below the top of piling providing an elevation of 6.4 ft. A value of 6.3 ft is used for this time.



Figure 1-9. Picture DSC02231.JPG taken at 0552:00 CDT on 8/29/05, elevation 6.6 ft. Looking southwest. Water level is 1.0 ft below lower rail.

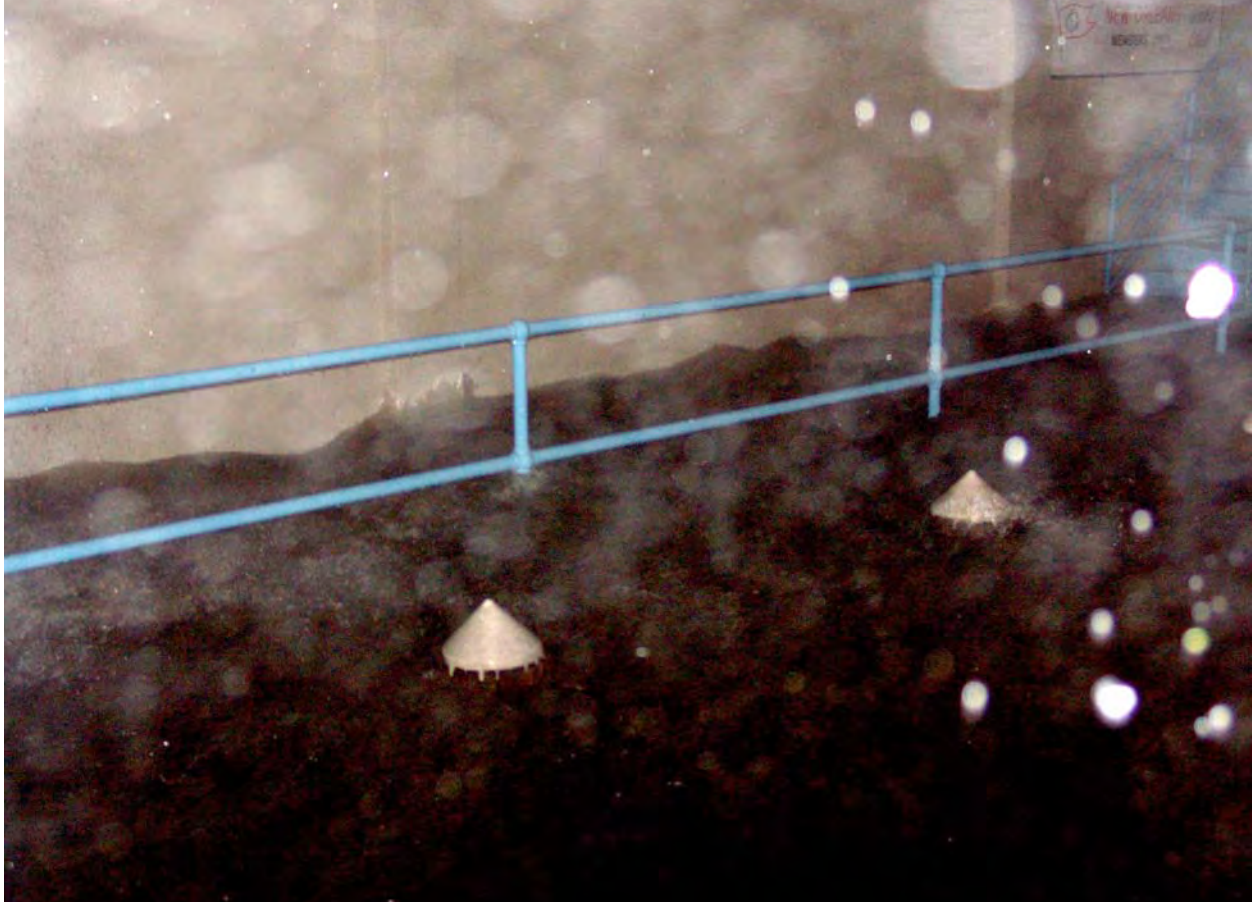


Figure 1-10. Picture DSC02232.JPG taken at 0552:22CDT on 8/29/05, elevation 6.6 ft. Looking southwest. Left vertical post: water level 0.2 ft below lower rail. Center vertical post: water level 0.6 ft below lower rail, right vertical post: water level 0.7 ft below lower rail. Average of all observations from DSC02231 and DSC02232 is 0.6 ft. Picture brightness and contrast adjusted.





Figure 1-11. Picture DSC02237.JPG taken at 0816:22 (CDT) on 8/29/05, elevation 9.1 ft. Looking southeast. Water level at upper rail. Brightness and contrast adjusted.



Figure 1-12. Picture DSC02238.JPG taken at 0816:28 (CDT) on 8/29/05, elevation 9.1 ft. Looking southeast. Water level at upper rail. Brightness and contrast adjusted



Figure 1-13. Picture DSC02239.JPG taken at 0816:52 (CDT) on 8/29/05, elevation 9.1 ft. Looking southeast. Water level at upper rail. Brightness and contrast adjusted.



Figure1-14. Picture DSC02240.JPG taken at 0826:32 (CDT) on 8/29/05, elevation 9.1 ft. Looking south. Water level at upper rail.



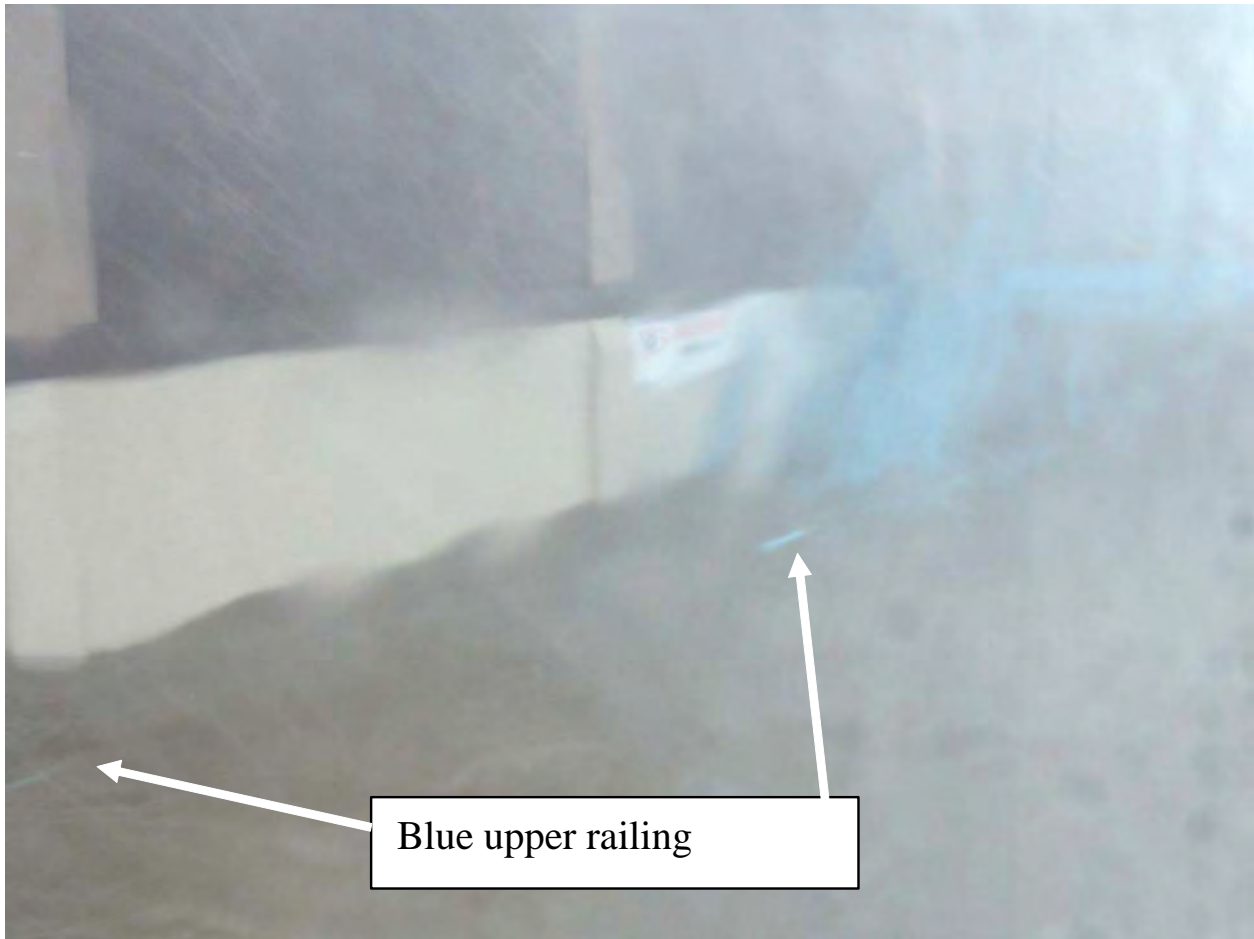


Figure 1-15. Picture DSC02241.JPG taken at 0826:36 (CDT) on 8/29/05, elevation 9.1 ft. Looking south. Water level at upper rail. Brightness and contrast adjusted.



Figure 1-16. Picture DSC02255.JPG taken at 1313 (CDT) on 8/29/05, elevation 6.3 ft. Looking northeast

- g. 1537 (CDT) – 1543 (CDT) on 8/29/05, elevation 6.5 ft: Numerous pictures provide rail evidence and top of piling evidence. Figure 1-17 (DSC02262- 1538:44) shows the water level at 5 vertical posts at 0.7, 0.8, 0.8, 0.7, and 0.6 ft below the lower rail that averages 0.7 ft. Figure 1-18 (DSC02263- 1538:54) show the water level at 4 vertical posts at 0.5, 0.7, 0.7, and 0.9 ft below the lower rail that averages 0.7 ft below the lower rail that gives an elevation of  $7.2 - 0.7 = 6.5$  ft. Figures 1-19 (DSC02267- 1539:34) and 1-20 (DSC02269- 1539:56) show the double piling with the orange cushion. Based on the photographs, the water level is about 0.1 ft below the top of piling giving an elevation of 6.5 ft.
- h. 1648 (CDT) – 1650 (CDT) on 8/29/05, elevation 6.7 ft: Numerous pictures (DSC02280- DSC02296) of fire in background and top of piles both close to the boat and far away. Figure 1-21 (DSC02287) shows a typical picture of top of piling relative to water level. Average distance of water level below tops of piling was about 0.1-0.3 ft. Based on surveyed average top of piling, average elevation was 6.7 ft.
- i. 1710 (CDT) – 1724 (CDT) on 8/29/05, elevation 6.9 ft: Pictures DSC02297 – DSC02327 show distance of water level below tops of highest pilings of about 0.1 ft or an elevation of 6.8 ft. Figures 1-22 (DSC02305- 1711:04) and 1-23 (DSC02306- 1711:14) show the chain link fence section west of the moored boat. The water level position on the fence

was determined by counting the openings in the chain link fence and measuring that location on the fence above the slab that was surveyed near the fence. The distances above the slab were 3.6 ft and 2.6 ft giving respective water surface elevations of 7.5 and 6.5 ft for the two photographs that were 10 sec apart. In this case, wave height was at least 1.0 ft. Average water surface elevation based on the chain link pictures is 7.0 ft. Average of chain link derived and top of piling derived water surface elevations is 6.9 ft. By averaging the chain link derived water surface elevations with the top of piling derived elevations, the effects of wave action is reduced but not eliminated.

- j.* 1757 (CDT) – 1758 (CDT) on 8/29/05, elevation 6.7 ft: Pictures DSC02328- DSC02337 show the water level at about 0.2 ft below the tops of the highest pilings giving an average elevation of about 6.7 ft. Figure 1-24 (DSC02333) shows a typical top of piling picture.
- k.* 1132 (CDT) on 8/30/05, elevation 4.55 ft: Figure 1-25 (DSC02338) shows electrical box where the water level on 8/30 is 4.0 ft above the water level on 11/8 based on measuring the location of the water on the box in the picture down to the water level on 11/8. This point was not surveyed in the initial survey. The electrical box is located on the east end of the third row of docks. The water level on 11/8 was 5.8 ft lower than a surveyed mark on a piling that was at elevation 6.15 giving a water level of  $6.2 - 5.8 = 0.4$  ft on 11/8. The water level on 8/30 =  $4.0 + 0.4 = 4.4$  ft. In the resurvey in 2006, this point was at an elevation of 4.55 ft.



Figure 1-17. Picture DSC02262.JPG taken at 1538:44 (CDT) on 8/29/05, elevation 6.5 ft. Looking east-southeast. From left to right vertical posts, water level is 0.7, 0.8, 0.8, 0.7, and 0.6 ft below the center of the lower rail.





Figure 1-18. Picture DSC02263.JPG taken at 1538:54 (CDT) on 8/29/05, elevation 6.5 ft. Looking southeast. From left to right, water level is 0.5, 0.7, 0.7, and 0.9 ft below the center of the lower rail.



Figure 1-19. Picture DSC02267.JPG taken at 1539:34 (CDT) on 8/29/05 elevation 6.5 ft. Looking northeast.



Figure 1-20. Picture DSC02269.JPG taken at 1539:56 (CDT) on 8/29/05, elevation 6.5 ft. Looking northeast.





Figure 1-21. Picture DSC02287.JPG taken at 1649 (CDT) on 8/29/05, elevation 6.7 ft. Looking northeast.





Figure 1-22. Picture DSC02305.JPG taken at 1711:04 (CDT) on 8/29/05, elevation 7.5 ft. Looking west



Figure 1-23. Picture DSC02306.JPG taken at 1711:14 (CDT) on 8/29/05, elevation 6.5 ft. Looking west.



Figure 1-24. Picture DSC02333.JPG taken at 1757 (CDT) on 8/29/05, elevation 6.7 ft. Looking northeast





Figure 1-25. Picture DSC02338.JPG taken at 1132 (CDT) on 8/30/05 elevation 4.4 ft. Electrical box at east end of third row of docks

**Log of Water Level Observations.** A second boat owner stayed on his boat in the Orleans Marina (Figure 1-7) during Hurricane Katrina on Sunday and Monday, August 28 and 29, 2005 and kept a log of water levels during the storm. The boat owner was interviewed by the IPET on 12-15-05 at his boat in the Orleans Marina. Log entries were as follows:

- a. Sunday 8/28/05, 16:00 hrs: Water level 1 ft above normal. No mark will be surveyed because uncertain how to quantify “normal.”
- b. Sunday 8/28/05. 23:00 hrs, elevation 3.0 ft: Water level at bottom side of the 2X6’s covering the deck of the finger pier. Survey point OM-01, Figure 1-26.
- c. Monday 8/29/05,01:30, elevation 3.7 ft: Water level at top of 1<sup>st</sup> step up from finger pier. Survey point OM-02, Figure 1-27.
- d. Monday 8/29/05,04:00, elevation 5.1 ft: Water level at top of concrete pile cap. Survey point OM-03, Figure 1-28.
- e. Monday 8/29/05,06:00, elevation 5.6 ft: Water level at top of steps equal to top of main concrete dock in Figure 1-28. Survey point OM-04.
- f. Monday 8/29/05,06:15, elevation 7.0 ft: Water level at 1<sup>st</sup> rail. Survey point OM-05, Figure 1-29.

- g. Monday 8/29/05,10:00, elevation 10.1 ft: Water level at top rail. Survey point OM-06, Figure 1-29.



Figure 1-26. Time 23:00 on 8/28/05, elevation 3.0 ft. Bottom of 2X6 deck board





Figure 1-27. Time 1:30 on 8/29/05, elevation 3.7 ft. Top of first step on finger dock

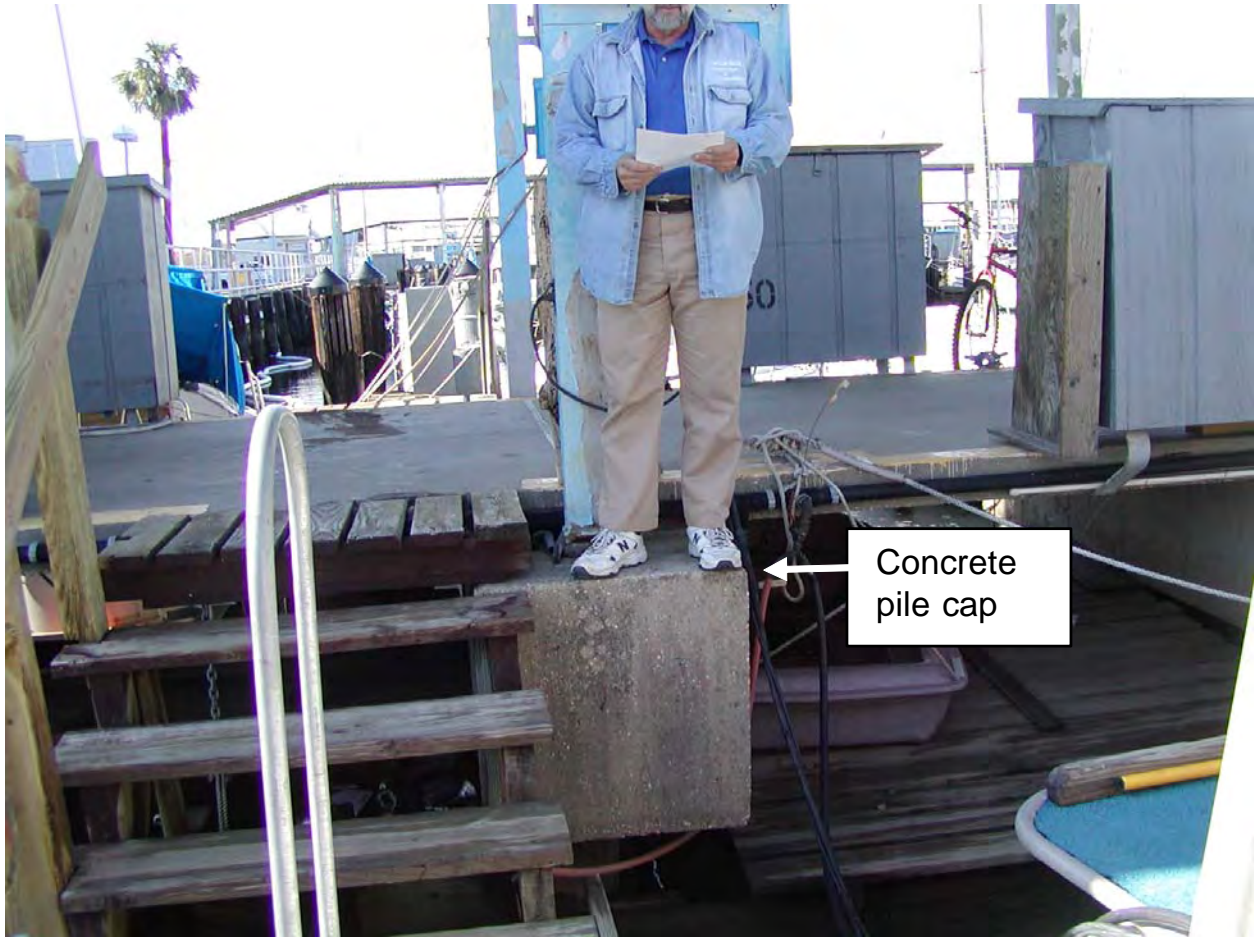


Figure 1-28. Time 4:00 on 8/29/05, elevation 5.1 ft. Top of concrete pile cap next to steps





Figure 1-29. Time 6:15 on 8/29/05, elevation 7.0 ft (bottom rail) and 10.1 ft (top rail)

- h. Monday 8/29/05, 11:00, elevation 9.2 ft: The boat owner stated that he observed the water on the floodwall was falling at 1100 hrs. He pointed to a location on the floodwall that was 2'3" below the top of floodwall (floodwall at 12.5 ft NAVD88, 2004.65) that was the location of the peak of the 2 ft waves being caused by the West wind. A survey point was placed at 3'3" below the top of wall and asked if this level would represent an average water level. He agreed that it was. Survey point OM-09, Figure 1-30, was the average level. This point has a high degree of uncertainty.
- i. Monday 8/29/05, from 12:45 to 15:00, elevation 6.5 ft: Water level at top of main walkway that supports metal railing. Elevation scaled from Figure 1-31 as 6.5 ft.
- j. Monday 8/29/05, unknown time, elevation 11.9 ft: HWM on a column near steps based on visual observation by boat owner and based on another boat owner's (who also stayed on his boat) depth sounder that resulted in the peak storm surge at 7 ft over the main pier. Because use of this mark would require checking the depth sounder and there are numerous HWM inside buildings in this area, this mark was not used.
- k. Monday 8/29/05, unknown time: The boat owner showed us a boat that had gouges on the stern where it had risen with the storm surge and hit the metal roof which gouged the boat. Boat located at Pier 5, slip 47 (2nd slip on left). Since the location on the bent roof



that caused the gouges is uncertain and the vertical extent of the gouges is about 1 ft, this HWM was not used.

- l. It must be noted that this individual believed the peak happened between 10:00 and 11:00 AM and closer to 11:00. His observations at 10:00 and 11:00 show the water level was falling. He was not able to make observations between 6:15 and 10:00 AM that contains the time interval of peak storm surge from the Lakefront Airport photographs.

**High water marks.** The high water mark (HWM) at the MYH was consistent at several locations inside the building and 5.2 ft above the floor. This mark, LA 1163, was surveyed as elevation 10.3 ft. This magnitude is compared in Table 1-2 to other HWMs in the 17th street area of Lake Pontchartrain. Figure 1-1 shows the locations of the high water marks. All of the HWMs are inside buildings and values in Table 1-2 are presented in NAVD88 (2004.65). Buildings are generally “tight” having brick walls and steel doors or “porous” having unsealed sheet metal walls attached to a metal framework. Based on the author’s field observations of each mark in Table 1-2, marks are labeled as (1) a likely high estimate of surge because of the presence of waves inside a porous building, (2) a possibly low estimate of surge because the mark was inside an undamaged tight building that may not have reached equilibrium, or (3) uncertain whether high or low because building was tight but damaged in the storm at an unknown time in the hydrograph. The four values for likely high estimate of surge range from 11.0 to 11.7 ft NAVD88 (2004.65). The 5 possibly low estimate of surge ranges from 10.0 to 10.9 ft NAVD88 (2004.65). Six values of 10.3 to 11.1 were classified as uncertain whether high or low. Three techniques were used to determine a representative value as follows:



Figure 1-30. Time 11:00 on 8/29/05, elevation 12.5 ft (top of floodwall), 10.2 ft (peak of 2 ft waves), 9.2 ft (average water level at OM-09)



Figure 1-31. Main walkway of Orleans Marina. Boat is just behind individual on the walkway.

**Table 1-2  
High Water Marks in 17th Street Canal and Vicinity**

LA ID#'s	Elevation, ft NAVD88 (2004.65)	Description
1007	10.8	Seed/debris line inside Coast Guard, brick and steel door room. Door had crease on backside indicating it was blown open but not known when. Uncertain whether this is low or high estimate of surge.
1031	10.9,10.3, 10.0, 10.4	Seed/debris line in Coast Guard rooms that had steel doors that were relatively tight and were intact. These points are possibly low estimates of surge because of building tightness.
1008,1009	10.7,11.0	Seed/debris line inside storage room of residential type construction, double door with wooden frame lying on floor, lower mark has less wave exposure. These points are unknown whether high or low because not certain when doors were damaged.
1010, 1020	11.7,11.0	Seed/debris line in sheet metal building which has many entry points for water and was severely damaged by Katrina. Lower mark set by COPRI after observing first mark had more wave exposure. These points are likely high estimates of surge because of wave exposure.
1032	10.2	Seed/debris line in Orleans Marina Men's restroom. Brick and steel door building. This point is possibly a low estimate of surge because of building tightness.
1034	10.8	Hong Kong restaurant. Seed/debris line on outside of building. Uncertain whether this point is high or low because the building was tight but damaged sometime during the storm.
1035	11.4	Seed/debris line inside severely damaged boathouse, definite wave exposure. This point is likely a high estimate of surge because of wave exposure.
1036	11.2	Seed/debris line inside sheet metal building that was severely damaged by Katrina. This point is likely a high estimate of surge because of wave exposure.
1038	11.1	Coast Guard, seed/debris line inside garage room with roll down door that had damage to the bottom during Katrina. Uncertain whether this is low or high estimate of surge.
1056	10.8	Levee Debris just west of Coast Guard. This is likely a high estimate of surge due to wave exposure. This is the only outside mark and is given no weight.
1163	10.3	Seed/debris line inside municipal yacht harbor. Steel door and brick building that was damaged by Katrina. Uncertain whether this is a low or high estimate of surge.

- a. Average of all points = 10.8 ft.
- b. Omit high category and low category HWMs. Average of uncertain points = 10.8 ft.
- c. Use one value for each location and average all locations. In buildings such as the Coast Guard where 5 points were taken, an average for each location was determined. The average of all locations was determined to be 10.9 ft.

Based on the above averaging techniques, a high water mark value of 10.8 ft is recommended for the 17th Street Canal entrance. Using all values in Table 1-2, the high water mark data has a standard deviation of 0.5 ft.

The timing of the high water mark is needed to position the high water mark in the hydrograph. Based on ADCIRC model results, the timing of peak high water at the 17th Street Canal and the Lakefront Airport is within 15-20 minutes of each other. The photographic record at Lakefront Airport is the best data available concerning when the peak occurred. Based on data from the Lakefront Airport and both marinas discussed herein, the peak water level occurred sometime between 9:00 AM and 10:00 AM. This time range will be shown on the hydrograph. This high water time range also agrees with the time estimate of an Orleans Avenue Canal Pump Station #7 operator who stated the short wall connecting the pump station to the floodwall started overflowing at 8:30-9:00 and lasted for about 1.5 hours.

**Hydrograph Plot-** The data derived from the boat owner pictures, log, and the high water mark are plotted in the Figure 1-32 hydrograph.

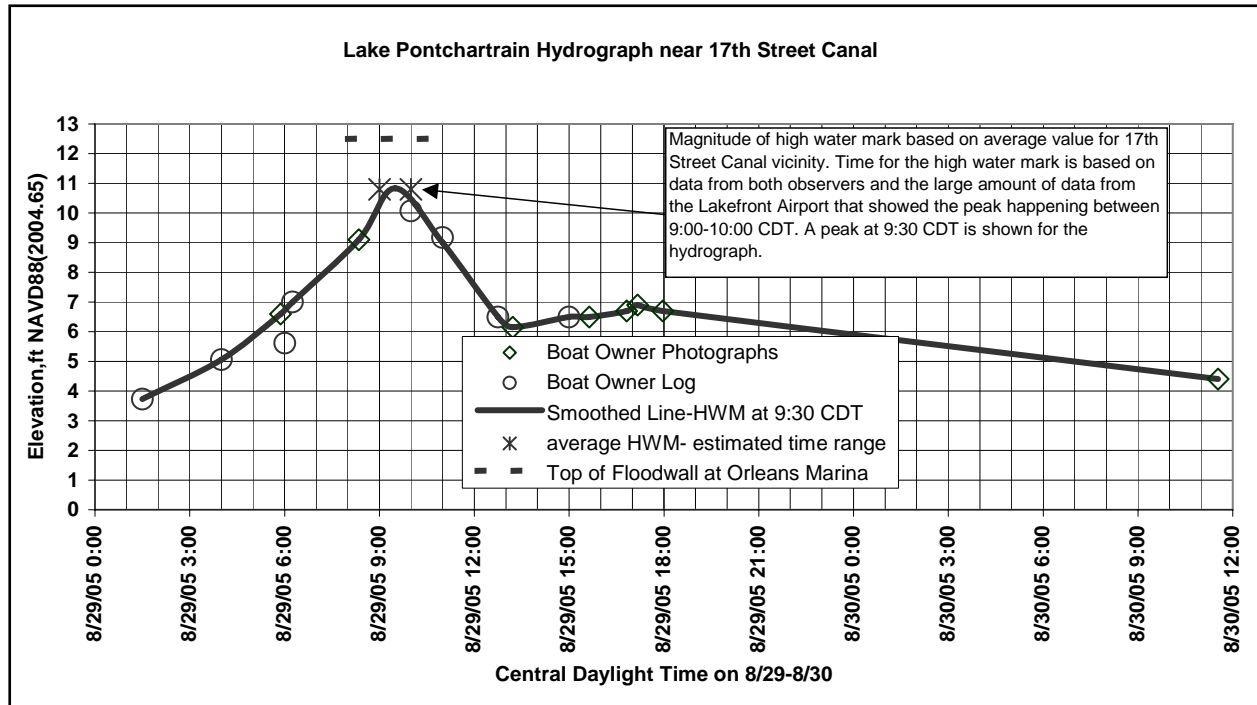


Figure 1-32. Hydrograph for Lake Pontchartrain at 17th Street Canal based on digital photographs, log of events, average HWM in vicinity, and HWM time based on boat owners and Lakefront Airport data.

## Constructed Hydrograph for New Orleans Lakefront Airport

**General Description.** During the passage of Hurricane Katrina on Monday August 29, 2005, personnel of the Orleans Levee District stayed in the terminal building of the Lakefront Airport (Figure 1-33). Levee District personnel used digital cameras to record events during the hurricane including the rise and fall of storm surge both inside and outside the terminal building. The digital photographs were used to identify water level locations that were subsequently surveyed. The surveyed elevations along with the time stamp on the digital picture files were used to construct a hydrograph for the Airport location.

**Water Level Data from Digital Photographs.** The digital cameras used by levee district personnel were an HP Photosmart 735, a Sony DSC P72, and a Sony FDMAVICA. The Sony DSC P72 had no automatic time update for daylight savings time (DST) whereas the HP Photosmart 735 has this feature as an option. The FDMAVICA has this feature on some cameras. The operator of the Sony DSC P72 camera confirmed that the time on this camera was 12 hr 9 min ahead during daylight savings time. The operator provided a cell phone picture on Dec 15, 2005 at 8:23 PM and the file information showing 9:32 AM on the 16th. When checked after DST in January 2006, the HP Photosmart 735 camera was 1 hour ahead that would have made the camera time correct during DST if the camera did not have this feature. The HP





and leaving the vicinity of the airport. (2) Wave activity in the terminal and surrounding buildings was reduced by the presence of the runways.

Table 1-3 shows the sequence of photographs and surveyed elevations that were used to construct the hydrograph. The table provides picture filenames as received from the Orleans Levee District. The following paragraphs describe each point in Table 1-3. Unless noted all points are in the time dependent datum of NAVD88 (2004.65).

- a. Time 7:29, Airport high water mark (APH)-01, elevation 6.7, Figure 1-34. Located south of terminal building on sloping wall. APH-01 is the earliest photograph providing stage data at the airport. Being on the south side of the terminal building, this mark is protected from direct wave activity from Lake Pontchartrain. Low wave action is evident.
- b. Time 7:29 AM, APH-22, elevation 6.6, Figure 1-35. On south wall of terminal building near east walkway. Horizontal joint in wall is 0.3 ft above floor of terminal which is at elevation 8.45 ft. Distance from bottom of light to joint was 6.3 ft. Scaled distance from joint to water surface was 2.2 ft. The influence of the surrounding bathymetry on water levels raises significant doubt about points APH-01 and APH-22.
- c. Time 8:27 AM, APH-21, elevation 10.8, Figure 1-36. Picture inside terminal lobby in which brightness and contrast have been adjusted to show water level. The window height was measured at 4.5 ft and the distance from the bottom of the window to the floor was 3.5 ft. Based on scaling the photograph, the distance from the bottom of the window to the water surface was 1.2 ft resulting in a 2.3 ft depth above the floor. The floor of the terminal is at elevation 8.45 giving a water level of 10.8.
- d. Time 8:28 AM, APH-15, elevation 10.8, Figure 1-37. Inside terminal on wall near south door in Figure 1-37. The distance on the wall above the bottom of the light switch was measured at 2.7 ft and the bottom of the light switch to floor was 4.2 ft. Based on scaling the photograph, the distance to the water surface was 1.9 ft below the bottom of the switch giving a depth above floor of 2.3 ft. Based on a terminal floor elevation of 8.45 ft, water level was 10.8 ft. Note that the column in the figure is brown whereas the same column in subsequent figures is white. According to Orleans Levee District personnel, the picture in Figure 1-37 was taken just before the fake marble covering fell off the column. The inside terminal elevation marks should have low wave activity and low uncertainty. The agreement of APH-15 and APH-21 elevations adds to the confidence in water level at this time in the hydrograph but some low wave activity can be seen inside the terminal in Figure 1-36.

**Table 1-3  
Water Levels at Lakefront Airport based on Digital Pictures**

Time	HWM#	Location	Photograph #	Camera	Elevation, ft NAVD88 (2004.65)
7:29 AM (7:38 PM)*	APH-01	Sloping wall south of entrance	DSC00943	DSC-P72	6.7
7:29 AM (7:38 PM)*	APH-22	South wall of building, east walkway	DSC00945	DSC-P72	6.6
8:27 AM (8:36 PM)*	APH-21	Window on inside wall of west side of lobby	DSC00948	DSC-P72	10.8
8:28 AM (8:37 PM)*	APH-15	Wall switch near south entrance door.	DSC00949	DSC-P72	10.8
9:40 AM	APH-04	Column on east side of balcony on north side of bldg	Gallery 4 KatG400003	Sony FDM AVICA	11.7
9:42 AM	APH-03	Wall just north of spiral staircase on east side of bldg	Gallery 4 KatG400004	Sony FDM AVICA	10.6
9:55 AM	APH-05	On chain link fence, north side of bldg, east of lobby	Gallery 1 KAT00021	HP Photosmart 735	11.3
9:56 AM	APH-16, based on APH-03	Wall just north of spiral staircase on east side of bldg	Gallery 1 KAT00022	HP Photosmart 735	10.9
10:30 AM (10:39 PM)*	APH-17, same elev as APH -03	Wall just north of spiral staircase on east side of bldg	DSC00952	DSC-P72	10.6
10:31 AM	APH-02	Wall just north of spiral staircase on west side of bldg	Gallery 4 KatG400007	Sony FDM AVICA	9.5
10:56 AM (11:05 PM)*	APH-08	Inside lobby, on column near director of aviation sign, 1.7 ft above floor	DSC00955 & Gallery 3 KatG300007	DSC-P72	10.2
10:56 AM (11:05 PM)*	APH-10	Elevator door facing on west side of lobby, 1.84 ft above floor	DSC00956 & Gallery 3 KatG300008	DSC-P72	10.3
11:48 AM (11:57 PM)*	APH-18, based on APH -13	At top of lowest window on building east of terminal building	DSC00961	DSC-P72	10.3
11:49 AM	APH-06	On switch box inside fence of APH-05	Gallery 1 KAT00026	HP Photosmart 735	9.7
12:08 PM	APH-09	Inside lobby, on column near director of aviation sign, 0.5 ft above floor	Gallery 4 KatG400011	Sony FDM AVICA	8.9
12:31 PM (12:40 AM on 8/30)*	APH-19, based on APH -13	On west side of bldg east of terminal building. 1.5 ft below top of lowest window near middle of west side of bldg.	DSC00979	DSC-P72	8.8
12:51 PM	APH-13	On west side of bldg east of terminal. 2.0 ft below top of lowest window near middle of west side of bldg.	Gallery 4 KatG400012	Sony FDM AVICA	8.3
2:46 PM	APH-12	On west side of bldg east of terminal. 0.5 ft below window sill near north west corner of bldg.	Gallery 1 KAT00042	HP Photosmart 735	7.1
5:14 PM (5:23 AM on 8/30)*	APH-20, based on APH-12	On west side of bldg east of terminal. 0.3 ft below bottom of lowest window.	DSC01010	DSC-P72	7.4
5:30 PM	APH-11	Bottom of metal railing on north side of building west of elec panel box ATS2	Gallery 1 KAT00048	HP Photosmart 735	7.4
6:30 PM	APH-14	Near corner of floodwall just north of flood gate on hand rail	Gallery 1 KAT00069	HP Photosmart 735	7.0

High water mark in Airport -No time	APH-07	High water mark inside Room 105, 3.35 feet above floor	No time stamped picture	NA	11.8
* DSC P72 camera operator confirmed this camera was 12 hrs 9 min ahead during daylight savings time.					



Figure 1-34. Time 7:29 AM, APH-01.





Figure 1-35. Time = 7:29, APH-22. Wall on south side of terminal building, east walkway

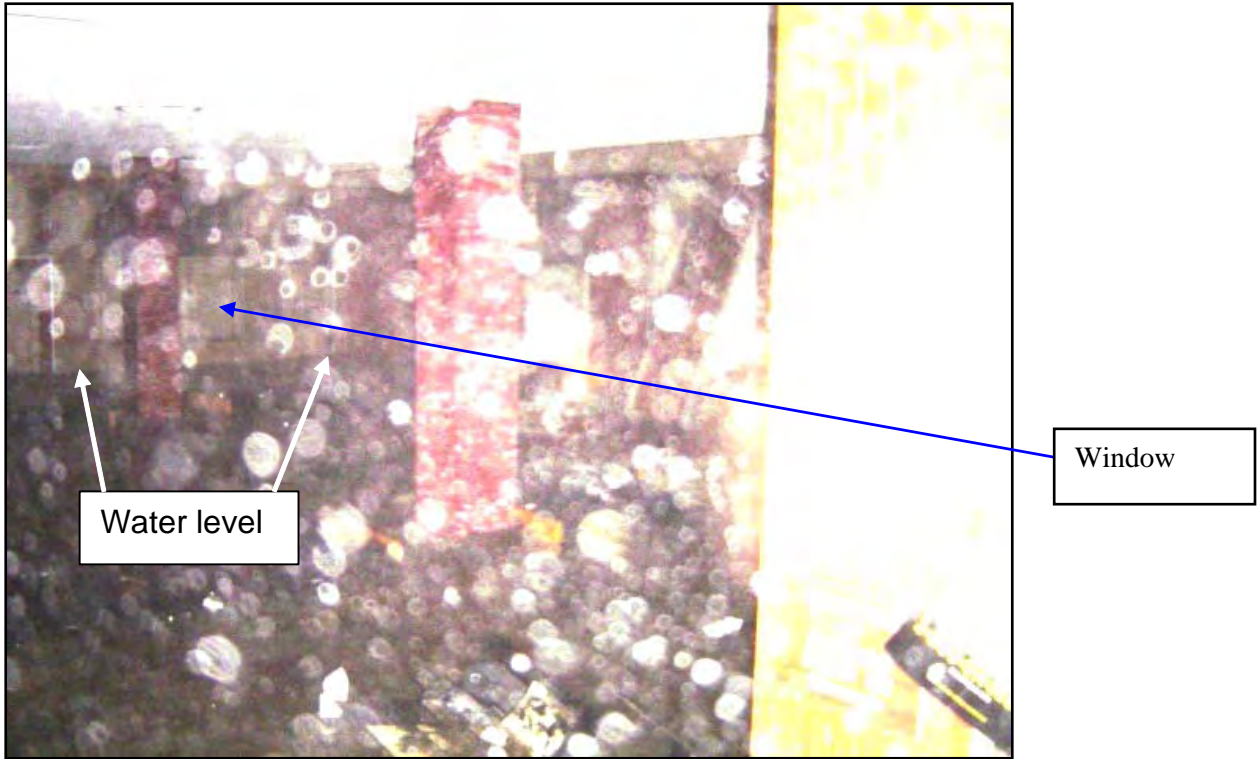


Figure 1-36. Time 8:27 AM, APH-21.



Figure 1-37. Time = 8:28 AM, APH-15. Door at south side of terminal building lobby

- e.* Time = 9:40 AM, APH-04, elevation 11.7 ft, Figure 1-38. On column outside northeast of lobby of terminal building. This mark was determined by measuring from the top of the metal rail to the bottom of the beam supporting the deck (a distance of 5.4 ft). The photograph was used to scale this distance in the photograph to the distance from the bottom of the deck beam to the water level. The distance from the photograph was 9.6 ft and this location on the column was surveyed as 12.0 ft. This value must be adjusted because the actual distance from the location of the camera and the 5.4 ft measurement is less than the actual distance from the camera location to the 9.6 ft measurement. Based on site measurements, the distance from the camera to the center of the 5.4 ft measurement is 47.2 ft versus the distance from the camera to the center of the 9.6 ft measurement was 48.4 ft. The actual distance of the 9.6 ft scaled from the photograph is  $9.6 \times 48.4 / 47.2 = 9.9$  ft. The location surveyed on the column should have been 0.3 ft lower resulting in an elevation of 11.7 ft. This was the only mark in the data set where the distance correction was felt to be important. The elevation of this mark has significant uncertainty because it is exposed to high wave activity (see Figure 1-38).
- f.* Time = 9:42 AM, APH-03, elevation 10.6 ft, Figure 1-39. On outside wall north of east spiral staircase where plaster is broken. The elevation of this mark has significant uncertainty because it is exposed to high wave activity.

- g.* Time = 9:55 AM, APH-05, elevation 11.3 ft, Figure 1-40. Mark is located on the chain link fence. This mark is exposed to high wave activity. The number of openings in the chain link fence between the top bar of the fence and the water surface were counted from the photograph. The same number was used in the field to determine the position to be surveyed.
- h.* Time = 9:56 AM, APH-16, elevation = 10.9 ft, Figure 1-41. Located on the outside wall north of east spiral staircase where plaster is broken. This mark is exposed to high wave activity.
- i.* Time = 10:30 AM, APH-17, elevation = 10.6 ft, Figure 1-42. On outside wall north of east spiral staircase where plaster is broken. This mark is exposed to high wave activity.
- j.* Time = 10:31 AM, APH-02, elevation 9.5 ft, Figure 1-43. On outside wall north of west spiral staircase. This mark is exposed to high wave activity. This mark was difficult to locate because the wall had no defined points to relate to the water level. One IPET member positioned himself in the window where the picture was taken and another IPET member placed his hand on the wall until his hand in the actual viewing and the water level in the photograph were at the same vertical position on the wall. This mark has significant uncertainty because of the method just described and the high waves present.



Figure 1-38. Time = 9:40 AM, APH-04. Water level on column northeast of lobby.





Figure 1-39. Time = 9:42 AM, APH-03. Wall north of east spiral staircase.



Figure 1-40. Time = 9:55 AM, APH-05. Chain link fence, north side of building, east of lobby.



Figure 1-41. Time = 9:56 AM, APH-16. Wall north of east spiral staircase.





Figure 1-42. Time = 10:30 AM, APH-17. Wall north of east spiral staircase.





Figure 1-43. Time = 10:31 AM, APH-02. Wall north of west spiral staircase.

- k.* Time = 10:56 AM, APH-08, elevation 10.2 ft, Figure 1-44. Located on the column just below the electrical outlet in the lobby of the terminal building. The mark was determined by scaling from the photograph the height of the outlet and the distance from the bottom of the outlet to the water surface. The height of the outlet was measured at the airport and the ratio of the photograph measurements were used to position the mark. The broken doors on the north side of the building provided limited openings to this room that should have resulted in low wave activity and low uncertainty of this mark. Some wave action is apparent in Figure 1-44.
- l.* Time = 10:56 AM, APH-10, elevation 10.3 ft, Figure 1-45. Mark was determined by scaling from the photograph the distance from the top of the white strip on the elevator door facing to the top of the elevator door opening and the distance from the top of the white strip to the water surface. The distance from the top of the white strip to the top of the elevator door opening was measured at the airport and the ratio of the photograph measurements were used to position the mark. The elevator is in a side hallway off the main lobby of the terminal building and should have little wave activity. The agreement of this mark and APH-08 is strong evidence supporting these two marks.
- m.* Time = 11:48 AM, APH-18, elevation 10.3 ft, Figure 1-46. On the west side of the building east of the terminal building, the water level is at the top of the lowest window.

Based on the survey of point APH-13, this places the top of the lowest window at 10.3 ft. As seen in the photograph, this mark is exposed to high wave activity.

- n.* Time = 11:49, APH-06, elevation 9.7 ft, Figure 1-47. Inside the chain link fence of the north side of the building east of the lobby of the terminal building. By zooming the picture, the water level is just below the 2<sup>nd</sup> row of switches on the electrical box in the middle of the picture. The location of the switches on the north side of the airport building and the 11:48 AM picture in Figure 1-46 show this point is exposed to significant wave activity.
- o.* Time = 12:08 PM, APH-09, elevation 8.9 ft, Figure 1-48. Used technique described for APH-08. Since water depth over lobby floor of the terminal building was about 0.5 ft and the lobby has limited door openings, waves in the lobby should be minor and this point has low uncertainty. The water surface around the column in Figure 1-48 has less wave activity than the earlier time in Figure 1-44.
- p.* Time = 12:31, APH-19, elevation 8.8 ft, Figure 1-49. The left side of the photograph was zoomed to the windows on the building east of the airport. Mark to be surveyed was determined by scaling from the photograph the height of the window and the distance from the top of the lowest window to the water surface. The height of the window (2.5 ft) was measured at the airport and the ratio of the photograph measurements were used to position the mark. The size of the windows and the haziness in the photograph along with the wave activity cause significant uncertainty in this mark.

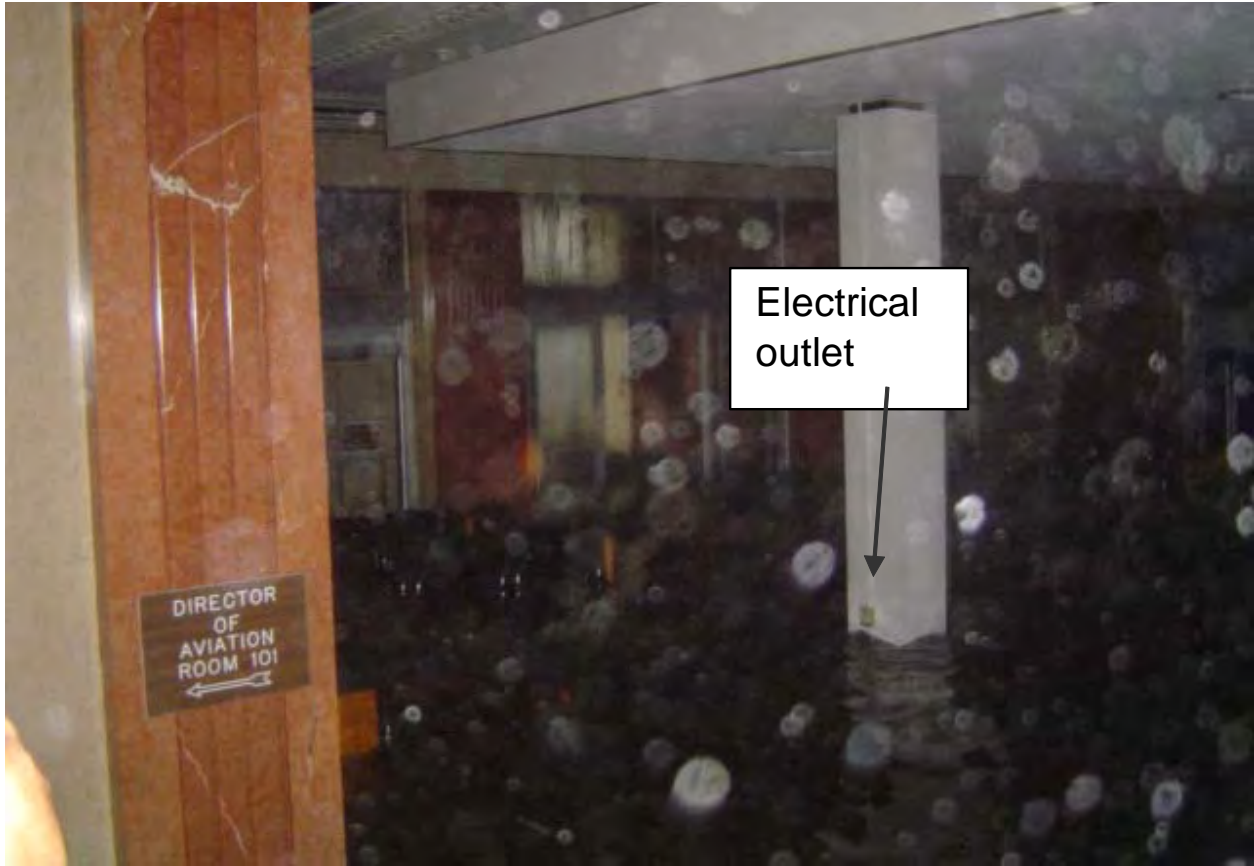


Figure 1-44. Time = 10:56 AM, APH-08. Column in terminal building lobby.



Figure 1-45. Time = 10:56 AM, APH-10, elevator east of lobby.





Figure 1-46. Time = 11:48 AM, APH-18. Top of lowest window on building east of terminal building.

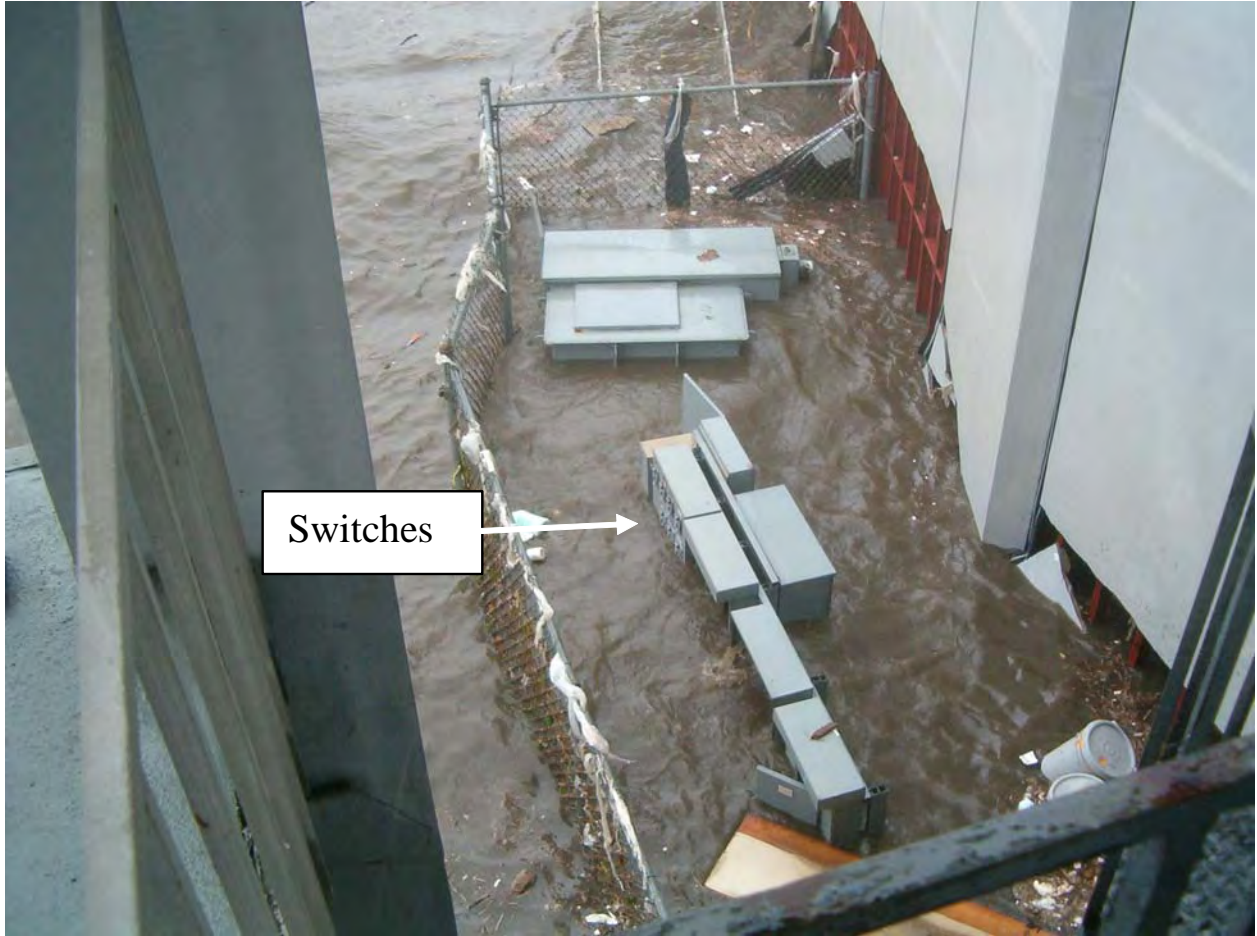


Figure 1-47. Time = 11:49 AM, APH-06. On switchbox in middle of picture.



Figure 1-48. Time = 12:08, APH-09. On column in terminal building lobby.



Figure 1-49. Time = 12:31 PM, APH-19. Windows on building just east of terminal building.

- q.* Time = 12:51 PM, APH-13, elevation 8.3 ft, Figure 1-50. Mark is on the windows on the building east of the terminal building. The mark to be surveyed was determined by scaling from the photograph the height of the window and the distance from the top of the lowest window to the water surface. The height of the window (2.5 ft) was measured at the airport and the ratio of the photograph measurements were used to position the mark which was 2.0 ft below the top of the lowest window. Even though wave activity is present, the water level can be determined at several windows that results in low uncertainty in this mark. The good agreement of this mark and the best fit line presented subsequently supports the validity of the assumed timing on the FDMAVICA camera.
- r.* Time = 2:46 PM, APH-12, elevation 7.1 ft, Figure 1-51. Mark is below the windows on the building east of the terminal building. The mark to be surveyed was determined by scaling from the photograph the height of the window and the distance from the bottom of the lowest window to the water surface. The height of the window (2.5 ft) was measured at the airport and the ratio of the photograph measurements were used to position the mark which was 0.5 ft below the bottom of the lowest window. This is the first photograph where the water is calmed significantly which makes this a mark with little uncertainty.



- s. Time = 5:14 PM, APH-20, elevation 7.3, Figure 1-52. Mark is below the windows on the building east of the terminal building. The mark to be surveyed was determined by scaling from the photograph the height of the window and the distance from the bottom of the lowest window to the water surface. The height of the window (2.5 ft) was measured at the airport and the ratio of the photograph measurements were used to position the mark which was 0.0 to 0.3 ft below the bottom of the window.
- t. Time = 5:30 PM, APH-11, elevation 7.4 ft, Figure 1-53. Located on north side of terminal building, west of lobby. Water level is at horizontal framework just to the west or right of the electrical panel box. Wave activity was low.
- u. Time = 6:30 PM, APH-14, elevation 7.0 ft, Figure 1-54. Located southwest of terminal building near floodwall opening. Mark to be surveyed was on sloping handrail that is below and slightly to the left of the jet engine. The absence of wave activity makes this a mark with little uncertainty.

**High Water Marks.** High water mark, APH-07, elevation 11.8 ft, has no definite time associated with it. Several highwater marks were found in the terminal building ranging from 3.1 to 3.75 ft above the floor of the lobby. The 3.1 ft mark was in the office on the northwest corner of the lobby that had a steel door. The level in this office may not have reached equilibrium during the brief peak storm surge. The best high water mark found at the airport was in Room 105 which had a louver at the bottom of the door that provided enough area to reach equilibrium. This room was in a hallway off the lobby of the terminal building. This mark was at 3.35 ft above the floor resulting in an elevation of 11.8 ft. Other high water marks in the Lakefront Airport vicinity are similar to APH-07. Highwater Mark (HWM) LA 1063 is inside the building east of the terminal building at elevation 12.1 ft. HWM LA1033 is inside the National Guard Bldg #103 about 0.25 mile east of terminal building at 11.7 ft. HWM 1074 is levee debris near the Marina east of the terminal building at 11.9 ft. The 3 inside points (11.8, 12.1, and 11.7) have an average value of 11.9 ft that will be used in the hydrograph.



Figure 1-50. Time = 12:51 PM, APH-13. Windows on building east of terminal building.



Figure 1-51. Time = 2:46 PM, APH-12. Below windows on building east of terminal building.





Figure 1-52. Time = 5:14 PM, APH-20. Below windows on building east of terminal building.



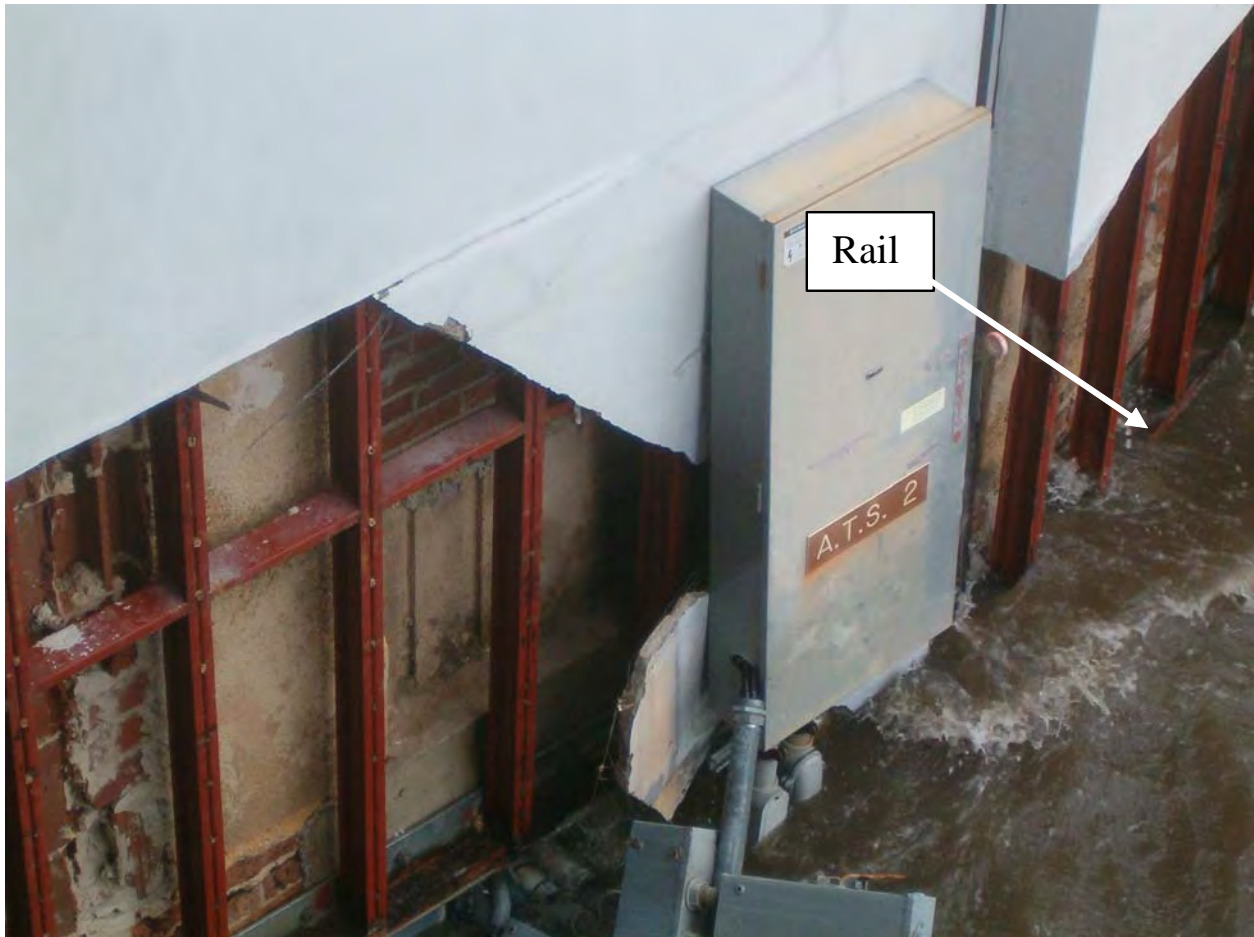


Figure 1-53. Time = 5:30 PM, APH-11. Bottom of horizontal rail to right of electrical panel box on north side of terminal building, east of lobby.



Figure 1-54. Time = 6:30 PM, APH-14. On slanted railing just below jet engine.

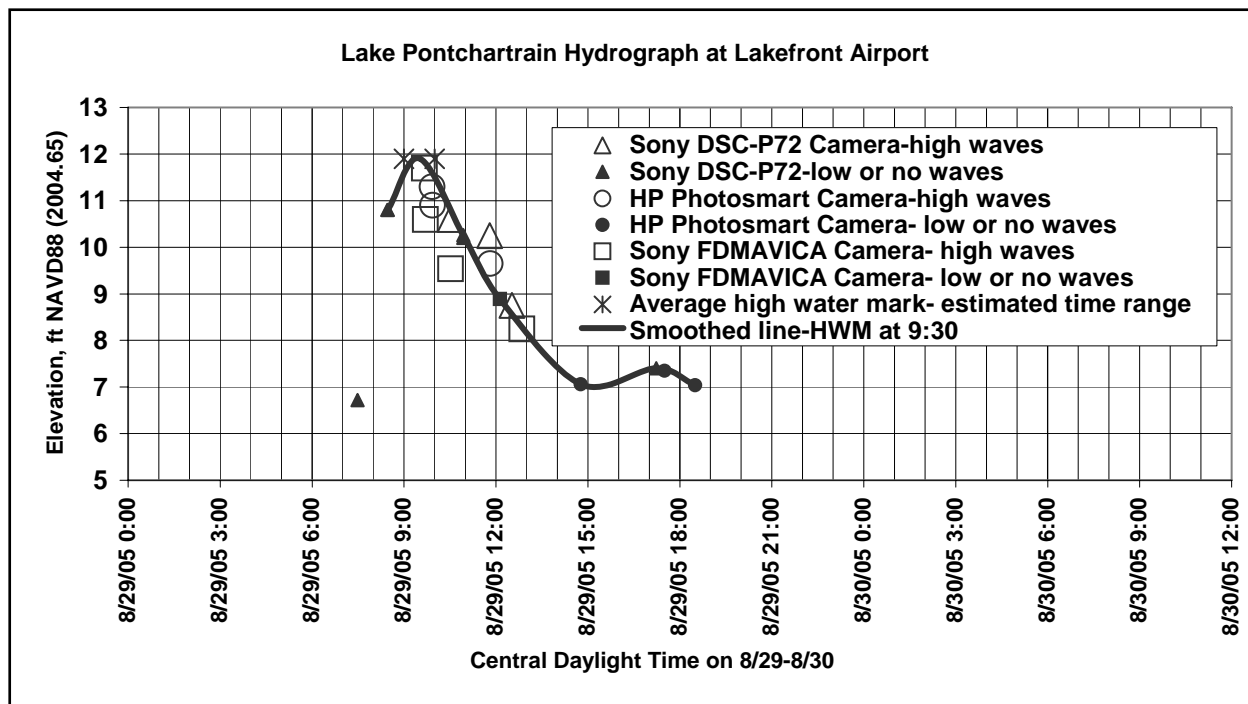


Figure 1-55. Constructed hydrograph at Lakefront Airport. Note that the point at 7:28 AM is not considered representative of Lake Pontchartrain because of relatively high topography around airport building (elevated runways) and is not included in the smoothed line of the hydrograph. The recession side may also have some of this effect but the lower rate of fall may reduce the impact.

**Hydrograph Plot.** The above data was used to construct a hydrograph as shown in Figure 1-55. Solid points are used to signify points with little or no wave effects. Larger open data points are used to signify points with significant uncertainty in elevation due to factors such as wave effects. Note that these open symbol points can be either high or low estimates of storm surge depending on the timing of the photograph relative to the wave crest or trough. The time of the high water mark in Figure 1-55 is based on extrapolating the digital photograph points along the recession of the storm surge up to a level of 11.9 ft while considering the 8:28 time of the two points at 10.8. The resulting time of peak storm surge is between 9:00 and 10:00. The smoothed line hydrograph is shown with a time of 9:30 AM on the plot. Due to the rapid rise of the storm surge and the presence of the runways and other high topographic features, the data at 7:28 AM should not be used in developing a hydrograph to represent levels in Lake Pontchartrain. The recession side of the hydrograph may have some effects of the high topography but the lower rate of fall may reduce these effects.

Orleans Levee District personnel are thanked for allowing use of these photographs.

## Observed Water Levels Along the IHNC and GIWW

**General Description.** This section summarizes hydrographs from self-recording gages, staff gages, and digital pictures along the Inner Harbor Navigation Canal (IHNC) and Gulf

Intracoastal Waterway (GIWW). This report also presents variation of peak water level along the IHNC from high water marks. All elevations presented herein are in the time dependent datum of NAVD88 (2004.65).

**Recorded Hydrographs at IHNC Lock.** Figure 1-56 shows a plot of data from two self-recording gages at I-10 on the IHNC, a self-recording gage at Paris Road (I-510) on the MRGO, staff gage readings at the IHNC Lock, and water levels derived from digital pictures taken at the IHNC Lock. Each source of data in Figure 1-56 is described in the following paragraphs.

During passage of Hurricane Katrina, water levels were recorded by an operator at the IHNC Lock from the staff gage at the lock. The operator stated that on each hour he would read the high and low and record an average value. Based on the recorded readings and the operator's statements, the gage was being read to the nearest 0.1 ft for elevations below about 12.5 ft and the nearest 0.5 ft while the stage was approaching the peak and wave variation was significant. The operator was observing the staff gage from the north end of the lock wall at the edge where it drops to the lower level. Figure 1-57 shows a closeup of the gage and Figure 1-58 shows a picture of the gage from the lock operator's observation location. Both figures are looking north. Note that the top of the framework in the background behind (north of) the staff gage is about 2.5 ft below the peak water level of 15 ft on the gage. This framework would have reduced wave activity at the gage. The operator appeared to be a reliable observer of the staff gage and stated that he had good eyesight. The staff gage was surveyed by IPET datum team and the 15 ft mark was equal to an elevation of 14.3 ft in NAVD88 (2004.65). All IHNC staff gage readings were reduced by 0.7 ft to convert to NAVD88 (2004.65).

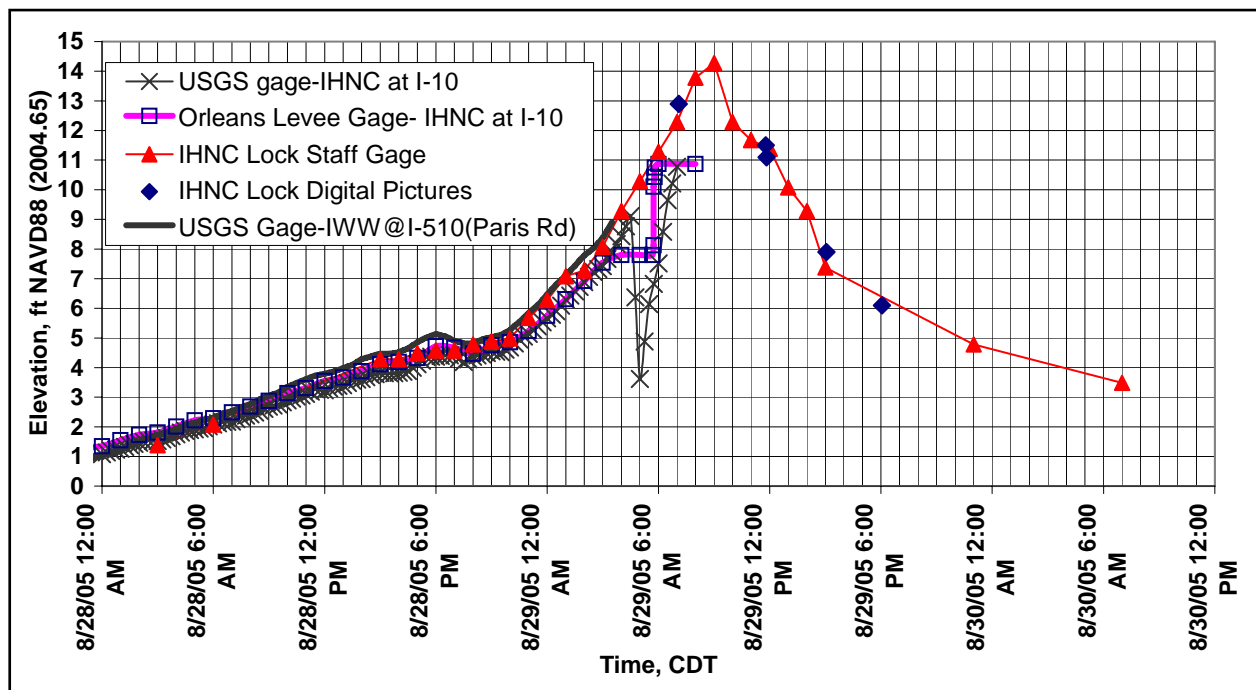


Figure 1-56. Hydrographs on the IHNC.





Figure 1-57. Staff gage at IHNC lock. Numbers were far more visible when the lock was visited in October 2005. Picture looking north.



Figure 1-58. Staff gage from viewing location during storm. Picture looking north. Claiborne Avenue bridge in the background.

**Water Level Data from Digital Pictures, IHNC Lock.** Digital pictures were taken by one of the IHNC Lock personnel on a Kodak DX6490 zoom digital camera. The camera time was checked on 7 Feb 2006 and found to be the correct time. The lockmaster stated he had loaned the camera out during the period since the storm and he could not be certain that the time had not been changed. The camera owner's manual was checked and no mention was found of any automatic update of time for Daylight Savings Time (DST). Without this camera option, the times on the camera could be 1 hour behind assuming that no changes have been made to the camera. However, agreement of times and elevations from the staff gage and the camera lead to accepting the camera times. Details of the pictures are as follows:

- a. File time 7:06 AM, Picture 100\_0498, Figure 1-59, looking southeast. Water level was based on distance below top of lockwall on east side of lock. Top of lockwall surveyed at 19.9 ft. Used height of post (3.55 ft) and height of top of yellow box (5.56 ft) to scale down to water surface at 4 points along wall. Distances below top of wall were 6.6 ft, 7.8 ft, 7.1 ft, and 6.5 ft for an average distance of 7.0 ft and a water level of 12.9 ft. The range of water level of 1.3 ft provides some information about wave height along the wall.





Figure 1-59. Time 7:06, file 100\_0498. Picture brightness and contrast adjusted to show water level. Looking southeast.

- b.* File time 11:47 AM, Picture 100\_0502, Figure 1-60, looking east-northeast into Lower Ninth Ward. Water level at location of sloping handrail. Elevation = 11.5 ft.
- c.* File time 11:50 AM, picture 100\_0507, Figure 1-61, looking north. Shows staff gage where water level is almost hidden by handrail. Using other objects in the picture such as tops of handrails, the staff gage reading is 11.8 ft, that is an elevation of 11.1 ft.
- d.* File time 3:03 PM, Picture 100\_0508, Figure 1-62, looking northeast into Lower Ninth Ward. Top of highest pile in cluster under arrow is at elevation 8.7 ft. Based on width of pile cluster of 4.8 ft, water level is 0.8 ft below top of highest pile for an elevation of 7.9 ft.
- e.* File time 6:03 PM, Picture 100\_0509, Figure 1-63, looking northeast into Lower Ninth Ward. Top of highest pile in cluster under arrow is at elevation 8.7 ft. Based on width of pile cluster of 4.8 ft, water level is 2.6 ft below top of highest pile for an elevation of 6.1 ft.

To determine the elevations used in the above paragraph, IPET members used a level to determine water surface elevations in pictures taken at the IHNC lock on 29 Aug 05. The survey was conducted on 7 Feb 06.



Figure 1-60. Time 11:47, picture 100\_0502. Red arrow shows location surveyed. Looking east-northeast into Lower Ninth Ward.





Figure 1-61. Time 11:50, picture 100\_0507, looking north.



Figure 1-62. Time 3:03 PM, picture 100\_0508. Breach on east side of IHNC in background. Looking northeast into Lower Ninth Ward.



Figure 1-63. Time 6:03 PM, file 100\_0509. Breach on east side of IHNC in background. Looking northeast into Lower Ninth Ward.

**High Water Marks, IHNC Lock.** High water marks in the vicinity of the lock are summarized in Table 1-4. Due to the perceived reliability of the operator who read the staff gage, the reading of 14.3 ft (2004.65) is considered the best estimate of the peak high water. High water mark data are up to about 0.5 ft lower.

<b>Table 1-4 High Water Marks in Vicinity of IHNC Lock</b>		
<b>Point ID</b>	<b>Description</b>	<b>Elevation, ft (NAVD88 (2004.65))</b>
LA 1171	The operator was reading the staff gage to the nearest 0.5 ft. Staff gage reading of 15 ft = 14.3 ft NAVD88 (2004.65)	14.3
LA 1005	Inside a sheet metal building which is typically very porous. Mark was consistent throughout building.	13.7
LA 1006	Inside galley of lock. This mark had uncertain connection to the outside water level and was not accepted.	13.2
LA1172	In coast guard building stairwell that had wall damage that should have allowed adequate entry of water if the damage occurred prior to the peak water level.	13.8

**Other IHNC and GIWW Recorded Hydrographs.** The USGS and Orleans Levee District (OLD) gages at I-10 on the IHNC and the USGS Paris Road gage were surveyed to convert to the NAVD88 (2004.65) datum. The USGS I-10 at IHNC readings had to be reduced by 0.41 ft and the OLD I-10 at IHNC readings had to be reduced by 0.45 ft. The USGS Paris Road gage, which had an unknown datum, had to be reduced by 3.5 ft to convert to NAVD88 (2004.65).

As shown in Figure 1-56, the USGS gage at I-10 on the IHNC (1-65) experienced a 5 ft drop in stage at about 4:30 AM on August 29 when the stage was about 9.5 ft. At first, this drop was interpreted to mean that a breach on the IHNC occurred at this time but most people doubted that the water level dropped 5 ft. Figure 1-64 shows that the white PVC pipe holding the USGS gage has a top elevation of about 9 ft on the staff gage. The larger PVC pipe is the OLD gage. The electronic cable holding the USGS pressure transducer inside the PVC pipe is exposed above the top of the pipe. One possible explanation of the 5 ft drop is that the high velocities through the railroad/I-10 bridge opening, along with debris, snagged the cable and pulled the transducer up out of the pipe giving it an apparent drop in water level. The OLD gage is a float gage and experienced identical 7.8 ft readings at 4:00 AM, 5:00 AM, and 5:40 AM followed by a rapid rise in 8 minutes to about 10.9 ft. The 10.9 ft reading is in agreement with the IHNC Lock readings. The constant readings followed by the rapid rise is consistent with a float gage that became stuck. Whether the OLD gage got stuck or the level readings indicate the time of a breach is unknown. Because the OLD and USGS gages are within 10 ft of each other, the difference in water levels after about 4:30 raises concerns about readings on both gages.



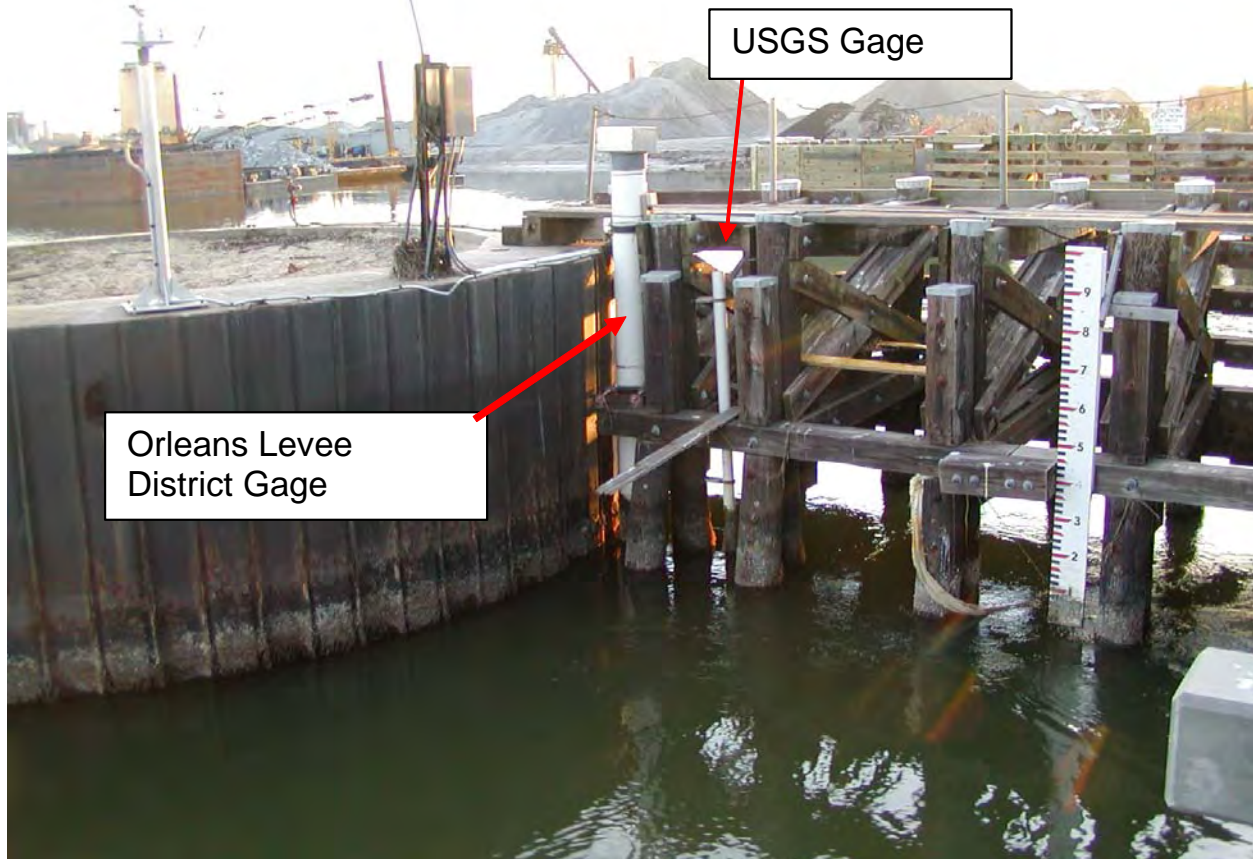


Figure 1-64. USGS and Orleans Levee District gages on east side of IHNC and south of railroad bridge at I-10. Picture looking southwest.

**Variation of High Water Marks along the IHNC.** The peak water level variation along the IHNC is complicated by railroad bridges that were in the down position and had relatively low chord elevations and the presence of the Port of New Orleans (PONO) floodwall that was never finished and does not tie into the USACE protection on the north end of the PONO. In addition, some or all of the floodgates on the PONO were either not closed or only partially closed during Katrina. Personnel of the OLD stated that these floodgates are generally not closed because of the lack of completion of the PONO floodwall on the north end. Low chord elevation on a bridge refers to the lowest elevation at which the bridge structure begins to block the flow area. The low chord elevations on the IHNC are as follows:

- a. Railroad bridge at Lakeshore Drive- elevation 2.4 ft
- b. Railroad bridge at I-10- elevation 3.5 ft
- c. Railroad bridge at Florida Avenue- elevation 4.1 ft

Figures 1-65, 1-66 and 1-67 show high water marks and a layout of the USACE protection along the west side of the IHNC. Figure 1-66 shows the layout of the PONO floodwall. On Figure 1-66 at the railroad south of I-10 on the west side is the floodwall opening that was

sandbagged prior to Katrina and failed sometime during Katrina. High water mark LA 1054 at 13.0 ft is close to this opening and may have been affected by the sandbag failure. The other marks in this area of 14.2-14.4 ft are believed to better represent water levels immediately south of the railroad bridge just south of the I-10 bridge. The railroad bridge was in the down position during Katrina. High water marks on the north and south sides of the railroad bridge show about a 1.5 ft drop in water level across the bridge. Evidence on the ground (Figure 1-68) showed vegetation laid down indicating high velocity through the I-10/railroad area of the IHNC.

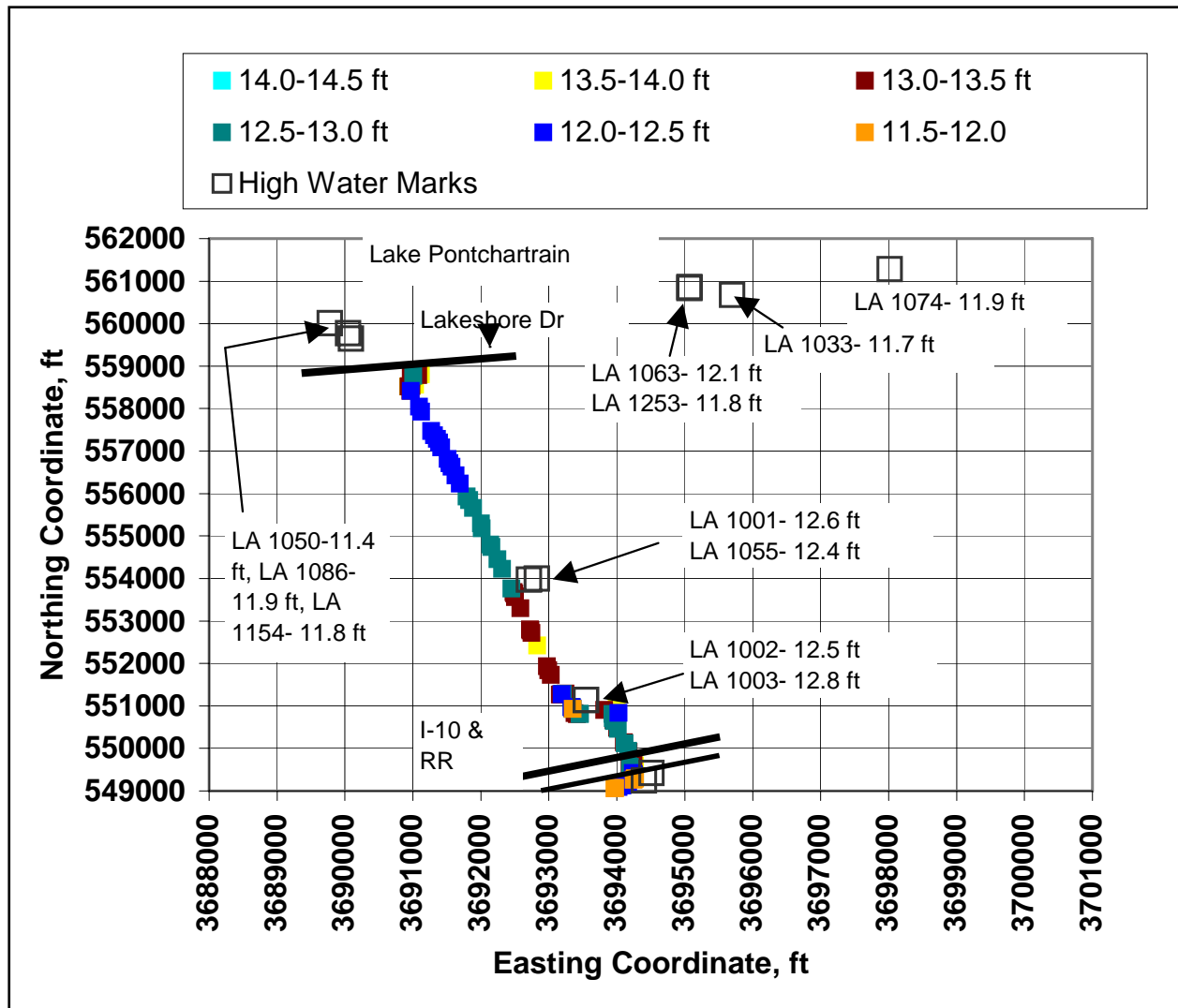


Figure 1-65. Floodwall layout, wall elevations, and high water marks along the west side of IHNC, Lake Pontchartrain to I-10.

In Figure 1-67 on the south end of the floodwall note that high water mark data are only available at the IHNC Lock and at the south end of the PONO floodwall. The elevation drops from 15.2 ft at the south end of the PONO floodwall to about 14.3 ft at the lock based on the staff gage or about 13.8 ft based on the high water marks. As stated above, this could have been the result of the breach. Another alternative or a contributing factor could have been the head loss across the Florida Avenue railroad bridge that was also reported to be in the down position

during the storm. Figure 1-69 shows the Florida Avenue Railroad bridge (blue bridge in foreground) in the down position on 7 Sept 05.

Figure 1-70 shows the variation of peak water level along the IHNC based on high water marks. Note that the area west of the PONO that experienced a levee and floodwall breaches is shown to have experienced a peak water level of about 14.2 to 14.3 ft. On the east side of the PONO, peak water levels were up to 15.4 ft at the junction of the MRGO. The difference in peak water level across the PONO floodwall is likely due to (1) the 1600 ft long east-west earth levee on the west side of the PONO that was at an elevation of about 11.0 ft and (2) USACE floodwall overtopping all along the reach west of the PONO.

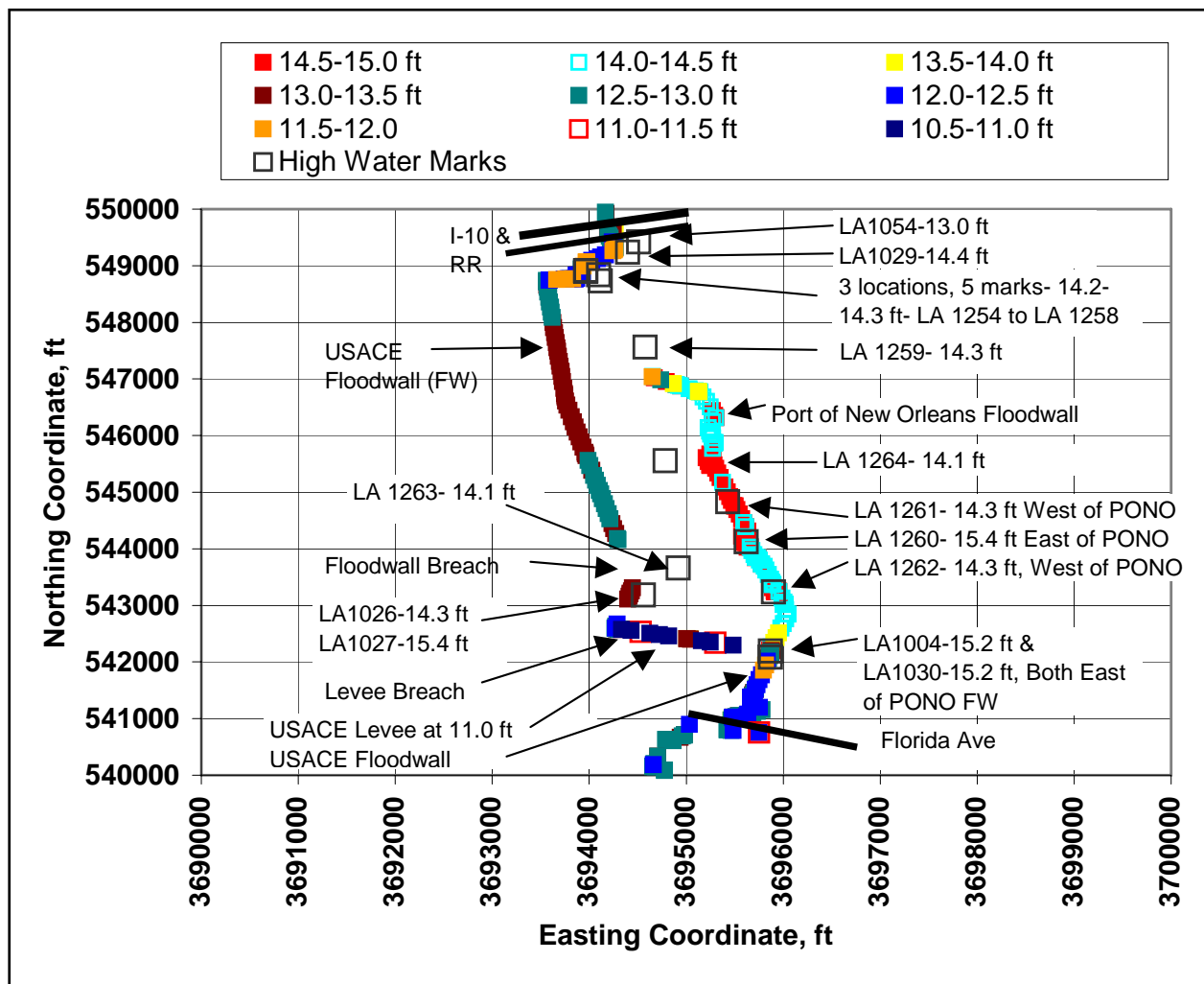


Figure 1-66. Floodwall layout, wall elevations, and high water marks along the west side of IHNC, I-10 to Florida Avenue railroad bridge.

One location west of the PONO floodwall has a single high water mark (LA 1027) that does not agree with the other high water mark data (See Figure 1-66). Mark LA 1027 is also shown on Figure 1-70 at latitude 29.987. Mark LA 1027 at elevation 15.4 ft is located in the same building as LA1026 at elevation 14.3 ft. Neither mark is a well-defined seed/debris line as are the other

marks in this area. Both marks are based on debris in the rafters of a heavily damaged building that is close to the floodwall and levee breach on the west side of the IHNC. Both LA 1026 and LA 1027 were described as possibly low. Subsequent visits to this building by other IPET members has not resolved the peak water level in this building. The agreement of LA 1026 at elevation 14.3 ft with 4 other marks west of the PONO is the reason LA 1027 is not accepted.

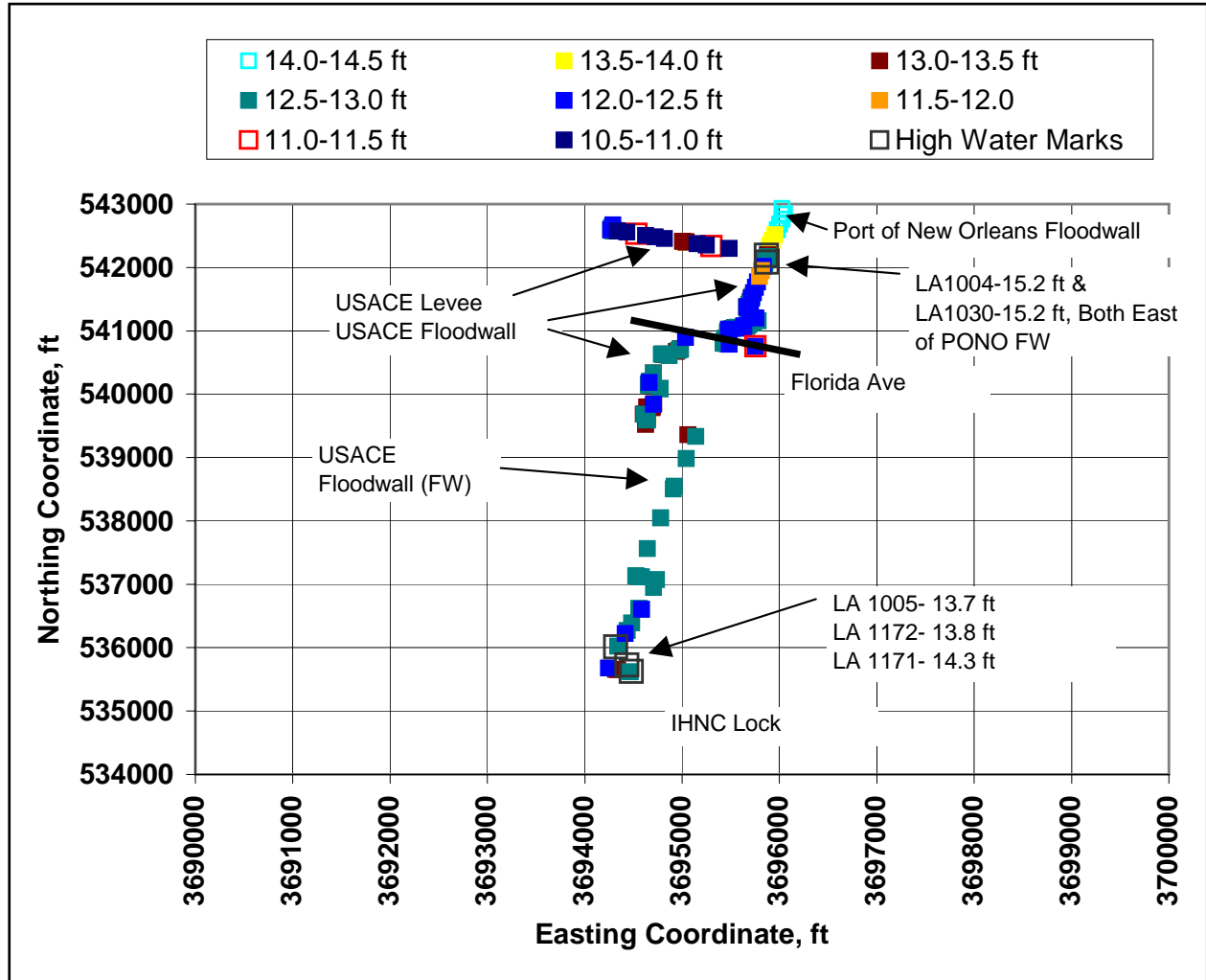


Figure 1-67. Floodwall layout, wall elevations, and high water marks along the west side of IHNC, Florida Avenue railroad bridge to IHNC Lock.





Figure 1-68. Vegetation at I-10 laid down in a northerly direction by flow in IHNC.



Figure 1-69. Florida Avenue railroad bridge (blue), two breaches on east side of IHNC into Lower 9<sup>th</sup> Ward, and IHNC lock at top of picture. Picture looking south-southwest. Note debris on railroad bridge.

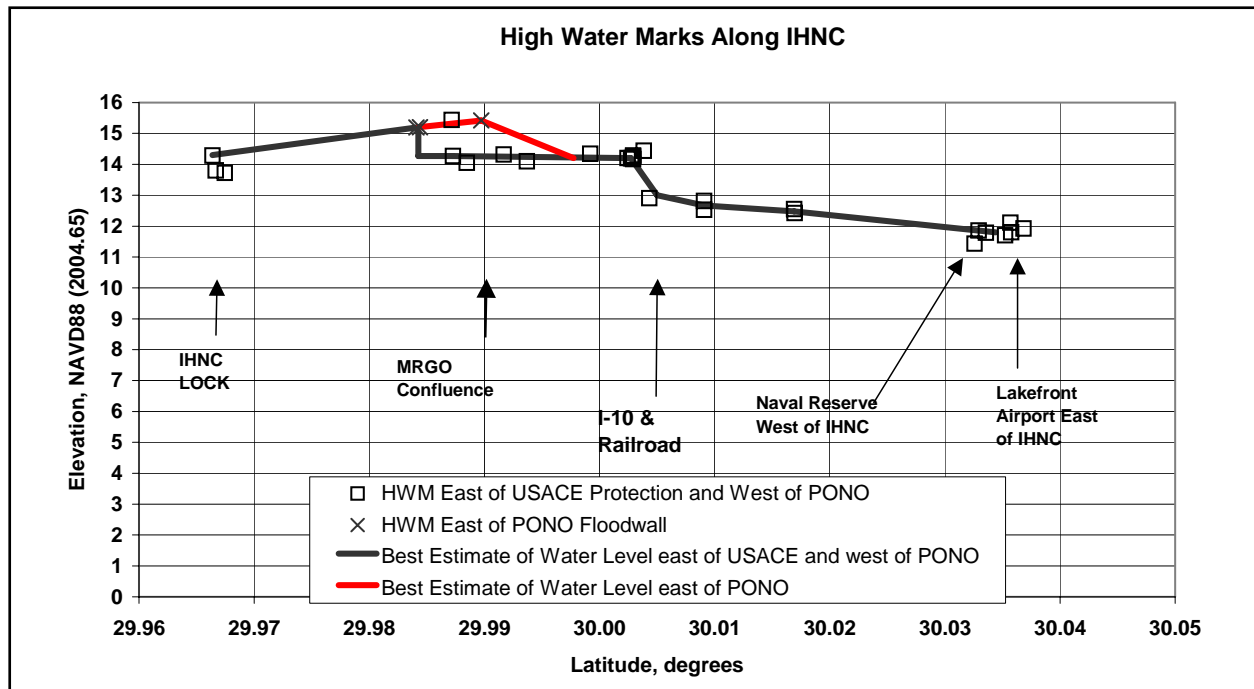


Figure 1-70. Variation of peak water level along IHNC based on high water marks. Red line is Port of New Orleans (PONO) Floodwall that is not complete and is not tied in to the USACE protection on the north end.

## Observed Water Levels in Orleans Parish Canal Interiors

**Introduction.** The data collection team of IPET visited various locations along the subject canals and made observations of high water marks and water levels and factors affecting those marks. At the pump stations and within the canals, high water marks were generally fair or poor marks with a few exceptions. Canal walls were subjected to intense rains from Hurricane Rita and yielded little information. At pump stations, several factors were present that complicated the interpretation of high water marks including:

- a. Backflow through the pumps- the pump stations on London Canal (OP#3) and Orleans Avenue Canal (OP#7) have not been upgraded with frontal protection that has been accomplished at the 17th Street Canal (OP#6). Frontal protection provides pump station walls that are the same elevation as the floodwalls and gates/valves that, if closed, prevent backflow through the pumps. Interviews with pump station operators have been varied and inconclusive regarding if frontal protection gates were closed or if backflow occurred. At OP#7, an operator stated that early on 8/29/05, he had pumps spinning backwards that means backflow was occurring at this station.
- b. Pumps being turned off and on- when large pumps are turned off and on, a significant surge is created in the discharge area that could have altered high water marks. This could be particularly significant when a station loses power and several pumps shut down at one time. Information shows that London and Orleans Canal pump stations were down

prior to the peak water level in the lake. The 17th Street Canal OP#6 may have come back online near the time when the peak water level was occurring in the Lake.

- c. Time of breach- the timing of breaches could have been the deciding factor on the height of the water level at the pump stations on the south end of the canals.
- d. Surging/seiching in the canals- No information has been found assess whether or not the canals were subject to significant surging.
- e. Debris and bridge losses- Debris on the Hammond Highway bridge over the 17th Street Canal almost certainly influenced the water level in the canal south of the bridge after significant flow started through the breach. Losses at other bridges on the canals could also be a factor in determining water levels.
- f. Wind and waves- eyewitness and photographic evidence shows that waves were present in the 17th Street Canal. Wind setup of the water level at the south end of the canals is also possible.

All elevations presented herein, unless otherwise noted, are in the time dependent datum of NAVD88 (2004.65). Times are presented in Central Daylight Time (CDT). UTC is 5 hours earlier than CDT.

### **Orleans Avenue Canal**

An operator who stayed at pump station OP#7 during the storm was interviewed on 9/29/05. Figure 1-71 shows the low pump station wall that connects OP#7 to the floodwall. Figure 1-72 shows a picture of the low wall, the earth levee, and the south end of the east floodwall. Figure 1-73 shows the low wall looking south towards the pump station. Figure 1-74 shows the layout of the wall around the station along with elevations. The low pump station wall is at about elevation 9.7 ft. The floodwall north of OP#7 is at elevation 14.0 ft. The earth levee on the east side connecting the low wall to the floodwall is at about elevation 8.3-8.7 ft. Future frontal protection at Orleans Avenue Canal Pump Station OP#7 will raise this wall and add valves/gates to prevent backflow through the pumps. The operator stated that the low pump station wall overtopped by about 6-12" (the 6-12" amount is based on an estimate of how high the operator held his hand above the low wall) and had flow over the wall for about 1½ hours starting at about 8:30 to 9:00 am on Monday. If the 1½-hour is assumed to begin at 8:45 AM, the flow over the wall lasted until 10:15 and the peak would have occurred at about 9:30 AM. This timing is consistent with the peak high water timing developed from digital photographs and an event log at the Marinas at the 17th Street Canal entrance and the Lakefront Airport. The water surface elevation based on 6-12" estimate would be about 10.2-10.7 ft that is consistent with an 11.1 ft peak water level at the Orleans Avenue Canal entrance that was estimated from high water marks along Lake Pontchartrain. A difference in water level between the lake and the pump station may have been due to a) drawdown from flow over the wall, b) possibly drawdown from backflow through the pumps, c) the low area in the levee profile just north of Robert E Lee Bridge (presented subsequently) if that area was low during Katrina, and d) losses at the bridges.





Figure 1-71. Low pump station wall at Orleans Avenue Pump station OP#7.



Figure 1-72. Low wall, earth levee, and floodwall in background on east side of Orleans Avenue Canal just north of pump station. Looking northwest.





Figure 1-73. Low wall that connects to OP#7 at Orleans Avenue Canal looking south-southeast standing on earth levee.

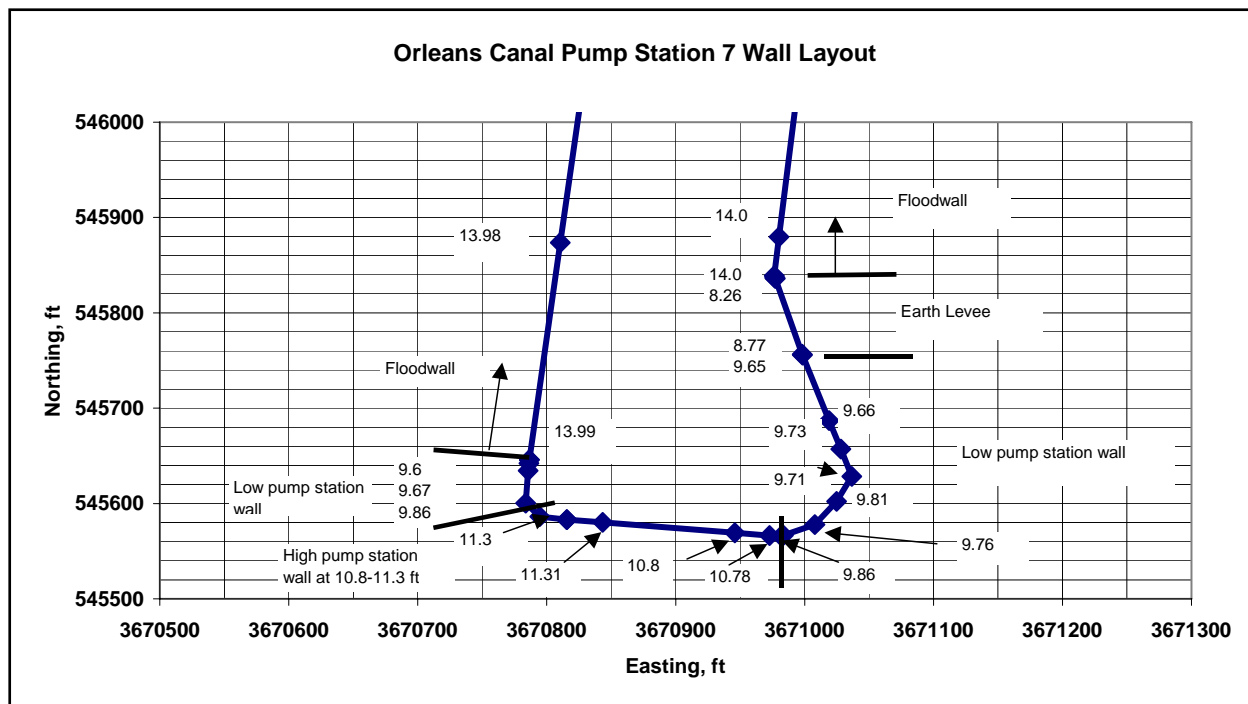


Figure 1-74. Floodwall, levee, and pump station wall elevations at OP#7.

The only high water mark at the pump station was debris around the south end of the east floodwall. The mark LA 1052 at 9.5 ft is a poor mark and represents a minimum level of the peak water.

Another operator on another visit to OP#7 stated that the wall did not overtop. Water levels in Lake Pontchartrain, scour, and limited high water marks near the pump station show the wall did overtop. Although not easily seen in Figure 1-71, minor scour occurred below the low wall on the east side of the station. Note the rise of about 1 ft in the low wall in Figure 1-71 behind the individual in the picture. The walls adjacent to the low wall that are at elevation 10.8 ft on the east side and elevation 11.3 ft on the west side had no evidence of scour on the protected side of the wall supporting the first operator’s account of the maximum amount of flow over the wall being about 1 ft. Figure 1-75 shows scour between the columns that could only have come from flow down the concrete slope that is adjacent to the low wall on the east side of the channel. Figure 1-76 shows scour around a power pole below the earth levee on east side of Orleans Ave Canal. Figure 1-77 shows scour below the concrete apron that is below the low wall on the east side of the canal. Figure 1-78 shows greater scour behind the low wall on the west side of Orleans Canal. Note that the west low pump station wall has a larger fall to the ground that is important in determining the amount of scour. Figure 1-79 shows where the west low wall ties into the higher pump station wall. Based on debris trapped in the vegetation, flow overtopped this wall by about 6” that supports the pump station operator’s lower estimate of 6-12” of flow over the wall.





Figure 1-75. Scour between columns below low pump station wall at OP#7. Low wall is at top of slope behind concrete columns.



Figure 1-76. Scour around power pole below earth levee on east side of Orleans Ave Canal.





Figure 1-77. Scour below concrete apron that is below low pump station wall on east side of Orleans Ave Canal.



Figure 1-78. Scour below OP#7 low pump station wall on west side. Note that fall distance and scour is greater on this side than on the east side. Note floodwall in background that is about 4.3 ft higher.





Figure 1-79. Debris caught in vegetation showing flow over low wall at OP#7. About 6" above low wall on west side.

Figures 1-80 and 1-81 show wall profiles along the west and east sides of Orleans Avenue Canal, respectively. The low levee elevation on the west side of the canal just north of Robert E. Lee bridge suggest that water may have flowed over the levee at this location since the peak water levels were about 11.0 ft.

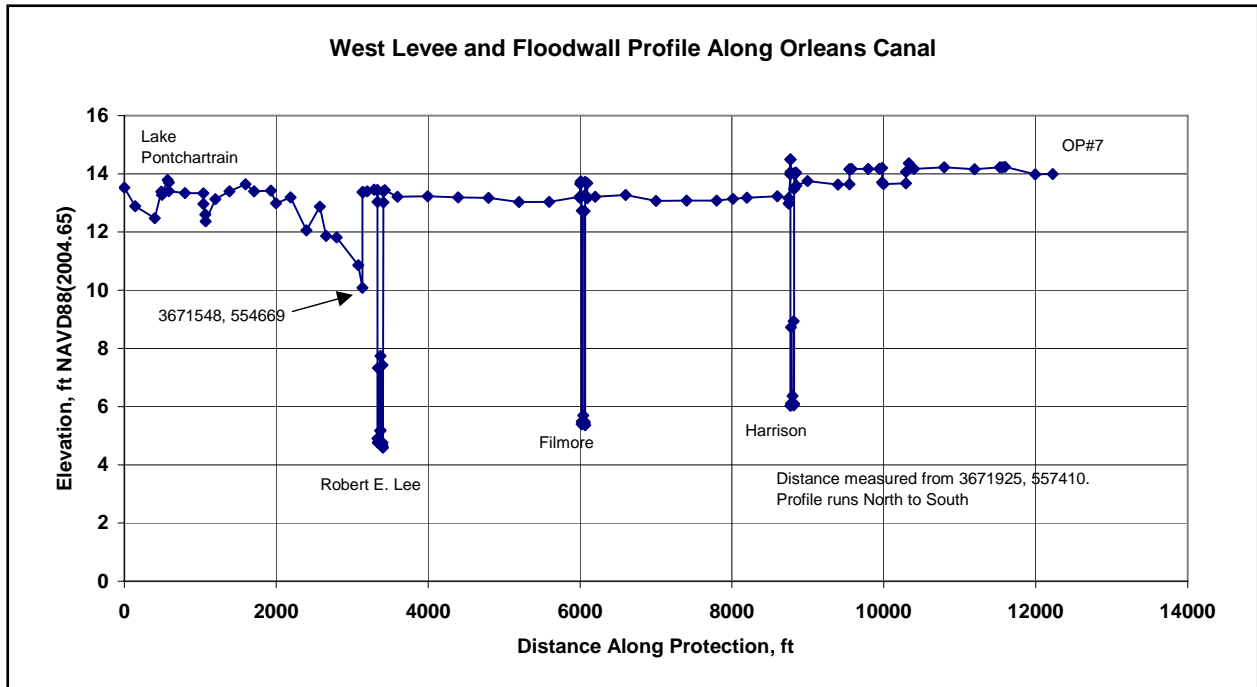


Figure 1-80. West Levee and Floodwall Profile for Orleans Avenue Canal. Note that low areas at bridges and pump stations are floodgate openings that were closed during the storm.

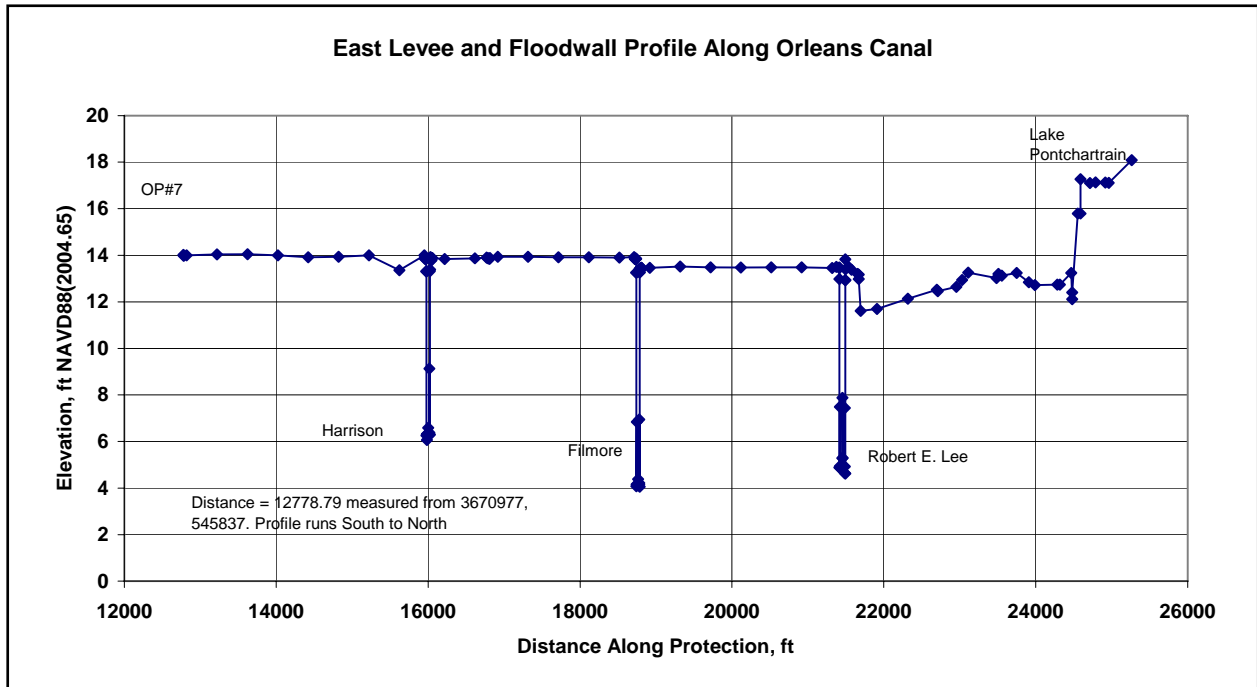


Figure 1-81. East Levee and Floodwall Profile for Orleans Avenue Canal. Note that low areas at bridges and pump stations are floodgate openings that were closed during the storm.

## 17th Street Canal

On 9/29/05, a location was observed about 200 ft south of the 17th Street Canal breach looked like ground that had flow over it. Further south of this location on the east side of the canal are the lowest wall elevations on 17th Street Canal of about 12.1 ft. The scour was possibly the result of minor wave overtopping but no visible scour was observed. A picture (Figure 1-82) was taken in this area but the effect on vegetation was so minor it does not show up.

The floodwall and fronting protection walls at the pump station OP#6 are at about elevation 13-13.2 ft as shown in Figure 1-83. On 9/29/05, debris was observed at the top of the fronting protection wall as shown in Figure 1-84. This debris was only observed at the center portion of the fronting protection wall as shown on Figure 1-83, a location where waves coming down the canal would be largest. On 11/9/05, a debris HWM LA 1252 was found (Figure 1-85) around two gate rods, both at about 2.1 ft below the top of the floodwall for an elevation of about 11.1 ft. This type of mark is best described as “at least this high” because the debris can wrap around the gate rod at a higher water level and fall down when the stage drops/waves subside and settle on the gate rod support. The location of this HWM is 50-ft east of the point on the fronting protection wall that is inline with the east floodwall (Figure 1-83). This high water elevation was confirmed at another HWM LA 1251 found on 9/29/05 and located in an area on the west side of the discharge area where top of debris at a crack in the wall was found at 2.2 ft below top of floodwall (at the 13.08 ft point in Figure 1-83) for an elevation of 10.9 ft. Both marks, LA 1251 and 1252 were in areas exposed to some wave action. A picture (Figure 1-86) taken in 4/06/06 shows the location of LA 1251. In this picture the debris in the crack was no longer at the level of 2.2 ft below the top of the wall. A third HWM LA 1019 at this general location was levee debris at 9.0 ft. Levee debris high water marks have been inconsistent when compared to nearby marks inside structures.



Figure 1-82. Attempt to show possibility of minor scour along west floodwall, south of 17th Street Canal breach.



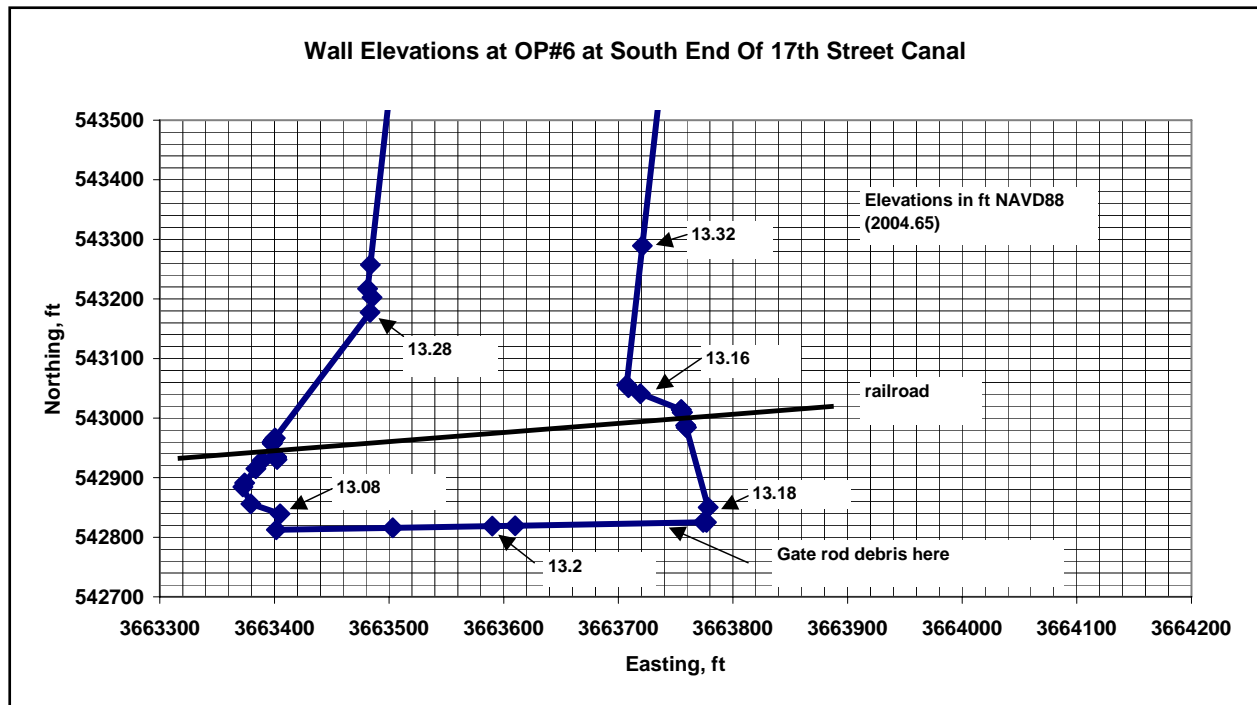


Figure 1-83. Wall elevation at OP#6 at south end of 17th Street Canal.



Figure 1-84. Debris on top of floodwall at OP#6 at 17th Street Canal.

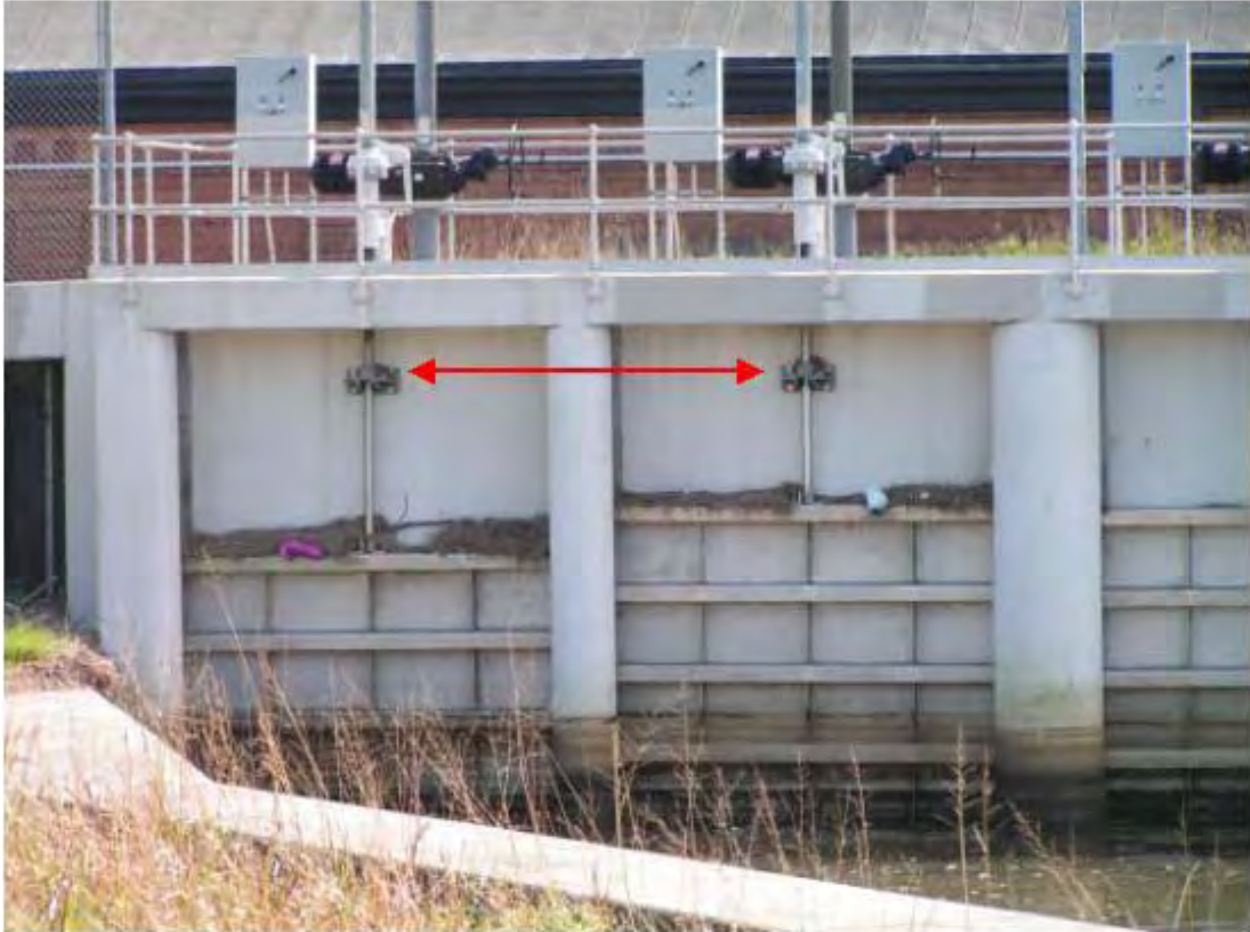


Figure 1-85. Debris high water mark at top of brackets holding gate rods on east side of discharge area.





Figure 1-86. LA 1251 at crack in wall. Picture taken 4/06/06. Debris in crack was 2.2 ft below top of wall on 9/29/05.



Several eyewitness accounts provide information about events in the canals including water levels as described in the following:

- a. Around 6:30 AM- Two witnesses observed a single floodwall panel leaned over. Several witnesses in houses near the breach report only water in the streets, with no significant flooding until about 9:00 AM. Based on the constructed hydrograph for the 17th Street Canal entrance, Lake Pontchartrain was at a water level of about 7.0 ft at 6:30 AM.
- b. 9:00 AM to 9:30 AM- Several witnesses in houses close to the breach report rapidly rising water with water moving at a fast pace down the street. This would suggest that the breach widened rapidly at this time. Based on the constructed hydrograph for the 17th Street Canal entrance, Lake Pontchartrain was at a water level of about 10.8 ft at 9-9:30 AM.
- c. An eyewitness in an apartment at 1161 Lake Avenue on the west side of the 17th Street Canal stayed during the storm with his family. This apartment is north of Veterans and about 0.9 mile south of the Hammond Bridge. He observed water and debris coming over the floodwall between 5:00 AM and 7:00 AM but he was uncertain about this timing. He was more certain that the water and debris stopped coming over the wall between 8:00 and 9:00 AM and far more certain that the water and debris were not coming over the wall after 9:00 AM.
- d. Another eyewitness lives in an apartment immediately next to the west side of the 17th Street Canal at 1111 Lake Avenue. His apartment is north of Veterans and about 1 mile south of the Hammond Bridge. The floodwall north of Veterans on the west side has an elevation of about 12.3 ft. He stayed during the storm and said he was the only person who stayed in his building. He stated the power went off around 5:00 am and he turned on his battery-powered radio/TV and heard that there was some flooding reported. At around 8:00 AM he went outside where he said the wind was high and reported seeing water from waves coming over the 17th Street Floodwall. Waves were moving in the canal from north to south. He stated that the waves could have been occurring before 8:00 AM but it only became light enough to see at 8:00 AM. He said the amount of water coming over the wall was not great because his patio did not flood. He took a picture (Figure 1-87) that shows the wave splash. He stated the picture was a case of unfortunate timing because the tree limb hides a wave crest. He stated the wave crests were clearly visible and up to 1 ft above the wall. He said this continued until around 10:00 AM. I asked him how far north and south the waves were coming over the wall. He stated that his field of view width was about 50 yards but water was coming over that entire width. At 10:00 AM, he walked to the wall and looked over the wall and observed the water level in the canal at about 2 ft below the top of the floodwall and moving rapidly toward the lake. He went to the Hammond Bridge on the afternoon of 8/29/05 and took pictures at 2:00 and 3:00 PM (Figures 1-88 and 1-89). Times in these pictures are based on the recollection of the observer and were not digital pictures. Based on the brown part of the floodwall being 65” high and the top of floodwall near the breach at elevation 12.5 ft, the water level at 2-3:00 PM was at elevation 4.0 ft. In the interview, the eyewitness described this as a high tide level.



Figure 1-87. Wave spray or splash (left of tree limb) at west wall of 17th Street Canal north of Veterans Blvd and 1.0 mile south of Hammond Hwy. The individual who took this picture stated that the tree limb obscures the crest of a wave.

- e.* Another eyewitness on the west side of the canal at 1161 Lake Avenue did not go out early but later in the day walked along the floodwall. The west side of the 17th Street Canal in this area has a paved walkway that is easily accessible. This eyewitness reported seeing fish that presumably came over the floodwall.
- f.* While at the 17th Street Canal in March 2006, an assistant superintendent with the East Jefferson Levee District Police Department was interviewed. He stated he stayed in the emergency operations center during the storm and that they had not received reports of water coming over the floodwall on the west side of the 17th Street Canal.
- g.* Two eyewitnesses reported that the water level in the canal was about 1-2 ft below the top of the wall near the breach at about 6:30 AM on the morning of 8/29/05.
- h.* The fireman's video shows water level in the canal at about 11:10 AM. Based on analysis of the picture, water level in the canal at this time was about 3-4 ft.



Figure 1-88. 17th Street Canal and breach at 2 pm on 8/29/05. Looking south.



Figure 1-89. North end of 17th Street Canal breach at 3 PM on 8/29/05.

If valid, the most complete information on the canal water levels is the log of water levels recorded at OP#6 on the south end of the 17th Street Canal. The water levels at the pump station differ significantly from the constructed hydrograph for the 17th Street Canal entrance as shown in Figure 1-90. The IPET data collection team spent considerable effort to determine if the logbook readings correctly describe the water level in the 17th Street Canal during Hurricane Katrina on the morning and afternoon of 8/29/05. The logbook data shows that the water level in the canal peaked at an elevation of 7.5 ft between 4:30 AM and 6:00 AM and fell after that time. The datum of the pump station logbook data was established using Lake Pontchartrain hydrographs that have water surface elevations in NAVD88 (2004.65). From 12:00 AM to 12:00 PM on 8/28/05, the Orleans Levee District gage at Southshore Marina averaged 1.25 ft, the Pass Manchac gage averaged 1.09 ft, and the Bayou Labranch gage averaged 1.27 ft. Based on averaging the 3 gages, Lake Pontchartrain averaged an elevation of 1.20 ft from 12:00 AM to 12:00 PM on 8/28/05. During this time, no significant pumping was taking place at OP#6. Based on the pump station logbook for the same time interval, the average reading at OP#6 was 22.6 ft in the Cairo datum. The conversion from Cairo datum to NAVD88 (2004.65) is  $22.6 - 1.2 \text{ ft} = 21.4 \text{ ft}$  for OP#6 logbook readings on the discharge side of the pump station. This conversion value is considered to be valid for this location in the system. The conversion is used in Figure 1-90 and the derived hydrograph at the Lake and the pump station log are in fair agreement on the morning of 8/29/05 before 4:00 AM.

The IPET data collection team visited the station numerous times, most recently on 3/02/06. The information determined is as follows:



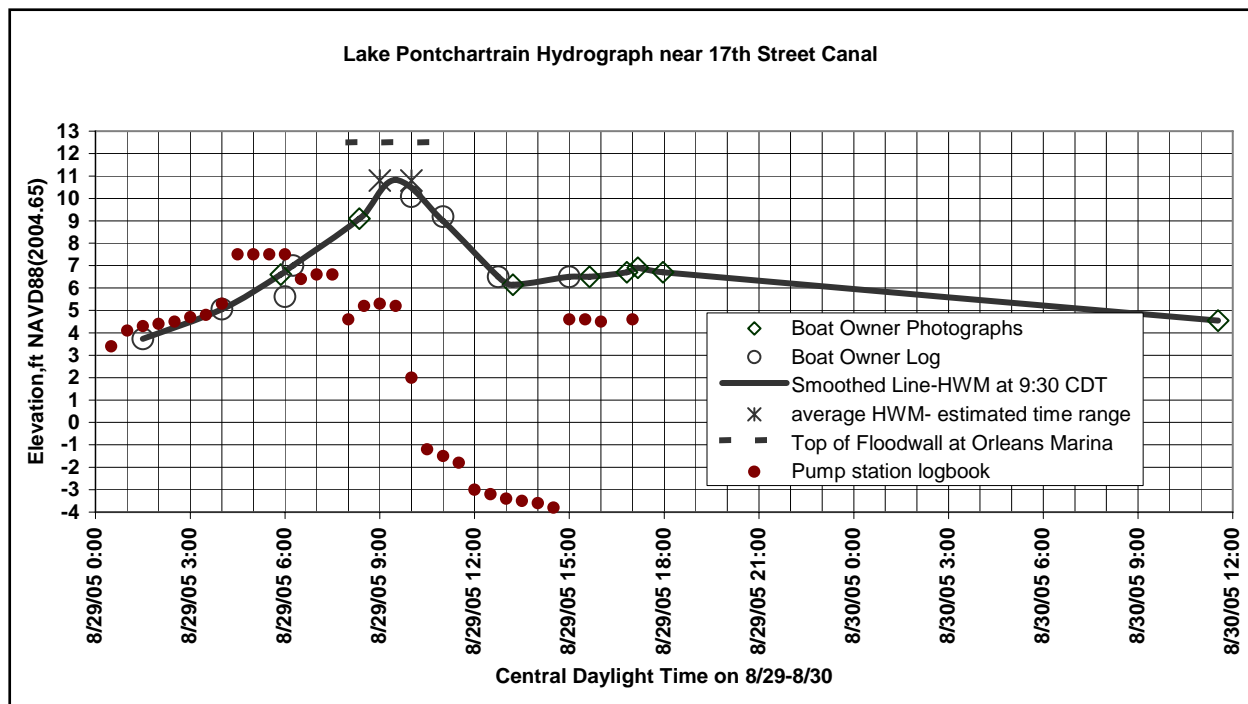


Figure 1-90. Pump station logbook values and constructed hydrograph at 17th Street Canal entrance.

- a. The logbook numbers on the 17th Street Canal (north or discharge) side of the pump station were taken from a mechanical air pressure gage connected to a bubbler system. The operators were not reading the discharge side staff gage on the outside of the pump station because of adverse weather conditions nor were they reading the strip chart recorder. Even if power is lost, the bubbler system will remain valid if the system does not lose air pressure. The bubbler system had a 5-gallon air tank connected to a compressor powered by 60 Hz electricity. The compressor and tank supply air to 2 bubbler systems on the suction side of the pump station and one system on the discharge side of the pump station. Based on interviews with station operators and the logbook, 60 Hz electrical power was lost beginning between 4:00 AM and 5:00 AM on 8/29/05. The 60 Hz electrical power was not restored until days after the storm.
- b. The compressor used during Katrina was present and still operating on 3/02/06. At 11:10 hrs on Thursday 3/02/06, the IPET team read 22.2 ft (Cairo datum) on the mechanical dial gage of the bubbler system and 21.8 ft (Cairo datum) on the outside staff gage indicating the bubbler system on the discharge side of the pump station was functioning. Later that day, the bubbler system was tested by unplugging the compressor to simulate the loss of electrical power on 8/29/05. The system began losing pressure after 2 hours and the mechanical gage on the discharge side bottomed out at a reading of 16 ft (Cairo datum) after 3 hours.
- c. It was observed that the suction side bubbler system had a damaged air tube that could have been the source of the loss of pressure. The operators did not know if the line was damaged before, during, or after Katrina. One reason this was unknown was that the operators could easily read a staff gage on the suction side of the pump station.

- d. The berm on the canal side of the floodwall at the 17th Street Canal breach did not erode and remained at an elevation of about 0.0 to -1.0 ft. Lack of berm erosion was also seen on the breach on the west side of the IHNC. By remaining intact, the berm should prevent water levels from going below the top of the berm. On 8/29/05, flow was going over the top of the berm that means the minimum canal levels would be greater than the top of the berm. As shown in Figure 1-90, the bubbler system gage shows 9 readings less than the top of the berm ranging from an elevation of -1.2 to -3.8 ft, thus at some point the logbook readings must not be valid. If readings are invalid for part of the record, this casts doubt over the entire record after power was lost.

The large drop in water level recorded in the pump station logbook at 9:30 to 10:30 is consistent with eyewitness information regarding the time of the breach and it is logical to conclude that the pump station data are capable of indicating time of changes even though the magnitudes may not be correct. This conclusion must be tempered by the fact that the bubbler gage showed a similar response to loss of air supply when tested on 2 March 2006.

As shown in Figure 1-90, the system appears to rebound to about correct values at about 3:00 PM. This appears impossible because the air compressor did not regain power. Close inspection of the logbook numbers indicated the possibility that a 2 had been written over the 1 in the logbook. For example, a value of 16 in the logbook became 26. It is possible that the outside staff gage was being read because winds had died down by this time.

Summarizing the bubbler system, the loss of electrical power beginning sometime between 4:00 to 5:00 AM on 8/29/05 along with the 2.2 ft increase in stage above the lake level from 4:00 AM to 4:30 AM followed by four identical 7.5 ft readings causes concern with the bubbler system. The rapid loss of pressure of the bubbler system when tested on 03/02/06 also causes concern for the 8/29/05 readings. Readings of the bubbler system below the berm elevation of 0 to -1 ft are likely not possible. These three problems with the bubbler system cast doubt on the entire set of readings after power was lost.

To accept the elevations from the pump station log, one must accept the bubbler system worked after loss of power and that other pictures, high water marks, and eyewitness data are incorrect. We have not been able to develop a scenario that accepts the pump station data and incorporates the other data. One unanswered question is how pump discharge and pump backflow affect this scenario. The records on these topics are unclear.

Integrating all data sources and considering the problems with the pump station data noted above indicates that it is more likely that stages continued to rise in the canal to a higher level before falling to the low levels observed at around 11:00 AM, 2:00 PM, and 3:00 PM.

Floodwall elevations along the 17th Street Canal are shown in Figures 1-91 and 1-92.

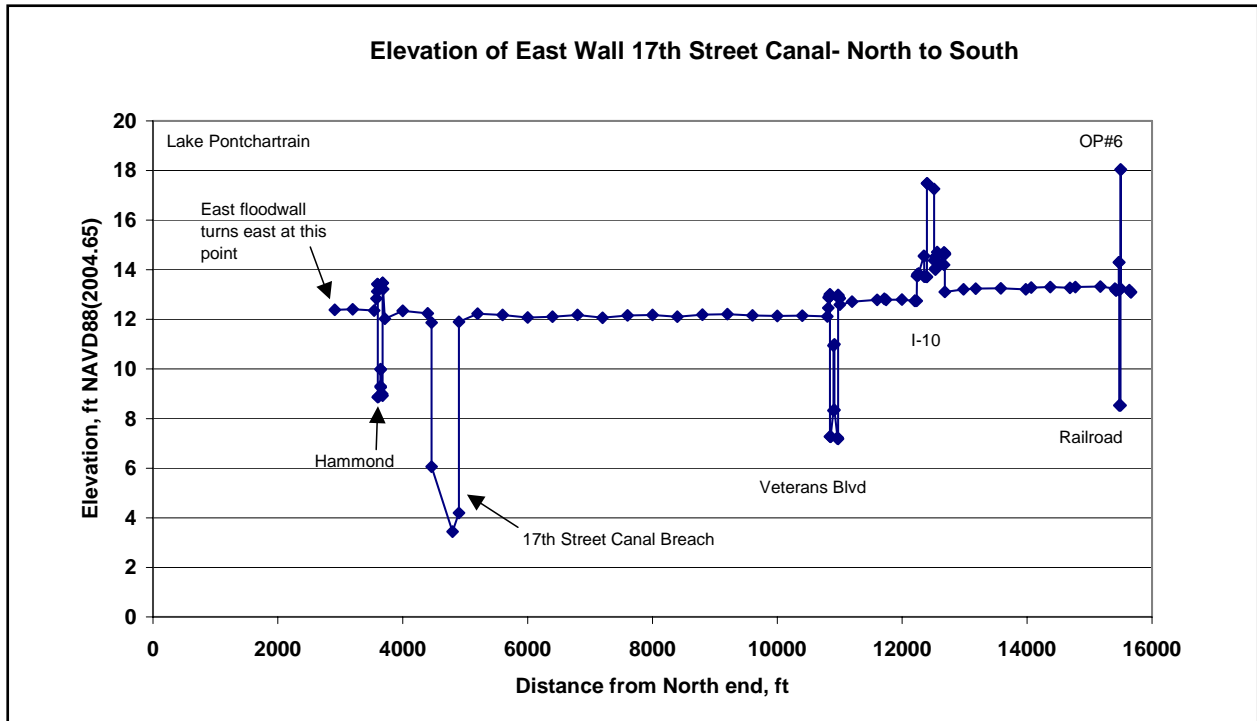


Figure 1-91. Floodwall profile along east side of 17th Street Canal. Note that low areas at bridges and pump stations are floodgate openings that were closed during the storm.

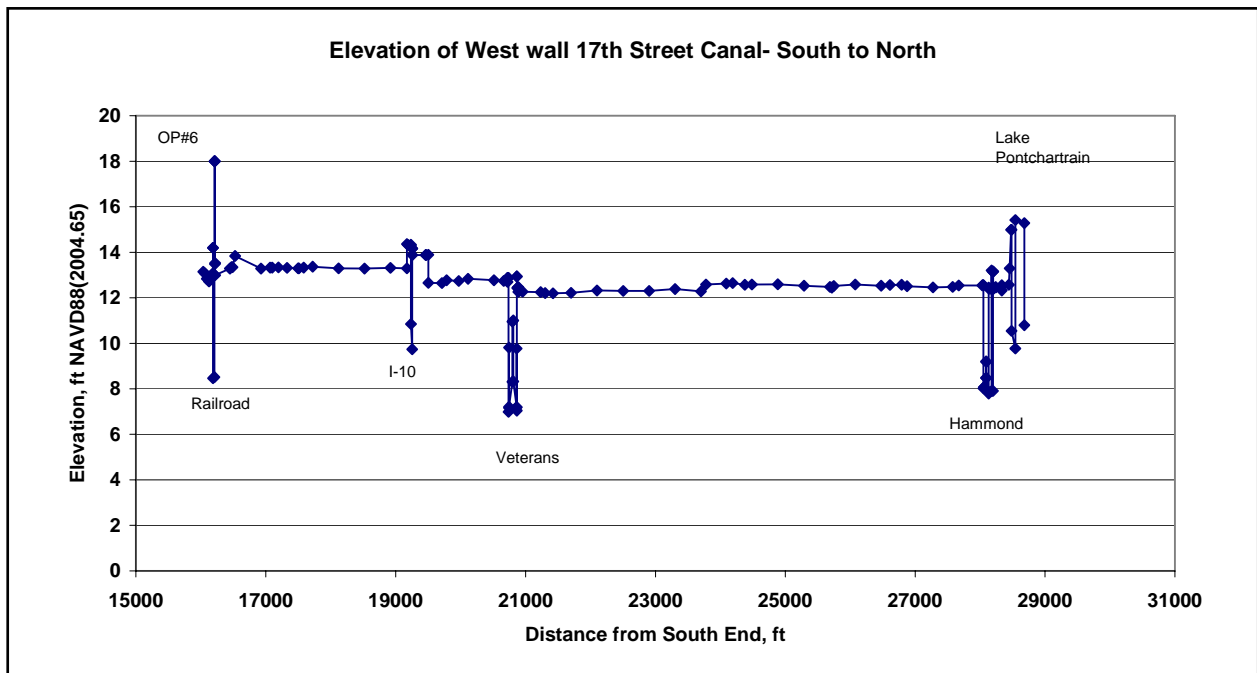


Figure 1-92. Floodwall and levee profile along west side of 17th Street Canal. Note that low areas at bridges and pump stations are floodgate openings that were closed during the storm.

## London Avenue Canal

Various factors but particularly the timing of the breaches complicate high water marks within the London Avenue Canal. Both the north breach near Robert E. Lee and the south breach near Mirabeau may have occurred before the peak high water in the lake, which would influence high water marks inside the canals. Marks south of Lakeshore Drive will have wave influence and will be lowered by the entrance loss at the north end of London Avenue Canal as well as head loss across the Lakeshore Drive Bridge because of flow through the breaches. The locations of levee debris marks near the entrance of the London Canal are shown in Figure 1-93. Observed high water marks inside London Avenue Canal were as follows:

- a.* LA 1015- 10.8 ft- Levee debris on west side of canal north of Robert E Lee Bridge. Figure 1-94 shows the location of this mark and demonstrates the difficulty of providing good photographs with the high grass. The debris line could be easily seen by looking straight down into the high grass.
- b.* LA 1017- 7.6 ft- Levee Debris on west side of canal south of Lakeshore Drive- ASCE COPRI felt a better mark was found south of this location.
- c.* LA 1018- 7.9 ft- debris on area near railroad track at OP#3, east side of discharge area. This area is shown in Figure 1-95.
- d.* LA 1022- 10.6 ft- this is the ASCE COPRI mark near LA 1017. See Figure 1-96.
- e.* LA 1059- 11.2 ft- Levee Debris on west side of canal just north of Leon C Simon Bridge.





Figure 1-93. Location of high water marks near entrance of London Avenue Canal.



Figure 1-94. Debris high water mark LA 1015 located on 10/02/05 on west side of London Avenue Canal. Looking north between Lakeshore Drive and Leon Simon Drive.





Figure 1-95. East floodgate at OP#3 at south end of London Avenue Canal. High water mark LA 1018 at top of painted concrete wall.



Figure 1-96. Debris high water mark LA 1022 on east levee of London Avenue Canal north of Leon C Simon Drive.

- f.* LA 1060- 9.8 ft- Levee debris on west side of canal, south of Leon C Simon Bridge, at bridge abutment.
- g.* LA 1061- 10.6 ft- Levee debris on west side of canal, north of Leon C Simon Bridge, at bridge abutment. Marks 1060 and 1061 suggest losses across this bridge of about 0.8 ft that would have been the result of flow through a breach but levee debris lines have significant variability.
- h.* LA 1069- 10.6 ft- Debris on southwest side of Robert E. Lee Bridge.
- i.* LA 1227- 9.5 ft- revisit to site of LA 1018 at OP#3 on east side of discharge area. This is a difficult mark to assess because of the factors listed in the beginning of this section. Observers believe debris between railroad rails suggest the water level was at least as high as the railroad ties that was the elevation surveyed. Mark location shown in Figure 1-97.
- j.* LA 1228- 10.0 ft- this mark is a debris mark on the west side of the discharge area. Debris is on a support for the floodgate and somewhat protected from any wave action in the canal as shown in Figure 1-98. The water level could have been higher as the debris may have been left behind as the water level dropped.



One eyewitness on London Avenue Canal just north of the Mirabeau Breach on the east side of the canal reported that at some time after 7:30 AM, he was hoisted up onto the floodwall and was able to reach over and touch the water with his hand. The time at which this happened is uncertain.



Figure 1-97. East floodgate at OP#3 at south end of London Avenue Canal. High water mark LA 1227 at top of railroad ties.



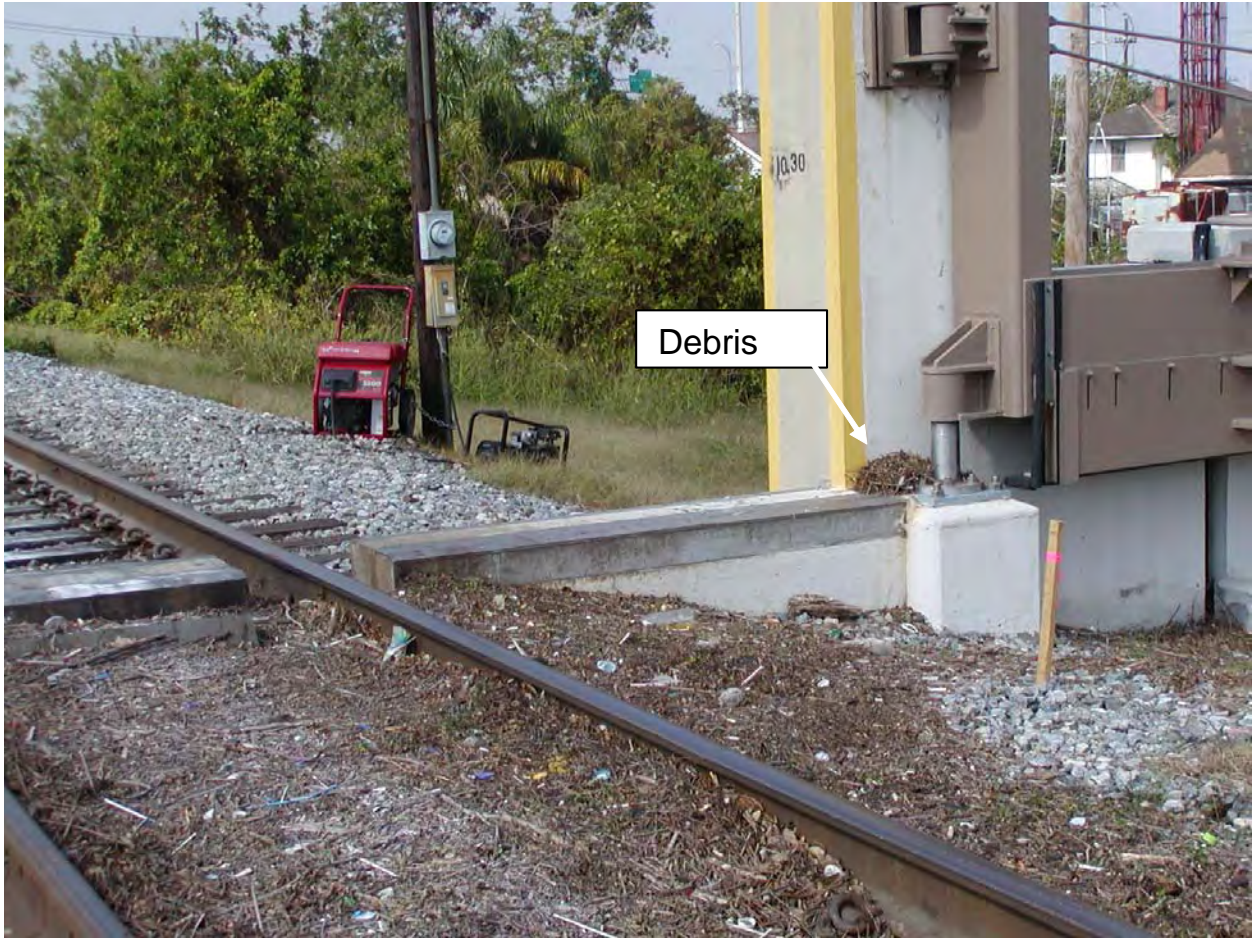


Figure 1-98. West floodgate at OP#3 at south end of London Avenue Canal. High water mark LA 1228 based on debris on top of sill at floodgate opening.

Floodwall and levee profiles for London Avenue Canal are shown in Figures 1-99 and 1-100.

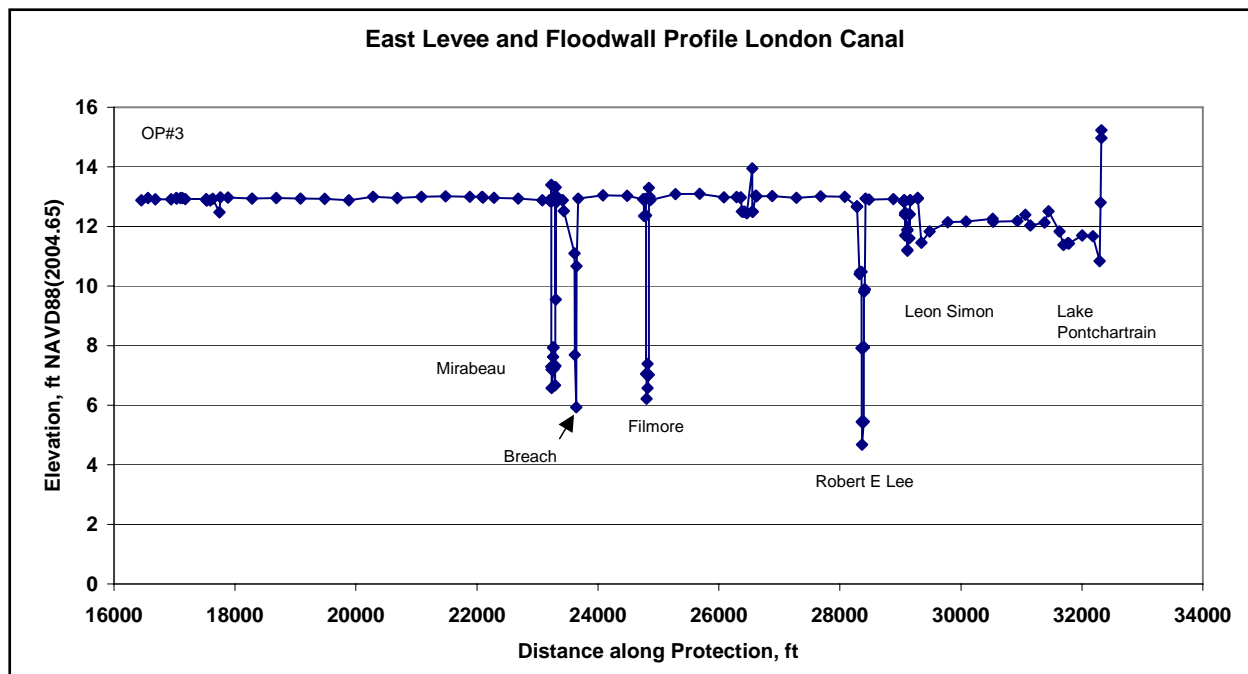


Figure 1-99. East levee and floodwall profile for London Avenue Canal. Note that low areas at bridges and pump stations are floodgate openings that were closed during the storm.

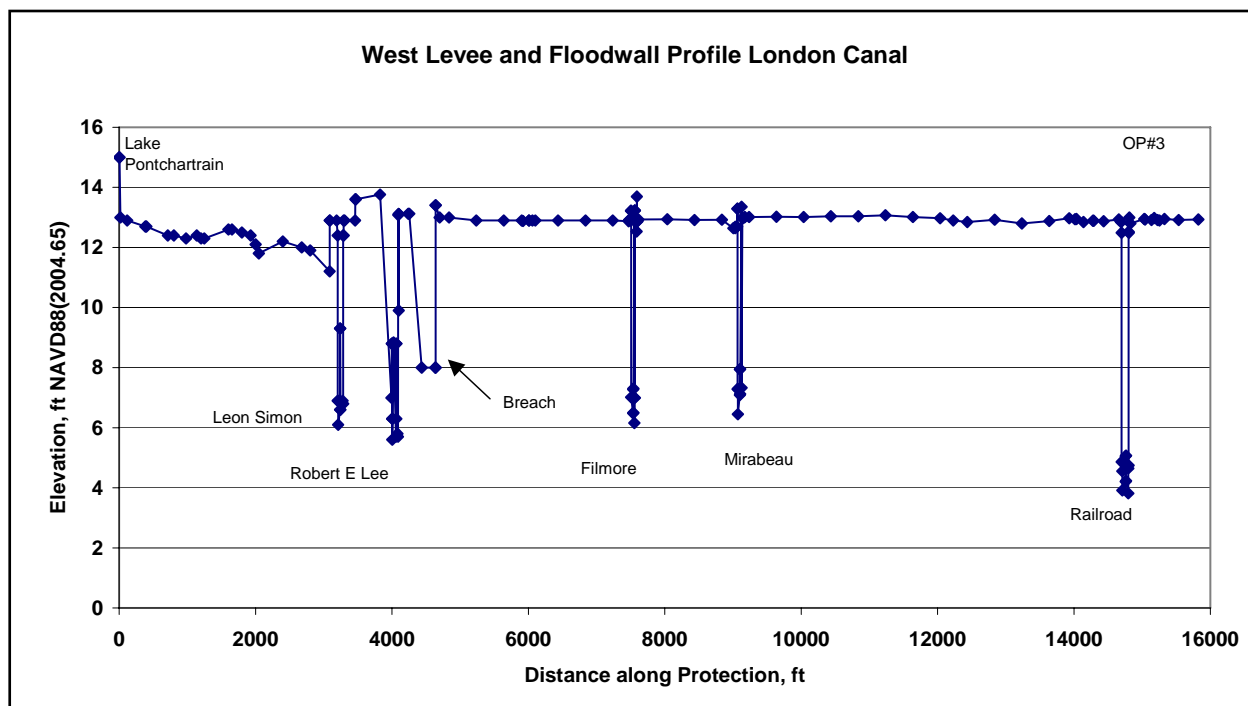


Figure 1-100. West levee and floodwall profile for London Avenue Canal. Note that low areas at bridges and pump stations are floodgate openings that were closed during the storm.

## Observed Water Levels along the GIWW and MRGO

High water marks collected along the GIWW and the MRGO are described in the following paragraph. Marks are presented beginning at the IHNC, east to the confluence of the GIWW and MRGO, and then southeast along the MRGO.

- a. LA 1004 (el 15.2 ft) - Mark is debris line on interior wall of Crane Building at Maersk/Sealand located at the intersection of the IHNC and the GIWW/MRGO. Structure is located on the east side of the Port of New Orleans floodwall.
- b. LA 1030 (el 15.2 ft) - Mark is debris line on interior wall of Crane Building at Maersk/Sealand located at the intersection of the IHNC and the GIWW/MRGO. Structure is located on the east side of the Port of New Orleans floodwall.
- c. LA 1260 (el 15.4 ft) - Mark is debris line on interior wall of bathroom located at the intersection of the IHNC and the GIWW/MRGO. Structure is located on the east side of the Port of New Orleans floodwall.
- d. LA 1039 (el 15.5 ft) - Mark is located at Boh Bros construction site on the north side of the GIWW/MRGO about 2.4 miles west of the confluence of the GIWW and MRGO. The mark was a debris line on an interior wall of the elevated office building. On the initial visit, the highest mark found was at 14.5 ft but it was a weak debris mark at 2.3 ft above the floor. On a subsequent visit, a better debris line was found at 3.3 ft above the floor giving an elevation of 15.5 ft.
- e. LA 1053 (el 15.5 ft) - Mark is at the Entergy power plant that is on the north side of the GIWW/MRGO and about 0.7 miles west of the confluence of the GIWW and MRGO. The mark was inside a building that is at the water's edge of the MRGO. The mark was a debris line inside an electrical panel box.
- f. LA 1093 (el 14.7 ft) - Mark is at the Entergy power plant that is on the north side of the GIWW/MRGO and about 0.7 miles west of the confluence of the GIWW and MRGO. Mark was debris on a chain link fence.
- g. LA 1043 (el 18.2 ft) - Located 1.1 mile southeast of the GIWW/ MRGO junction at the Bayou Bienvenue Structure. This mark is debris inside a radiator that is inside the gage house (Figure 1-101). The doors to this gage house were damaged by the storm surge and significant flow was passing through the gage house. The large amount of flow through the gage house and potential for wave effects within the gage house may cause this mark to be high.
- h. LA 1044 (el 18.5 ft) - Also at Bayou Bienvenue but was debris on the upper handrail outside the gage house and exposed to wave activity.
- i. LA 1045 (el 16.5 ft) - Also at Bayou Bienvenue but was debris on the lower handrail outside the gage house and exposed to wave activity.
- j. LA 1040 (el 20.8 ft)- At Bayou Dupre Structure on MRGO about 7.5 miles southeast of the GIWW/MRGO junction. Inside gage house that was heavily damaged, small amount of debris in window frame, likely high.
- k. LA 1041 (el 16.8 ft) - Also at Bayou Dupre. Debris on lower guardrail.
- l. LA 1042 (el 21.7 ft) - Also at Bayou Dupre. Debris on light standard on outside of gage house, likely high.
- m. The marks at Bayou Bienvenue and Bayou Dupre were difficult to interpret and inconclusive.



- n. LA 1155 - This mark was not surveyed and was only accessible by boat since it was on channel marker #107 (Figure 1-102). The marker is about 13.8 miles southeast of the GIWW/MRGO junction and about 0.7 miles southeast of where the levee protection leaves the MRGO. The debris on this tower was measured at 19.6 ft above the water level at 1345 hrs on 10/17/2005. The Bayou Dupre gage read about 1.8 ft on this same day giving an elevation of about 21.4 ft (relative to an uncertain datum). This debris elevation contains a large wave component. Water depth at the channel marker on the day of the inspection was about 12 ft.
- o. LA 1087 (el 18.1 ft) - Well-defined debris line inside bedroom of home (Figure 1-103) at Shell Beach that is about 19 miles southeast of the GIWW/MRGO junction. High water mark is 31" above second level floor.



Figure 1-101. Bayou Bienvenue Gage House.



Figure 1-102. LA 1155 on MRGO. Debris on tower.



Figure 1-103. Home in Shell Beach containing high water mark LA 1087 at 31" above second level floor.

- p. LA 1088 (el 18.7 ft) - Well-defined debris line inside pantry of a different home at Shell Beach. Of the three marks at Shell Beach, this house is closest to the MRGO.
- q. LA 1089 (el 17.1 ft) - Inside business at Shell Beach. Of the three marks at Shell Beach, this business is farthest from the MRGO.

Figure 1-104 shows a plot of the high water mark data along the GIWW/MRGO along with a best estimate line. The best estimate line ends at the Entergy Plant because of uncertainty of high water marks at Bayou Bienvenue and Bayou Dupre, the large wave component at channel marker 107, and the fact that Shell Beach is beyond the levee protection. Of all the marks southeast of the GIWW/MRGO junction, the marks at Shell Beach are the most reliable estimates of the peak “still” water level.

## Additional Relevant Hydrographs

Figures 1-105 and 1-106 are hydrographs acquired by NOAA National Ocean Service stations 8761724 at Grand Isle, Louisiana and 8760922 at Southwest Pass, Louisiana. The



instruments at these stations are among the few that functioned throughout Katrina's passage and recorded peak water levels. The Grand Isle station recorded a peak water level of 5.70 ft above mean lower-low water (MLLW) at 09:06 UTC on 29 August 2005. The Southwest Pass station recorded a peak water level of 7.61 ft above MLLW at 09:30 UTC on 29 August 2005.

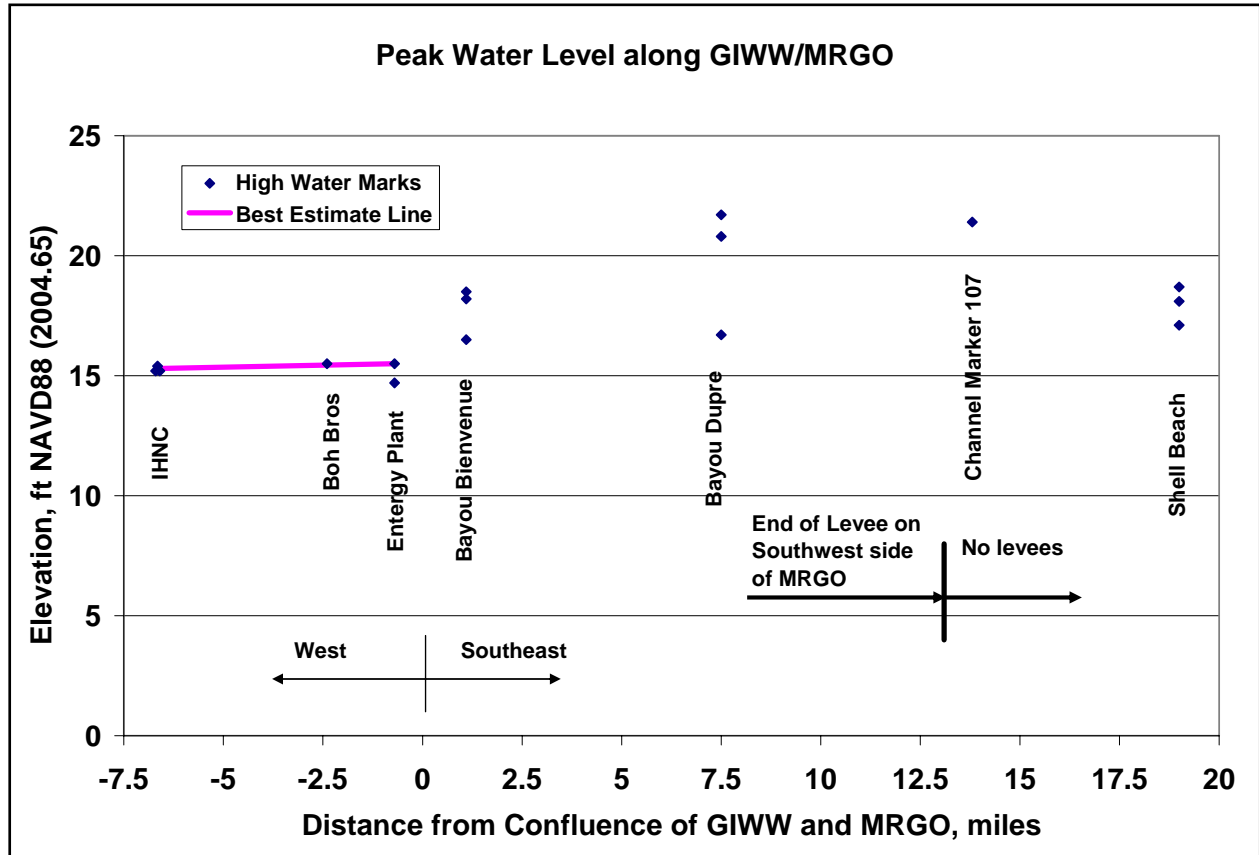


Figure 1-104. Peak water level along GIWW and MRGO based on high water marks.



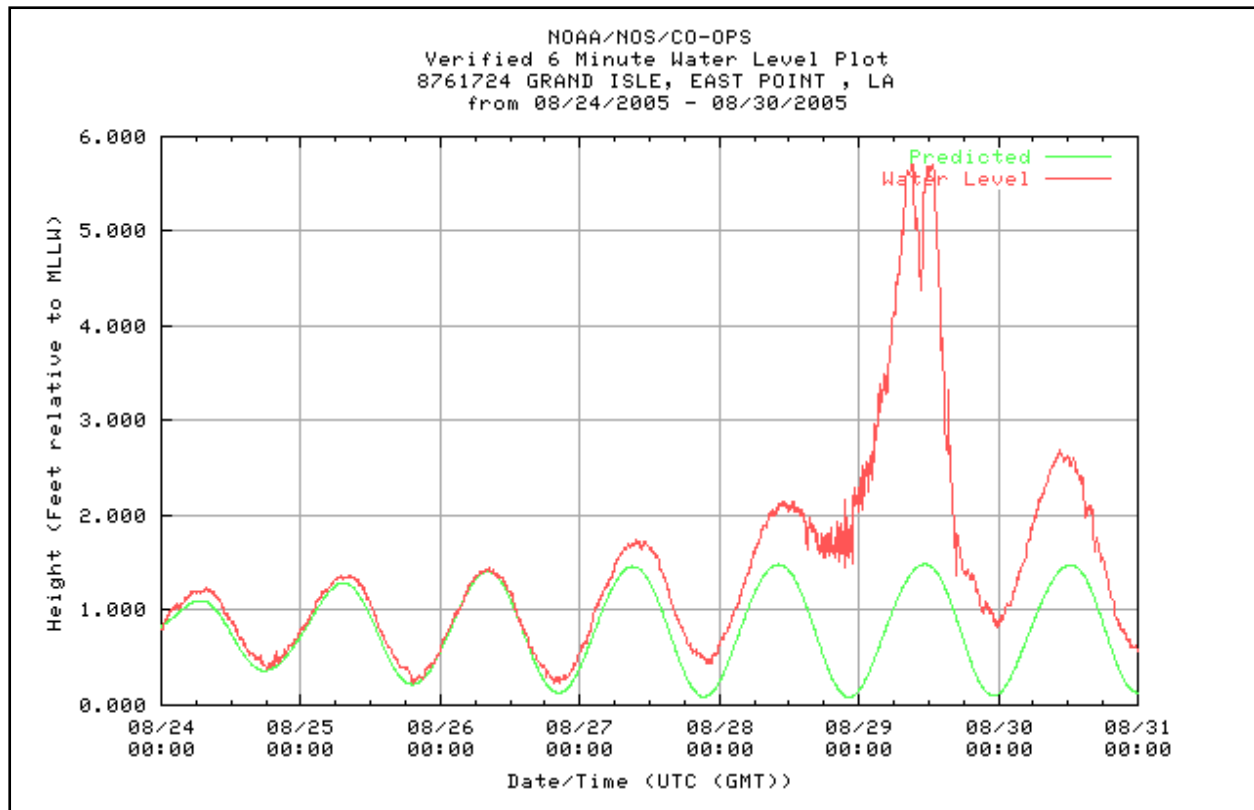


Figure 1-105. Hydrograph for NOAA National Ocean Service station at Grand Isle, Louisiana. Vertical datum relation between MLLW and NAVD88-2004.65 is uncertain.

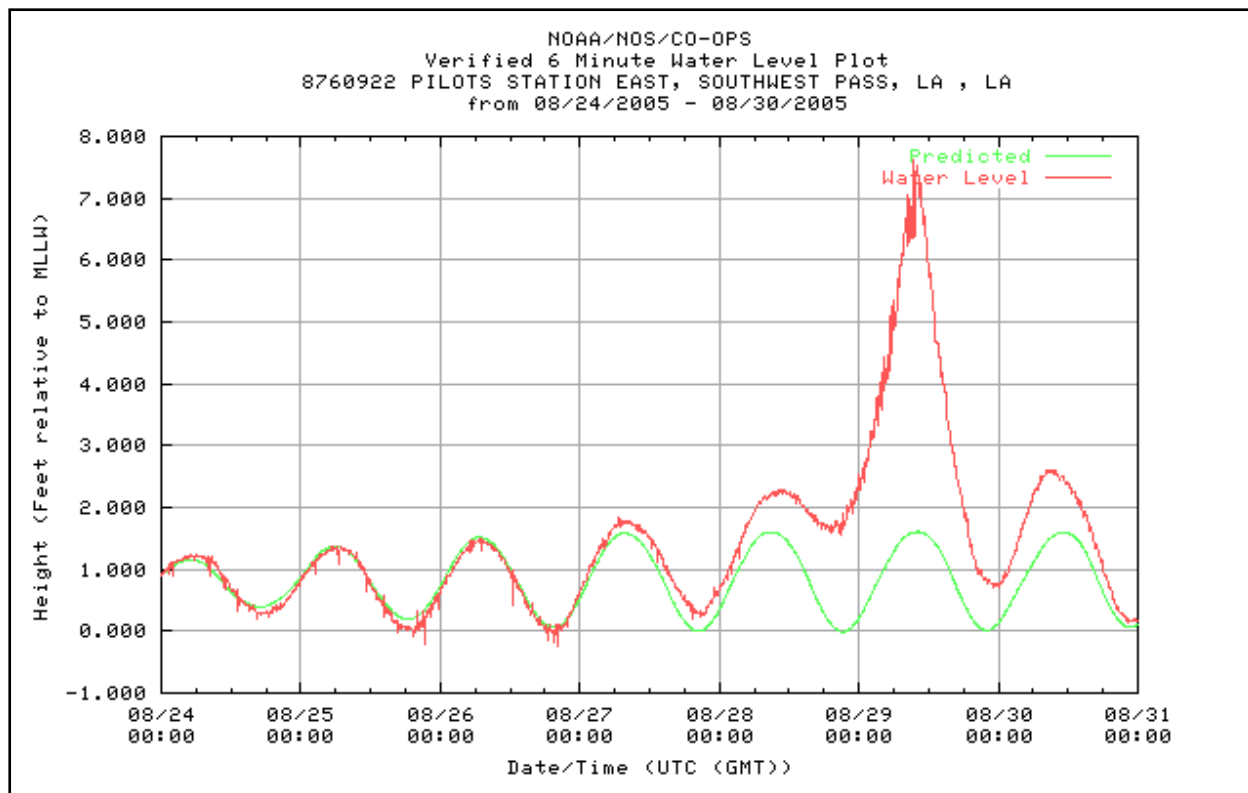
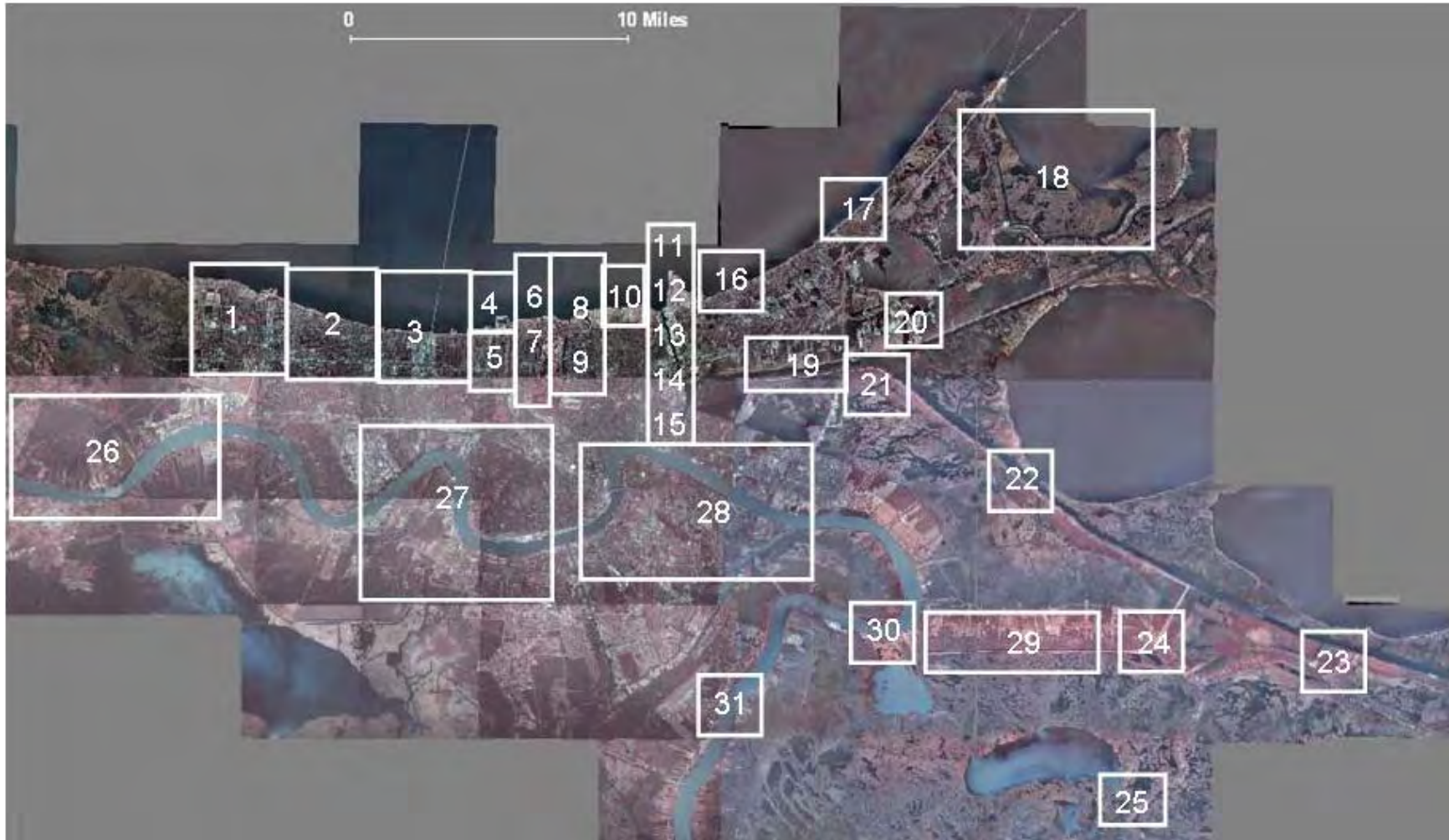


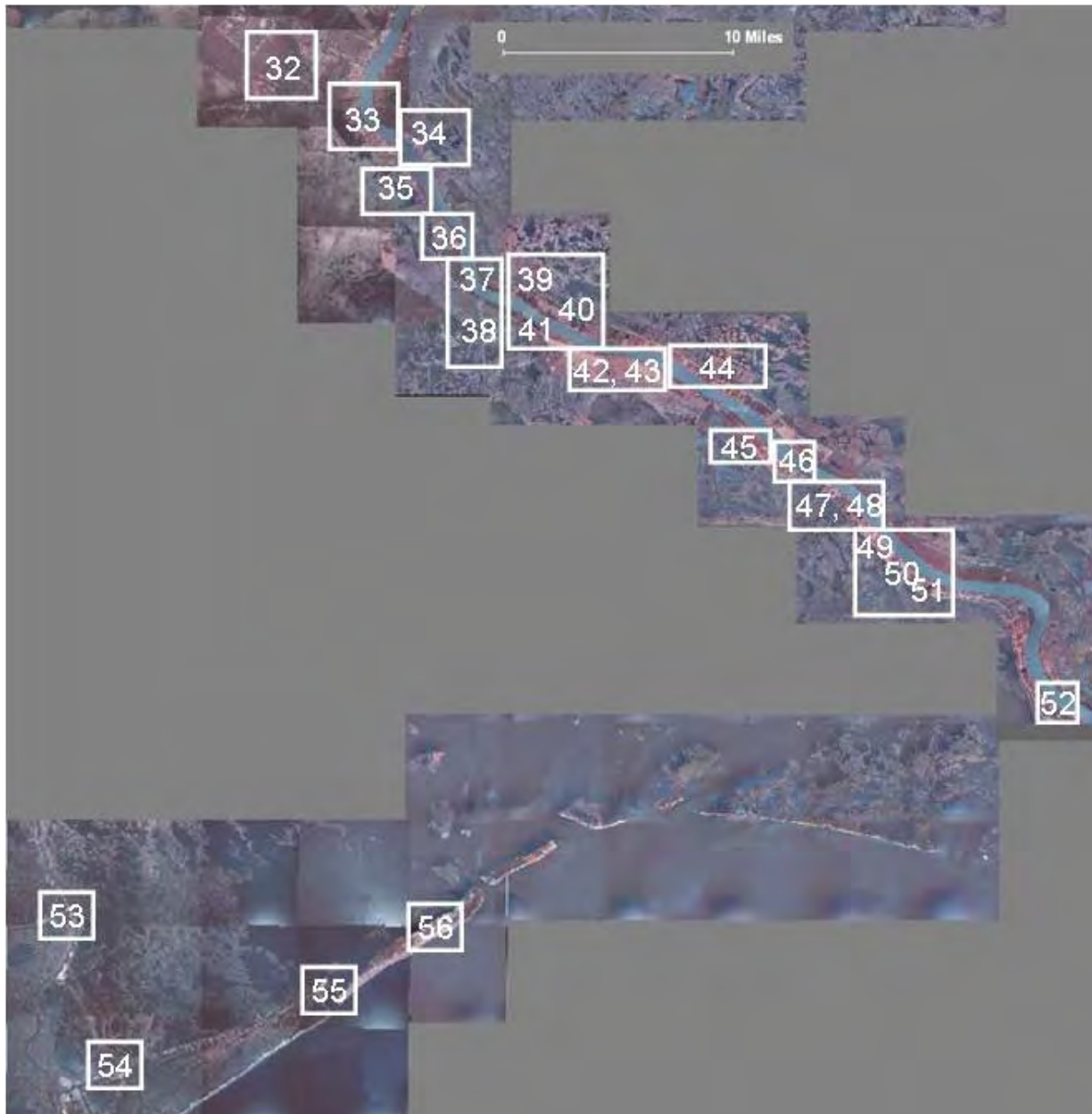
Figure 1-106. Hydrograph for NOAA National Ocean Service Station at Southwest Pass, Louisiana. Vertical datum relation between MLLW and NAVD88-2004.65 is unknown.

Note the double peak in the Grand Isle hydrograph. There was initial concern that the double peak may have been caused by movement of the gage or supporting structure. Inspection of the station shortly after Katrina's passage showed the gage and supporting structure to be intact and the gage vertical datum was confirmed as correct. The simplest, most obvious meteorological explanation for the double peak is a sudden, temporary shift in the local winds, but this has not been verified at this time. The data of these hydrographs have been verified as conforming to NOS standards.

## Images of High Water Mark Locations



Index to North Images



Index to South Images

Volume IV The Storm – Technical Appendix

This is a preliminary report subject to revision; it does not contain final conclusions of the United States Army Corps of Engineers.





**High Water Mark Quality**

- ▲ Excellent
- Good
- ◆ Fair/Poor
- Unknown

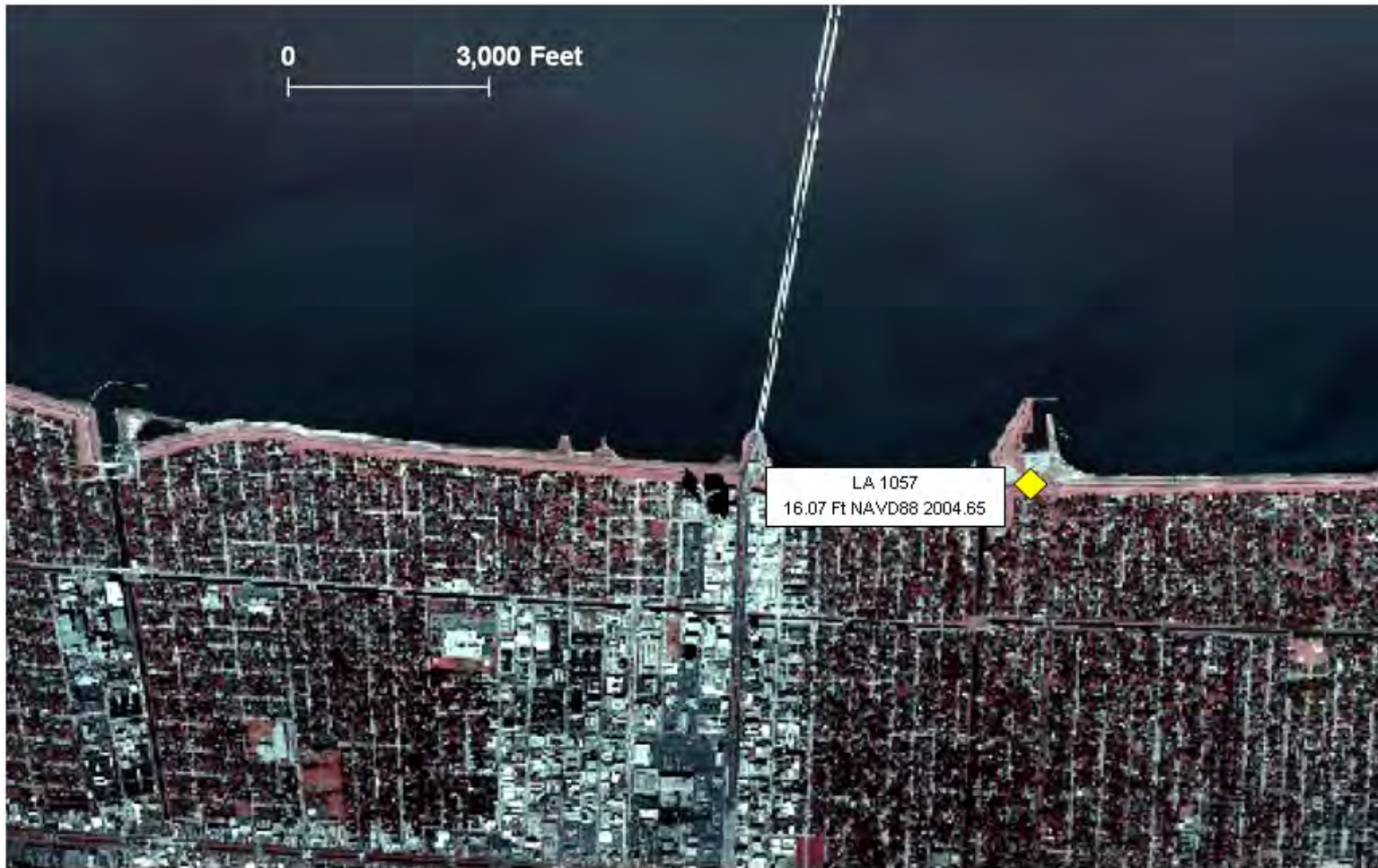


**High Water Mark Quality**

- ▲ Excellent
- Good
- ◆ Fair/Poor
- Unknown

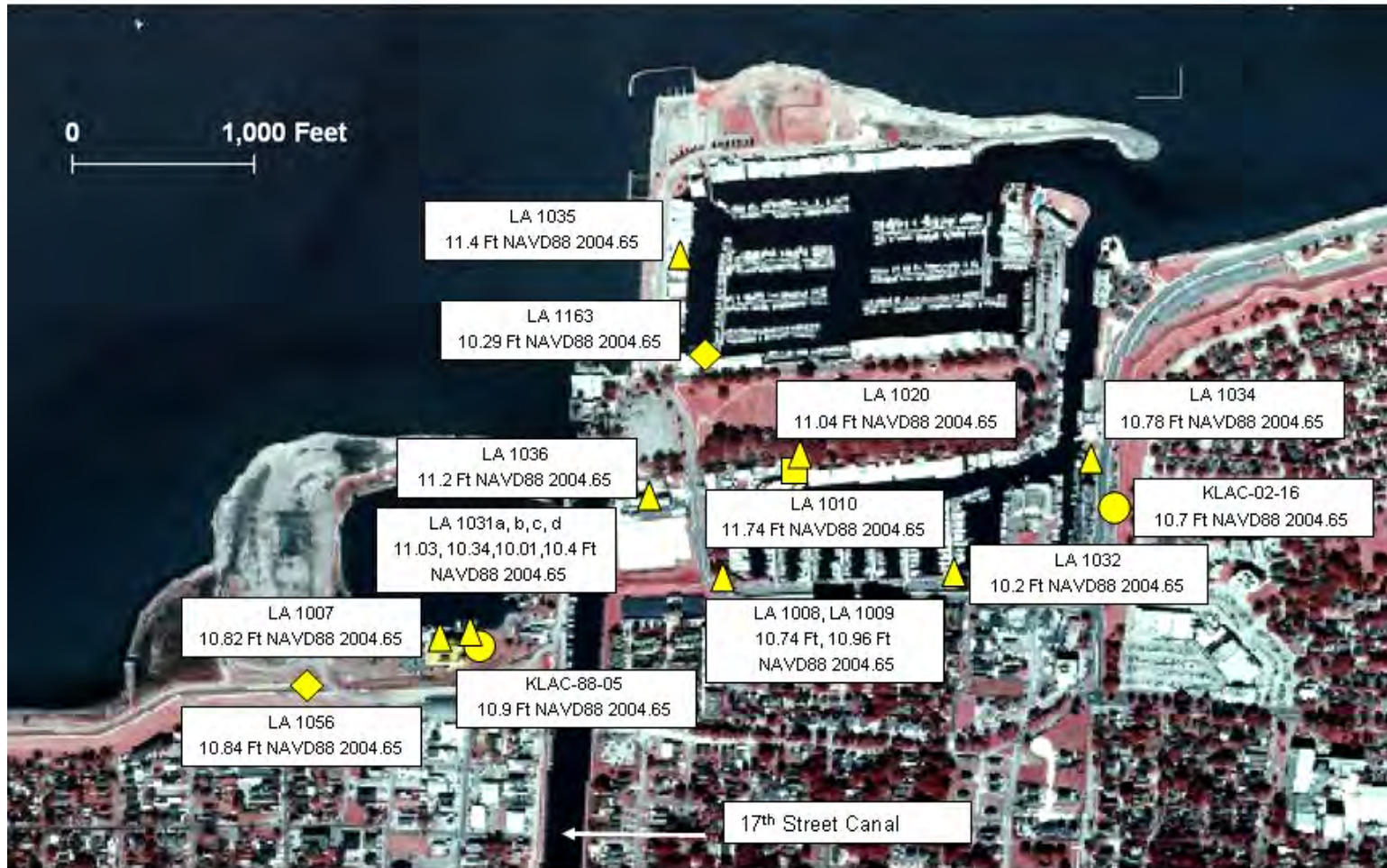


3



**High Water Mark Quality**

- ▲ Excellent    ■ Good    ◆ Fair/Poor    ● Unknown



**High Water Mark Quality**

- ▲ Excellent
- Good
- ◆ Fair/Poor
- Unknown





**High Water Mark Quality**

- ▲ Excellent
- Good
- ◆ Fair/Poor
- Unknown



**High Water Mark Quality**

- ▲ Excellent
- Good
- ◆ Fair/Poor
- Unknown





**High Water Mark Quality**

- ▲ Excellent
- Good
- ◆ Fair/Poor
- Unknown





**High Water Mark Quality**

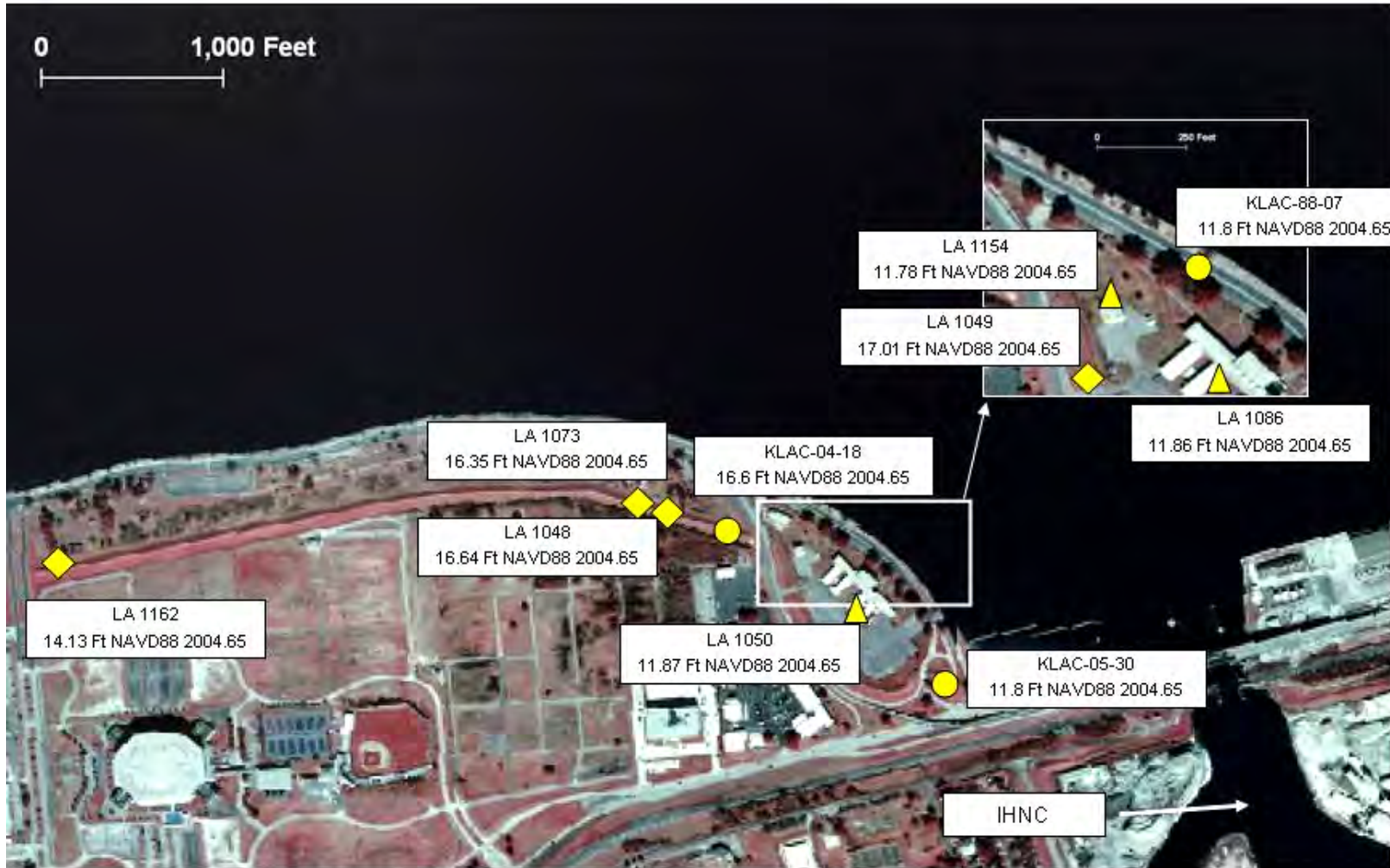
- ▲ Excellent
- Good
- ◆ Fair/Poor
- Unknown





**High Water Mark Quality**

- ▲ Excellent
- Good
- ◆ Fair/Poor
- Unknown



**High Water Mark Quality**

- ▲ Excellent
- Good
- ◆ Fair/Poor
- Unknown





**High Water Mark Quality**

- ▲ Excellent
- Good
- ◆ Fair/Poor
- Unknown





**High Water Mark Quality**

- ▲ Excellent
- Good
- ◆ Fair/Poor
- Unknown





**High Water Mark Quality**

- ▲ Excellent
- Good
- ◆ Fair/Poor
- Unknown



**High Water Mark Quality**

- ▲ Excellent
- Good
- ◆ Fair/Poor
- Unknown





**High Water Mark Quality**

- ▲ Excellent
- Good
- ◆ Fair/Poor
- Unknown





**High Water Mark Quality**

- ▲ Excellent
- Good
- ◆ Fair/Poor
- Unknown





**High Water Mark Quality**

- ▲ Excellent
- Good
- ◆ Fair/Poor
- Unknown





**High Water Mark Quality**

- ▲ Excellent
- Good
- ◆ Fair/Poor
- Unknown



**High Water Mark Quality**

- ▲ Excellent
- Good
- ◆ Fair/Poor
- Unknown





**High Water Mark Quality**

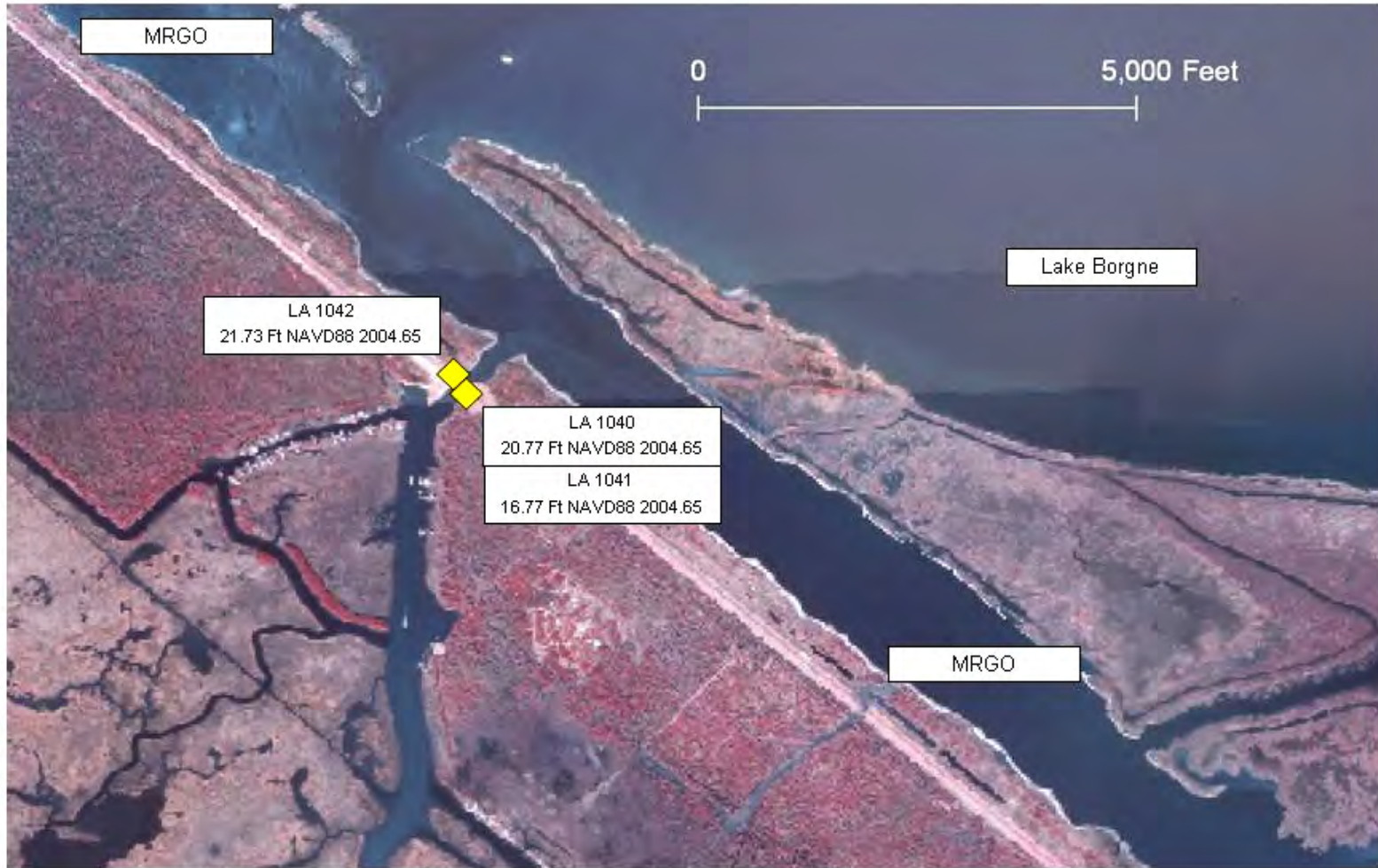
- ▲ Excellent
- Good
- ◆ Fair/Poor
- Unknown





**High Water Mark Quality**

- ▲ Excellent
- Good
- ◆ Fair/Poor
- Unknown



**High Water Mark Quality**

- ▲ Excellent
- Good
- ◆ Fair/Poor
- Unknown

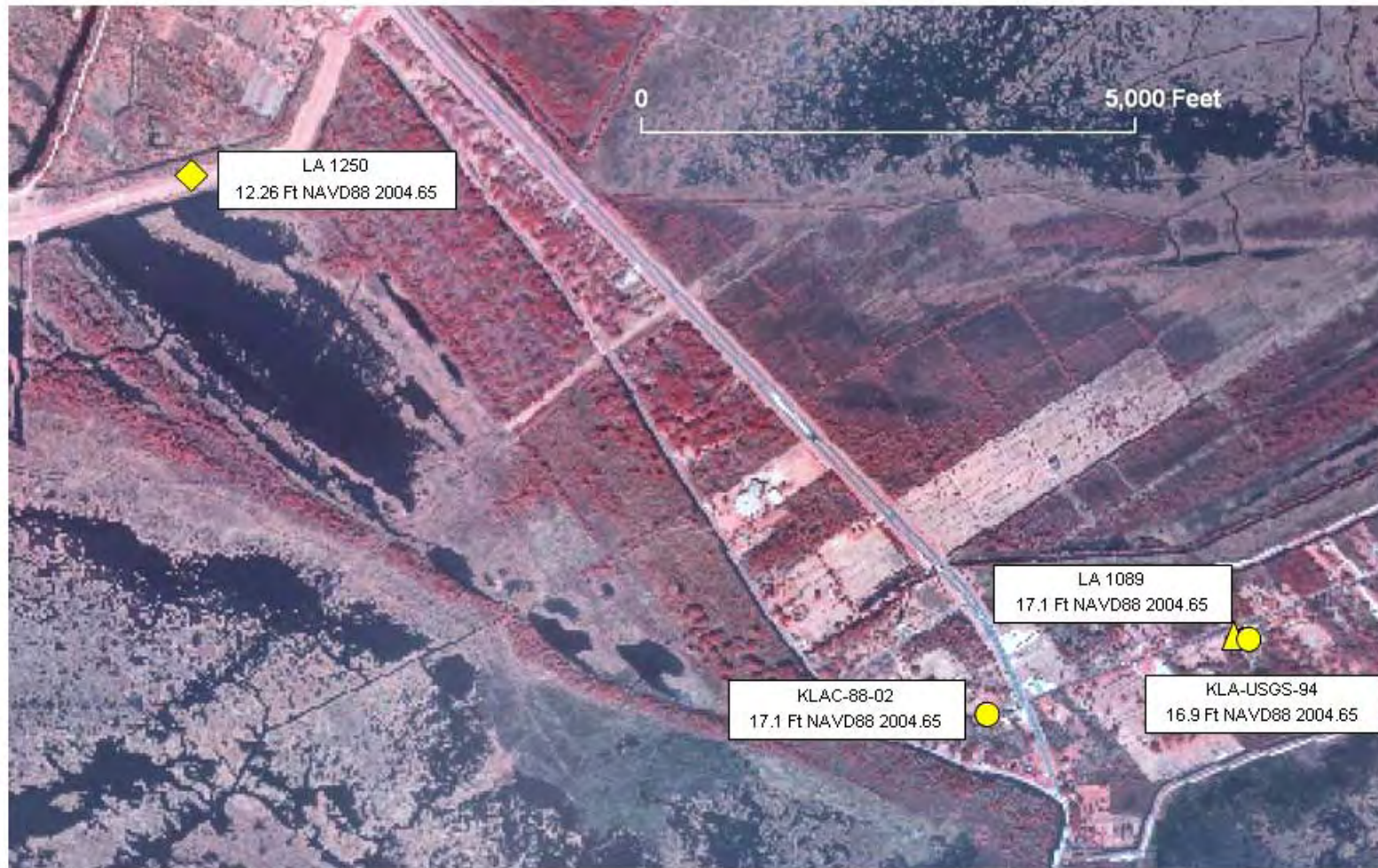




**High Water Mark Quality**

- ▲ Excellent
- Good
- ◆ Fair/Poor
- Unknown





**High Water Mark Quality**

- ▲ Excellent
- Good
- ◆ Fair/Poor
- Unknown





**High Water Mark Quality**

- ▲ Excellent
- Good
- ◆ Fair/Poor
- Unknown



**High Water Mark Quality**

- ▲ Excellent
- Good
- ◆ Fair/Poor
- Unknown





**High Water Mark Quality**

- ▲ Excellent
- Good
- ◆ Fair/Poor
- Unknown

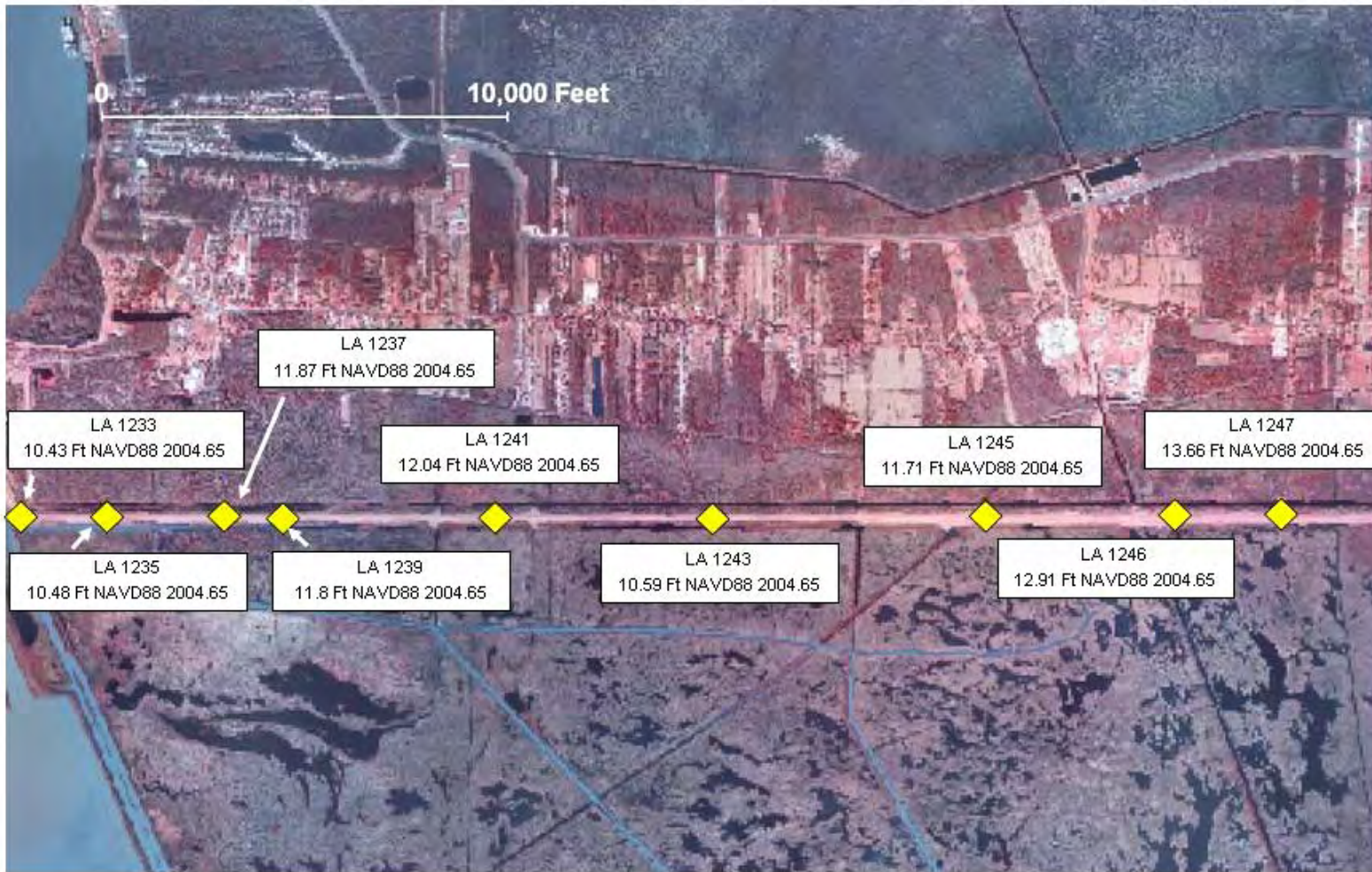




**High Water Mark Quality**

- ▲ Excellent
- Good
- ◆ Fair/Poor
- Unknown





**High Water Mark Quality**

- ▲ Excellent
- Good
- ◆ Fair/Poor
- Unknown





**High Water Mark Quality**

- ▲ Excellent
- Good
- ◆ Fair/Poor
- Unknown



**High Water Mark Quality**

- ▲ Excellent
- Good
- ◆ Fair/Poor
- Unknown





**High Water Mark Quality**

- ▲ Excellent
- Good
- ◆ Fair/Poor
- Unknown





**High Water Mark Quality**

- ▲ Excellent
- Good
- ◆ Fair/Poor
- Unknown



**High Water Mark Quality**

- ▲ Excellent
- Good
- ◆ Fair/Poor
- Unknown





**High Water Mark Quality**

- ▲ Excellent
- Good
- ◆ Fair/Poor
- Unknown





**High Water Mark Quality**

- ▲ Excellent
- Good
- ◆ Fair/Poor
- Unknown



**High Water Mark Quality**

- ▲ Excellent
- Good
- ◆ Fair/Poor
- Unknown





**High Water Mark Quality**

- ▲ Excellent
- Good
- ◆ Fair/Poor
- Unknown





**High Water Mark Quality**

- ▲ Excellent
- Good
- ◆ Fair/Poor
- Unknown



**High Water Mark Quality**

- ▲ Excellent
- Good
- ◆ Fair/Poor
- Unknown

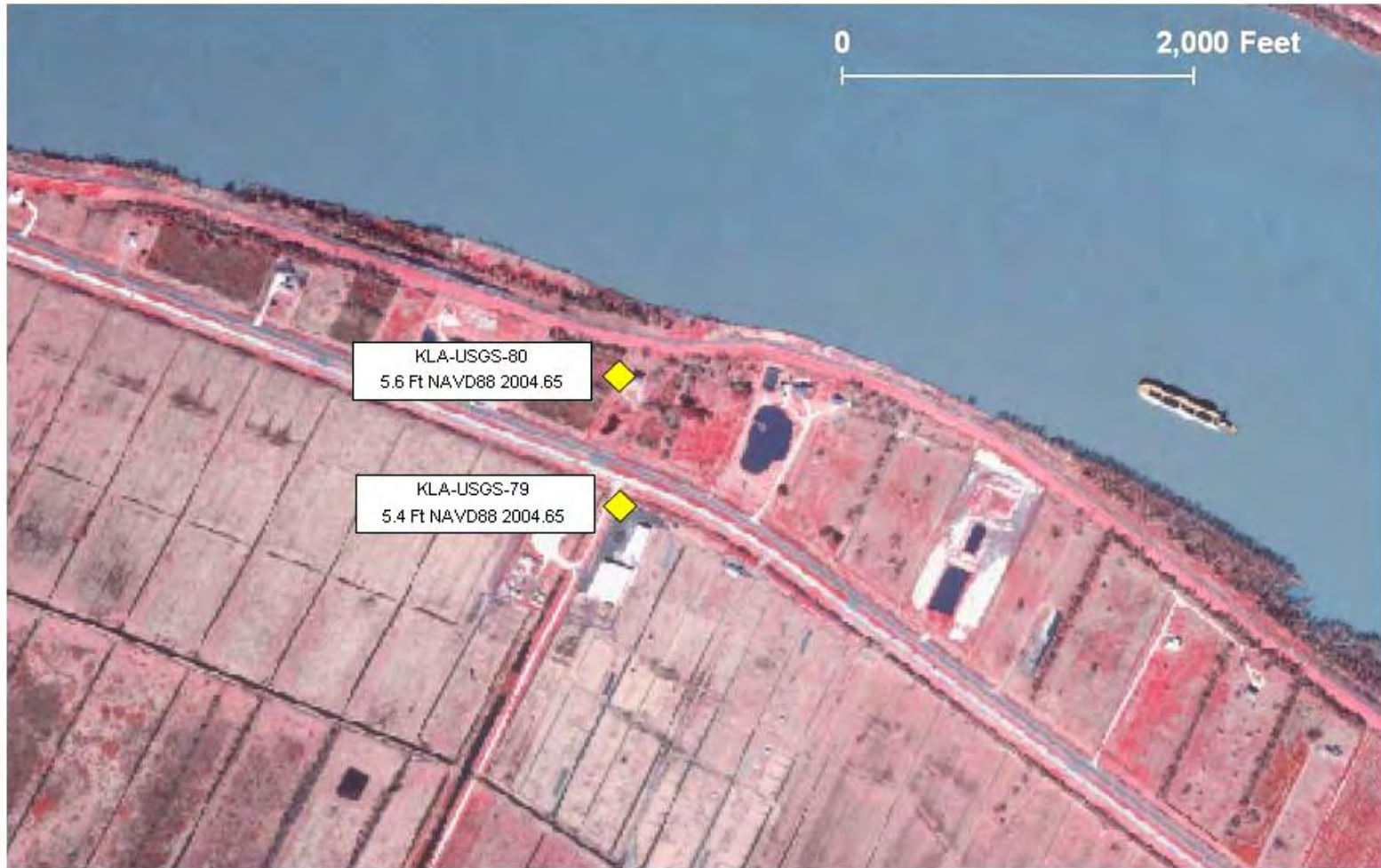




**High Water Mark Quality**

- ▲ Excellent
- Good
- ◆ Fair/Poor
- Unknown





**High Water Mark Quality**

- ▲ Excellent
- Good
- ◆ Fair/Poor
- Unknown



**High Water Mark Quality**

- ▲ Excellent
- Good
- ◆ Fair/Poor
- Unknown





**High Water Mark Quality**

- ▲ Excellent
- Good
- ◆ Fair/Poor
- Unknown





**High Water Mark Quality**

- ▲ Excellent
- Good
- ◆ Fair/Poor
- Unknown

46



**High Water Mark Quality**

- ▲ Excellent
- Good
- ◆ Fair/Poor
- Unknown





**High Water Mark Quality**

- ▲ Excellent
- Good
- ◆ Fair/Poor
- Unknown





**High Water Mark Quality**

- ▲ Excellent
- Good
- ◆ Fair/Poor
- Unknown



**High Water Mark Quality**

- ▲ Excellent
- Good
- ◆ Fair/Poor
- Unknown





**High Water Mark Quality**

- ▲ Excellent
- Good
- ◆ Fair/Poor
- Unknown





**High Water Mark Quality**

- ▲ Excellent
- Good
- ◆ Fair/Poor
- Unknown



**High Water Mark Quality**

- ▲ Excellent
- Good
- ◆ Fair/Poor
- Unknown





**High Water Mark Quality**

- ▲ Excellent
- Good
- ◆ Fair/Poor
- Unknown





**High Water Mark Quality**

- ▲ Excellent
- Good
- ◆ Fair/Poor
- Unknown



**High Water Mark Quality**

- ▲ Excellent
- Good
- ◆ Fair/Poor
- Unknown





**High Water Mark Quality**

- ▲ Excellent
- Good
- ◆ Fair/Poor
- Unknown



## Plate 1-1. Spreadsheet of FEMA and USGS High Water Marks for Louisiana

HWM_ID	County	Type of HWM	HWM Object	HWM Quality	Flood Type	Reliability of mark	Elev NAVD88 2004.65 (corrected)	Survey Latitude	Survey Longitude	Survey Comments
KLAC-01-01	St. Tammany	Mud Line	Exterior trailer	Good	Coastal - Surge Only	good	9.7	30.301813	-89.93886	NGS Control Used: ALCO.STENNIS CORS ARP.HAMMOND CORS MON
KLAC-01-02	St. Tammany	Mud Line	Exterior of front door	Good	Coastal - Surge Only	good	9.7	30.301163	-89.94365	NGS Control Used: ALCO.STENNIS CORS ARP.HAMMOND CORS MON
KLAC-01-03	St. Tammany	Debris Line	Next to road in ditch	Fair	Coastal - Wave Runup	poor	7.6	30.309747	-89.93982	NGS Control Used: ALCO.STENNIS CORS ARP.HAMMOND CORS MON
KLAC-01-04	St. Tammany	Mud Line	Exterior of house	Fair	Coastal - Surge Only	poor	5.2	30.329397	-90.003	NGS Control Used: STENNIS.ALCO.NICOLE.G 275.A 193
KLAC-01-05	St. Tammany	Mud Line	Exterior of shed / carport	Good	Coastal - Surge Only	fair	10.5	30.328688	-89.98737	NGS Control Used: STENNIS.ALCO.NICOLE.G 275.A 193
KLAC-01-06	St. Tammany	Mud Line	Exterior post back of car port	Poor		poor	27.9	30.394586	-89.89353	NGS Control Used: STENNIS.ALCO.NICOLE.G 275.A 193
KLAC-01-10	St. Tammany	Mud Line	Exterior Post of Boat House Bldg	Good	Riverine - Hurricane	fair	9.8	30.314372	-89.92729	NGS Control Used: ALCO.STENNIS CORS ARP.HAMMOND CORS MON
KLAC-01-11	St. Tammany	Debris Line	Next to wooden bridge at church	Fair	Riverine - Hurricane	fair	9.6	30.331819	-89.9459	NGS Control Used: ALCO.STENNIS CORS ARP.HAMMOND CORS MON
KLAC-01-12	St. Tammany	Mud Line	Exterior of trailer	Good	Coastal - Surge Only	fair	9.8	30.315155	-89.95477	NGS Control Used: ALCO.STENNIS CORS ARP.HAMMOND CORS MON
KLAC-01-13	St. Tammany	Debris Line	grass next to ditch	Good	Coastal - Surge Only	fair	10.8	30.326294	-89.98468	NGS Control Used: ALCO.STENNIS CORS ARP.HAMMOND CORS MON
KLAC-01-14	Jefferson	Mud Line	Apartment Fence	Good	tbd	protected	-1.2	29.893883	-90.14487	NGS Control Used: ZURFLUH.B 369.REGGIO 2.ALCO.WASTE WELL RESET 2
KLAC-01-15	Jefferson	Mud Line	Front of house - bay window	Good	tbd	protected	1.2	29.876847	-90.13436	NGS Control Used: B 369.L 278.S 188.ALCO.WASTE WELL RESET 2
KLAC-01-16	Jefferson	Wrack Line	Stake	Good	tbd	poor	2.4	29.76864	-90.08252	NGS Control Used: REGGIO 2.C 195.R 194.B 369.A 152.MILAN 2

HWM_ID	County	Type of HWM	HWM Object	HWM Quality	Flood Type	Reliability of mark	Elev NAVD88 2004.65 (corrected)	Survey Latitude	Survey Longitude	Survey Comments
KLAC-01-17	Jefferson	Mud Line	steel power pole next to Destrehan Ave, next to Woodmere Elementary School	Good	tbd	protected	-1.8	29.854061	-90.0703	NGS Control Used: B 369.L 278.S 188.ALCO.WASTE WELL RESET 2
KLAC-02-01	Terrebonne	Wrack Line	GROUND, STAKE	Good	Coastal - Surge Only	poor	2.1	29.469424	-90.55929	NGS Control Used: S 233.G 233
KLAC-02-02	St. Charles	Debris Line	ground	Good	Riverine - Hurricane	poor	13.6	29.938693	-90.37497	NGS Control Used: ALCO.G 275.S 379.G 165.HAMMOND CORS ARP
KLAC-02-03	St. Charles	Debris Line	ground	Good	Riverine - Hurricane	poor	15.7	29.935227	-90.36343	NGS Control Used: ALCO.G 275.S 379.G 165.HAMMOND CORS ARP
KLAC-02-04	Jefferson	Debris Line	spray paint on Levee - stake at bottom of levee	Good	Riverine - Hurricane	poor	17.8	29.96386	-90.27356	NGS Control Used: B 369.L 278.S 188.ALCO.WASTE WELL RESET 2
KLAC-02-05	St. Charles	Wrack Line	ground	Good	Riverine - Hurricane	poor	3.5	29.834727	-90.47595	NGS Control Used: ALCO.G 275.S 379.G 165.HAMMOND CORS ARP
KLAC-02-06	Livingston	Water Line	duct tape - front door step	Good	Coastal - Surge Only	good	3.1	30.262079	-90.6462	NGS Control Used: ALCO.G 275.S 379.G 165.HAMMOND CORS ARP
KLAC-02-07	Livingston	Water Line	fence - survey ground - vertical offset	Fair	Coastal - Surge Only	good	2.8	30.261999	-90.64758	NGS Control Used: ALCO.G 275.S 379.G 165.HAMMOND CORS ARP
KLAC-02-08	Livingston	Personal Account	ground	Fair	Coastal - Surge Only	fair	3.3	30.263901	-90.62395	NGS Control Used: ALCO.G 275.S 379.G 165.HAMMOND CORS ARP
KLAC-02-09	Livingston	Personal Account	ground	Fair	Coastal - Surge Only	good	5.4	30.310067	-90.60236	NGS Control Used: ALCO.G 275.S 379.G 165.HAMMOND CORS ARP
KLAC-02-16		Orleans				unknown	10.7(NAVD88)	30.02316	-90.113	NGS Control Used: B 369.L 278.S 188.ALCO.WASTE WELL RESET 2
KLAC-02-17		Orleans				unknown	14.5(NAVD88)	30.02672	-90.108	NGS Control Used: B 369.L 278.S 188.ALCO.WASTE WELL RESET 2
KLAC-02-18		Orleans				unknown	12.9(NAVD88)	30.02725	-90.098	NGS Control Used: B 369.L 278.S 188.ALCO.WASTE WELL RESET 2
KLAC-02-22		Orleans				unknown	12.6(NAVD88)	30.02786	-90.089	NGS Control Used: B 369.L 278.S 188.ALCO.WASTE WELL RESET 2
KLAC-02-35	Jefferson	Water Line	Interior garage wall - transferred to exterior	Good	Coastal - Surge Only	excellent	5.8	29.265225	-89.95735	NGS Control Used: B 369.L 278.S 188.ALCO.WASTE WELL RESET 2

HWM_ID	County	Type of HWM	HWM Object	HWM Quality	Flood Type	Reliability of mark	Elev NAVD88 2004.65 (corrected)	Survey Latitude	Survey Longitude	Survey Comments
KLAC-02-36	Jefferson	Water Line	Bottom level glass doors (front of house)	Good	Coastal - Surge Only	good	8.5	29.241738	-89.97881	NGS Control Used: H 359.Q 359.876 1724 TIDAL 11
KLAC-03-01	Jefferson	Water Line	Water line from inside wall transferred to outside wall	Good	Coastal - Surge Only	excellent	8.9	29.211475	-90.05154	NGS Control Used: H 359.Q 359.876 1724 TIDAL 11
KLAC-03-02	LaFourche	Water Line	On door jamb of outside bathroom under carport	Good	Coastal - Surge Only	fair	7.5	29.156245	-90.18039	NGS Control Used: H 359.Q 359.876 1724 TIDAL 11
KLAC-03-03	Tangipahoa	Water Line	Outside Building Wall	Good	Coastal - Surge Only	fair	6	30.404156	-90.32338	NGS Control Used: H 359.Q 359.876 1724 TIDAL 11
KLAC-03-04	Tangipahoa	Water Line	On the dock palen (Boat Dock)	Good	Coastal - Surge Only	poor	5.6	30.405803	-90.26204	NGS Control Used: H 359.Q 359.876 1724 TIDAL 11
KLAC-03-05	Tangipahoa	Water Line	Middendorf Restaurant (brown building) mark on back of building (watermark)	Good	Coastal - Surge Only	poor	3.5	30.290135	-90.40138	NGS Control Used: H 359.Q 359.876 1724 TIDAL 11
KLAC-03-06	St. John the Baptist	Personal Account	Post on Lakeside seafood. South side of bar door (Beacon Lounge)	Fair	Coastal - Wave Height	fair	6	30.281138	-90.39997	NGS Control Used: ALCO.A 193.STENNIS CORS ARP.COVINGTON CORS ARP.HAMMOND CORS MON
KLAC-03-07	St. John the Baptist	Water Line	guardrail on West side of interchange	Fair	Coastal - Surge Only	poor	2.8	30.194538	-90.43598	NGS Control Used: ALCO.G 275.S 379.G 165.HAMMOND CORS ARP
KLAC-03-09	St. John the Baptist	Water Line	exterior wall of house	Good	Coastal - Surge Only	poor	3.9	30.101686	-90.42541	NGS Control Used: ALCO.G 275.S 379.G 165.HAMMOND CORS ARP
KLAC-03-10	St. John the Baptist	Debris Line	pipe line mark/stake - stake taped to pipeline mark	Fair	Coastal - Surge Only	poor	5.7	30.101597	-90.42488	NGS Control Used: ALCO.G 275.S 379.G 165.HAMMOND CORS ARP
KLAC-03-29	St. Charles	Wrack Line	On ground debris on embankment	Good	Coastal - Surge Only	poor	6.4	30.055665	-90.3718	NGS Control Used: ALCO.G 275.S 379.G 165.HAMMOND CORS ARP



HWM_ID	County	Type of HWM	HWM Object	HWM Quality	Flood Type	Reliability of mark	Elev NAVD88 2004.65 (corrected)	Survey Latitude	Survey Longitude	Survey Comments
KLAC-03-30	St. Charles	Wrack Line	Wrack line on fence-personal account from head maint. Supervisor Jeff Parish	Good	Coastal - Surge Only	good	5.5	29.999022	-90.28475	NGS Control Used: B 369.L 278.S 188.ALCO.WASTE WELL RESET 2
KLAC-03-31	St. Charles	Wrack Line	Railroad track structure	Good	Coastal - Surge Only	poor	9.3	30.072671	-90.39937	NGS Control Used: ALCO.G 275.S 379.G 165.HAMMOND CORS ARP
KLAC-04-01	St. Tammany	Mud Line	On wheel of trailer transferred to stake	Good	Riverine - Hurricane	poor	12.8	30.477691	-90.08724	NGS Control Used: STENNIS.ALCO.NICOLE.G 275.A 193
KLAC-04-02A	St. Tammany	Mud Line	Flood Gage on side of Abita River	Good	Riverine - Hurricane	fair	9.7	30.461502	-90.08175	NGS Control Used: STENNIS.ALCO.NICOLE.G 275.A 193
KLAC-04-03	St. Tammany	Debris Line	Debris line	Good	Riverine - Hurricane	fair	7.7	30.438345	-90.11593	NGS Control Used: STENNIS.ALCO.NICOLE.G 275.A 193
KLAC-04-04	St. Tammany	Personal Account	Exterior SE wall of utility room under raised house transferred to Northwest column of carport	Good	Riverine - Hurricane	good	8.1	30.437713	-90.11628	NGS Control Used: STENNIS.ALCO.NICOLE.G 275.A 193
KLAC-04-05	St. Tammany	Mud Line	on post of homeowner's mailbox	Good	Riverine - Hurricane	poor	6.9	30.398989	-90.15579	NGS Control Used: STENNIS.ALCO.NICOLE.G 275.A 193
KLAC-04-06	St. Tammany	Mud Line	electrical meter panel on east side of Tchefuncte River south of LA 22	Good	Riverine - Hurricane	poor	4.3	30.402995	-90.15373	NGS Control Used: STENNIS.ALCO.NICOLE.G 275.A 193
KLAC-04-07	Jefferson	Water Line	exterior wall @ front door	Good	Levee - Interior	protected	-4.3	30.042867	-90.27493	NGS Control Used: ZURFLUH.B 369.REGGIO 2.ALCO.WASTE WELL RESET 2
KLAC-04-10	Jefferson	Wrack Line	ground (levee)	Good	Coastal - Wave Runup	poor	9.4	30.040061	-90.23809	NGS Control Used: ZURFLUH.B 369.REGGIO 2.ALCO.WASTE WELL RESET 2
KLAC-04-11	Jefferson	Wrack Line		Good	Coastal - Wave Runup	poor	11.6	30.032774	-90.21962	NGS Control Used: ZURFLUH.B 369.REGGIO 2.ALCO.WASTE WELL RESET 2
KLAC-04-13	Jefferson	Wrack Line	Wrack line on levee bank	Good	Levee - Interior	protected	-3.9	29.9948	-90.19442	NGS Control Used: B 369.L 278.S 188.ALCO.WASTE WELL RESET 2

HWM_ID	County	Type of HWM	HWM Object	HWM Quality	Flood Type	Reliability of mark	Elev NAVD88 2004.65 (corrected)	Survey Latitude	Survey Longitude	Survey Comments
KLAC-04-14	Jefferson	Debris Line	School fence transferred to stake (Top of debris equates to level of debris)	Good	Levee - Interior	protected	-3.7	29.984246	-90.19876	NGS Control Used: B 369.L 278.S 188.ALCO.WASTE WELL RESET 2
KLAC-04-15	Jefferson	Mud Line	Visible mud line on wooden fence transferred to power pole on SE corner 5" from bottom rail east face of power pole	Good	Levee - Interior	protected	-3.8	29.99597	-90.21629	NGS Control Used: ALCO.G 275.S 379.G 165.HAMMOND CORS ARP
KLAC-04-18		Orleans				unknown	16.6 (NAVD88)	30.03372	-90.042	NGS Control Used: B 369.L 278.S 188.ALCO.WASTE WELL RESET 2
KLAC-04-33	Jefferson	Wrack Line	Inside of levee	Good	Coastal - Surge Only	poor	8.5	30.049191	-90.27667	NGS Control Used: ZURFLUH.B 369.REGGIO 2.ALCO.WASTE WELL RESET 2
KLAC-04-34	Jefferson	Wrack Line	Levee		Coastal - Surge Only	poor	9.4	30.04081	-90.24307	NGS Control Used: V 375.S 188.ALCO.WASTE WELL RESET 2
KLAC-04-35	Jefferson	Wrack Line		Good	Coastal - Wave Runup	fair	6.8	30.027021	-90.19898	NGS Control Used: ZURFLUH.B 369.REGGIO 2.ALCO.WASTE WELL RESET 2
KLAC-05-01	St. Tammany	Water Line	Exterior condo wall on siding	Good	Coastal - Surge Only	good	13.2	30.219233	-89.81995	NGS Control Used: STENNIS.ALCO.NICOLE.G 275.A 193
KLAC-05-03	St. Tammany	Water Line	exterior wall line	Good	Riverine - Hurricane	fair	11.2	30.278714	-89.83856	NGS Control Used: STENNIS.ALCO.NICOLE.G 275.A 193
KLAC-05-04	St. Tammany	Water Line	inside window blind transferred to exterior wall	Good	Riverine - Hurricane	excellent	11	30.27216	-89.79514	NGS Control Used: STENNIS.ALCO.NICOLE.G 275.A 193
KLAC-05-05	St. Tammany	Water Line	Front Porch Wall SE Corner	Good	Riverine - Hurricane	good	10.5	30.272963	-89.79474	NGS Control Used: STENNIS.ALCO.NICOLE.G 275.A 193
KLAC-05-06	St. Tammany	Water Line	Exterior Wall of house (door jam) transferred from inside wall of house	Good	Riverine - Hurricane	excellent	11.4	30.263776	-89.79352	NGS Control Used: STENNIS.ALCO.NICOLE.G 275.A 193
KLAC-05-07	St. Tammany	Water Line	Interior wall transferred to exterior wall	Good	Coastal - Surge Only	excellent	15.3	30.195716	-89.75619	NGS Control Used: A 193.ALCO

HWM_ID	County	Type of HWM	HWM Object	HWM Quality	Flood Type	Reliability of mark	Elev NAVD88 2004.65 (corrected)	Survey Latitude	Survey Longitude	Survey Comments
KLAC-05-09	St. Tammany	Water Line	interior wall transferred to front right of door jam	Good	Coastal - Surge Only	excellent	16	30.203851	-89.69958	NGS Control Used: A 193.ALCO
KLAC-05-10	Jefferson	Wrack Line	ground	Good	tbd	protected	0.4	29.884566	-90.09947	NGS Control Used: ZURFLUH.B 369.REGGIO 2.ALCO.WASTE WELL RESET 2
KLAC-05-11	Jefferson	Wrack Line	ground	Good	tbd	protected	0.9	29.875315	-90.1099	NGS Control Used: ZURFLUH.B 369.REGGIO 2.ALCO.WASTE WELL RESET 2
KLAC-05-12	Jefferson	Wrack Line	ground	Good	tbd	protected	0.4	29.854456	-90.11716	NGS Control Used: ZURFLUH.B 369.REGGIO 2.ALCO.WASTE WELL RESET 2
KLAC-05-14	Jefferson	Wrack Line	Bank of canal-East side	Good	tbd	protected	-4.3	29.894341	-90.0145	NGS Control Used: ZURFLUH.B 369.REGGIO 2.ALCO.WASTE WELL RESET 2
KLAC-05-15	Jefferson	Water Line	Exterior wall between garage doors.	Good	tbd	protected	-3.7	29.906414	-90.02241	NGS Control Used: ZURFLUH.B 369.REGGIO 2.ALCO.WASTE WELL RESET 2
KLAC-05-16	Jefferson	Wrack Line	West bank of canal	Good	tbd	protected	-5.7	29.879582	-90.0343	NGS Control Used: ZURFLUH.B 369.REGGIO 2.ALCO.WASTE WELL RESET 2
KLAC-05-17	Plaquemines	Water Line	Exterior garage wall	Good	tbd	poor	2.9	29.74339	-90.0245	NGS Control Used: REGGIO 2.C 195.R 194.B 369.A 152.MILAN 2
KLAC-05-18	Plaquemines	Wrack Line	6 feet up from HWM on concrete revetment on riverside of levee	Fair	tbd	poor	16.3	29.81729	-90.00688	NGS Control Used: ZURFLUH.B 369.REGGIO 2.ALCO.WASTE WELL RESET 2
KLAC-05-30		Orleans				unknown	15.3 (NAVD88)	30.03142	-90.039	NGS Control Used: B 369.L 278.S 188.ALCO.WASTE WELL RESET 2
KLAC-05-43	St. Tammany	Water Line	Exterior wall of garage	Good	Coastal - Surge Only	good	7.8	30.389975	-90.20524	NGS Control Used: STENNIS.ALCO.NICOLE.G 275.A 193
KLAC-06-01	St. Tammany	Water Line	interior garage wall transferred to exterior wall	Good	Coastal - Surge Only	excellent	12.8	30.22262	-89.81597	NGS Control Used: STENNIS.ALCO.NICOLE.G 275.A 193
KLAC-06-02	St. Tammany	Wrack Line	ground	Good	Riverine - Hurricane	poor	17.1	30.325798	-89.8379	NGS Control Used: STENNIS.ALCO.NICOLE.G 275.A 193
KLAC-06-03	St. Tammany	Wrack Line	ground, bank of stream	Fair	Riverine - Hurricane	poor	12.6	30.309997	-89.77983	NGS Control Used: STENNIS.ALCO.NICOLE.G 275.A 193



HWM_ID	County	Type of HWM	HWM Object	HWM Quality	Flood Type	Reliability of mark	Elev NAVD88 2004.65 (corrected)	Survey Latitude	Survey Longitude	Survey Comments
KLAC-06-04	St. Tammany	Water Line	exterior wall	Good	Riverine - Hurricane	fair	12.1	30.285462	-89.72844	NGS Control Used: STENNIS.ALCO.NICOLE.G 275.A 193
KLAC-06-05	St. Tammany	Water Line	foundation pile of I-59 bridge	Good	Riverine - Hurricane	good	15.2	30.38148	-89.73736	NGS Control Used: STENNIS.ALCO.NICOLE.G 275.A 193
KLAC-06-06	St. Tammany	Water Line	red paint on light pole	Fair	Riverine - Hurricane	good	15.2	30.384245	-89.73483	NGS Control Used: STENNIS.ALCO.NICOLE.G 275.A 193
KLAC-06-08	St. Tammany	Wrack Line	ground (embankment of I-10 overpass)	Good	Riverine - Hurricane	poor	12.4	30.247756	-89.76381	NGS Control Used: STENNIS.ALCO.NICOLE.G 275.A 193
KLAC-06-09	St. Tammany	Wrack Line	ground	Good	Riverine - Hurricane	poor	13.4	30.290653	-89.76771	NGS Control Used: STENNIS.ALCO.NICOLE.G 275.A 193
KLAC-06-10	Jefferson	Wrack Line	red paint on levee	Good	Riverine - Hurricane	poor	17.9	29.965889	-90.25818	NGS Control Used: E 191.S 379.S 188.HAMMOND CORS ARP
KLAC-06-11	Jefferson	Wrack Line	red paint on roadway over levee	Good	Riverine - Hurricane	poor	17.9	29.917806	-90.14178	NGS Control Used: V 375.S 188.ALCO.WASTE WELL RESET 2
KLAC-06-13	Jefferson	Wrack Line	ground	Good	tbd	protected	-3.6	29.897037	-90.20696	NGS Control Used: ZURFLUH.B 369.REGGIO 2.ALCO.WASTE WELL RESET 2
KLAC-06-14	Plaquemines	Wrack Line	Levee	Good	tbd	poor	13.2	29.480648	-89.69368	NGS Control Used: REGGIO 2.C 195.R 194.B 369.A 152.MILAN 2
KLAC-06-15	Plaquemines	Wrack Line	Levee	Good	tbd	poor	11.9	29.524854	-89.73995	NGS Control Used: REGGIO 2.C 195.R 194.B 369.A 152.MILAN 2
KLAC-06-17	Plaquemines	Wrack Line	Levee	Good	tbd	poor	3.2	29.638149	-89.94847	NGS Control Used: REGGIO 2.C 195.R 194.B 369.A 152.MILAN 2
KLAC-06-18	Plaquemines	Wrack Line	Levee	Good	tbd	poor	17	29.697418	-89.98234	NGS Control Used: REGGIO 2.C 195.R 194.B 369.A 152.MILAN 2
KLAC-06-19	Plaquemines	Water Line	Exterior wall facing Hwy 23 (door jam)	Good	tbd	good	5.4	29.747804	-90.02397	NGS Control Used: REGGIO 2.C 195.R 194.B 369.A 152.MILAN 2
KLAC-06-20	Plaquemines	Wrack Line	Levee	Good	tbd	poor	12.5	29.540295	-89.75253	NGS Control Used: REGGIO 2.C 195.R 194.B 369.A 152.MILAN 2
KLAC-06-21	Plaquemines	Wrack Line	Levee	Good	tbd	poor	12	29.585034	-89.80633	NGS Control Used: REGGIO 2.C 195.R 194.B 369.A 152.MILAN 2
KLAC-06-22	Plaquemines	Wrack Line	Levee	Good	tbd	poor	13.7	29.615051	-89.88299	NGS Control Used: REGGIO 2.C 195.R 194.B 369.A 152.MILAN 2
KLAC-06-23	Plaquemines	Wrack Line	Levee	Good	tbd	poor	16.1	29.647733	-89.94561	NGS Control Used: REGGIO 2.C 195.R 194.B 369.A 152.MILAN 2
KLAC-06-24	Plaquemines	Mud Line	Levee	Good	tbd	poor	4.3	29.718877	-89.98194	NGS Control Used: REGGIO 2.C 195.R 194.B 369.A 152.MILAN 2

HWM_ID	County	Type of HWM	HWM Object	HWM Quality	Flood Type	Reliability of mark	Elev NAVD88 2004.65 (corrected)	Survey Latitude	Survey Longitude	Survey Comments
KLAC-06-27		Orleans				unknown	12 (NAVD88)	30.03688	-90.015	NGS Control Used: ZURFLUH.B 369.REGGIO 2.ALCO.WASTE WELL RESET 2
KLAC-07-01	Livingston	Personal Account	Pre-existing stake marked per personal account	Good	Riverine - Hurricane	poor	4	30.271941	-90.75152	NGS Control Used: E 191.S 379.S 188.HAMMOND CORS ARP
KLAC-07-02	St. Tammany	Other	Exterior wall	Good	Coastal - Surge Only	poor	8.8	30.351446	-90.05033	NGS Control Used: A 193.ALCO
KLAC-07-03	St. Tammany	Mud Line	Exterior wall - front door of house	Good	Coastal - Surge Only	fair	9.2	30.354669	-90.06762	NGS Control Used: ALCO.STENNIS CORS ARP.HAMMOND CORS MON
KLAC-07-04	St. Tammany	Mud Line	Exterior door	Good	Coastal - Surge Only	fair	9.3	30.35969	-90.07084	NGS Control Used: ALCO.STENNIS CORS ARP.HAMMOND CORS MON
KLAC-07-05	St. Tammany	Mud Line	Mud line on garage door	Good	Coastal - Surge Only	fair	9.1	30.362328	-90.0798	NGS Control Used: ALCO.STENNIS CORS ARP.HAMMOND CORS MON
KLAC-07-07	St. Tammany	Wrack Line	On ground	Good	Coastal - Wave Runup	poor	6.6	30.364935	-90.09184	NGS Control Used: ALCO.STENNIS CORS ARP.HAMMOND CORS MON
KLAC-07-08	St. Tammany	Mud Line	Exterior wall	Good	Coastal - Surge Only	fair	9.2	30.363178	-90.07756	NGS Control Used: ALCO.STENNIS CORS ARP.HAMMOND CORS MON
KLAC-07-09	St. Tammany	Personal Account	Exterior front steps	Fair	Coastal - Surge Only	good	10.3	30.357811	-90.06549	NGS Control Used: ALCO.STENNIS CORS ARP.HAMMOND CORS MON
KLAC-07-10	St. Tammany	Mud Line	Exterior wall of shed in back	Good	Coastal - Surge Only	fair	8.4	30.371039	-90.10491	NGS Control Used: A 193.ALCO
KLAC-07-11	St. Tammany	Mud Line	Exterior brick piling	Good	Coastal - Surge Only	poor	7.8	30.396049	-90.1217	NGS Control Used: A 193.ALCO
KLAC-07-12	St. Tammany	Wrack Line	Stake-debris line in backyard	Good	Riverine - Hurricane	fair	7.8	30.419672	-90.10429	NGS Control Used: A 193.ALCO
KLAC-07-13	St. Tammany	Mud Line	Exterior Wall	Good	Coastal - Surge Only	poor	9	30.425247	-90.08152	NGS Control Used: A 193.ALCO
KLAC-07-14	Jefferson	Mud Line	Exterior column by front door	Good	Levee - Interior	protected	-3.4	30.02291	-90.18743	NGS Control Used: ZURFLUH.B 369.REGGIO 2.ALCO.WASTE WELL RESET 2

HWM_ID	County	Type of HWM	HWM Object	HWM Quality	Flood Type	Reliability of mark	Elev NAVD88 2004.65 (corrected)	Survey Latitude	Survey Longitude	Survey Comments
KLAC-07-15	Jefferson	Mud Line	Exterior garage door on left	Good	Levee - Interior	protected	-3.5	30.020022	-90.1743	NGS Control Used: ZURFLUH.B 369.REGGIO 2.ALCO.WASTE WELL RESET 2
KLAC-07-16	Jefferson	Mud Line	Exterior wall - Northern frame of garage door.	Good	Levee - Interior	protected	-3.6	30.018831	-90.15917	NGS Control Used: ZURFLUH.B 369.REGGIO 2.ALCO.WASTE WELL RESET 2
KLAC-07-18	Jefferson	Mud Line	Exterior wall - frame of garage door	Good	Levee - Interior	protected	2.4	29.983684	-90.14265	NGS Control Used: ZURFLUH.B 369.REGGIO 2.ALCO.WASTE WELL RESET 2
KLAC-07-19	Jefferson	Mud Line	Exterior wall - cement around door - front of house	Good	Levee - Interior	protected	2.5	29.976499	-90.14049	NGS Control Used: ZURFLUH.B 369.REGGIO 2.ALCO.WASTE WELL RESET 2
KLAC-07-20	Jefferson	Mud Line	Exterior wall - front right column of house (facing house)	Good	Levee - Interior	protected	2.6	29.976465	-90.12681	NGS Control Used: ZURFLUH.B 369.REGGIO 2.ALCO.WASTE WELL RESET 2
KLAC-07-21	Jefferson	Mud Line	Exterior column of fence	Good	Levee - Interior	protected	-3.2	30.012813	-90.12372	NGS Control Used: ZURFLUH.B 369.REGGIO 2.ALCO.WASTE WELL RESET 2
KLAC-07-23	Jefferson	Mud Line	Exterior - front door.	Good	Levee - Interior	protected	-3.3	30.016298	-90.14337	NGS Control Used: ZURFLUH.B 369.REGGIO 2.ALCO.WASTE WELL RESET 2
KLAC-07-24	Jefferson	Mud Line	Exterior wall	Good	Levee - Interior	protected	-3.1	30.011497	-90.13486	NGS Control Used: ZURFLUH.B 369.REGGIO 2.ALCO.WASTE WELL RESET 2
KLAC-07-25	Jefferson	Mud Line	Exterior - Frame of front door	Good	Levee - Interior	protected	-3.3	30.014168	-90.16827	NGS Control Used: ZURFLUH.B 369.REGGIO 2.ALCO.WASTE WELL RESET 2
KLAC-07-28	Jefferson	Mud Line	Exterior - garage door	Good	Levee - Interior	protected	-3.8	30.014035	-90.18593	NGS Control Used: ZURFLUH.B 369.REGGIO 2.ALCO.WASTE WELL RESET 2
KLAC-07-29	Jefferson	Mud Line	Exterior - Cement front step	Good	Levee - Interior	protected	-3.6	29.989979	-90.16455	NGS Control Used: B 369.L 278.S 188.ALCO.WASTE WELL RESET 2
KLAC-07-30	Jefferson	Mud Line	Exterior - wooden frame of front door	Good	Levee - Interior	protected	-3.4	29.992	-90.15776	NGS Control Used: B 369.L 278.S 188.ALCO.WASTE WELL RESET 2
KLAC-07-31	Jefferson	Mud Line	Frame of front door	Good	Levee - Interior	protected	1.5	29.960933	-90.21074	NGS Control Used: B 369.L 278.S 188.ALCO.WASTE WELL RESET 2
KLAC-07-32	Jefferson	Mud Line	Brick exterior	Fair	Levee - Interior	protected	4.3	29.956418	-90.21918	NGS Control Used: B 369.L 278.S 188.ALCO.WASTE WELL RESET 2



HWM_ID	County	Type of HWM	HWM Object	HWM Quality	Flood Type	Reliability of mark	Elev NAVD88 2004.65 (corrected)	Survey Latitude	Survey Longitude	Survey Comments
KLAC-08-01	Jefferson	Personal Account	Interior Wall transferred to Exterior	Good	Coastal - Surge Only	good	8.6	29.208757	-90.03385	NGS Control Used: H 359.Q 359.876 1724 TIDAL 11
KLAC-08-02	LaFourche	Personal Account	Porch Bottom, left side if facing restaurant	Good	Coastal - Surge Only	good	4.1	29.257687	-90.21436	NGS Control Used: H 359.Q 359.876 1724 TIDAL 11
KLAC-08-06	Plaquemines	Water Line	Coastal Hurricane Protection Levee	Good	tbd	poor	1.4	29.474219	-89.69721	NGS Control Used: REGGIO 2.C 195.R 194.B 369.A 152.MILAN 2
KLAC-08-08	Plaquemines	Wrack Line	Wrack/debris line on Coastal Hurricane Protection Levee	Good	tbd	poor	7.1	29.522635	-89.741	NGS Control Used: REGGIO 2.C 195.R 194.B 369.A 152.MILAN 2
KLAC-08-09	Plaquemines	Water Line	Stake in levee	Good	tbd	poor	3	29.543527	-89.77808	NGS Control Used: REGGIO 2.C 195.R 194.B 369.A 152.MILAN 2
KLAC-08-10	Plaquemines	Mud Line	Exterior wall front corner of building;	Good	tbd	poor	8.3	29.518947	-89.73203	NGS Control Used: REGGIO 2.C 195.R 194.B 369.A 152.MILAN 2
KLAC-08-11	Plaquemines	Wrack Line	Stake at wrack line on marsh side of Coastal Hurricane Protection Levee	Good	tbd	poor	5.9	29.527769	-89.76299	NGS Control Used: REGGIO 2.C 195.R 194.B 369.A 152.MILAN 2
KLAC-08-12	Plaquemines	Wrack Line	Stake in ground at wrack line on marsh side of Coastal Hurricane Protection Levee	Good	tbd	poor	5.8	29.54315	-89.77909	NGS Control Used: REGGIO 2.C 195.R 194.B 369.A 152.MILAN 2
KLAC-08-13	Plaquemines	Water Line	Stake in ground marking water line on marsh side of levee	Good	tbd	poor	0.4	29.625983	-89.9497	NGS Control Used: REGGIO 2.C 195.R 194.B 369.A 152.MILAN 2
KLAC-08-14	Plaquemines	Wrack Line	Stake in ground at wrack line on Estate side of levee	Good	tbd	poor	4.2	29.625942	-89.95043	NGS Control Used: REGGIO 2.C 195.R 194.B 369.A 152.MILAN 2
KLAC-08-16	Plaquemines	Wrack Line	Stake with yellow tape at wrack line in coastal hurricane protection levee.	Good	tbd	poor	13.6	29.624711	-89.87833	NGS Control Used: REGGIO 2.C 195.R 194.B 369.A 152.MILAN 2
KLAC-08-17	Plaquemines	Water Line	Water mark on levee	Good	tbd	poor	8.9	29.648495	-89.94456	NGS Control Used: REGGIO 2.C 195.R 194.B 369.A 152.MILAN 2
KLAC-08-18	Plaquemines	Wrack Line	Wrack line on levee	Good	tbd	poor	16.2	29.648567	-89.94467	NGS Control Used: REGGIO 2.C 195.R 194.B 369.A 152.MILAN 2

HWM_ID	County	Type of HWM	HWM Object	HWM Quality	Flood Type	Reliability of mark	Elev NAVD88 2004.65 (corrected)	Survey Latitude	Survey Longitude	Survey Comments
KLAC-20-01	St. Charles	Wrack Line	ground	Good	Riverine - Hurricane	fair	13.5	29.979332	-90.40267	NGS Control Used: E 191.S 379.S 188.HAMMOND CORS ARP
KLAC-20-02	St. John the Baptist	Wrack Line	ground	Good	Riverine - Hurricane	poor	12.9	30.044764	-90.54956	NGS Control Used: E 191.S 379.S 188.HAMMOND CORS ARP
KLAC-20-03	St. James	Wrack Line	ground		Riverine - Hurricane	poor	13.6	30.028047	-90.6942	NGS Control Used: E 191.S 379.S 188.HAMMOND CORS ARP
KLAC-88-01		St. Bernard				unknown	12 (NAVD88)	29.86042	-89.913	NGS Control Used: E 191.S 379.S 188.HAMMOND CORS ARP
KLAC-88-02		St. Bernard				unknown	17.1 (NAVD88)	29.84059	-89.758	NGS Control Used: V 375.REGGIO 2.WASTE WELL RESET 2
KLAC-88-04	Jefferson	Water Line	Still water mark inside of restroom.			good	6.6	30.040939	-90.23858	NGS Control Used: V 375.S 188.ALCO.WASTE WELL RESET 2
KLAC-88-05		Jefferson/Orleans				unknown	10.9 (NAVD88)	30.02101	-90.123	NGS Control Used: V 375.S 188.ALCO.WASTE WELL RESET 2
KLAC-88-06		Orleans				unknown	11.8 (NAVD88)	30.02978	-90.091	NGS Control Used: V 375.S 188.ALCO.WASTE WELL RESET 2
KLAC-88-07		Orleans				unknown	11.8 (NAVD88)	30.0338	-90.04	NGS Control Used: V 375.S 188.ALCO.WASTE WELL RESET 2
KLAC-88-08		Orleans				unknown	13.8 (NAVD88)	30.05768	-89.969	NGS Control Used: V 375.S 188.ALCO.WASTE WELL RESET 2
KLAC-88-09		Orleans				unknown	13.8 (NAVD88)	30.05772	-89.969	NGS Control Used: V 375.S 188.ALCO.WASTE WELL RESET 2
KLAC-88-10		Orleans				unknown	13.7 (NAVD88)	30.05776	-89.969	NGS Control Used: V 375.S 188.ALCO.WASTE WELL RESET 2
KLAC-88-11		Orleans				unknown	13.5 (NAVD88)	30.05778	-89.969	NGS Control Used: V 375.S 188.ALCO.WASTE WELL RESET 2
KLAC-88-12		Orleans				unknown	12.7 (NAVD88)	30.05783	-89.969	NGS Control Used: V 375.S 188.ALCO.WASTE WELL RESET 2
KLAC-88-13		Orleans				unknown	12.7 (NAVD88)	30.05786	-89.969	NGS Control Used: V 375.S 188.ALCO.WASTE WELL RESET 2
KLAC-88-14		Orleans				unknown	13.1 (NAVD88)	30.05791	-89.969	NGS Control Used: V 375.S 188.ALCO.WASTE WELL RESET 2
KLAC-88-15		Orleans				unknown	13 (NAVD88)	30.05793	-89.969	NGS Control Used: V 375.S 188.ALCO.WASTE WELL RESET 2
KLAC-88-16		Orleans				unknown	13.2 (NAVD88)	30.05797	-89.968	NGS Control Used: V 375.S 188.ALCO.WASTE WELL RESET 2
KLAC-88-17		Orleans				unknown	13.6 (NAVD88)	30.05801	-89.968	NGS Control Used: V 375.S 188.ALCO.WASTE WELL RESET 2
KLAC-88-18		Orleans				unknown	13.8 (NAVD88)	30.05805	-89.968	NGS Control Used: V 375.S 188.ALCO.WASTE WELL RESET 2

HWM_ID	County	Type of HWM	HWM Object	HWM Quality	Flood Type	Reliability of mark	Elev NAVD88 2004.65 (corrected)	Survey Latitude	Survey Longitude	Survey Comments
KLAC-88-20		Orleans				unknown	11.4 (NAVD88)	30.03679	-90.017	NGS Control Used: V 375.S 188.ALCO.WASTE WELL RESET 2
KLAC-99-01		Orleans				unknown	11.7 (NAVD88)	30.04179	-90.023	NGS Control Used: B 369.L 278.S 188.ALCO.WASTE WELL RESET 2
KLA-USGS-01	St. Tammany	Debris Line	Front of house	Fair		fair	7.9	30.399072	-90.1571	NGS Control Used: ALCO.STENNIS CORS ARP.HAMMOND CORS MON
KLA-USGS-03	St. Tammany	Debris Line	Door	Good		fair	7.5	30.404488	-90.15816	NGS Control Used: ALCO.STENNIS CORS ARP.HAMMOND CORS MON
KLA-USGS-04	St. Tammany	Debris Line	Glass door	Good		good	7.6	30.410498	-90.16853	NGS Control Used: ALCO.STENNIS CORS ARP.HAMMOND CORS MON
KLA-USGS-05	St. Tammany	Debris Line	House exterior	Good		fair	7.5	30.409486	-90.16215	NGS Control Used: ALCO.STENNIS CORS ARP.HAMMOND CORS MON
KLA-USGS-06	St. Tammany	Scum and Debris Line	Piling	Good		fair	7.6	30.413102	-90.15987	NGS Control Used: ALCO.STENNIS CORS ARP.HAMMOND CORS MON
KLA-USGS-07	St. Tammany	Scum and Debris Line		Good		fair	7.7	30.406241	-90.15531	NGS Control Used: ALCO.STENNIS CORS ARP.HAMMOND CORS MON
KLA-USGS-08	St. Tammany	Debris Line	Interior wall transferred to exterior door frame	Good		excellent	7.9	30.400375	-90.15297	NGS Control Used: ALCO.STENNIS CORS ARP.HAMMOND CORS MON
KLA-USGS-09	St. Tammany	Debris Line	Fence	Fair		poor	12.8	30.408792	-90.1401	NGS Control Used: ALCO.STENNIS CORS ARP.HAMMOND CORS MON
KLA-USGS-10	St. Tammany	Debris Line	Fence	Fair		fair	8.6	30.36721	-90.0976	NGS Control Used: ALCO.STENNIS CORS ARP.HAMMOND CORS MON
KLA-USGS-101	Plaquemines	Debris Line		Excellent	tbd	poor	12.8	29.586328	-89.80684	NGS Control Used: V 375.S 188.ALCO.WASTE WELL RESET 2
KLA-USGS-102	Plaquemines	Seed Line		Good	tbd	poor	13.1	29.586142	-89.80753	NGS Control Used: V 375.S 188.ALCO.WASTE WELL RESET 2
KLA-USGS-103	Plaquemines	Debris Line	Concrete levee wall	Good	tbd	poor	13.4	29.583721	-89.79296	NGS Control Used: REGGIO 2.C 195.R 194.B 369.A 152.MILAN 2



HWM_ID	County	Type of HWM	HWM Object	HWM Quality	Flood Type	Reliability of mark	Elev NAVD88 2004.65 (corrected)	Survey Latitude	Survey Longitude	Survey Comments
KLA-USGS-105	Plaquemines	Seed Line		Good	tbd	poor	13.2	29.64296	-89.93042	NGS Control Used: REGGIO 2.C 195.R 194.B 369.A 152.MILAN 2
KLA-USGS-106	Plaquemines	Seed Line	Exterior wall	Good	tbd	poor	7.2	29.858856	-89.91498	NGS Control Used: V 375.REGGIO 2.WASTE WELL RESET 2
KLA-USGS-107	Plaquemines	Seed Line		Good	tbd	poor	7	29.85877	-89.91498	NGS Control Used: V 375.REGGIO 2.WASTE WELL RESET 2
KLA-USGS-109	Terrebonne	Debris Line		Good		poor	6.3	29.38475	-90.73036	NGS Control Used: S 233.G 233
KLA-USGS-11	St. Tammany	Debris Line		Good		fair	7.9	30.415975	-90.13586	NGS Control Used: ALCO.STENNIS CORS ARP.HAMMOND CORS MON
KLA-USGS-12	St. Tammany	Debris Line	Garage door	Good		fair	8.1	30.402588	-90.131	NGS Control Used: ALCO.STENNIS CORS ARP.HAMMOND CORS MON
KLA-USGS-13	St. Tammany	Debris Line	Frame of garage door	Not Provided By USGS		fair	8.8	30.369432	-90.10732	NGS Control Used: ALCO.STENNIS CORS ARP.HAMMOND CORS MON
KLA-USGS-14	St. Tammany			Good		poor	8.8	30.36671	-90.11085	NGS Control Used: ALCO.STENNIS CORS ARP.HAMMOND CORS MON
KLA-USGS-15	St. Tammany	Debris Line	Exterior concrete wall	Good		fair	8.7	30.36488	-90.08302	NGS Control Used: ALCO.STENNIS CORS ARP.HAMMOND CORS MON
KLA-USGS-16	St. Tammany	Debris Line	House	Excellent		fair	9.3	30.358349	-90.07855	NGS Control Used: ALCO.STENNIS CORS ARP.HAMMOND CORS MON
KLA-USGS-17	St. Tammany	Debris Line		Good		fair	9.1	30.361793	-90.07633	NGS Control Used: ALCO.STENNIS CORS ARP.HAMMOND CORS MON
KLA-USGS-18	St. Tammany	Debris Line		Good		fair	9.1	30.352383	-90.05769	NGS Control Used: A 193.ALCO
KLA-USGS-19	St. Tammany	Debris Line		Not Provided By USGS		fair	9.4	30.350002	-90.0601	NGS Control Used: A 193.ALCO

HWM_ID	County	Type of HWM	HWM Object	HWM Quality	Flood Type	Reliability of mark	Elev NAVD88 2004.65 (corrected)	Survey Latitude	Survey Longitude	Survey Comments
KLA-USGS-20	St. Tammany	Debris Line	Exterior wall	Good		fair	10	30.339285	-90.03978	NGS Control Used: A 193.ALCO
KLA-USGS-21	St. Tammany	Debris Line	Interior wall	Good		excellent	8.4	30.335535	-90.04498	NGS Control Used: A 193.ALCO
KLA-USGS-22	St. Tammany	Debris Line		Good		poor	9.5	30.329096	-90.00401	NGS Control Used: A 193.ALCO
KLA-USGS-23	St. Tammany			Not Provided By USGS		poor	9.6	30.300184	-89.9573	NGS Control Used: A 193.ALCO
KLA-USGS-24	St. Tammany	Debris Line	Door frame	Good		poor	6	30.302465	-89.92252	NGS Control Used: A 193.ALCO
KLA-USGS-25	St. Tammany	Debris Line		Good		poor	2.9	30.284085	-89.91699	NGS Control Used: A 193.ALCO
KLA-USGS-26	St. Tammany	Debris Line	Exterior window frame	Good		fair	11.7	30.273698	-89.85962	NGS Control Used: A 193.ALCO
KLA-USGS-27	St. Tammany	Debris Line	Fence	Not Provided By USGS		poor	8	30.280911	-89.86094	NGS Control Used: A 193.ALCO
KLA-USGS-28	Livingston	Seed Line	Bridge piles	Good		fair	3.9	30.307745	-90.60859	NGS Control Used: ALCO.G 275.S 379.G 165.HAMMOND CORS ARP
KLA-USGS-29	Livingston	Seed Line		Good		fair	5.7	30.37286	-90.55118	NGS Control Used: ALCO.G 275.S 379.G 165.HAMMOND CORS ARP
KLA-USGS-30	Livingston	Mud Line	Bridge piles	Poor		poor	6.8	30.43138	-90.54706	NGS Control Used: ALCO.G 275.S 379.G 165.HAMMOND CORS ARP
KLA-USGS-31	Tangipahoa	Seed Line		Fair		poor	5	30.404156	-90.32338	NGS Control Used: STENNIS.ALCO.NICOLE.G 275.A 193
KLA-USGS-32	St. Tammany		Steel bridge support	Not Provided By USGS		fair	11	30.271359	-89.79349	NGS Control Used: ALCO.STENNIS CORS ARP.HAMMOND CORS MON

HWM_ID	County	Type of HWM	HWM Object	HWM Quality	Flood Type	Reliability of mark	Elev NAVD88 2004.65 (corrected)	Survey Latitude	Survey Longitude	Survey Comments
KLA-USGS-33	St. Tammany	Seed Line		Excellent		fair	10.5	30.270442	-89.78379	NGS Control Used: STENNIS.ALCO.NICOLE.G 275.A 193
KLA-USGS-34	St. Tammany			Not Provided By USGS		poor	11.3	30.248595	-89.79394	NGS Control Used: STENNIS.ALCO.NICOLE.G 275.A 193
KLA-USGS-35	St. Tammany	Seed Line	Interior wall	Good		excellent	13.4	30.229114	-89.80674	NGS Control Used: STENNIS.ALCO.NICOLE.G 275.A 193
KLA-USGS-36	St. Tammany			Fair		fair	11.3	30.277091	-89.80732	NGS Control Used: ALCO.STENNIS CORS ARP.HAMMOND CORS MON
KLA-USGS-37	St. Tammany		Interior wall	Good		excellent	12.2	30.265562	-89.84415	NGS Control Used: STENNIS.ALCO.NICOLE.G 275.A 193
KLA-USGS-38	St. Tammany		Interior wall	Good		poor	10	30.226541	-89.67755	NGS Control Used: STENNIS.ALCO.NICOLE.G 275.A 193
KLA-USGS-39	St. Tammany			Not Provided By USGS		fair	15.2	30.230726	-89.71151	NGS Control Used: STENNIS.ALCO.NICOLE.G 275.A 193
KLA-USGS-40	St. Tammany		Stud	Good		good	16	30.231136	-89.66929	NGS Control Used: STENNIS.ALCO.NICOLE.G 275.A 193
KLA-USGS-41	Mississippi	Debris Line	Bridge support	Very Poor		good	21.9	30.239215	-89.61394	NGS Control Used: STENNIS.ALCO.NICOLE.G 275.A 193
KLA-USGS-42	St John the Baptist		Interior wall	Not Provided By USGS		excellent	16.8	30.157315	-89.73773	NGS Control Used: STENNIS.ALCO.NICOLE.G 275.A 193
KLA-USGS-43	Tangipahoa		Post	Not Provided By USGS		poor	3.8	30.28938	-90.40211	NGS Control Used: ALCO.A 193.STENNIS CORS ARP.COVINGTON CORS ARP.HAMMOND CORS MON
KLA-USGS-44	Tangipahoa		Post	Not Provided By USGS		fair	5	30.289241	-90.40201	NGS Control Used: ALCO.A 193.STENNIS CORS ARP.COVINGTON CORS ARP.HAMMOND CORS MON
KLA-USGS-45	Tangipahoa		Support post	Not Provided By USGS		poor	2.9	30.289675	-90.40132	NGS Control Used: ALCO.A 193.STENNIS CORS ARP.COVINGTON CORS ARP.HAMMOND CORS MON



HWM_ID	County	Type of HWM	HWM Object	HWM Quality	Flood Type	Reliability of mark	Elev NAVD88 2004.65 (corrected)	Survey Latitude	Survey Longitude	Survey Comments
KLA-USGS-46	Tangipahoa		Support post	Not Provided By USGS		poor	2.9	30.289679	-90.40135	NGS Control Used: ALCO.A 193.STENNIS CORS ARP.COVINGTON CORS ARP.HAMMOND CORS MON
KLA-USGS-47	Tangipahoa		PVC pipe	Not Provided By USGS		fair	4	30.293711	-90.40416	NGS Control Used: ALCO.A 193.STENNIS CORS ARP.COVINGTON CORS ARP.HAMMOND CORS MON
KLA-USGS-48	Tangipahoa		Post	Not Provided By USGS		poor	2.4	30.302949	-90.40506	NGS Control Used: ALCO.A 193.STENNIS CORS ARP.COVINGTON CORS ARP.HAMMOND CORS MON
KLA-USGS-49	Tangipahoa		Post	Not Provided By USGS		poor	2.3	30.308865	-90.40469	NGS Control Used: ALCO.A 193.STENNIS CORS ARP.COVINGTON CORS ARP.HAMMOND CORS MON
KLA-USGS-50	St. Tammany		Sign	Not Provided By USGS		poor	6.4	30.396116	-90.1571	NGS Control Used: ALCO.STENNIS CORS ARP.HAMMOND CORS MON
KLA-USGS-51	St. Tammany		2x4	Not Provided By USGS		poor	7.8	30.397819	-90.15604	NGS Control Used: ALCO.STENNIS CORS ARP.HAMMOND CORS MON
KLA-USGS-52	St. Tammany	Scum Line	Signpost	Fair		fair	7.7	30.400775	-90.15696	NGS Control Used: ALCO.STENNIS CORS ARP.HAMMOND CORS MON
KLA-USGS-53	St. Tammany	Seed Line	Support post	Good		poor	6.8	30.401321	-90.15848	NGS Control Used: ALCO.STENNIS CORS ARP.HAMMOND CORS MON
KLA-USGS-54	Tangipahoa	Debris Line	Timber post	Fair		poor	5.1	30.404078	-90.32401	NGS Control Used: ALCO.STENNIS CORS ARP.HAMMOND CORS MON
KLA-USGS-56	St. Tammany	Scum Line		Fair		good	7.6	30.387738	-90.20932	NGS Control Used: STENNIS.ALCO.NICOLE.G 275.A 193
KLA-USGS-57	St. Tammany	Mud Line	Tree	Poor		poor	4.5	30.309137	-89.9297	NGS Control Used: ALCO.STENNIS CORS ARP.HAMMOND CORS MON
KLA-USGS-59	St. Tammany		Garage door frame	Fair		good	9.8	30.286559	-89.9535	NGS Control Used: STENNIS.ALCO.NICOLE.G 275.A 193
KLA-USGS-60	St. Tammany		Roofing timber	Not Provided By USGS		good	9.6	30.297754	-89.93985	NGS Control Used: ALCO.STENNIS CORS ARP.HAMMOND CORS MON

HWM_ID	County	Type of HWM	HWM Object	HWM Quality	Flood Type	Reliability of mark	Elev NAVD88 2004.65 (corrected)	Survey Latitude	Survey Longitude	Survey Comments
KLA-USGS-61	St. Tammany	Stain Line	Interior wall	Good		excellent	9.7	30.293306	-89.93545	NGS Control Used: STENNIS.ALCO.NICOLE.G 275.A 193
KLA-USGS-73	Plaquemines	Debris Line	Ground	Not Provided By USGS	tbd	poor	3.8	29.626077	-89.95134	NGS Control Used: REGGIO 2.C 195.R 194.B 369.A 152.MILAN 2
KLA-USGS-74	Plaquemines	Debris Line	Ground	Fair	tbd	poor	4.4	29.633632	-89.94939	NGS Control Used: REGGIO 2.C 195.R 194.B 369.A 152.MILAN 2
KLA-USGS-75	Plaquemines	Debris Line	Fence	Poor	tbd	poor	4.2	29.670619	-89.9709	NGS Control Used: REGGIO 2.C 195.R 194.B 369.A 152.MILAN 2
KLA-USGS-76	Plaquemines		Gate post	Not Provided By USGS	tbd	poor	4.2	29.649179	-89.96566	NGS Control Used: REGGIO 2.C 195.R 194.B 369.A 152.MILAN 2
KLA-USGS-77	Plaquemines	Seed and Debris Line	Door frame	Good	tbd	poor	7	29.583893	-89.8281	NGS Control Used: REGGIO 2.C 195.R 194.B 369.A 152.MILAN 2
KLA-USGS-78	Plaquemines	Debris Line	levee	Poor	tbd	poor	5.6	29.61738	-89.91564	NGS Control Used: REGGIO 2.C 195.R 194.B 369.A 152.MILAN 2
KLA-USGS-79	Plaquemines	Debris Line	Fence	Good	tbd	poor	5.4	29.595853	-89.84867	NGS Control Used: REGGIO 2.C 195.R 194.B 369.A 152.MILAN 2
KLA-USGS-80	Plaquemines	Debris Line		Fair	tbd	poor	5.6	29.597849	-89.84868	NGS Control Used: REGGIO 2.C 195.R 194.B 369.A 152.MILAN 2
KLA-USGS-81	Plaquemines	Debris Line	Ground	Fair	tbd	poor	3.5	29.618379	-89.91054	NGS Control Used: REGGIO 2.C 195.R 194.B 369.A 152.MILAN 2
KLA-USGS-82	Plaquemines			Not Provided By USGS	tbd	poor	3.2	29.638149	-89.94847	NGS Control Used: REGGIO 2.C 195.R 194.B 369.A 152.MILAN 2
KLA-USGS-83	Plaquemines		Exterior wall	Very Good	tbd	poor	4.3	29.647637	-89.96369	NGS Control Used: REGGIO 2.C 195.R 194.B 369.A 152.MILAN 2
KLA-USGS-84	Plaquemines	Debris Line	Levee	Fair	tbd	poor	14.8	29.462508	-89.67112	NGS Control Used: REGGIO 2.C 195.R 194.B 369.A 152.MILAN 2

HWM_ID	County	Type of HWM	HWM Object	HWM Quality	Flood Type	Reliability of mark	Elev NAVD88 2004.65 (corrected)	Survey Latitude	Survey Longitude	Survey Comments
KLA-USGS-85	Plaquemines	Debris Line		Poor	tbd	poor	11.8	29.468431	-89.6803	NGS Control Used: REGGIO 2.C 195.R 194.B 369.A 152.MILAN 2
KLA-USGS-87	Plaquemines	Debris Line		Poor	tbd	poor	11.8	29.480121	-89.69319	NGS Control Used: REGGIO 2.C 195.R 194.B 369.A 152.MILAN 2
KLA-USGS-88	Plaquemines	Debris Line		Not Provided By USGS	tbd	poor	15	29.490806	-89.70266	NGS Control Used: REGGIO 2.C 195.R 194.B 369.A 152.MILAN 2
KLA-USGS-89	Plaquemines	Debris Line		Poor	tbd	poor	12.1	29.506911	-89.71594	NGS Control Used: REGGIO 2.C 195.R 194.B 369.A 152.MILAN 2
KLA-USGS-91	Plaquemines	Debris Line	Levee slope	Fair	tbd	poor	7	29.525419	-89.75335	NGS Control Used: REGGIO 2.C 195.R 194.B 369.A 152.MILAN 2
KLA-USGS-92	Plaquemines	Debris Line	Interior door	Fair	tbd	good	11.4	29.545586	-89.77367	NGS Control Used: REGGIO 2.C 195.R 194.B 369.A 152.MILAN 2
KLA-USGS-93							unknown	29.8399	-89.688	NGS Control Used: REGGIO 2.C 195.R 194.B 369.A 152.MILAN 2
KLA-USGS-94						unknown	16.9 (NAVD88)	29.84266	-89.751	Description for this point has a measure up of 14.0 ft from finish floor, field survey recorded 10.3 ft from finish floor - HWM elevation is based on 10.3 ft) NGS Control Used: REGGIO 2.C 195.R 194.B 369.A 152.MILAN 2
KLA-USGS-95		Seed Line		Good		poor	11.8	29.873418	-89.85357	NGS Control Used: ZURFLUH.B 369.REGGIO 2.ALCO.WASTE WELL RESET 2
KLA-USGS-96		Debris Line	Interior wall	Excellent		poor	0.8	29.911314	-89.89827	NGS Control Used: ZURFLUH.B 369.REGGIO 2.ALCO.WASTE WELL RESET 2
KLA-USGS-97		Debris Line	Interior wall	Excellent		poor	0.5	29.936323	-89.92337	NGS Control Used: ZURFLUH.B 369.REGGIO 2.ALCO.WASTE WELL RESET 2
KLA-USGS-98		Debris Line	Interior wall	Excellent		poor	11.9	29.945682	-89.97176	NGS Control Used: ZURFLUH.B 369.REGGIO 2.ALCO.WASTE WELL RESET 2



HWM_ID	County	Type of HWM	HWM Object	HWM Quality	Flood Type	Reliability of mark	Elev NAVD88 2004.65 (corrected)	Survey Latitude	Survey Longitude	Survey Comments
KLA-USGS-99		Debris Line		Excellent		poor	10.7	29.960582	-90.00123	NGS Control Used: V 375.S 188.ALCO.WASTE WELL RESET 2

## Plate 1-2. Spreadsheet of USACE High Water Marks for Louisiana

HWM_ID	Reliability of mark	Elev NAVD88 2004.65	Elev NAVD88	Survey Latitude	Survey Longitude	Survey Comments					
LA 1001	excellent	12.55	12.87	30.0169	-90.0319	Based on Kemp, Smith, Maynard, Chapman evaluation, this point was in a building exposed to some wave activity. At an office in this same building, another point was located.	Holcim, west bank IHNC, 8 ft above concrete floor in warehouse.	unprotected	CEMVN	IHNC	Periera, Alette
LA 1002	excellent	12.53	12.85	30.0091	-90.0293	Slab elevation of 4.65 ft was surveyed. A/C unit removed. High Water Mark is sum of 4.65 and 8.2 ft	Trinity Yachts, West bank IHNC, mark is 8.2 ft above concrete floor in "NC" shop on a/c at northwest corner of office.	unprotected	CEMVN	IHNC	Periera, Alette
LA 1003	good	12.81	13.13	30.0091	-90.0293	Mark was added	Trinity Yachts, mark on wall east of LA 1002, Trinity Yachts.	unprotected	CEMVN	IHNC	Pereira, Alette
LA 1004	excellent	15.2	15.52	29.9843	-90.0223	Maynard, Kemp, Smith, and Chapman believe this is a valid point.	Maersk Sealand, 2700 France Rd, West Bank IHNC, 5.1 ft above concrete floor in Crane Department Bldg.	unprotected	CEMVN	IHNC	Pereira, Alette
LA 1005	excellent	13.72	14.04	29.9674	-90.0274	Maynard, Kemp, Smith, and Chapman believe this is a valid point.	USCG, West Bank IHNC, 9.2 ft above floor in Industrial Mechanical Div Engine shop, Bldg 12.	unprotected	CEMVN	IHNC	Pereira, Alette
LA 1006	excellent	13.2	13.52	29.9662	-90.0271	Maynard, Kemp, Smith, and Chapman did not believe this point reached an equilibrium water level.	IHNC Lock, 2.9 ft above engine room floor, on west wall electrical panel boxes.	unprotected	CEMVN	IHNC	Pereira, Alette
LA 1007	excellent	10.82	11.12	30.0210	-90.1234		Inside Coast Guard station near 17th St Canal on NW side of building in room with double door. HWM found on back of shelves and moved from shelves to wall because office was being cleaned. Orange paint on floor. Mark is 22" above floor.	unprotected	ERDC and LSU	17th St Canal	Kemp, Biedenharn, Maynard

HWM_ID	Reliability of mark	Elev NAVD88 2004.65	Elev NAVD88	Survey Latitude	Survey Longitude	Survey Comments					
LA 1008	excellent	10.74	11.54	30.0219	-90.1192		East side of 17th St Canal, inside storage room of building that had double door completely removed but there was another structure between Lake and storage room to block waves. HWM was near door and was less exposed to any sloshing and was 1.55 ft from	unprotected	ERDC and LSU	17th St Canal	Kemp, Biedenham, Maynord
LA 1009	excellent		11.29	30.0220	-90.1192		East side of 17th St Canal, Inside storage room of building that had double door completely removed but there was another structure between Lake and storage room to block waves. HWM was near wall air conditioner and was more exposed to any sloshing and w	unprotected	ERDC and LSU	17th St Canal	Kemp, Biedenham, Maynord
LA 1010	good	11.74	12.24	30.0236	-90.1181		East side of 17th St Canal, Inside business at 402 South Roadway St at back wall of building. 7.9 ft above concrete dock. Subsequent visit by COPRI team resulted in observation by one member that HWM may be high because of wave exposure. Another mark set	unprotected	ERDC and LSU	17th St Canal	Kemp, Biedenham, Maynord
LA 1011	fair	10.79	11.41	30.0251	-90.0980		Debris HWM on east levee of Orleans Ave Canal, near end of Snipe St, 2.07 ft below top of levee crest.	unprotected	ERDC and LSU	Orleans Ave Cana	Kemp, Biedenham, Maynord
LA 1012	excellent	11.73	12.31	30.0297	-90.0914		Inside west bathroom at Shelter No 2 on Lakeshore Dr between Orleans Ave Canal and Bayou St John, 4.28 ft above floor.	unprotected	ERDC and LSU	New Orleans lake	Kemp, Biedenham, Maynord
LA 1013	poor	12.59	14.99	30.0279	-90.0892		FEMA HWM "KLAC-02-22, 9/16/05", debris HWM on Lakeshore Dr between Bayou St John and Orleans Ave Canal.	unprotected	ERDC and LSU	New Orleans lake	Kemp, Biedenham, Maynord



HWM_ID	Reliability of mark	Elev NAVD88 2004.65	Elev NAVD88	Survey Latitude	Survey Longitude	Survey Comments					
LA 1014	poor	12.52	13.07	30.0247	-90.0823		Debris HWM on east levee of Bayou St John, 1.05 ft below levee crest.	unprotected	ERDC and LSU	Bayou St John	Kemp, Biedenbarn, Maynord
LA 1015	fair	10.82	11.38	30.0250	-90.0721		Debris HWM on west levee of London Ave Canal, north of Robert E. Lee Blvd, 1.5 ft below crest of levee.	unprotected	ERDC and LSU	London Ave Canal	Kemp, Biedenbarn, Maynord
LA 1016	poor	10.73	11.40	30.0308	-90.0746		Debris mark on west side of London Ave Canal, on north side of Lake Pontchartrain levee, about 4 ft below crest of levee. This mark was felt to be influenced by waves by COPRI team. New point located about 100-150 ft west that had a higher road embankmen	unprotected	ERDC and LSU	London Ave Canal	Kemp, Biedenbarn, Maynord
LA 1017	poor	7.61	8.41	30.0288	-90.0725		Debris mark on east levee of London Ave Canal, south of Lakeshore Dr, 4.8 ft below levee. COPRI team felt that HWM should be moved and new point was set about 400 ft south on same levee.	unprotected	ERDC and LSU	London Ave Canal	Kemp, Biedenbarn, Maynord
LA 1018	protected	8.1	8.79	29.9889	-90.0677		At London Ave Canal pump station, pump station #3, east side of discharge area on top of concrete wall along railroad track, this could be high estimate. Levee debris HWM is 4.67 ft below adjacent floodwall.	unprotected	ERDC and LSU	London Ave Canal	Kemp, Biedenbarn, Maynord
LA 1019	protected	8.74	8.99	29.9878	-90.1239		Levee debris HWM, east side of London Ave Canal pump station discharge area, pump station #3.	unprotected	ERDC and LSU	London Ave Canal	Kemp, Biedenbarn, Maynord
LA 1020	excellent	11.04	12.12	30.0236	-90.1181		Inside business at 402 South Roadway St at back wall of building. Same building as LA 1010.	unprotected	COPRI and ERDC	17th St Canal	COPRI, Biedenbarn, Maynor

HWM_ID	Reliability of mark	Elev NAVD88 2004.65	Elev NAVD88	Survey Latitude	Survey Longitude	Survey Comments					
LA 1021	poor	10.03	10.50	30.0309	-90.0750		Debris HWM on west side of London Ave Canal, on north side of Lake Pontchartrain levee.	unprotected	COPRI and ERDC	London Ave Canal	COPRI, Biedenham, Maynor
LA 1022	fair	10.59	10.95	30.0278	-90.0727		Debris HWM on east levee of London Ave Canal, south of Lakeshore Dr.	unprotected	COPRI and ERDC	London Ave Canal	COPRI, Biedenham, Maynor
LA 1023	protected	3.04	3.36	29.9891	-90.0282		IHNC, Cold Storage site, between two containers, on tire.	protected	COPRI and ERDC	IHNC	COPRI, Biedenham
LA 1024	protected	4.45	4.77	29.9877	-90.0285		IHNC, HWM on chain link fence to Kerney Co.	protected	COPRI and ERDC	IHNC	COPRI, Biedenham
LA 1025	protected	4.94	5.26	29.9872	-90.0280		IHNC, Inside Kerney Bldg, SE corner, in secretary office.	protected	COPRI and ERDC	IHNC	COPRI, Biedenham
LA 1026	Poor	14.34	14.34	29.9872	-90.0264		IHNC, Puerto Rico Marine Compound, debris in rafters, may be low estimate.	unprotected	COPRI and ERDC	IHNC	COPRI, Biedenham
LA 1027	poor	15.44	15.76	29.9872	-90.0264		IHNC, Puerto Rico Marine Compound, dot in rafters, may be low estimate.	unprotected	COPRI and ERDC	IHNC	COPRI, Biedenham
LA 1029	poor	14.44	14.76	30.0038	-90.0267		IHNC, south of I-10. HWM on large gravel pile not marked with orange.	unprotected	COPRI and ERDC	IHNC	COPRI, Biedenham
LA 1030	excellent	15.19	15.51	29.9843	-90.0223	Maynard, Kemp, Smith, and Chapman believe this is a valid point.	IHNC, Crane Machine Shop. HWM is under 2 big black cranes.	unprotected	COPRI and ERDC	IHNC	COPRI, Biedenham
LA 1031a	excellent	10.846	11.03	30.0211	-90.1230		West side of 17th Street Canal at Coast Guard Station. HWMs are 12-22" above slab at 4 places in 1st floor.	unprotected	CEMVN	17th St Canal	Bellocq,Winer
LA 1031b	excellent	10.34	10.52	30.0211	-90.1230		West side of 17th Street Canal at Coast Guard Station. HWMs are 12-22" above slab at 4 places in 1st floor.	unprotected	CEMVN	17th St Canal	Bellocq,Winer
LA 1031c	excellent	10.01	10.19	30.0211	-90.1230		West side of 17th Street Canal at Coast Guard Station. HWMs are 12-22" above slab at 4 places in 1st floor.	unprotected	CEMVN	17th St Canal	Bellocq,Winer

HWM_ID	Reliability of mark	Elev NAVD88 2004.65	Elev NAVD88	Survey Latitude	Survey Longitude	Survey Comments					
LA 1031d	excellent	10.405	10.58	30.0211	-90.1230		West side of 17th Street Canal at Coast Guard Station. HWMs are 12-22" above slab at 4 places in 1st floor.	unprotected	CEMVN	17th St Canal	Bellocq,Winer
LA 1032	excellent	10.2	10.56	30.0220	-90.1157		East side of 17th Street Canal, Orleans Levee Board Marina, Mens' Restroom. HWM is 42"above floor on south wall just inside the door.	unprotected	CEMVN	17th St Canal	Bellocq,Winer
LA 1033	excellent	11.7	12.24	30.0352	-90.0222	Maynard, Kemp, Smith, and Chapman believe this is a valid point.	National Guard Bldg near Lakefront Airport, bldg 103, left center portion of bldg inside stairwell. HWM is 83" above floor, on south side of building close to road.	unprotected	CEMVN, ERDC	New Orleans lake	Blodgett, Pereira
LA 1034	excellent	10.78	11.14	30.0237	-90.1136		East side of 17th St Canal, 7400 Lakeshore Dr, Hong Kong Restaurant. HWM is 68.5" above floor.	unprotected	CEMVN	17th St Canal	Alette,Frost
LA 1035	excellent	11.4	11.76	30.0268	-90.1172	Maynard, Biedenham, Smith, and Chapman believe this is a valid point.	East side of 17th St Canal, 7734 Breakwater Dr, 18th boathouse. HWM is 0.7 ft above carpet in back bedroom, 2nd floor elevation above concrete in front is 7.0 ft.	unprotected	CEMVN,ERDC	17th St Canal	Alette, Frost
LA 1036	excellent	11.2	11.56	30.0232	-90.1203	Maynard, Kemp, Smith, and Chapman believe this is a valid point.	East side of 17th St Canal, between 7352 and 7358 W Roadway St, inside building. HWM is 7.15 ft above floor.	unprotected	CEMVN, ERDC	17th St Canal	Alette, Frost
LA 1037	poor	9.51	9.26	30.0401	-90.2381	Maynard, Kemp, Smith, and Chapman believe this is a valid point.	Williams Boat Launch, Levee Debris HWM, stake in levee about even with front of Pontchartrain Center.	unprotected	CEMVN	Jefferson Parish	Alette, Frost
LA 1038	excellent	11.07	11.25	30.0211	-90.1230		West of 17th St Canal at Coast Guard Station. HWM is 2.4 ft above floor at second bolt from bottom of the NE garage door, lakeside.	unprotected	CEMVN	17th St Canal	Alette, Frost



HWM_ID	Reliability of mark	Elev NAVD88 2004.65	Elev NAVD88	Survey Latitude	Survey Longitude	Survey Comments					
LA 1039	excellent	14.45	14.20	30.0030	-89.9607		On GIWW, at Boh Bros Construction. HWM is inside office, 2.25 ft above floor. Mark moved to outside of building, 3.22 ft 3.22 ft below HWM. Surveyed mark at 10.9. Must add 3.2	Unprotected	ERDC	GIWW	Maynard, Dunbar, Smith, Ch
LA 1040	poor	20.77	20.09	29.9347	-89.8368		Bayou Dupre Floodgate, east gate house, small debris in window frame, painted, probably high.	Unprotected	ERDC	MRGO	COPRI, Biedenbarn
LA 1041	poor	16.77	16.90	29.9347	-89.8368		Bayou Dupre Floodgate, east gate house, lower guardrail debris, painted.	Unprotected	ERDC	MRGO	COPRI, Biedenbarn
LA 1042	poor	21.73	21.60	29.9349	-89.8369		Bayou Dupre Floodgate, east gate house, light standard, painted metal plate, probably high.	Unprotected	ERDC	MRGO	COPRI, Biedenbarn
LA 1043	poor	18.17	18.42	29.9986	-89.9156		Bayou Bienvenue Floodgate, west gate house, top of radiator, painted orange, 3.3 ft above floor, best estimate.	Unprotected	ERDC	MRGO	Maynard, Biedenbarn
LA 1044	poor	18.47	18.68	29.9986	-89.9156		Bayou Bienvenue Floodgate, top rail of handrail closest to gate house, upper limit of surge.	Unprotected	ERDC	MRGO	Maynard, Biedenbarn
LA 1045	poor	16047	16.70	29.9986	-89.9155		Bayou Bienvenue, bottom rail of handrail closest to gate house, lower limit of surge.	Unprotected	ERDC	MRGO	Maynard, Biedenbarn
LA 1046	poor	14.97	15.44	30.0314	-90.0715		Levee Debris HWM on levee, Lakeshore Dr, east of London Ave Canal- has wave component.	Unprotected	ERDC	London Ave Canal	Smith, Chapman, Maynard,
LA 1047	poor	14.4	14.87	30.0314	-90.0716		Levee Debris HWM on levee, Lakeshore Dr, east of London Ave Canal- has lesser wave component because protected by downed tree	Unprotected	ERDC	London Ave Canal	Smith, Chapman, Maynard,

HWM_ID	Reliability of mark	Elev NAVD88 2004.65	Elev NAVD88	Survey Latitude	Survey Longitude	Survey Comments					
LA 1048	poor	16.64	17.16	30.0340	-90.0429		Top of levee, obtain levee crest elevation, every 50 ft for 200 ft east and west of GPS location.	Unprotected	ERDC		Smith, Chapman, Maynord,
LA 1049	poor	16.57	17.01	30.0329	-90.0411		HWM at top of floodwall. Survey top of floodwall.	Unprotected	ERDC		Smith, Chapman, Maynord,
LA 1050	excellent	11.43	11.87	30.0326	-90.0399	Accepted by Kemp	Naval Reserve building west of IHNC. At backside in 3rd building from east side. HWM is 3.7 ft above floor. Must call Joe Peters at 985-703-1692 for access.	Unprotected	ERDC	IHNC	Smith, Chapman, Maynord,
LA 1052	poor	9.16	9.52	29.9952	-90.1008		Survey arrow in orange paint at south end of east floodwall at Orleans pump station, pumping station #7. HWM is 0.5 ft below arrow. Also survey 3 points along levee between this HWM and beginning of short wall attached to station. Survey points at ends a	unprotected	ERDC	Orleans Ave Canal	Smith, Chapman, Maynord
LA 1053	excellent	15.54	16.31	30.0069	-89.9368		Entergy power plant at MRGO. HWM is in pump area next to MRGO in most eastern building in an electrical panel box. HWM is 3.55 ft above concrete floor. Rough measurements place this HWM 15.9 ft above water level in MRGO.	unprotected	ERDC & LSU	MRGO	Smith, Chapman, Maynord,
LA 1055	excellent	12.42	12.83	30.0168	-90.0316		Inside "Holcim" bldg office on west side of bldg near SW corner. HWM is 2.44 ft above slab on counter on left after entering office. This is a revision to LA 1001. Marked on counter with arrow but not with orange paint.	unprotected	ERDC & LSU	IHNC	Smith, Chapman, Maynord,
LA 1056	poor	10.84	11.20	30.0203	-90.1255		Debris line on levee just west of Coast Guard building at 17th St Canal.	unprotected	ERDC & LSU	17th St Canal	Smith, Chapman, Maynord,

HWM_ID	Reliability of mark	Elev NAVD88 2004.65	Elev NAVD88	Survey Latitude	Survey Longitude	Survey Comments					
LA 1057	poor	11.74	12.19	30.0195	-90.1428		Debris line on levee near Bonnabel boat launch	unprotected	ERDC & LSU	Jefferson Parish	Smith, Chapman, Maynard,
LA 1058	good	6.76	6.51	30.0410	-90.2386		Williams Blvd near Lake Pontchartrain center, on lake side of levee, inside ladies restroom, 2.27 ft above slab.	unprotected	ERDC & LSU	Jefferson Parish	Smith, Chapman, Maynard,
LA 1059	poor	11.16	11.63	30.0267	-90.0729		Debris HWM on west levee of London Ave Canal north of Leon C Simon Dr bridge. Marked with orange paint and 3" long bolt driven into levee.	unprotected	ERDC	London Ave Canal	Biedenham, Maynard, Pink
LA 1060	fair	9.75	10.22	30.0228	-90.0713		West Flood wall/abutment wall that is south of Leon C Simon Dr bridge over London Ave Canal. Survey top of wall near GPS location. Debris HWM on levee is 0.9 m below top of flood wall. HWM is not marked by paint.	unprotected	COPRI	London Ave Canal	COPRI
LA 1061	fair	10.64	11.11	30.0236	-90.0713		West Flood wall/abutment wall that is north of Leon C Simon Dr bridge over London Ave Canal. Survey top of wall near GPS location. Debris HWM on levee is 0.67 m below top of flood wall. HWM is not marked by paint.	unprotected	COPRI	London Ave Canal	COPRI
LA 1062	poor	-1.8	-0.95	30.0334	-90.0272	New Orleans East Lakefront Levee	North side of center support pier under the railroad overpass over Downman Rd, just north of Hayne Blvd. HWM is 2.81 ft above the concrete median at a gage reading of 3.5 ft on the staff gage on the peir.		Corps MVN		Alette, Bellocq



HWM_ID	Reliability of mark	Elev NAVD88 2004.65	Elev NAVD88	Survey Latitude	Survey Longitude	Survey Comments					
LA 1063	excellent	12.11	12.63	30.0358	-90.0241	lat and long is just outside the exterior door that is closest to the HWM	New Orleans Lakefront Airport, in the Taylor Energy hangar, the westernmost hangar, the first one to the east of the main terminal building. HWM is located in the stairway behind the wall at the sound end of the open area in the hangar. The entrance to		Corps MVN	New Orleans lake	Alette, Bellocq
LA 1064	protected	-1.49	-0.98	30.0580	-89.9656		Garage door of single family home at 7963 Jahncke Road, just off Hayne Blvd and just to the southeast of the Jahncke Pumping Station. Mark is 8 inches above the driveway slab on the garage door.	protected	Corps MVN	New Orleans East	Alette, Bellocq
LA 1065	poor	11.4	11.71	30.1316	-89.8721	Appears that the peak stage during Katrina slightly overtopped the levee at this location as evidenced by debris near the landside toe that appears to have been swept over the top of the levee from the floodside.	Debris HWM about 3 ft below levee crown along the South Point to GIWW levee just south of I-10. This appears to be an interim HWM, where the water stood for a time during Katrina. May be worthwhile to shoot top of levee at this location.	unprotected	Corps MVN	New Orleans East	Alette, Bellocq
LA 1066	poor	13.79	14.10	30.1240	-89.8659	Appears that the peak stage during Katrina slightly overtopped the levee at this location as evidenced by debris near the landside toe that appears to have been swept over the top of the levee from the floodside.	Debris HWM along the South Port to GIWW levee just east of US Hwy 11.	unprotected	Corps MVN	New Orleans East	Alette, Bellocq
LA 1067	fair	10.1	10.57	30.0276	-90.0743		Debris HWM on levee approximately 29 inches from top of each wheel track on top of levee	unprotected	Corps MVN	New Orleans lake	Pereira, Blodgett

HWM_ID	Reliability of mark	Elev NAVD88 2004.65	Elev NAVD88	Survey Latitude	Survey Longitude	Survey Comments					
LA 1069a	fair	10.64	11.11	30.0236	-90.0713		Debris HWM on southwest side of Robert E. Lee Blvd bridge over the London Ave Canal, approximately 3.0 ft below top of wingwall	unprotected	Corps MVN	London Ave Canal	Pereira, Blodgett
LA 1069b	poor	4.96	5.43	30.0236	-90.0713	Rita	Debris HWM on southwest side of Robert E. Lee Blvd bridge over the London Ave Canal, approximately 3.0 ft below top of wingwall	unprotected	Corps MVN	London Ave Canal	Pereira, Blodgett
LA 1070a	protected	3.17	3.63	29.9883	-90.0678	Two marks at this location, LA 1070A and LA 1070B	Pumping Station 3 at North Broad St. Two marks, first mark is on metal cabinet 11 inches above floor in office. Second mark is 23.5 inches above concrete floor on door outside of office in pump building	protected	Corps MVN	New Orleans Metr	Pereira, Blodgett
LA 1070b	protected	3.15	3.61	29.9883	-90.0678	Two marks at this location, LA 1070A and LA 1070B	Pumping Station 3 at North Broad St. Two marks, first mark is on metal cabinet 11 inches above floor in office. Second mark is 23.5 inches above concrete floor on door outside of office in pump building	protected	Corps MVN	New Orleans Metr	Pereira, Blodgett
LA 1071	poor	10.74	11.21	30.0309	-90.0746		Debris HWM on lake side of levee, south of Lakeshore Dr. HWM is 43 inches below top of levee. Note - drove stake with 2 inch PVC pipe painted orange at high water mark	unprotected	Corps MVN	New Orleans lake	Pereira, Blodgett
LA 1072	poor	11.93	12.40	30.0320	-90.0653		Debris HWM on lake side of levee on Lakeshore Dr, across from Kurshmann Hall. Debris line is 30 inches below top of levee. Did not mark.	unprotected	Corps MVN	New Orleans lake	Pereira, Blodgett
LA 1073	poor	16.35	16.87	30.0341	-90.0433		Debris HWM on top of levee	unprotected	Corps MVN	New Orleans lake	Pereira, Blodgett
LA 1074	good	11.92	12.50	30.0369	-90.0148		Marina at Lakefront Airport. Debris line approximately 2 ft below top of levee.	unprotected	Corps MVN	New Orleans East	Pereira, Blodgett

HWM_ID	Reliability of mark	Elev NAVD88 2004.65	Elev NAVD88	Survey Latitude	Survey Longitude	Survey Comments					
LA 1075	poor	9.52	10.20	29.9447	-90.0028		Painted orange mark located on steel I-beam forming the platform for grated walkway of wingwall, 63 inches below concrete base of platform at Mississippi River at Chalmette gage	unprotected	Corps MVN	Mississippi Rive	Pereira, Servay
LA 1077	excellent	14.18	14.59	29.3889	-89.5965		HWM is in control house of Empire Lock, 4 inches above floor on back of door. Line very faint, but there was mud on floor.	unprotected	Corps MVN	Mississippi River	Pereira, Servay
LA 1078	excellent	14.39	14.80	29.3889	-89.5966		HWM is in bathroom downstairs in control house of Empire Lock, 85.5 inches above cement floor	unprotected	Corps MVN	Mississippi River	Pereira, Servay
LA 1079	poor	4.27	4.61	30.1006	-90.4287		HWM on chain link fence 2.21 ft above ground. Use middle of orange paint line on fence post	unprotected	Corps MVN	St John the Bapt	Pereira
LA 1080	excellent	7.16	7.01	30.1066	-90.4241		HWM on quonset hut located at the corner of Peavine Road and Ponch Road. Mark is located on a white wooden door inside the Quonset, near floor	unprotected	Corps MVN	St John the Bapt	Pereira
LA 1081	excellent	3.91	5.12	30.2812	-90.3999		HWM is located in a building approximately 100 ft south of the Pass Manchac DCP gage. The mark is on the inside of the back door of the Beacon Lounge, 0.45 ft above the bottom of the door.	unprotected	Corps MVN	St John the Bapt	Pereira
LA 1082	poor	4.6	4.76	29.9857	-90.3496		HWM is located on the northwest portion of the sheet pile at Cross Bayou Structure. Mark is 90 inches below the top of the sheetpile	unprotected	Corps MVN	St Charles Paris	Pereira
LA 1083	excellent	15.71	15.93	30.0668	-89.8063		HWM is located on sheetrock in stairwell of house at 4300 Fort Mcomb. Mark is 112 inches above floor (concrete slab)	unprotected	Corps MVN	New Orleans East	Pereira, Servay



HWM_ID	Reliability of mark	Elev NAVD88 2004.65	Elev NAVD88	Survey Latitude	Survey Longitude	Survey Comments					
LA 1084	fair	12.52	12.52	30.0280	-90.0891	Recovered as in Corps photo. Stake reads KLAC not KLAL. Tied to NGS PBM Essex published superceded 6.43 ft. Found 5.78 ft	Debris line about 4 to 8 inches below the top of the levee on the lake front of Lake Pontchartrain, marked by FEMA stake FEMA KLAC-02-22	unprotected	Corps MVN	New Orleans lake	Blodgett and Taylor
LA 1085	poor	16.85	16.85	30.0285	-90.0936	See photo, may have been splash line	Debris line along lake front of Lake Pontchartrain.	unprotected	Corps MVN	New Orleans lake	Blodgett and Taylor
LA 1086	excellent	11.86	11.86	30.0329	-90.0401	LA1156 in same vicinity	High water mark is located in the old Naval Reserve Center. Mark is located at approximately 75 ft from the back of the building on the second of the four wings starting from the left. No information provided as to measurement from floor	unprotected	Corps MVN	New Orleans lake	Blodgett and Taylor
LA 1087	excellent	18.12	18.12	29.8510	-89.6801		Mark is located on inside of home in Shell Beach at the corner of West Indies Drive and Caribbean Blvd. Should be one mark in each bedroom located upstairs on the end of the house opposite the kitchen. Mark is approximately 31 inches above carpet	unprotected	Corps MVN	New Orleans East	Blodgett and Taylor
LA 1088	excellent	18.67	18.67	29.8538	-89.6777		Mark is located on inside of home in Shell Beach at the end of West Indies St opposite to the house above. Mark is located in a pantry in the kitchen, 28 inches above the 2nd story floor or about 142 inches above the ground slab	unprotected	Corps MVN	New Orleans East	Blodgett and Taylor
LA 1089	excellent	17.1	17.10	29.8427	-89.7509		Mark is located on inside of Dixie Well Service and Supply. Mark is located about 11 ft above the slab by the stairs leading to a second level.	unprotected	Corps MVN	New Orleans East	Blodgett and Taylor

HWM_ID	Reliability of mark	Elev NAVD88 2004.65	Elev NAVD88	Survey Latitude	Survey Longitude	Survey Comments					
LA 1090	excellent	15.77	15.77	30.0697	-89.8139	Sheetrock has been removed. HWM measured from third step of inside stairs. Elevation of third step = 10.69 ft	Mark is located on inside of home at 4620 Murano Road. Mark is 2 ft below slab of second floor, 61 inches above the third step.	unprotected	Corps MVN	New Orleans East	Bellocq and Donnelly
LA 1091	poor	2.61	2.61	30.0285	-89.8931		Mark is on Industrial Parkway in New Orleans. Mark measures 39 inches above train tracks.		Corps MVN	New Orleans East	Bellocq and Donnelly
LA 1092	poor	12.85	12.85	30.0063	-89.9393	Top of levee, low spot	Debris overtopping GIWW levee by Paris Road Bridge.	unprotected	Corps MVN	New Orleans East	Bellocq and Donnelly
LA 1093	poor	14.71	14.71	30.0093	-89.9386	Low point in levee at Paris Rd Bridge = Elev 12.85 ft	Entergy Michoud Power Plant. Debris along fence under Paris Road Bridge.	unprotected	Corps MVN	New Orleans East	Bellocq and Donnelly
LA 1094	poor	12.4	12.40	30.0086	-90.0264	Floodside toe = 10.37 ft, protected side toe = 9.37 ft	Under east side of Danzinger Bridge over Chef Menteur Highway. Water overtopped floodwall.	unprotected	Corps MVN	New Orleans East	Bellocq and Donnelly
LA 1095a	poor	12.08	12.08	30.0173	-90.0271	First elevation is floodgate, second elevation is floodwall	top of floodgate and top of floodwall at Dwyer Road floodgate E11	unprotected	Corps MVN	New Orleans East	Bellocq and Donnelly
LA 1095b	poor	13.02	13.02	30.0173	-90.0271	First elevation is floodgate, second elevation is floodwall	top of floodgate and top of floodwall at Dwyer Road floodgate E11	unprotected	Corps MVN	New Orleans East	Bellocq and Donnelly
LA 1096	poor	3.79	3.79	30.0317	-90.0317	Elevation needs to be checked, surveyor measured 2 marks. Top of floodwall is 11.19 ft	Mark on floodgate located at Jourdan Road and Hayne Blvd. Mark is 58 inches from bottom of steel floor	Unprotected?	Corps MVN	New Orleans East	Bellocq and Donnelly
LA 1097	poor	6.42	6.42	30.0041	-89.9492		Debris line at 28 mark of staff gage at Grand St Pumping Station	Unprotected	Corps MVN	New Orleans East	Bellocq and Donnelly
LA 1098	poor	18.6	18.60	30.0276	-89.9060	Fence removed. Elevation is for top of floodwall at Gate M3, Eastside Maxent Canal. Air Products will send photos of water overtopping floodwall	Debris on chain link fence and razor wire on the Maxent Canal on the east side of Air Products Corps.	Unprotected	Corps MVN	New Orleans East	Bellocq and Donnelly

HWM_ID	Reliability of mark	Elev NAVD88 2004.65	Elev NAVD88	Survey Latitude	Survey Longitude	Survey Comments					
LA 1099	good	16.46	16.50	29.7685	-89.7899		Administrative building in Delacroix. Mark painted orange on slab in front of building must add 13.35 ft to slab elev of 3.11 ft	Unprotected	Corps MVN	New Orleans East	Bellocq and Donnelly
LA 1100	good	16.7	16.70	29.7587	-89.7844		House on main highway in Delacroix, with number address 6623. Nail in fifth post on right side as you face house. Nail is approximately 4.8 ft off ground. HWM is 8.8 ft above nail at elev 7.9 ft	Unprotected	Corps MVN	New Orleans East	Bellocq and Donnelly
LA 1101	protected	-1.39	-1.39	30.0413	-89.9478		Main Developer's House at 5690 Eastover Drive New Orleans. Mark is on front porch to the right of the front door, 43 inches from ground.	Protected	Corps MVN	New Orleans East	Bellocq and Donnelly
LA 1102	protected	-1.31	-1.31	30.0470	-89.9444		The Golf Club of New Orleans Eastover. Mark is 38 inches from ground outside of building on grounds	Protected	Corps MVN	New Orleans East	Bellocq and Donnelly
LA 1103	protected	-1.43	-1.43	30.0539	-89.9671		7601 Bullard, New Orleans. Mark on concrete porch on front of house, 22 inches from ground	Protected	Corps MVN	New Orleans East	Bellocq and Donnelly
LA 1104	protected	-1.39	-1.39	30.0543	-89.9674		11901 Curran Road, New Orleans. Mak on north edge of fence, 12 inches from ground.	Protected	Corps MVN	New Orleans East	Bellocq and Donnelly
LA 1105	protected	-1.44	-1.44	30.0260	-89.9502		11611 N Adams Court, New Orleans. House at N Adams and W Adams Ct. Mark is next to front window left of front door, 33 inches from ground	Protected	Corps MVN	New Orleans East	Bellocq and Donnelly
LA 1106	protected	2.73	2.73	29.9554	-90.1210		2331 S Carrollton Ave New Orleans. Corner of S Claiborne Ave and South Carrollton Ave. Mark is located outside of Chase Bank building on S Claiborne Ave, 34 inches from ground	Protected	Corps MVN	New Orleans Metr	Bellocq and Donnelly



HWM_ID	Reliability of mark	Elev NAVD88 2004.65	Elev NAVD88	Survey Latitude	Survey Longitude	Survey Comments					
LA 1107	protected	2.6	2.60	29.9504	-90.1068		4401 Fountainebleau Dr New Orleans. Mark is on side of building located at corner of Napoleon Ave and Broad St, 89 inches from ground	Protected	Corps MVN	New Orleans Metr	Bellocq and Donnelly
LA 1108	protected	1.96	1.96	29.9288	-90.1001		4219 Baronne St, New Orleans. Mark on wooden fence to right of gate, 14.5 inches from ground	Protected	Corps MVN	New Orleans Metr	Bellocq and Donnelly
LA 1109	protected	1.96	1.96	29.9270	-90.0990		9 Palm Terrace, New Orleans. Southern most edge of flooding in Broadmoor. Mark on white cinder block wall, to the left of the driveway, 10 inches from ground	Protected	Corps MVN	New Orleans Metr	Bellocq and Donnelly
LA 1110	protected	2.49	2.49	29.9360	-90.0945	Tied to NGS PBM 'X-49' Flint Goodridge Hosp. Published superceded EI = 3.69' found 3.29'	3328 LaSalle St New Orleans. Mark is on building for Mo Hair Design on corner of LaSalle St and Louisiana Ave, 48.5 inches from ground	Protected	Corps MVN	New Orleans Metr	Bellocq and Donnelly
LA 1111	protected	2.52	2.52	29.9423	-90.0954		South Claiborne Ave and Toledano. Mark is on building 52.5 inches from ground	Protected	Corps MVN	New Orleans Metr	Bellocq and Donnelly
LA 1112	protected	2.52	2.52	29.9444	-90.0908		2841 South Claiborne Ave. Mark in on front of Winn Dixie building, 59 inches from ground.	Protected	Corps MVN	New Orleans Metr	Bellocq and Donnelly
LA 1113	protected	2.52	2.52	29.9498	-90.1003		3933 Washington Ave New Orleans. Mark is on Rhodes Funeral Home building, 63 inches from ground	Protected	Corps MVN	New Orleans Metr	Bellocq and Donnelly
LA 1114	protected	2.38	2.38	29.9528	-90.0979		Pumping station at South Broad and Martin Luther King Blvd. Mark is 44 inches below top of flood wall located on west side of pumping station off bridge.	Protected	Corps MVN	New Orleans Metr	Bellocq and Donnelly
LA 1115	protected	2.55	2.55	29.9498	-90.1003		3609 Toledano St, New Orleans. Mark is on Captain Sal Seafood building, 70.5 inches from ground.	Protected	Corps MVN	New Orleans Metr	Bellocq and Donnelly

HWM_ID	Reliability of mark	Elev NAVD88 2004.65	Elev NAVD88	Survey Latitude	Survey Longitude	Survey Comments					
LA 1116	protected	2.54	2.54	29.9624	-90.0901		425 Broad St New Orleans. Mark is on Israel Augustine Middle School, 46 inches from ground	Protected	Corps MVN	New Orleans Metr	Bellocq and Donnelly
LA 1117	protected	2.6	2.60	29.9646	-90.0881		200 S Broad, New Orleans. Mark is at right corner of building housing McKenna and Medley Eye Clinic, 74.5 inches from concrete pavement	Protected	Corps MVN	New Orleans Metr	Bellocq and Donnelly
LA 1118	protected	2.32	2.32	29.9688	-90.0845		Old Pumping station at North Broad and St Louis. Mark in right of garage door 21 inches from ground.	Protected	Corps MVN	New Orleans Metr	Bellocq and Donnelly
LA 1119	protected	2.52	2.52	29.9708	-90.0826		711 N Broad St New Orleans. Mark on side of building housing Ruth Chris Steak House, on top of grey curb, 49 inches from grey curb	Protected	Corps MVN	New Orleans Metr	Bellocq and Donnelly
LA 1120	protected	1.93	1.93	29.9820	-90.0996		718 N Alexander St. New Orleans. Mark on Orleans Ave side of building, 19.5 inches from ground.	Protected	Corps MVN	New Orleans Metr	Bellocq and Donnelly
LA 1121	protected	1.94	1.94	29.9863	-90.1221		441 Fairway Drive. New Orleans. Mark is on white wooden fence 50.5 inches from ground.	Protected	Corps MVN	New Orleans Metr	Bellocq and Donnelly
LA 1122	protected	-3.22	-3.22	30.0046	-90.1073		724 Harrison Ave Metairie LA. Mark is 2.5 inches from step.	Protected	Corps MVN	Jefferson Parish	Bellocq and Donnelly
LA 1123	fair	9.93	9.93	29.9466	-89.9592		St. Avide and Tournefort mark on Metal Light Pole 10 ft from ground	Protected	Corps MVN	St Bernard Paris	Jones
LA 1124	fair	10.97	10.97	29.9443	-89.9522		St. Avide and Decomine mark on Metal Light Pole 12 ft from ground	Protected	Corps MVN	St Bernard Paris	Jones
LA 1125	fair	9.39	9.39	29.9480	-89.9534		Marietta and Josephine mark on Metal Light Pole 12 ft from ground	Protected	Corps MVN	St Bernard Paris	Jones
LA 1126	fair	9.08	9.08	29.9511	-89.9490		Eagle and Dauterive mark on Metal Light Pole 10 ft from ground	Protected	Corps MVN	St Bernard Paris	Jones

HWM_ID	Reliability of mark	Elev NAVD88 2004.65	Elev NAVD88	Survey Latitude	Survey Longitude	Survey Comments					
LA 1127	fair	10.29	10.29	29.9416	-89.9509		2909 Palmisano mark on tree in neutral ground 9 ft from ground	Protected	Corps MVN	St Bernard Paris	Jones
LA 1128	fair	9.47	9.47	29.9356	-89.9178		2809 St. Marie mark on Metal Light Pole 15 ft from ground	Protected	Corps MVN	St Bernard Paris	Jones
LA 1129	fair	9.09	9.09	29.9408	-89.9162		Van Cleave and Ehrhard mark on Metal Light Pole 14 feet from ground	Protected	Corps MVN	St Bernard Paris	Jones
LA 1130	fair	10.25	10.25	29.9428	-89.9139		4218 Florida Ave in Lexington mark on Wood Light Pole 15 ft from ground	Protected	Corps MVN	St Bernard Paris	Jones
LA 1131	fair	11.11	11.11	29.9297	-89.9280		Hannan Blvd near Hwy 46 mark on tree on west side 8 ft from ground	Protected	Corps MVN	St Bernard Paris	Jones
LA 1132	fair	8.65	8.65	29.9653	-89.9988		1519 Alexander mark on wood light pole 10 ft from ground	Protected	Corps MVN	St Bernard Paris	Jones
LA 1133	fair	7.08	7.08	29.9586	-89.9737		Creole and Evangeline mark on Metal Light Pole 12 ft from ground	Protected	Corps MVN	St Bernard Paris	Jones
LA 1134	poor	9.02	9.02	29.9480	-89.9881		2209 Pirate Drive mark on Metal Light Pole 12 ft from ground	Protected	Corps MVN	St Bernard Paris	Jones
LA 1135	fair	8.86	8.86	29.9571	-89.9792		Packenhams and W Claiborne Sq mark on cement light pole 12 ft from ground	Protected	Corps MVN	St Bernard Paris	Jones
LA 1136	fair	9.91	9.91	29.9460	-89.9379		3709 Jacob Drive mark on Metal Light Pole 9.4 ft from ground	Protected	Corps MVN	St Bernard Paris	Jones
LA 1137	fair	9.94	9.94	29.9702	-89.9917		Rose and Center St mark on Wood Pole 11 ft from ground	Protected	Corps MVN	St Bernard Paris	Jones
LA 1138	fair	11.01	11.01	29.9505	-90.0049		448 Friscoville mark on Wood Pole 6 ft from ground	Protected	Corps MVN	St Bernard Paris	Jones
LA 1139	fair	10.87	10.87	29.9415	-89.9702		2300 Victor St mark on Wood Pole 8 ft from ground	Protected	Corps MVN	St Bernard Paris	Jones
LA 1140	fair	9.29	9.29	29.9453	-89.9645		219 Urquart mark on Wood Pole 6 ft from ground	Protected	Corps MVN	St Bernard Paris	Jones
LA 1141	fair	9.95	9.95	29.9524	-89.9616		3812 Fenelon mark on Wood Pole 6.3 ft from ground	Protected	Corps MVN	St Bernard Paris	Jones



HWM_ID	Reliability of mark	Elev NAVD88 2004.65	Elev NAVD88	Survey Latitude	Survey Longitude	Survey Comments					
LA 1142	fair	10.74	10.74	29.9352	-89.9449		2316 Despaux mark on Wood Pole 6 ft from ground	Protected	Corps MVN	St Bernard Paris	Jones
LA 1143	fair	10.01	10.01	29.9469	-89.9280		3217 Munster mark on Wood Pole 13 ft from ground	Protected	Corps MVN	St Bernard Paris	Jones
LA 1144	fair	10.51	10.51	29.9276	-89.9053		3032 Maureen mark on Wood Pole 10.72 ft from ground	Protected	Corps MVN	St Bernard Paris	Jones
LA 1145	fair	9.98	9.98	29.9102	-89.8921		3012 Lakewood mark on Metal Pole 13 ft from ground	Protected	Corps MVN	St Bernard Paris	Jones
LA 1146	fair	11.72	11.72	29.9048	-89.9002		Colonial @ 3rd mark on Metal Pole in neutral ground 10 ft from ground	Protected	Corps MVN	St Bernard Paris	Jones
LA 1147	fair	10.07	10.07	29.8792	-89.8958		Corner of River Park Dr. & STB Hwy mark on Wood Pole 4 ft from ground	Protected	Corps MVN	St Bernard Paris	Jones
LA 1148	fair	10.39	10.39	29.8689	-89.8907		2020 E Christie mark on Metal Pole 5 ft from ground	Protected	Corps MVN	St Bernard Paris	Jones
LA 1149	fair	10.84	10.84	29.8738	-89.8748		2700 Torres mark on Wood Pole 6 ft from ground	Protected	Corps MVN	St Bernard Paris	Jones
LA 1150	fair	10.88	10.88	29.8787	-89.8898		#5 South Lake Blvd mark on metal pole 7 ft from ground	Protected	Corps MVN	St Bernard Paris	Jones
LA 1151	fair	10.86	10.86	29.9103	-89.9046		Corner of Edgar & Kenneth mark on cement pole 15 ft from ground	Protected	Corps MVN	St Bernard Paris	Jones
LA 1152	fair	10.81	10.81	29.9199	-89.9120		Corner of Landry Ct & Birch St. - Parc Oaks Sub mark on metal pole 10 ft from ground	Protected	Corps MVN	St Bernard Paris	Jones
LA 1153	fair	9.81	9.81	29.9319	-89.9308		2208 Etienne mark on metal pole, 10 feet from ground	Protected	Corps MVN	St Bernard Paris	Jones
LA 1154	excellent	11.78	11.78	30.0336	-90.0409		In first building west of NAVAL Reserve just west of IHNC at Lake P. Survey mark in side room 4.88 ft above slab	Unprotected	Corps MVN	New Orleans Lake	MVN
LA 1156	fair	9.54	9.54	30.1080	-90.4239		In Frenier, on side of house facing lake. FEMA mark KLAC-03-08.	Unprotected	ERDC, LSU	Frenier	Maynard, Kemp, Garcia, Dar

HWM_ID	Reliability of mark	Elev NAVD88 2004.65	Elev NAVD88	Survey Latitude	Survey Longitude	Survey Comments					
LA 1157	good	7.3	7.30	30.1077	-90.4246		In Frenier, on foundation post on SE corner of storage building. HWM is 3.0 ft above arrow on post. Survey arrow. Arrow = 4.3 ft	Unprotected	ERDC, LSU	Frenier	Maynard, Kemp, Garcia, Dar
LA 1158	excellent	7.08	7.08	30.1067	-90.4241		In Frenier, in Quonset Hut. Moved to outside building on right side of door. Mark is at about 7.65 ft on owners gage.	Unprotected	ERDC, LSU	Frenier	Maynard, Kemp, Garcia, Dar
LA 1159	good	6.02	6.00	30.0500	-90.3678		At Marsh Hunting Club on Bayou LaBranche. Drive along levee and then along railroad track to get there. Building at back, survey concrete foundation pad at front left corner of building where painted. Two distinct HWM. Owner said Katrina higher. Katrina	Unprotected	ERDC, LSU	West Lake p	Maynard, Kemp, Garcia, Dar
LA 1160	excellent	5.75	5.75	30.0500	-90.3678	Crew did not find arrow on pipe. Elevation is for finished floor elevation.	At Marsh Hunting Club on Bayou LaBranche. Drive along levee and then along railroad track to get there. HWM moved to back NW corner of main building from inside in closet. HWM is shown by arrow on pipe on corner. Katrina mark only because Rita did not g	Unprotected	ERDC, LSU	West Lake p	Maynard, Kemp, Garcia, Dar
LA 1161	poor	15.15	15.15	30.0315	-90.0709		Levee debris, 2.44 ft below levee.	Unprotected	ERDC	Orleans	Maynard, Garcia
LA 1162	poor	14.13	14.13	30.0332	-90.0521		Lakefront levee debris, between UNO and Naval Reserve. 1.9 ft below top of levee.	Unprotected	ERDC	Orleans	Maynard, Garcia
LA 1163	fair	10.29	10.29	30.0254	-90.1194	Measured 4.15 ft above wood deck	Municipal Yacht Club, HWM on outside of east side of bldg. About 5.2 ft above wood deck.	Unprotected	ERDC	Orleans	Maynard, Garcia

HWM_ID	Reliability of mark	Elev NAVD88 2004.65	Elev NAVD88	Survey Latitude	Survey Longitude	Survey Comments					
LA 1171	good	14.28	14.28	29.9664	-90.0269		Inner Harbor Navigation Canal Lock, survey gage installed by lockmaster. Use 15 ft mark on gage. 15.0 was highest level recorded on staff gage	Unprotected	ERDC	IHNC	Maynard, Garcia
LA 1172	excellent	13.8	13.80	29.9667	-90.0269	Elevation of slab below HWM = 3.80 ft	Near Inner Harbor Navigation Canal Lock at coast guard bldg 13, SW corner, stairwell, 5.6 ft above 5th step. Survey HWM.	Unprotected	ERDC	IHNC	Maynard, Garcia
LA 1173	protected	2.4	2.4	29.9339	-90.0921	2119 Harmony. On gate, scum line is 28" above sidewalk		Protected	MVN	Orleans	Blodgett. Hickerson
LA 1174	protected	2.0	2.0	29.9426	-90.0810	1416 Simon Blvd. Mark is 10" above sidewalk.		Protected	MVN	Orleans	Blodgett. Hickerson
LA 1175	protected	2.4	2.4	29.9489	-90.0775	Girod St near Superdome. Mark is inside parking garage, 13" above concrete.		Protected	MVN	Orleans	Blodgett. Hickerson
LA 1176	protected	2.6	2.6	29.9543	-90.0813	Laboratory of Environmental Medicine. Mark is on column 37 inches above footing.		Protected	MVN	Orleans	Blodgett. Hickerson
LA 1177	protected	2.4	2.4	29.9544	-90.0813	Laboratory of Environmental Medicine. Two marks, Mark 1177A is on parking meter, 57 inches above sidewalk. Scum line is 6 inches below HWM.		Protected	MVN	Orleans	Blodgett. Hickerson
LA 1178	protected	2.6	2.6	29.9685	-90.0843	Orange Building on N Broad across from pumping station. Address may be 470 N Broad. Scum line 40 inches above parking lot.		Protected	MVN	Orleans	Blodgett. Hickerson



HWM_ID	Reliability of mark	Elev NAVD88 2004.65	Elev NAVD88	Survey Latitude	Survey Longitude	Survey Comments					
LA 1179	protected	2.6	2.6	29.9709	-90.0824	Zulu Social and Pleasure Club. Address may be 730 N Broad. Scum line 59 inches above walk on southwest side of building		Protected	MVN	Orleans	Blodgett. Hickerson
LA 1180	protected	2.7	2.7	29.9871	-90.0676	2837 AP Tureaud Ave. Mark 1180 is 69 inches above walk. Scum line is 0.7 ft below HWM.		Protected	MVN	Orleans	Blodgett. Hickerson
LA 1181	protected	2.7	2.7	29.9861	-90.0620	3518 Pauger St. Mark is on glass 64.5 inches above driveway		Protected	MVN	Orleans	Blodgett. Hickerson
LA 1182	protected	3.2	3.2	29.9861	-90.0620	3520 Pauger St. Original mark is inside garage. Mark moved outside to right door post, Mark is 71 inches above driveway		Protected	MVN	Orleans	Blodgett. Hickerson
LA 1183	protected	3.4	3.4	29.9886	-90.0587	2936 Elysian Fields. Original mark is inside bar. Mark moved outside next to window. Mark is 87 inches above wall footing, which is about 6 inches above sidewalk.		Protected	MVN	Orleans	Blodgett. Hickerson
LA 1184	protected	2.6	2.6	29.9759	-90.0587	1811 Frenchmen St. Mark is 29.5 inches above sidewalk at corner.		Protected	MVN	Orleans	Blodgett. Hickerson
LA 1185	protected	2.6	2.6	29.9716	-90.0536	1336 Spain St. Mark is 18 inches above walk.		Protected	MVN	Orleans	Blodgett. Hickerson
LA 1186	protected	2.0	2.0	29.9686	-90.0395	3423 Urquhart St. Mark is 54 inches above walk to house.		Protected	MVN	Orleans	Blodgett. Hickerson
LA 1187	protected	4.9	4.9	29.9693	-90.0334	4034 N Robertson. Mark is inside building. Mark moved outside to left window post 64 inches above ground. Scum line 37 inches below HWM.		Protected	MVN	Orleans	Blodgett. Hickerson

HWM_ID	Reliability of mark	Elev NAVD88 2004.65	Elev NAVD88	Survey Latitude	Survey Longitude	Survey Comments					
LA 1188	protected	4.8	4.8	29.9750	-90.0338	1938 Alvar St. Mark is inside building, copied to siding above door 86.5 inches above floor. Mark moved outside to 88 inches above porch. Scum line 3 ft below HWM.		Protected	MVN	Orleans	Blodgett. Hickerson
LA 1189	protected	4.8	4.8	29.9796	-90.0350	2344 Congress St. Mark is inside building, 2 inches above top of door. Mark moved outside 119 inches above ground on corner of house. Scum line 38 inches below HWM.		Protected	MVN	Orleans	Blodgett. Hickerson
LA 1190	protected	5.3	5.3	29.9818	-90.0372	2518 Louisa St. Mark is inside building, 89 inches above floor. Mark moved outside 131 inches above ground. Scum line 31 inches below HWM.		Protected	MVN	Orleans	Blodgett. Hickerson
LA 1191	protected	1.8	1.8	30.0048	-90.0525	4484 Painters St. Mark is 14 inches up fireplace curtain. Mark moved outside 5 inches above outside walk. Scum line 1 inch below HWM.		Protected	MVN	Orleans	Blodgett. Hickerson
LA 1192	protected	2.9	2.9	30.0120	-90.0638	5158 Cameron St. Mark is 74 inches above front porch. Mark 1192B is scum line 15 inches below HWM.		Protected	MVN	Orleans	Blodgett. Hickerson
LA 1193	protected	2.6	2.6	30.0121	-90.0726	5363 Chatham Drive. Mark 1193 is 90.5 inches above front walk.		Protected	MVN	Orleans	Blodgett. Hickerson
LA 1194	protected	2.8	2.8	30.0144	-90.0793	1360 Mendez Drive. Mark is 85.5 inches above front porch.		Protected	MVN	Orleans	Blodgett. Hickerson

HWM_ID	Reliability of mark	Elev NAVD88 2004.65	Elev NAVD88	Survey Latitude	Survey Longitude	Survey Comments					
LA 1195	protected	2.8	2.8	30.0065	-90.0828	4840 St Bernard Ave. Mark is inside building, 62 inches above subfloor. Scum line 24 inches below HWM.		Protected	MVN	Orleans	Blodgett. Hickerson
LA 1196	protected	2.8	2.8	30.0124	-90.0961	City Park Equine Center. Mark is 68.5 inches above concrete walk at entrance.		Protected	MVN	Orleans	Blodgett. Hickerson
LA 1197	protected	2.9	2.9	29.9995	-90.0984	City Park Marconi Meadows. Mark on outside refrigerator, 54 inches above slab.		Protected	MVN	Orleans	Blodgett. Hickerson
LA 1198	protected	2.1	2.1	29.9906	-90.0933	City Park Bayou Oaks Golf Club. Mark is 47 inches above ground on left side of entrance. Scum line 0.7 ft below HWM.		Protected	MVN	Orleans	Blodgett. Hickerson
LA 1199	protected	3.4	3.4	30.0052	-90.1035	6327 Marshall Foch St. Mark is 96 inches above ground, 5 inches above soffit.		Protected	MVN	Orleans	Blodgett. Hickerson
LA 1200	protected	3.4	3.4	30.0102	-90.1133	6546 Catina St. Mark is inside building, copied outside, 84.5 inches above entry floor at top of left door post. Scum line is 24 inches below HWM.		Protected	MVN	Orleans	Blodgett. Hickerson
LA 1201	protected	3.4	3.4	30.0060	-90.1198	331 Harrison St, Acrus Electrolux. Mark is 103.5 inches above inside floor. Scum line is 26 inches below HWM.		Protected	MVN	Orleans	Blodgett. Hickerson
LA 1202	protected	3.2	3.2	29.9918	-90.1101	620 Hopedale St. Mark is in stairwell 79 inches above floor, about 7 inches above outside walk. Scum line 1.8 ft below HWM.		Protected	MVN	Orleans	Blodgett. Hickerson



HWM_ID	Reliability of mark	Elev NAVD88 2004.65	Elev NAVD88	Survey Latitude	Survey Longitude	Survey Comments					
LA 1203	protected	2.6	2.6	29.9738	-90.1019	4110 Cleveland Ave. Mark is 65 inches above ground.		Protected	MVN	Orleans	Blodgett. Hickerson
LA 1204	protected	2.5	2.5	29.9673	-90.1133	8338 Stroelitz St. Mark is 63.5 inches above ground.		Protected	MVN	Orleans	Blodgett. Hickerson
LA 1205	protected	2.5	2.5	29.9691	-90.1203	8936 Olive. Mark is 64 inches above ground.		Protected	MVN	Orleans	Blodgett. Hickerson
LA 1206	protected	2.5	2.5	29.9719	-90.1199	9129 Airline Highway. Mark is on downspout 84 inches above ground. Scum line is 6 inches below HWM.		Protected	MVN	Orleans	Blodgett. Hickerson
LA 1207	protected	2.4	2.4	29.9749	-90.1402	206 Maple Ridge Dr. Mark is 43.5 inches above porch.		protected	MVN	Orleans	Blodgett. Hickerson
LA 1208	protected	2.5	2.5	29.9810	-90.1398	409 Ridgewood Drive. Mark is on front window, 44.5 inches above ground.		protected	MVN	Orleans	Blodgett. Hickerson
LA 1209	protected	2.5	2.5	29.9530	-90.1083	4100 Vendome St. Mark copied to left post 54 inches above ground. Scum line is 8 inches below HWM.		protected	MVN	Orleans	Blodgett. Hickerson
LA 1210	protected	4.4	4.4	29.9970	-90.0347	3756 Louisa St. Mt Kingdom Church. Mark inside building 86 inches above floor, moved outside. Scum line 30 inches below HWM.		protected	MVN	Orleans	Blodgett. Hickerson
LA 1211	protected	4.5	4.5	29.9874	-90.0366	2926 Louisa St. Mark is 120 inches above ground. Scum line at 34 inches below HWM.		protected	MVN	Orleans	Blodgett. Hickerson
LA 1212	protected	4.4	4.4	29.9825	-90.0374	3240 Law St, Johnson Lockett Public School. Mark at 89.5 inches above porch. Scum lime 23 inches below HWM.		protected	MVN	Orleans	Blodgett. Hickerson

HWM_ID	Reliability of mark	Elev NAVD88 2004.65	Elev NAVD88	Survey Latitude	Survey Longitude	Survey Comments					
LA 1213	protected	3.6	3.6	29.9805	-90.0465	2211 Almonaster St. Mark is 49 inches above porch. Scum line 22 inches below HWM.		protected	MVN	Orleans	Blodgett, Hickerson
LA 1214	protected	3.5	3.5	29.9892	-90.0495	2940 Franklin St, Vic's Auto Glass. Mark is 96.5 inches above front walk. Scum line 12 inches below HWM.		protected	MVN	Orleans	Blodgett, Hickerson
LA 1215	protected	2.9	2.9	30.0192	-90.0478	6422 Peoples. Seed line at front door, 107 ft above driveway. Mark is 19 inches above oil line.		protected	ERDC & MVN	Orleans	Maynard, Biedenham, Powell
LA 1216	protected	2.2	2.2	30.0163	-90.0449	5544 St Ferdinand. Seed line on eave on right side of house, 94 to 95 inches above ground.		protected	ERDC & MVN	Orleans	Maynard, Bienenham, Powell
LA 1217	protected	3.6	3.6	29.9927	-90.0451	House at corner of Peoples and Edge. No house number. Mark on door frame on inside of front door to the left. Mark is 89 inches above step to the door		protected	ERDC & MVN	Orleans	Maynard, Bienenham, Powell
LA 1218	protected	4.1	4.1	29.9851	-90.0421	2930 Florida Ave		protected	ERDC & MVN	Orleans	Maynard, Bienenham, Powell
LA 1219	protected	11.9	11.9	29.2595	-89.3629	Miswaco Venice II Warehouse, McDermott Rd, Mark on wall in northeast corner of closet in office.		protected	USGS	Plaquemines	MLD JRF
LA 1220	protected	11.9	11.9	29.3399	-89.4960	Chevron Pipeline Co, Buras District. Corner of pipeline and Hwy 11. Seedline 13 ft 9 in above ground in front stairwell facing road.		protected	USGS	Plaquemines	MLD JRF

HWM_ID	Reliability of mark	Elev NAVD88 2004.65	Elev NAVD88	Survey Latitude	Survey Longitude	Survey Comments					
LA 1221	protected	13.7	13.7	29.3535	-89.5258	Burras High School, Hwy 11. Mark is 13 ft above 1 <sup>st</sup> floor in stairwell behind main entrance on north side of building.		protected	USGS	Plaquemines	MLD JRF
LA 1222	protected	13.7	13.7	29.3545	-89.5271	Old Buras Auditorium, Hwy 11. Mark is 7 ft above stairwell landing in front northwest stairwell of building.		protected	USGS	Plaquemines	MLD JRF
LA 1223	protected	13.9	13.9	29.3583	-89.5320	Buras Volunteer Fire Dept, Hwy 11. Mark is 2 inches from baseboard of south door jam in south stairwell to 2 <sup>nd</sup> floor.		protected	USGS	Plaquemines	MLD JRF
LA 1224	protected	15.3	15.3	29.3688	-89.5358	Buras Middle School, Hwy 11. Mark is about 2 ft above 2 <sup>nd</sup> floor in closet above southwest stairwell of auditorium.		protected	USGS	Plaquemines	MLD JRF
LA 1225	protected	16.2	16.2	29.3939	-89.6031	Water Treatment Plan, Hwy 11. Mark is about 3 ft above 2 <sup>nd</sup> floor in northwest corner of 2 <sup>nd</sup> floor.		protected	USGS	Plaquemines	MLD JRF
LA 1226	protected	14.7	14.7	29.4486	-89.6282	Delta Outboard Sales and Service, Hwy 23. Mark is in southeast corner of loft near south side entrance.		protected	USGS	Plaquemines	MLD JRF
LA 1227	Fair	9.54	9.54	29.9889	90.0677	Debris HWM between railroad rails crossing London Canal just north of pump station OP#3, HWM at bottom of rail, east side of station.	On this revisit to LA 1018A, the collectors believe the mark to be a minimum of 0.8 ft higher than the original mark. This mark is not intended to replace the original mark, only to provide an additional observation.	Unprotected	ERDC	London Canal-OP#3	Maynard, Garcia
LA 1228	Fair	10.04	10.04	29.9891	90.0682	Debris HWM on railroad floodgate on west side of pump station OP#3 discharge area.		Unprotected	ERDC, Vicksburg District	London Canal-OP#3	Maynard, Goldman, Smith



HWM_ID	Reliability of mark	Elev NAVD88 2004.65	Elev NAVD88	Survey Latitude	Survey Longitude	Survey Comments					
LA 1229	excellent	11.01	11.01	29.8631	89.9083	Inside Office on South side of building, about 4" below top of door.		Unprotected	ERDC, LSU	St Bernard E-W Levee	Maynard, Kemp
LA 1231	fair	10.67	10.67	29.8581	89.9055	HWM on south side of levee	Forest away from levee	Unprotected	ERDC, LSU	St Bernard E-W Levee	Maynard, Kemp
LA 1233	fair	10.43	10.43	29.8541	89.9037	HWM on south side of levee	Forest away from levee	Unprotected	ERDC, LSU	St Bernard E-W Levee	Maynard, Kemp
LA 1235	fair	10.48	10.48	29.8540	89.8975	HWM on south side of levee	Open	Unprotected	ERDC, LSU	St Bernard E-W Levee	Maynard, Kemp
LA 1237	fair	11.87	11.87	29.8540	89.8895	HWM on south side of levee	Open	Unprotected	ERDC, LSU	St Bernard E-W Levee	Maynard, Kemp
LA 1239	fair	11.80	11.80	29.8540	89.8859	HWM on south side of levee	Open	Unprotected	ERDC, LSU	St Bernard E-W Levee	Maynard, Kemp
LA 1241	fair	12.04	12.04	29.8540	89.8712	HWM on south side of levee	open	Unprotected	ERDC, LSU	St Bernard E-W Levee	Maynard, Kemp
LA 1243	fair	10.59	10.59	29.8540	89.8561	HWM on south side of levee	open	Unprotected	ERDC, LSU	St Bernard E-W Levee	Maynard, Kemp
LA 1245	fair	11.71	11.71	29.8541	89.8378	HWM on south side of levee	open	Unprotected	ERDC, LSU	St Bernard E-W Levee	Maynard, Kemp
LA 1246	fair	12.91	12.91	29.8541	89.8254	HWM on south side of levee	open	Unprotected	ERDC, LSU	St Bernard E-W Levee	Maynard, Kemp
LA 1247	fair	13.66	13.66	29.8541	89.8183	HWM on south side of levee	open	Unprotected	ERDC, LSU	St Bernard E-W Levee	Maynard, Kemp
LA 1250	fair	12.26	12.26	29.8553	89.7799	HWM on south side of levee	open	Unprotected	ERDC, LSU	St Bernard E-W Levee	Maynard, Kemp
LA 1251	fair	10.90	10.90	29.9871	90.1248	Debris HWM in crack on SW corner of discharge area 26" below top of floodwall which is at elev 13.1 ft.		Unprotected	ERDC	17th Street Canal-OP#6	Maynard
LA 1252	good	11.10	11.10	29.9871	90.1238	Debris HWM on top of gate rods on east side of station. 2.1 ft below floodwall that is at elevation 13.2 ft at this location.		Unprotected	ERDC	17th Street Canal-OP#6	Maynard
LA 1253	excellent	11.80	11.80	30.0360	90.0256	High water mark inside Room 105, 3.35 feet above floor	No picture, based on surveyed floor elevation of 8.45 ft.	Unprotected	ERDC & Task 6	Lakefront Airport	Maynard, Bergen

HWM_ID	Reliability of mark	Elev NAVD88 2004.65	Elev NAVD88	Survey Latitude	Survey Longitude	Survey Comments					
LA 1254	excellent	14.20	14.20	30.0024	90.0276	HWM in Control Room of Boh Bros on west side of IHNC just south of I-10. mark is 26" above floor.		Unprotected	ERDC	IHNC west	Maynard, Abraham
LA 1255	excellent	14.17	14.17	30.0029	90.0281	HWM in shed with sheet metal room of Boh Bros on west side of IHNC just south of I-10. mark is on wall near roof.		Unprotected	ERDC	IHNC west	Maynard, Abraham
LA 1256	excellent	14.28	14.28	30.0029	90.0281	HWM#3 in shed with sheet metal room of Boh Bros on west side of IHNC just south of I-10. mark is on wall near roof.		Unprotected	ERDC	IHNC west	Maynard, Abraham
LA 1257	excellent	14.25	14.25	30.0029	90.0281	HWM#2 in shed with sheet metal room of Boh Bros on west side of IHNC just south of I-10. mark is on wall near roof.		Unprotected	ERDC	IHNC west	Maynard, Abraham
LA 1258	excellent	14.19	14.19	30.0027	90.0277	HWM inside yellow freight container at Boh Bros just below ceiling.		Unprotected	ERDC	IHNC west	Maynard, Abraham
LA 1259	excellent	14.34	14.34	29.9992	90.0262	HWM inside office in trailer at Mechanical Equipment Co. Mark moved to outside of building		Unprotected	ERDC	IHNC west	Maynard, Abraham
LA 1260	excellent	15.42	15.42	29.9897	90.0230	HWM on unprotected (east) side of Port of New Orleans floodwall in storage room at back of mens restroom 5.44 ft above slab.	unprotected side of USACE protection	Unprotected	ERDC	IHNC west	Maynard, Abraham
LA 1261	excellent	14.32	14.32	29.9917	90.0236	HWM on protected (west) side of Port of New Orleans floodwall in 2nd stall at back of mens restroom 3.4 ft above slab.	unprotected side of USACE protection	Unprotected	ERDC	IHNC west	Maynard, Abraham

HWM_ID	Reliability of mark	Elev NAVD88 2004.65	Elev NAVD88	Survey Latitude	Survey Longitude	Survey Comments					
LA 1262	excellent	14.27	14.27	29.9873	90.0222	HWM on protected (west) side of Port of New Orleans floodwall in storage room at back of mens restroom 3.22 ft above slab.	unprotected side of USACE protection	Unprotected	ERDC	IHNC west	Maynard, Abraham
LA 1263	excellent	14.05	14.05	29.9885	90.0253	HWM on protected (west) side of Port of New Orleans floodwall in paper storage warehouse at 4.2 ft above slab in closet.	unprotected side of USACE protection	Unprotected	ERDC	IHNC west	Maynard, Abraham
LA 1264	excellent	14.10	14.10	29.9937	90.0256	HWM on protected (west) side of Port of New Orleans floodwall in Container Freight Station, Inc warehouse at 4.32 ft above slab in closet.	unprotected side of USACE protection	Unprotected	ERDC	IHNC west	Maynard, Abraham



### Plate 1-3. Spreadsheet of High Water Marks for Mississippi

HWM ID	HWM Address	Flaggers Original HWM Surface - RAW	County	Type of HWM	HWM Object	Location_Directions to HWM Object_RAW	Type of Marker RAW	Reliability of mark for surge	NAVD-88	Survey Latitude	Survey Longitude	Survey Comments
KMS_USGS_100	Pascagoula River at Gulf side of I-10 east bridge end	Not Provided By USGS	Jackson	Seed and drift	Bridge	Centerline at east end of eastbound lane bridge	Centerline	poor	11.6	30.4382	-88.5499	Shot seed line
KMS_USGS_16	Old Fort Bayou at I-10	Not Provided By USGS	Jackson	Seed Line	Bridge	Downstream right (southwest) end of eastbound I-10 bridge crossing Old Fort Bayou, about 1,600 ft west of I-10/SR 57 interchange	Top of handrail	poor	14.4	30.4431	-88.7221	Debris line
KMS_USGS_17	West Pascagoula River at Gulf side of I-10 West bridge end	Not Provided By USGS	Jackson	Debris Line	Bridge	West end of eastbound lane bridge	Centerline	poor	17.3	30.4375	-88.6174	Shot debris line
KMS_USGS_18	West Pascagoula River at Inland side of I-10 West bridge end	Not Provided By USGS	Jackson	Debris Line	Bridge	East end of eastbound lane bridge	Centerline	poor	16.8	30.4374	-88.6173	Shot debris line
KMS_USGS_21	Pascagoula River at SR 614 (34.4 mi upstream of mouth)	Not Provided By USGS	Jackson	Gage reading from first peak on stage hydro-graph	Bridge	Top of wheel guard at upstream side of right (west) bridge abutment (elev. 59.665 ft--5/22/94 GPS survey)	NOAA/NOS Tidal BM "2187A"	poor	15.4	30.6106	-88.6417	Shot hydrograph line
KMS_USGS_88	Fraziers Nursery and Florist on Lemoyne Blvd., West of Hwy 609 on Ocean Springs Quad.	Not Provided By USGS	Jackson	Seed Line	Pole	Far left front pole holding up awning in front of Fraziers Nursery and Florist	Threaded bolt	poor	21.4	30.4434	-88.8549	Mark on window @ front door
KMS_USGS_89	Corner of Washington Avenue and Calhoun st., South of Catholic church on Ocean Springs Quad.	Not Provided By USGS	Jackson	Seed Line	Power pole	2 ft above ground into power pole just North of Yellow and white house at corner of Washington Ave. and Calhoun St.	Nail	poor	21.3	30.4090	-88.8281	Seed line on exterior wall

HWM ID	HWM Address	Flaggers Original HWM Surface - RAW	County	Type of HWM	HWM Object	Location_Directions to HWM Object_RAW	Type of Marker RAW	Reliability of mark for surge	NAVD-88	Survey Latitude	Survey Longitude	Survey Comments
KMS_USGS_90	House no. 16 on side street off of road leading to Gulf Coast Research Lab On Ocean Springs Quad.	Not Provided By USGS	Jackson	Seed/Water Line	Tree	Large oak tree in front lawn of Blue house no. 16	Nail	good	20.68	30.4002	-88.7986	Mark on window
KMS_USGS_91	House no. 1000 on Magnolia Bayou Blvd.North of Heron Bayou, on Ocean Springs Quad.	Not Provided By USGS	Jackson	Seed/Water Line	Tree	North side of oak tree on the South side of House no. 1000 Near garage entrance	Nail	poor	20	30.4029	-88.7771	Mark on wall inside garage @ window
KMS_USGS_92	House no. 2720 at corner of Beachview Dr. and Spring Avenue on the bottom right of Ocean Springs Quad.	Not Provided By USGS	Jackson	Water Lines	Tree	North side of oak tree in the front lawn of House No. 2720	Nail	poor	19.1	30.3816	-88.7593	Water mark on wallboard inside foyer
KMS_USGS_94	Old Fort Bayou (02481299) at SR 609 (Washington Ave)	Not Provided By USGS	Jackson	Seed Line	Concrete pier footer	Top of concrete pier footer below gage junction box at control tower	Not Provided By USGS	poor	20.4	30.4192	-88.8281	Red mark on gear housing
KMS_USGS_99	Pascagoula River at I-10 east bridge end	Not Provided By USGS	Jackson	Seed Line	Bridge	Centerline at east end of eastbound lane bridge	Centerline	poor	11.9	30.4382	-88.5505	Chalk mark on column
KMSC-02-01	3807 Torres Ave.	House piling	Jackson	Water Line	House piling	South side of stairs , west porch piling	Duct tape on house piling	fair	13.6	30.4166	-88.5471	Shot duct tape on wood pile
KMSC-02-02	4806 Ridgewood Dr.	Exterior wall of garage	Jackson	Water Line	Exterior wall of garage	Looking south, east side of garage door	Duct tape	fair	14.6	30.4126	-88.5698	Shot bottom of duct tape
KMSC-02-03	5037 Pecan St.	Front Porch Column	Jackson	Water Line	Front Porch column	Looking west, north front porch column	Duct tape	fair	13	30.4146	-88.5046	Shot bottom of duct tape
KMSC-02-05	3132 W. Rollins	Lawn	Jackson	Debris Line	Lawn	Flagged stake east side of house on lawn	Flagged stake	poor	12.8	30.4043	-88.5571	Shot ground at wood stake

HWM ID	HWM Address	Flaggers Original HWM Surface - RAW	County	Type of HWM	HWM Object	Location_Directions to HWM Object_RAW	Type of Marker RAW	Reliability of mark for surge	NAVD-88	Survey Latitude	Survey Longitude	Survey Comments
KMSC-02-06	3913 Griffin St.	Exterior wall	Jackson	Water Line	Exterior wall	Front of house looking west	Duct tape	fair	14.7	30.3979	-88.5524	Shot bottom of duct tape
KMSC-02-07	6300 Gardenia St.	Front exterior	Jackson	Water Line	Exterior wall	Looking south, west end of house	Duct tape	fair	12.1	30.4097	-88.5040	Shot bottom of duct tape
KMSC-02-08	7731 Albert Dr.	Exterior wall, SE side	Jackson	Water Line	Exterior wall, S.E. side	NE side of house near garage entrance	Duct tape	good	11.5	30.4119	-88.4799	Shot bottom of duct tape
KMSC-02-09	4435 Blackwell St.	East side of house, front at north end	Jackson	Water Line	East side of house, front at north end	Looking west, north end of house	Duct tape on front of house	good	11.7	30.4059	-88.4876	Shot bottom of duct tape
KMSC-02-10	5601 Sound Bluff Rd.	Exterior wall	Jackson	Water Line	Exterior wall	Looking south, toward center of house	Duct tape	fair	20.5	30.3442	-88.7023	Shot ground at mark
KMSC-02-11	4920 Beach St. (Fountainebleau Vol. Fire Dept.)	South wall of Fire Station, approx. midway	Jackson	Water Line	Exterior wall	Looking NE at front of Fire Station	Duct tape	fair	16.9	30.3558	-88.6919	Shot ground at mark
KMSC-02-12	1322 Dorothy St.	SW corner of garage	Jackson	Water Line	Exterior garage door	Looking NE towards garage doors	Duct tape	fair	18.4	30.3613	-88.6991	Shot surface of concrete drive at mark
KMSC-02-13	1201 Oak St.	Exterior wall, front of house	Jackson	Water Line	Exterior wall, front of house	Looking toward front of house, left side of door next to shutter.	Duct tape	good	19	30.3587	-88.7092	Shot ground next to porch
KMSC-02-14	413 Inverness Court	Exterior wall, front of garage door, south end of house	Jackson	Water Line	Exterior wall, front of garage door	Looking at front	Duct tape	good	19.9	30.3483	-88.7119	Shot driveway at mark
KMSC-02-15	7112 Pinehurst Dr.	Front of house, exterior wall	Jackson	Water Line	Exterior wall	Looking east at front of house, north side of front door	Duct tape	fair	19.2	30.3681	-88.7278	Shot porch slab
KMSC-02-16	5800 Olde Oak View	Exterior wall between garage doors	Jackson	Water Line	Exterior wall between garage doors	Looking NW toward garage doors, standing on driveway	Duct tape	good	19.4	30.3769	-88.7043	Shot driveway slab



HWM ID	HWM Address	Flaggers Original HWM Surface - RAW	County	Type of HWM	HWM Object	Location_Directions to HWM Object_RAW	Type of Marker RAW	Reliability of mark for surge	NAVD-88	Survey Latitude	Survey Longitude	Survey Comments
KMSC-02-30	5940 Shingle Mill Rd.	Exterior brick wall	Jackson	Water Line	Exterior brick wall	Looking at north end of house, duct tape on southwest corner	Duct tape	fair	10.6	30.4289	-88.4623	Shot bottom of duct tape
KMSC-02-31	10808 Pecan St.	Exterior brick wall	Jackson	Water Line	Exterior brick wall	Looking west toward house, duct tape on north side of door	Duct tape	fair	14.2	30.4434	-88.4291	Shot bottom of duct tape
KMSC-02-32	2615 Convent Ave.	Front exterior wall	Jackson	Water Line	Exterior wall	Looking toward front of house, west end of garage exterior wall	Duct tape	good	16	30.3641	-88.5353	Shot bottom of duct tape
KMSC-02-33	3917 Sherwood Dr.	Exterior wall under carport between doors	Jackson	Water Line	Exterior wall under carport between doors	Looking west toward house. Exterior wall storage room door	Duct Tape	fair	14.4	30.3737	-88.5216	Shot bottom of duct tape
KMSC-02-34	814 13th St.	Exterior wall	Jackson	Water Line	Exterior wall	Looking east front exterior brick wall	Duct tape	good	16.6	30.3469	-88.5402	Shot bottom of duct tape
KMSC-02-40	3228 Willis Dr.	Water line 11'8" above ground	Jackson	Water Line	Exterior wall	Looking SE toward house, HWM located at back corner of the house 11'8" above ground.	See photo	fair	15.2	30.3885	-88.6146	Shot ground at duct tape
KMSC-03-05	1590 Collin J. Mcrae Rd.	Interior wall transferred to exterior column on front porch	Jackson	Mud Line	Interior wall transferred to exterior column on front porch	Front porch of 1590 Collin J. Mcrae Rd., on column to left of front entry	Tape	Fair	21.1	30.3648	-88.6320	Shot bottom of duct tape
KMSC-03-06	115 Halstead Rd.	On the garage door	Jackson	Mud Line	Garage door	115 Halstead Rd., east side of temporary garage door (Plywood)	Duct tape	poor	19.9	30.3962	-88.8001	Shot bottom of duct tape
KMSC-03-10	Empty lot near end of Clamshell Ave.	On ground	Jackson	Wrack Line	Ground	Right side at end of Clamshell Road, in front of empty lot	Wood stake	Fair	18.2	30.3579	-88.7380	Shot ground at wood stake
KMSC-03-11	8908 Mermaid Rd	Interior wall transferred to exterior	Jackson	Mud Line	Interior wall transferred to exterior wall	S.E. corner of house, east side of garage door	Tape on wall	excellent	18.6	30.3628	-88.7581	Shot bottom of duct tape

HWM ID	HWM Address	Flaggers Original HWM Surface - RAW	County	Type of HWM	HWM Object	Location_Directions to HWM Object_RAW	Type of Marker RAW	Reliability of mark for surge	NAVD-88	Survey Latitude	Survey Longitude	Survey Comments
KMSC-03-12	3108 Magnolia Ln.	Interior wall transferred to exterior pile	Jackson	Mud Line	Interior wall transferred to exterior pile	South side of house on Marina Ave.	Duct tape	excellent	18.8	30.3867	-88.7706	Shot bottom of duct tape
KMSC-03-13	12000 Poin Auxchenes Rd.	Exterior wall	Jackson	Mud Line	Exterior wall	On side of garage door	Duct tape	Fair	20.4	30.3721	-88.7793	Shot bottom of duct tape
KMSC-03-14	111 Port Rd.	Exterior wall transferred from interior	Jackson	Mud Line	Exterior wall transferred from interior	South side of office building, west of front entry	Tape	good	17	30.3621	-88.5680	Shot bottom of duct tape
KMSC-06-11	Exit #57 going east on I-10	Ground	Jackson	Wrack Line	Ground	HWM is 77 feet from birm	Stake w/pink flag & white paint	poor	15.3	30.4408	-88.7170	Shot ground at wood stake
KMSC-06-13	423 East Beach Dr.	Wood siding	Jackson	Water Line	Exterior wall	N.W. corner of house, on wood siding	Duct tape with permanent marker	good	20.8	30.3967	-88.8125	Shot bottom of duct tape
KMSC-06-14	402 Maginnis Ave.	Exterior wall transferred to exterior wall located in front porch	Jackson	Water Line	Exterior wall transferred to exterior wall located in front porch	N.E. corner of porch	Duct tape with permanent marker	good	21.4	30.4109	-88.8381	Shot bottom of duct tape
KMSC-06-15	1215 Harbor Rd.	Exterior wall inside porch	Jackson	Water Line	Exterior wall inside porch	S.E. corner of entry way. HWM on wood wall	None	good	20.5	30.4062	-88.8240	Shot top of planter box
KMSC-06-16	102 Boise Bryant Lane	Interior HWM transferred to exterior column on north side of home	Jackson	Water Line	Interior wall transferred to exterior column	First Column on left side when walking up backyard steps	Duct tape with Black permanent marker	excellent	20.7	30.4229	-88.8463	Shot bottom of duct tape
KMSC-06-17	3600 Gollott Rd	Exterior wall	Jackson	Water Line	Exterior wall	Bottom left of gray block next to exterior wall	Duct tape w/ black permanent marker	Fair	18.9	30.3928	-88.7813	Shot bottom of duct tape
KMSC-06-18	120 Watersedge Dr.	Exterior door	Jackson	Water Line	Exterior door	HWM located on white main entrance door	Duct tape with black permanent marker	good	20.1	30.3963	-88.8059	Shot brick(duct tape gone)

HWM ID	HWM Address	Flaggers Original HWM Surface - RAW	County	Type of HWM	HWM Object	Location_Directions to HWM Object_RAW	Type of Marker RAW	Reliability of mark for surge	NAVD-88	Survey Latitude	Survey Longitude	Survey Comments
KMSC-06-19	211 Wheaton Ct.	Doorway, west side of home	Jackson	Personal Account	Doorway, west side of home	Exterior slab at west side doorway near carport	Duct tape with permanent black marker	Fair	22.4	30.4047	-88.8087	Shot bottom of duct tape
KMSC-06-21	114 Braeburn Dr.	Window	Jackson	Water Line	Window	First window to the left of front door	None	poor	17.1	30.3575	-88.7158	Shot porch slab
KMSC-06-22	6804 Ocean Springs Rd.	NE post of deck on 2nd floor	Jackson	Water Line	Post	Back of house, 2nd floor deck	Duct tape with black permanent marker	good	16.4	30.4411	-88.7228	Shot tape on deck railing
KMSC-06-23	6808 Ocean Springs Rd.	Interior wall transferred to exterior west railing	Jackson	Water Line	Interior wall transferred to exterior railing	W. side corner of 2nd floor deck	Duct tape with pink and permanent black marker	excellent	16.4	30.4411	-88.7228	Shot tape on deck railing
KMSC-06-24	6812 Ocean Springs Rd.	South exterior main door transferred to south exterior wall	Jackson	Water Line	Exterior main door transferred to exterior wall	Wall located to the east of steps to main entrance	Duct tape with pink flag and permanent black marker	good	16.1	30.4416	-88.7232	Shot duct tape on side of house
KMSC-06-25	7004 Ocean Springs Rd.	Exterior corner of most northern garage door	Jackson	Water Line	Exterior garage door	East side of house, top right corner of garage door to the north	Duct tape with pink flag and permanent black marker	poor	18.1	30.4401	-88.7250	Shot duct tape on corner of house
KMSC-07-01	13347 Pascagoula St. (Chateau Tourraine Apt.)	Exterior wall	Jackson	Water Line	Exterior wall	Apartment Building exterior East from Pascagoula St.	Tape	good	16.9	30.3518	-88.5533	Shot bottom of duct tape
KMSC-07-02	1340 S. Market St., (Thunders Tavern)	Exterior wall, in front of business	Jackson	Water Line	Exterior wall, front of business	Exterior wall on the north side of the tavern	Tape	good	16.8	30.3516	-88.5481	Shot point 3.64' above finished floor
KMSC-07-03	Washington St. and Pascagoula St.	Water line on exterior wall	Jackson	Water Line	Exterior wall	Exterior wall in front of home	Duct tape	good	18	30.3450	-88.5538	Shot bottom of duct tape
KMSC-07-04	2101 Choctaw Avenue	Exterior wall in front of home	Jackson	Water Line	Exterior wall in front of home	Intersection Choctaw Ave. and 11th St./Water line on exterior wall in front of home	Duct tape	Fair	17.2	30.3477	-88.5429	Shot point 7.6' above finished floor
KMSC-07-05	805 Warren St.	Water line on exterior wall	Jackson	Water Line	Exterior wall	Exterior wall in front of home, next to front door	Duct tape	Fair	17.3	30.3463	-88.5332	Shot bottom of duct tape



HWM ID	HWM Address	Flaggers Original HWM Surface - RAW	County	Type of HWM	HWM Object	Location_Directions to HWM Object_RAW	Type of Marker RAW	Reliability of mark for surge	NAVD-88	Survey Latitude	Survey Longitude	Survey Comments
KMSC-07-06	2502 Ingalls Ave. (Eastlawn United Methodist Church)	Water line on exterior wall	Jackson	Water Line	Exterior wall	Exterior wall in front of the church, next to the chapel	Duct tape	good	16.6	30.3547	-88.5371	Shot bottom of duct tape
KMSC-07-07	4401 Washington Ave.	Exterior wall	Jackson	Water Line	Exterior wall	Exterior wall in front of home	Duct tape	good	16.8	30.3468	-88.5173	Shot bottom of duct tape
KMSC-07-08	3721 Mercier St.	Exterior wall	Jackson	Water Line	Exterior wall	Exterior wall next to garage, SE corner of house	Tape	good	16.2	30.3540	-88.5219	Shot bottom of duct tape
KMSC-07-09	2003 Roosevelt	Exterior wall	Jackson	Water Line	Exterior wall	Exterior wall in front of home	Duct tape	poor	20	30.3562	-88.5574	Shot bottom of duct tape
KMSC-07-10	520 Watts Ave. (Resurrection Catholic School)	Water line on exterior wall	Jackson	Water Line	Exterior wall	Main entrance hallway, facing South.	Duct tape	good	16.7	30.3660	-88.5598	Shot bottom of duct tape
KMSC-07-11	525 Spanish Dr.	Water line on exterior wall	Jackson	Water Line	Exterior wall	Exterior wall in front of home 75' S. from front door	Duct tape	Fair	14.9	30.3798	-88.5589	Shot bottom of duct tape
KMSC-07-27	3304 Oak St.	On an interior wall transferred to the exterior of camper, camper stands on a concrete slab	Jackson	Water Line	Interior wall transferred to exterior wall	6'3" Above concrete slab	Tape, paint on concrete slab	excellent	14.4	30.3892	-88.6128	Shot ground near X mark on slab
KMSC-07-28	701 Homestill Blvd.	Ground	Jackson	Personal Account	Ground	33'8" from utility pool, 5' 10" from gravel pavement	Stake	poor	19.5	30.4157	-88.6201	Shot ground at wood stake
KMSC-08-02	6005 Bayou Heron Rd.	Grass, ground at edge of parking area and in trees.	Jackson	Wrack Line	Ground	Take Bayou Heron Rd., to dead end at boat ramp, look for stake 280 degrees west.	Fema stake with red ribbon and red paint on road	poor	18.7	30.4131	-88.4033	Shot ground near tree
KMSC-08-03	6005 Bayou Heron Rd.	Roof	Jackson	Wrack Line	Roof	Take Bayou Heron Rd. to dead end. Shed on right side of road.	Duct tape with arrow points to roof just above wood column where debris rest from flood	poor	19.1	30.4123	-88.4038	Shot point 15' above slab
KMSC-08-05	1600 Indian pkwy.	Glass	Jackson	Wrack Line	Glass	Overflow trailer parking #9/of 9 Fema stake with red ribbon	Red ribbon on FEMA stake	Fair	14.5	30.4082	-88.6300	Shot ground at wood stake

HWM ID	HWM Address	Flaggers Original HWM Surface - RAW	County	Type of HWM	HWM Object	Location_Directions to HWM Object_RAW	Type of Marker RAW	Reliability of mark for surge	NAVD-88	Survey Latitude	Survey Longitude	Survey Comments
KMSC-08-06	1600 Indian Point pkwy.	Interior wall moved to exterior wall	Jackson	Mud Line	Interior wall transferred to exterior wall	Take I-10 to exit 61. Turn south toward Gautier, go approx. 1.75 miles to Indian Point Rd., in the let and follow Indian Point on the right side.(club house)	Duct tape on glass front door	excellent	14.3	30.4059	-88.6345	Shot bottom of tape
KMSC-08-07	7116 Ocean Springs Rd.	Right side front door	Jackson	Personal Account	Exterior door	West side home, right side front door, duct tape stake	Duct tape next to front door	Fair	14.6	30.4381	-88.7283	Shot bottom of tape
KMSC-08-08	36 Davis Bayou Dr.	Pole near wood fence-stake with red ribbon	Jackson	Mud Line	Pole near wood fence	North side near wood fence- duct tape stake	Duct tape	poor	17.7	30.4073	-88.7512	Shot bottom of tape
KMSC-08-09	3000 Magnolia Ln.	Garage door	Jackson	Mud Line	Garage door	Right side of garage door	Duct tape	poor	18.1	30.3849	-88.7739	Shot bottom of tape
KMSC-08-10	8201 Fountain Rd.	Slab in front of the house	Jackson	Personal Account	Concrete slab	8201 Fountain Rd. off of Fountain Blvd. after turns in from Government St.	Stake in ground	Fair	19.4	30.3822	-88.7460	Shot concrete slab
KMSC-08-11	1812 Seashore Ave.	Water line on exterior wall of the house	Jackson	Water Line	Exterior wall	1812 Seashore Ave. Pointe Aux Chenes to Seashore Ave.	Paint on road, stake on driveway	Fair	19.7	30.3680	-88.7697	Shot window sill
KMSC-08-12	Beach area near south end of 6th street	Piece Debris flooded to tree top	Jackson	Debris Line	Tree	Beach area to the east of south end of 6th St.	Stake near tree, paint on road	poor	21.2	30.3616	-88.7641	Shot ground
KMSC-08-13	8517 Clamshell Ave.	Exterior wall of house	Jackson	Water Line	Exterior wall of house	8517 Clamshell Ave., off of 12st	Paint mark on road	poor	17.6	30.3608	-88.7518	Shot water line on wall
KMSC-10-01	Fishing Pier at North end of Prestly Outing Campground	Mud line on railing post of pier	Jackson	Water Line	Exterior railing post	HWM on railing post at Fishing pier at prestly Outing Campground	Duct tape on railing	Fair	9.3	30.4909	-88.4325	Shot wood deck
KMSC-10-02	Back of bridge caution marker at Pollucks Ferry Landing	Fine silt and leaf fragments stuck to back of caution bar sign on bridge	Jackson	Water Line	Caution sign on bridge	Back of caution sign on bridge (NW corner) at Pollucks ferry Landing	Duct tape on backside of caution sign	Fair	10	30.4358	-88.4518	Shot ground at sign

HWM ID	HWM Address	Flaggers Original HWM Surface - RAW	County	Type of HWM	HWM Object	Location_Directions to HWM Object_RAW	Type of Marker RAW	Reliability of mark for surge	NAVD-88	Survey Latitude	Survey Longitude	Survey Comments
KMSC-10-03	8400 Cochrane Ave.	Exterior wall on east side of house	Jackson	Water Line	Exterior wall on east side of house	From Hwy 613 go west on hill about 1 mile to Graham, turn right then left onto Cochrane, go south at river. HWM is near left window seal, 109.5" from concrete base.	Not flagged, no marks, ground covered with mud on gravel	Fair	12.3	30.4643	-88.5590	Shot concrete slab
KMSC-10-04	2233 Pascagoula River Road	Support post on elevated house, center post on driveway	Jackson	Water Line	Support post	From Hwy 63 at Three Rivers west of river. HWM is located on center support post on driveway (on a bluff).	Center post on driveway	Fair	10	30.5814	-88.5728	Shot concrete slab
KMSC-10-06	HWY 614 and Pascagoula River, behind Visitors Permit Station on Graham Lake Road)	Mud line	Jackson	Mud Line	Tree	NE side of Graham Lake Road, behind Visitors permit Station, approximately 100 feet north of hwy 64	Red paint with mark of a triangle and a horizontal line underneath it on tree trunk.	poor	13.4	30.6124	-88.6381	Shot bottom of paint line
KMSC-10-07	Hickory Hill Drive (Hickory Hill Country Club) 3 miles north of Guatier	Asphalt parking lot	Jackson	Wrack Line	Asphalt parking lot	HWM is located on the parking lot at back of Hickory Hill Golf Course Club house (approx. 150')	Red paint water mark (triangle with horizontal line underneath) on top edge of debris line.	poor	13.2	30.4572	-88.6230	Shot paint line
KMSC-10-08	5543 Dead River Road	West wall of house	Jackson	Water Line	Exterior wall	HWM is located at west side of house, near electrical box.	N/A	good	14	30.4216	-88.6255	Shot ground at electrical box
KMSC-10-09	1409 E. Village Parkway	Water line on exterior wall	Jackson	Water Line	Exterior wall	On siding of front porch facing street	None	good	14.4	30.4076	-88.6322	Shot concrete porch slab
KMSC-10-10	Log Cabin Style House at corner of Souix Bayou and E. Village Parkway (across street from 1409 E. Village Parkway).	Ground	Jackson	Wrack Line	Ground	In front yard of house	Debris line in yard 29.5' from house (12' from road curb)	good	14.3	30.4080	-88.6320	Shot ground in yard 12' north of curb

HWM ID	HWM Address	Flaggers Original HWM Surface - RAW	County	Type of HWM	HWM Object	Location_Directions to HWM Object_RAW	Type of Marker RAW	Reliability of mark for surge	NAVD-88	Survey Latitude	Survey Longitude	Survey Comments
KMSC-10-11	Ecatawpa River Access via Pollock Ferry Rd. (South of I-10)	Mud line on tree	Jackson	Mud Line	Tree	Access via Pollock Ferry Rd. from Helena crossover I-10 and turn left to river on dirt road (approx. 100' from river)	Wooden stake with flagging red paint on tree trunk	poor	7.2	30.4548	-88.4532	Shot ground at wood stake
KMSC-10-12	2905 Indian Town Rd.	Water line on front porch.	Jackson	Water Line	Front porch.	End of Indian Town Rd., HWM is located at top of porch.	None	Fair	11.2	30.5114	-88.5613	Shot ground at wood stake
KMSC-10-14	12312 Clark Bayou rd.	Water line at SW corner of garage.	Jackson	Personal Account	Garage door	SW corner of garage	None	Fair	10.6	30.5212	-88.5523	Shot driveway
KMSC-10-15	3109 River Band Rd.	Water line at left garage door frame 14" above driveway	Jackson	Personal Account	Garage door frame	From HWY 613; West on Donnie Brook, left on River Bend, go to end, last house on the right. HWM at left garage door frame 14" above driveway.	None	Fair	11.7	30.4942	-88.5581	Shot point 0.33' above garage finished floor
KMSC-10-16	3118 or 3120 River Bend Rd. (No street # on house)	East wall of house/ water line was 8" down from porch	Jackson	Water Line	East exterior wall	From HWY 613, turn west onto Donnie Brook, then left on River Bend Rd., go to end. HWM on NE of house, near porch.	None	poor	10.4	30.4939	-88.5578	Shot point 0.7' down from porch
KMSC-10-17	Hexagonal house in Shady Pines Camp	Mud line on trees between house and river	Jackson	Mud Line	Tree	HWM on pine tree, in front of hexagonal house.	Silver duct tape wrapped around large pine tree with "private Beach" sign	poor	9.4	30.5216	-88.6802	Shot bottom of tape
KMSC-10-19	11720 Potocaw Landing	Water line on retainer post.	Jackson	Water Line	Exterior retaining post	HWM on retainer post on right side of house.	Silver duct tape on retainer wall post to top of 2"x8" board	poor	10.7	30.5139	-88.6195	Shot bottom of tape



HWM ID	HWM Address	Flaggers Original HWM Surface - RAW	County	Type of HWM	HWM Object	Location_Directions to HWM Object_RAW	Type of Marker RAW	Reliability of mark for surge	NAVD-88	Survey Latitude	Survey Longitude	Survey Comments
KMSC-10-20	13139 Hanover Dr.	Interior rear wall at kitchen and living room area. HWM was transferred to back porch.	Jackson	Water Line	Interior wall transferred to back porch.	From Hwy 609 turn east on Winsor Porte then south on Hanover, 3rd house from end on left. HWM was located back of house near kitchen door.	No mark inside house, duct tape placed on exterior wall on porch near kitchen door.	excellent	20.1	30.4252	-88.8269	Shot bottom of tape
KMSC-10-22	5809 Morton Place	Base of brick ledge on attic window over garage	Jackson	Water Line	Base of brick ledge on attic window over garage	From HWY 609, take Windsor Porte to Hanover, turn left to Morton Place, right on Morton go to end and turn right on unnamed Rd. to dead end.	Duct tape placed at HWM	good	19.7	30.4281	-88.8157	Shot bottom of tape
KMSC-10-23	11433 Bayou Place	Inside Garage	Jackson	Water Line	Interior wall	Right side of garage at 11433 bayou place	Duct tape	excellent	18.4	30.4370	-88.8029	Shot bottom of tape
KMSC-10-24	Sanctuary (a gated community, off of Kippie Cut Off Road)	Ground	Jackson	Wrack Line	Ground	From Old Fort Bayou Rd., take Yellow Jacket Road south, past St. Martin High School, left onto Kippie Cut Off Rd.	Wooden stake at top of wrack line	poor	18.9	30.4268	-88.7756	Shot ground at wood stake
KMSC-10-25	6717 Woodlake Lane, about 0.25 mile down a private road	On sheetrock inside house transferred to outside wall for survey	Jackson	Water Line	Interior wall transferred to exterior wall	From Hwy 609, go east on Old Fort Bayou Rd., turn right at Elgen/Woodgate, go to end of Woodlake Lane and take private drive 0.25 mile. HWM is located on SW corner of house (2nd level) right side of stairs by front door.	Duct tape	Good	21	30.4358	-88.7459	Shot duct tape on corner of house
KMSC-10-26	Old Fort Bayou Road bridge on Old Fort Bayou	Plant debris and silt floated onto trees and brush	Jackson	Mud Line	Plants	From HWY 609 take Old Fort Bayou Road east, go under interstate I-10 2 miles to bridge	Red painted HWM on bridge support, SW side of bridge	Poor	21	30.4844	-88.7497	Shot paint line on bridge support

HWM ID	HWM Address	Flaggers Original HWM Surface - RAW	County	Type of HWM	HWM Object	Location_Directions to HWM Object_RAW	Type of Marker RAW	Reliability of mark for surge	NAVD-88	Survey Latitude	Survey Longitude	Survey Comments
KMSC-10-27	Semmes Rd.	Tree	Jackson	Water Line	Tree	From hwy 609, take Old Fort Bayou Road east under I-10, to Semmes Road, turn right go to end where golf course is under construction	Purple duct tape wrapped around tree	Poor	11.4	30.4719	-88.7253	Shot tape on tree
KMSC-10-30	7809 Utopia St.	On garage door supports	Jackson	Water Line	Garage door supports	HWM at west side of 1st garage.	Purple duct tape	Poor	17.2	30.4324	-88.7399	Shot duct tape outside garage door
KMSC-10-31	9012 Dixie Street	Front wall of house, above windows	Jackson	Water Line	Front wall of house, above windows	From I-10, take Hwy 57 south 0.25mile, turn right on to Ocean Springs Road, go right to Southland, take left on Dixie Street. Yellow with green metal roof house.	No marker left	Poor	16.5	30.4269	-88.7603	Shot finished floor
KMSC-10-32	4037 Dunsinane St.	Water line on right side of garage	Jackson	Water Line	Exterior wall	From intersection of HWY 90 and Ocean Springs Road, turn north on Guildford and continued to Diller Road, turn right to Queen Elizabeth to Dunshinane St., house on cul-de-sac. HWM is on bricks right side of garage door.	Purple duct tape	Fair	22	30.4218	-88.7775	Shot duct tape on brick
KMSC-10-33	3205 Cumberland St.	Inside wall in kitchen dinging area	Jackson	Water Line	Interior wall	HWM was transferred to back porch on brick wall, adjacent to support post.	Purple duct tape outside of deck railing	excellent	21.4	30.4187	-88.7922	Shot duct tape on brick
KMSC-10-34	1224 Nelson DR.	Water line	Jackson	Water Line	Exterior railing	HWM on back of porch (east side), adjacent to the left side of the stairs.	Purple duct tape on left side of stair railing on eastside of house	Fair	19.5	30.4204	-88.8101	Shot duct tape on balcony rail
KMSC-10-35	Nelson Rd. (next door to 1224 Nelson Rd.)	Ground	Jackson	Wrack Line	Ground	In backyard of unoccupied house next to 1224 Nelson Rd.	Wooden stake with orange flagging	Poor	18.6	30.4207	-88.8108	Shot debris line

HWM ID	HWM Address	Flaggers Original HWM Surface - RAW	County	Type of HWM	HWM Object	Location_Directions to HWM Object_RAW	Type of Marker RAW	Reliability of mark for surge	NAVD-88	Survey Latitude	Survey Longitude	Survey Comments
KMSC-10-36	1219 Sunset St.	Water line on back porch.	Jackson	Water Line	Exterior wall	HWM is located on back porch, SW corner of house adjacent to stairway	Bottom of purple duct tape, SW corner of house, back side of house	good	20.1	30.4199	-88.8233	Shot bottom of tape
KMSC-10-45	St. Martin St. and Lemoine	On interior wall of Wood Shop Building	Jackson	Water Line	Interior wall	From exit 2 on I-10, take Rodriguez St. east, turn left on Lemoine, go about 0.75 mile, St. Martin Middle school on left. HWM located inside Wook Shop Building on northeastern yellow brick wall.	None	excellent	20	30.4387	-88.8816	Shot finished floor
KMSC-10-46	13541 Paso Rd.	Debris line, 15'4" from brick wall at pool, 38' from marker on Paso Road	Jackson	Debris Line	Ground	From Exit 50 on I-10, take HWY 609 south about 3 miles, turn west on Pine Road, turn right on Shore Dr., than turn left on to Fairway Dr. Debris line, 15'4" from brick wall at pool, 38' from marker on Paso Road	Marker on Paso Road	Poor	19	30.4254	-88.8360	Shot debris line
KMSC-10-47	14004 Baysweep Dr.	Exterior wall at rear of house next to power meters	Jackson	Water Line	Exterior wall at rear of house next to power meters	From exit 50 on I-10, take 609 south, turn west on Lemoine, then south on Corto Road, right on Shore Orchard, then right onto Baysweep Dr.; house on right near end	Purple duct tape	Good	19.8	30.4408	-88.8430	Shot bottom of tape
KMSC-10-48	15182 Lemoyne Dr. (Sun Palace)	Waterline on sheetrock near back door of Sun Palace	Jackson	Water Line	Interior wall	At Martinique Shopping Center, 15182 Lemoyne. HWM is located in NW corner of bldg, behind Sun Palace	Purple duct tape	excellent	20.2	30.4425	-88.8741	Shot bottom of tape

HWM ID	HWM Address	Flaggers Original HWM Surface - RAW	County	Type of HWM	HWM Object	Location_Directions to HWM Object_RAW	Type of Marker RAW	Reliability of mark for surge	NAVD-88	Survey Latitude	Survey Longitude	Survey Comments
KMSC-20-01	3807 Washington Avenue	Interior wall transferred to exterior wall	Jackson	Water Line	Interior wall transferred to exterior wall	Right of front door entrance on brick wall	Vertical offset	excellent	16.5	30.3463	-88.5231	Shot concrete slab
KMSR-10-02	Near intersection of Gautier-Vancleave Rd. and Collins Wood	Debris line on ground.	Jackson	Wrack Line	Ground	From exit 61 of I-10, go south on Gautier-Vancleave Road, about 1 mile to Fast track Gas Station at corner of Collins Wood. HWM located on east side of Gautier-Vancleave Rd. south of Fast Track Gas Station parking lot. 20'4" south of light pole, 6'1" from	Wooden stake at top of debris line, locator mark on road side edge of side walk measure 6'1" east from base of location mark	Poor	14.5	30.4207	-88.6491	Shot debris line
KMSR-10-03	Hwy 57 @ Little Bluff Creek	Plant debris line on bridge embankment	Jackson	Wrack Line	Bridge embankment	From exit 61 of I-10, take Gautier-Vancleave Rd. north to Hwy 57, turn right on Hwy 57 go to Little Bluff Creek. HWM on north east side of Little Bluff and Hwy57 intersections	Wooden stake with flagging next to concrete drainage gutter. 40' east from gutter at rd.	Poor	11.7	30.5170	-88.6936	Ground shot at wood stake
KMSR-10-04	Hwy 57 and Bluff Creek Bridge	Plant and debris line on north bank of bluff creek, east side of hwy 57	Jackson	Wrack Line	Ground	From Exit 51 of I-10, take Hwy57 north to bluff creek in Vancleave, about 7 miles. HWM down 14'8" from top of bridge railing (red mark)	Red locator mark on top of bridge railing east side of Hwy 57.	Poor	11	30.5313	-88.6874	Shot top of concrete bridge rail



HWM ID	HWM Address	Flaggers Original HWM Surface - RAW	County	Type of HWM	HWM Object	Location_Directions to HWM Object_RAW	Type of Marker RAW	Reliability of mark for surge	NAVD-88	Survey Latitude	Survey Longitude	Survey Comments
KMSR-10-05	Bridge at Burney Rd. and Smith Rd. crossing	Debris line in creek banks below bridge level	Jackson	Wrack Line	Ground	Turn left from Hwy 57 to Burney Rd. and go 0.5 mile west on Burney Rd. to Smith Rd. HWM on SW side of bridge adj. to Smith Rd.	Wooden stake placed on west bank, south side of rd., 8'8" from rd. sign (unlawful to litter) with orange flagging at end of bridge	Poor	19.6	30.5435	-88.6967	Ground shot at wood stake
KMSR-10-06	McGregor Rd. and Monger creek	Debris line along east bank of Mongers Creek below bridge level	Jackson	Wrack Line	Ground	From Exit 57 of I-10, take Hwy 57 north past Vancleare, go east on McGregor to Monger Creek	Red location mark on bridge railing 14.5' from road sign on east end of bridge	Poor	29.6	30.5803	-88.6707	Shot paint mark on bridge rail
KMSR-10-07	Soley Road	On post near pink house	Jackson	Mud Line	Post	Exit 69 of I-10, go north on Hwy 63 about 21 miles to Old Americus Rd., go left on Ceder Creek Rd. turn left on Soley Rd. gravel till end.	Silver duct tape on post	Poor	17.5	30.6840	-88.6309	Shot tape on 4"x4" wood post at boat ramp
KMSR-10-08	13206 Fairly Rd.	Silt line on plants	Jackson	Mud Line	Plant	From Hwy 57 in Van Cleare go west on Jim Ramsay Rd. about 2miles, then take right at Fairly Rd. and go 0.25 mile and take right at first driveway on the right	Wooden stake with flagging, use PVC pipe located approximate 10' from stake location as an alternate	Poor	7.1	30.5354	-88.6944	Ground shot at wood stake

HWM ID	HWM Address	Flaggers Original HWM Surface - RAW	County	Type of HWM	HWM Object	Location_Directions to HWM Object_RAW	Type of Marker RAW	Reliability of mark for surge	NAVD-88	Survey Latitude	Survey Longitude	Survey Comments
KMSR-10-11	Big Creek and Constitution Rd. crossing	Plant debris and silt line in plants	Jackson	Wrack Line	Plants	From Exit 75 of I-10, take Fonts Lake Rd. north, turn west on Cherry Valley, then left at Constitution Rd.	Wooden stake located on NW side of Creek Rd. inter section, stake is 23'8" from red paint locator mark in road	Poor	18.4	30.5489	-88.4086	Shot ground
KMSR-10-12	Boat Launch Area @ Exit 5A on I-59 north (Frontage Road)	Silt line in grass bank under I-59 bridge	Pearl River	Mud Line	Ground	Exit 5A on I-59 North, boat launch area go under bridge near Frontage Road	Wooden stake located 24' north of Frontage Rd. loop under bridge	Fair	14.9	30.3815	-89.7379	Shot Ground at wood stake
KMSR-10-13	I-59 and Pearl River, on MS-LA state line	On bridge supports. Silt line in grass on embankment, dead fish	Pearl River	Mud Line	Bridge supports	Exit 11, Pearl River turnaround on I-59 at MS-LA state line.	Red line painted at HWM on 1st bridge support under south I-59 bridge	Poor	20	30.4624	-89.6957	Shot bottom of paint line
KMS_USGS_10	Wolf River at I-10 west bridge end	Not Provided By USGS	Harrison	Seed Line	Bridge seat	Southwest bridge seat of eastbound lane bridge (Br. No. 28.7B)	Top of pile cap at abutment	Poor	18.7	30.4146	-89.2038	Shot seed line
KMS_USGS_101	Biloxi River at Three Rivers Road (02481130)	Not Provided By USGS	Harrison	Line on crest-stage gage	Bridge seat	Top of aluminum tee (elev. 29.01 ft) in crest-stage gage attached to downstream side of right(south) main bridge pier.	Chiseled square	Poor	26.2	30.4881	-89.0358	Shot 2" pipe on side of bridge (USGS point not found)
KMS_USGS_102	House at 13066 Husley Road	Not Provided By USGS	Harrison	Seed Line	Not Provided By USGS	TBM 29 is downstream left (southeast) bridge seat of Woolmarket road bridge crossing Parker Creek	Not Provided By USGS	Poor	18.9	30.4728	-88.9616	Shot seed line
KMS_USGS_103	D&L Body Shop	Not Provided By USGS	Harrison	Seed/ Stain Lines	Handrail	Downstream (south) handrail of old State Highway 67 bridge crossing Howard Creek	Orange paint	Poor	18.2	30.4693	-88.9384	Shot seed line

HWM ID	HWM Address	Flaggers Original HWM Surface - RAW	County	Type of HWM	HWM Object	Location_Directions to HWM Object_RAW	Type of Marker RAW	Reliability of mark for surge	NAVD-88	Survey Latitude	Survey Longitude	Survey Comments
KMS_USGS_104	House at 3296 Sandy Bluff Drive near Lameybridge Road crossing of Tchoutacabouffa River	Not Provided By USGS	Harrison	Seed Line	Handrail	Downstream (south) handrail at Lameybridge Road bridge crossing Tchoutacabouffa River	Chiseled square	Poor	15.9	30.4745	-88.8926	Shot seed line
KMS_USGS_11	Wolf River at I-10 east bridge end	Not Provided By USGS	Harrison	Seed/Debris Line	Bridge seat	Southeast bridge seat of eastbound lane bridge (Br. No. 28.7B)	Top of pile cap at abutment	Poor	19	30.4152	-89.2020	Shot seed line
KMS_USGS_12	Turkey Creek at I-10	Not Provided By USGS	Harrison	Seed Line	Bridge seat	Southeast bridge seat of eastbound lane bridge (Br. No. 32.1B).	Top of pile cap at abutment	Poor	27.4	30.4221	-89.1494	Shot seed line
KMS_USGS_13	Bernard Bayou at I-10	Not Provided By USGS	Harrison	Seed Line	Bridge seat	Downstream left (southeast) bridge seat of bridge on westbound lanes of I-10 crossing Bernard Bayou (Bridge No. 35.9B)	Not Provided By USGS	Poor	19.1	30.4337	-89.0901	Shot seed line
KMS_USGS_14	Fritz Creek at Cowan-Lorraine Road Extension (Under Construction)--Upstream of Biloxi River at I-10	Not Provided By USGS	Harrison	Debris Line	Bridge	Centerlines at right (south) ends of newly constructed dual bridges crossing Fritz Creek (NW 1/4 of Sec 7, T7S, R10W)	Centerlines	Poor	18.8	30.4545	-89.0292	Shot debris line
KMS_USGS_15	Tchoutacabouffa River at I-10	Not Provided By USGS	Harrison	Debris Line	Bridge abutment	Downstream left (southeast) abutment of eastbound I-10 bridge crossing Tchoutacabouffa River	Painted 'X' labeled "BM 45"	Poor	16.1	30.4527	-88.9423	Shot debris line
KMS_USGS_27	Pass Christian High School	Not Provided By USGS	Harrison	Seed Line	Cinder block window frame	Top of cinder block window frame, 40 ft east of north covered entrance to main building and about 300 ft south of gymnasium	Not Provided By USGS	Fair	24.6	30.3154	-89.2543	Inside school bathroom
KMS_USGS_28	105 Timber Ridge Boulevard	Not Provided By USGS	Harrison	Seed Line	Curb	Directly across the street from 105 Timber Ridge Boulevard	Orange square	Poor	23.4	30.3191	-89.2728	Shot seed line

HWM ID	HWM Address	Flaggers Original HWM Surface - RAW	County	Type of HWM	HWM Object	Location_Directions to HWM Object_RAW	Type of Marker RAW	Reliability of mark for surge	NAVD-88	Survey Latitude	Survey Longitude	Survey Comments
KMS_USGS_29	108 Timber Ridge Boulevard	Not Provided By USGS	Harrison	Seed Line	Curb	Directly across the street from 105 Timber Ridge Boulevard	Orange square	Poor	23.7	30.3199	-89.2725	Shot seed line
KMS_USGS_33	South Edge Biloxi Bay at I-110 (Bayview Pawn Shop)	Not Provided By USGS	Harrison	Seed Line	Concrete foundation	Northwest corner of concrete foundation of junction box located about 120 ft southeast of Bayview Pawn	Orange square	Poor	19.7	30.4121	-88.8950	Shot seed line
KMS_USGS_35	566 Howard Avenue	Not Provided By USGS	Harrison	Seed Line	Curb	North curb along Howard Avenue about 100 ft south of SE corner of old Central High School building and about 75 feet west of residence	Orange square	Poor	21	30.3967	-88.8800	Seed line on interior wall
KMS_USGS_36	Front entrance to Beau Rivage Casino	Not Provided By USGS	Harrison	Seed Line	Concrete lamp post base	Northeast corner of square concrete lamp post base, 15 ft east of northeast column supporting awning in front of Beau Rivage Casino	Black square	Poor	22	30.3931	-88.8917	Mark on wall inside entrance of Beau Rivage
KMS_USGS_37	St. John Neumann Residence, 1044 Beach Boulevard	Not Provided By USGS	Harrison	Seed Line	Concrete pad	About 75 ft north of north entrance to residence	Black square	Poor	22.5	30.3953	-88.9007	Seed line on wall at front of building
KMS_USGS_38	Saxony Apartments, 1282 Beach Boulevard	Not Provided By USGS	Harrison	Seed Line	Concrete slab	Northwest corner of small concrete slab about 140 ft south of apartment complex	Orange square	Poor	22.5	30.3953	-88.9134	Seed line on wall
KMS_USGS_39	1611 Glennswetman Street	Not Provided By USGS	Harrison	Seed Line	Power pole	About 120 ft northeast of garage, at northeast corner of intersection of Glennswetman Street and Clower Street	Nail with pink flagging	Fair	22.5	30.3953	-88.9340	Shot seed line
KMS_USGS_40	Treasure Bay Hotel	Not Provided By USGS	Harrison	Seed Lines	Curb	South of hotel, about 150 ft south of entrance	Orange square	Poor	23.1	30.3940	-88.9550	Shot seed line
KMS_USGS_41	My Oh My at Edgewater Mall	Not Provided By USGS	Harrison	Seed Line	Curb	About 250 ft south of main entrance to Edgewater Mall	Orange square	Poor	23.2	30.3907	-88.9902	Shot seed line



HWM ID	HWM Address	Flaggers Original HWM Surface - RAW	County	Type of HWM	HWM Object	Location_Directions to HWM Object_RAW	Type of Marker RAW	Reliability of mark for surge	NAVD-88	Survey Latitude	Survey Longitude	Survey Comments
KMS_USGS_42	House on Kennedy Lane near Dampman Point	Not Provided By USGS	Harrison	Seed Line	Power pole	West side of county road about 300 ft west of residence	Nail	Poor	18.7	30.4290	-88.9375	Shot seed line
KMS_USGS_43	Isle of Capri Casino	Not Provided By USGS	Harrison	Seed Line	Column	Base of northwest column supporting awning in front of main entrance to casino	Black square	Poor	23.6	30.3906	-88.8602	Mark on wall of 2nd level lobby
KMS_USGS_62	Brickyard Bayou at 30th Street	Not Provided By USGS	Harrison	Debris Line	Wingwall	Top of upstream left wingwall.	Not Provided By USGS	Poor	14.4	30.3787	-89.0976	Shot deris line
KMS_USGS_63	Pops Ferry Bridge, South abutment	Not Provided By USGS	Harrison	Seed Lines	Bridge seat	BM Brass disk on southeast bridge seat 1979 - 4671A.	Brass disk	Poor	19.2	30.4142	-88.9759	Seed line on concrete beam
KMS_USGS_66	House no.807, on Pass Christian Quad., South of Rail Road on Louise Ave. Below U.S. Naval Reservation	Not Provided By USGS	Harrison	Seed Line	Tree	Third oak tree North of House no 807 just inside fence, 3 ft above ground	Nail	Poor	24.8	30.3577	-89.1266	Seed line on window
KMS_USGS_67	Mark on shop in rear of house No. 109, Beach Park Place, South of Rail Road Tracks, Next to Gulf Park College, On Pass Christian Quad.	Not Provided By USGS	Harrison	Seed Line	Power pole	Front of house no.809, set 3 ft above ground on the North side	Nail	Poor	25	30.3551	-89.1361	Seed line on door
KMS_USGS_68	Long Beach Barber Shop across from Public Library,3 blocks south of Rail Road tracks, on Pass Christian Quad.	Not Provided By USGS	Harrison	Seed/Water Line	Power pole	3 ft above the ground on the north side of pole, South of Library and across the street from Prestige Printing	Nail	Poor	25	30.3489	-89.1505	Seed line on window

HWM ID	HWM Address	Flaggers Original HWM Surface - RAW	County	Type of HWM	HWM Object	Location_Directions to HWM Object_RAW	Type of Marker RAW	Reliability of mark for surge	NAVD-88	Survey Latitude	Survey Longitude	Survey Comments
KMS_USGS_69	House no.136 , South of Rail Road tracks, South East of Mt. Pilgrim Church , on Pass Christian Quad.	Not Provided By USGS	Harrison	Seed Line	Tree	3 ft above ground on the west side of large oak in the front yard of house	Nail	Poor	25	30.3423	-89.1703	Shot seed line
KMS_USGS_70	House no. 218,216 on White Harbor Rd., South of Rail Road, 2nd street goes west from there, Pass Christian Quad.	Not Provided By USGS	Harrison	Seed Line	Tree	1 ft above ground on the south side of oak tree, North of House no. 218	Nail	Poor	24.9	30.3377	-89.1837	Shot seed line
KMS_USGS_71	Large White house on point of Camellia Dr. in rear of house, on Pass Christian Quad.	Not Provided By USGS	Harrison	Seed Line	Tree	North side of very large Oak tree in front lawn of large white house on point of road	Nail	Poor	25.3	30.3294	-89.2066	Seed line on AC duct
KMS_USGS_72	House no. 107 on east scenic across from small tennis court, On Pass Christian Quad.	Not Provided By USGS	Harrison	Seed Line	Tree	2 ft above ground on the north east side of tree in the front yard of House no.107	Nail	Poor	24.5	30.3258	-89.2182	Seed line on door
KMS_USGS_73	House no. 4103 Menge Avenue, across the street and south of Dixie White House Nursing Home	Not Provided By USGS	Harrison	Seed Line	Tree	SouthWest side of small oak in the front yard of House no.4103	Nail	Poor	23.3	30.3423	-89.2172	Shot seed line
KMS_USGS_74	Corner of Courtview Avenue and 2nd St. across the street from some apartments, north of Rail Road tracks, on Pass Christian Quad.	Not Provided By USGS	Harrison	Seed Line	Slab	Garage on the East side of the home just to the left of the stairs on that side of the house	Not Provided By USGS	Poor	23.5	30.3327	-89.2284	Shot water mark on window

HWM ID	HWM Address	Flaggers Original HWM Surface - RAW	County	Type of HWM	HWM Object	Location_Directions to HWM Object_RAW	Type of Marker RAW	Reliability of mark for surge	NAVD-88	Survey Latitude	Survey Longitude	Survey Comments
KMS_USGS_75	House at 38th avenue and 11th st. just south of Rail Road tracks, on Gulfport south Quad.	Not Provided By USGS	Harrison	Seed Line	Tree	2.5 ft above the ground, on the West side of tree in the yard of the first house on the left once you cross 11th st.	Nail	Poor	24.3	30.3646	-89.1069	Seed line on window
KMS_USGS_76	Sign in front of Gulf South Outpatient Center, on corner of 13st and 31 avenue across from church on Gulfport South Quad.	Not Provided By USGS	Harrison	Seed Line	Tree	2 ft above the ground in the west side of a large oak tree, East of church and North of Gulf South Outpatient Center	Nail	Poor	24.3	30.3669	-89.0988	Seed line on sign
KMS_USGS_77	Just below Rail Road Tracks, at corner of Thorton Avenue and 2nd street, across from apartments, on Gulfport south Quad.	Not Provided By USGS	Harrison	Debris Line	Power pole	2 ft above the ground on the south side of a large Power pole ,South of the rail Road tracks and across from apartment on Thorton Rd.	Nail	Poor	24.2	30.3733	-89.0782	Shot seed line
KMS_USGS_78	Apartment building just south of Rail Road tracks, off of Court House rd., on Gulfport North Quad.	Not Provided By USGS	Harrison	Seed/Water Line	Power pole	2 ft above the ground in a power pole , located on the corner of the apartment building parking lot ,Nail is on the East side of pole	Nail	Fair	24.2	30.3820	-89.0424	
KMS_USGS_79	Across from Teagarden Park apartments, at crossing of Rail Road St. and Teagarden Rd., on Gulfport North Quad	Not Provided By USGS	Harrison	Debris Line	Power pole	West side of Power pole on Rail Road St. South of Rail Road and East on Teagarden Rd. across from Teagarden Park Apartments	Nail	Poor	23.9	30.3843	-89.0354	Shot debris line

HWM ID	HWM Address	Flaggers Original HWM Surface - RAW	County	Type of HWM	HWM Object	Location_Directions to HWM Object_RAW	Type of Marker RAW	Reliability of mark for surge	NAVD-88	Survey Latitude	Survey Longitude	Survey Comments
KMS_USGS_80	Collins Woodworks, just south of Wolf River Bridge, on Gulfport NW Quad.	Not Provided By USGS	Harrison	Seed Line	Tree	2 ft above the ground on the North side of the tree, directly in front of blue shop just before Wolf River on the right	Nail	Poor	23.5	30.3751	-89.2289	Shot seed line
KMS_USGS_81	Pineville Elementary School Gym, Aprox 1 mile Southeast of Wolf river on Pass Christian Quad.	Not Provided By USGS	Harrison	Seed Line	Tree	2 ft above the ground into large Oak tree located north of Gym next to gravel service Rd.	Nail	Poor	22.5	30.3596	-89.2170	Shot seed line
KMS_USGS_82	Magic River Campground, on Bells Ferry Rd, East of Wolf River, on Gulfport NW Quad.	Not Provided By USGS	Harrison	Seed Line	Power pole	2 ft above the ground just right of magic river camping entrance	Nail	Poor	13.4	30.3889	-89.1991	Shot seed line
KMS_USGS_83	Debris Line Just north of Turkey Creek on US 49, on Gulfport North Quad.	Not Provided By USGS	Harrison	Debris Line	Drainage top cover	Center of drainage top cover just north of Turkey creek on the west side off of US 49	Orange paint dot	Poor	16.9	30.4143	-89.0932	Shot debris line
KMS_USGS_84	California Motor Sports no. 3503, just south of airport, on Gulfport North Quad.	Not Provided By USGS	Harrison	Seed/Water Line	Power pole	2 ft above ground on the North side of pole located in front af California Motor Sports	Nail	Good	17.4	30.3926	-89.0611	Shot seed line
KMS_USGS_85	House no. 1423, just south of Handsboro Bridge across from Kremer Marine, on Gulfport North Quad.	Not Provided By USGS	Harrison	Seed/Water Line	Tree	Small Magnolia tree just in front of garage 2 ft above ground on house no.1423, across from Kremer Marine	Nail	Fair	18.8	30.4026	-89.0256	Seed line on inside window



HWM ID	HWM Address	Flaggers Original HWM Surface - RAW	County	Type of HWM	HWM Object	Location_Directions to HWM Object_RAW	Type of Marker RAW	Reliability of mark for surge	NAVD-88	Survey Latitude	Survey Longitude	Survey Comments
KMS_USGS_86	House no 1809 on Curcor Dr. just south of Rail Road Tracks, just over a mile below Handsboro on Gulfport North Quad.	Not Provided By USGS	Harrison	Seed/Water Line	Tree	1 ft above the ground in a huge oak tree in front lawn of House no.1809	Nail	Fair	23.8	30.3865	-89.0260	Seed line on exterior wall
KMS_USGS_93	Tchoutacabouffa River (02480599) at SR 15 & 67 at D'Iberville (north bridge end)	Not Provided By USGS	Harrison	Seed Line	Wingwall	Top of wingwall at upstream right (north) abutment of upstream bridge	NGS BM "15V5 1986"	Poor	17.7	30.4610	-88.9014	Red mark on bottom side of bridge abutment
KMS_USGS_96	1310 Scenic Drive	Not Provided By USGS	Harrison	Seed Line	Fire hydrant	In front of house near road	Orange paint	Poor	26	30.3216	-89.2273	Shot seed line
KMS_USGS_97	1310 Scenic Drive	Not Provided By USGS	Harrison	Seed Line	Fire hydrant	In front of house near road	Orange paint	Poor	26	30.3216	-89.2273	Shot seed line
KMS_USGS_98	1320 Scenic Drive	Not Provided By USGS	Harrison	Seed Line	Fire hydrant	In front of house near road	Orange paint	Poor	26.1	30.3218	-89.2267	Seed line in doorway of house
KMSC-02-17	East Oaklawn Rd.	Shoulder of road, north side	Harrison	Wrack Line	Ground	East end of East Oaklawn Rd. on north side	Flagged stake with orange tape	Poor	8.7	30.4599	-88.9576	Shot ground at wood stake
KMSC-02-18	8332 West Oaklawn Rd.	Exterior brick wall, east end of building	Harrison	Water Line	Exterior brick wall	Looking north toward front of building	Duct tape	Fair	15.5	30.4574	-88.9761	Shot bottom of duct tape
KMSC-02-19	10497 Shore Crest Rd.	Exterior brick wall	Harrison	Water Line	Exterior brick wall	Looking west, south end of house	Duct tape	Fair	18.7	30.4384	-89.0069	Shot bottom of duct tape
KMSC-02-20	Popps Ferry Rd. (at north end of Popps Ferry Rd. Bridge)	West shoulder of Popps ferry Rd., about 15' from curb	Harrison	Wrack Line	Ground	Looking south toward bridge, west shoulder of road app. 15' from curb	Orange tape on stake	Poor	19	30.4262	-88.9737	Shot ground at wood stake
KMSC-02-21	2556 Southshore Dr.	Exterior front brick wall	Harrison	Water Line	Exterior front brick wall	Looking south toward house west side	Duct tape	Good	18.6	30.4352	-88.9905	Shot bottom of tape
KMSC-02-23	656 Watersview Dr.	Front porch column	Harrison	Water Line	Front Porch column	Looking north at front of house, east column	Duct tape	Good	18.9	30.4259	-88.9500	Shot bottom of tape

HWM ID	HWM Address	Flaggers Original HWM Surface - RAW	County	Type of HWM	HWM Object	Location_Directions to HWM Object_RAW	Type of Marker RAW	Reliability of mark for surge	NAVD-88	Survey Latitude	Survey Longitude	Survey Comments
KMSC-02-24	Across the street from 1098 Campbell Dr.	Front exterior wall	Harrison	Water Line	Exterior wall	Looking at front of house (north), west side of door	Duct tape	Poor	12.1	30.4525	-88.9515	Shot bottom of tape (NOTE: Owner stated that HWM was 5.85' above bottom of duct tape)
KMSC-02-25	6194 Whitman Rd.	Front of house, looking east on south corner	Harrison	Water Line	Exterior wall	Looking east at front of house	Duct tape	Good	24.6	30.3749	-89.2679	Shot bottom of duct tape
KMSC-02-26	Last house on right side of Midway Dr.	Water line on exterior wall.	Harrison	Water Line	Exterior wall	Looking North 10'7" above concrete driveway	See photo	Poor	17.1	30.3595	-89.2635	Shot Waterline
KMSC-02-27	23554 Woodland Way	Water line on exterior wall	Harrison	Water Line	Exterior wall	HWM located 18" above carport gable bottom.	See photo	Good	24.1	30.3544	-89.2350	Shot ground near HWM
KMSC-02-28	25302 Cuevas Delisle Rd.	Lawn at south end of house	Harrison	Water Line	Lawn	Looking North, flagged stake at south end of house	Flagged stake	Good	24.7	30.3809	-89.2654	Shot ground at wood stake
KMSC-02-29	23335 Bells Perry Rd.	Exterior front brick wall	Harrison	Water Line	Exterior front brick wall	Looking south toward front of house, west side of living room window	Duct tape	Good	23	30.3887	-89.2275	Shot bottom of duct tape
KMSC-03-01	461 Parker St.	Interior transferred to exterior	Harrison	Mud Line	Interior wall transferred to exterior wall	From Red mark on Bay View Dr., 126' to the front of 461 Bldg.	Duct tape	excellent	20.8	30.4108	-88.8889	Shot mud line on wall
KMSC-03-02	116 Rue Magnolia	Front of brunet fourchey house	Harrison	Mud Line	Exterior wall	Left side of 116 house facing south	Duct tape	Poor	25.8	30.3947	-88.8889	Shot bottom of tape
KMSC-03-04	910 W. Beach Blvd.	Interior wall transferred into exterior column	Harrison	Water Line	Interior wall transferred into exterior column	On left column of front entry stairs	Tape and orange	excellent	27.8	30.3066	-89.2746	Shot bottom of duct tape
KMSC-03-07	Lorraine Rd. and I-10	Ground	Harrison	Wrack Line	Ground	See Sketch	Stake with orange tape	Poor	26.2	30.4316	-89.0178	Shot ground at wood stake

HWM ID	HWM Address	Flaggers Original HWM Surface - RAW	County	Type of HWM	HWM Object	Location_Directions to HWM Object_RAW	Type of Marker RAW	Reliability of mark for surge	NAVD-88	Survey Latitude	Survey Longitude	Survey Comments
KMSC-03-08	13410 River Rd.	On wall	Harrison	Mud Line	Wall	In front of the house	Duct tape	Fair	16.7	30.4813	-89.0264	Shot bottom of duct tape
KMSC-03-09	11857 Lorraine Rd.	Ground	Harrison	Wrack Line	Ground	Back of the house, 77' east from eastern edge of breeze way (approximate 200 yds from Biloxi River)	Wood stake	Poor	17.4	30.4537	-89.0152	Shot debris line (stake not found)
KMSC-04-09	West 2nd Ave.	Outside of building, on brick	Harrison	Water Line	Exterior brick wall	Located in the NW corner of building of nursing Home/ Hospital	Duct tape with red line	Fair	25	30.3143	-89.2511	Shot finished floor
KMSC-04-10	Apt. #65-68 Pine Ave.	Brick wall	Harrison	Water Line	Brick wall	Go down Pine Ave., toward 90 look for Apt. 65-68 on right. HWM located in stairwell on 2nd floor	Red paint located in 2nd floor of black metal stairwell plus duct tape mark	Fair	25	30.3171	-89.2630	Shot paint mark on wall
KMSC-04-11	Apt.5, 590 W. Royal Oak St.	Outside of building on tin roof	Harrison	Water Line	Roof	Go down Royal Oak street. look for red Apt. on left of road, traveling north. HWM on the tin roof marked with red paint	Red paint with duct tape	Fair	22.6	30.3212	-89.2751	Shot bottom of duct tape
KMSC-04-12	207 Alabama St.	On outside railing of house	Harrison	Water Line	Exterior railing	Heading west on Alabama St., 2 story house on right. HWM located on railing post facing the road. Directly in front of front door.	Marked with duct tape and yellow marking tape	Fair	25.8	30.3153	-89.2812	Shot bottom of duct tape
KMSC-04-13	108 Elm Ln.	Outside front of building/ vinyl siding	Harrison	Water Line	Exterior wall	Go down Elm Lane, 2nd house from the corner. HWM located above the front door up front stairs.	Duct tape with flag	Fair	22.7	30.3232	-89.2846	Shot bottom of duct tape
KMSC-04-14	300 Forest St.	Outside wooden siding of house	Harrison	Water Line	Porch Column	Go down Forest St., St. Louis Bay behind you, blue wooden 2 story house with white railing. HWM in front of front door	Duct tape and yellow flagging	Poor	20.9	30.3276	-89.2812	Shot bottom of duct tape

HWM ID	HWM Address	Flaggers Original HWM Surface - RAW	County	Type of HWM	HWM Object	Location_Directions to HWM Object_RAW	Type of Marker RAW	Reliability of mark for surge	NAVD-88	Survey Latitude	Survey Longitude	Survey Comments
KMSC-04-15	492 Royal Oak Blvd	Outside surface of vinyl siding	Harrison	Water Line	Exterior wall	Go down Royal Oak Blvd., looking for tan vinyl sided house. Looking at front of house, HWM on right side.	Duct tape on outside of window	Good	22.2	30.3284	-89.2714	Shot bottom of duct tape
KMSC-04-16	555 Henderson Ave.	Offset off of wrap around deck	Harrison	Mud Line	Roof	555 Henderson Ave. (green house, shape of octagon) At the top of stairs, HWM around deck measure up 10.33'	Off set from deck around house	Good	24.1	30.3323	-89.2631	Shot wood deck
KMSC-04-17	830 Clark Ave.	Pilling on west side of front stairs	Harrison	Mud Line	Pilling	Go to top of stairs at pilling on west side of stairs, the HWM is 8.1' up	Duct tape	Good	24.9	30.3395	-89.2628	Shot bottom of duct tape
KMSC-04-18	494 N. Market St.	Exterior wall of east side of maintenance garage	Harrison	Mud Line	Exterior wall of east side of maintenance garage	Go to maintenance garage and HWM is located at east side 7.55' above concrete slab	Duct tape	Good	24	30.3346	-89.2541	Shot bottom of duct tape
KMSC-04-19	371 Woodman Ave.	Exterior wall transferred on yellow building	Harrison	Mud Line	Exterior wall	At 371 Woodman Ave. (yellow house), HWM is marked with tape 13.9' above slab	Duct tape	Fair	22.7	30.3238	-89.2497	Shot bottom of duct tape
KMSC-04-20	205 Lynn Circle	On 2nd story interior wall	Harrison	Water Line	Interior wall (2nd story)	Go down E. North St., left on Oak Park Drive, left into Lynn Circle. 3rd house on left 2 story house	Red paint on roadway in front of house	excellent	25.5	30.3279	-89.2366	Shot finished floor
KMSC-04-21	805 Deer Trail Ln.	Interior wall	Harrison	Water Line	Interior wall	Goto down deer trail lane untill you reach 805 address. White house with navy blue shutters. Marking tape on railing of front porch and orange paint on roadway. Duct tape placed on inside water mark	Duct tape and marking tape, orange paint on roadway	excellent	23.9	30.3329	-89.2225	Shot wood deck



HWM ID	HWM Address	Flaggers Original HWM Surface - RAW	County	Type of HWM	HWM Object	Location_Directions to HWM Object_RAW	Type of Marker RAW	Reliability of mark for surge	NAVD-88	Survey Latitude	Survey Longitude	Survey Comments
KMSC-04-22	901 East Scenic Dr.	Located on exterior wall	Harrison	Water Line	Exterior wall	HWM on SW corner of house, 2.1' below screened proch window. Facing Menge Ave and Gulf, directly off of 90	Duct tape	Fair	27.2	30.3252	-89.2178	Shot bottom of duct tape
KMSC-04-23	119 Espy Ave.	Outside garage	Harrison	Water Line	Exterior wall	Heading south on Espy Ave., residence is located on right side of road. HWM located on east entrance of garage	Duct tape	Good	26.2	30.3302	-89.2044	Shot bottom of duct tape
KMSC-04-24	23027 Woodland Way	On exterior brick wall	Harrison	Water Line	Exterior wall	Go down woodland way traveling south. HWM located next to front door on brick house with brown and white shutters.	Duct tape	Good	23.5	30.3590	-89.2202	Shot bottom of duct tape
KMSC-04-25	3510 Olga Dr.	Exterior wall on 2nd floor window	Harrison	Water Line	Exterior wall on 2nd floor window	Travel west on Jones Dr., south on Olga Dr., look for address on mailbox	No marking used	Fair	23.3	30.3393	-89.2308	Shot finished floor
KMSC-04-26	151 Beach Blvd.	Pillion of vehicle check-in, west of main entrance	Harrison	Mud Line	Pilling	@ 151 Beach Blvd, go to vehicle check-in, which is west of main entrance, HWM is 0.6' above concrete @ NW pillion	Duct tape	Fair	22.6	30.3908	-88.8606	Shot bottom of duct tape
KMSC-04-27	Apt #104 Back Bay Place	Edge of second floor breeze way	Harrison	Mud Line	Second floor breeze way	Go to Apt #104 Back Bay Place, off of Bay View Ave. HWM is 9' above slab @ first floor marked with duct tape between first and second floor	Duct tape	Fair	18.5	30.4065	-88.8689	Shot bottom of duct tape

HWM ID	HWM Address	Flaggers Original HWM Surface - RAW	County	Type of HWM	HWM Object	Location_Directions to HWM Object_RAW	Type of Marker RAW	Reliability of mark for surge	NAVD-88	Survey Latitude	Survey Longitude	Survey Comments
KMSC-04-28	260 5th St.	West side of building (exterior)	Harrison	Mud Line	Exterior wall	@ 260 5th St (white building, oyster cleaning house), go to SW corner of building @ Middle Loading Bay measure up 5.53' from first floor (marked with tape)	Duct tape	Good	20	30.4005	-88.8652	Shot bottom of duct tape
KMSC-04-29	507 Roy St.	Exterior wall	Harrison	Mud Line	Exterior wall	@ 507 Roy St., go to NW front door and measure up 8.5 from slab @ front door	Duct tape	Good	19.6	30.4048	-88.8770	Shot bottom of duct tape
KMSC-04-30	641 Bay View Ave.	Exterior wall	Harrison	Mud Line	Exterior wall	@AAA Transfer and Storage Inc. 641 Bayview Dr., @ NW corner go to door labeled 641 A on loading dock	Duct tape	Fair	19.4	30.4113	-88.8834	Shot bottom of duct tape
KMSC-04-32	220 Caillavet St.	Exterior wall of metal building	Harrison	Water Line	Exterior wall of metal building	Traveling South on Caillquet St. look for Shaughnessy Printing (2 story brick front), go around to back door and HWM is located right on back door.	Duct tape on backside of building	Fair	18.8	30.4004	-88.8916	Shot bottom of duct tape
KMSC-05-11	110 Holiday Ave.	Electrical wire (debris in)	Harrison	Debris Line	Electrical wire	Wire from first utility pole on Holiday ave. NW corner of intersection between Holiday Ave. and E. Beach Blvd.	Paint on road and stake at bottom of pole	Poor	27.7	30.3325	-89.1874	Shot ground at wood stake
KMSC-05-12	822 E. Beach Blvd.	Exterior of home	Harrison	Personal Account	Exterior of home		N/A	Poor	33	30.3522	-89.1326	Shot bottom of eave
KMSC-05-13	109 W. 3rd St.	Interior water line transferred to exterior wall	Harrison	Water Line	Interior wall transferred to exterior wall	109 W. 3rd St. off of Geff Davis Ave. which is off 90 (Beach Blvd.)	Paint in road and stake at edge of front lawn	excellent	25.3	30.3483	-89.1509	Shot ground at wood stake at EP
KMSC-05-14	404 S. Girard Ave.	Interior wall	Harrison	Water Line	Interior wall	W. Beach Blvd. (HWY 90) to S. Girard Ave. HWM on left	Magic marker	excellent	25.6	30.3456	-89.1561	Shot marker line

HWM ID	HWM Address	Flaggers Original HWM Surface - RAW	County	Type of HWM	HWM Object	Location_Directions to HWM Object_RAW	Type of Marker RAW	Reliability of mark for surge	NAVD-88	Survey Latitude	Survey Longitude	Survey Comments
KMSC-05-15	223 Boggs Dr.	Carport wall	Harrison	Water Line	Carport wall	223 Boggs Dr.	Paint in street and stake in ground	Good	25.9	30.3428	-89.1693	Shot faint marker line
KMSC-05-16	332 Bldg. R Arbor Station Dr.	Interior of unit #332 Building R	Harrison	Water Line	Interior wall	Hwy. 90 W (or W. Beach Blvd.). right to Arbor Station Dr. 0.4 mile to HWM on right	Magic marker on stud in door frame	Good	25.4	30.3397	-89.1761	Shot marker line
KMSC-05-17	127 English Village Dr.	Interior wall	Harrison	Water Line	Interior wall	Highway 90 west to english Village Dr. (right)	Magic marker	excellent	25	30.3545	-89.1314	Shot marker line
KMSC-05-18	131 Trautman Ave.	Interior wall	Harrison	Water Line	Interior wall	West on 90 and turn right on Trautman Ave.	N/A	excellent	25.2	30.3449	-89.1613	Shot water line on wall
KMSC-05-22	112 Olsen Ave	Ground	Harrison	Water Line	Ground	Highway 90 West ro Runnels Ave (right) to Magnolia St (Left) Olsen Ave right	Paint Mark / PK Nail	Poor	22.9	30.3443	-89.1653	Shot nail near edge of pavement in front of 112 Olsen Ave
KMSC-05-23	106 South Lang Ave	N/A	Harrison	Water Line	N/A	Head west on Highway 90 (Magnolia) turn right on South Lang Avenue	Paint on centerline on road	Good	25.5	30.3433	-89.1706	Shot road
KMSC-05-24	159 Markham Dr.	Water line on road	Harrison	Water Line	Road	Head west on West Beach Blvd. (HWY 90), turn right on Markham Dr., HWM on left side of road in front of house	Paint on road	Poor	22.7	30.3398	-89.1801	Shot pavement
KMSC-05-25	221 White Harbor Rd.	Water/debris line on road	Harrison	Water Line	Road	Head west on hwy 90, turn right on White Harbor Dr. and head north, HWM on road, in front of 221 house.	Paint on road	Poor	23.2	30.3382	-89.1839	Shot pavement
KMSC-05-26	South Girard	Water/debris line on ground	Harrison	Water Line	Ground	Head north on Highway 90 (Magnolia St.) turn right on South Girard, head north cementary on left side of street	Paint on road	Poor	22.3	30.3480	-89.1570	Shot pavement

HWM ID	HWM Address	Flaggers Original HWM Surface - RAW	County	Type of HWM	HWM Object	Location_Directions to HWM Object_RAW	Type of Marker RAW	Reliability of mark for surge	NAVD-88	Survey Latitude	Survey Longitude	Survey Comments
KMSC-05-27	200 South Nickelson	Water/debris line on ground	Harrison	Water Line	Ground	Head west on hwy 90, turn right on South Nickelson, on left hand side of road before passing east 22 St.	Tape	Poor	24.3	30.3522	-89.1424	Shot ground
KMSC-05-28	501 East First St.	Water/debris line on ground	Harrison	Water Line	Ground	Head west on highway 90, turn right on South Nickelson, then turn right on East 1st St., wind water debris line between train track and baseball field	Wood stake	Poor	23.6	30.3545	-89.1395	Shot ground at wood stake
KMSC-05-29	West Railroad St.	Water/debris line on ground	Harrison	Water Line	Ground	Head west on highway 90, turn right on Louis St., turn left on West Railroad St., HWM located at the intersection of West Railroad St. and Louis Ave. between west railroad and train track	Wood stake	Poor	23.2	30.3586	-89.1272	Shot ground at wood stake
KMSC-06-08	24384 Clubhouse Dr.	Ground	Harrison	Debris Line	Ground	Next to sandtrap between the 14th hole & the 15th tee. White paint mark on the cart path, which is 37 feet to the HWM	Stake w/pink flag & white paint	Poor	23	30.3846	-89.2502	Shot ground at wood stake
KMSC-06-09	East Bound I-10, East of Exit #38 ( 0.6mi East of Exit #38 - Lorraine Rd.)	Ground	Harrison	Debris Line	Ground	HWM located on HWY I10 by Exit #38 & 19 feet from birm	Stake w/pink flag & white paint	Poor	11.7	30.4462	-89.0211	Shot ground at wood stake
KMSC-06-10	East bound on I-10 before Exit #44 ( Beauvoir-Jefferson Davis home) west of Tchoutacabouffa River	Ground	Harrison	Debris Line	Ground	East bound on I-10, HWM located 21 feet from birm	Stake w/pink flag & white paint	Poor	11.6	30.4570	-88.9498	Shot ground at wood stake
KMSC-07-12	1600 Pratt st.	Exterior wall	Harrison	Water Line	Exterior wall	Exterior wall next to 2 car garage	Tape, paint on Road	Fair	24.9	30.3719	-89.0802	Shot bottom of duct tape



HWM ID	HWM Address	Flaggers Original HWM Surface - RAW	County	Type of HWM	HWM Object	Location_Directions to HWM Object_RAW	Type of Marker RAW	Reliability of mark for surge	NAVD-88	Survey Latitude	Survey Longitude	Survey Comments
KMSC-07-14	3215 West Beach Blvd.	Exterior wall	Harrison	Water Line	Exterior wall	Exterior wall- hotel casino front entrance	Tape	Good	24.5	30.3635	-89.1021	Shot bottom of duct tape
KMSC-07-15	801 Lewis St.	Exterior wall	Harrison	Water Line	Exterior wall	Exterior wall in front of home, 25' from front door	Tape, paint on road	Good	24.9	30.3573	-89.1264	Shot bottom of duct tape
KMSC-07-16	615 Camp Ave.	Exterior wall	Harrison	Water Line	Exterior wall	Exterior wall in front of the home, front door	Tape	Good	24.6	30.3600	-89.1151	Shot bottom of duct tape
KMSC-07-17	1101 2nd street	Exterior wall	Harrison	Water Line	Exterior wall	Exterior wall in front of home	Tape	Fair	24.8	30.3740	-89.0700	Shot bottom of duct tape
KMSC-07-18	1816 3rd. Street	Exterior wall	Harrison	Water Line	Exterior wall	Exterior wall behind home N. wall	Tape	Fair	23.4	30.3769	-89.0620	Shot bottom of duct tape
KMSC-07-19	143 Bilmarsan Dr.	Exterior wall	Harrison	Water Line	Exterior wall	Exterior wall in front of home	Tape	Good	22.2	30.3952	-88.9350	Shot bottom of tape
KMSC-07-20	156 Camillia St.	Exterior wall	Harrison	Water Line	Exterior wall	Exterior wall in front of church, south concrete column	Tape	Fair	21	30.3955	-88.9533	Shot bottom of tape
KMSC-07-21	183 Beauvoir Rd.	Exterior wall	Harrison	Water Line	Exterior wall	Exterior NW wall, 2 ft from contactor door entrance	Tape	Fair	21.6	30.3955	-88.9729	Shot bottom of tape
KMSC-07-22	100 S. Marshall	Exterior wall	Harrison	Water Line	Exterior wall	Exterior wall, south end of building	Tape	Fair	22.7	30.3911	-88.9869	Shot bottom of tape
KMSC-07-23	1 Colonial Drive Apt.4	Exterior wall	Harrison	Water Line	Exterior wall	Exterior wall of condo N., 3' from back door	Tape	Fair	22.2	30.3895	-89.0023	Shot bottom of tape
KMSC-07-24	473 Jord Drive	Exterior wall	Harrison	Water Line	Exterior wall	Exterior wall of garage, 1ft north of garage door	Duct tape	fair	19.2	30.4149	-88.9706	Shot bottom of tape
KMSC-07-25	2523 Provence Place	Exterior wall	Harrison	Water Line	Exterior wall	Exterior wall in front of home, facing N., 2 ft E. of front door	Duct tape	Good	18.8	30.4128	-88.9830	Shot bottom of tape
KMSC-07-26	474 Channel Mark Dr.	Exterior wall	Harrison	Water Line	Exterior wall	Exterior wall in front of home, 3 ft north of front door	Duct tape	Good	19.1	30.4115	-88.9975	Shot bottom of tape
KMSC-08-14	237 Graham Ave.	Water line mark on exterior wall of the front house	Harrison	Water Line	Exterior wall	237 Graham Ave. 2nd Street to South of Division St.	Paint on the road red	Poor	18.2	30.4005	-88.8994	Shot top of brick

HWM ID	HWM Address	Flaggers Original HWM Surface - RAW	County	Type of HWM	HWM Object	Location_Directions to HWM Object_RAW	Type of Marker RAW	Reliability of mark for surge	NAVD-88	Survey Latitude	Survey Longitude	Survey Comments
KMSC-08-15	159 Azalea Dr.	Ground	Harrison	Water Line	Ground	Head west on Hwy 90, turn right on Azalea Dr. and go 0.5 mile, house on left hand side. HWM between 155 and 159.	Pointed stake	Fair	21.7	30.3971	-88.9045	Shot ground at wood stake
KMSC-08-16	251 Iroquois St.	Ground	Harrison	Water Line	Ground	Take I-10 to Division St., head west on Division St., turn left on Iroquois St.	Stake to point	Poor	19	30.4012	-88.8983	Shot ground at red paint
KMSC-08-17	157 St. Charles Ave.	Ground	Harrison	Water Line	Ground	Head west from I-10 on Irish Hill Rd, turn left onto St. Charles Ave.	Stake to point	Good	22.2	30.3961	-88.9303	Shot ground at red paint
KMSC-08-18	139 McDonnell Ave	Ground	Harrison	Water Line	Ground	Head west on Irish Hill Rd. turn left on McDonnell Ave.	Stake pointer	Good	21.8	30.3952	-88.9455	Shot pavement
KMSC-09-07	200 E. Beach Port Blvd.	Exterior wall	Harrison	Mud Line	Exterior wall	Main entrance last building in left, back wall facing railroad tracks	Duct tape	Fair	23.7	30.3796	-89.0533	Shot bottom of duct tape
KMSC-09-08	233 Courthouse Rd.	Exterior wall	Harrison	Mud Line	Exterior wall	Rear wall of Coldwell Banker, facing railroad tracks	Duct tape	Fair	24.2	30.3818	-89.0442	Shot bottom of duct tape
KMSC-09-09	745 S. Railroad St.	Exterior wall	Harrison	Mud Line	Exterior wall	Front of house, left of front door on porch	Duct tape	Fair	23.8	30.3834	-89.0378	Shot bottom of duct tape
KMSC-09-10	Corner of Railroad and Tegarden	Side of road	Harrison	Wreck Line	Side of road	Corner of Railroad and Tegarden	Flag and paint	Poor	23.3	30.3843	-89.0354	Shot ground at wood stake
KMSC-09-11	1806 Curcor	Exterior wall	Harrison	Mud Line	Exterior wall	Right of front door	Duct tape	Fair	24.7	30.3860	-89.0264	Shot bottom of duct tape
KMSC-09-12	13 Venetian Gardens	Exterior wall	Harrison	Mud Line	Exterior wall	Left of front door	Duct tape	Fair	23.6	30.3885	-89.0060	Shot bottom of duct tape
KMSC-09-13	Corner of Railroad and Hewes St. (Blue house)	Exterior wall of house	Harrison	Mud Line	Exterior wall of house	Side of house	Duct tape	Fair	23.9	30.3776	-89.0602	Shot bottom of duct tape
KMSC-09-14	Intersection of Dolan Ave. and Railroad	Debris line	Harrison	Debris Line	Ground	Intersection of Dolan Ln. and Railroad. HWM with flag.	Flag	Poor	22	30.3836	-89.0382	Shot bottom of duct tape
KMSC-09-15	198 Paradise Ave.	Exterior wall	Harrison	Mud Line	Exterior wall	Wall facing Township Rd.	Duct tape	Fair	23.5	30.3842	-89.0316	Shot bottom of duct tape

HWM ID	HWM Address	Flaggers Original HWM Surface - RAW	County	Type of HWM	HWM Object	Location_Directions to HWM Object_RAW	Type of Marker RAW	Reliability of mark for surge	NAVD-88	Survey Latitude	Survey Longitude	Survey Comments
KMSC-09-16	217 Cowan Rd.	Exterior wall	Harrison	Mud Line	Exterior wall	K.L. Young Real estate, left side of building	Duct tape	Fair	23.8	30.3849	-89.0273	Shot bottom of duct tape
KMSC-09-17	1458A Magnolia St.	Exterior wall	Harrison	Mud Line	Exterior wall	Right of front door	Duct tape	Fair	15.5	30.4034	-89.0246	Shot bottom of duct tape
KMSC-09-18	1162 John Evans Rd.	Transfer from interior wall to exterior wall	Harrison	Mud Line	Interior wall transferred to exterior wall	Right of front door	Duct tape	excellent	18.2	30.4075	-89.0132	Shot bottom of duct tape
KMSC-09-19	11272 Sundown Dr.	Exterior wall right of garage	Harrison	Mud Line	Exterior wall right of garage	Right side wall of garage	Duct tape	Poor	18	30.4092	-89.0261	Shot bottom of duct tape
KMSC-09-20	1230 W. Pine St.	Exterior wall	Harrison	Mud Line	Exterior wall	Left side of front door	Duct tape	Poor	16.6	30.4024	-89.0286	Shot bottom of duct tape
KMSC-09-21	1111 Magnolia St.	Interior wall	Harrison	Mud Line	Interior wall	Rear of house 2nd story left window (back to water)	Duct tape	Fair	15.9	30.4037	-89.0310	Shot bottom of duct tape
KMSC-09-22	948 Mary Ruth	Exterior wall	Harrison	Mud Line	Exterior wall	Front of house left of door	Duct tape	Poor	15.4	30.4000	-89.0325	Shot bottom of duct tape
KMSC-09-23	6 Pouenia Place	Exterior wall	Harrison	Personal Account	Exterior wall	Rear of home right of french door	Duct tape	Poor	16.6	30.4103	-89.0411	Shot bottom of duct tape
KMSC-09-24	13 Colonel Wink Dr.	Exterior wall	Harrison	Mud Line	Exterior wall	Left of front door	Duct tape	Fair	18.1	30.4180	-89.0428	Shot bottom of duct tape
KMSC-09-25	17 Poplar Cir.,	Exterior wall	Harrison	Mud Line	Exterior wall	Right side of house	Duct tape	Fair	16.8	30.4015	-89.0493	Shot bottom of duct tape
KMSC-09-26	44 Poplar Cir.,	Exterior wall	Harrison	Mud Line	Exterior wall	Right wall of garage	Duct tape	Fair	15.1	30.4039	-89.0505	Shot bottom of duct tape
KMSC-09-27	117 Canal St.	Transfer from interior wall to exterior wall	Harrison	Mud Line	Interior wall transferred to exterior wall	Right exterior wall of garage	Duct tape	Fair	17.1	30.3993	-89.0469	Shot bottom of duct tape
KMSC-09-28	Behind 933 Parkview Place	Ground	Harrison	Wrack Line	Ground	Behind building, 75' from road to wrack line	Red paint in red flag	Poor	18.2	30.4058	-89.0175	Shot wood stake
KMSC-09-29	122 Euia Dr.	Exterior wall	Harrison	Mud Line	Exterior wall	Right of door	Duct tape	Good	18.6	30.4043	-88.9981	Shot bottom of duct tape
KMSC-10-37	12056 Cedar Lake Road	Water line on second floor	Harrison	Water Line	Exterior wall	HWM on western wall of bailshop adjacent to window.	Purple duct tape	Fair	17.9	30.4592	-88.9387	Shot bottom of tape

HWM ID	HWM Address	Flaggers Original HWM Surface - RAW	County	Type of HWM	HWM Object	Location_Directions to HWM Object_RAW	Type of Marker RAW	Reliability of mark for surge	NAVD-88	Survey Latitude	Survey Longitude	Survey Comments
KMSC-10-38	11471 Old HWY 67	Water line inside building	Harrison	Water Line	Interior wall	HWM is located on north outside metal wall by front entrance	Purple duct tape on left side of door, outside	excellent	17.1	30.4681	-88.9187	Shot bottom of tape
KMSC-10-39	3293 Sandy Bluff Drive	On concrete columns supports	Harrison	Water Line	Concrete column supports	From I-10 exit 46, HWY 15 N. to Lick Skillet Rd., turn right on to Lane Bridge Rd., turn right onto Sandy Bluff Dr., house on right. HWM on support column by front stairway (near treatment system).	Purple duct tape	Good	15.9	30.4744	-88.8926	Shot bottom of tape
KMSC-10-40	15369 Old HWY 15	Road embankment	Harrison	Wrack Line	Road embankment	Wrack line located 25'9" north of HWM on roadway.	Wooden stake	Poor	20.9	30.5103	-88.9114	Shot ground at wood stake
KMSC-10-42	739 Hengen Lane	Sand line on front door	Harrison	Water Line	Front door	From I-10, take Ceder Lake south, turn right on to Brodie, take 1st left onto the Hengen Lane, last house on road next to bay	Purple duct tape on front wall right side of door	Good	21.1	30.4319	-88.9322	Shot bottom of tape
KMSC-10-43	4361 Brodie rd.	Right front edge of carport	Harrison	Water Line	Carport	From exit 44 on I-10, take Ceder Lake south, turn east onto Brodie Rd. House is on short NS stretch of Brodie Rd. past high school	Purple duct tape on right side of carport	Fair	20.1	30.4334	-88.9110	Shot bottom of tape
KMSC-10-44	10221 Rodriguez Street	Water line on brick wall	Harrison	Water Line	Exterior brick wall	From exit 2 on I-10, take Rodrigues St. west. Looking for Suburban Extended Stay Hotel. HWM located adj. to blue door at AC unit, 10' north of guest laundry area.	Purple duct tape, top of tape	Fair	20.2	30.4306	-88.8976	Shot top of tape



HWM ID	HWM Address	Flaggers Original HWM Surface - RAW	County	Type of HWM	HWM Object	Location_Directions to HWM Object_RAW	Type of Marker RAW	Reliability of mark for surge	NAVD-88	Survey Latitude	Survey Longitude	Survey Comments
KMSC-10-50	13610 River Rd	On bricks, front side of house	Harrison	Water Line	Exterior wall	From Hwy 49 South of I-10, take Creosote Road east, turn north on Three Rivers Road. Turn south on River Road at Biloxi River 0.5 mile	None	Fair	16.6	30.4836	-89.0307	Shot of window sill
KMSC-10-51	3536 River Bluff Road	On molding over door to storage shed	Harrison	Water Line	Exterior door	Take exit 50 of I-10, go north to Cook Rd, turn west, go to end, turn north on Daisy Vestry Rd, about 0.75 mile, turn west onto River Bluff Rd, 3rd house from end	None	Fair	14.6	30.4711	-88.8935	Shot concrete slab at storage room door
KMSC-10-52	3504 Stephen Earl RD	Silt line in trees	Harrison	Water Line	Trees	From exit 50 of I-10, go north on Hwy 609 to Stephen Earl Rd, go to end, pink brick house on right.	Purple duct tape wrapped around tree	Poor	21	30.5096	-88.8881	Shot bottom of tape around 10" pine tree
KMSC-10-53	Exit ramp at Exit 2 of I-110, 200' down west side	Ground	Harrison	Wrack Line	Ground	Exit 2 on I-110, 200' down west side of exit ramp, wrack line located 14' 5" from mark at base of light pole.	Locator mark and light pole	Poor	20.1	30.4321	-88.8952	Shot ground 14.5' west of light pole base
KMSC-10-54	11015 Old Highway 49	Silt line in fence and shrubs	Harrison	Mud Line	Fence and plants	From exit 34 on I-10, take Hwy 49 North turn west onto Landon Road then north on old Hwy 49. House is on North side	Purple tape placed on fence post between two "square" shaped shrubs	Poor	18.7	30.4421	-89.1008	Shot bottom of tape
KMSC-10-62	#2 Riverbend Dr.	Waterline by stair leading to second floor	Harrison	Water Line	Interior wall	From exit 38 on I-10, take Lorraine Rd. south, turn right on Magnolia St., turn right on Mill Rd. House is at corner of Mill and Riverbend Drive. HWM on sheetrock by inside stairway	None	excellent	19.9	30.4083	-89.0394	Shot concrete slab below stairs

HWM ID	HWM Address	Flaggers Original HWM Surface - RAW	County	Type of HWM	HWM Object	Location_Directions to HWM Object_RAW	Type of Marker RAW	Reliability of mark for surge	NAVD-88	Survey Latitude	Survey Longitude	Survey Comments
KMSC-10-63	80 Bayou Circle	Inside garage/kitchen door	Harrison	Water Line	Interior door	From ext 38 on I-10, take Lorraine Rd. south, turn right on W. Pine St. (name will change to W. Magnolia St.), turn right on Courthouse Rd., turn left on Bayou Circle. House at intersection of Bayou Circle and E. 52nd St.	None	Fair	24.6	30.4224	-89.0438	Shot slab in front of garage
KMSC-10-64	Tramark Golf Course	Ground	Harrison	Wrack Line	Ground	From exit 34 of I-10, take hwy 49 south, turn left on Airport Road toward Washington Ave., cross Wahington Ave. onto Tramark Golf Course Rd.. HWM located 67" from arrow on golf car path, wrackline circles putting 18th green	Locator arrow on golf cart path, red paint sprayed on grass at survey point	poor	17.9	30.4232	-89.0634	Shot debris line near putting green
KMSC-10-65	Tramark Golf Course	Inside walls of clubhouse	Harrison	Water Line	Interior wall	From exit 34 of I-10, take hwy 49 south, turn left on Airport Road toward Washington Ave., cross Wahington Ave. onto Tramark Golf Course Rd..	Silver duct tape on outside wall next to door	excellent	19.1	30.4238	-89.0632	Shot bottom of tape
KMSC-10-66	9506 Creosote rd.	Water line in warehouse area,	Harrison	Water Line	Interior wall	From I-10, take Hwy 49 south, turn left onto Creosote Road, go to right turn in road. HWM at A/C closet and coke machine in garage on north side of building	Silver duct tape on right side of garage	excellent	19.3	30.4268	-89.0772	Shot bottom of tape
KMSC-10-67	14108 Airport Rd.	Waterline on inside walls	Harrison	Water Line	Interior walls	From I-10 take Hwy 49 south. Turn left on Airport Road. Building on left across from airport entrance. HWM on right side of front door	Purple duct tape, HWM @ top of duct tape.	excellent	18.7	30.4158	-89.0759	Shot bottom of tape

HWM ID	HWM Address	Flaggers Original HWM Surface - RAW	County	Type of HWM	HWM Object	Location_Directions to HWM Object_RAW	Type of Marker RAW	Reliability of mark for surge	NAVD-88	Survey Latitude	Survey Longitude	Survey Comments
KMSC-10-68	606 35th street	Water line on front door glass	Harrison	Water Line	Exterior door	HWM on front glass door adj. stucco wall	None	good	18	30.3927	-89.0616	Shot slab surface (finished floor)
KMSC-10-69	930 Courthouse Rd. Apt#4	Inside walls of Apt. #4 bldg. 930	Harrison	Water Line	Interior wall	From I-10, take Lorraine Rd. south to E. Pass Rd. turn right on Courthouse Rd., turn right on Commerce St., 3rd building on left. HWM on sheetrock located approximate 4' inside front door of Apt. #4.	None	excellent	20	30.3984	-89.0440	Shot slab surface (finished floor)
KMSC-10-70	1510 28th Street	Waterline on glass windows and door	Harrison	Water Line	Windows and Door	From I-10 take hwy 49 south to 28th street, turn east , cross brickyard and bayou, building located on north side of road	Silver duct tape on outside brick wall, right of door	good	18.6	30.3844	-89.0810	Shot duct tape
KMSC-10-71	2600 Pass Rd.	Water line on sheetrock and painting inside building	Harrison	Water Line	Interior wall	HWM is located on metal siding adj. to west side at door	None	excellent	18.6	30.3806	-89.0942	Shot duct tape
KMSC-10-72	8477 Old Hwy 49	On interior wall and pegboard	Harrison	Water Line	Interior wall	From I-10, take Hwy 49 south to Russell Blvd., turn west goto Old Hwy 49, go south 0.2miles building on right. HWM on red metal wall by glass entrance door.	Silver duct tape on outside, left side of front	excellent	18	30.4113	-89.0947	Shot duct tape
KMSC-10-73	7685 Kiln Delisle Rd.	Waste water pond on bay side of plant	Harrison	Debris Line	Ground	HWM on west side of solids pond by eye wash station.	Wooden stake with orange flagged by solids pond on west side	poor	25.1	30.3811	-89.3130	Shot ground at wood stake
KMSC-15-01	279 Hopkins Blvd.	Interior wall transferred to exterior wall	Harrison	Mud Line	Interior wall transferred to exterior wall	Left door jamb front foor of house	N/A	excellent	20.6	30.4023	-88.8956	Shot front porch floor

HWM ID	HWM Address	Flaggers Original HWM Surface - RAW	County	Type of HWM	HWM Object	Location_Directions to HWM Object_RAW	Type of Marker RAW	Reliability of mark for surge	NAVD-88	Survey Latitude	Survey Longitude	Survey Comments
KMSC-15-02	241 Hopkins Blvd.	Interior wall transferred to exterior front door jamb	Harrison	Water Line	Interior wall transferred to exterior front door jamb	27.5" up from front porch stoop on left door jamb of front door	N/A	excellent	20.5	30.4008	-88.8956	Shot taken on concrete slab
KMSC-15-04	134 Seal Avenue	Brick wall inside carport	Harrison	Mud Line	Brick wall inside carport	Carport on north end of house. Brick wall in carport	Duct tape on wall	poor	19.9	30.3962	-88.8969	Shot duct tape
KMSC-15-05	In field on SW corner of Intersection of White Ave. and Father Ryan Ave.	On ground	Harrison	Wrack Line	Ground	73' due west from paint on Road	Red paint on road	poor	22.5	30.3962	-88.9116	Shot ground
KMSC-15-06	2555 Marshall Rd. (Mississippi Casino Operators Association, next to Edgewater Mall)	Interior wall transferred to exterior wall	Harrison	Water Line	Interior wall transferred to exterior wall	Interior wall transferred to exterior wall, most NW corner of building	N/A	good	25.7	30.3907	-88.9869	Shot concrete slab
KMSC-20-05	141 Pine Crest Drive	Roof line of house	Harrison	Water Line	Roof line of house	Front of house, right side is garage floor slab	Vertical offset	Fair	29.8	30.3395	-89.2678	Shot concrete floor
KMSR-02-01	Beatline Rd. and Canal 3 Bridge	On ground, west side of bridge	Harrison	Wrack Line	Ground	Looking south, west side of bridge at Canal 3 and Beatline Rd.	Flagged stake	poor	19	30.3690	-89.1872	Shot ground at wood stake
KMSR-02-02	Canal 1 Bridge and Bealine Rd.	Bridge support column	Harrison	Water Line	Bridge support column	Looking east at bridge, water line 5' below bridge surface	None	fair	19	30.3447	-89.1868	Shot east corner concrete bridge
KMSR-10-09	CC Rd. and Tchoutacabouffa River	Silt line in plants and grass along side road. Traces of debris line present.	Harrison	Mud Line	Ground	From exit 48 I-10, take Hwy 15 north about 7 miles to CC Rd., turn right goto creek near county line	Wooden stake with flagging 10' from red painted marker on road	poor	32.5	30.5604	-88.8848	Ground shot at wood stake



HWM ID	HWM Address	Flaggers Original HWM Surface - RAW	County	Type of HWM	HWM Object	Location_Directions to HWM Object_RAW	Type of Marker RAW	Reliability of mark for surge	NAVD-88	Survey Latitude	Survey Longitude	Survey Comments
KMSR-10-10	Hwy 15 and Hurricane Creek	Silt line in plants	Harrison	Mud Line	Plants	From I-10 in D'lberville at exit 46 go north for approximate 13 miles. (Bridge @ Hwy 15 crosses Hurricane Creek)	Red painted marker on top of bridge rail	poor	57.4	30.6152	-88.9225	Shot paint mark on guardrail on bridge deck
KMSR-10-19	Seaway Road at Northrup Gruman	Plant debris hanging on chain link fence.	Harrison	Wrack Line	Chain link fence.	From Exit 38 of I-10, take Lorraine Road south, turn west on Seaway Road.	Duck tape place on chain link fence gate post, left side of gate	poor	18.2	30.4340	-89.0672	Shot tape on gate post
KMSR-10-20	Canal Road and Bernard Bayou	Silt line in plants under bridge	Harrison	Mud Line	Plants	Exit 31 of I-10, go north on Canal Road about 1.3 mile to Bernard Bayou	Silver duct tape wrapped around guard rail post on north east end of bridge.	poor	7.7	30.4252	-88.8266	Duct tape on concrete post at bridge
KMSR-10-21	Old Hwy 49 and Biloxi River	Water line on bridge deck support, silt on plants and debris on banks.	Harrison	Water Line	Bridge deck support	Exit 34 of I-10, take Hwy 49 north about 9 miles, turn left (west) on W. Wortham Road, turn right (north) on Old Hwy 49 to bridge	Red paint on bridge rail, south west corner of bridge	poor	48	30.5697	-89.1360	Shot paint mark on bridge rail
KMS_USGS_01	West Pearl River at I-10 west bridge end	Not Provided By USGS	Hancock	Seed Line	Bridge	Centerline at west end of eastbound lane bridge	Centerline	poor	15.9	30.2978	-89.6980	Shot seed line
KMS_USGS_03	Devils Swamp @ Box culvert at I-10 (Drains Stennis)	Not Provided By USGS	Hancock	Seed/Debris Line	Box culvert headwall	Top of box culvert headwall at downstream southeast end at eastbound lanes	Orange paint	poor	14.29	30.3336	-89.5127	Shot debris line
KMS_USGS_04	Gulf side of I-10 overpass of SR 43	Not Provided By USGS	Hancock	Debris Line	Bridge seat	Southeast bridge seat of eastbound lane bridge (Br. No. 14.5B)	Top of pile cap at abutment	poor	22.1	30.3584	-89.4230	Shot debris line
KMS_USGS_05	Inland side of I-10 overpass of SR 43	Not Provided By USGS	Hancock	Debris Line	Bridge seat	Northeast bridge seat of westbound lane bridge (Br. No. 14.5A)	Top of pile cap at abutment	poor	24.7	30.3580	-89.4236	Shot debris line
KMS_USGS_06	Jourdan River at I-10 West bridge end	Not Provided By USGS	Hancock	Seed Line	Bridge seat	Northwest bridge seat	Top of pile cap at abutment	poor	20.1	30.3628	-89.4093	Shot seed line

HWM ID	HWM Address	Flaggers Original HWM Surface - RAW	County	Type of HWM	HWM Object	Location_Directions to HWM Object_RAW	Type of Marker RAW	Reliability of mark for surge	NAVD-88	Survey Latitude	Survey Longitude	Survey Comments
KMS_USGS_07	Jourdan River at Inland side of I-10 east bridge end	Not Provided By USGS	Hancock	Debris Line	Bridge seat	Northeast bridge seat	Top of pile cap at abutment	poor	23.9	30.3663	-89.3985	Shot debris line
KMS_USGS_08	Jourdan River at Gulf side of I-10 east bridge end	Not Provided By USGS	Hancock	Debris Line	Bridge seat	Southeast bridge seat	Top of pile cap at abutment	poor	26.6	30.3658	-89.3982	Shot debris line
KMS_USGS_09	Jourdan River at SR 43 gage (02481660)	Not Provided By USGS	Hancock	Seed Line	Bridge abutment	Top of wingwall at downstream left (north) bridge abutment	NGS BM "B-365 1993"	poor	19.7	30.3873	-89.4415	Shot seed line
KMS_USGS_105	Stennis Space Center	Not Provided By USGS	Hancock	Seed Line	Not Provided By USGS	Cinder Block Building on East Bank of Pearl River	Not Provided By USGS	poor	14.8	30.3475	-89.6417	Shot seed line
KMS_USGS_20	Pearl River at I-59 at Pearl River, LA	Not Provided By USGS	Hancock	Gage reading from first peak on stage hydro graph	Not Provided By USGS		Not Provided By USGS	poor	15	30.3804	-89.7391	Shot mark on staff guage
KMS_USGS_23	819 Central Avenue	Not Provided By USGS	Hancock	Seed Line	Power pole	Across street from residence, about 30 ft north of centerline of Central Avenue and about 50 ft south of railroad	Nail with pink flagging	poor	27	30.3002	-89.3501	Shot seed line
KMS_USGS_24	708 6th Street	Not Provided By USGS	Hancock	Seed Line	Interior floor	Inside back (northwest) door of house at northwest corner of St. Jude Street and Sixth Street	Not Provided By USGS	poor	26.2	30.2963	-89.3632	Shot seed line
KMS_USGS_25	Dunbar Village Retirement Home @ 725 Dunbar Avenue	Not Provided By USGS	Hancock	Seed Line	Interior floor	Inside west entrance to retirement home	Not Provided By USGS	poor	23.6	30.3253	-89.3380	Shot seed line
KMS_USGS_26	Rotten Bayou at county road in SE1/4 Sec24, T7S, R14W	Not Provided By USGS	Hancock	Seed Line	Bridge seat	Upstream left (northeast) bridge seat of bridge crossing Rotten Bayou on DeLisle-Kiln Road	Not Provided By USGS	poor	24.8	30.4196	-89.3435	Shot seed line
KMS_USGS_31	Casino Magic Inn	Not Provided By USGS	Hancock	Seed Line	Power pole	About 70 ft northeast of northeast corner of Casino Magic Inn	Nail with pink flagging	poor	25	30.3319	-89.3528	Shot seed line

HWM ID	HWM Address	Flaggers Original HWM Surface - RAW	County	Type of HWM	HWM Object	Location_Directions to HWM Object_RAW	Type of Marker RAW	Reliability of mark for surge	NAVD-88	Survey Latitude	Survey Longitude	Survey Comments
KMS_USGS_32	Casino Magic (main building)	Not Provided By USGS	Hancock	Seed Line	Concrete light pole	Directly in front of Casino Magic	Black square	poor	24.2	30.3350	-89.3538	Shot seed line
KMS_USGS_45	84 Lumber Showroom SE corner or Hwy 43/90 intersection	Not Provided By USGS	Hancock	Seed Line	Concrete footing	Corner of concrete footing for Rite Aid sign at intersection	Orange paint	poor	23	30.3050	-89.3771	Shot seed line
KMS_USGS_47	Al Capone's house on Bayou LaTerre	Not Provided By USGS	Hancock	Seed Line	Concrete handrail	Top of concrete handrail at downstream left abutment.	Chiseled square	poor	24.2	30.4149	-89.3807	Shot seed line
KMS_USGS_48	Jack's Firestone west side of HWY 603, south of Bayou LaCroix	Not Provided By USGS	Hancock	Seed Line	Slab	Inside the business next to the only second story interior wall.	Not Provided By USGS	poor	22.3	30.3179	-89.4098	Shot seed line
KMS_USGS_49	Performance Marine on HWY 90 East (4093 Hwy 90)	Not Provided By USGS	Hancock	Seed Line	Slab	Inside bay doors next to steel frame	Not Provided By USGS	poor	22.2	30.2985	-89.4061	Shot seed line
KMS_USGS_50	Sport Trail Trailer Parts and Repairs, Hwy 90 West near Bayside Park	Not Provided By USGS	Hancock	Seed/Mud Lines	Slab	Inside boat shop, located in the back of the compound, next to steel structure.	Not Provided By USGS	good	21.6	30.3002	-89.4182	Seed line on wall inside structure
KMS_USGS_51	Whitney Bank SE corner of HWY90 and Waveland Ave.	Not Provided By USGS	Hancock	Seed Line	Slab	Outside of the bank at the right inside corner of the entrance porch	Not Provided By USGS	poor	22.4	30.2992	-89.3972	Shot seed line
KMS_USGS_52	Communications building on Whites Bayou (HWY90)	Not Provided By USGS	Hancock	Seed Line	BM USCGS G122	Brass disk on left, downstream curb, Whites Bayou bridge HWY 90.	Brass disk	fair	18.6	30.2525	-89.5879	Shot seed line
KMS_USGS_53	First Southern Baptist Church inside the sanctuary	Not Provided By USGS	Hancock	Seed/Stain Line	Slab	Inside the church at the entrance	Not Provided By USGS	excellent	18.3	30.2535	-89.6157	Shot seed line
KMS_USGS_54	Bogue Homa Tributary near	Not Provided By USGS	Hancock	Seeds in trees	Bridge seat	Downstream right bridge seat.	Orange paint	poor	10.9	30.2866	-89.6075	Shot seed line
KMS_USGS_55	Bogue Homa	Not Provided By USGS	Hancock	Seed/Sand Line	Bridge seat	Downstream right bridge seat.	Not Provided By USGS	poor	8.86	30.3021	-89.6139	Shot seed line

HWM ID	HWM Address	Flaggers Original HWM Surface - RAW	County	Type of HWM	HWM Object	Location_Directions to HWM Object_RAW	Type of Marker RAW	Reliability of mark for surge	NAVD-88	Survey Latitude	Survey Longitude	Survey Comments
KMS_USGS_56	Bayou LaCroix Trib at Holy Cross Church on gravel road nr I-10	Not Provided By USGS	Hancock	Seed Line	Bridge seat	Downstream left bridge seat.	Not Provided By USGS	poor	7.6	30.3235	-89.4880	Ink mark on bridge
KMS_USGS_57	Gulf View School gymnasium North entrance	Not Provided By USGS	Hancock	Mud Line	Not Provided By USGS	Inside the North entrance to the gym at corner near the door	Not Provided By USGS	excellent	23.6	30.2684	-89.4494	Shot mud line
KMS_USGS_58	Pearlington Road building 5117 at Jackson Marsh	Not Provided By USGS	Hancock	Seed Line	Slab	Inside the building just inside the entrance	Not Provided By USGS	poor	23	30.2897	-89.4098	Shot seed line
KMS_USGS_59	610 Taylor Trail	Not Provided By USGS	Hancock	Seed Line	Slab	In the kitchen area	Not Provided By USGS	poor	25.1	30.2743	-89.3905	Shot seed line
KMS_USGS_60	Waveland United Methodist Church, inside entrance to sanctuary	Not Provided By USGS	Hancock	Seed Line	Slab	Inside the sanctuary beside the "Servant's Exit"	Not Provided By USGS	poor	25.3	30.2842	-89.3805	Shot seed line
KMS_USGS_61	57146 Diamondhead Drive East	Not Provided By USGS	Hancock	Mud Line	Slab	Inside garage at corner of wall by entrance to living area.	Not Provided By USGS	good	25.3	30.3812	-89.3590	Shot mud line
KMS_USGS_64	SNF Polychemie Business Port Bienville inside storage and office buildings	Not Provided By USGS	Hancock	Seed Line	Concrete slab	Front, right corner of 20 x 24 ft concrete slab to the right of building (used to be gated entrance)	Not Provided By USGS	poor	19	30.2417	-89.5548	Shot seed line
KMS_USGS_65	GE Plastics at Port Bienville inside admin/security entrance	Not Provided By USGS	Hancock	Seed Line	Ditch culvert	Center of headwall of ditch culvert, second furthest from fenced entrance.	Square chipped out of paint	fair	20.1	30.2160	-89.5752	Shot seed line
KMSC-02-35	425 Skyline Dr.	See photo	Hancock	Water Line	Exterior wall	Looking SE, HWM located 16' 6" Above Ground (see photo)	See photo	fair	19.2	30.3308	-89.3762	Shot concrete slab
KMSC-02-36	64 Wolf St.	See photo	Hancock	Water Line	Exterior wall	See photo	See photo	fair	19.5	30.3334	-89.3637	Shot concrete slab
KMSC-02-37	10200 Chapman Rd.	See photo	Hancock	Water Line	Exterior wall	See photo	See photo	fair	25.8	30.3179	-89.3807	Shot water line mark on wall



HWM ID	HWM Address	Flaggers Original HWM Surface - RAW	County	Type of HWM	HWM Object	Location_Directions to HWM Object_RAW	Type of Marker RAW	Reliability of mark for surge	NAVD-88	Survey Latitude	Survey Longitude	Survey Comments
KMSC-04-01	16463 HWY 90	Side of building	Hancock	Water Line	Side of building	East of intersection 604 and Hwy 90. Go to South West Corner of building (Turtle Landing). HWM is 4' above 2nd Floor and 13.5 above concrete slab.	Duct tape	good	20.1	30.2420	-89.6057	Shot bottom of duct tape
KMSC-04-02	3531 Port and Harbor Dr.	Side of Visitors Check in Building	Hancock	Water Line	Exterior wall	Pull into visitors parking lot. Go to front door of visitors office. HWM is 0.75" from slab to right of the front door.	Used vertical offset measurement only	fair	18.3	30.2160	-89.5754	Shot finish floor plus 0.06 feet
KMSC-04-03	5095 Bud Landner Rd.	On outside front of building above doorway.	Hancock	Water Line	Exterior wall above doorway	House on left of road. Brick house with new tin roof.	Duct tape located directly under eave.	poor	16.6	30.2439	-89.4858	Shot bottom of duct tape
KMSC-04-04	Lakeshore Rd. and Lower Bay Rd.	inside right concrete wall	Hancock	Mud Line	Concrete wall	Located building to right of gym. Kindergarten School Building HWM directly inside door that faces Lakeshore Rd.	Duct tape used	excellent	23.7	30.2677	-89.4493	Shot mud line on wall
KMSC-04-05	11010 Old Lower Bay Rd.	Side of Carport	Hancock	Water Line	Side of carport	Drive into driveway, house directly ahead with garage on right. HWM on backside of garage.	Duct tape on north side of garage	good	20.4	30.2519	-89.5118	Shot bottom of duct tape
KMSC-04-06	3025 Port and Harbor Dr.	Outside of metal building	Hancock	Water Line	Exterior wall	Go down Port and Harbor Dr. left into.	Duct tape on outside of Building	good	20.1	30.2401	-89.5467	Shot bottom of duct tape
KMSC-04-07	@ Exit I-10 E. from N. of SR43/603	On ground marked with stake	Hancock	Wrack Line	Ground	Head north on SR-43/603, take the I-10 exit, heading East, HWM is located half way up ramp marked with stake in west side of road.	Flagged survey stake in ground	poor	21	30.3586	-89.4214	Shot ground at wood stake

HWM ID	HWM Address	Flaggers Original HWM Surface - RAW	County	Type of HWM	HWM Object	Location_Directions to HWM Object_RAW	Type of Marker RAW	Reliability of mark for surge	NAVD-88	Survey Latitude	Survey Longitude	Survey Comments
KMSC-05-01	Buccaneer State Park	Side of electric pole	Hancock	Debris Line	Side of electric pole	Buccaneer State Park off of Beach Blvd. Light pole in parking lot to the North of water slide.	Flagged stake at base of pole	poor	19.8	30.2635	-89.4048	Shot ground at wood sake
KMSC-05-02	409 St. Josepa St.	Exterior front wall of house @ eave to roof	Hancock	Water Line	Exterior front wall of house @ eave to roof	Hwy. 90 left to Nicholson Ave., right to N. Central Ave., left to St. Joseph St., 410' to HWM(HSE#409)	Nail set on road/see offset point	fair	24.4	30.2860	-89.3751	Shot eave of roof
KMSC-05-03	630 Cali Ct.	Exterior wall of house	Hancock	Water Line	Exterior wall of house	630 Cali Ct., Close to corner of Cali Ct. and N. Central Ave.	Paint mark and flag in middle of N. Central Ave. Mark in 73' from centerline intersection of N. Cent and Cali Ct. in NE direction.	fair	25.5	30.2945	-89.3612	Shot Ground (paint mark not found)
KMSC-05-04	234 Washington Ave.	Exterior wall (front porch)	Hancock	Water Line	Exterior wall (front porch)	Hwy. 90 west to Washington Ave. (left) follow Washington Ave. to house #234.	Prop. Owner marked wall w/marker	good	25.9	30.3052	-89.3356	Shot marker line on wall
KMSC-05-05	410 McDonald Lane	Side of utility pole	Hancock	Personal Account	Side of utility pole	410 McDonald Lane, East of N 2nd St. which is south of Hwy 90	Stake at bottom of pole; paint mark on pole	good	25.8	30.3150	-89.3239	Shot ground at wood sake
KMSC-05-06	661 N. Beach Blvd.	Tree	Hancock	Debris Line	Tree	Hwy. 43 south from I-10 to hwy 90 east to bridge, left on N. Beach Blvd. to address	Chiseled "X" in concrete	fair	25.8	30.3230	-89.3266	Shot ground at base of tree
KMSC-05-07	1380 N. Beach Blvd.	Piece of debris, floating into a tree	Hancock	Other	Tree	1380 N. Beach Blvd.	Chinsel mark and paint to east of road also, stake at same location.	poor	21.7	30.3385	-89.3346	Shot ground at base of tree
KMSC-05-08	N. Beach Blvd. and Blakemore, St.	Tree	Hancock	Debris Line	Tree	Hwy. 90 to St. Louis Bay, Left on N. Beach Blvd. to address	Chiseled "X" in concrete	poor	22.3	30.3428	-89.3476	Shot ground at base of tree

HWM ID	HWM Address	Flaggers Original HWM Surface - RAW	County	Type of HWM	HWM Object	Location_Directions to HWM Object_RAW	Type of Marker RAW	Reliability of mark for surge	NAVD-88	Survey Latitude	Survey Longitude	Survey Comments
KMSC-05-09	Unnamed street close to 1371 Blue Meadow Rd., Bay St. Louis, MS 39520	Wall Exterior	Hancock	Water Line	Exterior wall	Wall of new sub division, right of off Blue Meadow Rd. which is off Hwy 90.	Stake in front of wall. Also a black line in the inside corner of the NW wall	poor	16.3	30.3248	-89.3556	Shot marker line on line
KMSC-06-01	7250 Stennis Airport Dr.,	Ground	Hancock	Debris Line	Ground	Off Hwy. 10 going west, and get off onto Hwy 603, follow to Stennis Airport Dr. to the left. Surge line North of end of Airport Apron.	Stake with pink flag	poor	19.4	30.3743	-89.4518	Shot ground at wood stake
KMSC-06-03	Across street from 16038 Hart Lane, residence	Interior HWM transferred to exterior NW coner in back of shop. Metal green wall.	Hancock	Water Line	Interior wall transferred to exterior wall	Off Hwy. I-10 go north and take Hwy 603/43 heading towards Kiln. Shop will be on left with a concrete gorilla at entrance.	Duct tape and black permanent marker.	excellent	20.6	30.4071	-89.4392	Shot bottom of tape
KMSC-06-04	HWY I-10, 321' pass NE of Pearl River Bridge	Ground	Hancock	Debris Line	Ground	HWM is located 36' from paint. Paint mark is located 321' NE of the NE corner of the bridge	Stake with pink flag. White paint	poor	8.5	30.3055	-89.6315	Shot ground at wood stake
KMSC-06-05	Hwy I-10	Ground	Hancock	Wrack Line	Ground	HWM is 12' from birm of road	Stake and pink flag and White paint on birm	poor	11.9	30.3318	-89.5199	Shot ground at wood stake
KMSC-06-06	I-10 HWY	Ground	Hancock	Wrack Line	Ground	HWM is 9' from birm	Stake with pink flag and white paint	poor	15.4	30.3449	-89.4673	Shot ground at wood stake
KMSC-06-07	I-10	Ground	Hancock	Debris Line	Ground	Going west on I-10 HWM is 44 feet from paintmark on the birm. 61 feet from the sign post to HWM. (0.15 mile to I-10 Exit 16)	Stake w/pink flag & white paint	poor	25.2	30.3751	-89.3701	Shot ground at wood stake
KMSC-09-01	100 Central Ave.	Back Exterior wall	Hancock	Mud Line	Back Exterior wall	Left of front door	Duct tape bottom of tape	fair	26.6	30.3062	-89.3392	Shot duct tape on wall

HWM ID	HWM Address	Flaggers Original HWM Surface - RAW	County	Type of HWM	HWM Object	Location_Directions to HWM Object_RAW	Type of Marker RAW	Reliability of mark for surge	NAVD-88	Survey Latitude	Survey Longitude	Survey Comments
KMSC-09-02	Corner of Central and Bay Oaks Dr. (Power Transfer Station)	Exterior wall	Hancock	Mud Line	Exterior wall	Side door facing road	Duct tape bottom of tape	fair	22.7	30.2980	-89.3544	Shot bottom of duct tape
KMSC-09-03	120 Lakeside Dr.	Exterior wall	Hancock	Mud Line	Exterior wall	Mud line on exterior wall, facing railroad tracks.	Duct tape	fair	25.2	30.2950	-89.3603	Shot bottom of duct tape
KMSC-09-04	436 Waveland Ave.	Exterior wall	Hancock	Mud Line	Exterior wall	HWM is on left of front door.	Duct tape	fair	19.6	30.2792	-89.3878	Shot bottom of duct tape
KMSC-09-05	5117 Lower Bay Rd.	Exterior wall, transfer from interior wall	Hancock	Mud Line	Interior wall transferred to exterior wall	HWM on right side of front door	Duct tape		22.6	30.2897	-89.4099	Shot bottom of duct tape
KMSC-09-06	230 Old Spanish Trail	Mud line on exterior wall	Hancock	Mud Line	Exterior wall	HWM on left of front door.	Duct tape	good	22.5	30.3017	-89.3722	Shot bottom of duct tape
KMSC-10-74	1.6 miles east of Hwy I-10 exit 16 (Diamondhead exit) on embankment on west bound lane	Northside of I-10 between exits 16 and 20	Hancock	Wrack Line	Ground	56' from outside white line on west bound I-10 to stake on embankment 1.6 miles east of exit 16	Stake marks top of HWM	fair	25.3	30.3823	-89.3468	Shot ground at wood stake
KMSC-10-75	104219 Bayou	On ground	Hancock	Wrack Line	Ground	On Bayou Drive 1 lot past 104219 house, 18'8" north of 104227 Bayou driveway, even with telephone pole. Wrack line approximate 200' of 104219 house.	Red paint line in road at HWM	poor	20.4	30.4077	-89.3725	Shot paint line on road
KMSC-20-02	404 HWY 90	Interior wall transferred to exterior wall.	Hancock	Mud Line	Interior wall transferred to exterior wall.	Front entrance of Motel on right side of front door.	Vertical offset from set point	excellent	23.3	30.3059	-89.3800	Shot slab surface at mark
KMSC-20-03	At corner of Nicholson and Beach Blvd.	On road	Hancock	Water Line	Road	Approximate at corner of Nicholson and Beach Blvd.	Red mark on side of road. Looks like a circle with cross	fair	26.9	30.2899	-89.3596	Shot edge of pavement



HWM ID	HWM Address	Flaggers Original HWM Surface - RAW	County	Type of HWM	HWM Object	Location_Directions to HWM Object_RAW	Type of Marker RAW	Reliability of mark for surge	NAVD-88	Survey Latitude	Survey Longitude	Survey Comments
KMSC-20-04	South Beach Blvd.	Exterior wall	Hancock	Personal Account	Exterior wall	Facing house, right end of porch	Vertical offset	fair	21	30.3022	-89.3342	Shot concrete slab

# Appendix 2

## Wind and Atmospheric Pressures

---

### Introduction

This section describes the methodology that is used to generate the final (95-percent solution) wind and pressure fields for Hurricane Katrina. These fields were used to drive the wave and hydrodynamic modeling discussed in Appendices 3, 4, and 5. All results presented here utilize the final H\*Wind/IOKA wind product. At times references are made to the *95% winds*, or *OWI95*. Final winds and the *95-percent winds* are synonymous. The final winds represent the best that could be produced in the time allocated for the project, realizing that they could be improved possibly with more time and effort.

### Approach

Accurate modeling of wave and storm surge levels is highly dependent on the quality of wind and pressure field input to the models. The techniques used to construct these fields rely on point-source measurements (buoys and land-based meteorological platforms), hurricane reconnaissance data consisting of Drop Windsonde (radio transmitting gauges measuring wind speed, pressure and other meteorological information), satellite-based scatterometer wind estimates (e.g., QuikScat, SSMI) and Step Frequency Microwave Radiometer (SFMR, Uhlhorn et al. 2003), a new measurement device for estimating the winds at the air-sea boundary (the most reliable wind estimate).

The inner core of a hurricane is constructed using a method developed at NOAA's Hurricane Research Division (HRD) called the HRD Surface Wind Field Analysis System (H\*Wind [http://www.aoml.noaa.gov/hrd/Storm\\_pages/katrina2005/wind\\_realtime.html](http://www.aoml.noaa.gov/hrd/Storm_pages/katrina2005/wind_realtime.html)). All measurements are transformed to a standard 10-m elevation, averaging period (1-minute sustained wind speed) and set exposure (marine or land). The data are scrutinized for quality. The product of this man-machine mix is a streamline and isotach contour plot (Figure 2-1). These products were specifically generated for the Hurricane Katrina IPET study.

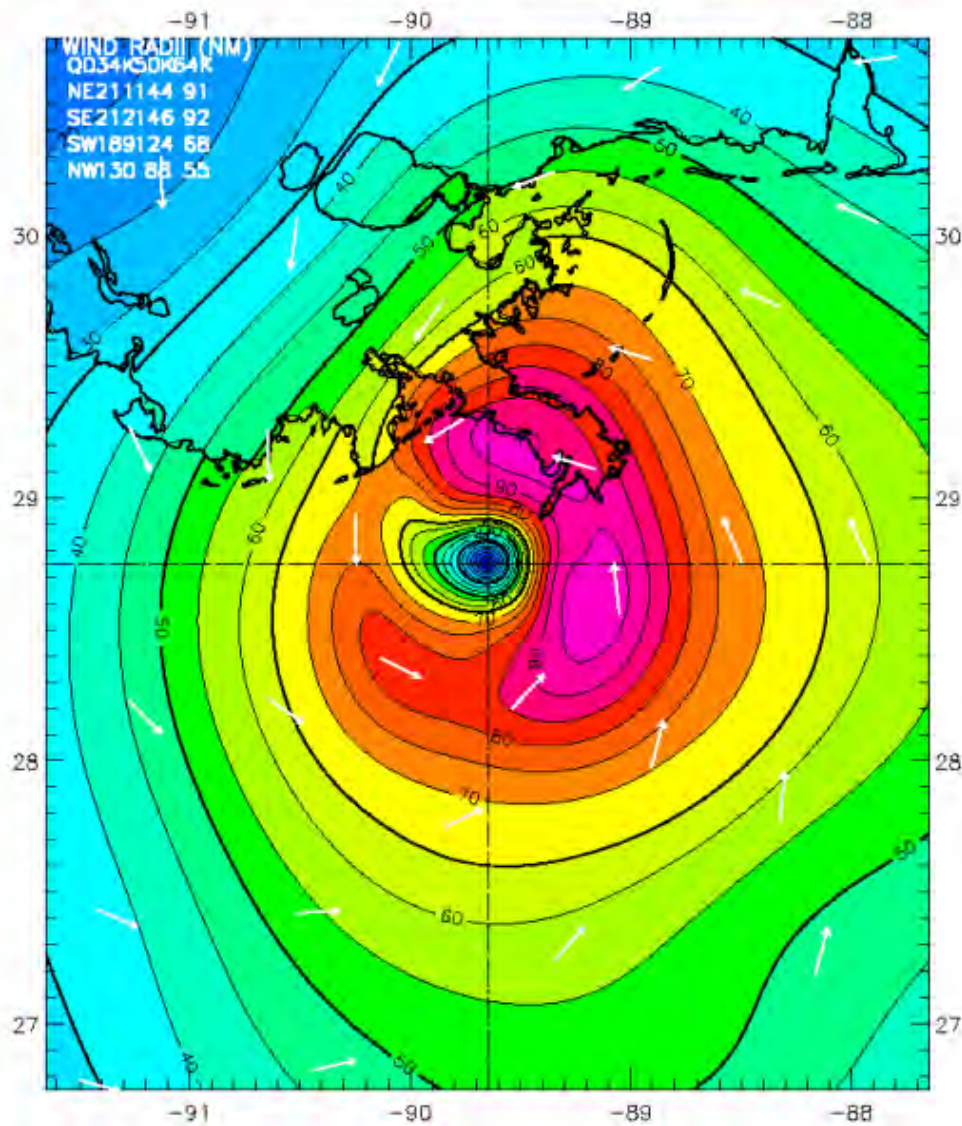
## Hurricane Katrina 0900 UTC 29 AUG 2005

Max 1-min sustained surface winds (kt)

Valid for marine exposure over water, open terrain exposure over land

Analysis based on SHIP from 0707 - 1010 z; FCMP\_TOWER from 0703 - 1059 z; MESONET from 0700 - 1100 z;  
SFMR43 from 0712 - 1059 z; DUAL\_DOPPLER from 1010 - 1010 z;  
ASOS from 0700 - 1100 z; CMAN from 0700 - 1100 z;  
GOES\_SWIR from 1002 - 1002 z; METAR from 0712 - 1058 z;  
MOORED\_BUOY from 0700 - 1059 z; MADIS from 0707 - 1049 z;  
VAD\_88D from 0804 - 1012 z; TAIL\_DOPPLER43 from 0921 - 1020 z;  
GPSSONDE\_WL150 from 0847 - 1058 z;

0900 z Army Corps fix; mslp = 917.0 mb



Observed Max. Surface Wind: 99 kts, 30 nm SE of center based on 1032 z SFMR43 sfc measurement  
Analyzed Max. Wind: 99 kts, 31 nm NE of center

Figure 2-1. Example of H\*Wind snapshot on 29 August 2005 0900 UTC. The wind speeds are color contoured in knots, representing 1-minute sustained wind speeds. Note this wind field includes marine and land exposures identified by the abrupt change in color contours over the land.

There are 33 H\*Wind analysis snapshots, generated at 3-hour intervals for the duration of this storm. These are fixed (storm centered) in space and time (see Figure 2-2 and Figures 2-11 to 2-43). The snapshots represent the best wind estimate for the 4-deg by 4-deg longitude/latitude target domain.

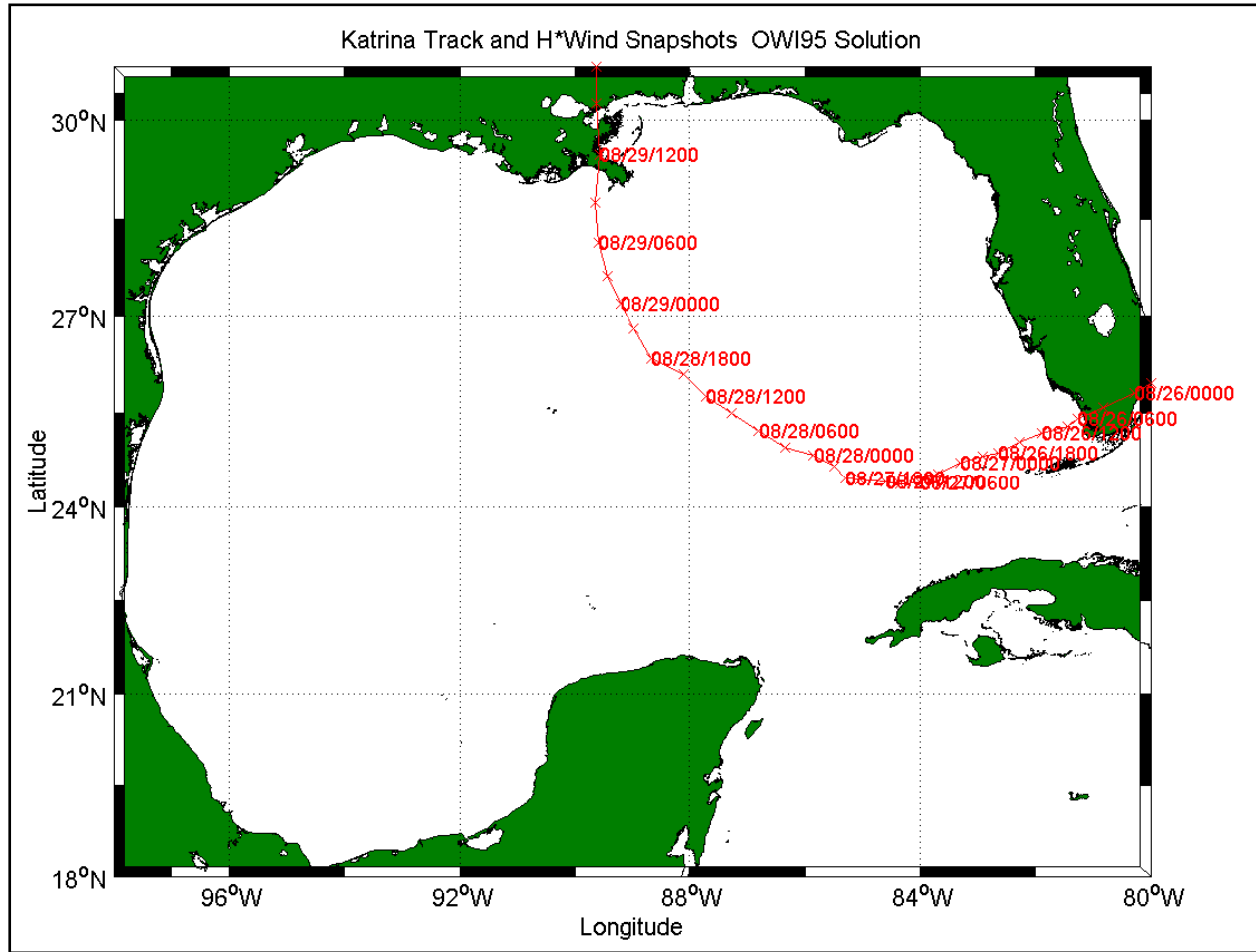


Figure 2-2. Spatial and temporal locations of the 33 H\*Wind snapshots relative to the forecast official storm track of Hurricane Katrina.

The development of the full domain winds requires two straightforward procedures. In an analysis mode, information in a forward-track direction is known as is information in a back-track direction. Snapshot H\*Wind fields are time interpolated to a three-hour interval and positioned to the NHC Official Hurricane Katrina Storm Track (Figure 2-2, red symbols). A moving center interpolation algorithm is applied to preserve the characteristics of the tropical storm wind core in space and time. The wave and surge modeling activities require complete wind field specification for the entire target domain (the area shown in Figure 2-2). Accomplishing this task requires background estimates which are derived from the NOAA National Centers for Environmental Prediction/National Center for Atmospheric Research (NCEP/NCAR) Reanalysis Project (Kalany et al. 1996). The NCEP/NCAR winds are rigorously analyzed and rely on assimilation methods with data not originally used in the NCEP operational forecast. A final step is to inject local marine data (adjusted to a consistent 10-m elevation and



adjusted for neutral stability). This procedure uses an Interactive Objective Kinematic Analysis System (Cox et al. 1995) performed by Oceanweather, Inc. (OWI).

Generation of the surface pressure fields follows a slightly different approach using the TC96 model (Thompson and Cardone 1996). The model solves, by numerical integration, the vertically averaged equations of motion that govern a boundary layer subject to horizontal and vertical shear stresses. Upgrades and modifications of the TC96 have been made over the development cycle (Cox and Cardone 2000). The pressure fields generated for the Katrina study are built from parameters derived from data in meteorological records and the ambient pressure field. The symmetric part of the pressure field is described by an exponential pressure profile from Holland (1980). The pressure field snapshots aligned to the storm track are spatially and temporally interpolated in a similar fashion as described in the wind field preparation and placed on the identical fixed latitude/longitude grid. No synoptic-scale inputs were considered in this application. All wind and pressure fields used in the Hurricane Katrina study were produced by OWI (<http://www.oceanweather.com>) on two domains that are summarized in Table 2-1 and depicted in Figures 2-3 and 2-4.

<b>Table 2-1 Wind and Pressure Field Domain Characterization</b>							
Domain	Longitude (deg)		Latitude (deg)		Res. (deg)	Duration (yr/mth/day/hr)	Interval (sec)
	West	East	South	North			
Basin	98 W	80 W	18 N	30.8 N	0.1	2005082500 – 2005083100	900 30-min ave
Region	91 W	88 W	28.5 N	30.8 N	0.025	2005082800 - 2005083000	900 30-min ave

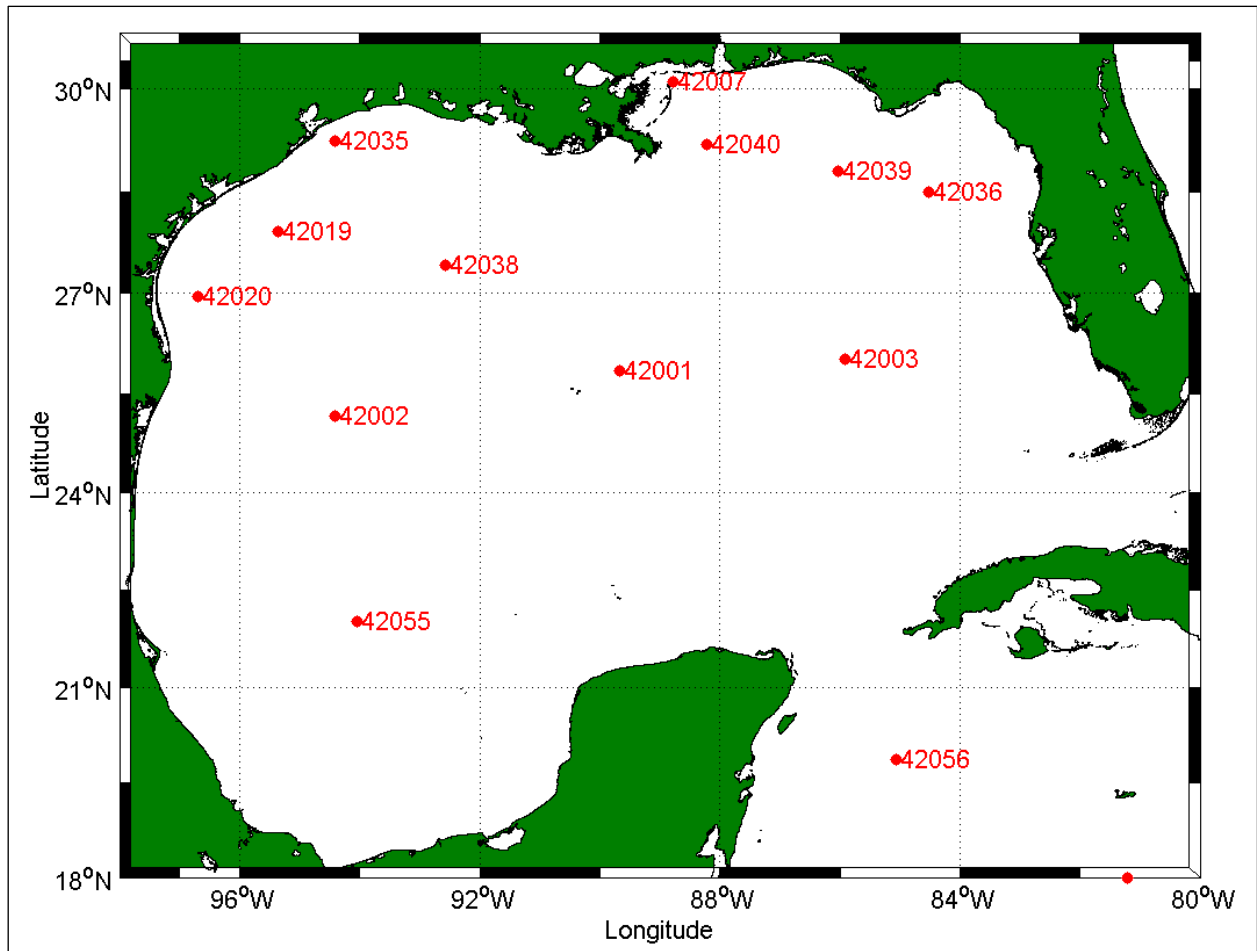


Figure 2-3. Domain of the basin-scale OWI wind and pressure fields for Hurricane Katrina simulations. Buoy measurement sites are identified in red

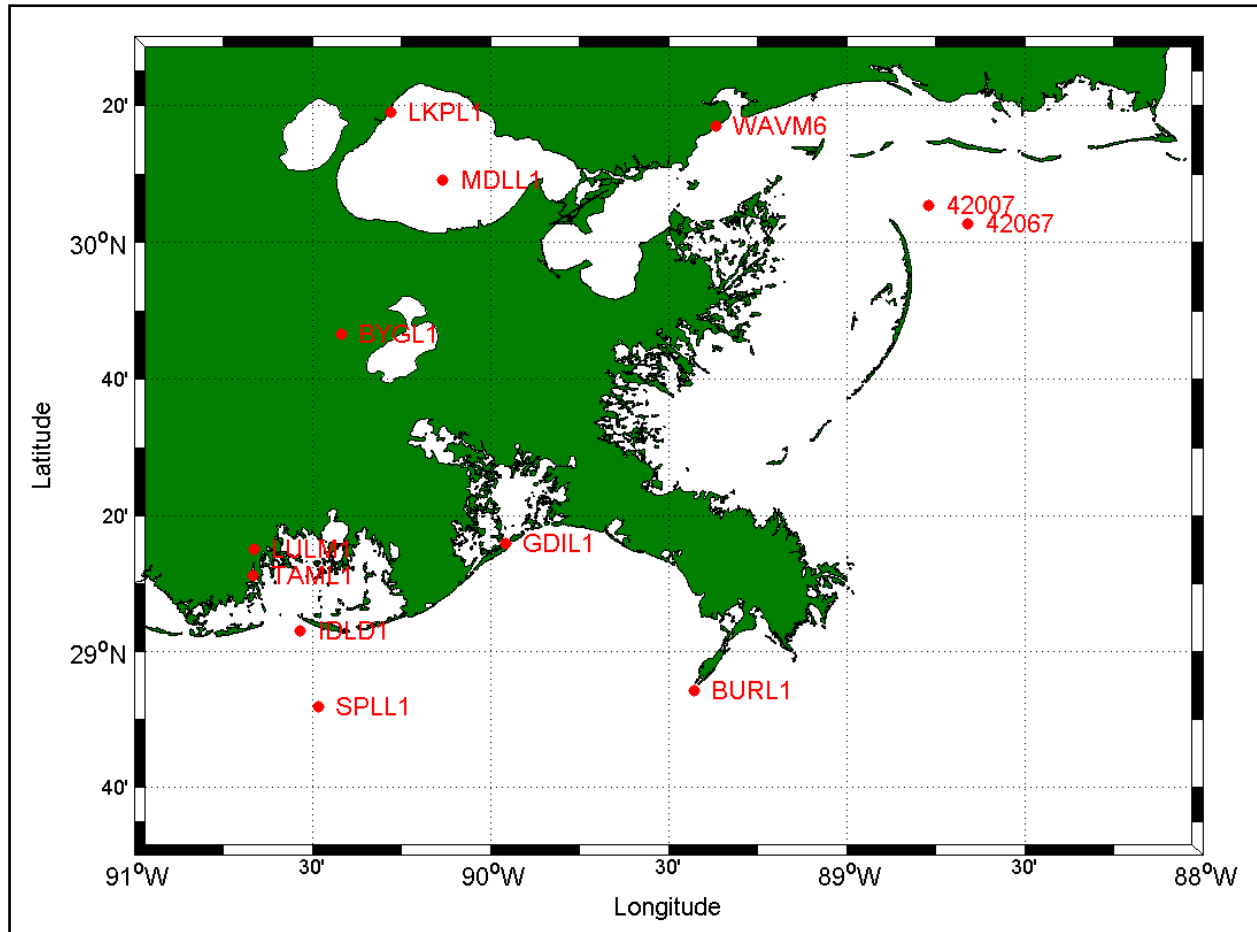


Figure 2-4. Domain of the region-scale OWI wind and pressure fields for Hurricane Katrina simulations. Point source measurement sites are identified in red.

## Discussion

Graphical representations of the maximum sustained 30-min averaged wind speed over the duration of each simulation at each grid point are presented for the basin-scale domain (Figure 2-5) and the region-scale domain (Figure 2-6). The wind results plotted in these two figures reflect wind input to the wave modeling, which uses the 30-min wind averaging that is reflected in the final H\*Wind/IOKA wind product.

Conversion from a 30-min average to a 1-min (sometimes termed a *gust factor*) is made with a multiplication factor on the order of  $1.24 \cdot U_{30\text{-min}} = U_{1\text{-min}}$ . A 30-min average wind speed has been commonly applied and is the standard used in wave modeling efforts (Cardone et al. 1996). A 10-min average wind speed is commonly used in surge modeling ( $1.09 \cdot U_{30\text{-min}} = U_{10\text{-min}}$ ). Scaling the absolute maximum wind speed in Figure 2-5 (which shows 30-min average winds) to a 1-min average value using the 1.24 factor yields a maximum value of 145 knots. In the main text of Volume IV there are references to the peak 1-min wind speeds during Katrina, of 139 knots derived from individual H\*Wind snapshots (Figures 2-11 to 2-43). The discrepancy

between the final OWI based wind fields and the H\*Wind snapshot results is a result of resolution, and slight adjustments in the *gust factor* used in the construction of the final winds. H\*Wind snapshots are based on 2-km resolution. There will be some loss of wind intensity associated with placing these results onto the 0.1-deg grid adopted for the final basin-scale wind product. However OWI accounted for this by varying the multiplication factor over time, and minimized the errors between the final winds and the individual H\*Wind snapshots.

The color contours of the maximum winds for the basin-scale domain show the rapid deepening of Katrina's central pressure reflected in a maximum wind speed increase of 44 knots (73 knots at 27 August 1930 UTC to the maximum of 117 knots at 28 August 1500 UTC, see Figure 2-2 for the storm position on these dates). From that point onward to landfall, the winds steadily decreased, however the lateral extent of the storm varied only modestly. Two offshore oil platforms equipped with wind and wave measurement sensors recorded peak winds of 53.7 knots during the time of Katrina. These values are compared to coincident final wind field estimates of 51.9 and 56.7 knots. These data are proprietary and cannot be provided here.

By the time Katrina entered into the regional domain (Figure 2-6) the winds were decaying. There were two zones of 80-kt winds, one close to the entrance of the Mississippi River and east of Grand Isle, LA. The second lobe covers an area from Breton and Chandeleur Sounds extending north through Bay St. Louis and Pass Christian, MS. The absolute maximum wind speed in the grid was slightly over 87 kt. Wind speeds exceeded 80 kt along Mississippi Sound, and well into Lake Borgne. Lake Pontchartrain winds were nominally in the 60-kt range.



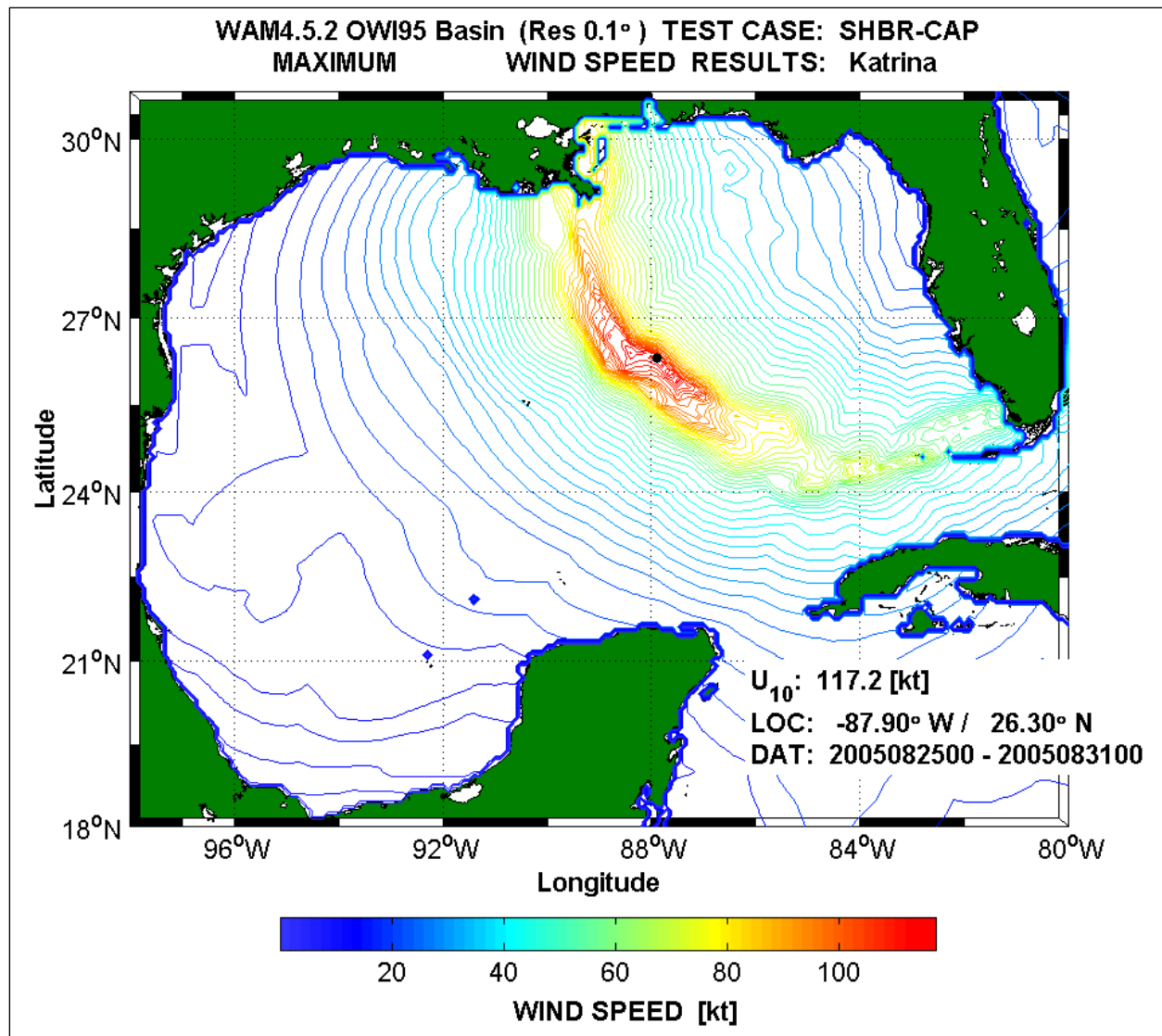


Figure 2-5. Wind speed maxima for the simulation period of Hurricane Katrina in the basin-scale domain

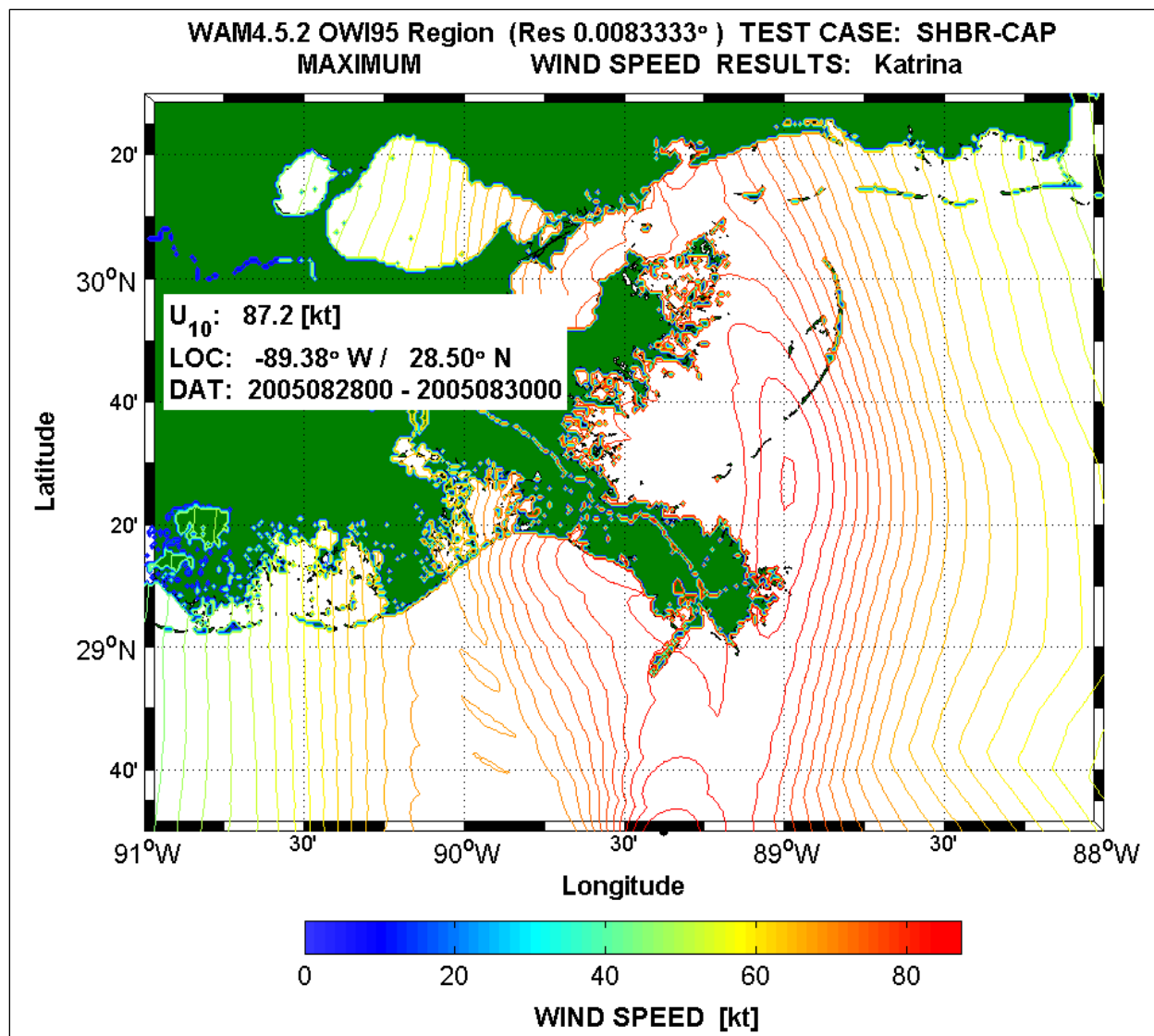


Figure 2-6. Wind speed maxima for the simulation period of Hurricane Katrina in the regional-scale domain.

Verification of the modeled winds is an important factor for the wave and surge modeling efforts. The wave height estimates (first moment of the energy density spectrum) are related to the square of the wind speed. Thus, a 10-percent error in the winds could, by scaling principles, force as much as 20-percent error for the waves.

Of 19 locations, ten residing in NOAA’s National Data Buoy Center (NDBC) offshore buoy network (Figure 2-3) and nine land-based meteorological stations (Figure 2-4), only ten survived during Hurricane Katrina (see <http://www.ndbc.noaa.gov>). Of those ten locations only 42036 and 42039 were situated in the right-quadrant of the storm, whereas 42001, 42038, 42002, 42019, 42020, and 42035 only marginally felt the effects of tropical wind forcing. One additional site MDLL1, the Lake Pontchartrain Causeway anemometer, survived through the peak of the storm. However, soon after the storm peak, there was a significant gap in the causeway wind records,

and this is assumed to be resulting from a loss of power. Recently acquired data from Lakefront Airport cast some doubt on the accuracy of the mid-Lake wind data. The focus of the wind speed and directional accuracy evaluation presented here is concentrated in the regional domain.

Table 2-2 summarizes the wind measurement sites used for comparison purposes, anemometer elevation, and when each site ultimately failed.

<b>Table 2-2 Point Source Measurements of Winds and Waves</b>						
LOC. No.	Location (deg/min/sec)		Domain Tested	Parameters		Date Failed
	Longitude (W)	Latitude (N)		Wind elev (m)	Water dep (ft)	
42067	88 39 30	30 02 40	Reg	5.0		2005 08 29 11 30
42007	88 46 07	30 05 25	Reg/Bas	5.0	43.9	2005 08 29 05 50
GDIL1	89 57 24	29 16 00	Reg	15.8		2005 08 29 10 00
LKPL1	90 16 50	30 18 54	Reg	13.0		WIND DIR
WAVM6	89 22 00	30 16 54	Reg	---		2005 08 29 09 36
MDLL1	90 08 00	30 09 00	Reg	5.49		2005 08 29 15 20 GAP
BURL1	89 25 42	28 54 18	Reg	30.5		2005 08 29 05 00
BYGL1	90 25 06	29 46 36	Reg	9.1		2005 08 26 19 42 (WS)
ILDL1	90 32 00	29 03 12	Reg	19.2		2005 08 29 11 00
SPILL1	90 29 00	28 52 00	Reg	40.4		2005 08 28 17 00
TAML1	90 39 55	29 11 15	Reg	10.0		2005 08 29 11 00
LULM1	90 39 48	29 15 12	Reg	13.2		2005 08 29 09 00
42040	88 12 49	29 11 05	Bas	5.0	900	-----
42039	86 01 17	28 47 38	Bas	5.0	954	-----
42036	84 31 00	28 30 00	Bas	5.0	179	-----
42003	85 54 50	26 00 32	Bas	5.0	10617	2005 08 28 04 50
42001	89 39 30	25 50 30	Bas	10.0	10739	-----
42038	92 34 31	27 25 12	Bas	5.0	3780	2005 08 31 07 50
42002	94 25 00	25 10 00	Bas	10.0	10496	-----

Time plots of modeled winds and measurements at four locations (BURL1, GDIL1, WAVM6, and MDLL1) are provided in Figures 2-7 to 2-10. These are selected based on their location relative to Katrina's track. BURL1 (Southwest Pass, LA) and GDIL1 (Grand Isle, LA) are located in close proximity to the Louisiana landfall. MDLL1 (Lake Pontchartrain Causeway, LA) is selected to evaluate the accuracy in the modeled winds in Lake Pontchartrain. WAVM6 (Waveland, MS) is selected as being near the landfalling point in Mississippi. The remaining plots are contained in the Figures 2-44 to 2-50 at the end of this section. Wind directions are plotted in a meteorological coordinate system where 0 deg represent a wind from the North and 90 deg represent a wind from the East

Rather than convert the measurements to an equivalent neutral stable 10-m wind, they are plotted as raw data. In these types of analyses, a 1:1:1 running average is generally applied to the U (east/west component), V (north/south component), and W (the square root of the sum of the squares of the two components). For these comparisons no smoothing was used. There are differences in the anemometer heights as shown in Table 2-2, varying from 40.4 m to 5.0 m. Generation of the equivalent neutral stable wind requires the air and water temperatures. At most

sites only one of the two temperatures exist so interpreting the net effect would be subjective. Both of these effects would marginally affect the wind speed ( $\pm 10$  percent or less). This would fall into the range of geophysical variability and within the confidence limits associated with measuring winds at high velocities. Figures 2-7 and 2-8 display the comparison between the basin- and regional-scale winds to measurements obtained at Southwest Pass and Grand Isle, LA. The modeled results are taken at the closest grid node to the point measurements, potentially generating some slight phase lags between the two data sets. Studies were conducted using four surrounding model grid points; however, the variation in speed and direction deviated only on the order of 5 percent.

Modeled winds show very good agreement with the magnitude and direction measurements at both sites. There are subtle differences, for example the diurnal oscillation in the speed and directions is not replicated in the modeled winds. There is a slight under-estimation in the wind speed at Southwest Pass (Figure 2-7) prior to the peak winds of Hurricane Katrina; however, differences are on the order of about 5 kt. Up until the wind sensor failed, both the basin and regional winds emulated the measurements well. The drop in speed seen near the peak is due to Katrina's eyewall passing in close proximity to Southwest Pass, and is also evident in the 150 deg directional shift. In the left quadrant, (see Figure 2-8 at Grand Isle) the opposite holds true. The magnitude is lower, and the directional shift is counter-clockwise (rotation from 45 to 255 deg). Despite only a limited data around this peak, the model winds do remarkably well.

The last two examples are from Waveland, MS (WAVM6) and the Lake Pontchartrain Causeway, LA (MDLL1). For the Waveland site (Figure 2-9), like all other meteorological sites shown thus far, the instrument failed long before the peak of the wind. Prior to failure, the modeled winds emulate the measurements quite well, including the rapid increase in magnitude accompanied by the clockwise rotation in direction, evident of the right-quadrant position relative to Katrina's eyewall. At the peak, modeled winds were in excess of 80 kt with a southerly direction, or straight into the coastline.



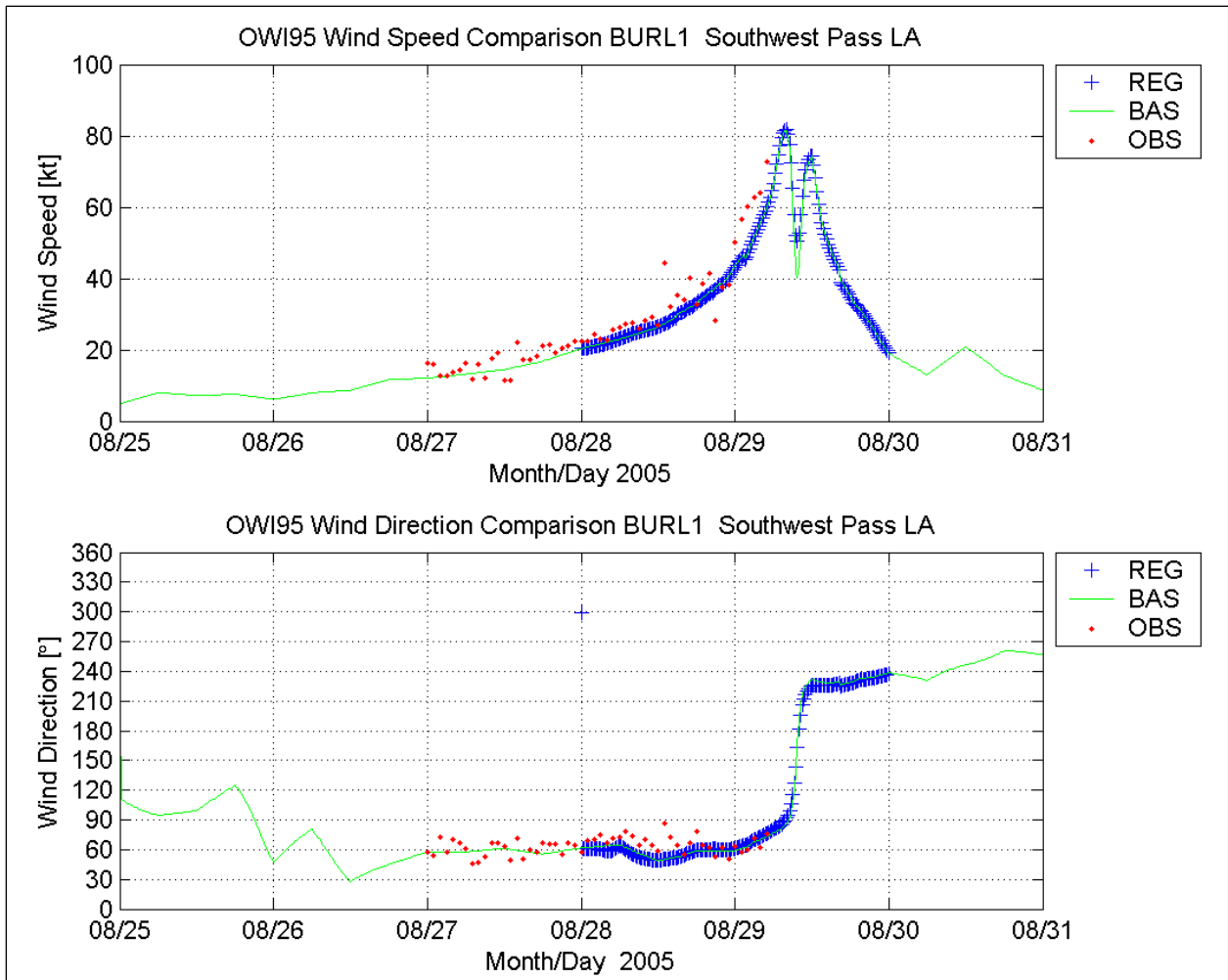


Figure 2-7. Comparison of wind speed (upper panel) and direction (bottom panel) at Southwest Pass, LA

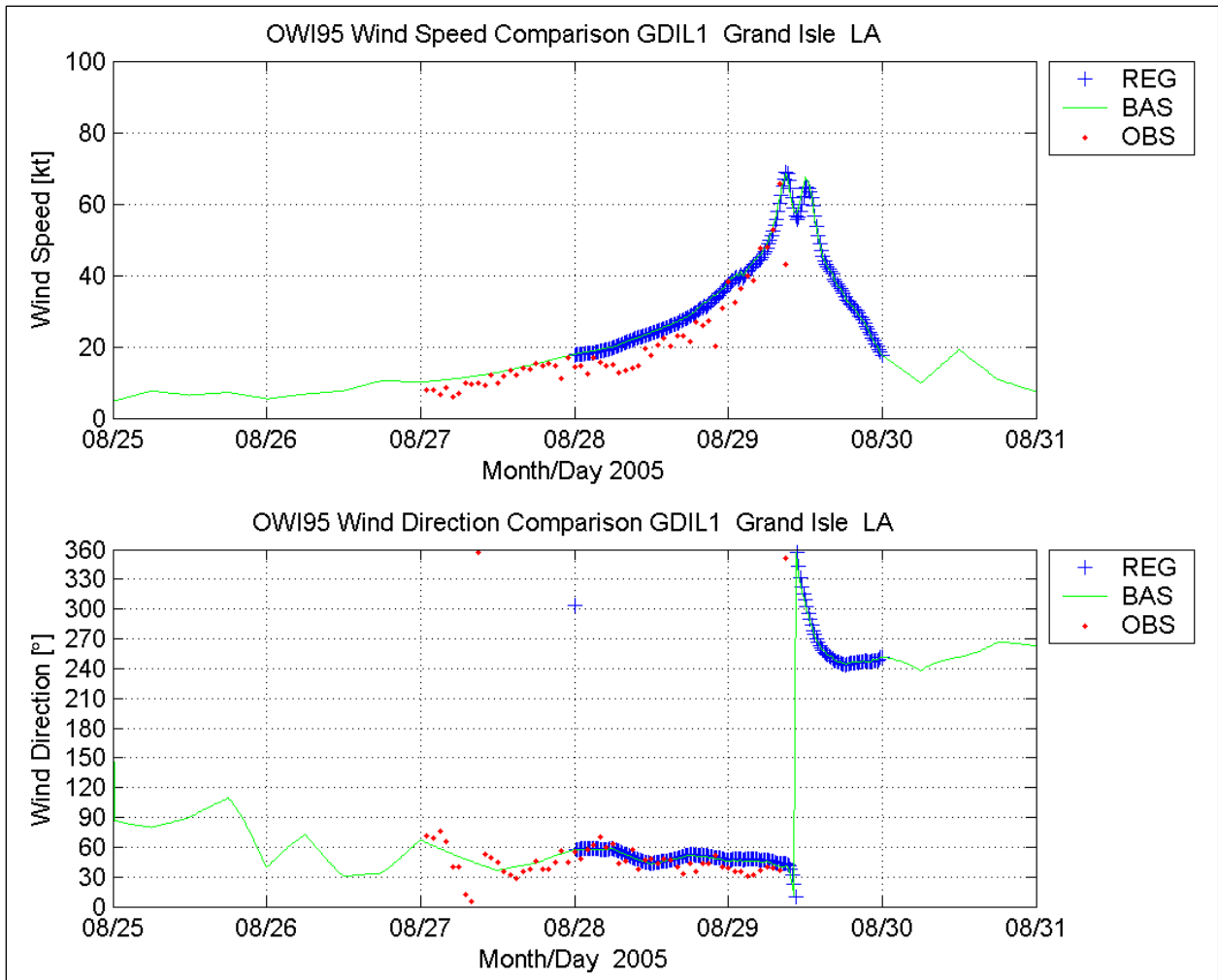


Figure 2-8. Comparison of wind speed (upper panel) and direction (bottom panel) at Grand Isle, LA

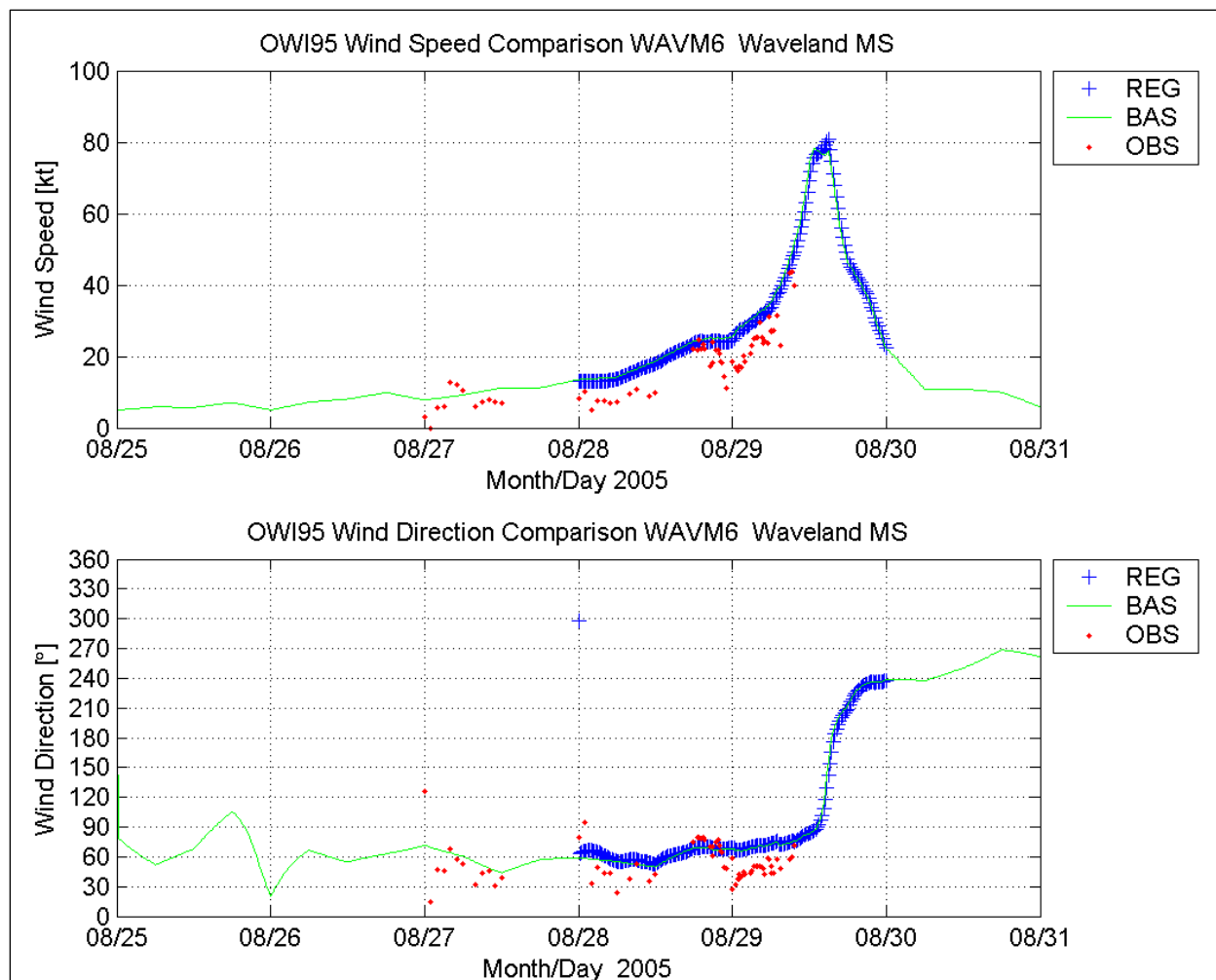


Figure 2-9. Comparison of wind speed (upper panel) and direction (bottom panel) at Waveland, MS.

The only meteorological site that survived through the storm peak was located at the Lake Pontchartrain Causeway (Figure 2-10). The velocity trace at this site is unusual. From about 29 August 0000 UTC the magnitude is about one half of the other sites, averaging around 10 kt, compared to Waveland (Figure 2-9) at nearly 20 kt. The winds are coming off the land at Waveland, whereas the causeway's winds would be classified as a marine exposure which would suggest the winds should have a higher magnitude. Anemometer differences could play a role in these differences; however, the Waveland site did not include any specific information about the anemometer. The modeled wind speed over-estimated the causeway measurements by about 10 to 20 kt. The modeled increase in wind speed during the growth stage is slower than the measurements, by nearly a factor of two. However, at the peak of the wind speed trace, the model results compare favorably. One might suspect errors are due to the combination of differences in sampling (1-minute sustained for the measurements versus a 30-minute average wind speed for the model), stability (air-sea temperature differences), and anemometer elevations (5.49 versus 10 m). However, these adjustments are merely multiplication factors on the order of 7 to 10 percent, and would only move the measurement data up or down relative to the data in Figure 2-10. These adjustments would not alter the time rate of change in the wind speed.

Comparing sustained winds over Lake Pontchartrain, the measurements show a 3-hr duration of winds in excess of 40-kt, whereas the modeled wind during is nearly 5.5 hrs. Wind speed measurements from the mid-lake Lake Pontchartrain site on the causeway (Figure 2-10) show an unusually abrupt increase in wind speed. The rapid change was not seen in any other data that were acquired in the region, and data from Lakefront Airport (also shown in Figure 2-10) along the south shore of Lake Pontchartrain suggest a more gradual increase in wind speed, so the data from the mid-lake measurement site were considered to be suspect, likely due to the causeway obstructing the flow for wind directions from the north.

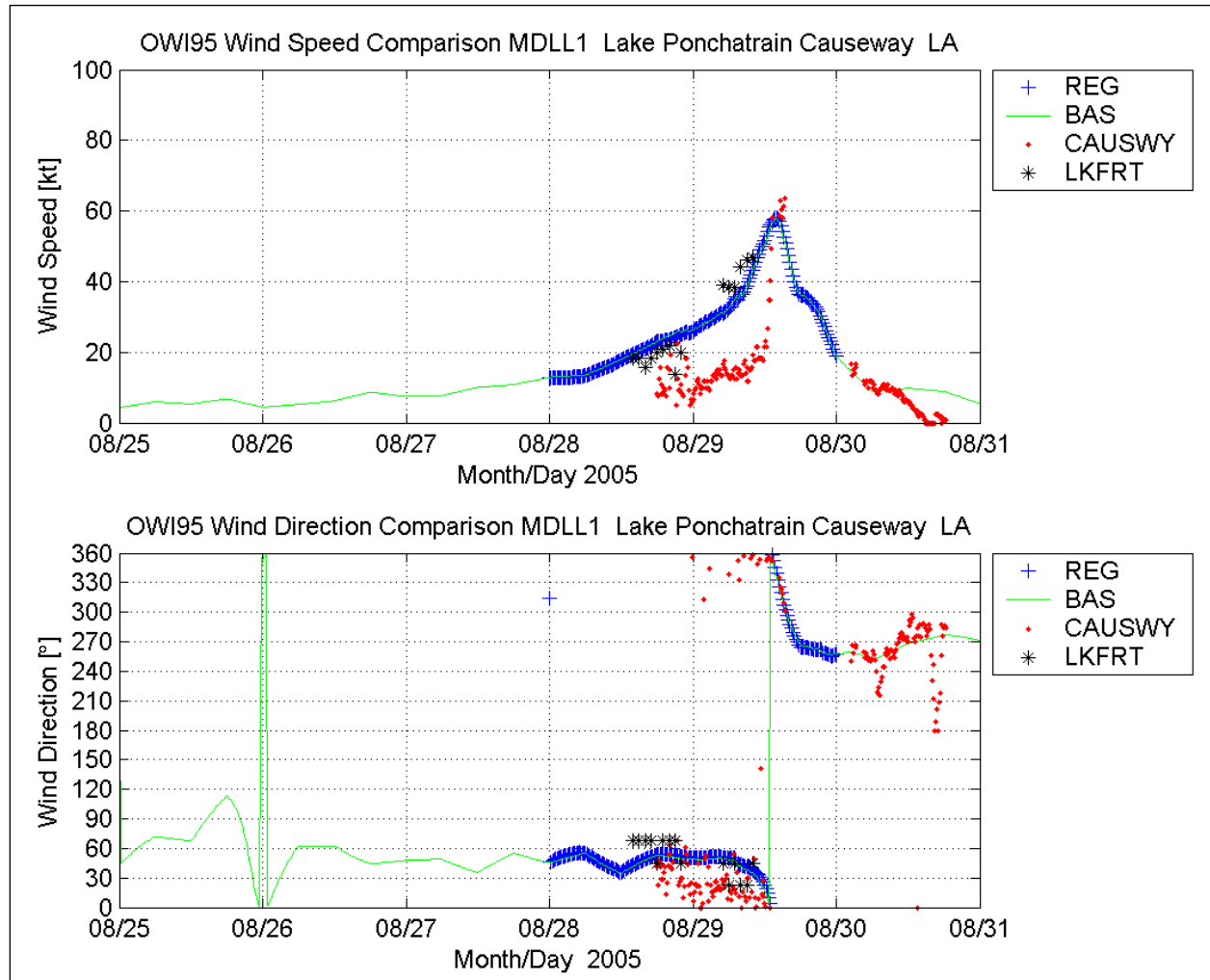


Figure 2-10. Comparison of wind speed (upper panel) and direction (bottom panel) at Lake Pontchartrain Causeway, LA.

Consistency in the land-based wind estimates have been established in the time plots for the various point source measurements made within the model domain. Evaluation of the overall performance can be assessed with statistical testing. Because of the population size for time-paired model to measurements is small (generally less than 100), any variation from the measurement comparisons will be amplified. In light of the limited data, and understanding that



all results could potentially be altered by the population size, the results of certain tests can be informative and diminish the uncertainties in the generation of the wave estimates for Katrina.

As previously cited, only one land-based meteorological station survived Katrina, and questions regarding the accuracy of the Mid-Lake Pontchartrain Causeway data mean that these data will not provide the needed insights of the accuracy in the wind fields. Hence, attention is turned toward data in the Gulf of Mexico obtained from the NDBC buoy array. All but two stations survived Katrina. All stations represent a marine exposure winds, identical to the basis of the final wind fields.

Eight NDBC locations are selected as evaluation points (42055, 42001, 42003, 42036, 42038, 42039, 42040, and 42007 in Figure 2-3). The corresponding time plots will be presented in Appendix 3 with the wave data analysis, because of the dependencies between wind and wave estimates.

The statistical tests are defined below. Note that in all cases, the independent variable is defined as the measurement, and the dependent variable is the model output. All results of the wind speed statistical tests are presented in Table 2-3, along with the number of observations considered in the analysis.

The measured wind parameters are denoted  $B$  and modeled wind parameters are denoted as  $M$ , where triangular bracket represent the arithmetic mean.

$$\bar{B} = \langle B \rangle \quad ; \quad \bar{M} = \langle M \rangle$$

$$BIAS = \langle M - B \rangle$$

$$\text{Absolute Error: } Abs\ Err = \langle |M - B| \rangle$$

$$\text{Root Mean Square Error (RMSE): } RMSE = \langle (M - B - BIAS)^2 \rangle^{1/2}$$

$$\text{Scatter Index: } SI = 100 * \frac{RMSE}{\bar{M}}$$

$$\text{Correlation Coefficient: } r = \frac{\langle (B - \bar{B})(M - \bar{M}) \rangle}{\left[ \langle (B - \bar{B})^2 \rangle \langle (M - \bar{M})^2 \rangle \right]^{1/2}}$$

$$\text{Slope and Intercept of Linear Regression: } M = a + b * B$$

A secondary linear regression is applied where the intercept  $a$  is forced to zero, and termed herein as the symmetric  $r$  value (Symm  $r$ ). For the range of values, the Scatter Index is defined as a percentage, where a lower value indicates a more reliable estimate. The mean values are

presented to position the bias, absolute error, and RMSE in the context of the distribution in population. There has been no adjustment or added analyses performed to examine if the model and measurements are phase lagged. No averaging technique is used on either data set, and as previously mentioned, the model and measurements are time paired. The measurement times identify the end time when the data were taken or 50-minutes into the hour, so for this analysis, the buoy data were adjusted to the even hour.

The statistical results for the wind estimates at the eight offshore buoy locations (see Figure 2-3) show remarkable agreement to the measurements. This is not surprising because IOKA uses all available measurements in the final blending step. For the large variation in the wind speeds in the near- and far-field of Hurricane Katrina, the biases in the modeled winds range from -1.16 to +1.05 kt (Note that a negative bias is model under-estimation and a positive bias is an over-estimation.). The absolute error is more or less a factor of two greater. The RMSE, a measure of the error variability, is slightly less than 3.5 kt, demonstrating the high-degree of accuracy in the wind fields. The greatest error is in the Bay of Campeche well over 400-nautical miles from the storm track. The Scatter Index (SI) falls into a range that is consistent with that of research quality wind products (Cardone et al. 1995). The correlation coefficient is no less than 0.92 in the area surrounding Katrina’s path. Results from the linear regression again typify the accuracy of the wind fields at these point source measurements, diverging from -8 to +5 percent estimation. For the standard linear regression (MODEL= $a+b \cdot \text{BUOY}$ ), the slope is relatively consistent with the forced zero intercept. However as the intercept increases, as in the case at 42003, 42038, 42039, 42040 and the far-field station of 42055, the slope suggests a model underestimate. The likelihood of these deviations is resulting from the limited population size, and amplified by the majority of those time-paired data consisting of low wind speeds. , The range of these values is quite acceptable, from a low of nearly 0.04 kt to the high at 42055 (far-field location) of 6.4 kt.

**Table 2-3. Statistical Results: Basin-Scale Hurricane Katrina Wind Speed (kt)**

Buoy ID	Mean Cond.		Bias (kt)	Abs. Err (kt)	RMS Error (kt)	Scat Indx	Linear Regression Estimators				No. Obs
	Meas (kt)	Model (kt)					Corr (r)	Symm r	Slope (b)	Intercp (a).	
42001	18.08	18.58	0.50	1.52	1.90	10	0.99	1.03	1.03	0.04	82
42003	22.97	21.81	-1.16	2.53	3.03	13	0.99	0.92	0.82	3.05	42
42007	15.92	15.49	-0.43	2.60	3.42	21	0.92	0.98	0.93	0.62	57
42036	21.36	21.01	-0.35	1.32	1.73	8	0.95	0.98	0.89	1.92	83
42038	12.97	13.41	0.44	1.94	2.35	18	0.95	1.01	0.90	1.71	82
42039	21.71	22.32	0.61	1.94	2.58	12	0.95	1.01	0.87	3.38	84
42040	20.74	21.62	0.87	2.06	2.72	13	0.98	1.01	0.93	2.27	84
42055	9.43	10.48	1.05	2.92	3.48	37	0.64	1.05	0.44	6.36	84

In summary, the wind and accompanying pressure fields used to force the surge and wave modeling efforts have been documented. The results at selected points in the Gulf of Mexico and at land-based meteorological stations uniquely define the detailed structure of Hurricane Katrina. Despite the limited population size used in a formal statistical evaluation, errors in the wind speeds show neither a trend to over- nor underestimate the wind speeds. The RMSE is well

within a range defined by a geophysical variation in the measurements with a magnitude of about 2.5 kt.

## References

- Cardone, V. J., R. E. Jensen, D. T. Resio, V. R. Swail, and A. T. Cox. 1996. Evaluation of contemporary ocean wave models in rare extreme events: the “Halloween Storm” of October 1991 and the “Storm of the Century” of March 1993. *J. Atmos. Oceanic. Technol.*, **13**, 198-230.
- Cox, A. T., and V. J. Cardone. 2000. Operational system for the prediction of tropical cyclone generated winds and waves. *6th International Workshop on Wave Hindcasting and Forecasting*, November 6-10, 2000, Monterey, CA
- Cox, A. T., J. A. Greenwood, V. J. Cardone, and V. R. Swail, 1995. An interactive objective kinematic analysis system. Preprints, *Fourth International Workshop on Wave Hindcasting and Forecasting*, Banff, Alberta, Canada, Atmospheric Environment Service, 109-118.
- Holland, G. L. 1980. An analytical model of the wind and pressure profiles in hurricanes. *Mon. Wea. Rev.*, **108**, 1212-1218.
- Kalany, E., M. Kanamitsu, R. Kistler, W. Collins, D. Deaven, L. Gandin, M. Iredell, S. Saha, G. White, J. Woollen, Y. Zhu, M. Chelliah, W. Ebisuzaki, W. Higgins, J. Janowiak, K.C. Mo, C. Ropelewski, J. Wang, A. Leetmaa, R. Reynolds, R. Jenne, and D. Joseph, 1996. The NCEP/NCAR 40-year reanalysis project. *Bull. American Met. Society*, Vol. 77, No. 3, 437-471.
- Thompson, E. F., and V. J. Cardone. 1996. Practical modeling of hurricane surface wind fields. *ASCE J. of Waterway, Port, Coastal and Ocean Engineering*. 122, 4, 195-205.
- Uhlhorn, E.W., and P.G. Black. 2003. Verification of remotely sensed sea surface winds in hurricanes. *J. Atmos. Oceanic. Technol.*, **20**, 99-116.

# H\*Wind Snapshots

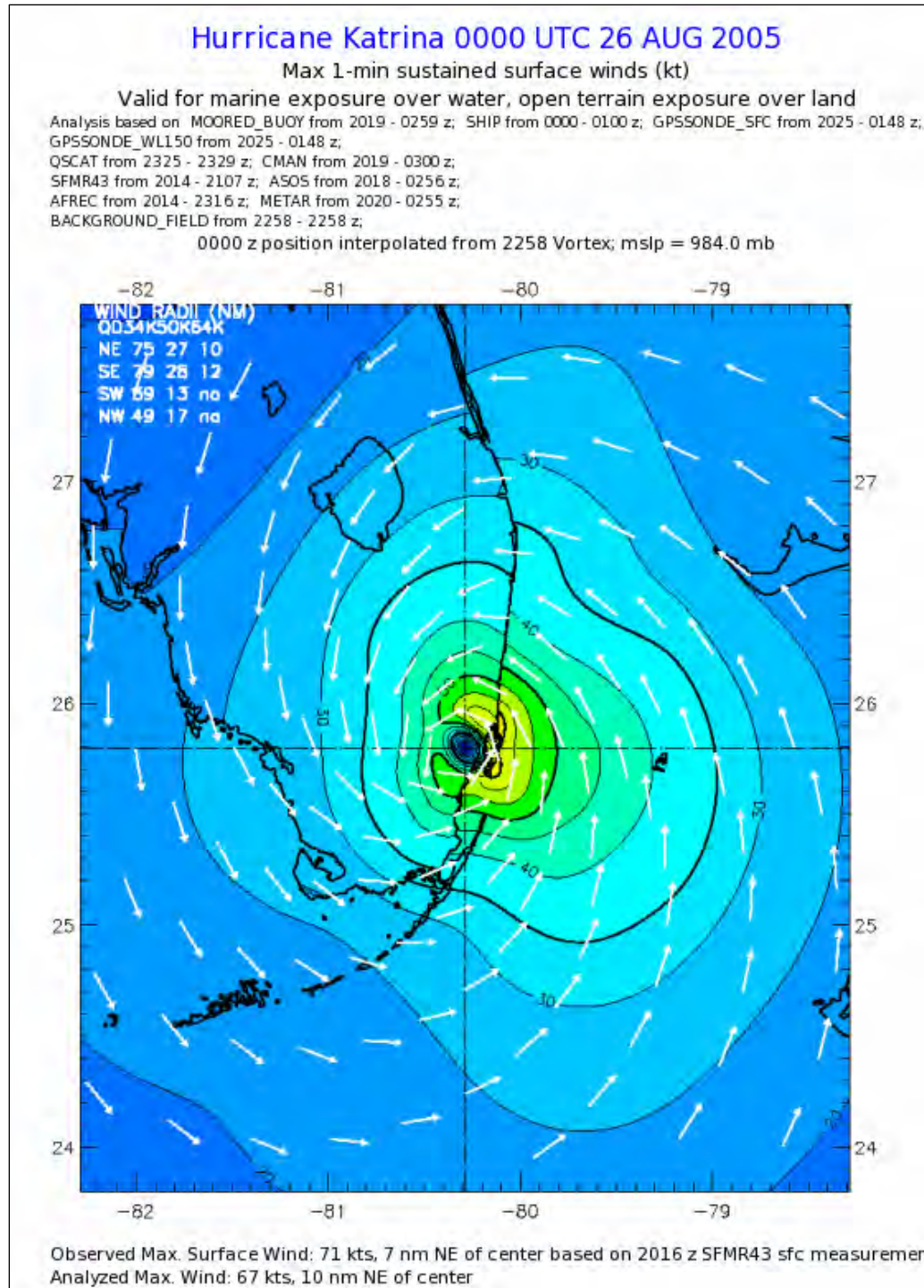


Figure 2-11. H\*Wind snapshot on 26 August 2005 0000 UTC. The wind speeds are color contoured in knots, representing 1-minute sustained wind speeds. Note this wind field includes marine and land exposures identified by the abrupt change in color contours over the land.



## Hurricane Katrina 0300 UTC 26 AUG 2005

Max 1-min sustained surface winds (kt)

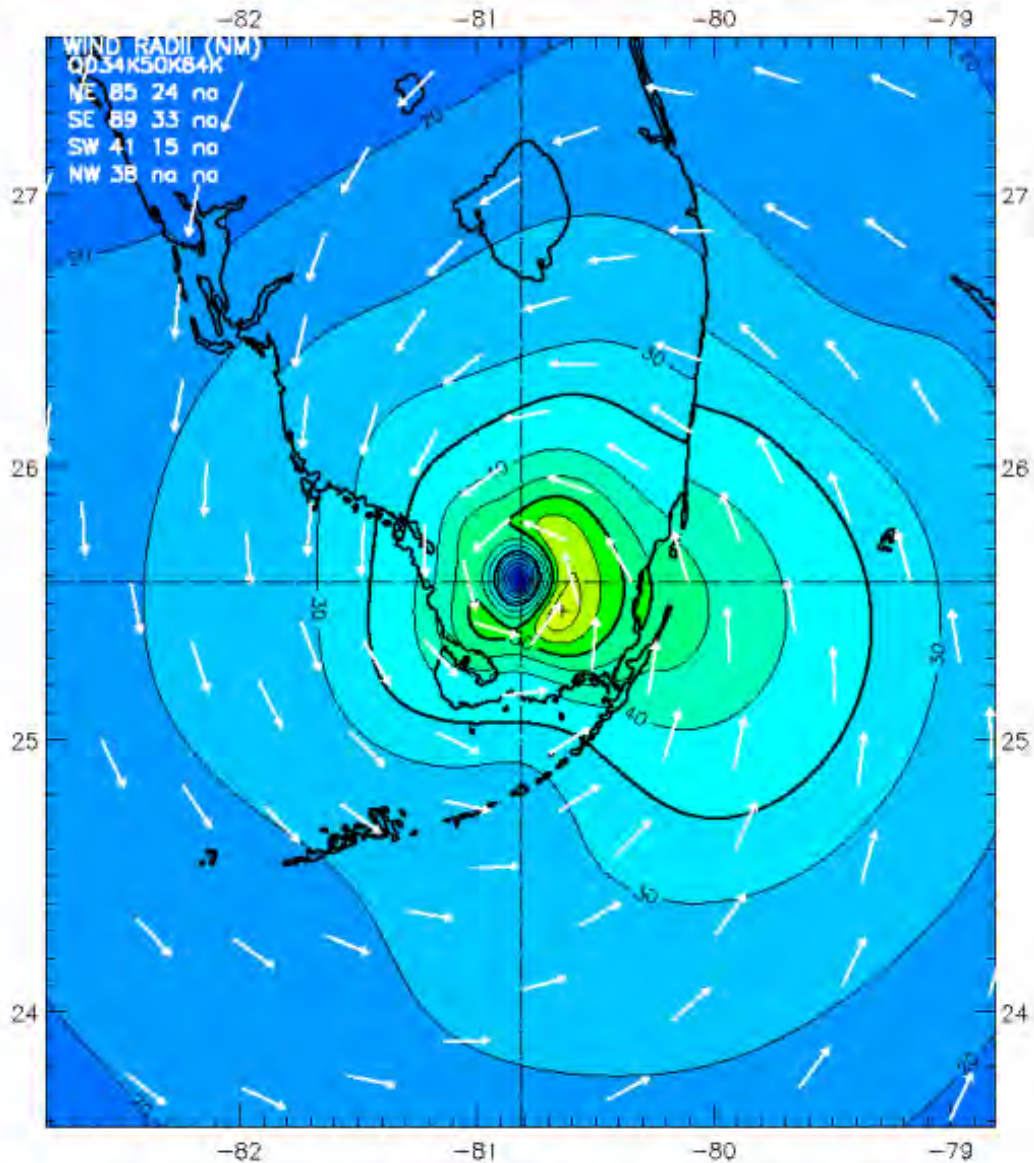
Valid for marine exposure over water, open terrain exposure over land

Analysis based on CMAN from 0000 - 0700 z; GPSSONDE\_SFC from 0040 - 0148 z; SHIP from 0000 - 0607 z; GOES\_SWIR from 0102 - 0102 z; GPSSONDE\_WL150 from 0040 - 0148 z;

METAR from 0000 - 0658 z; ASOS from 0000 - 0659 z;

MOORED\_BUOY from 0009 - 0659 z; BACKGROUND\_FIELD from 0300 - 0300 z;

0300 z position interpolated from 0201 Army Corps; mslp = 984.0 mb



Observed Max. Surface Wind: 71 kts, 13 nm SE of center based on 0000 z CMAN sfc measurement  
Analyzed Max. Wind: 63 kts, 12 nm SE of center

Figure 2-12. H\*Wind snapshot on 26 August 2005 0300 UTC. The wind speeds are color contoured in knots, representing 1-minute sustained wind speeds. Note this wind field includes marine and land exposures identified by the abrupt change in color contours over the land.

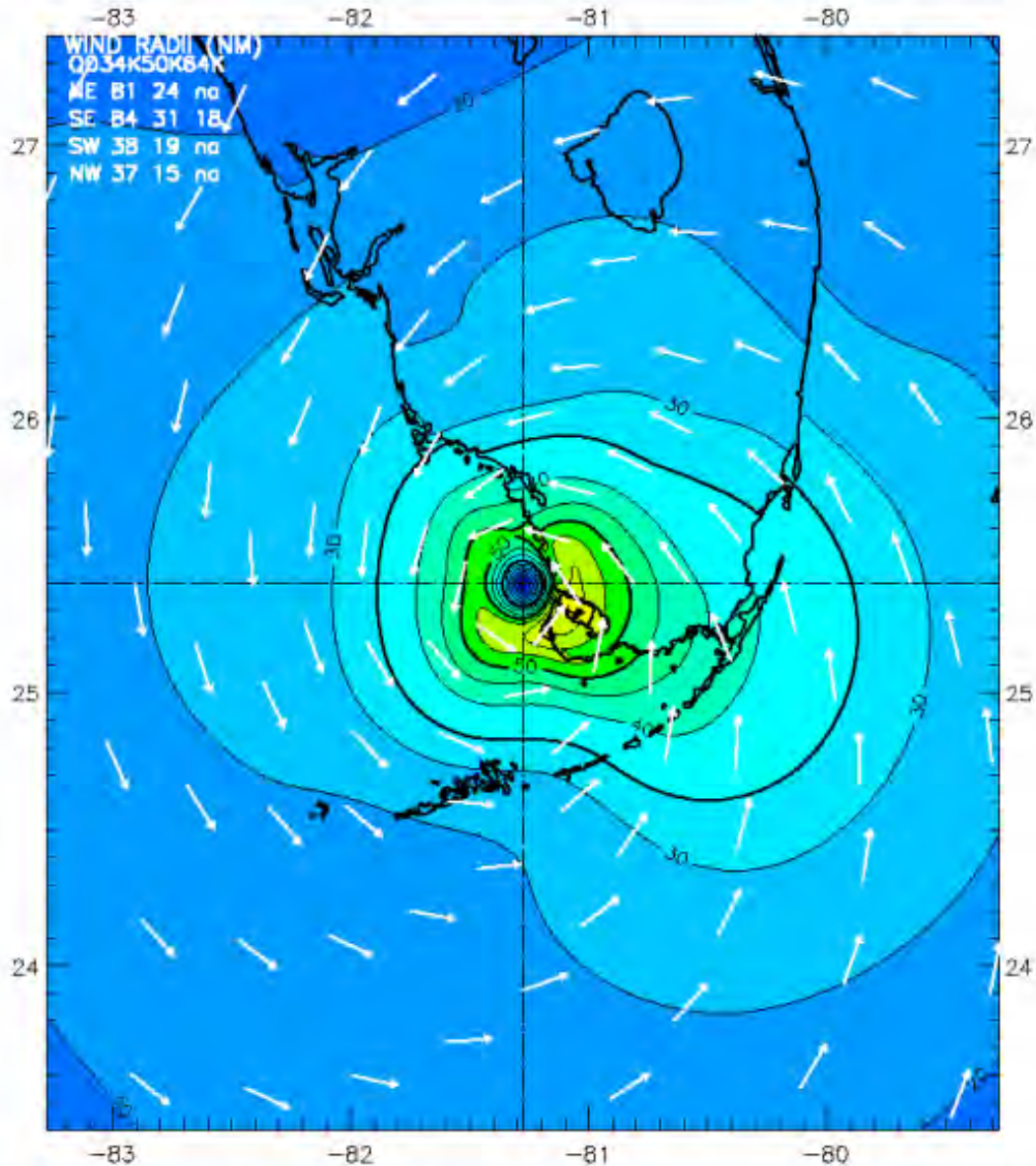
## Hurricane Katrina 0600 UTC 26 AUG 2005

Max 1-min sustained surface winds (kt)

Valid for marine exposure over water, open terrain exposure over land

Analysis based on MOORED\_BUOY from 2259 - 0450 z; METAR from 2319 - 0455 z; CMAN from 2259 - 0454 z; SHIP from 0000 - 0100 z; BACKGROUND\_FIELD from 2258 - 2258 z; ASOS from 2317 - 0456 z;

0600 z position interpolated from 0457 Army Corps; mslp = 987.0 mb



Observed Max. Surface Wind: 71 kts, 8 nm SE of center based on 0000 z CMAN sfc measurement  
Analyzed Max. Wind: 69 kts, 13 nm SE of center

Figure 2-13. H\*Wind snapshot on 26 August 2005 0600 UTC. The wind speeds are color contoured in knots, representing 1-minute sustained wind speeds. Note this wind field includes marine and land exposures identified by the abrupt change in color contours over the land.



## Hurricane Katrina 0900 UTC 26 AUG 2005

Max 1-min sustained surface winds (kt)

Valid for marine exposure over water, open terrain exposure over land

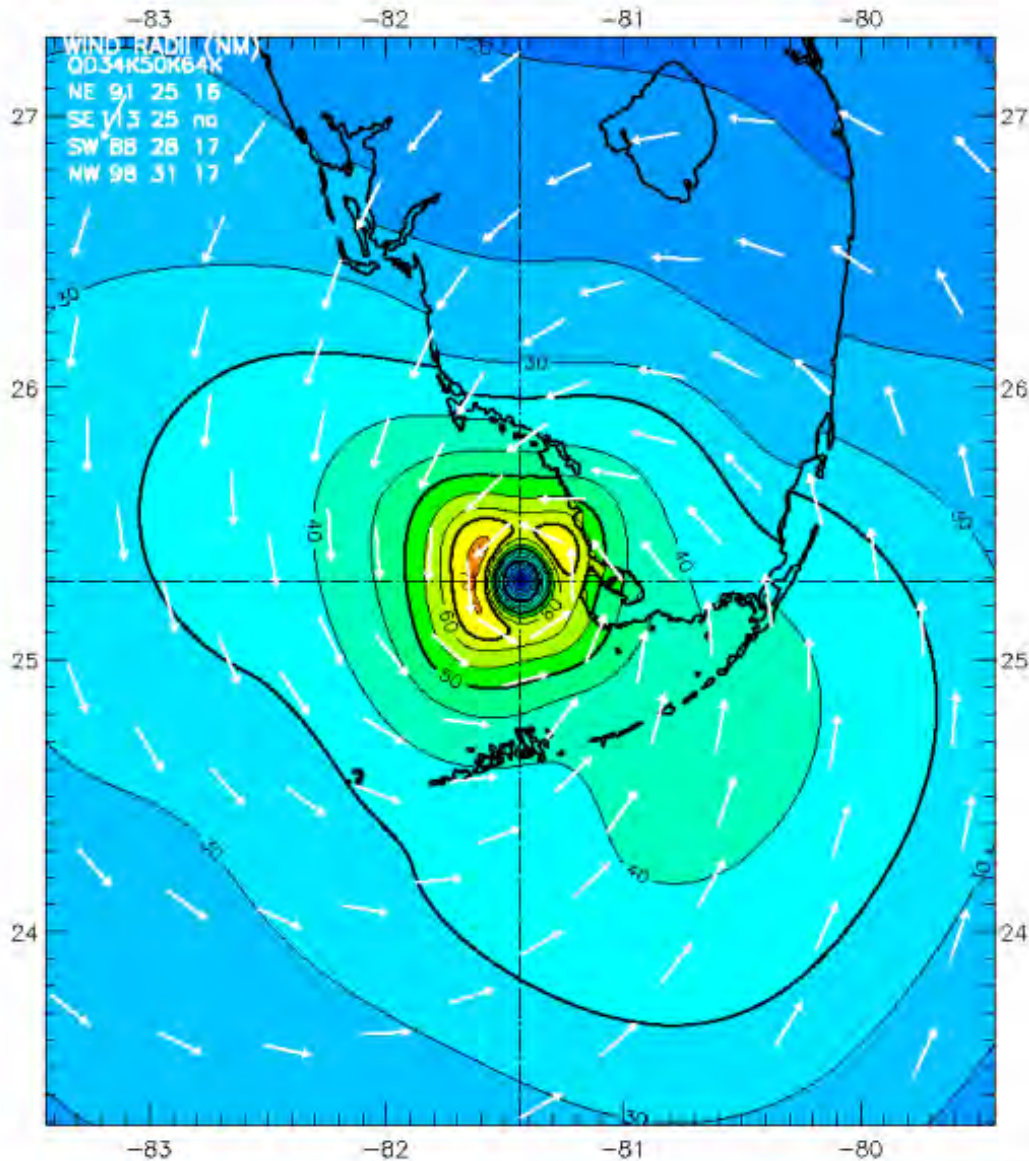
Analysis based on CMAN from 0605 - 1200 z; QSCAT from 1037 - 1040 z; SHIP from 0606 - 0607 z;

GOES\_SWIR from 0702 - 0702 z; METAR from 0640 - 1200 z;

ASOS from 0605 - 1156 z; MOORED\_BUOY from 0609 - 1159 z;

BACKGROUND\_FIELD from 1202 - 1202 z;

0900 z position interpolated from 0858 Army Corps; mslp = 987.0 mb



Observed Max. Surface Wind: 72 kts, 12 nm NW of center based on 1202 z BACKGROUND\_FIELD sfc measurement  
Analyzed Max. Wind: 72 kts, 12 nm NW of center

Figure 2-14. H\*Wind snapshot on 26 August 2005 0900 UTC. The wind speeds are color contoured in knots, representing 1-minute sustained wind speeds. Note this wind field includes marine and land exposures identified by the abrupt change in color contours over the land.

## Hurricane Katrina 1200 UTC 26 AUG 2005

Max 1-min sustained surface winds (kt)

Valid for marine exposure over water, open terrain exposure over land

Analysis based on CMAN from 1205 - 1500 z; AFREC from 1354 - 1459 z;

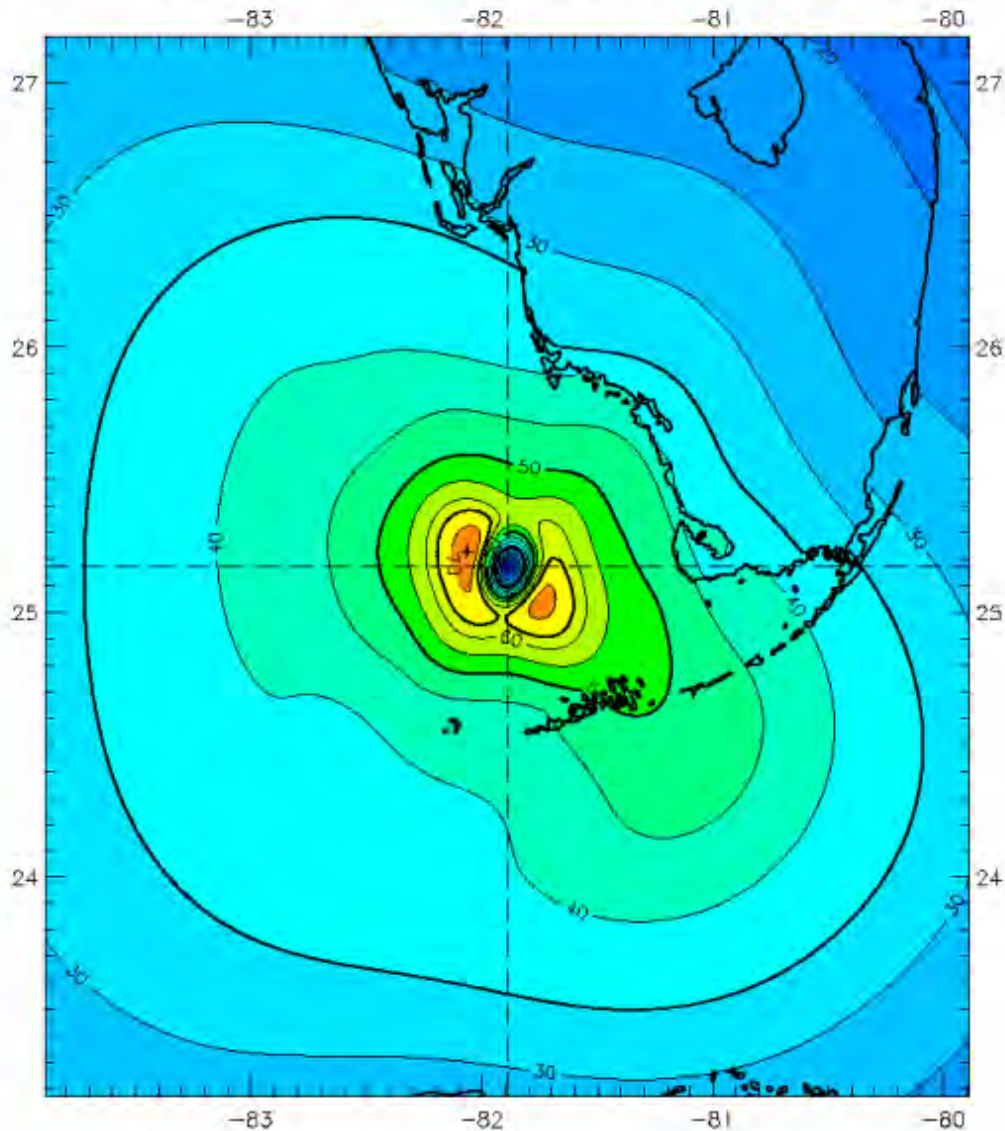
SHIP from 1210 - 1414 z; GPSSONDE\_WL150 from 1338 - 1444 z;

METAR from 1232 - 1500 z; GOES from 1302 - 1302 z;

ASOS from 1206 - 1456 z; MOORED\_BUOY from 1209 - 1459 z;

BACKGROUND\_FIELD from 1200 - 1200 z;

1200 z position interpolated from 1058 Army Corps; mslp = 987.0 mb



Observed Max. Surface Wind: null sfc measurement  
Analyzed Max. Wind: 75 kts, 10 nm NW of center

Figure 2-15. H\*Wind snapshot on 26 August 2005 1200 UTC. The wind speeds are color contoured in knots, representing 1-minute sustained wind speeds. Note this wind field includes marine and land exposures identified by the abrupt change in color contours over the land.



## Hurricane Katrina 1500 UTC 26 AUG 2005

Max 1-min sustained surface winds (kt)

Valid for marine exposure over water, open terrain exposure over land

Analysis based on CMAN from 1205 - 1800 z; AFREC from 1354 - 1759 z;

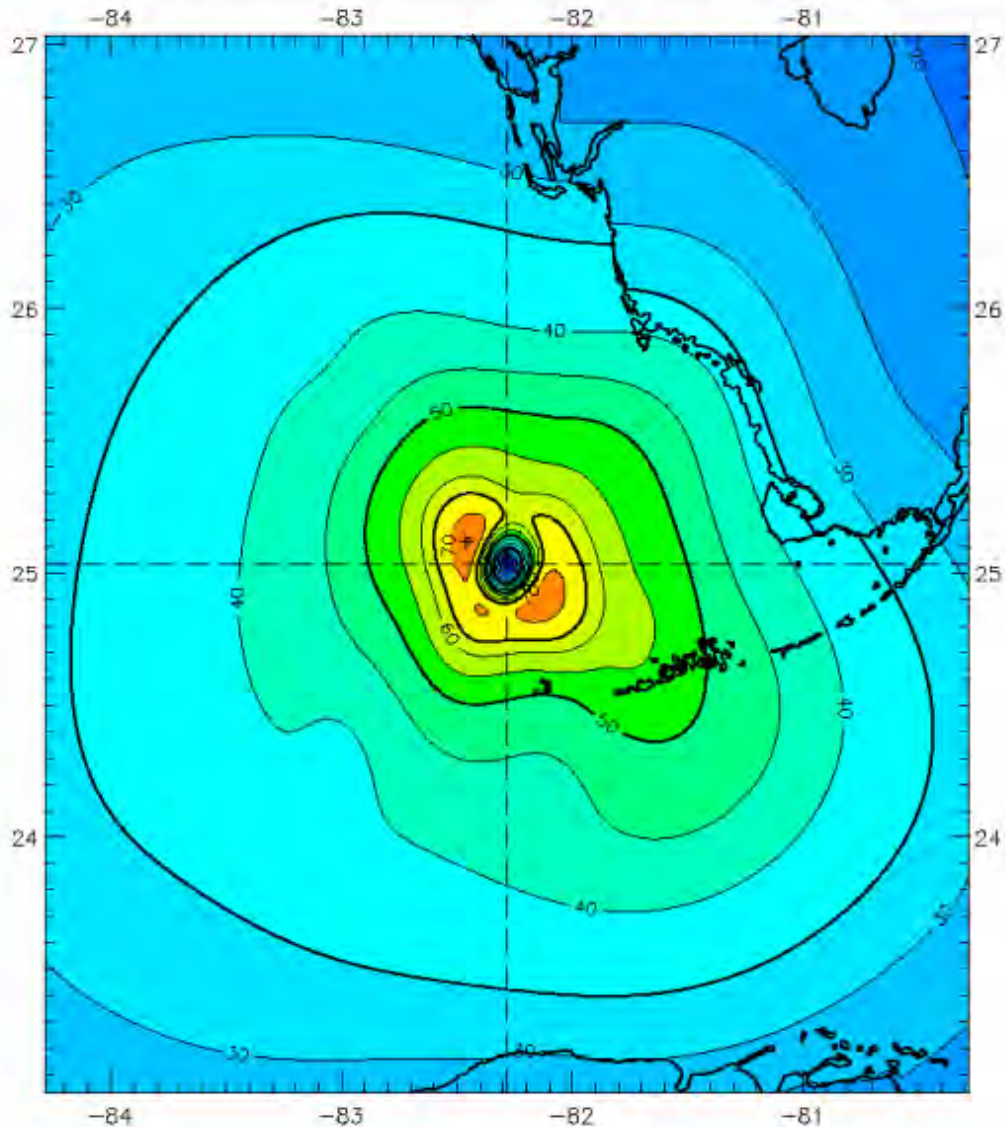
SHIP from 1210 - 1717 z; GPSSONDE\_WL150 from 1338 - 1705 z;

METAR from 1232 - 1755 z; GOES from 1302 - 1302 z;

ASOS from 1206 - 1800 z; MOORED\_BUOY from 1209 - 1800 z;

MADIS from 1505 - 1747 z;

1500 z position interpolated from 1434 Army Corps; mslp = 971.0 mb



Observed Max. Surface Wind: null sfc measurement  
Analyzed Max. Wind: 75 kts, 12 nm NW of center

Figure 2-16. H\*Wind snapshot on 26 August 2005 1500 UTC. The wind speeds are color contoured in knots, representing 1-minute sustained wind speeds. Note this wind field includes marine and land exposures identified by the abrupt change in color contours over the land.

## Hurricane Katrina 1800 UTC 26 AUG 2005

Max 1-min sustained surface winds (kt)

Valid for marine exposure over water, open terrain exposure over land

Analysis based on CMAN from 1500 - 2100 z; AFREC from 1500 - 2033 z;

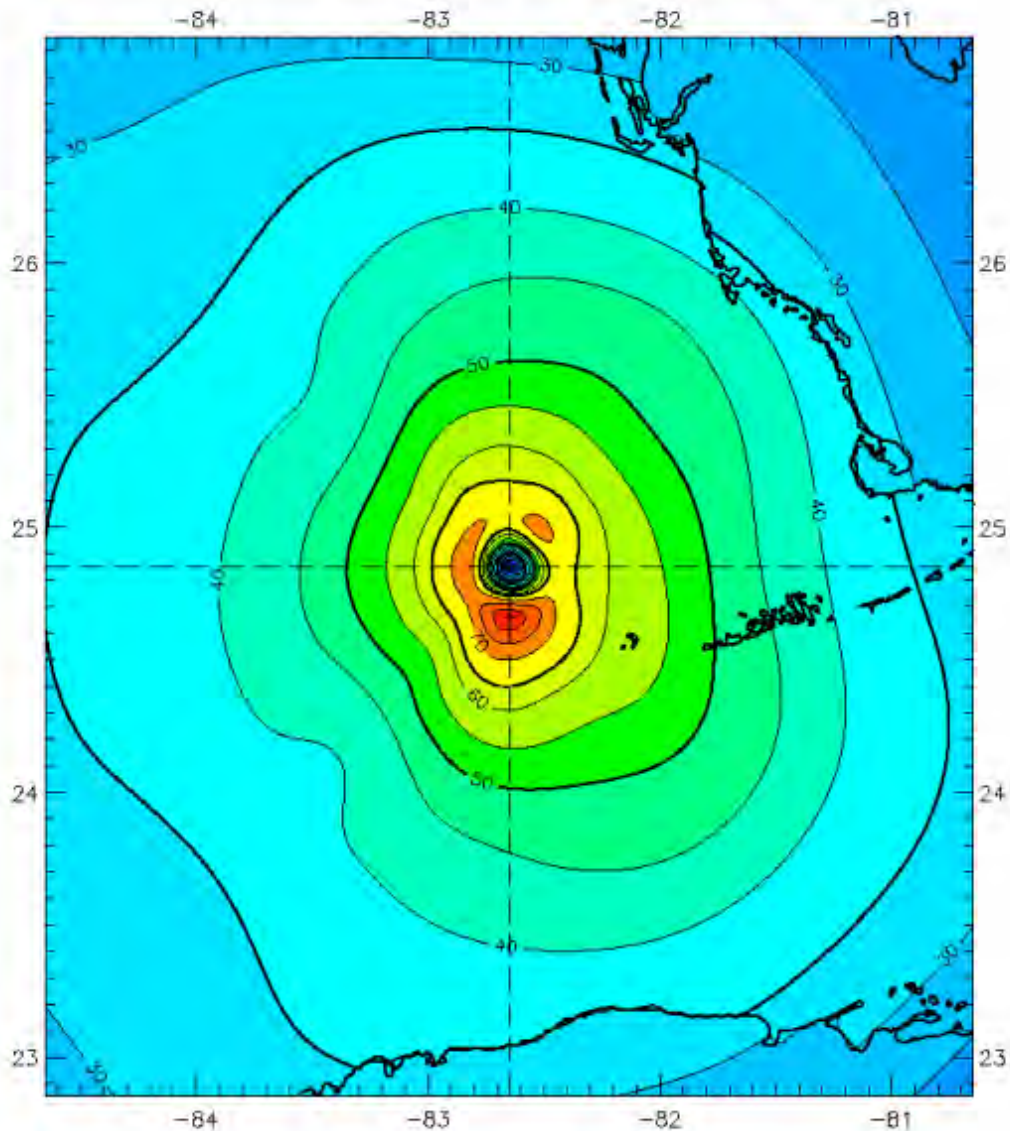
SHIP from 1616 - 1919 z; GPSSONDE\_WL150 from 1550 - 2031 z;

METAR from 1500 - 2100 z; GOES from 1902 - 1902 z;

ASOS from 1502 - 2056 z; MOORED\_BUOY from 1509 - 2059 z;

MADIS from 1505 - 2040 z;

1800 z position interpolated from 1703 Army Corps; mslp = 969.0 mb



Observed Max. Surface Wind: null sfc measurement

Analyzed Max. Wind: 82 kts, 13 nm SE of center

Figure 2-17. H\*Wind snapshot on 26 August 2005 1800 UTC. The wind speeds are color contoured in knots, representing 1-minute sustained wind speeds. Note this wind field includes marine and land exposures identified by the abrupt change in color contours over the land.



## Hurricane Katrina 2100 UTC 26 AUG 2005

Max 1-min sustained surface winds (kt)

Valid for marine exposure over water, open terrain exposure over land

Analysis based on BACKGROUND\_FIELD from 2100 - 2100 z; SHIP from 1817 - 0000 z;

METAR from 1840 - 0000 z;

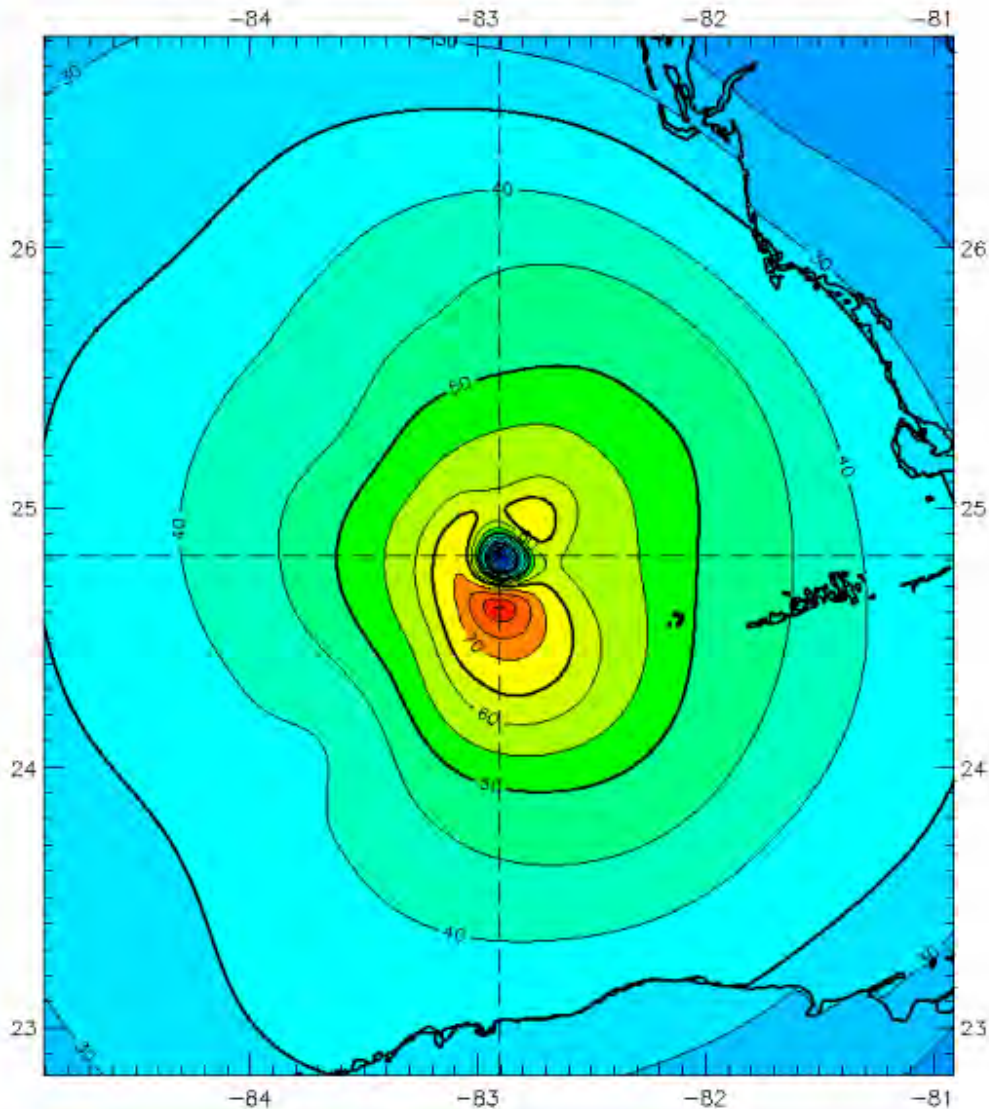
CMAN from 1800 - 0000 z; AFREC from 1800 - 2033 z;

GPSSONDE\_WL150 from 1844 - 2334 z; GOES from 1902 - 2202 z;

ASOS from 1800 - 2356 z; QSCAT from 2300 - 2303 z;

MOORED\_BUOY from 1800 - 2359 z;

2100 z position interpolated from 2023 Army Corps; mslp = 965.0 mb



Observed Max. Surface Wind: null sfc measurement  
Analyzed Max. Wind: 83 kts, 13 nm SE of center

Figure 2-18. H\*Wind snapshot on 26 August 2005 2100 UTC. The wind speeds are color contoured in knots, representing 1-minute sustained wind speeds. Note this wind field includes marine and land exposures identified by the abrupt change in color contours over the land.

## Hurricane Katrina 0000 UTC 27 AUG 2005

Max 1-min sustained surface winds (kt)

Valid for marine exposure over water, open terrain exposure over land

Analysis based on BACKGROUND\_FIELD from 0000 - 0000 z; SHIP from 2212 - 0101 z;

METAR from 2100 - 0300 z;

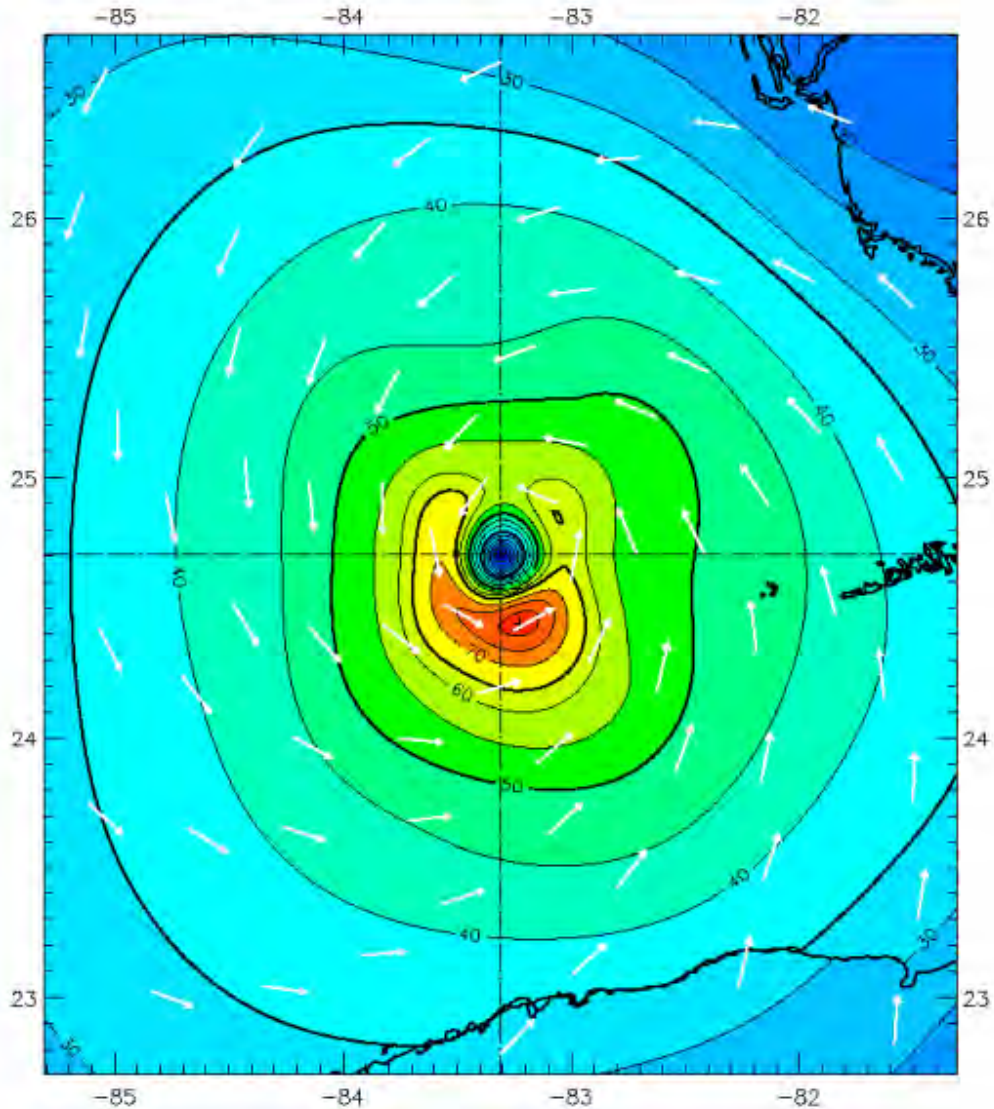
CMAN from 2100 - 0300 z; GPSSONDE\_WL150 from 2106 - 0056 z;

GOES\_SWIR from 0102 - 0102 z;

GOES from 2202 - 2202 z; ASOS from 2117 - 0256 z;

QSCAT from 2300 - 0043 z; MOORED\_BUOY from 2109 - 0259 z;

0000 z position interpolated from 2357 Army Corps; mslp = 965.0 mb



Observed Max. Surface Wind: null sfc measurement  
Analyzed Max. Wind: 82 kts, 18 nm SE of center

Figure 2-19. H\*Wind snapshot on 27 August 2005 0000 UTC. The wind speeds are color contoured in knots, representing 1-minute sustained wind speeds. Note this wind field includes marine and land exposures identified by the abrupt change in color contours over the land.



## Hurricane Katrina 0300 UTC 27 AUG 2005

Max 1-min sustained surface winds (kt)

Valid for marine exposure over water, open terrain exposure over land

Analysis based on MOORED\_BUOY from 0009 - 0559 z; SHIP from 0000 - 0404 z;

GPSSONDE\_SFC from 0023 - 0557 z;

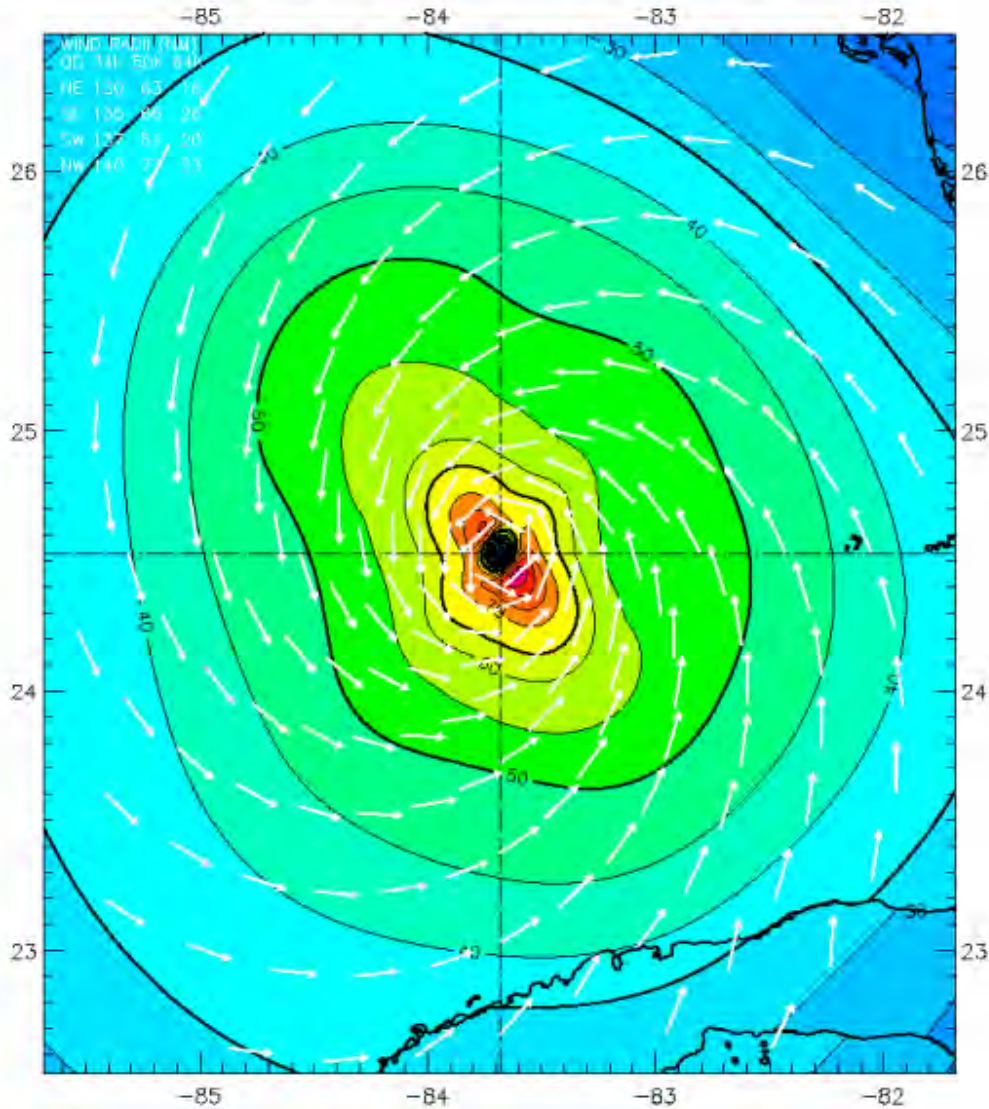
GPSSONDE\_WL150 from 0023 - 0559 z; QSCAT from 0040 - 0043 z;

CMAN from 0000 - 0600 z; GOES\_SWIR from 0102 - 0102 z;

ASOS from 0029 - 0559 z; AFREC from 0511 - 0559 z;

METAR from 0000 - 0600 z; BACKGROUND\_FIELD from 0300 - 0300 z;

0300 z position interpolated from 0200 Army Corps; mslp = 965.0 mb



Observed Max. Surface Wind: null sfc measurement  
Analyzed Max. Wind: 87 kts, 7 nm SE of center

Figure 2-20. H\*Wind snapshot on 27 August 2005 0300 UTC. The wind speeds are color contoured in knots, representing 1-minute sustained wind speeds. Note this wind field includes marine and land exposures identified by the abrupt change in color contours over the land.

## Hurricane Katrina 0600 UTC 27 AUG 2005

Max 1-min sustained surface winds (kt)

Valid for marine exposure over water, open terrain exposure over land

Analysis based on CMAN from 0300 - 0900 z; AFREC from 0511 - 0859 z;

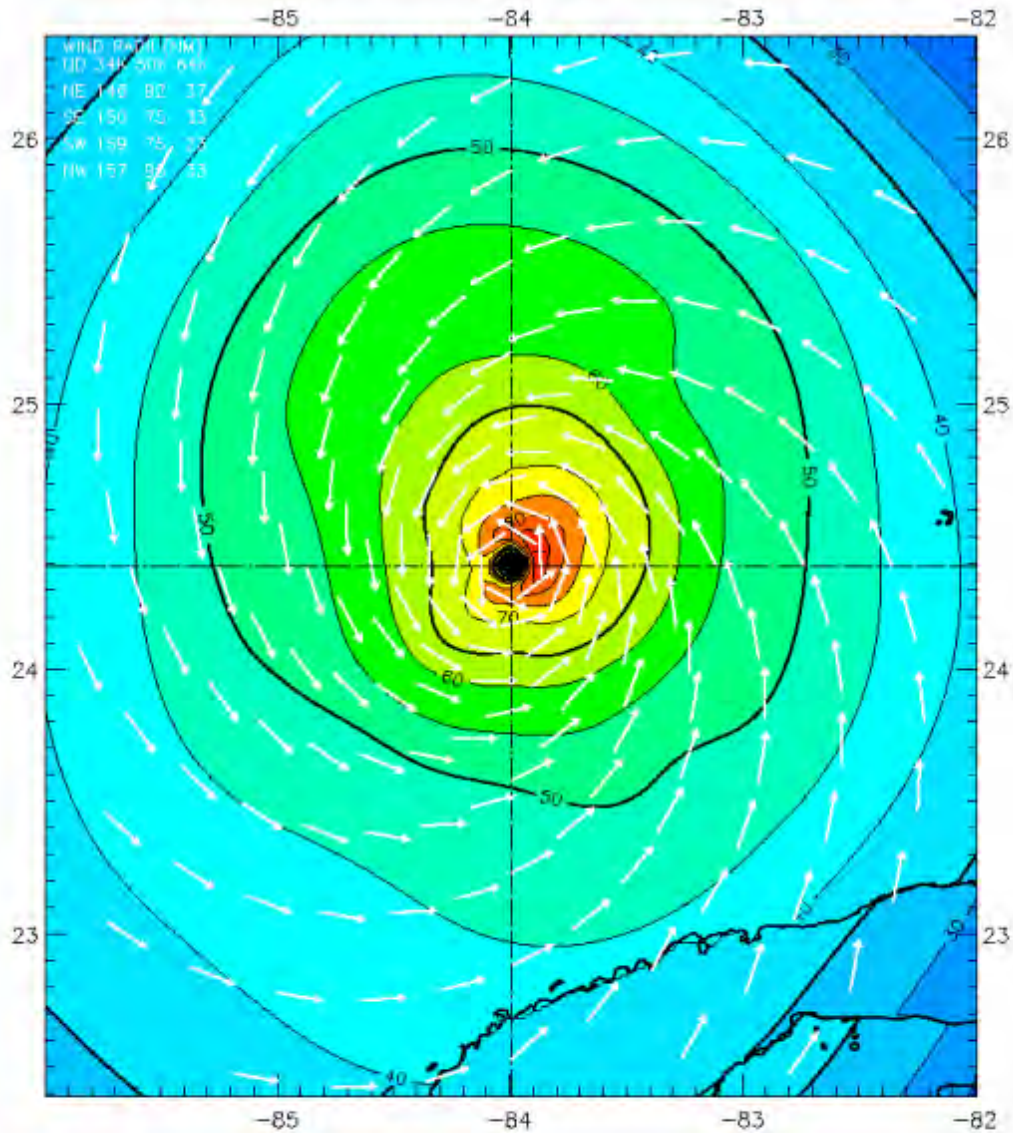
GPSSONDE\_SFC from 0557 - 0809 z;

SHIP from 0404 - 0706 z; GOES\_SWIR from 0702 - 0702 z;

GPSSONDE\_WL150 from 0557 - 0812 z; METAR from 0300 - 0855 z;

ASOS from 0317 - 0856 z; MOORED\_BUOY from 0309 - 0859 z;

0600 z position interpolated from 0553 Army Corps; mslp = 950.0 mb



Observed Max. Surface Wind: null sfc measurement

Analyzed Max. Wind: 90 kts, 7 nm NE of center

Figure 2-21. H\*Wind snapshot on 27 August 2005 0600 UTC. The wind speeds are color contoured in knots, representing 1-minute sustained wind speeds. Note this wind field includes marine and land exposures identified by the abrupt change in color contours over the land.



## Hurricane Katrina 0900 UTC 27 AUG 2005

Max 1-min sustained surface winds (kt)

Valid for marine exposure over water, open terrain exposure over land

Analysis based on SHIP from 0606 - 0906 z; METAR from 0600 - 1200 z;

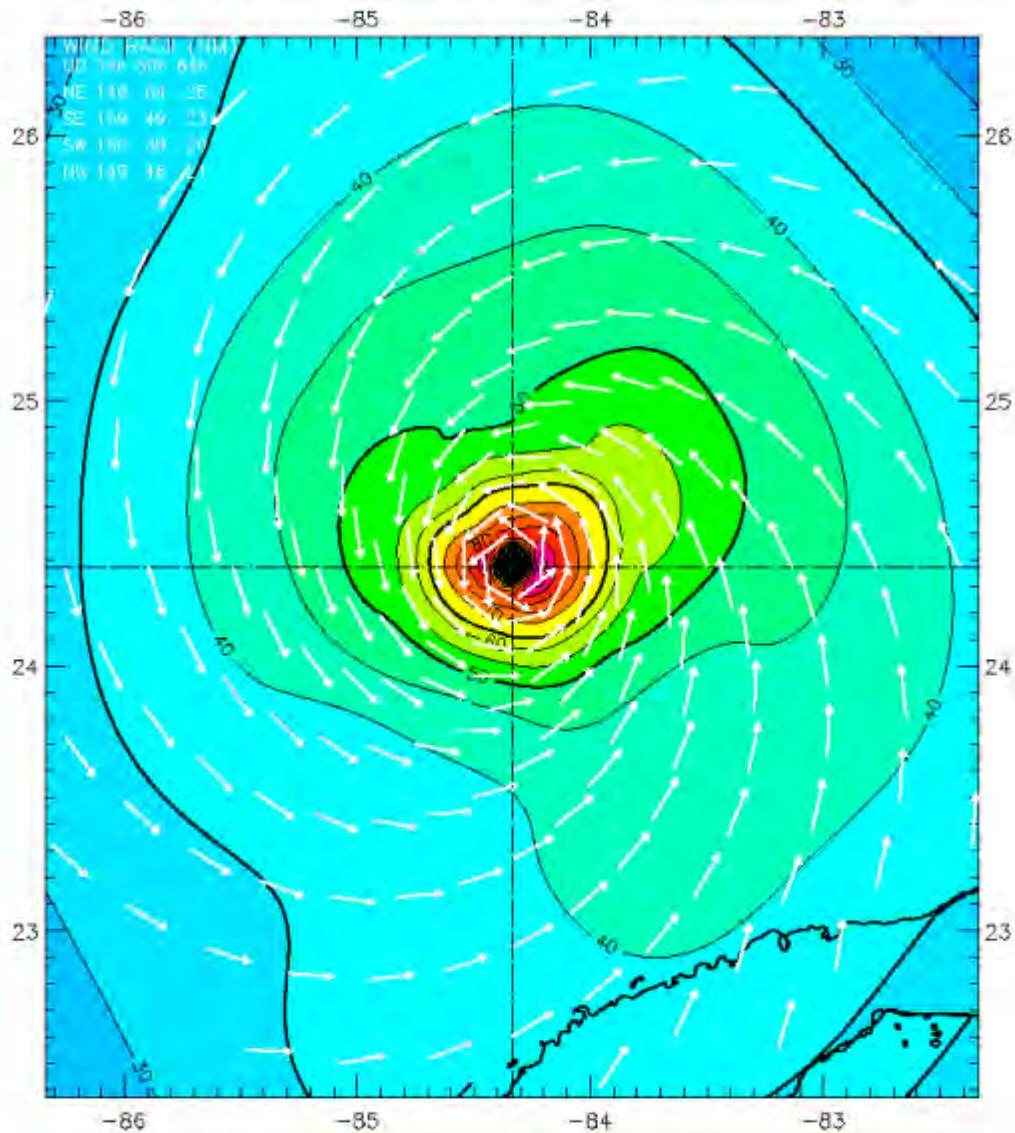
CMAN from 0600 - 1200 z; GPSSONDE\_SFC from 0714 - 1110 z;

AFREC from 0600 - 1145 z; GPSSONDE\_WL150 from 0714 - 0937 z;

GOES\_SWIR from 0702 - 1002 z; ASOS from 0606 - 1056 z;

QSCAT from 1151 - 1154 z; MOORED\_BUOY from 0609 - 1159 z;

0900 z position interpolated from 0825 Army Corps; mslp = 945.0 mb



Observed Max. Surface Wind: 94 kts, 7 nm NE of center based on 0937 z GPSSONDE\_WL150 sfc measurement  
Analyzed Max. Wind: 93 kts, 6 nm NE of center

Figure 2-22. H\*Wind snapshot on 27 August 2005 0900 UTC. The wind speeds are color contoured in knots, representing 1-minute sustained wind speeds. Note this wind field includes marine and land exposures identified by the abrupt change in color contours over the land.

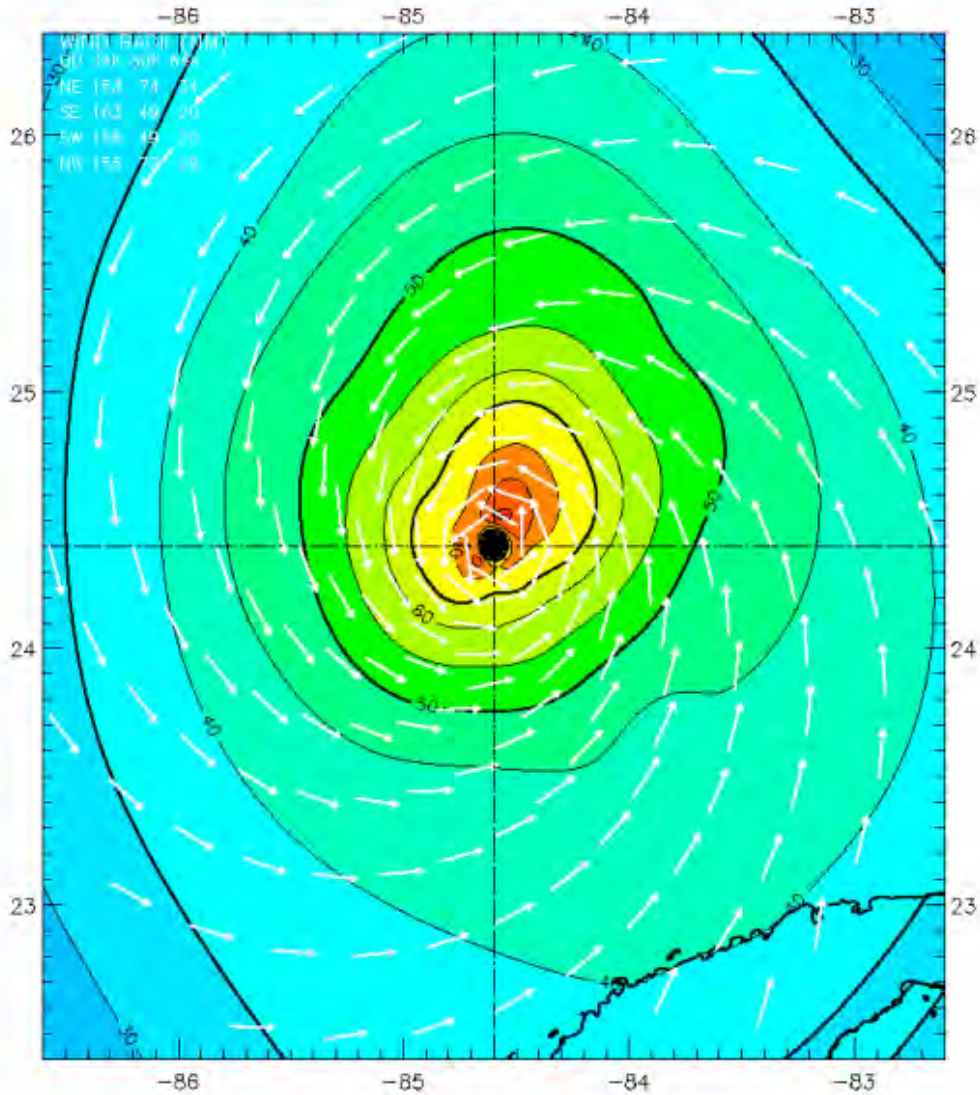
## Hurricane Katrina 1200 UTC 27 AUG 2005

Max 1-min sustained surface winds (kt)

Valid for marine exposure over water, open terrain exposure over land

Analysis based on AFREC from 0600 - 1145 z; SFMR43 from 1336 - 1529 z;  
CMAN from 0936 - 1530 z; ASOS from 0951 - 1520 z;  
GOES\_SWIR from 1002 - 1002 z; BACKGROUND\_FIELD from 1200 - 1200 z;  
QSCAT from 1151 - 1154 z; SHIP from 1212 - 1512 z;  
GPSSONDE\_WL150 from 0933 - 1517 z; METAR from 0940 - 1515 z;  
MOORED\_BUOY from 0939 - 1529 z; TAIL\_DOPPLER43 from 1513 - 1513 z;  
GOES from 1302 - 1302 z;

1200 z Army Corps fix; mslp = 942.0 mb



Observed Max. Surface Wind: 81 kts, 7 nm SW of center based on 1513 z TAIL\_DOPPLER43 sfc measurement  
Analyzed Max. Wind: 81 kts, 7 nm NE of center

Figure 2-23. H\*Wind anpsnapshot on 27 August 2005 1200 UTC. The wind speeds are color contoured in knots, representing 1-minute sustained wind speeds. Note this wind field includes marine and land exposures identified by the abrupt change in color contours over the land.



## Hurricane Katrina 1500 UTC 27 AUG 2005

Max 1-min sustained surface winds (kt)

Valid for marine exposure over water, open terrain exposure over land

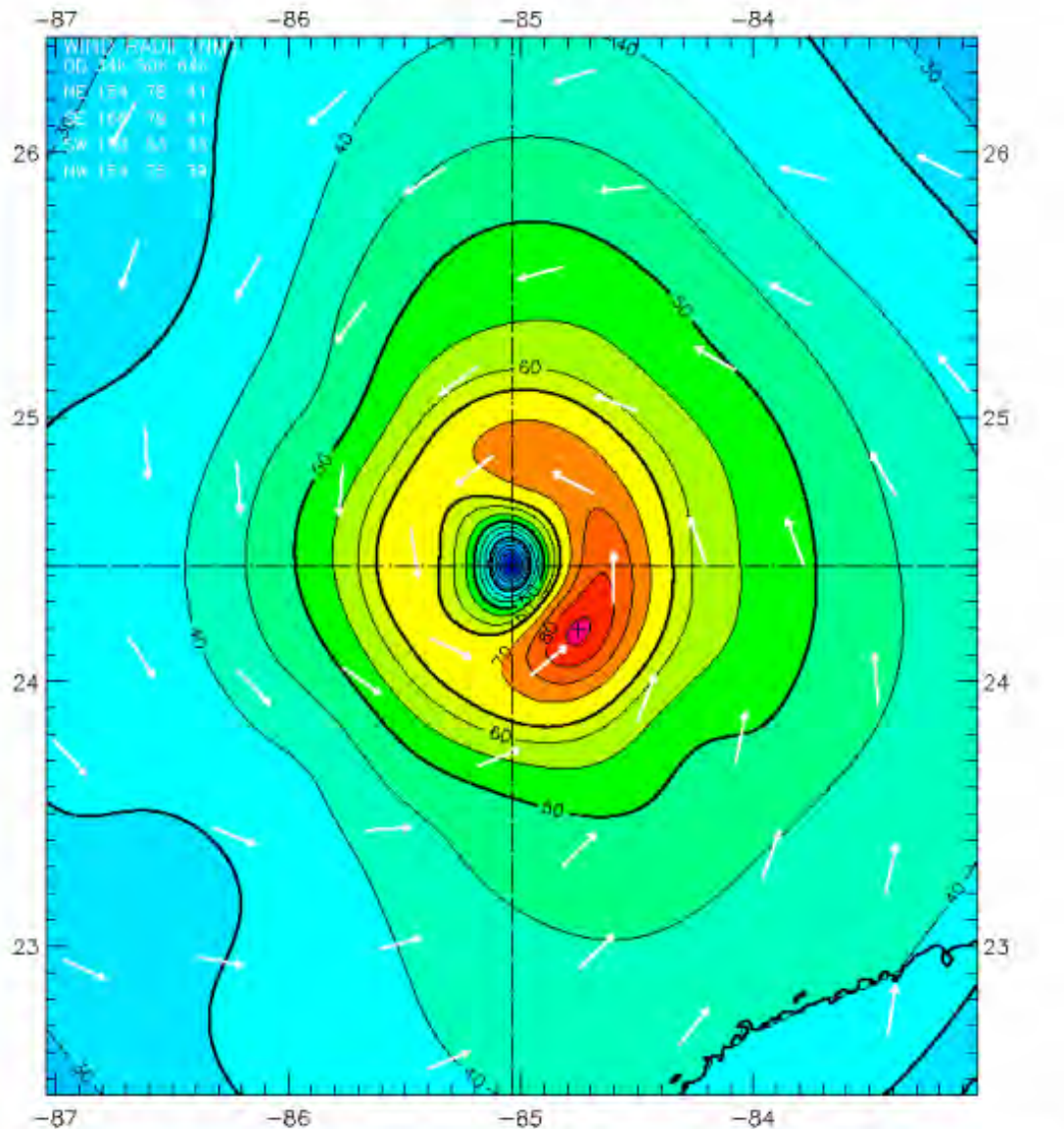
Analysis based on CMAN from 1200 - 1819 z; SFMR43 from 1336 - 1824 z;

SHIP from 1212 - 1818 z; METAR from 1200 - 1755 z;

GOES from 1302 - 1602 z; GPSSONDE\_WL150 from 1427 - 1823 z;

ASOS from 1235 - 1823 z; MOORED\_BUOY from 1209 - 1820 z;

1500 z position interpolated from 1425 Army Corps; mslp = 942.0 mb



Observed Max. Surface Wind: 86 kts, 24 nm SE of center based on 1644 z SFMR43 sfc measurement  
Analyzed Max. Wind: 86 kts, 23 nm SE of center

Figure 2-24. H\*Wind snapshot on 27 August 2005 1500 UTC. The wind speeds are color contoured in knots, representing 1-minute sustained wind speeds. Note this wind field includes marine and land exposures identified by the abrupt change in color contours over the land.

## Hurricane Katrina 1800 UTC 27 AUG 2005

Max 1-min sustained surface winds (kt)

Valid for marine exposure over water, open terrain exposure over land

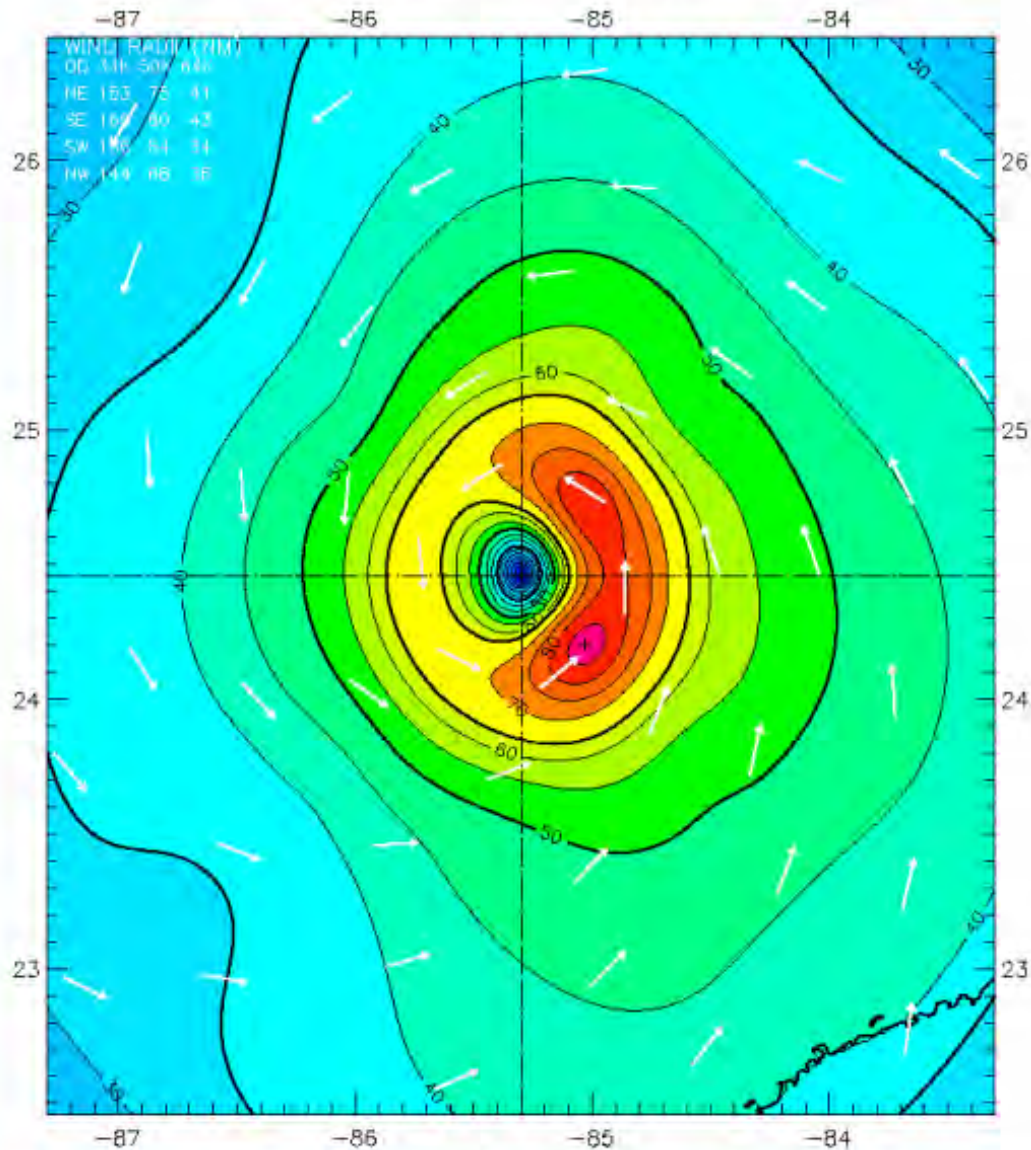
Analysis based on CMAN from 1500 - 2100 z; SFMR43 from 1500 - 2059 z;

SHIP from 1500 - 1919 z; METAR from 1500 - 2055 z;

GOES from 1602 - 1602 z; GPSSONDE\_WL150 from 1517 - 2042 z;

ASOS from 1504 - 2056 z; MOORED\_BUOY from 1509 - 2059 z;

1800 z position interpolated from 1759 Army Corps; mslp = 948.0 mb



Observed Max. Surface Wind: 87 kts, 24 nm NE of center based on 2014 z SFMR43 sfc measurement  
Analyzed Max. Wind: 87 kts, 23 nm SE of center

Figure 2-25. H\*Wind snapshot on 27 August 2005 1800 UTC. The wind speeds are color contoured in knots, representing 1-minute sustained wind speeds. Note this wind field includes marine and land exposures identified by the abrupt change in color contours over the land.



## Hurricane Katrina 2100 UTC 27 AUG 2005

Max 1-min sustained surface winds (kt)

Valid for marine exposure over water, open terrain exposure over land

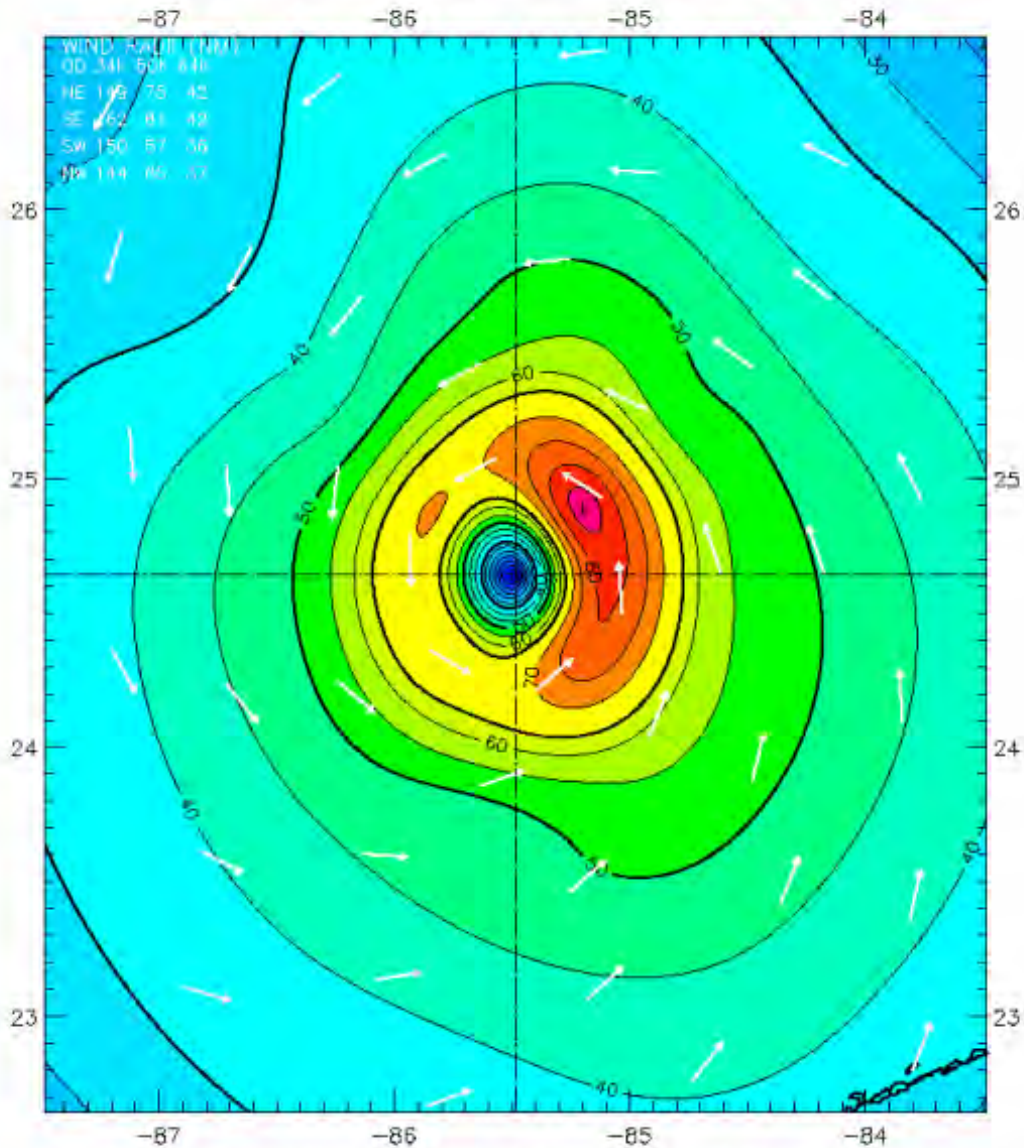
Analysis based on CMAN from 1800 - 0000 z; SFMR43 from 1800 - 2108 z;

SHIP from 1818 - 0000 z; METAR from 1843 - 2355 z;

GPSSONDE\_WL150 from 1802 - 0001 z; ASOS from 1800 - 2356 z;

MOORED\_BUOY from 1809 - 2359 z; BACKGROUND\_FIELD from 2100 - 2100 z;

2100 z position interpolated from 2054 Army Corps; mslp = 949.0 mb



Observed Max. Surface Wind: 87 kts, 24 nm NE of center based on 2104 z SFMR43 sfc measurement  
Analyzed Max. Wind: 87 kts, 23 nm NE of center

Figure 2-26. H\*Wind snapshot on 27 August 2005 2100 UTC. The wind speeds are color contoured in knots, representing 1-minute sustained wind speeds. Note this wind field includes marine and land exposures identified by the abrupt change in color contours over the land.

## Hurricane Katrina 0000 UTC 28 AUG 2005

Max 1-min sustained surface winds (kt)

Valid for marine exposure over water, open terrain exposure over land

Analysis based on CMAN from 2100 - 0300 z; AFREC from 2100 - 0259 z;

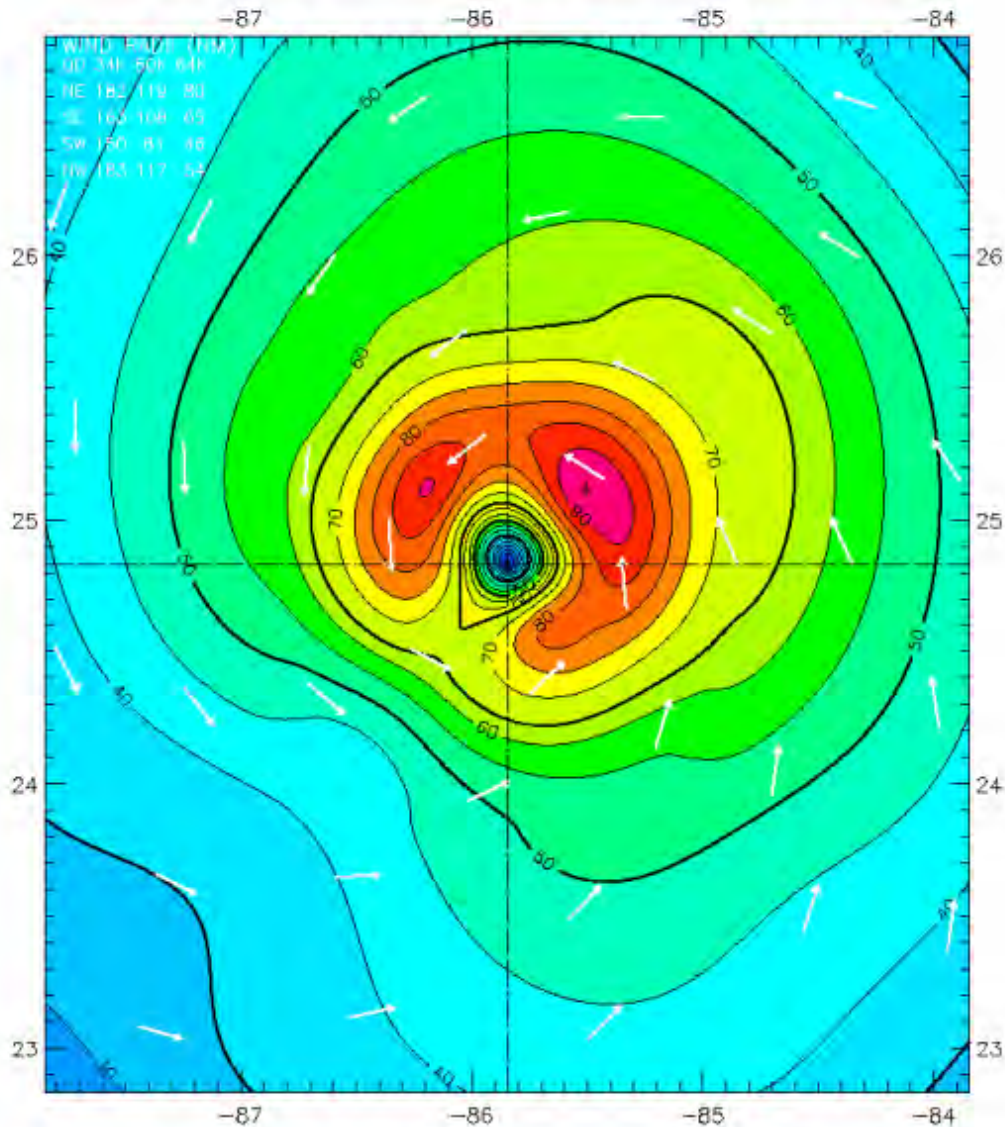
SHIP from 2118 - 0000 z; GOES\_SWIR from 0102 - 0102 z;

GPSSONDE\_WL150 from 2119 - 0001 z; METAR from 2125 - 0259 z;

GOES from 2202 - 2202 z; ASOS from 2104 - 0255 z;

MOORED\_BUOY from 2109 - 0259 z;

0000 z position interpolated from 2325 Army Corps; mslp = 949.0 mb



Observed Max. Surface Wind: 95 kts, 27 nm NE of center based on 0017 z AFREC sfc measurement  
Analyzed Max. Wind: 95 kts, 28 nm NE of center

Figure 2-27. H\*Wind snapshot on 28 August 2005 0000 UTC. The wind speeds are color contoured in knots, representing 1-minute sustained wind speeds. Note this wind field includes marine and land exposures identified by the abrupt change in color contours over the land.



## Hurricane Katrina 0300 UTC 28 AUG 2005

Max 1-min sustained surface winds (kt)

Valid for marine exposure over water, open terrain exposure over land

Analysis based on CMAN from 0000 - 0600 z; AFREC from 0000 - 0359 z;

SHIP from 0000 - 0000 z; GOES\_SWIR from 0102 - 0102 z;

METAR from 0035 - 0558 z; GPSSONDE\_WL150 from 0001 - 0001 z;

ASOS from 0003 - 0556 z; MOORED\_BUOY from 0009 - 0559 z;

0300 z position interpolated from 0149 Army Corps; mslp = 939.0 mb

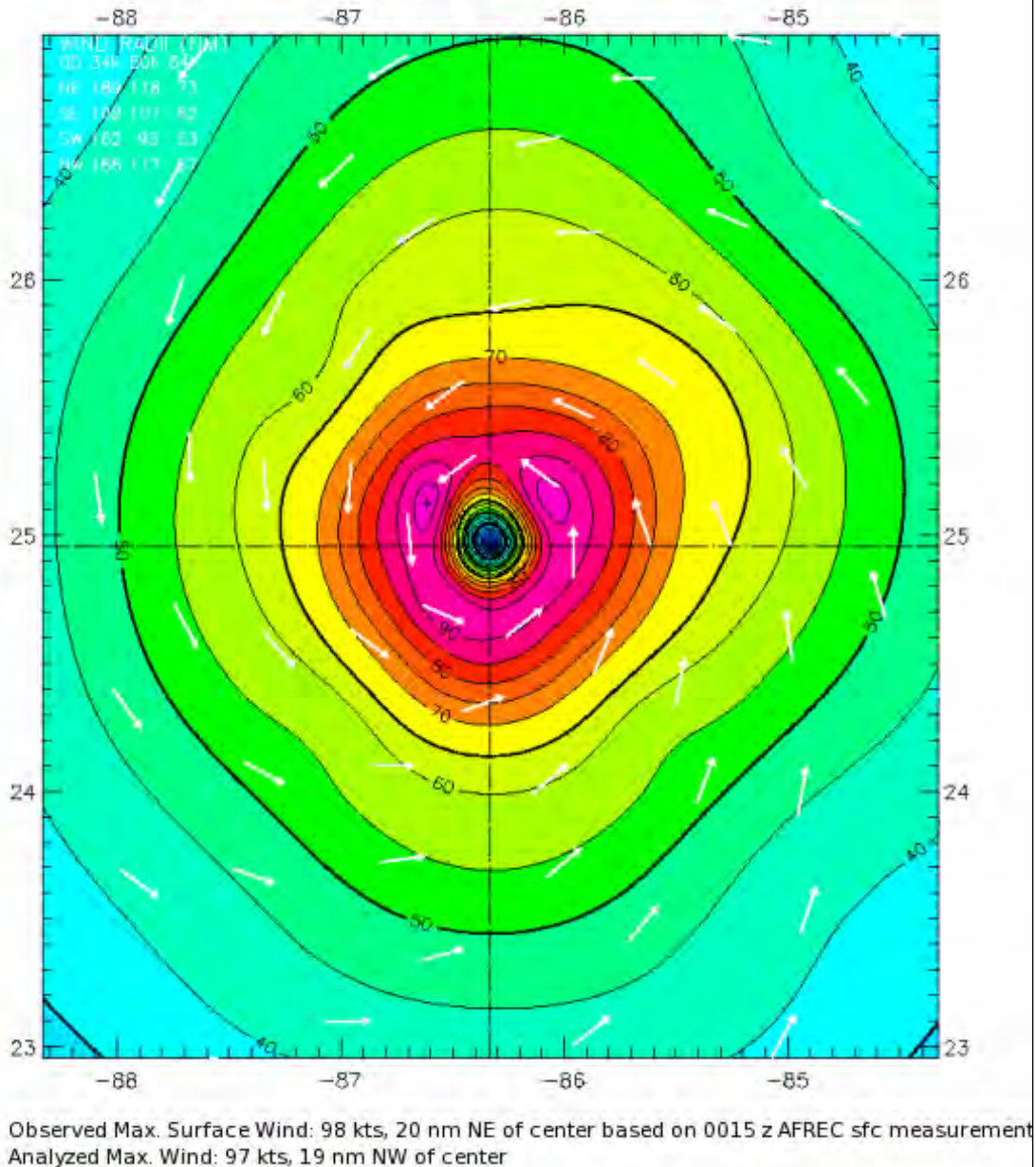


Figure 2-28. H\*Wind snapshot on 28 August 2005 0300 UTC. The wind speeds are color contoured in knots, representing 1-minute sustained wind speeds. Note this wind field includes marine and land exposures identified by the abrupt change in color contours over the land.

## Hurricane Katrina 0600 UTC 28 AUG 2005

Max 1-min sustained surface winds (kt)

Valid for marine exposure over water, open terrain exposure over land

Analysis based on CMAN from 0300 - 0900 z; AFREC from 0300 - 0859 z;

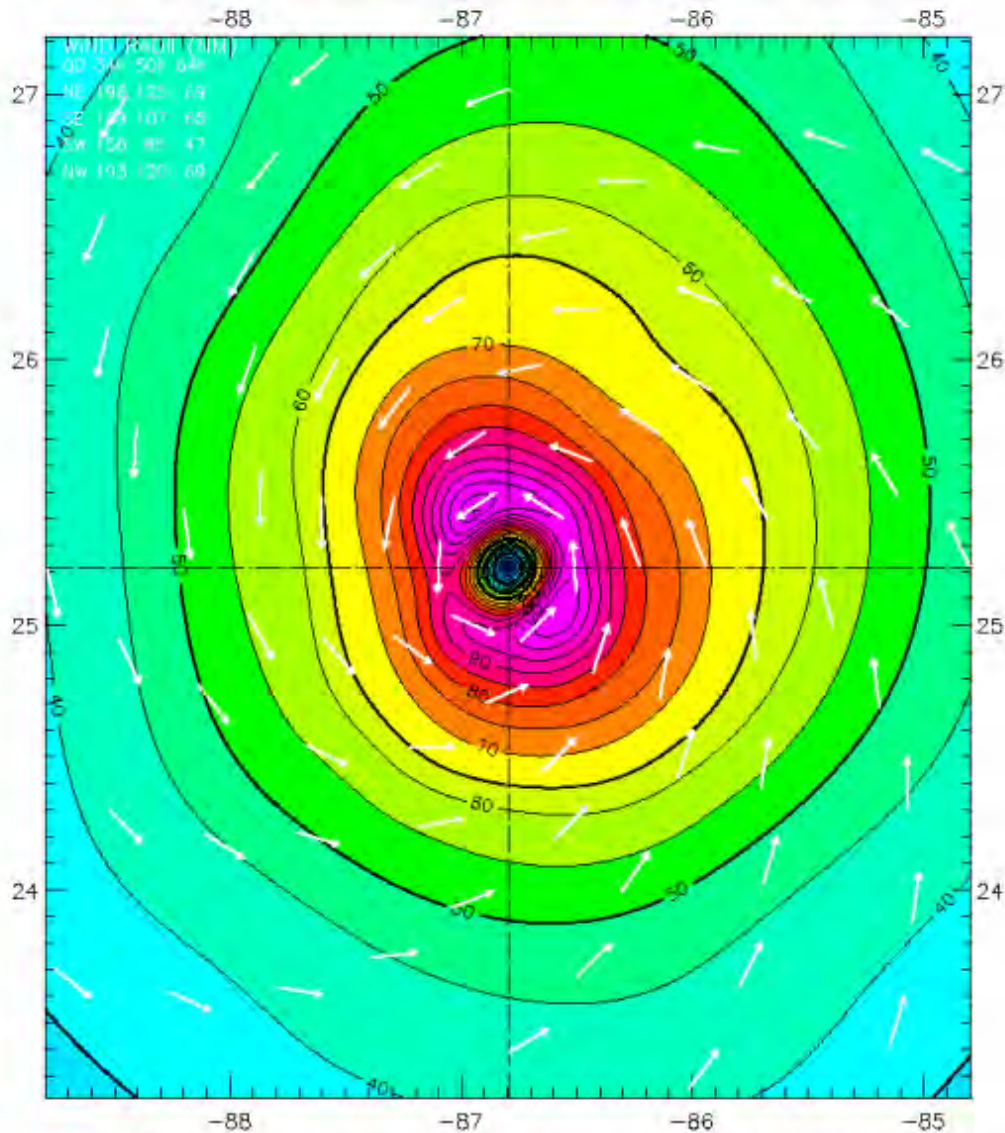
SHIP from 0606 - 0606 z; GOES\_SWIR from 0702 - 0702 z;

GPSSONDE\_WL150 from 0625 - 0830 z; METAR from 0315 - 0857 z;

ASOS from 0351 - 0900 z; MOORED\_BUOY from 0309 - 0859 z;

BACKGROUND\_FIELD from 0600 - 0600 z;

0600 z position interpolated from 0512 Army Corps; mslp = 935.0 mb



Observed Max. Surface Wind: 113 kts, 16 nm NW of center based on 0516 z AFREC sfc measurement  
Analyzed Max. Wind: 113 kts, 16 nm NW of center

Figure 2-29. H\*Wind snapshot on 28 August 2005 0600 UTC. The wind speeds are color contoured in knots, representing 1-minute sustained wind speeds. Note this wind field includes marine and land exposures identified by the abrupt change in color contours over the land.



## Hurricane Katrina 0900 UTC 28 AUG 2005

Max 1-min sustained surface winds (kt)

Valid for marine exposure over water, open terrain exposure over land

Analysis based on CMAN from 0600 - 1200 z; AFREC from 0806 - 1159 z;

QSCAT from 1125 - 1128 z; SHIP from 0606 - 0606 z;

GOES\_SWIR from 0702 - 1002 z; GPSSONDE\_WL150 from 0625 - 1107 z;

METAR from 0635 - 1155 z; ASOS from 0651 - 1200 z;

MOORED\_BUOY from 0609 - 1159 z;

0900 z position interpolated from 0600 Interpolation; mslp = 915.0 mb

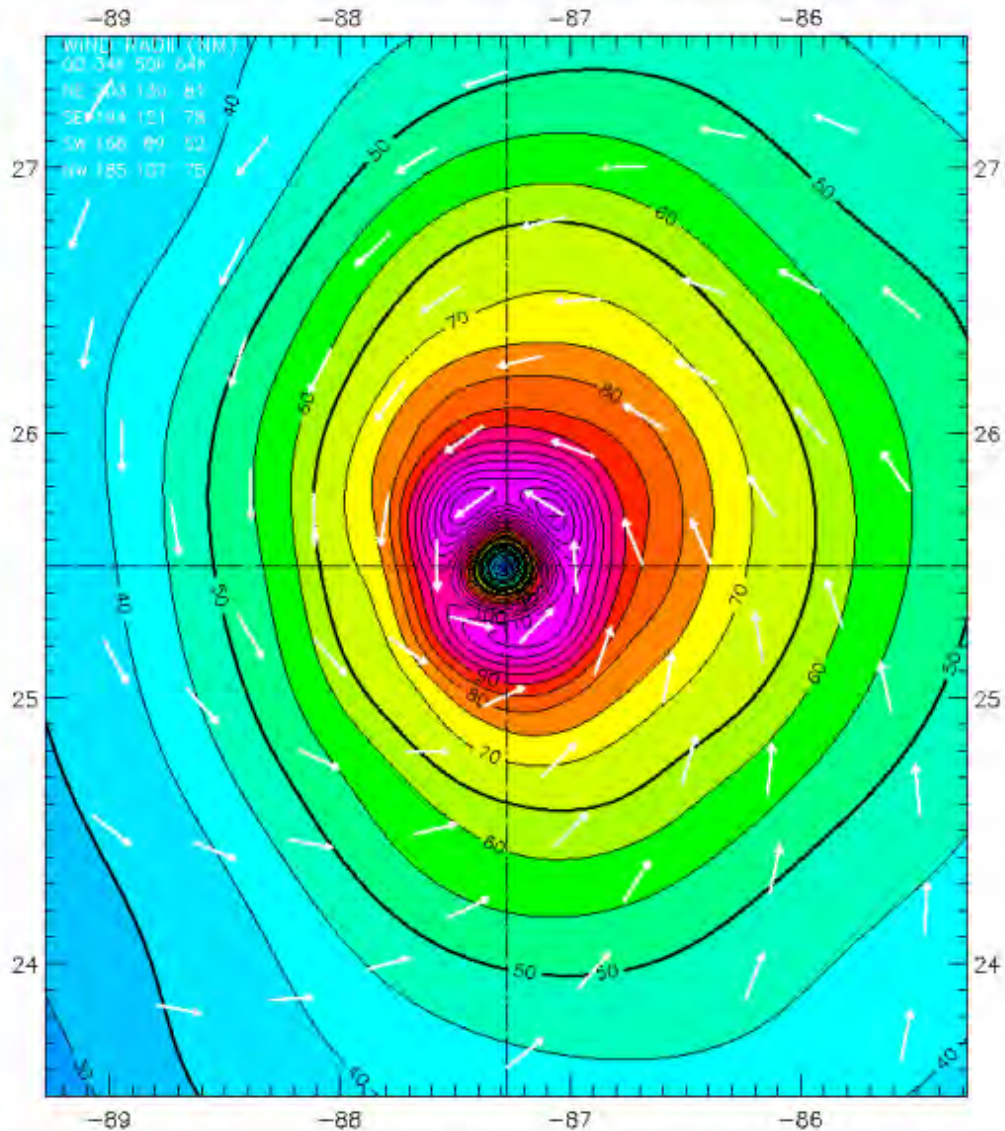


Figure 2-30. H\*Wind snapshot on 28 August 2005 0900 UTC. The wind speeds are color contoured in knots, representing 1-minute sustained wind speeds. Note this wind field includes marine and land exposures identified by the abrupt change in color contours over the land.

## Hurricane Katrina 1200 UTC 28 AUG 2005

Max 1-min sustained surface winds (kt)

Valid for marine exposure over water, open terrain exposure over land

Analysis based on CMAN from 0900 - 1500 z; AFREC from 0907 - 1459 z;

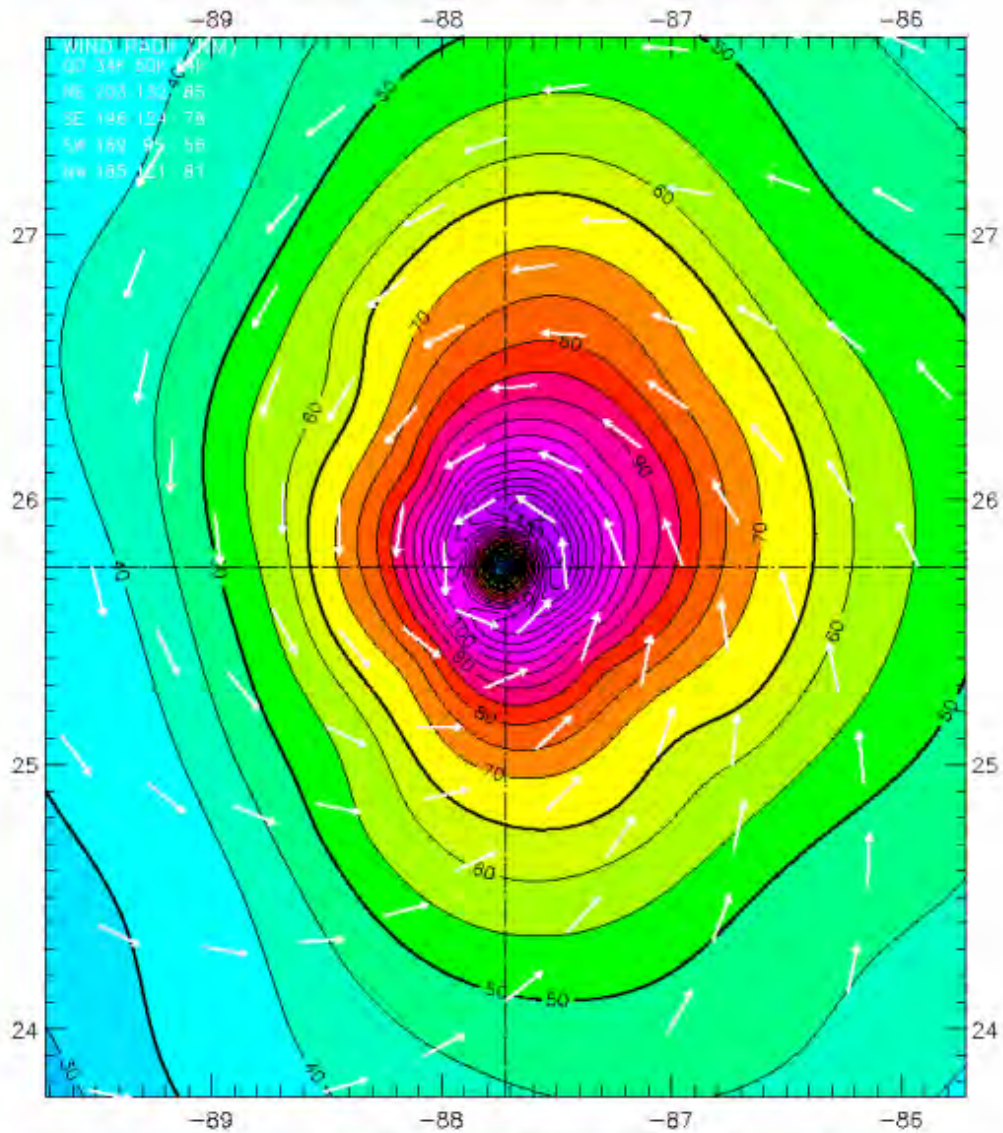
QSCAT from 1125 - 1128 z; SHIP from 1208 - 1312 z;

MESONET from 1418 - 1458 z; GPSSONDE\_WL150 from 0900 - 1458 z;

METAR from 0915 - 1500 z; ASOS from 0904 - 1500 z;

MOORED\_BUOY from 0909 - 1459 z;

1200 z position interpolated from 1104 Army Corps; mslp = 908.0 mb



Observed Max. Surface Wind: 139 kts, 14 nm NE of center based on 1422 z AFREC sfc measurement  
Analyzed Max. Wind: 139 kts, 14 nm NE of center

Figure 2-31. H\*Wind snapshot on 28 August 2005 1200 UTC. The wind speeds are color contoured in knots, representing 1-minute sustained wind speeds. Note this wind field includes marine and land exposures identified by the abrupt change in color contours over the land.



## Hurricane Katrina 1500 UTC 28 AUG 2005

Max 1-min sustained surface winds (kt)

Valid for marine exposure over water, open terrain exposure over land

Analysis based on AFREC from 0907 - 1459 z; SFMR43 from 1622 - 1829 z;

CMAN from 1230 - 1830 z; FCMP\_TOWER from 1510 - 1827 z;

ASOS from 1246 - 1756 z; BACKGROUND\_FIELD from 1500 - 1500 z;

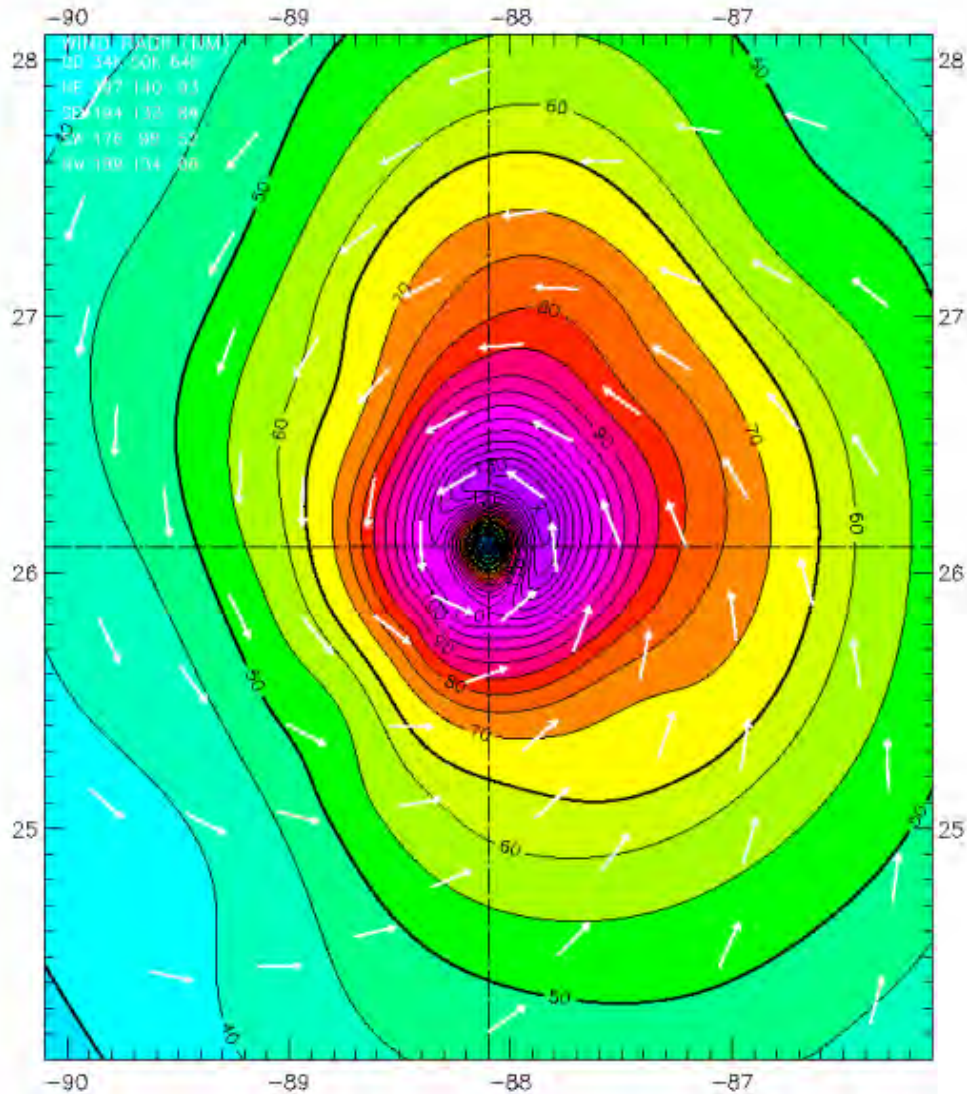
SHIP from 1312 - 1818 z; GPSSONDE\_WL150 from 1236 - 1827 z;

METAR from 1245 - 1805 z; MOORED\_BUOY from 1230 - 1830 z;

TAIL\_DOPPLER43 from 1755 - 1755 z; GOES from 1302 - 1602 z;

MESONET from 1418 - 1830 z;

1500 z Army Corps fix; mslp = 907.0 mb



Observed Max. Surface Wind: 139 kts, 16 nm NE of center based on 1744 z SFMR43 sfc measurement  
Analyzed Max. Wind: 139 kts, 16 nm NE of center

Figure 2-32. H\*Wind snapshot on 28 August 2005 1500 UTC. The wind speeds are color contoured in knots, representing 1-minute sustained wind speeds. Note this wind field includes marine and land exposures identified by the abrupt change in color contours over the land.

## Hurricane Katrina 1800 UTC 28 AUG 2005

Max 1-min sustained surface winds (kt)

Valid for marine exposure over water, open terrain exposure over land

Analysis based on AFREC from 0907 - 1459 z; SFMR43 from 1622 - 2100 z;

CMAN from 1500 - 2100 z; FCMP\_TOWER from 1510 - 2055 z;

ASOS from 1500 - 2056 z; BACKGROUND\_FIELD from 1800 - 1800 z;

SHIP from 1612 - 1818 z; GPSSONDE\_WL150 from 1503 - 2041 z;

METAR from 1500 - 2059 z; MOORED\_BUOY from 1509 - 2100 z;

TAIL\_DOPPLER43 from 1755 - 2038 z; GOES from 1602 - 1902 z;

MESONET from 1500 - 2058 z;

1800 z position interpolated from 1755 Army Corps; mslp = 902.0 mb

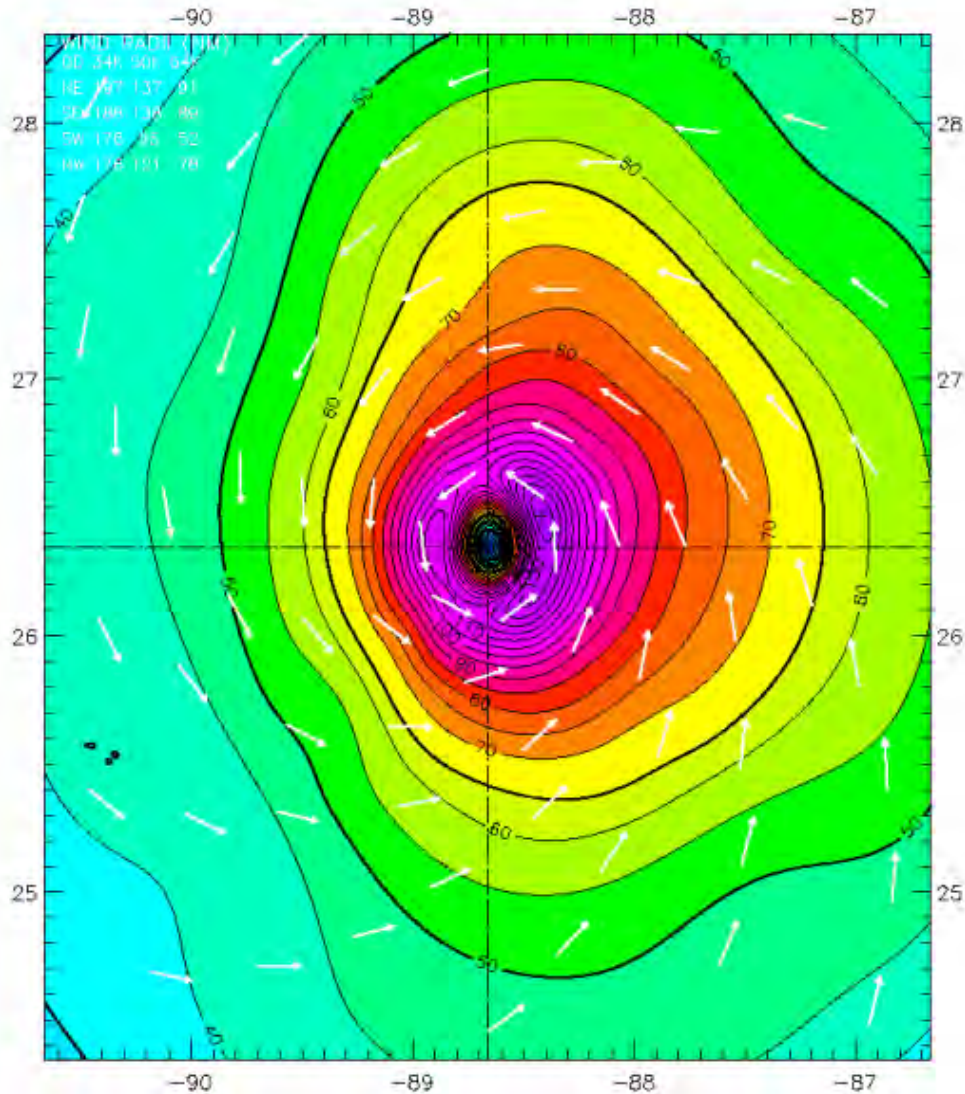


Figure 2-33. H\*Wind snapshot on 28 August 2005 1800 UTC. The wind speeds are color contoured in knots, representing 1-minute sustained wind speeds. Note this wind field includes marine and land exposures identified by the abrupt change in color contours over the land.



## Hurricane Katrina 2100 UTC 28 AUG 2005

Max 1-min sustained surface winds (kt)

Valid for marine exposure over water, open terrain exposure over land

Analysis based on SFMR43 from 1800 - 0000 z; CMAN from 1800 - 0000 z;

ASOS from 1849 - 2356 z; FCMP\_TOWER from 1809 - 2355 z;

QSCAT from 2349 - 2351 z; SHIP from 1814 - 0000 z;

GPSSONDE\_WL150 from 1801 - 2353 z; METAR from 1805 - 2359 z;

MOORED\_BUOY from 1800 - 2359 z; TAIL\_DOPPLER43 from 1923 - 2326 z;

GOES from 1902 - 2202 z; MESONET from 1800 - 0000 z;

2100 z position interpolated from 2038 Army Corps; mslp = 903.0 mb

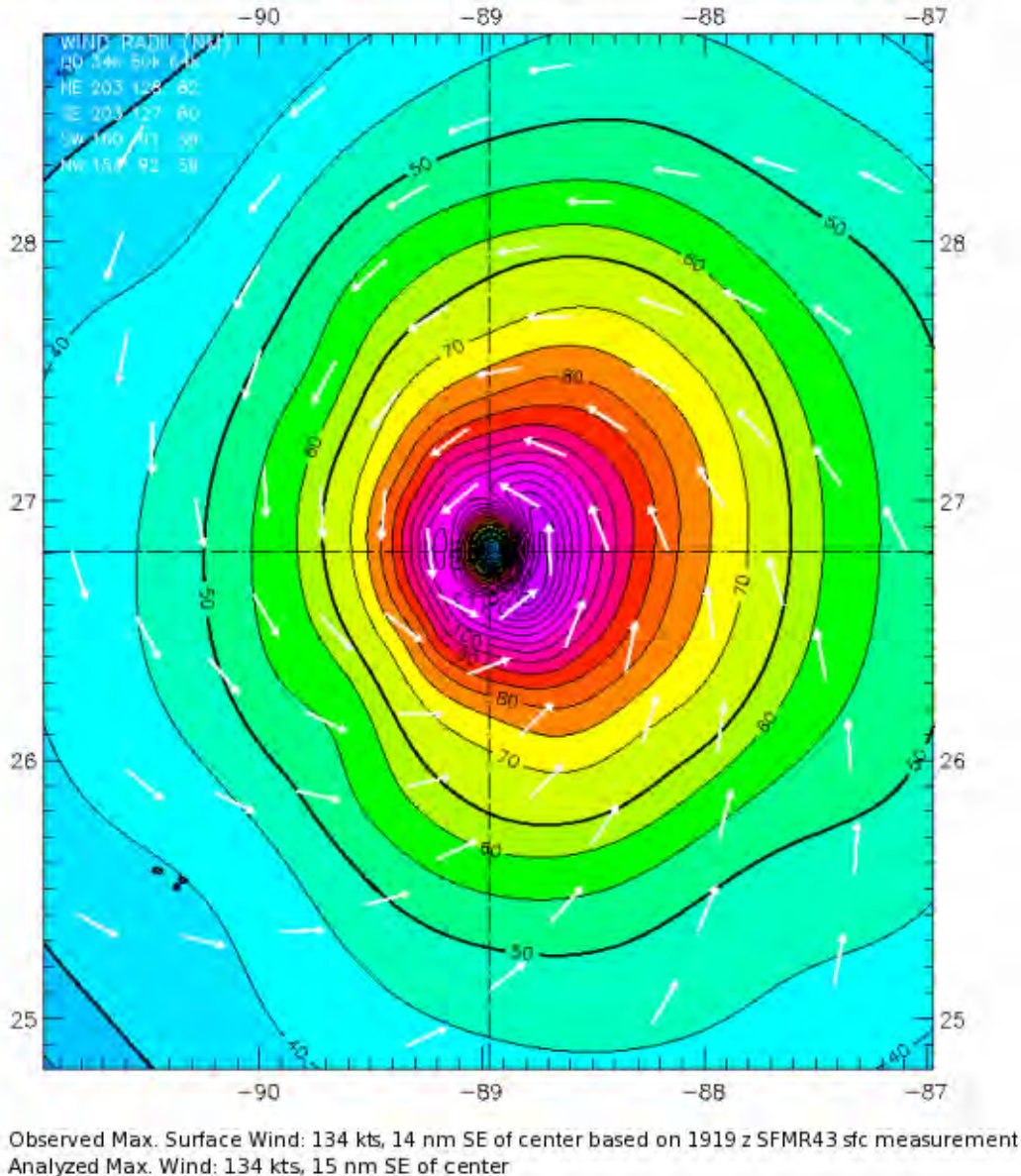


Figure 2-34. H\*Wind snapshot on 28 August 2005 2100 UTC. The wind speeds are color contoured in knots, representing 1-minute sustained wind speeds. Note this wind field includes marine and land exposures identified by the abrupt change in color contours over the land.

## Hurricane Katrina 0000 UTC 29 AUG 2005

Max 1-min sustained surface winds (kt)

Valid for marine exposure over water, open terrain exposure over land

Analysis based on AFREC from 0105 - 0259 z; SFMR43 from 2100 - 0120 z;

CMAN from 2100 - 0300 z; FCMP\_TOWER from 2109 - 0255 z;

ASOS from 2105 - 0259 z; BACKGROUND\_FIELD from 0000 - 0000 z;

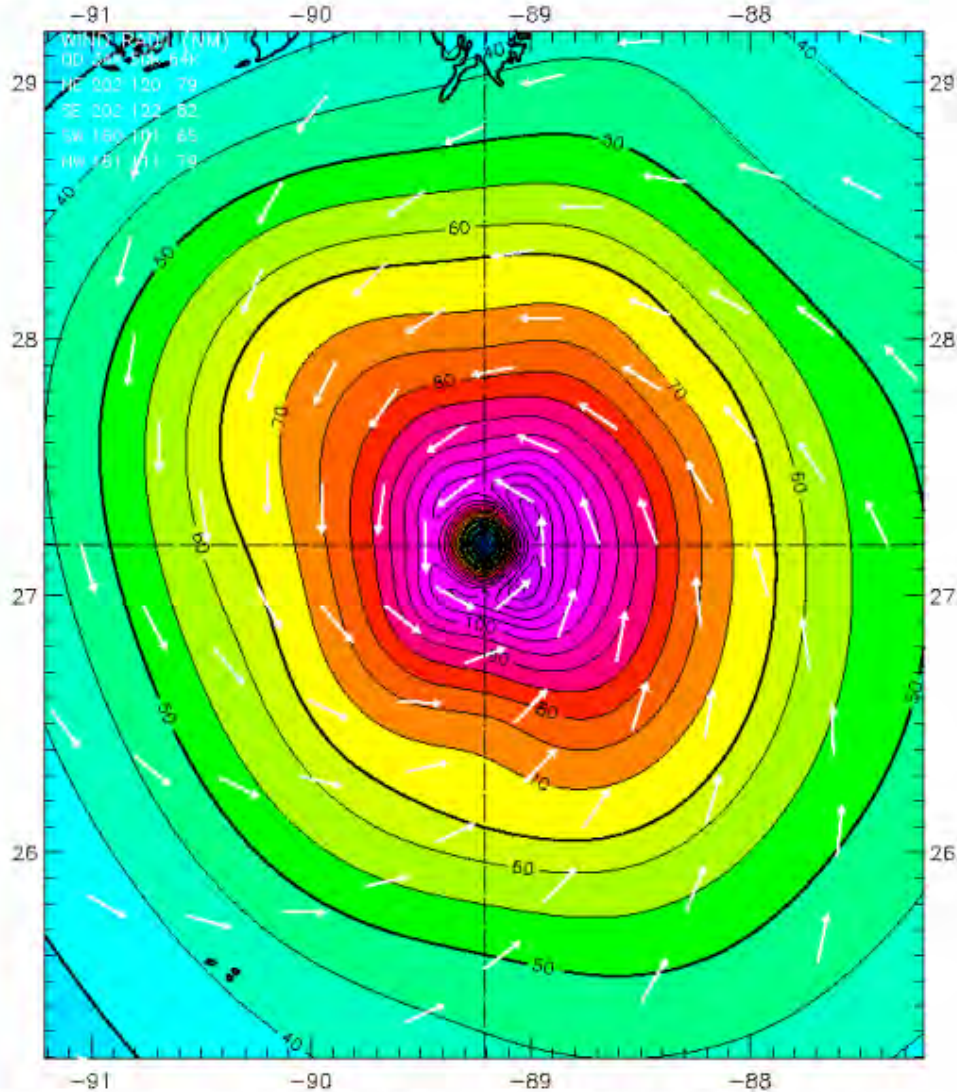
QSCAT from 2349 - 2351 z; SHIP from 2118 - 0300 z;

GPSSONDE\_WL150 from 2103 - 0239 z; METAR from 2105 - 0255 z;

MOORED\_BUOY from 2100 - 0300 z; TAIL\_DOPPLER43 from 2231 - 2326 z;

MESONET from 2100 - 0300 z;

0000 z position interpolated from 2326 Army Corps; mslp = 904.0 mb



Observed Max. Surface Wind: 124 kts, 14 nm NE of center based on 2326 z TAIL\_DOPPLER43 sfc measurement:  
Analyzed Max. Wind: 124 kts, 14 nm SE of center

Figure 2-35. H\*Wind snapshot on 29 August 2005 0000 UTC. The wind speeds are color contoured in knots, representing 1-minute sustained wind speeds. Note this wind field includes marine and land exposures identified by the abrupt change in color contours over the land.



## Hurricane Katrina 0300 UTC 29 AUG 2005

Max 1-min sustained surface winds (kt)

Valid for marine exposure over water, open terrain exposure over land

Analysis based on BACKGROUND\_FIELD from 0300 - 0300 z; FCMP\_TOWER from 0004 - 0556 z;

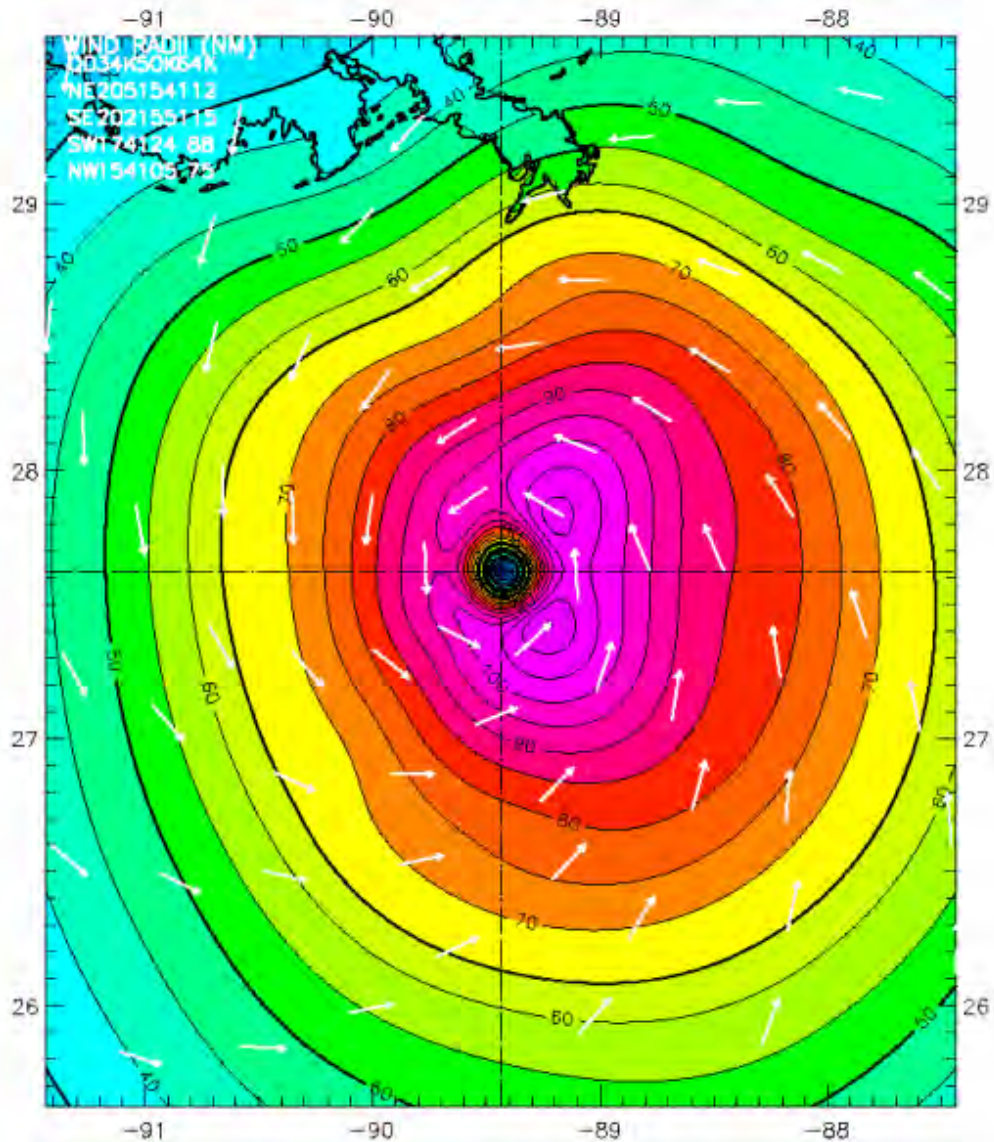
SHIP from 0000 - 0404 z; METAR from 0037 - 0559 z;

CMAN from 0000 - 0600 z; AFREC from 0105 - 0552 z;

GPSSONDE\_WL150 from 0016 - 0538 z; MESONET from 0000 - 0600 z;

ASOS from 0001 - 0600 z; MOORED\_BUOY from 0009 - 0600 z;

0300 z position interpolated from 0236 Army Corps; mslp = 908.0 mb



Observed Max. Surface Wind: 116 kts, 17 nm NE of center based on 0300 z BACKGROUND\_FIELD sfc measurement  
Analyzed Max. Wind: 115 kts, 18 nm SE of center

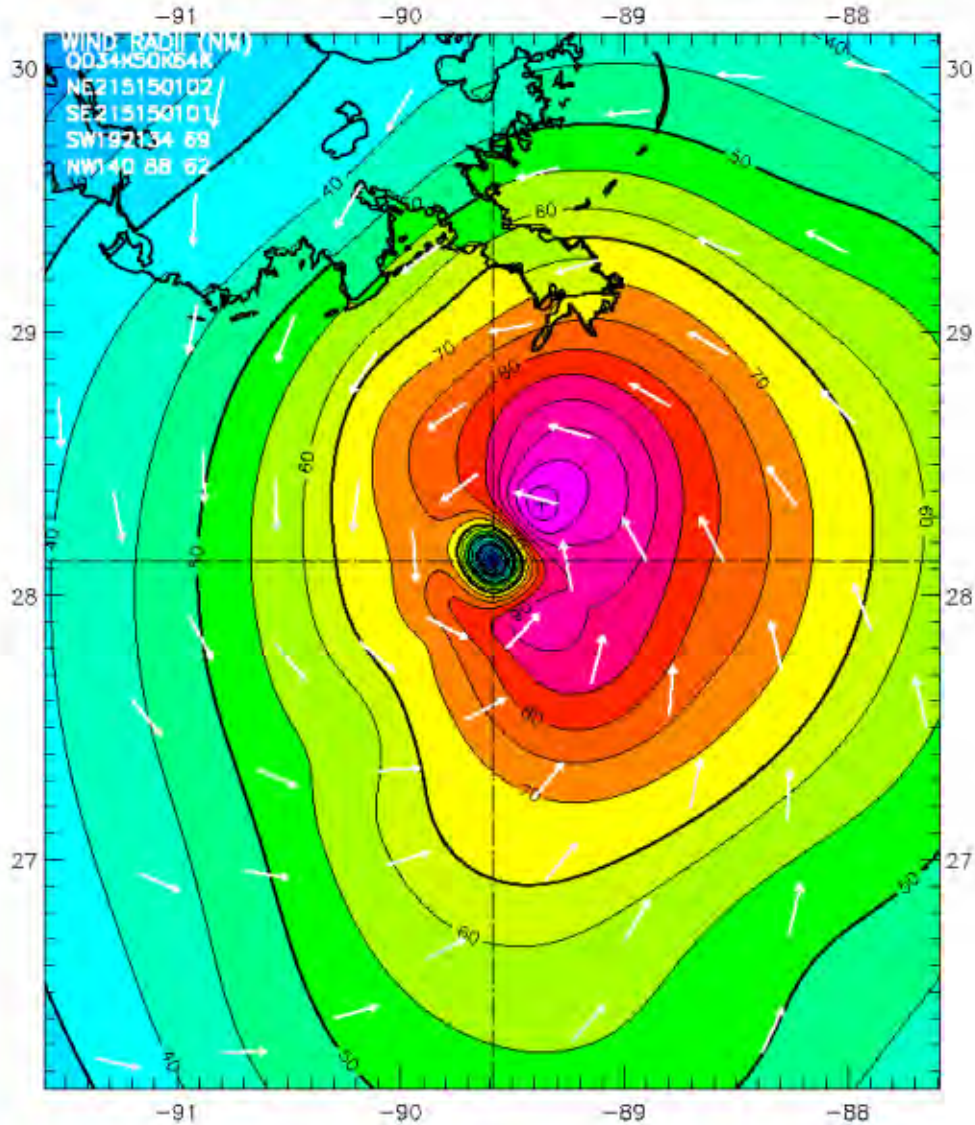
Figure 2-36. H\*Wind snapshot on 29 August 2005 0300 UTC. The wind speeds are color contoured in knots, representing 1-minute sustained wind speeds. Note this wind field includes marine and land exposures identified by the abrupt change in color contours over the land.

## Hurricane Katrina 0600 UTC 29 AUG 2005

Max 1-min sustained surface winds (kt)

Valid for marine exposure over water, open terrain exposure over land

Analysis based on AFREC from 0300 - 0859 z; SFMR43 from 0711 - 0858 z; CMAN from 0300 - 0900 z;  
FCMP\_TOWER from 0300 - 0857 z; ASOS from 0302 - 0900 z;  
SHIP from 0300 - 0707 z; MADIS from 0306 - 0835 z;  
GPSSONDE\_WL150 from 0428 - 0855 z; METAR from 0320 - 0856 z;  
MOORED\_BUOY from 0300 - 0900 z; GPSSONDE\_SFC from 0438 - 0855 z;  
VAD\_88D from 0804 - 0859 z; MESONET from 0300 - 0900 z;  
0600 z position interpolated from 0549 Army Corps; mslp = 910.0 mb



Observed Max. Surface Wind: 108 kts, 18 nm SE of center based on 0705 z AFREC sfc measurement  
Analyzed Max. Wind: 108 kts, 18 nm NE of center

Figure 2-37. H\*Wind snapshot on 29 August 2005 0600 UTC. The wind speeds are color contoured in knots, representing 1-minute sustained wind speeds. Note this wind field includes marine and land exposures identified by the abrupt change in color contours over the land.



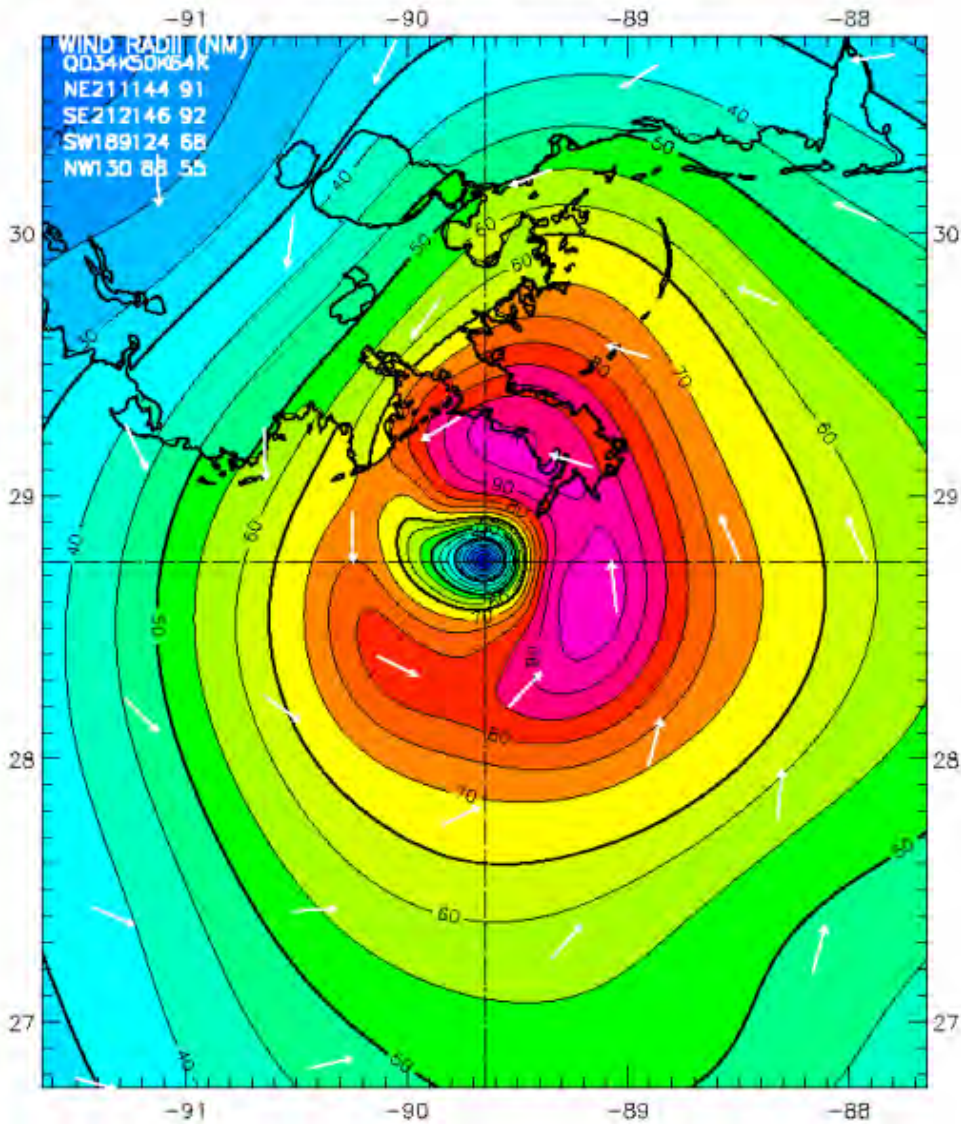
## Hurricane Katrina 0900 UTC 29 AUG 2005

Max 1-min sustained surface winds (kt)

Valid for marine exposure over water, open terrain exposure over land

Analysis based on SHIP from 0707 - 1010 z; FCMP\_TOWER from 0703 - 1059 z; MESONET from 0700 - 1100 z;  
SFMR43 from 0712 - 1059 z; DUAL\_DOPPLER from 1010 - 1010 z;  
ASOS from 0700 - 1100 z; CMAN from 0700 - 1100 z;  
GOES\_SWIR from 1002 - 1002 z; METAR from 0712 - 1058 z;  
MOORED\_BUOY from 0700 - 1059 z; MADIS from 0707 - 1049 z;  
VAD\_88D from 0804 - 1012 z; TAIL\_DOPPLER43 from 0921 - 1020 z;  
GPSSONDE\_WL150 from 0847 - 1058 z;

0900 z Army Corps fix; mslp = 917.0 mb



Observed Max. Surface Wind: 99 kts, 30 nm SE of center based on 1032 z SFMR43 sfc measurement  
Analyzed Max. Wind: 99 kts, 31 nm NE of center

Figure 2-38. H\*Wind snapshot on 29 August 2005 0900 UTC. The wind speeds are color contoured in knots, representing 1-minute sustained wind speeds. Note this wind field includes marine and land exposures identified by the abrupt change in color contours over the land.

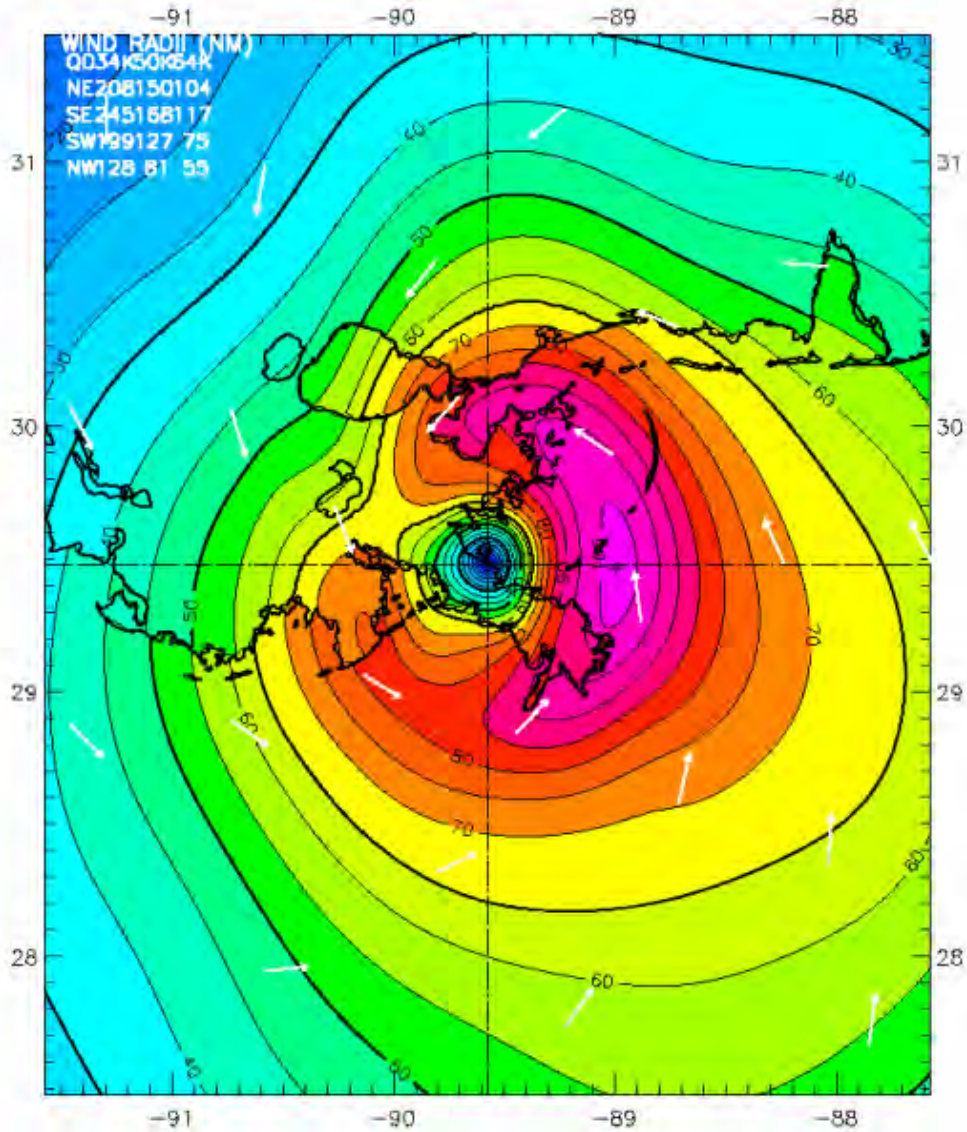
## Hurricane Katrina 1200 UTC 29 AUG 2005

Max 1-min sustained surface winds (kt)

Valid for marine exposure over water, open terrain exposure over land

Analysis based on GPSSONDE\_WL150 from 0959 - 1357 z; FCMP\_TOWER from 0942 - 1359 z; VAD\_88D from 0959 - 1354 z;  
QSCAT from 1100 - 1102 z;  
SHIP from 1010 - 1212 z; ASCS from 0936 - 1359 z;  
SFMR43 from 0936 - 1359 z; MOORED\_BUOY from 0939 - 1400 z;  
METAR from 0950 - 1355 z; CMAN from 0936 - 1400 z;  
GOES\_SWIR from 1002 - 1002 z; TAIL\_DOPPLER43 from 1020 - 1346 z;  
MADIS from 0936 - 1359 z; DUAL\_DOPPLER from 1010 - 1302 z;  
MESONET from 0937 - 1400 z;

1200 z position interpolated from 1132 Army Corps; mslp = 923.0 mb



Observed Max. Surface Wind: 102 kts, 35 nm SE of center based on 1020 z TAIL\_DOPPLER43 sfc measurement  
Analyzed Max. Wind: 102 kts, 36 nm NE of center

Figure 2-39. H\*Wind snapshot on 29 August 2005 1200 UTC. The wind speeds are color contoured in knots, representing 1-minute sustained wind speeds. Note this wind field includes marine and land exposures identified by the abrupt change in color contours over the land.



## Hurricane Katrina 1500 UTC 29 AUG 2005

Max 1-min sustained surface winds (kt)

Valid for marine exposure over water, open terrain exposure over land

Analysis based on SHIP from 1512 - 1717 z; FCMP\_TOWER from 1326 - 1800 z; MESONET from 1323 - 1800 z; AFREC from 1323 - 1802 z; SFMR43 from 1324 - 1506 z; ASOS from 1323 - 1800 z; CMAN from 1324 - 1800 z; METAR from 1325 - 1759 z; MOORED\_BUOY from 1329 - 1800 z; MADIS from 1324 - 1759 z; VAD\_88D from 1349 - 1548 z; TAIL\_DOPPLER43 from 1346 - 1346 z; GPSSONDE\_WL150 from 1326 - 1449 z; GBVTD from 1548 - 1548 z;

1500 z position interpolated from 1443 Army Corps; mslp = 932.0 mb

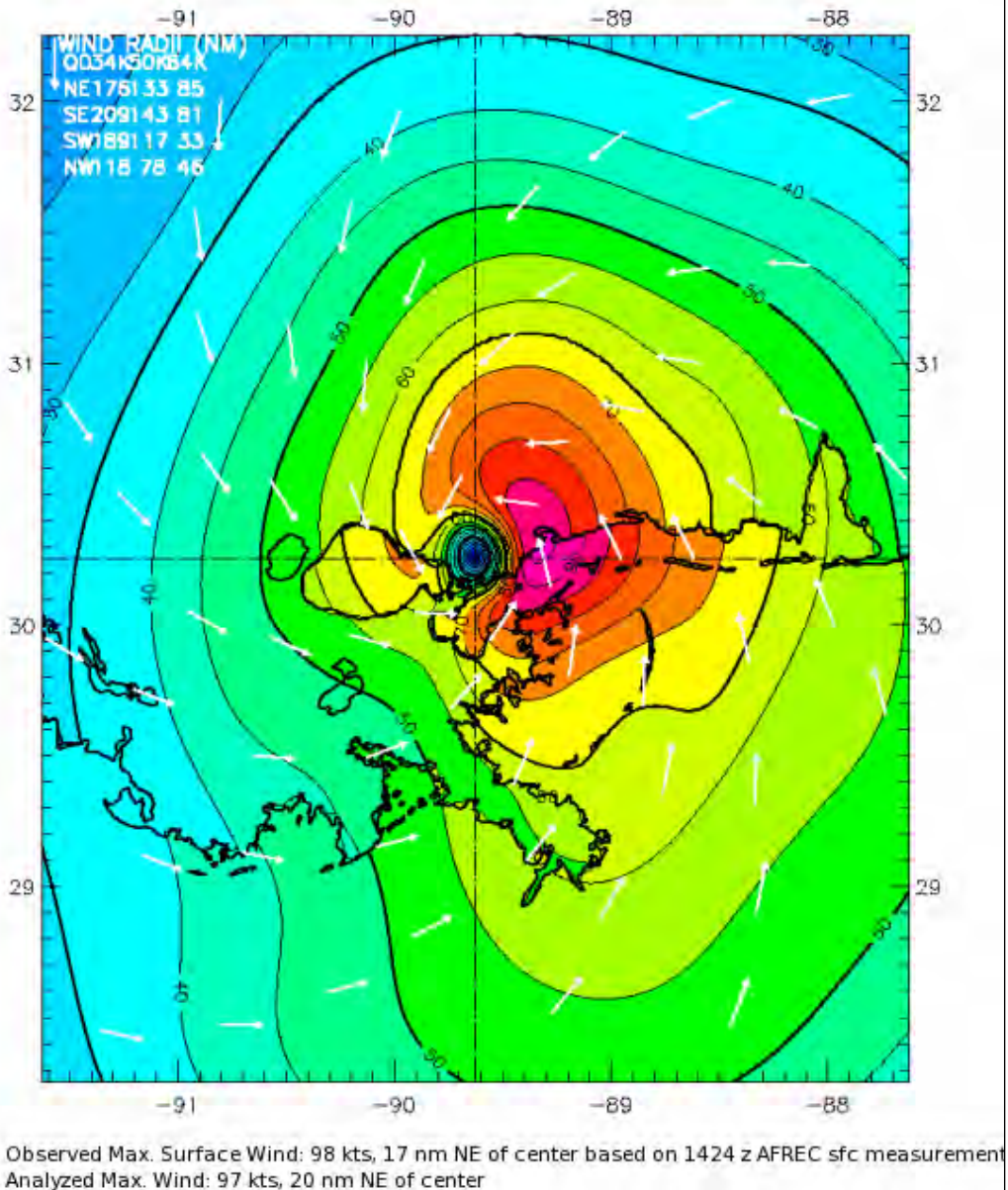


Figure 2-40. H\*Wind snapshot on 29 August 2005 1500 UTC. The wind speeds are color contoured in knots, representing 1-minute sustained wind speeds. Note this wind field includes marine and land exposures identified by the abrupt change in color contours over the land.

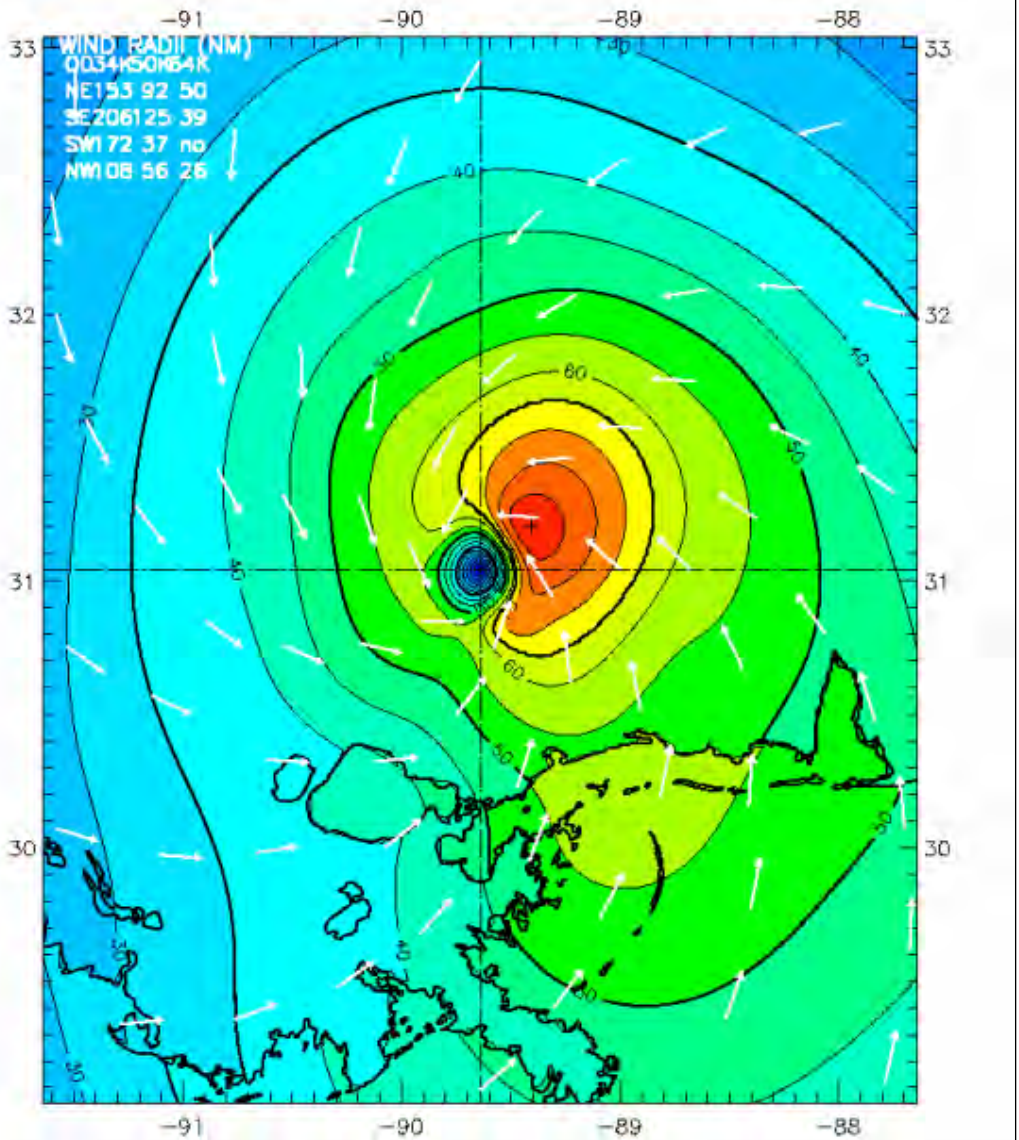
## Hurricane Katrina 1800 UTC 29 AUG 2005

Max 1-min sustained surface winds (kt)

Valid for marine exposure over water, open terrain exposure over land

Analysis based on AFREC from 1548 - 1802 z; CMAN from 1329 - 2300 z; FCMP\_TOWER from 1553 - 1952 z;  
ASOS from 1323 - 1958 z; BACKGROUND\_FIELD from 1800 - 1800 z;  
SHIP from 1616 - 1818 z; MADIS from 1324 - 1914 z;  
METAR from 1325 - 1958 z; MOORED\_BUOY from 1549 - 2000 z;  
GBVTD from 1548 - 1548 z; GOES from 1902 - 1902 z;  
MESONET from 1330 - 2000 z;

1800 z position interpolated from 1704 Army Corps; mslp = 948.0 mb



Observed Max. Surface Wind: 92 kts, 17 nm NE of center based on 1548 z AFREC sfc measurement  
Analyzed Max. Wind: 84 kts, 16 nm NE of center

Figure 2-41. H\*Wind snapshot on 29 August 2005 1800 UTC. The wind speeds are color contoured in knots, representing 1-minute sustained wind speeds. Note this wind field includes marine and land exposures identified by the abrupt change in color contours over the land.



## Hurricane Katrina 2100 UTC 29 AUG 2005

Max 1-min sustained surface winds (kt)

Valid for marine exposure over water, open terrain exposure over land

Analysis based on BACKGROUND\_FIELD from 2100 - 2100 z; FCMP\_TOWER from 1904 - 2251 z;

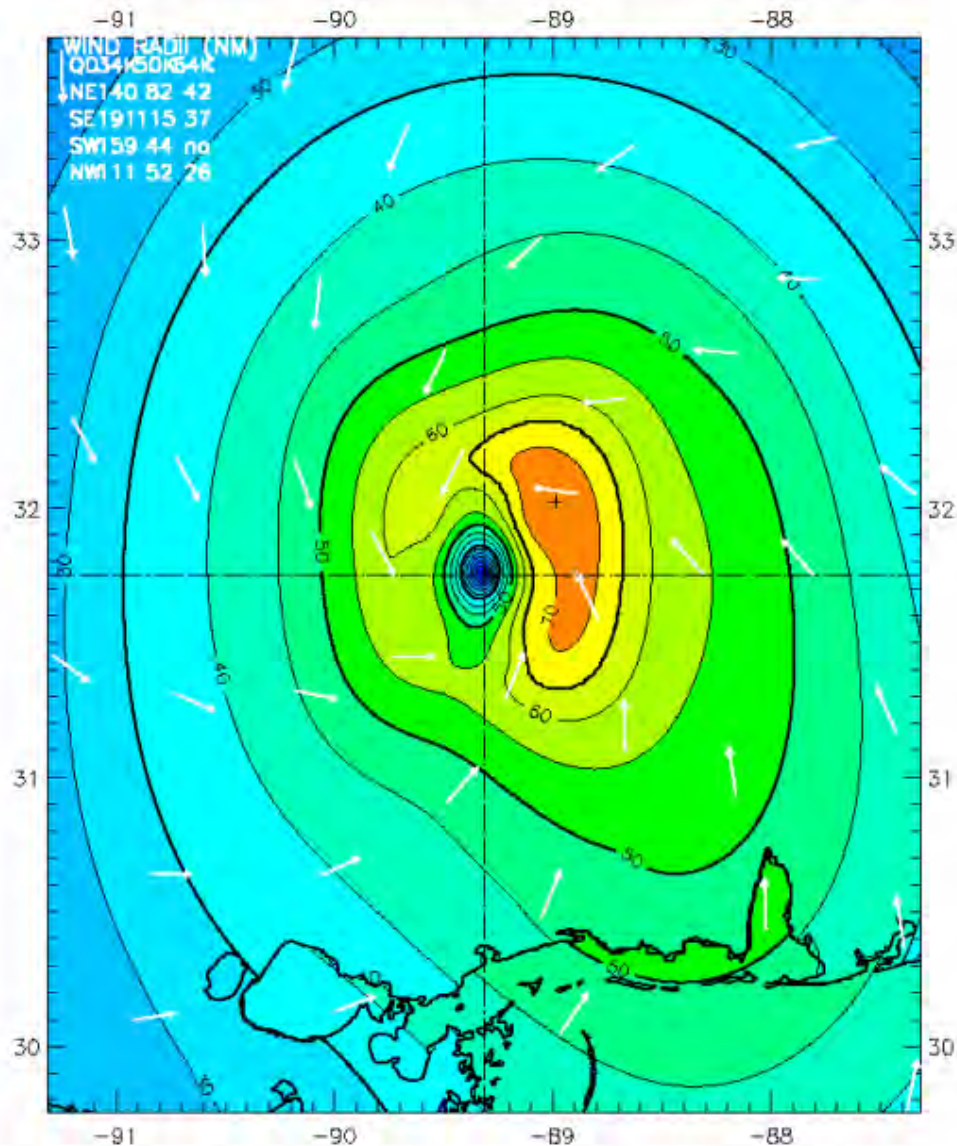
SHIP from 2222 - 2222 z; METAR from 1325 - 1958 z;

CMAN from 1329 - 2000 z; MADIS from 1324 - 1914 z;

MESONET from 1330 - 2000 z; GOES from 1902 - 2202 z;

ASOS from 1323 - 1958 z; MOORED\_BUOY from 1859 - 2300 z;

2100 z position interpolated from 2052 Army Corps; mslp = 954.0 mb



Observed Max. Surface Wind: 82 kts, 26 nm NE of center based on 2100 z BACKGROUND\_FIELD sfc measurement  
Analyzed Max. Wind: 75 kts, 25 nm NE of center

Figure 2-42. H\*Wind snapshot on 29 August 2005 2100 UTC. The wind speeds are color contoured in knots, representing 1-minute sustained wind speeds. Note this wind field includes marine and land exposures identified by the abrupt change in color contours over the land.

## Hurricane Katrina 0000 UTC 30 AUG 2005

Max 1-min sustained surface winds (kt)

Valid for marine exposure over water, open terrain exposure over land

Analysis based on MOORED\_BUOY from 2159 - 0200 z; SHIP from 2222 - 0101 z; FCMP\_TOWER from 2206 - 2333 z;

MADIS from 2159 - 0159 z; QSCAT from 0103 - 0104 z;

GOES\_SWIR from 0102 - 0102 z; MESONET from 2158 - 0200 z;

ASOS from 2158 - 0156 z; GOES from 2202 - 2202 z;

METAR from 2157 - 0156 z; BACKGROUND\_FIELD from 0000 - 0000 z;

0000 z position interpolated from 2256 Army Corps; mslp = 963.0 mb

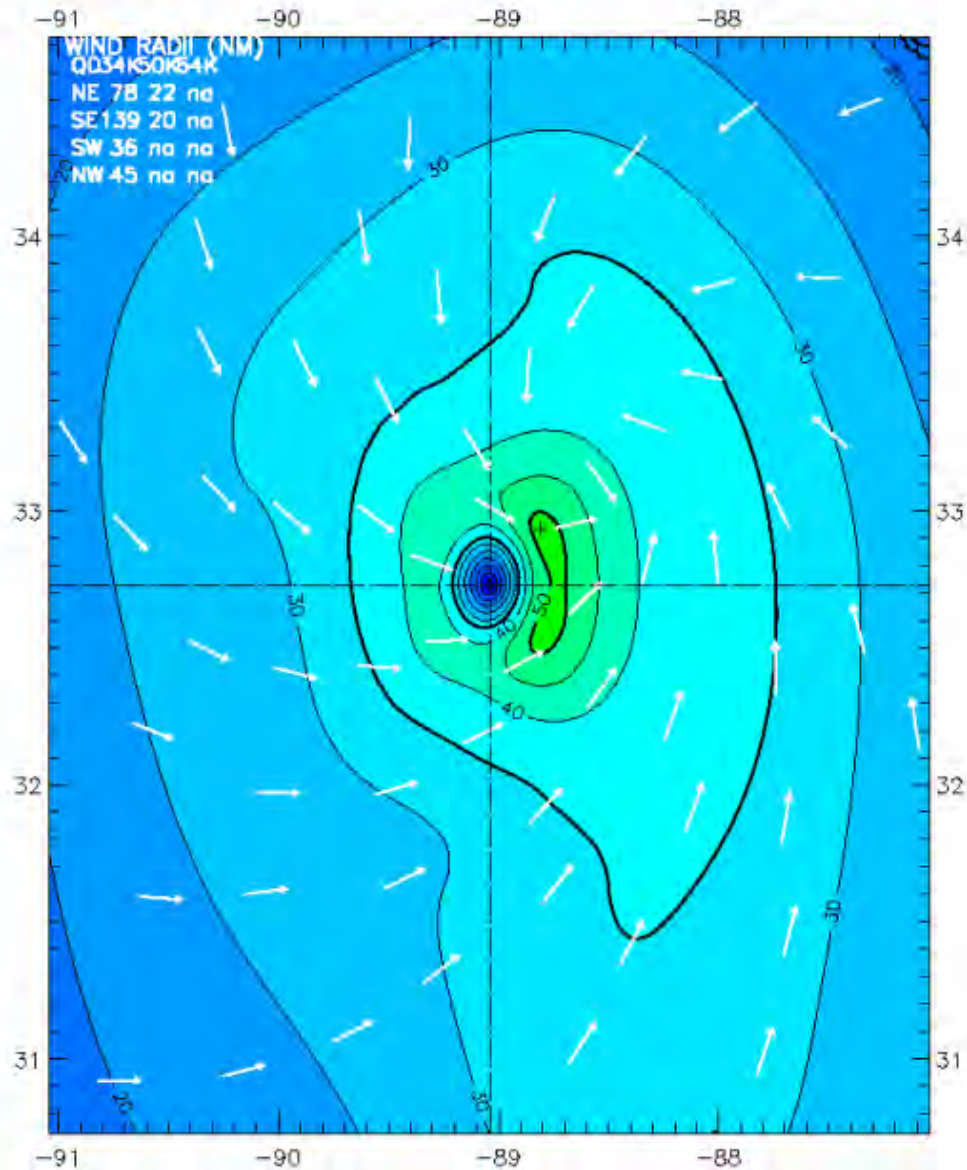


Figure 2-43. H\*Wind snapshot on 30 August 2005 0000 UTC. The wind speeds are color contoured in knots, representing 1-minute sustained wind speeds. Note this wind field includes marine and land exposures identified by the abrupt change in color contours over the land.



## Wind Speed and Direction Comparisons

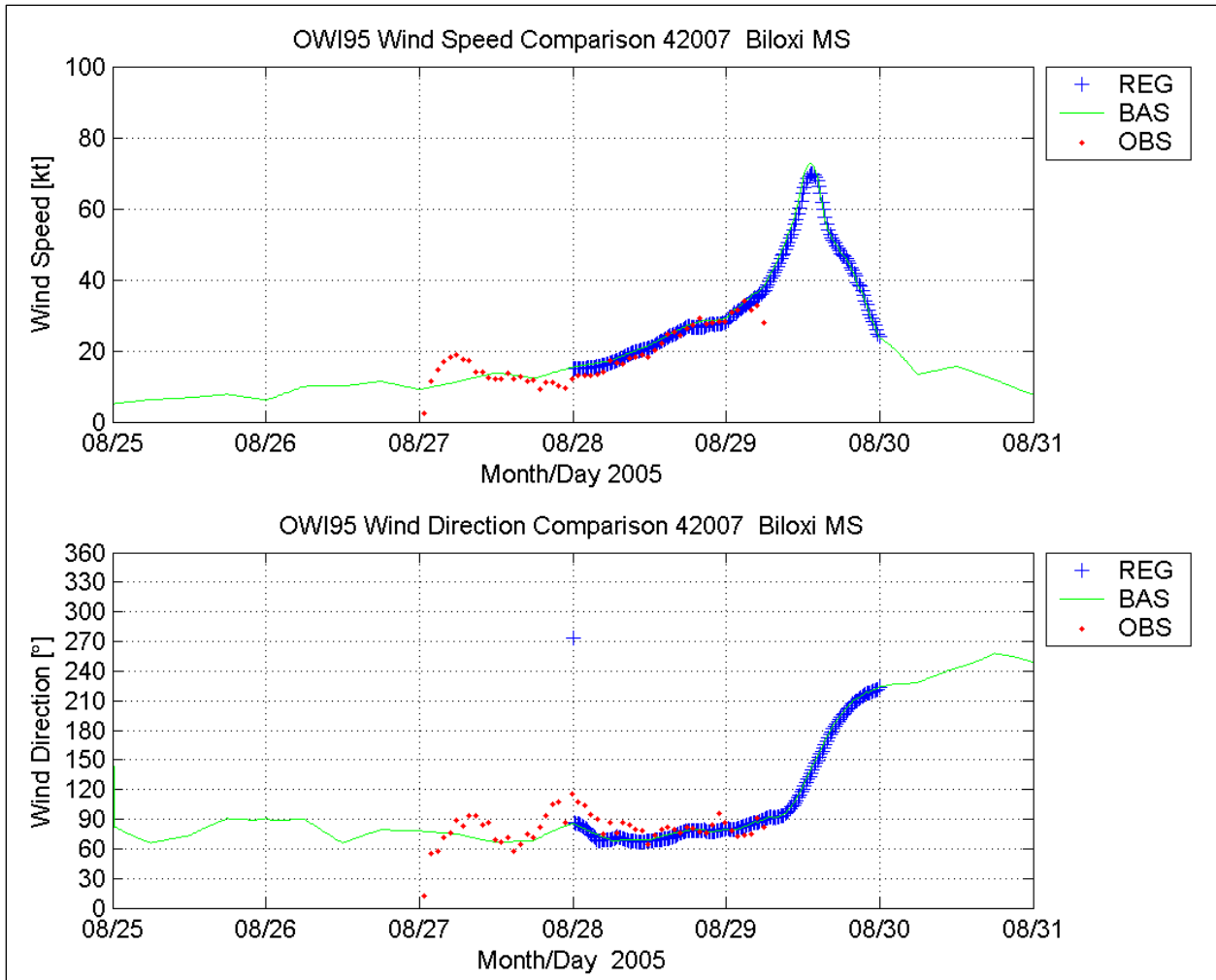


Figure 2-44. Comparison of wind speed (upper panel) and direction (bottom panel) at NDBC 42007

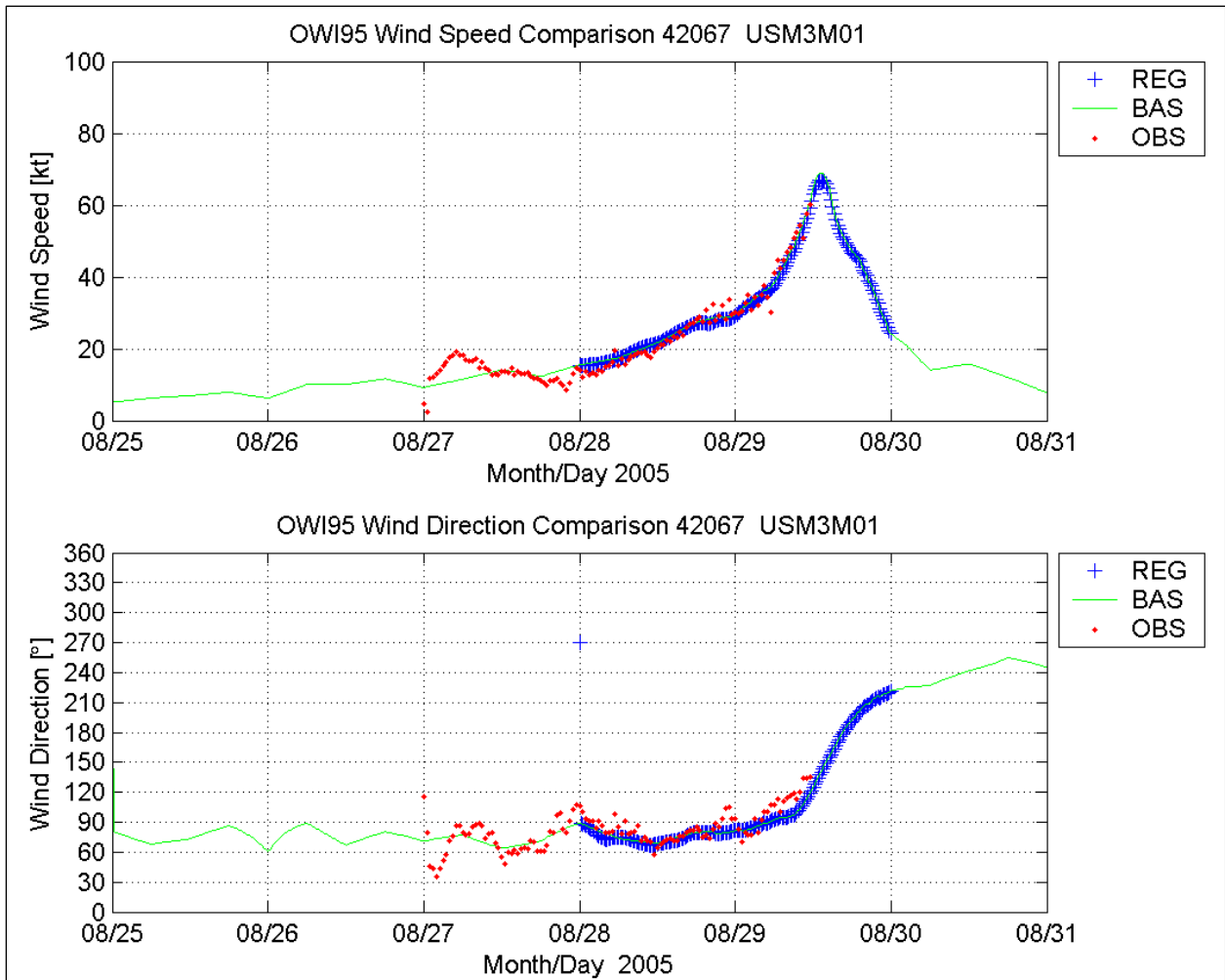


Figure 2-45. Comparison of wind speed (upper panel) and direction (bottom panel) at NDBC 42067

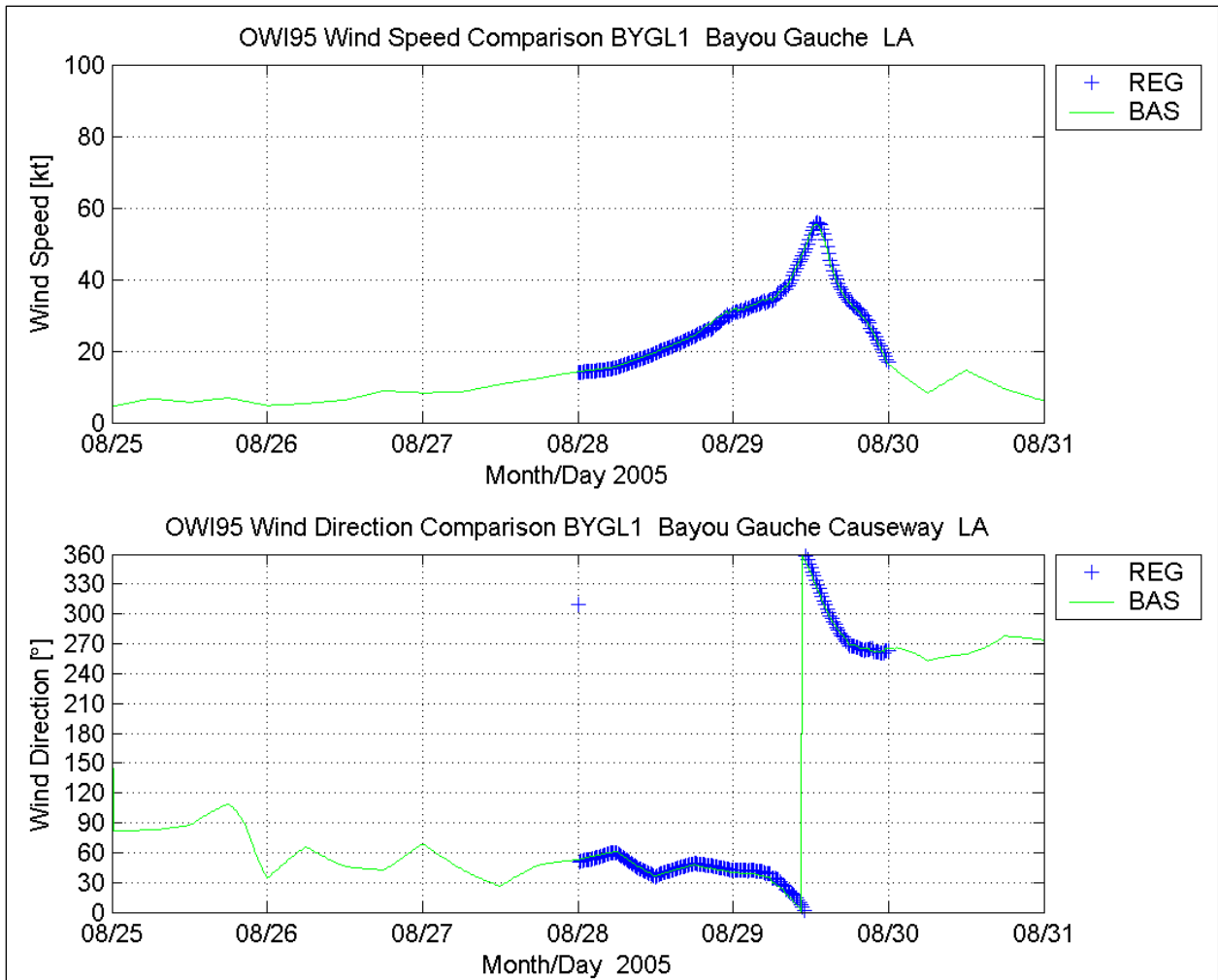


Figure 2-46. Comparison of wind speed (upper panel) and direction (bottom panel) at Bayou Gauche, LA

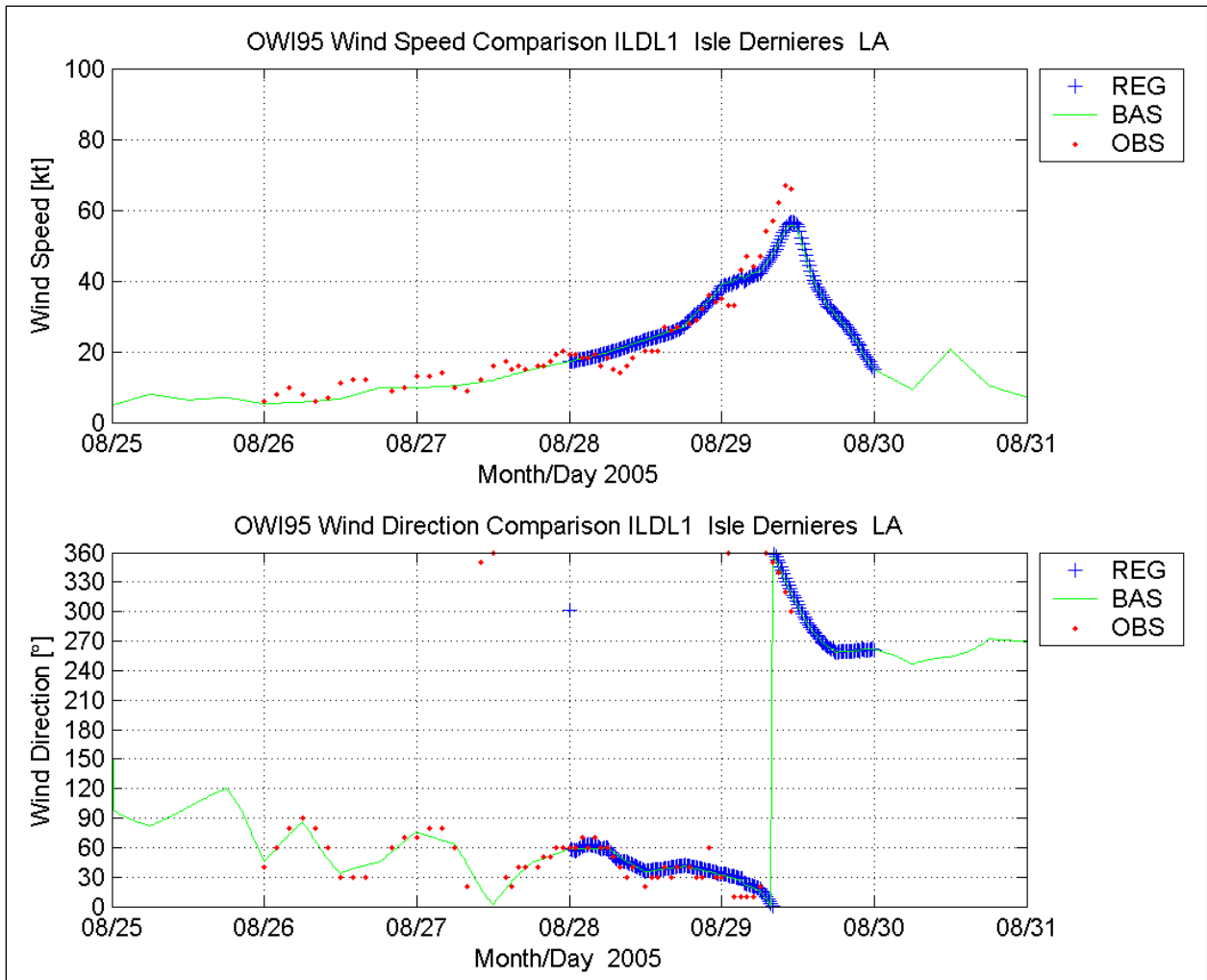


Figure 2-47. Comparison of wind speed (upper panel) and direction (bottom panel) at Isle Dernieres, LA



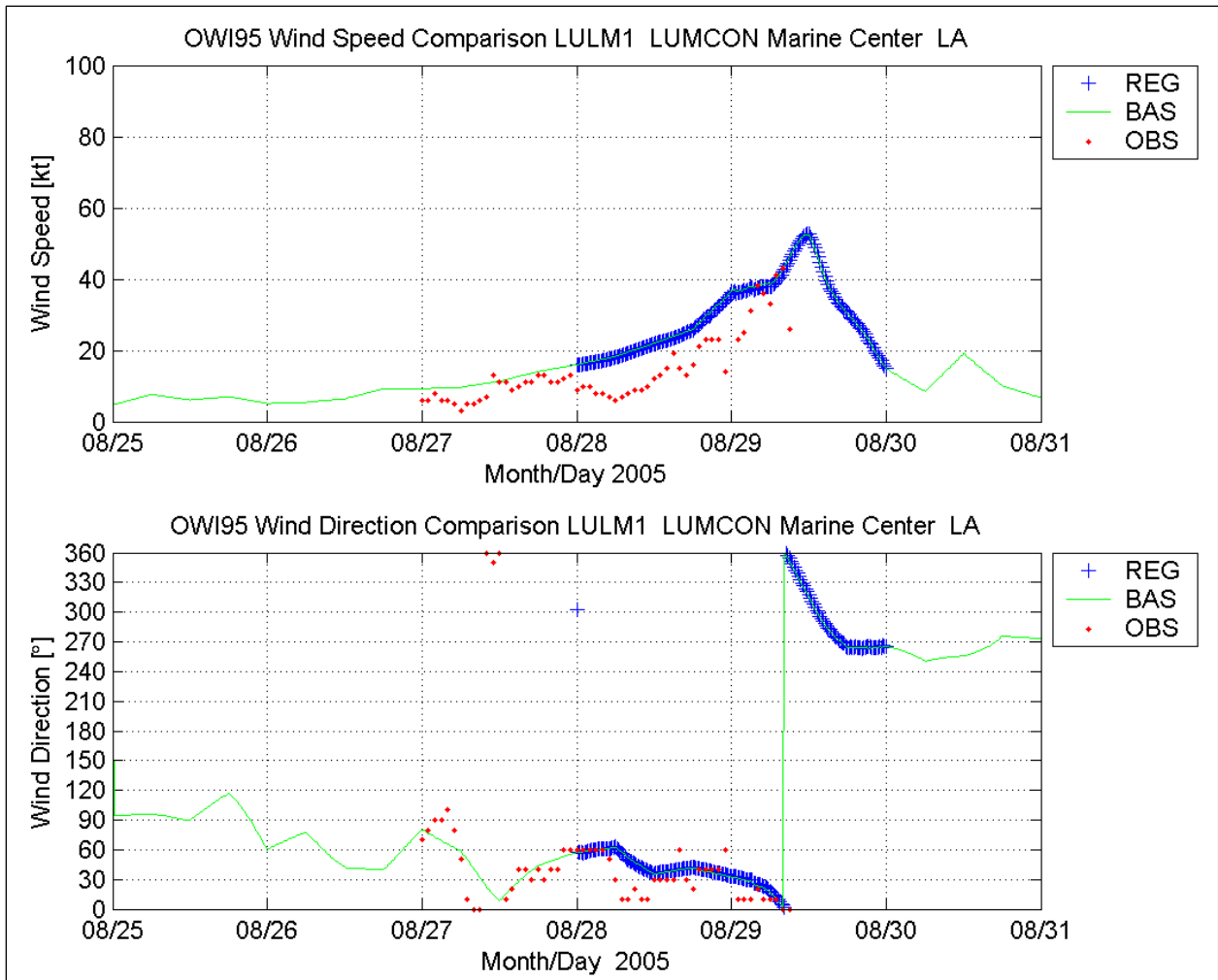


Figure 2-48. Comparison of wind speed (upper panel) and direction (bottom panel) at LUMCON Marine Center, LA

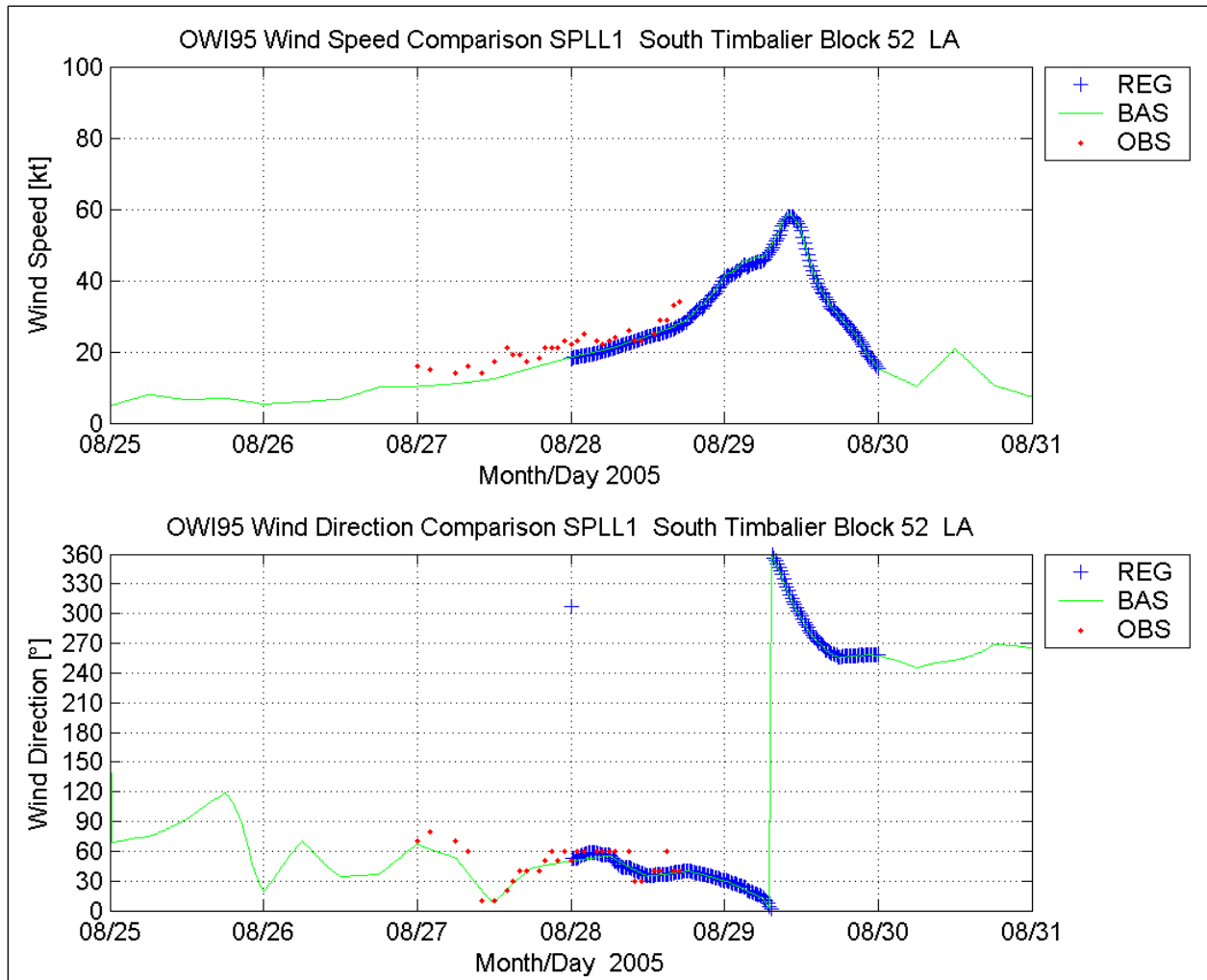


Figure 2-49. Comparison of wind speed (upper panel) and direction (bottom panel) at South Timbalier Block 52, LA

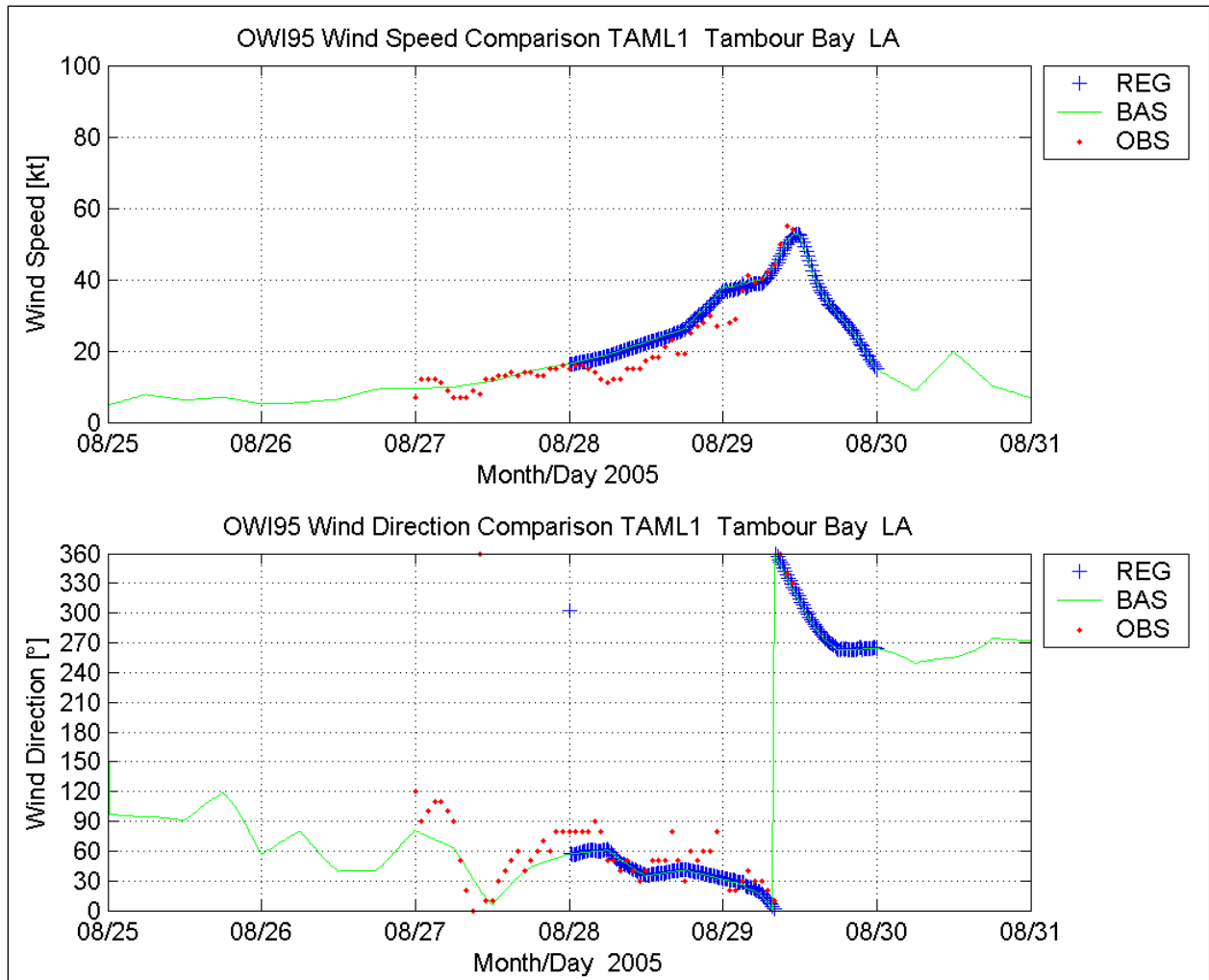


Figure 2-50. Comparison of wind speed (upper panel) and direction (bottom panel) at Tambour Bay, LA

# Appendix 3

## Offshore Waves

---

### Introduction

The methodologies for generation of basin- and regional-scale offshore wave fields resulting from Hurricane Katrina are presented. This appendix describes the model selection process, a summary of the modeling approach, input conditions, and the resulting wave computations. In this context, the basin-scale is defined as the Gulf of Mexico. The regional-scale encompasses the offshore domain of Louisiana, Mississippi, and Alabama. All results presented here utilize the final H\*Wind/IOKA wind product discussed in Appendix 2. At times references are made to the *95% winds*, or *OWI95*. Final winds and the *95-percent winds* are synonymous. The final winds and waves represent the best that could be produced in the time allocated for the project, realizing that they could be improved possibly with more time and effort.

The quality of the wave estimates is strongly dependent on the quality of the wind fields. Growth characteristics of the significant wave height (defined as the zero<sup>th</sup> moment of the energy density spectrum) are proportional to the wind speed squared. Hence, quality is primarily dictated by the accuracy of the forcing function, i.e., the wind. Secondary influences on accuracy are geographical effects (grid resolution) and resolution of the shoreline and offshore islands. Accurate water depth information is important, because many wave parameters are related to water depth through the linear dispersion relation ( $\omega^2 = g\kappa \tanh(\kappa h)$  where  $\omega$  is the radial frequency,  $\kappa$  is the wave number,  $g$  the gravitational acceleration and  $h$  the water depth). Theoretical scaling of the wavenumber spectrum is  $\kappa^{-5/2}$ , hence any substantial inaccuracy in the water depth will have an impact on the wave results. More importantly, close to the coast water depth becomes very important in the spectral collapse due to depth-limited wave breaking.

### Wave Model Selection

Selection of an appropriate wave modeling technology is critical to provide quality estimates. The spatial and temporal scales associated with tropical systems are very short compared to synoptic-scale events (e.g., Northeasters along the Atlantic coast). The physical processes inherent to these tropical systems, extremely high wind speeds and rapid turning winds, coupled with active wind-sea and swell interactions, must be accurately modeled. Ultimately the selection is based on historical performance in the estimation of hurricane-generated waves.



There are many wave models that can satisfy these requirements, whether they are second-generation or more recently developed third-generation models. For example, the Wave Information Study ([http://frf.usace.army.mil/cgi-bin/wis/atl/atl\\_main.html](http://frf.usace.army.mil/cgi-bin/wis/atl/atl_main.html)) has used a second-generation wave model WISWAVE (Hubertz 1992) for the generation of a long-term wave climate along the U.S. coastlines. As an outcrop of the Sea Wave Modeling Project (SWAMP Group 1985) third-generation wave models were developed. The main difference in this class of models compared to their predecessors is no a priori assumption governing the wave spectrum and inclusion of discrete source terms posed with the same number of degrees of freedom found in the resulting directional wave spectrum. Models of this class include WAM (Komen et al. 1994), WAVEWATCH III (Tolman 1997, 1999), and most recently SWAN (Ris 1997, Holthuijsen et al. 1993).

For the most part, WAM, WAVEWATCH III and SWAN are very similar. There are slight variations in the numerical scheme used, specification of the source-sink terms that at times produce different results using the same input conditions. Over the past three years WAM has undergone major improvements, not only cosmetic (formulation in pure FORTRAN90 schema), but also revisions to source term specification, multi-grid nesting, ice coverage implementation and, more importantly, depth-limited breaking. These improvements and three years of critical evaluation for the 2003 through the 2005 hurricane seasons (Real-Time Forecasting System of Winds, Waves and Surge in Tropical Cyclones <http://www.hurricanewaves.org>), including a battery of historical tropical storm simulations, have contributed to the choice of WAM Cycle 4.5 (Gunther 2002) as the primary technology used in this project. It is not suggested that WAVEWATCH III, SWAN or WISWAVE would provide inferior results, but WAM has recently been through a rigorous testing cycle for hurricane situations. WAVEWATCH III was run and comparisons between WAM and WAVEWATCH III are provided.

These wave models solve the Action Balance Equation,

$$\frac{\partial N}{\partial t} + c_G \vec{\nabla} \frac{\partial N}{\partial x} = \omega^{-1} \cdot \sum_i S_i \quad (3-1)$$

where  $N$  is the action density defined by  $F(f, \theta, x_i, t)/\omega$ , where  $F$  is the energy density spectrum defined in frequency ( $f$ ) direction ( $\theta$ ) over space ( $x_i$ ) and time ( $t$ ),  $c_G$  is the group speed dependent on the water depth and frequency  $f$ , and the radial frequency  $\omega$  is equal to  $2\pi f$ .  $S_i$  represents the source-sink terms:

$$\sum_i S_i = S_{in} + S_{nl} + S_{ds} + S_{w-b} + S_{bk} \quad (3-2)$$

where  $S_{in}$  is the atmospheric input,  $S_{nl}$  is the nonlinear wave-wave interactions,  $S_{ds}$  is the high-frequency breaking (white-capping),  $S_{w-b}$  is wave bottom effects (bottom friction), and  $S_{bk}$  is depth-limited wave breaking. The model solves for the spatial and temporal variation of action in frequency and direction over a fixed grid defined in  $x_i$  (generally a fixed longitude-latitude geospatial grid).

Computationally, Equation 3-1 is solved in two steps. The advection term (second term in Equation 3-1) is solved first accounting for the propagation of wave energy. Each packet of energy in frequency and direction is moved based on the group speed of that particular frequency band and water depth. This assumes linear theory and superposition of wave packets. In a fixed longitude- latitude grid system curvature effects are resolved where the energy is propagated in a spherical coordinate system (or along great circle paths). As the water depth decreases, the full dispersion relationship is applied. Wave shoaling and refraction effect the propagation of the energy packets.

After each propagation step the time rate change of the action density is solved including the source term integration. The wind field is read, and the atmospheric input source ( $S_{in}$ ) is applied. The nonlinear wave-wave interaction source term is the mechanism that self-stabilizes the spectral energy, transferring portions of the energy to the forward face and high-frequency tail. Dissipation ( $S_{ds}$ ) removes portions of energy that become too energetic for the given frequency band. For application in arbitrary depths, energy is removed via the wave-bottom sink ( $S_{w-b}$ ) and ultimately, in very shallow water, the spectrum loses its energy through breaking ( $S_{bk}$ ). A more complete theoretical derivation and formulation of the source terms can be found in Komen et al. (1994).

## Wave Model Input Requirements

To perform any wave model simulation, input data are required. These input data consist of a water depth field; wind input fields (over space and time) and general numerical information defining the time steps, output files to be generated, grid nesting and options defining the simulation.

As previously mentioned, accurate water depth information is needed to specify certain model parameters (those based on linear dispersion), and definition of the shoreline and offshore islands are important; both influence the computed wave fields. Recently NOAA's National Geophysical Data Center (known as GEODAS, <http://www.ngdc.noaa.gov/mgg/coastal/>) have assembled gridded topography-bathymetry by merging many different digital data bases together at a 3-arc sec resolution and the bathymetric elevations are resolved to 0.328 ft (0.1 m). These digital databases are a compilation of many individual sets of soundings and span tens of years, or more. Changes in the offshore bathymetry that have taken place may not be reflected in these data sets; however changes should only influence at most the littoral zone (out to roughly depths of 15 to 20 ft). For the basin and regional wave modeling applications, these deficiencies should not significantly influence the final results. All water depths are referenced to Mean Sea Level.

Setting the land/sea boundary is accomplished by using the NOAA National Geophysical Data Center's Global Self-consistent, Hierarchical, High-resolution Shoreline Database (GSHHS, Wessel and Smith 1996 or <http://www.ngdc.noaa.gov/mgg/shorelines/gshhs.html>). Combining both the land/sea boundary, depicting the shoreline location, and the water depth grids necessitated a certain amount of hand editing. Also some of the islands not contained in the digital water depth database were set based on the GSHHS data set, on a manual basis.

Two wave-modeling domains were generated, one for the basin-scale (Gulf of Mexico) and a more refined domain for the regional-scale modeling effort. The final water depth grids for each domain are displayed in Figure 3-1 and 3-2. Both target domains are fixed in geographical space identical to the wind fields domains described in Appendix 2. For convenience, the color contours are limited to 500 ft to focus on the shallow shelf region.

In general, there is a substantial shelf area west of Florida and along northern Texas and western Louisiana coasts. This gentle slope also exists along the Mississippi-Alabama gulf coast. Offshore of the southeastern portion of Louisiana (at the entrance of the Mississippi River) there is a strong water depth gradient (Figure 3-2) that has a significant impact on the wave results. It is an area of focusing of the wave energy (associated with the process of refraction).

Considerable editing of the original 30-sec (Figure 3-3) digital bathymetry in the vicinity of Chandeleur and Breton Sounds was required. Note the color contouring in Figures 3-1 and 3-2 differs, amplifying bathymetric changes in this area. The unusual straight-line features, located at 30-deg N latitude and 89-deg W longitude, were suspected to be errors in the database as shown in Figure 3-3. It was believed west and north of the discontinuities, data were accurate. A smoothing algorithm was used from north to south and east to west, correcting this problem. The final regional-scale grid is displayed in Figure 3-2.

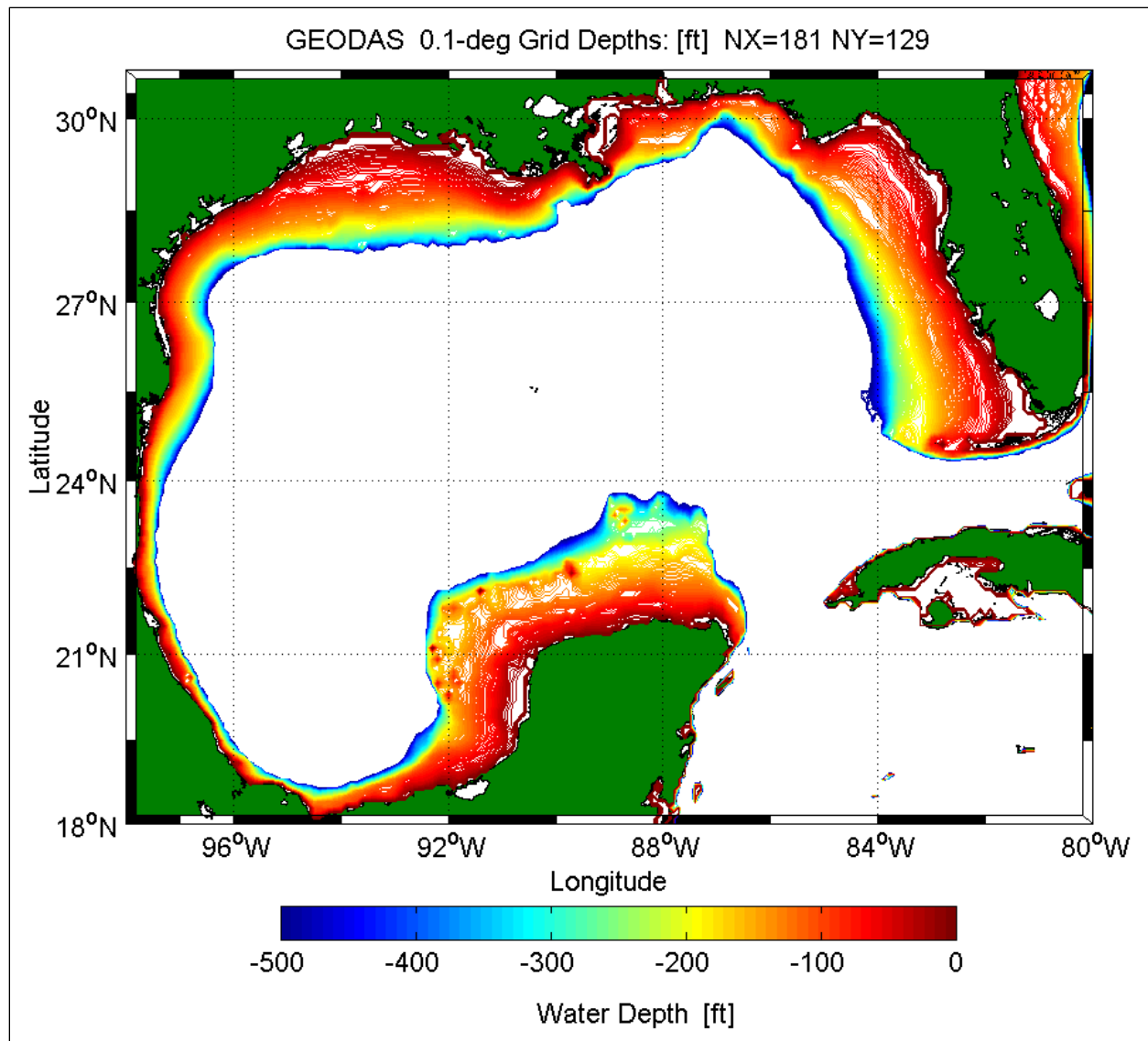


Figure 3-1. Color contour of the basin-scale wave model domain



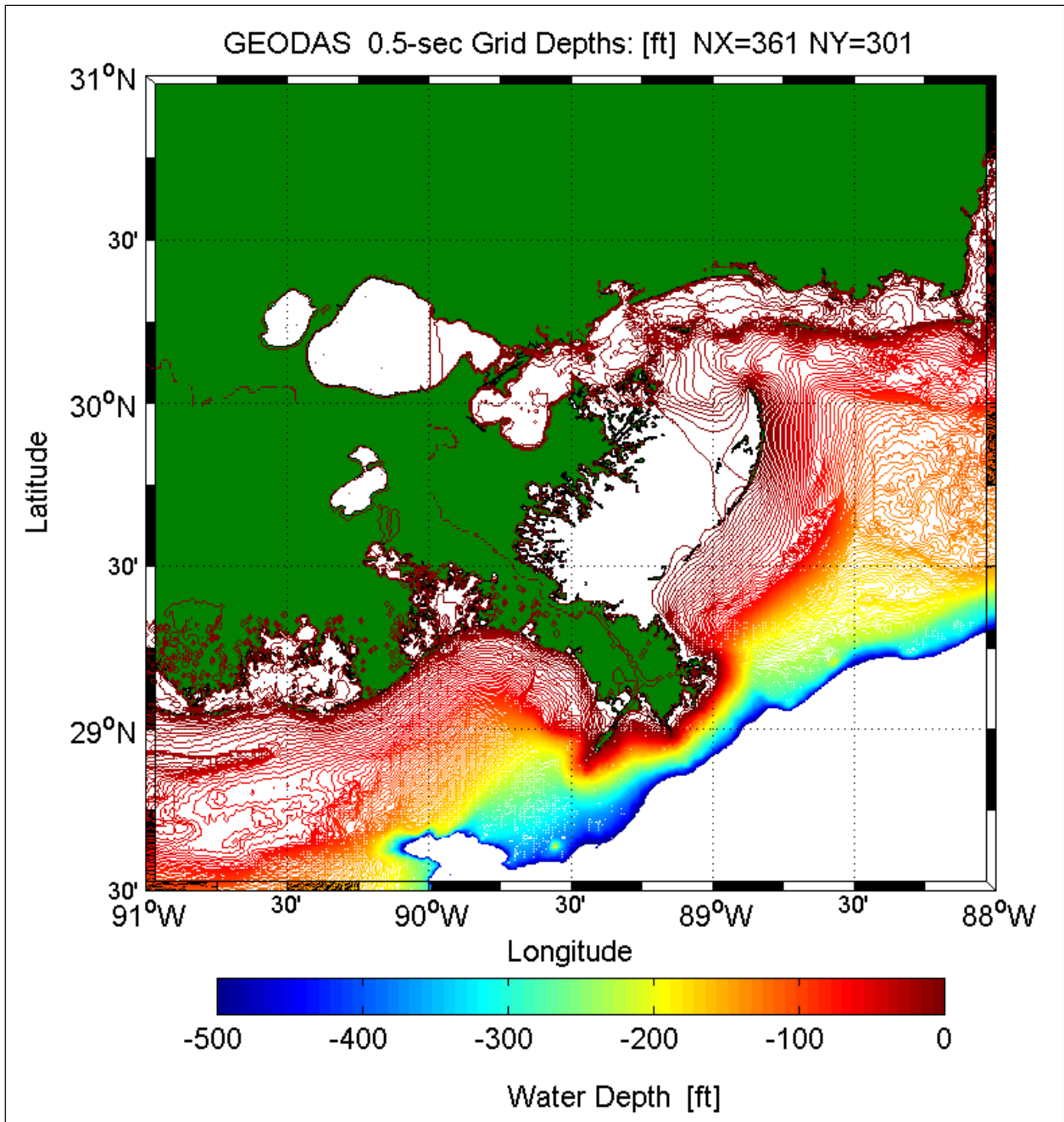


Figure 3-2. Color contour of regional-scale wave modeling domain

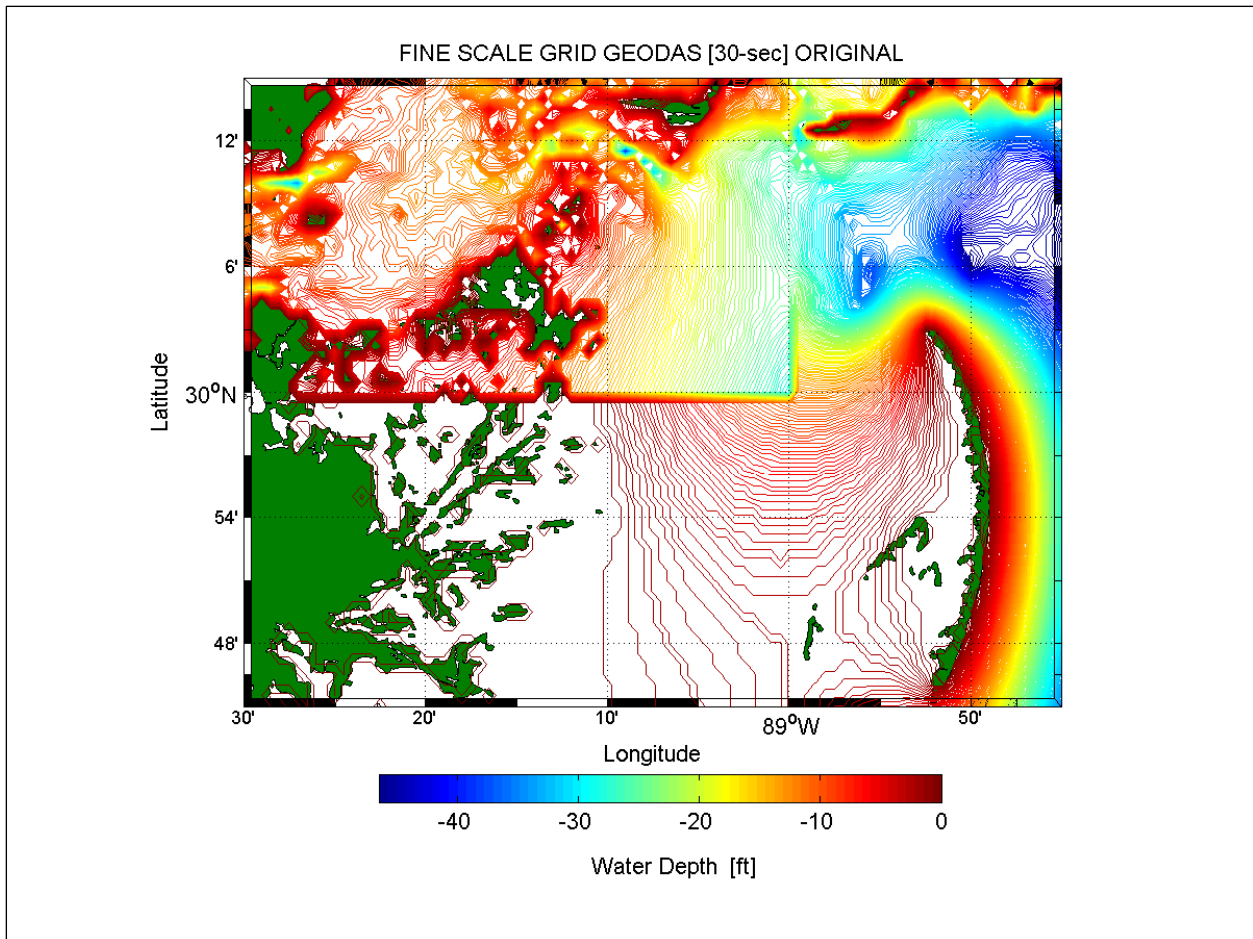


Figure 3-3. Color contour of suspect GEODAS 30-sec digital bathymetry

The wind fields used for the basin and regional wave model simulations are documented in Appendix 2. These files were then re-formatted to satisfy WAM input standards.

A summary table defining the domains, simulation period, time steps, and options used in the two WAM simulations are provided in Table 3-1. Specific time step and auxiliary options are contained in Table 3-2. The selection of a 0.5-min (or 0.08333-deg) regional wave model grid that is three times finer than the input wind fields (provided at 0.025-deg) was made to resolve the Chandeleur Island chain and Cat, Ship, Horn and Dauphin Islands offshore of the Mississippi/Alabama gulf coast. Quantification of the large depth gradient offshore of the Mississippi River entrance is critical to the Katrina wave simulation. All of the original wind field information is retained in the finer scale regional wave model domain because the resolutions are integer multiples. Within WAM, wind fields are spatially interpolated in terms of  $U$  (the longitude component),  $V$  (the latitude component) and  $W$  (the magnitude), thus removing any convergence or divergence artifacts that are generally an outcome of standard interpolation routines.

**Table 3-1  
Wave Model Input and Simulation Values**

Domain	Simulation Period	Forcing	Domain		Resolution
			Long	Lat	
Basin	2005082500 2005083100	WINDS ONLY	98 – 80 W	18 - 30.8 N	0.1 deg
Region	2005082800 2005083000	WINDS PLUS BC from Basin	91 – 88 W	28.5 - 30.5N	0.00833 deg

**Table 3-2  
Wave Model Specific Input Conditions**

Domain	Wind Input Time Step	Time Steps		Options
		Prop	Source	
Basin	900 sec	150 sec	600 sec	BC Out Shoal, Dep-Break
Region	900 sec	10 sec	600 sec	BC In Shoal, Ref, Dep-Break

## WAM Simulations Description

WAM Cycle 4.5 is posed in the CGS (centimeter, gram, second) system. All input and output are generated in this system; however, the information provided here is converted to the FPS (foot, pound, second) system.

The WAM Cycle 4.5 simulations were performed on the specified grids defined in Tables 3-1 and 3-2 with the two-dimensional wave spectrum defined by 28 frequencies, and 24 direction bins. The directions are at a 15-deg resolution starting at 7.5-deg while the frequency bands are defined as:

$$f_{n+1} = 1.1 * f_n \quad \text{where } f_1 = 0.03138. \quad (3-3)$$

This assures finite frequency bands accepting energy at very low frequency values, and falls within the domain specified in Komen et al. (1994) to retain the accuracy in the nonlinear wave-wave interaction source function approximation.

The initiation of the wave model simulation for both grids assumes local wind wave growth specified by the first wind field. This at times elevates the wave heights in the domain proper; however, this is generally damped quickly (about four time steps). The time step for propagation is dictated by numerical stability that is dependent on the group speed of the lowest frequency, water depth, location (latitudinal variation in the physical distance of a grid), and when applicable, the water depth gradient influencing the refraction of the wave energy. The source term time step is dependent on the physical processes modeled. This is loosely coupled to relaxation times of the source term specifications. This is the time at which the winds can affect the wave system and the nonlinear wave-wave interactions move the energy about the wave spectrum. For deepwater applications relaxation times are on the order of 3600 sec. In shallow

water, the relaxation times reduce to about 900 sec. Hurricane Katrina spans both deep and arbitrary depths, so the source term time step was conservatively set to 600 sec. The water depth for the basin and regional wave model simulations were held constant. Depths were not modified to reflect changes in depth due to storm surge. This was handled in the nearshore wave transformation modeling.

The basin-scale WAM Cycle 4.5 simulation was performed for the duration of Katrina noted in Table 3-1. Boundary condition directional wave spectra were saved along the four sides defined by the regional domain, at a time step of 150 sec (defined by the basin propagation time step). Output, which consist of two-dimensional wave spectra, were saved at 900-sec intervals for verification purposes at locations corresponding to all available NOAA National Data Buoy Center (NDBC) wave buoys. Integral wave parameter estimates, significant wave height, peak and mean spectral wave period, and vector mean wave direction were generated for the entire domain at 1800-sec intervals. These parameters are defined as:

Significant Wave Height:

$$H_{mo} = 4 * \sqrt{\iint E(f, \theta) df d\theta} \quad (3-4)$$

Mean Wave Period:

$$T_{mean} = \left[ \frac{\int f E(f) df}{\int E(f) df} \right]^{-1} \quad (3-5)$$

where:  $E(f) = \int E(f, \theta) d\theta$

Peak Spectral Wave Period:

$$T_p = [\max[E(f_i)]]^{-1}, \text{ for } i=1, \text{ no. frequencies} \quad (3-6)$$

Vector Mean Wave Direction:

$$\theta_{mean} = \tan^{-1} \left[ \frac{\iint \sin\theta E(f, \theta) d\theta df / \iint E(f, \theta) d\theta df}{\iint \cos\theta E(f, \theta) d\theta df / \iint E(f, \theta) d\theta df} \right] \quad (3-7)$$



The maximum significant wave heights for the entire hurricane Katrina simulation are shown in Figure 3-4. This graphic is based on the maximum height occurring at each individual point in the basin-scale WAM grid for the entire simulation period. As Katrina moved off the western Florida coastline and rapidly intensified, so too did the wave heights. There is a clearly defined hook at 86W, 24.5N where the net effect of increasing wind speeds dramatically increases the wave energy. Figure 3-4 also shows the path of Katrina and the absolute maximum  $H_{mo}$  of nearly 54.6 ft occurring at 88.8W, 26.9N. Two offshore oil platforms equipped with wave measurement sensors recorded peak significant wave heights of 38.6 ft and 38.7 ft with  $T_p$  values of 10.5 sec and 12.6 sec, respectively. These values are similar to coincident WAM estimates corresponding to the platform measurements of 33.3 ft and 38.6 ft with peak period estimates of 14.9 sec and 13.5 sec, respectively. These data are proprietary, so additional documentation is not provided here.

By comparison, Hurricane Camille wave model simulations reached approximately 47.2 ft as an absolute maximum (Jensen and Cardone 2005). This is not to suggest Katrina was more powerful than Camille. Although the results contained in Figure 3-4 are derived purely from a numerical wave model, when Katrina reached Category-5 strength (Knabb 2005) it produced wave heights commensurate with that strength.

The swath of heights exceeding 45 ft (the red contours) widened as Katrina moved in a more northerly direction. The lateral expanse of this swath is roughly 2 deg in width, or 150 miles. The 20-ft contour (aqua contours) covers the areas of Louisiana, Mississippi, and Alabama, to the Florida Panhandle. As Katrina decreased in intensity as it approached the coastline, the  $H_{mo}$  values remained relatively constant until they reached decreasing water depths. This occurred abruptly at the Mississippi River entrance to the Gulf of Mexico, and more gradually along the Mississippi/Alabama coast. In either case the relative amount of wave energy remains in the system until depth-limited wave breaking limits the height.

The mean wave period ( $T_{mean}$ ) maximum graphic is shown in Figure 3-5. The mean wave period is selected for presentation over the standard peak spectral wave period (defined in Equation 3-6) because it is a more stable wave parameter, especially in a mixed wind-sea/swell energy environment typical of tropical systems, and it is an integral wave property (Equation 3-5) comparable to the  $H_{mo}$

WAM OWI95 SHBR-CAP Basin (Res 0.1°): MAXIMUM

Total Wave Height  $H_{mo}$  [ft] RESULTS: Katrina

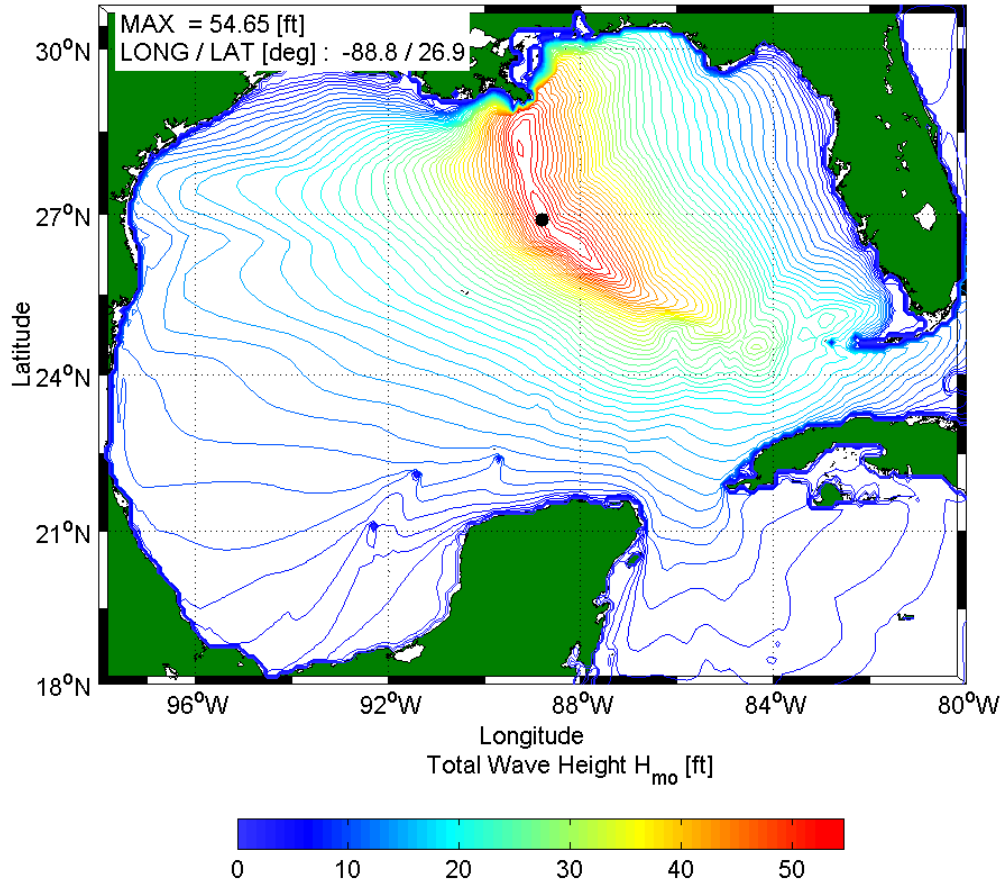


Figure 3-4. Color contour of the maximum wave height conditions in the Basin domain for the simulation period 2005082500 through 2005083100

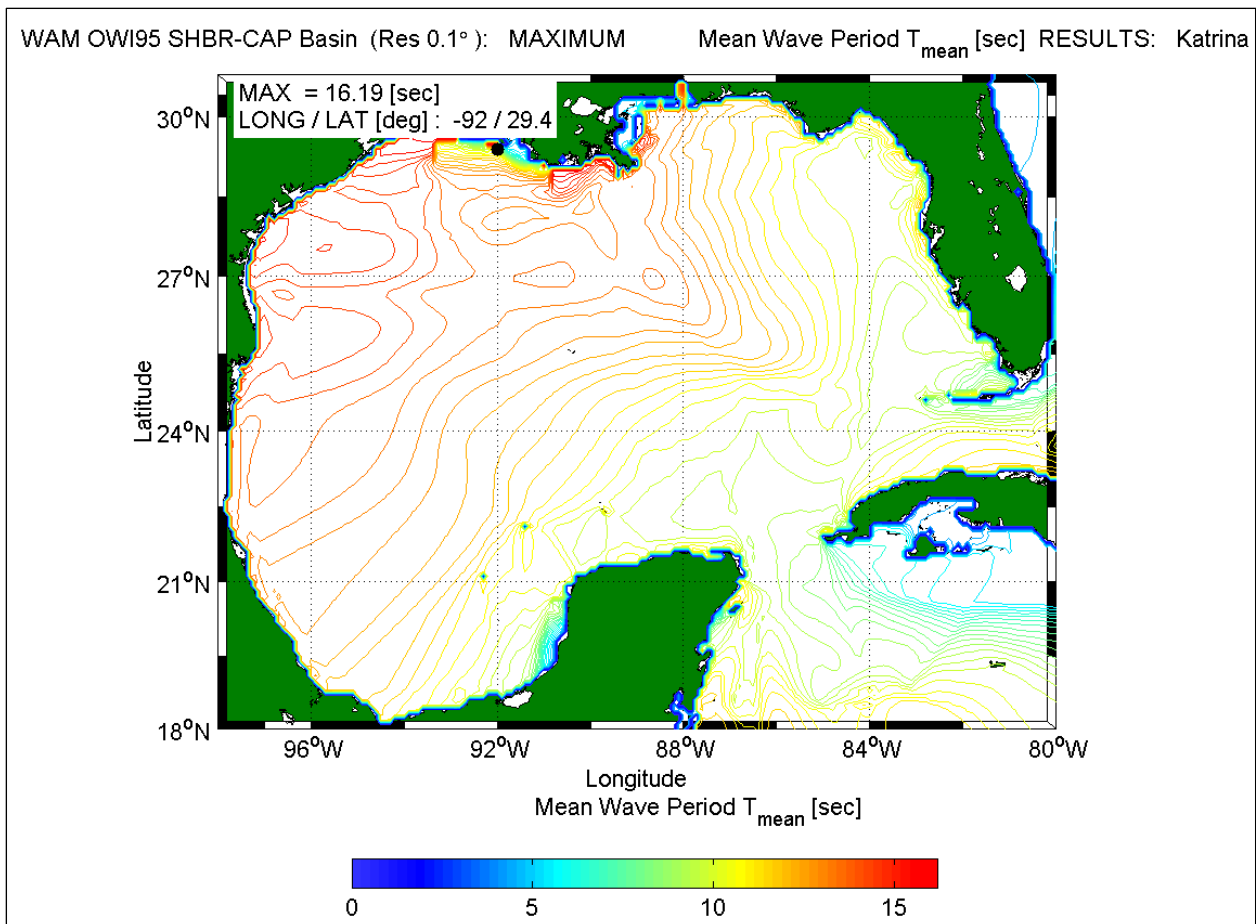


Figure 3-5. Color contour of the maximum mean wave period conditions in the Basin domain for the simulation period 2005082500 through 2005083100.

There is only a slight indication of Katrina's path in the maximum  $T_{mean}$  results because this wave parameter is not as sensitive to the wind speeds (linearly related to them) whereas the significant wave height is related to wind speed squared. However the graphic does show the net impact of the long-period swells impinging on the Louisiana coastline where 15-sec (red colors) wave periods were computed. Most noticeable are lobes of swells to the east of the Chandeleur Island chain, inside the Mississippi Sound, in Mobile Bay, and to the west of the Mississippi Delta just offshore of Atchafalaya Bay where the absolute maximum  $T_{mean}$  value occurs. The local maxima result from a combination of sheltering by the Mississippi Delta, and depth-induced wave refraction and shoaling. These anomalies are also amplified by the contouring routines used in the analysis. The long-period results in Mobile Bay are a model artifact that most likely is due to the coarseness in the grid resolution and should be taken as approximate. To the right of the path of Katrina there is preponderance of 10- to 12-sec wave periods, indicative of strong wind-sea conditions.

Similar graphics are generated for the region-scale WAM Cycle 4.5 simulations. To reiterate, the region-scale simulations were forced by basin-scale directional wave spectra (at 150-sec intervals) along the lateral extent of the regional domain. In addition, the winds generated by OWI (based on  $H^*Wind$  specifying the core of the hurricane, and blended with NRA background

winds) were also used for this simulation. Increasing the wave model's grid resolution by a factor of 12 (0.1-deg defined for the basin and 0.00833-deg for the region) provided a better representation of the offshore island chains, quantified the dramatic depth gradient of the Mississippi River delta, and provided an enhanced depiction of the shoreline configuration.

Figure 3-6 illustrates the complexities of the wave field generated by hurricane Katrina within the regional domain. The entire simulation period is 48 hrs, starting on 28 August 0000 UTC and completing at 30 August 0000 UTC. The overall maximum significant wave height occurs at 89.1417W 28.975N with a value of 53.6 ft. Shallow-water effects of shoaling and more importantly refraction focus the offshore energy toward very distinct capes. The entire tip of southeastern Louisiana is in the high-energy environment. There is another convergence zone at Southwest Pass (Burrwood, LA). The wave height maxima follow the bathymetry (Figure 3-2) remarkably well, an indication of depth-limited breaking effects. To the west of Southwest Pass the  $H_{mo}$  values tend to decay rapidly with distance away from the storm center compared to those in the front right quadrant of Katrina. The northern motion of Katrina also forces waves through the gap between the Chandeleur, Cat, Ship and Horn Islands. The WAM simulation assumes stationary water depths (neglecting surge) and the results will be lower compared to expected results in the areas landward of these offshore islands where surge levels increase the potential for larger wave heights (through increases in water depth).

The maximum mean wave period results for the regional WAM Cycle 4.5 simulation are provided in Figure 3-7. This again illustrates the diverging wave field east and west of hurricane Katrina's path. To the west, the mean wave period is dominated by swells, as evidenced by higher period values (ranging from 12 to more than 20 sec); whereas in the front right hand quadrant of Katrina, there local wind seas abound with limited, yet distinct long-period swell lobes. Shadow zones appear (larger  $T_{mean}$  values) in the lee of geographical capes or offshore islands. Also evident are zones of large mean period values that are landward of island gaps (around Horn and Dauphin Islands) in the eastern portion of Mississippi Sound. The highest  $T_{mean}$  conditions reside in the West Bay region (west of the lower Mississippi River). This area is geographically sheltered from Katrina's offshore energy. This region is influenced by very low wave energy and a limited number of grid points.

These graphics provide an overview of the maximum energy level contained in the wave field resulting from Katrina. To assess model accuracy, comparisons between model results and measurements were made and they are presented in the next section.



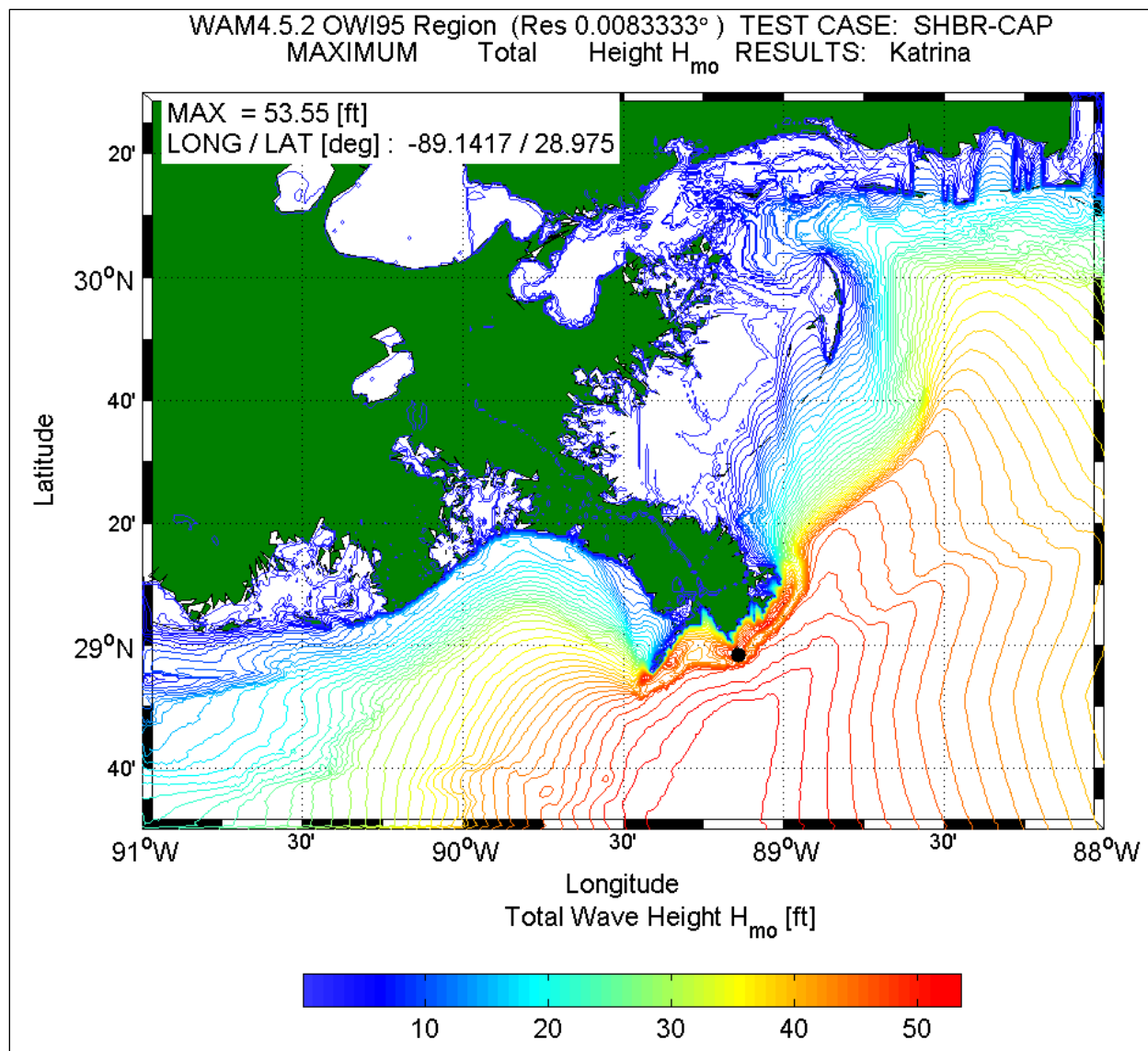


Figure 3-6. Color contour of the maximum wave height conditions in the Region domain for the simulation period 2005082800 through 2005083000

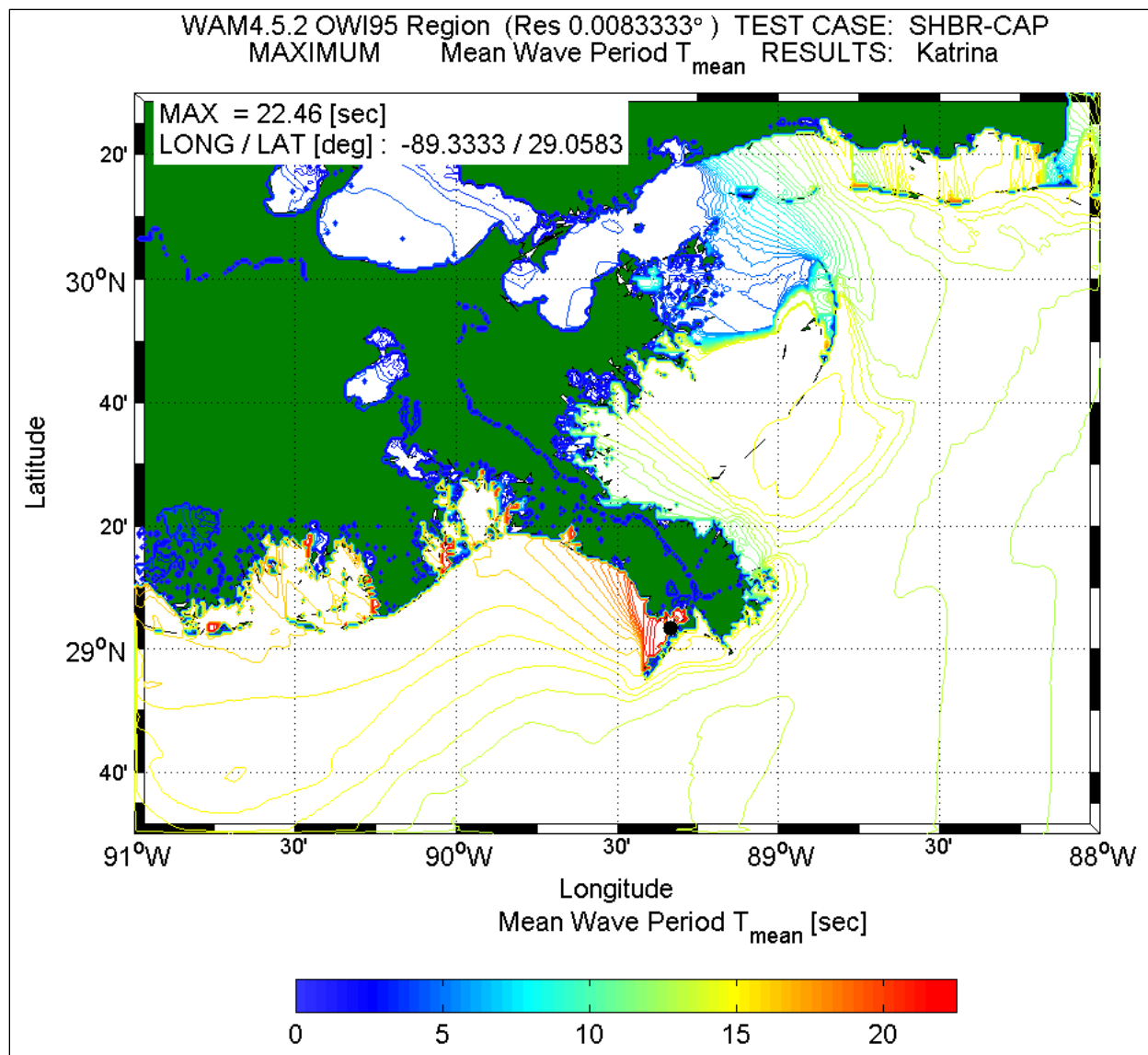


Figure 3-7. Color contour of the maximum mean wave period conditions in the Basin domain for the simulation period 2005082800 through 2005083000.

## Discussion

Any wave model simulation has a degree of error and uncertainty. Uncertainty pertaining to deficiencies in the input and methodology can be estimated by a careful comparison of the model results to measurements. For hurricane Katrina, there were numerous NOAA National Data Buoy Center (NDBC, <http://www.ndbc.noaa.gov/>) point measurements in the Gulf of Mexico. Of the 13 sites available (Figure 3-8), five were located in the right front quadrant of Katrina, while the remaining eight were positioned in the left front quadrant. Two NDBC buoys failed (42003 flipped over and the mooring of 42007 failed) before the peak of the wave conditions; one buoy (42040) provided erroneous directional wave information, however the other integral wave

parameters are considered to be accurate. Directional wave measurements at 42002 were discovered to be incorrect and removed from the NDBC archive.

The various hardware configurations comprising the NDBC buoy network complicated the evaluation process. The 10- and 12-m discus buoys (42001, 42002 and 42003), because of their size, cannot identify short period energy less than about 5 seconds. The HIPPI sensors have been proven measurement devices over the last two decades, while the Magnetometer Only (MO) and Angular Rate Sensor (ARS) systems are relatively new. This does not mean the MO and ARS systems are inferior devices compared to a HIPPI sensor. It only suggests the systems differ in their response and measurement of directional wave characteristics. Table 3-3 summarizes the various platform related information (also see Teng and Bouchard 2005).

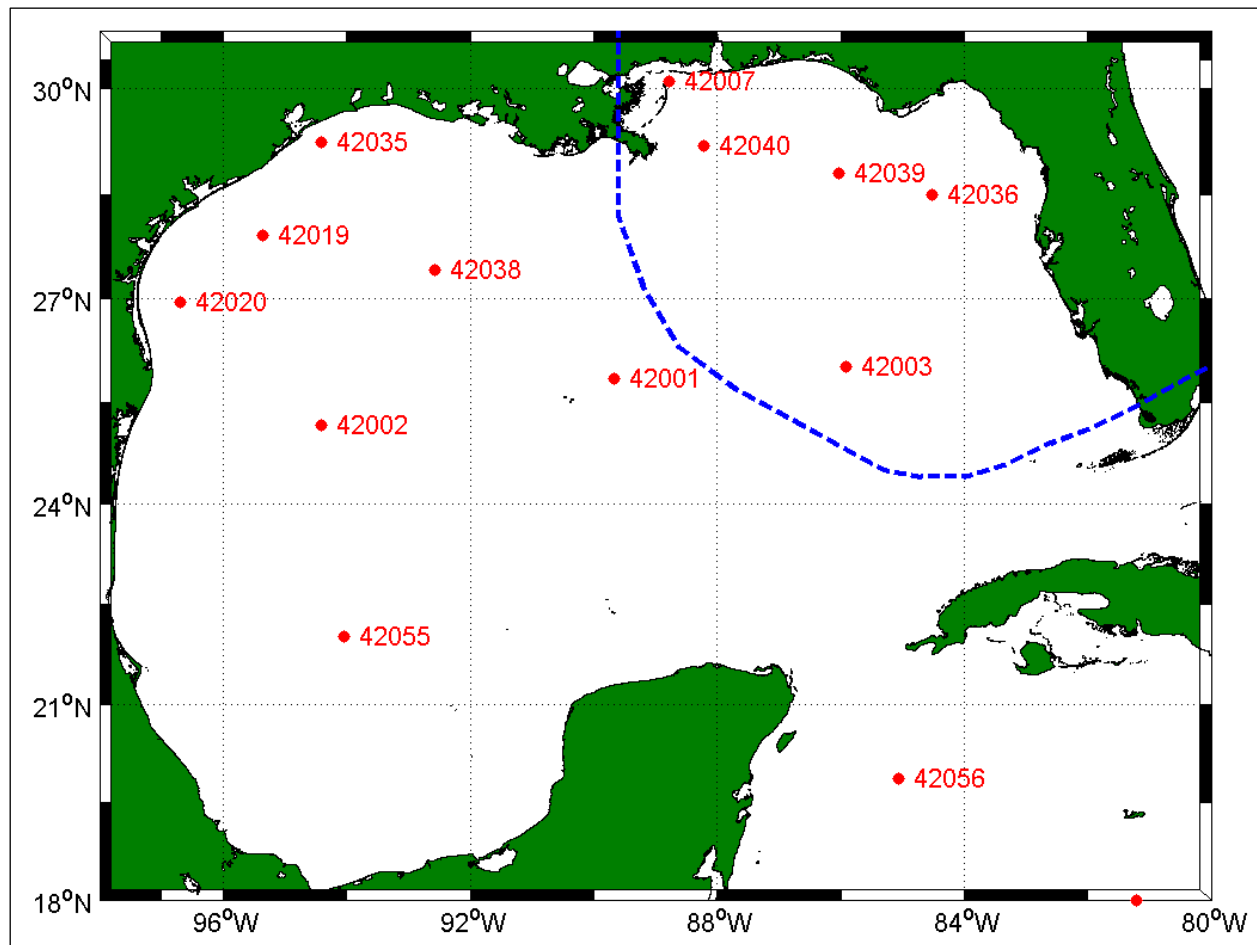


Figure 3-8. Location of NOAA's NDBC buoy network in the Gulf of Mexico. The blue dashed line is the NOAA NHC Official Track (Knabb et al. 2005).

**Table 3-3  
NOAA NDBC Buoy Summary**

Station Id	Location (Deg/Min/Sec)		Water Depth (ft)	Hull (m)	Sensor <sup>1</sup>
	Longitude (West)	Latitude (North)			
42001	89 / 39 / 30	25 / 50 / 30	10739	10	HIPPY
42002	94 / 25 / 00	25 / 20 / 00	10496	12	HIPPY
42003	85 / 54 / 50	26 / 00 / 32	10617	10	HIPPY
42007	88 / 46 / 10	30 / 05 / 25	44	3	MO
42036	84 / 31 / 00	28 / 30 / 00	179	3	MO
42038	92 / 34 / 01	27 / 25 / 12	3778	3	ARS
42039	86 / 01 / 17	28 / 47 / 38	956	3	ARS
42040	88 / 12 / 49	29 / 11 / 05	900	3	MO
42055	94 / 02 / 45	22 / 01 / 02	11088	12	ARS
42019	95 / 21 / 36	27 / 54 / 47	275	3	MO
42020	96 / 41 / 47	26 / 56 / 39	289	3	MO
42035	94 / 24 / 30	29 / 14 / 47	45	3	MO
42056	85 / 03 / 32	19 / 52 / 27	14583	12	ARS

<sup>1</sup> HIPPY Accelerometer; MO: Magnetometer Only; ARS: Angular Rate Sensor.

Verification of the WAM Cycle 4.5 wave estimates was examined using time plots, scatter plots, quartile-quartile plots, and statistical tests. Because of limited population size, the results derived from the statistical tests may be weighted disproportionately high. A concerted effort in the evaluation process focused on the locations near Katrina’s storm track. For brevity only five locations (42001, 42003, 42040, 42039, and 42007) are presented in the context of this section while the remaining information is provided in the figures at the end of this chapter (Figures 3-37 through 3-40). All wind and wave directional information are plotted in a meteorological coordinate system where 0 deg represents a wind or wave coming from the north; 90 deg represents a wind or wave coming from the east.

Beginning offshore and progressing along Katrina’s path, Figures 3-9 to 3-13 display comparisons of integral wave properties:  $H_{mo}$ ,  $T_p$ ,  $T_{mean}$ , and  $\theta_{mean}$  (defined in Equations 3-4 to 3-7) as well as the wind speed and direction. Note for the wind speed comparisons, the measurements were adjusted to a 10-m equivalent neutral stable wind speed to be consistent with the modeled winds. Comparing 42003 and 42001, it is interesting to note the differences between the wave results on the more active right quadrant (42003) versus the less-active left quadrant (42001). Wave heights are about 10-ft higher at 42003; however both buoys show similar growth characteristics toward their respective peak values. The wind and wave directions vary considerably between the two measurement sites. In the active right front quadrant, the winds rotate clockwise at 42003, while at 42001 the rotation is counter-clockwise. The mean and peak wave periods are indicative of the very rapid wave development in Katrina as it moved into the Gulf of Mexico. There is rapid change of the  $T_p$  values just after 27 August 0300 UTC or approximately 18 hrs after Katrina cleared the western Florida coastline. An oscillating pattern in the  $T_{mean}$  results, around 27 August 1800 UTC at 42003 and 28 August 0600 UTC at 42001 in which the wave periods decrease then rapidly increase toward the storm peak, is characteristic of eyewall replacement cycling or weakening/strengthening processes in Katrina.



WAM Cycle 4.5 results compare favorably to these offshore measurements. The general growth, establishment of the peak conditions (less than 2-ft difference at the maximum), and for 42001 the decay cycles, are all well replicated. There is a tendency for the WAM results to underestimate the  $H_{mo}$  and  $T_{mean}$  values associated with low wind speeds during the initial development of Katrina in the Gulf of Mexico. This could be due to the lack of resolution in the wave model grid, where the winds in the core of Katrina generated by H\*Wind are correct, but sub-sampling at 0.1 deg may omit the strength of the winds. The wind speed and direction comparisons for 42003 (Figure 3-9) and 42001 (Figure 3-10) clearly show the local modeled winds do not have appreciable errors. There appears to be a strong difference in the wind directions at 42003; however the differences are amplified by the circular nature in the parameter plotted. These differences are only a few degrees on either side of 0 deg. Comparing the modeled vector mean wave direction ( $\theta_{mean}$ ) results to the buoy measurements shows good agreement, with up to about 40-deg differences. Only during the latter stages of the decay cycle do the model results diverge significantly from the measurements. WAM results follow the wind direction whereas the buoy results show slower migration toward the winds. There is an indication of a very substantial difference in the wind and wave results at NDBC 42002 (Figure 3-38). The model results indicate the peak of the waves leads the measurements by over 18 hrs. These discrepancies were confirmed by other wave modeling efforts performed by the private sector. Questions regarding the validity in the measurements were discussed with staff from NDBC. The directional wave data were eliminated from the NDBC archive records. The other wave parameter data at 42002 passed the NDBC reliability tests and were deemed correct. To date, the reason for phase lag inconsistency between model and measurements remains unknown.

Moving toward the coastline, comparisons for NDBC buoys 42040, 42039 and 42036 (Figure 3-11, 3-12, and 3-40, respectively) are examined. Results show differing wave conditions. Close to Katrina's path at 42040 the  $H_{mo}$  and wind speed show a pronounced storm peak. The maximum height measured at 42040 is 55.4 ft, whereas east of the storm's center (42039) an isolated peak is replaced by nearly 24 hrs of sustained wave heights of 23 ft or more. This condition is also found at 42036 (Figure 3-40), however the magnitude of the plateau is in the range of 16 to 17 ft. The peak spectral wave periods for all three sites are consistent, displaying the early swell arrival around 27 August 1200 UTC, climbing to about 12 sec and then to upwards of 15 sec (the latter result found at 42040, closer to the hurricane path). The 55.4 ft measurement at Buoy 42040 was the largest significant wave height ever measured at an NDBC Buoy in the Gulf of Mexico.

The mean wave period variation shows the slight pulsation evident in the offshore buoy records, and generally levels off at 10 to 12 sec. These conditions suggest uni-modal spectra, downshifting to the leading swell energy through growth to the storm peak. The  $\theta_{mean}$  wave direction results are nearly invariant for these buoys. There are oscillations of the  $\theta_{mean}$  results at 42040 (Figure 3-11) around the storm peak. These particular records have been subsequently recalled by NDBC and are considered incorrect. The suspected cause of these inconsistencies was abundance of yaw (rotation about the center of the buoy) signal in a carrier frequency of the waves during this extremely high-energy condition. NDBC does not believe this problem contaminated any other wave related records.

The WAM results for the three inner buoys follow the measured trends in integral wave parameters. In general though, the model slightly underestimates the energy level in the early swells (low height and mean wave period). WAM underpredicted the peak wave conditions at all three buoys, with differences reaching nearly 14.4 ft. At 42040 the modeled versus measured wave height is 41.5 ft versus 55.4 ft; for 42039 21.3 ft versus 26.7 ft; and at buoy 42036 14.0 ft versus 18.0 ft. It is believed that local winds, despite some low values in the model results, could not explain these differences. The peak wave period model results are consistent with the measurements, and at times are slightly higher (at 42040 for example); suggesting either a far-field wind problem (magnitude and/or domain size of the storm's most intense winds) or that swell energy dissipation is too strong in the wave model. The mean model wave direction results are well replicated, with exception of the erroneous NDBC buoy results at 42040. There does seem to be a bias in the model results at 42036 (Figure 3-40), again with computed directions aligning to the wind direction rather than remaining with the swells as is seen in the measurements.

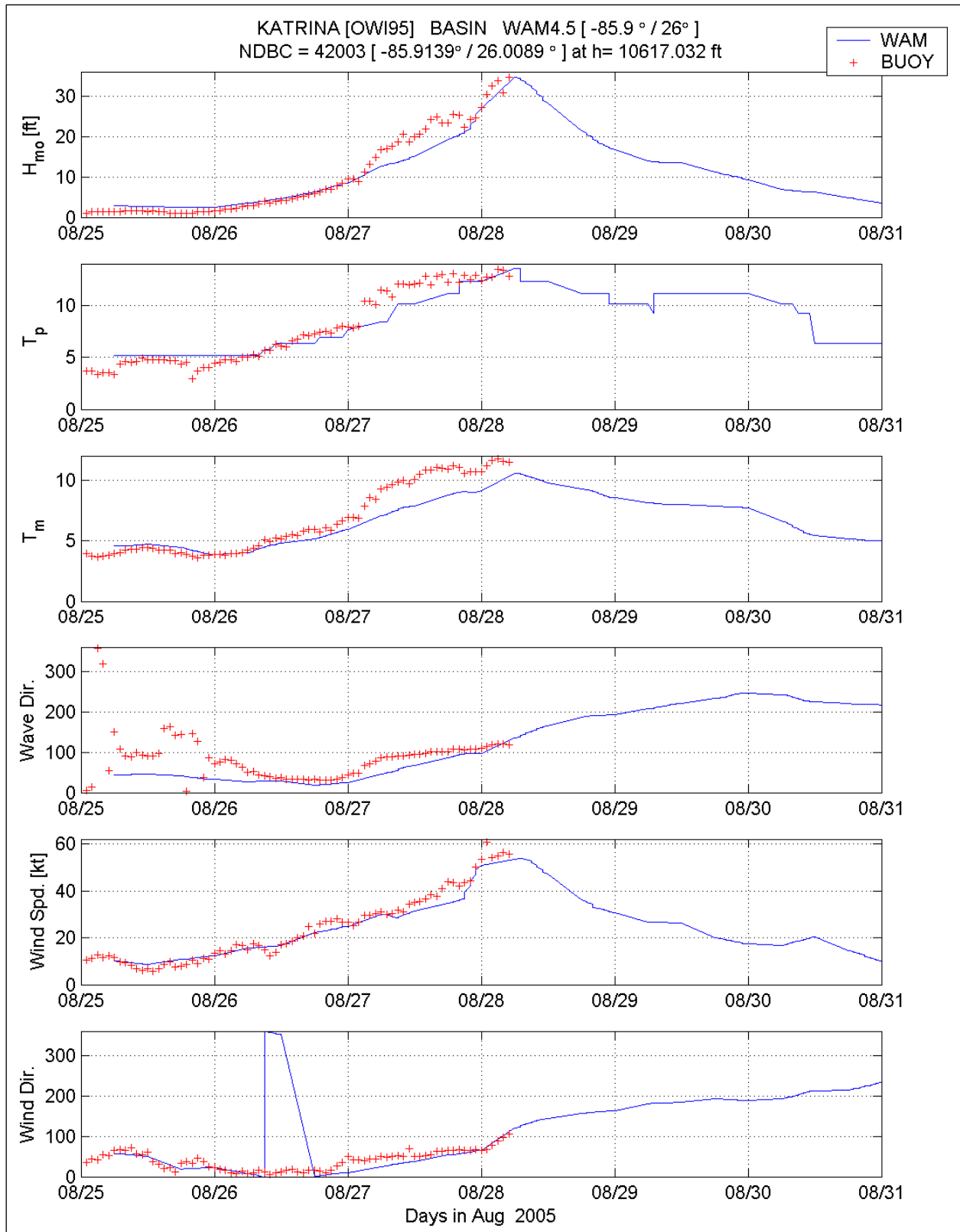


Figure 3-9. Comparison of WAM Cycle 4.5 basin-scale (blue line) to the measurements at NDBC 42003

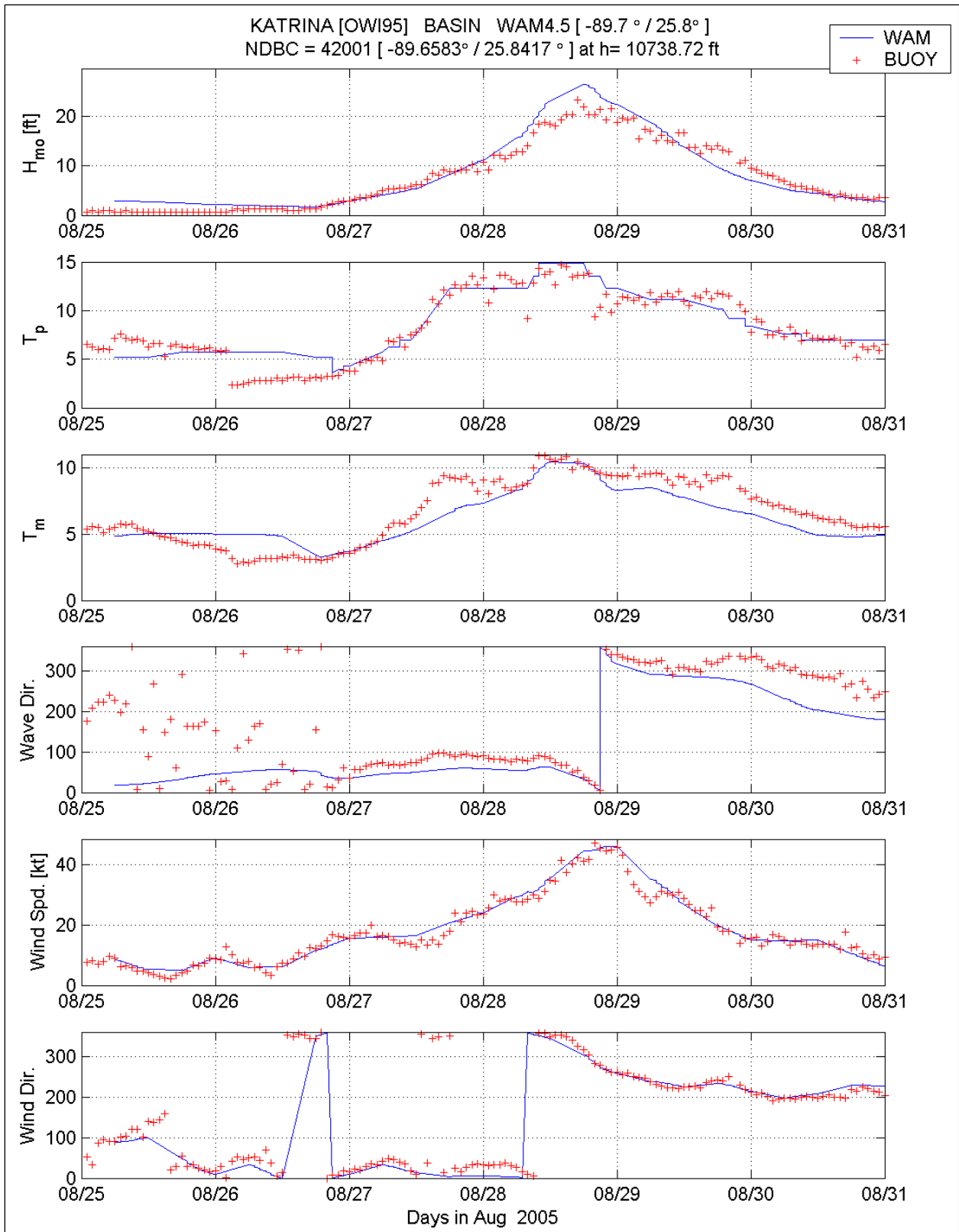


Figure 3-10. Comparison of WAM Cycle 4.5 basin-scale (blue line) to the measurements at NDBC 42001



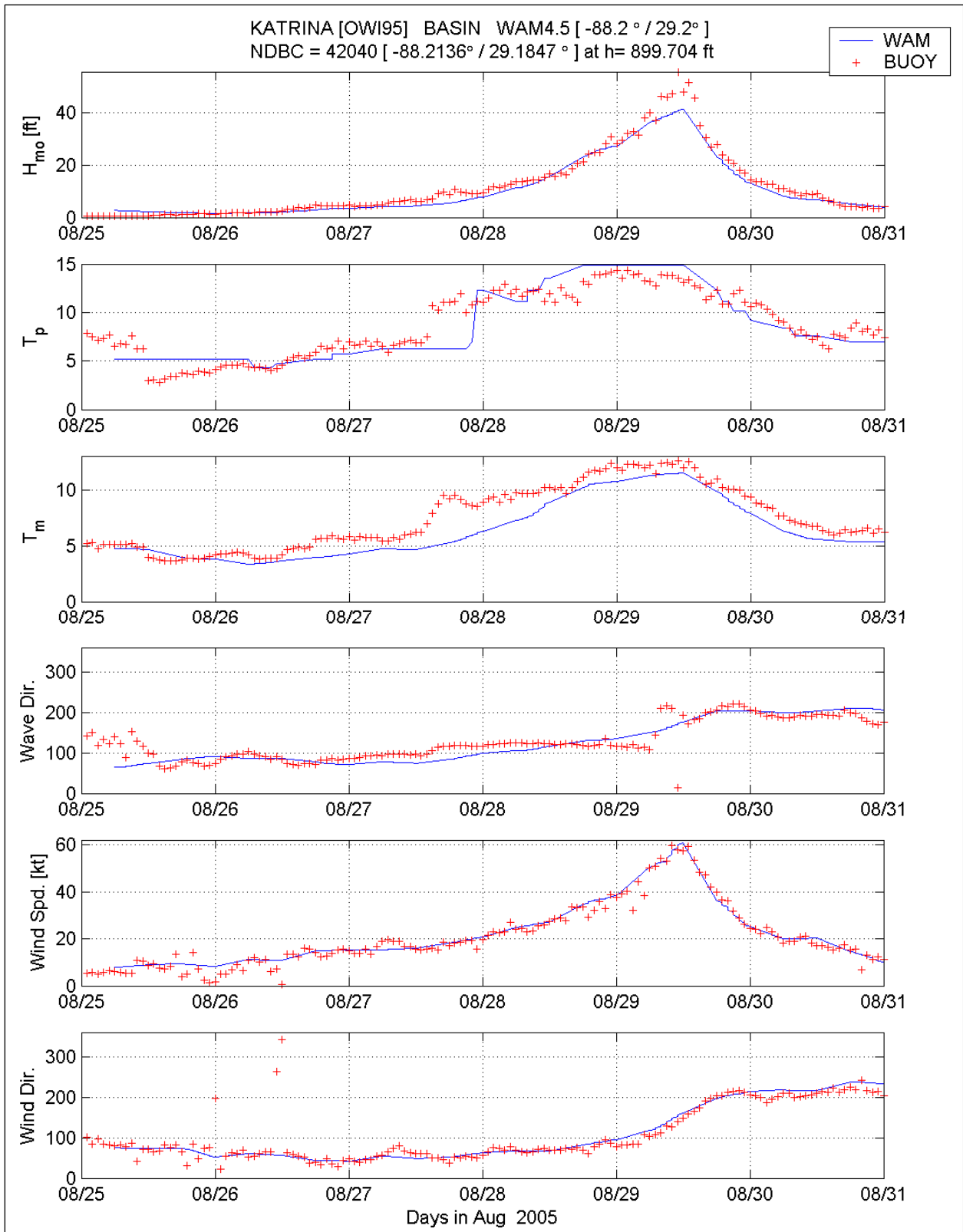


Figure 3-11. Comparison of WAM Cycle 4.5 basin-scale (blue line) to the measurements at NDBC 42040

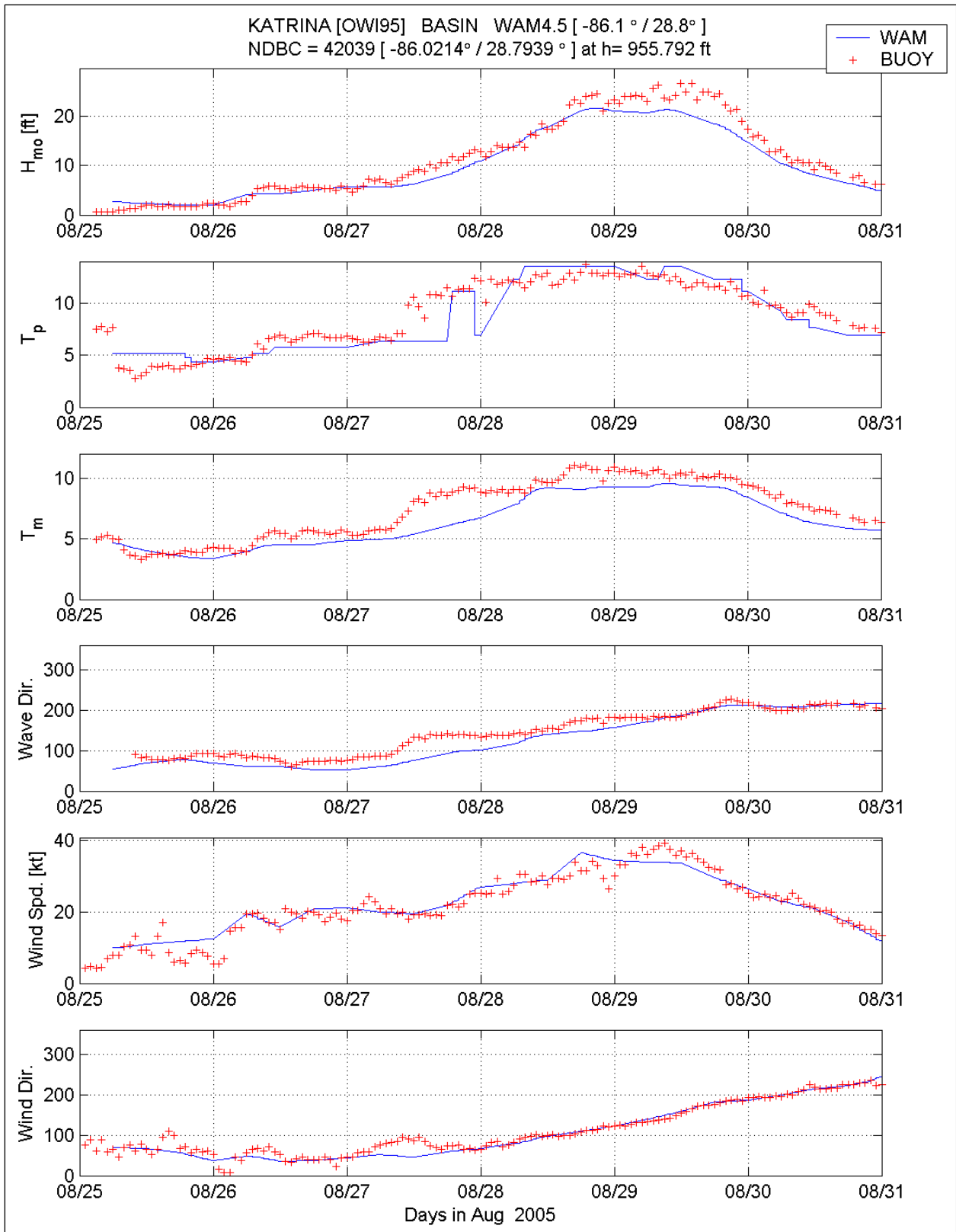


Figure 3-12. Comparison of WAM Cycle 4.5 basin-scale (blue line) to the measurements at NDBC 42039

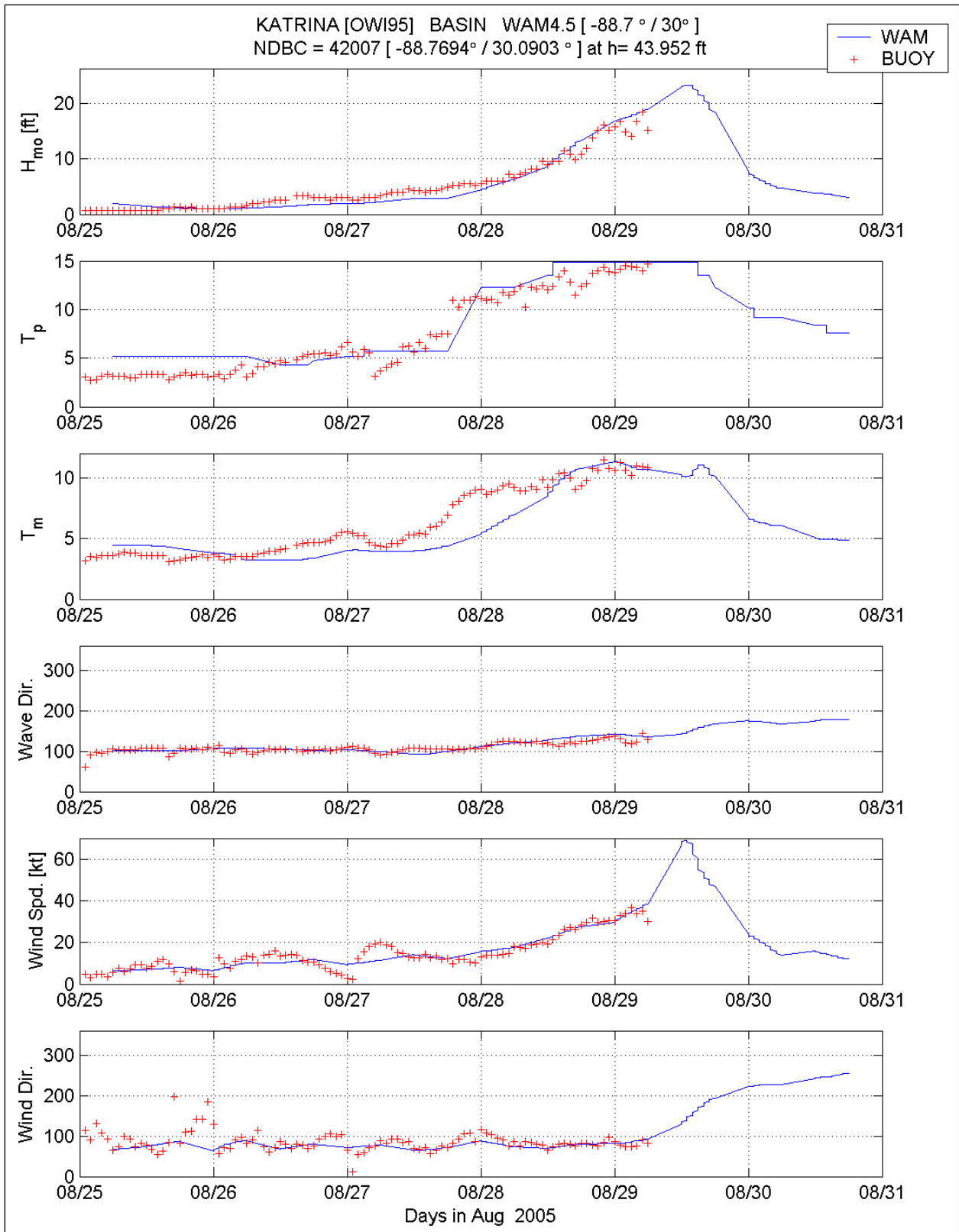


Figure 3-13. Comparison of WAM Cycle 4.5 basin-scale (blue line) to the measurements at NDBC 42007.

The final comparison is made to the most landward buoy, located in the shallowest water depth in the NDBC Gulf of Mexico array. Buoy 42007 is located just north of the Chandeleur Island chain in a water depth of 44 ft. Seaward of this area the bathymetry (Figure 3-2) is complex, and refraction, shoaling and depth-limited breaking will dominate the physical processes. It is unfortunate though that this buoy did not survive Katrina, and as evidenced by the wave record (Figure 3-13). It failed well before the storm peak. Documentation from NDBC stated that buoy 42007 broke its mooring on 29 August 2005 0000 UTC. Hence, all measurements provided in Figure 3-13 beyond this date should not be considered as valid points.

The growth stage is indicated by a methodical increase in wave height and is dominated by wind-seas until 27 August 1800 UTC when there is a dramatic shift in  $T_p$ , an indication of the early arriving swell energy combined with local wind-seas. The downshifting in frequency (or increasing  $T_p$ ) continues, with the increase in wave energy until the failure of the buoy. Approaching failure there is only a modest change in the vector mean wave direction of at most 30 deg. This should not be surprising because to the south, west, and north there is considerable sheltering due to geographical constraints (land masses), and thus a small window available to receive wave energy.

The basin-scale WAM Cycle 4.5 results generated for 42007 are shown in Figure 3-13. Results for the region-scale simulation effort provided nearly identical results compared to the basin simulation. As in the previous comparisons, the early arriving swell energy is low by about 2 ft in height, however when the transformation of wind-sea to swell dominance occurs, the errors markedly decrease. Growth up to the buoy failure is well approximated in height, peak wave period and eventually the mean wave period. The vector mean wave direction is the most consistent of these integral properties showing little or no bias. The modeled winds do not show the small variations compared to the buoy measurements, however the magnitude of these winds is low (on the order of about 10-knots at most and would only provide a modest change in the wave characteristics. Overall, for the location, complex nature of the bathymetry and the location of Katrina's storm center, WAM results proved to be quite consistent with the measurements.

Consistency in the wind (see Appendix 2) and wave estimates have been established in the time plots for the various point source measurements in the model domain. Evaluation of the overall performance can be assessed with statistical testing. As previously mentioned, because the population size for model/measurement pairs is low (generally less than 100), any variation from the measurements will be amplified. The selected statistical tests are provided below. Note that in all cases, the independent variable is defined as the measurements and the dependent variable is the model output. All results of these tests are presented in Tables 3-4 and 3-5 for the significant wave height, and mean wave period, respectively. Results of the wind speed statistical validation tests are presented in Table 2-3 (Appendix 2).

The measured wave parameters are denoted  $B$  and modeled wave parameters are denoted as  $M$ , where triangular bracket represent the arithmetic mean.

$$\bar{B} = \langle B \rangle \quad ; \quad \bar{M} = \langle M \rangle$$

$$BIAS = \langle M - B \rangle$$



$$\text{Absolute Error: } Abs\ Err = \langle |M - B| \rangle$$

$$\text{Root Mean Square Error (RMSE): } RMSE = \langle (M - B - BIAS)^2 \rangle^{1/2}$$

$$\text{Scatter Index: } SI = 100 * \frac{RMSE}{\bar{M}}$$

$$\text{Correlation Coefficient: } r = \frac{\langle (B - \bar{B})(M - \bar{M}) \rangle}{\left[ \langle (B - \bar{B})^2 \rangle \langle (M - \bar{M})^2 \rangle \right]^{1/2}}$$

$$\text{Slope and Intercept of Linear Regression: } M = a + b * B$$

A secondary linear regression is applied where the intercept  $a$  is forced to zero, and termed herein as the symmetric  $r$  value (“Symm  $r$ ” column in Table 3-4). For the range of values, the Scatter Index is defined as a percentage, where a lower value indicates a more reliable estimate. The mean values are presented to cast the bias, absolute error, and RMSE in the context of the distribution in population. There were no adjustments made or added analyses performed to examine whether or not the model and measurements are phase-lagged. No averaging technique was used on either data set, and as previously mentioned, the model and measurements are time paired. The measurements identify the end time when the data were taken or 50-minutes into the hour. All buoy data were adjusted to the even hour for this analysis.

The wave field statistics rely on two principle integral wave parameters, the significant wave height and the mean wave period. It is unfortunate that despite directional wave measurements, the reliability of those data still remain in question, especially in the context of statistical testing. Also, there are few statistical tests that are appropriate for vector quantities, and in the context of the limited population size, none were performed. Tables 3-4 and 3-5 provide the statistical results for the  $H_{mo}$ , and  $T_{mean}$ , respectively, for the offshore wave conditions in the Katrina study. Testing follows the same principles outlined in Appendix 2.

The wave conditions generated from Katrina are highly variable, as is evident from the mean measured significant wave heights found in Table 3-4. However some of the statistical variations are a result of buoy failures limiting the record length and the small population size in general. The biases reflected in the model estimates are generally negative; despite a more positive bias in the wind speeds (see Table 2-3). This is important because the wave height is proportional to the wind speed squared. One would expect the errors to remain consistent with respect to the sign. In general, the wave height biases are less than 1.5 ft, and RMSE values are less than 2.5 ft.

**Table 3-4  
Statistical Results: Basin-Scale Hurricane Katrina Significant Wave Height**

Buoy ID	Mean Cond.		Bias (ft)	Abs Err (ft)	RMS Error (ft)	Scatter Index	Linear Regression Estimators				No. Obs
	Meas (ft)	Model (ft)					Corr (r)	Symm r	Slope (a)	Intercp (b).	
42001	7.74	8.30	0.59	1.61	2.03	26	0.96	1.09	1.08	-0.01	83
42003	9.48	8.68	-0.79	1.84	2.46	26	0.98	0.86	0.77	1.34	42
42007	5.54	5.35	-0.19	1.02	1.28	23	0.98	1.05	1.13	-0.92	56
42036	9.48	8.04	-1.48	1.67	1.38	15	0.97	0.85	0.82	0.29	82
42038	5.97	5.18	-0.79	1.41	1.61	27	0.97	0.88	0.87	0.00	83
42039	11.94	10.46	-1.48	1.74	1.70	14	0.98	0.87	0.85	0.33	78
42040	12.10	10.59	-1.51	2.00	2.52	21	0.99	0.87	0.85	0.26	84
42055	4.30	4.56	0.26	0.75	0.85	19	0.95	1.05	0.96	0.43	69

The scatter index reflects the quality of the wave estimates. Wave hindcast efforts with near perfect winds (Cardone et al. 1995) produced SI values on the order of 10. The results from this study are somewhat larger, yet are considered acceptable. The correlation coefficient value is no less than 0.95, showing a strong tendency for the model to emulate the measurements. Linear regression demonstrates again the limited biases in the model estimates of about 13 percent, about a factor of two greater than that calculated for the winds (Table 2-3). The slopes and intercept again reflect the general trend in WAM to slightly underestimate the measured wave heights, however the magnitude of the differences is relatively small.

The mean wave period, an integral model estimate, is selected for the wave period statistics instead of peak period because the mean period characterizes the entire distribution of wave energy. The results provided in Table 3-5 typify the same trend shown in the  $H_{m0}$  statistics. One of the glaring errors in wave modeling even in 3rd Generation wave models is the tendency to underestimate the wave periods. This was found for the Katrina study. However, given the complexities of the event, the negative biases of 1.2 sec or less are very good. These results also reflect the tendency for WAM to “favor” the wind-seas over swells during swell migration out of Katrina; swell is being dissipated to a higher degree than is reflected in the measurements. The RMSE is on the order of 0.7 to 1.3 sec, more accurate than values commonly found in documented studies. Scatter Indices of 10 to 20 percent shows that the variability in the model results are close to the geophysical variation in the measurements themselves. The correlation coefficient  $r$  is near 1 for all cases, while the linear regression shows from the slope results (either systematic, or the standard  $a$  value) a tendency for underestimation.

**Table 3-5  
Statistical Results: Basin-Scale Hurricane Katrina Mean Wave Period**

Buoy ID	Mean Cond.		Bias (sec)	Abs. Err (sec)	RMS Error (sec)	Scat Indx	Linear Regression Estimators				No. Obs
	Meas (sec)	Model (sec)					Corr. r	Sysm r	Slope	Intercp.	
42001	6.68	6.16	-0.53	2.02	1.09	16	0.90	0.90	0.70	1.51	82
42003	6.59	5.85	-0.74	0.98	1.01	15	0.98	0.86	0.65	1.58	42
42007	6.45	5.80	-0.66	1.16	1.29	20	0.89	0.91	0.89	0.06	56
42036	7.21	6.00	-1.22	1.30	0.82	11	0.93	0.83	0.75	0.58	82
42038	6.37	5.72	-0.65	1.14	1.32	21	0.89	0.88	0.71	1.20	83
42039	7.41	6.42	-0.99	1.06	0.75	10	0.95	0.87	0.83	0.27	82
42040	7.52	6.37	-1.15	1.18	0.86	11	0.95	0.85	0.87	-0.17	84
42055	6.42	6.70	0.29	0.59	0.66	10	0.97	1.03	0.91	0.83	83

The outcome of this statistical analysis reflects quality in the wind and wave modeling efforts used in the simulation of Hurricane Katrina. In general the winds are of exceptional quality, and the wave model reflects that in its results. No model is perfect; however the results from the time plot comparisons and statistical tests, despite the limited population size, demonstrate that WAM Cycle 4.5 produces a quality wave hindcast.

Thus far the verification has concentrated on temporal comparisons to point source measurements. The results though only reflect a limited number of measurement points within the entire Gulf of Mexico. Additional wave height estimates from satellite based altimeters provide a useful source of data over space but for selected time intervals. Use of both data sets (temporally varying point source measurements, and spatially varying measurements at discrete times) enable better assessment of the capability of a wave model's performance in this complex meteorological situation.

Wave height altimeter results were available from two sources: Envisat (ENVSAT) operated by the European Space Agency and Jason (JS1) operated jointly by NASA and the French Space Agency CNES. Three distinct tracks, two from ENVSAT and one from JS1 are used here. The WAM wave heights are color contoured, and the colored symbols are the estimates from the various altimeter data sets. The altimeter estimates are spatially filtered, eliminating the near-coast/land contaminated estimates and any other spurious data. As shown in Figure 3-14, the altimeter cannot accurately estimate wave heights though the core of Hurricane Katrina. However, in the remainder of the Gulf of Mexico it provides useful data with which to compare to the WAM results. It is very apparent WAM replicates the ENVSAT data until it reaches about the 27-ft wave height contour in the left front quadrant of Katrina. As the satellite passes out of the core, WAM overestimates wave heights by 5 to at most 10 ft. This comparison is also shown in the upper panel of Figure 3-17; however note that WAM estimates in the core of Katrina (not visible in the altimeter data) have been removed from the plot.

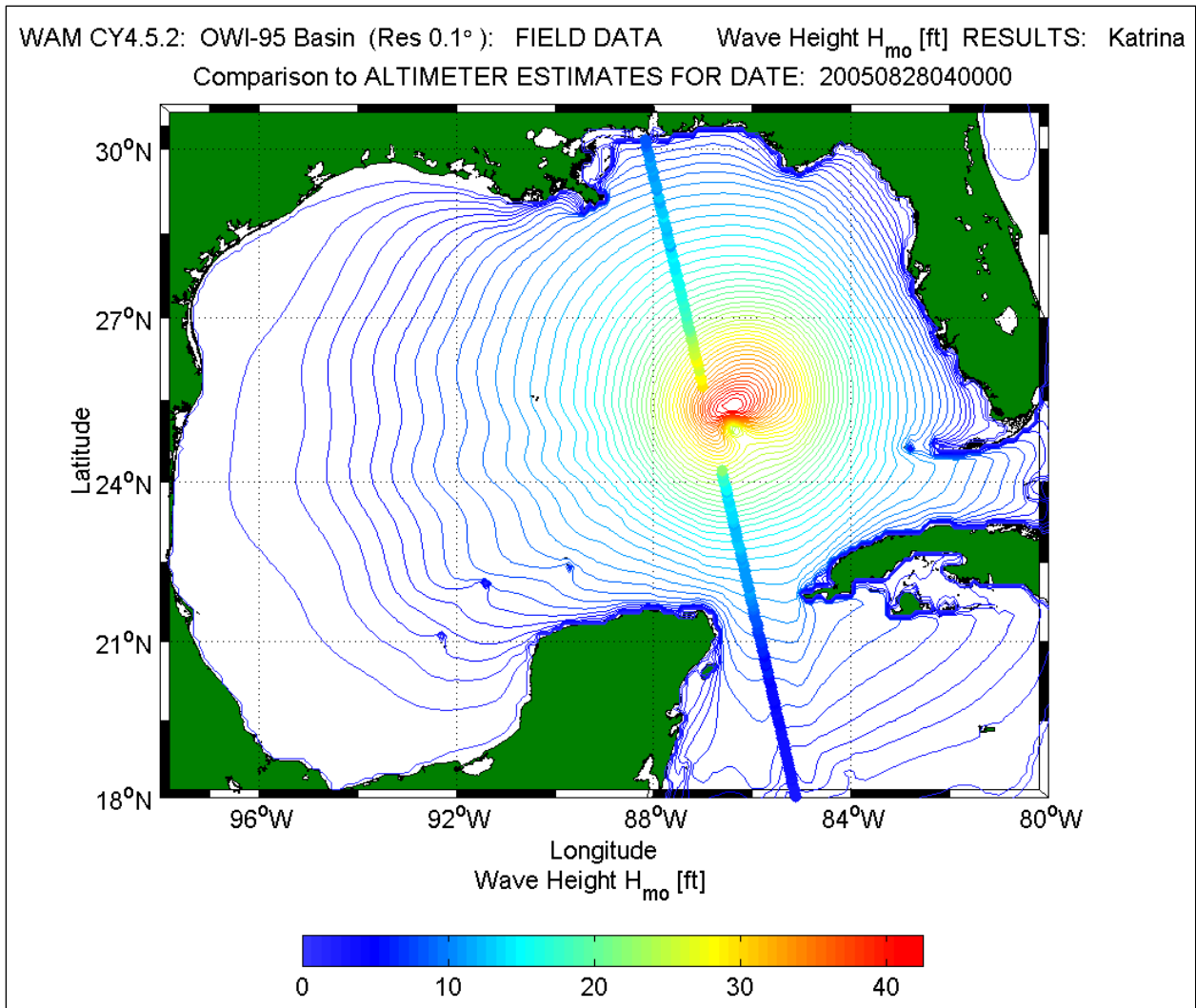


Figure 3-14. WAM wave height color contour overlaying ENVSAT altimeter wave height estimates at 28 August 2005 0400 UTC.

Approximately 12 hrs later the second ENVSAT pass takes place southeast of Katrina as shown in Figure 3-15. In this area the wave heights are on the order of 15 ft, slightly increasing to its maximum at about 26.5 deg N, then falling off as it passes south of the tip of Cuba. Over this track WAM does very well matching the slight spatial variation. This is an area consisting of decaying swells with an influx of locally generated wind-seas caused by the “backwash” of Katrina’s counter-clockwise rotating wind field.



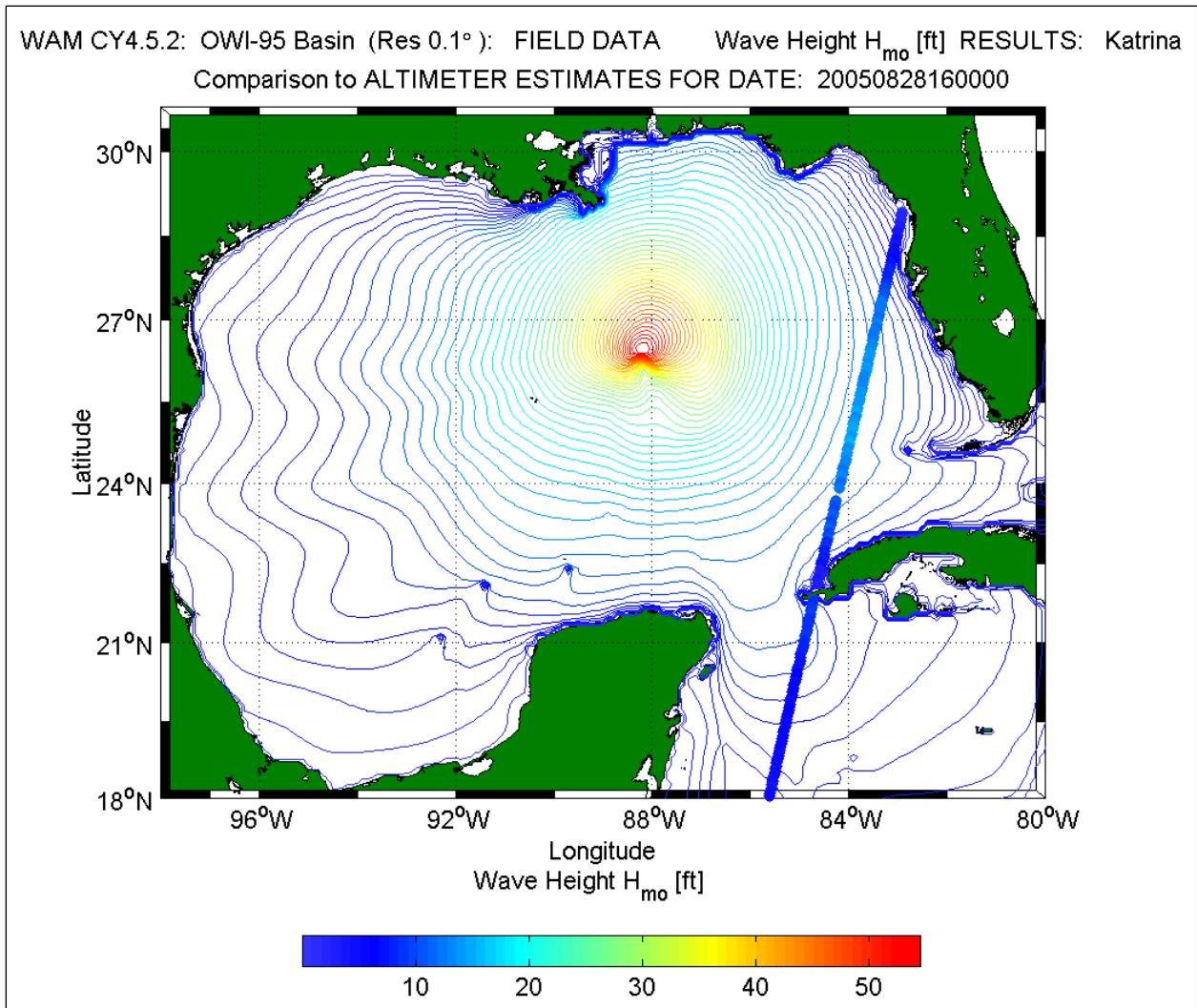


Figure 3-15. WAM wave height color contour overlaying ENVISAT altimeter wave height estimates at 28 August 2005 1600 UTC.

The last altimeter track is derived from a Jason (JS1) satellite flight that is about 2 hrs after Katrina's initial landfall. The results of the WAM and altimeter comparison are found in Figure 3-16. The track is located southeast of Katrina's position. As in the previous case, the altimeter and WAM results for this area are quite similar and they reflect a near homogeneous wave field. Variations in the  $H_{mo}$  estimates range from lows on each end of the track of about 5 ft to a predominance of 10 to 15 ft wave heights. WAM results again emulate these slight variations over space.

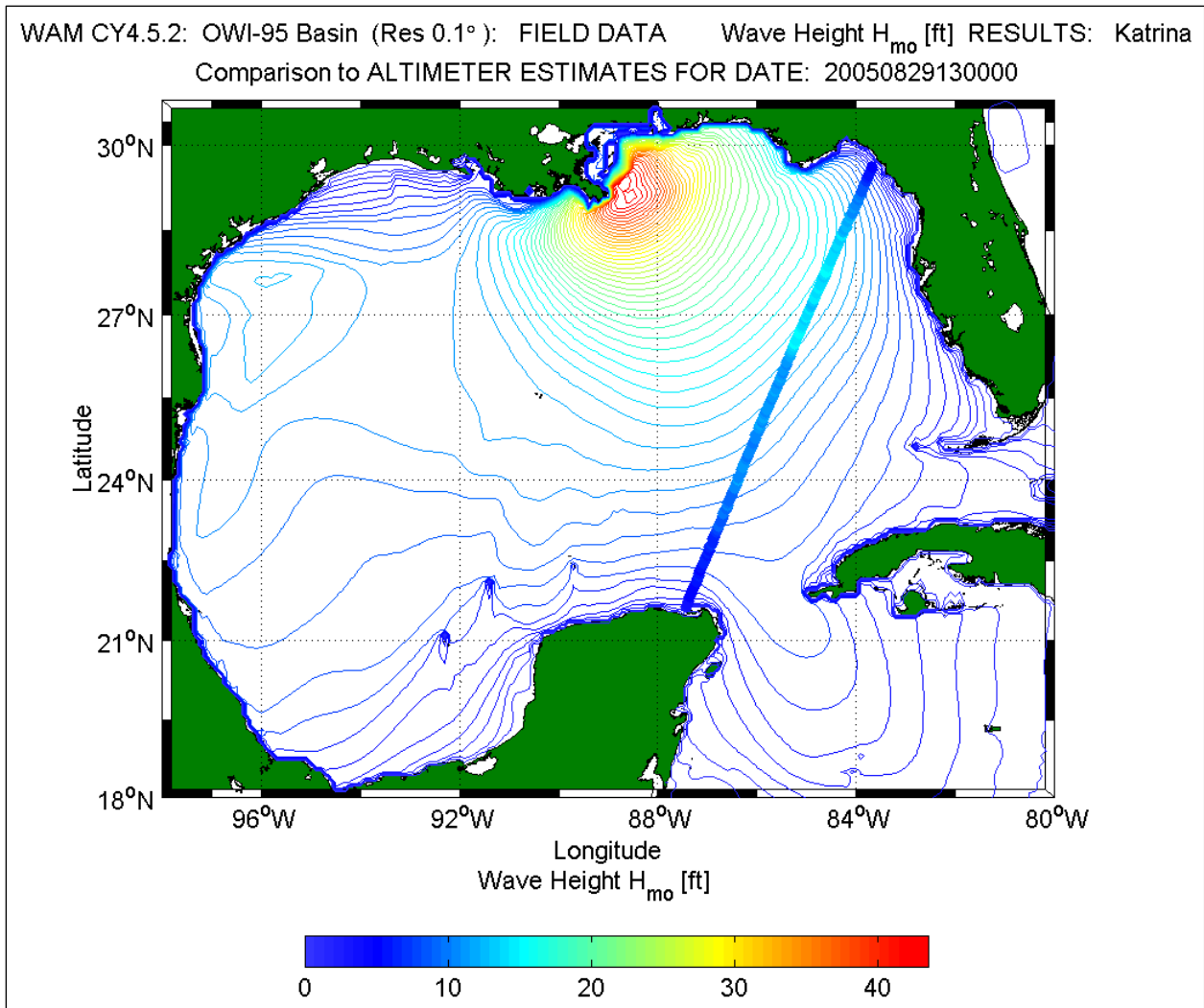


Figure 3-16. WAM wave height color contour overlaying Jason altimeter wave height estimates at 29 August 2005 1300 UTC.

The comparisons of all three tracks of data to the WAM output are summarized in Figure 3-17. The model estimates are taken directly from Figures 3-14 through 3-17, and plotted over a station number. For all three cases the plotted model results are co-located to the altimeter data set, and omitted when the satellite data are not present. The first case (top panel of Figure 3-17) shows reasonably good agreement of the WAM simulation with the altimeter data. There is a tendency to overestimate the wave conditions north of Katrina's core by about 7 ft. However with regard to the remainder of the altimeter track, WAM emulates these wave estimates quite well. At the peak values in the altimeter data set the maximum differences are only about 3 ft.

The second ENVSAT pass occurring on 28 August 2005 at 1600 UTC is shown in the middle panel of Figure 3-17. As in the case of the previous comparison, the model results emulate the trend found in the altimeter data set. There is one area consisting of a positive bias,

and the magnitude of the bias is on the order of 2.5 ft. As the altimeter track crosses the western tip of Cuba, WAM matches the measurements quite well.

The final track results are derived from the Jason (JS1) around the time of Katrina's second landfall (Figure 3-17 bottom panel). The track is in an area where swells are coming from the back-wash of Katrina's wind pattern. WAM predicts the general spatial variability in the data extremely well, yielding smoother variation in wave heights compared to the altimeter oscillations. There is no discernable bias in the WAM results, as was evident in the previous two cases. In general the patterns of these three unique altimeter passes are well represented by the model. These results also indicate the wind field specification used in the simulation is of excellent quality. There were occurrences in which some of the inconsistencies in the WAM simulations could have been caused by lack of wave model grid resolution. However at the level of analysis here, a major percentage of the inconsistencies found in the WAM results are within the geophysical variability of the measurements themselves.

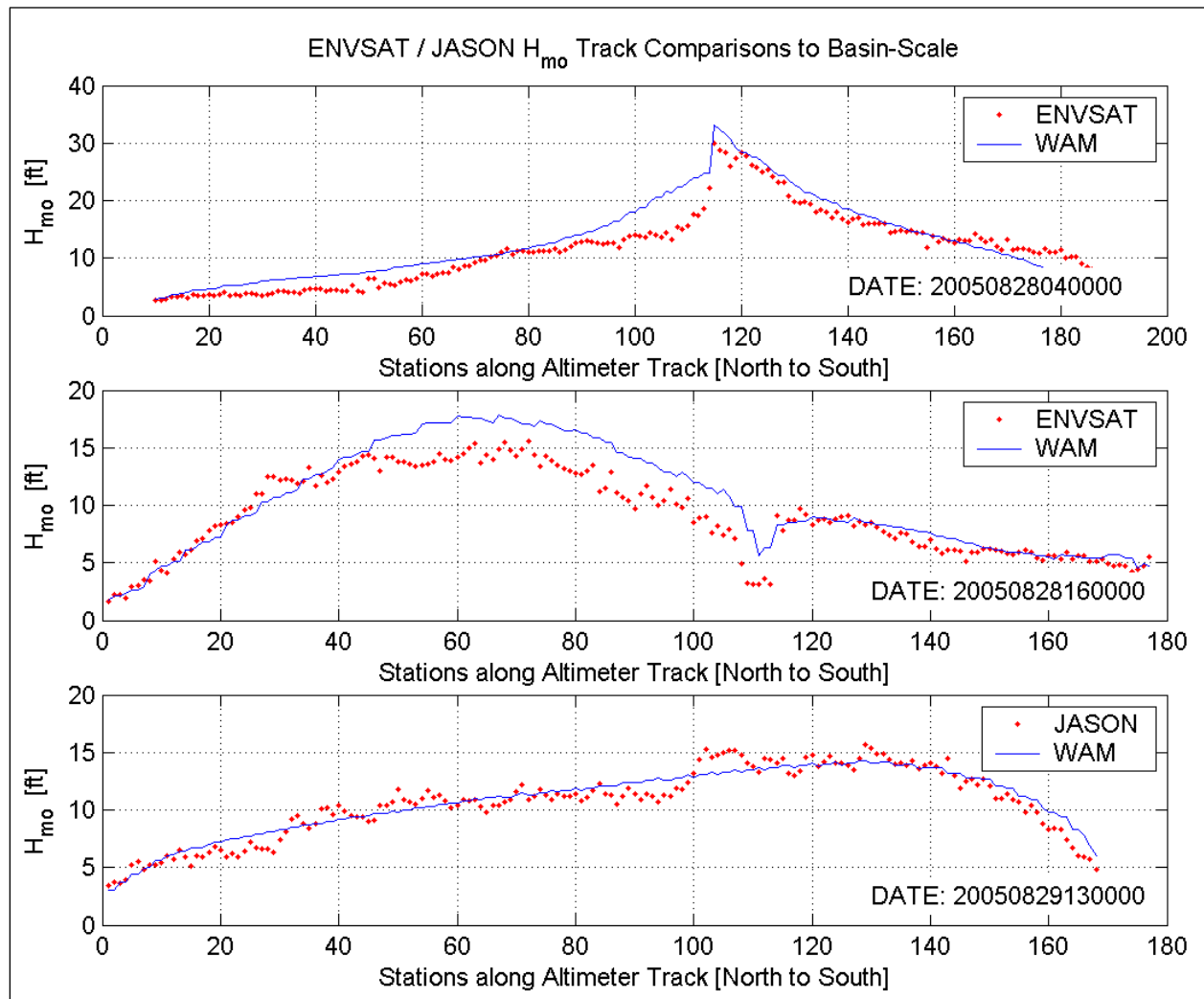


Figure 3-17. Comparison of WAM wave heights for the two ENVSAT and Jason altimeter passes.

## Sensitivity of Wave Estimates to Wind Field Specification

In general, the largest source of error in a wave model simulation originates from the wind fields. In all wave models, scaling of the significant wave height is proportional to the wind speed squared. Hence, a simple study is posed to assess the effect of potential errors in the specification of the wind fields for Hurricane Katrina.

The premise is as follows, what would happen to the wave estimates if the wind fields are subjected to a  $\pm 5$ -percent change in magnitude over the entire domain and over the duration of the simulation? The final wind fields were multiplied by 1.05 for Test Case 1 and multiplied by 0.95 for Test Case 2. The wave model results are then evaluated over the full grid, and at specific point measurement locations. In addition, results of these tests were then provided to the nearshore wave model in the form of two-dimensional wave spectra to force the sensitivity runs in the nearshore domains. This modeling approach of a simple multiplication factor produces the largest change in the wind forcing function in the core of the hurricane, and less so in the far field.

The final wind magnitudes are subjected to a multiplication factor of 1.05 and 0.95. WAM Cycle 4.5 is run again with identical input criteria (grids, time steps, and boundary conditions) as previously defined. The results are post-processed and graphically presented below. The significant wave height field estimates are presented as the maximum wave height distribution over the entire model domain. The products are identical to those presented for the original simulations (Basin-scale results in Figure 3-4 and the Region-scale results in Figure 3-6).

Figure 3-18 shows the wave height results for Test Case 1 using the 5-percent increase in wind magnitude. It is not surprising to see the distribution in maximum wave heights between this case and the original run (Figure 3-4) is nearly identical. The magnitude of the largest  $H_{mo}$  increases from 54.7 ft to 57.0 ft and its location is moved slightly north (from 26.7 deg to 27.0 deg). The migration toward the north would be characteristic of the increased growth processes resulting from the increased wind speed. Also, because of the change in the wind speed, there would be a slight downshifting of the peak frequency sending increased swells outward from the front right quadrant in Katrina. A plot of the differences between Test Case 1 and the original Base-case solution is shown in Figure 3-19, where a simple difference is applied. The Base case reflects the final wind solution and the Test Case 1 is the result of applying the  $1.05 \cdot U_{10}$ . The color contouring shows these differences in shades of red and blue (Test case minus Base case), where the red reflects increased  $H_{mo}$  estimates for the Test Case 1 compared to the Base case and blue identifies areas where the Base case result is greater.

In general, as expected, the entire Gulf of Mexico is contoured in red signifying a net increase in wave energy resulting from the increase in wind speed. The overall average increase in significant wave height is about 3 ft. There are lobes of concentrated red areas along the Mississippi Delta where depth effects focus the added energy. However, there is a distinct lobe of blue in the Atchafalaya and Vermilion Bay area. This suggests that by increasing the wind speed, wave heights are reduced, which is counter-intuitive. What seems to take place is the following. There is an increase in wave energy caused by the increased wind speed. There is also an increase in wave period. As Katrina passes, longer period swells radiate outward in a



northwestern direction. These longer period waves refract due to the local bathymetry and are focused further west as indicated by the strong local red contours just to the west. Refraction causes focusing of energy, producing higher wave conditions in some areas and lower wave conditions in others.

Test Case 2 consists of reducing the overall wind speed by 5 percent. The results of the WAM run are presented in Figure 3-20 which shows color contours of the maximum wave height over the domain for the simulation period. The overall maximum wave height for this case is 52.3 ft or a net reduction of 2.4 ft compared to the base case, and its location has moved in a southerly direction, residing at 88.1deg W / 26.4 deg N. This reflects the overall reduction in the wind magnitude.

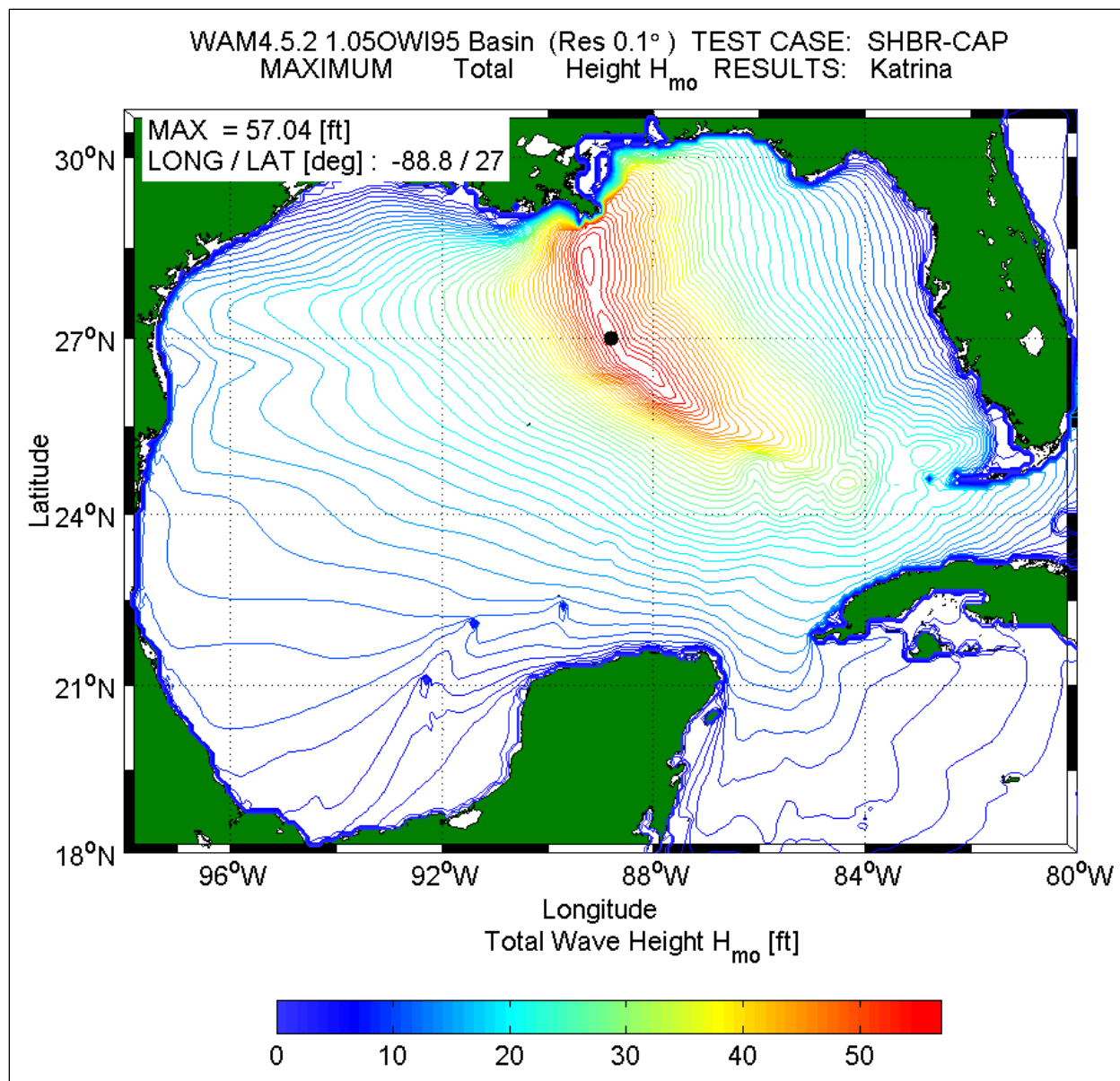


Figure 3-18. Color contour of the maximum wave height conditions in the Basin domain for the 5-percent wind magnitude increase

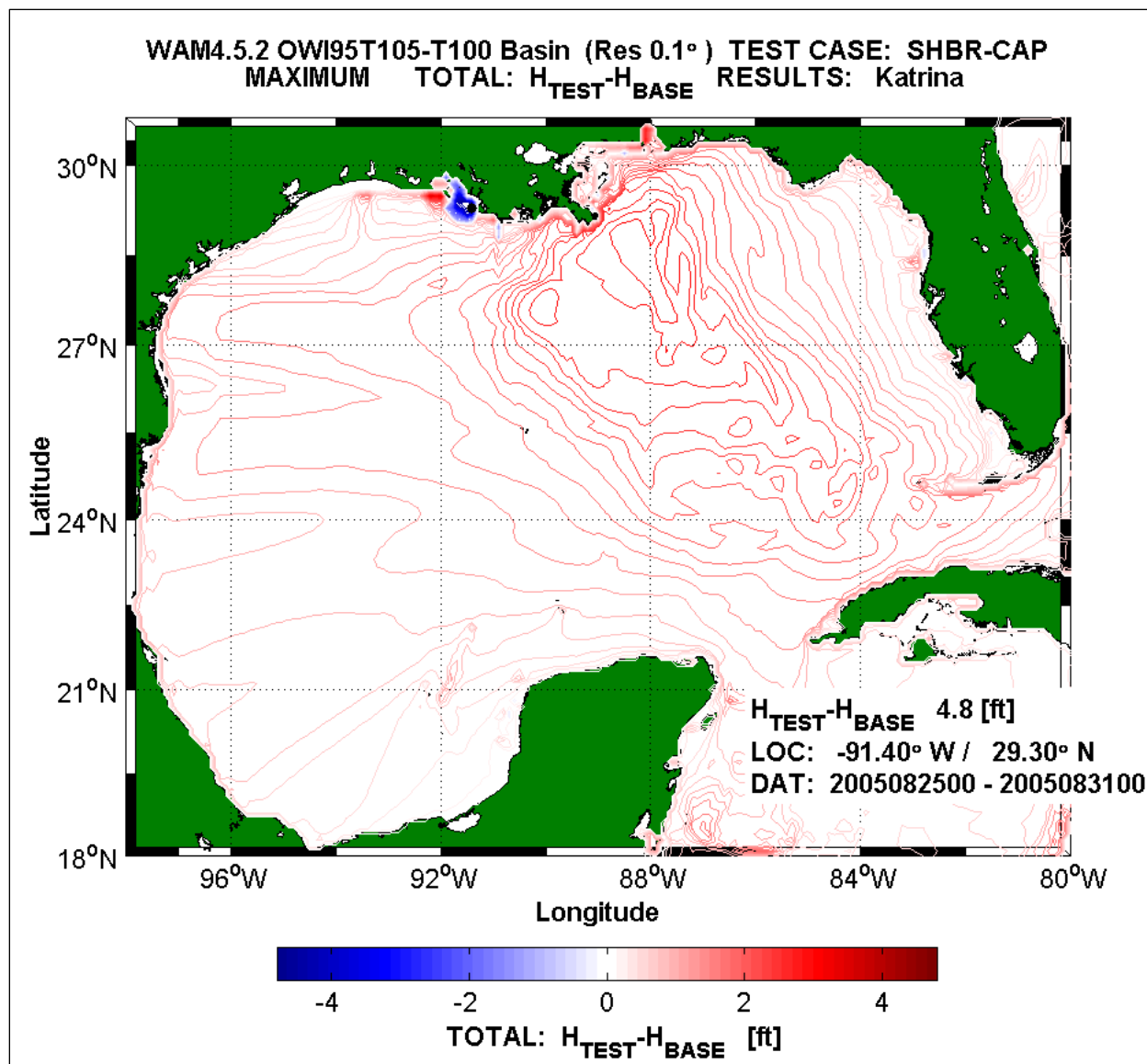


Figure 3-19. Color contour of the difference between Test Case 1 ( $1.05*U_{10}$ ) minus the Base Case maximum wave height conditions in the Basin domain.

The difference between the maximum wave heights for Test Case 2 ( $0.95*U_{10}$ ) and the Base case is shown in Figure 3-21. In general the entire domain is covered by blue contours signifying the reduction in wave energy for this simulation compared to the base case. The maximum difference is 3.4 ft in Mobile Bay. This is most likely an artifact in the contouring software, and not reflective of the overall differences, which on average are 2 ft. There again are two very small areas with a positive change; however these are locally amplified by the contouring. One does see a concentration of blue contours just offshore of the Mississippi Gulf Coast, extending westward through the Mississippi Delta and the Louisiana coastal domain. The large “L” feature west of Atchafalaya Bay is caused by a lowering of Katrina’s wind and thus wave energy, amplified by sheltering of the Mississippi Delta and depth effects. The wind-reduction case, Test

Case 2, generates a nearly symmetric change pattern (but a change in sign) relative to Test Case 1 the wind-increase case.

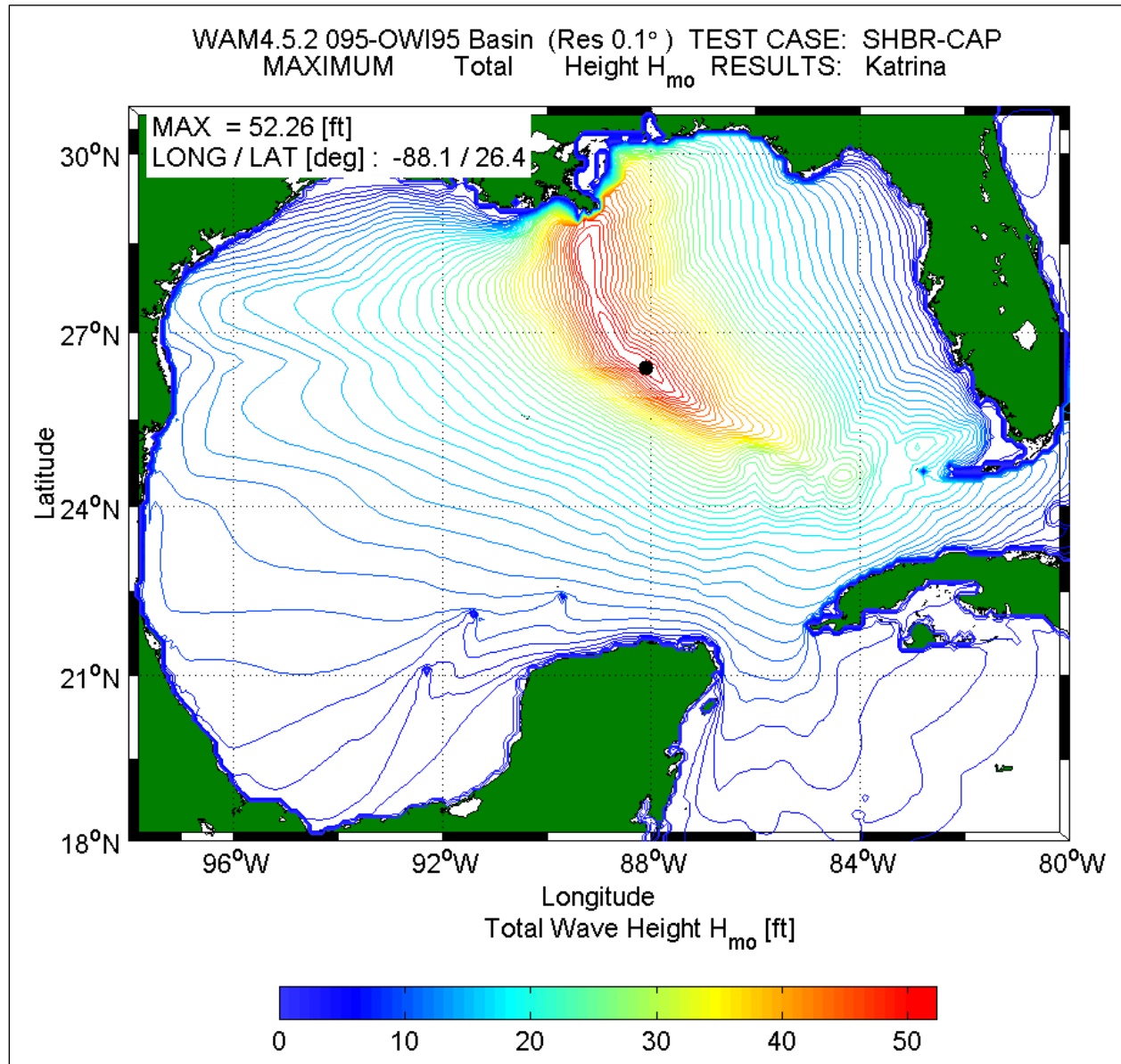


Figure 3-20. Color contour of the maximum wave height conditions in the Basin domain for the 5-percent wind magnitude reduction



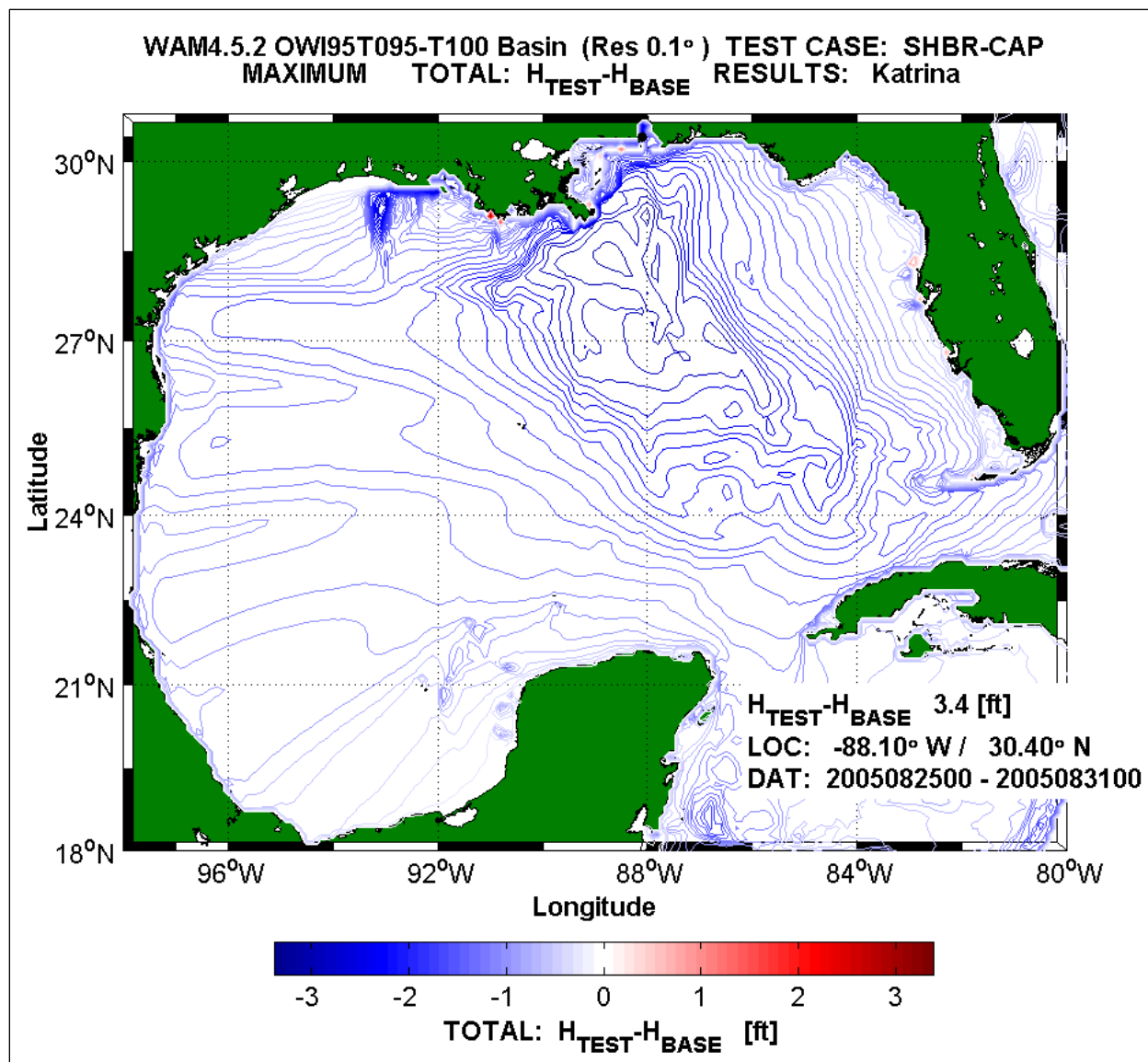


Figure 3-21. Color contour of the difference between Test Case 2 ( $0.95*U_{10}$ ) minus the Base Case maximum wave height conditions in the Basin domain.

The analysis is carried out for the Region-scale domain too. The Base case simulation is presented in Figure 3-6 for reference. For Test Case 1 (Figure 3-22), increasing the wind magnitude by 5 percent again increases the  $H_{m0}$  value from 53.6 ft to 56.1 ft or by about 3 ft, and translates the maximum location in a southerly direction placing it one grid point north of the boundary condition. The overall distribution of significant wave height for Test Case 1 and the base case solution is quite similar. A simple difference of the Test ( $1.05*U_{10}$ ) minus the Base case solution is shown in Figure 3-23. There are large areas covered by increased wave heights, with a maximum difference of 6 ft occurring west of the Mississippi Delta. This is not surprising considering that more energy is available and in light of the radiation outward of the swell energy in a westerly direction long before Katrina makes its first landfall. As in the case of the Basin-scale sensitivity tests, the Region-scale simulation with increased wind speeds

demonstrates that the wave energy can be reduced as well. Longer period energy exists, and it is more susceptible to depth effects, refraction, shoaling and wave breaking. The latter mechanism produces a net decrease in energy level compared to the Base case in places, generally in the areas landward of the offshore island chains.

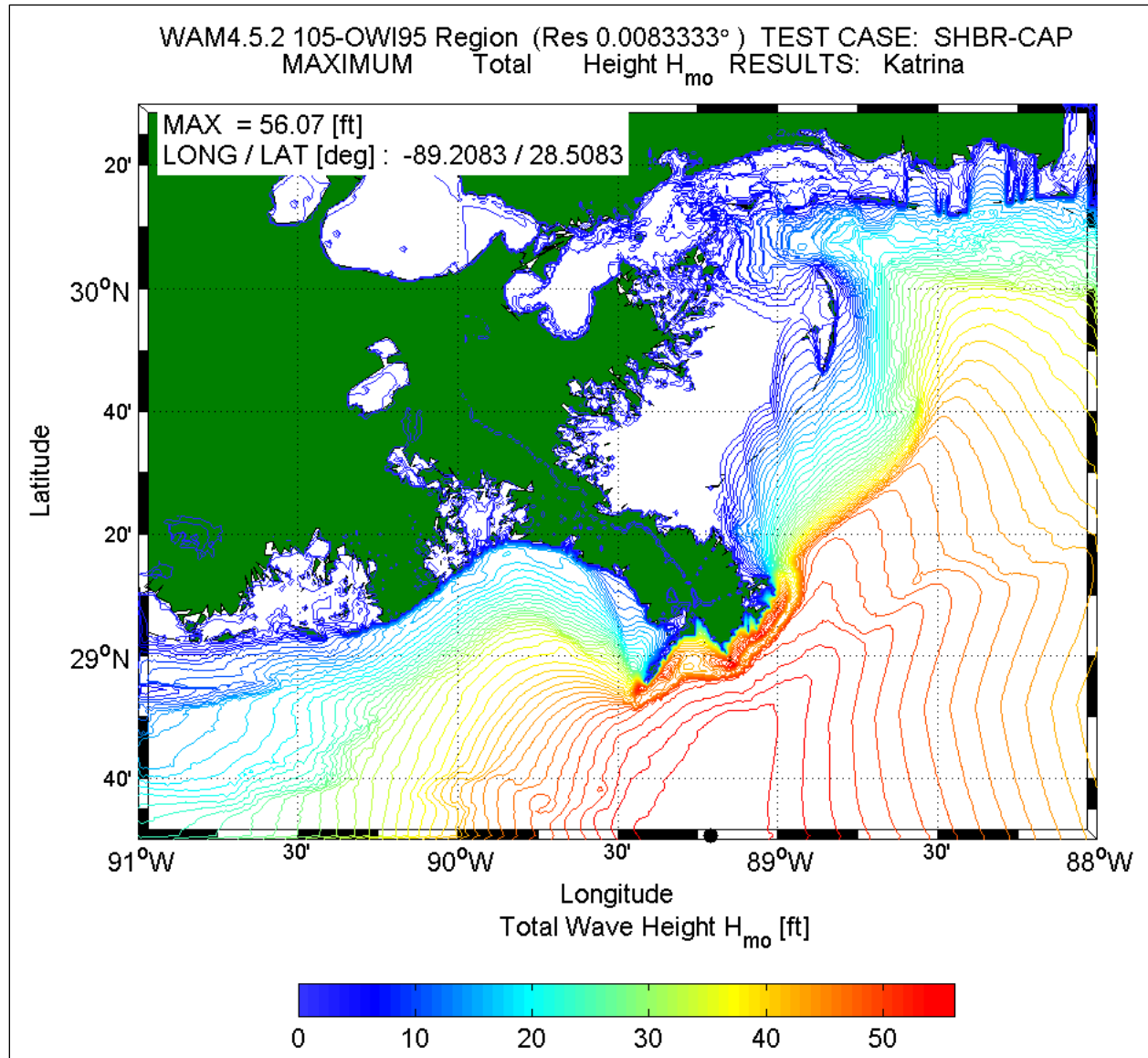


Figure 3-22. Color contour of the maximum wave height conditions in the Region domain for the 5-percent wind magnitude increase

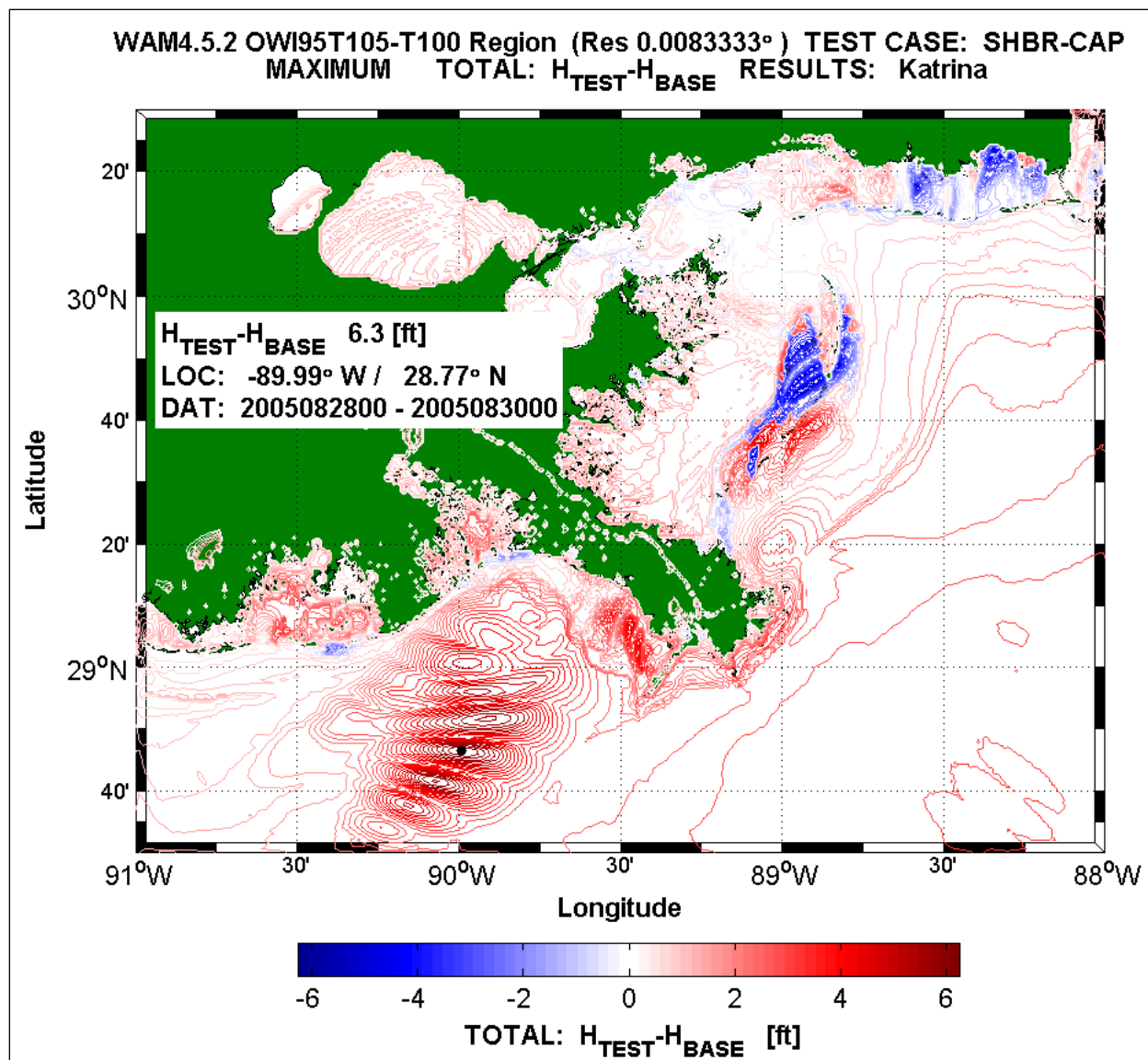


Figure 3-23. Color contour of the difference between Test Case 1 ( $1.05 \cdot U_{10}$ ) minus the Base Case maximum wave height conditions in the Region domain

Continuing the sensitivity analysis for the Region-scale domain, the maximum wave height distribution for the reduced wind speed case is provided in Figure 3-24. For this case, the maximum significant wave height is found to be 50.8 ft compared to the Base-case result of 53.6 ft, or a net reduction of slightly over 3 ft. The location of the maximum wave height is identical to that of the original run, which is not surprising because depth-dependent mechanisms will control the wave energy at this location. Because of these effects, there is no translation of the location of maximum height in a northerly direction as found in the Basin-scale results.

The difference plot, Test Case 2 ( $0.95 \cdot U_{10}$ ) minus the Base Case is shown in Figure 3-25. The results nearly emulate Test Case 1 results, inverting the values from positive (red) to negative (blue). The maximum difference in this analysis is -5.2 ft located to the east of the Chandeleur Islands. The domain to the west of the Mississippi Delta is negative, and intervals of

positive-negative lobes are evident along the Mississippi Gulf Coast. These results suggest that wind errors of the magnitude considered here can affect the wave energy more in bathymetrically controlled wave environments. The effect is further amplified (from a 3.5-5 ft difference in the Basin scale to 5.2-6.3 ft in the Regional scale) because of strong dependence of wave transformation on wave period and water depth. These simulations do not include surge and the interaction of the wave transformation with surge in shallow areas.

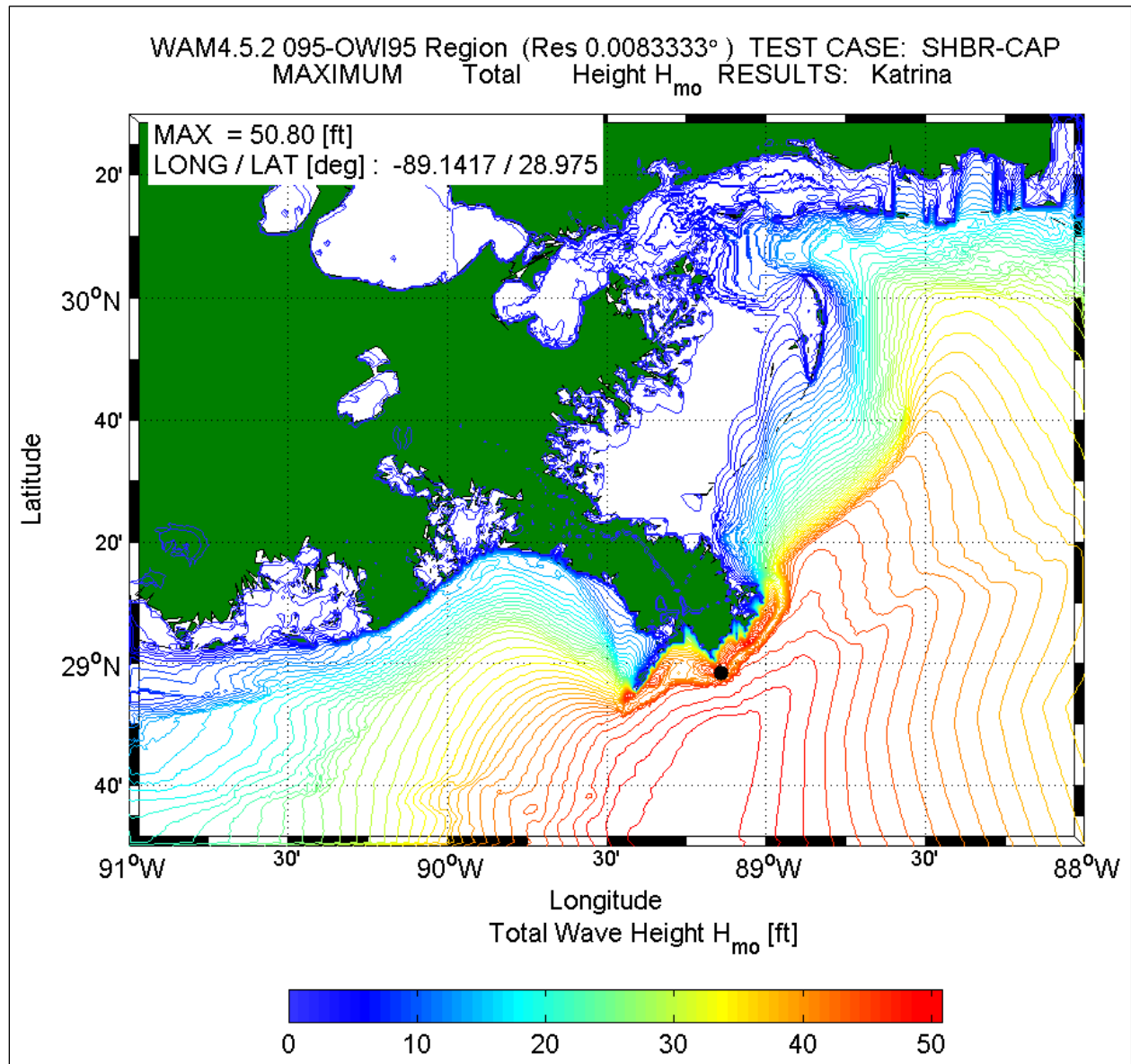


Figure 3-24. Color contour of the maximum wave height conditions in the Basin domain for the 5-percent wind magnitude reduction



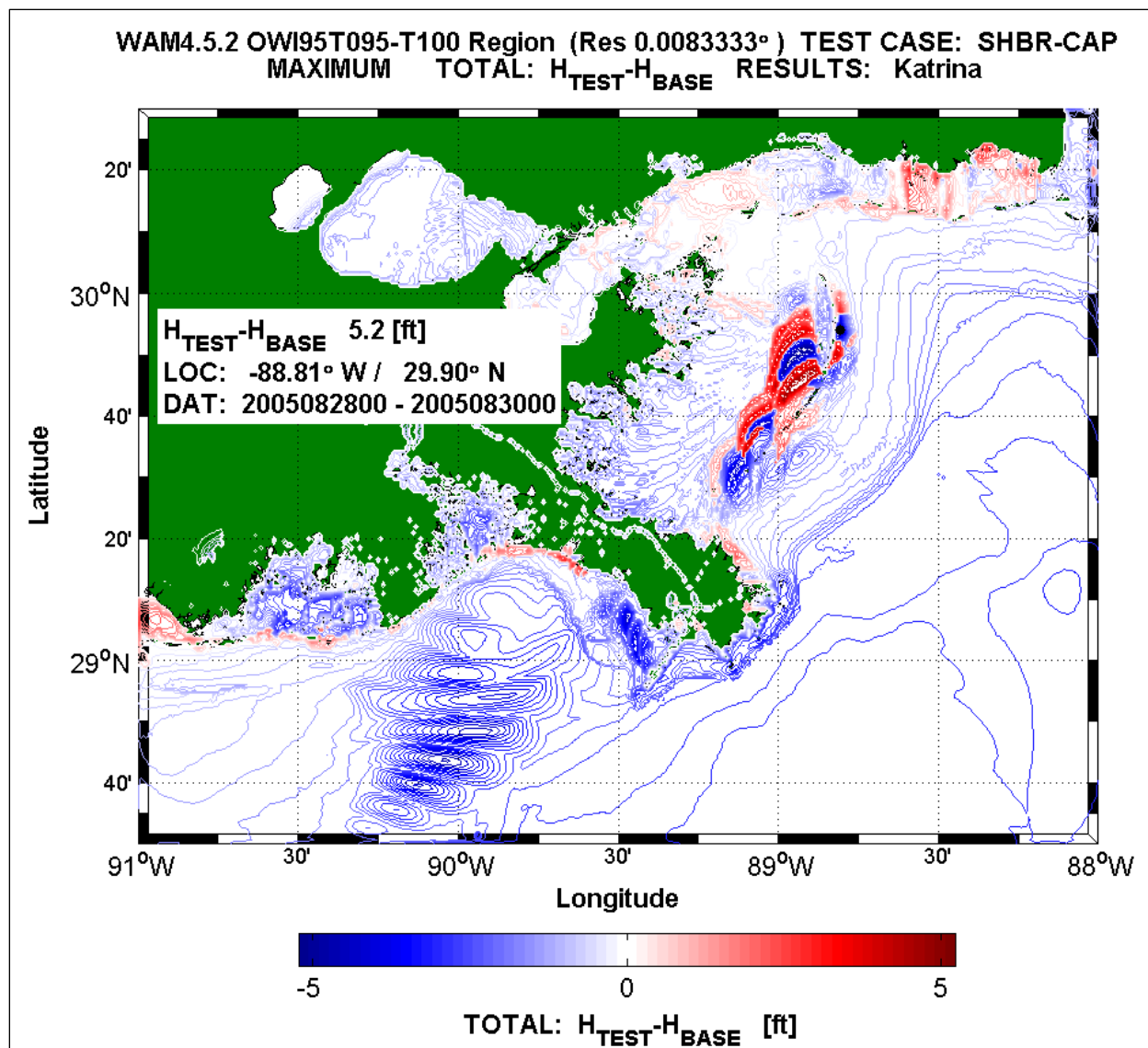


Figure 3-25. Color contour of the difference between Test Case 2 ( $0.95 \cdot U_{10}$ ) minus the Base Case maximum wave height conditions in the Region domain.

Quantification of the temporal variation resulting from the sensitivity tests at selected sites is also an important issue in the evaluation of the wave modeling effort for the Katrina study. Previous analyses were restricted to the variation in maximum wave results over the entire domain, and thus do not consider the time scale. Four NDBC buoy sites are used for this evaluation which do consider the time scale: 42003, 42001, 42040, and 42007 (see Figure 3-8 for the buoy locations). All results are derived from the Basin-scale simulation because only one buoy is located in the Region-scale domain (42007). These locations were selected based on their position relative to the storm track, water depth, and also to determine if an increase/decrease in the wind speed would significantly alter the WAM-buoy comparisons. Scaling principles in all wave models adhere to the relationship that significant wave height is proportional to the wind speed squared; wave period is linearly related to the wind speed. Therefore, with a 5-percent change in wind speed, one would expect the wave height to be

altered by about 10 percent. Based on the maximum  $H_{mo}$  results (Figure 3-4) one would expect no more than 5.5 ft change. This has, in general been verified in the full domain comparisons; however results can be distorted when depth-dependent mechanisms control the model results.

Two locations 42003 and 42001 reside in deep water located on the right and left quadrants of Hurricane Katrina, respectively. These results are provided in Figures 3-26 and 3-27. Figure 3-26 shows the WAM results for both Test Cases 1 and 2. As previously cited, if the overall wind speed is increased (or decreased) the integral wave parameters will show a very similar trend. These tests demonstrate a near uniform shift in the  $H_{mo}$  and  $T_{mean}$  results, reflecting the scaling principles. As base wind speed increases, wave height deviations increase in magnitude and are on the order of 3 to 4 ft in magnitude. The mean wave period, an integral variable also reflects this trend, but the deviations are much smaller. The variation is generally less than 1 sec separating Test Case 1 and Test Case 2 when the wind speed reaches its maximum. Only the peak spectral wave period (third panel from the top) shows significant change. As the wind magnitude increases, there is an earlier downshifting toward lower frequencies (or increased in the  $T_p$ ). However, the underestimation in the pre-swell conditions (around 27 August 0600 UTC) persists in the model results for  $H_{mo}$ ,  $T_{mean}$ , and  $T_p$ . The vector-mean wave directions for the three simulations are nearly identical, and are weighted toward the direction of the local wind-sea rather than direction of the mature swells.

NDBC buoy 42001 resides on the less-energetic left-hand quadrant of Hurricane Katrina (Figure 3-27). This location reflects a more complex situation, crossing locally generated wind-seas with mature swell energy, rapid wind shifts, and a lower wind environment. Given these conditions the sensitivity tests show similar trends as exhibited in the wave height traces. The uniform offsets between the 1.05 and 0.95 sensitivity tests are again nearly identical, for all but the vector-mean wave directions which show little differences. There are very similar trends in the peak wave period results, where increasing the wind magnitude results in a shift to frequencies that are one frequency band lower.

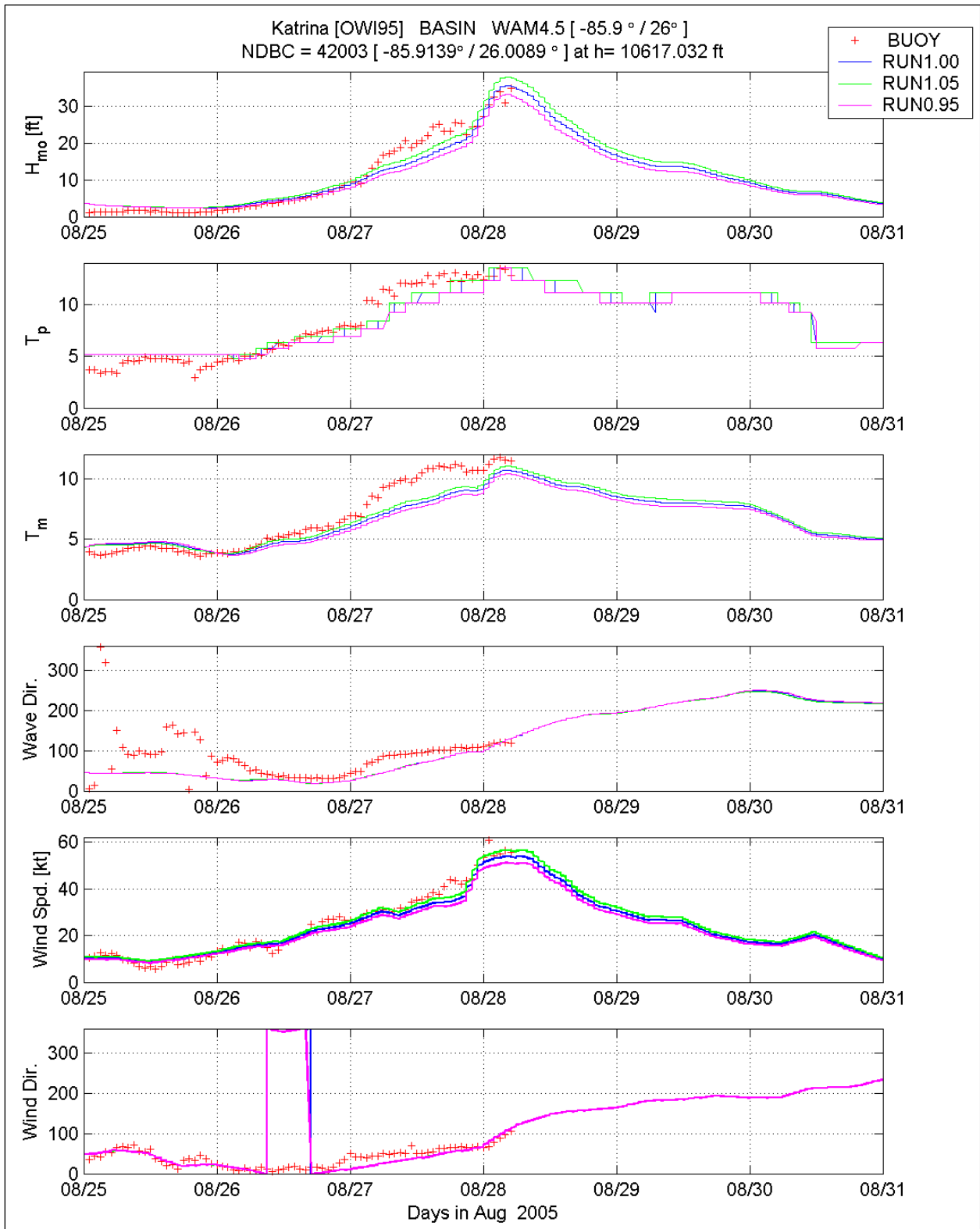


Figure 3-26. Comparison of WAM Cycle 4.5 basin-scale (blue line), sensitivity tests for  $1.05 \cdot U_{10}$  (green line)  $0.95 \cdot U_{10}$  (magenta line) to the measurements at NDBC 42003

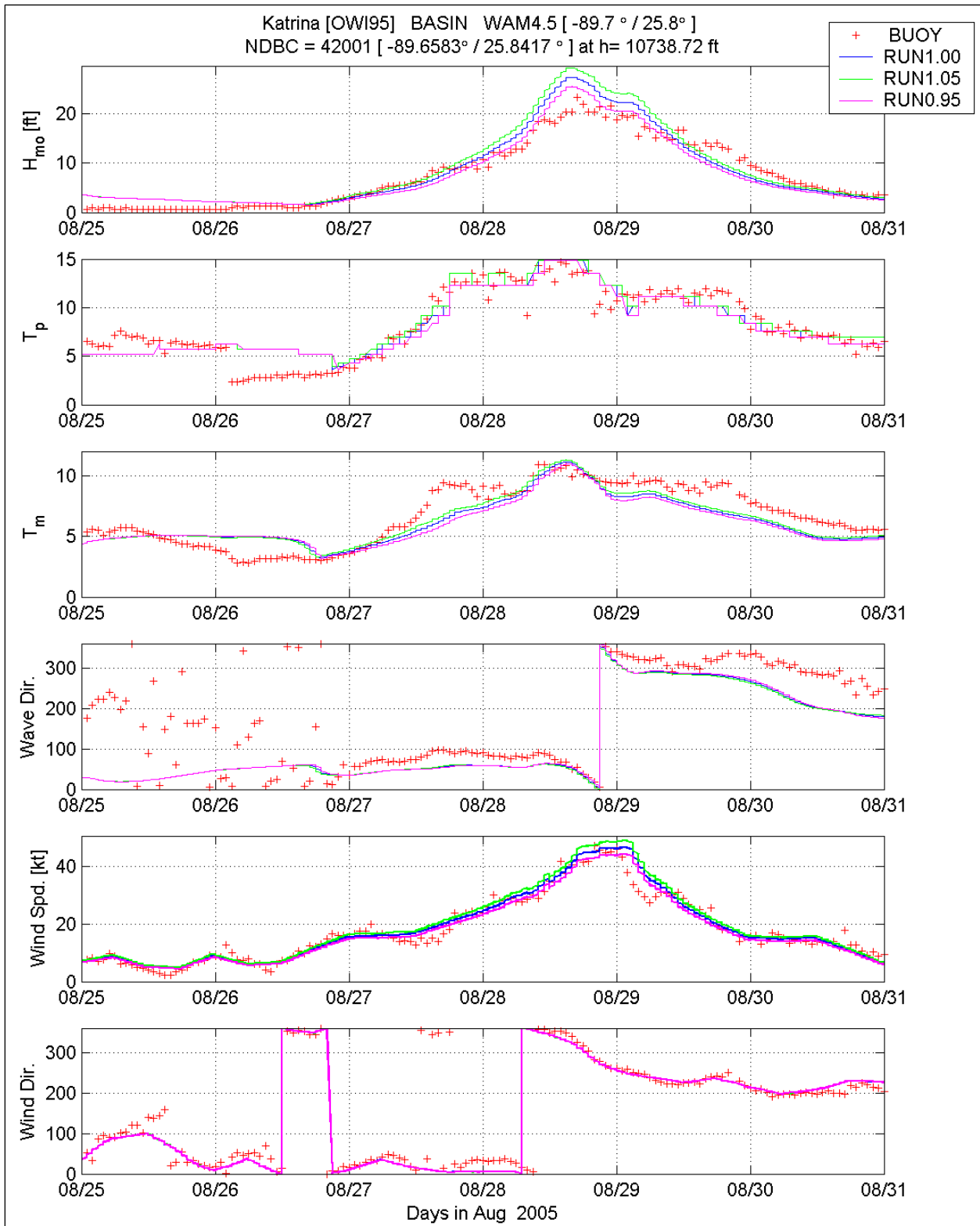


Figure 3-27. Comparison of WAM Cycle 4.5 basin-scale (blue line), sensitivity tests for  $1.05 \cdot U_{10}$  (green line)  $0.95 \cdot U_{10}$  (magenta line) to the measurements at NDBC 42001



Moving toward the coast, NDBC 42040 is the next site selected in the sensitivity study. Recall the WAM results were found to underestimate wave height by nearly 14 ft during the peak conditions of Katrina (Figure 3-11). This is also reflected in Figure 3-28. Increasing and decreasing the wind magnitude over the entire modeling domain has the same net effect on the integral wave parameters as evident in data from all the other central Gulf of Mexico buoy sites that were examined. Increasing the wind magnitude influences the wave estimates, reducing the underestimation by only 2.7 ft. The downshifting in frequency for the increased wind speed occurs about an hour earlier, again not to the degree that is required to match the measurements (occurring about 7 hrs earlier). The mean period results reflect similar trends as the wave height results, a near uniform offset between the  $1.05$  and  $0.95 \cdot U_{10}$  simulations, remaining biased low compared to the buoy data. The model vector mean wave direction again shows little change between the two sensitivity simulations.

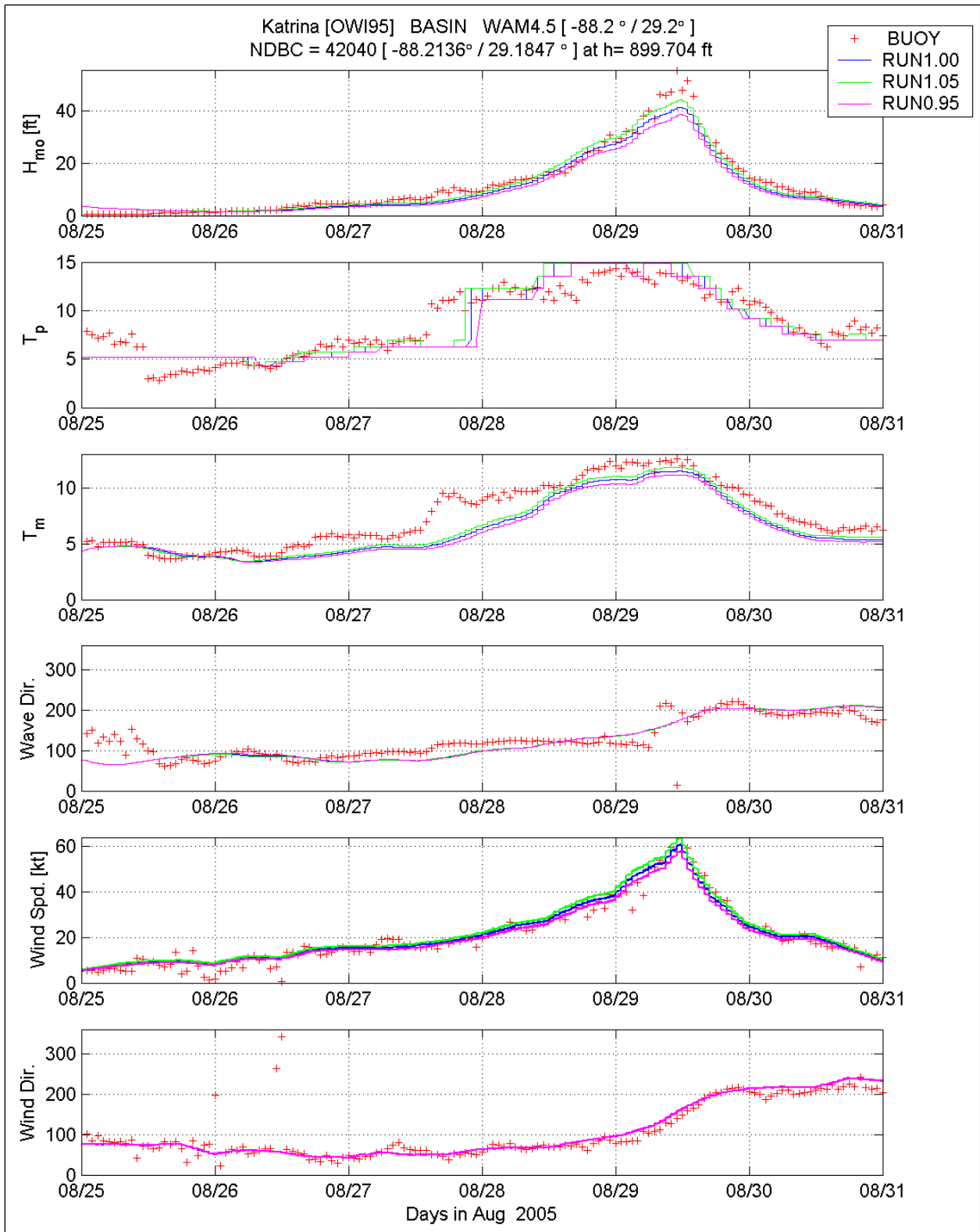


Figure 3-28. Comparison of WAM Cycle 4.5 basin-scale (blue line), sensitivity tests for  $1.05 \cdot U_{10}$  (green line)  $0.95 \cdot U_{10}$  (magenta line) to the measurements at NDBC 42040.

The final test site, NDBC site 42007 is the most nearshore site, located in roughly 44-ft water depth. This site will reflect local depth-dependent effects, (refraction, shoaling, and wave-bottom interaction) and depth-limited wave breaking. The comparisons between the two sensitivity runs display slightly different trends compared to those evident for the three prior sites. First, the offset in wave height between the 5-percent increase and 5-percent decrease in wind speed is relatively small from 25 August to 28 August. The wind speeds during this time period are relatively low and range from about 5 to 15 kts; and thus modestly influence the local wind-sea contribution. As the wind speed increases so does the offset in height, consistent with the previous three study sites. As the model results reach the storm peak, the results tend to converge toward one value. This is the result of depth-limited wave breaking, where the difference between the wind-increase and the wind-decrease cases are on the order of 0.6 ft.

In summary, the sensitivity tests adhere to scaling principles inherent to all wind-generated wave modeling technologies. Increasing or decreasing the wind speed will result generally in a net increase or a reduction in the significant wave height and mean wave period, respectively. For the case of Katrina, there are exceptions to this rule that are governed by local bathymetry that influences depth-dependent mechanisms as well as geographical sheltering that can influence the change in approach angle defined by the wind field. At most sites temporal variations in integral wave parameters tend to follow scaling principles very well. The exception to this rule is depth-limited conditions where the solutions converge toward one unique solution independent of the wind forcing.

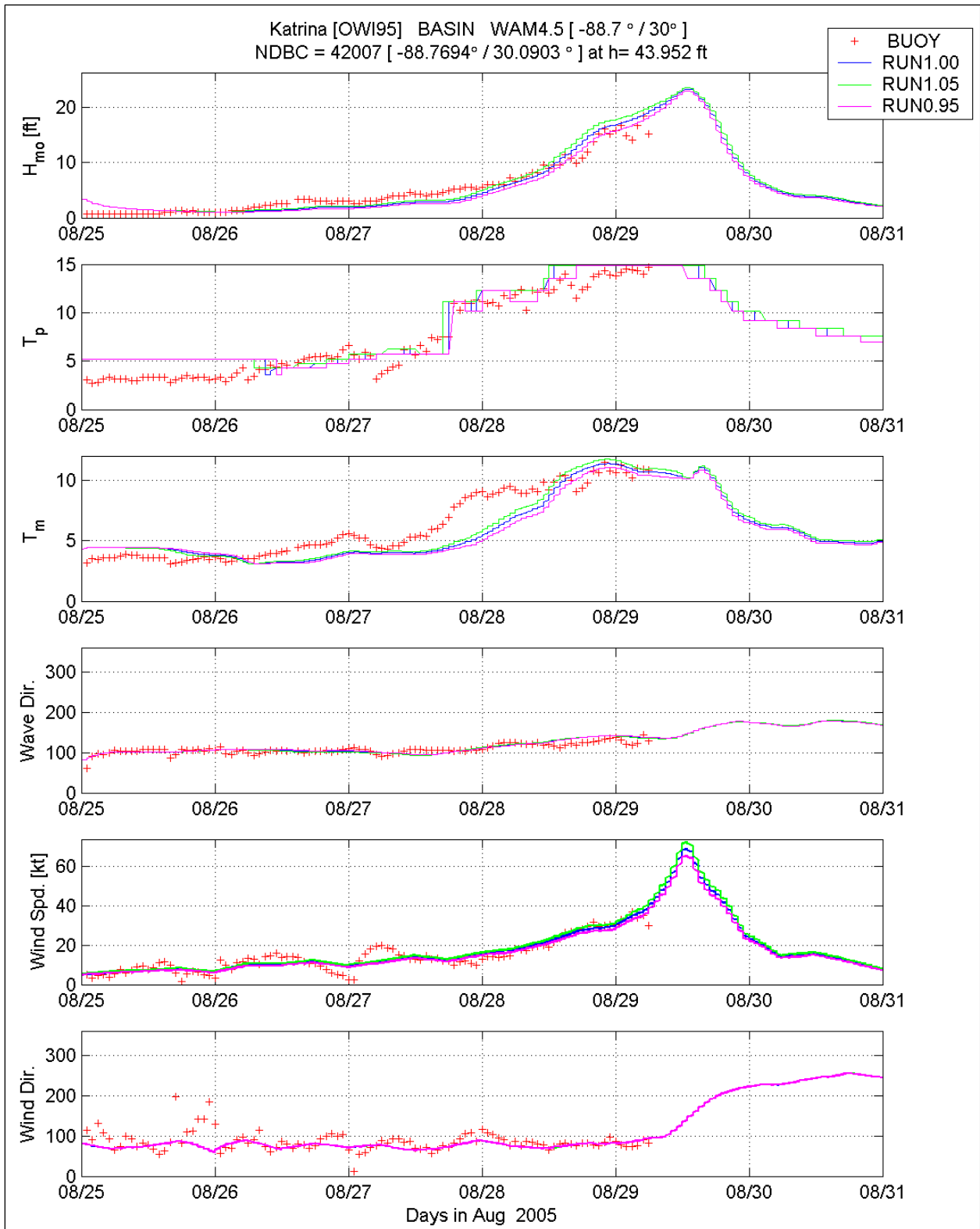


Figure 3-29. Comparison of WAM Cycle 4.5 basin-scale (blue line), sensitivity tests for  $1.05 \cdot U_{10}$  (green line) and  $0.95 \cdot U_{10}$  (magenta line) to the measurements at NDBC 42007



## Boundary Conditions to STWAVE

The culmination of this task is to provide boundary conditions from the Base case Katrina hindcast to the nearshore wave modeling effort. Accomplishing this task requires a decision on where to save boundary information relative to selection of the STWAVE model domains. The selection process was bound by the nearshore model domain size, the number of WAM points available, and most importantly assurances these results would be seaward of depth-limited breaking. A boundary was constructed along the 100-ft (30-m) water depth contour. A total of 60 individual stations from the regional scale WAM simulation were defined and directional wave spectra (28 frequency bands and 24 directional bands) every 900 sec from 28 August 0030 UTC to 30 August 0000 UTC were saved at these points. This provides adequate coverage of the offshore conditions and captures the spatial variation evident from offshore wave model simulations. An example of the directional wave spectrum is shown in Figure 3-30 and the output station locations are provided in Figure 3-31.

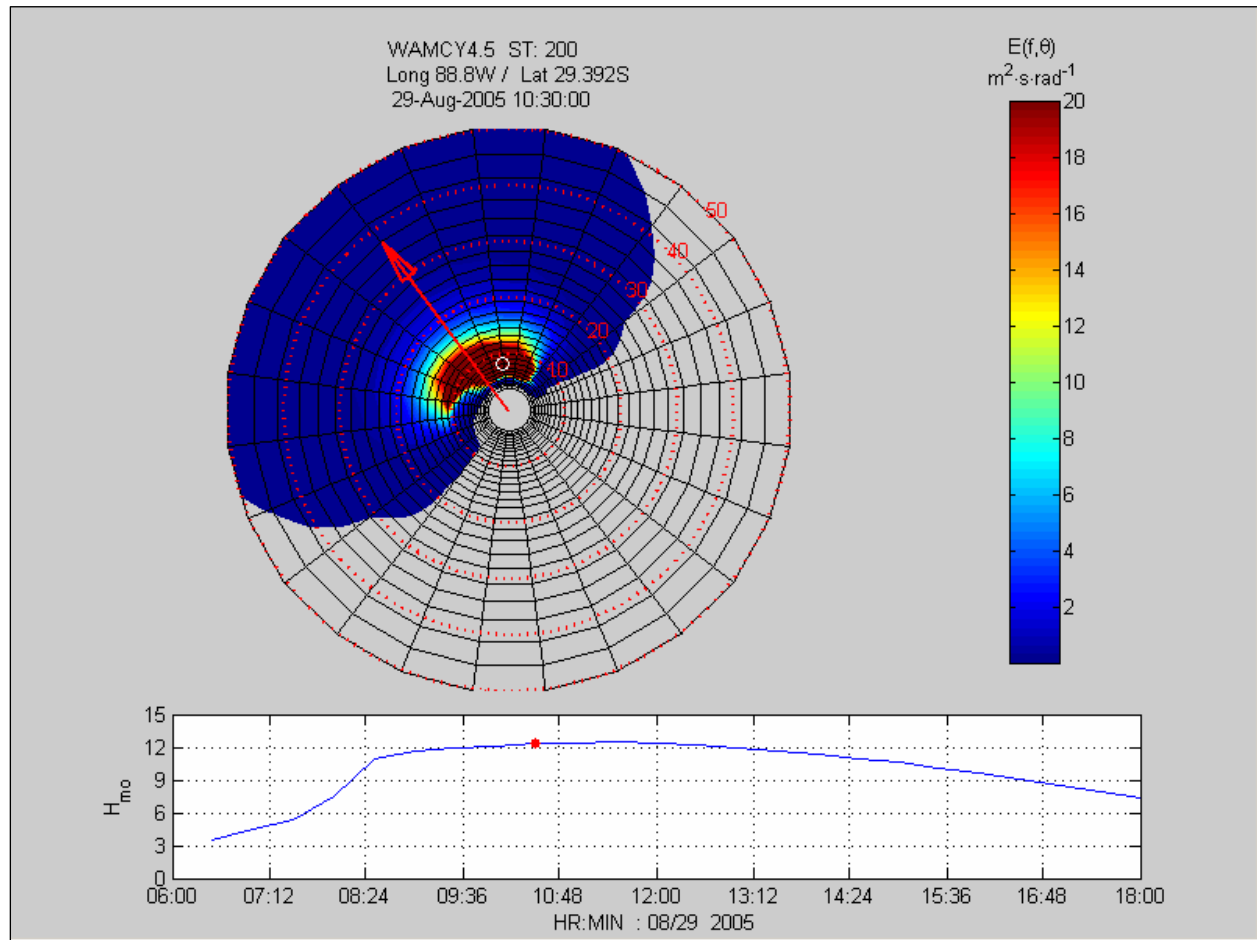


Figure 3-30. Example of the directional wave spectra color contoured in the upper panel and the wave height trace in the lower panel. Note units are in CGS

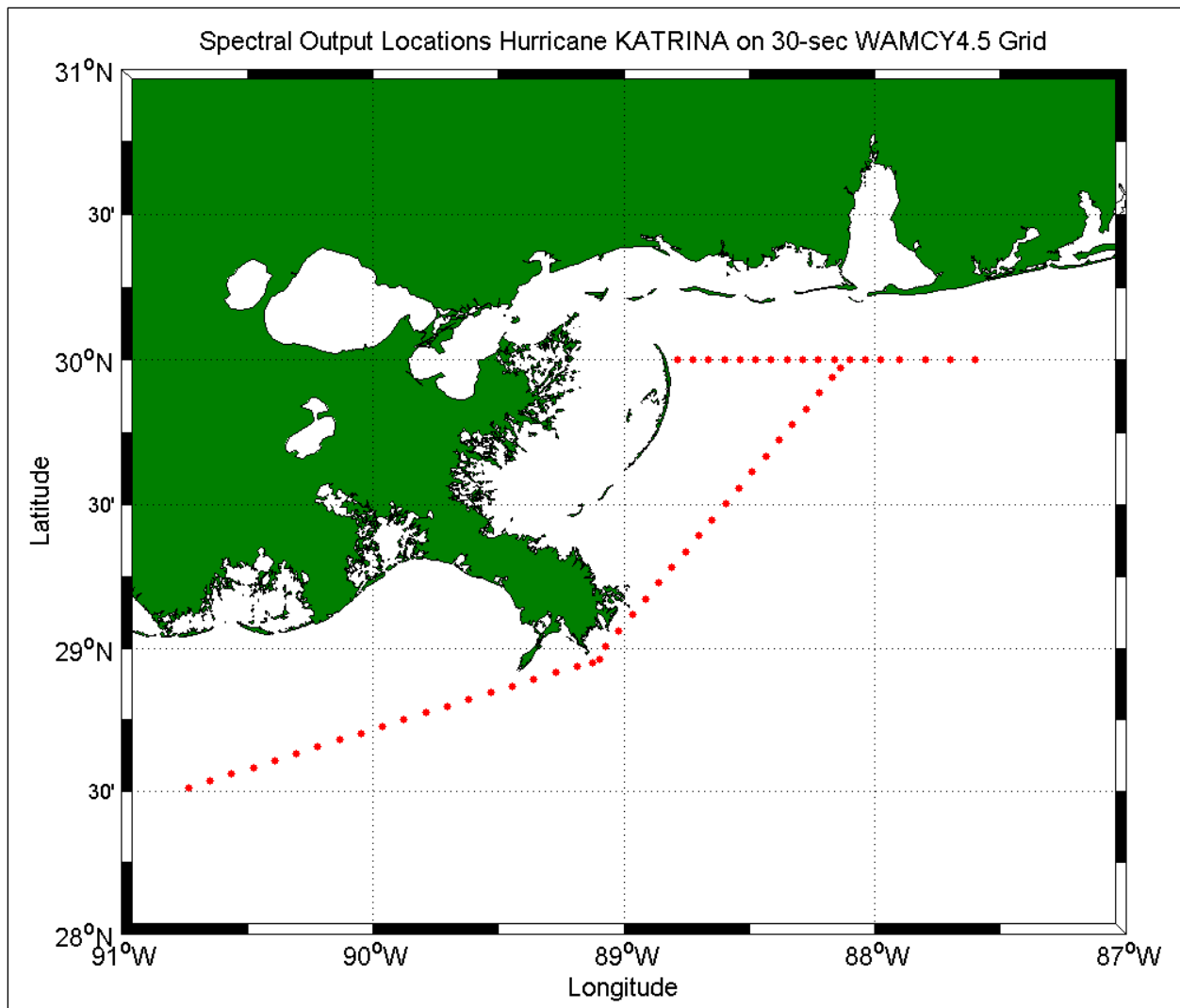


Figure 3-31. Location of the 60 output sites consisting of two-dimensional wave spectra output every 900-sec from the regional WAM Cycle 4.5 nested simulation.

## WAVEWATCH III Simulations

### Description

The third-generation numerical wave model WAVEWATCH III Version 2.22 was used to generate a Hurricane Katrina hindcast to compare with output hindcast results from WAM. WAVEWATCH III was developed at the NOAA National Centers for Environmental Prediction (NCEP), Marine Modeling and Analysis Branch, and is used by NOAA for operational numerical wave simulations. Tolman (2002) presents a user manual describing model physics, computer installation procedures, and input-output files. For the Katrina hindcast, WAVEWATCH III was run with default settings which include the Tolman and Chalikov (1996) source functions. The basin-level Gulf of Mexico grid was used with the same bathymetry and spatial resolution as the WAM simulation (see Figure 3-1). WAM and WAVEWATCH III used

identical input wind fields, the final wind fields from OWI. Input frequencies and directions were set to the values used in the WAM simulation. The WAVEWATCH III run used temporally constant water depths with no input surge information. WAVEWATCH III requires four input time steps. The global time step that propagates the entire solution in time for the basin level run was set to 450 sec. The spatial propagation time step was set to 300 sec. The third time step that relates to refraction effects for shallow water grids was set to 225 sec, and the final time step for integration of the source terms was set to 5 sec to reflect Katrina’s quickly changing wind and wave conditions. WAVEWATCH III was designed for deep and intermediate water conditions and does not include steepness- and depth-induced breaking for shallow areas. Hourly wave parameter and spectral information were saved for all Gulf of Mexico measurement stations impacted by Hurricane Katrina. Complete grid information was saved at 30-min intervals for comparison with available altimeter measurements.

## Discussion

Hindcast results from WAVEWATCH III were compared to measurements at NDBC stations 42001, 42003, 42007, 42036, 42038, 42039, and 42040. These locations are noted in Figure 3-8 and listed in Table 3-3. A complete set of comparison plots appears in Figures 3-41 to 3-47. Bulk wave height statistics indicate WAVEWATCH III hindcast results are biased lower than the measurements at all the sites. The mean wave height bias for the seven NDBC stations listed above is -1.87 ft indicating WAVEWATCH III wave height results are slightly low when compared to measurements. Wave height bias statistics range from -0.8 ft at NDBC 42001 to -3.5 ft at 42007. Peak period results are biased low by 1-2 sec. The maximum hindcast wave height difference with measurements was 17 ft at 42040 and 10.4 ft at 42007. See the WAM section for discussions relevant to these differences. A thorough evaluation of the WAVEWATCH III and WAM Katrina final hindcasts follows in the Wave Model Performance section.

<b>Table 3-6 Satellite Altimeter Passes used for Hurricane Katrina Hindcast Evaluation</b>		
<b>Pass</b>	<b>Satellite</b>	<b>Date and Time (UTC)</b>
1	ENVSAT	28 August 0400
2	ENVSAT	28 August 1600
3	JS1	29 August 1600

Satellite altimetry data was used as an additional validation of the Hurricane Katrina basin-level final wave model hindcast results. Wave height altimeter results were available from three sources: 1) Envisat (ENVSAT) operated by European Space Agency, 2) Jason (JS1) operated jointly by NASA and French Space Agency CNES, and 3) Geosat Follow-On (GFO) operated by the U.S. Navy. Of the satellite passes over the Gulf of Mexico during Hurricane Katrina, the three events listed in Table 3-6 produced information that was co-located with the severe portion of the storm. Data from all three passes are compared to WAVEWATCH III hindcast results in Figures 3-48 to 3-50. Of these, the ENVSAT pass on 28 August was the closest to a “direct hit” on the storm center and measured significant wave heights up to 26 ft. A comparison of the

observed and hindcast wave heights for this event appears in Figure 3-32. Figure 3-32 plots the consecutive satellite observations (red) with collocated points from the Wavewatch III Katrina final hindcast (blue). The satellite moved from the back of Katrina in a northwest direction and observations 100 and above show comparisons with the left front quadrant of the storm. As with the NDBC buoy data, the altimetry data indicates that the model wave heights are biased low especially in the right front quadrant of the storm, with this event exhibiting a mean bias of -1.57 ft.

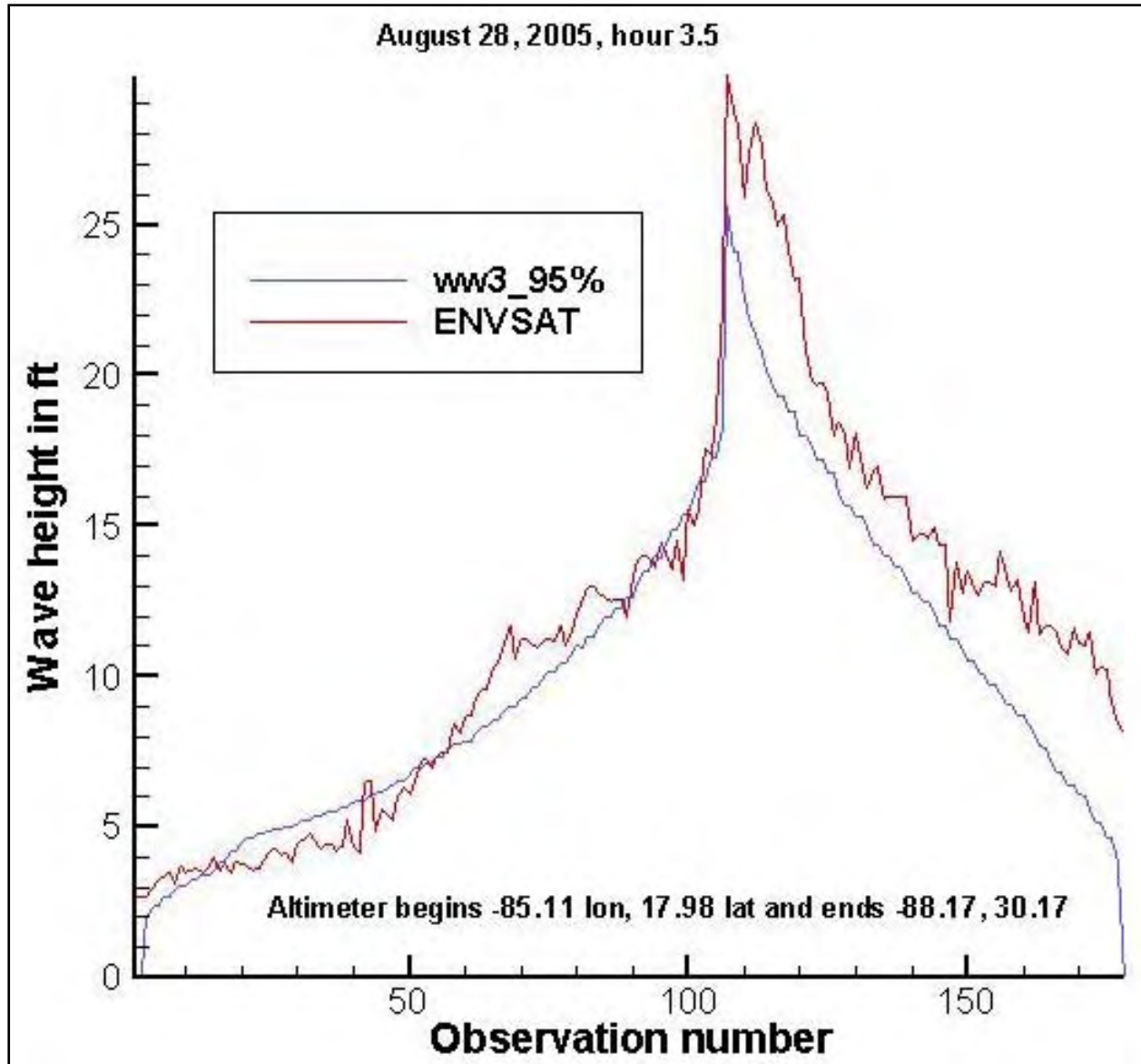


Figure 3-32. ENVSAT satellite altimetry track for 28 August 0330 UTC with co-located points from the WAVEWATCH III significant wave height hindcast. Observation numbers refer to consecutive measurements as the satellite passed over the storm. Altimeter measurements begin at 85.11 W Longitude, 17.98 Latitude and end 88.17 W Longitude, 30.17 Latitude.



## Wave Model Performance

The performance of the final solution WAM and WAVEWATCH III simulations was evaluated using the available NDBC buoy observations. The USACE Wave Model Evaluation and Diagnostics System (WaveMEDS) was employed to make the model-data comparisons. WaveMEDS uses a variety of performance metrics to determine hindcast accuracy at the wave component (wind sea, mature swell, and young swell) level. The final wind field results indicate that the overall performance of both models is quite similar, with the WAM hindcast slightly outperforming the WAVEWATCH III hindcast for this hurricane event.

### Approach

Output wave spectra from the basin-scale runs of both WAM and WAVEWATCH III were compared to the results of NDBC buoy observations at stations 42001, 42003, 42007, 42036, 42038, 42039, and 42040. These locations are identified in Figure 3-8 and listed in Table 3-3. The approach employs a spectral partitioning algorithm to isolate individual wind sea and swell wave components in the buoy spectra (Hanson and Phillips 2001). The frequency and direction domains associated with each dominant peak in a wave spectrum form a spectral partition that is associated with that particular wave component. The significant wave height, peak wave period, and mean wave direction of each of these spectral components are then statistically compared to the identical regions in the model output spectra (Hanson and Jensen 2005). The original intent was to perform this analysis on the full directional wave spectra. However, mooring-induced motions during the hurricane corrupted the directional data at most of the buoy stations. Hence this analysis was limited to the one-dimensional (energy-frequency) spectra  $E(f)$ .

The WaveMEDS analyses allows for the computation of model performance for a variety of wind sea and swell parameters. First, the isolated wave components at each station are divided into three wave component classes: wind sea, young swell, and mature swell. A wave age criterion is used to classify spectral peaks that are forced by the existing wind as wind sea. Remaining wave components that have a peak frequency of 0.09 Hz or greater are classified as young swell, and those with a peak frequency less than 0.09 Hz are classified as mature swell. This frequency division was found to be a somewhat natural separation between regionally-generated young swell and swell that has traveled significant distances (Hanson, unpublished data). For each wave component spectral domain, WaveMEDS computes the total wave energy

$$E = \int S(f)df ;$$

the significant wave height, approximated by  $H_{mo}$

$$H_s \approx H_{mo} = 4\sqrt{E} ;$$

and the peak wave period

$$T_p = \frac{1}{f_p},$$

with the peak wave frequency  $f_p$  computed from a 3-point parabolic fit to the  $S(f)$  spectral peak.

These computations are performed over the identical wave partition frequency domains in both the observed and hindcast spectra. This results in a unique set of paired wave component parameters for each model run. The hindcast wave component parameters are evaluated against the observed quantities using both temporal correlation (TC) and quantile-quantile (QQ) distributions. The TC analysis provides an indication of how well the hindcast quantities match the observed quantities in absolute time. For example, a time offset in identical hindcast magnitudes would degrade the TC results. In contrast, the QQ analysis is used to indicate if the correct parameter magnitudes are reached, regardless of occurrence time. For an assessment of engineering loading, a correct time sequence may not be as important as having a proper distribution of parameter magnitudes.

A variety of established metrics are used to quantify the TC and QQ comparisons. For the series of buoy measurements  $m$  and hindcasts  $h$  these metrics include the bias (hindcast-buoy)

$$b = \frac{1}{n} \sum h - m;$$

root-mean-square (RMS) error

$$E_{RMS} = \left[ \frac{\sum (h - m)^2}{n} \right]^{0.5};$$

and the scatter index

$$SI = \frac{\sigma_d}{\langle m \rangle},$$

where the standard deviation of difference is given by

$$\sigma_d = \left[ \frac{\sum_i (h_i - m_i - b)^2}{n - 1} \right]^{0.5}$$

(Cardone et al. 1996). The definition of the SI above differs from the versions cited in Appendix 2 and earlier in this Appendix by a factor of 100 only. These error statistics are computed over the entire duration of the hurricane hindcast at each station.

The evaluation metrics are converted into performance scores that are normalized to mean quantities. These scores provide a basis for combining the results from multiple stations into an overall model performance for each parameter (wave height and period). These estimators include the RMS Error performance

$$\hat{E}_{RMS} = \left( 1 - \frac{E_{RMS}}{m_{RMS}} \right);$$

the bias performance

$$\hat{b} = \left( 1 - \frac{|b|}{m_{RMS}} \right);$$

and the scatter index performance

$$\hat{SI} = (1 - SI),$$

where the root-mean-square of the measurements is given by

$$m_{RMS} = \left( \frac{\sum m^2}{n} \right)^{0.5}.$$

The non-dimensional performance scores range from 0 (uncorrelated) to 1 (perfect correlation) and are averaged across metrics and stations using sample size weighting factors. Hence for a particular parameter, the station performance would be given by

$$P_s = \frac{\hat{E}_{RMS} + \hat{b} + \hat{SI}}{3},$$

with the weighted overall performance across stations

$$\bar{P} = \frac{\sum n_i P_{s_i}}{n_c},$$

where  $n$  denotes the total number of observations at each station ( $i$  subscript) and for all stations combined ( $c$  subscript).

## Basin-Scale Model Performance

The WaveMEDS technique was applied to the basin-scale final solution WAM and WAVEWATCH III results at the NDBC buoy ground truth stations 42001, 42003, 42036, 42038, 42039, and 42040 (See Figure 3-8 and Table 3-3). The overall (across-station) model performance scores for significant wave height and peak wave period appear in Tables 3-7 and 3-8, respectively. In each table, the results of the temporal correlations (TC) and the quantile-quantile (QQ) distributions are given for each wave system component.

<b>Table 3-7 Wave Height Performance Summary</b>				
<b>Component</b>	<b>Temporal Correlations</b>		<b>Quantile-Quantile</b>	
	<b>WAM</b>	<b>WW3</b>	<b>WAM</b>	<b>WW3</b>
Windsea	0.86	0.85	0.87	0.88
Young Swell	0.75	0.74	0.76	0.78
Mature Swell	0.85	0.72	0.87	0.73
Combined	0.83	0.80	0.84	0.82

<b>Table 3-8 Wave Period Performance Summary</b>				
<b>Component</b>	<b>Temporal Correlations</b>		<b>Quantile-Quantile</b>	
	<b>WAM</b>	<b>WW3</b>	<b>WAM</b>	<b>WW3</b>
Windsea	0.93	0.89	0.95	0.92
Young Swell	0.90	0.85	0.91	0.86
Mature Swell	0.93	0.87	0.95	0.89
Combined	0.92	0.88	0.94	0.90

The final combined scores provide a weighted performance across all wave system components.

Overall, the wave height performance scores are reasonably good for both models. The combined wave height and peak period scores for WAM show a 2-4 percent improvement over WAVEWATCH III for both TC and QQ statistical analyses. WAM and WAVEWATCH III wind sea heights depict only 1 percent difference, while WAM wind sea periods exhibit a 3-4 percent improvement over WAVEWATCH III. Most significant for this study, however, are a 14 percent improvement in mature swell heights by WAM over WAVEWATCH III, and a corresponding 6 percent improvement in WAM mature swell wave periods. These large waves propagated away from Katrina as the hurricane moved north across the Gulf of Mexico.

Further detail on model performance is given by the WAM and WAVEWATCH III station wave height summary plots in Figures 3-33 and 3-34, respectively. Here the wave model TC performance scores at each station are compared in each of the wave component classes. In these plots, Swell 1 refers to the young swell class and Swell 2 refers to the mature swell class. The absence of a bar in a wave component plot, for example young swell at station 42003, indicates



that no wave observations of that wave component were made at that particular station. The gross features of the WAM and WAVEWATCH III results are very similar, suggesting only minor differences between the models. Furthermore, the variation in wave model performance across stations is also fairly consistent with the exception of the Station 42038, which exhibited consistently poorer performance in both models. It should be noted that Station 42038 was the furthest west of the storm track.

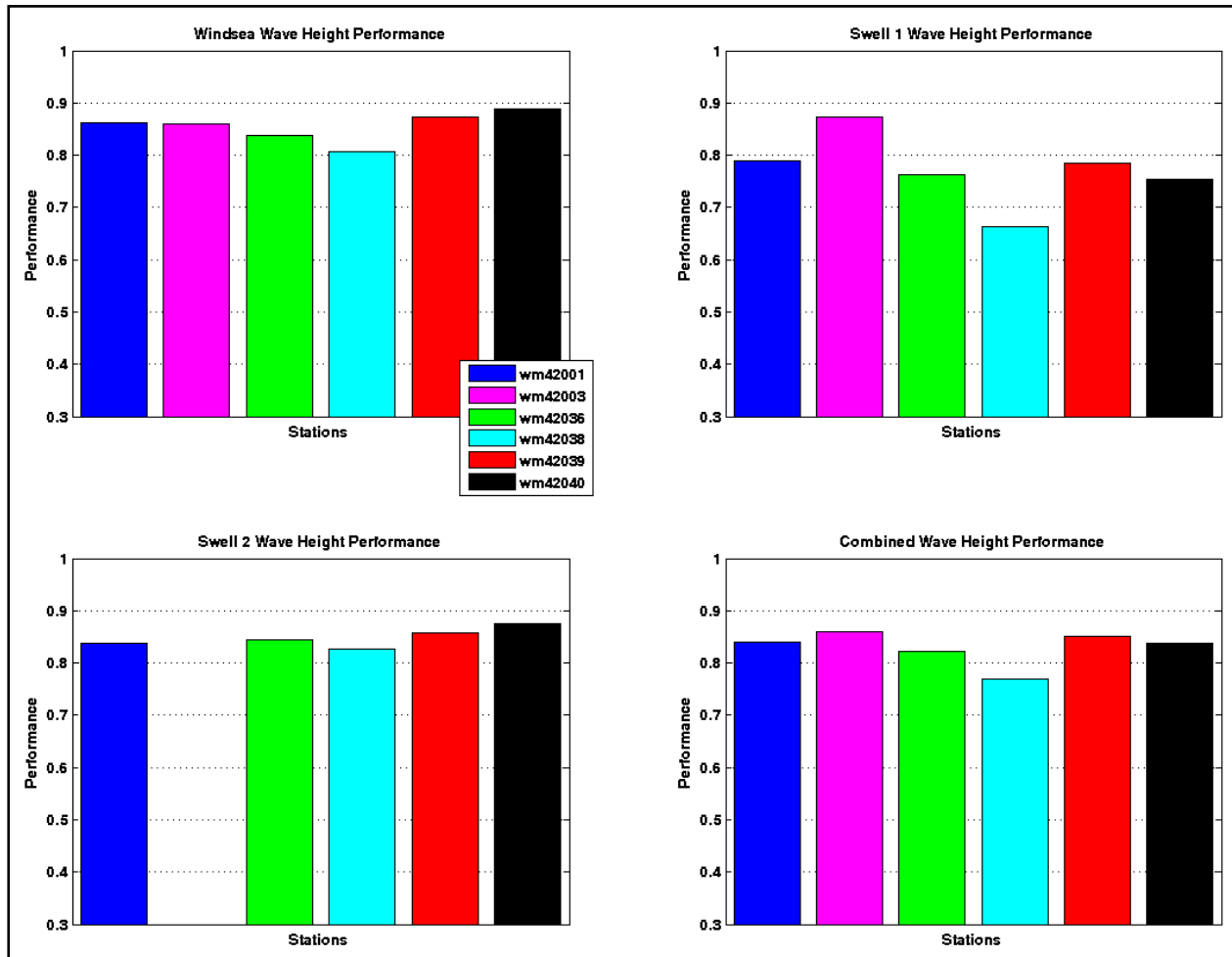


Figure 3-33. WAM temporal correlation wave height performance by station.

The best combined performance in both models was at stations 42001 and 42003, which are mid-gulf buoys that are furthest away from the coast. A summary of observed and predicted wave height at each validation station appears in Figure 3-35. A diagnostic evaluation of the model-observation discrepancies appears in the following section.

### Model Diagnostics

Although the performance scores provide a unique assessment of model skill by station and by wave component class, they provide little insight into the mechanics behind the performance of each model. The nature of these hindcast errors can best be visualized through inspection of

the temporal correlation (TC) and quantile-quantile (QQ) analysis results that were used to compute the performance scores. The attributes of the hindcast errors are summarized below for selected stations. The full set of statistical results for WAM and WAVEWATCH III appears in Figure 3-51 to 3-94.

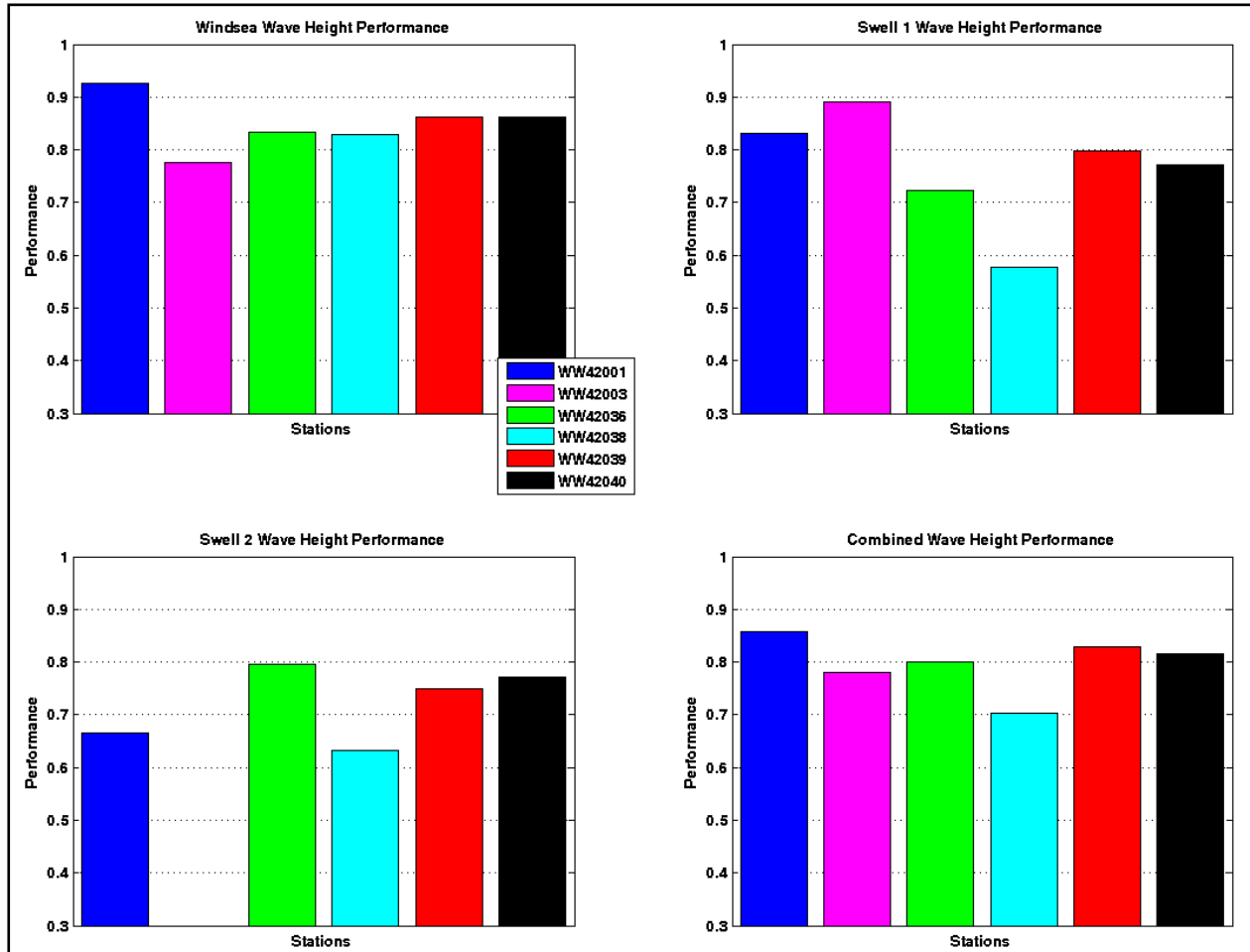


Figure 3-34. WAVEWATCH III temporal correlation wave height performance by station.

Example WAM and WAVEWATCH III QQ distributions from three observation stations appear in Figure 3-36. The subplots of Figure 3-36 separately display the QQ distribution of each wave component class for that station and model run. A solid diagonal black line indicates where the data would lie for a perfect match of hindcast and observed wave heights. When data fall above the line the model is predicting values that are too high (biased high), and when data fall below the line the model is predicting values that are too low.

Even a cursory glance at Figure 3-36 reveals that both models predict lower than observed wave heights most of the time. The first station represented in Figure 3-35 is the mid-gulf station 42001, which have high combined performance scores for both WAM and WAVEWATCH (Figures 3-33 and 3-34). The WAM QQ distributions for this station are reasonable for wave heights up to 13 ft (4 m), and are biased high for the extreme wave heights. This is the only station where WAM hindcast wave heights were too high. In contrast, the WAVEWATCH III

mature swell (Swell 2) heights at station 42001 are biased low. In contrast to this station, station 42038 received the worst performance scores in both wave models and is the second station featured in the QQ plots of Figure 3-36. At this station the wave heights in both models tend to be biased low, with the mature swells in WAVEWATCH III under-predicted by nearly 5 ft in height at times. The remaining stations all reveal a general trend of hindcast wave heights biased low, with WAM exhibiting slightly improved results over WAVEWATCH III (Figure 3-36 and Figures 3-51 to 3-94).

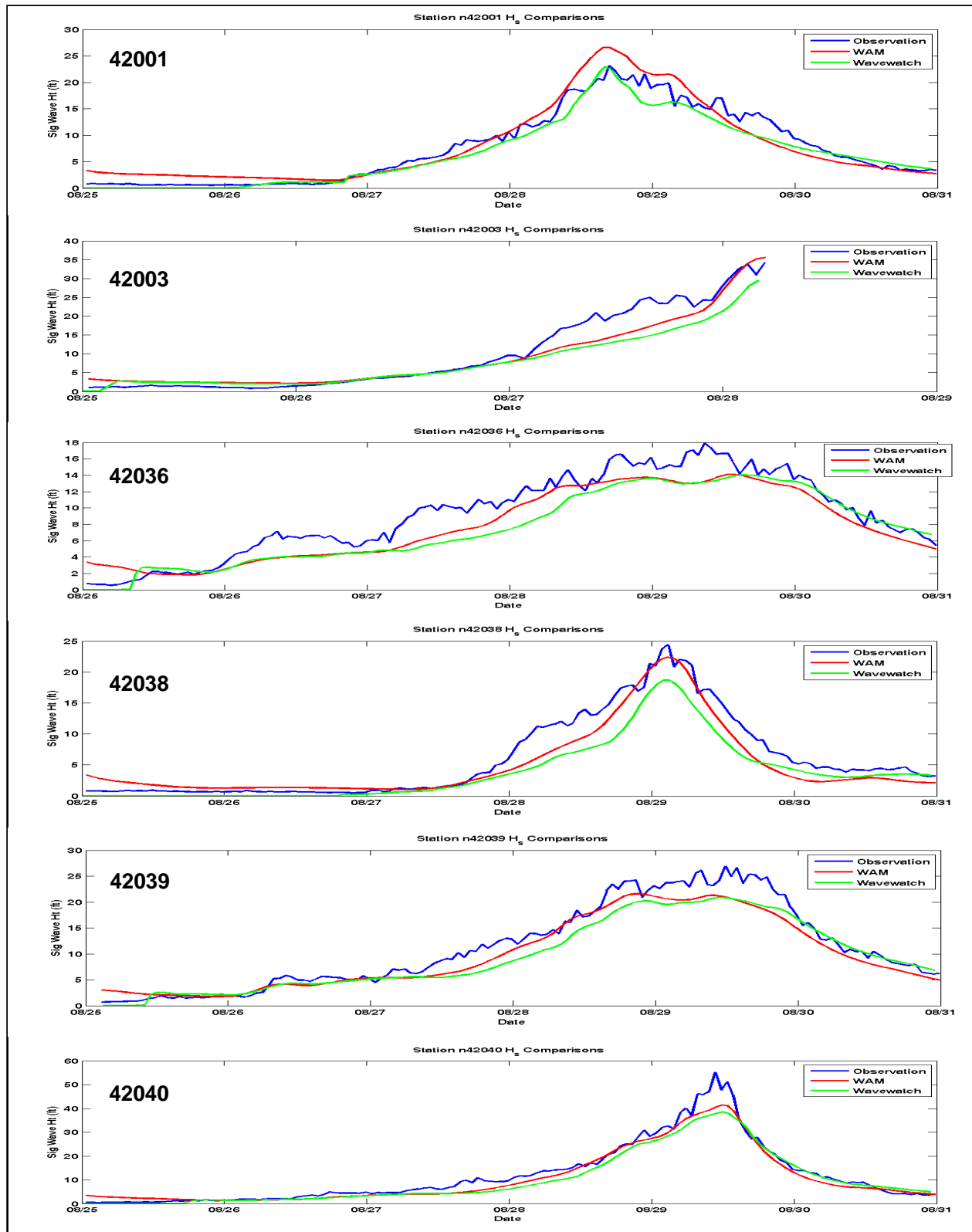


Figure 3-35. Comparison of significant wave heights (ft) from observation stations (blue), WAM hindcast (red), and WAVEWATCH III hindcast (green)



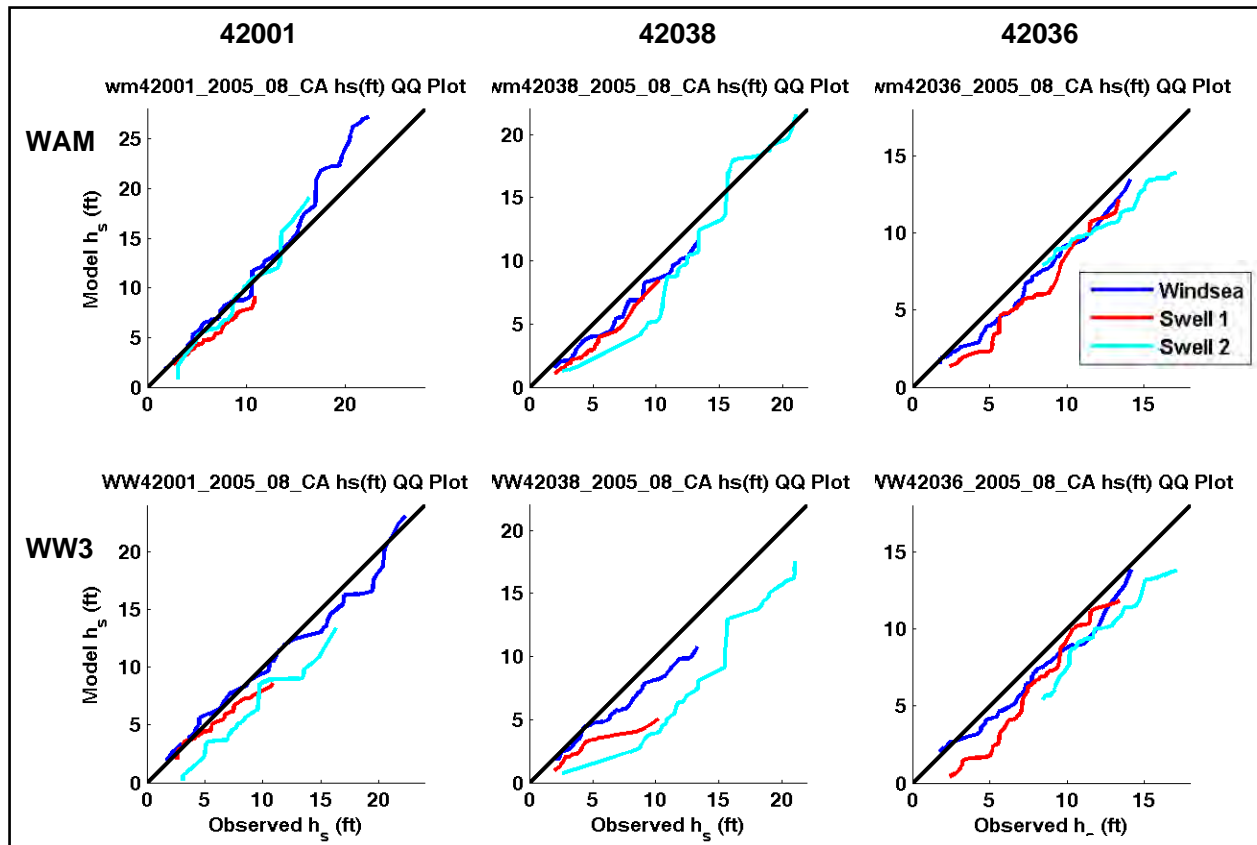


Figure 3-36. Quantile-quantile wave height distributions at 3 buoy stations. Top row: WAM hindcast. Bottom row: WAVEWATCH III hindcast

As the TC and QQ results reveal, the most significant issue with the WAM and WAVEWATCH III basin-scale hindcast results is a negative swell height bias at most of the observation stations.

## References

- Cardone, V. J., R. E. Jensen, D. T. Resio, V. R. Swail, and A. T. Cox. 1996. Evaluation of contemporary ocean wave models in rare extreme events: the “Halloween Storm” of October 1991 and the “Storm of the Century” of March 1993. *J. Atmos. Oceanic. Technol.*, **13**, 198-230.
- Cardone, V. J., H.C. Graber, R.E. Jensen, S. Hasselmann and M.J. Caruso. 1995. In search of the true surface wind field in SWADE IOP-1: Ocean waev modeling perspective. *Global Atmosp. And Ocean System*, **3(2-3)**, 107-150.
- Gunther, H. 2002. WAM Cycle 4.5, Institute for Coastal Research, GKSS Research Centre Geesthacht, 43 pp.
- Gunther, H. 2005. WAM Cycle 4.5 Version 2.0, Institute for Coastal Research, GKSS Research Centre Geesthacht, 38 pp.

- Hanson, J. L., and O. M. Phillips, 2001. Automated analysis of ocean surface directional wave spectra. *J. Atmos. Oceanic. Technol.*, **18**, 277-293.
- Hanson, J. L., and R. Jensen, 2005. Wave system diagnostics for numerical wave models. *Proceedings, 8<sup>th</sup> International Symposium on Wave Hindcasting and Forecasting*, Turtle Bay Resort, Honolulu, HI.
- Holthuijsen, L. H., N. Booij, and R. C. Ris. 1993. A spectral wave model for the coastal zone, *Proc. of 2<sup>nd</sup> Int. Symposium on Ocean Wave Measurement and Analysis*, New Orleans, USA, 630-641.
- Hubertz, J. A. 1992. User's guide to the Wave Information Studies (WIS) wave model, version 2.0. WIS Report 27, U.S. Army Engineer Waterways Experiment Station, Vicksburg, MS.
- Jensen, R. E. and V. J. Cardone. 2005. Modeling in the Core of Hurricanes: Perspectives from the 2004 Hurricane Season. Waves in Shallow Water Environments Presentation.
- Knabb, R. D. Rhone, J. R. and D. P. Powell. 2005. Tropical Cyclone Report Hurricane Katrina 23-30 August 2005. NOAA, National Hurricane Center, 42 pp.
- Komen, G. J., L. Cavaleri, M. Donelan, K. Hasselmann, S. Hasselmann, and P. A. E. M. Janssen. 1994. Dynamics and modelling of ocean waves. Cambridge University Press, Cambridge, UK, 560 pp.
- Powell, M. D., S. H. Houston, L. R. Amat, N. Morisseau-Leroy. 1998. The HRD real-time hurricane wind analysis system. *J. Wind Engineer. Ind. Aerody.*, **77&78**, 53-64.
- Ris, R. C. 1997. Spectral modeling of wind waves in coastal areas, (Ph.D. Dissertation Delft University of Technology, Department of Civil Engineering), Communications on Hydraulic and Geotechnical Engineering, Report No. 97-4, Delft, The Netherlands.
- SWAMP Group. 1985. Ocean Wave Modeling, Plenum, New York, 256 p.
- Teng, C. C., and R. H. Bouchard. 2005. "Directional wave data measured from data buoys using angular rate sensors and magnetometers," *Ocean Wave Measurements and Analysis*, Barcelona Spain, ASCE.
- Tolman, H. L. 1997. A New Global Wave Forecast System at NCEP. In: *Ocean Wave Measurements and Analysis*, Vol. 2, (Ed: B. L. Edge and J. M. Helmsley), ASCE, 777-786.
- Tolman, H. L. 1999: User Manual and System Documentation of WAVEWATCH-III version 1.18. Technical Note, 110 pp.
- Tolman, H. L. 2002. User manual and system documentation of WAVEWATCH-III version 2.22. Technical Note, U.S. Department of Commerce, NOAA, NWS, NCEP, Washington, DC.
- Tolman, H. L. and D. V. Chalikov. 1996. Source terms in a third-generation wind-wave model. *J. Phys. Oceanogr.*, **26**, 2497-2518.
- Uhlhorn, E.W., and P.G. Black. 2003. Verification of remotely sensed sea surface winds in hurricanes. *J. Atmos. Oceanic. Technol.*, **20**, 99-116.
- Wessel, P., and W. H. F. Smith. 1996 A Global Self-consistent, Hierarchical, High-resolution Shoreline Database, *J. Geophys. Res.*, **101**, #B4, 8741-8743.

# Verification of the Final WAM Wave Model Estimates during Hurricane Katrina

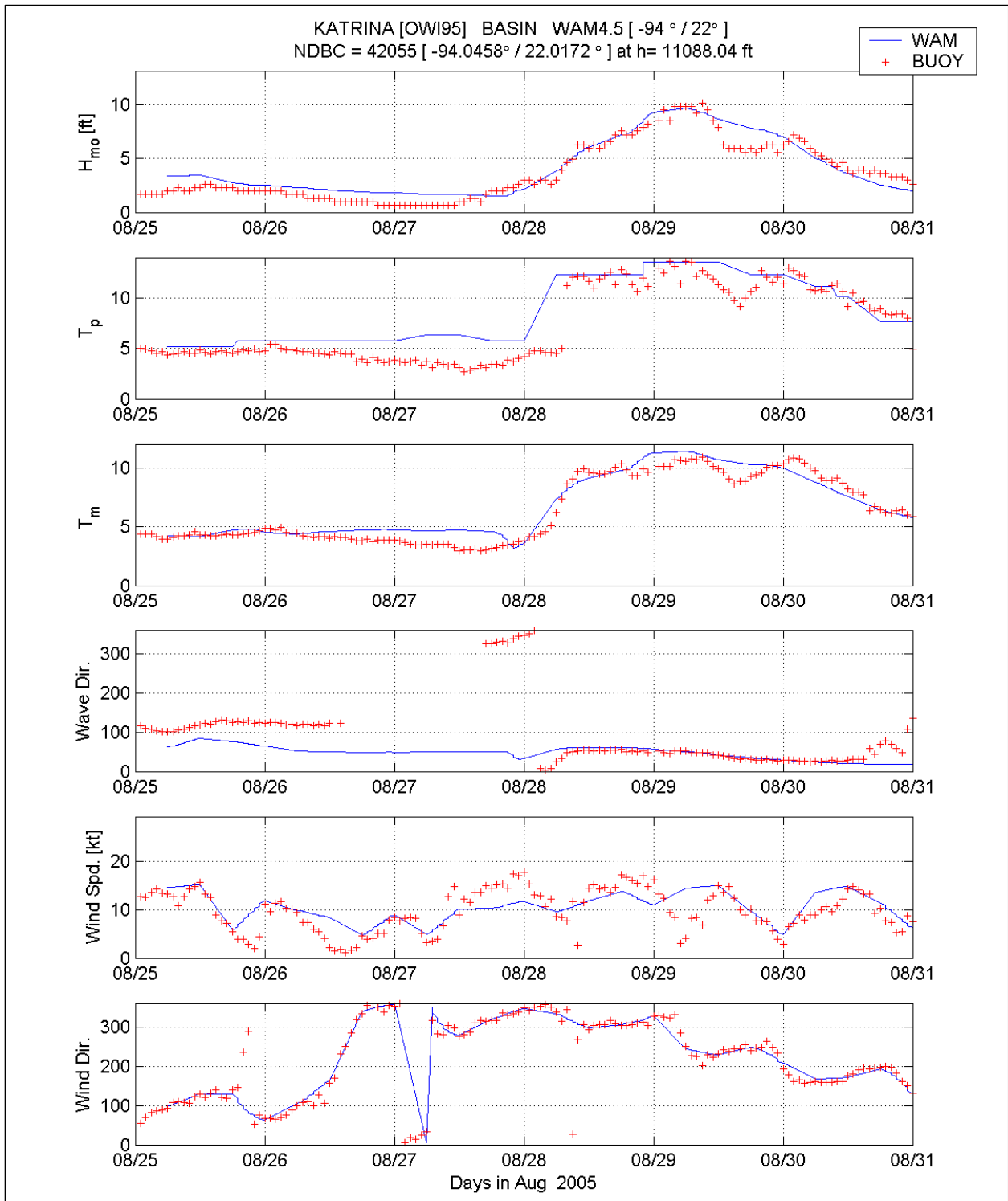


Figure 3-37. Comparison of WAM Cycle 4.5 basin-scale (blue line) to the measurements at NDBC 42055

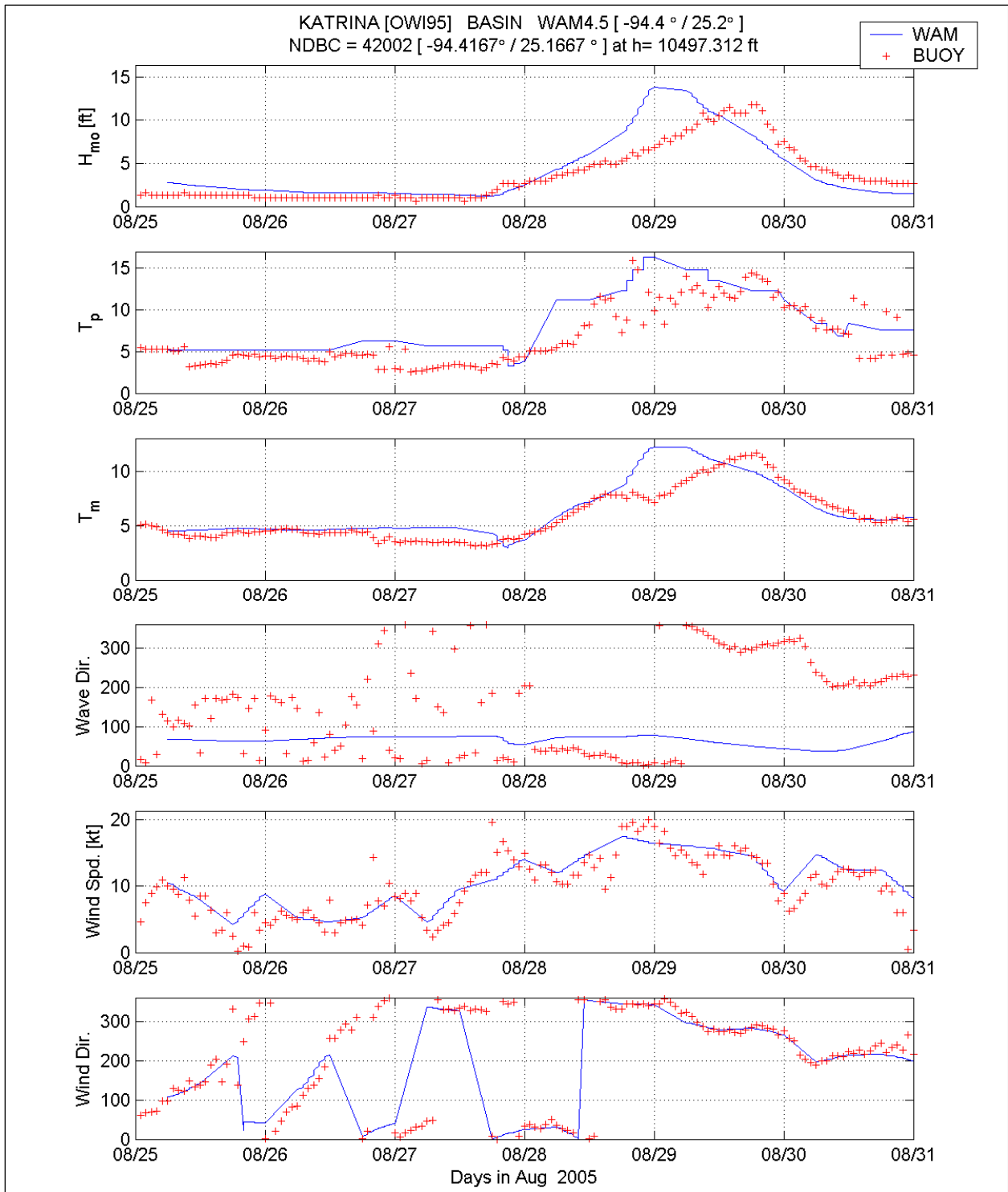


Figure 3-38. Comparison of WAM Cycle 4.5 basin-scale (blue line) to the measurements at NDBC 42002



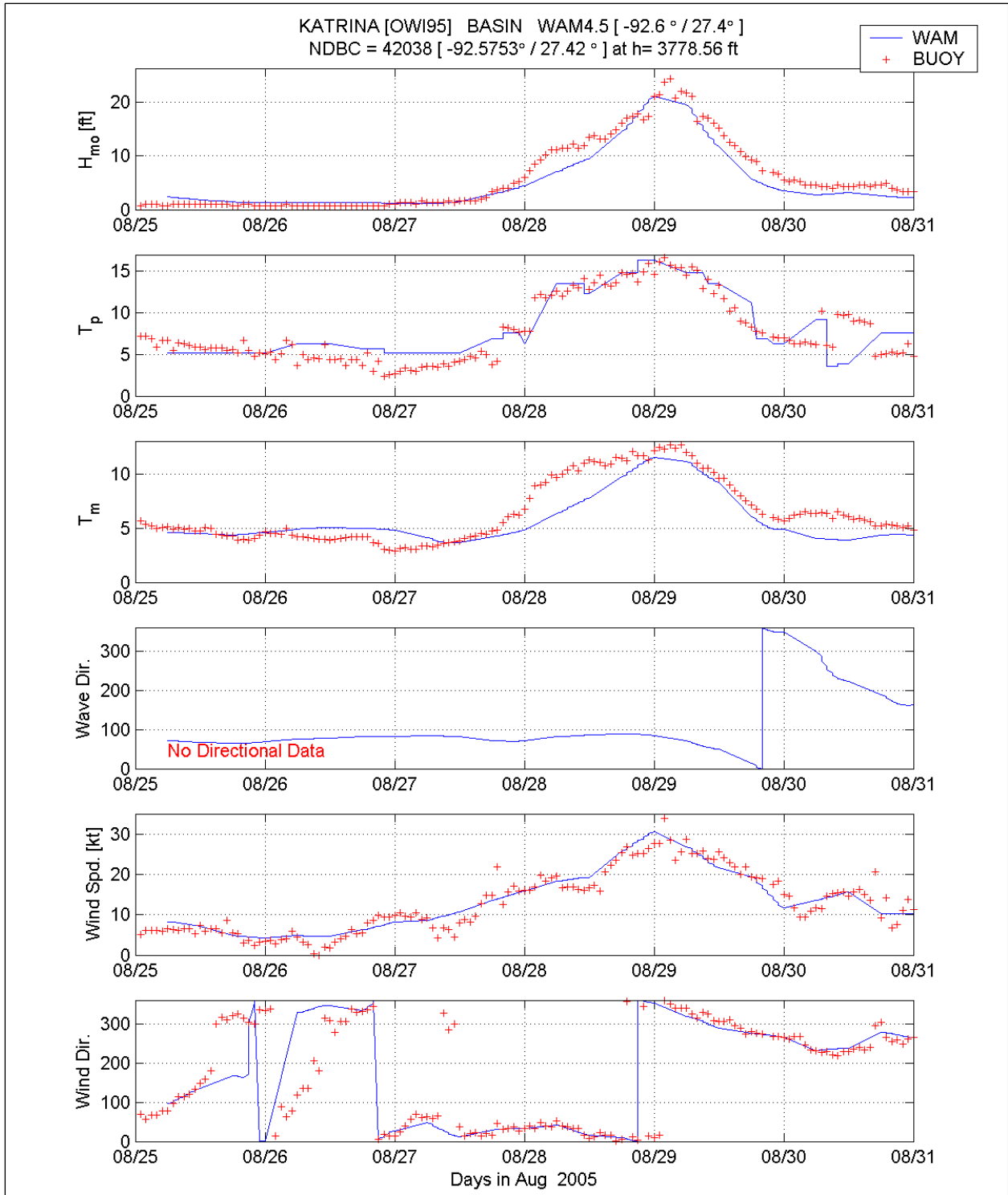


Figure 3-39. Comparison of WAM Cycle 4.5 basin-scale (blue line) to the measurements at NDBC 42038

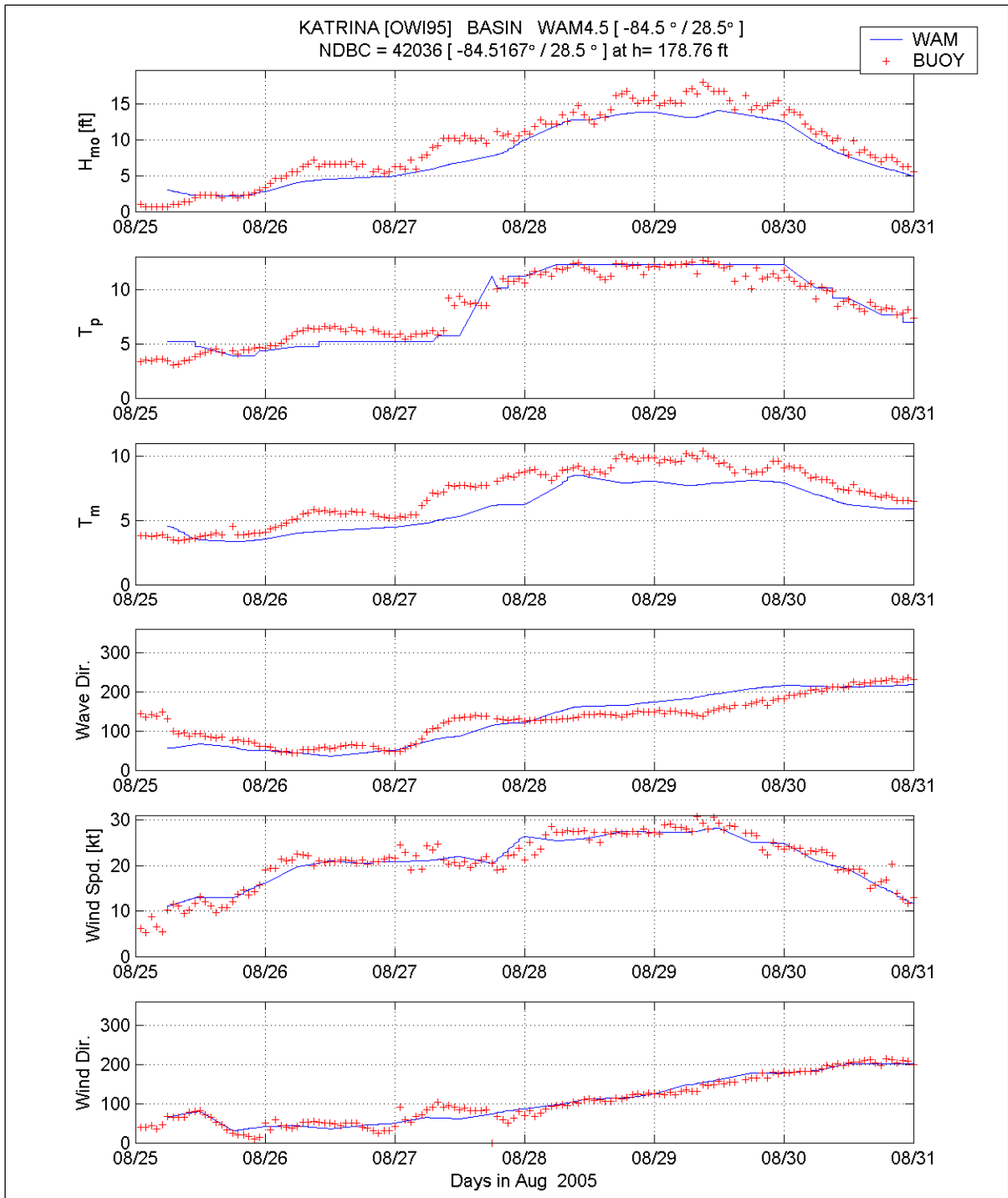


Figure 3-40. Comparison of WAM Cycle 4.5 basin-scale (blue line) to the measurements at NDBC 42036.

# Comparison of NDBC Buoy Observations with Final WAVEWATCH III Estimates during Hurricane Katrina

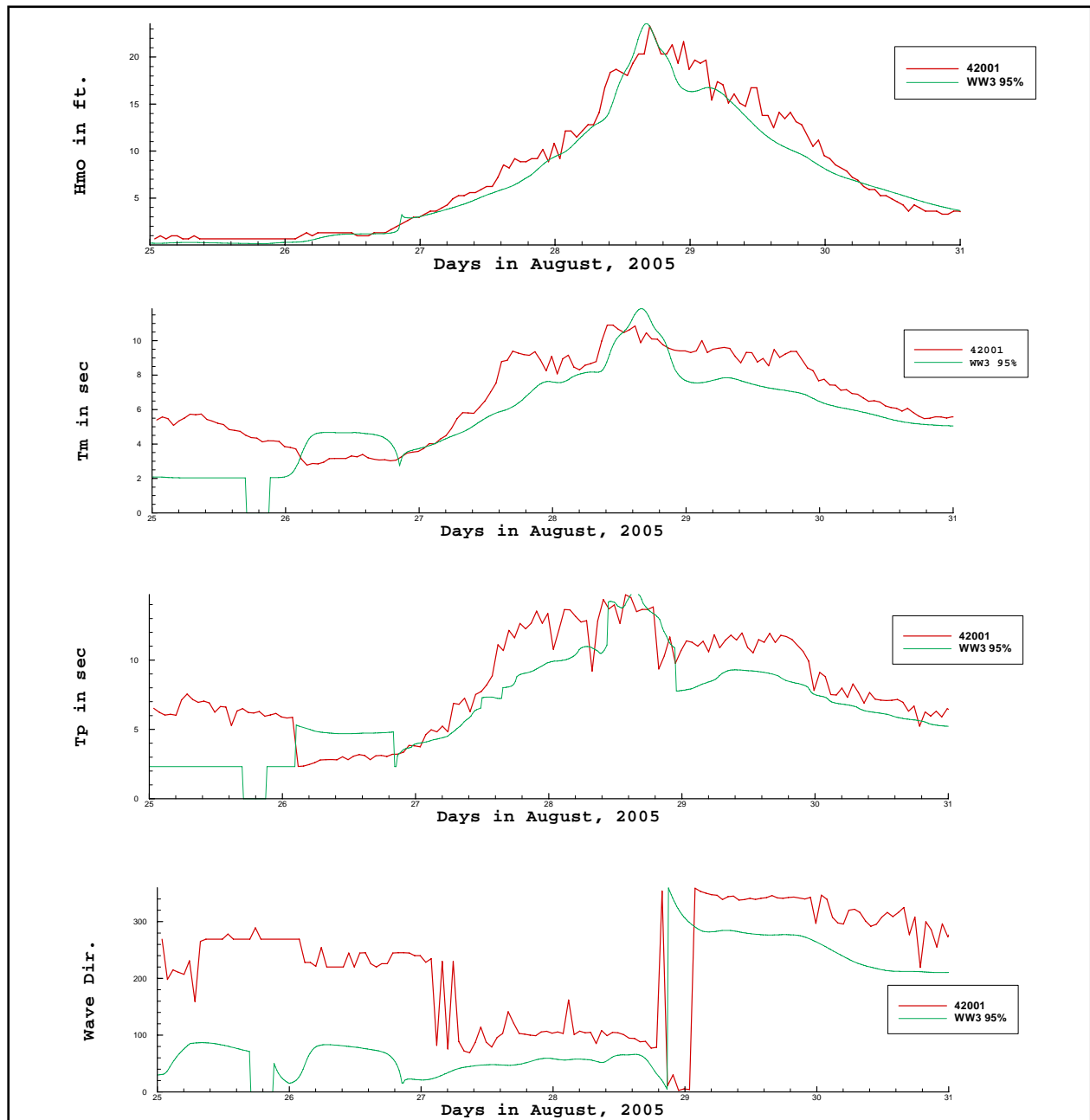


Figure 3-41. Comparison of NDBC buoy and WAVEWATCH III parameters at Station 42001

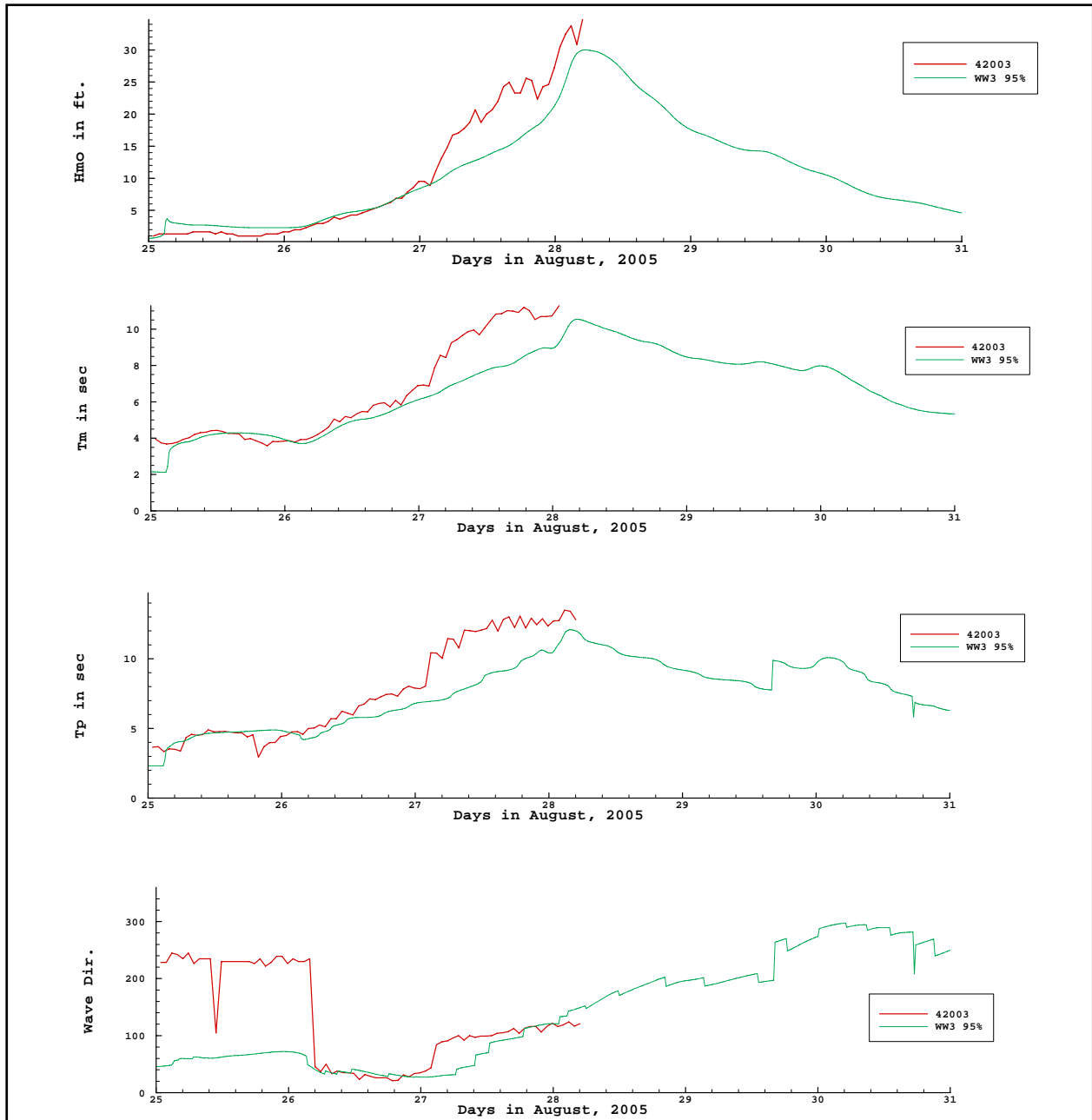


Figure 3-42. Comparison of NDBC buoy and WAVEWATCH III parameters at Station 42003



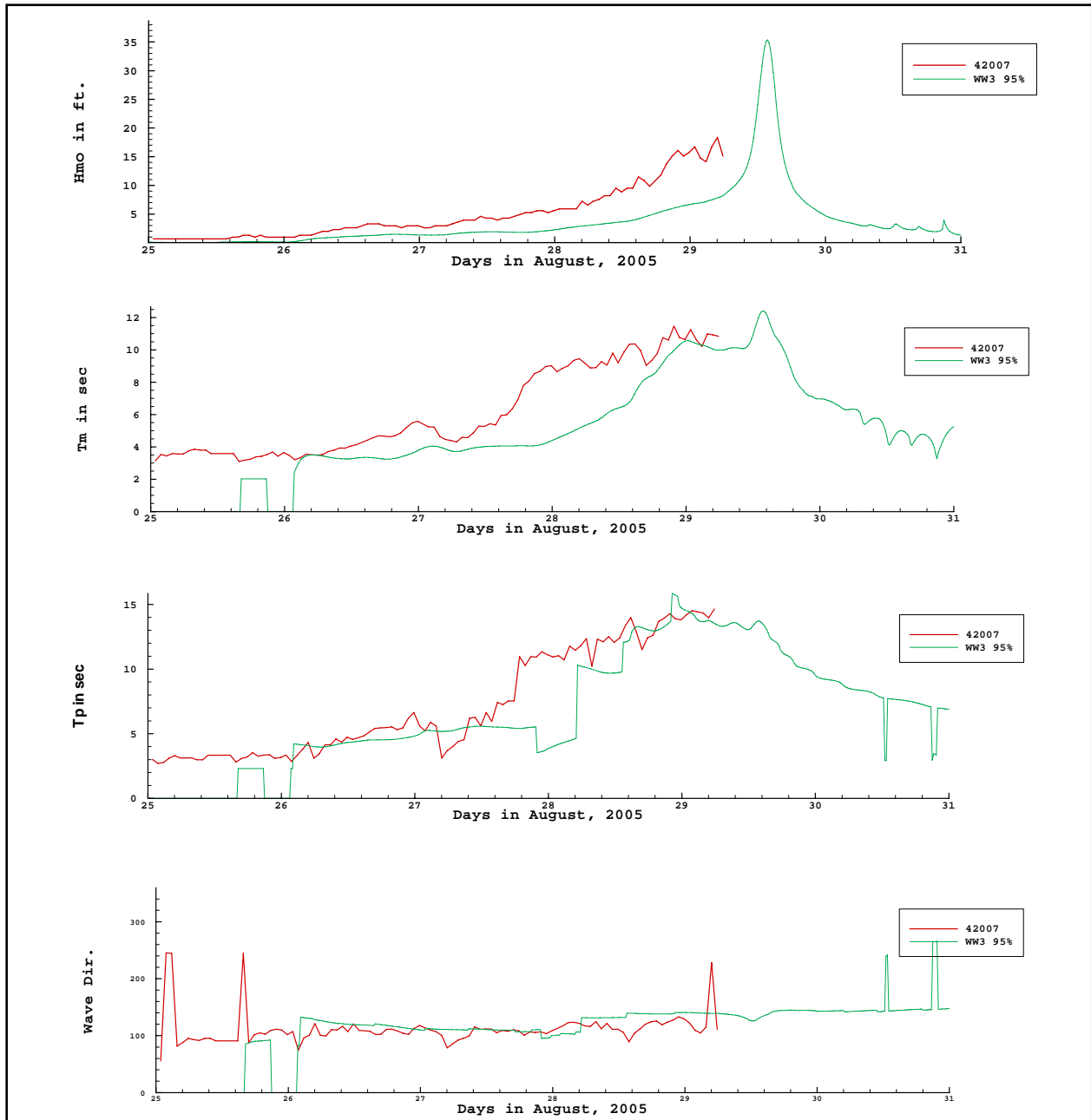


Figure 3-43. Comparison of NDBC buoy and WAVEWATCH III parameters at Station 42007

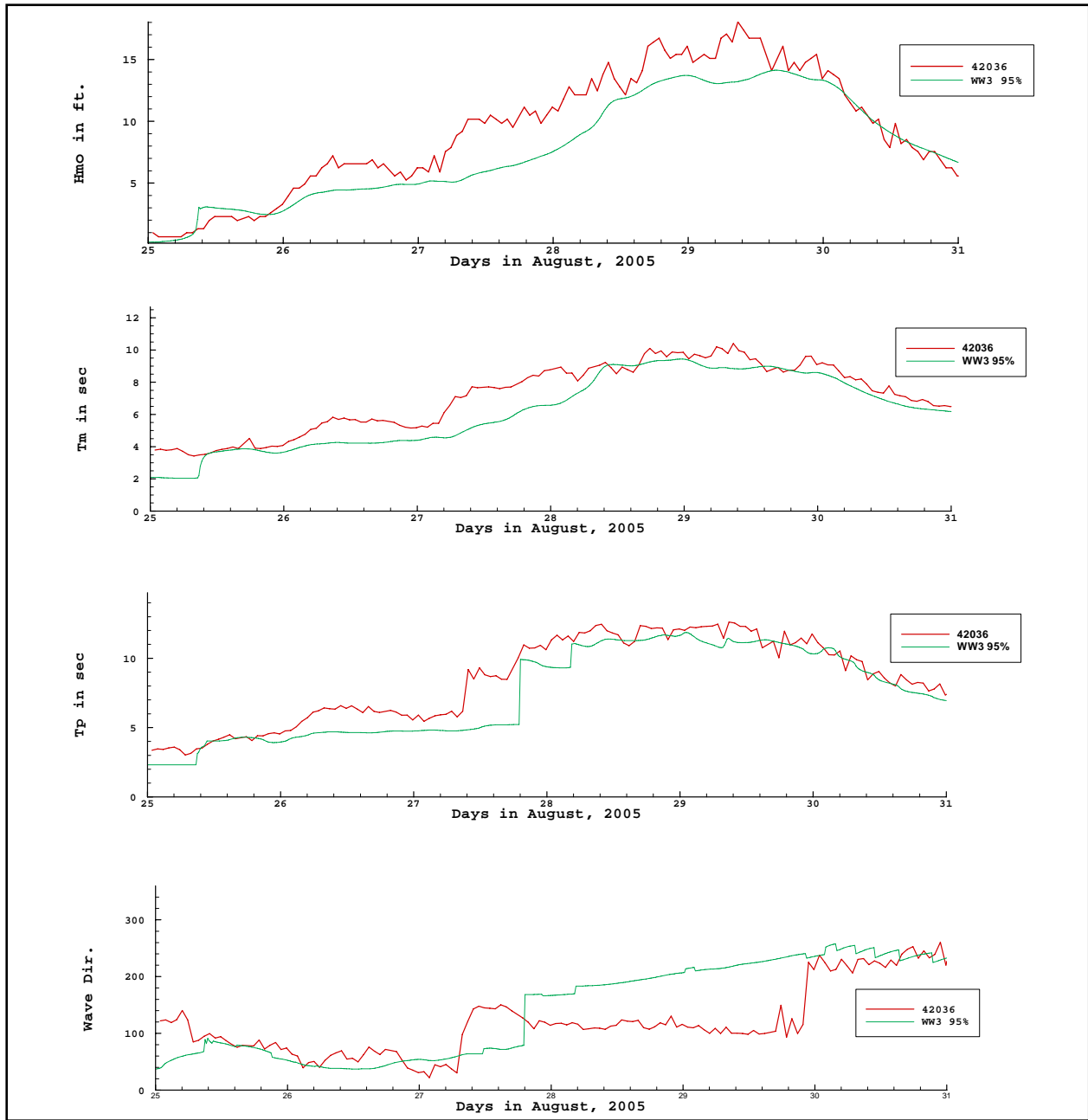


Figure 3-44. Comparison of NDBC buoy and WAVEWATCH III parameters at Station 42036

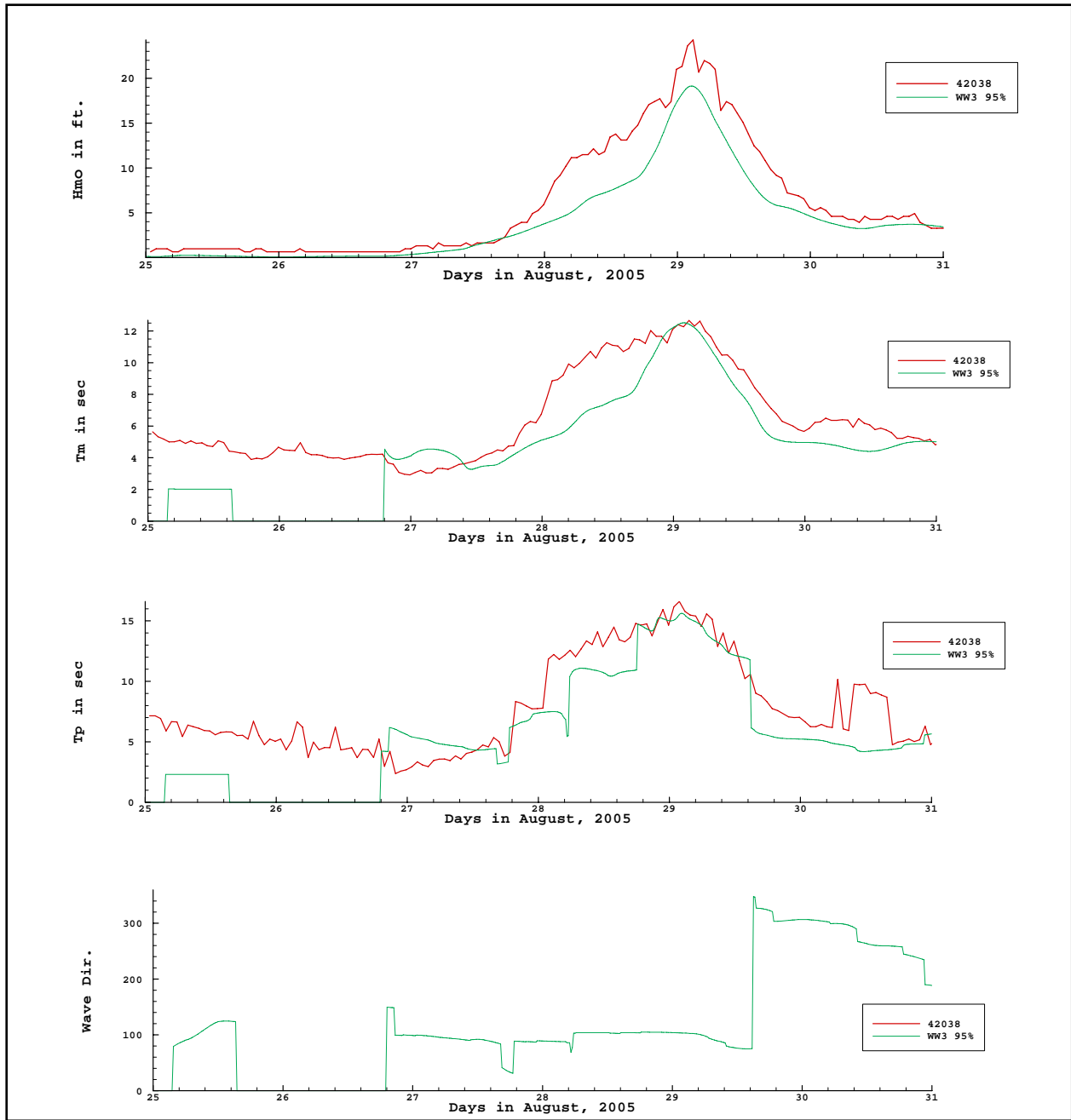


Figure 3-45. Comparison of NDBC buoy and WAVEWATCH III parameters at Station 42038

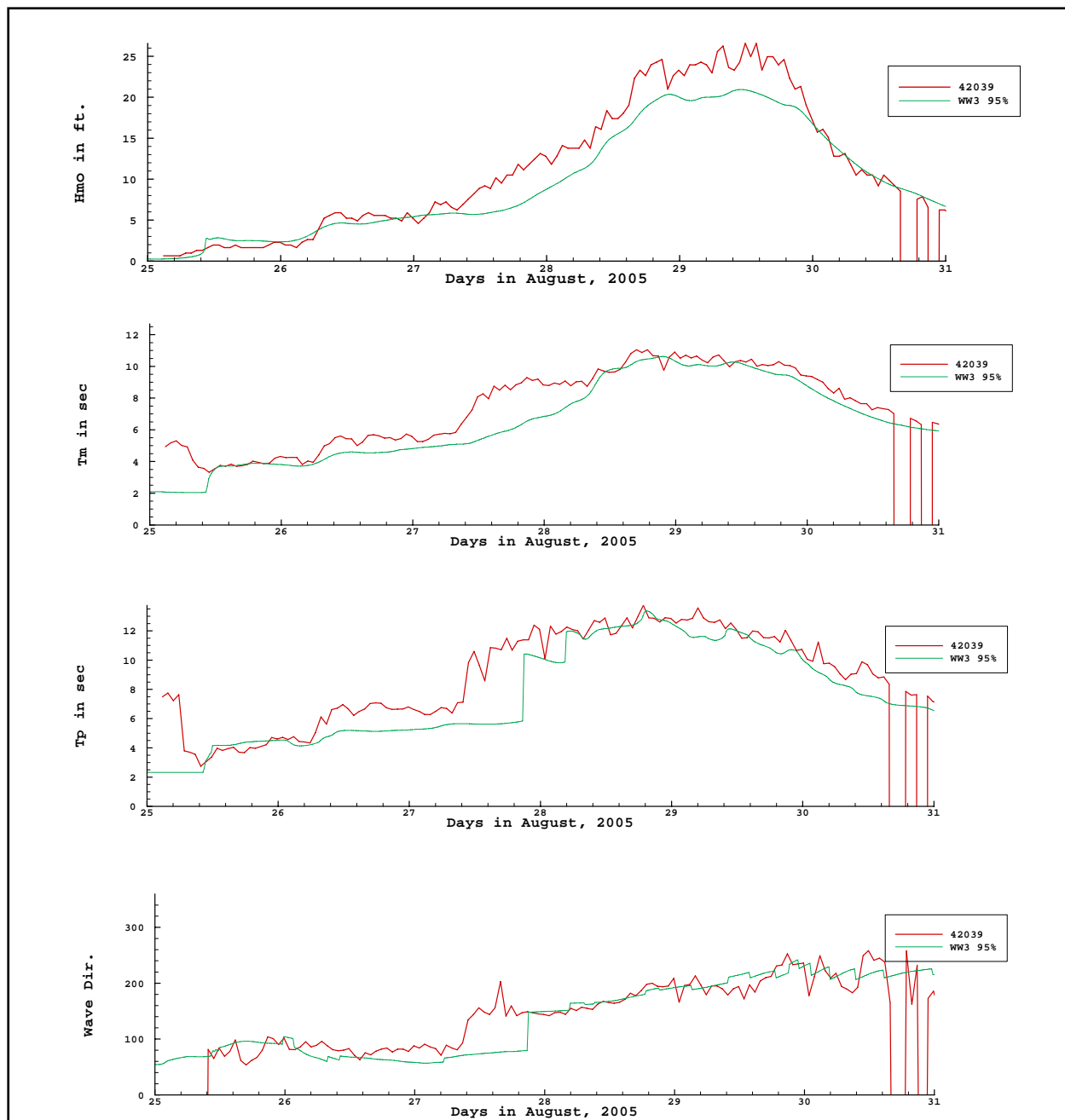


Figure 3-46. Comparison of NDBC buoy and WAVEWATCH III parameters at Station 42039



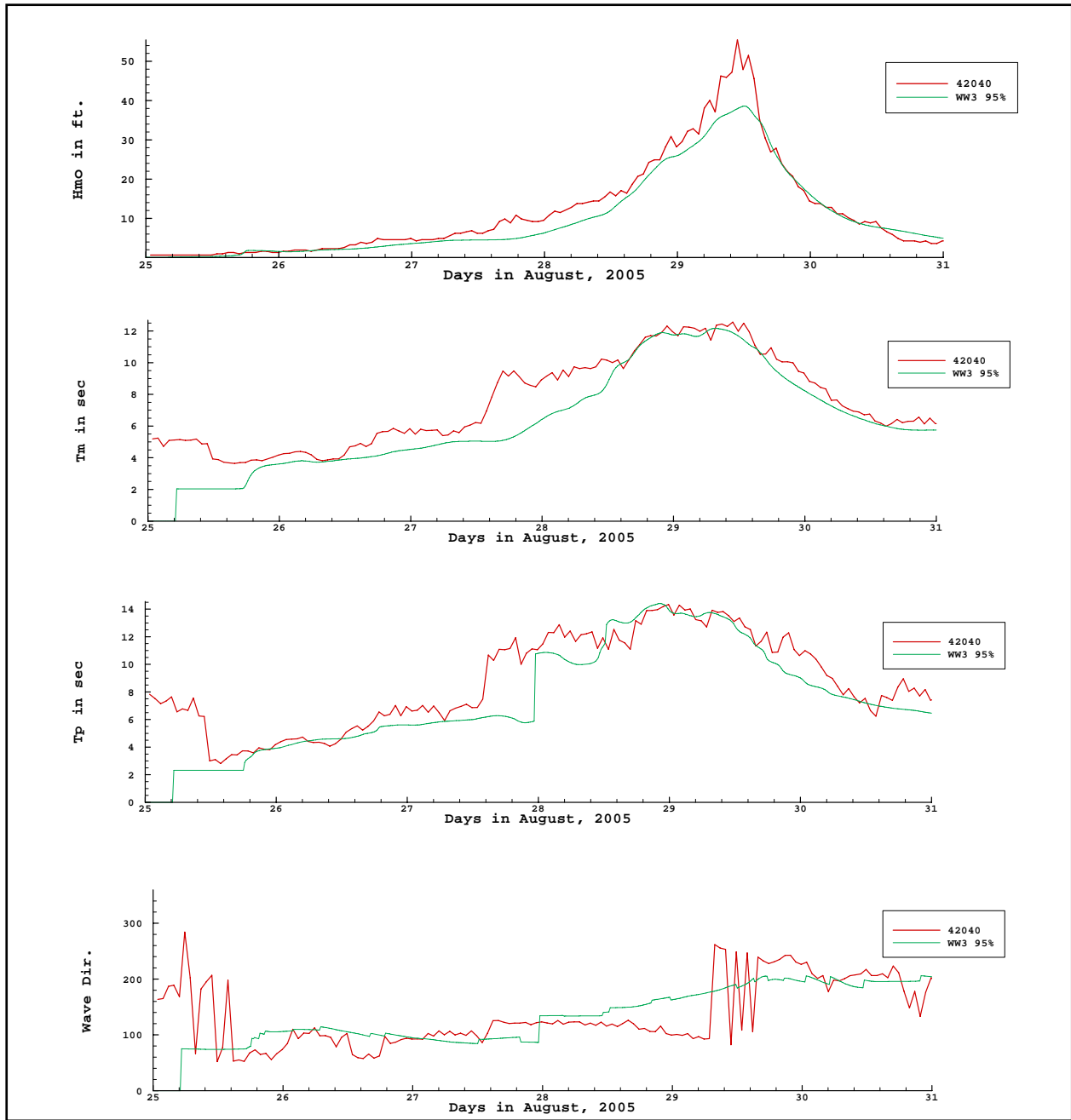


Figure 3-47. Comparison of NDBC buoy and WAVEWATCH III parameters at Station 42040

## Altimeter Comparisons with WAVEWATCH III

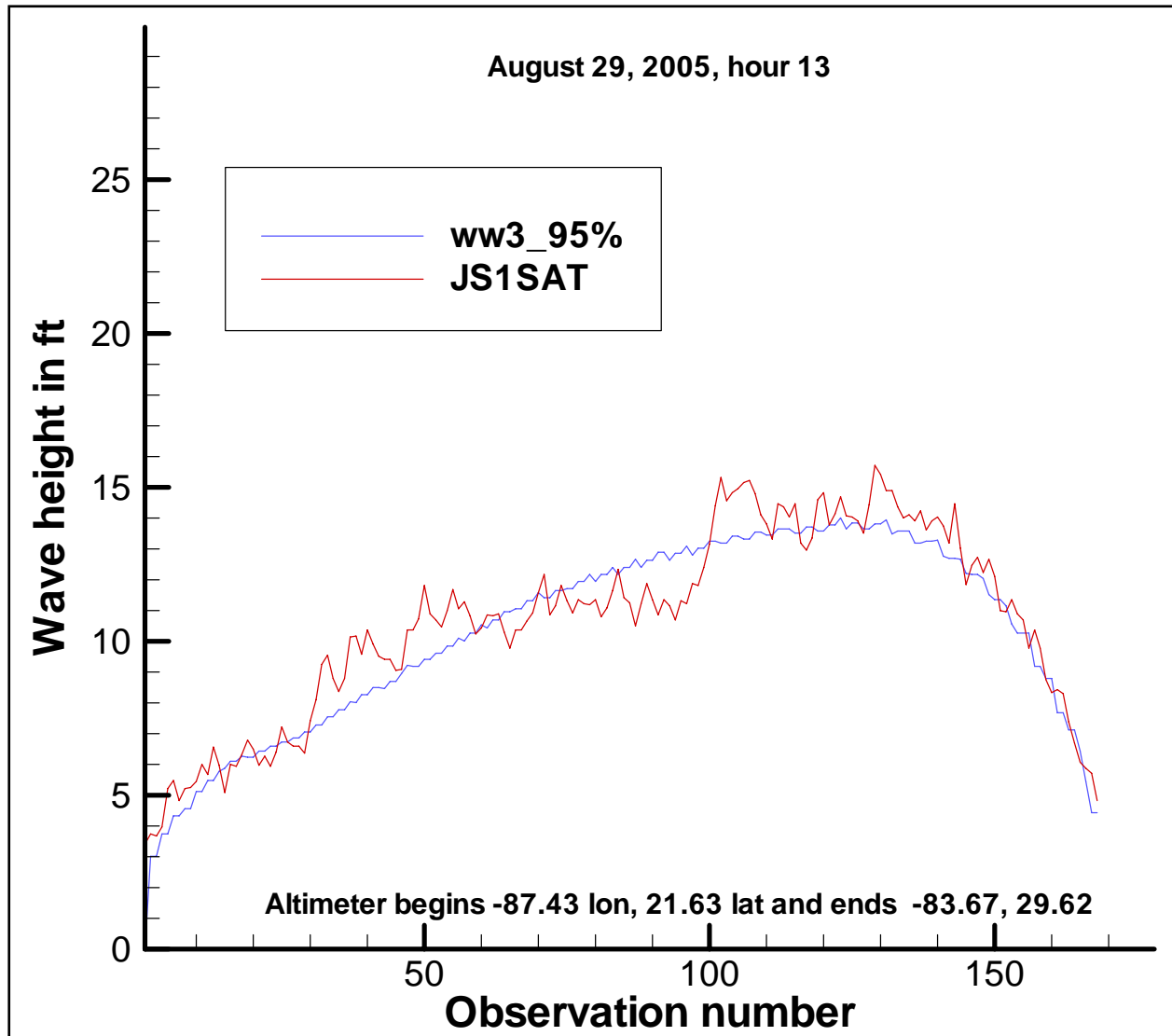


Figure 3-48. JS1 satellite altimetry track for 29 August 1300 UTC with co-located points from the final WAVEWATCH III significant wave height hindcast. Observation numbers refer to consecutive measurements as the satellite passed over the storm. Altimeter measurements begin at 87.43 W Longitude, 21.63 Latitude and end 83.67 W Longitude, 29.62 Latitude. Mean difference between WW3 and altimeter measurements is -0.31ft indicating WW3 is slightly lower than measurements.

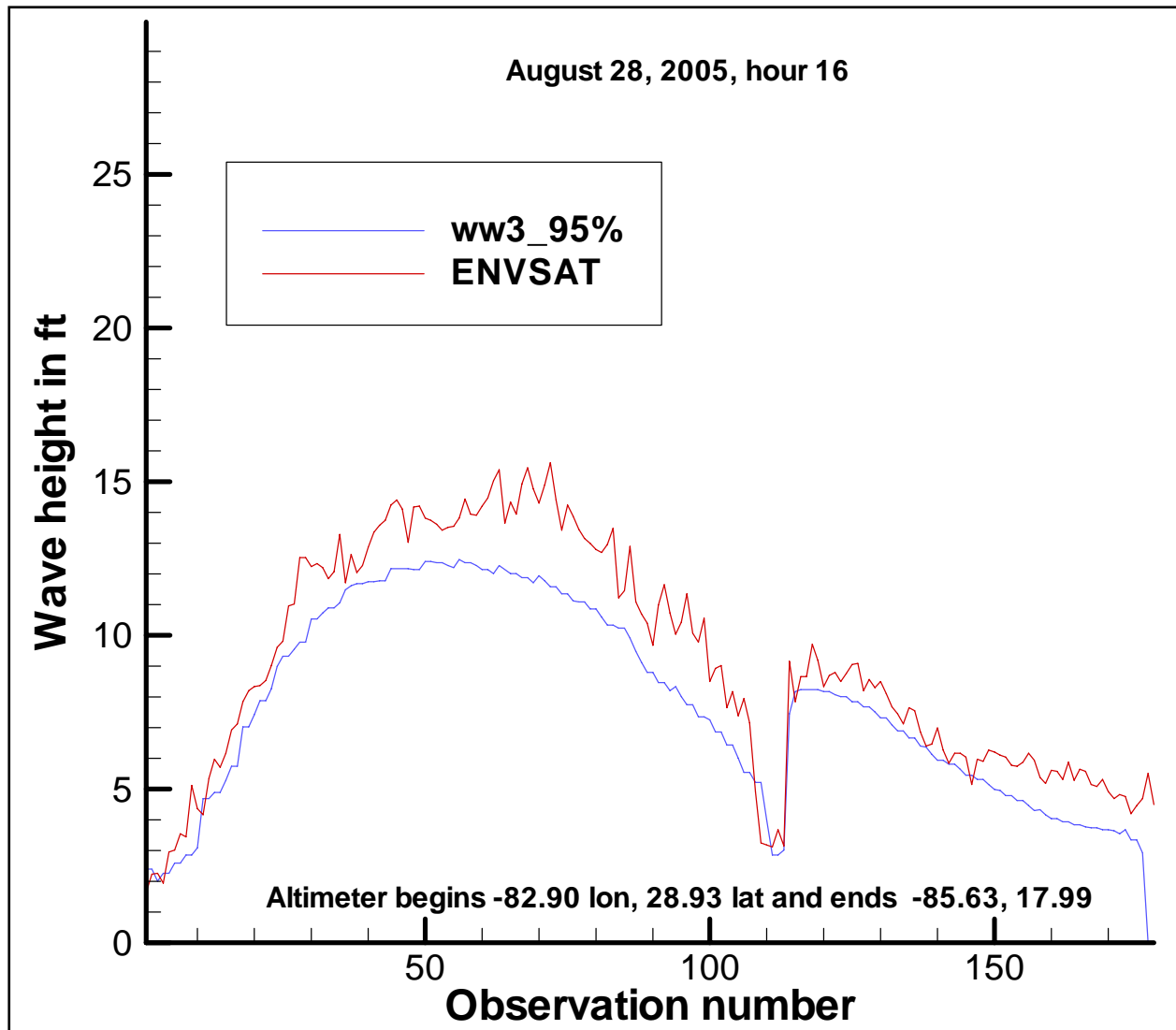


Figure 3-49. ENVSAT satellite altimetry track for 28 August 1600 UTC with co-located points from the final WAVEWATCH III significant wave height hindcast. Observation numbers refer to consecutive measurements as the satellite passed over the storm. Altimeter measurements begin at 82.90 W Longitude, 28.93 Latitude and end 85.63 W Longitude, 17.99 Latitude. Mean difference between WW3 and altimeter measurements is -1.34ft indicating WW3 is slightly lower than measurements

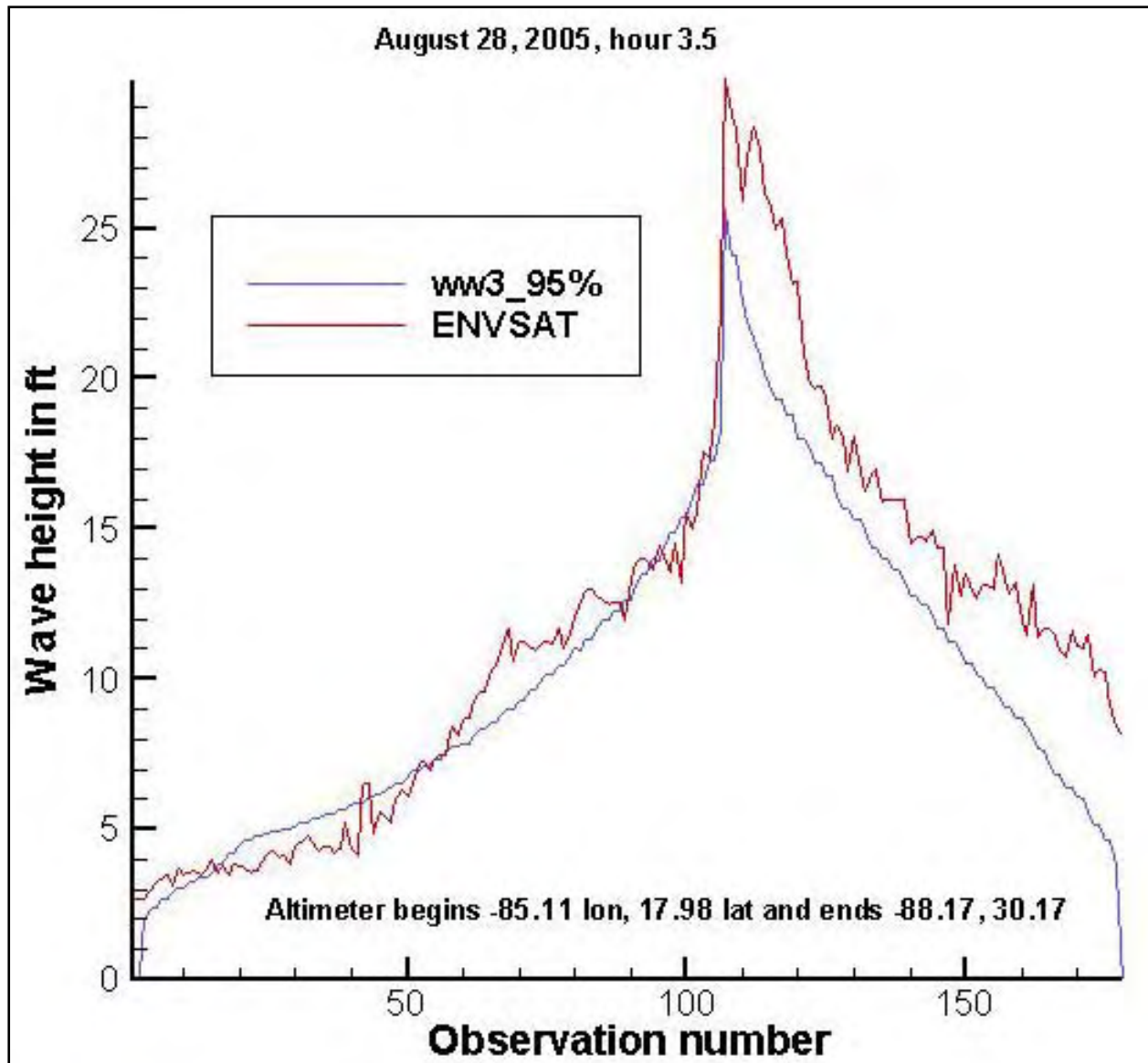


Figure 3-50. ENVSAT satellite altimetry track for 28 August 0330 UTC with co-located points from the final WAVEWATCH III significant wave height hindcast. Observation numbers refer to consecutive measurements as the satellite passed over the storm. Altimeter measurements begin at 85.11 W Longitude, 17.98 Latitude and end 88.17 W Longitude, 30.17 Latitude. Mean difference between WW3 and altimeter measurements is -1.57ft indicating WW3 is lower than measurements



# WAM WaveMEDS Validation Data

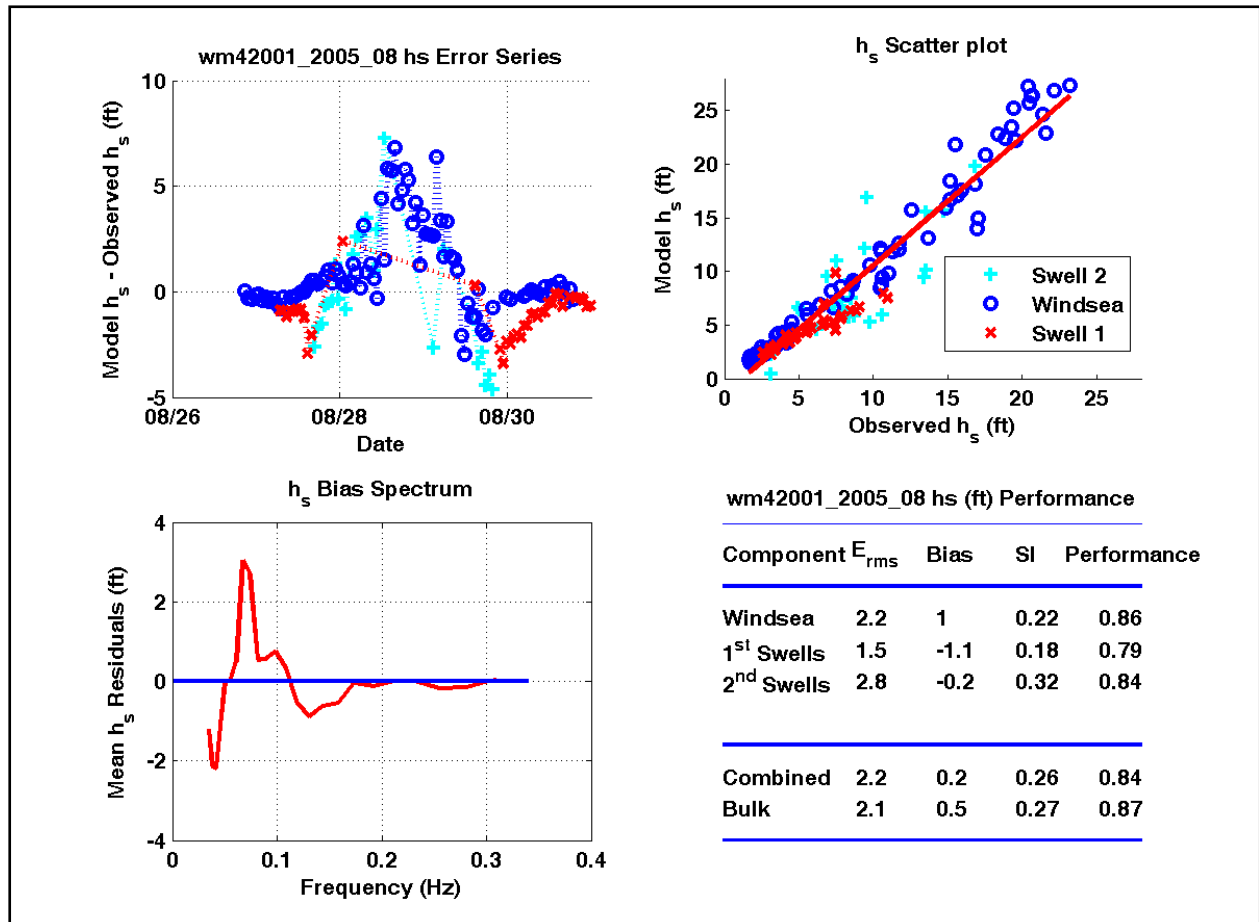


Figure 3-51. Wave height temporal correlation results for WAM hindcast at station 42001

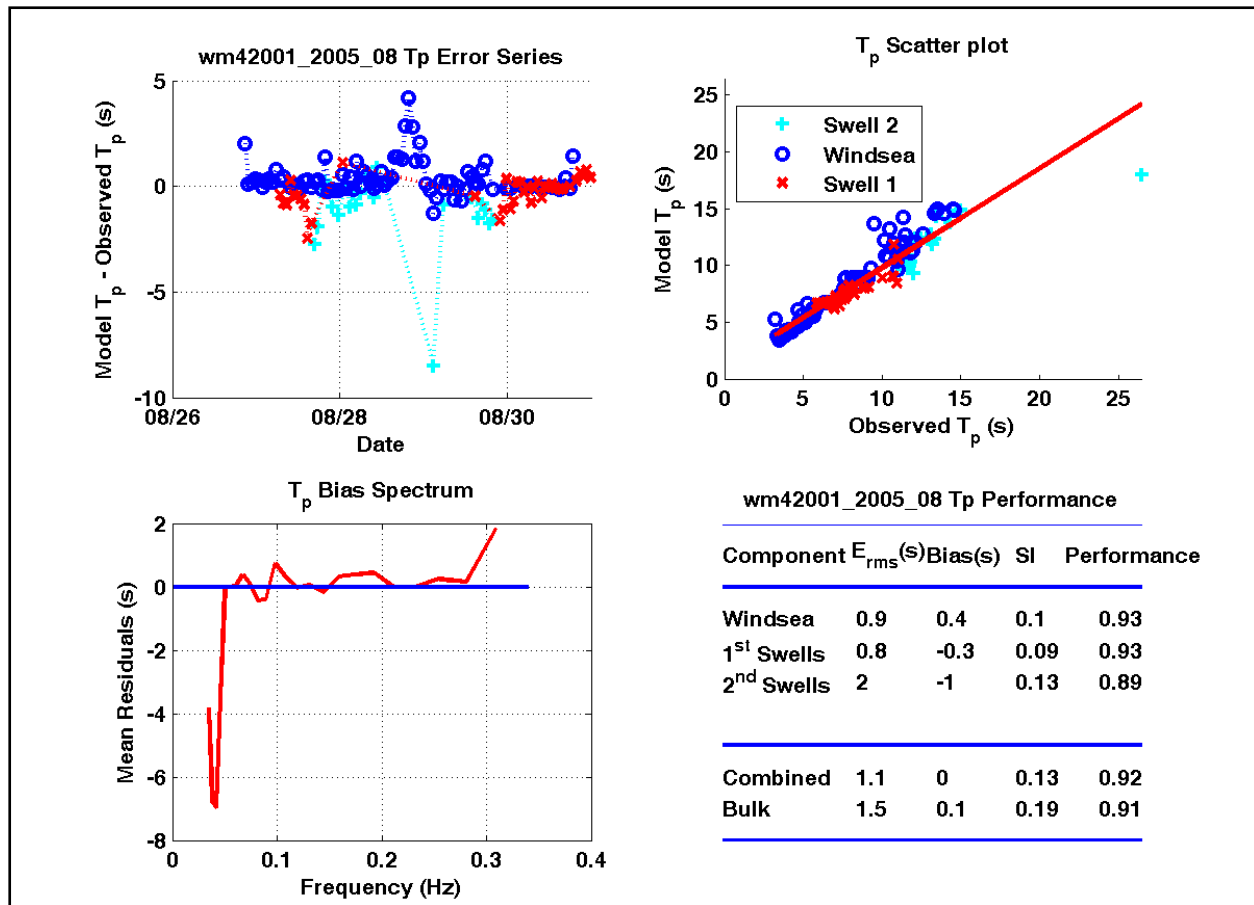


Figure 3-52. Wave period temporal correlation results for WAM hindcast at station 42001

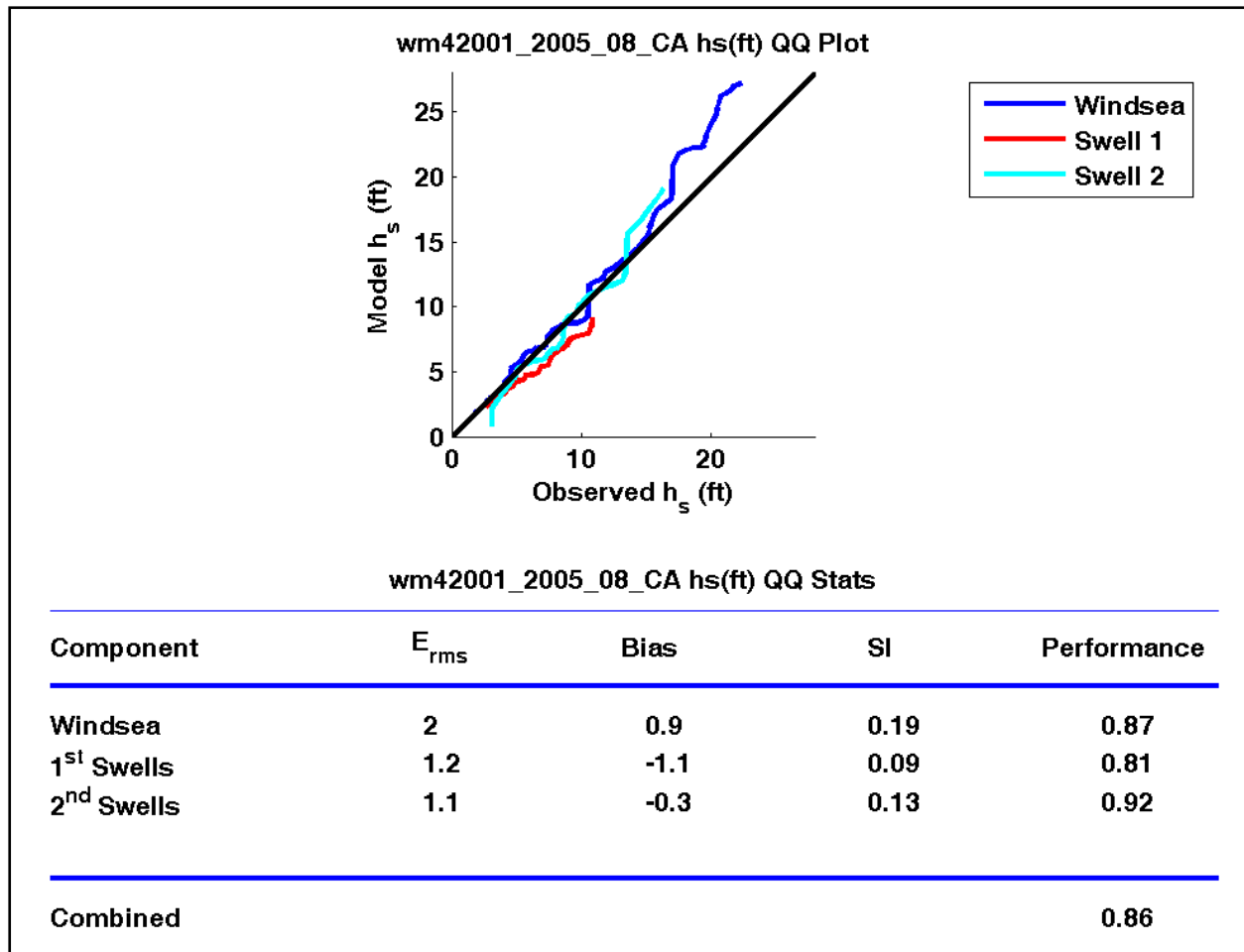


Figure 3-53. Wave height quantile-quantile results for WAM hindcast at station 42001

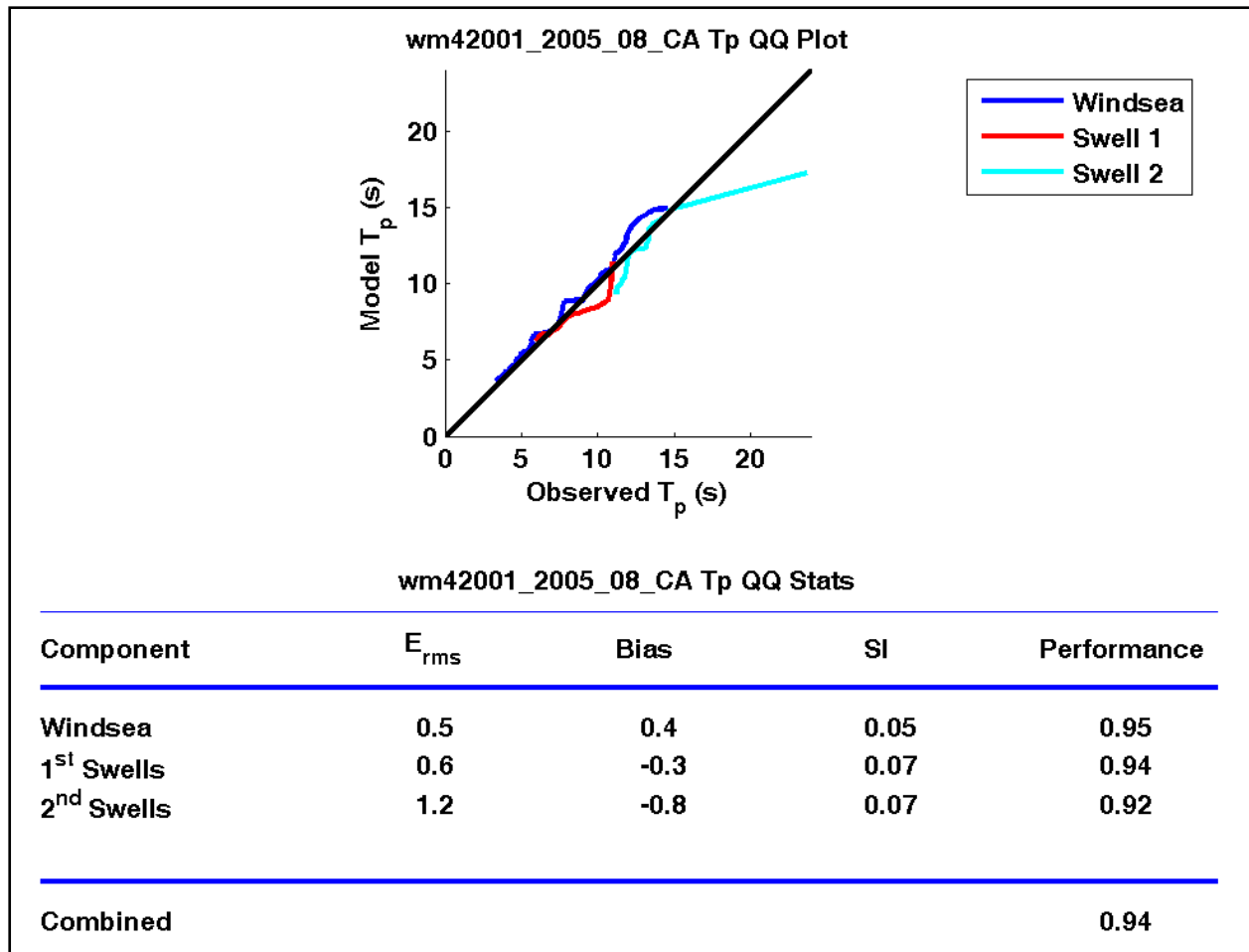


Figure 3-54. Wave period quantile-quantile results for WAM hindcast at station 42001



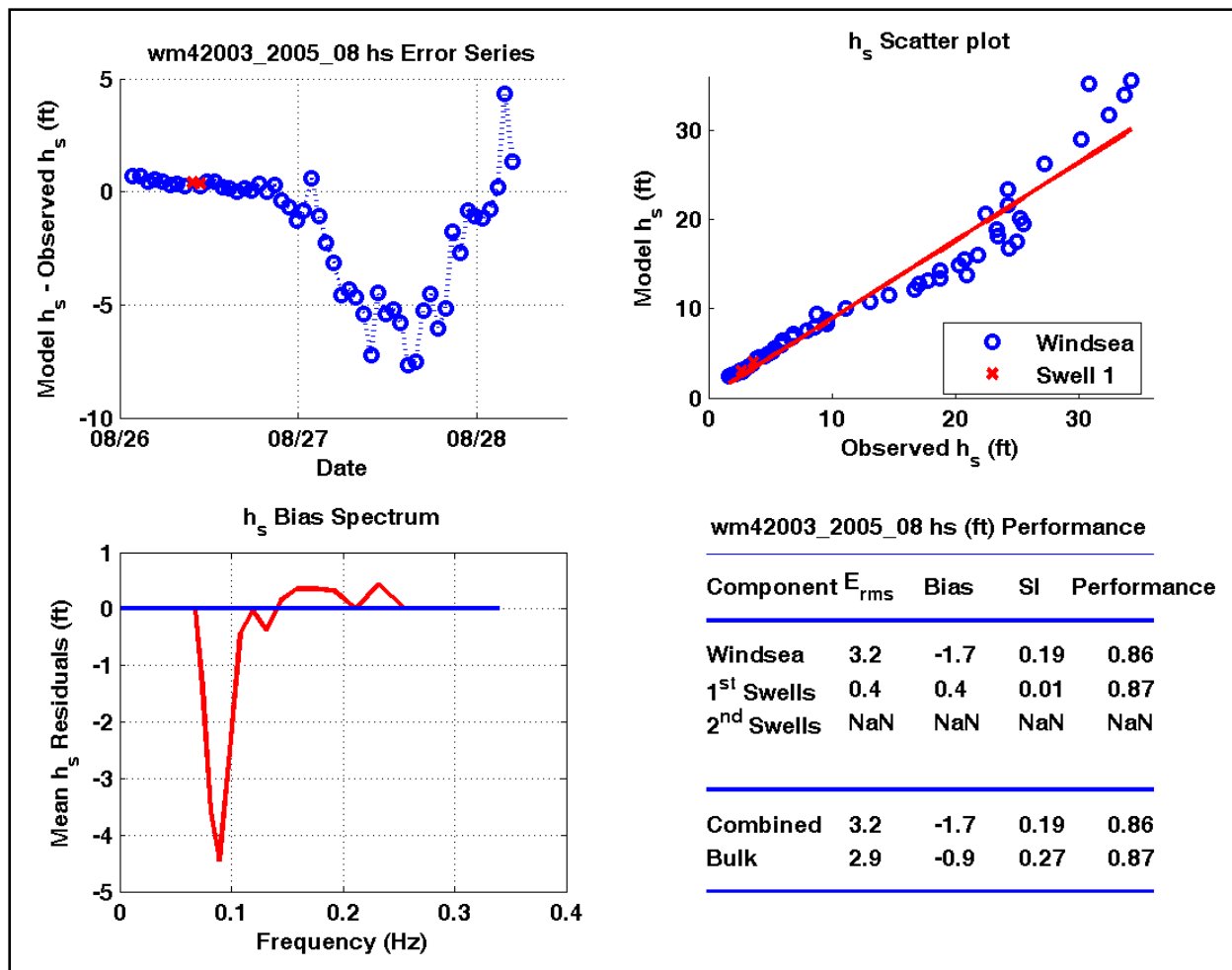


Figure 3-55. Wave height temporal correlation results for WAM hindcast at station 42003

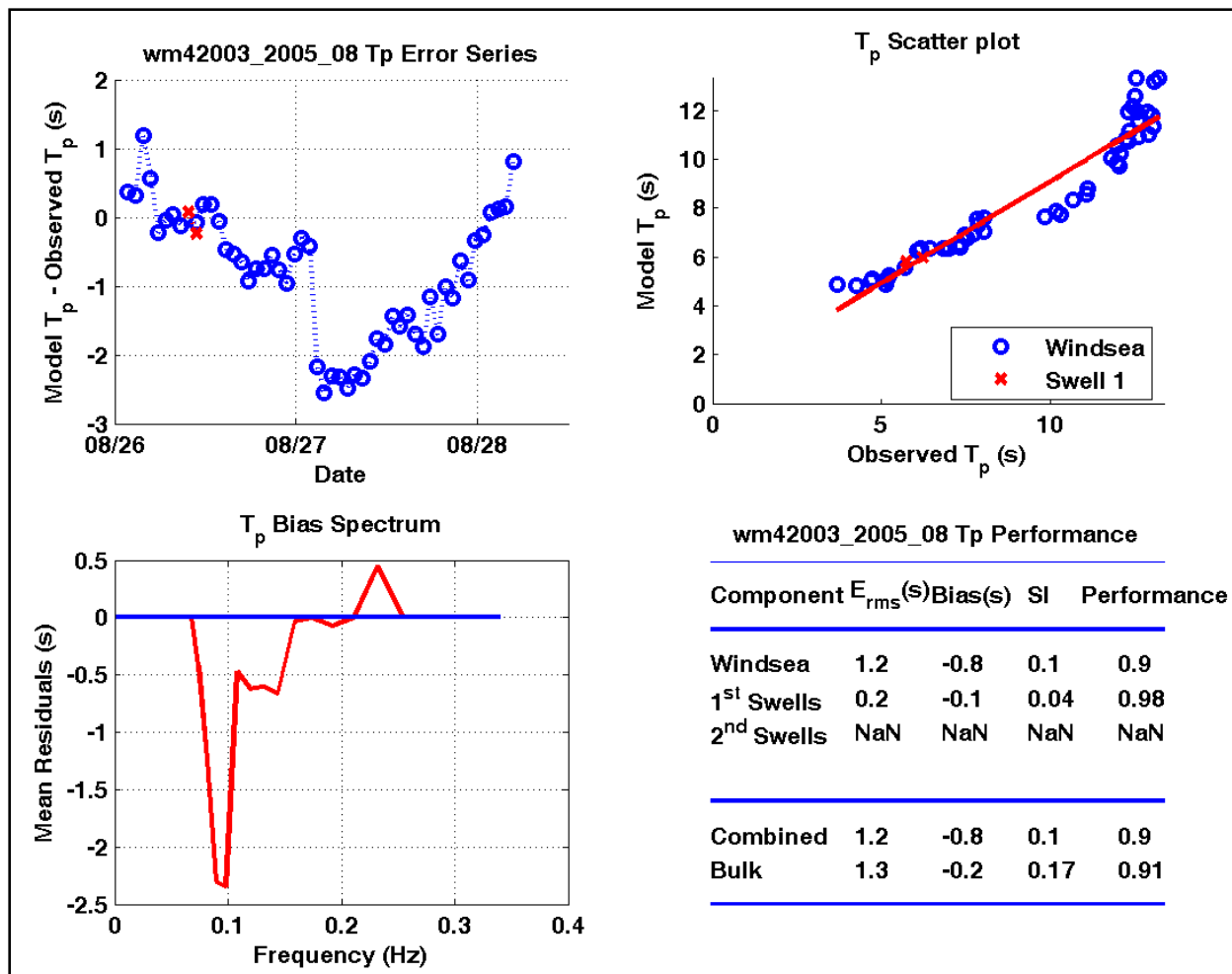


Figure 3-56. Wave period temporal correlation results for WAM hindcast at station 42003

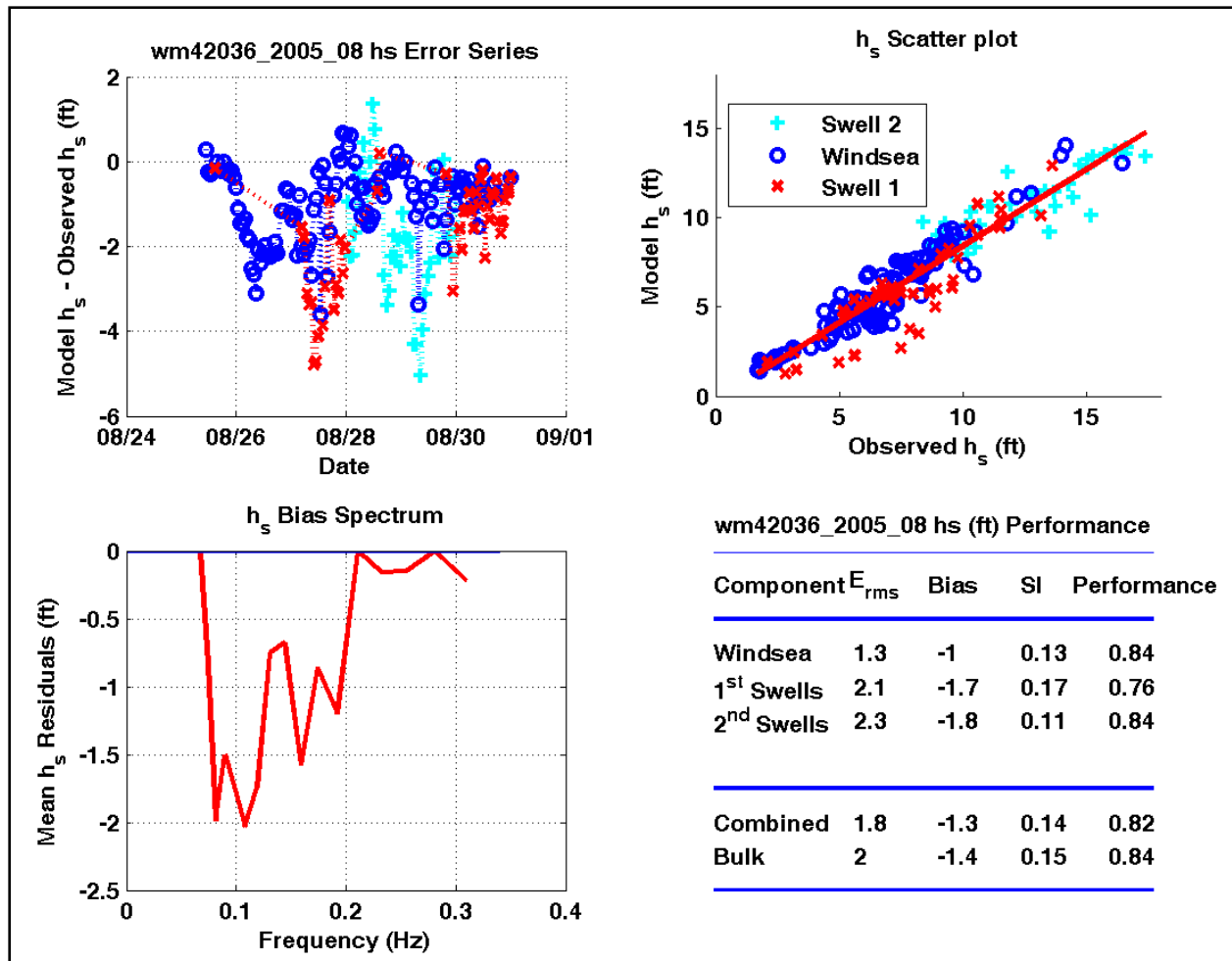


Figure 3-57. Wave height temporal correlation results for WAM hindcast at station 42036

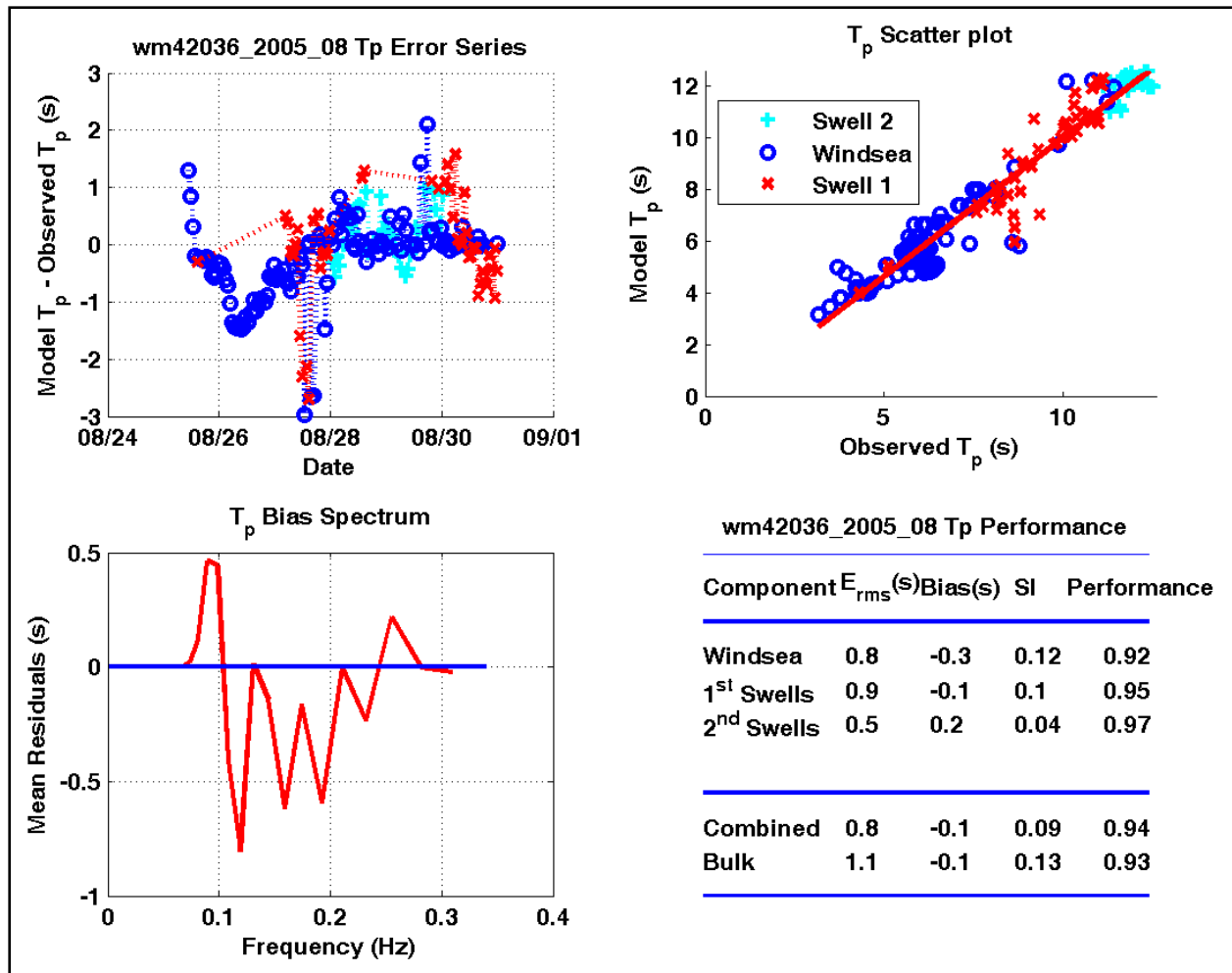


Figure 3-58. Wave period temporal correlation results for WAM hindcast at station 42036

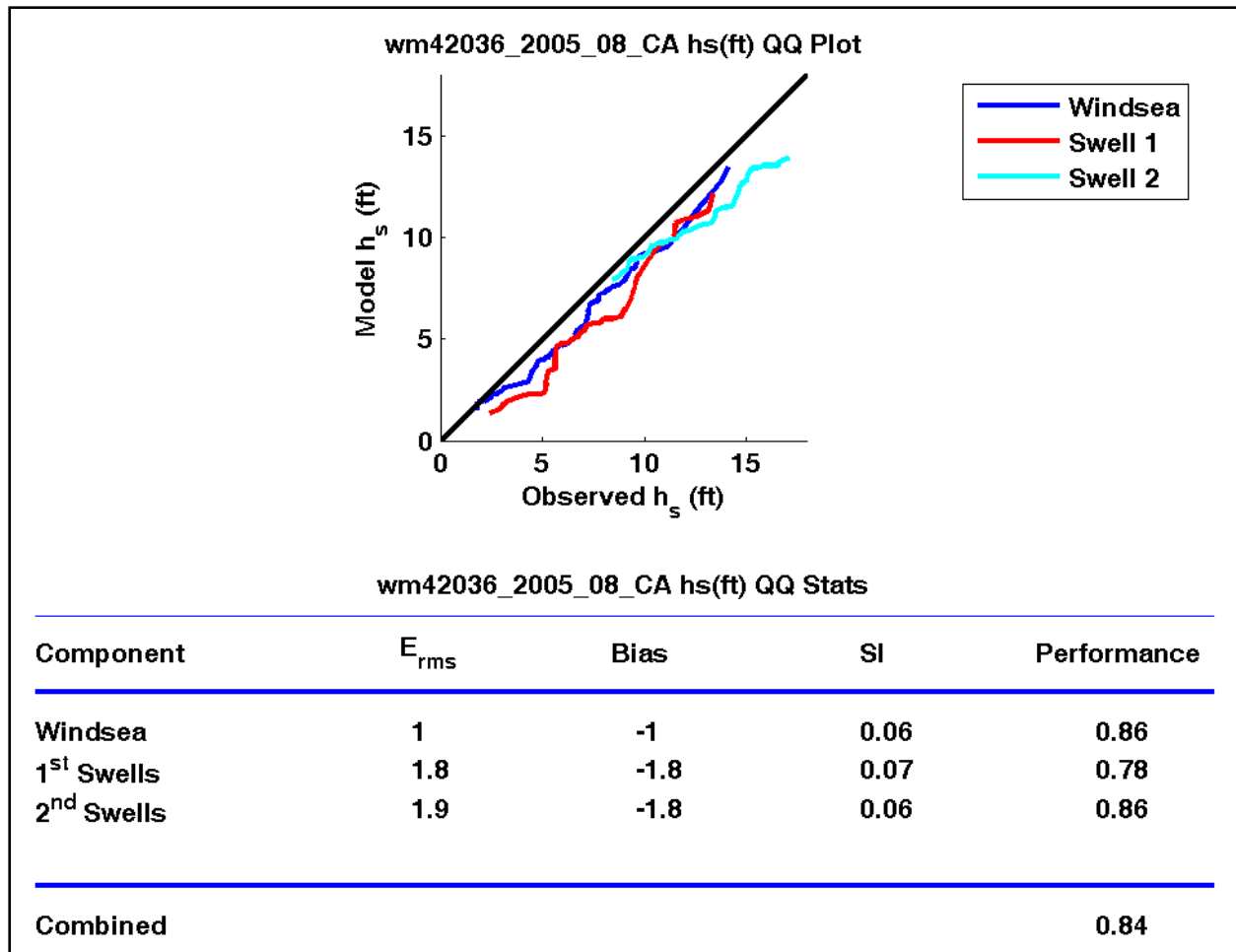


Figure 3-59. Wave height quantile-quantile results for WAM hindcast at station 42036



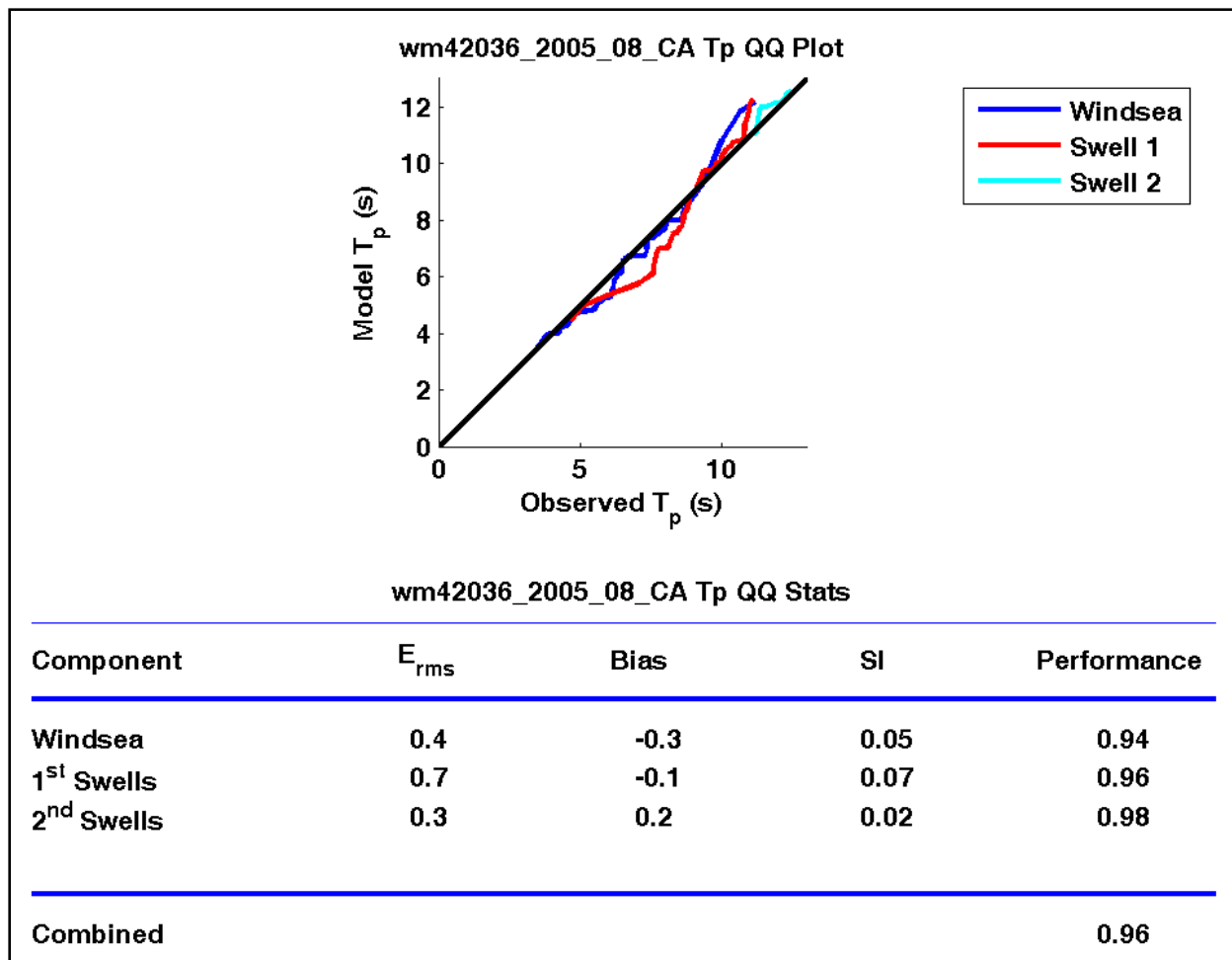


Figure 3-60. Wave period quantile-quantile results for WAM hindcast at station 42036

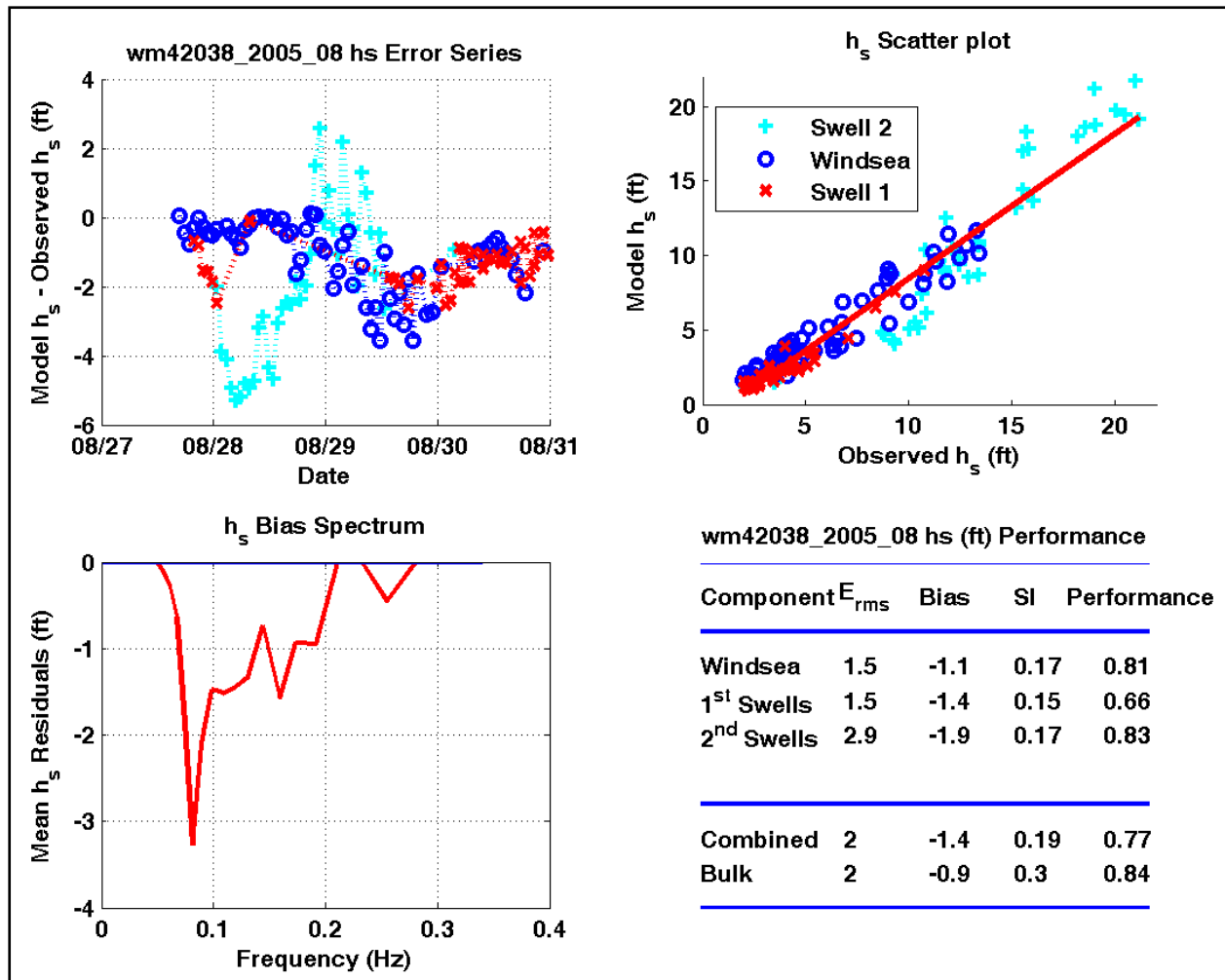


Figure 3-61. Wave height temporal correlation results for WAM hindcast at station 42038

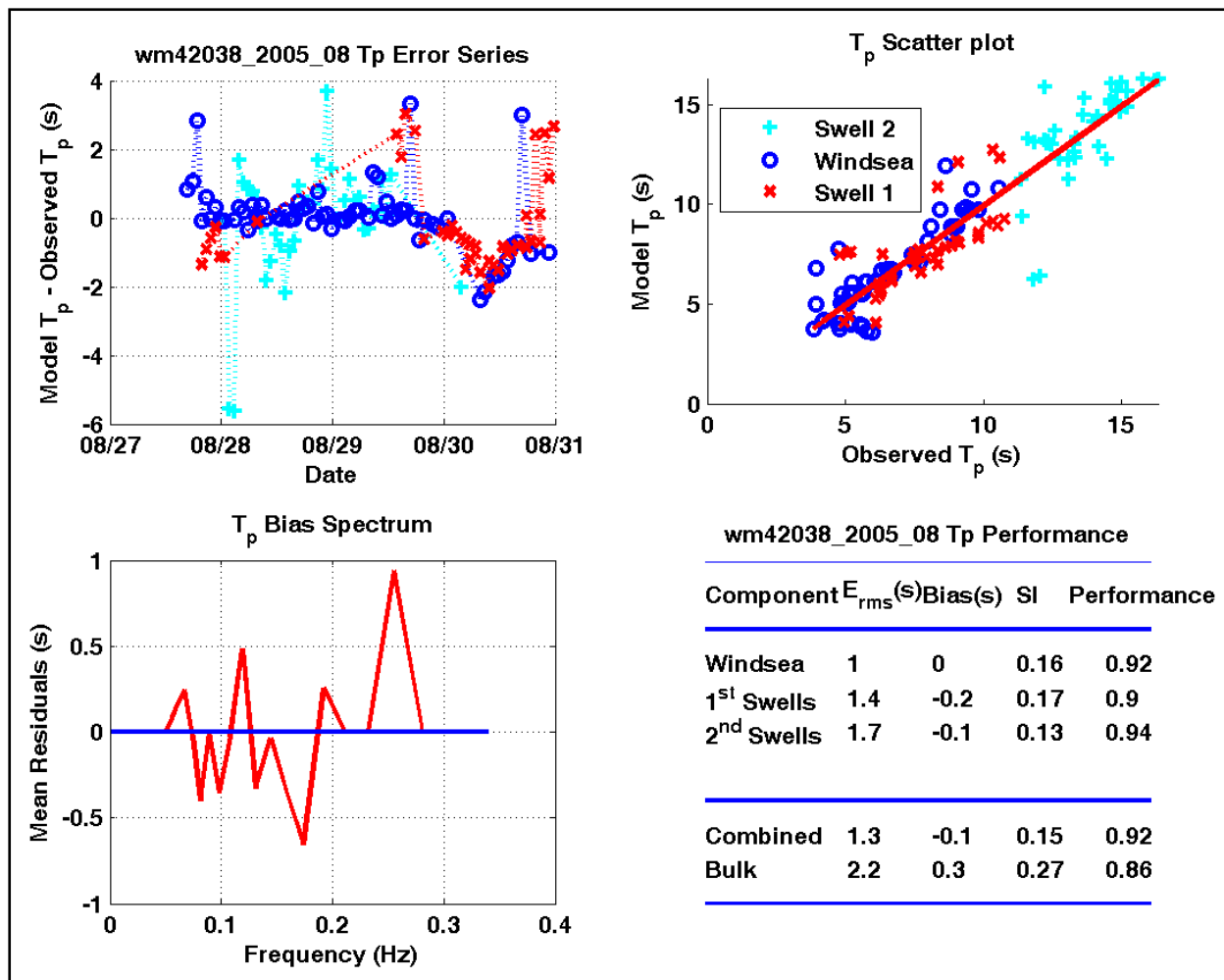


Figure 3-62. Wave period temporal correlation results for WAM hindcast at station 42038

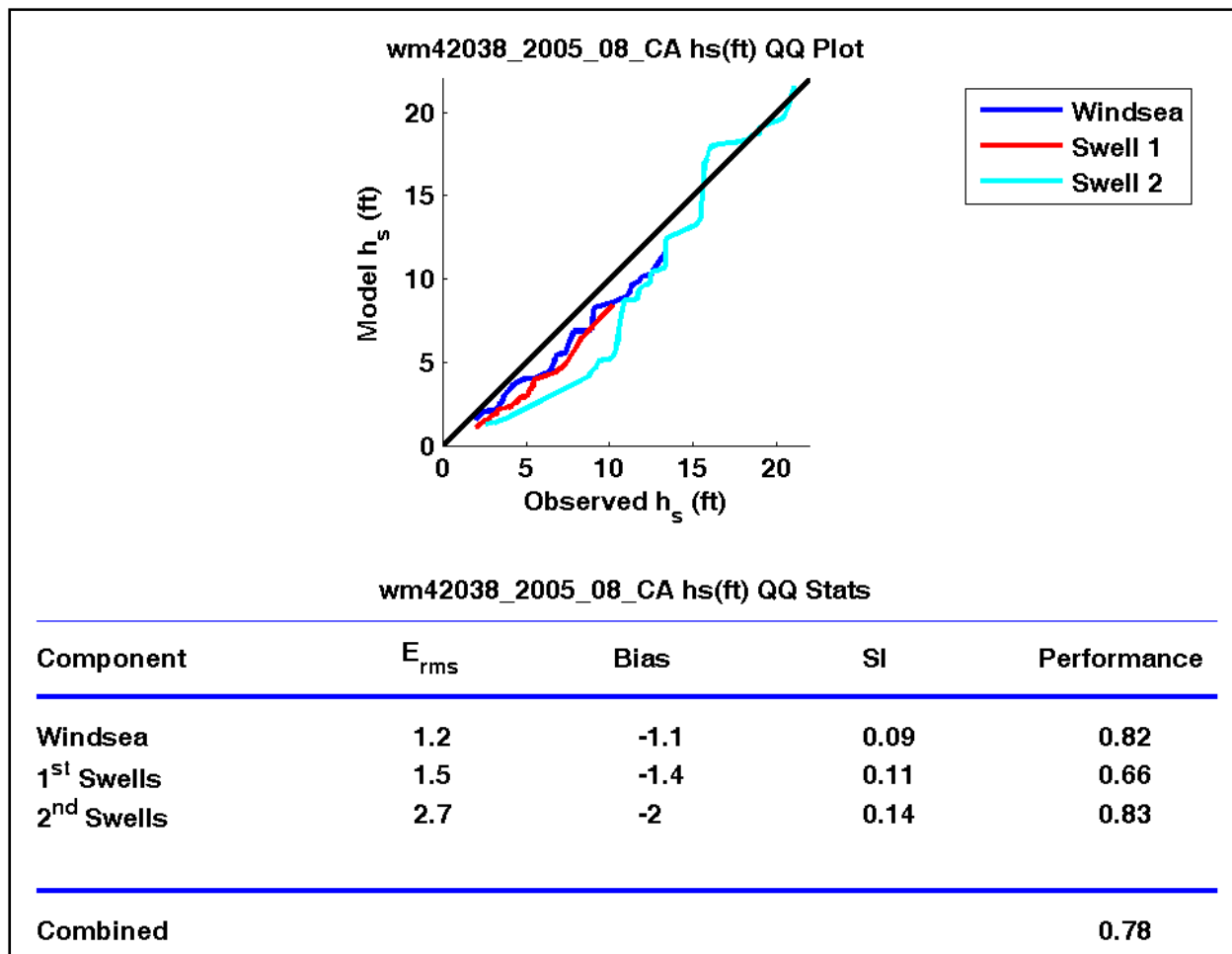


Figure 3-63. Wave height quantile-quantile results for WAM hindcast at station 42038

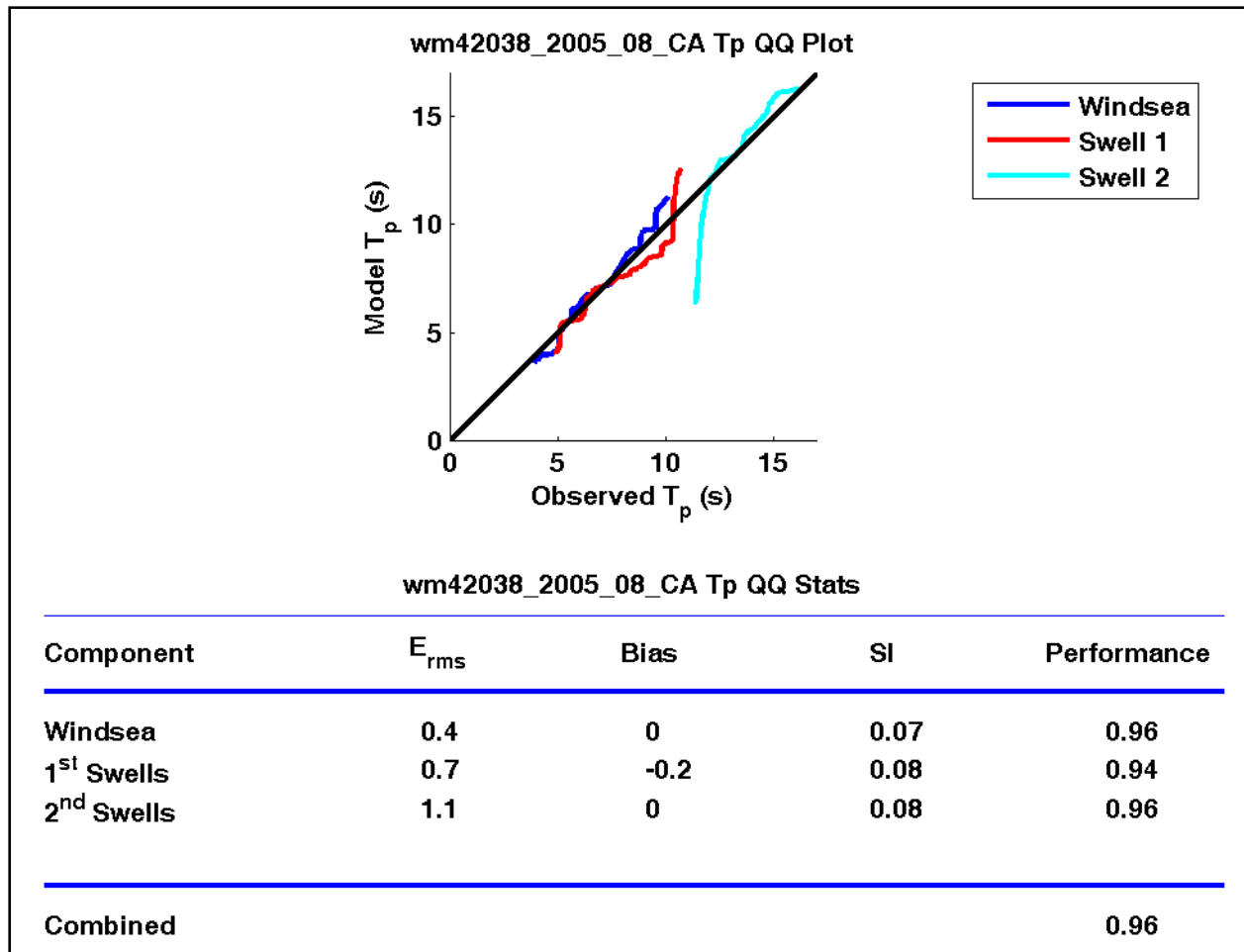


Figure 3-64. Wave period quantile-quantile results for WAM hindcast at station 42038



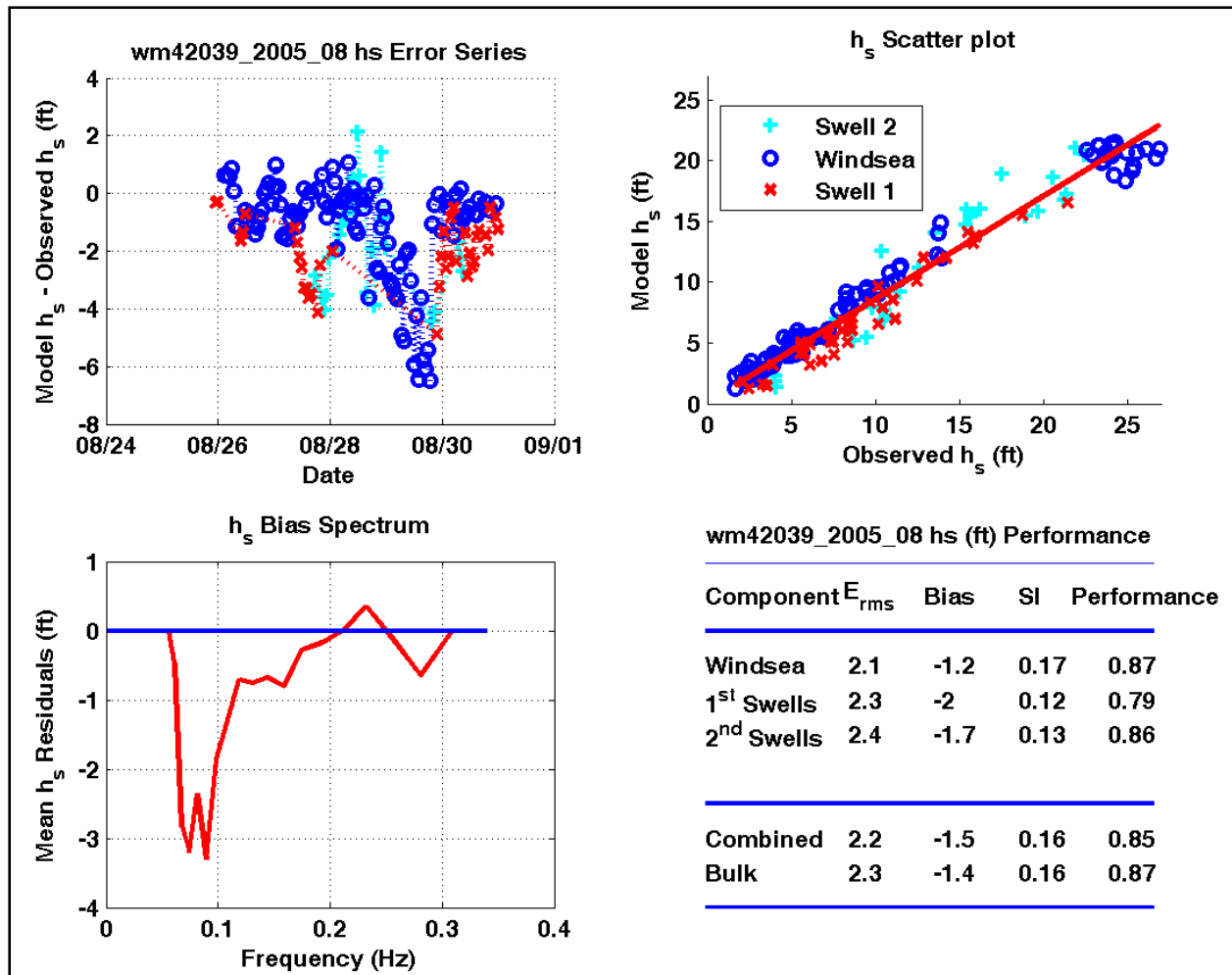


Figure 3-65. Wave height temporal correlation results for WAM hindcast at station 42039

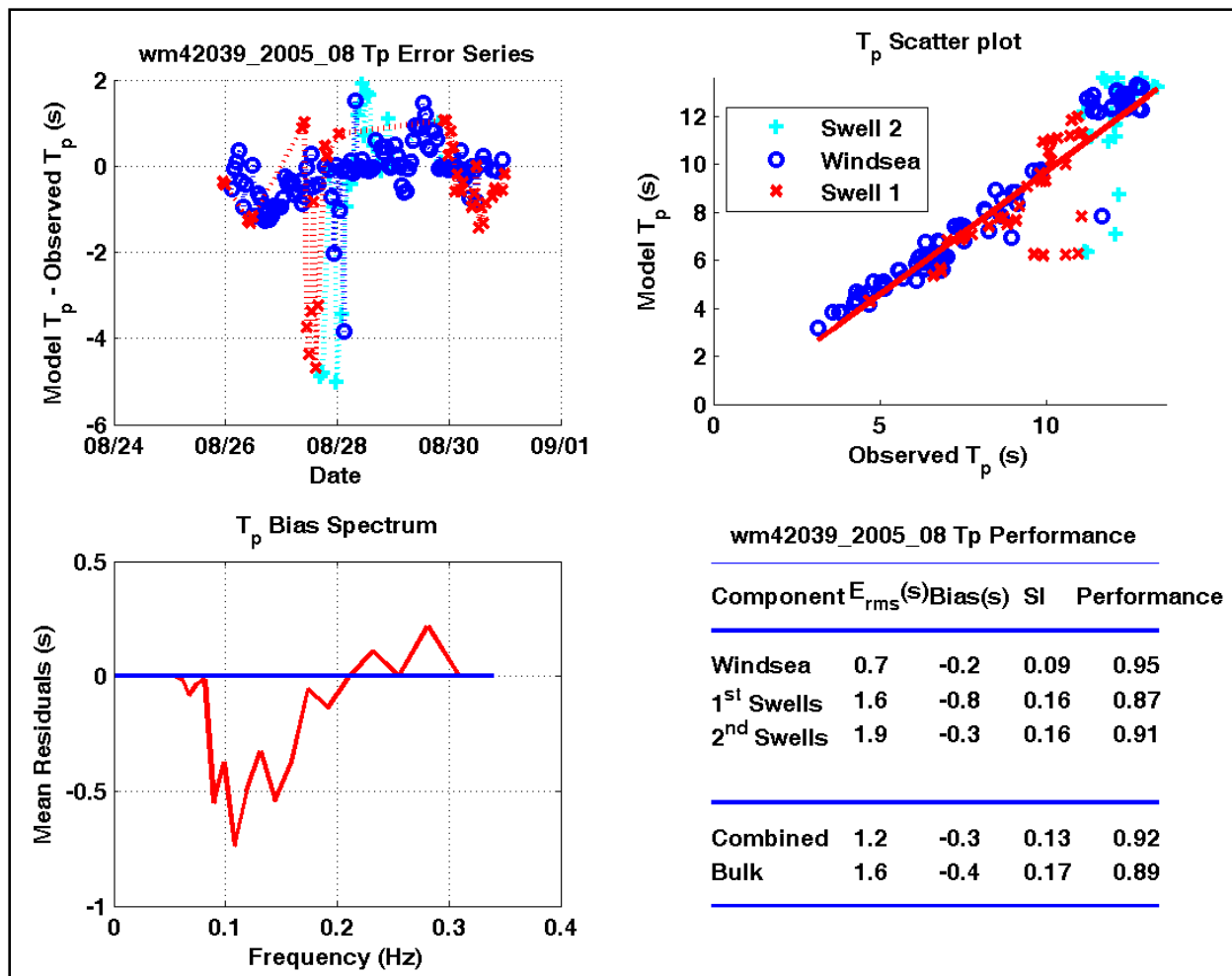


Figure 3-66. Wave period temporal correlation results for WAM hindcast at station 42039

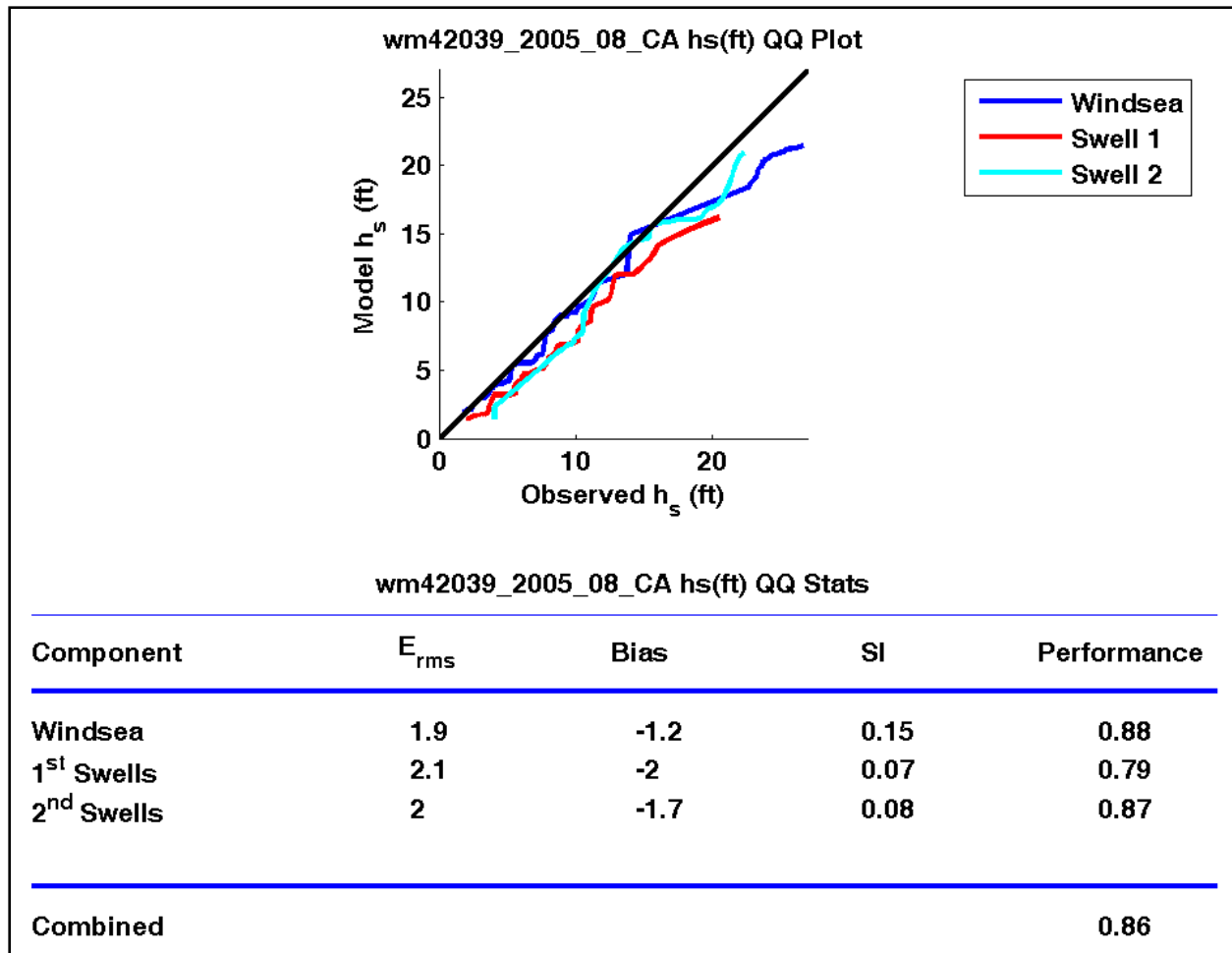


Figure 3-67. Wave height quantile-quantile results for WAM hindcast at station 42039

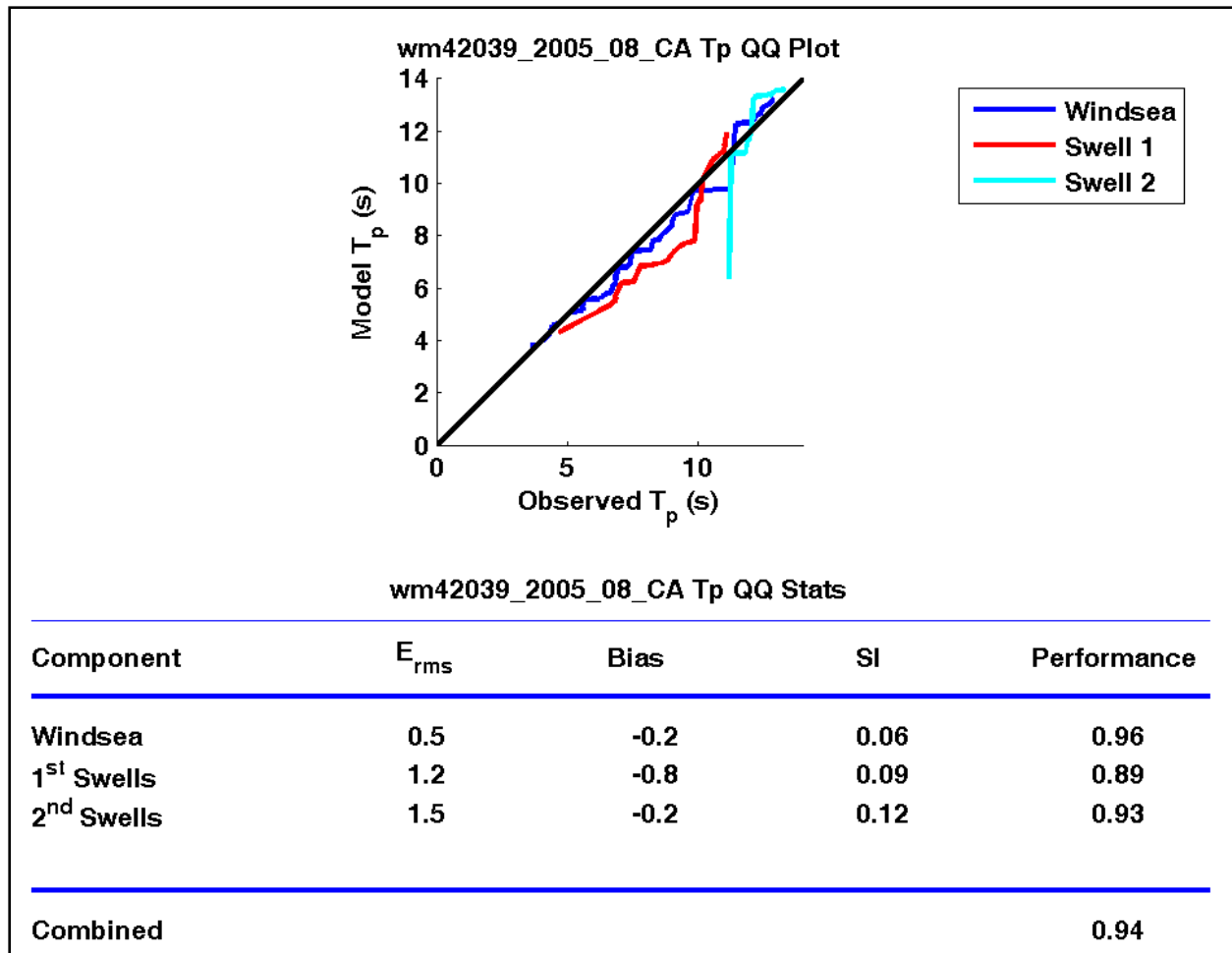


Figure 3-68. Wave period quantile-quantile results for WAM hindcast at station 42039

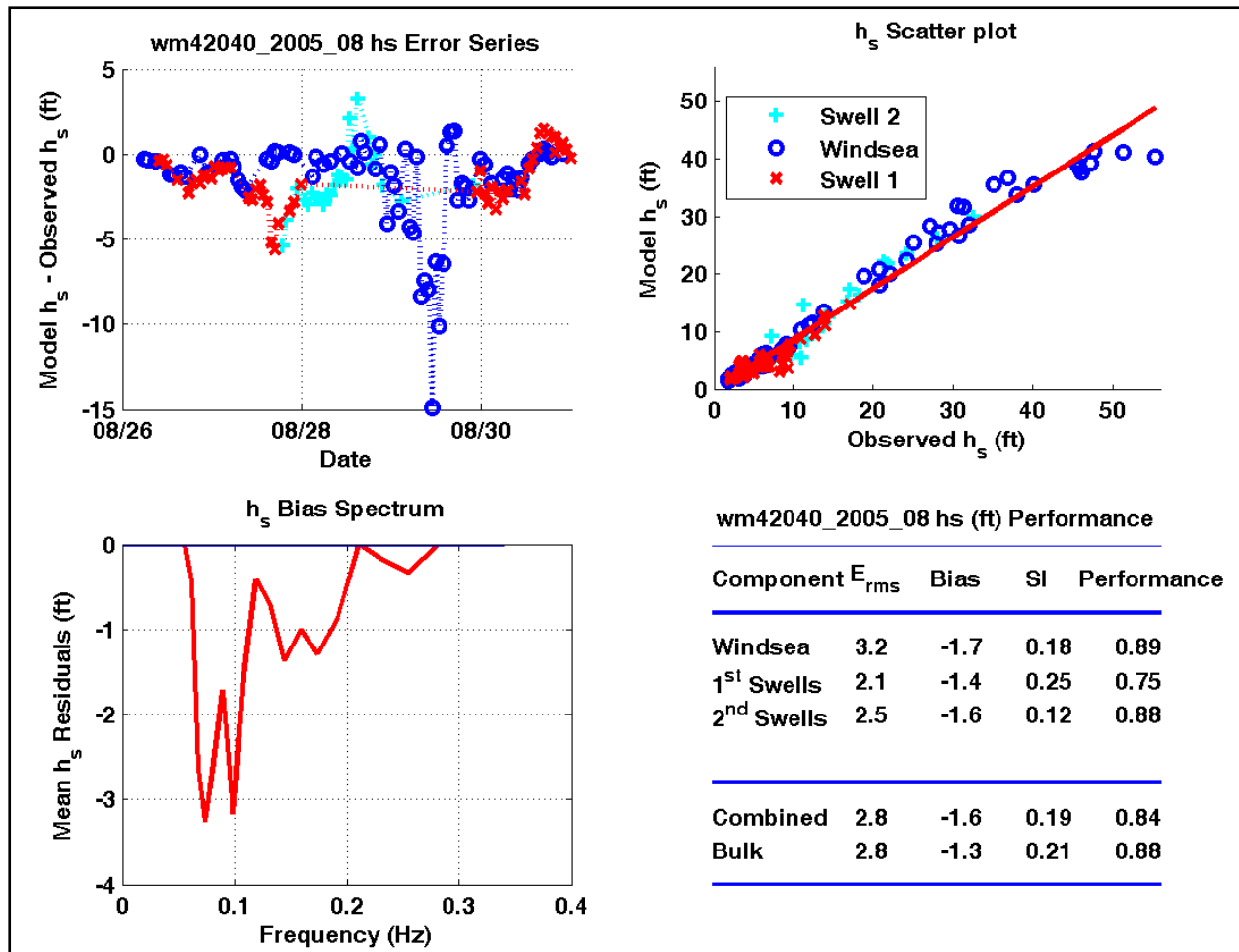


Figure 3-69. Wave height temporal correlation results for WAM hindcast at station 42040



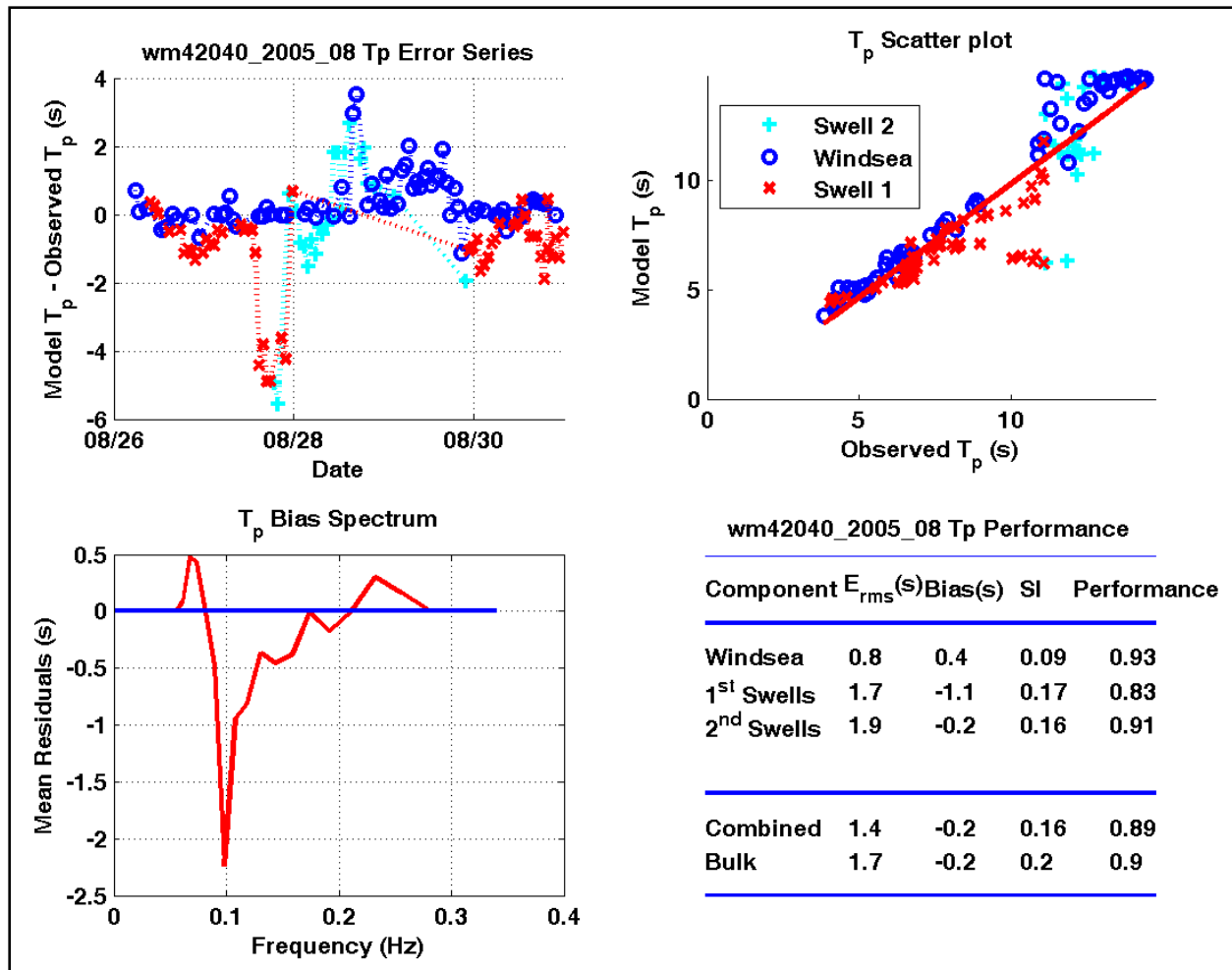


Figure 3-70. Wave period temporal correlation results for WAM hindcast at station 42040

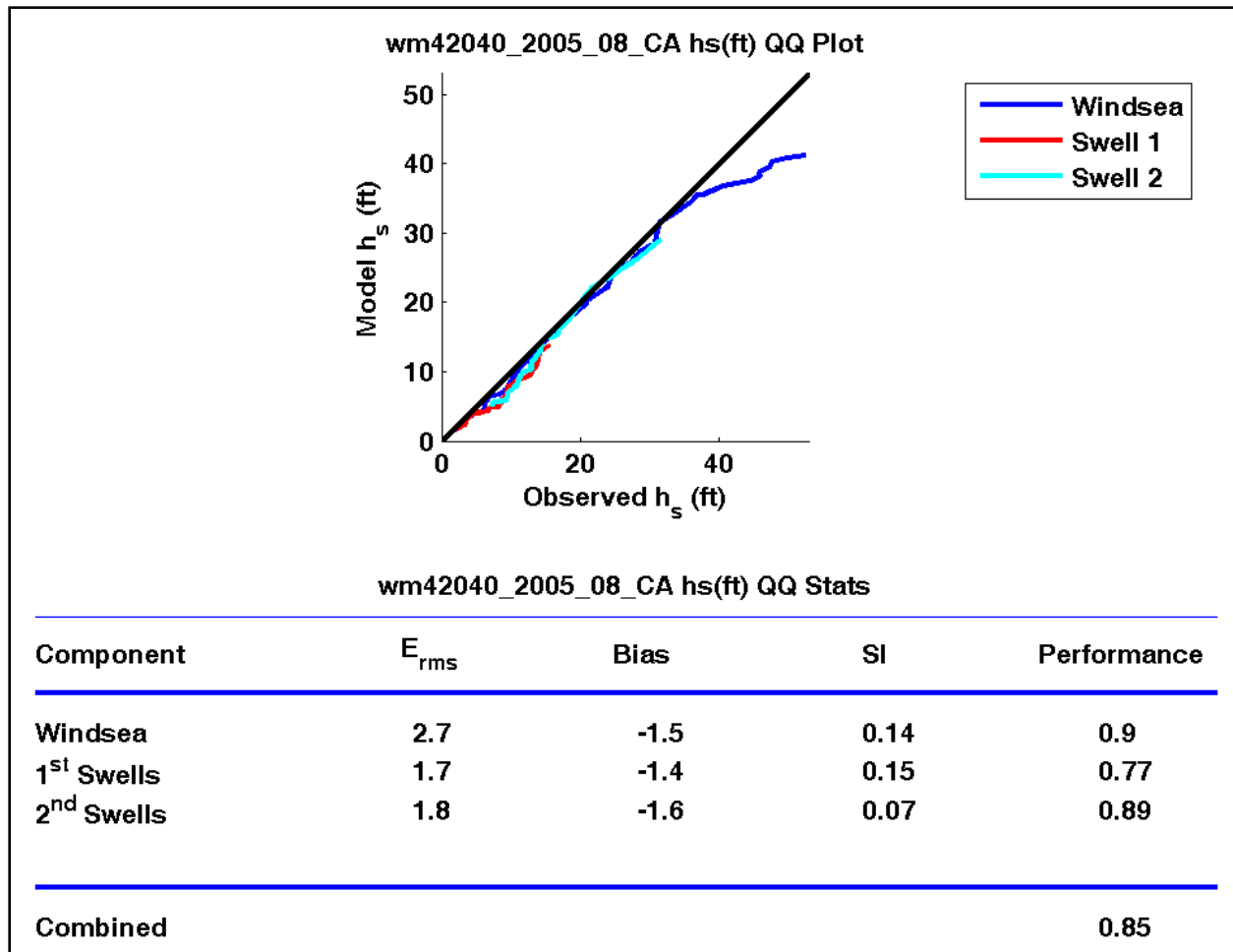


Figure 3-71. Wave height quantile-quantile results for WAM hindcast at station 42040

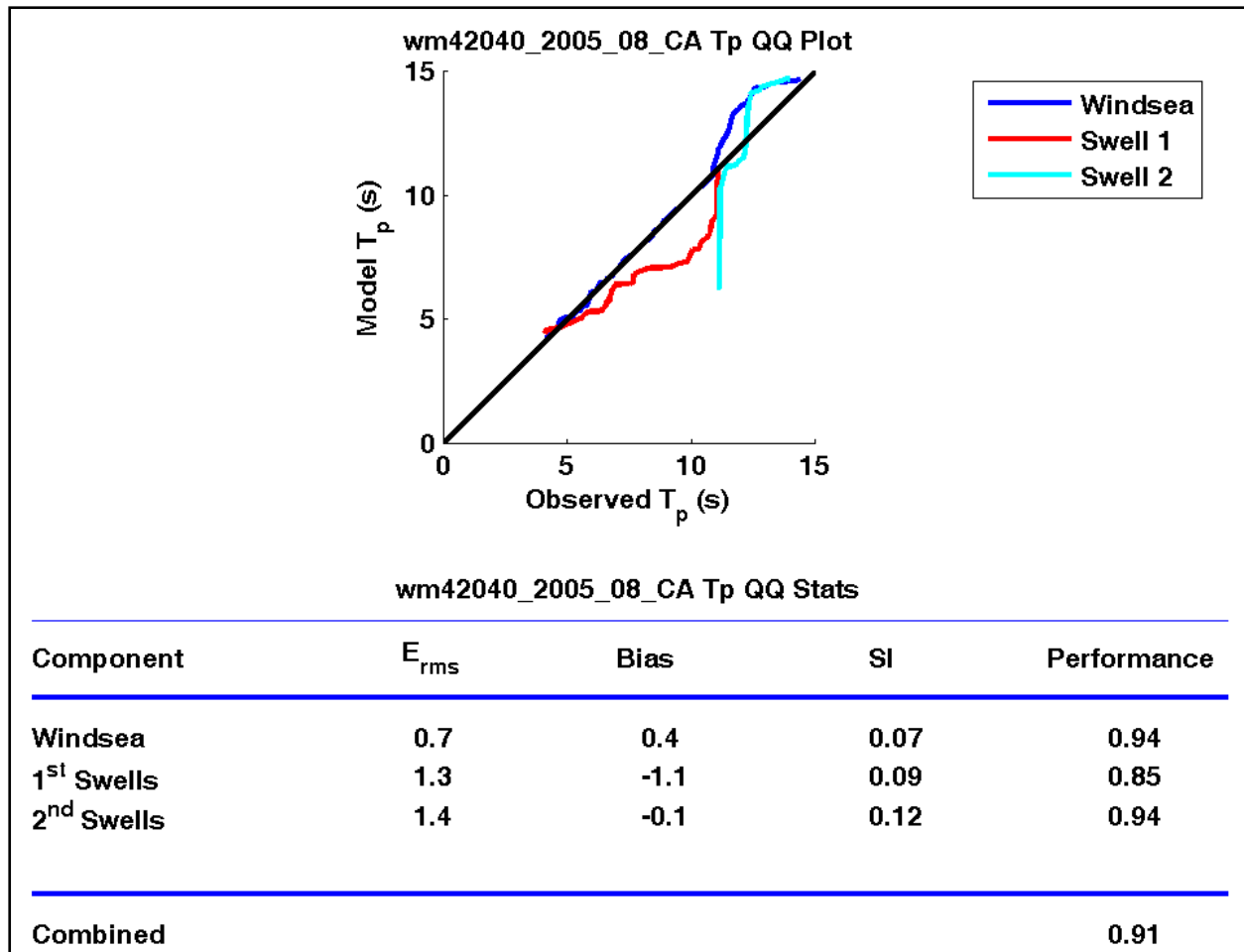


Figure 3-72. Wave period quantile-quantile results for WAM hindcast at station 42040.

# WAVEWATCH III WaveMEDS Validation Data

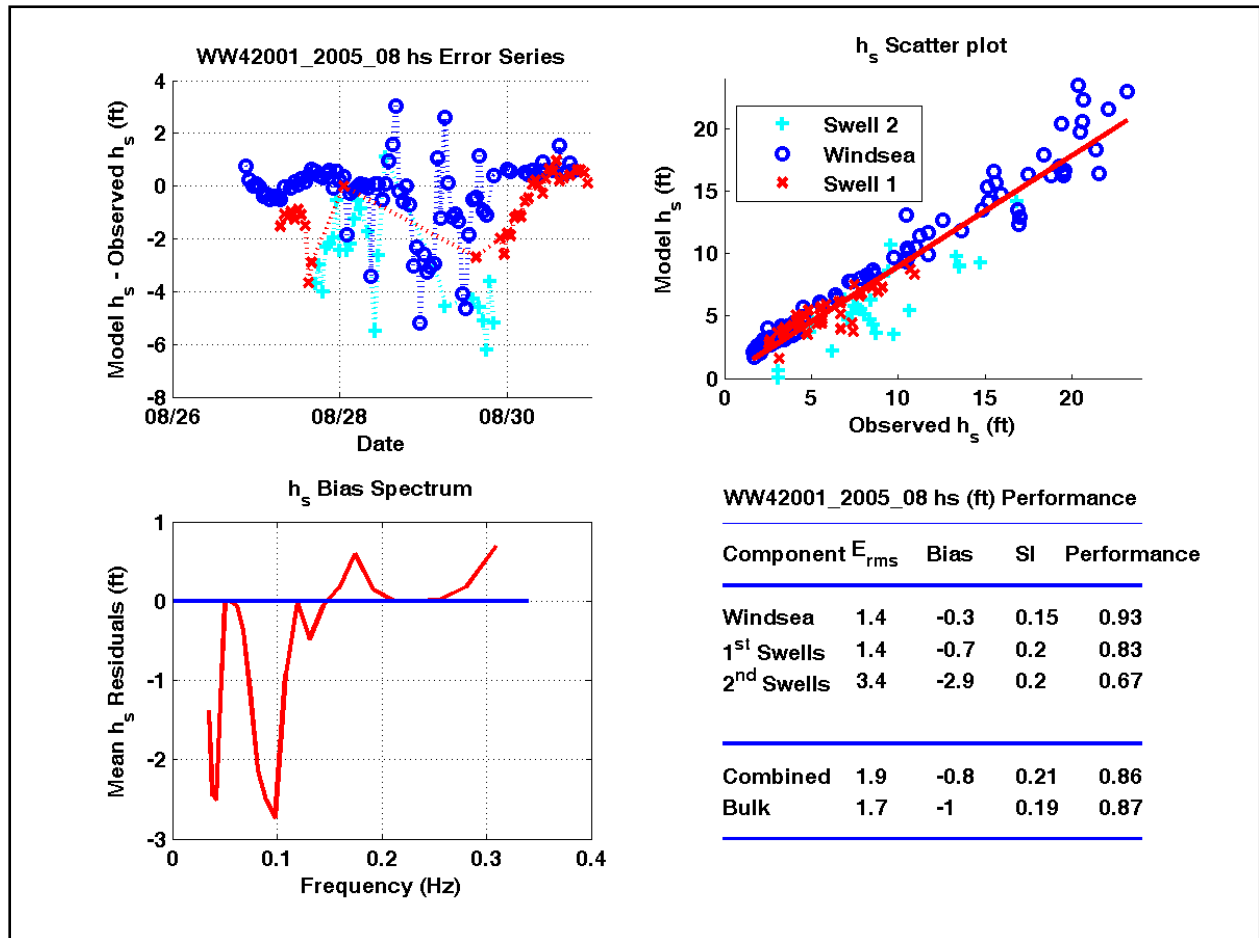


Figure 3-73. Wave height correlation results for WAVEWATCH hindcast at station 42001

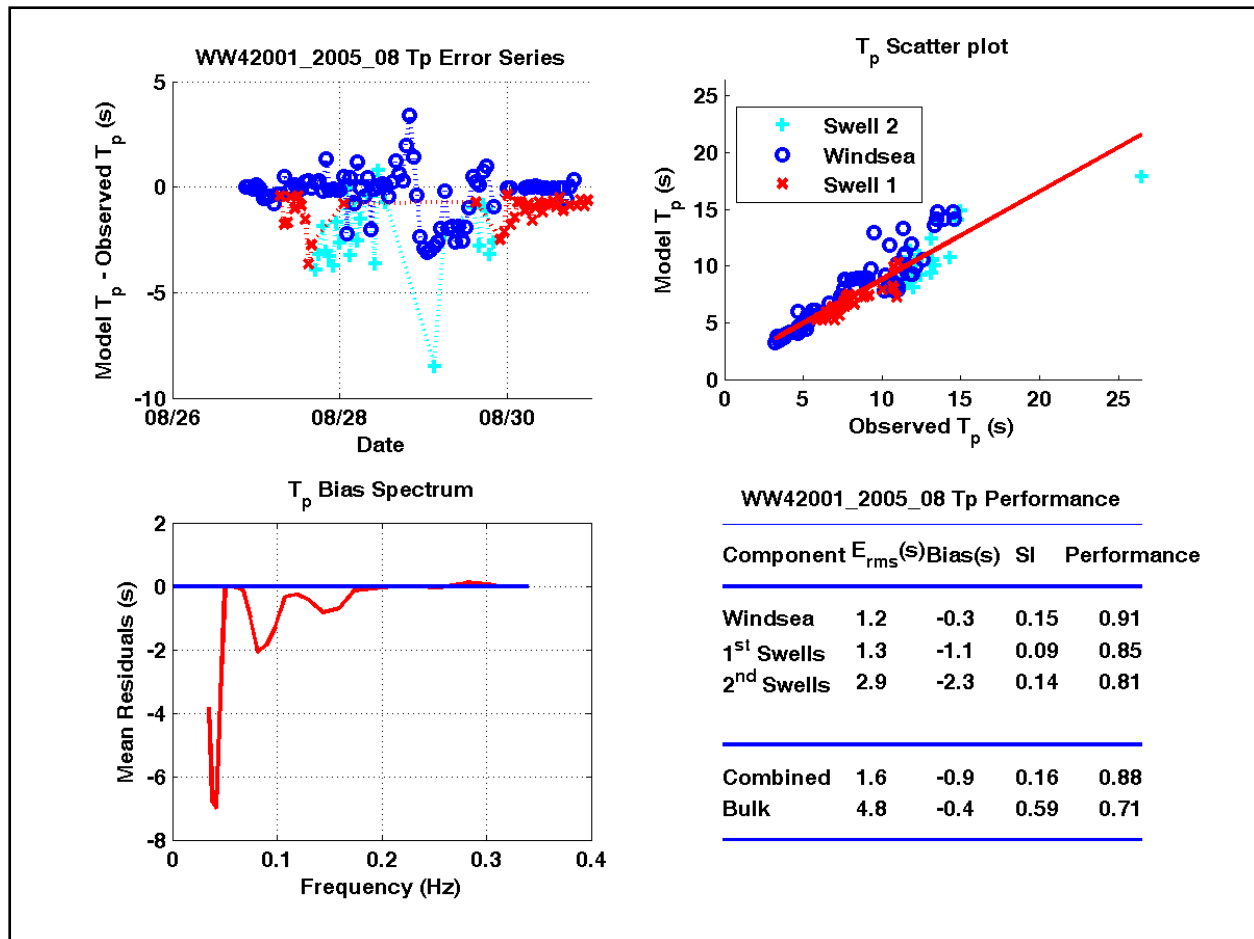


Figure 3-74. Wave period correlation results for WAVEWATCH hindcast at station 42001



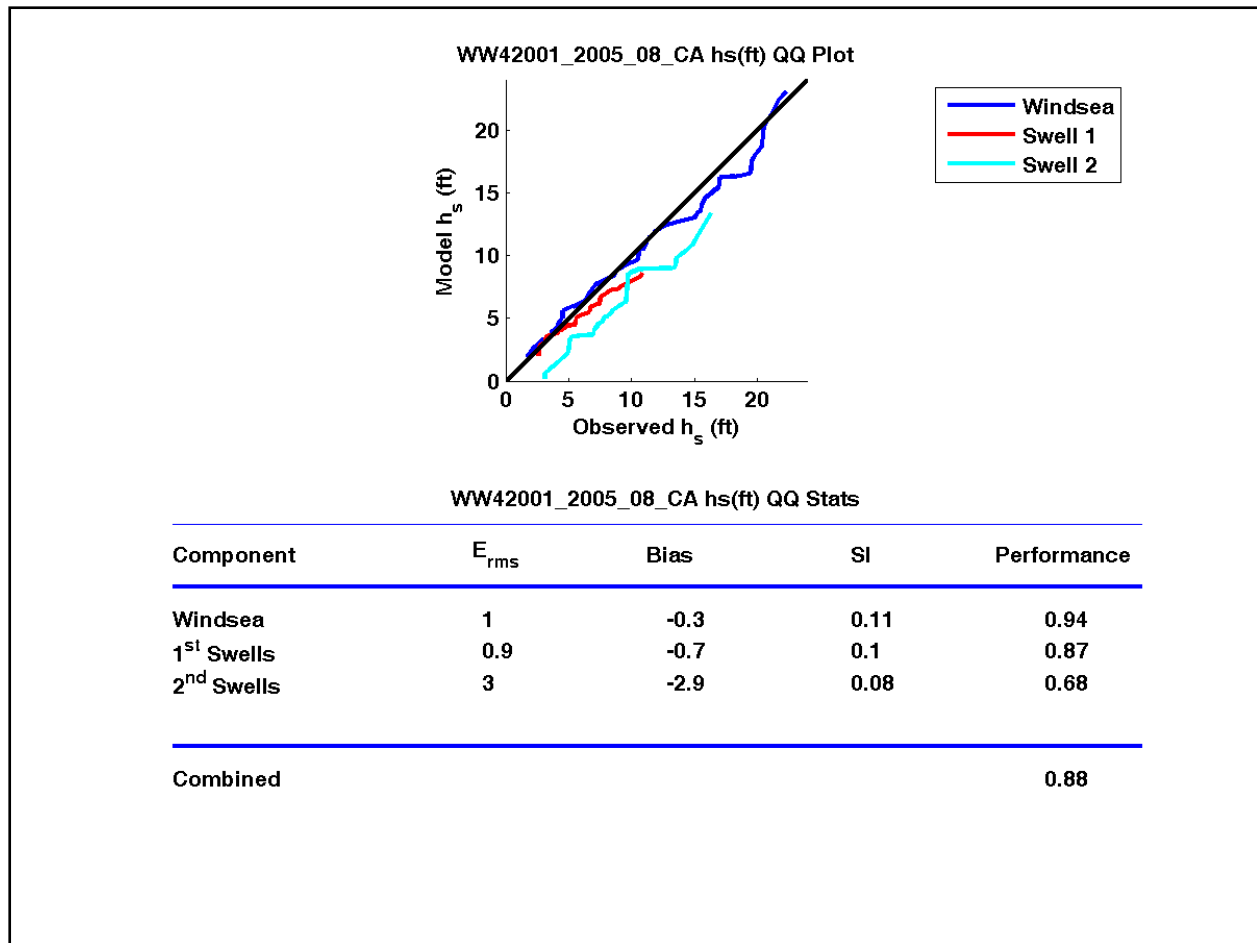


Figure 3-75. Wave height quantile-quantile results for WAVEWATCH hindcast at station 42001

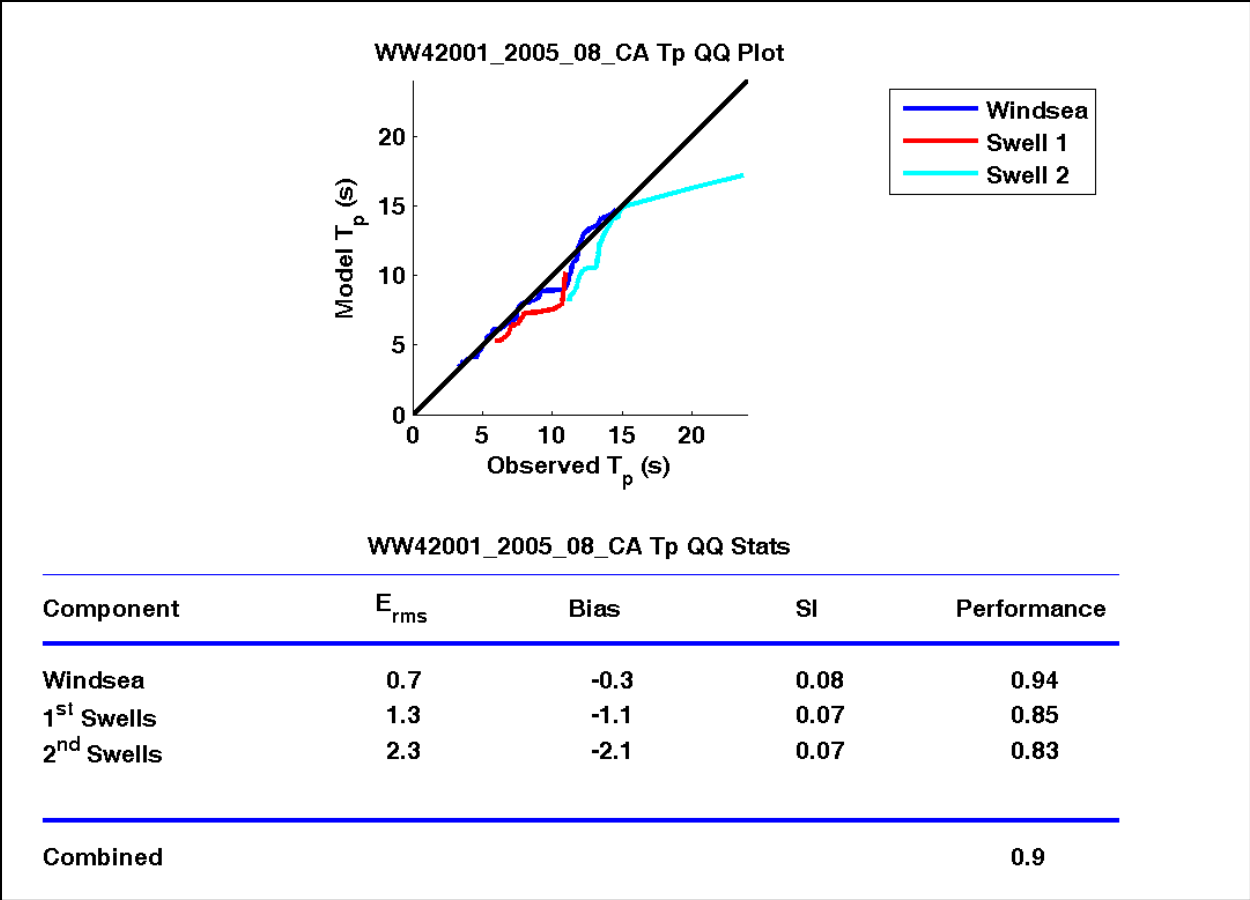


Figure 3-76. Wave period quantile-quantile results for WAVEWATCH hindcast at station 42001

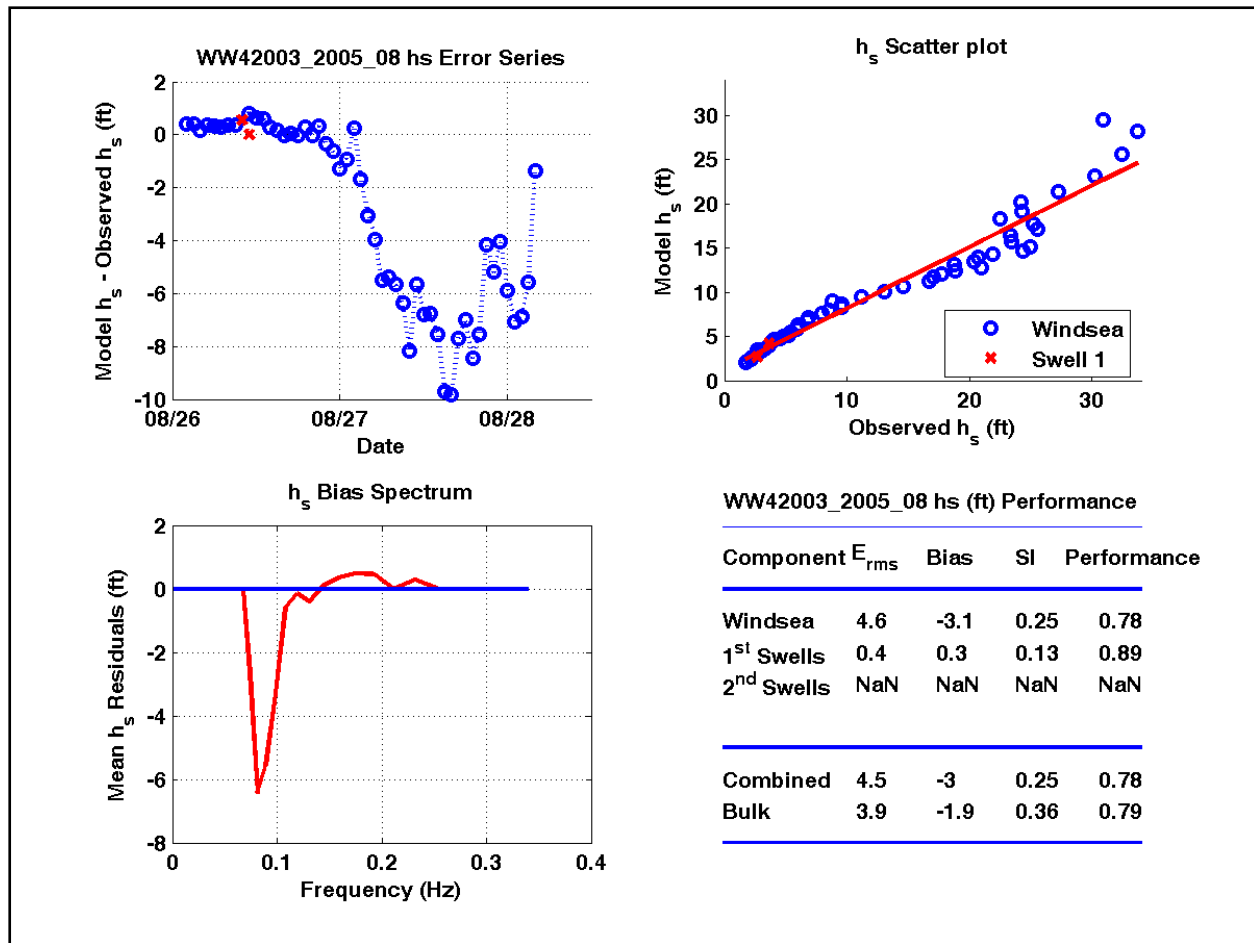


Figure 3-77. Wave height correlation results for WAVEWATCH hindcast at station 42003

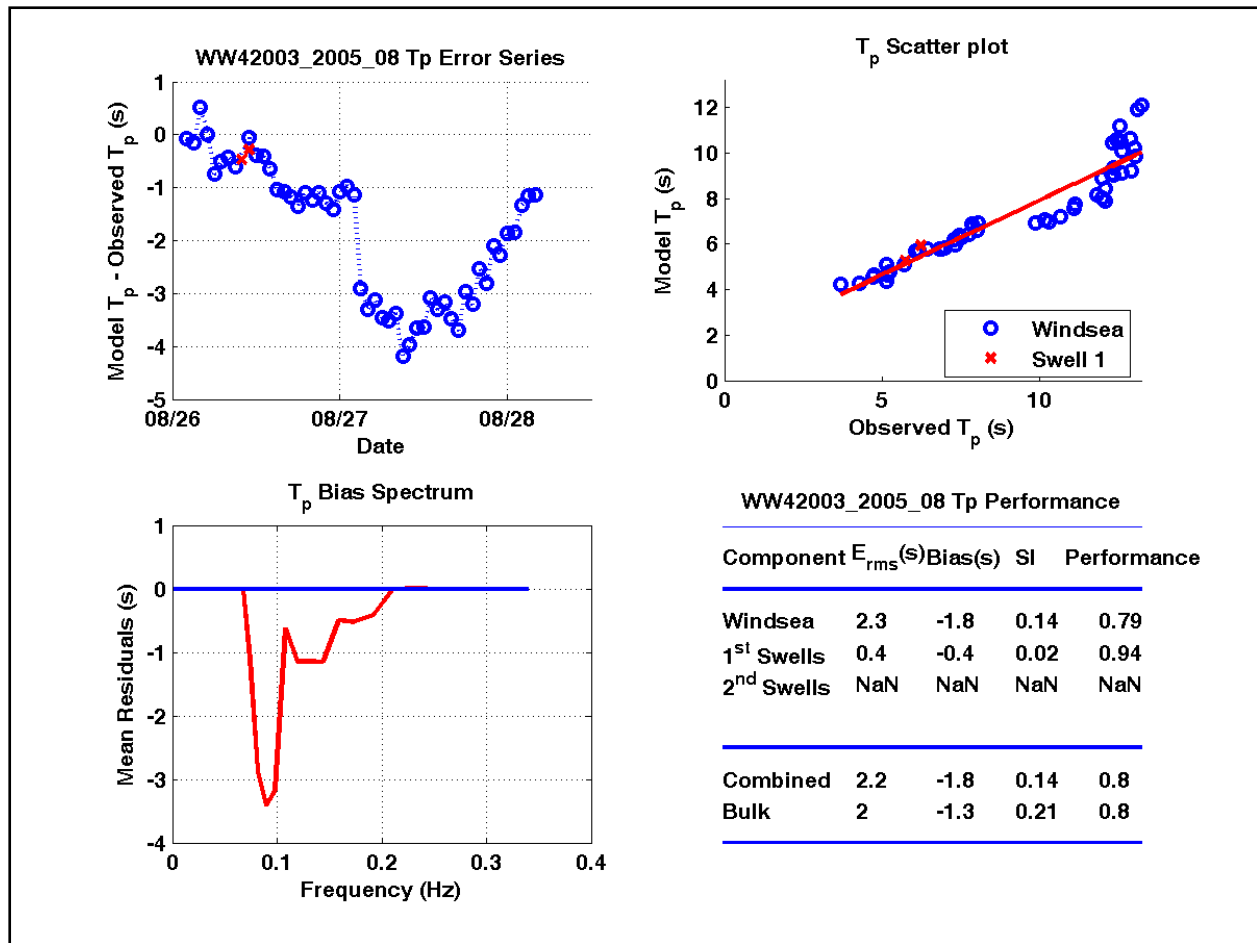


Figure 3-78. Wave period correlation results for WAVEWATCH hindcast at station 42003

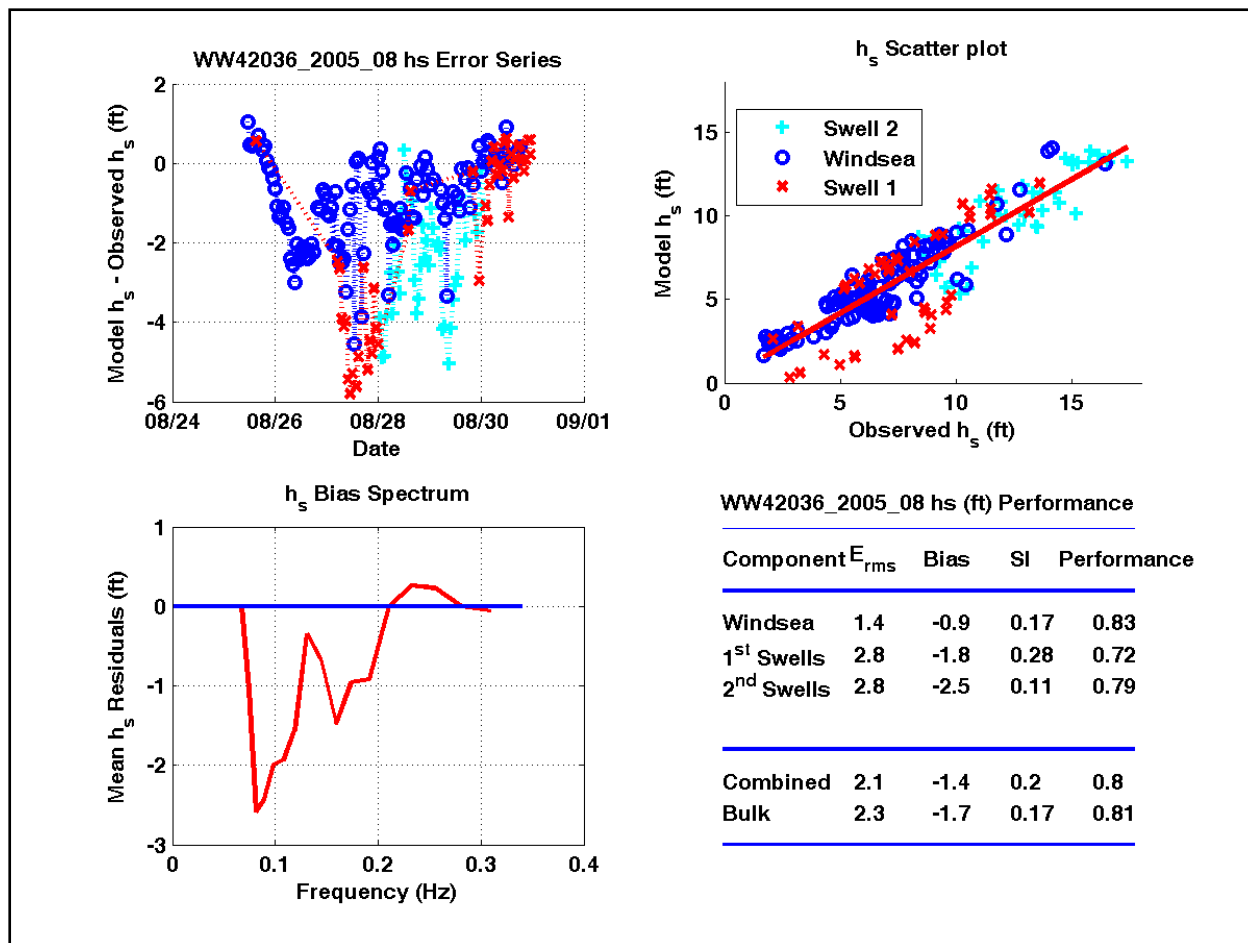


Figure 3-79. Wave height correlation results for WAVEWATCH hindcast at station 42036



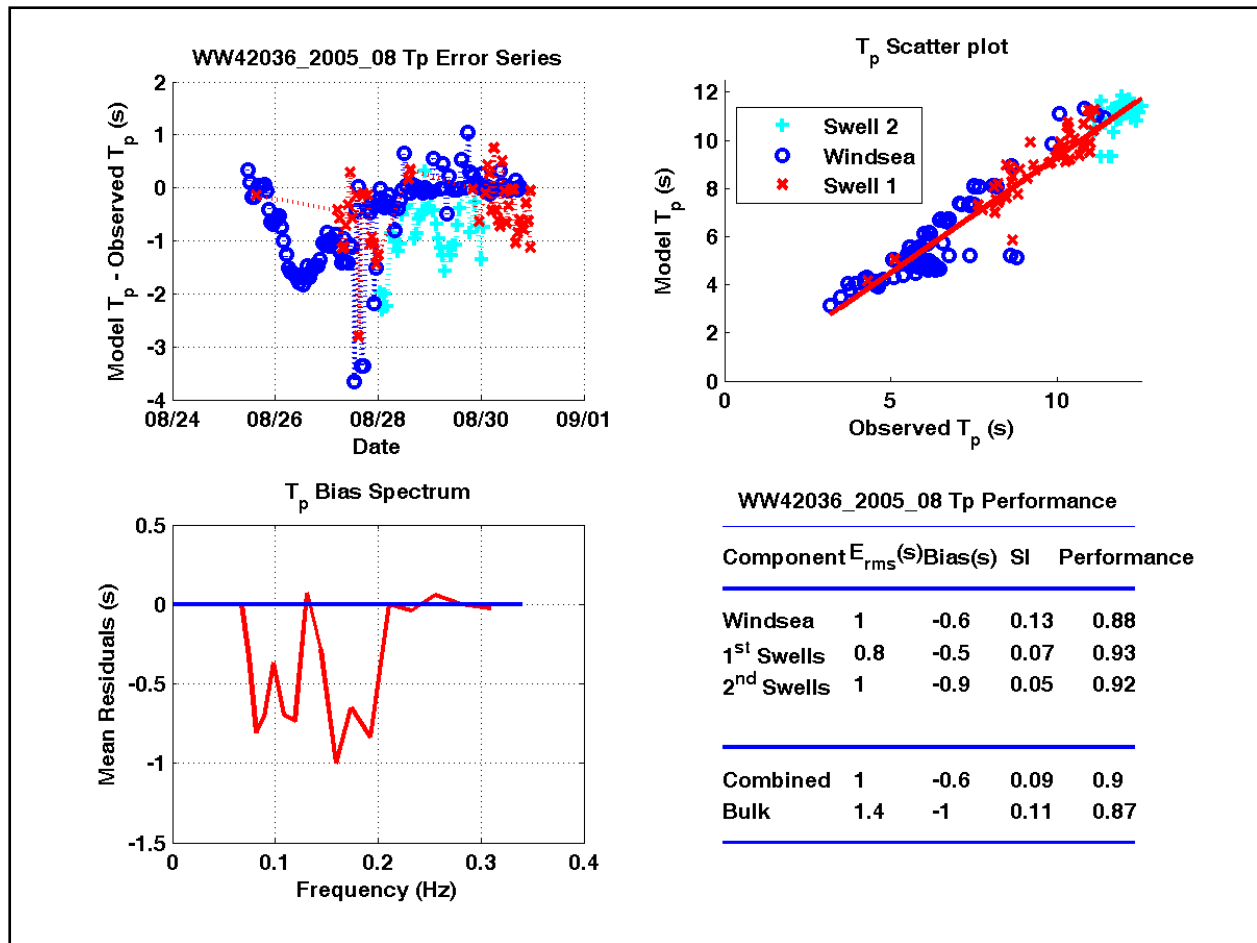


Figure 3-80. Wave period correlation results for WAVEWATCH hindcast at station 42036

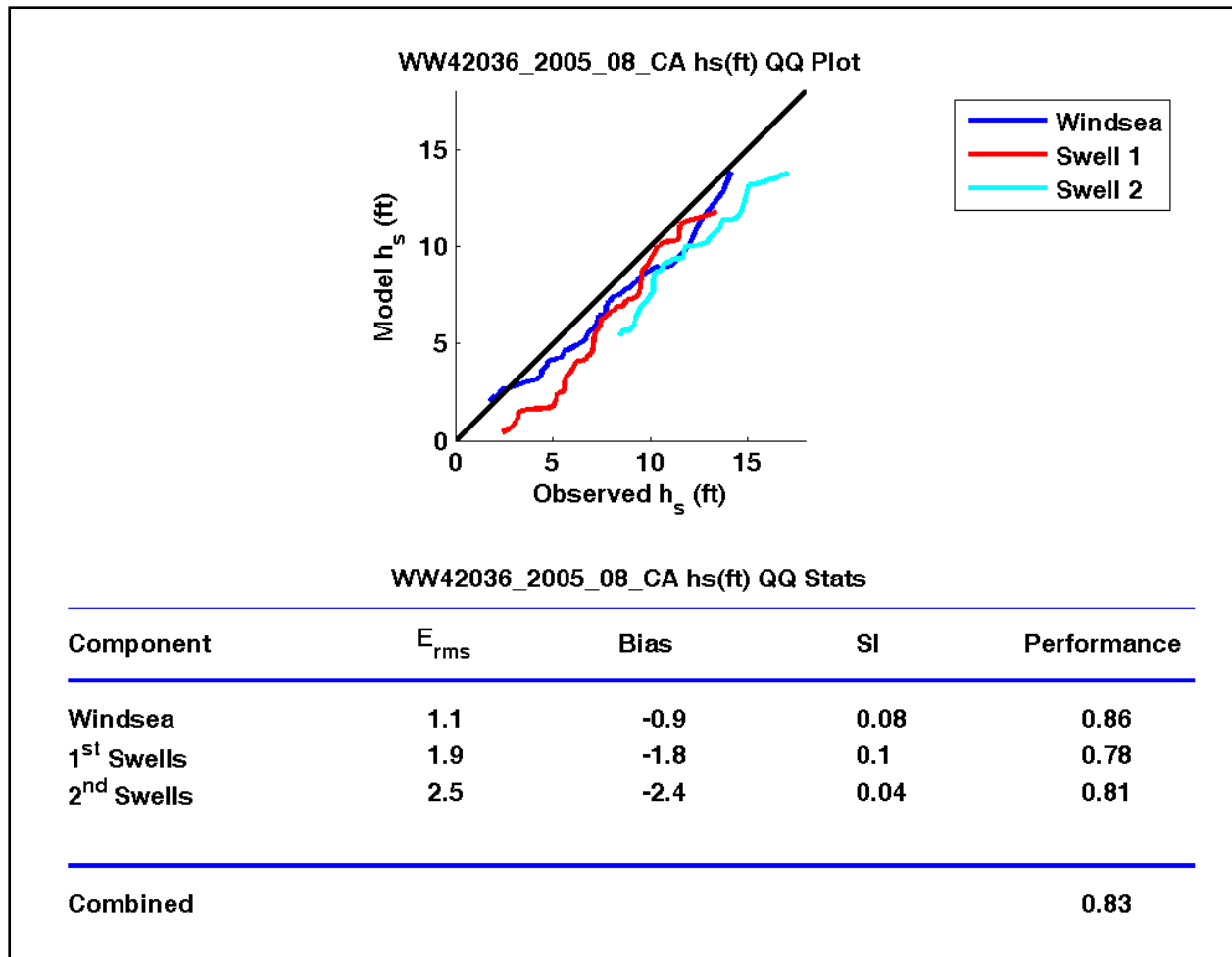


Figure 3-81. Wave height quantile-quantile results for WAVEWATCH hindcast at station 42036

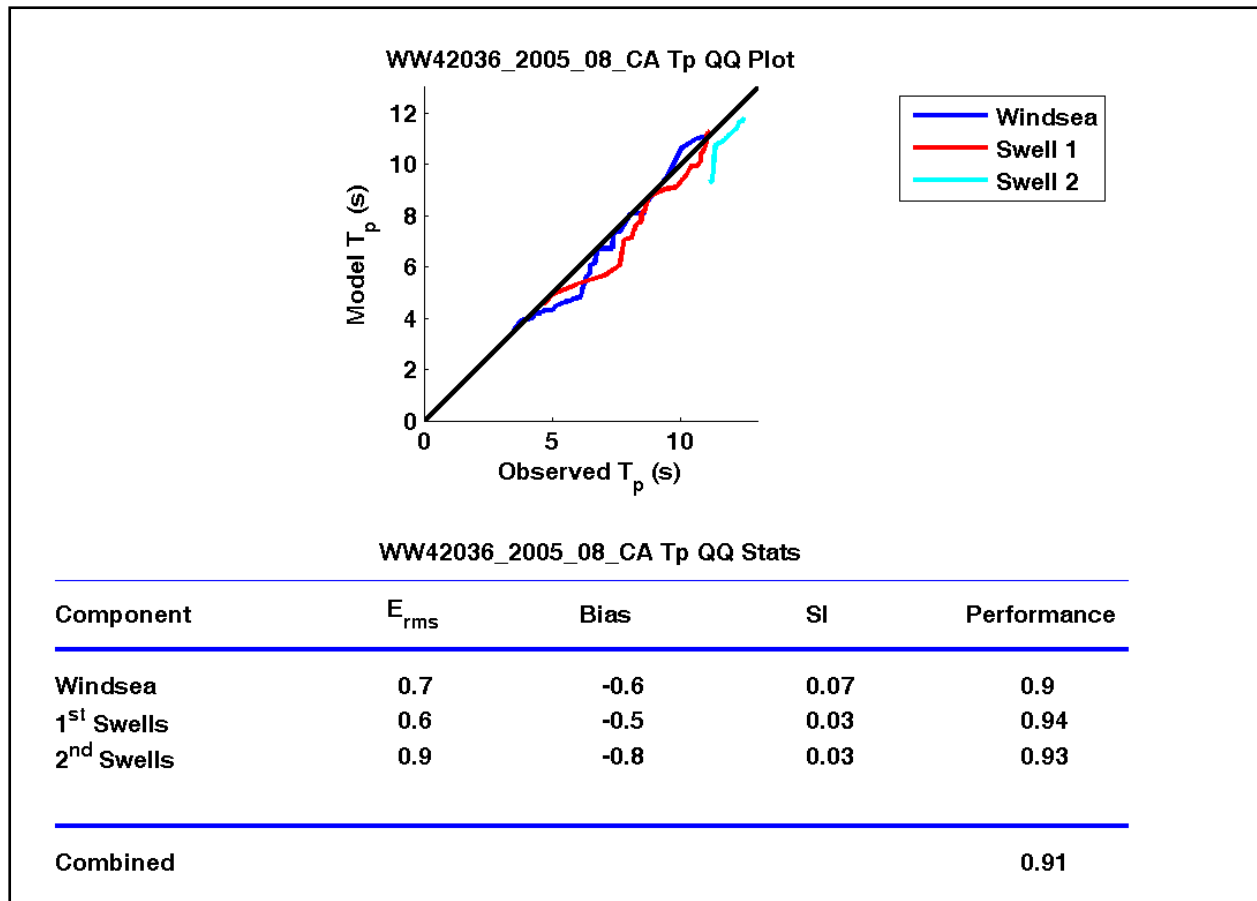


Figure 3-82. Wave period quantile-quantile results for WAVEWATCH hindcast at station 42036

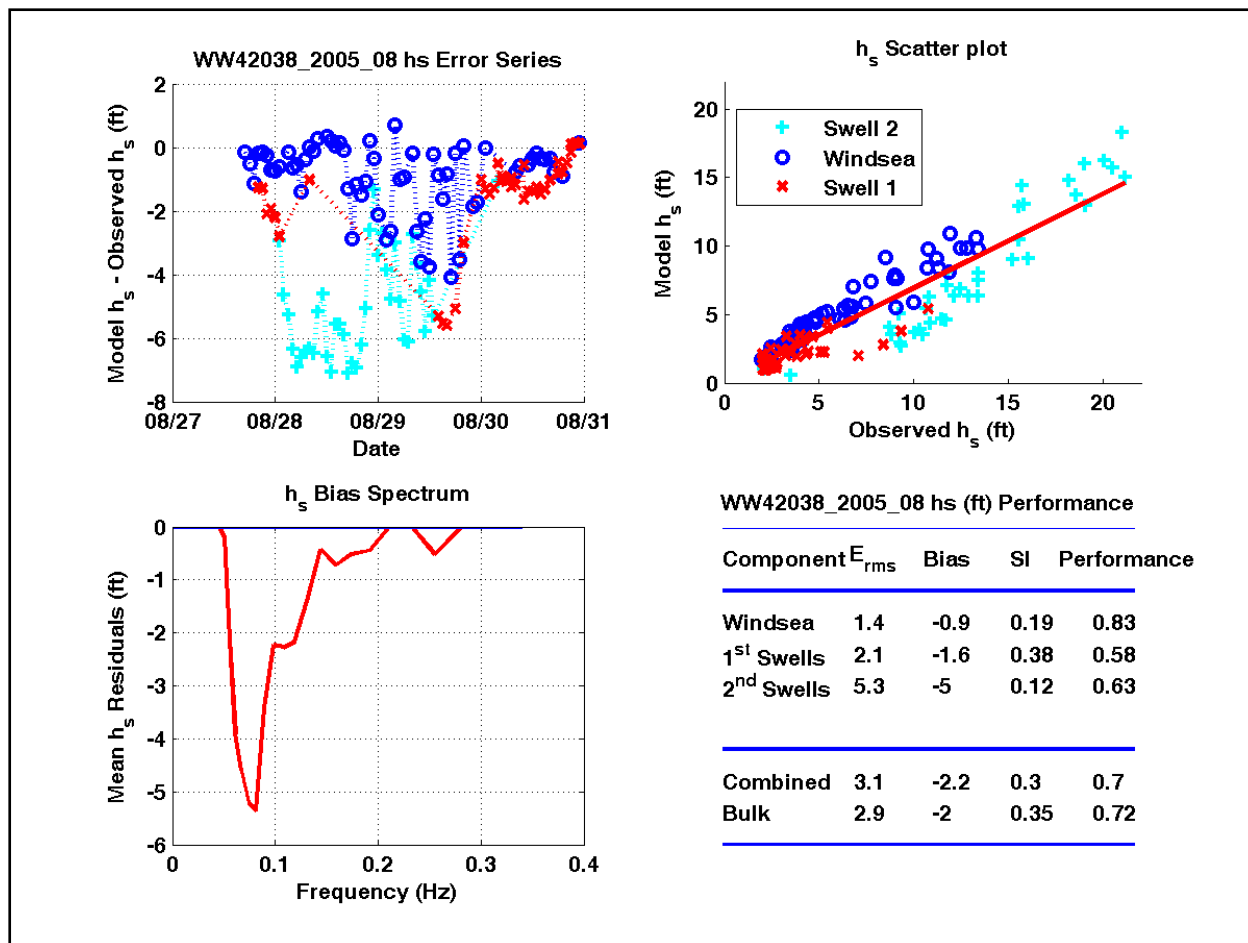


Figure 3-83. Wave height correlation results for WAVEWATCH hindcast at station 42038

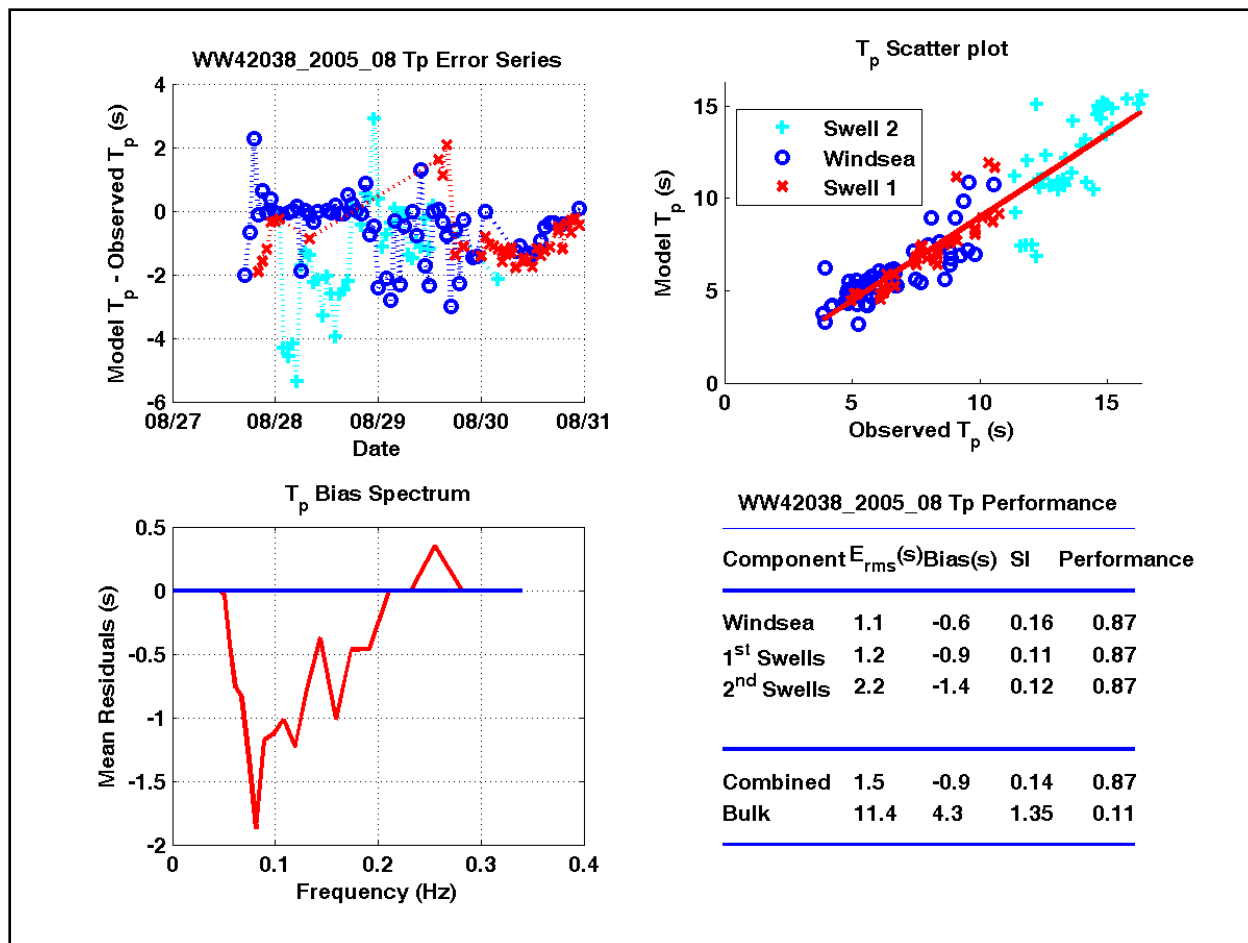


Figure 3-84. Wave period correlation results for WAVEWATCH hindcast at station 42038



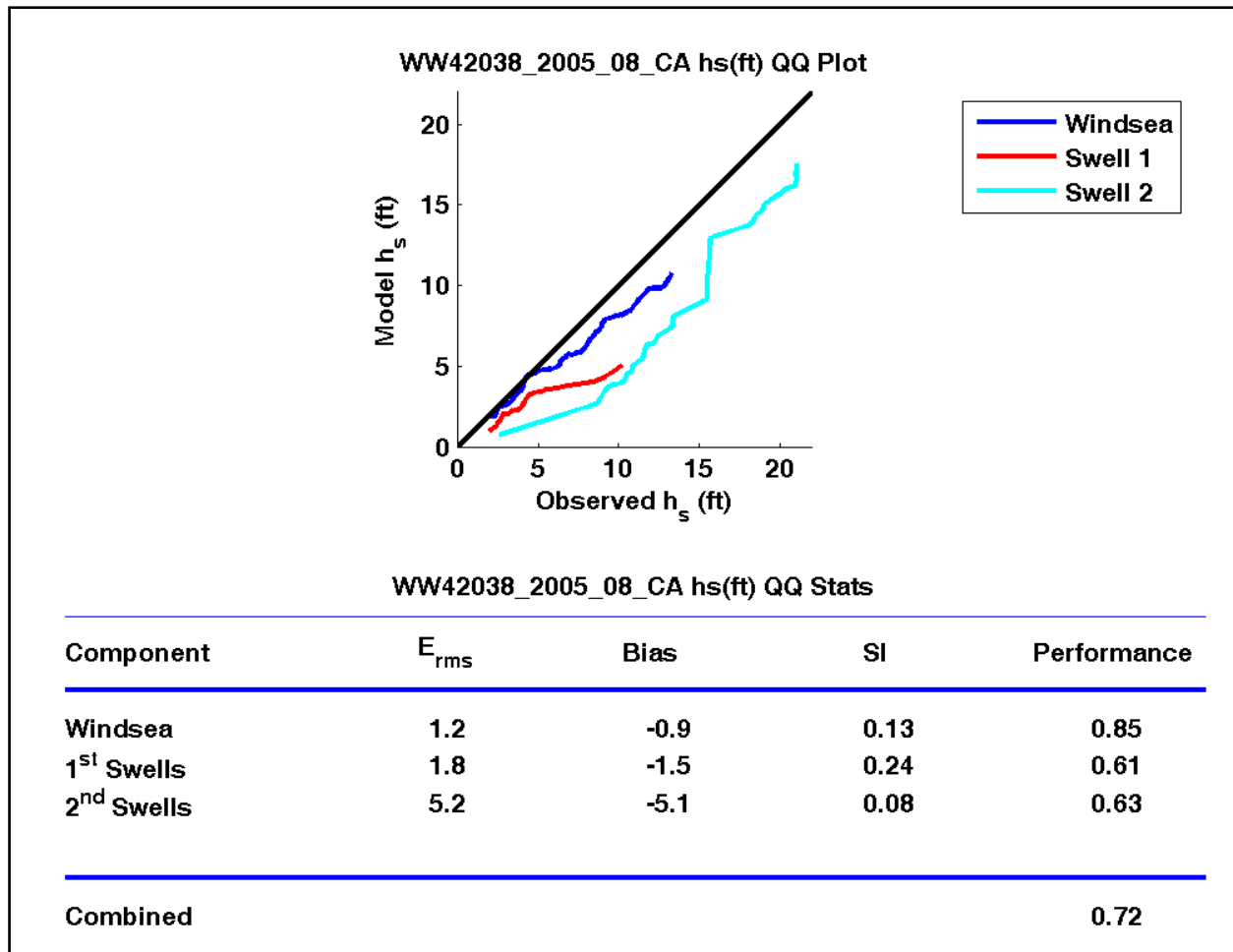


Figure 3-85. Wave height quantile-quantile results for WAVEWATCH hindcast at station 42038

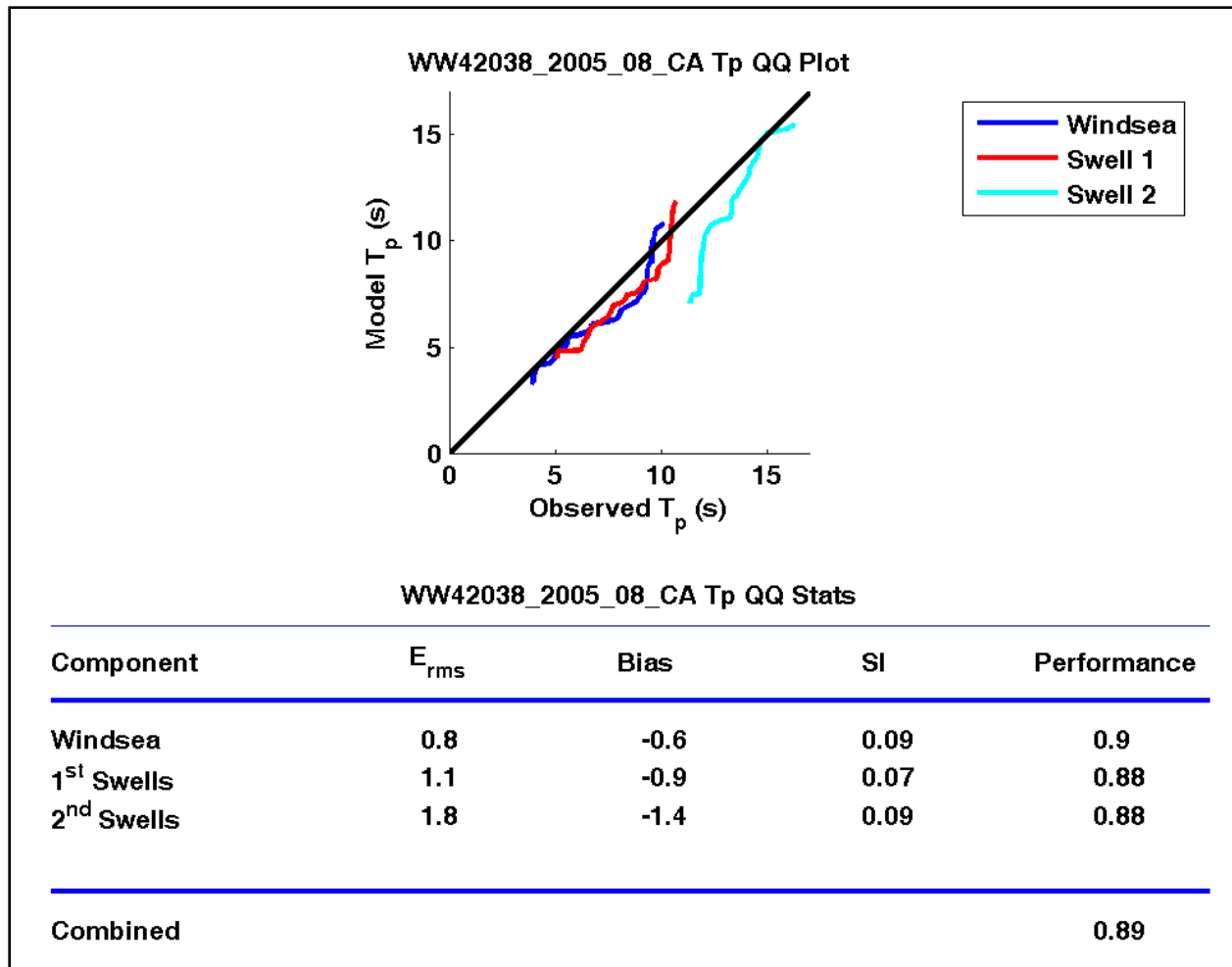


Figure 3-86. Wave period quantile-quantile results for WAVEWATCH hindcast at station 42038

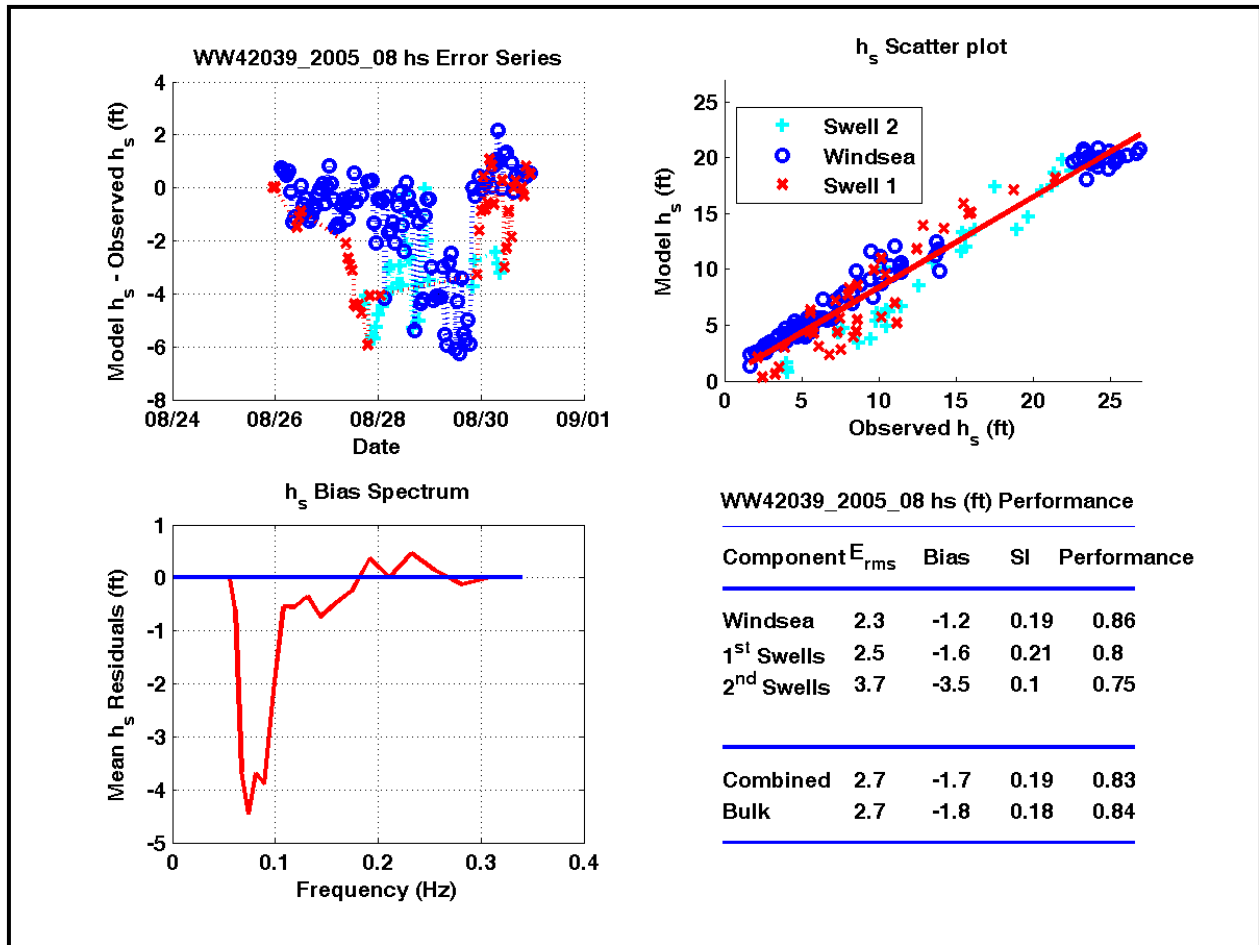


Figure 3-87. Wave height correlation results for WAVEWATCH hindcast at station 42039

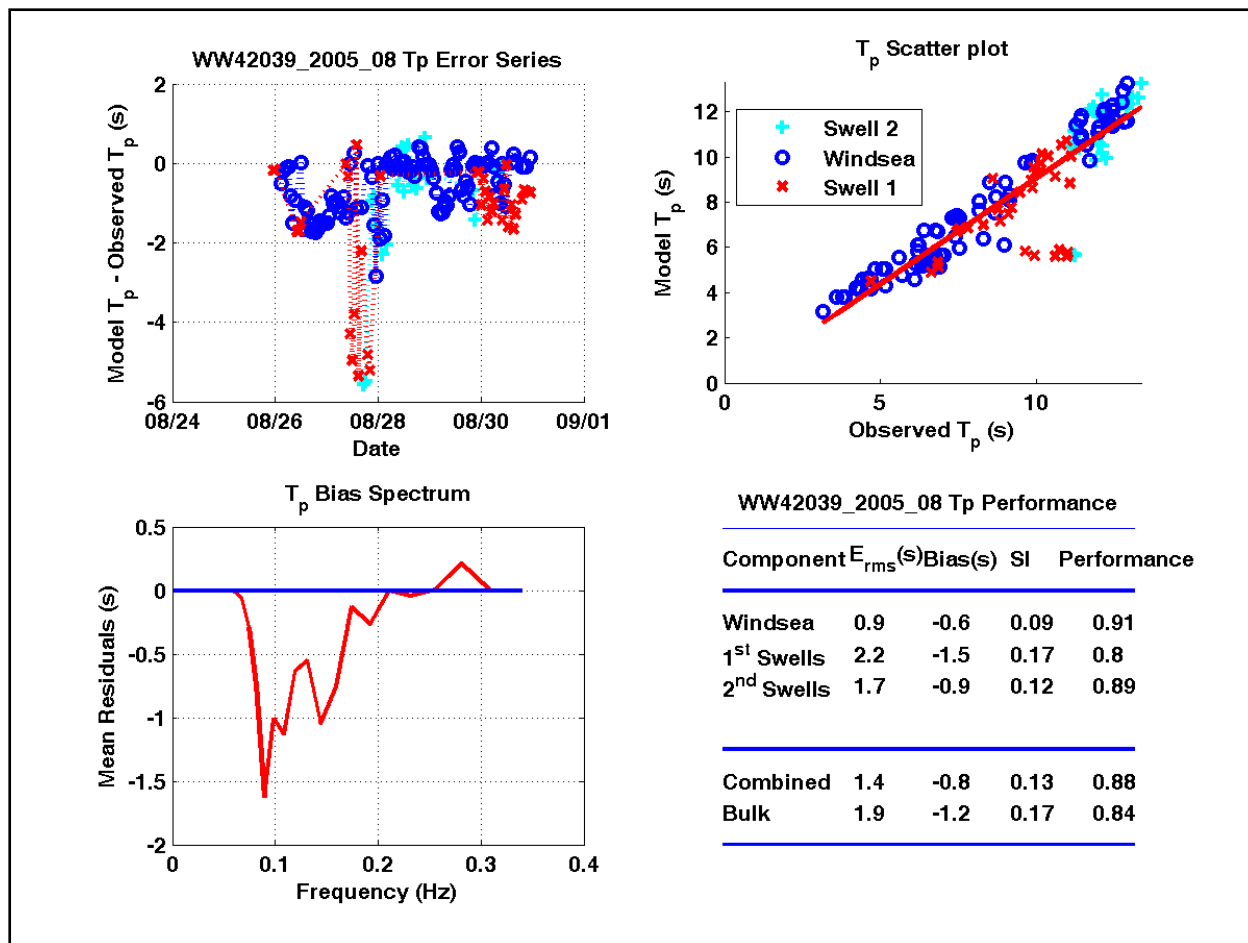


Figure 3-88. Wave period correlation results for WAVEWATCH hindcast at station 42039

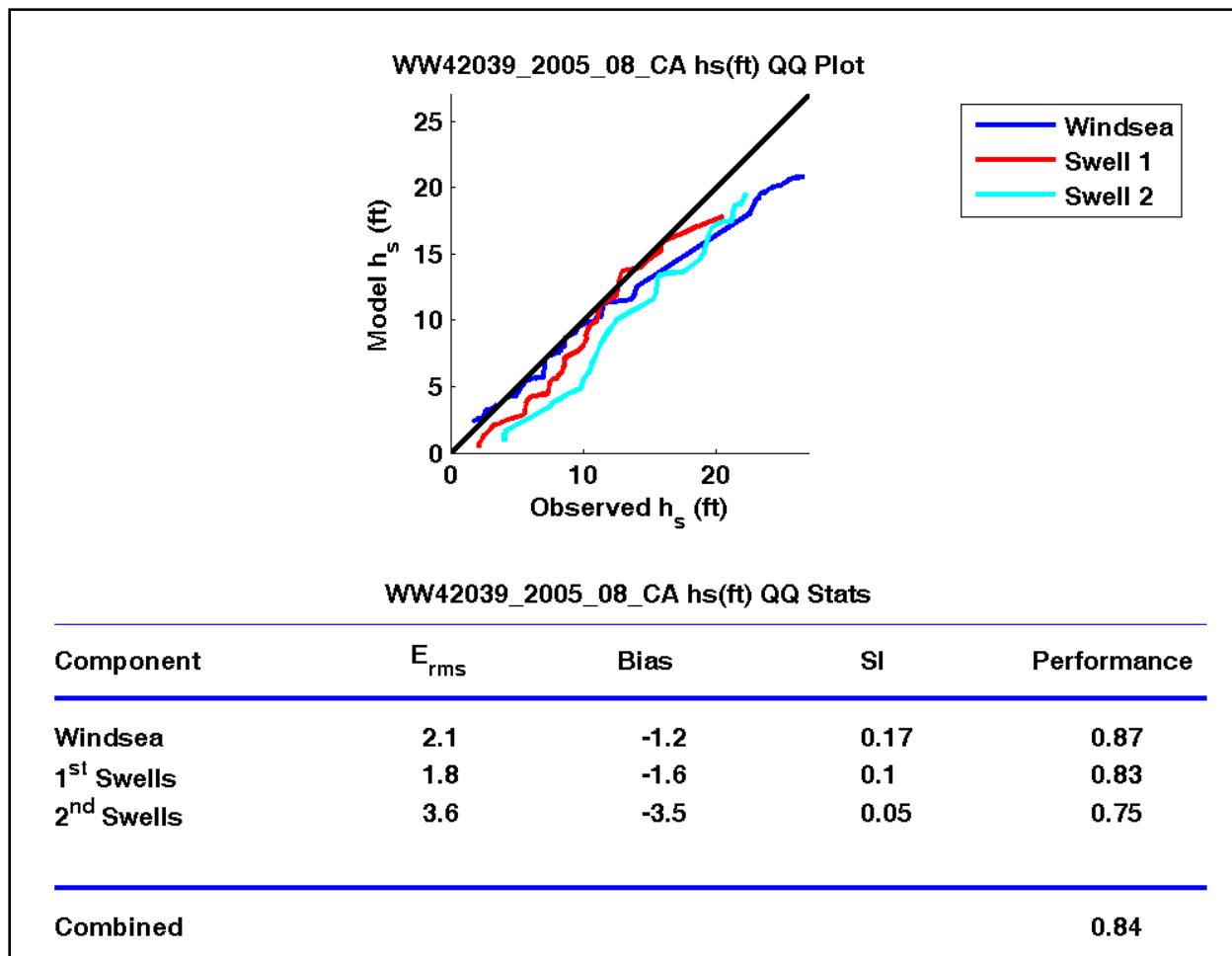


Figure 3-89. Wave height quantile-quantile results for WAVEWATCH hindcast at station 42039



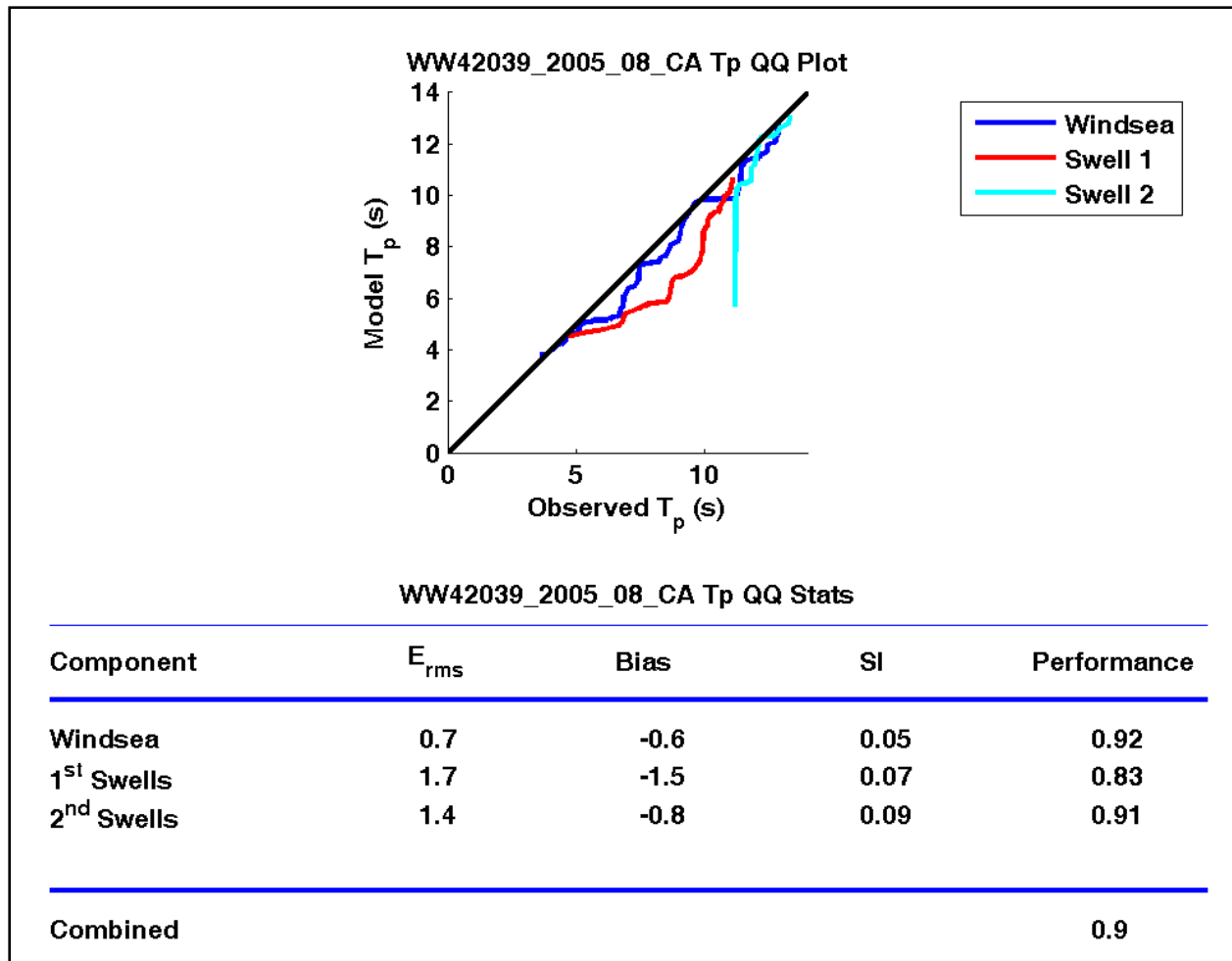


Figure 3-90. Wave period quantile-quantile results for WAVEWATCH hindcast at station 42039

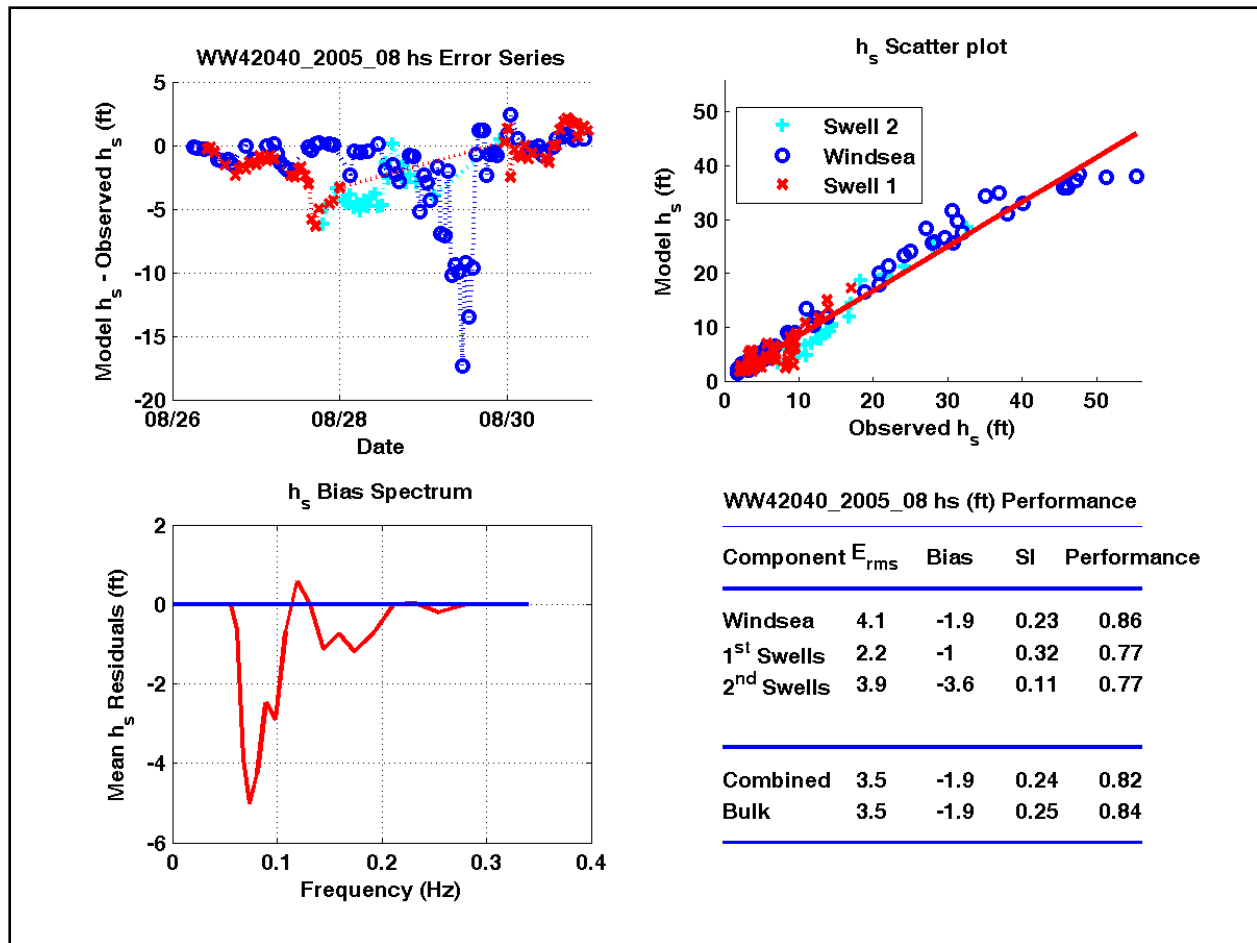


Figure 3-91. Wave height correlation results for WAVEWATCH hindcast at station 42040

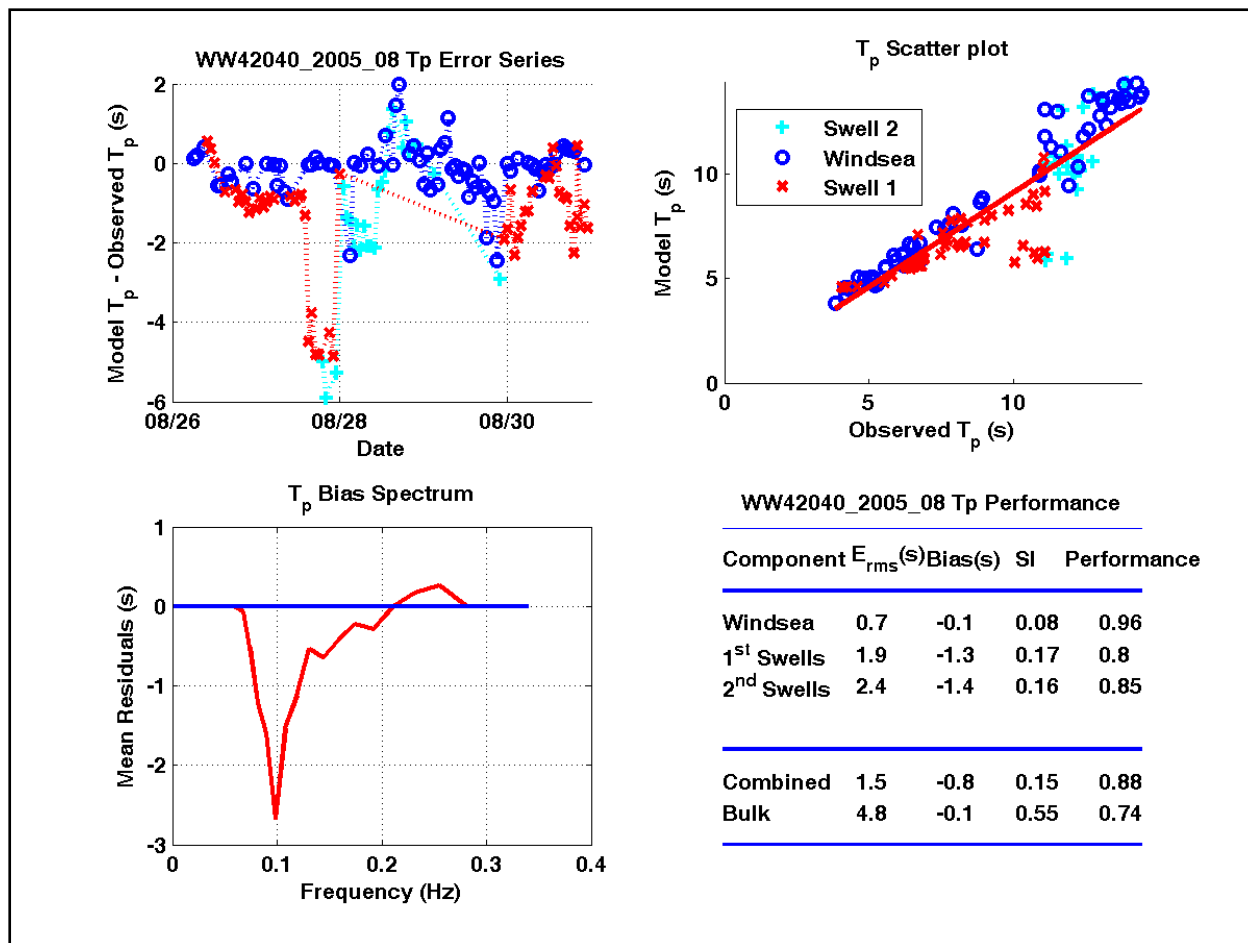


Figure 3-92. Wave period correlation results for WAVEWATCH hindcast at station 42040

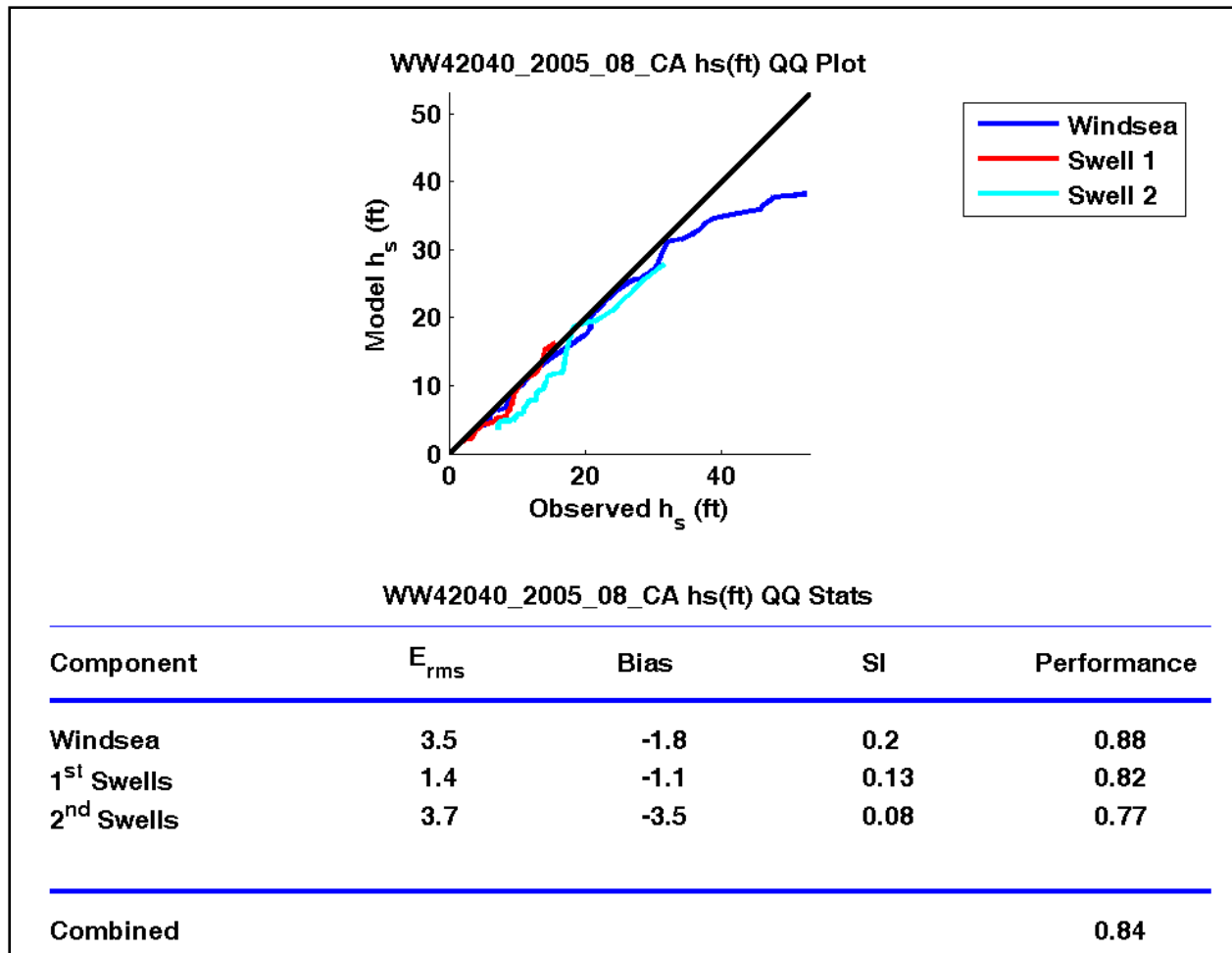


Figure 3-93. Wave height quantile-quantile results for WAVEWATCH hindcast at station 42040

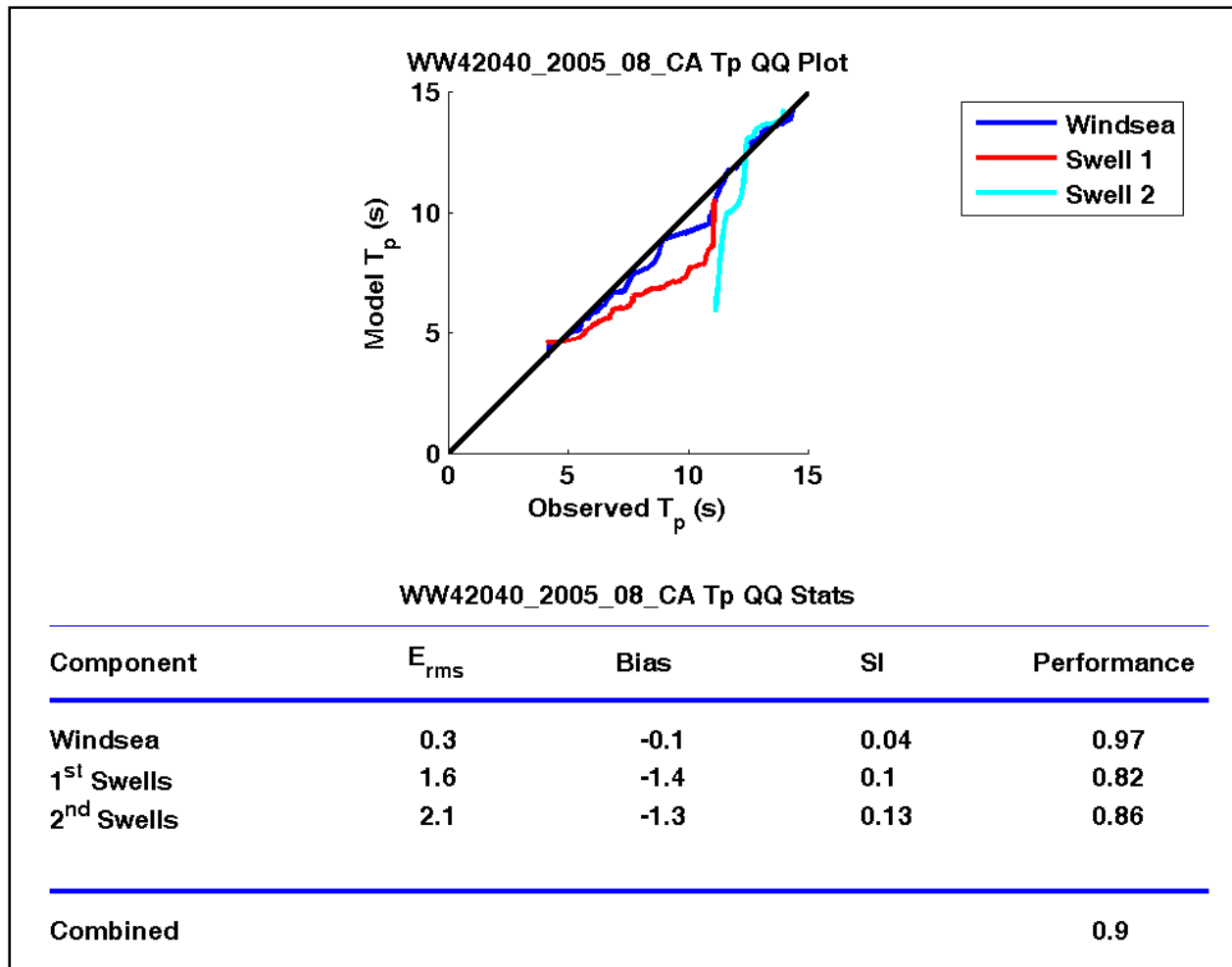


Figure 3-94. Wave period quantile-quantile results for WAVEWATCH hindcast at station 42040



# Appendix 4

## Nearshore Waves

---

### Introduction

This section describes the numerical modeling of nearshore wave transformation and generation for Hurricane Katrina within IPET Task 4. Nearshore waves are required to calculate wave runup and overtopping on structures, the wave momentum (radiation stress) contribution to elevated water levels (wave setup), and wave forces on structures. First the nearshore wave model STWAVE is briefly described, then the modeling methodology is outlined, and finally, results and sensitivity analyses are presented.

### Nearshore Wave Model STWAVE

The numerical model STWAVE (Smith 2000; Smith, Sherlock, and Resio 2001; Smith and Smith 2001; Thompson, Smith, and Miller 2004) was used to generate and transform waves to the shore for Hurricane Katrina. STWAVE numerically solves the steady-state conservation of spectral action balance along backward-traced wave rays:

$$(C_{ga})_x \frac{\partial}{\partial x} \frac{C_a C_{ga} \cos(\mu - \alpha) E(f, \alpha)}{\omega_r} + (C_{ga})_y \frac{\partial}{\partial y} \frac{C_a C_{ga} \cos(\mu - \alpha) E(f, \alpha)}{\omega_r} = \sum \frac{S}{\omega_r} \quad (4-1)$$

where

$C_{ga}$  = absolute wave group celerity

$x, y$  = spatial coordinates, subscripts indicate  $x$  and  $y$  components

$C_a$  = absolute wave celerity

$\mu$  = current direction

$\alpha$  = propagation direction of spectral component

$E$  = spectral energy density

$f$  = frequency of spectral component

$\omega_r$  = relative angular frequency (frequency relative to the current)

$S$  = energy source/sink terms

The source terms include wind input, nonlinear wave-wave interactions, dissipation within the wave field, and surf-zone breaking. The terms on the left-hand side of Equation 4-1 represent wave propagation (refraction and shoaling), and the source terms on the right-hand side of the equation represent energy growth and decay in the spectrum.

The assumptions made in STWAVE are as follows:

- a. Mild bottom slope and negligible wave reflection.
- b. Steady waves, currents, and winds.
- c. Linear refraction and shoaling.
- d. Depth-uniform current.

STWAVE can be implemented as either a half-plane model, meaning that only waves propagating toward the coast are represented, or a full-plane model, allowing generation and propagation in all directions. Wave breaking in the surf zone limits the maximum wave height based on the local water depth and wave steepness:

$$H_{m_{o,max}} = 0.1L \tanh kd$$

where

$H_{m_o}$  = zero-moment wave height

$L$  = wavelength

$k$  = wave number

$d$  = water depth

STWAVE is a finite-difference model and calculates wave spectra on a rectangular grid. The model outputs zero-moment wave height (Equation 3-4), peak wave period ( $T_p$ , Equation 3-6), and mean wave direction ( $\alpha_m$ , Equation 3-7) at all grid points and two-dimensional spectra at selected grid points. For Katrina applications, an option has been added to input spatially variable surge fields. The surge significantly alters the wave transformation and generation for the hurricane simulations in shallow areas (such as Lake Pontchartrain) and where low-laying areas are flooded. Spatially varying wind input has also been added as an option to STWAVE for Katrina applications.

## Wave Model Inputs

The inputs required to execute STWAVE include:

- a. Bathymetry grid (including shoreline position and grid size and resolution).
- b. Incident frequency-direction wave spectra on the offshore grid boundary.
- c. Current field (optional).
- d. Surge and/or tide fields, wind speed, and wind direction (optional).
- e. Bottom friction coefficients (optional).

## Wave Model Outputs

The outputs generated by STWAVE include:

- a.* Fields of energy-based, zero-moment wave height, peak spectral wave period, and mean direction.
- b.* Wave spectra at selected locations.
- c.* Fields of radiation stress gradients to use as input to ADCIRC (to calculate wave setup).

## Nearshore Wave Modeling Methodology

STWAVE was applied on four grids for the southern Louisiana area: Lake Pontchartrain, Louisiana Southeast, Louisiana South, and Mississippi/Alabama (Figure 4-1). Four grids were used to take advantage of the efficient half-plane version of STWAVE for the three outer grids (which must approximately align with the shoreline) and to concentrate grid coverage in the areas of interest. The input for each grid includes the bathymetry (interpolated from the ADCIRC domain), surge fields (interpolated from ADCIRC surge fields), and wind (interpolated from the ADCIRC wind fields, which apply land effects to the OWI wind fields). The wind applied in STWAVE is spatially and temporally variable for all domains. STWAVE was run at 30-min intervals from 0030 UTC on 28 August 2005 to 0000 UTC on 30 August 2005.

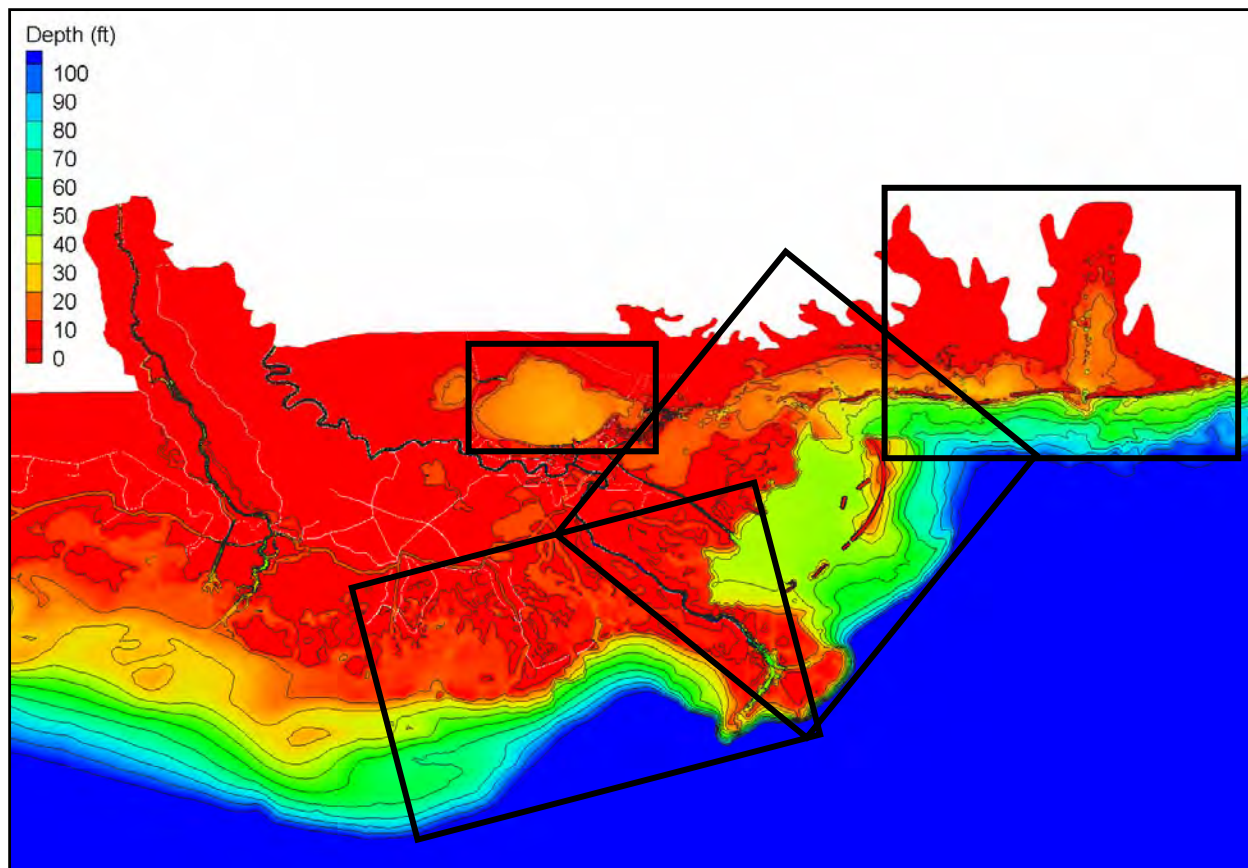


Figure 4-1. STWAVE modeling domains.

### Lake Pontchartrain Grid

The first grid covers Lake Pontchartrain at a resolution of 656 ft (200 m). Earlier runs were made at finer resolution 164 ft (50 m) by 328 ft (100 m), but the results were essentially the same, so the more efficient coarse grid is used for these simulations. The domain is approximately 25.8 by 41.9 miles (41.6 by 67.4 km). Lake Pontchartrain is run with the full-plane STWAVE to include generation and transformation along the entire lake shoreline. The grid parameters are given in Table 4-1. Figure 4-2 shows the bathymetry for the Lake Pontchartrain Grid relative to NAVD 88 (2004.65). Brown/red areas in the bathymetry plots indicate land areas at 0 ft or higher elevation.

<b>Table 4-1 STWAVE Grid Specifications</b>								
<b>Grid</b>	<b>State Plane</b>	<b>X origin, ft</b>	<b>Y origin, ft</b>	<b><math>\Delta x</math>, ft</b>	<b><math>\Delta y</math>, ft</b>	<b>Orient, Deg</b>	<b>X cells</b>	<b>Y cells</b>
Lake Pontchartrain	LA South	3563779.5	690485.6	656	656	270	208	337
Louisiana Southeast	LA Offshore	4294586.6	1639491.5	656	656	141	683	744
Louisiana South	LA Offshore	3997126.0	1264895.0	656	656	108	664	839
Mississippi/ Alabama	LA Offshore	4463976.4	1653950.1	656	656	90	563	605

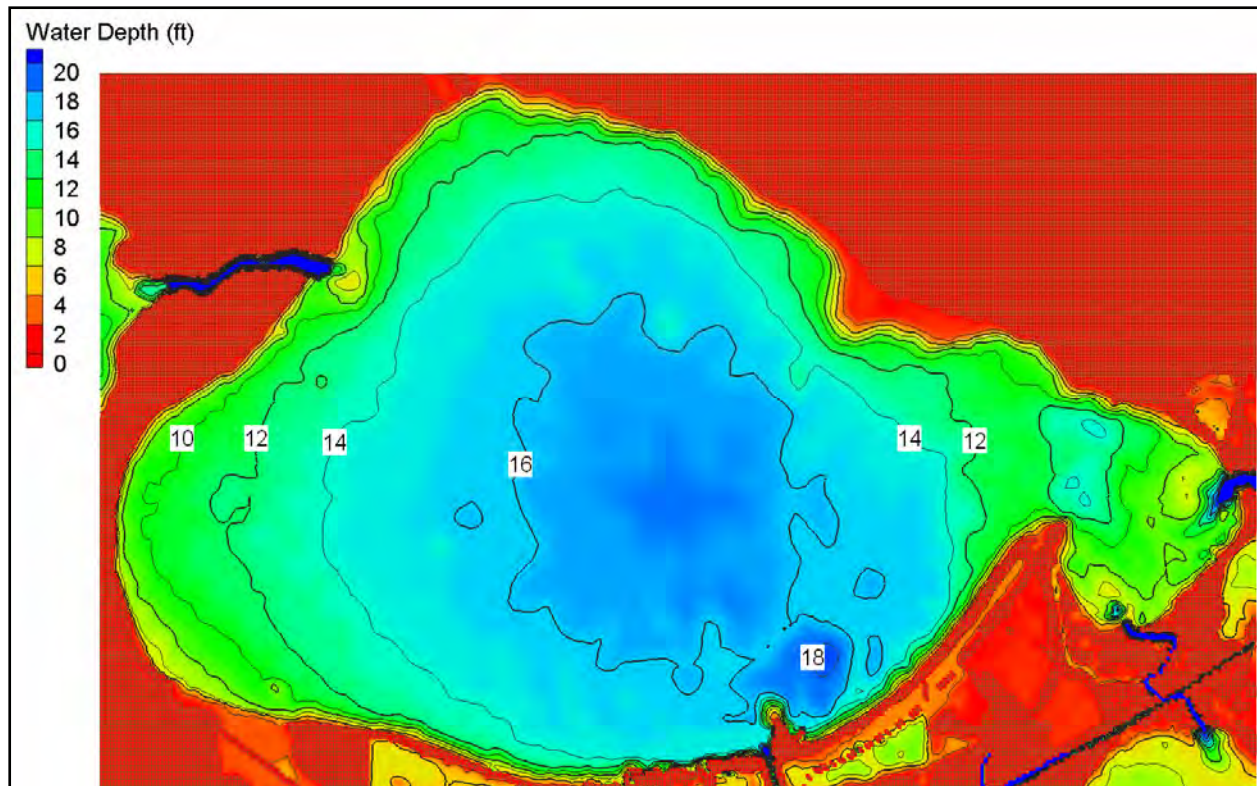


Figure 4-2. Lake Pontchartrain bathymetry grid (NGVD 88 2004.65).

### Louisiana Southeast and South Grids and Mississippi/Alabama Grid

The second, third, and fourth grids cover the coastal area east, southeast, and south of New Orleans at a resolution of 656 ft (200 m). The domain for the Louisiana southeast grid is approximately 84.9 by 92.4 miles (136.6 by 148.8 km) and extends from Mississippi Sound in the northeast to the Mississippi River in the southwest. The domain for the Louisiana south grid is approximately 82.5 by 104.2 miles (132.8 by 167.8 km) and extends from the Mississippi River in the east to the Atchafalaya River in the west. The domain for the Mississippi and Alabama coasts was added to simulate the wave momentum fluxes that increase the surge in Mississippi Sound and Lake Pontchartrain. The Mississippi/Alabama domain is approximately 70.0 by 75.2 miles (112.6 by 121.0 km) and extends from east of Mobile Bay to Biloxi, Mississippi. These three grids were run with the half-plane STWAVE for computational efficiency. The grid parameters are given in Table 4-1. Figures 4-3 to 4-5 show the bathymetry for the Louisiana southeast, Louisiana south, and Mississippi/Alabama grids, respectively. These simulations are forced with both the local winds and wave spectra interpolated on the offshore boundary from the regional WAM model described in Appendix 3.



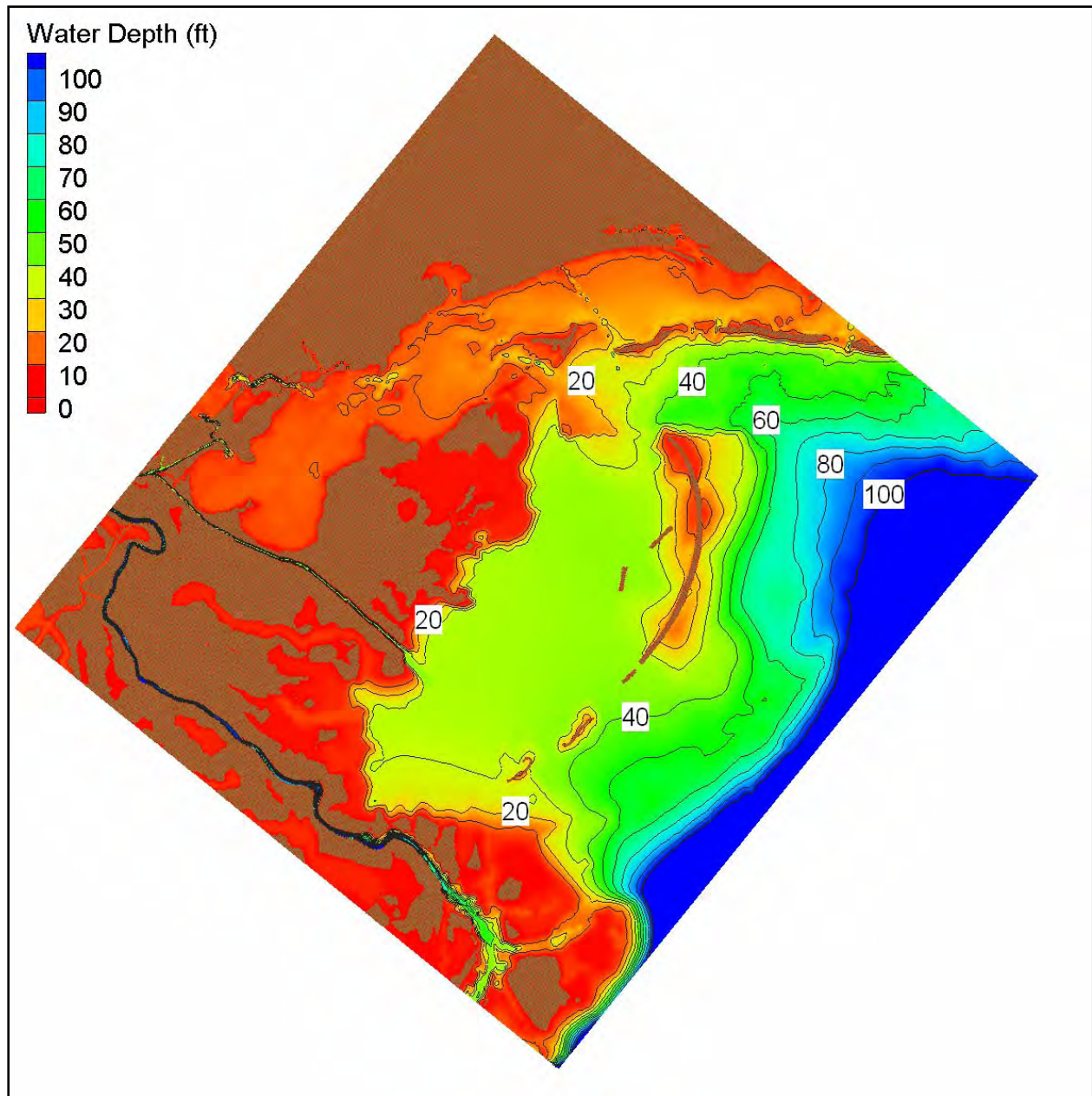


Figure 4-3. Louisiana Southeast bathymetry grid (NGVD 88 2004.65).

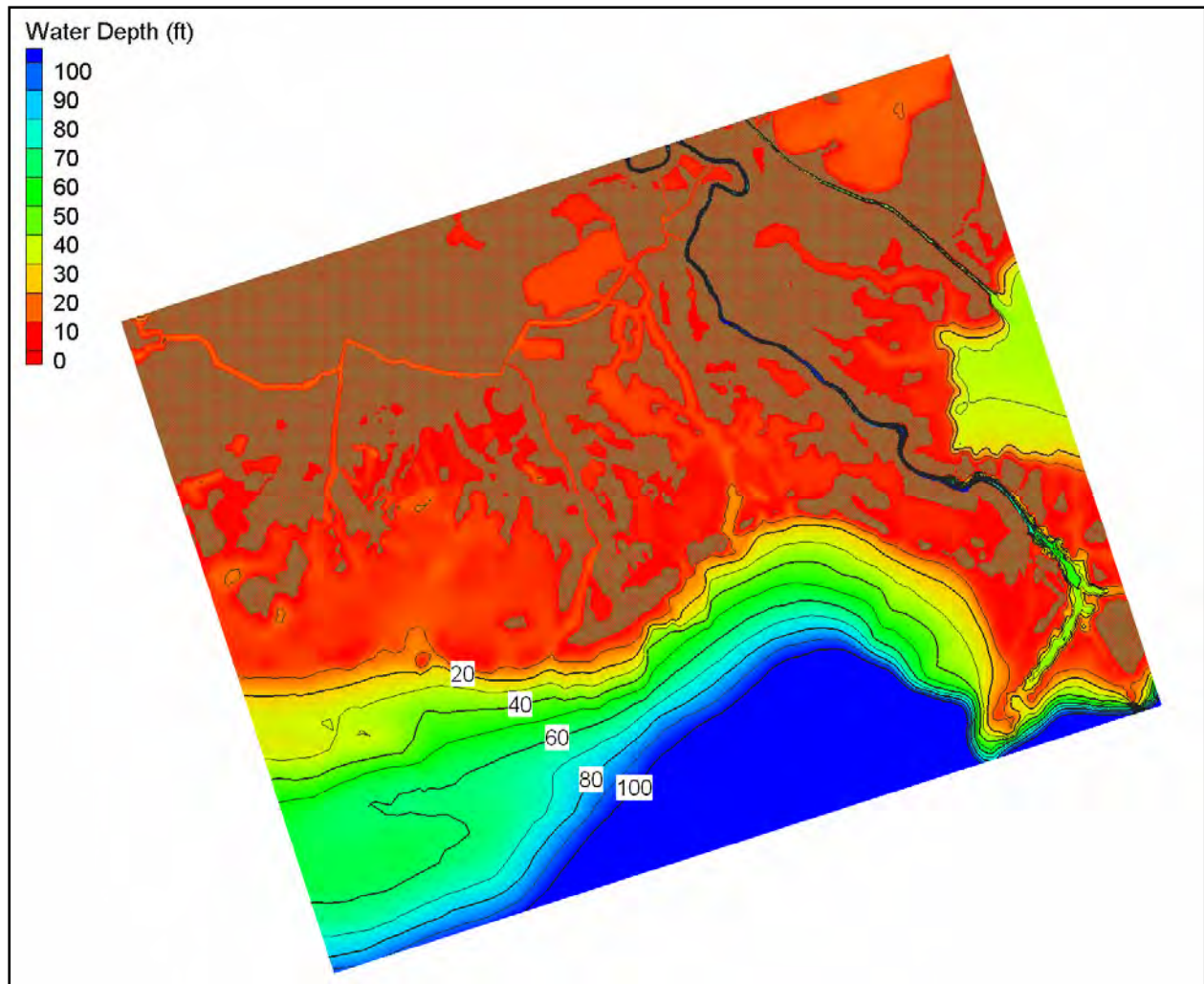


Figure 4-4. Louisiana South bathymetry grid (NGVD 88 2004.65).

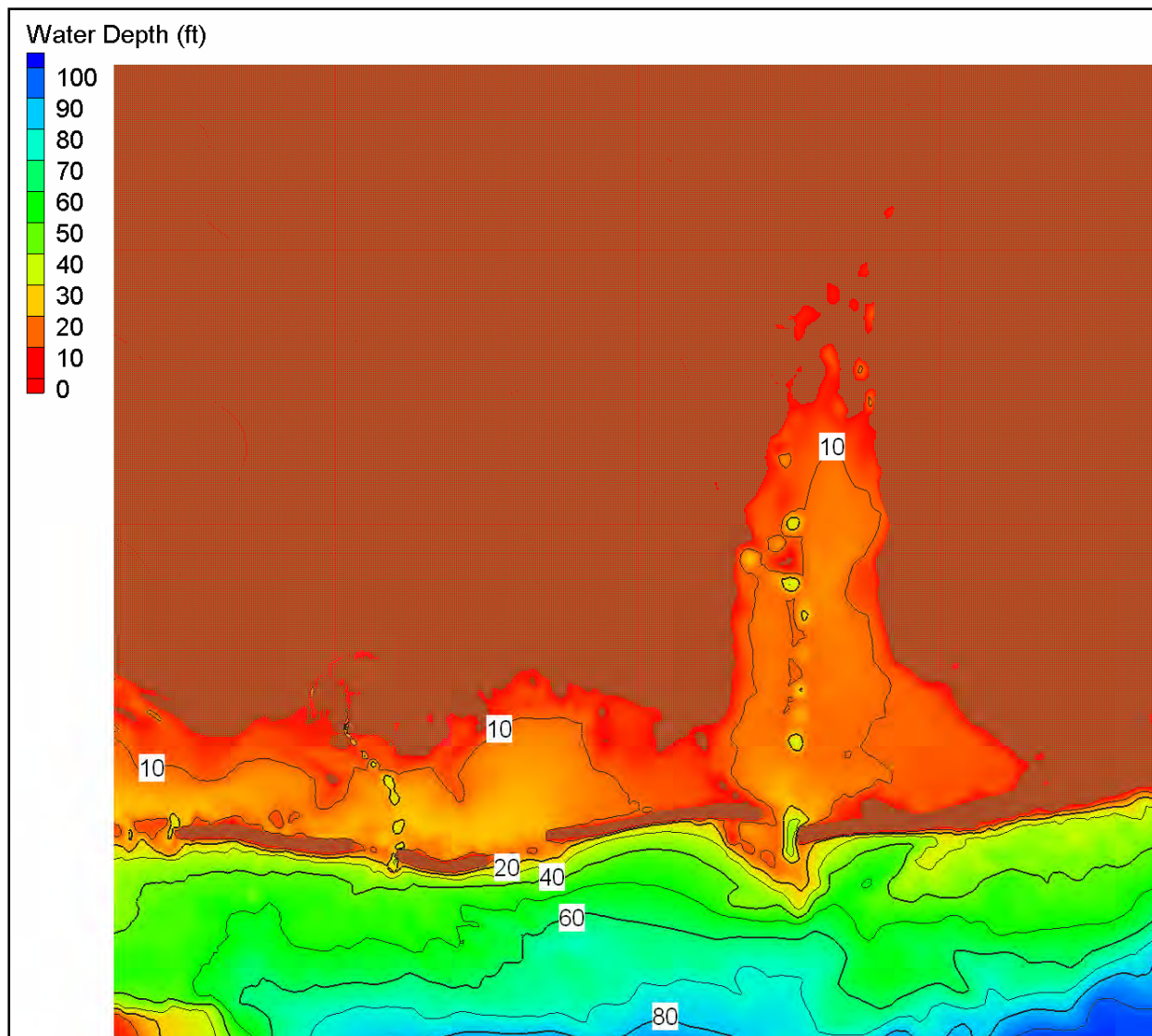


Figure 4-5. Mississippi/Alabama bathymetry grid (NGVD 88 2004.65).

## Results

### Lake Pontchartrain

The peak wave conditions on the south shore of Lake Pontchartrain occur at approximately 1330-1430 UTC on 29 August 2005. Figure 4-6 shows a snapshot of wave height and wave direction at 1430 UTC. The wind is approximately 60 knots (30 m/sec) from the north through northwest. The maximum wave height is 8.7 ft with a peak wave period of 7 sec. Figure 4-7 shows the maximum wave height for each grid cell within the domain for the entire simulation period. Areas contoured in darkest blue with no vectors (zero wave height or period) are land areas. Figure 4-8 shows the peak wave period corresponding to the maximum wave height for



each cell. The maximum wave heights range from 8.0 to 8.7 ft on the New Orleans lakefront and the associated peak periods are 7-8 sec.

Three small wave buoys were deployed in Lake Pontchartrain on 27 August 2005 to capture wave conditions in Hurricane Katrina. Two of those gauges were recovered and provide valuable comparison data. The deployment locations were 30 deg 2.053' North, 90 deg 7.358' West for Gauge 22 and 30 deg 1.989' North, 90 deg 7.932' West for Gauge 23. Gauge 22 was directly north of the 17th Street Canal entrance and Gauge 23 was west of Gauge 22. Both gauges were in approximately 13 ft (4 m) water depth. The sampling records were a relatively short 8.5 min, so there is a lot scatter in the data. At the peak of the storm (~29 August 2005 1200 to 1530 UTC), the measured wave heights drop from approximately 8 ft to 5 ft. This is the time of maximum wind speed and thus the time when the maximum wave height would be expected. The wave height measurements do not appear to be reliable during the storm peak. The buoys may have experienced excesses tilt due to the extreme winds or been submerged or overturned. Figures 4-9 and 4-10 show comparisons of significant wave height and peak period, respectively, for the buoy locations. The blue lines are the measurements with the spectra averaged over 3 records (25.5 min), and the red line is the modeled parameters (30-min average). The STWAVE results are essentially the same for the two gauge sites. The modeled wave heights are an average of 1.04 ft (0.32 m) lower than the measurements in the growth stage of the storm (0000-1200 UTC 29 August 2005) and 0.26 ft (0.08 m) lower than the measurements in the decaying stage of the storm (1530-2400 UTC 29 August 2005). Comparisons at the storm peak are not meaningful. The modeled peak periods are consistent with the measurements, but 1.6 sec shorter in the decaying stage of the storm.

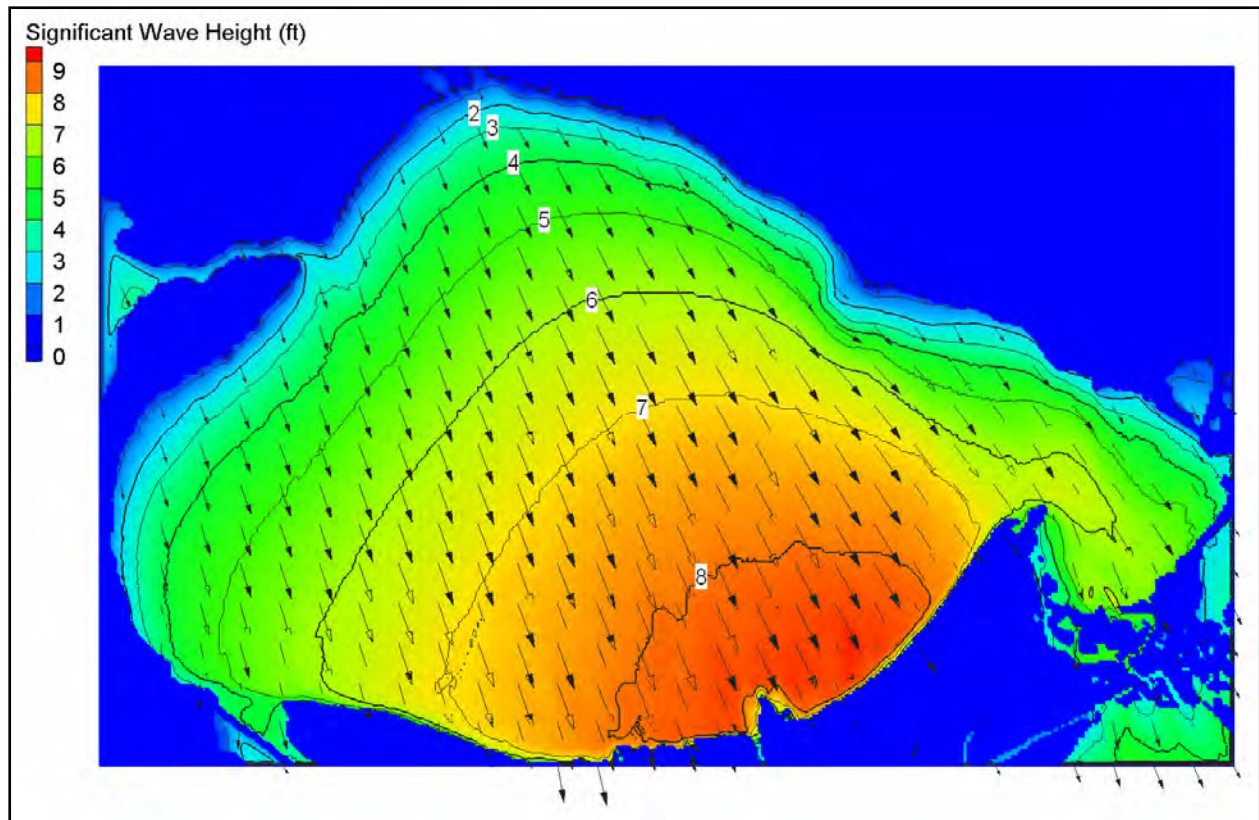


Figure 4-6. Lake Pontchartrain modeled wave height and direction for 1430 UTC on 29 August 2005 (wave heights in feet).



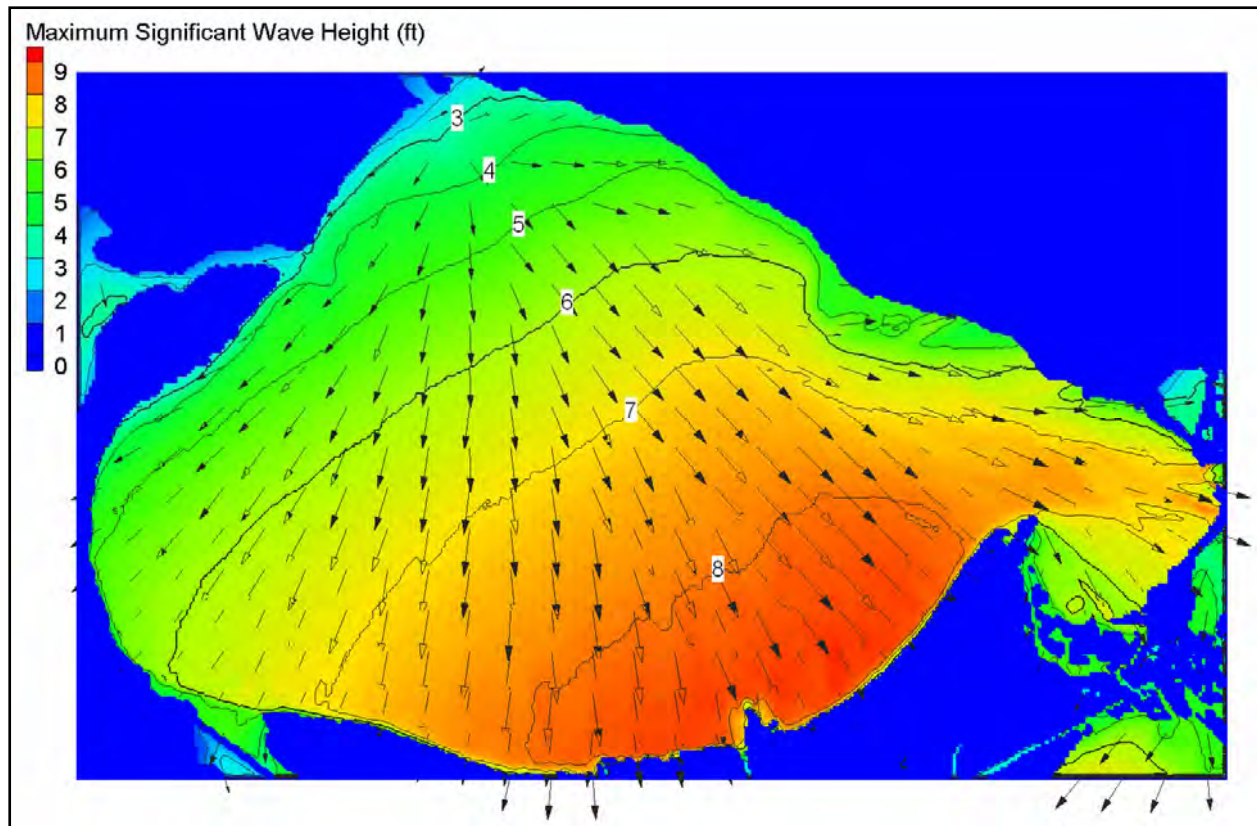


Figure 4-7. Lake Pontchartrain maximum modeled significant wave height and corresponding mean direction for 0030 UTC on 28 August to 0000 UTC on 30 August 2005 (wave heights in feet).

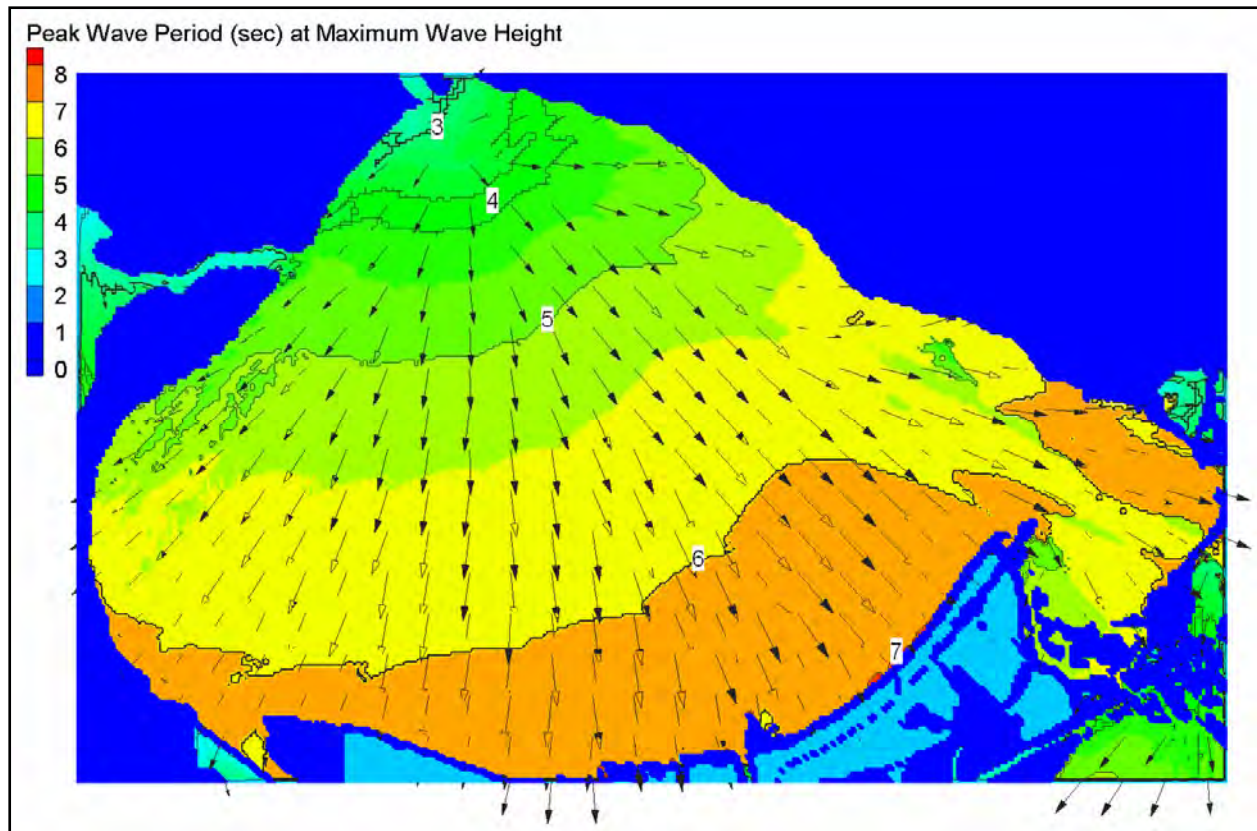


Figure 4-8. Lake Pontchartrain modeled peak wave period corresponding to the maximum wave height for 0030 UTC on 28 August to 0000 UTC on 30 August 2005 (periods in sec).

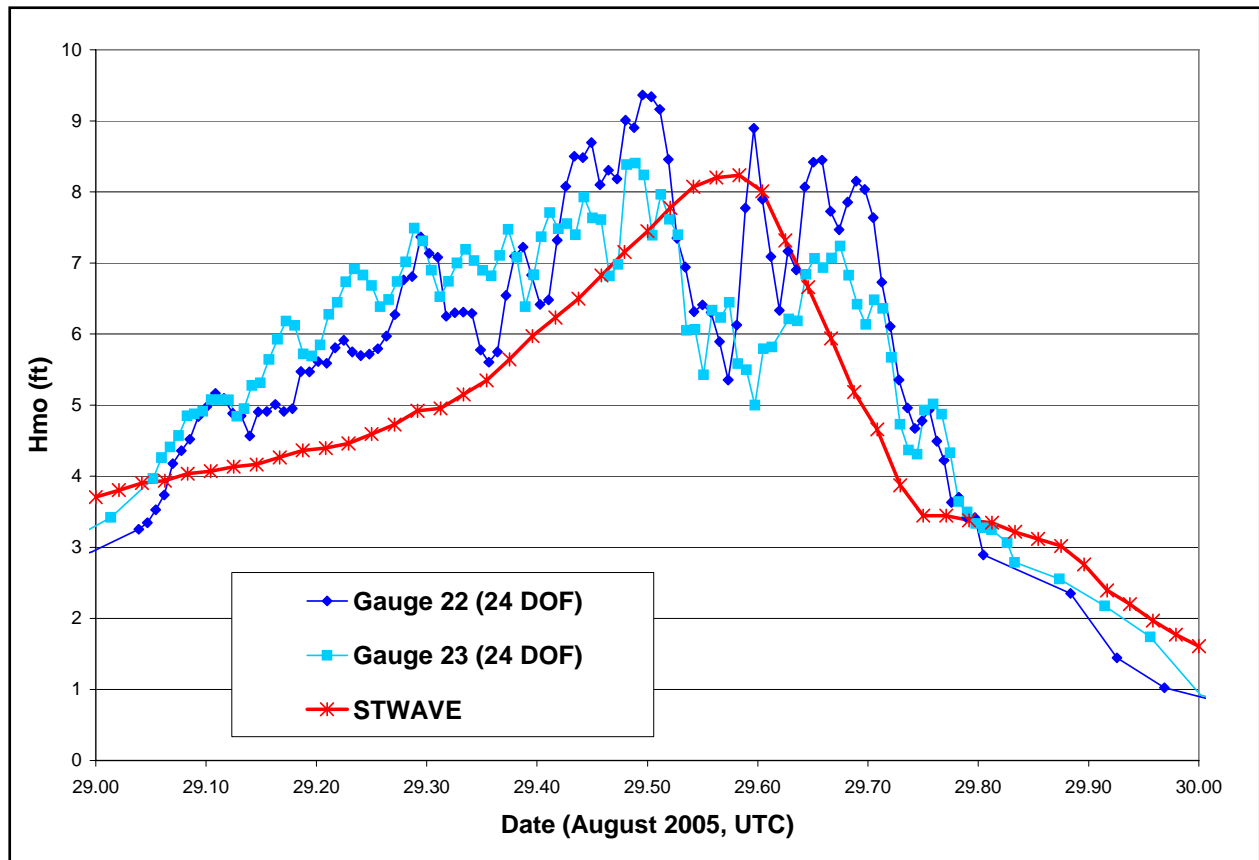


Figure 4-9. Lake Pontchartrain measured and modeled significant wave height.

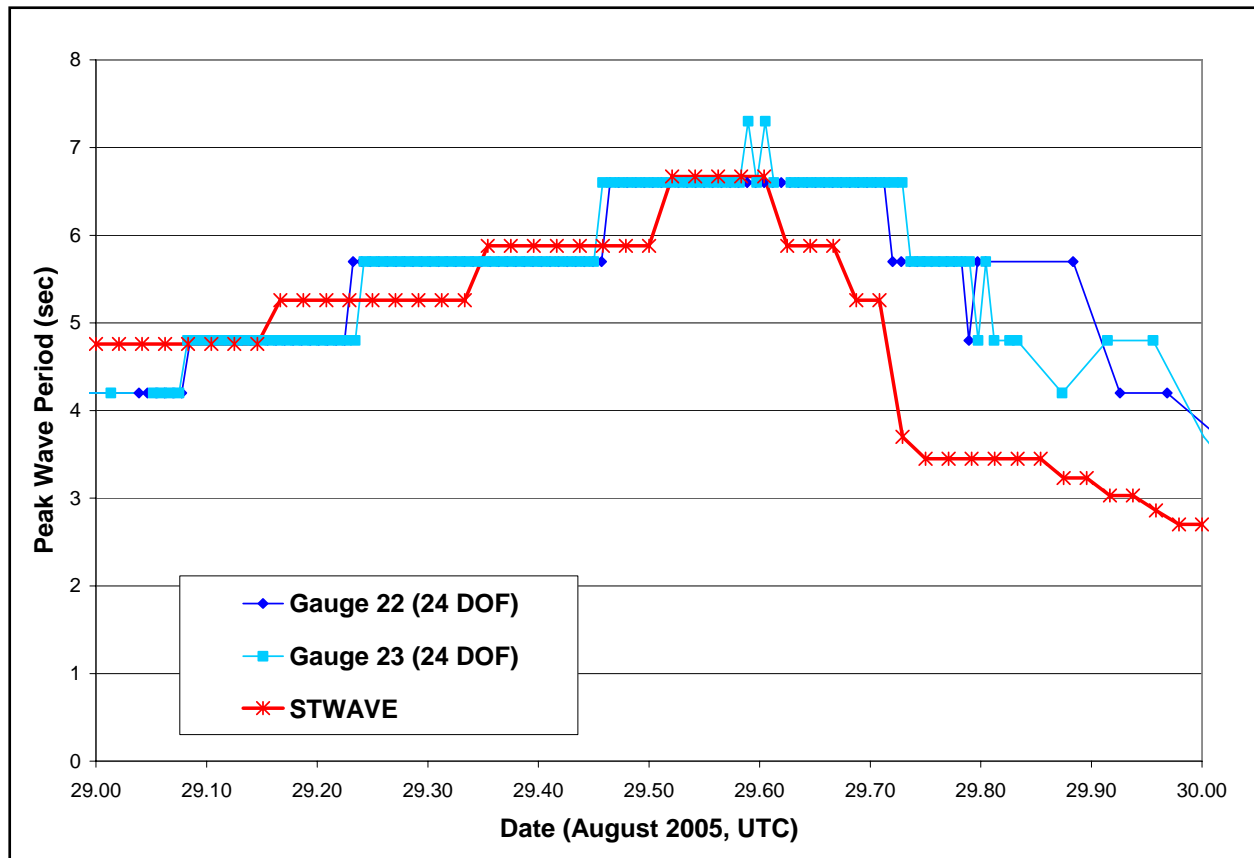


Figure 4-10. Lake Pontchartrain measured and modeled peak wave period.

### Louisiana Southeast

The peak wave conditions on the southeast grid occur between approximately 1000 and 1500 UTC on 29 August 2005. The highest waves along the Mississippi River levees occur around 1000-1200 UTC and along the Lake Borgne shoreline around 1400-1500 UTC. Figure 4-11 shows a snapshot of wave height and direction at 1200 UTC. Figures 4-12 and 4-13 show the maximum wave heights and corresponding wave periods for the entire simulation period for each grid cell within the domain. The maximum wave heights range from 4 to 10 ft along the shoreline and the associated periods are 7-16 sec. The longer wave periods originate from wave energy traveling between or over the islands from the Gulf of Mexico. Figure 4-13 shows only the periods corresponding to the maximum wave height, so peak period at the shoreline can change appreciably as the offshore wave direction and the surge vary, allowing swell to propagate through the island gaps or over the islands. Larger wave heights occur in lower Plaquemines Parish (6-10 ft) and smaller heights in upper Plaquemines and St. Bernard Parishes (4-6 ft). The peak periods are relatively large (up to 16 sec) because of wave penetration through and over the barrier islands. Expanded views of the maximum significant wave heights and peak periods are provided in Figures 4-28 through 4-31 at the end of this appendix. Time history and selected wave spectra for Lake Pontchartrain, and Orleans, St. Bernard, and Plaquemines Parishes are given in Attachment 1.

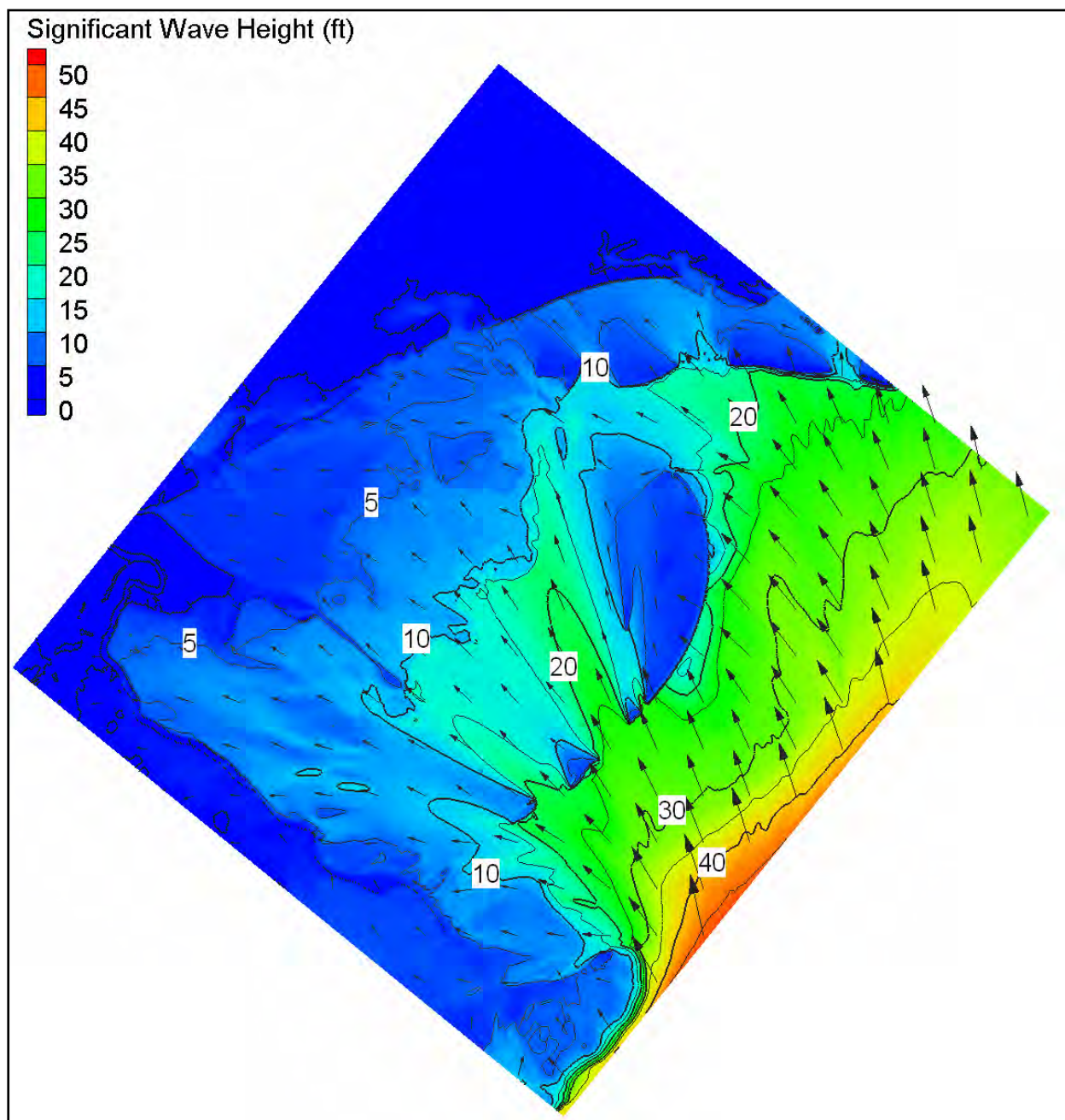


Figure 4-11. Southeast Louisiana modeled wave height and direction for 1200 UTC on 29 August 2005 (wave heights in feet).



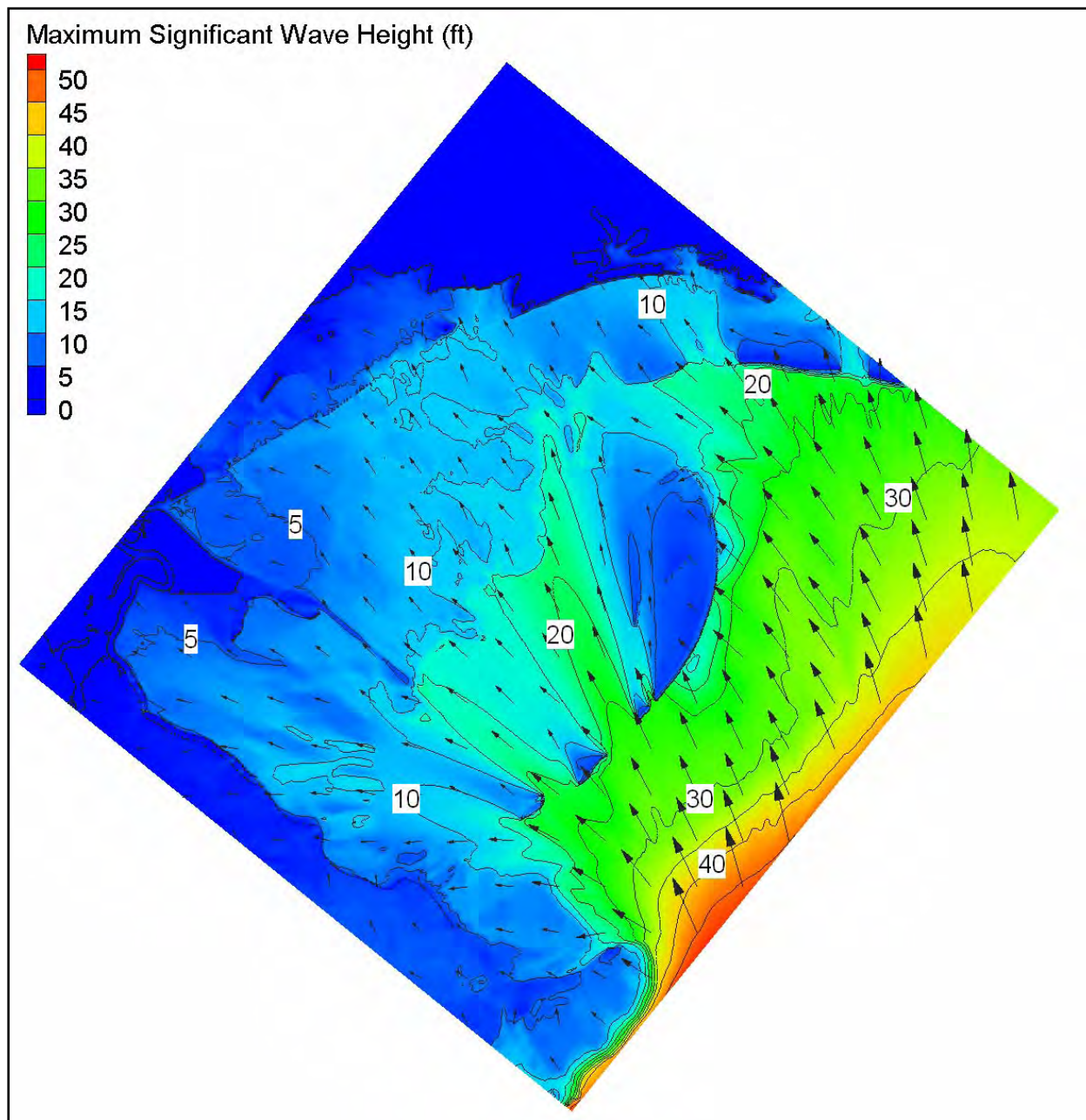


Figure 4-12. Southeast Louisiana maximum modeled wave height for for 0030 UTC on 28 August to 0000 UTC on 30 August 2005 (wave heights in feet).

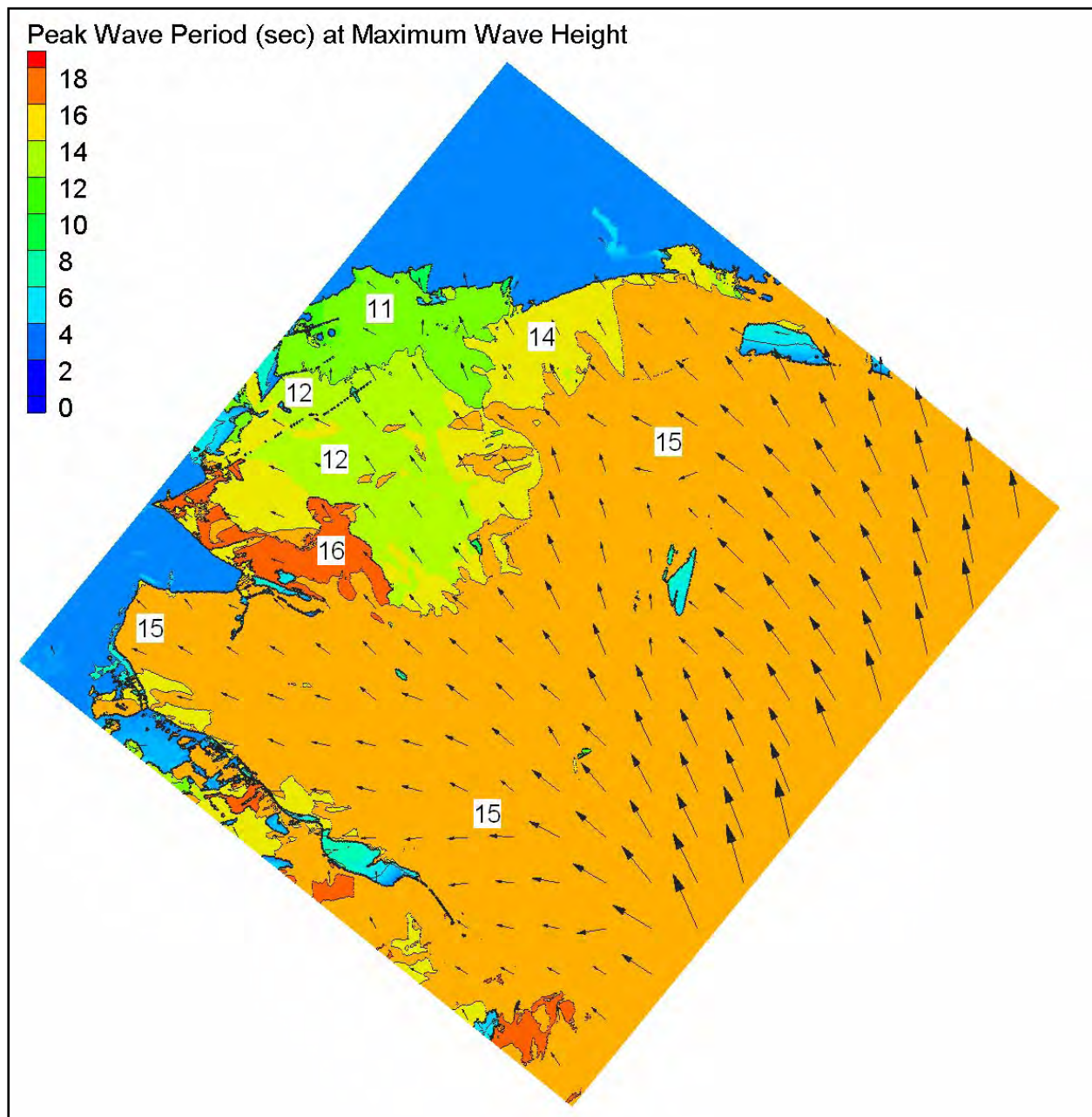


Figure 4-13. Southeast Louisiana modeled peak wave period corresponding to the maximum wave height for 0030 UTC on 28 August to 0000 UTC on 30 August 2005 (periods in sec).

### Louisiana South

The peak wave conditions on the south grid occur between 0800 and 1030 UTC on 29 August 2005. The water level changes due to surge on this grid are generally less than the Southeast Louisiana grid, so the wave penetration over the marsh is less severe. Figure 4-14 shows a snapshot of wave height and direction at 0800 UTC. Figures 4-15 and 4-16 show the maximum wave heights and corresponding wave periods for the entire simulation period for each

grid cell within the domain. The maximum wave heights at the barrier islands are approximately 10-14 ft (depth limited) and associated periods are 15-16 sec. Wave heights were significantly lower along the west bank Mississippi River levees. The barrier islands dissipated much of the wave energy arriving from the Gulf of Mexico and help protect the interior shorelines. These simulations were made with pre-Katrina bathymetry, so as barriers eroded, this protection may be overstated in the modeling results. The local winds were not important on this grid because the winds generally blow along the shore or offshore in the area. The portion of the south Louisiana grid east of the Mississippi River should be disregarded because the model is not forced along the lateral boundary (that area is modeled with the southeast Louisiana grid).

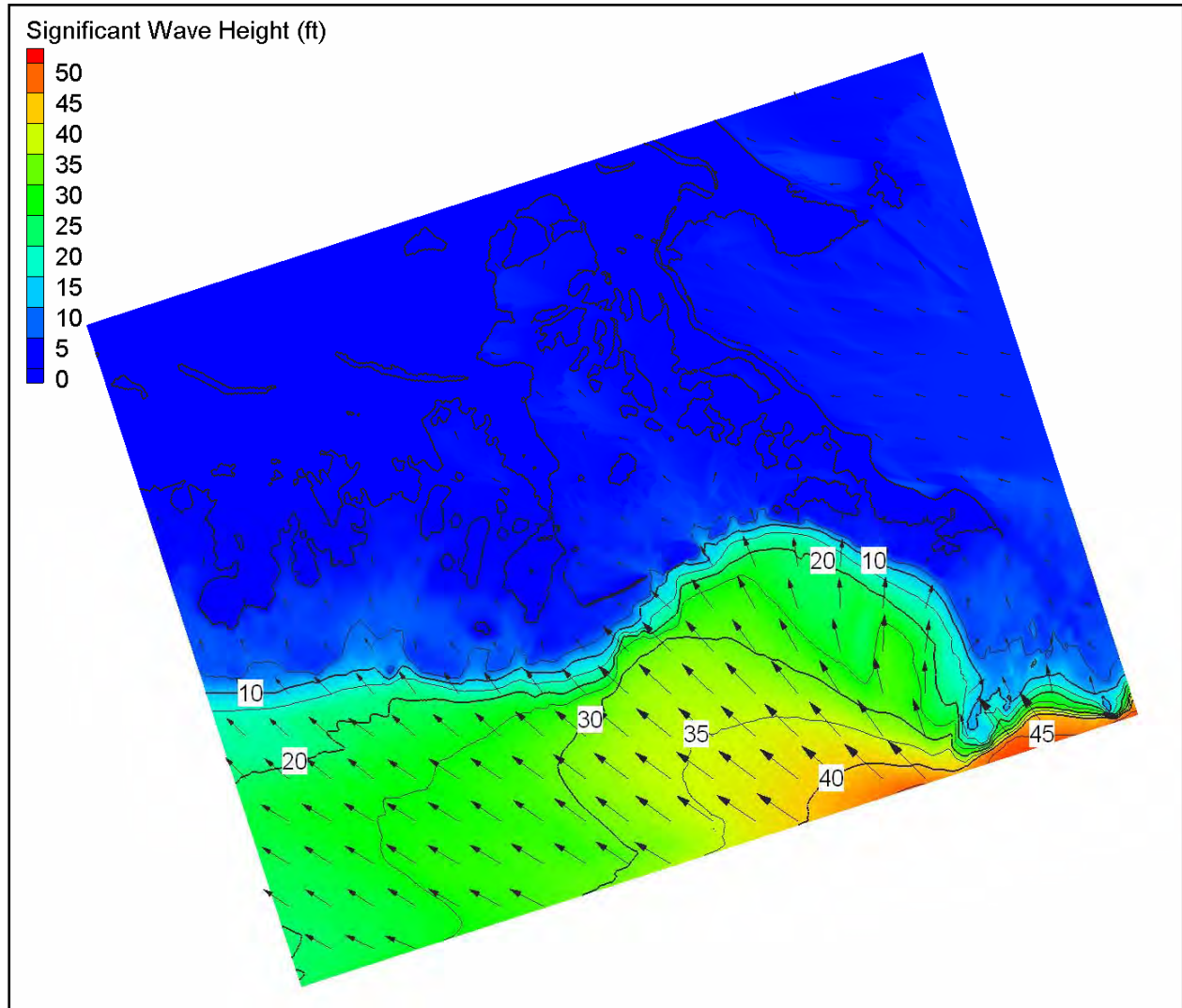


Figure 4-14. South Louisiana modeled wave height and direction for 0800 UTC on 29 August 2005 (wave heights in feet).



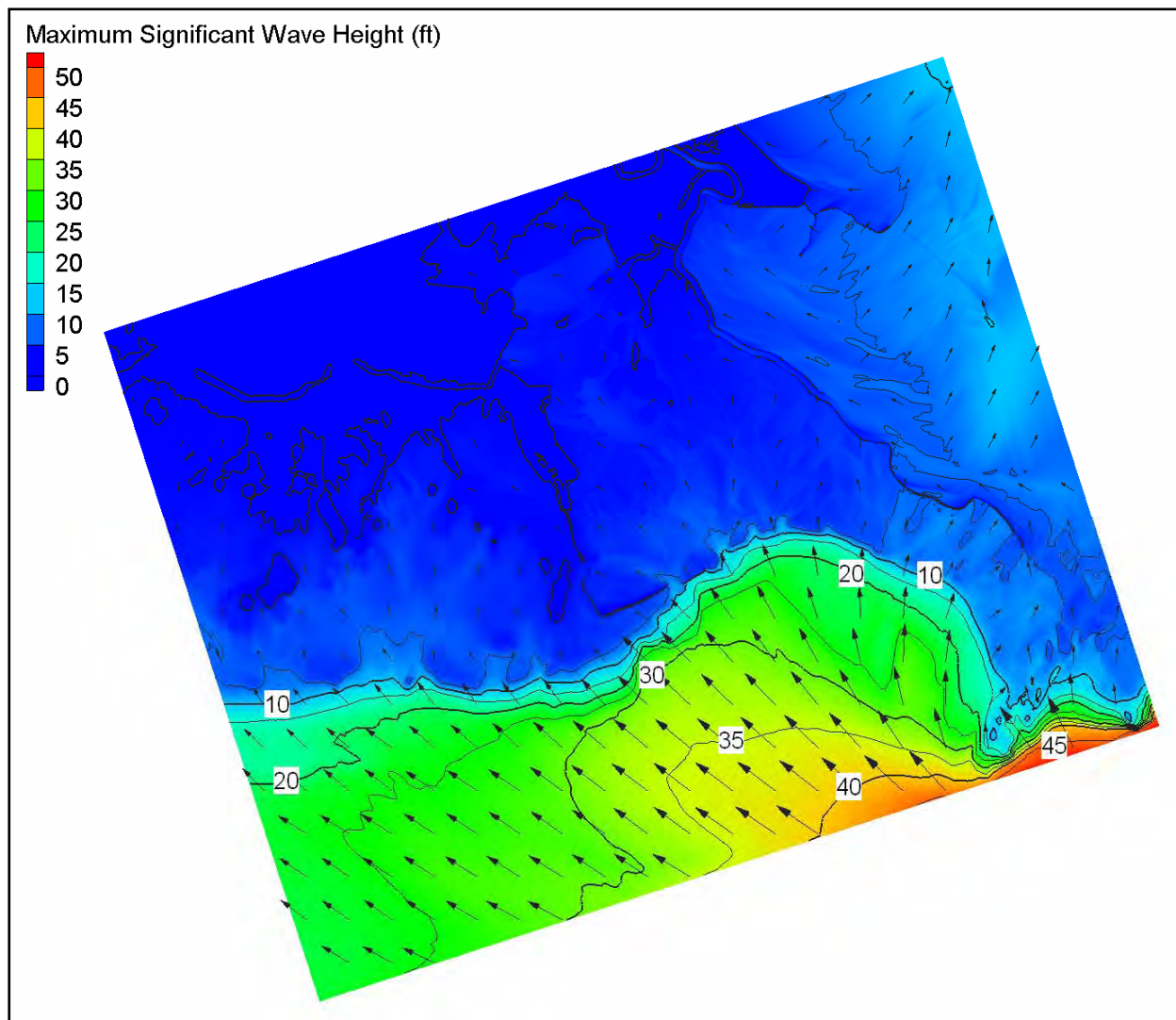


Figure 4-15. South Louisiana maximum modeled wave height for 0030 28 August 2005 to 0000 UTC on 30 August 2005 (wave heights in feet).

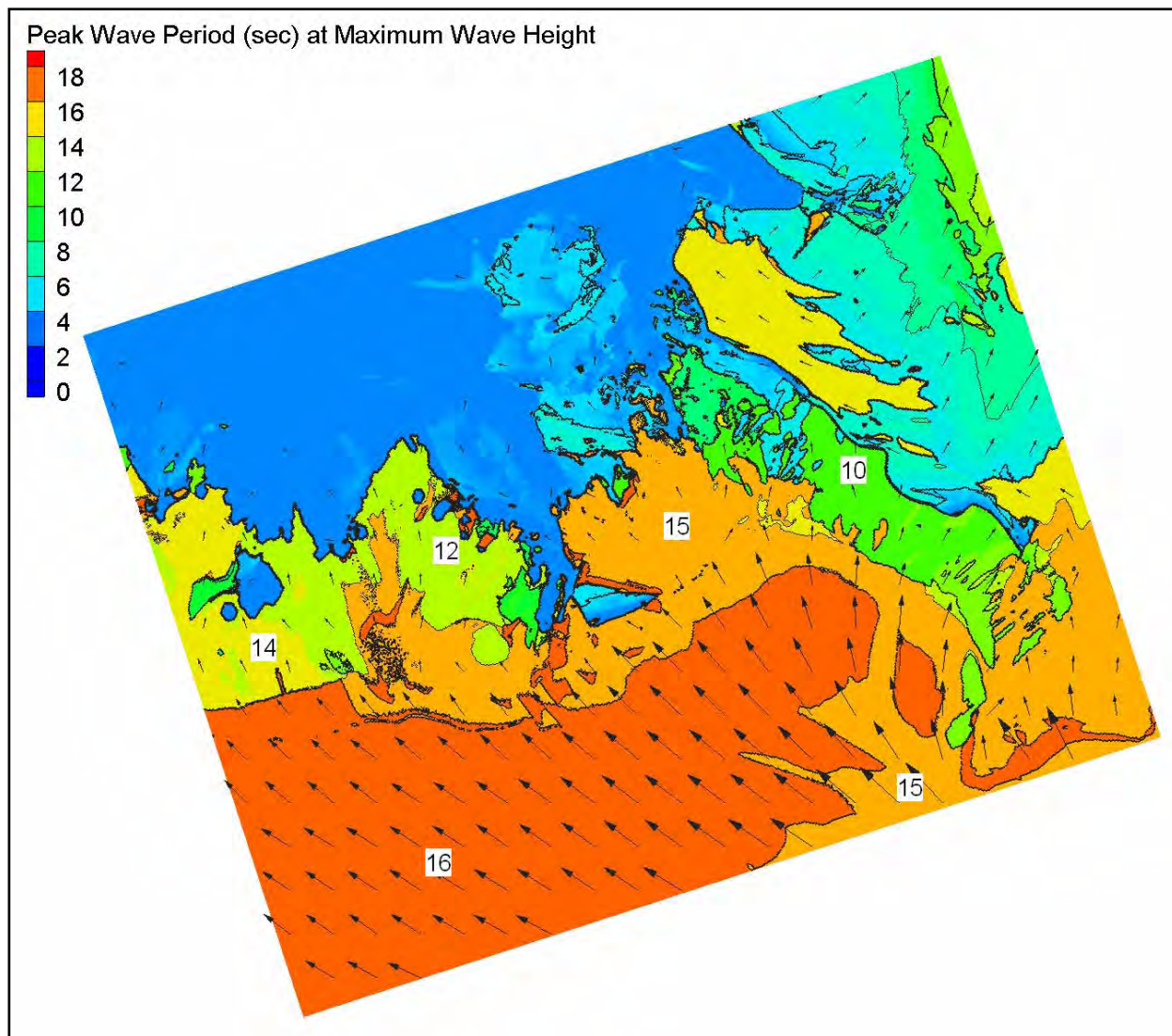


Figure 4-16. South Louisiana modeled peak wave period corresponding to the maximum wave height for 0030 28 August 2005 to 0000 UTC on 30 August 2005 (periods in sec).

### Mississippi-Alabama

The peak wave conditions on the Mississippi-Alabama grid occur around 1430 UTC on 29 August 2005, near the time of the hurricane landfall in Mississippi. Figure 4-17 shows a snapshot of wave height and direction at 1430 UTC. Figures 4-18 and 4-19 show the maximum wave heights and corresponding wave periods for the entire simulation for each grid cell within the domain. The maximum wave heights at the barrier islands are approximately 20 ft (depth limited) and associated periods are 15 sec. The barrier islands dissipated much of the wave energy arriving from the Gulf of Mexico and help protect the interior shorelines. These simulations were made with pre-Katrina bathymetry, so as barriers eroded, this protection may be overstated. Wave heights in Mississippi Sound and Mobile Bay generally range from 5 to 10 ft, but are 10-20 ft in the lee of the inlets on the Mississippi coast. Similar to the Louisiana



south domain, the barrier islands on the Mississippi and Alabama coasts dissipated much of the wave energy arriving from the Gulf of Mexico and help protect the interior shorelines. These simulations were made with pre-Katrina bathymetry, so as barriers eroded, this protection may be overstated. Large wave periods (15 sec) penetrate to the interior shorelines. The depth-limited wave breaking on the Mississippi and Alabama coasts generates wave setup in Mississippi Sound and Lake Borgne, which then forces additional water into Lake Pontchartrain (simulated with ADCIRC).

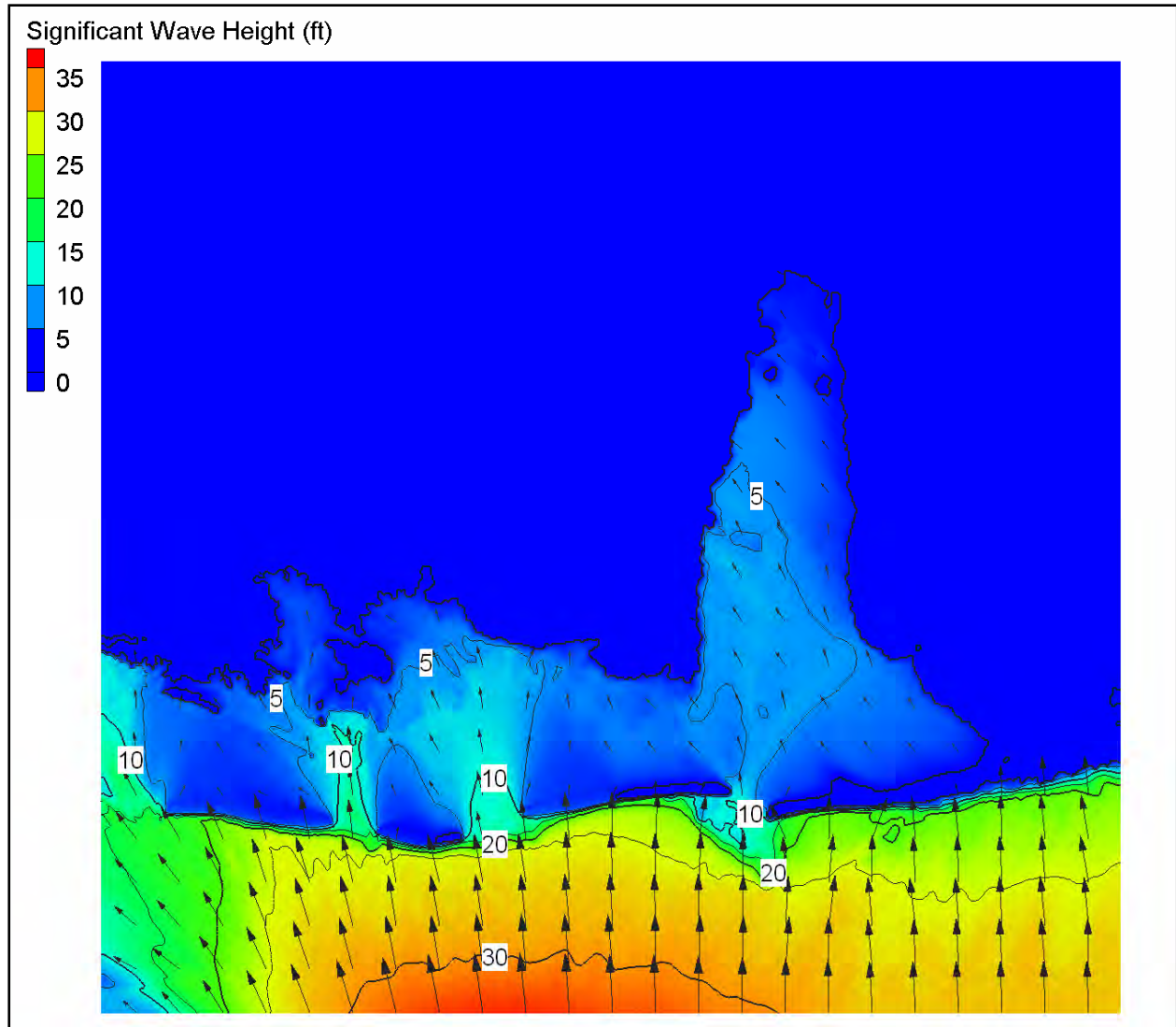


Figure 4-17. Mississippi-Alabama modeled wave height and direction for 1430 UTC on 29 August 2005 (wave heights in feet).

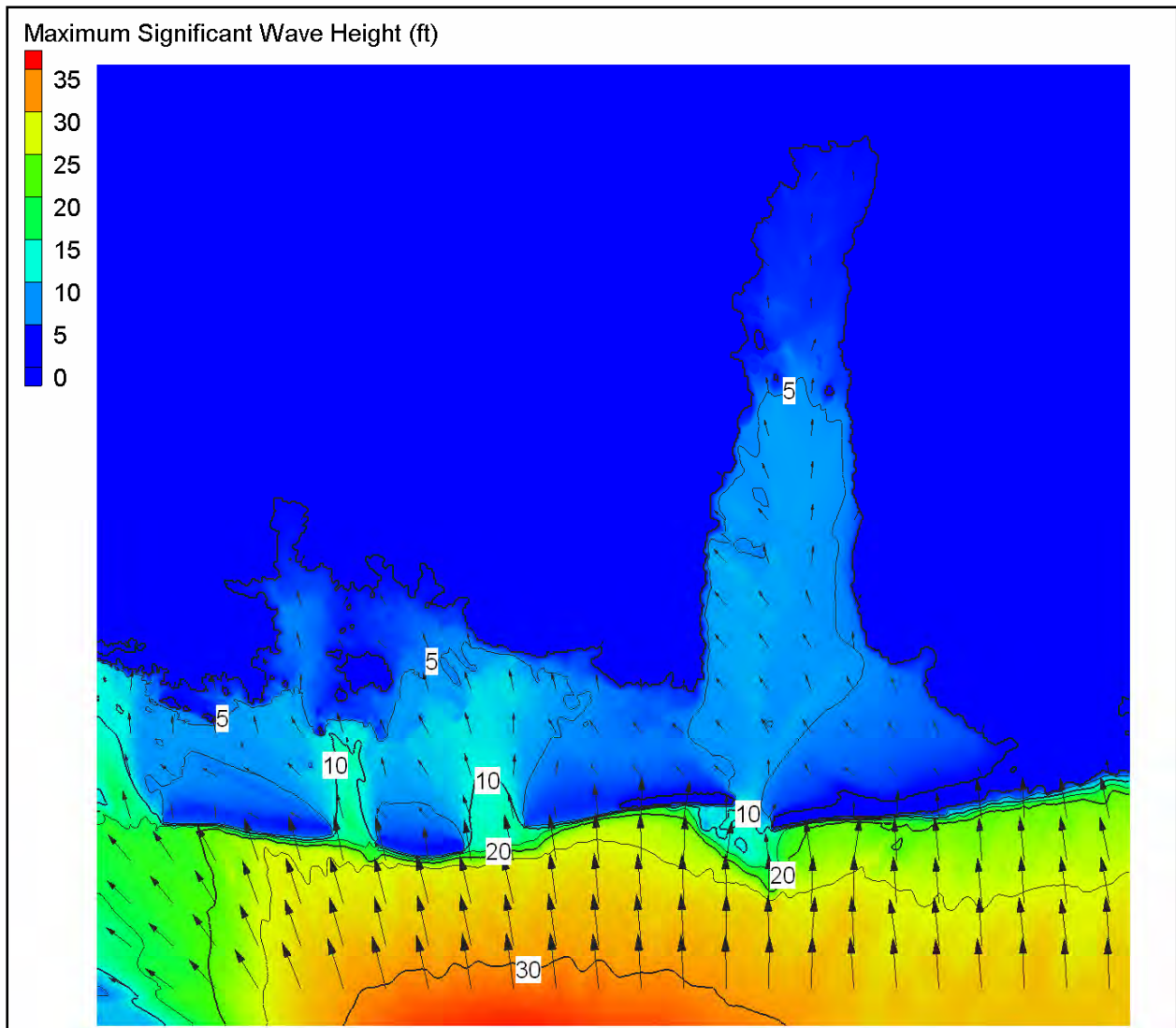


Figure 4-18. Mississippi-Alabama maximum modeled wave height for 0030 on 28 August 2005 to 0000 UTC on 30 August 2005 (wave heights in feet).

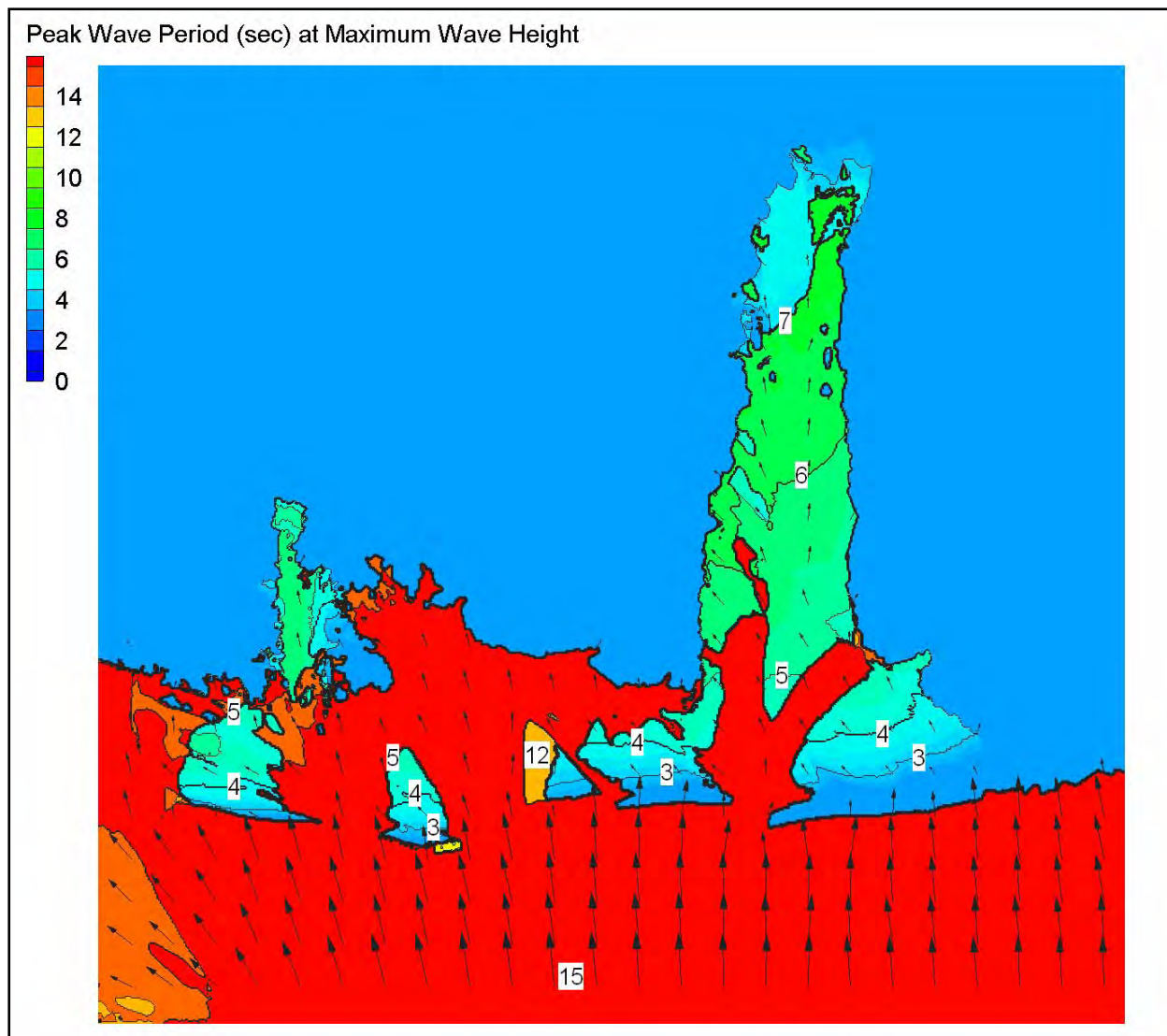


Figure 4-19. Mississippi-Alabama modeled peak wave period corresponding to the maximum wave height for 0030 on 28 August 2005 to 0000 UTC on 30 August 2005 (periods in sec).

### Sensitivity Analysis

STWAVE was not calibrated or turned in any way for the Hurricane Katrina applications, but all numerical models are sensitive to the quality of the input data. For STWAVE, these inputs include offshore waves, winds, surge, bathymetry, and bottom roughness. To investigate the sensitivity of the STWAVE results to critical input, three sets of sensitivity runs were made: wind input, degradation of the Chandeleurs Islands, and bottom roughness. These runs were made in coordination with the offshore wave and surge modeling, so modifications were made consistently in all three models: WAM, ADCIRC, and STWAVE.

Wind Input Sensitivity. Wind input enters into STWAVE in three ways: through the offshore waves input at the boundary, through the surge, and through the local wave generation within the



STWAVE grids. The importance of each component varies with location in the grid (offshore areas are influenced more by the offshore input and nearshore, protected areas by the local winds and surge). Two wind sensitivity runs were run, one increased the wind speed by 5 percent and one decreased the wind speed by 5 percent. Wind errors are likely to be random and partially cancel out through the integration of modeling, but a simplistic approach was selected to put realistic bounds on the solution. STWAVE was run for all four grids with the plus and minus 5 percent winds (and the offshore wave and surge generated from the same plus and minus 5 percent wind fields).

In Lake Pontchartrain, the maximum increase in wave height due to the plus 5 percent winds is approximately 0.8 ft on the southeast shore of the lake (Figure 4-20) and the maximum decrease due to the minus 5 percent winds is approximately 0.4 ft (Figure 4-21). For both cases there are some larger differences on the periphery of the lake, particularly the northeast shore, where the surge is a large percentage of the water depth. The differences in wave height increase across the lake (northwest to southeast), then decrease where the waves are locally depth limited, and then increase again very near the shore due to the increase in local water depth due to the differences in surge in very shallow water.

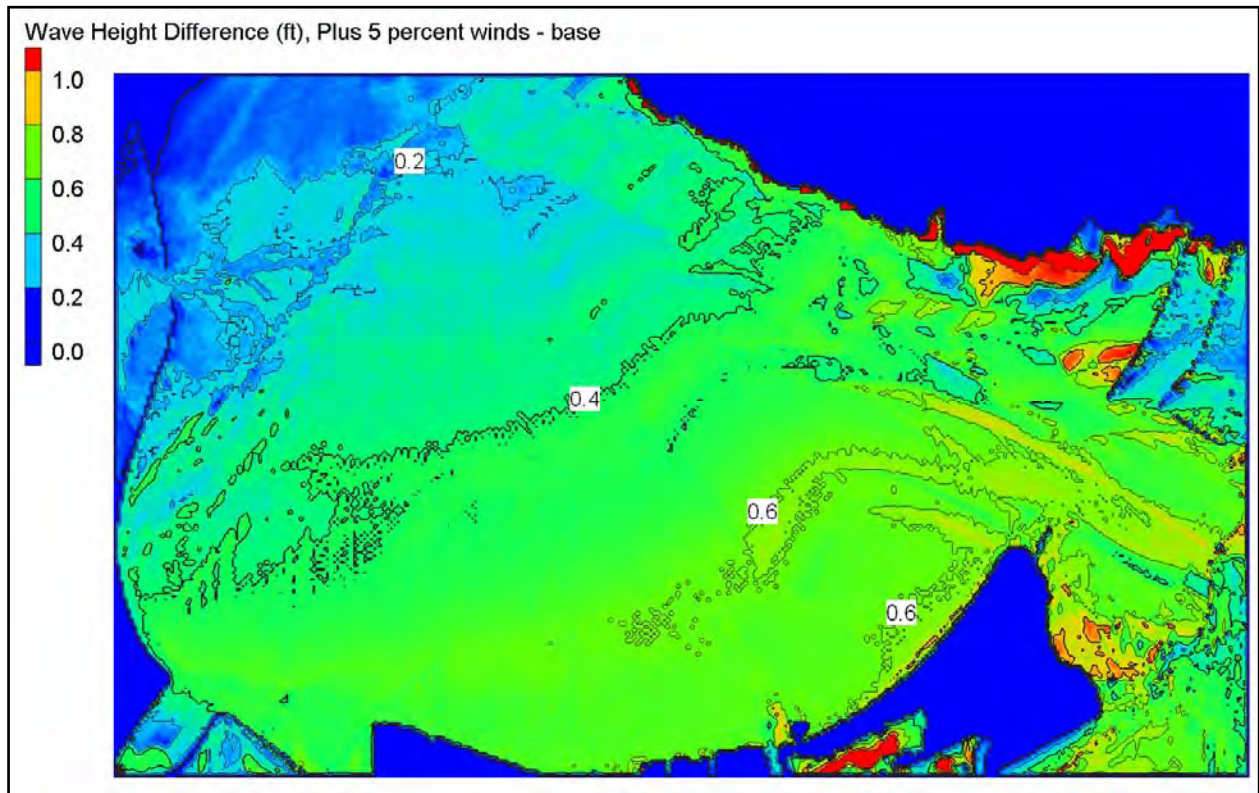


Figure 4-20. Differences in maximum wave height for sensitivity run with 5 percent increase in wind speed for Lake Pontchartrain (plus 5 percent – base).

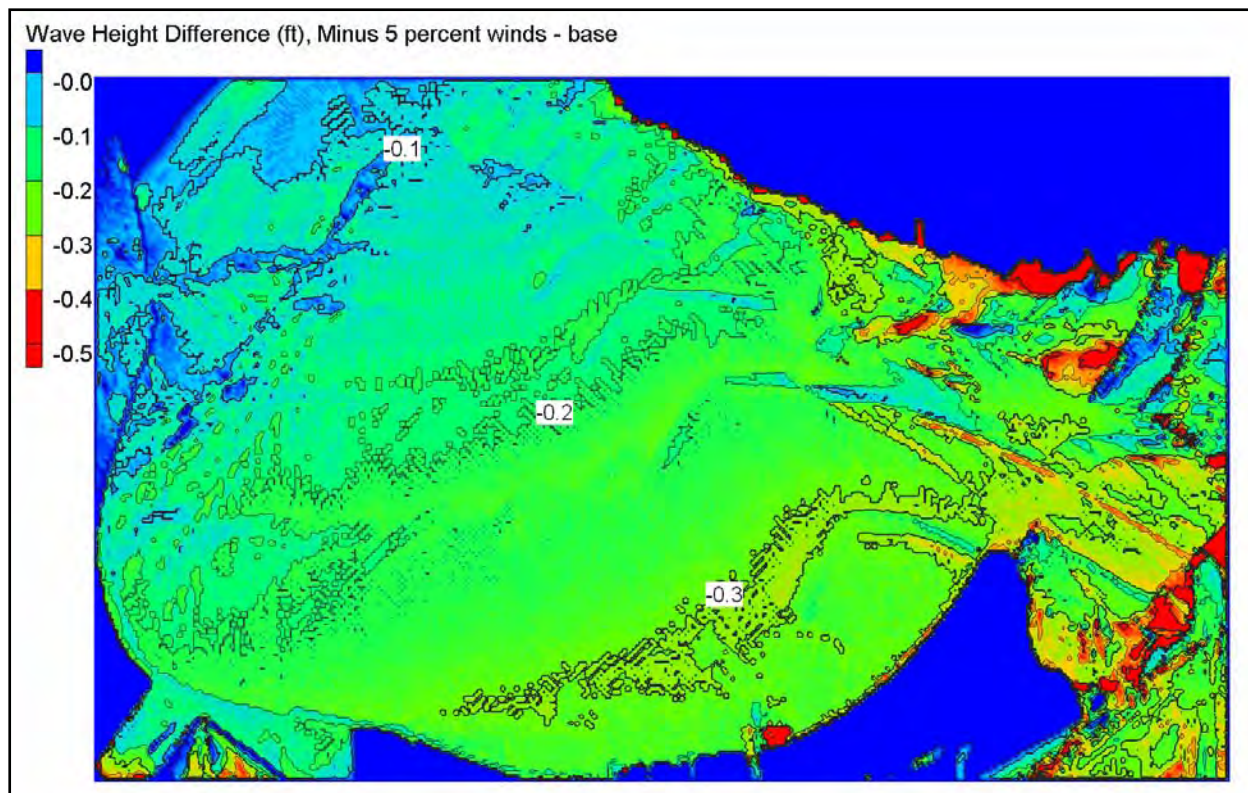


Figure 4-21. Differences in maximum wave height for sensitivity run with 5 percent decrease in wind speed for Lake Pontchartrain (minus 5 percent – base).

For the southeast grid, the maximum increase in wave height due to the plus 5 percent winds is approximately 0.5 to 1 ft along the levees (Figure 4-22), and the maximum decrease due to the minus 5 percent winds is approximately 0.5 to 1 ft. There are larger differences outside the Chandeleurs (increase of 2-3 ft for the plus 5 percent winds and 1.5 to 2.5 ft decrease for the minus 5 percent winds). For the south grid, the maximum increase along the barrier islands was approximately 2 ft due to the plus 5 percent winds and the maximum decrease along the barrier islands was approximately 2 ft for the minus 5 percent winds. Along the Mississippi River levees, waves increased approximately 0.5 ft for the plus 5 percent winds and the decrease was 0.5 to 1 ft for the minus 5 percent winds. In the wetland areas behind the barrier islands there was a decrease in wave height of 0.5 to 1 ft for both the plus and minus 5 percent winds, most likely because winds were blowing offshore locally (reducing surge for the plus 5 percent winds). At the grid boundary, the wave heights increased 1.5 to 3.5 ft for the plus 5 percent winds and decreased 1.5 to 3 ft for the minus 5 percent winds. For the Mississippi-Alabama grid, the maximum increase in wave height due to the plus 5 percent winds is 1 to 2 ft at the barrier islands (locally up to 2.6 ft offshore of Horn Island) and 0 to 1 ft at the interior shorelines (average of approximately 0.5 ft). The maximum decrease in wave height due to the minus 5 percent winds is 1 to 2 ft at the barrier islands and 0 to 1 ft at the shore line. The differences in peak wave period over all grids were generally 1 sec or less (increase in peak period for the plus 5 percent winds and decrease in peak period for minus 5 percent winds).



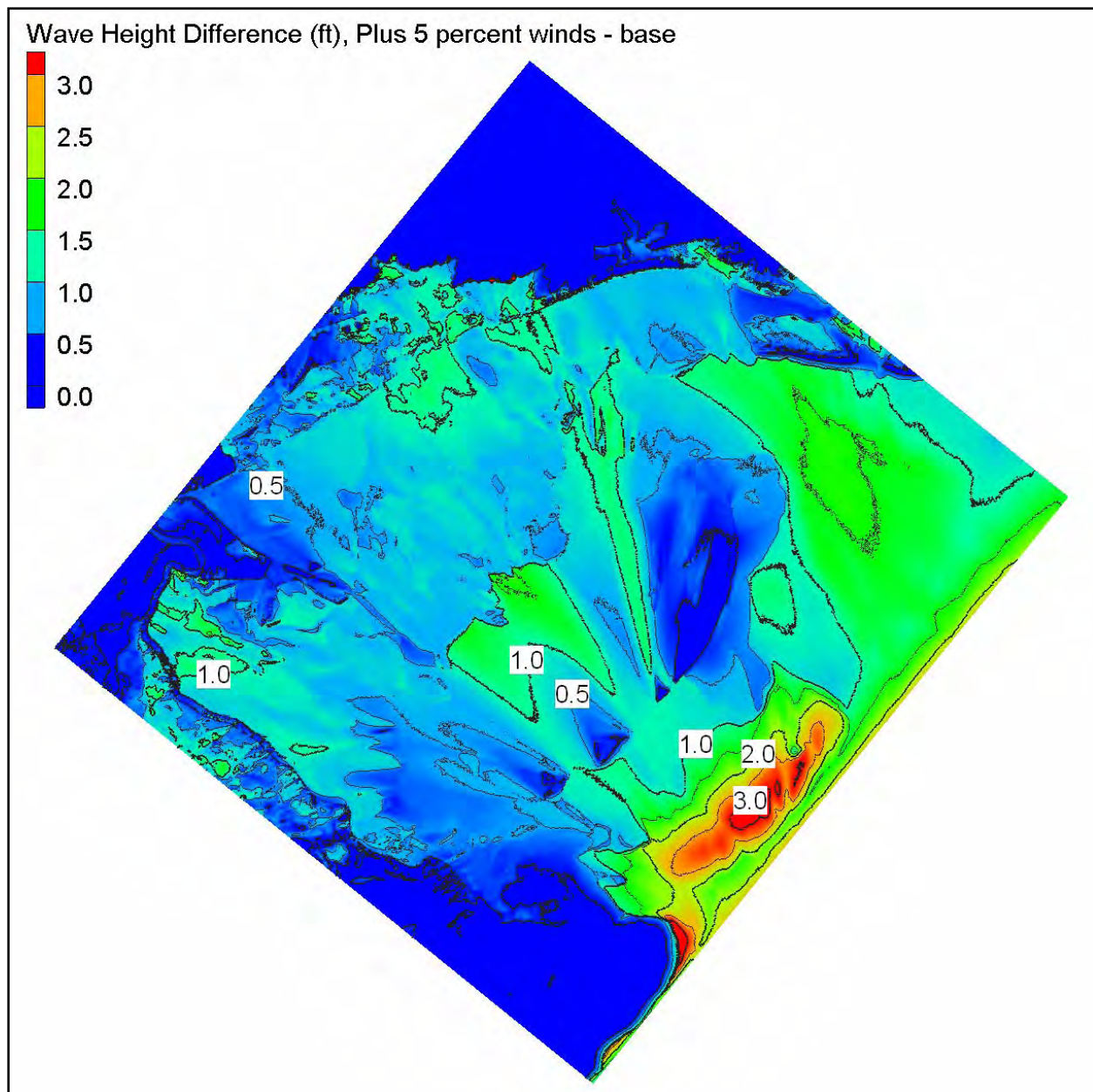


Figure 4-22. Differences in maximum wave height for sensitivity run with 5 percent increase in wind speed for Southeast Louisiana (plus 5 percent – base).

Although wind is the critical parameter for predicting waves and surge, the 5 percent increase and decrease in winds for the coupled simulations generally produced nearshore waves at the shoreline of  $\pm 1$  ft (or less) of the base simulations. The differences were larger,  $\pm 1$  to 3 ft, offshore of the barrier islands.

Bathymetry Sensitivity. Southern Louisiana is geomorphically active (wetland and barrier island loss, subsidence, and development). For the base case, an effort was made to use the most up-to-date and accurate bathymetry information to construct the STWAVE grids. These grids were derived from the ADCIRC bathymetry grids. Bathymetry interacts with wave processes

through shoaling (which generally increases waves in shallower depths), refraction (which turns waves more shore normal in shallower depths), and depth-limited breaking (which reduces wave height when the breaking threshold is reached). In general, small errors in water depth result in small errors in wave parameters (shoaling is a function of depth to exponent  $\frac{1}{4}$  and breaking is approximately linear with depth) and the impact is typically local. A possible exception to this is wave attenuation across the barrier islands, which protect the areas in their shadow. The Chandeleur Islands experienced significant degradation during Katrina. To investigate the impact of that degradation on the nearshore waves and surge, STWAVE was run with the Chandeleurs in a degraded state. The Chandeleurs are on the Southeast STWAVE grid, so only that grid was run. Surge values from ADCIRC with the degraded Chandeleurs were used as input together with offshore waves and winds from the base runs. Figure 4-23 shows the differences in maximum significant wave height for the degraded Chandeleur run minus the base run. The maximum increase in wave height is approximately 6 ft directly in the lee of the island. Close the shoreline, the difference are reduced to near zero. There are (very) small differences in other parts of the grid resulting from small differences in the surge. The barrier islands do significantly reduce the wave height in the nearshore area, even in a degraded state. The degraded islands allow more wave energy to pass over them and propagate into the sound. For the Chandeleurs, the impact on the shoreline of the degraded the islands was relatively small (because the wave height is depth limited in the shallow wetland areas between Chandeleur Sound and Lake Borgne), but increased wave energy in Chandeleur Sound would likely cause further degradation of these wetlands. The protection afforded by barrier islands for the shoreline is dependent on the elevation of the islands, submergence of the islands during the storm, distance from the shore, and characteristics of the storm.

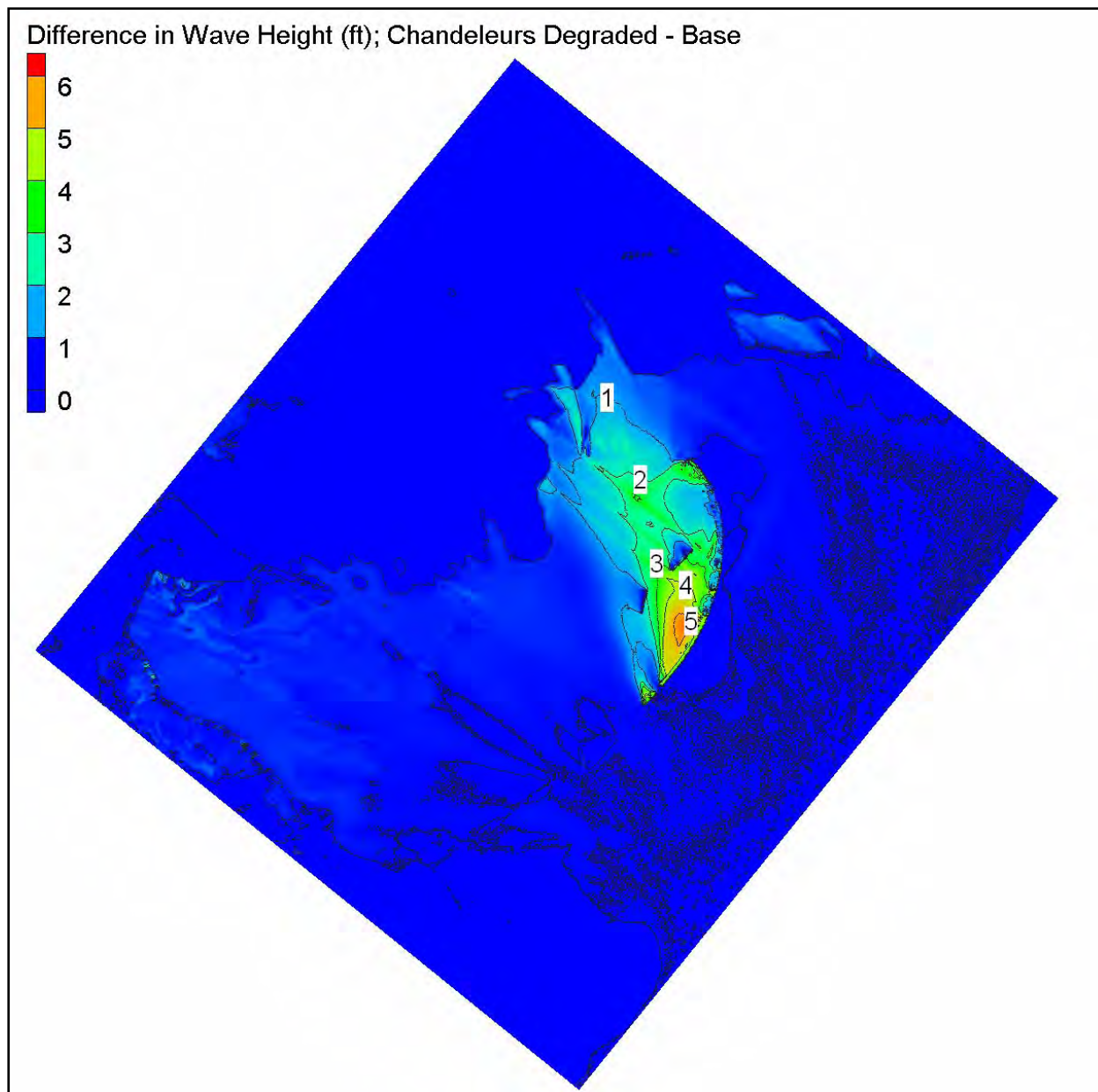


Figure 4-23. Differences in maximum wave height for sensitivity run with Chandeleur Islands degraded for Southeast Louisiana (degraded bathymetry – base).

Bottom Roughness. All STWAVE base simulations neglected wave energy dissipation due to bottom friction. Generally, dissipation due to bottom friction in the nearshore is relatively small because the propagation distances are small, so frictional dissipation is neglected. Within the Southeast grid, the propagation distances are significant, the water depths are relatively shallow, and vegetation in flooded areas may be highly dissipative, thus bottom friction may be significant. The bottom friction coefficient in STWAVE was specified as

$$C_f = g \frac{n^2}{d^{1/3}}$$

where  $g$  is acceleration of gravity,  $n$  is the Manning roughness coefficient, and  $d$  is total water depth (including surge). To investigate the impacts of bottom dissipation, STWAVE was run for two cases with bottom friction. These cases represent spatially-varying bottom roughness for the pre-Katrina vegetation cover and the post-Katrina cover (background Manning's  $n$  value of 0.02). A table of Manning's  $n$  values is provided in Appendix 5. During Katrina, vegetation was stripped from some wetland areas, so the post-Katrina roughness values are reduced in some areas. ADCIRC was run with the same Manning's  $n$  values and those surge fields were used as input to STWAVE. For the base case, ADCIRC was run with a constant friction coefficient and STWAVE neglected bottom friction.

Figures 4-24 and 4-25 show the differences in maximum significant wave height for the simulation with the pre-Katrina frictional loss minus the base case and post-Katrina frictional loss minus the base case, respectively. The patterns for the two simulations are very similar, with increases in wave height in Chandeleur Sound and Lake Borgne and decreases in wave height along Plaquemines and St. Bernard Parishes and in the flooded areas between Bay St. Louis and Slidell. The maximum reductions in wave height were 3.7 ft near the Louisiana-Mississippi border and 3.5 ft near Dalcour in upper Plaquemines Parish. The maximum increases in wave height in Chandeleur Sound are 1.8 ft. It is counterintuitive that adding bottom friction would increase wave heights over large areas. The increase in wave height results from increased surge of 1-2.5 ft in these shallow areas (see Appendix 5). The waves in these areas are generally depth limited, so increasing the water depth decreases the wave dissipation due to depth-limited breaking and increases the wave height. The largest differences in wave heights between the post- and pre-Katrina bottom friction runs were reductions in wave heights of up to 1.6 ft on the Mississippi River delta, 0.7 ft across the Chandeleurs, and 0.4 ft in Chandeleur Sound and Lake Borgne. Wave heights increased in very limited areas (St. Bernard-Plaquemines border and directly in the lee of the Chandeleur and Ship Islands) by 0.3 to 0.5 ft.

The inclusion of spatially variable bottom friction tied to the vegetation type reduced wave height in very limited areas by up to 3.7 ft. Somewhat surprisingly, though, the simulations show increased wave height over broad areas in Chandeleur Sound and Lake Borgne on the order of 1-1.8 ft, which occurs because the surge increased in these areas and dissipation due to depth-limited breaking was reduced. The change in wave heights between the post-Katrina Manning's  $n$  values and the pre-Katrina values were relatively small (maximum decrease of 1.6 ft and maximum increase of 0.5 ft) and limited to small areas. The interaction of waves and surge in wetlands will be an important topic for continued study.



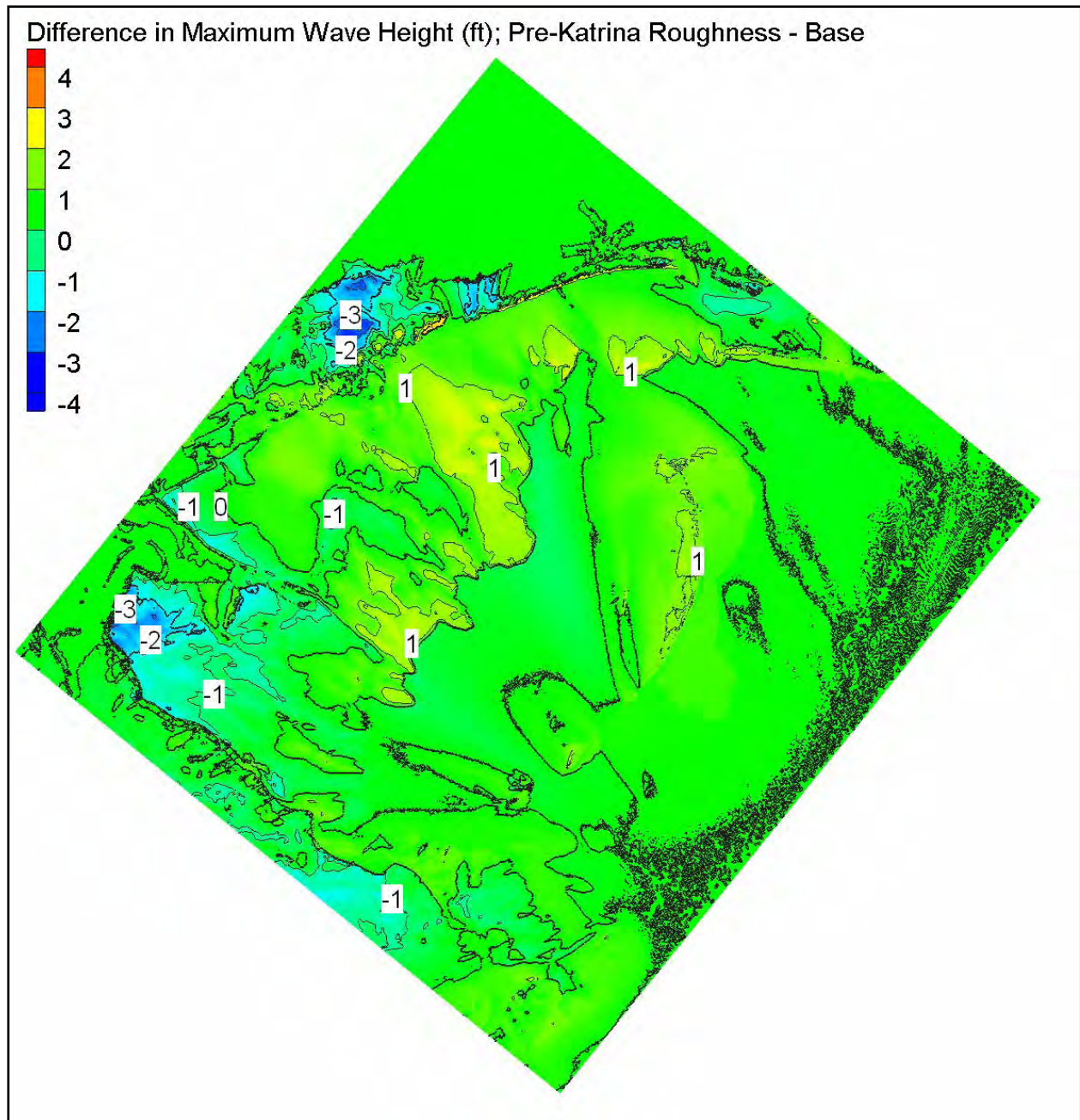


Figure 4-24. Differences in maximum wave height for sensitivity run with pre-Katrina bottom friction for Southeast Louisiana (with bottom friction – base).



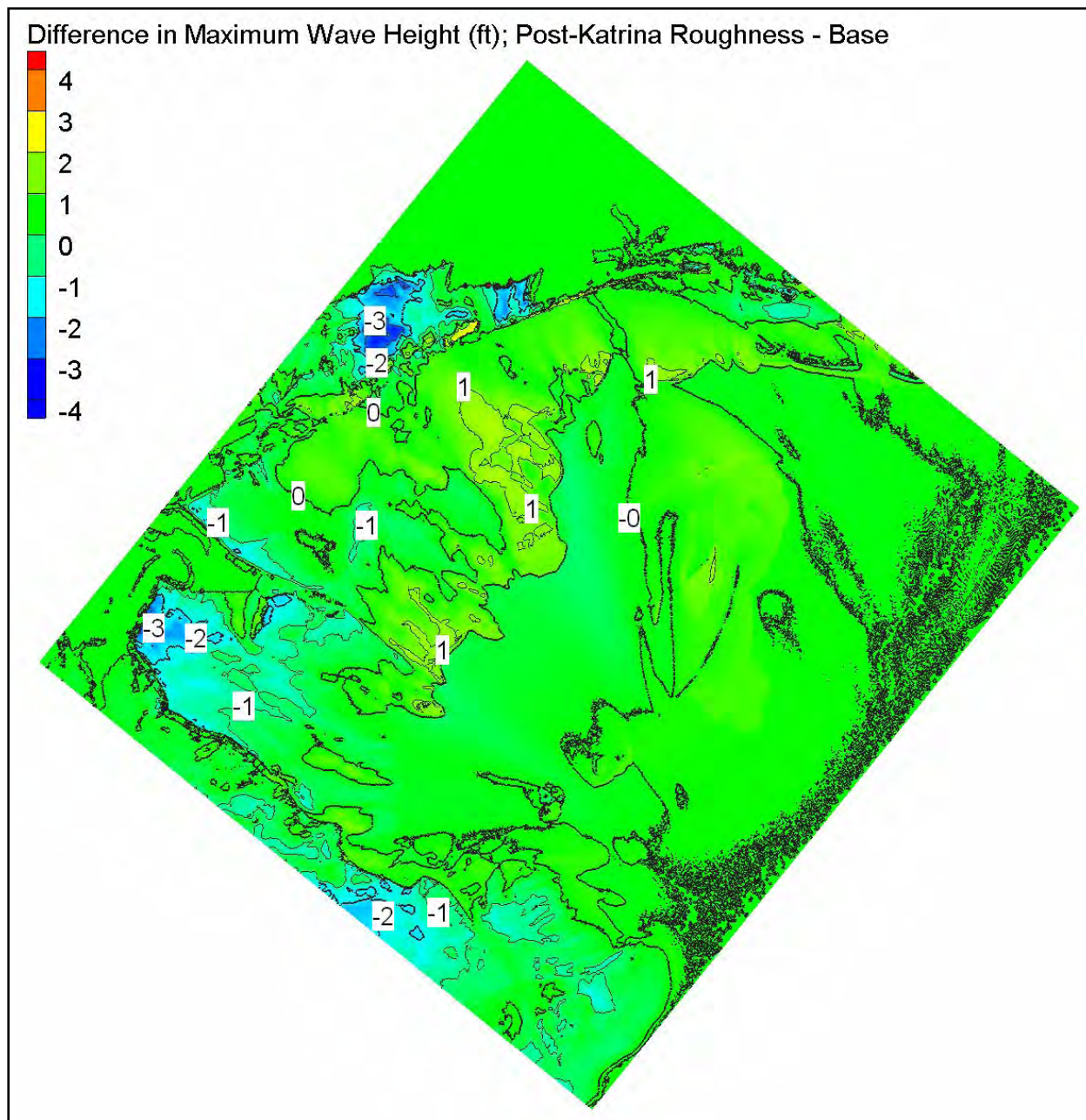


Figure 4-25. Differences in maximum wave height for sensitivity run with post-Katrina bottom friction for Southeast Louisiana (with bottom friction – base).

### Time-Dependent Simulations

STWAVE is a steady-state wave model, which means that the waves reach equilibrium with the local forcing conditions (wind, surge, and boundary waves). Thus, the STWAVE modeling assumes that the winds and surge vary slowly enough for the waves to reach quasi steady state. For Hurricane Katrina, the winds are time varying and the grid domains are relatively large, so the time-dependent SWAN model (Booij, Ris, and Holthuijsen 1999; Booij et al. 2004) was used

to evaluate the importance of time variation. Lake Pontchartrain was chosen for this test because the waves are all locally generated and time dependence is expected to have the greatest impact there. To test the time dependence, SWAN was run in time-dependent and steady-state mode for 29 August 2005 from 0000 UTC to 30 August 2005 0000 UTC. The simulation was made using 1-min time steps for the time-dependent run and forcing the steady-state run to an accuracy of 99 percent with a maximum of 15 iterations (this is more stringent than the default). All other SWAN model defaults were used. SWAN was run with the same spatially varying surge and wind as STWAVE.

Figures 4-26 and 4-27 show the SWAN and STWAVE results with the data measured in Lake Pontchartrain. The time-dependent and steady-state SWAN give essentially the same results through the peak of the storm, after a 3-hr model spin up. Thus, the steady-state solution is adequate for the simulations. STWAVE wave heights are 4 percent higher than SWAN at the peak of the storm and lower height on the building (11 percent) and waning (24 percent) legs of the storm. SWAN results are closer to the measurements on the building portion of the storm and STWAVE results are closer on the waning portion of the storm. The measurements are not reliable at the peak of the storm, when the wave heights are most critical. STWAVE peak periods are 8 percent longer than the SWAN peak periods through the peak of the storm and 23 percent shorter than SWAN periods after the storm peak. STWAVE shows better agreement with the wave period measurements through the storm peak, but both models are generally within 1 sec of each other.

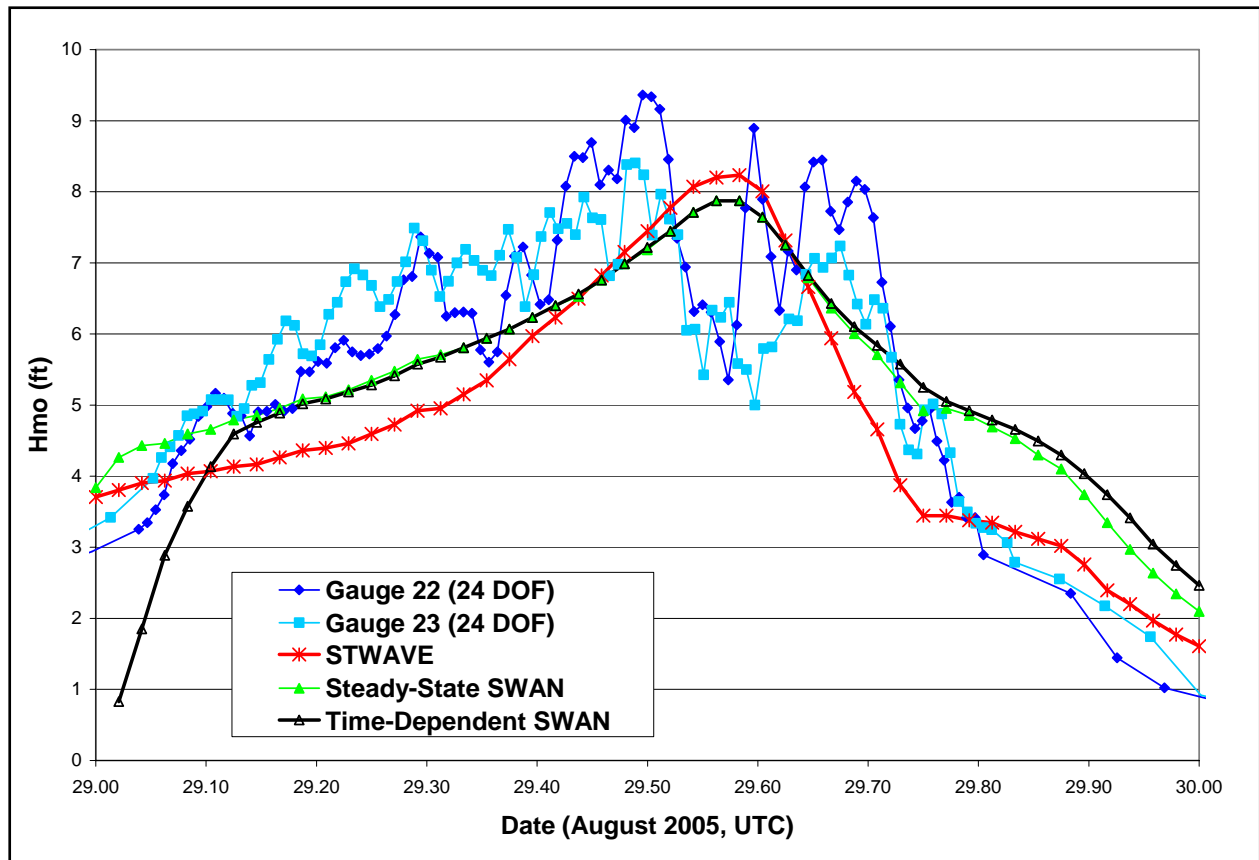


Figure 4-26. Time-dependent and steady-state SWAN and STWAVE modeled significant wave heights for Lake Pontchartrain measured and measured wave height.

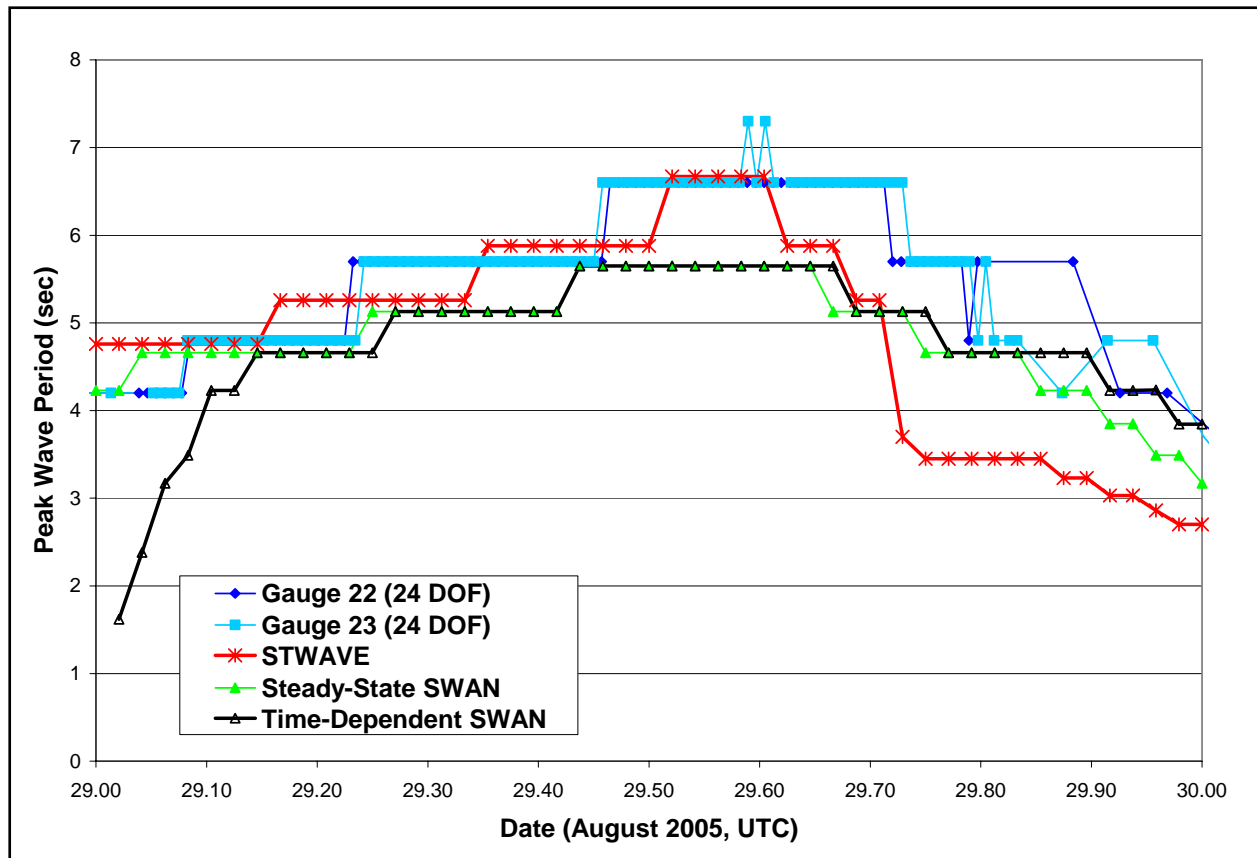


Figure 4-27. Time-dependent and steady-state SWAN and STWAVE modeled peak wave periods for Lake Pontchartrain measured and measured periods.

## References

- Booij, N., Haagsma, I J. G., Holthuijsen, L. H., Kieftenburg, A.T.M.M., Ris, R. C., van der Westhuysen, A. J., and Zijlema, M. 2004. "SWAN Cycle III Version 40.41 Users Manual," Delft University of Technology, Delft, The Netherlands, 118 p, <http://fluidmechanics.tudelft.nl/swan/index.htm>.
- Booij, N., Ris, R. C., and Holthuijsen, L. H. 1999. "A Third-Generation Wave Model for Coastal Regions, Part I: Model Description and Validation," *J. Geophys. Res.*, 104(C4), 7649-7666.
- Smith, S. J., and Smith, J. M. 2001. "Numerical Modeling of Waves at Ponce de Leon Inlet, Florida." *J. Waterway, Port, Coastal and Ocean Engineering*, 127(3), 176-184.
- Smith, J. M., Sherlock, A. R. and Resio, D. T. 2001. "STWAVE: Steady-State Spectral Wave Model User's manual for STWAVE, Version 3.0," ERDC/CHL SR-01-1, US Army Corps of Engineers Engineer Research and Development Center, Vicksburg, MS.
- Thompson, E. F., Smith, J. M., and Miller, H. C. 2004. "Wave Transformation Modeling at Cape Fear River Entrance, North Carolina." *J. Coastal Research*, 20 (4), 1135-1154.

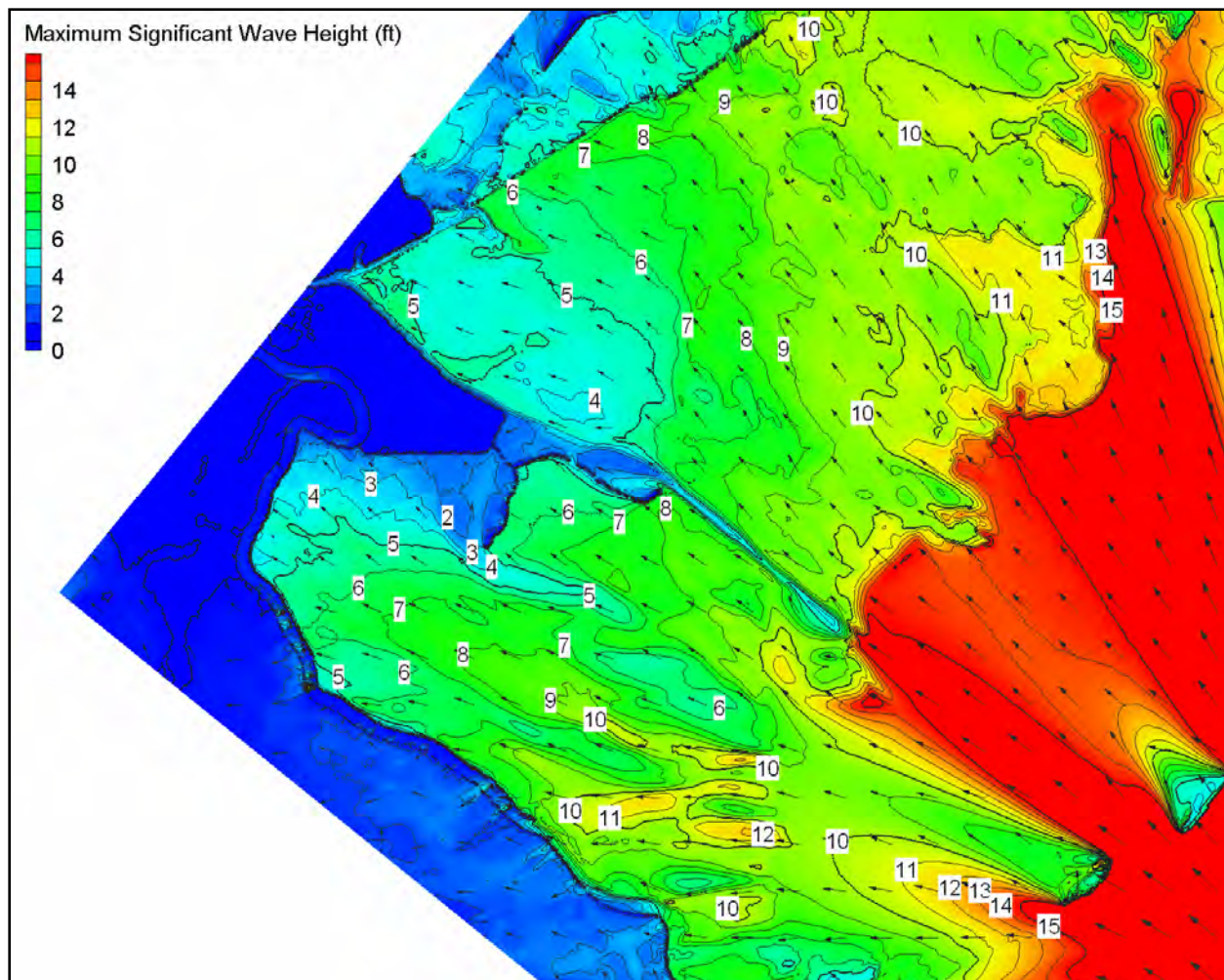


Figure 4-28. Southeast Louisiana modeled wave height and direction for 1200 UTC on 29 August 2005 (wave heights in feet); expanded view for St. Bernards and upper Plaquemines Parishes.



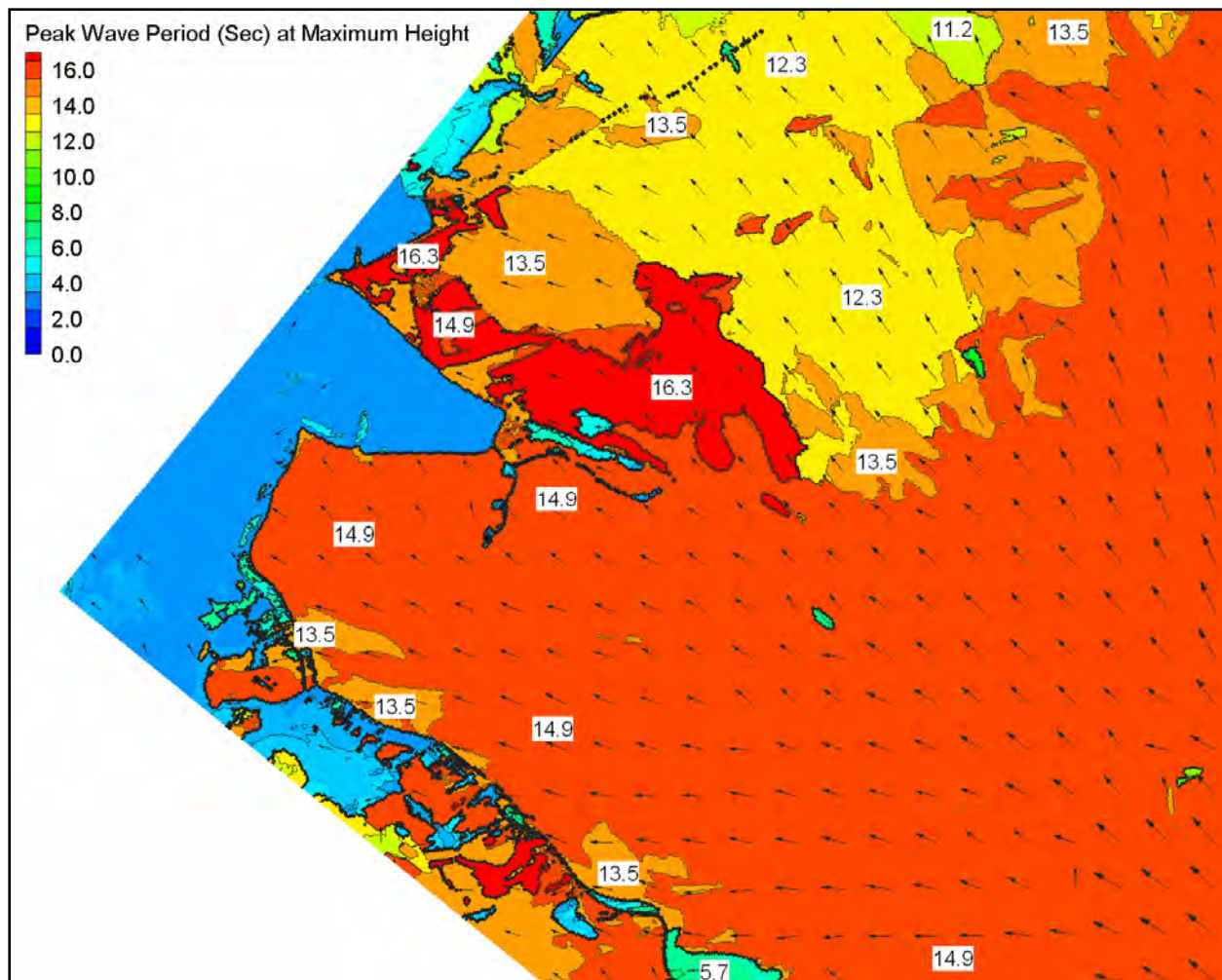


Figure 4-29. Southeast Louisiana modeled peak wave period corresponding to the maximum wave height for 0030 UTC on 28 August to 0000 UTC on 30 August 2005 (periods in sec); expanded view for St. Bernards and upper Plaquemines Parishes.

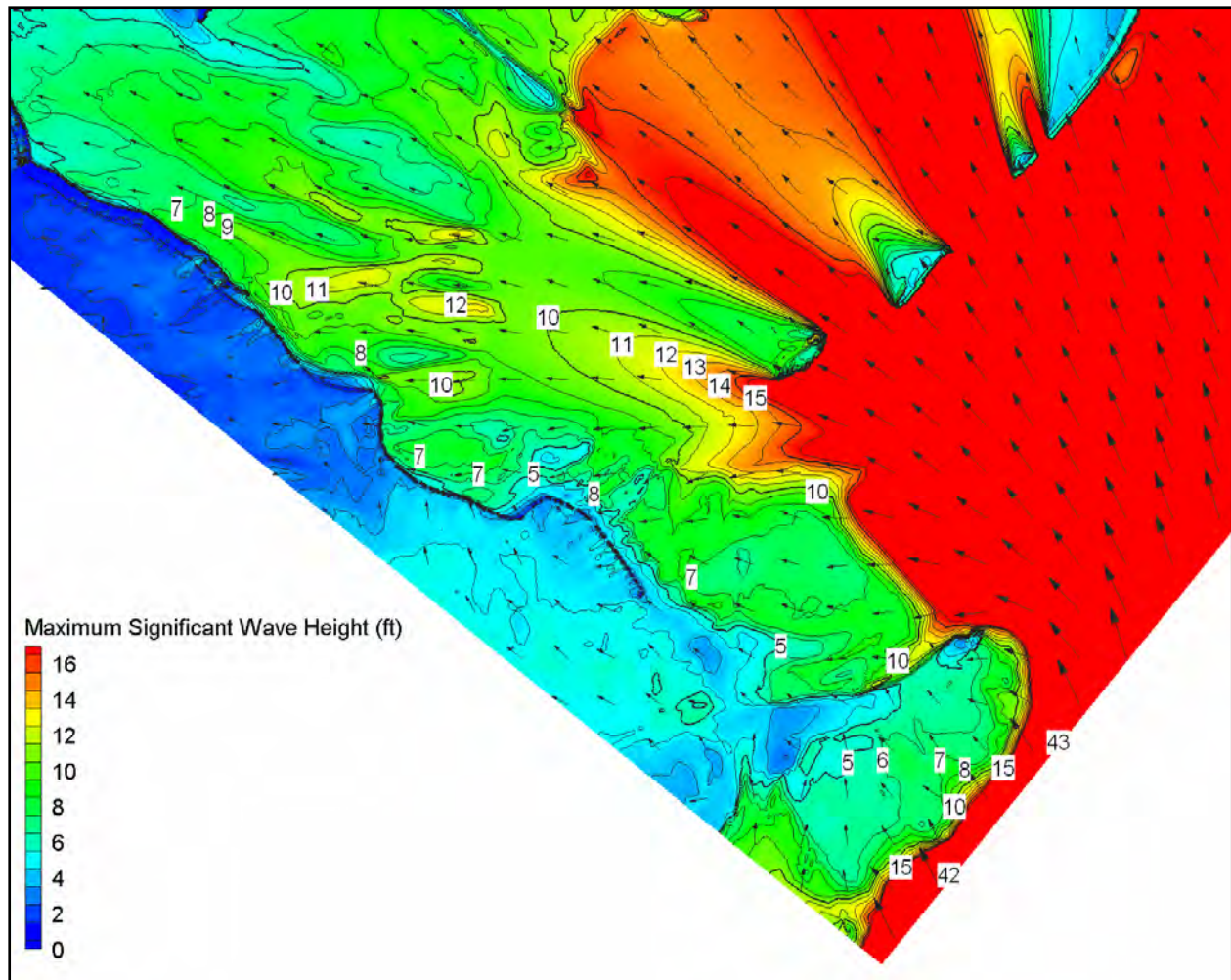


Figure 4-30. Southeast Louisiana modeled wave height and direction for 1200 UTC on 29 August 2005 (wave heights in feet); expanded view for lower Plaquemines Parish.

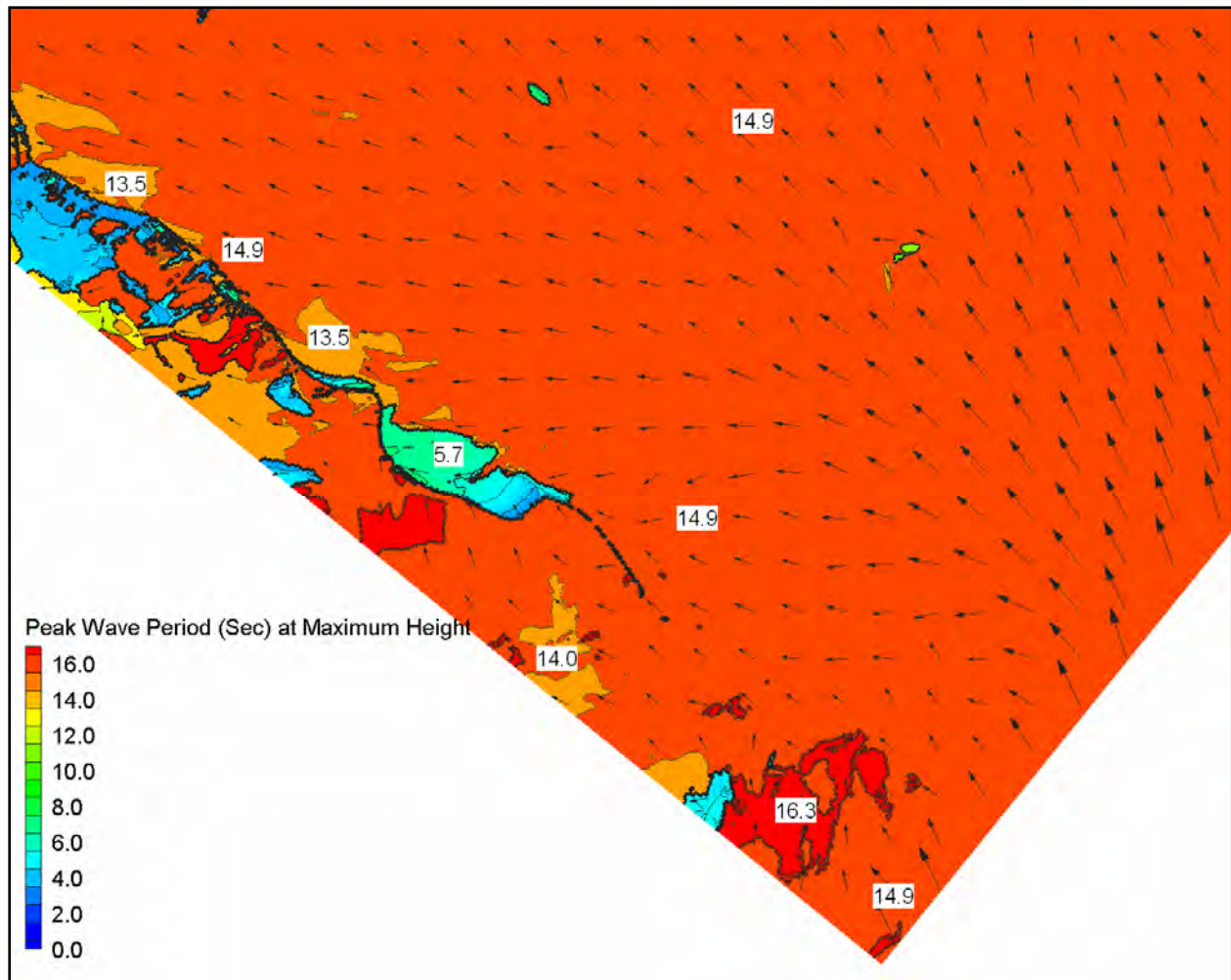


Figure 4-31. Southeast Louisiana modeled peak wave period corresponding to the maximum wave height for 0030 UTC on 28 August to 0000 UTC on 30 August 2005 (periods in sec); expanded view for lower Plaquemines Parish.

## Attachment 1. STWAVE Wave Time Histories and Spectra for Selected Locations

Time histories of significant wave height, peak wave period, and mean wave direction and peak two-dimensional wave spectra for 16 selected save points are provided in this attachment. Figure 1 shows the locations of the selected save points. All the even numbered figures in the attachment are time history plots and the odd numbered figures (after Figure 1) are peak wave spectra. Figures 2 through 13 represent locations modeled on the Pontchartrain grid, and the spectra cover the full-plane (360 deg). Figures 14 through 33 represent locations modeled on the Southeast Louisiana grid and the spectra cover a half plane (wave directions from 39 deg, clockwise to 219 deg). Spectral energy density is given in  $m^2/Hz/rad$  and the scale changes from plot to plot. Wave direction is the direction from which the waves come (a wave from north is 0 deg and from the east is 90 deg). The wave spectral shapes in Lake Pontchartrain are generally fairly similar (relatively broad wind sea). The peak wave direction changes somewhat based on the local fetch lengths and wind speed and direction. The peak spectra in St Bernard Parish are generally broad in direction because waves are propagating through various island gaps. In Plaquemines Parish, the spectra are generally very narrow in direction. For the full-plane spectra (Lake Pontchartrain grid), the frequencies (which radiate outward on the plot) range from 0.05 to 0.63 Hz, incremented by 0.02 Hz. For the half-plane spectra (Southeast Louisiana grid), the frequencies are: 0.031399999, 0.034499999E, 0.037999999, 0.041800000, 0.045899998, 0.050500002, 0.055599999, 0.061200000, 0.067299999, 0.074000001, 0.081400000, 0.089500003, 0.098499998, 0.1083000, 0.1192000, 0.1311000, 0.1442000, 0.1586000, 0.1745000, 0.1919000, 0.2111000, 0.2323000, 0.2555000, 0.2810000, 0.3091000, 0.3400000, 0.3740000, and 0.4114000 Hz.



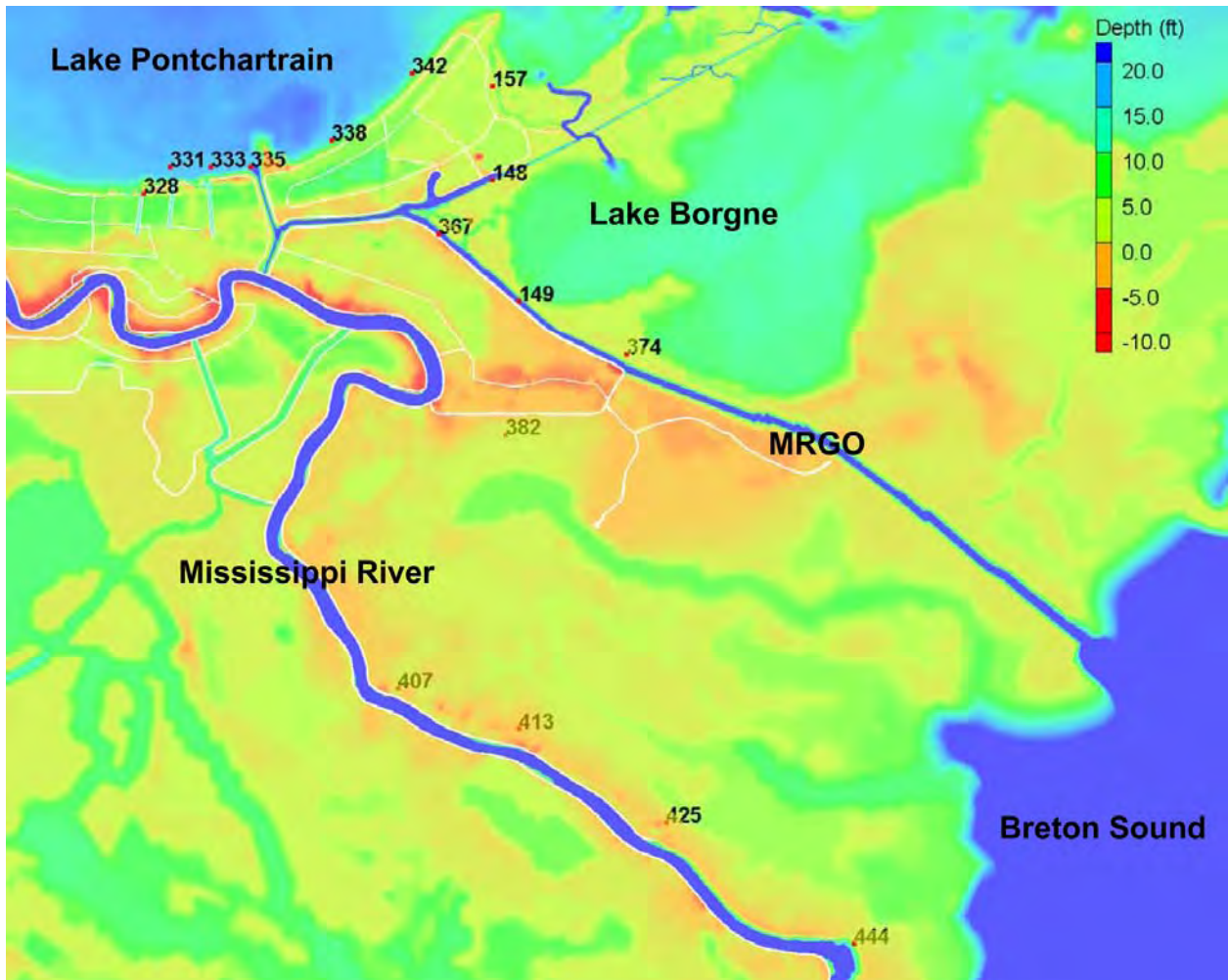


Figure 1. Locations of Selected Save Points.



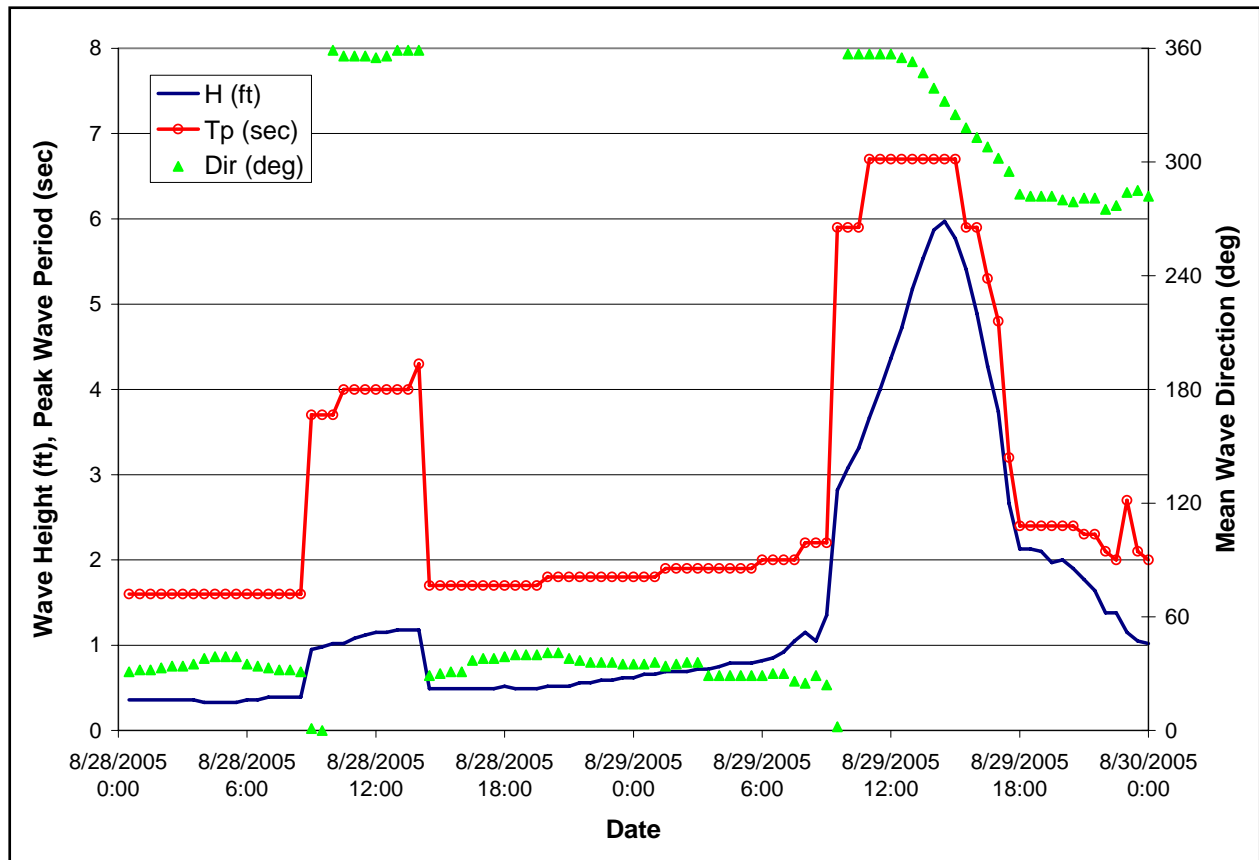


Figure 2. Time History of Wave Parameters for Station 328 (Entrance to 17th Street Canal).

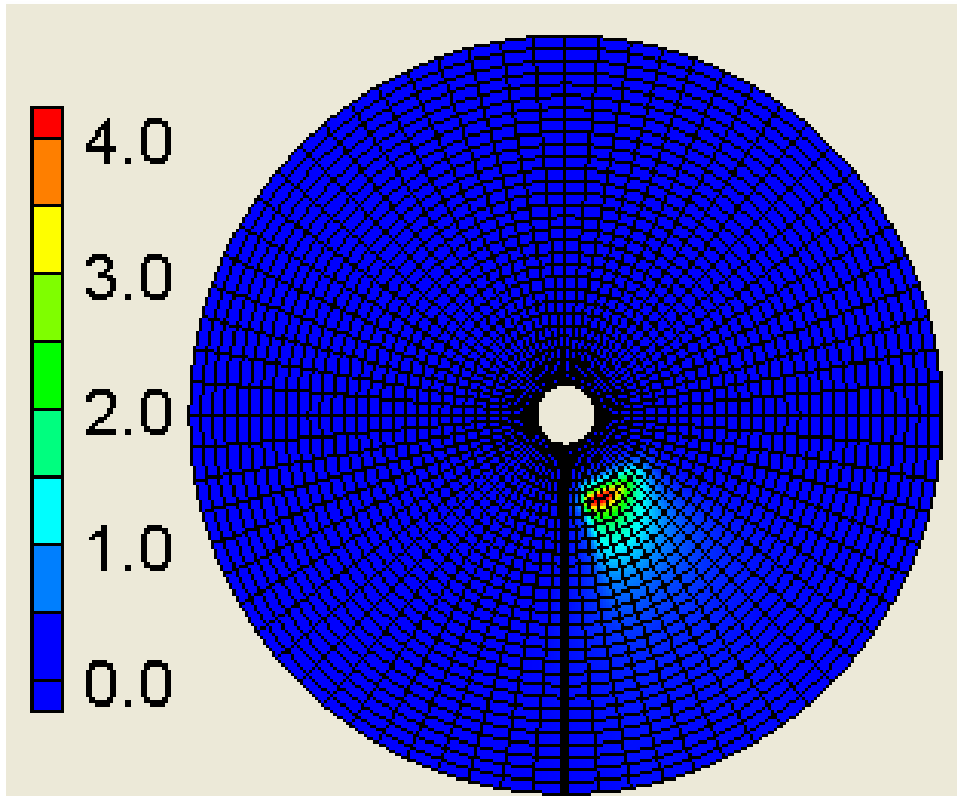


Figure 3. Wave Spectrum ( $\text{m}^2/\text{Hz}/\text{rad}$ ) for Station 328 (Entrance to 17th Street Canal) at 29 August 2005 1430 UTC. Frequencies radiate out from center (0.05 to 0.63 Hz), and directions are plotted clockwise with 0 deg (waves from north) pointing straight down (solid black line).

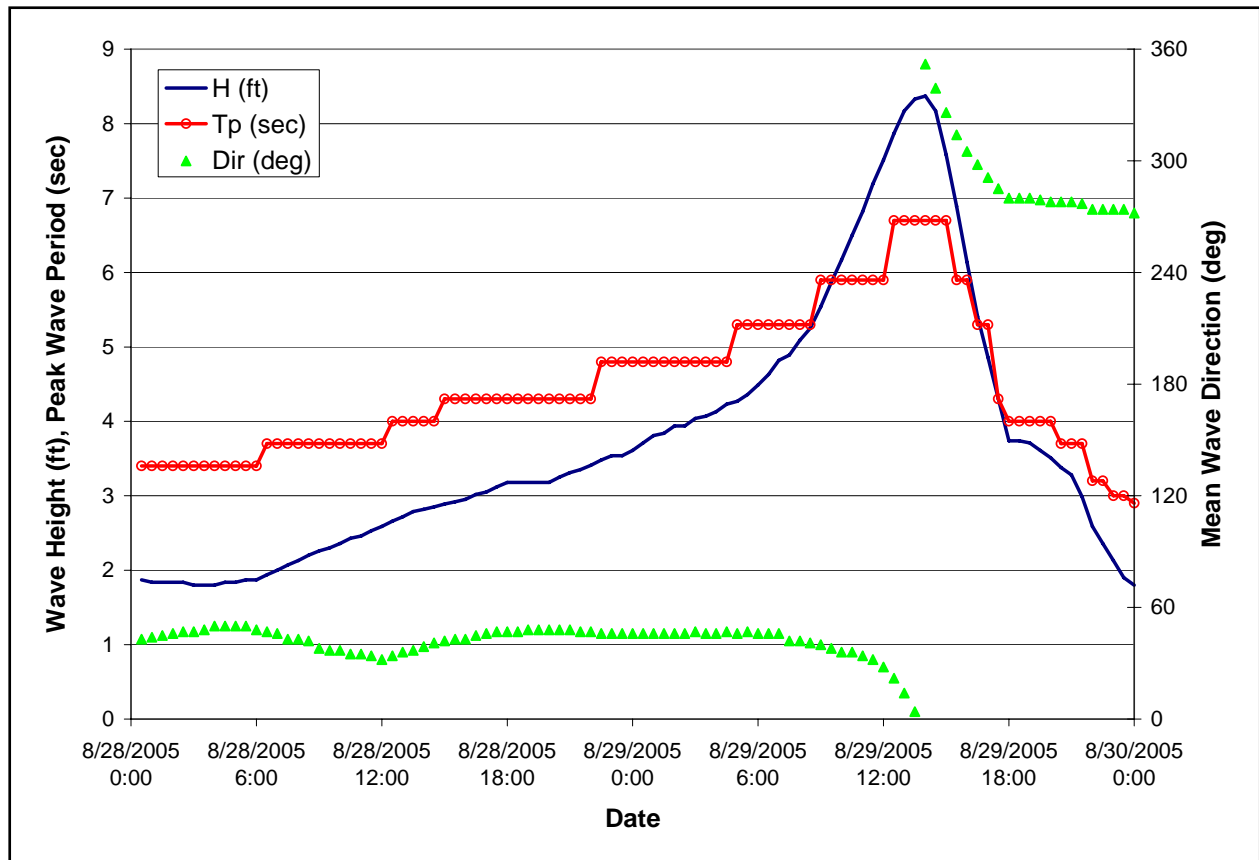


Figure 4. Time History of Wave Parameters for Station 331 (Entrance to Orleans Avenue Canal).

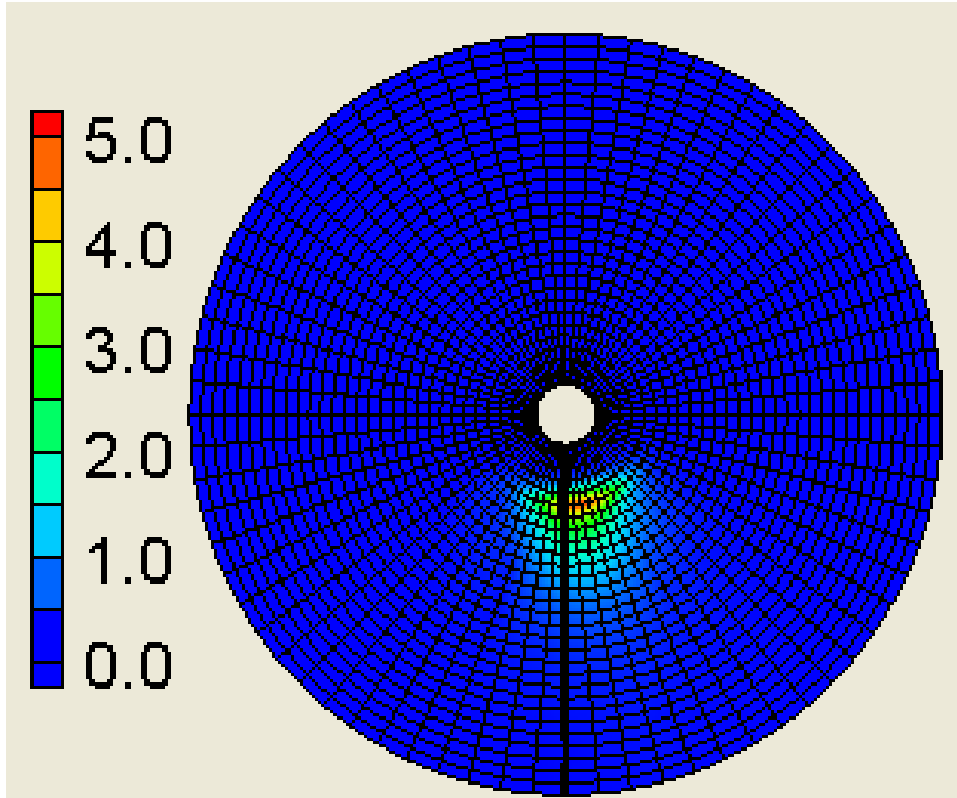


Figure 5. Wave Spectrum ( $\text{m}^2/\text{Hz}/\text{rad}$ ) for Station 331 (Entrance to Orleans Avenue Canal) at 29 August 2005 1400 UTC. Frequencies radiate out from center (0.05 to 0.63 Hz), and directions are plotted clockwise with 0 deg (waves from north) pointing straight down (solid black line).

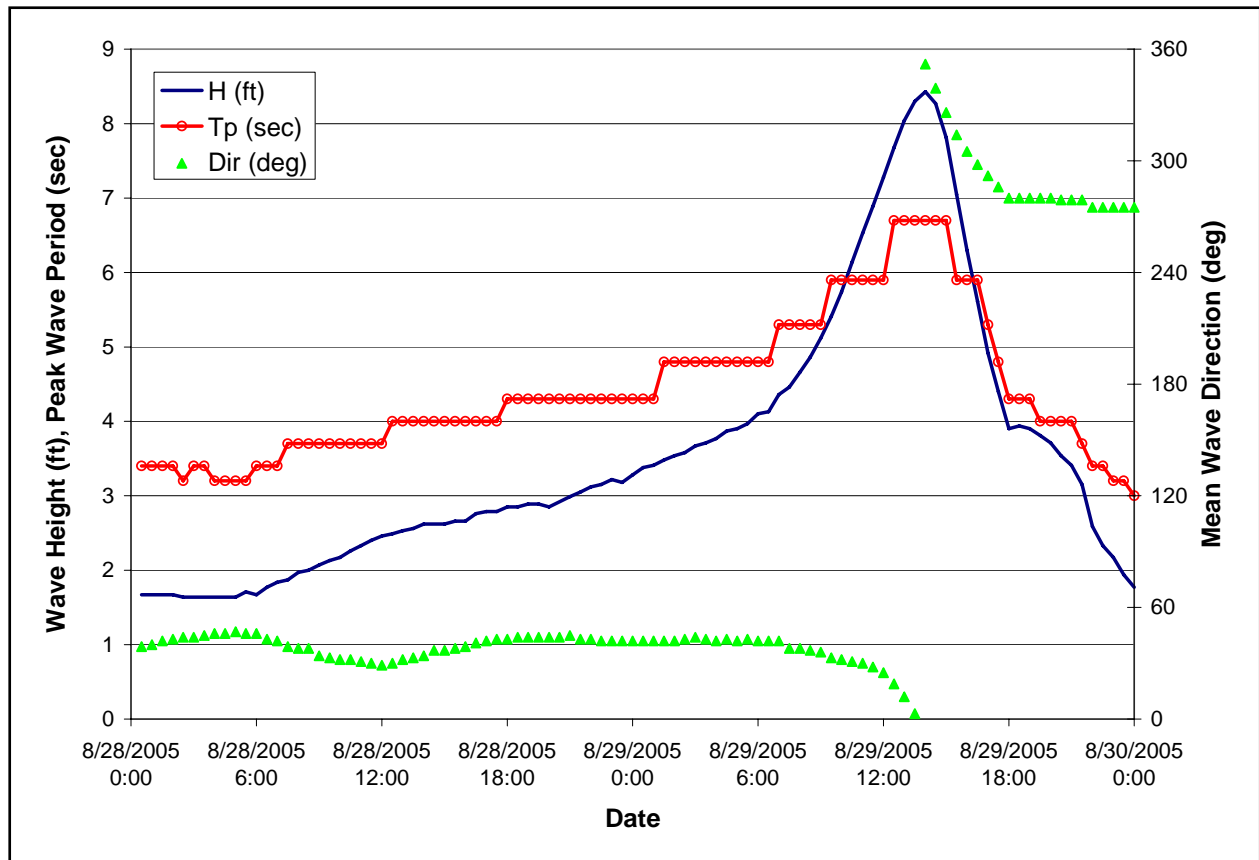


Figure 6. Time History of Wave Parameters for Station 333 (Entrance to London Avenue Canal).



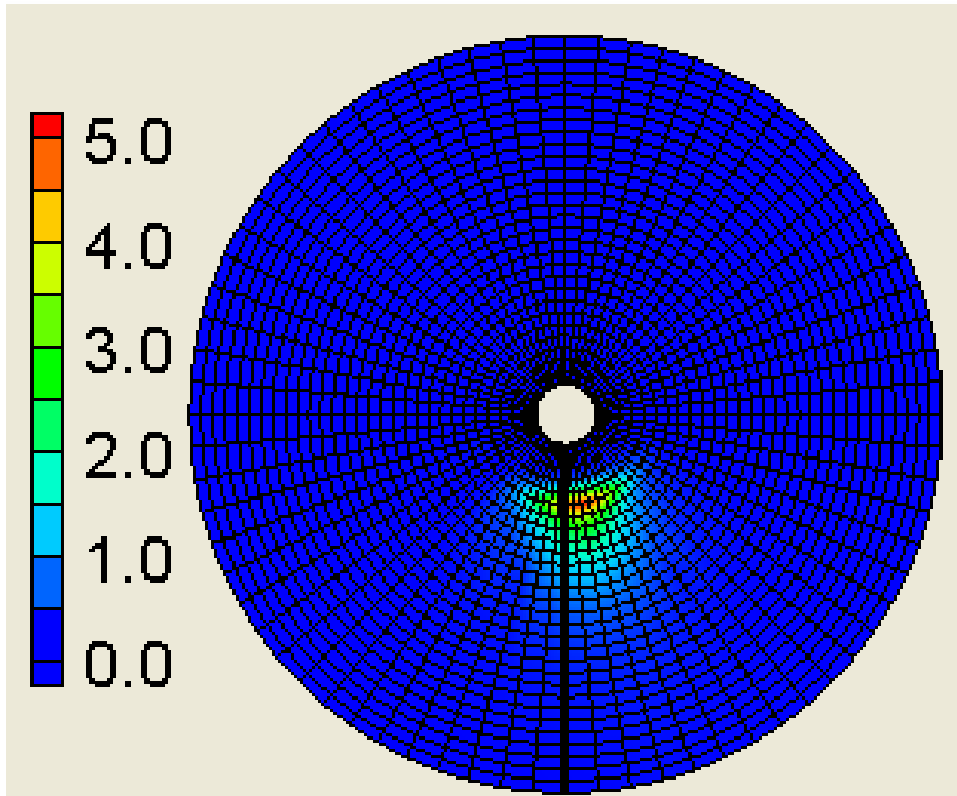


Figure 7. Wave Spectrum ( $\text{m}^2/\text{Hz}/\text{rad}$ ) for Station 333 (Entrance to London Avenue Canal) at 29 August 2005 1400 UTC. Frequencies radiate out from center (0.05 to 0.63 Hz), and directions are plotted clockwise with 0 deg (waves from north) pointing straight down (solid black line).

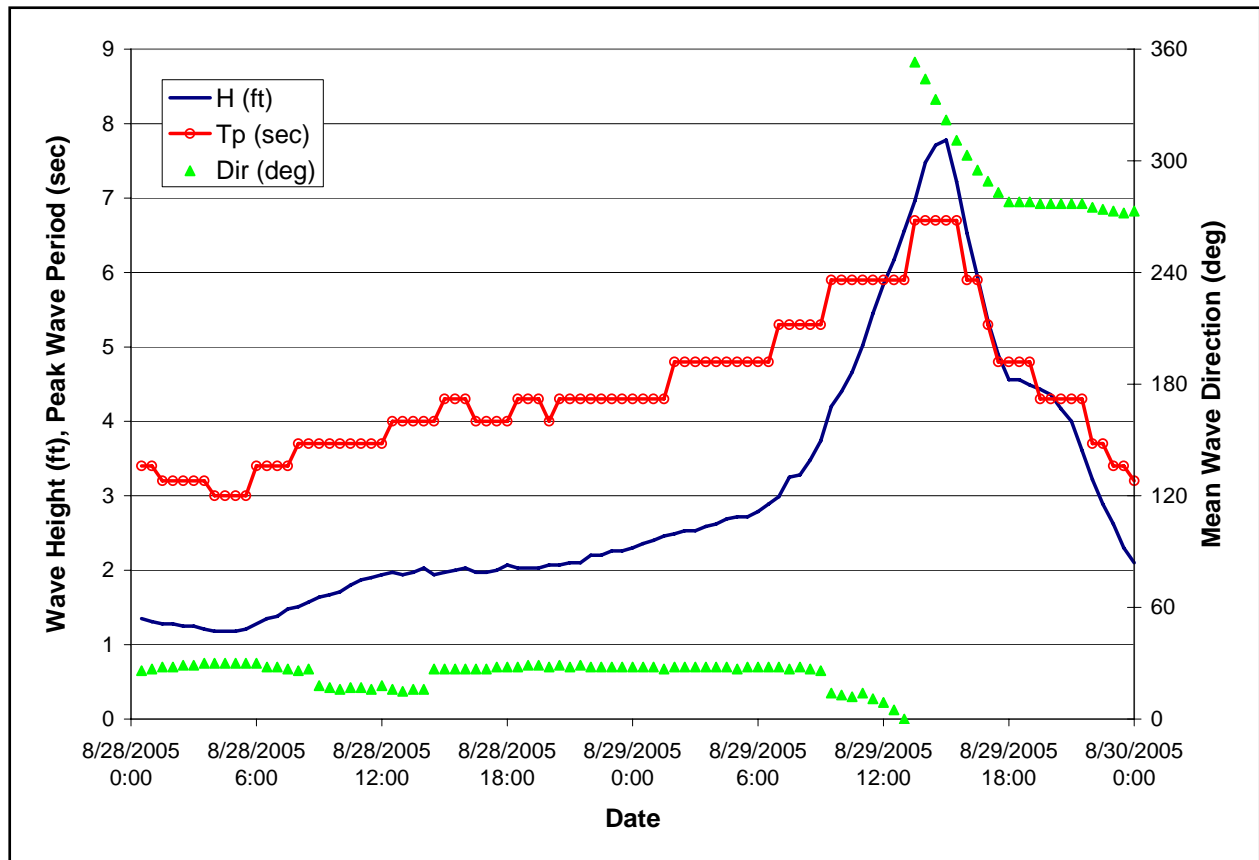


Figure 8. Time History of Wave Parameters for Station 335 (Entrance to IHNC).

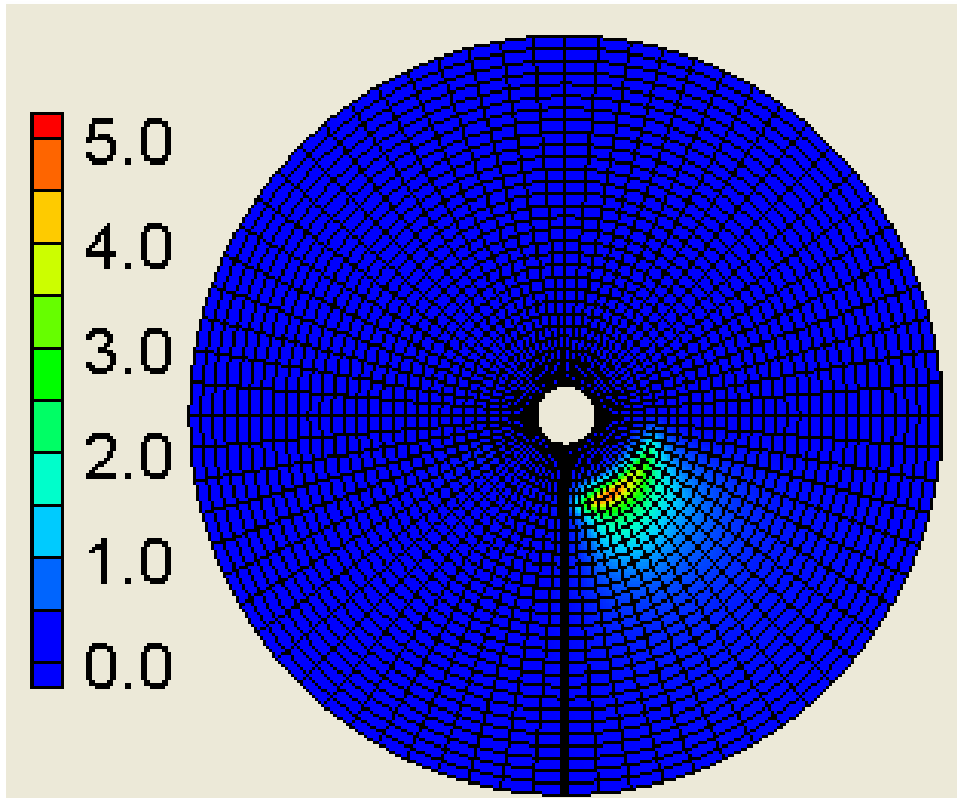


Figure 9. Wave Spectrum ( $\text{m}^2/\text{Hz}/\text{rad}$ ) for Station 335 (Entrance to IHNC) at 29 August 2005 1500 UTC. Frequencies radiate out from center (0.05 to 0.63 Hz), and directions are plotted clockwise with 0 deg (waves from north) pointing straight down (solid black line).

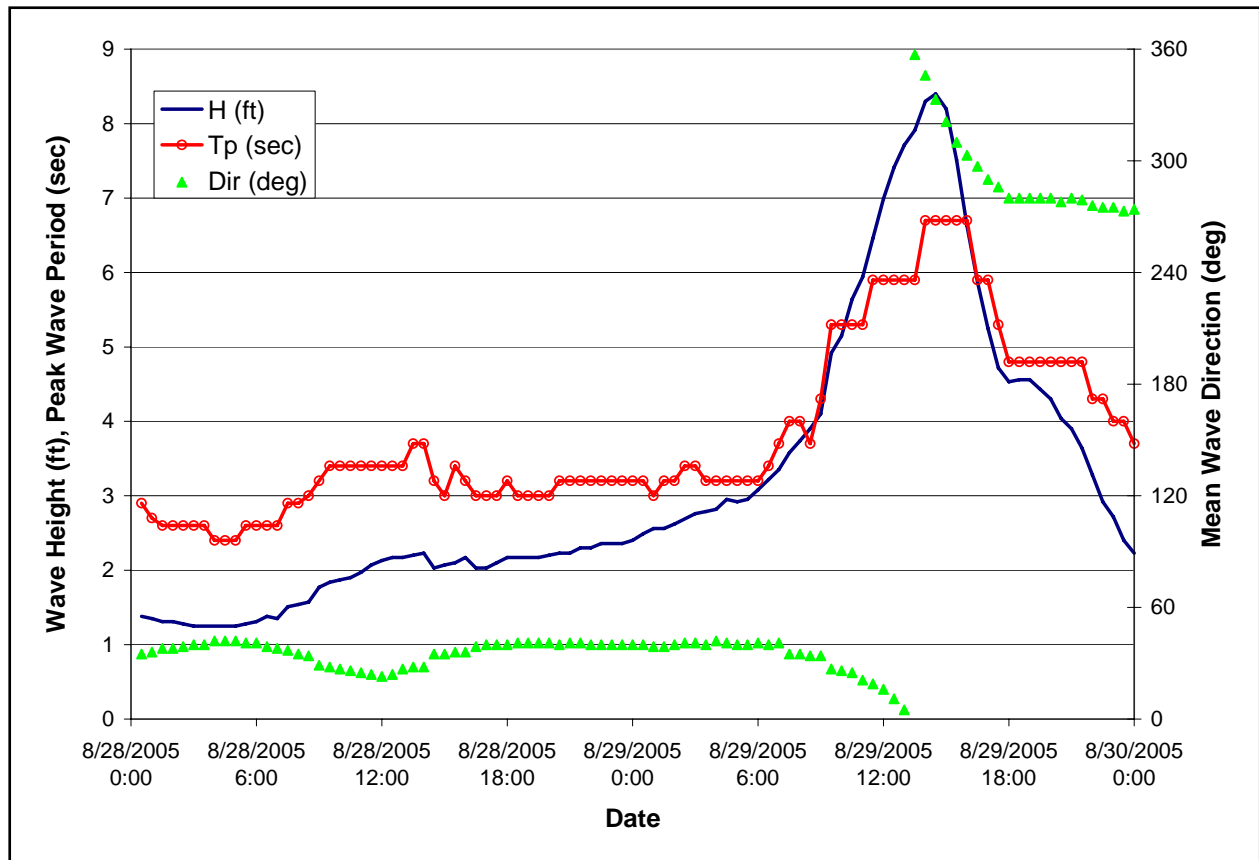


Figure 10. Time History of Wave Parameters for Station 338 (Lake Pontchartrain, Orleans Parish).

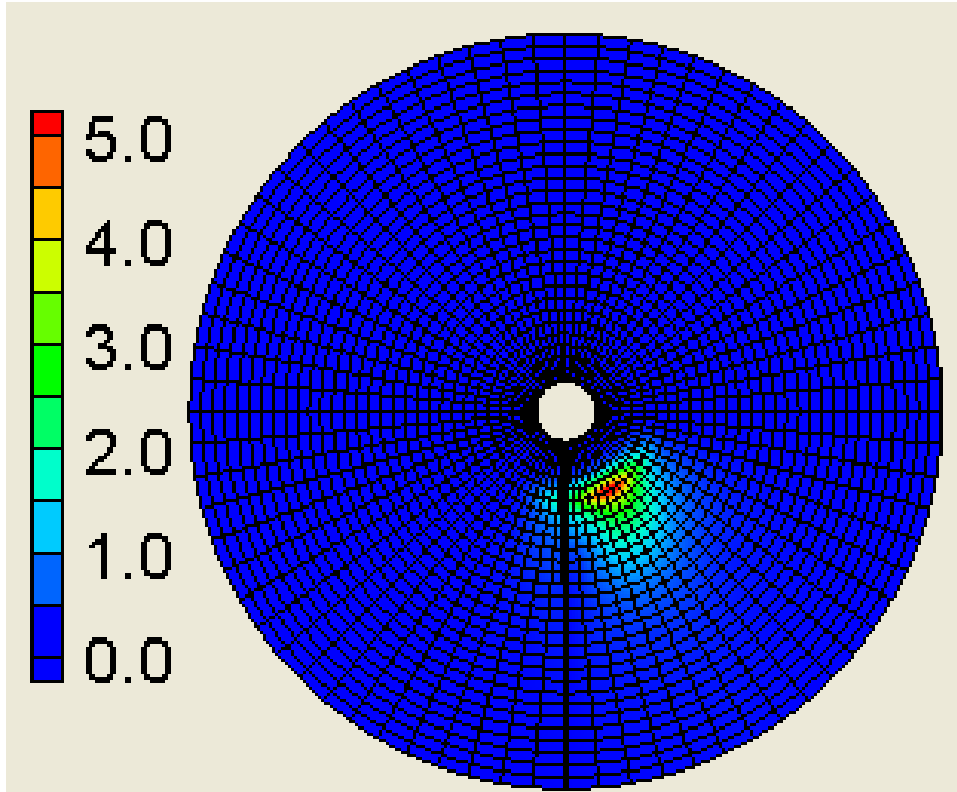


Figure 11. Wave Spectrum ( $\text{m}^2/\text{Hz}/\text{rad}$ ) for Station 338 (Lake Pontchartrain, Orleans Parish) at 29 August 2005 1430 UTC. Frequencies radiate out from center (0.05 to 0.63 Hz), and directions are plotted clockwise with 0 deg (waves from north) pointing straight down (solid black line).



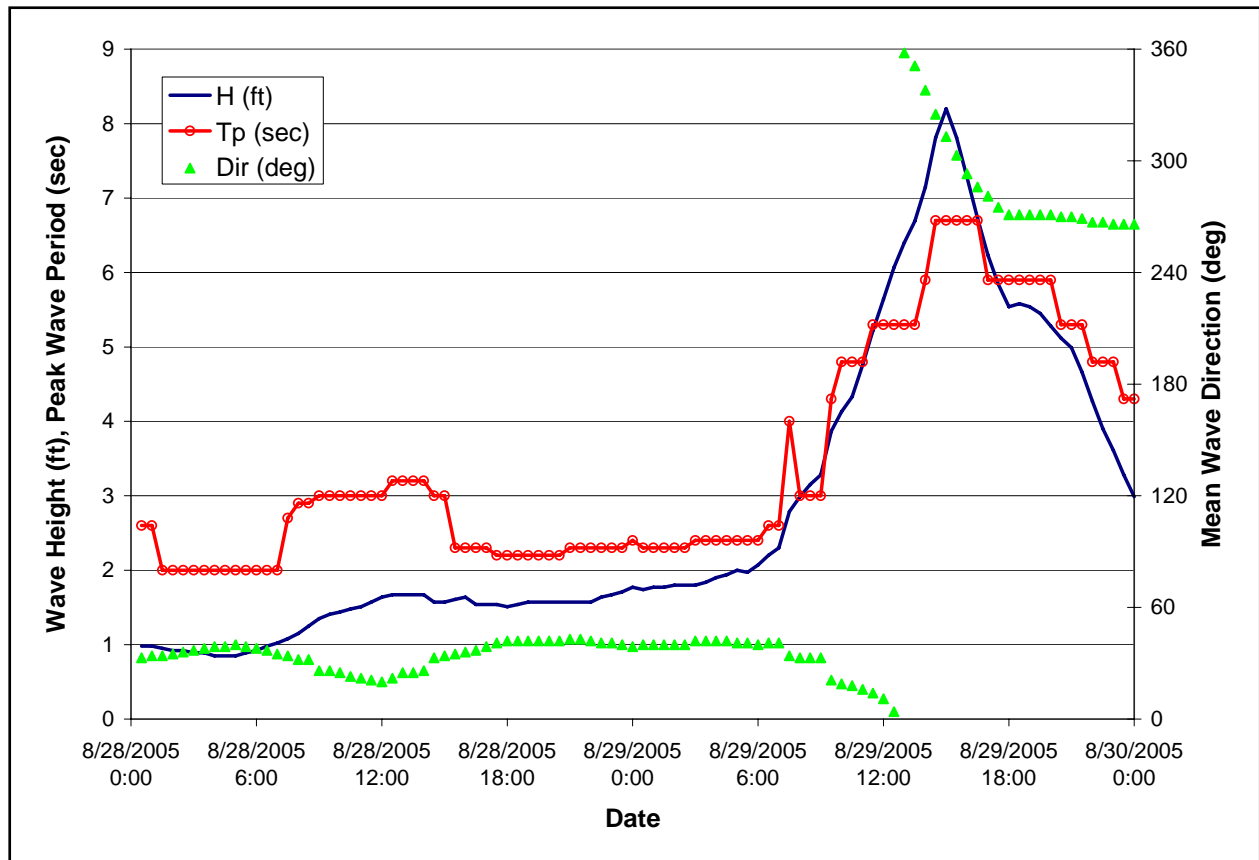


Figure 12. Time History of Wave Parameters for Station 342 (West of Black Bayou Lagoon, Orleans Parish).

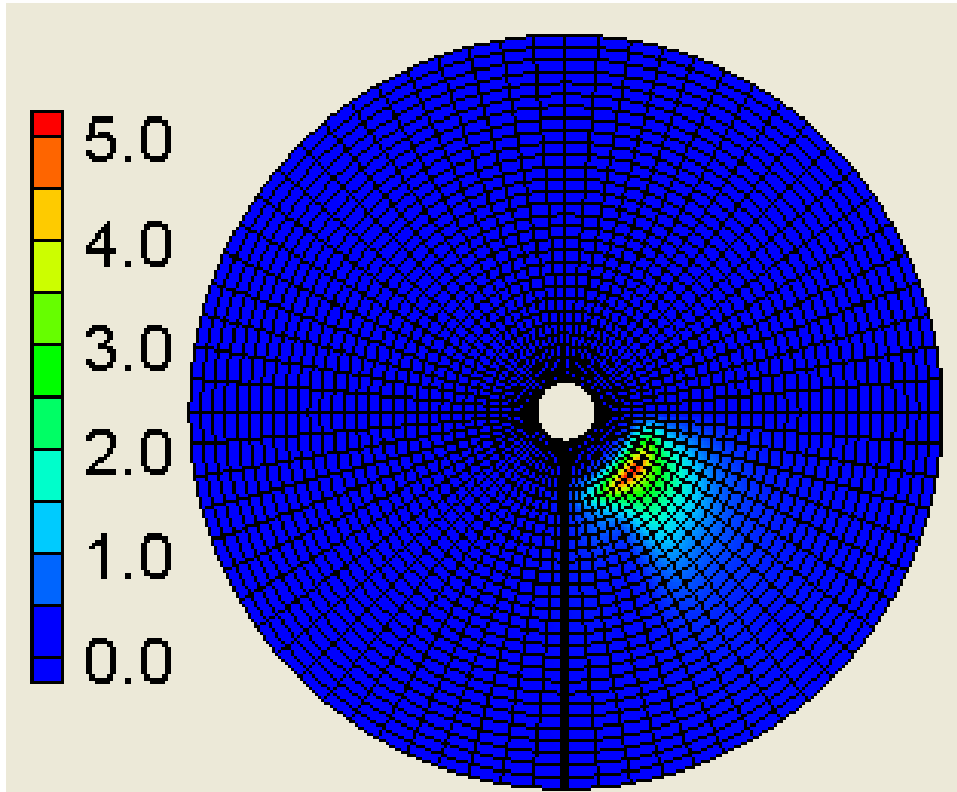


Figure 13. Wave Spectrum ( $m^2/Hz/rad$ ) for Station 342 (West of Black Bayou Lagoon, Orleans Parish) at 29 August 2005 1500 UTC. Frequencies radiate out from center (0.05 to 0.63 Hz), and directions are plotted clockwise with 0 deg (waves from north) pointing straight down (solid black line).

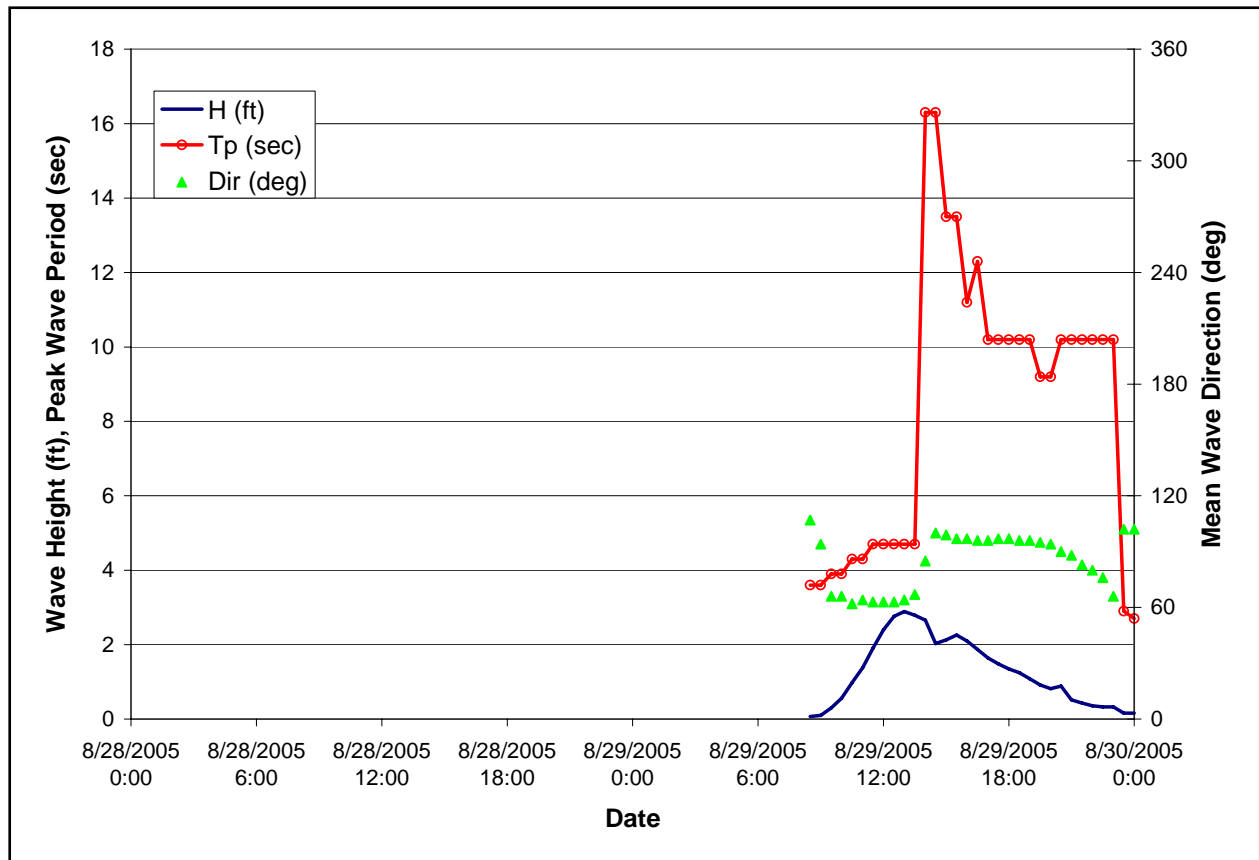


Figure 14. Time History of Wave Parameters for Station 157 (South Point at US 90 Levee, Orleans Parish).

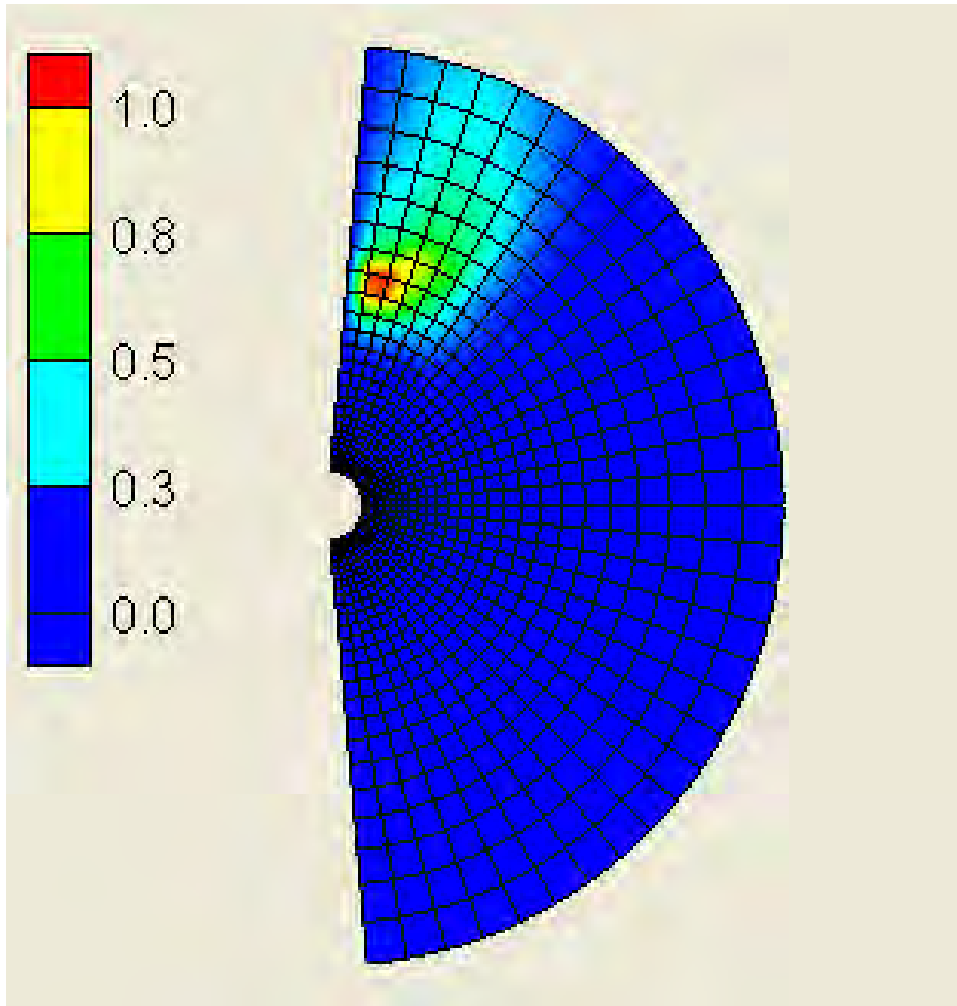


Figure 15. Wave Spectrum ( $\text{m}^2/\text{Hz}/\text{rad}$ ) for Station 157 (South Point at US 90 Levee, Orleans Parish) at 29 August 2005 1300 UTC. Frequencies radiate out from center (0.03 to 0.41 Hz), and directions are plotted clockwise from 39 deg (top, waves from 39 deg east of north) to 231 deg (at the bottom).

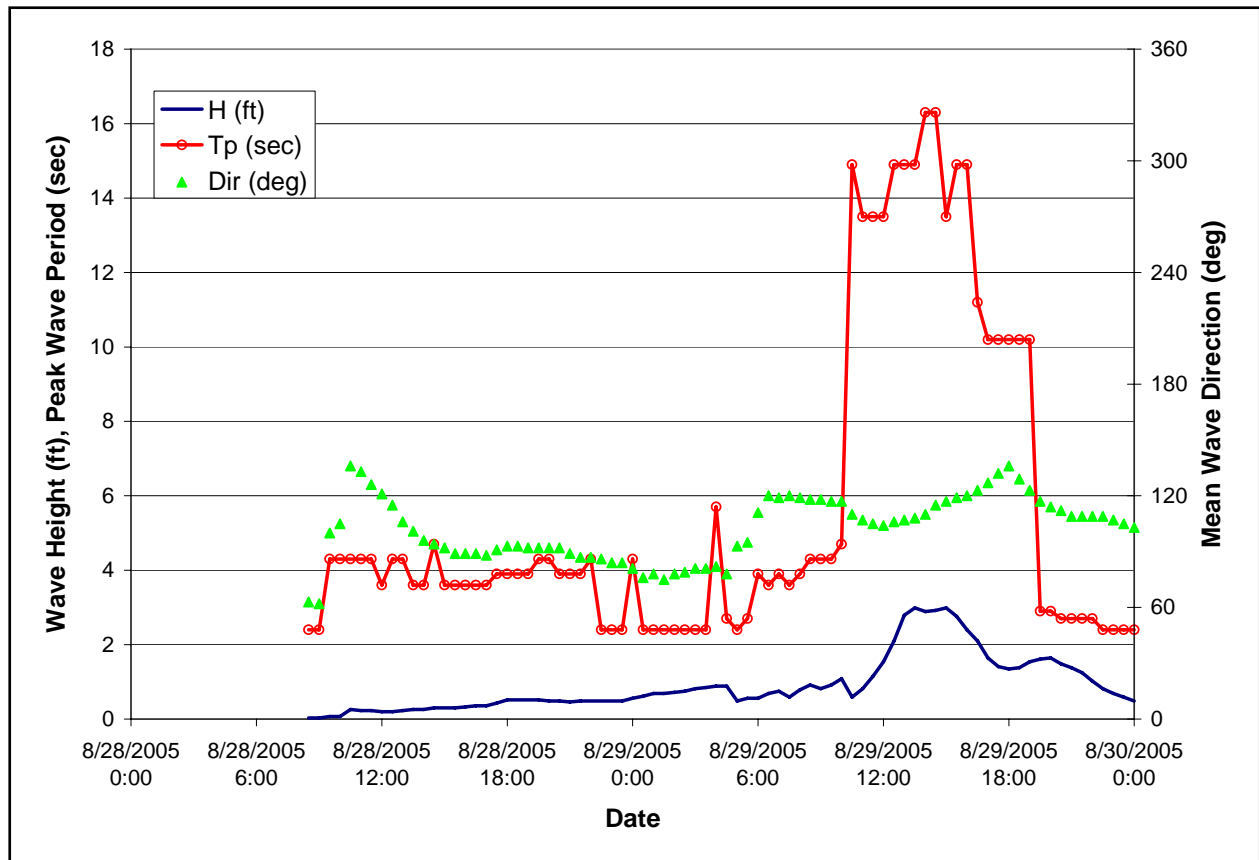


Figure 16. Time History of Wave Parameters for Station 148 (Northeast Back Levee, Orleans Parish).



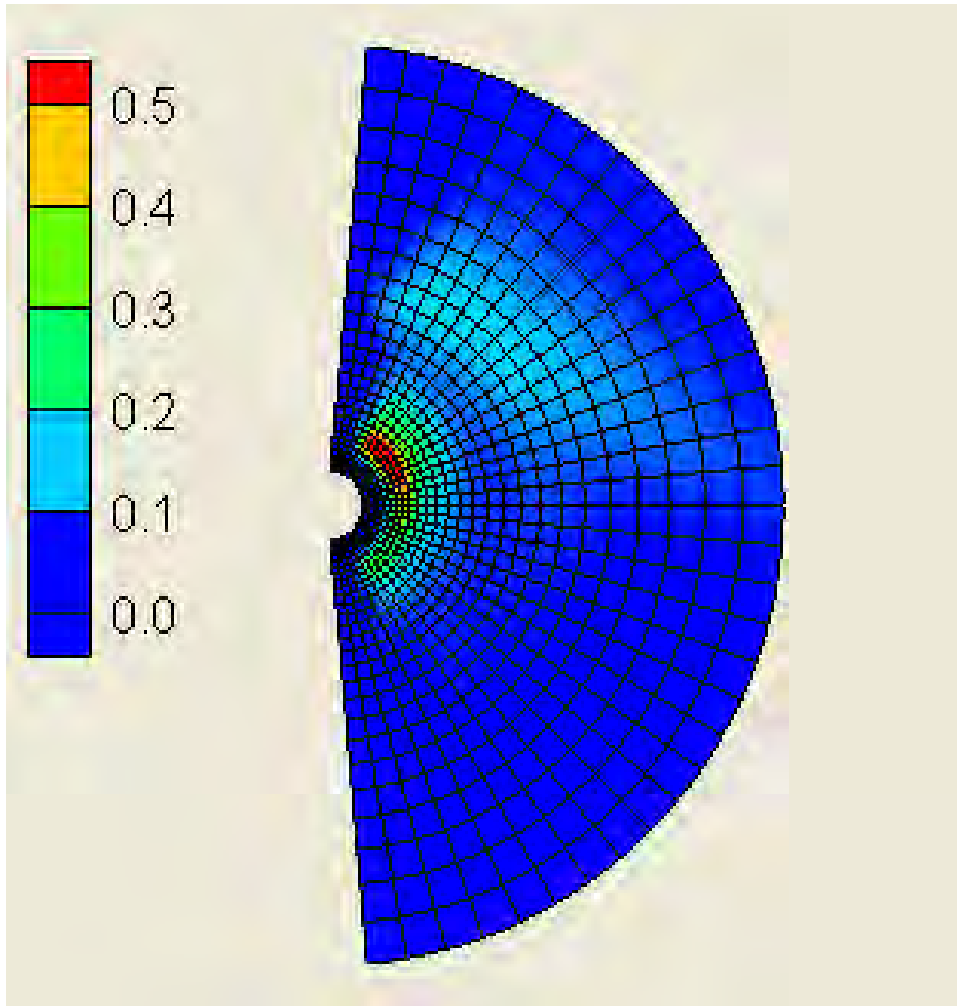


Figure 17. Wave Spectrum ( $\text{m}^2/\text{Hz}/\text{rad}$ ) for Station 148 (Northeast Back Levee, Orleans Parish) at 29 August 2005 1330 UTC. Frequencies radiate out from center (0.03 to 0.41 Hz), and directions are plotted clockwise from 39 deg (top, waves from 39 deg east of north) to 231 deg (at the bottom).

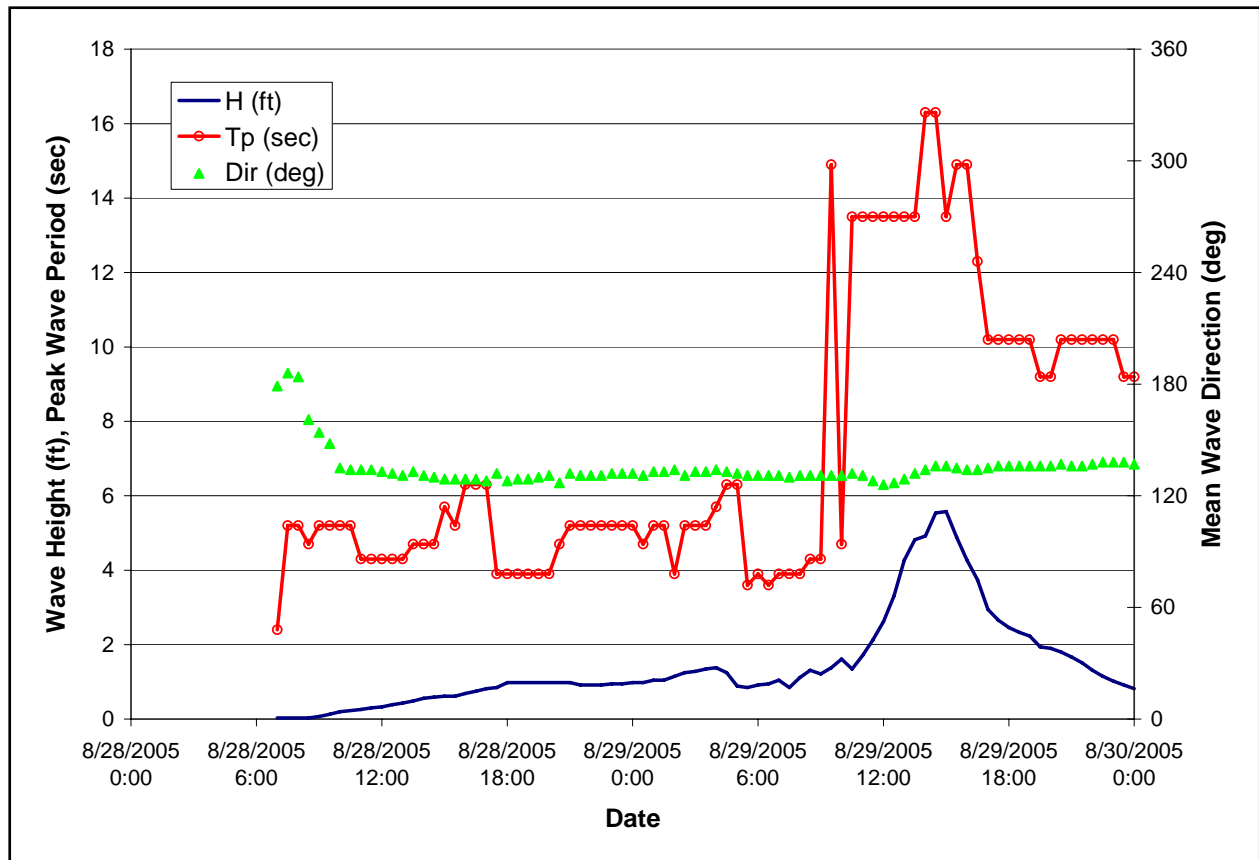


Figure 18. Time History of Wave Parameters for Station 367 (MRGO near Bayou Bienvenue, St. Bernard Parish).

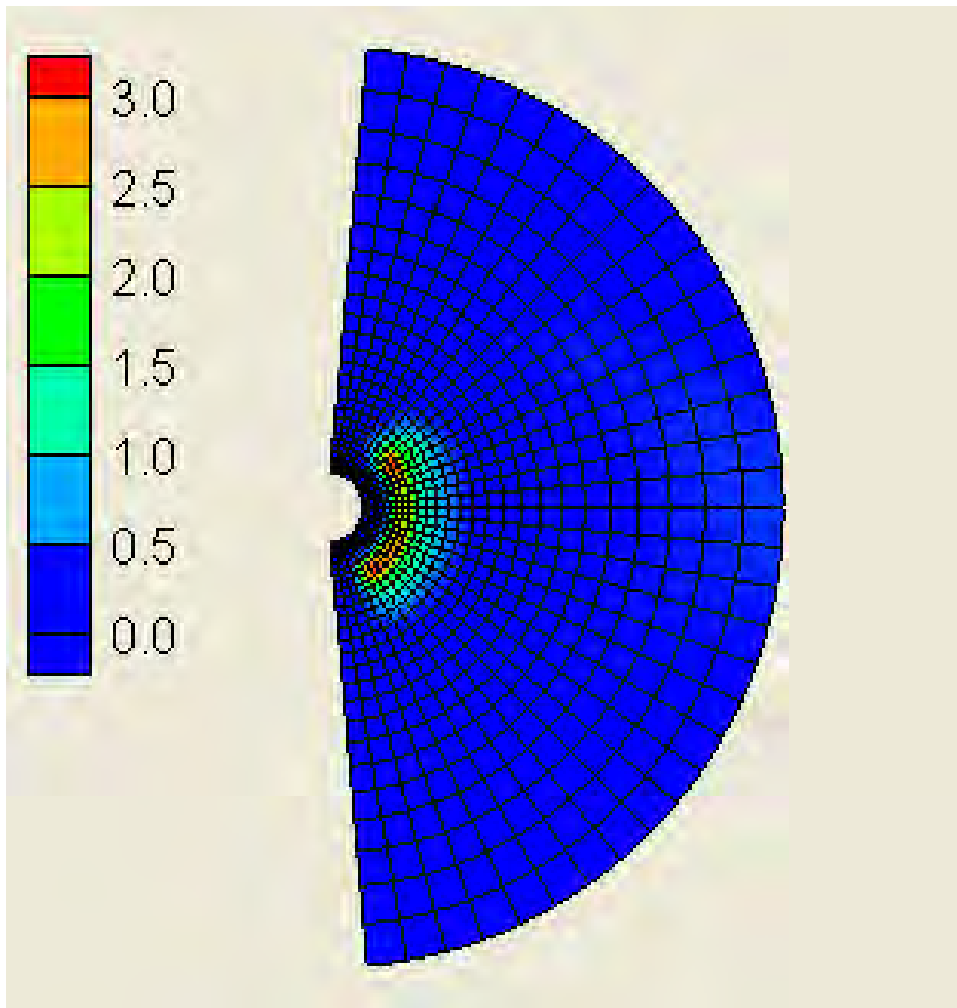


Figure 19. Wave Spectrum ( $m^2/Hz/rad$ ) for Station 367 (MRGO near Bayou Bienvenue, St. Bernard Parish) at 29 August 2005 1500 UTC. Frequencies radiate out from center (0.03 to 0.41 Hz), and directions are plotted clockwise from 39 deg (top, waves from 39 deg east of north) to 231 deg (at the bottom).

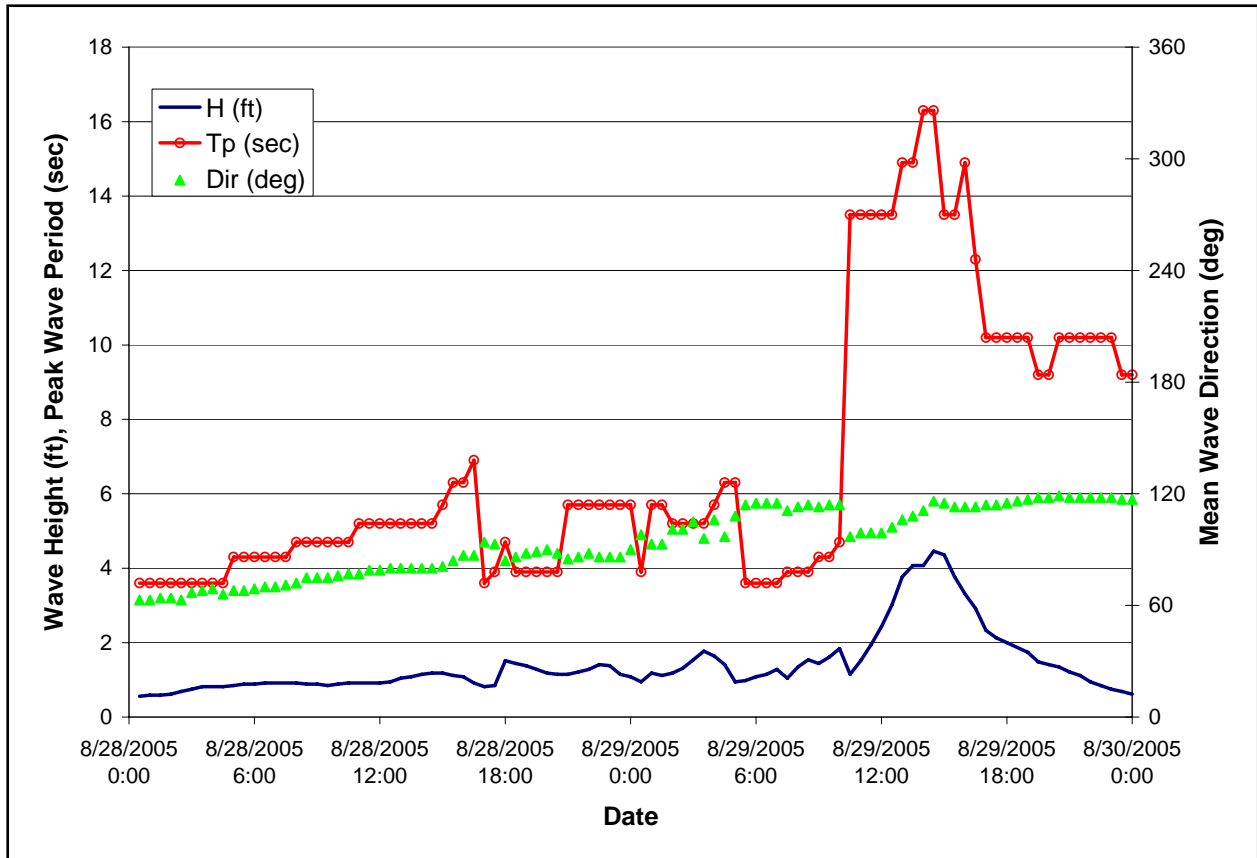


Figure 20. Time History of Wave Parameters for Station 149 (Bayou Dupree at Floodgate East, St. Bernard Parish).

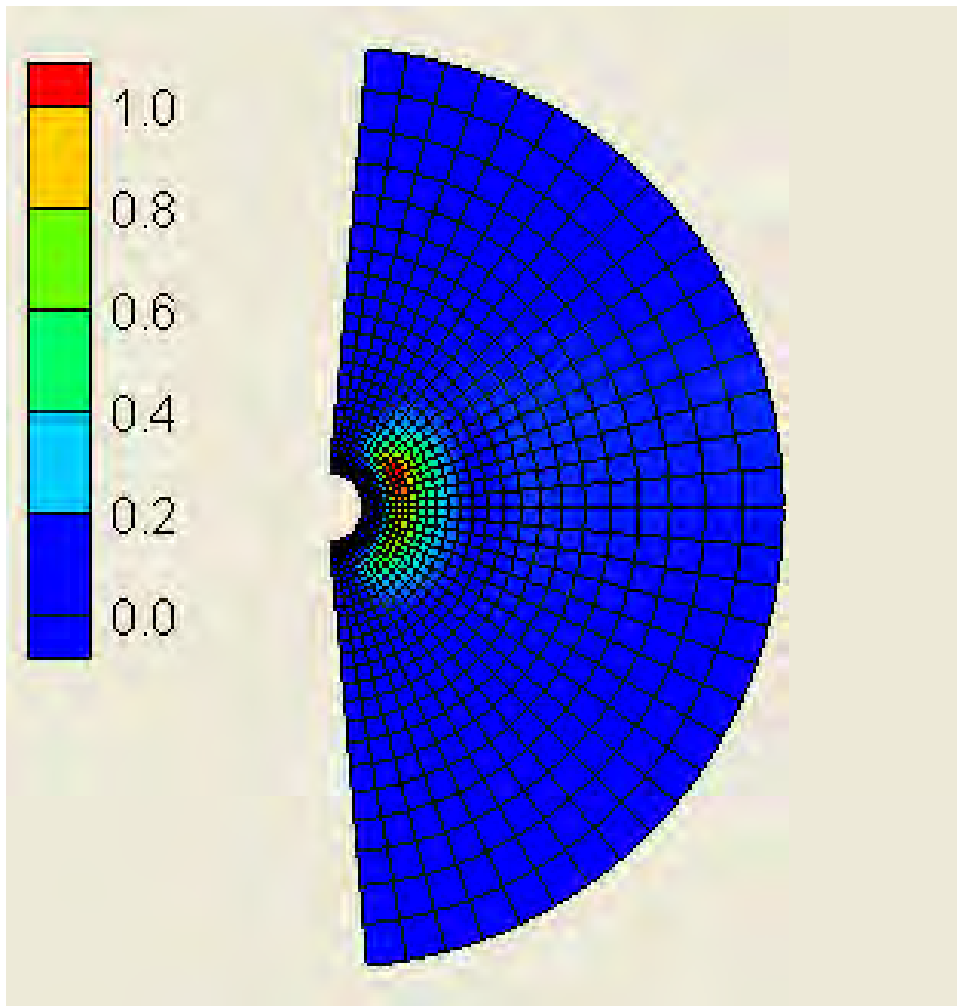


Figure 21. Wave Spectrum ( $\text{m}^2/\text{Hz}/\text{rad}$ ) for Station 149 (Bayou Dupree at Floodgate East, St. Bernard Parish) at 29 August 2005 1430 UTC. Frequencies radiate out from center (0.03 to 0.41 Hz), and directions are plotted clockwise from 39 deg (top, waves from 39 deg east of north) to 231 deg (at the bottom).



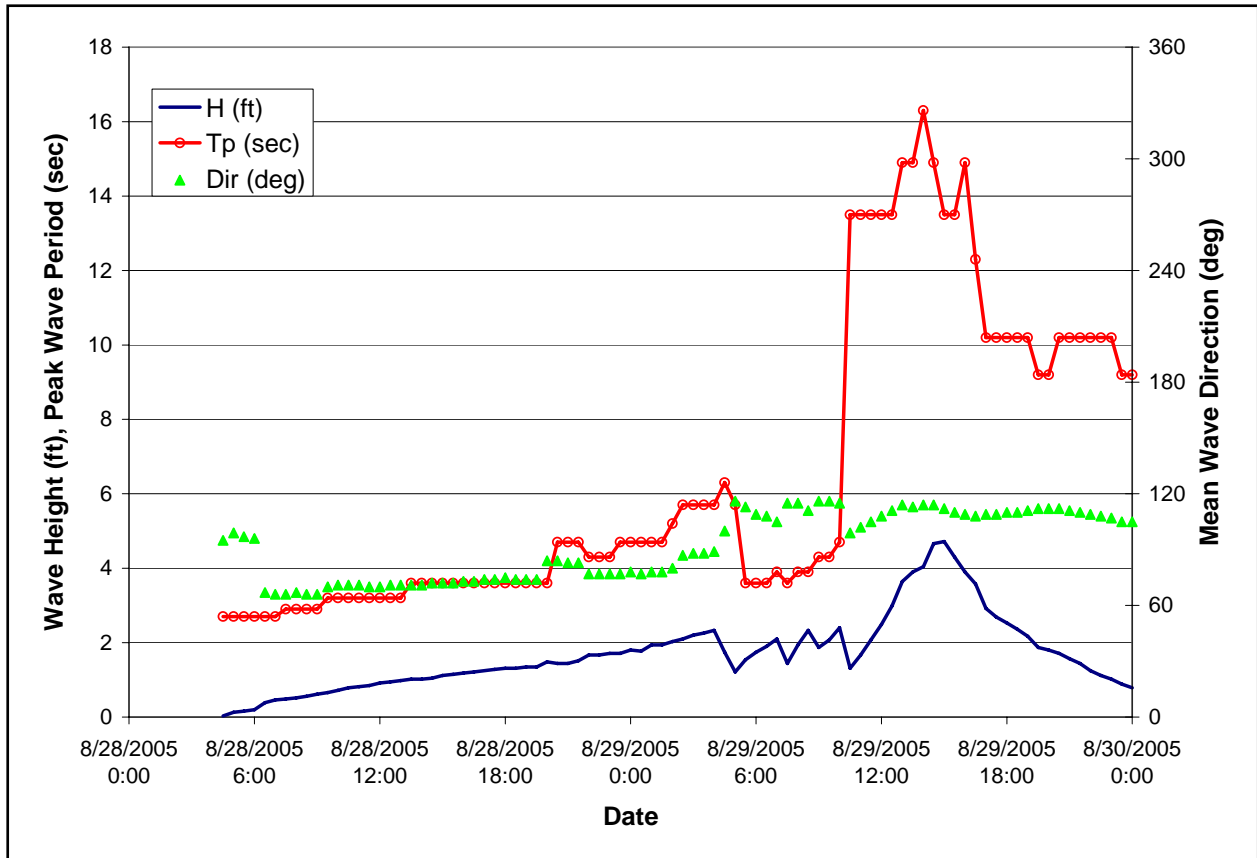


Figure 22. Time History of Wave Parameters for Station 374 (MRGO near Grand Bayou, St. Bernard Parish).

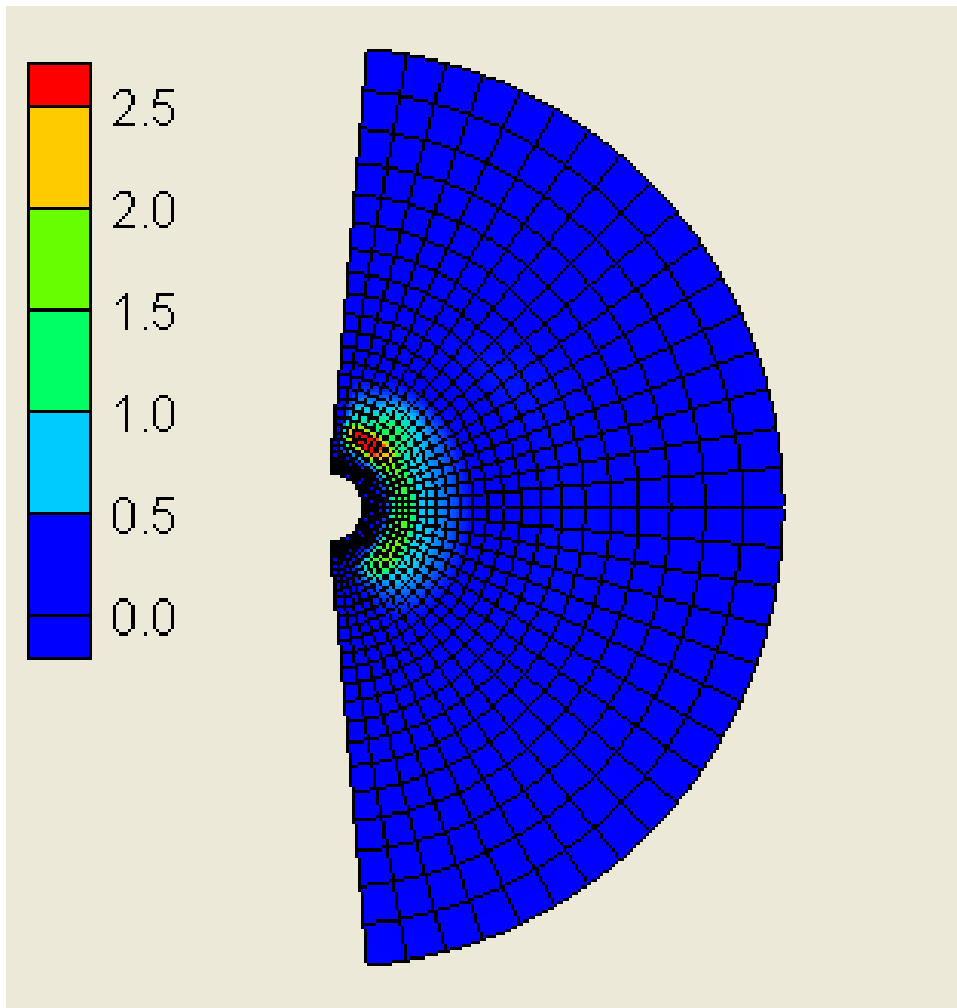


Figure 23. Wave Spectrum ( $\text{m}^2/\text{Hz}/\text{rad}$ ) for Station 374 (MRGO near Grand Bayou, St. Bernard Parish) at 29 August 2005 1500 UTC. Frequencies radiate out from center (0.03 to 0.41 Hz), and directions are plotted clockwise from 39 deg (top, waves from 39 deg east of north) to 231 deg (at the bottom).

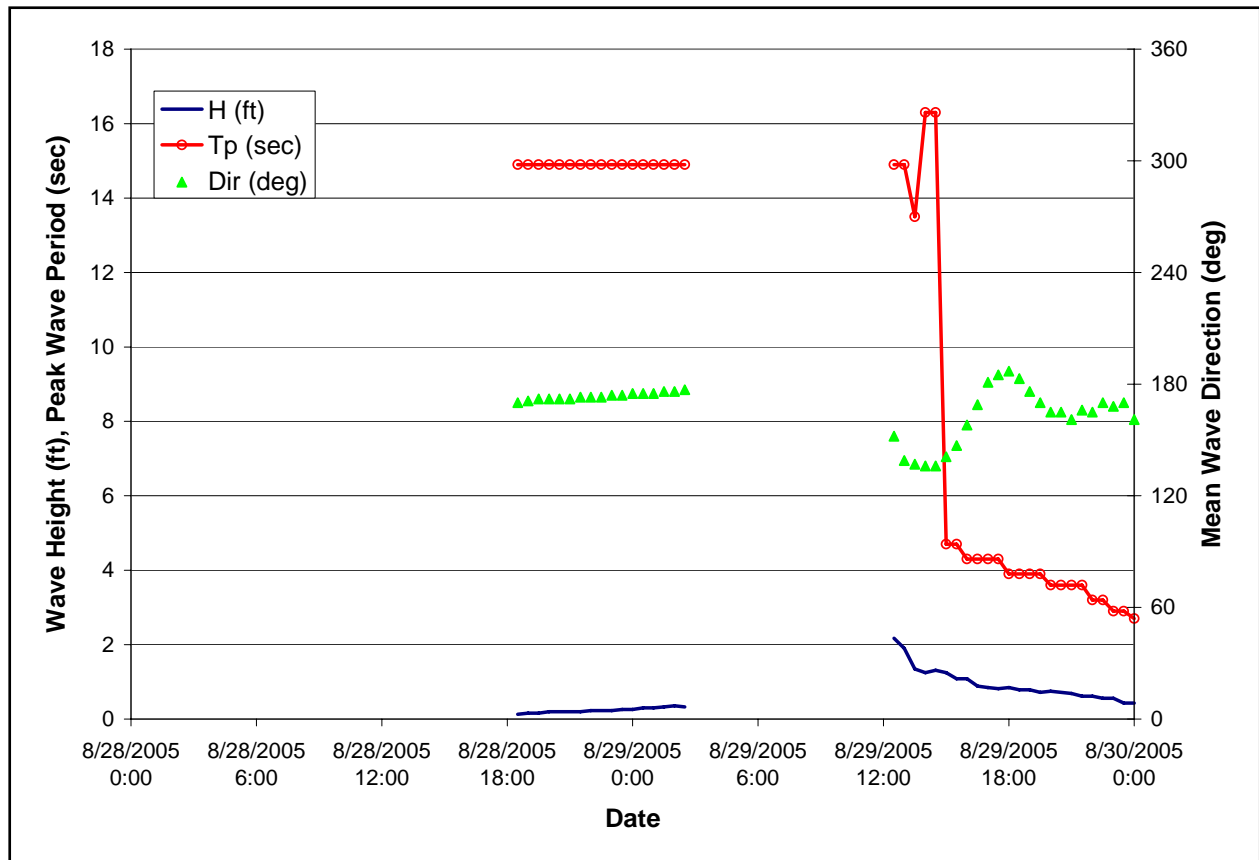


Figure 24. Time History of Wave Parameters for Station 382 (Between MRGO and MS River west of Magnolia Canal, St. Bernard Parish).

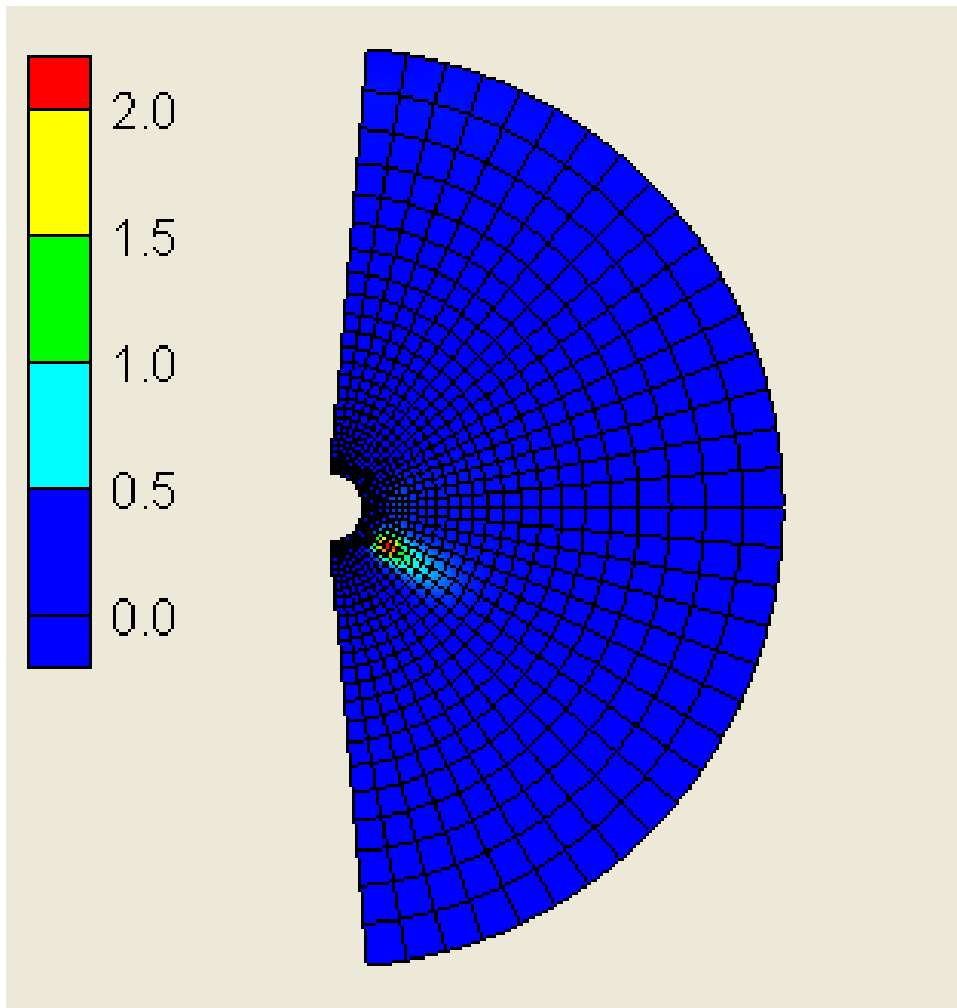


Figure 25. Wave Spectrum ( $\text{m}^2/\text{Hz}/\text{rad}$ ) for Station 382 (Between MRGO and MS River west of Magnolia Canal, St. Bernard Parish) at 29 August 2005 1230 UTC. Frequencies radiate out from center (0.03 to 0.41 Hz), and directions are plotted clockwise from 39 deg (top, waves from 39 deg east of north) to 231 deg (at the bottom).

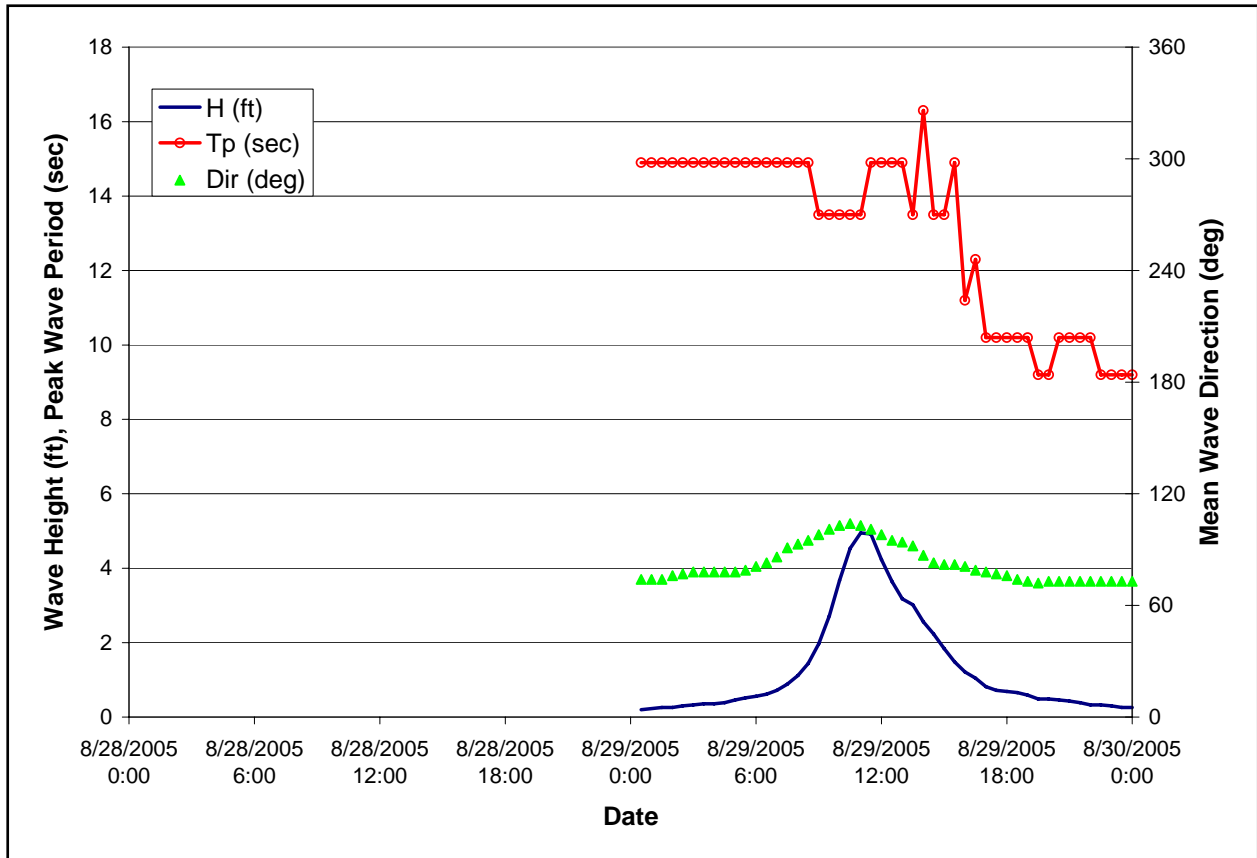


Figure 26. Time History of Wave Parameters for Station 407 (Plaquemines Parish at Phoenix).



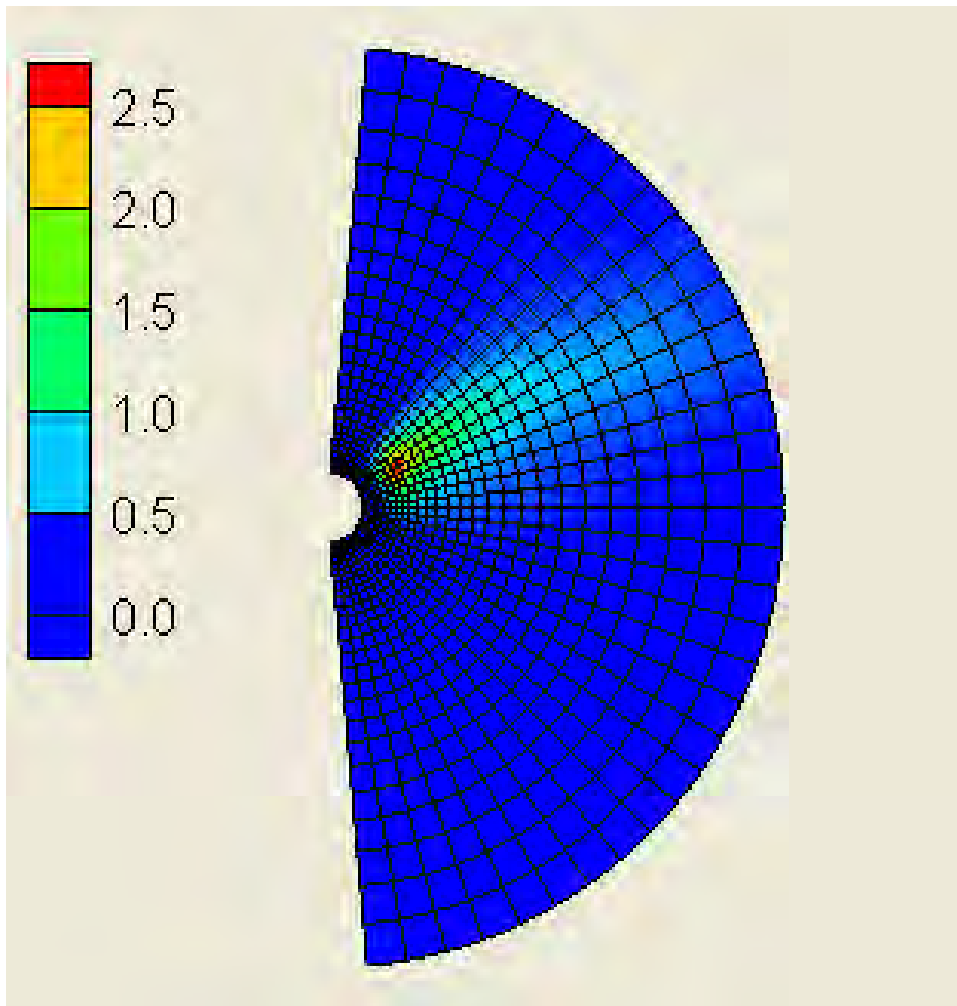


Figure 27. Wave Spectrum ( $\text{m}^2/\text{Hz}/\text{rad}$ ) for Station 407 (Plaquemines Parish at Phoenix) at 29 August 2005 1100 UTC. Frequencies radiate out from center (0.03 to 0.41 Hz), and directions are plotted clockwise from 39 deg (top, waves from 39 deg east of north) to 231 deg (at the bottom).

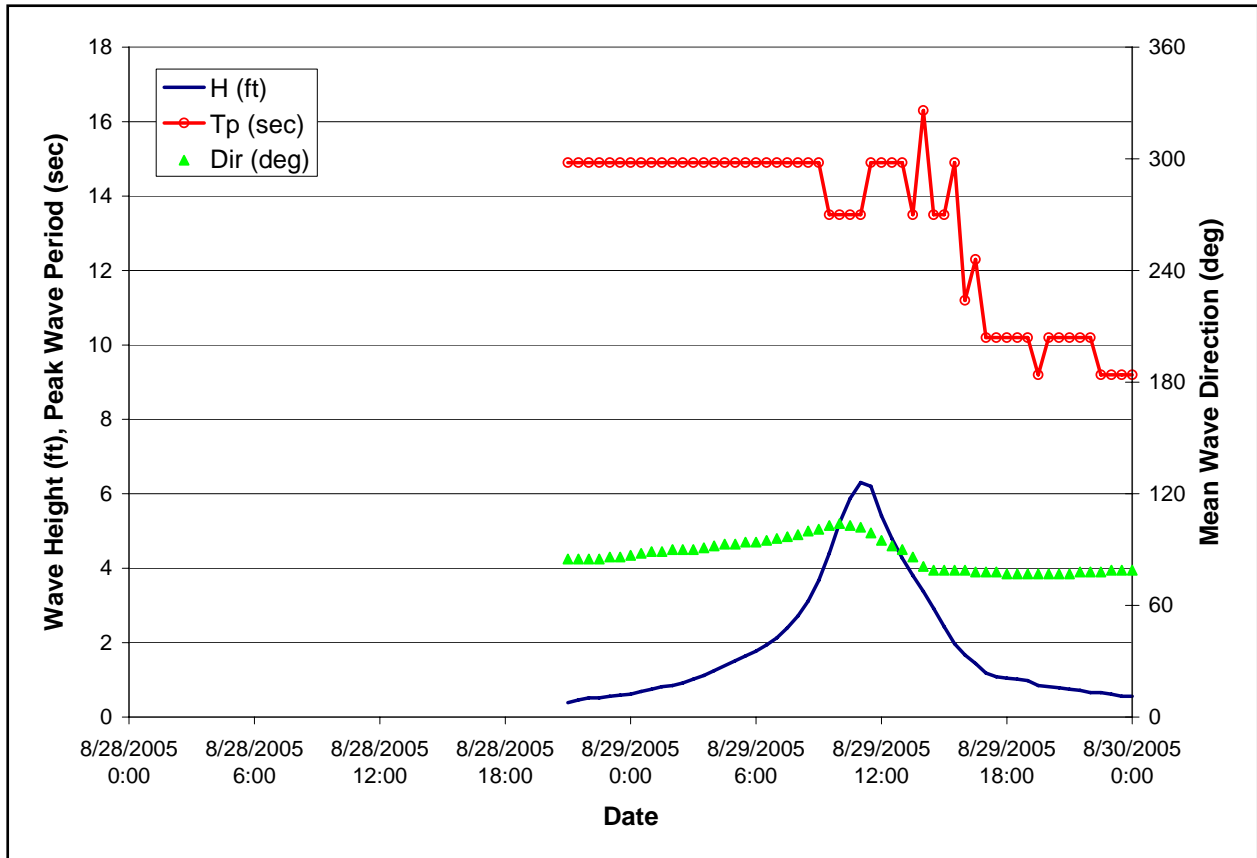


Figure 28. Time History of Wave Parameters for Station 413 (Plaquemines Parish north of Davant).

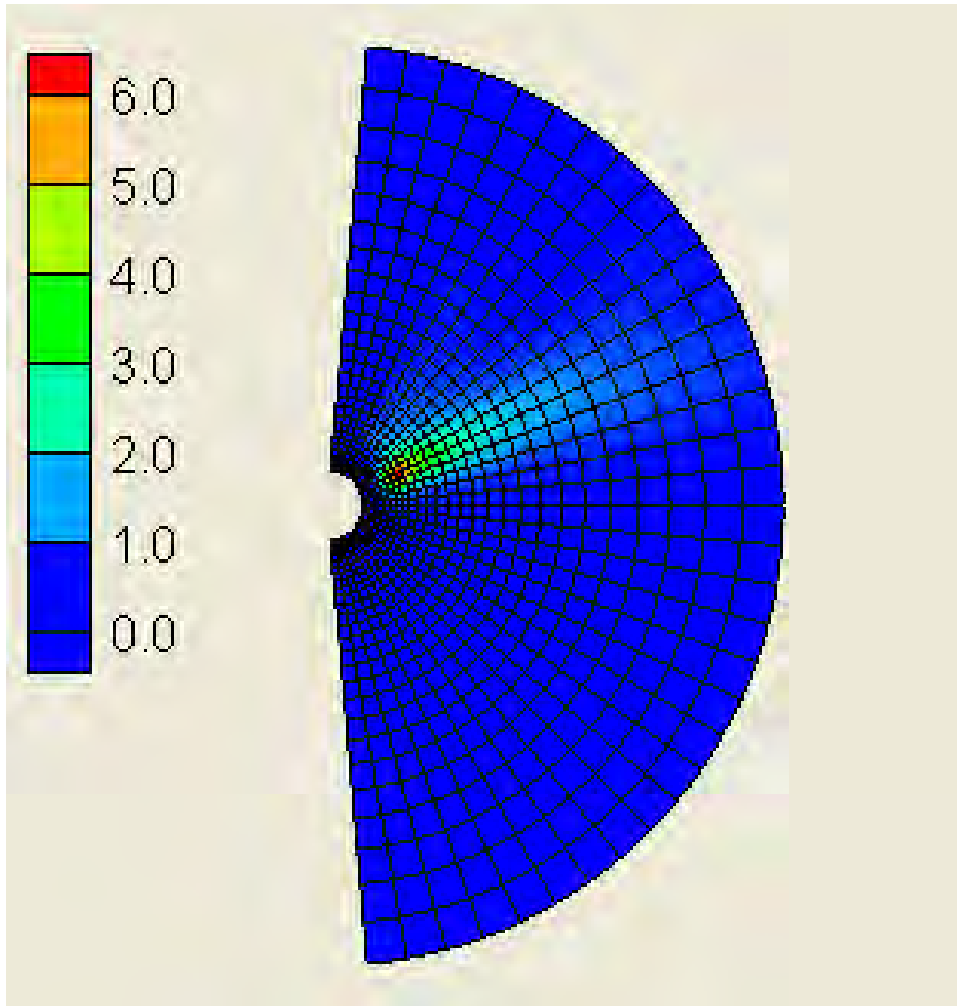


Figure 29. Wave Spectrum ( $\text{m}^2/\text{Hz}/\text{rad}$ ) for Station 413 (Plaquemines Parish north of Davant) at 29 August 2005 1100 UTC. Frequencies radiate out from center (0.03 to 0.41 Hz), and directions are plotted clockwise from 39 deg (top, waves from 39 deg east of north) to 231 deg (at the bottom).

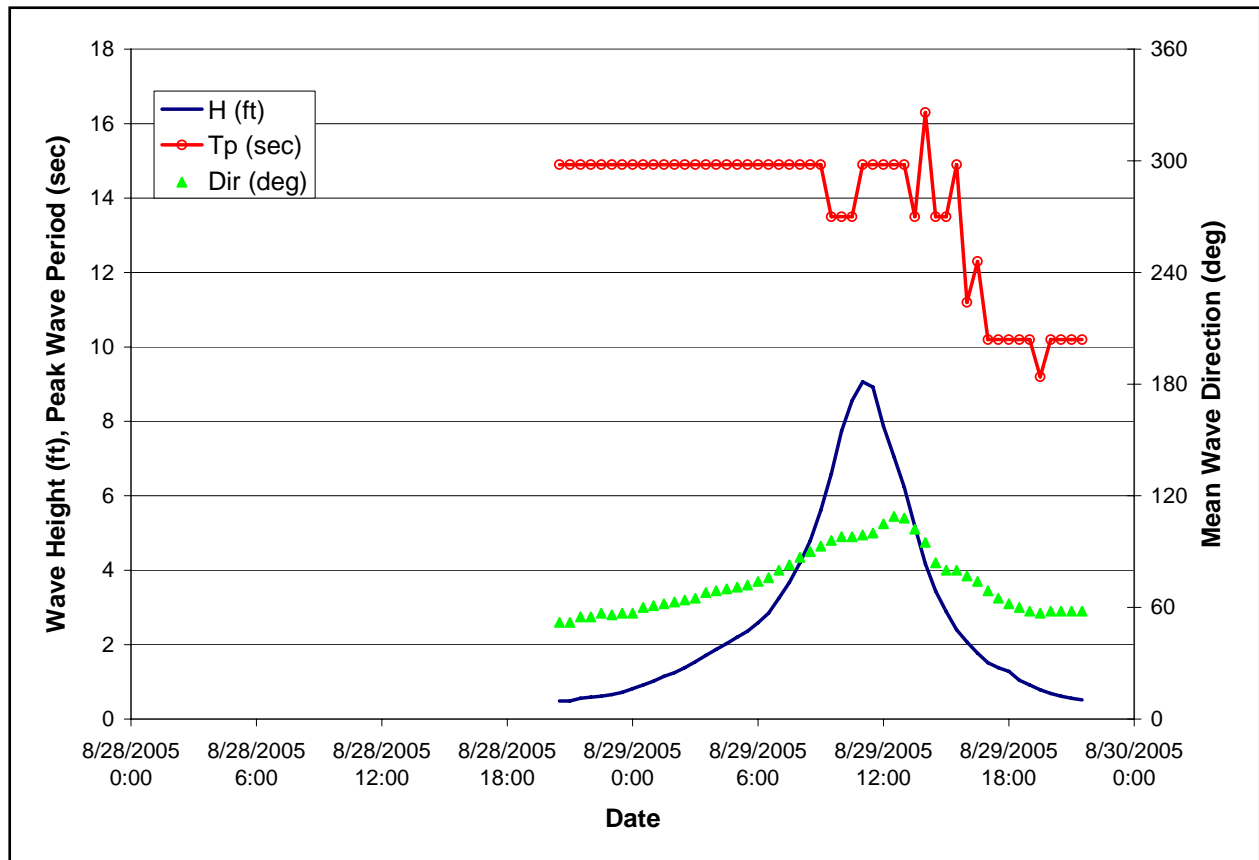


Figure 30. Time History of Wave Parameters for Station 425 (Plaquemines Parish at end of East Levee).

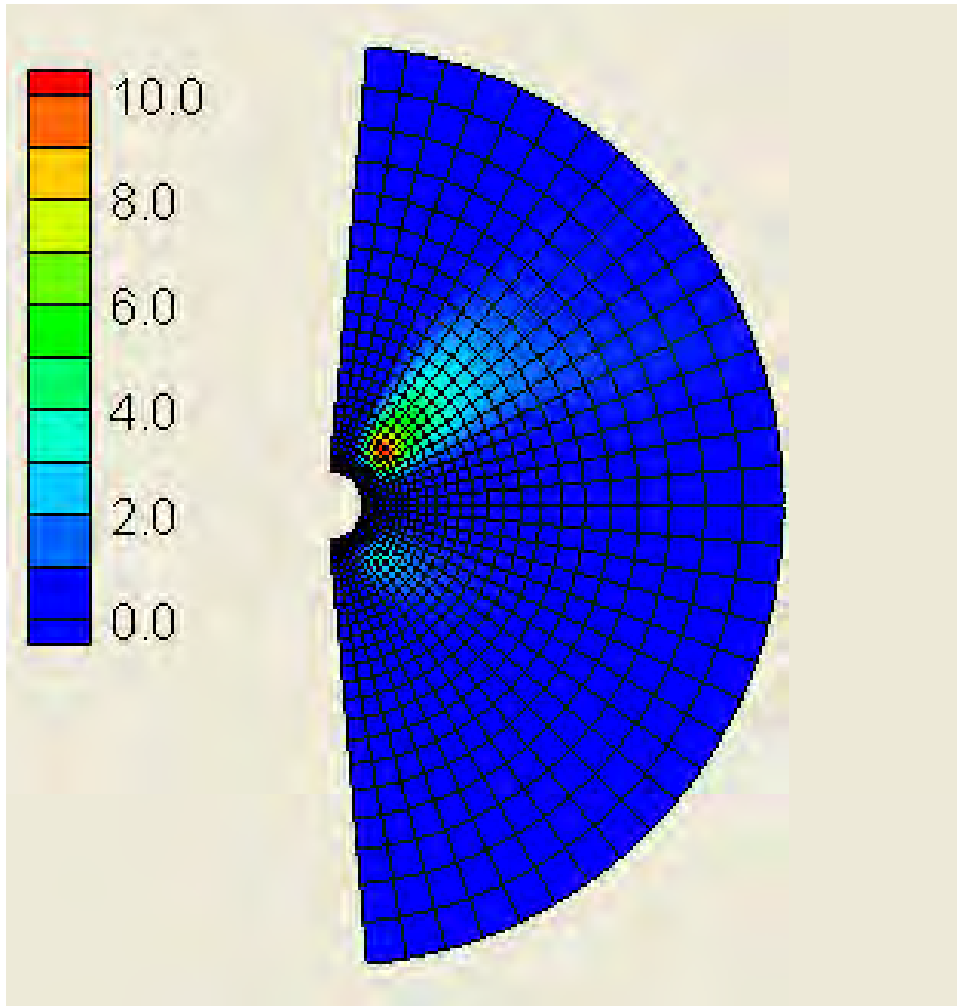


Figure 31. Wave Spectrum ( $\text{m}^2/\text{Hz}/\text{rad}$ ) for Station 425 (Plaquemines Parish at end of East Levee) at 29 August 2005 1100 UTC. Frequencies radiate out from center (0.03 to 0.41 Hz), and directions are plotted clockwise from 39 deg (top, waves from 39 deg east of north) to 231 deg (at the bottom).



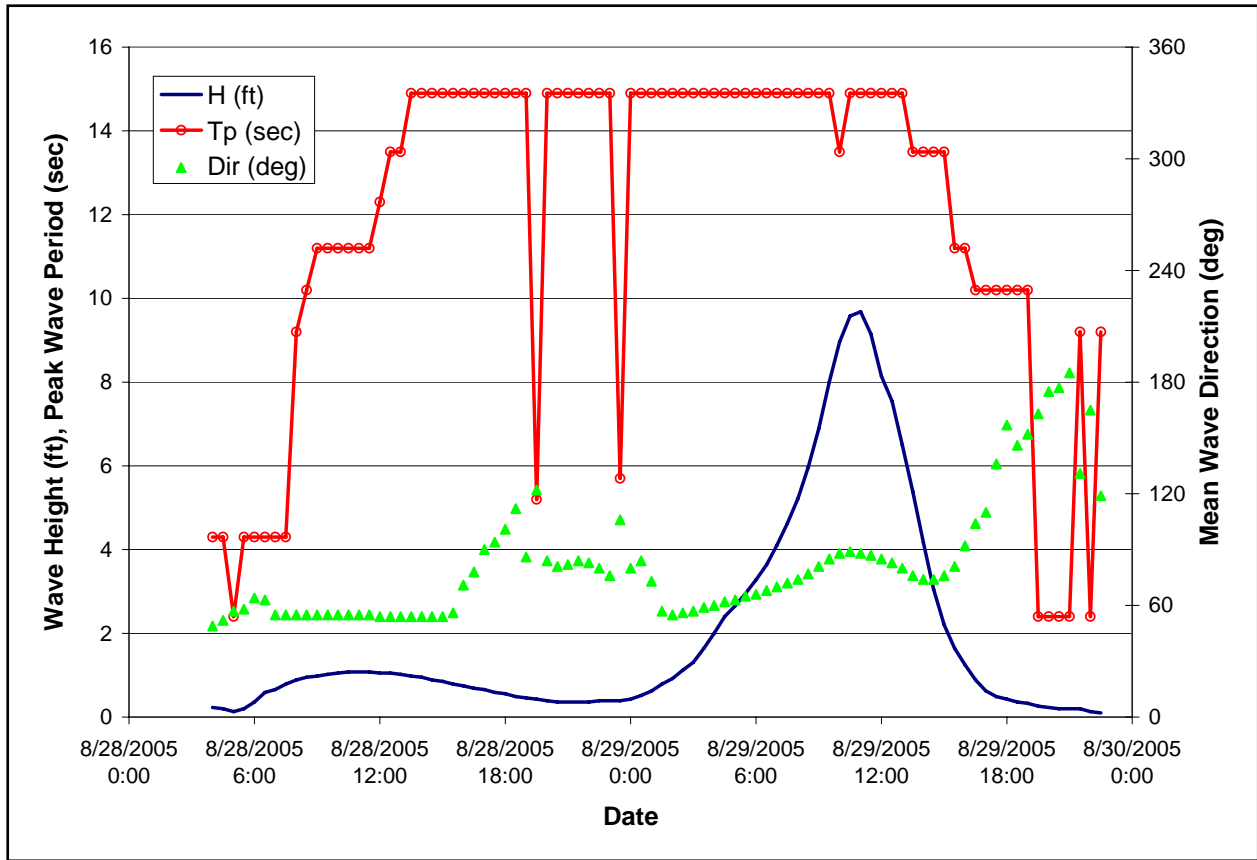


Figure 32. Time History of Wave Parameters for Station 444 (Plaquemines Parish east of MS River between Harris Bayou and Bayou Lamogue).

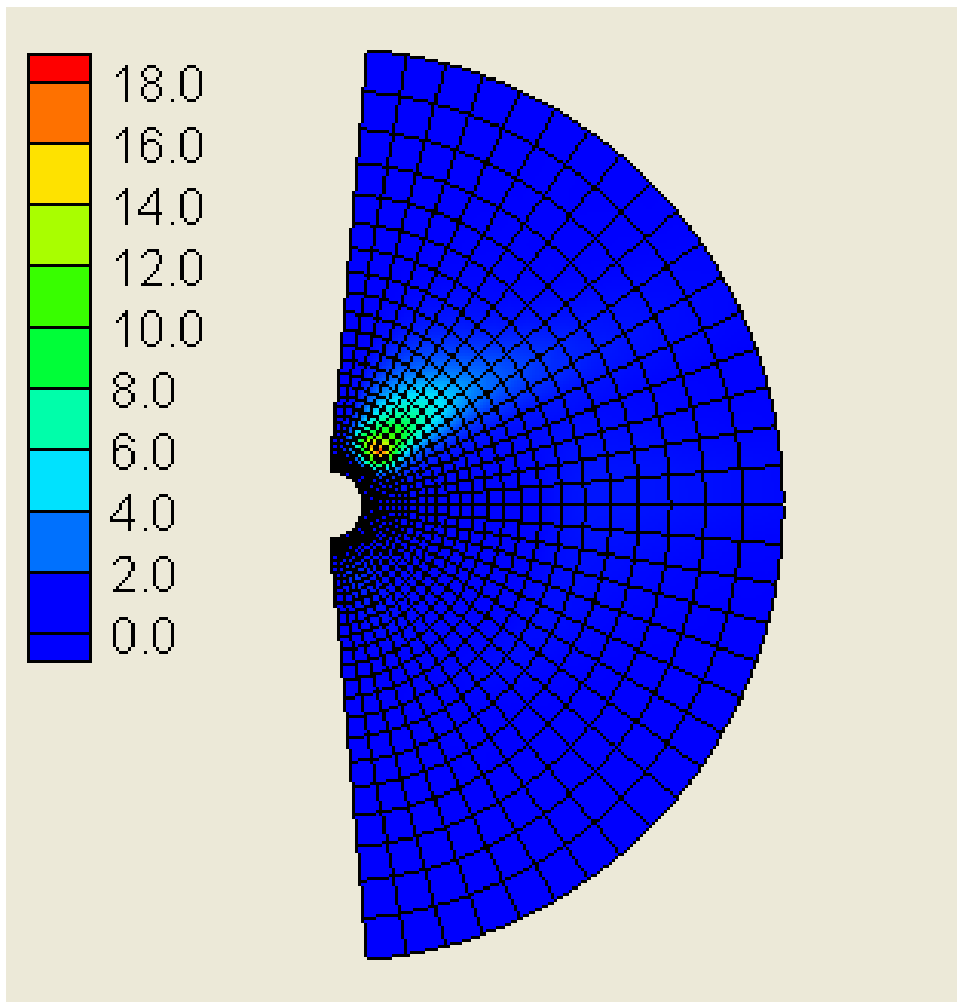


Figure 33. Wave Spectrum ( $m^2/Hz/rad$ ) for Station 444 (Plaquemines Parish east of MS River between Harris Bayou and Bayou Lamogue) at 29 August 2005 1100 UTC. Frequencies radiate out from center (0.03 to 0.41 Hz), and directions are plotted clockwise from 39 deg (top, waves from 39 deg east of north) to 231 deg (at the bottom).

# Appendix 5

## Storm Surge

---

### Introduction

Hurricane Katrina was a relatively fast moving storm characterized by its low pressure, its intensity and especially its large size. Katrina approached the Mississippi shelf as a category 5 storm and made landfall as a strong Category 3 storm on August 29 at 1110 UTC along the southern reach of the Mississippi river in Plaquemines Parish just south of Buras, LA (Knabb, Rhome and Brown, 2005). The storm then tracked straight north through Empire, passing through Lake Borgne and making a second Gulf landfall as a Category 3 hurricane on August 29 at 1445 UTC near Little Lake just west of the Louisiana-Mississippi state line and approximately 1.5 mi east of the Lake Borgne entrance to the Rigolets strait.

It is noted that the center of the storm tracked largely east of the city of New Orleans (about 28 miles due east at its closest point). However the storm was in the vicinity of critical features of the hurricane protection system, the center track being as close as 10 miles due east of the St. Bernard Parish/Chalmette protection levee which runs along the Mississippi River – Gulf Outlet (MRGO) and as close as 20 miles due east of the confluence of the Gulf Intracoastal Waterway (GIWW) and the MRGO. This confluence in particular, is a critical feature since it has adjacent protection levees that form a funnel shape, which can focus and amplify storm surge from the east.

Over the past decade, extensive storm surge model development, application, and validation efforts have been made in Southern Louisiana. This work has improved storm surge modeling capabilities within a physics based framework that correctly accounts for and simulates the forcing and response processes (Westerink et al. 2006, Feyen et al. 2006). These efforts have taken advantage of the evolution of unstructured grid computational algorithms as well as massively parallel software and hardware.

In this appendix, we describe the application of the ADCIRC unstructured grid hydrodynamic model to hindcast the surge development and propagation during the Katrina event. We have advanced the description of the significant physical features and topography/bathymetry relative to earlier ADCIRC Southern Louisiana models to more realistically simulate the flow and accumulation of water during the surge event. The forcing functions include the final H\*Wind/IOKA wind fields, OWI atmospheric pressure fields, tides, riverine flows and

STWAVE based wave radiation stress gradients. A comparison to the available excellent and good high water marks as well as available hydrographs quantifies the performance of the surge calculation.

The Katrina hindcast computation is based entirely on defining the best representation of the physical system and by applying standard coefficients widely used in modeling to represent parameterized processes such as air-sea momentum transfer, bottom friction, lateral sub-grid scale momentum diffusion and dispersion as well as levee overtopping. The winds and waves inputs were applied exactly as they came from separately validated model applications. The progressive refinements that were made in the TF01x2 model and simulations were to improve the physical features, to increase resolution were necessary and to incorporate all the forcing functions available. Thus no tuning of parameters was done to improve the fit to the measured data. An examination of the sensitivity of the surge computation to the bottom friction formulation and to the air-sea drag relationships was made. An investigation of the influence of physical features such as the Chandeleur Islands and the MRGO on storm water levels was also made.

## **TF01x2 Computational Model**

The TF01x2 model domain/grid used in the Katrina hindcast has evolved from the earlier S08 model (Westerink et al. 2006, Feyen et al. 2006). The S08 model incorporates the western North Atlantic Ocean, the Gulf of Mexico and Caribbean Sea to allow for full dynamic coupling between oceans, continental shelves, and the coastal floodplain without necessitating that these complicated couplings be defined in the boundary conditions (Blain et al. 1994).

Application of unstructured finite element grids to resolve the energetic scales of motion on a localized basis enables accurate solution of the governing equations while minimizing degrees of freedom, making the computations feasible from a cost perspective. In general the highest levels of grid resolution are necessary on the shelf and on the feature dominated coastal floodplain. It has been shown that under-resolution of the shelf leads to over-prediction of surge by as much as 30% (Blain et al. 1998). Furthermore, it is clear that under-resolution of critical small scale features in the coastal floodplain prevents the accurate propagation of the flood wave. Therefore, the grid is refined locally to resolve features such as inlets, rivers, navigation channels, levee systems and local topography/bathymetry. Unstructured grids can resolve the critical features and processes with orders of magnitude fewer computational nodes than a structured grid, since the latter is limited in its ability to provide resolution on a localized basis and fine resolution generally extends far outside the necessary area.

The S08 domain/grid has been extensively applied and validated in a number of hindcast studies. A complete description of the S08 model and its validation using hurricanes Betsy and Andrew is presented by Westerink et al., 2006 and Feyen et al., 2006. These previous S08 model hindcasts included atmospheric, riverine and tidal forcing. However wave-current interaction was not taken into account.

For the Katrina hindcast, the S08 model/domain was extended and refined to represent additional important hydraulic features and to accommodate wave radiation stress gradient forcing from the STWAVE model. The resulting TF01x2 model is shown in Figures 5-1 and Figures 5-2. Significant detail along the north shore of Lake Pontchartrain as well as the inlets and the coastal floodplain (up to the 60 ft contour) along the Mississippi and Alabama coasts was added. The extensive inlets, waterways and floodplain in Mississippi and Alabama attenuate the surge along the coast. This in turn will affect the piling up of water in Lake Borgne which controls the flow of water into Lake Ponchartrain. In addition, significant detail was added in the area between Lake Borgne and Lake Ponchartrain to more accurately represent the exchange of water between these shallow waterbodies. This entailed adding a representation of the CSX railway, highway US 90 as well the Gulf Intracoastal Waterway and a number of significant channels that were not included in the S08 model. Further improvements were made along the south shore of Lake Ponchartrain by including the details of the West End Lake Shore Park and its marina and the New Orleans Lakefront Airport. Finally, we accommodated the STWAVE forcing function by adding a high level of resolution where there were significant gradients in the wave radiation stresses and forcing of surge through wave transformation and breaking are the largest. We accommodated the four STWAVE grids shown earlier in this report and added resolution as fine as 300 ft in these transformation/breaking zones along Terrebonne Bay, Timbalier Bay, Barataria Bay, Breton Sound, Chandeleur Sound, Mississippi Sound and along the shores of Lake Ponchartrain. The Chandeleur Islands as well as the Mississippi Sound islands have all been directly included in the computational mesh as compute nodes at 300 ft resolution instead of as sub-grid scale internal barrier boundaries. This allows for the strong wave radiation stress gradients to fully force the water body in these important regions.

Geometry, topography and bathymetry in the Katrina hindcast were all defined to replicate the prevailing conditions prior to the storm. The elevation data was interpolated to the computational mesh by moving progressively from the coarsest to finest areas of the domain. Deep water bathymetric depths were first interpolated from a 5° x 5° regular grid based on the ETOPO5 values. Subsequently values were obtained from the National Oceanic and Atmospheric Administration (NOAA) depth sounding database and the U.S. Army Corps of Engineers (USACE) New Orleans District (MVN), the U.S. Geological Survey (USGS) DEM and Atlas Lidar topographic survey. Topographic/bathymetric values were evaluated at computational nodes using an element-based gathering/averaging procedure instead of a direct interpolation procedure. The gathering/averaging procedure searches for all available sounding/topographic survey values within the cluster of elements connected to one specific node, averages these values and assigns the average value as the depth/topographic elevation to that node. This gathering/averaging procedure essentially implements grid scale filtering to the bathymetric/topographic data and ensures that bathymetry/topography is consistent with the scale of the grid. Bathymetry/topography was locally-checked with available NOAA charts and elevation contour maps; in regions with missing or incorrect data, supplemental data from the USACE MVN, USGS or National Ocean Service (NOS) bathymetric charts was applied. Bathymetry was typically specified to tidal mean lower low water (MLLW). In addition, where USGS DEM topographic was applied it was adjusted to NAVD 88 using Corpscon based adjustments. Where Atlas Lidar data was applied, the previous epoch of NAVD 88 is the vertical reference. The IPET NAVD 88 2004.65 adjustments to the Atlas Lidar data defined relative to the previous NAVD 88 epoch could not be applied to southern Louisiana as a whole because of



the insufficient density of control points through portions of southern Louisiana. The large distances in the control point grid which are the basis of the adjustment surface leads to possibly significant errors in the sparse datum control point areas.

In order to represent mean sea level MSL in the model, the initial water level was raised across the entire domain as well as at elevation boundary forcing locations to accommodate the offset between tidal mean low low water (MLLW) and local mean sea level (LMSL) and between NAVD 88 2004.65 and LMSL based on values at stations throughout southern Louisiana. Examination of NOAA benchmarks by the IPET geodetic survey task in Southern Louisiana shows that on average LMSL is approximately 0.5 ft above MLLW. The average offset between LMSL and NAVD88 2004.65 at 11 stations examined by IPET within southern Louisiana is 0.44 ft (see volume II for more information on LMSL and vertical datum relationships). Thus LMSL regionally lies above NAVD 88 2004.65 by 0.44 ft which has been added to the initial ADCIRC water level. It is noted that the NAVD 88 2004.65 datum is a geodetic equipotential surface and therefore provides a sound reference for our computations when adjusted for the offset to LMSL. This is not the case for the NGVD 29 datum. This technique does not account for the 0.06 ft difference between the NAVD 88 2004.65 offsets to MLLW and LMSL. However this error is well within the margin of error of the bathymetric sounding data. It is also noted that since the computations are barotropic and only the Mississippi and Atchafalaya Rivers have been included in the model, this offset will not account for any increases in inland LMWL due to localized annual differences in water temperature or due to localized gradients due to regional rivers. These latter effects will be small. Thus model output will be relative to NAVD 88 2004.65.

Levee and road crown height are important in that they stop or slow the flow of water and lead to localized storm surge buildup. Levees and roads are included in the model as sub-grid scale features and are handled as weirs that accommodate both super- and sub-critical overflows. All levee heights are defined using the most recent surveys available from the USACE MVN. Road and railroad crown heights in Louisiana were generally taken from the Atlas Lidar surveys. Note that the CSX railway between the Rigolets and Chef Menteur Pass in particular was important to understand and represent correctly due to it being an important control in the flow of water between Lake Borgne and Lake Ponchartrain. In the Atlas Lidar surveys, the railway can be seen to have a height of 11 to 12 feet NAVD 88. However, CSX railway personnel involved in the reconstruction said that the gravel bed was entirely washed out during the storm and that the remaining compacted bed was at no more than 6 ft (Personal Communication). It is believed that the bed will rapidly wash out under combined high water and wave action and is therefore included in the model at an approximate value of the crown of the railroad (6 ft). In addition, US 90 sustained some damage although it was difficult to assess to what level it was lowered. Therefore Atlas Lidar based crown values for this highway were retained. Road heights were applied relative to NAVD 88 and levee heights were applied relative to NAVD 88 2004.65 from adjusted Atlas Lidar, localized 1 ft by 1 ft Lidar data, and pre- and post-storm surveys carried out by the USACE.

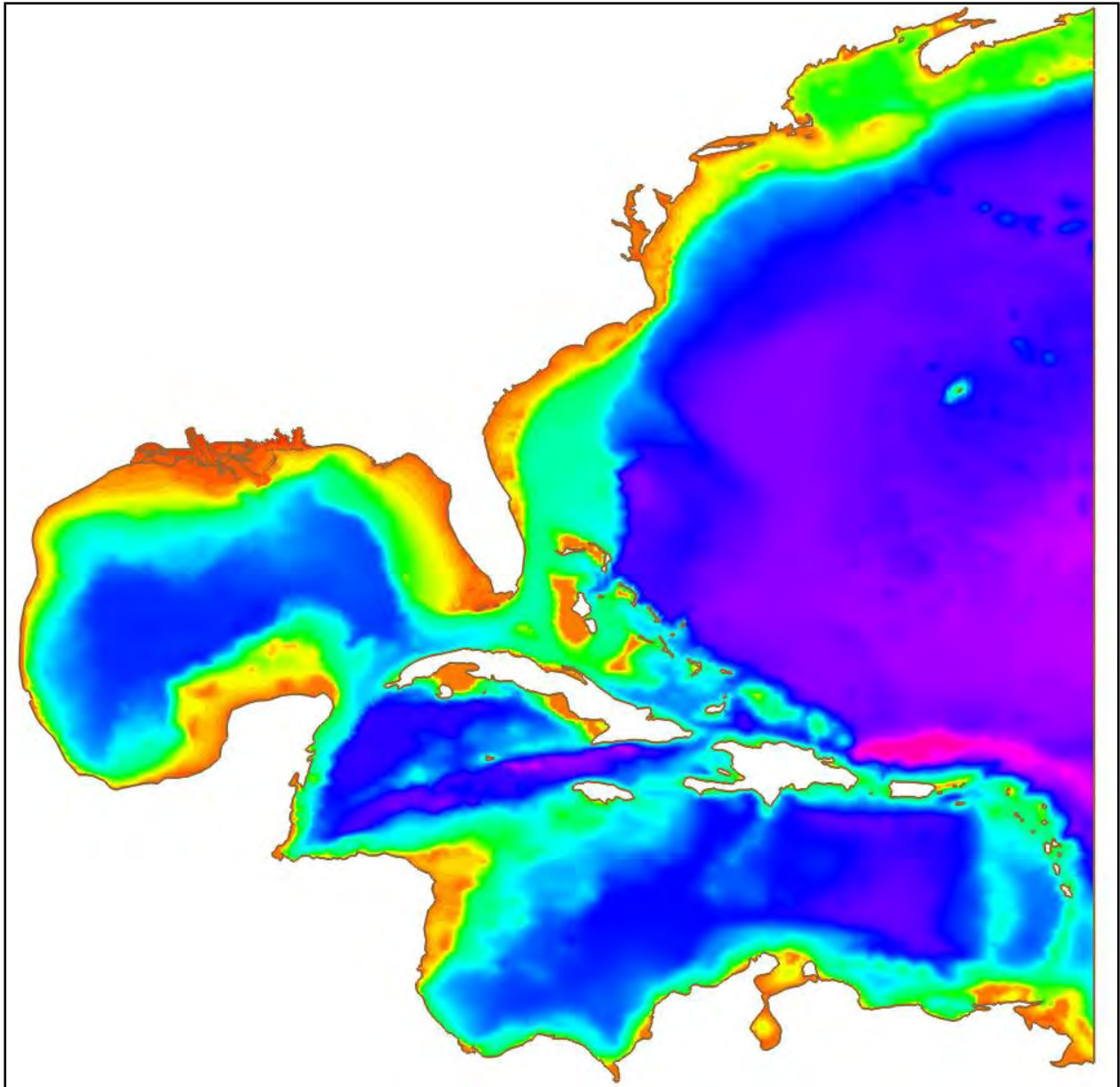


Figure 5-1a. TF01x2 computational domain showing the western North Atlantic, Gulf of Mexico, and Caribbean Sea with bathymetry (ft)

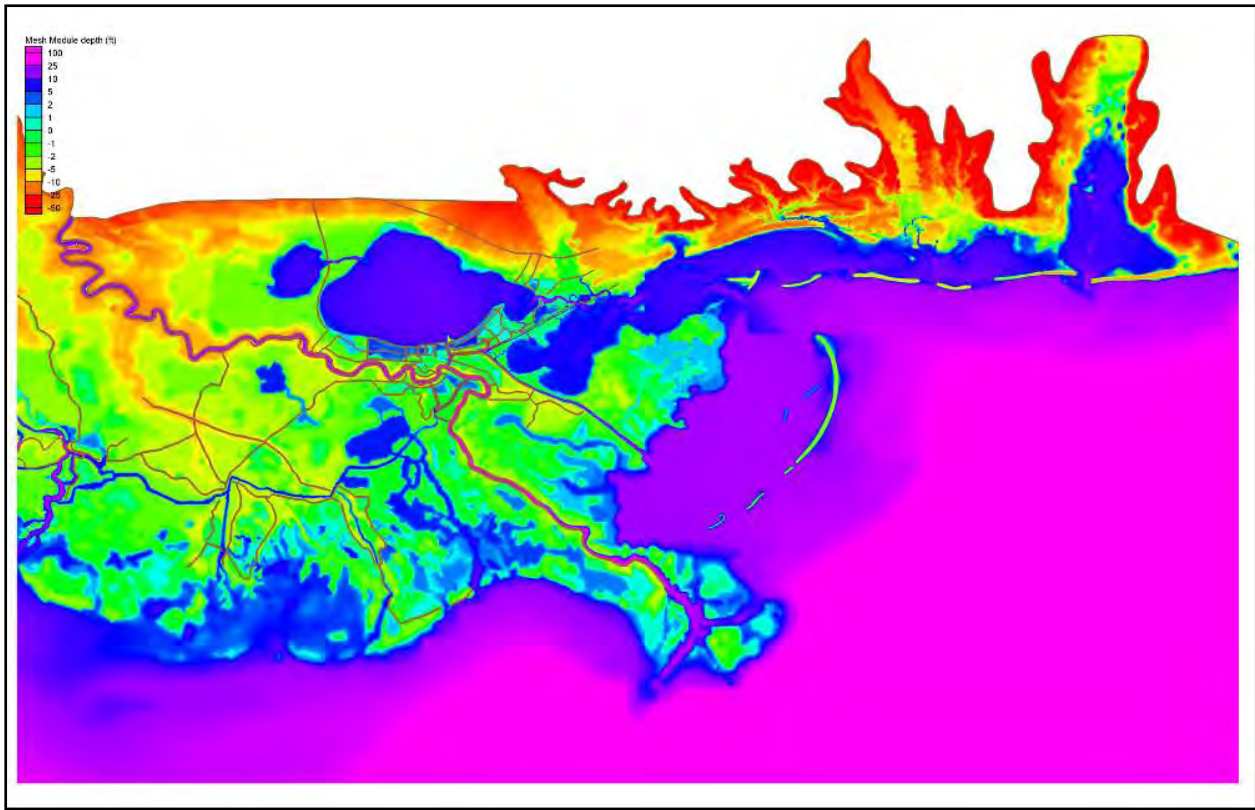


Figure 5-1b. Detail of TF01x2 domain with bathymetry and topography (ft) across Southern Louisiana to Alabama with raised features shown in brown

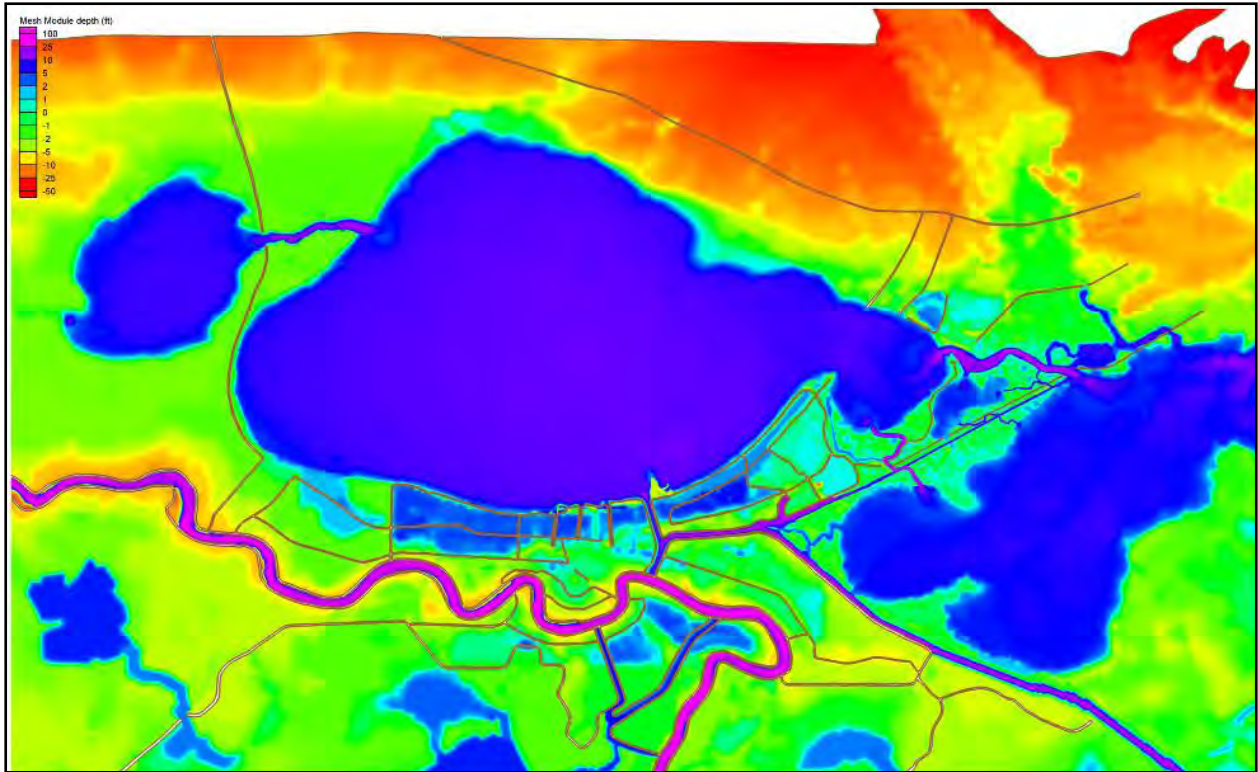


Figure 5-1c. Detail of TF01x2 domain with bathymetry and topography (ft) in the vicinity of Lakes Borgne and Ponchartrain and Metropolitan New Orleans with raised features shown in brown



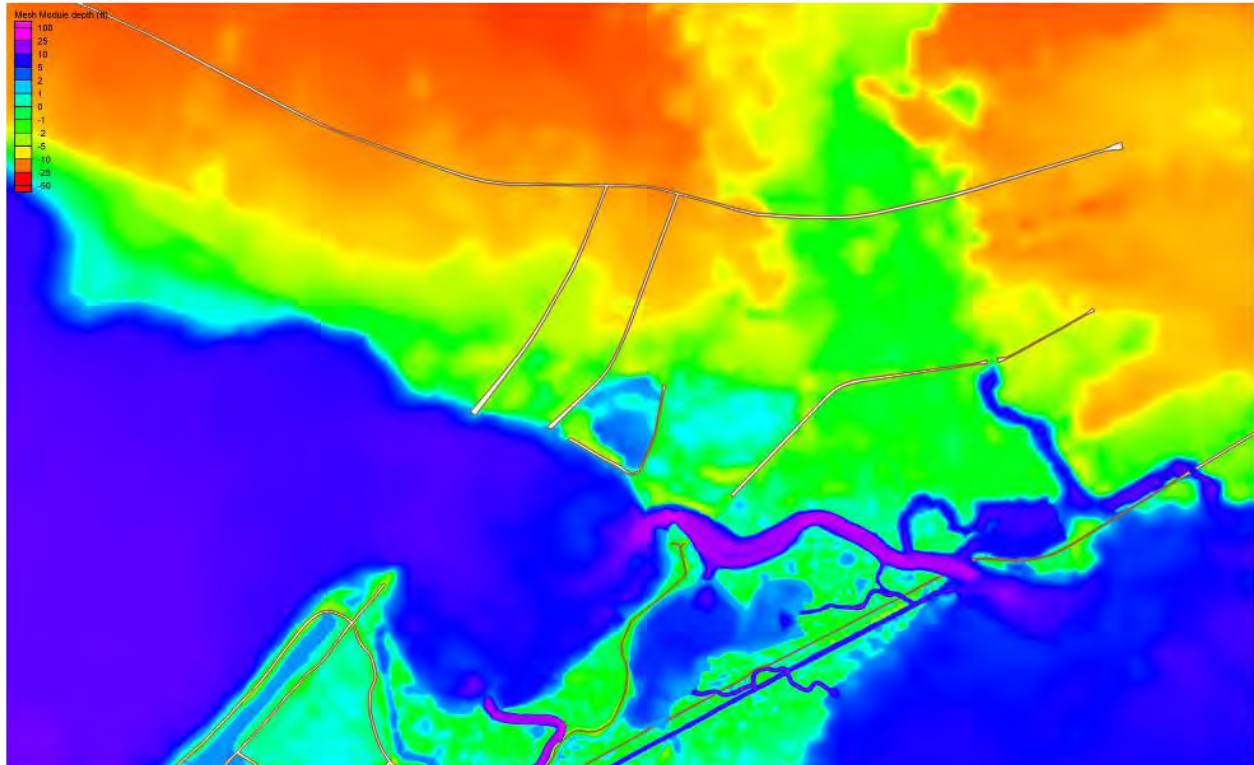


Figure 5-1d. Detail of TF01x2 domain with bathymetry and topography (ft) between Lake Borgne and Lake Ponchartrain with raised features shown in brown



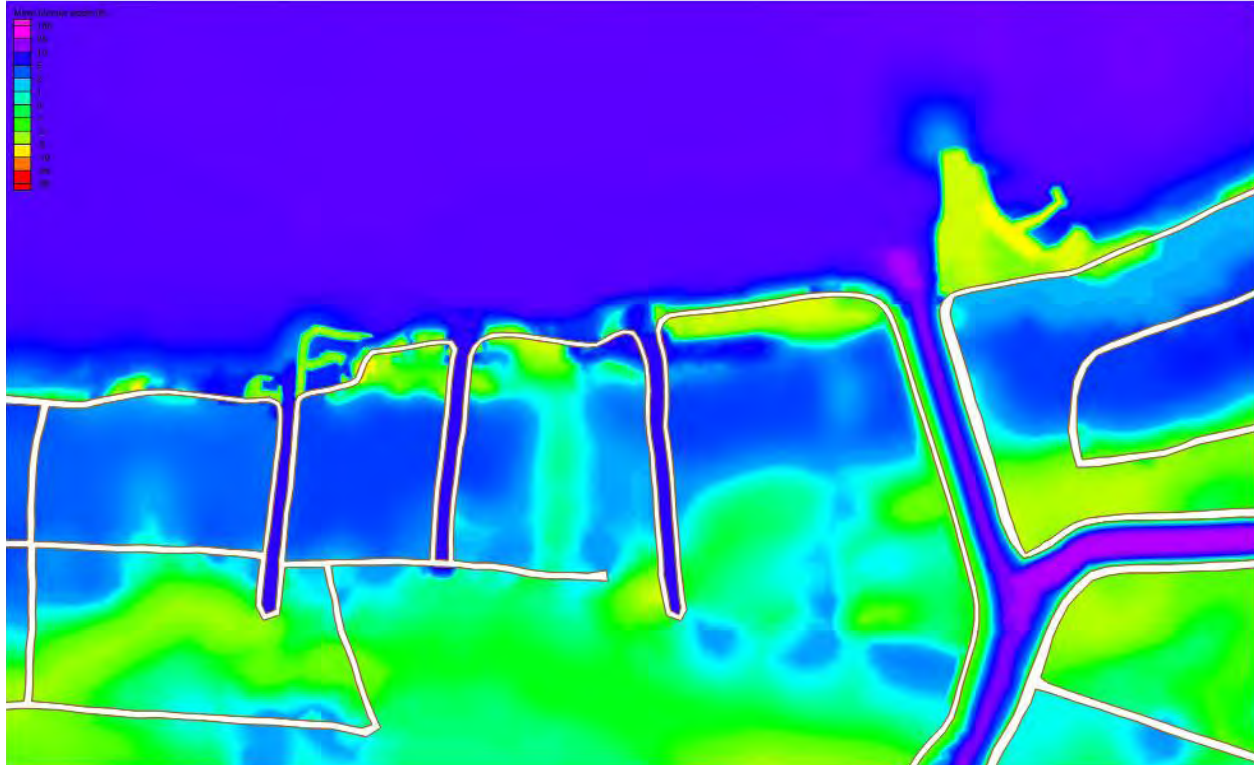


Figure 5-1e. Detail of TF01x2 domain with bathymetry and topography (ft) in Lake Ponchartrain between the 17th Street Canal and the IHNC with raised features shown in brown

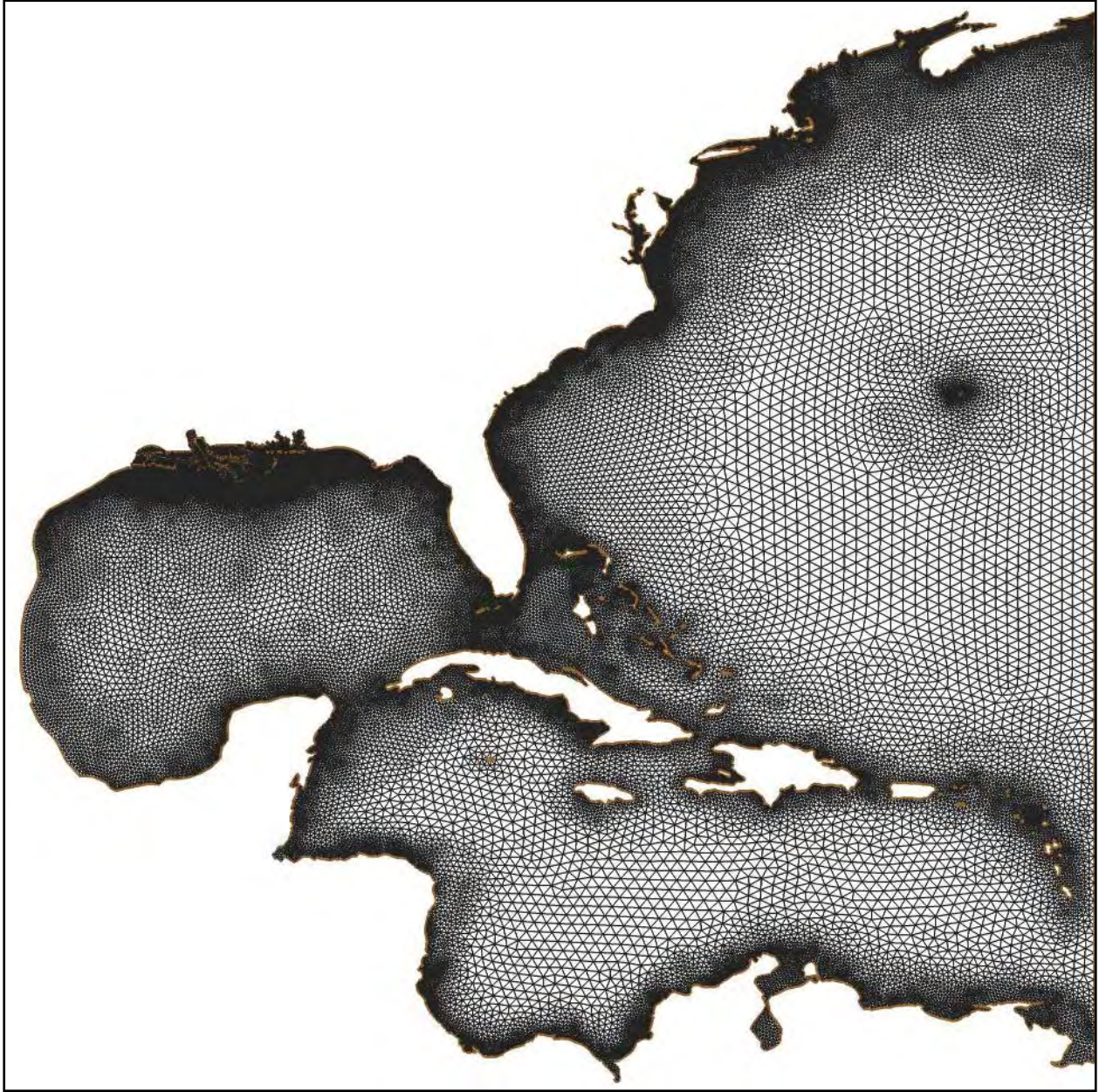


Figure 5-2a. Unstructured TF01x2 grid of the entire domain



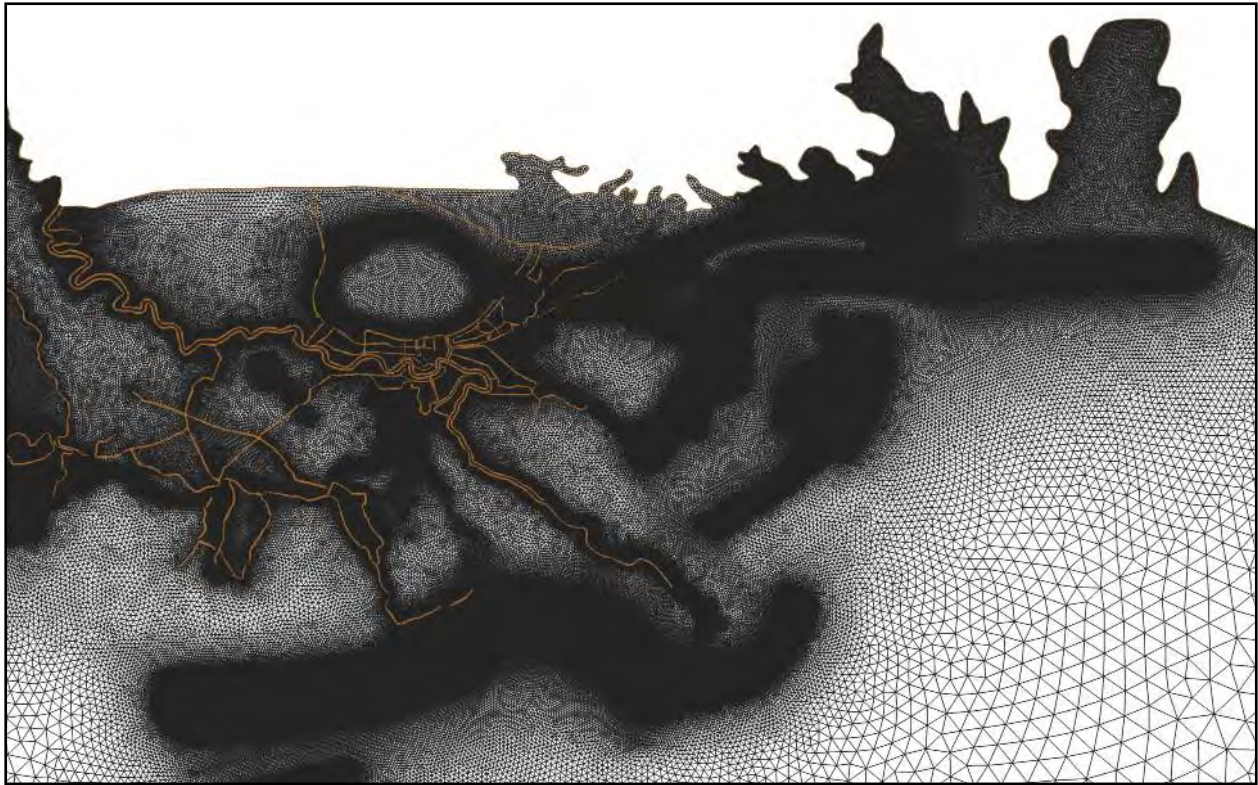


Figure 5-2b. Detail of the unstructured TF01x2 grid in Southern Louisiana to Alabama with raised features shown in brown

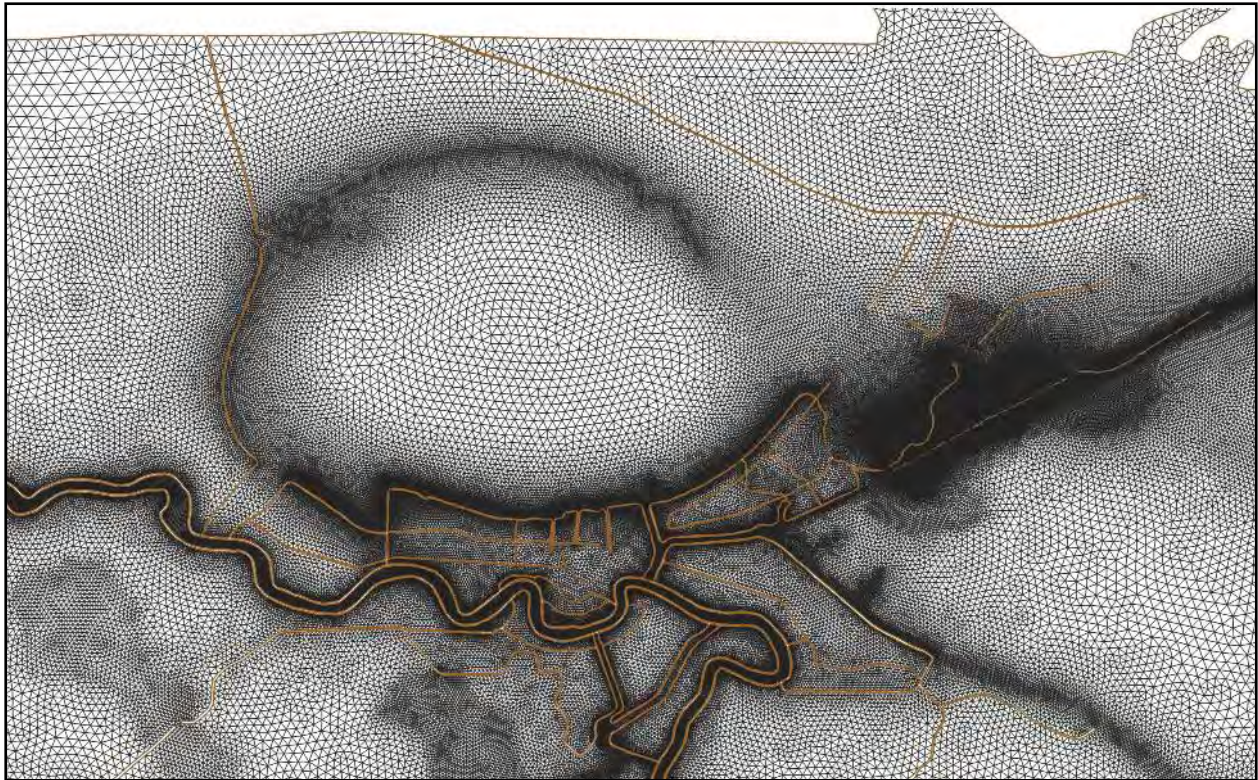


Figure 5-2c. Detail of the unstructured TF01x2 grid in the vicinity of Lakes Borgne and Ponchartrain and Metropolitan New Orleans with raised features shown in brown



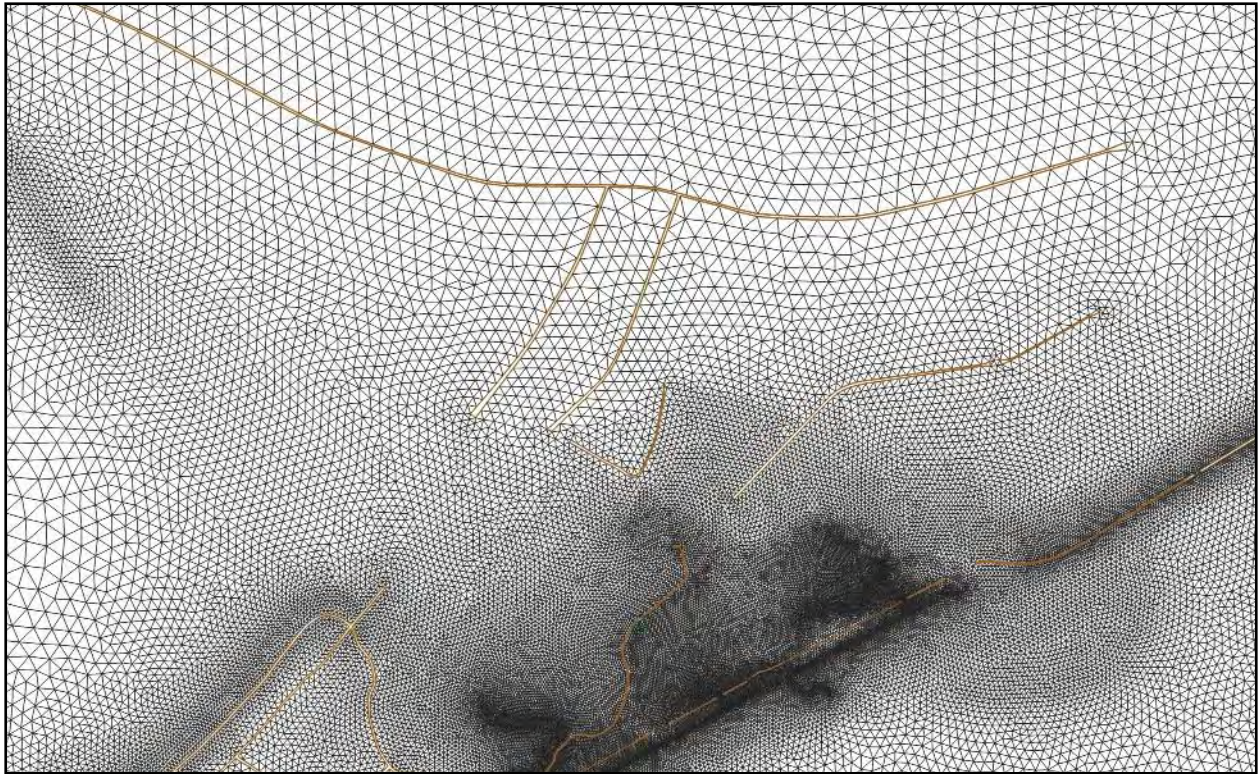


Figure 5-2d. Detail of the unstructured TF01x2 grid between Lake Borgne and Lake Ponchartrain with raised features shown in brown



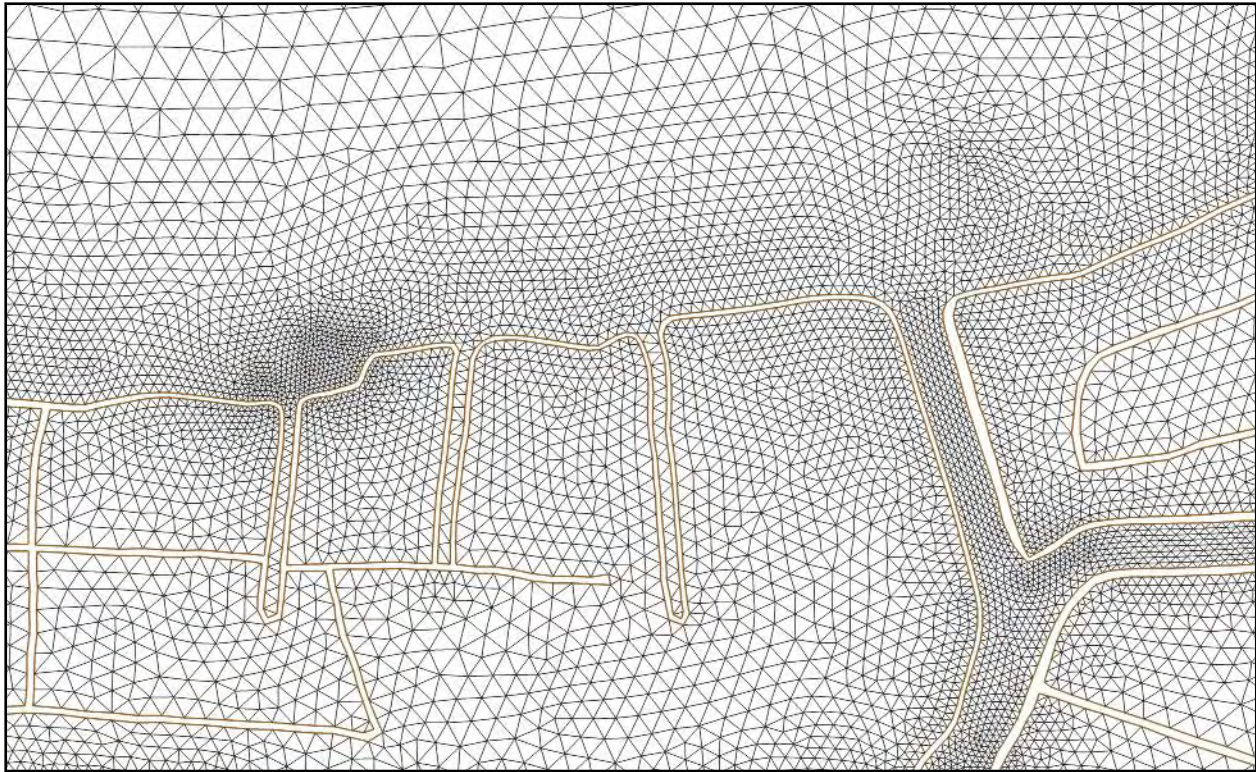


Figure 5-2e. Detail of the unstructured TF01x2 topography in Lake Ponchartrain between the 17th Street Canal and the IHNC with raised features shown in brown

## Storm Forcing and Other Details

Forcing functions for tides, wind and waves for the Katrina surge computation are all defined to replicate the prevailing conditions during the storm. Tides were forced in the simulation on the open Atlantic boundary as well as within the interior domain for the  $K_1$ ,  $O_1$ ,  $M_2$ ,  $S_2$  and  $N_2$  tidal constituents. Amplitudes and phases from Le Provost's (1998) global tidal model were specified on the Atlantic open ocean boundary. Tidal potential functions were specified throughout the domain to represent interior domain lateral gravitational forcing and earth wobble. The interior potential functions are particularly important in the resonant Gulf of Mexico. Nodal factors and equilibrium arguments were computed for both boundary and interior tidal forcing functions. Earth tidal potential reduction factors were applied to the interior tidal forcing functions (Luettich and Westerink, 2004).

The Mississippi and Atchafalaya rivers are forced with steady flows of 220,000 ft<sup>3</sup>/s and 67,000 ft<sup>3</sup>/s respectively. Actual flow rates in the Mississippi river ranged from 170,000 ft<sup>3</sup>/s to 208,000 ft<sup>3</sup>/s between August 27 and August 31. Actual flow rates in the Atchafalaya River ranged from 75,000 ft<sup>3</sup>/s to 80,000 ft<sup>3</sup>/s between August 27 and August 31. Steady flows are applied to work with the river radiation boundary conditions used in these rivers. These river radiation boundary conditions force the specified flow into the system while allowing tides and surge that propagate up these rivers to proceed upstream out of the computational domain (Westerink et al., 2006). Note that the application of standard elevation or flux specified

boundary condition would result in the unphysical reflection of tides and surge back into the computational domain.

Steric effects due to the thermal expansion of surface ocean water during late summer are pronounced in the Gulf of Mexico. This expansion is approximately captured in the long term solar annual and semiannual (*Sa* and *Ssa*) harmonic constituents. Examination of the harmonic constants computed by NOAA for tidal stations in the vicinity (Waveland, MS; Grande Isle, East Point LA; Galveston Channel, TX; Galveston Pleasure Pier, TX) shows that the combined amplitude of the *Sa* and *Ssa* constituents is on average just over 0.52 ft. It is assumed that the hurricanes generally take place during the times when the expansion is at its largest in the late summer. Therefore, the water level is adjusted above MSL by the addition of a steric adjustment of 0.52 ft.

Wind and atmospheric pressure fields were generated with increasing levels of refinement during the IPET investigation. The first set of winds were developed using the 5-level version of the Planetary Boundary Layer (PBL) model (Thompson and Cardone 1996). The model is based on the equations of horizontal motion, vertically averaged through the PBL and is driven by specification of the storm location, minimum central pressure, and maximum wind speed. The second set of wind fields were based on NOAA's Hurricane Research Division's (HRD) H\*Wind data assimilated wind model (Powell and Houston 1996, Powell et al. 1996, Powell et al. 1998) with further enhancements by Ocean Weather Inc. (OWI). The core winds were based on the H\*Wind nowcast. The HRD core snapshots were then embedded by OWI within a background field derived from the NCEP/NCAR Reanalysis Project 10-meter winds with assimilation of local marine data adjusted for neutral stability using the IOKA (Interactive Objective Kinematic Analysis) system. The final set of winds applied in the hindcast of Hurricane Katrina were based on the H\*Wind hindcast, which incorporated additional data sources as compared to the earlier nowcast, and then again had far field winds embedded and blended in using the IOKA procedure. The wind and pressure fields were developed on a basin scale 0.1 x 0.1 degree grid and on a finer regional scale 0.025 x 0.025 degree grid at 15-minute intervals. The winds are relative to a 10-meter reference height, are for a marine exposure and are averaged to 30 minutes. The resulting fields were interpolated onto the TF01x2 unstructured grid using bi-quadratic linear interpolation within the structured grids and selecting the regional grid values when available. Note that core winds based on the H\*Wind product were originally based on 1 minute averaged peak winds and were converted to 30-minute averaged winds by OWI using a conversion multiplier of 0.80645.

Since the air-sea drag laws have been developed assuming 10-minute-averaged winds, a conversion to 10-minute-averaged winds must be implemented. In all previous ADCIRC hindcasts, a standard procedure to convert to 10-minute winds by multiplying 30-minute winds by a factor equal to 1.04 and multiplying 1-minute winds by 0.8928 was applied (Powell et al., 1996). The OWI-recommended conversions to 10-minute winds are based on multiplying 30-minute winds by a factor equal to 1.09 and multiplying 1-minute winds by 0.8787. In order to be consistent with previous ADCIRC simulations and since the core winds are based on the H\*Wind product, a conversion factor equal to 1.107 to convert the combined H\*Wind/IOKA wind fields to 10-minute averaging was applied. This assures reproduction of the original 1-minute peak wind field using the previous standard 1- to 10-minute conversion factor of 0.8928.

A directional land masking procedure that alters the H\*Wind/IOKA wind fields, which assume open ocean marine conditions, was implemented to account for the wind boundary layer re-adjustment due to the higher surface roughness that exists over land. Land roughness in overland regions is characterized by land use conditions such as urban, forested, agricultural, or marsh. The land use type in Southern Louisiana was determined by a USGS Land Cover Classification raster map based upon Landsat imagery shown in Figure 5-3a with land use types defined in Table 5-1. Since the USGS land use maps do not specifically distinguish the ubiquitous Cypress forests from herbaceous wetlands, supplemental information from the National Wetlands Research Center (2004) was merged into the USGS land use map resulting in the composite map shown in Figure 5-3b with the hard red classification indicating the Cypress forest. This information is then combined with land roughness lengths,  $z_{0_{land}}$ , defined in Table 5-2 (Federal Emergency Management Association 2005). Wind boundary layer re-adjustments depend upon roughness conditions upwind of the location since the wind boundary layer does not adjust to a new roughness instantaneously. Therefore, upwind wind reduction factors are computed for 12 directions by examining all roughness coefficients up to 10 km away. Then the directional roughness used at each computational point within the mesh is based upon the existing wind direction. This upwind effect is particularly important in the nearshore region where winds are traveling either off or onshore and transitioning to or from open marine conditions. The directional roughness/wind reduction factors were computed with a weighted average of the roughness lengths for all pixels upwind of the computational mesh node in the USGS land classification raster image. Twelve upwind directions are chosen (every 30° about the compass) so that each computational node chooses the closest of the 12 directional roughness/reduction factor directions to the current wind direction.

The weighted pixel land roughness  $z_{0_{land}}$  within 10 km upwind of the computational node are added together to get the weighted upwind land roughness coefficient:

$$z_{0_{land-directional}} = \frac{\sum_{i=0}^n w(i) z_{0_{land}}(i)}{\sum_{i=0}^n w(i)} \quad (5-1)$$

where the normalization parameter is defined by

$$w(i) = \frac{1}{\sqrt{2\pi\sigma}} e^{\left(-\frac{d(i)^2}{2\sigma^2}\right)}. \quad (5-2)$$

The distance from the computational mesh node and the pixel,  $d(i)$ , is limited to 10 km in each of the 12 directions.  $z_{0_{land}}$  values for various land covers are defined in Table 5-2. The weighting parameter  $\sigma$  determines the importance of the closest pixels and is set to 3 km. Finally, the wind reduction factor,  $f_r$ , is calculated in proportion to the ratio of the surface roughness for open marine conditions to the weighted upwind land roughness. The marine roughness length can be computed based on the Charnock relationship (Charnock 1955) and the relationship between the friction velocity and the applied drag law (Hsu 1988):

$$z_{0_{marine}} = \frac{\alpha_c C_d W_{10}^2}{g} \quad (5-3)$$

where the Charnock parameter,  $\alpha_c$ , is set to a value of 0.018,  $C_d$  is the applied air-sea drag coefficient,  $W_{10}$  is wind speed sampled at a 10 meter height over a 10 minute time period, and  $g$  equals the acceleration due to gravity. The directional wind reduction coefficient is then computed for each of the 12 directions as (Powell et al. 1996, Simiu and Scanlan 1986).

$$f_{r-directional} = \left( \frac{z_{0_{marine}}}{z_{0_{land-directional}}} \right)^{0.0706} \quad (5-4)$$

The resulting upwind effect is particularly important in the near shore region and results in reduced winds offshore when winds come from land and results in sustained marine winds overland when winds come off of the water. Standard non-directional land masking procedures would incorrectly produce full marine winds in the near-offshore zone when winds come from land and result in reduced marine winds in the near-overland zone when winds come off of the water. Accurate winds are critical in these near-shore and low-lying overland regions that experience either drawdown or flooding because the wind stress term in the shallow water equations is inversely proportional to total water column height and thus the sensitivity to these winds is the greatest. Figures 5-4a and 5-4b show directional wind reduction coefficients for a steady uniform northerly and southerly wind. These figures illustrate the wind boundary layer lag for winds coming off and onto land in nearshore regions.

The directional changes in surface roughness from open marine conditions do not fully characterize the changes in surface stress on the water column during storm surge inundation. As inundation takes place, the land roughness elements (e.g. marsh grass, crops, bushes) are slowly submerged and the drag is reduced. Therefore, the large land surface roughness elements become less rough as they are inundated and the overland roughness length is reduced in the model dependent upon the local water column height, based on an assumption that the roughness length is 1/30 the physical roughness scale (Simiu and Scanlan, 1986). The reduced roughness length  $z_0'$  is limited to the marine roughness value, which is reached as the water depth  $H$  increases:

$$z_0' = z_0 - \frac{H}{30} \text{ for } z_0' \geq z_{0_{marine}} \quad (5-5)$$

Finally, the application of the directional wind boundary layer adjustments and inundation account for how the wind boundary layer is affected but do not characterize how the wind penetrates the physical roughness elements. There are large-scale features that shelter the water surface from the wind stress. These areas describe conditions such as heavily forested canopies, and they are in effect two-layered systems. Since these large roughness elements are exposed to the hurricane winds, shear stress at the water column surface is much smaller. It can be demonstrated that little momentum transfer occurs from the wind field to the water column in

heavily canopied areas (Reid and Whitaker 1976). Therefore, in heavily canopied regions defined as forest (land use types 41, 42 and 43) or as Cypress forest (the additional 95 classification) in the composite land use map shown in Figure 5-3, no wind stress is applied to model the limited impact wind shear stress has on the water column in these areas. Note that urban areas were not considered to be canopied.

The maximum interpolated H\*Wind/IOKA wind swaths during the entire Katrina event in Southern Louisiana are shown in Figures 5-5. These maximum event winds are averaged to the peak 1 minute sampling period, are at 10 meters height and include directional wind reduction effects, inundation effects as well as the inherent reduction in forested canopies.

The wind surface stress is computed by a standard quadratic drag law:

$$\frac{\tau_{s\lambda}}{\rho_0} = C_d \frac{\rho_{air}}{\rho_0} |W_{10}| W_{10-\lambda}, \quad (5-6)$$

$$\frac{\tau_{s\phi}}{\rho_0} = C_d \frac{\rho_{air}}{\rho_0} |W_{10}| W_{10-\phi}. \quad (5-7)$$

$W_{10}$  is wind speed sampled at a 10 meter height over a 10 minute time period (Hsu 1988). The ratio of the density of air to that of water,  $\rho_{air}/\rho_0$ , is 0.001293. The drag coefficient,  $C_d$ , in our computations is defined by Garratt's drag formula which defines the drag coefficient as a linear function of wind speed (Garratt 1977).

$$C_d = (0.75 + 0.067W_{10}) \times 10^{-3} \quad (5-8)$$

We do not apply any upper limit to this air-sea drag coefficient. This is consistent with all our previous hindcasts.

Wind-waves influence surge height with wind-wave radiation stress forcing, modifying bottom friction as well as determining the sea surface roughness. Modeling studies have shown that the surge increase due to wind-wave set-up can be proportionally significant for weaker winds and steep bathymetric profiles (Komen et al. 1994, Weaver and Slinn 2005, manuscript submitted to *Coastal Eng.*). Although wind-waves tend to be proportionately less important for strong storms on wide shallow shelves, they do influence the total surge away from the center of the storm, affect the time of arrival of the peak surge and tend to reduce draw-down (Weaver and Slinn 2005, manuscript submitted to *Coastal Eng.*). Wind-waves reach shore prior to the peak surge driven by the strongest hurricane winds, so combined wind and wind-wave surge builds up earlier than solely wind driven surge. Furthermore draw-down caused by winds coming from shore tends to be reduced by waves that are still coming into shore. In our Katrina hindcast we consider wave radiation stress forcing but do not include the effect on bottom friction or the influence of waves on surface roughness as they affect air-sea interaction. We force the ADCIRC computations with wave radiation stresses from the four localized STWAVE computations west



of the Mississippi river, east of the Mississippi river, south of the Mississippi-Alabama coasts and within Lake Ponchartrain. The level of resolution in the STWAVE forcing models is 600 ft and is consistent with the level of resolution that we have incorporated into the TF01x2 grid. Although the WAM model is used to force the open water STWAVE computations, no forcing information is directly applied from these models to the ADCIRC circulation computation. We note that a preliminary ADCIRC simulation without wave forcing provided preliminary water level and current information for the STWAVE computations. This establishes a reasonable level of 2 way coupling between the 2 models. The resulting STWAVE wave radiation stress gradients computed every ½ hour were then interpolated to the unstructured ADCIRC grid using bi-quadratic interpolation within the structured wave grid. Since the four STWAVE grids overlap, a hierarchy was defined in order to define ADCIRC nodal wave radiation stress gradient values. The Lake Ponchartrain STWAVE was given the lowest priority in overlapping regions, followed by the Mississippi-Alabama grid, then the Southeast Louisiana grid and finally the South Louisiana grid has the highest priority. The maximum wave radiation stress gradients during the entire Katrina event in Southern Louisiana are shown in Figure 5-6. We note that the strongest gradients exist along the Mississippi delta, along the barrier islands and along exposed shoreline.

Throughout most of the domain, the standard quadratic parameterization of bottom stress is applied. In order to model the high frictional losses associated with very shallow flows and at the inundation front that occurs as storm surge floods previously dry areas, a hybrid friction relationship is used that varies the bottom friction coefficient with the water column depth,

$$C_f = C_{f\min} \left[ 1 + \left( \frac{H_{break}}{H} \right)^{\theta_f} \right]^{\frac{\gamma_f}{\theta_f}} \quad (5-9)$$

This formulation applies a depth-dependent, Manning-type friction law below the break depth ( $H_{break}$ ), and a standard quadratic friction law when the depth is greater than the break depth (Luettich and Westerink 1999, Luettich and Westerink 2005). The break depth is set at 2.0 m, and the minimum friction factor,  $C_{f\min}$ , which is approached in deep water, is 0.003. The parameter  $\theta_f$  determines how rapidly the hybrid relationship approaches the asymptotic limit, and is set to a value of 10. Also, the parameter  $\gamma_f$ , which determines how the friction factor increases as water depth decreases, is set to 1.3333.

Momentum diffusion and dispersion due to unresolved lateral scales of motion as well as the effects of depth averaging are accounted for by an eddy viscosity type closure model. A simple version of the standard isotropic and homogeneous eddy viscosity model implemented by Kolar and Gray (1990) is used, where  $\nu_T$  is the constant depth-averaged horizontal eddy viscosity coefficient. A horizontal eddy viscosity value equal to  $50 \text{ m}^2 \text{ s}^{-1}$  was found to accurately model flow-stage relationships in the Mississippi and Atchafalaya Rivers as well as correctly model the tidal exchange in the Lake Pontchartrain – Lake Borgne system through the Rigolets and Chef Menteur Pass. It is necessary to define slip conditions at the wet/dry element interfaces since lateral boundary layers cannot be resolved at the defined grid scales and no-slip conditions

unrealistically restrict flows with the defined grids and lateral eddy viscosity values (Feyen et al. 2000).

Levee and road systems that are barriers to flood propagation are features that generally fall below the defined grid scale and represent a non-hydrostatic flow scenario. It is most effective to treat these structures as sub-grid scale parameterized weirs within the domain. ADCIRC defines these as barrier boundaries by a pair of computational nodes with a specified crown height (Westerink et al. 2001). Once water level reaches a height exceeding the crown height, the flow across the structure is computed according to basic weir formulae. This is accomplished by examining each node in the defined pair for their respective water surface heights and computing flow according to the difference in water elevation. The resulting flux is specified as a normal flow from the node with the higher water level to the node with the lower water level for each node pair. Weir boundary conditions also are implemented for external barrier boundaries, which permit surge that overtops levee structures at the edge of the domain to transmit flow out of the computational area.

Modeling storm surge inundation requires that the model accurately represent wetting and drying processes at the mesh scale. ADCIRC applies a wet/dry algorithm that is applicable to a continuous Galerkin FE discretization that utilizes Lagrange basis functions with nodally defined variables (Luettich and Westerink 1999, Dietrich et al. 2005). The wet/dry algorithm is based on a combination of nodal and elemental criteria. The algorithm requires all nodes within an element to be wet in order for hydrodynamic computations to be calculated at that element. Two parameters are used to define the wetting/drying criteria. First,  $H_0$  defines the nominal water depth for a node to be considered wet. Second, a minimum velocity  $U_{min}$  is specified that must be exceeded for water to propagate from a wet node to a dry node. Nodes are defined as initially dry if they lie above the defined starting water level or if they are within pre-defined regions, such as ring levees (e.g. New Orleans).

The algorithm proceeds through the following steps to update the wet and dry elements for the next time level. Wetting is accomplished by examining each dry element with at least 2 wet nodes with depth greater than  $1.2 H_0$  (ensuring sufficient water depth to sustain flow to the adjacent node). The velocity of the flow from the wet nodes towards the dry node along each element edge is computed based on a balance between the surface gradient and friction. If this velocity exceeds  $U_{min}$ , then the third node and the element are wetted. Finally, a check is made for elements that are bordered by elements with wet nodes but with insufficient water column height (not greater than  $1.2 H_0$ ) that they were not toggled wet themselves. If they exist, they are implicitly wet due the fact that the wet/dry algorithm is nodal. However, an elemental check ensures that elements that do not meet the wetting criteria are forced dry. For hurricane storm surge inundation, wet/dry parameters that are relatively unrestrictive have been found to be most effective:  $H_0 = 0.10$  m, and  $U_{min} = 0.01$  m s<sup>-1</sup>. It is critical that all wet/dry checks be done at a small enough time interval so that the wetting/drying algorithm is not Courant surpassing. This latter condition artificially retards the wetting front as the surge progresses inland and the surge height will artificially build up behind the wetting front. Practically, this implies performing wet/dry checks at each model time step.

All sub-grid scale parameters have been specified using standard physically relevant values as applied in previous S08 simulations. No tuning or optimization was performed with respect to the selected values and, with the exception of the domain/grid enhancements, all model parameters were defined as in previous hindcasts.

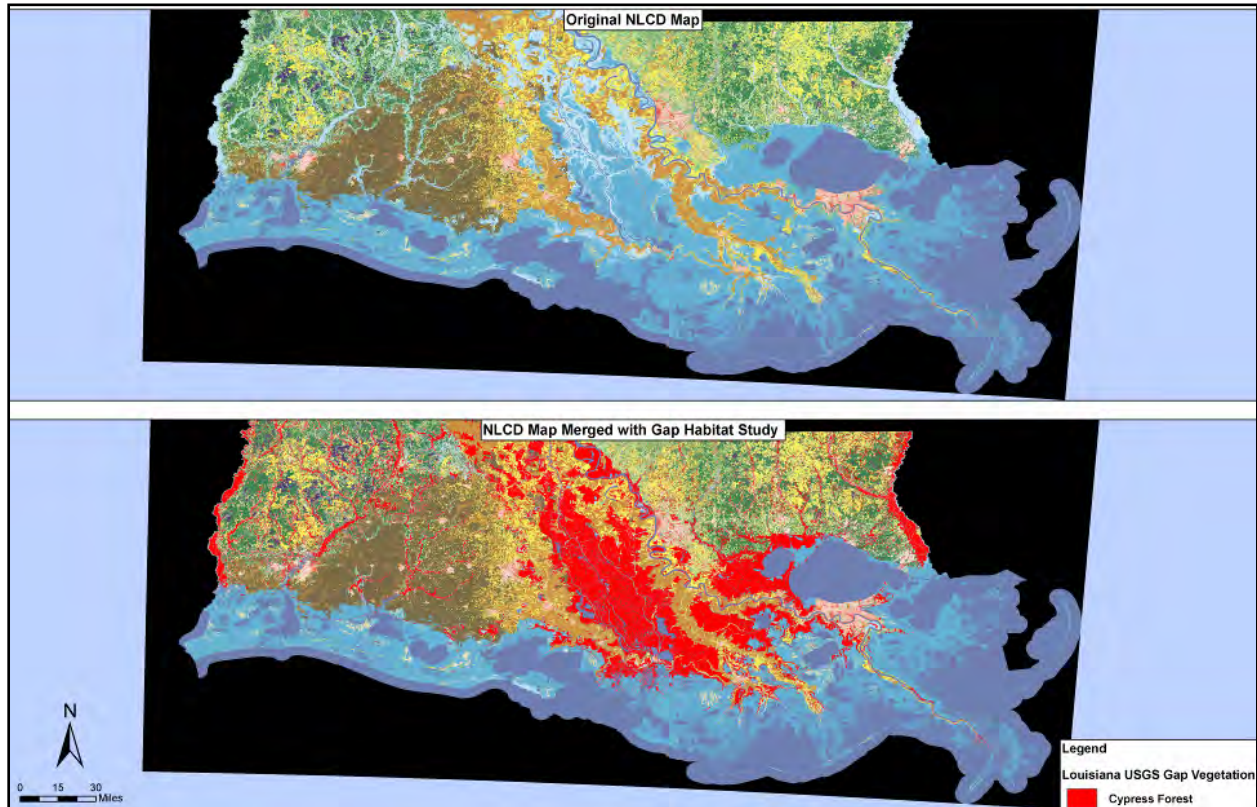

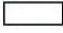















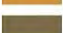





Figure 5-3. USGS land use data in Southern Louisiana is shown above. Cypress forests in red have been merged into the lower image.

**Table 5-1: USGS Land Cover Classifications**

<b>National Land Cover Dataset Classification System Legend</b>		
<b>Color Key</b>	<b>RGB Value</b>	<b>Class Number and Name</b>
	102, 140, 190	11 - Open Water
	255,255,255	12 - Perennial Ice/Snow
	253, 229, 228	21 - Low Intensity Residential
	247, 178, 159	22 - High Intensity Residential
	231, 86, 78	23 - Commerical/Industrial/Transportation
	210, 205, 192	31 - Bare Rock/Sand/Clay
	175, 175, 177	32 - Quarries/Strip Mines, Gravel Pits
	83, 62, 118	33 - Transitional
	134, 200, 127	41 - Deciduous Forest
	26, 129, 78	42 - Evergreen Forest
	212, 231, 177	43 - Mixed Forest
	220, 202, 143	51 - Shrubland
	187, 174, 118	61 - Orchards/Vineyards
	253, 233, 170	71 - Grasslands/Herbaceous
	252, 246, 93	81 - Pasture/Hay
	202, 145, 71	82 - Row Crops
	121, 108, 75	83 - Small Grains
	244, 238, 203	84 - Fallow
	240, 156, 054	85 - Urban/Recreational Grasses
	201, 230, 249	91 - Woody Wetlands
	144, 192, 217	92 - Emergent Herbaceous Wetlands

<b>Table 5-2</b>		
<b>Z<sub>0-land</sub> factors for NLCD classifications</b>		
<b>NLCD Class</b>	<b>Description</b>	<b>Z<sub>0-land</sub></b>
11	Open Water	0.001
12	Ice/Snow	0.012
21	Low Residential	0.330
22	High Residential	0.500
23	Commercial	0.390
31	Bare Rock/Sand	0.090
32	Gravel Pit	0.180
33	Transitional	0.180
41	Deciduous Forest	0.650
42	Evergreen Forest	0.720
43	Mixed Forest	0.710
51	Shrub Land	0.120
61	Orchard/Vineyard	0.270
71	Grassland	0.040
81	Pasture	0.060
82	Row Crops	0.060
83	Small Grains	0.050
84	Fallow	0.050
85	Recreational Grass	0.050
91	Woody Wetland	0.550
92	Herbaceous Wetland	0.110
95	Cypress Forest	0.550



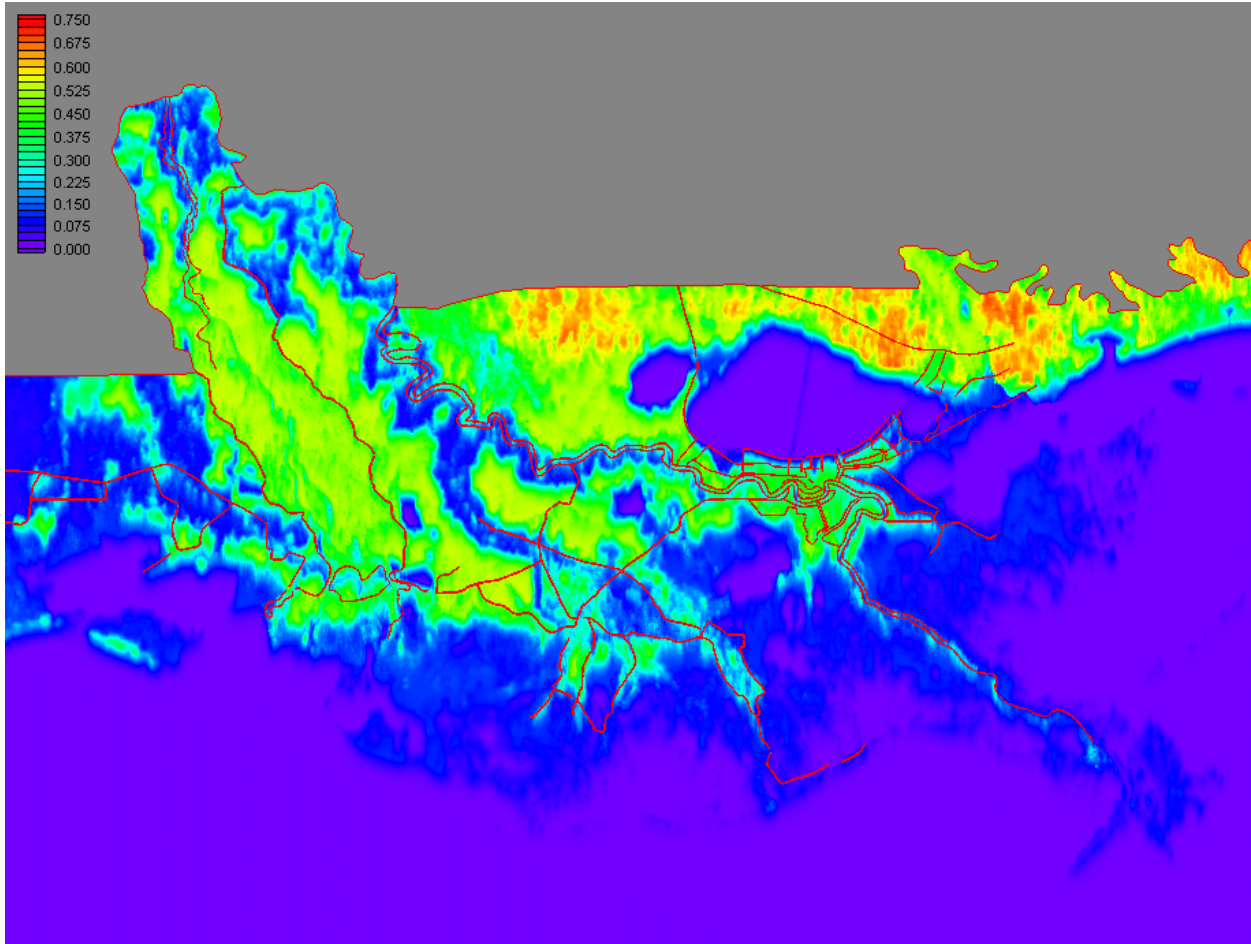


Figure 5-4a. Directional wind reduction values with a uniform northerly wind

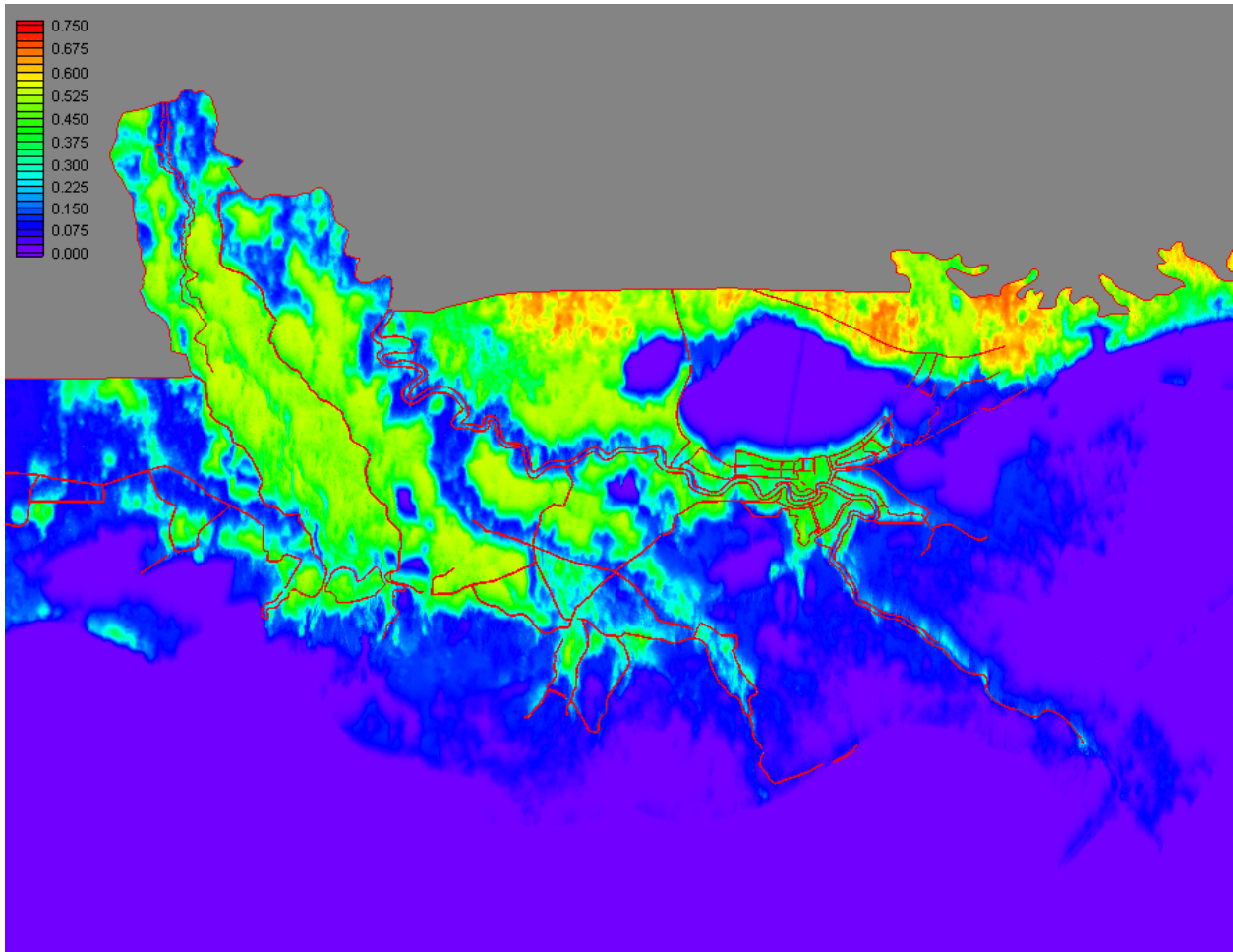


Figure 5-4b. Directional wind reduction values with a uniform southerly wind

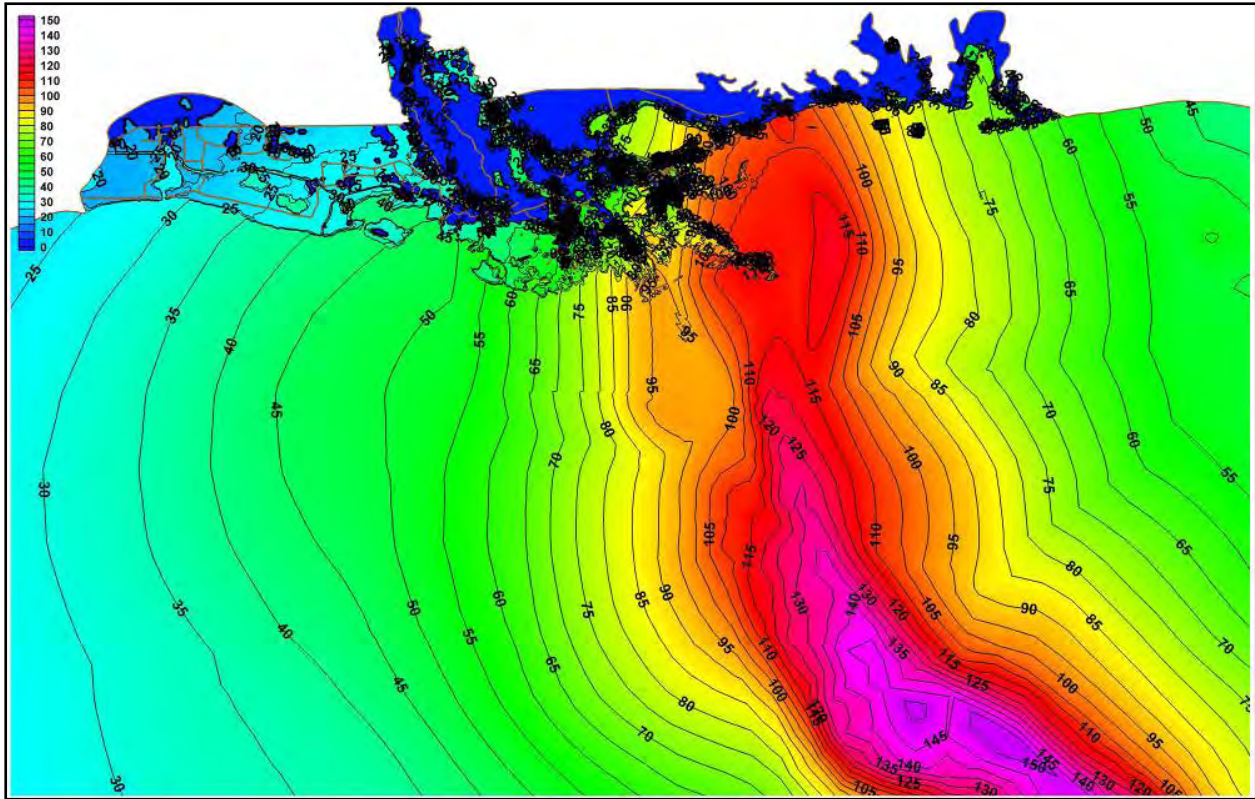


Figure 5-5a. The maximum H\*Wind/IOKA 1 minute averaged wind swaths adjusted for directional land roughness boundary layer effects and canopies during the entire Katrina event in the northern Gulf of Mexico



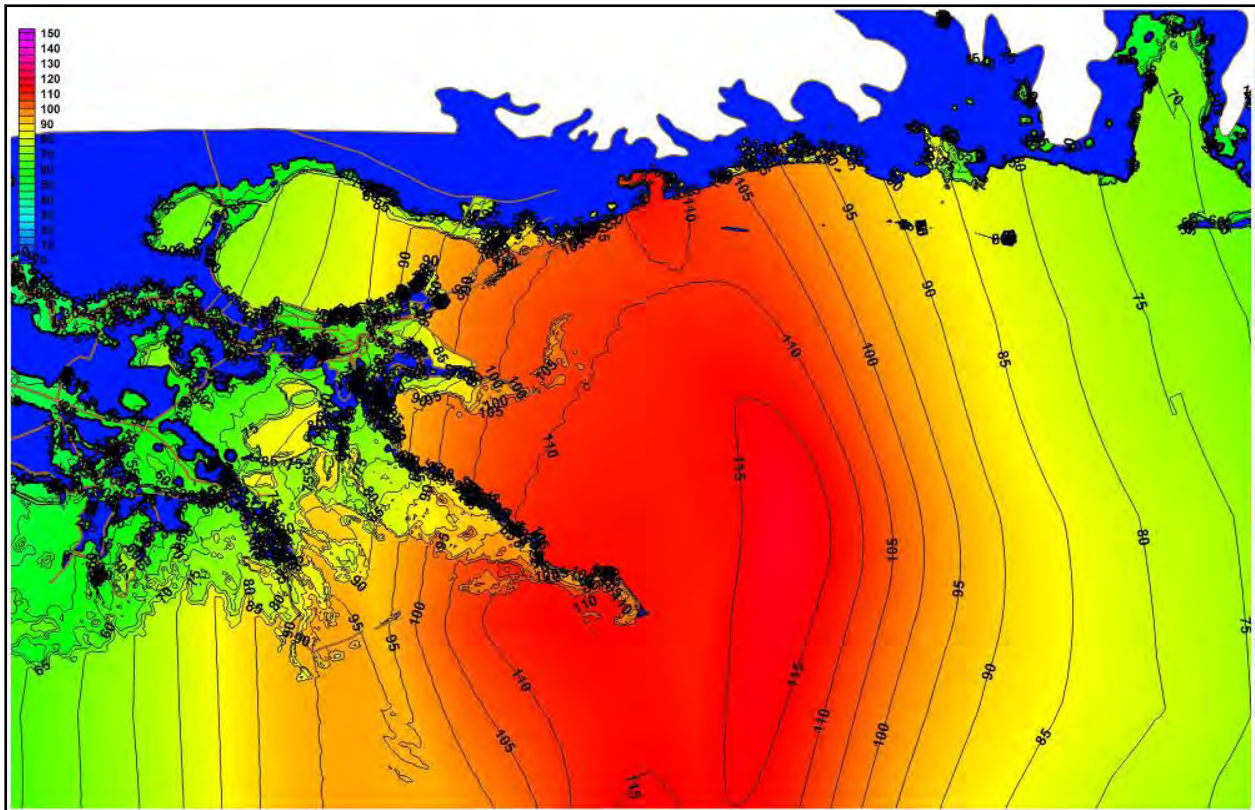


Figure 5-5b. The maximum H\*Wind/IOKA 1 minute averaged wind swaths adjusted for directional land roughness boundary layer effects and canopies during the entire Katrina event in Southeastern Louisiana

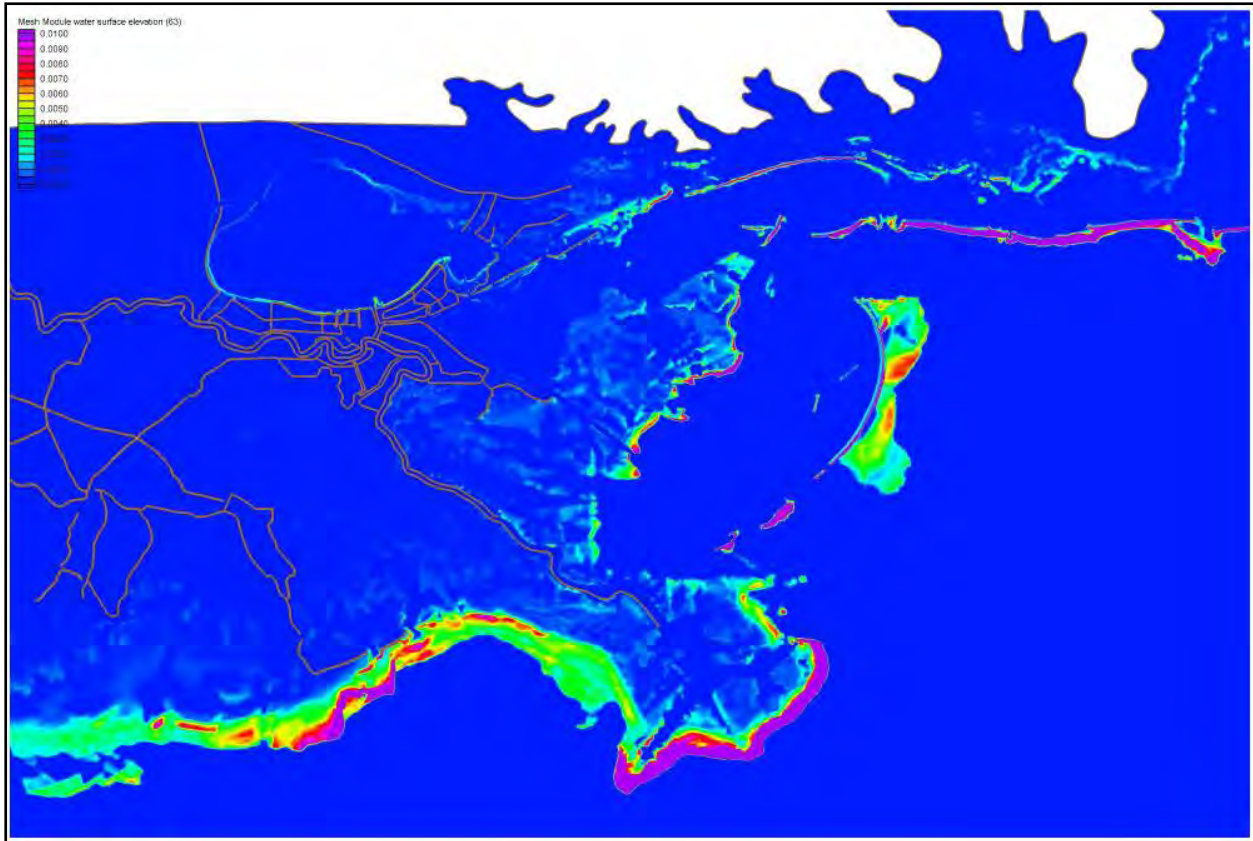


Figure 5-6. The maximum Katrina event wave radiation stress gradients used as wave forcing functions in the ADCIRC model and computed using the STWAVE model. The maximum of the legend is adjusted to 0.01 to better visualize the distribution. The maximum over the domain is 0.123

## Description of the Physics of the Hurricane Katrina Storm Surge

The progression and physics of the Katrina surge event is shown in a sequence of surface water elevation contour maps with superimposed wind vectors (knots) between 8/29/0700 UTC and 8/29/2300 UTC shown in Figure 5-7a to 5-7k and with water currents (ft/s) in Figures 5-8a to 5-8k. A more detailed view of the surface water contours and currents showing Lake Ponchartrain and metropolitan New Orleans is shown in Figures 5-9a to 5-9k. It is clear that storm response over southern Louisiana is highly localized and varies rapidly over even a few kilometers. Surge is dominated by physical features such as levees, river berms, raised roads as well as by breaks in these features, inlets, channels and rivers. Furthermore the shallower the water, the more effective a given wind stress is at increasing surface water gradients and in piling up water against obstructions.

On 8/29/0700 UTC (2:00 a.m. CDT) Katrina has just been downgraded to a Category 4 storm with the eye approximately 80 miles south of the initial landfall location. Figures 5-7a, 5-8a and 5-9a show the predominantly easterly winds blowing water into Breton and Chandeleur sounds



as well as into Lake Borgne. In particular, water is being stopped by the Mississippi River levees and by the St. Bernard/Chalmette protection levee where surge is building up to 10 ft.

Water level is also raised on the southwest end of Lake Pontchartrain where the railroad berm holds the water while water levels are suppressed in eastern Lake Pontchartrain. The combined water level rise in Lake Borgne and the drawdown of water in eastern Lake Pontchartrain causes a strong surface water gradient across the inlets which connect these two water bodies, Chef Menteur Pass and the Rigolets Strait. This gradient moves a current which drives water into Lake Pontchartrain which is further reinforced by the easterly winds. This process initiates the critical rise of the mean water level within Lake Pontchartrain. Finally, note that the predominantly easterly and northerly winds to the west of the Mississippi River force a drawdown of water away from the west-facing levees in these regions.

On 8/29/1000 UTC (Figures 5-7b, 5-8b and 5-9b) Katrina is located 30 miles south of its initial landfall location and the winds over the critical regions are still predominantly from the east. Surge is building up to more than 18 feet along the Mississippi levees between Buras and Pointe A La Hache.

On 8/29/1100 UTC (Figures 5-7c, 5-8c and 5-9c) Katrina is nearing landfall and surge continues to build up against the levees of lower Plaquemines Parish reaching elevations up to 19 ft. The surge in this region has started to propagate up the Mississippi River and also extends broadly into Breton Sound. Further north, surge continues to build up against the St. Bernard/Chalmette protection levee due to the now north-easterly winds, up to 13 feet.

On 8/29/1200 UTC (Figures 5-7d, 5-8d and 5-9d), the eye location has caused a significant shift in the wind patterns. Surge has started to be blown off the southernmost east-facing levees of Plaquemines Parish although surge continues to build up further north along the river levees. Surge has now reached 16 ft along the St. Bernard/Chalmette protection levee and is being driven through the GIWW into the IHNC and Lake Pontchartrain. In addition, the northeasterly winds over Lake Pontchartrain are building up surge against the lake levees of Jefferson Parish and Orleans Parish. In addition the continued strong surface water gradient aided by the winds between Lake Borgne and Lake Pontchartrain continue to drive water from Lake Borgne into Lake Pontchartrain. This process is still enhanced by the drawdown in the northeast corner of Lake Pontchartrain.

On 8/29/1300 UTC (Figures 5-7e, 5-8e and 5-9e), the surge that built up against the lower Mississippi River levees is rapidly propagating in a north-easterly direction towards the Chandeleur Sound. The component of the surge propagating up the Mississippi River reaches 16 ft. Surge is now also being driven from the west in southern Plaquemines Parish near Venice. Surge is peaking along the St. Bernard Parish/ Chalmette protection levee and in the funnel defined by levees along the GIWW and the MRGO. Within Lake Pontchartrain, surge is now strongly focused on the south side of the lake and a well defined drawdown exists along the north shore. It is noted that surge has not built up along the concavity in the Mississippi River along English Turn, due to the change in the direction of the winds.

On 8/29/1400 UTC (Figures 5-7f, 5-8f and 5-9f), Katrina is now located over Lake Borgne. The surge originating along the levees of lower Plaquemines continues to propagate across Chandeleur Sound towards the Mississippi Sound in a northeasterly direction. Surge is attenuating along lower Plaquemines on the east side of the river as is the surge that is propagating up the Mississippi River itself, due to winds from the west and north. Water continues to pile up from the west along the levees near Venice. Surge along the St. Bernard/Chalmette protection levee and in the GIWW/MRGO funnel are attenuating. Water is being blown from the north of Lake Ponchartrain and continues to build up along the southern shores of Lake Pontchartrain to around 9 ft. Water is accumulating from the east and overtopping the CSX railroad between Lake Borgne and Lake Ponchartrain.

On 8/29/1500 UTC (Figures 5-7g, 5-8g and 5-9g), Katrina continues to move north. The surge that propagated from Southern Plaquemines Parish has now combined with the local surge being generated by the strong southerly winds and is dramatically increasing water levels between Bay St. Louis and Biloxi with peaks reaching 24 ft. Water is blown from the west to the east in Lake Ponchartrain. In addition water is overtopping the CSX railroad west of Lake Borgne and the Mississippi Sound. Water is also driven in a westerly direction across Mobile Bay.

On 8/29/1600 UTC (Figures 5-7h, 5-8h and 5-9h), Katrina is near its second landfall. Surge along the State of Mississippi shoreline is spreading inland and continues to build up driven by the winds from the south to levels reaching 29 ft. Water still is being blown from west to east across Lake Ponchartrain and water continues to move from Lake Borgne into Lake Ponchartrain from the east, overtopping the CSX railroad and U.S. 90.

On 8/29/1700 UTC (Figures 5-7i, 5-8i and 5-9i), surge continues to propagate inland along the State of Mississippi shore. Winds are still blowing from the west across Lake Pontchartrain causing a drawdown in the west and a surge in the east and water very forcefully penetrates from Lake Borgne.

On 8/29/20 UTC (Figures 5-7j, 5-8j and 5-9j), Katrina has moved well inland. Surge along the State of Mississippi coast is subsiding. However high water remains in Lake Pontchartrain as well as Lake Maurepas. In addition, water is withdrawing from Lake Borgne.

This process continues as is shown on 8/29/23 UTC (Figures 5-7k, 5-8k and 5-9k). However note that Lake Pontchartrain is at 7 ft and is only slowly subsiding due to the lack of strong water surface elevation gradients between Lake Pontchartrain and Lake Borgne.

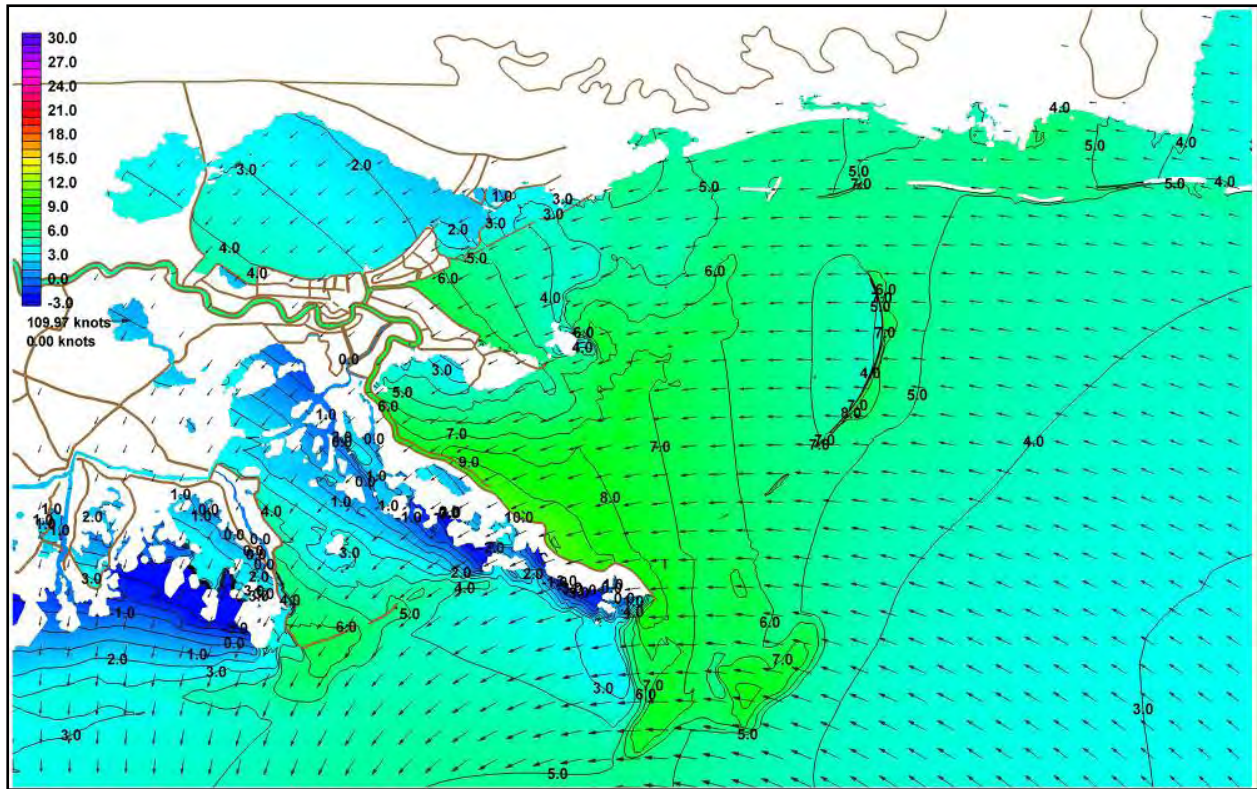


Figure 5-7a. Water surface elevation with respect to the NAVD 88 (ft) with boundary layer adjusted wind velocity vectors (knots) during Hurricane Katrina on August 29, 2005 at 700UTC

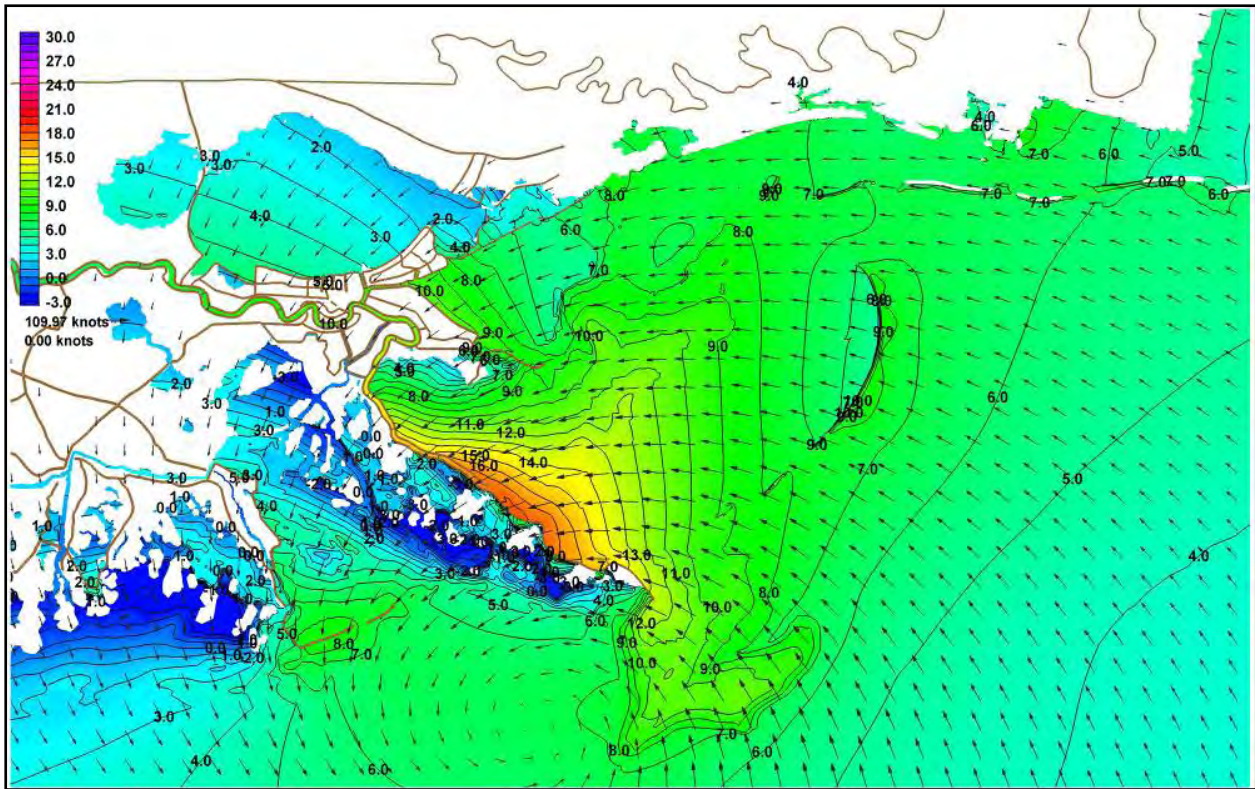


Figure 5-7b. Water surface elevation with respect to the NAVD 88 (ft) with boundary layer adjusted wind velocity vectors (knots) during Hurricane Katrina on August 29, 2005 at 1000UTC



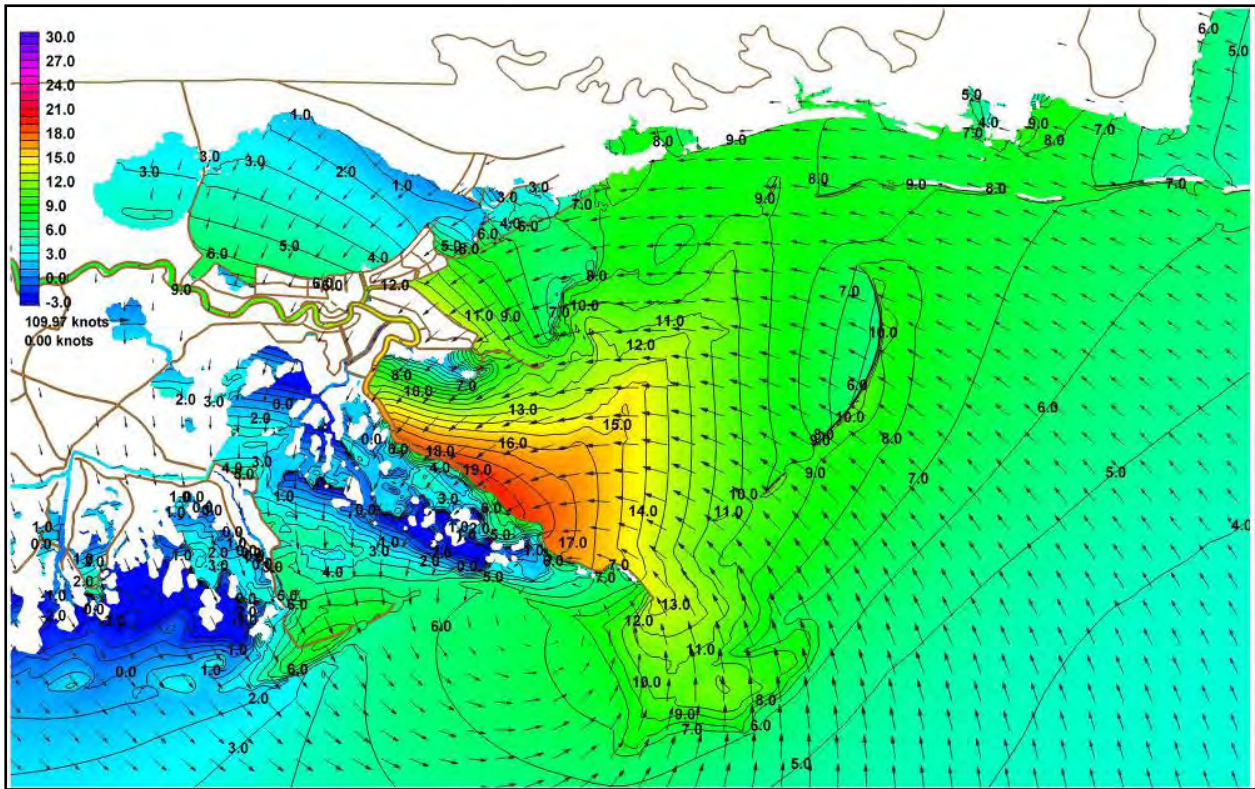


Figure 5-7c. Water surface elevation with respect to the NAVD 88 (ft) with boundary layer adjusted wind velocity vectors (knots) during Hurricane Katrina on August 29, 2005 at 1100UTC



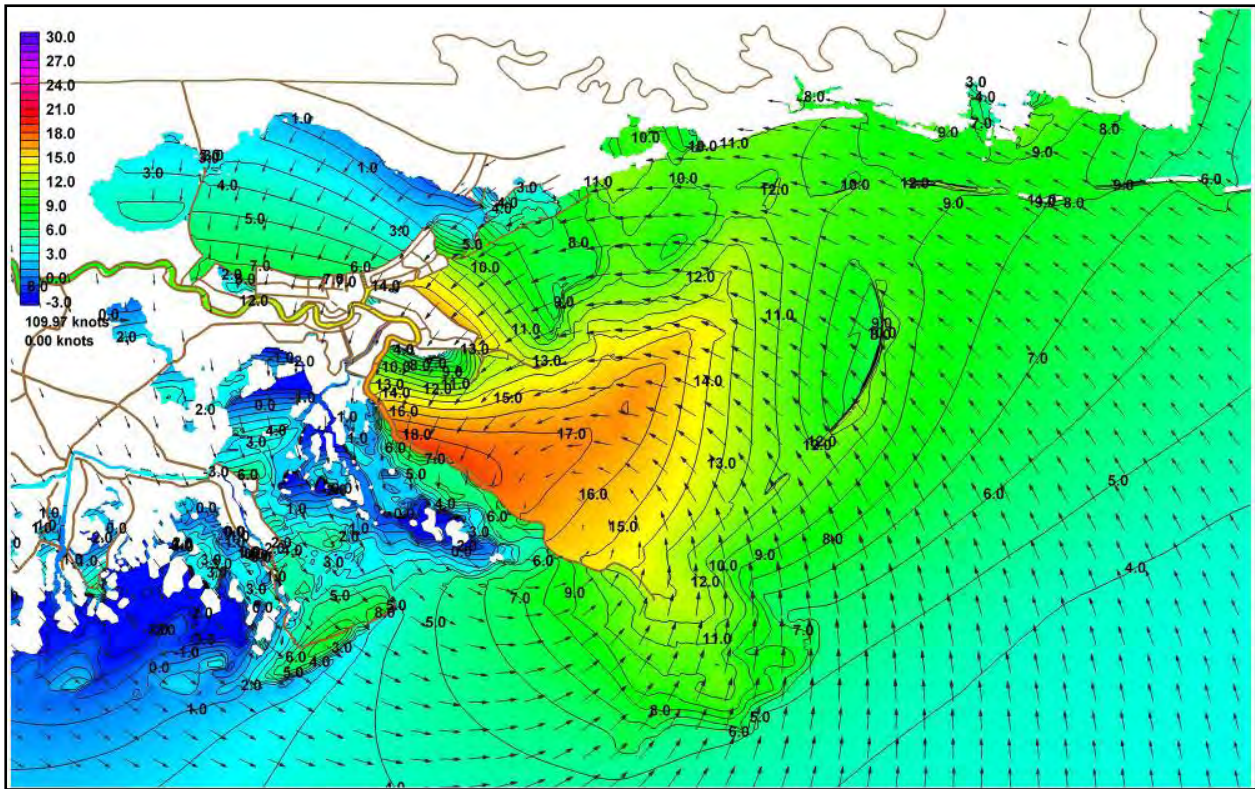


Figure 5-7d. Water surface elevation with respect to the NAVD 88 (ft) with boundary layer adjusted wind velocity vectors (knots) during Hurricane Katrina on August 29, 2005 at 1200UTC

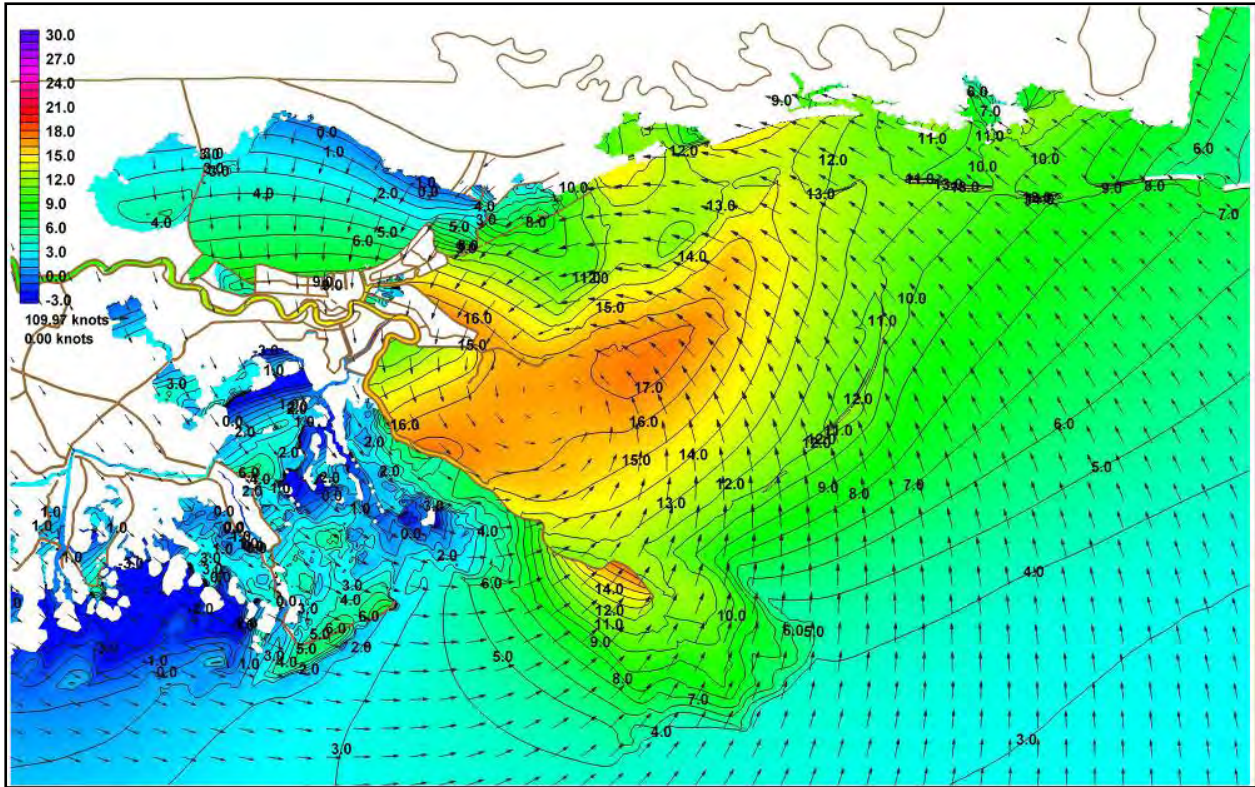


Figure 5-7e. Water surface elevation with respect to the NAVD 88 (ft) with boundary layer adjusted wind velocity vectors (knots) during Hurricane Katrina on August 29, 2005 at 1300UTC



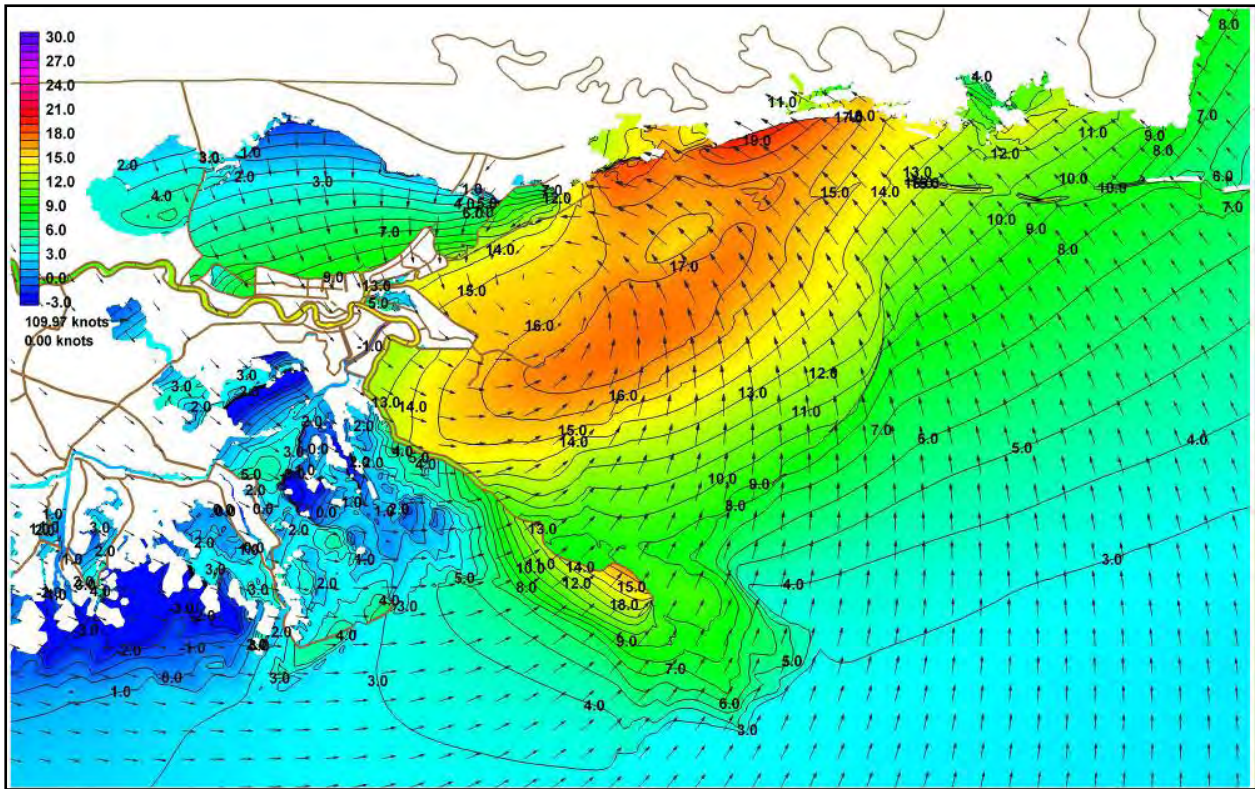


Figure 5-7f. Water surface elevation with respect to the NAVD 88 (ft) with boundary layer adjusted wind velocity vectors (knots) during Hurricane Katrina on August 29, 2005 at 1400UTC

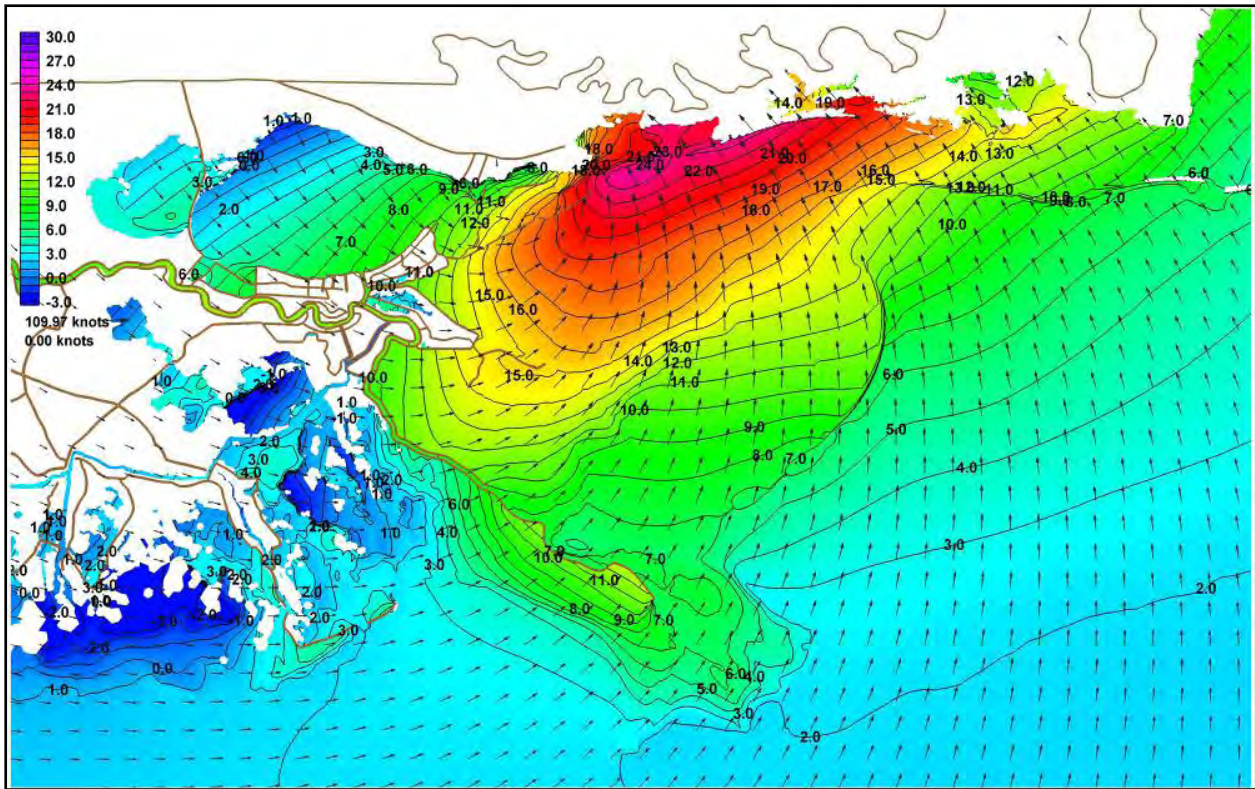


Figure 5-7g. Water surface elevation with respect to the NAVD 88 (ft) with boundary layer adjusted wind velocity vectors (knots) during Hurricane Katrina on August 29, 2005 at 1500UTC



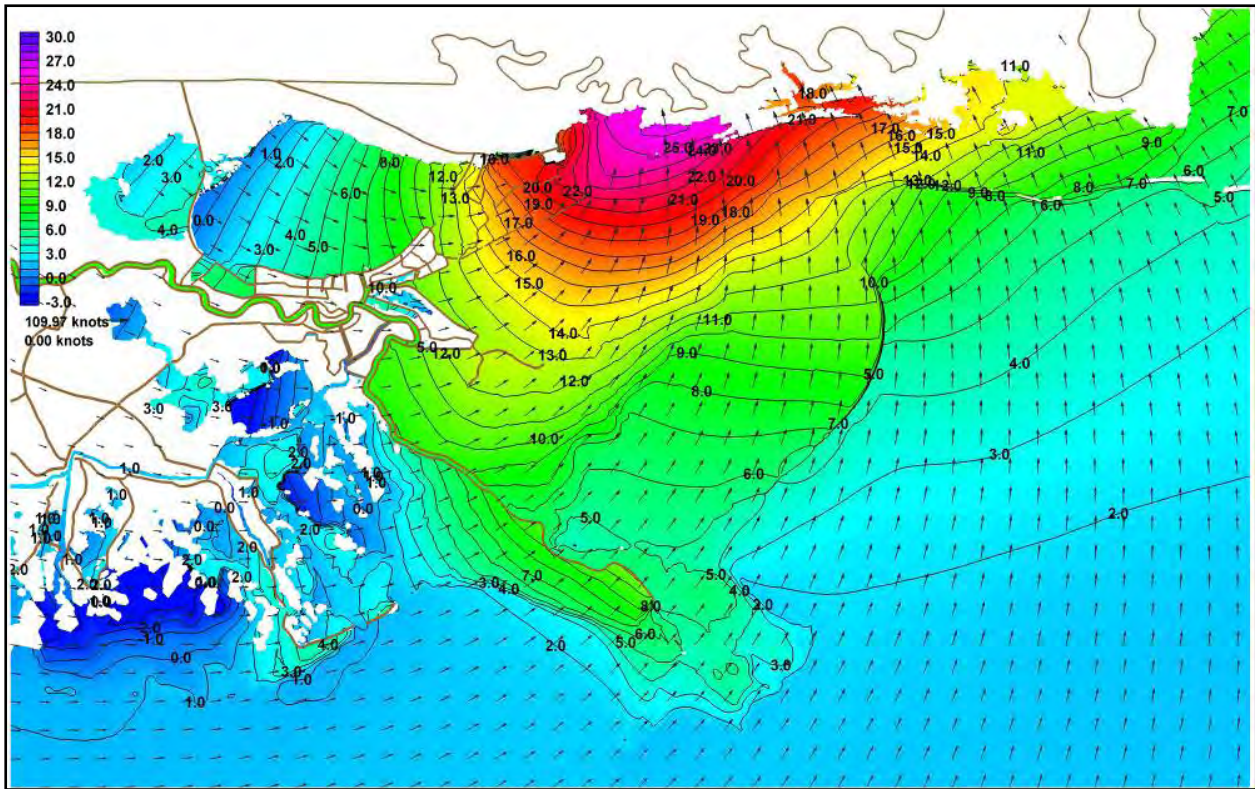


Figure 5-7h. Water surface elevation with respect to the NAVD 88 (ft) with boundary layer adjusted wind velocity vectors (knots) during Hurricane Katrina on August 29, 2005 at 1600UTC



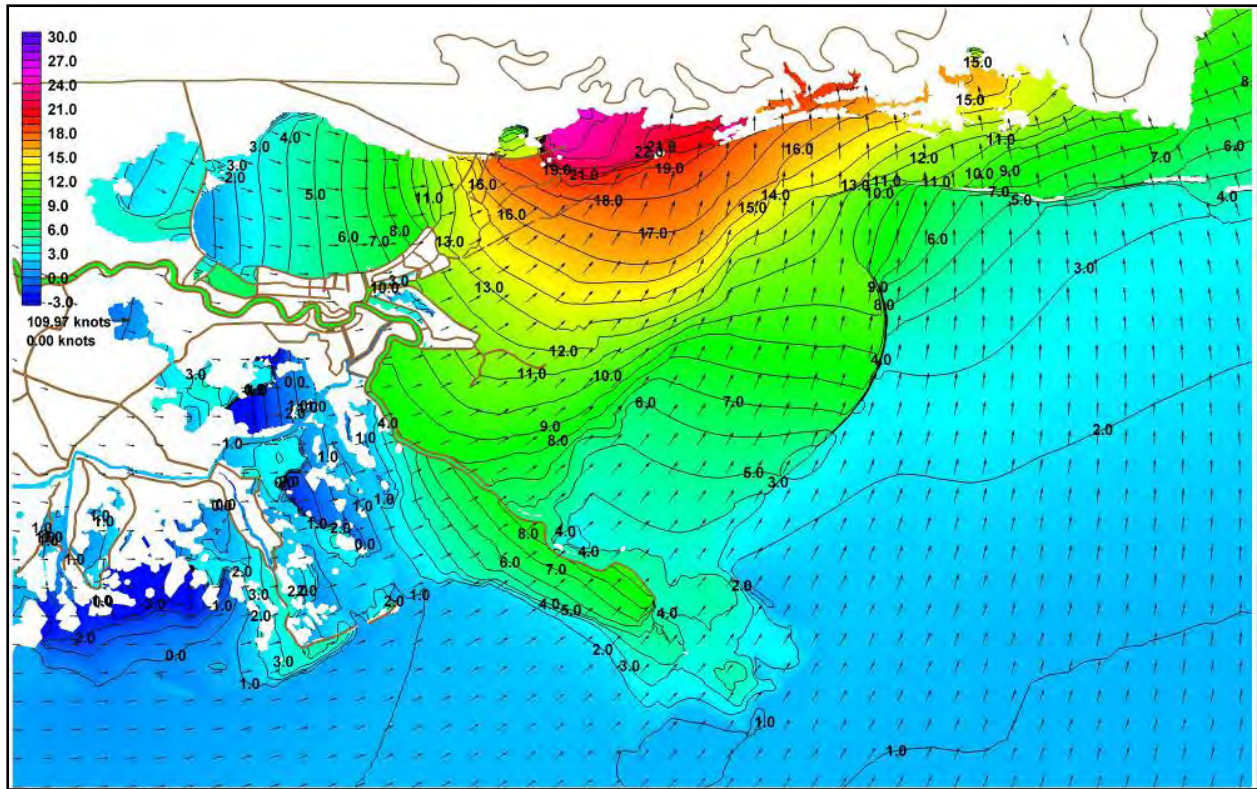


Figure 5-7i. Water surface elevation with respect to the NAVD 88 (ft) with boundary layer adjusted wind velocity vectors (knots) during Hurricane Katrina on August 29, 2005 at 1700UTC

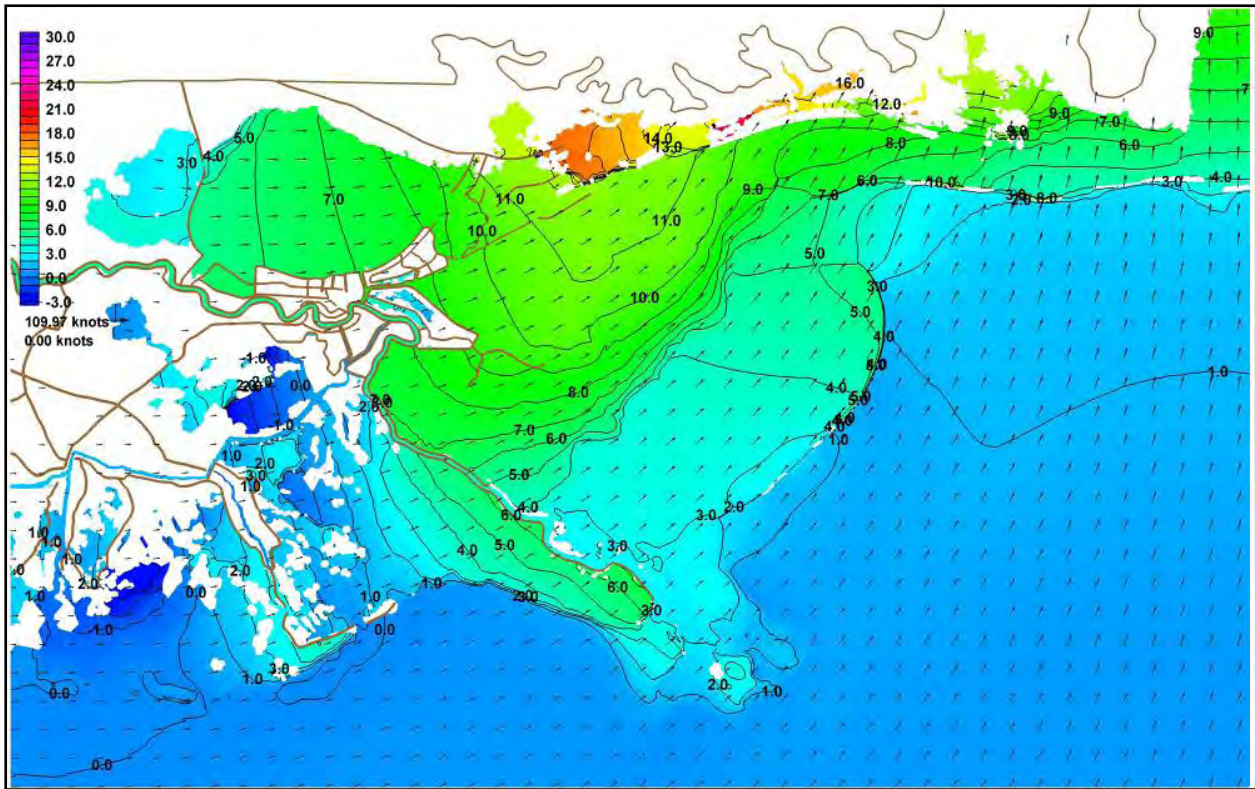


Figure 5-7j. Water surface elevation with respect to the NAVD 88 (ft) with boundary layer adjusted wind velocity vectors (knots) during Hurricane Katrina on August 29, 2005 at 2000UTC



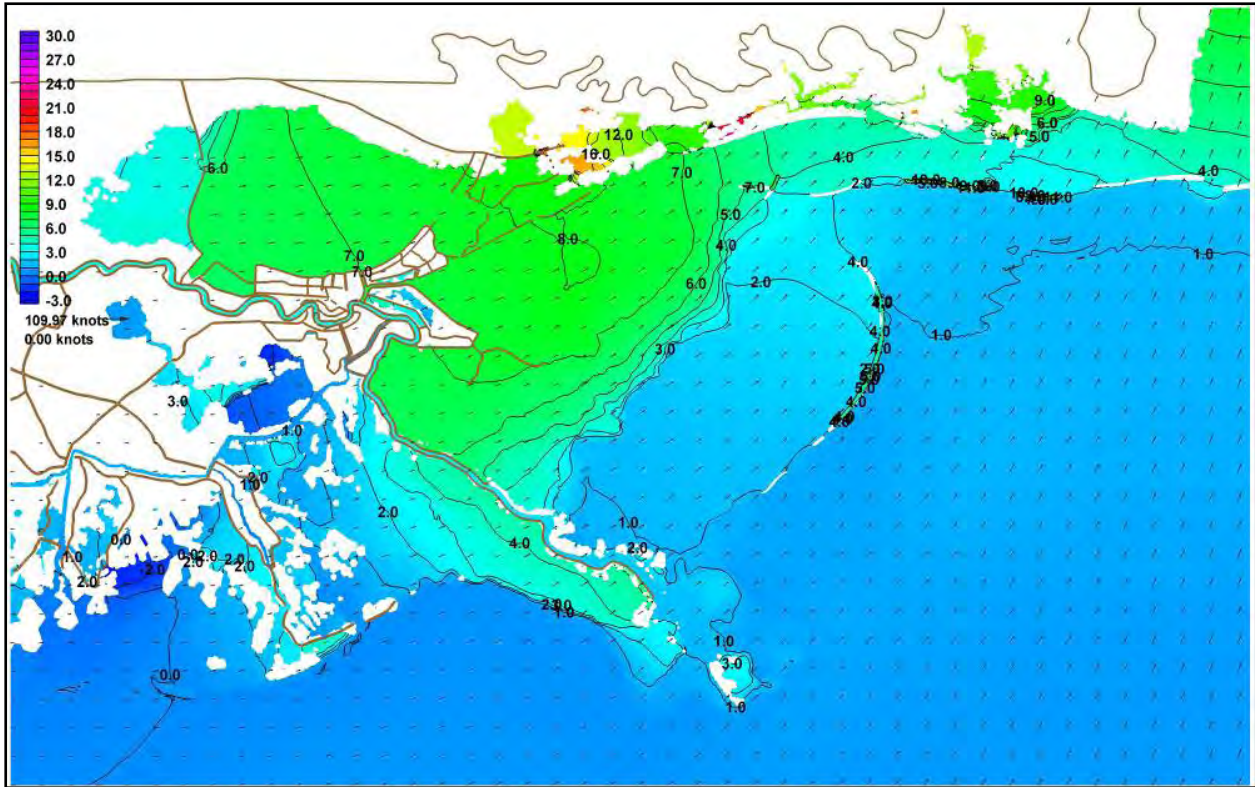


Figure 5-7k. Water surface elevation with respect to the NAVD 88 (ft) with boundary layer adjusted wind velocity vectors (knots) during Hurricane Katrina on August 29, 2005 at 2300UTC

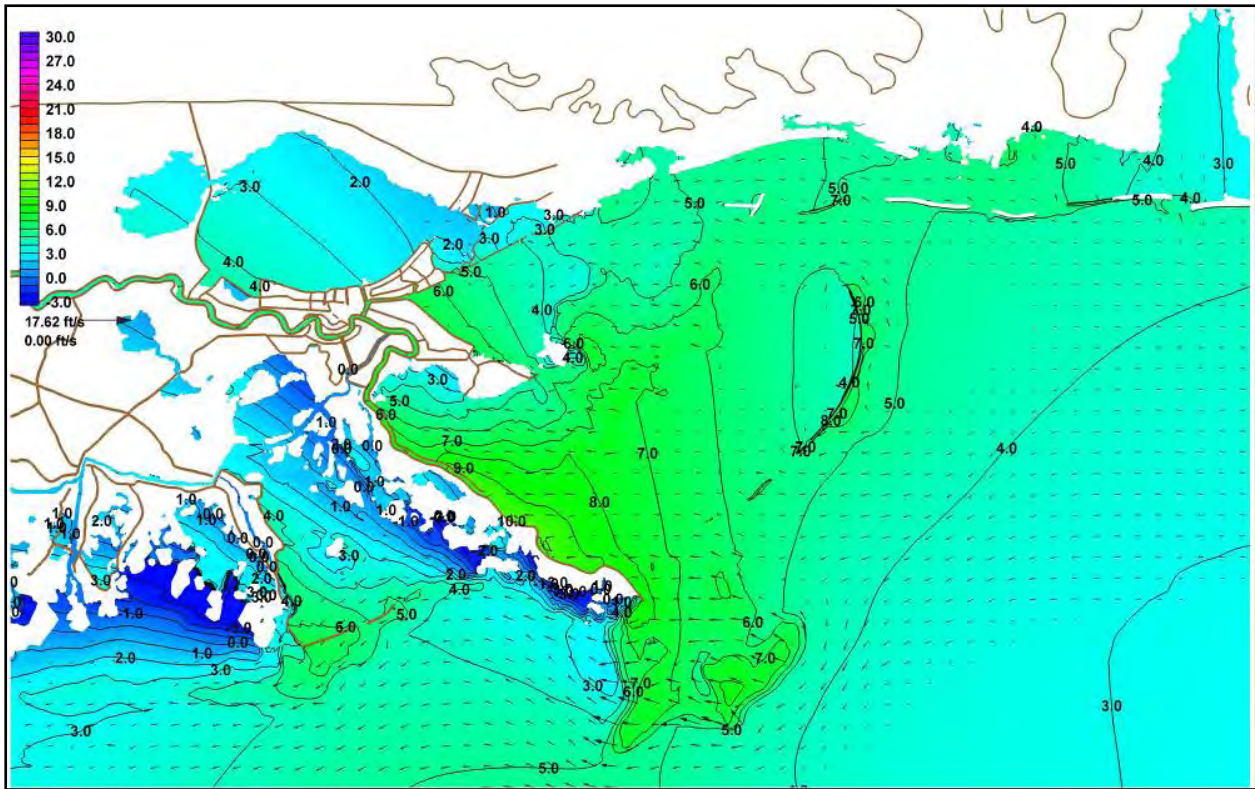


Figure 5-8a. Water surface elevation with respect to the NAVD 88 (ft) with labeled contours and currents (ft/sec) during Hurricane Katrina on August 29, 2005 at 0700UTC

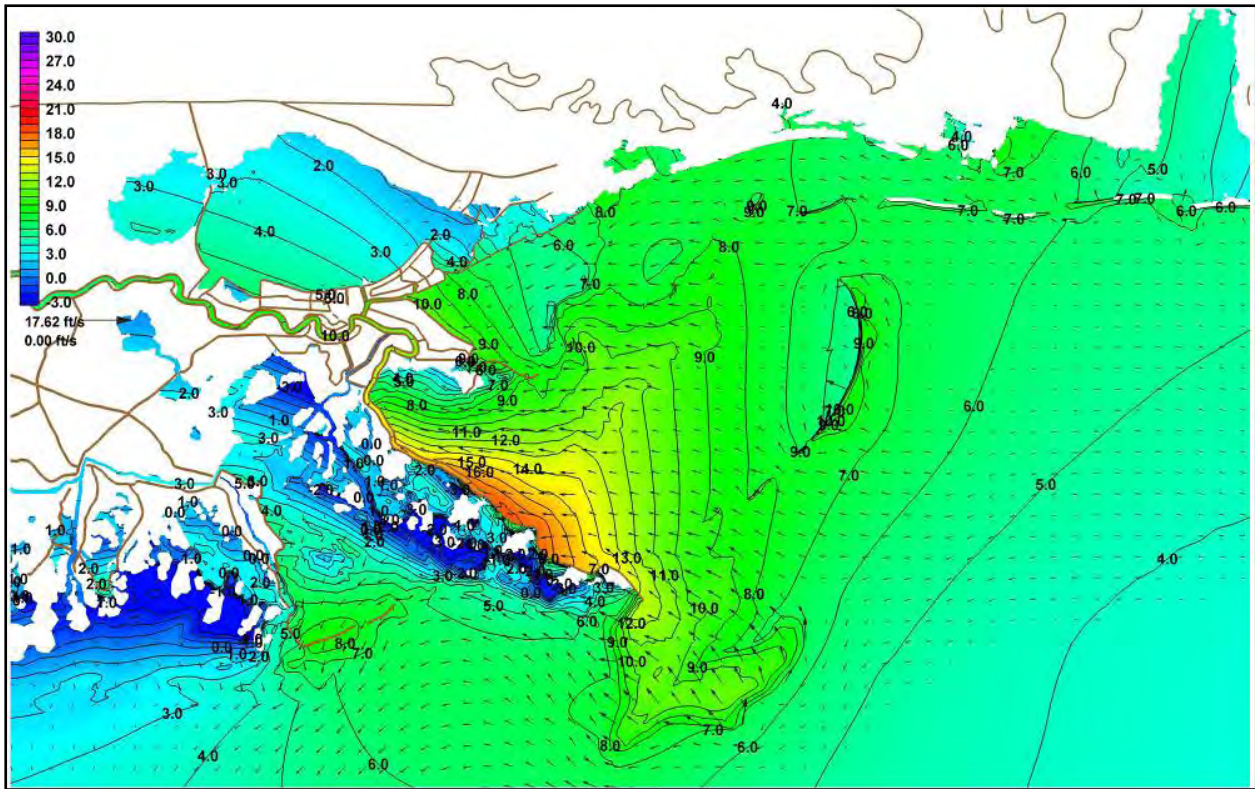


Figure 5-8b. Water surface elevation with respect to the NAVD 88 (ft) with labeled contours and currents (ft/sec) during Hurricane Katrina on August 29, 2005 at 1000UTC



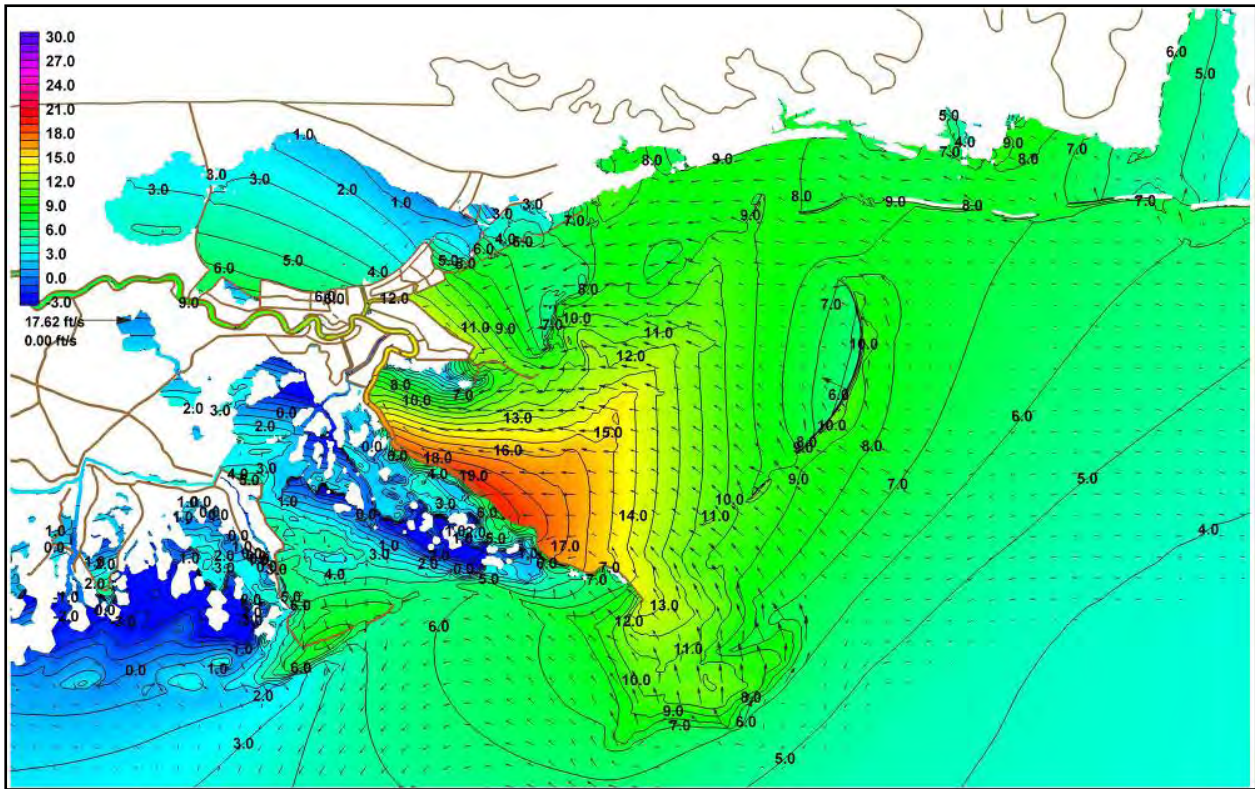


Figure 5-8c. Water surface elevation with respect to the NAVD 88 (ft) with labeled contours and currents (ft/sec) during Hurricane Katrina on August 29, 2005 at 1100UTC

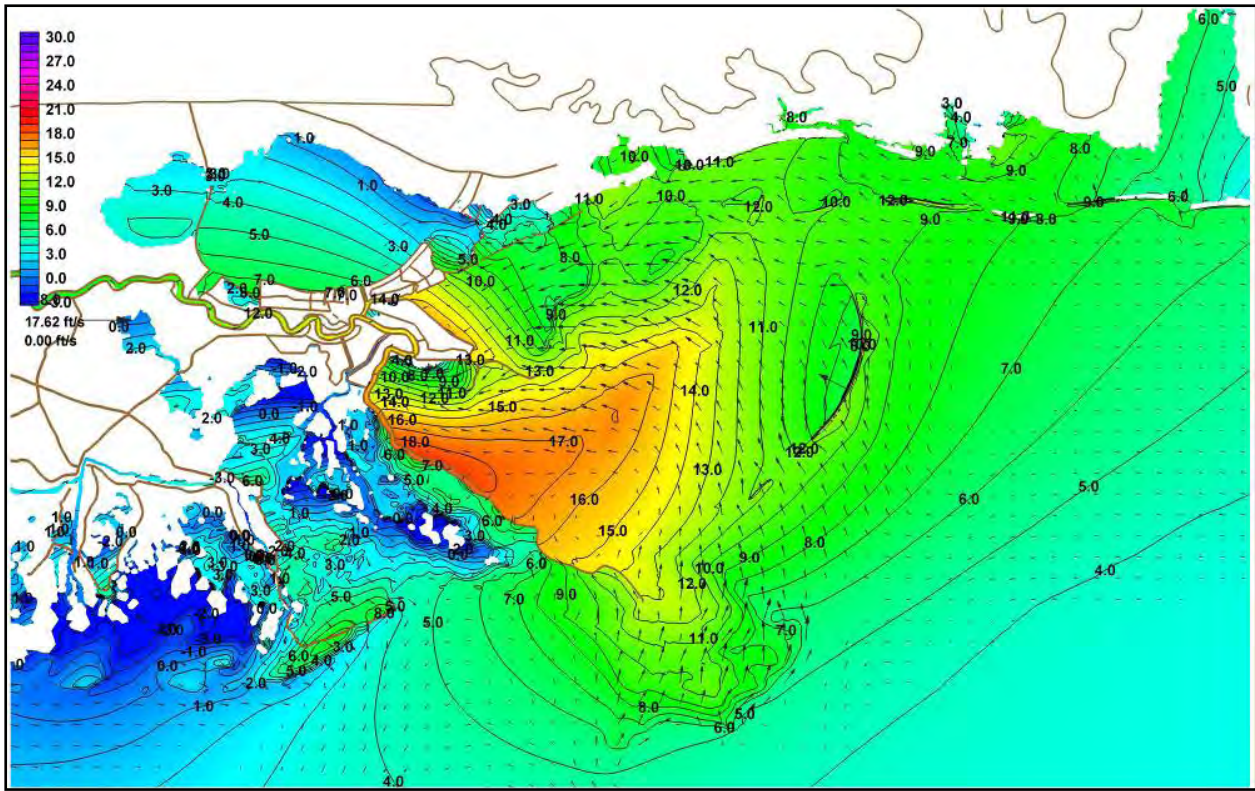


Figure 5-8d. Water surface elevation with respect to the NAVD 88 (ft) with labeled contours and currents (ft/sec) during Hurricane Katrina on August 29, 2005 at 1200UTC



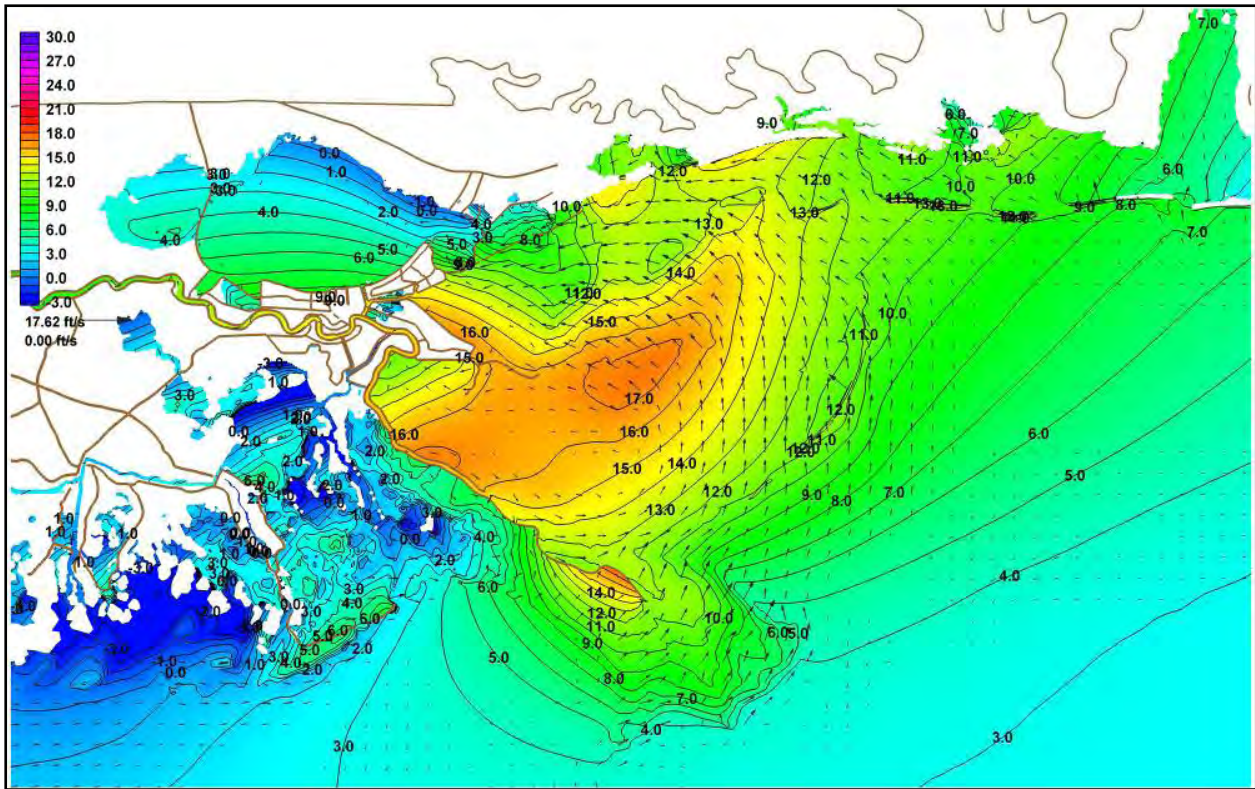


Figure 5-8e. Water surface elevation with respect to the NAVD 88 (ft) with labeled contours and currents (ft/sec) during Hurricane Katrina on August 29, 2005 at 1300UTC

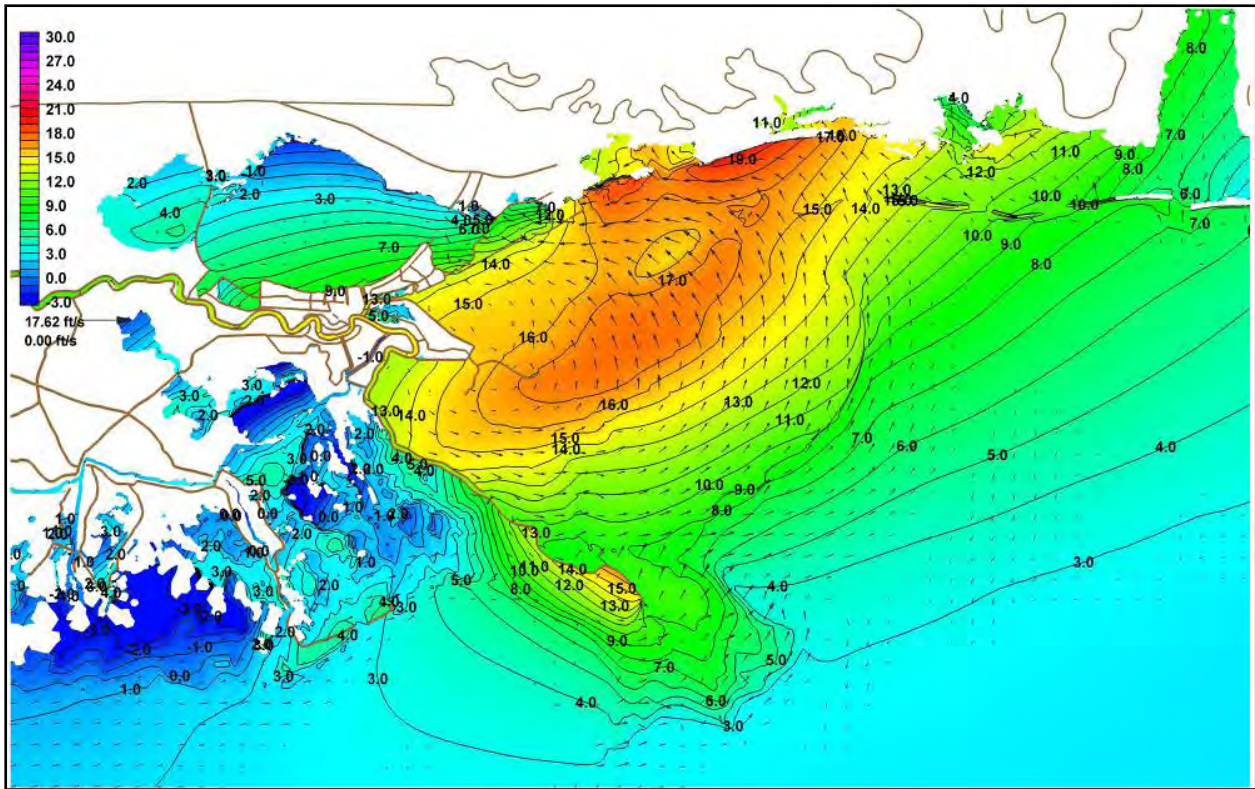


Figure 5-8f. Water surface elevation with respect to the NAVD 88 (ft) with labeled contours and currents (ft/sec) during Hurricane Katrina on August 29, 2005 at 1400UTC



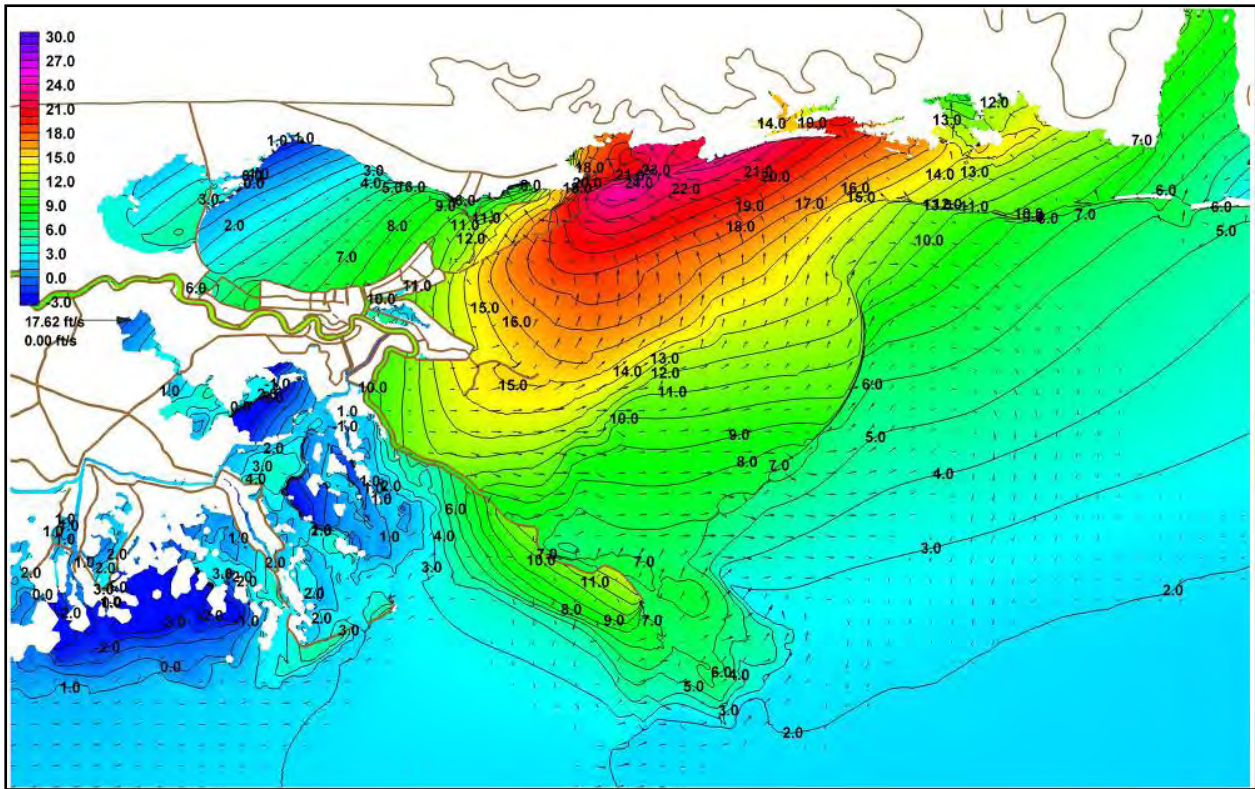


Figure 5-8g. Water surface elevation with respect to the NAVD 88 (ft) with labeled contours and currents (ft/sec) during Hurricane Katrina on August 29, 2005 at 1500UTC



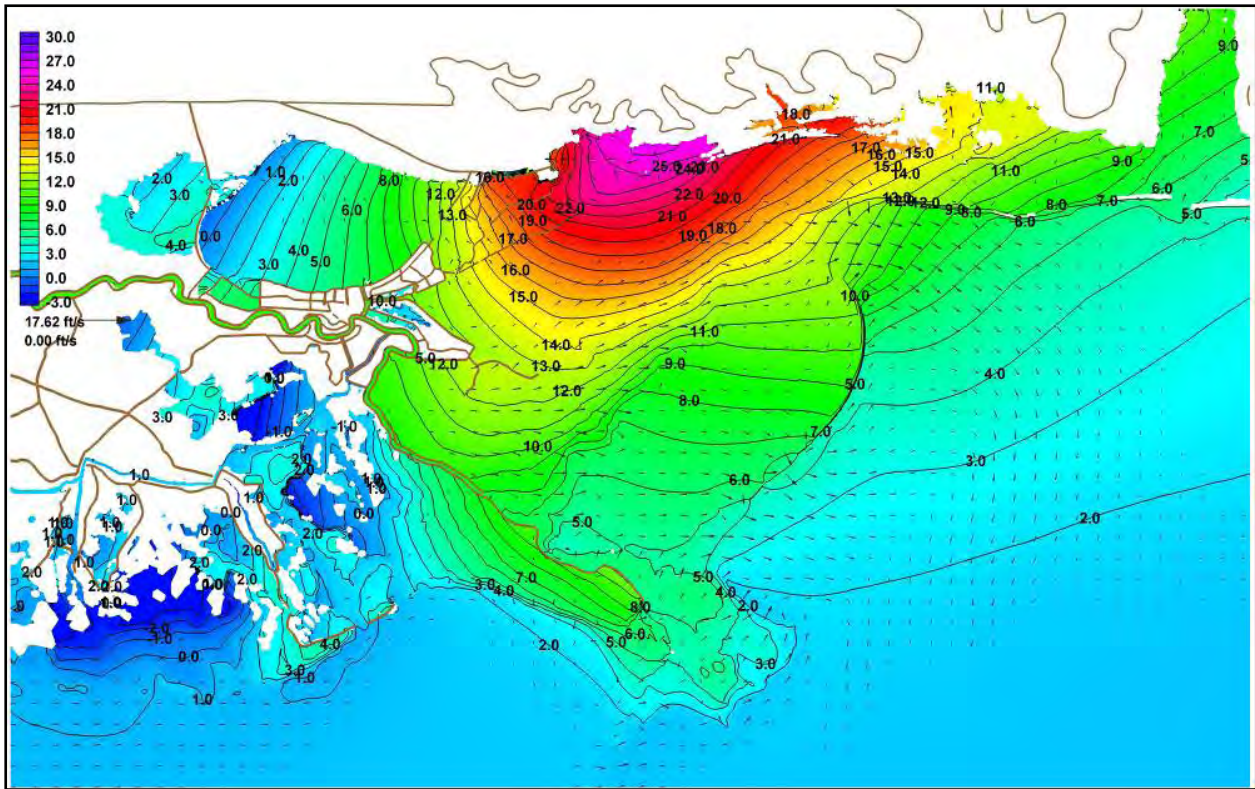


Figure 5-8h. Water surface elevation with respect to the NAVD 88 (ft) with labeled contours and currents (ft/sec) during Hurricane Katrina on August 29, 2005 at 1600UTC

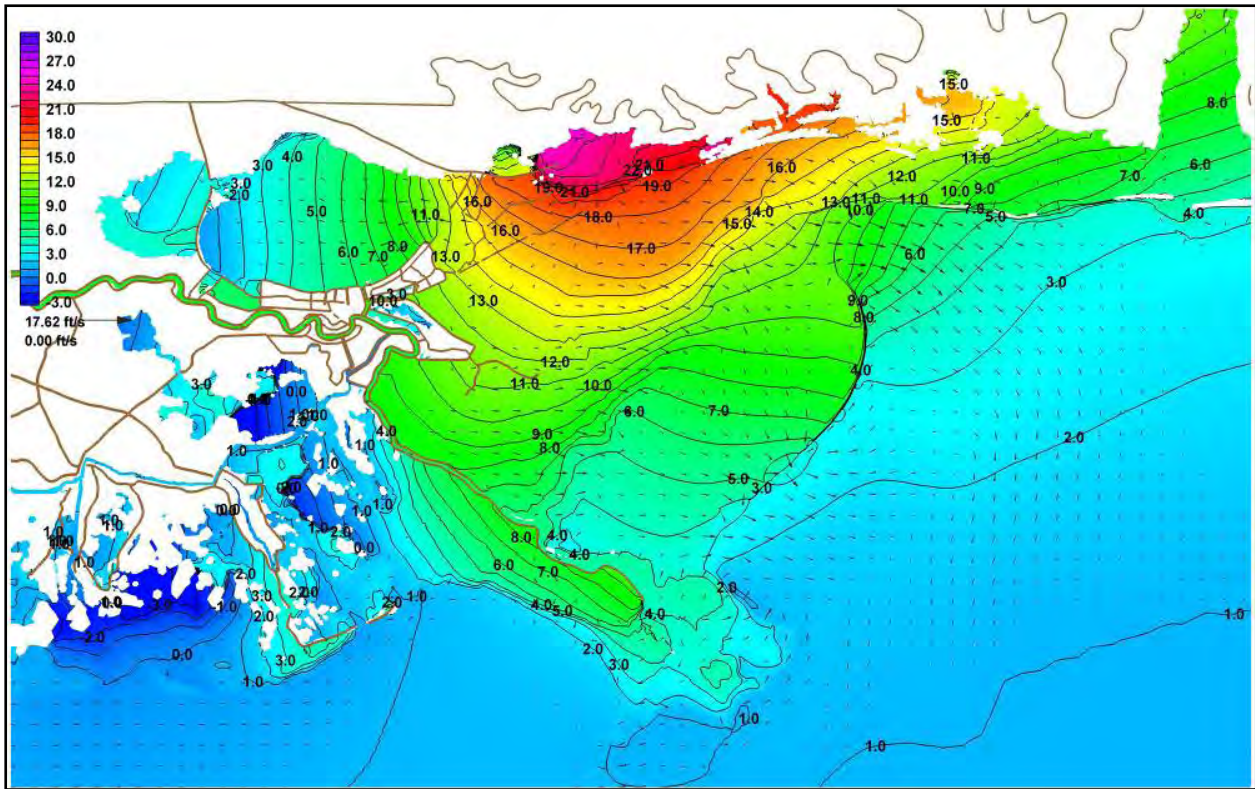


Figure 5-8i. Water surface elevation with respect to the NAVD 88 (ft) with labeled and currents (ft/sec) contours during Hurricane Katrina on August 29, 2005 at 1700UTC

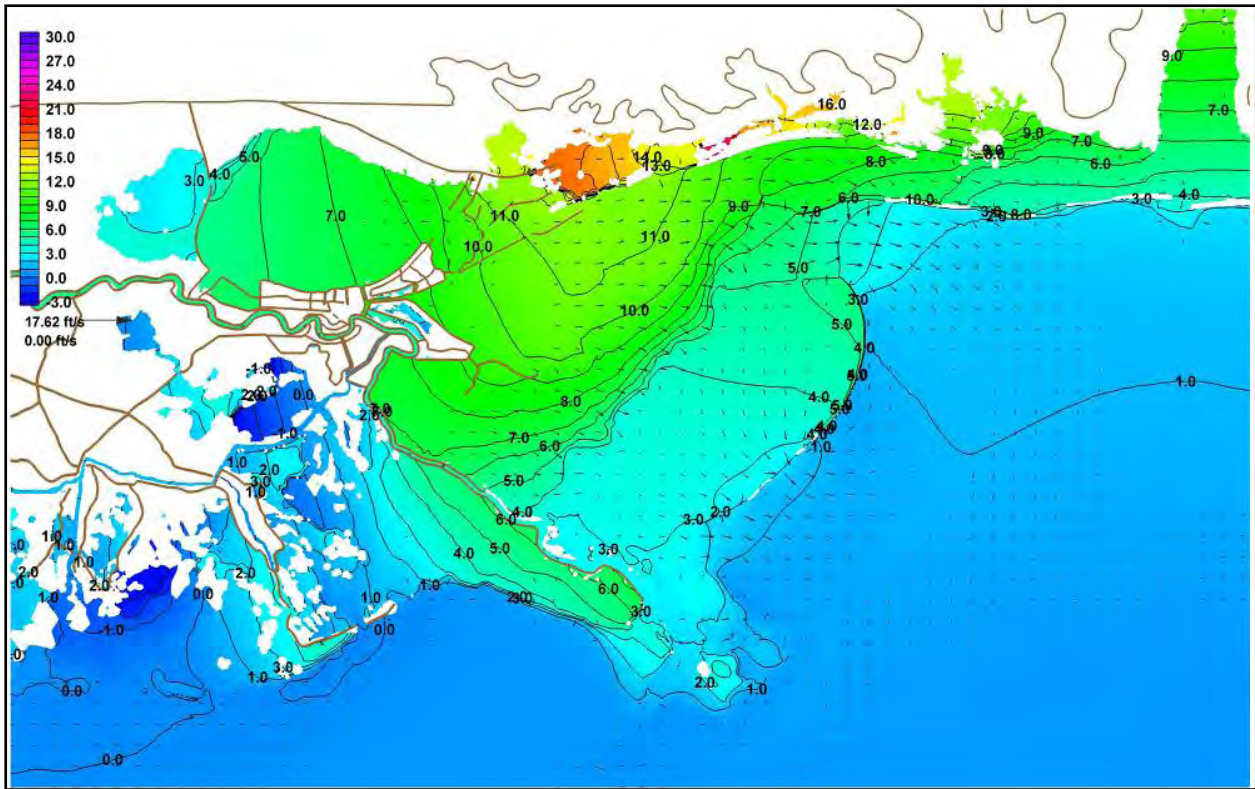


Figure 5-8j. Water surface elevation with respect to the NAVD 88 (ft) with labeled contours and currents (ft/sec) during Hurricane Katrina on August 29, 2005 at 2000UTC



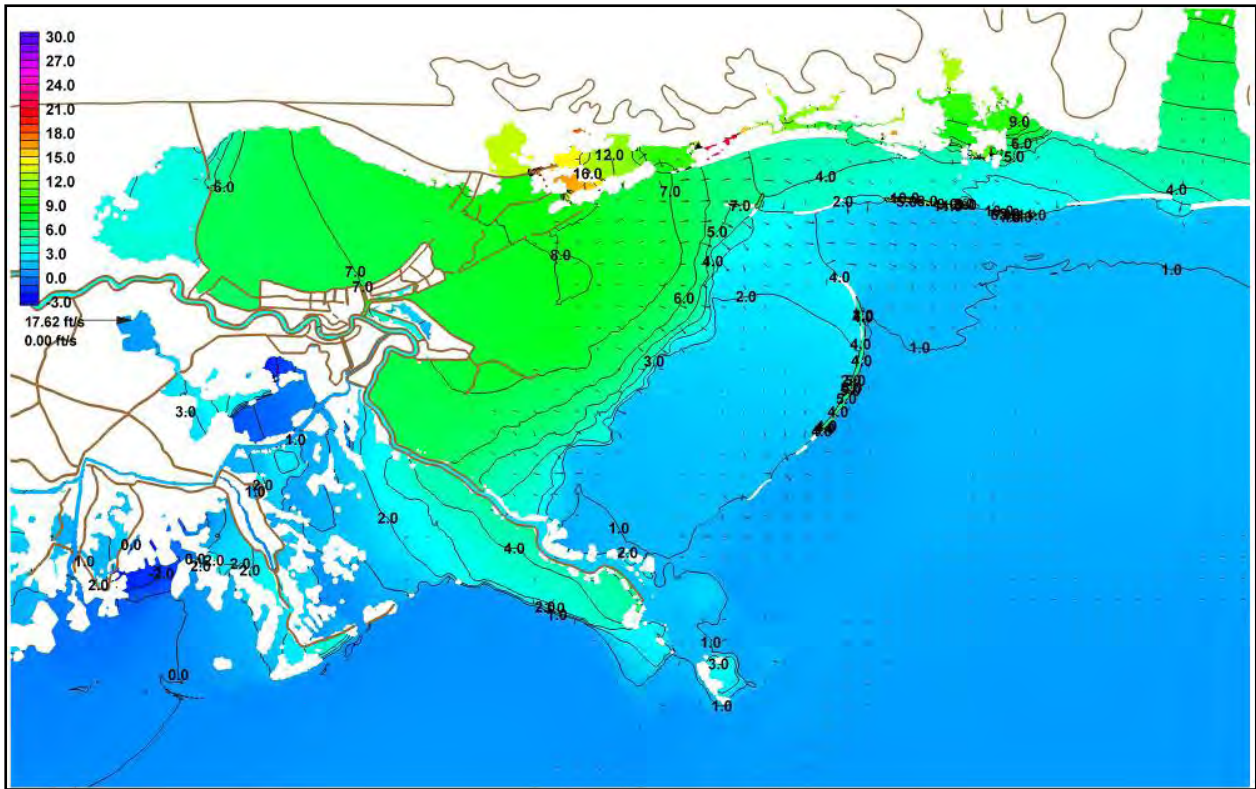


Figure 5-8k. Water surface elevation with respect to the NAVD 88 (ft) with labeled contours and currents (ft/sec) during Hurricane Katrina on August 29, 2005 at 2300UTC

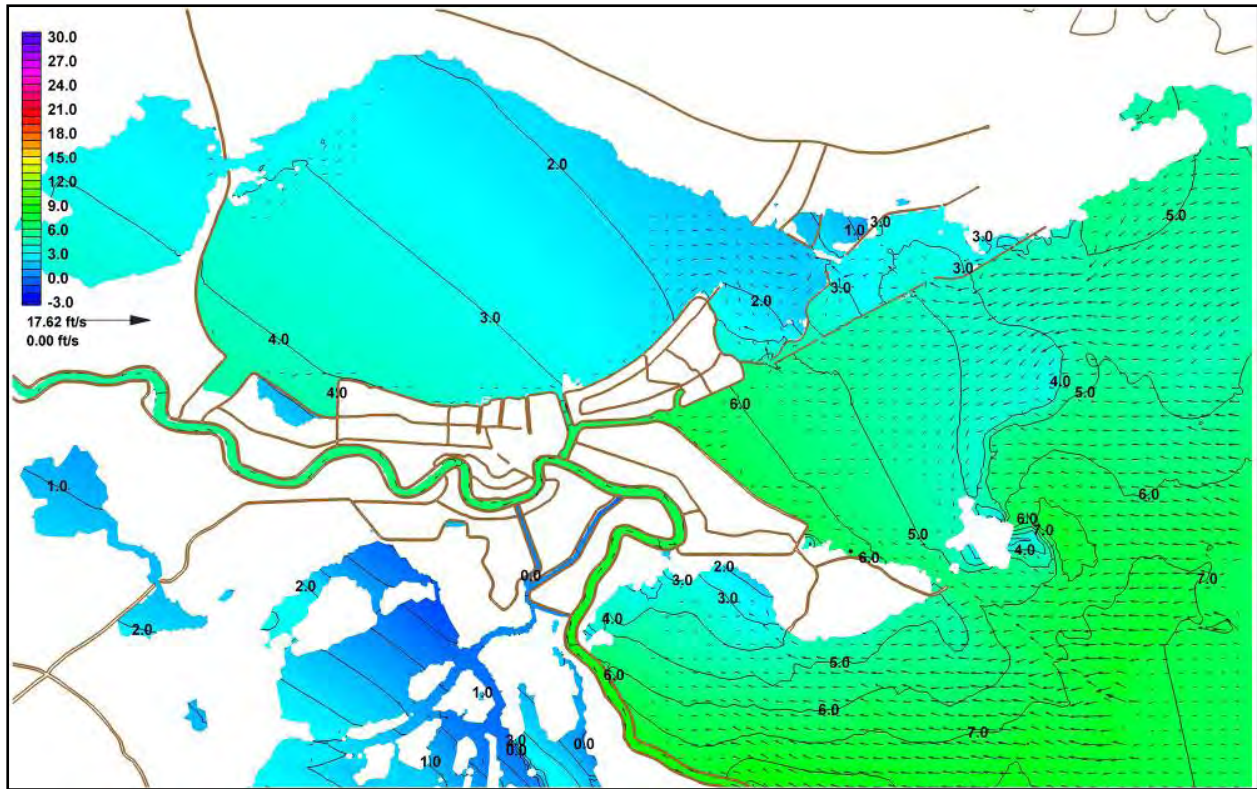


Figure 5-9a. Detail of water surface elevation in the vicinity of New Orleans with respect to the NAVD 88 (ft) with labeled contours and currents (ft/sec) on August 29, 2005 at 0700UTC



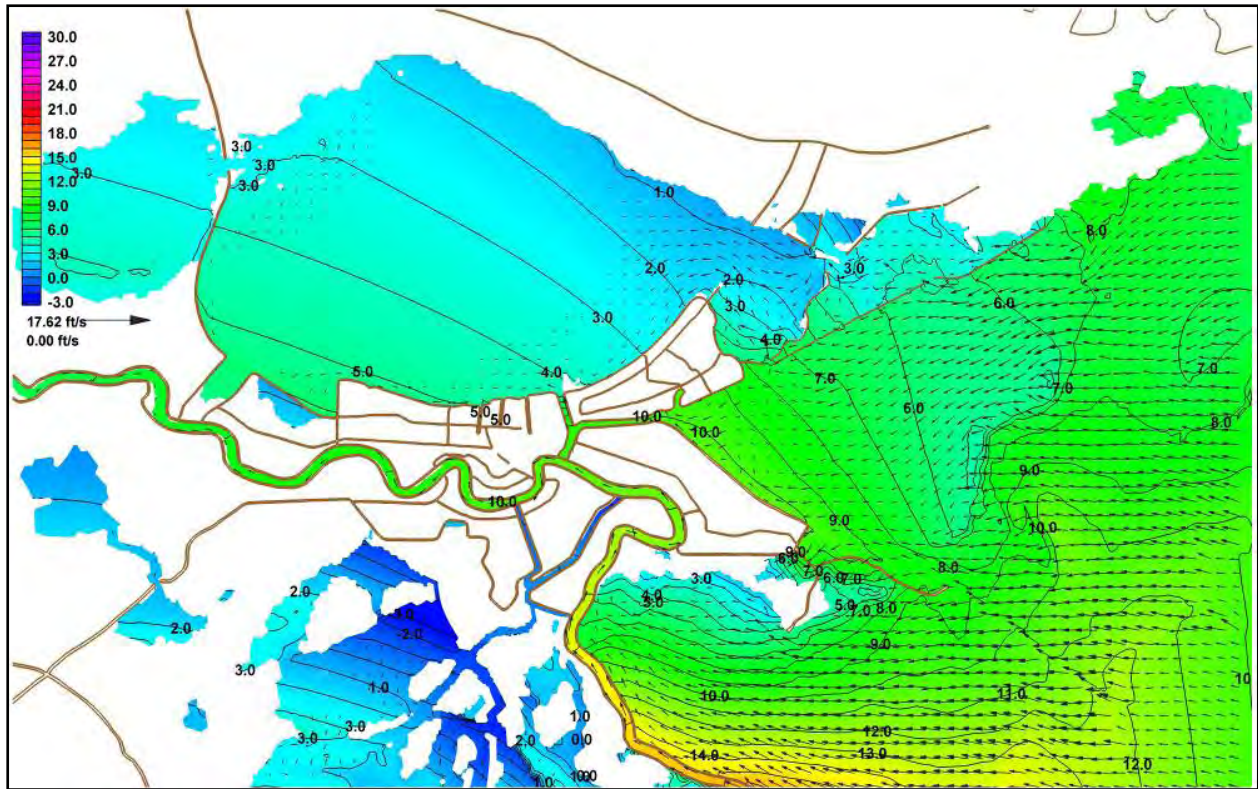


Figure 5-9b. Detail of water surface elevation in the vicinity of New Orleans with respect to the NAVD 88 (ft) with labeled contours and currents (ft/sec) on August 29, 2005 at 1000UTC

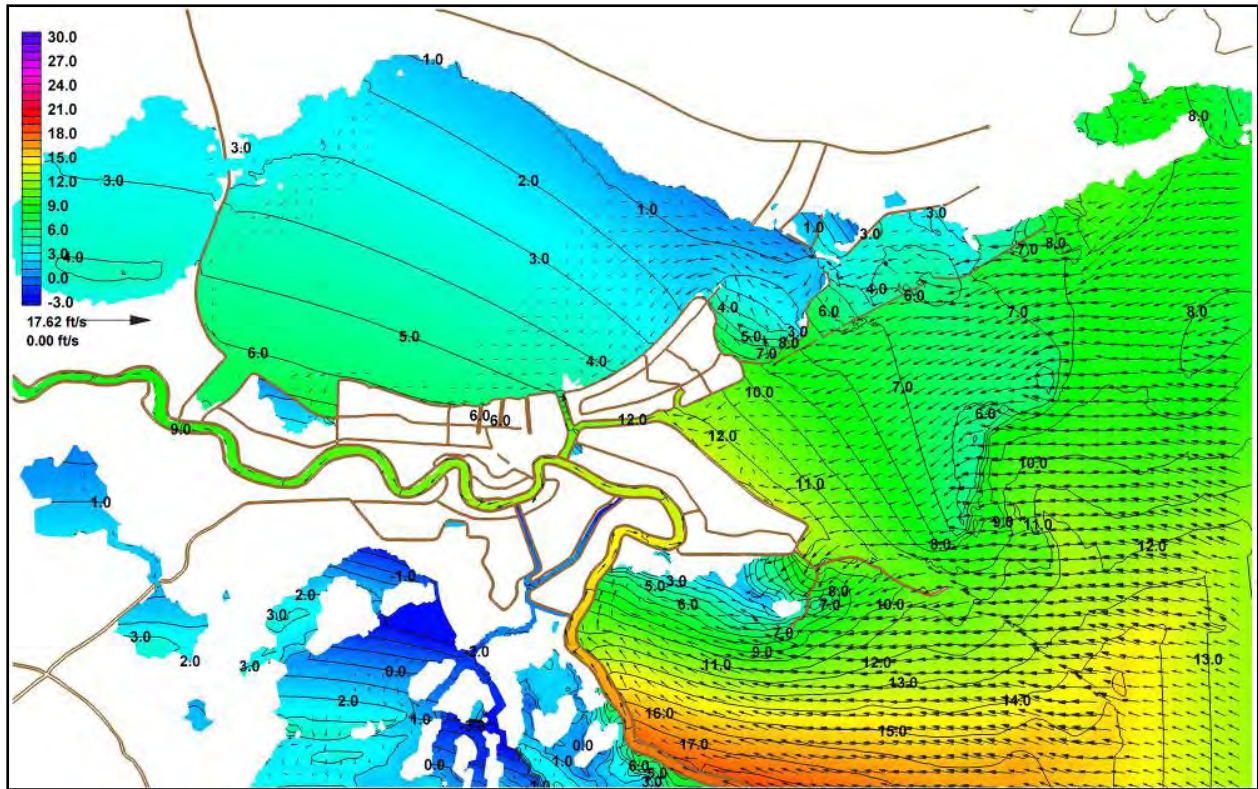


Figure 5-9c. Detail of water surface elevation in the vicinity of New Orleans with respect to the NAVD 88 (ft) with labeled contours and currents (ft/sec) on August 29, 2005 at 1100UTC



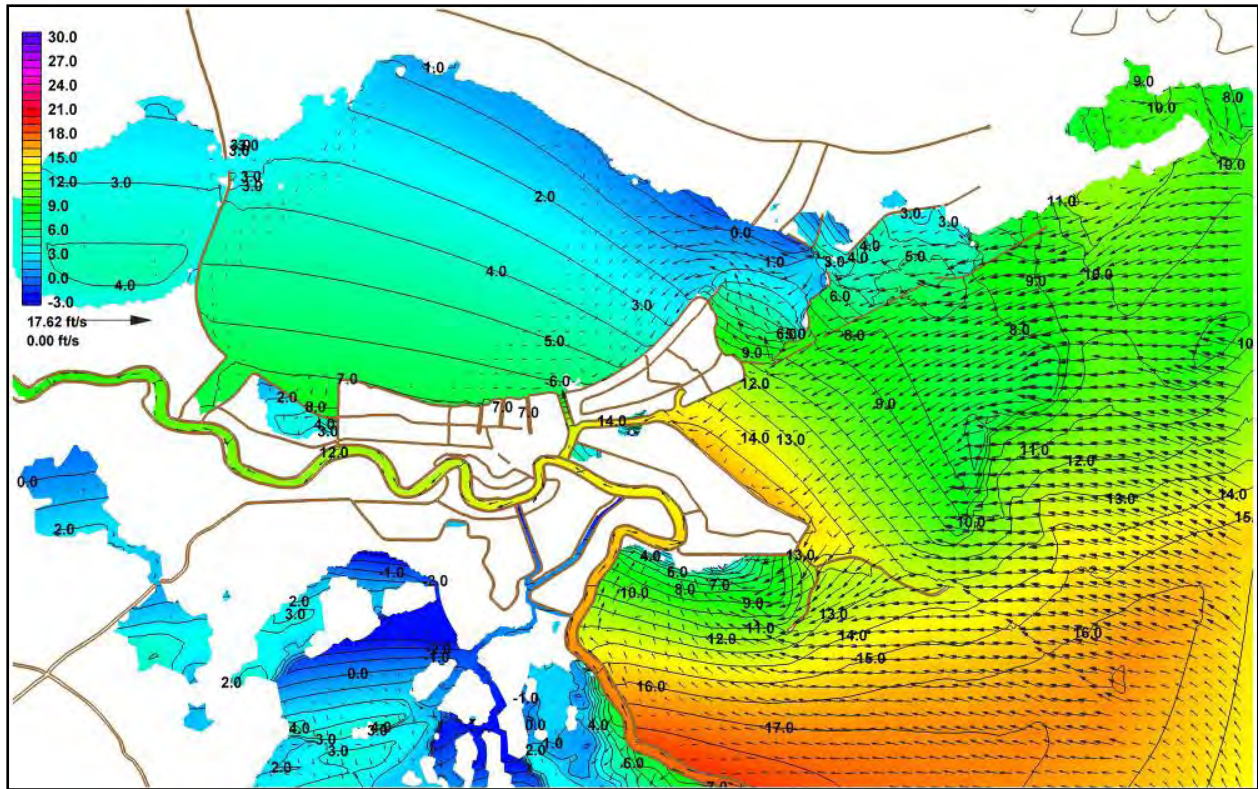


Figure 5-9d. Detail of water surface elevation in the vicinity of New Orleans with respect to the NAVD 88 (ft) with labeled contours and currents (ft/sec) on August 29, 2005 at 1200UTC

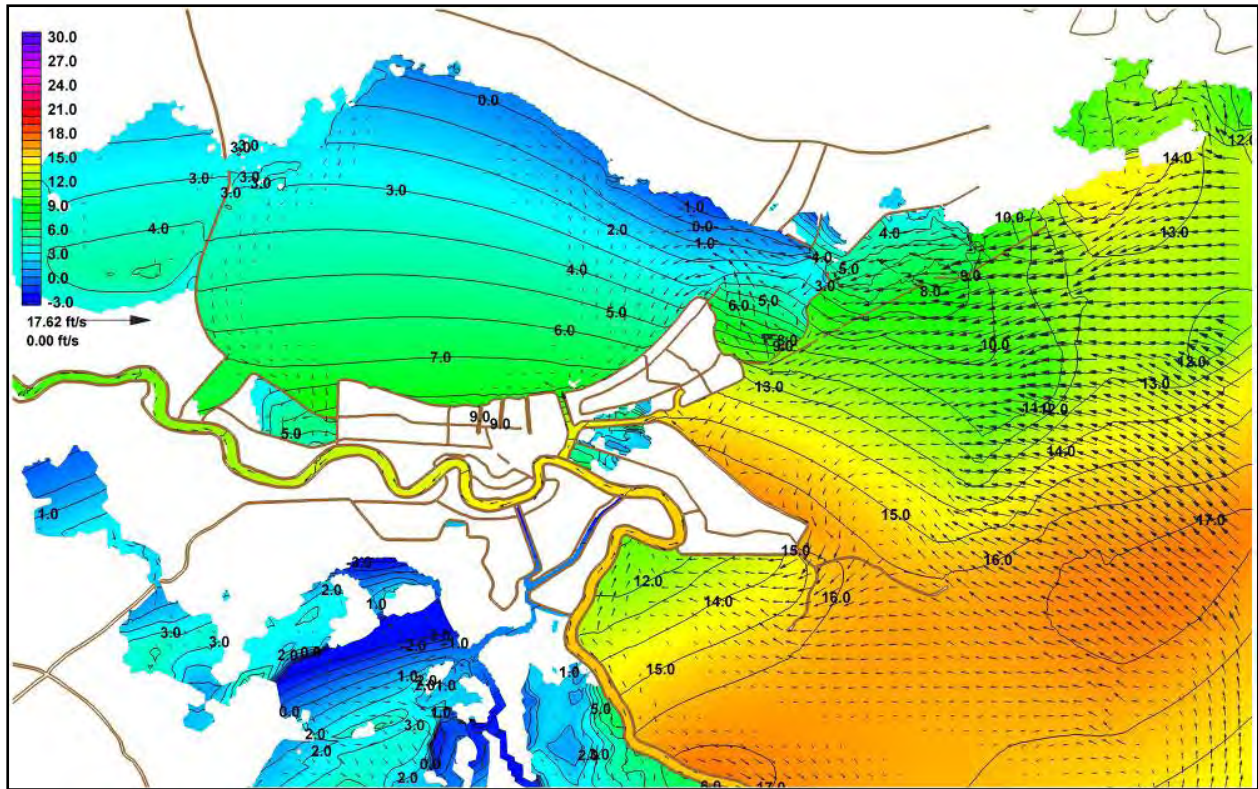


Figure 5-9e. Detail of water surface elevation in the vicinity of New Orleans with respect to the NAVD 88 (ft) with labeled contours and currents (ft/sec) on August 29, 2005 at 1300UTC



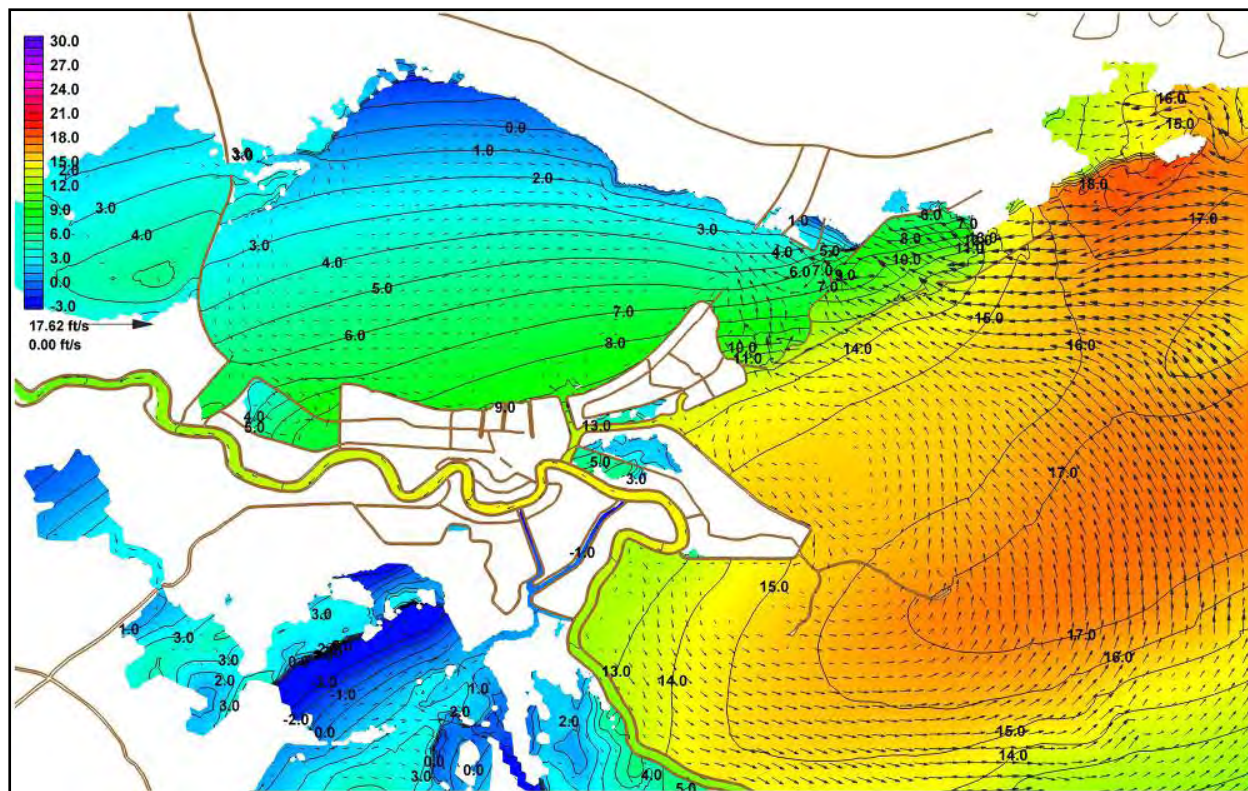


Figure 5-9f. Detail of water surface elevation in the vicinity of New Orleans with respect to the NAVD 88 (ft) with labeled contours and currents (ft/sec) on August 29, 2005 at 1400UTC



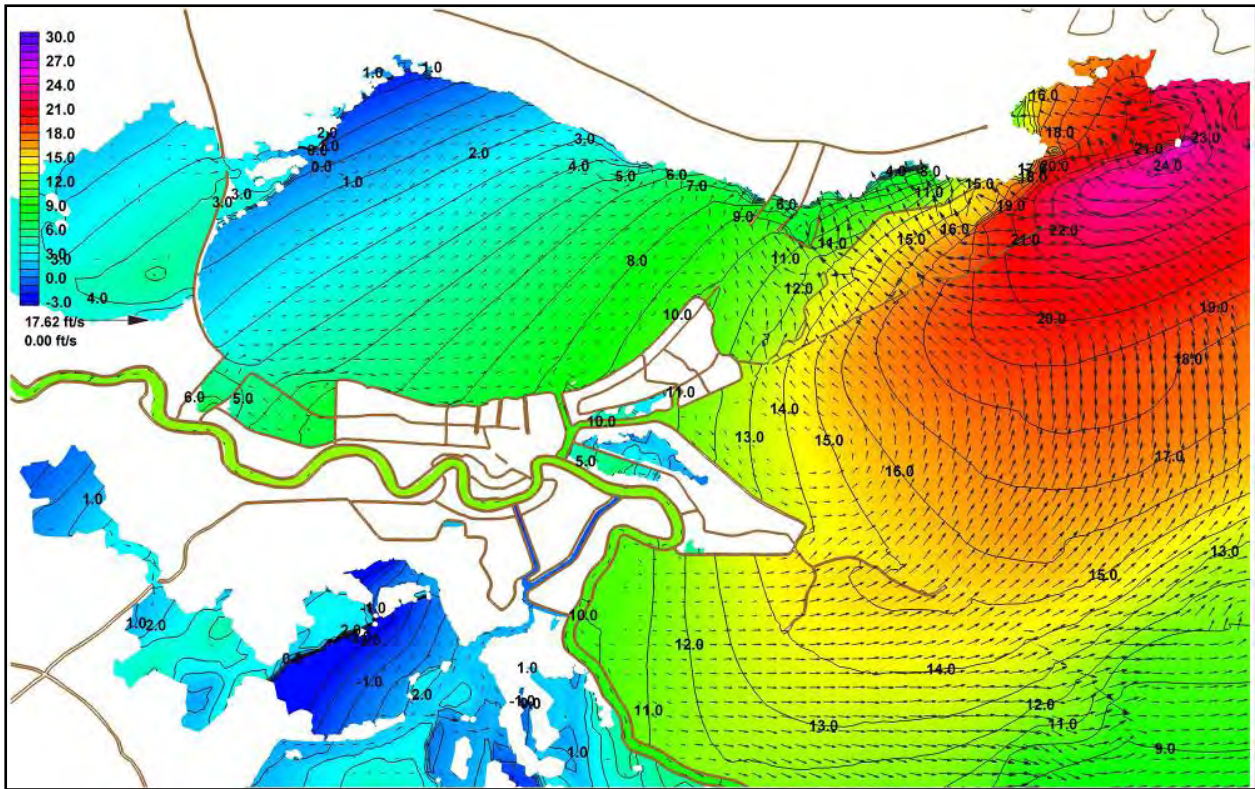


Figure 5-9g. Detail of water surface elevation in the vicinity of New Orleans with respect to the NAVD 88 (ft) with labeled contours and currents (ft/sec) on August 29, 2005 at 1500UTC

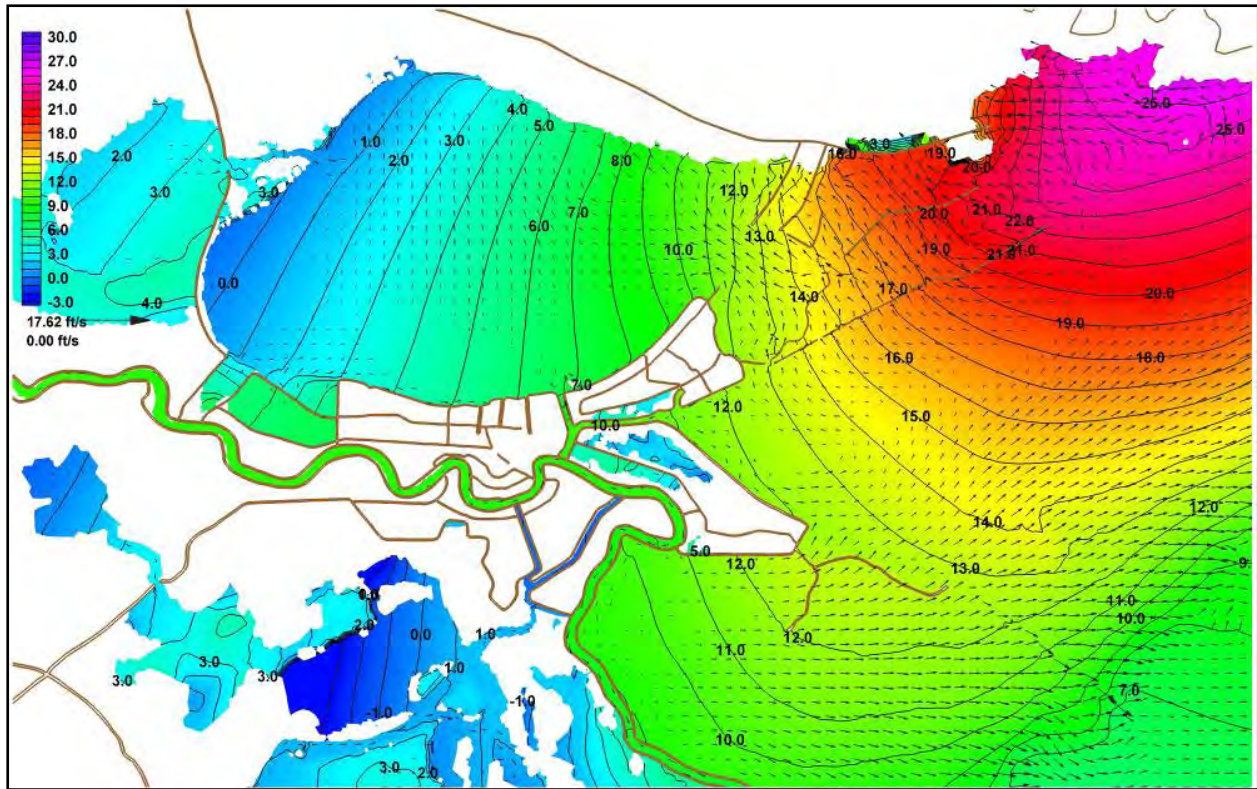


Figure 5-9h. Detail of water surface elevation in the vicinity of New Orleans with respect to the NAVD 88 (ft) with labeled contours and currents (ft/sec) on August 29, 2005 at 1600UTC



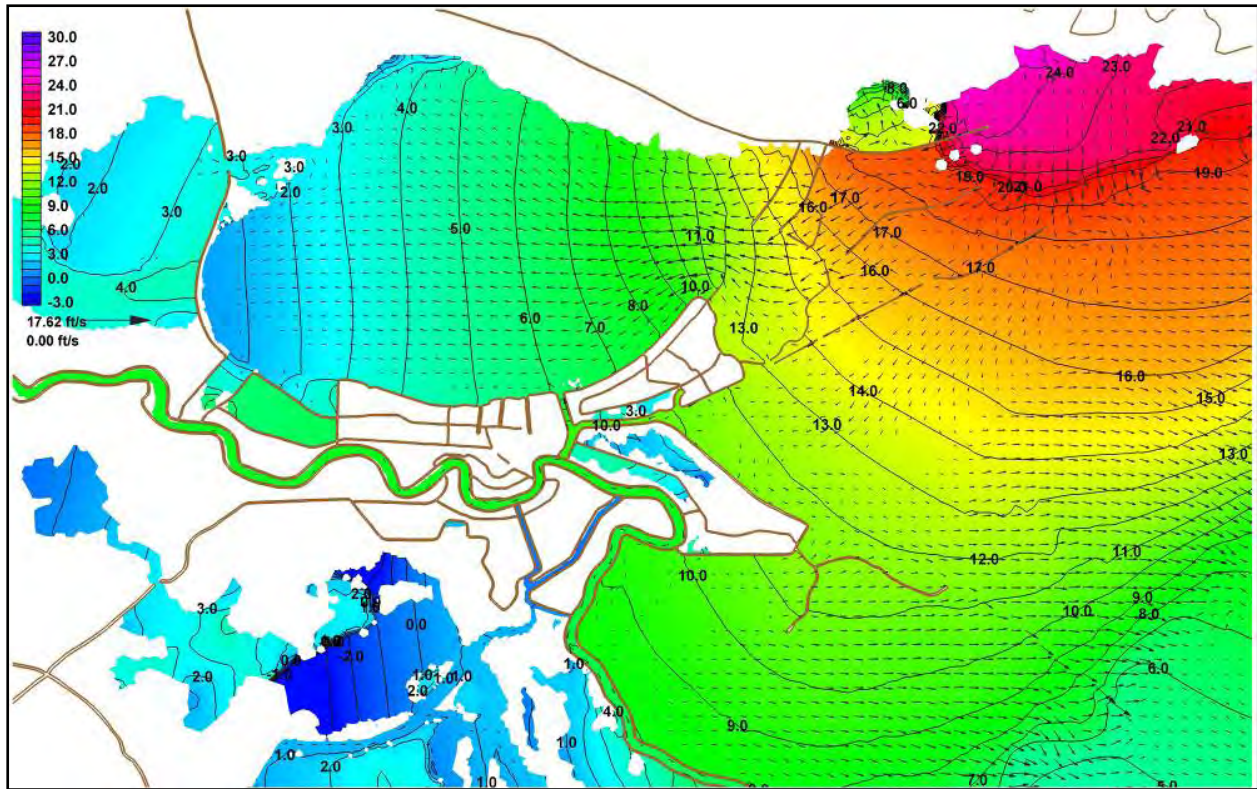


Figure 5-9i. Detail of water surface elevation in the vicinity of New Orleans with respect to the NAVD 88 (ft) with labeled contours and currents (ft/sec on August 29, 2005 at 1700UTC

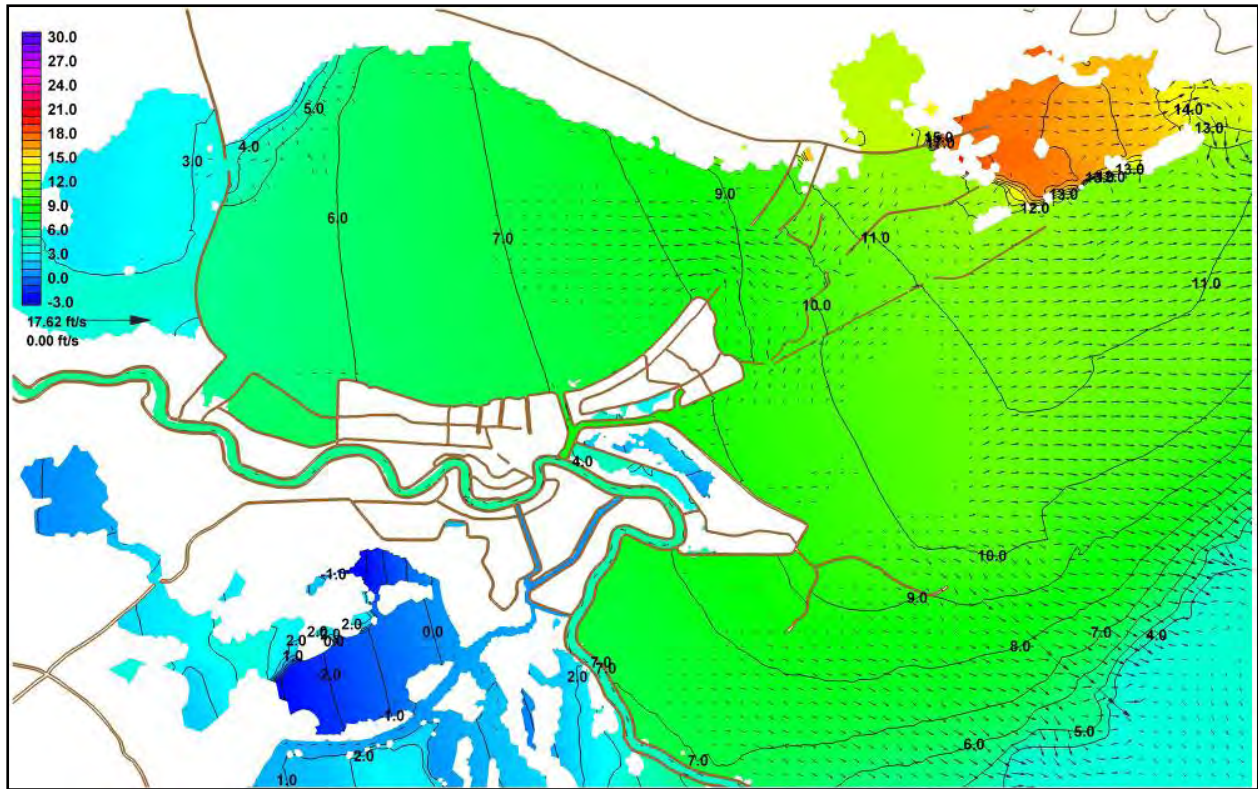


Figure 5-9j. Detail of water surface elevation in the vicinity of New Orleans with respect to the NAVD 88 (ft) with labeled contours and currents (ft/sec) on August 29, 2005 at 2000UTC



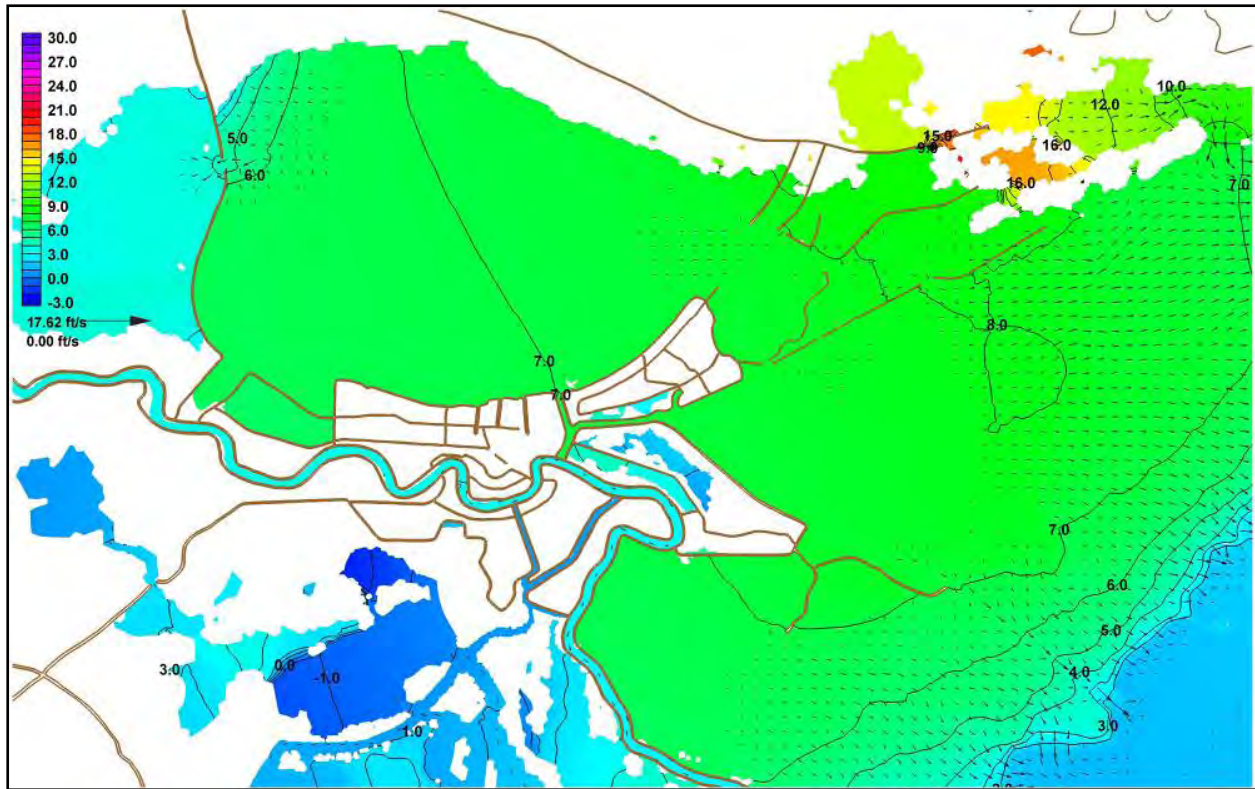


Figure 5-9k. Detail of water surface elevation in the vicinity of New Orleans with respect to the NAVD 88 (ft) with labeled contours and currents (ft/sec) on August 29, 2005 at 2300UTC

## Model Validation

The ADCIRC Katrina hindcast was validated by comparing computed water elevations to available hydrographs as well as to available excellent and good high water marks in Louisiana and Mississippi. All water level values were computed with respect to NAVD 88 2004.65 and were compared to observed water levels and high water marks relative to the same datum.

Time series of model response during Hurricane Katrina are compared to water level data at the tidal and river gauges. Hydrographs at 7 stations are plotted with the data records and model output in Figure 5-10. The model shows a very good match to both the tidal signal and the storm surge. Furthermore the datums appear to be well matched. The comparison at the mouth of the Mississippi River at South Pass indicates that the modeled tides are well represented in the region. The peak storm surge is under-predicted by about 1.8 ft. However nearby high water marks indicate that the observed peak value may somewhat under-represent the surge in the region. Specifically there are three nearby high water marks that indicate peak still water levels of 8.9, 8.6 and 8.5 ft. This more closely matches the ADCIRC predicted value. The gauge at Carrollton in the Mississippi River adjacent to New Orleans indicates that the model correctly captures the propagation of tides and surge up the Mississippi River. The tides are slightly under-damped; the computed peak water level is approximately 1.5 ft less than the measured value. It is noted that the recording station failed after the peak surge passed New Orleans. The



model results at Little Irish Bayou on Lake Ponchartrain side of Chef Menteur Pass shows rising water levels matching recorded levels. This gauge failed well before high water levels were reached. Model results at the location of the gauge in Lake Ponchartrain, Midlake, appear to match with the portion of the record that is available. The gauge failed in the middle of the storm but started recording again. It is noted that the ADCIRC model shows two peaks occurring in the lake. The first corresponds to high water being driven by winds from the north and northeast piling water against the south shore of the lake. The second and slightly larger and broader peak corresponds to the massive intrusion of water coming in from Lake Borgne driven by high waters associated with the second landfall of the storm on the Louisiana – Mississippi coast. It is noted that the drainage rate at Midlake is slightly slower in the model than the measured rate. The comparison at the 17th Street Canal indicates that the model is under-predicting peak surge by about 2 ft. More detailed local Boussinesq models have indicated that there is more wave set up than computed with this regional model, as much as 1.5-2 ft. Note that simulating wave setup properly would require grid resolution on the order of 3 to 10 m (10 to 30 ft) in order to capture the interaction of the breaking waves with the local roads (e.g. Lake Shore Drive), topography and the levee structures themselves. For this study, that interaction was considered in the high resolution hydrodynamics component of the project. The measured hydrograph compared to the ADCIRC hydrograph does show a good correspondence between the timing of the two peaks. The first is again associated with the wind driven peak from the westerly and northerly winds while the second is associated with the intrusion of high water from Lake Borgne. Again modeled drainage rates are slightly lower than measured. The comparison at Bayou Labranche is markedly different. While the model indicates that water levels abruptly rise and do not recede, the measured water levels indicate a gradual rise and a gradual recession. This is related to the fact that the TF01x2 model has included the railroad that runs along Lake Ponchartrain between the Kenner's western protection levee and the Bonnet Carre Spillway as a solid structure. The actual railroad includes a number of porous truss/piling based openings to the lake. Note that this also affects water levels against the protection levee to the west of Kenner since water is being unrealistically kept within the system, more water can be blown up against the system when winds are coming from the west towards the end of the storm. Finally water levels at Pass Manchac on the west side of the Lake compare to within 1 ft of the measured values, showing excellent agreement in terms of timing and reproduction of all hydrograph features.

Plots of modeled versus recorded peak storm surge values at all Katrina high water mark locations identified as either excellent or good are presented in Figures 5-11 for Louisiana and Mississippi. The data points are expected to lie along a 1:1 line. If a data point is above this line it indicates over-prediction in storm surge by the model, and a point under the line indicates under-prediction. Linear regression analysis of the data is used to generate a best fit line through the data and the origin. The results of this analysis can be used to compare the slope of the best fit line to the expected 1:1 line. This best fit line is generated in a least squares manner, and the overall quality of fit is given by the correlation coefficient  $R^2$ . For Louisiana, comparisons were made to 101 high water marks and are shown in Figure 5-11a. The slope of the line through all data points is 0.954, indicating that the model is on average under-predicting surge by 4.6 %. The average error is -0.48 ft while the average absolute error is 1.4 ft. The correlation coefficient ( $R^2$ ) is 0.81 for the entire Louisiana data set, demonstrating that the modeled peak surge is closely related to the recorded peak surge and the results are clustered about the 1:1 line. For Mississippi, comparisons were made to 105 high water marks which are shown in Figure 5-11b.

The slope of the line through all data points is 0.99, indicating that the model is on average under-predicting surge by less than 1%. The average error is -0.23 ft while the average absolute error is 1.3 ft. We note that in general surge values in Mississippi were quite high falling between 15 ft and 26 ft. The correlation coefficient ( $R^2$ ) is 0.81 for the entire Mississippi data set.

Figures 5-12a through 5-12i show the ADCIRC maximum water surface contours plotted together with all observed excellent and good high water marks. The colors within the circles indicate observed water level using the same elevation colors as the ADCIRC computed contours. Thus the closer the color within the circle to the adjacent color contour, the better the prediction. The numbers plotted next to each circle indicate the difference between the ADCIRC computed value and the observed high water mark. Negative value indicates under-prediction by the model and positive values indicate over-prediction. The error values have also been plotted onto topographic/bathymetric contours in Figure 5-13a through 5-13i. The circle colors in these plots indicate the level of error and are the difference between the ADCIRC computed value and the observed high water mark. The numeric value of this error is again plotted adjacent to each high water mark. These plots allow identification of the level of error associated with each high water mark. In general, note that there are typically missing features, processes and/or poor grid resolution associated with the more substantial errors. For example in Plaquemines Parish, the missing back levees lead to over-prediction when the surge comes from Barataria Bay and under-prediction when the water comes from over-topping of river levees as it does further north. In Mississippi, missing railroads and roads lead to under-prediction adjacent to the coast since these features tend to allow more water to collect seaward of the feature. Inadequate resolution in the circulation and wave models as well as missing features such as Lake Shore Drive lead to the under-prediction of wave induced setup on the south shore of Lake Ponchartrain. Further inland, the model generally tends to over-predict surge unless the area is connected to a well defined inland waterway. This over-prediction is likely related to missing features such as raised roads or railroads (particularly in Mississippi) and/or not accounting for the increased bottom friction and dissipation associated with inland land cover.

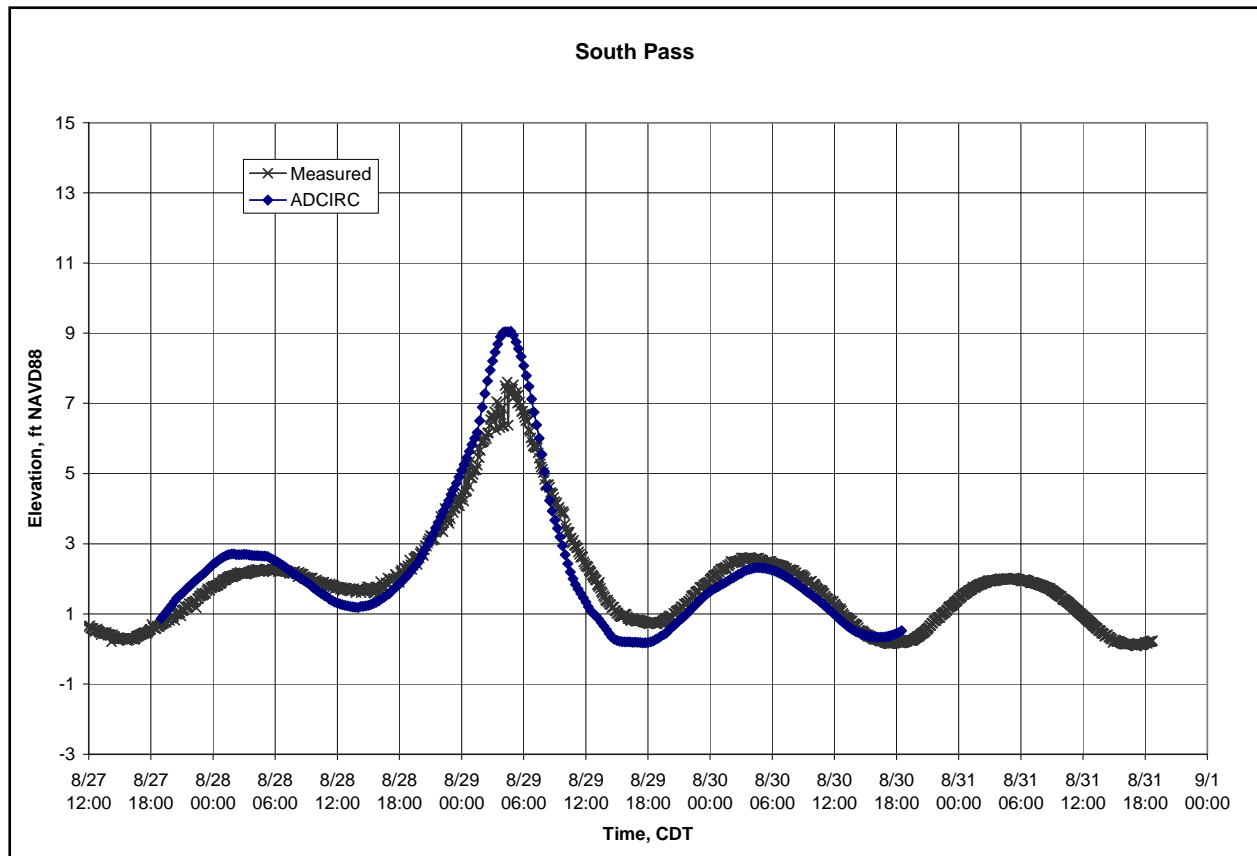


Figure 5-10a. Comparison of modeled versus measured storm surge hydrograph (ft NAVD88 2004.65) at the South West Pass, LA

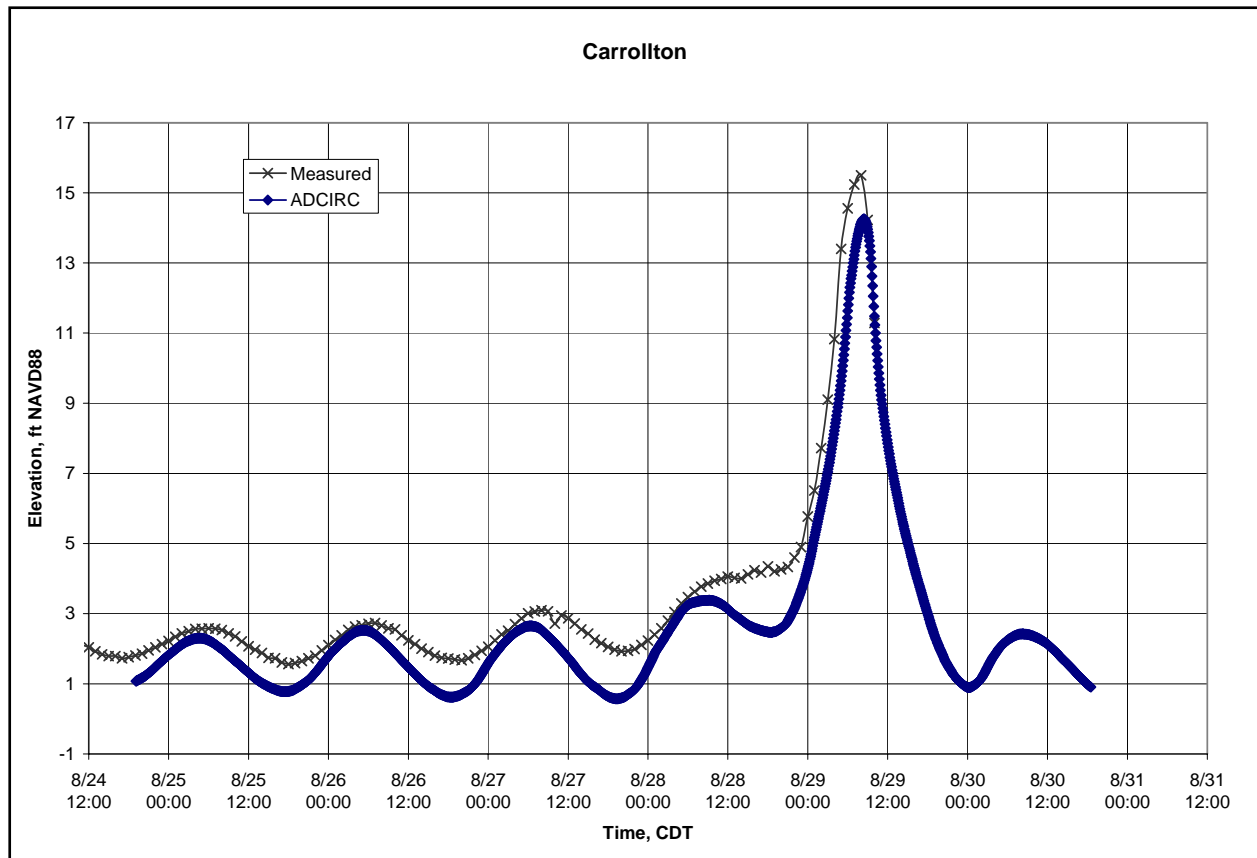


Figure 5-10b. Comparison of modeled versus measured storm surge hydrograph (ft NAVD88 2004.65) at the Carrollton gauge at New Orleans within the Mississippi River

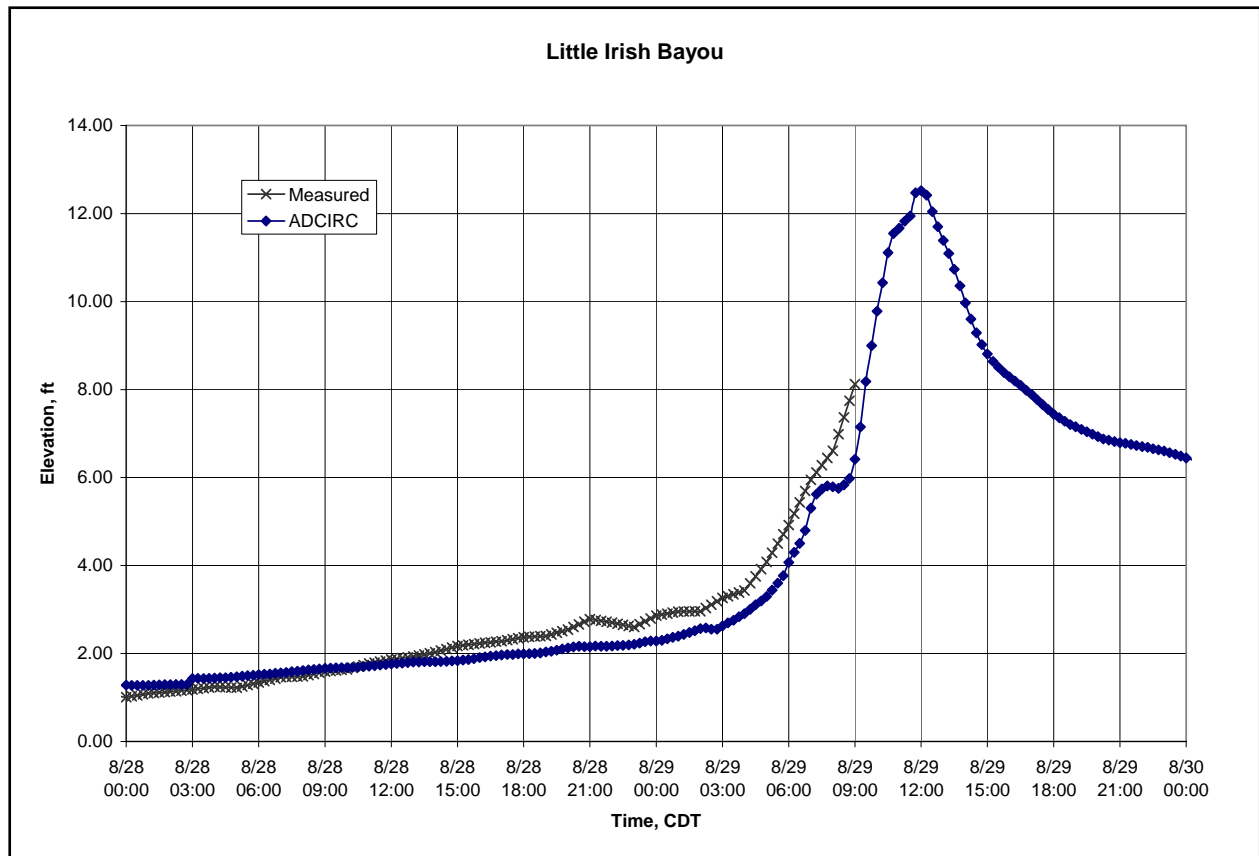


Figure 5-10c. Comparison of modeled versus measured storm surge hydrograph (ft NAVD88 2004.65) at Little Irish Bayou near Lake Pontchartrain



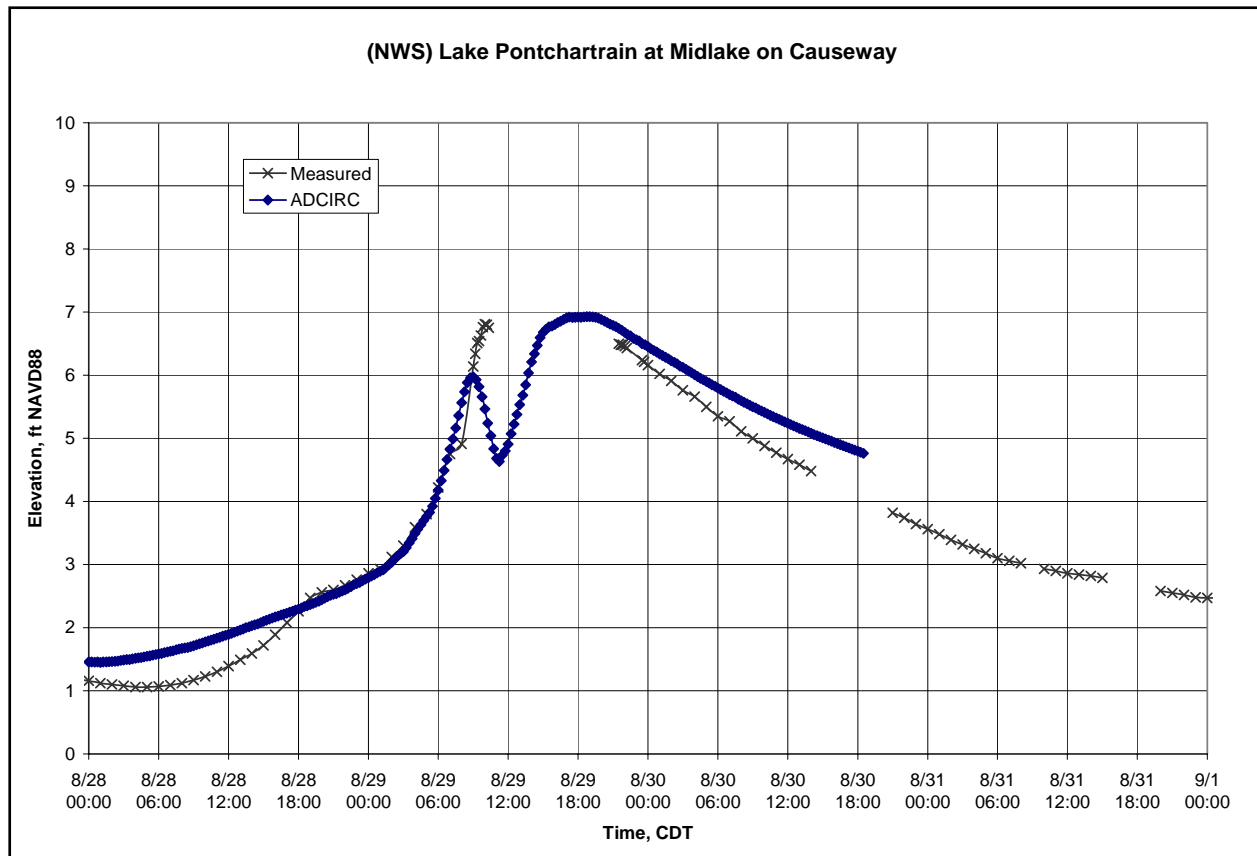


Figure 5-10d. Comparison of modeled versus measured storm surge hydrograph (ft NAVD88 2004.65) at Lake Pontchartrain at Midlake on the Causeway

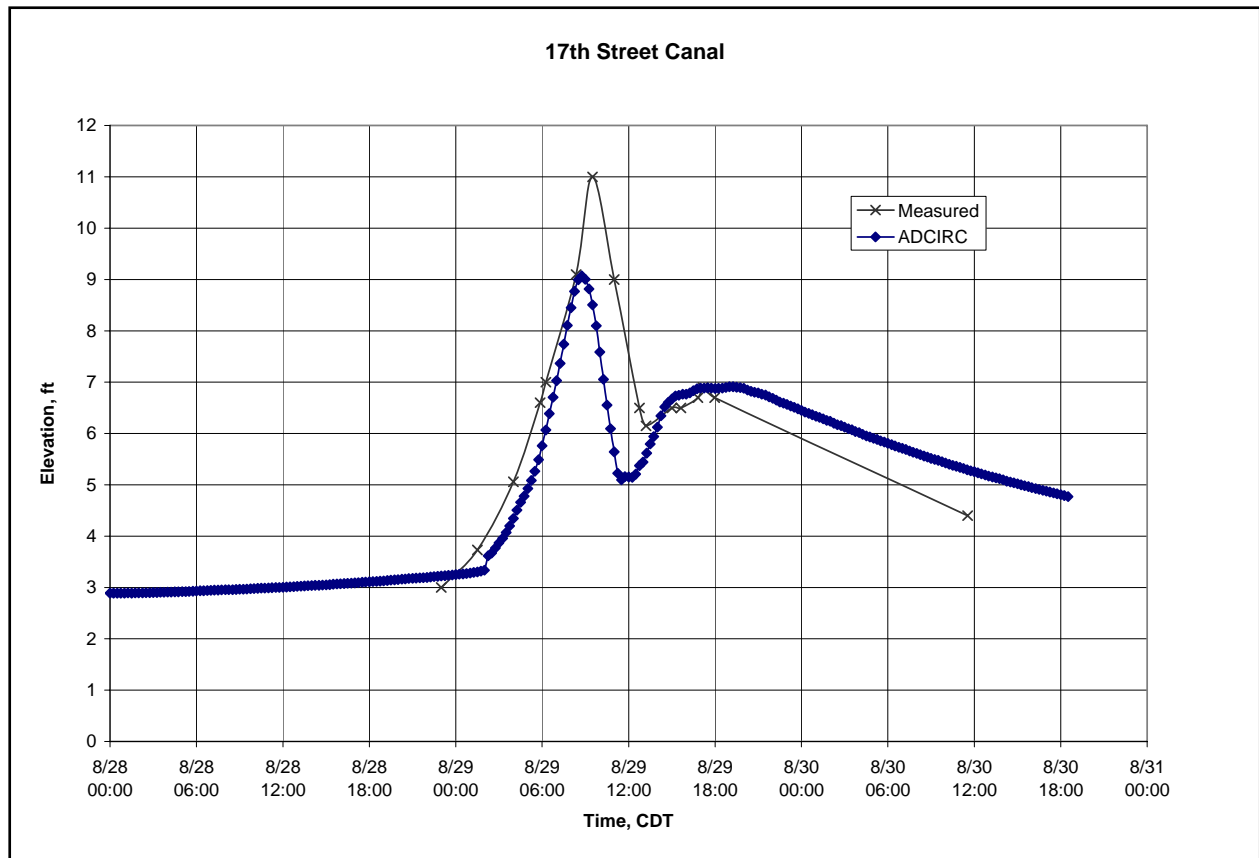


Figure 5-10e. Comparison of modeled versus measured storm surge hydrograph (ft NAVD88 2004.65) in Lake Ponchartrain at the 17th Street Canal

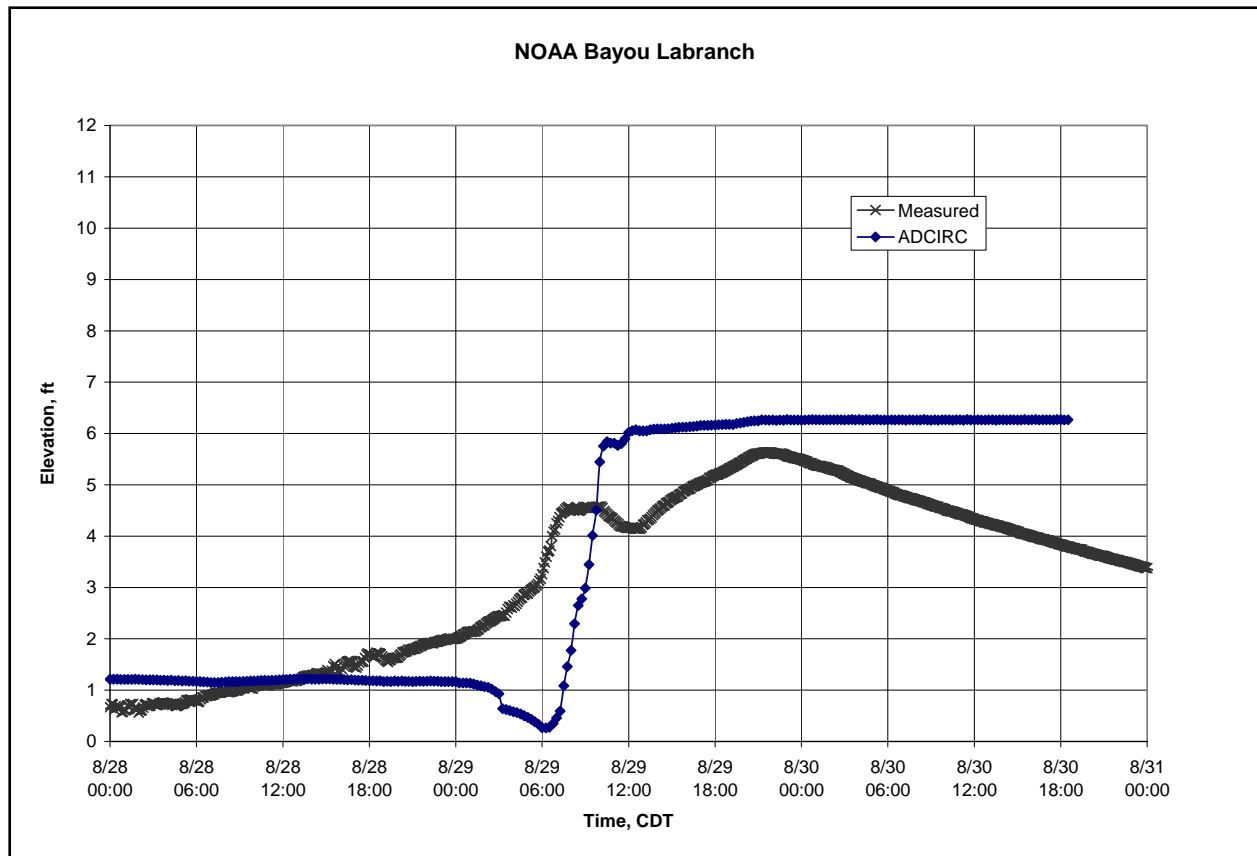


Figure 5-10f. Comparison of modeled versus measured storm surge hydrograph (ft NAVD88 2004.65) at Bayou Labranch behind the railroad near the Bonnet Carre spillway

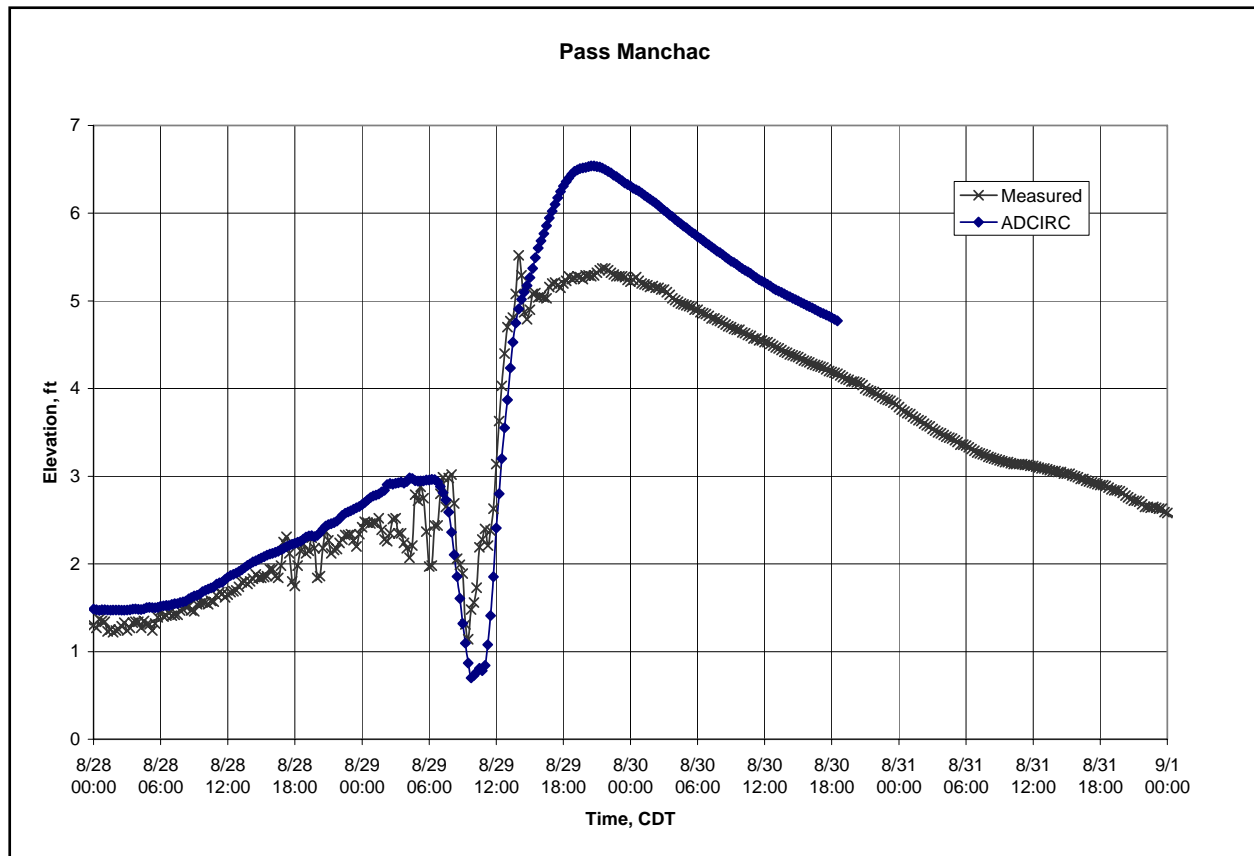


Figure 5-10g. Comparison of modeled versus measured storm surge hydrograph (ft NAVD88 2004.65) at Pass Manchac

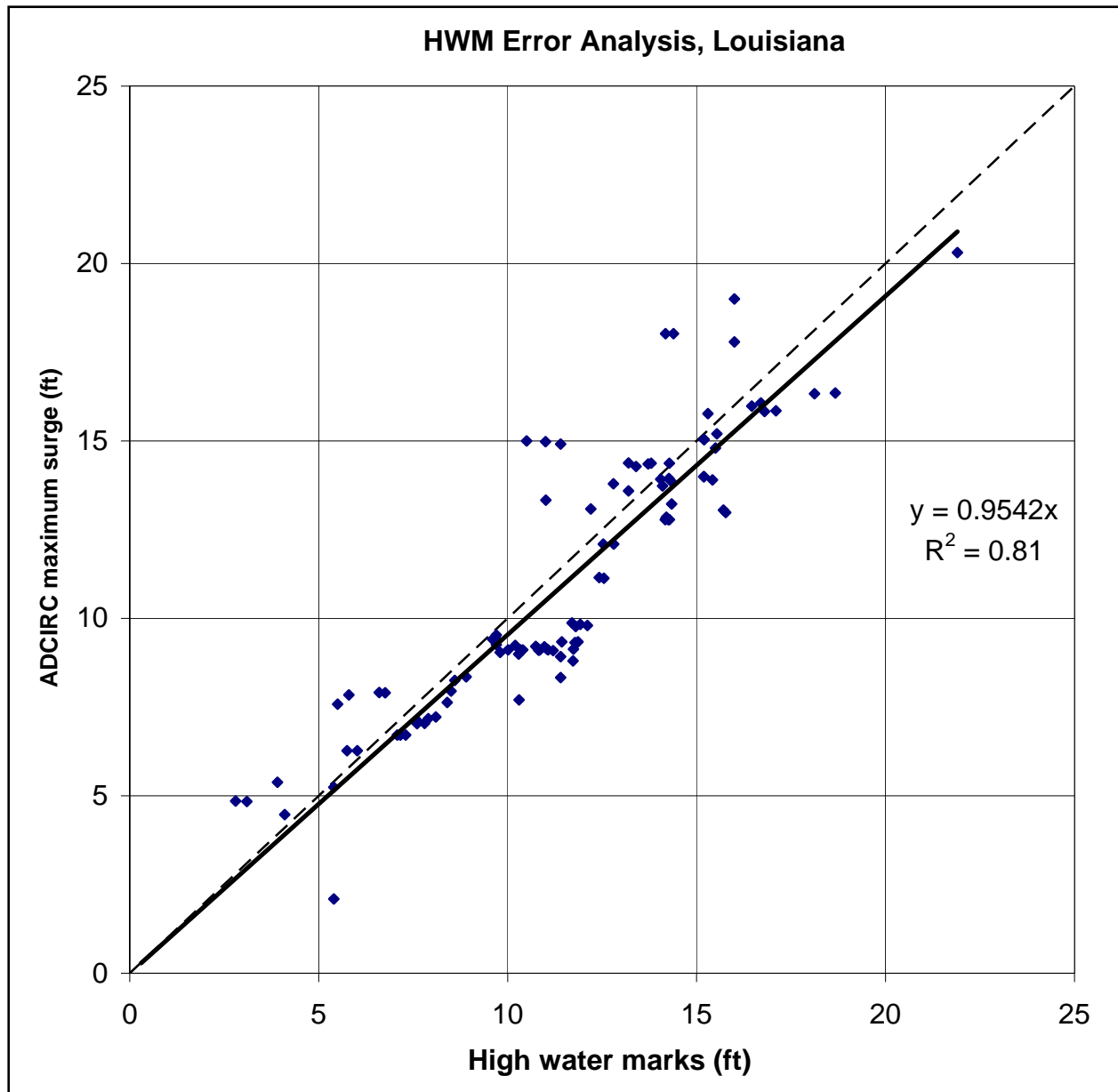


Figure 5-11a. Comparison of modeled versus observed peak storm surge elevation (ft NAVD88 2004.65) using good and excellent high water marks in Louisiana



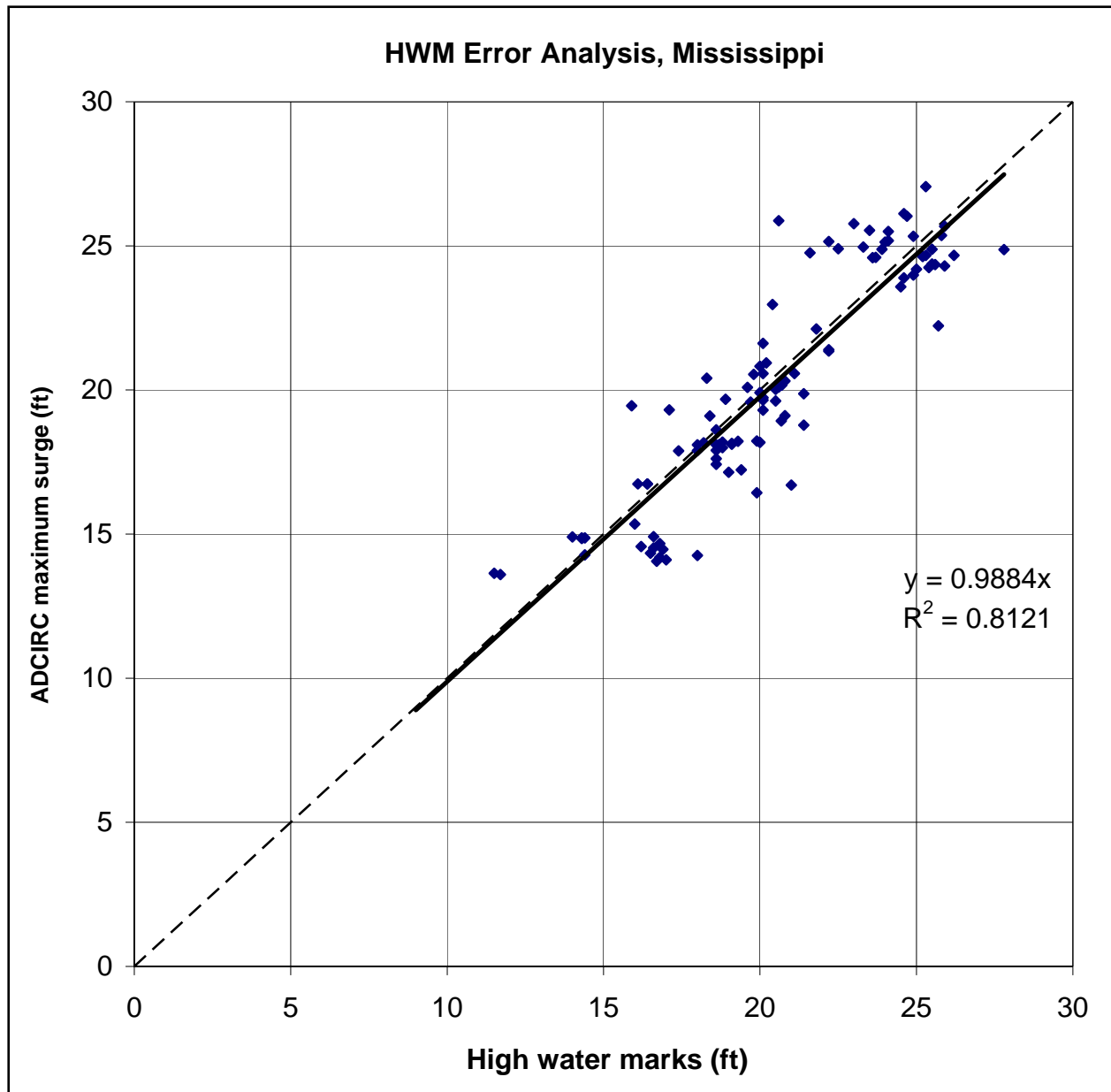


Figure 5-11b. Comparison of modeled versus observed peak storm surge elevation (ft NAVD88 2004.65) using good and excellent high water marks in Mississippi

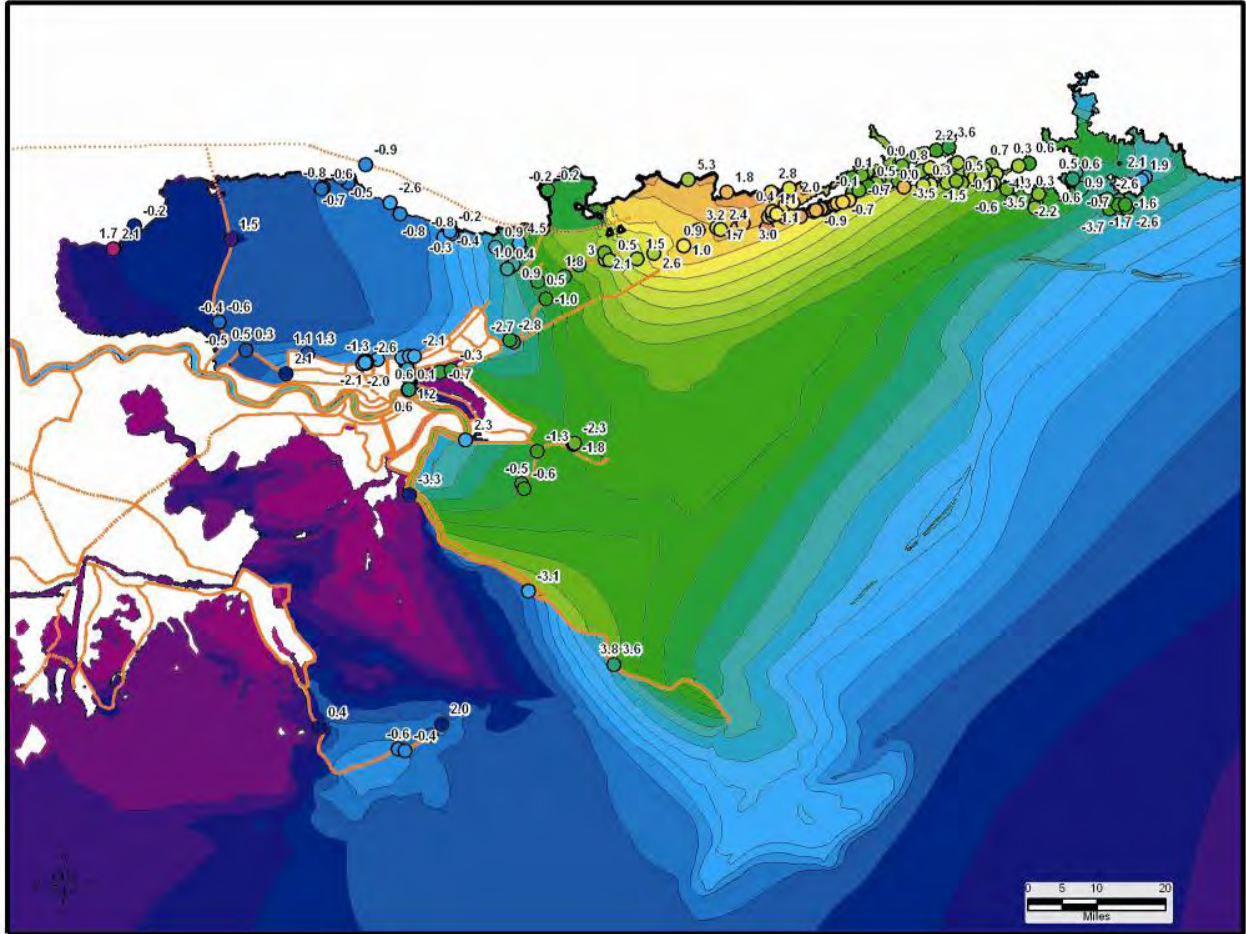


Figure 5-12a. Modeled maximum event elevation contours and HWM elevations in circles (ft NAVD 88 2004.65) with errors (ft) in Southern Louisiana and Mississippi

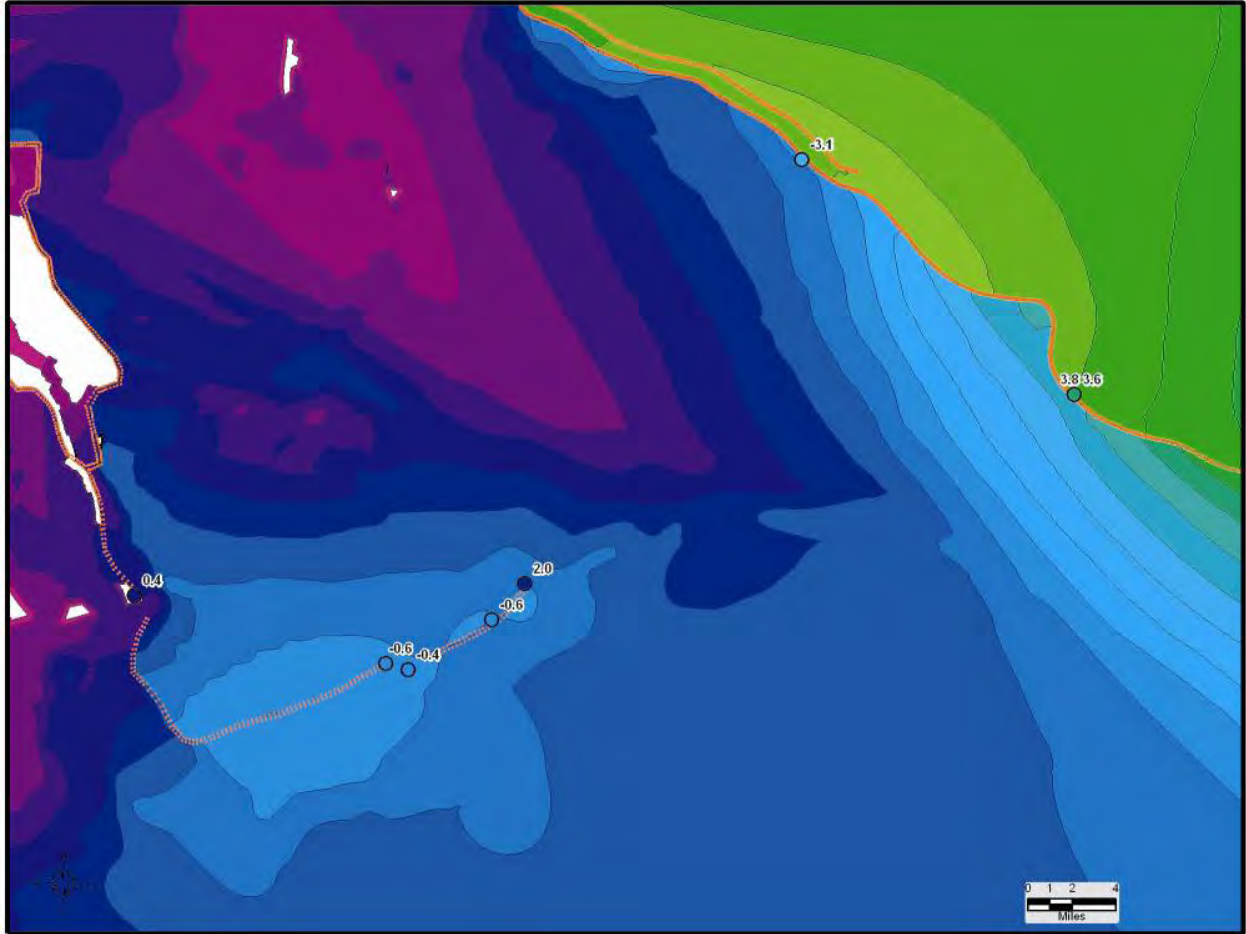


Figure 5-12b. Modeled maximum event elevation contours and HWM elevations in circles (ft NAVD 88 2004.65) with errors (ft). Detail between Grande Isle and western Plaquemines Parish



Figure 5-12c. Modeled maximum event elevation contours and HWM elevations in circles (ft NAVD 88 2004.65) with errors (ft). Detail in the vicinity of metropolitan New Orleans





Figure 5-12d. Modeled maximum event elevation contours and HWM elevations in circles (ft NAVD 88 2004.65) with errors (ft). Detail in the vicinity of the GIWW and IHNC



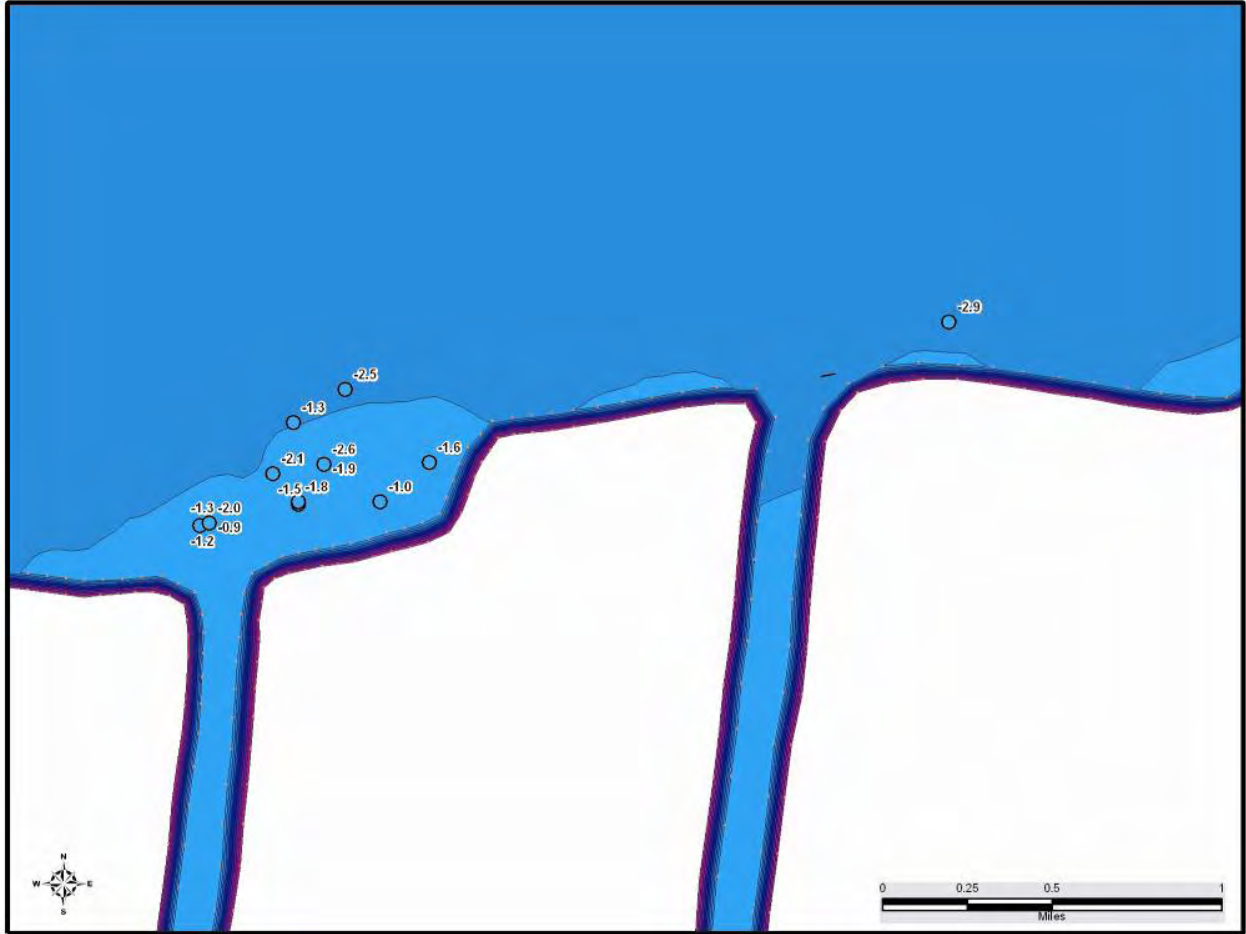


Figure 5-12e. Modeled maximum event elevation contours and HWM elevations in circles (ft NAVD 88 2004.65) with errors (ft). Detail of Orleans Parish, Lake Pontchartrain shore

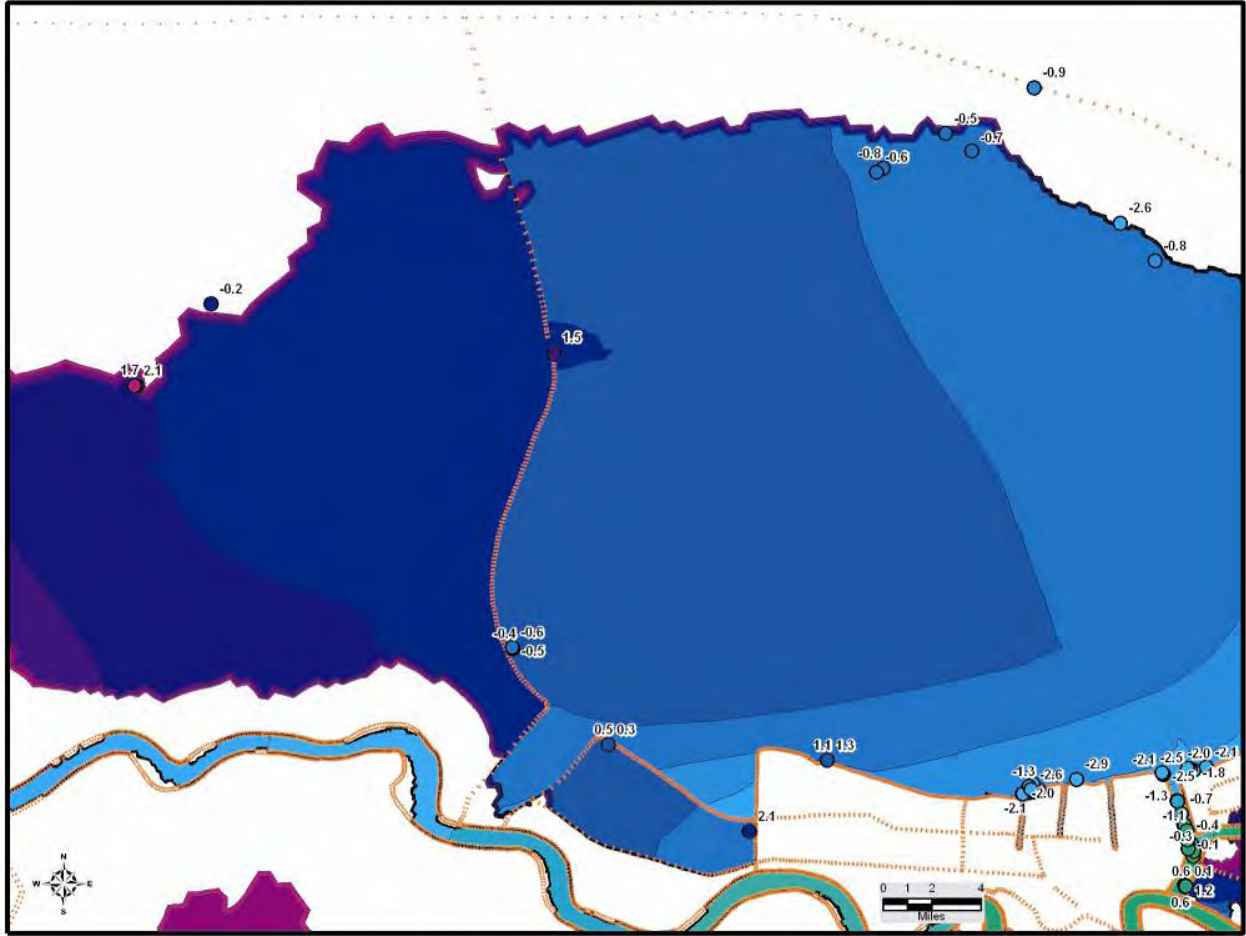


Figure 5-12f. Modeled maximum event elevation contours and HWM elevations in circles (ft NAVD 88 2004.65) with errors (ft). Detail of Lake Pontchartrain

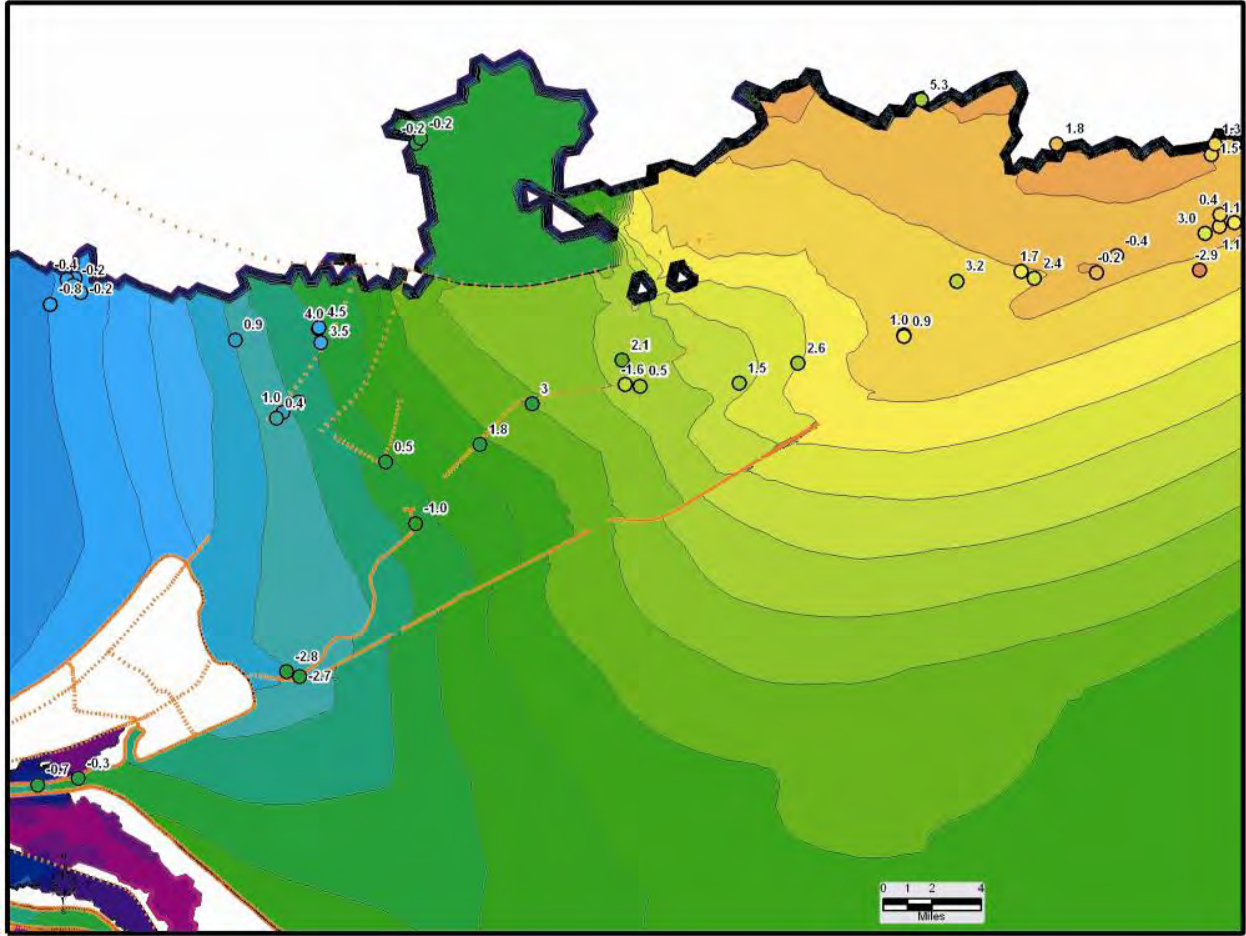


Figure 5-12g. Modeled maximum event elevation contours and HWM elevations in circles (ft NAVD 88 2004.65) with errors (ft). Detail of New Orleans East and Slidell, MS

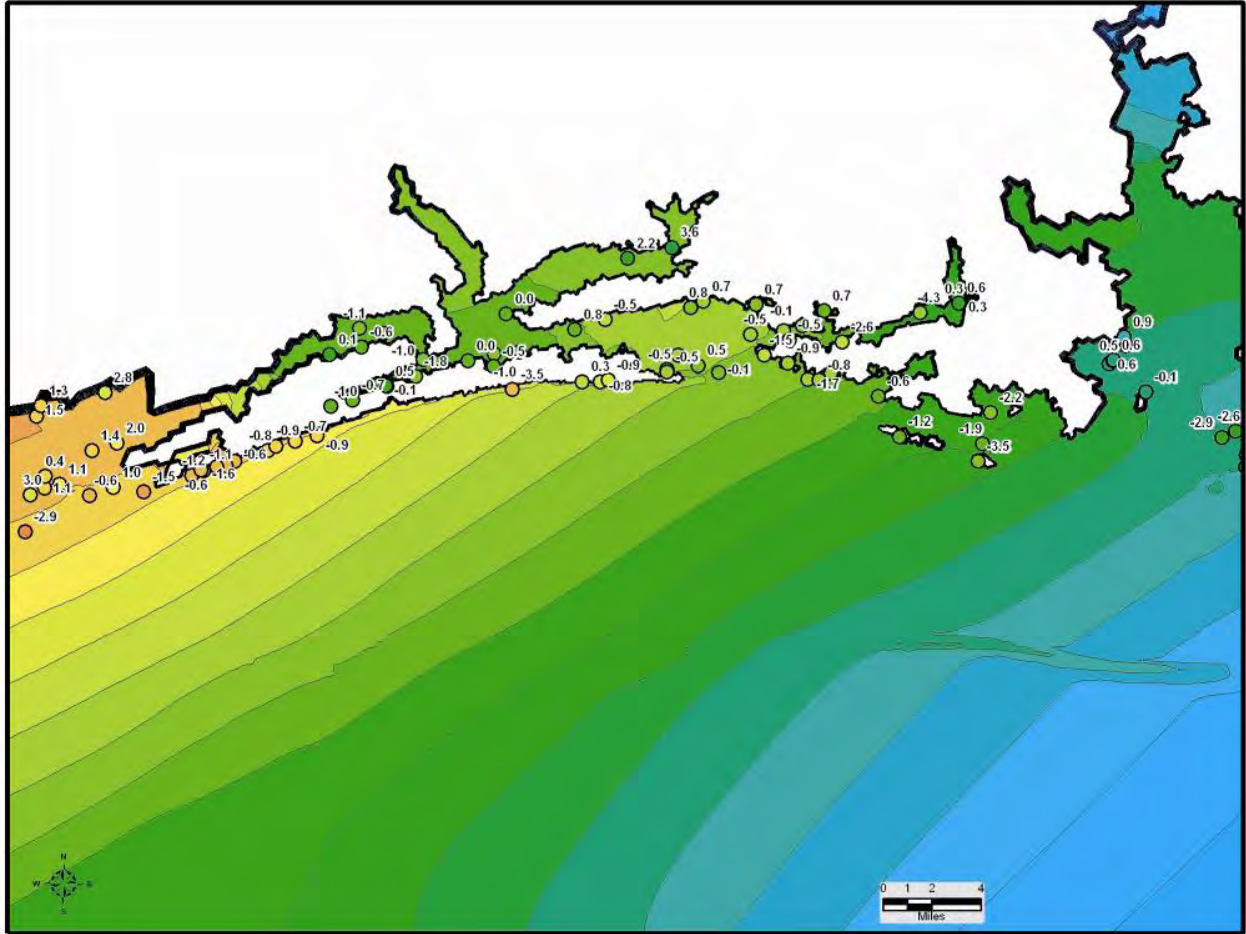


Figure 5-12h. Modeled maximum event elevation contours and HWM elevations in circles (ft NAVD 88 2004.65) with errors (ft). Detail of Mississippi coast



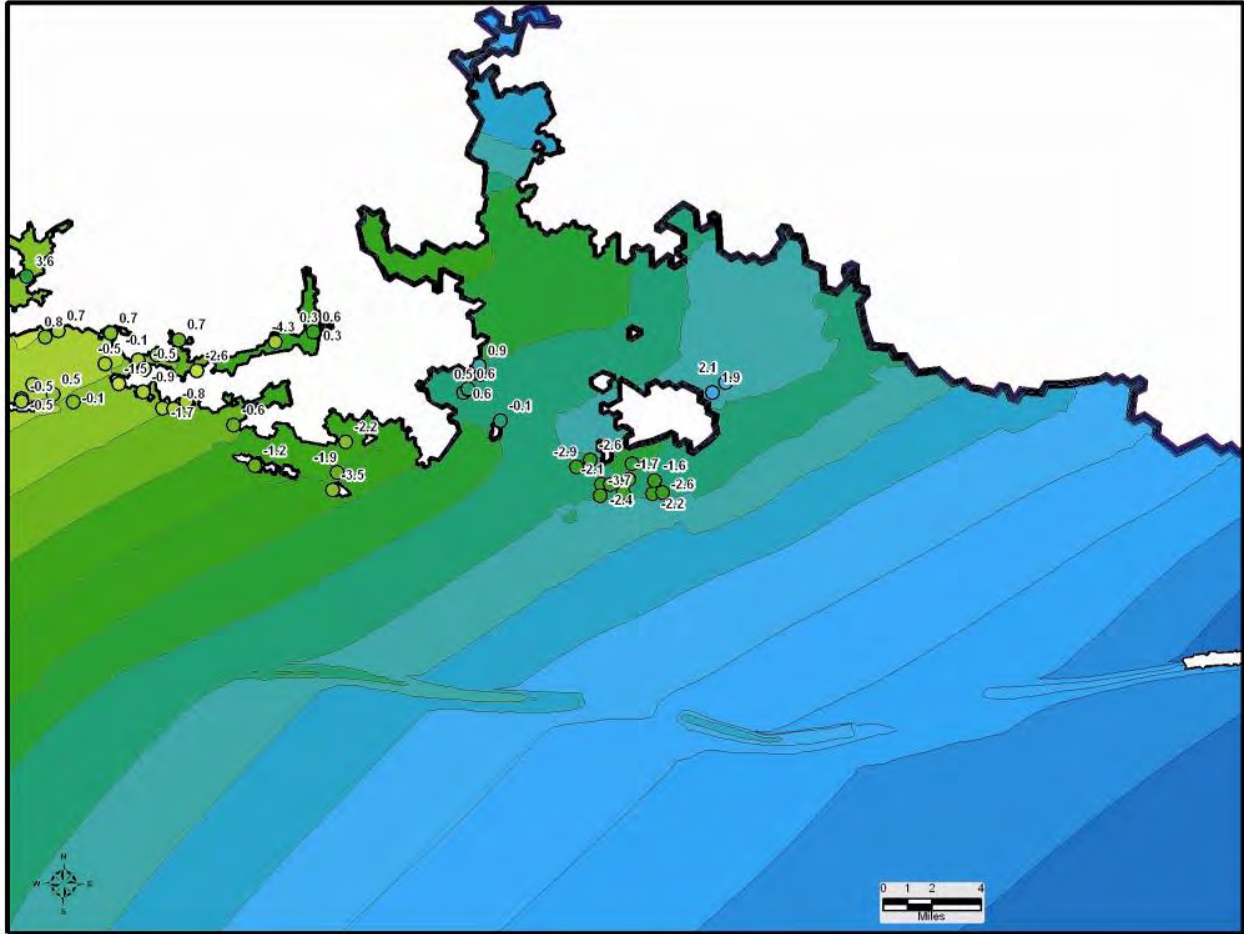


Figure 5-12i. Modeled maximum event elevation contours and HWM elevations in circles (ft NAVD 88 2004.65) with errors (ft). Detail of Jackson County, MS



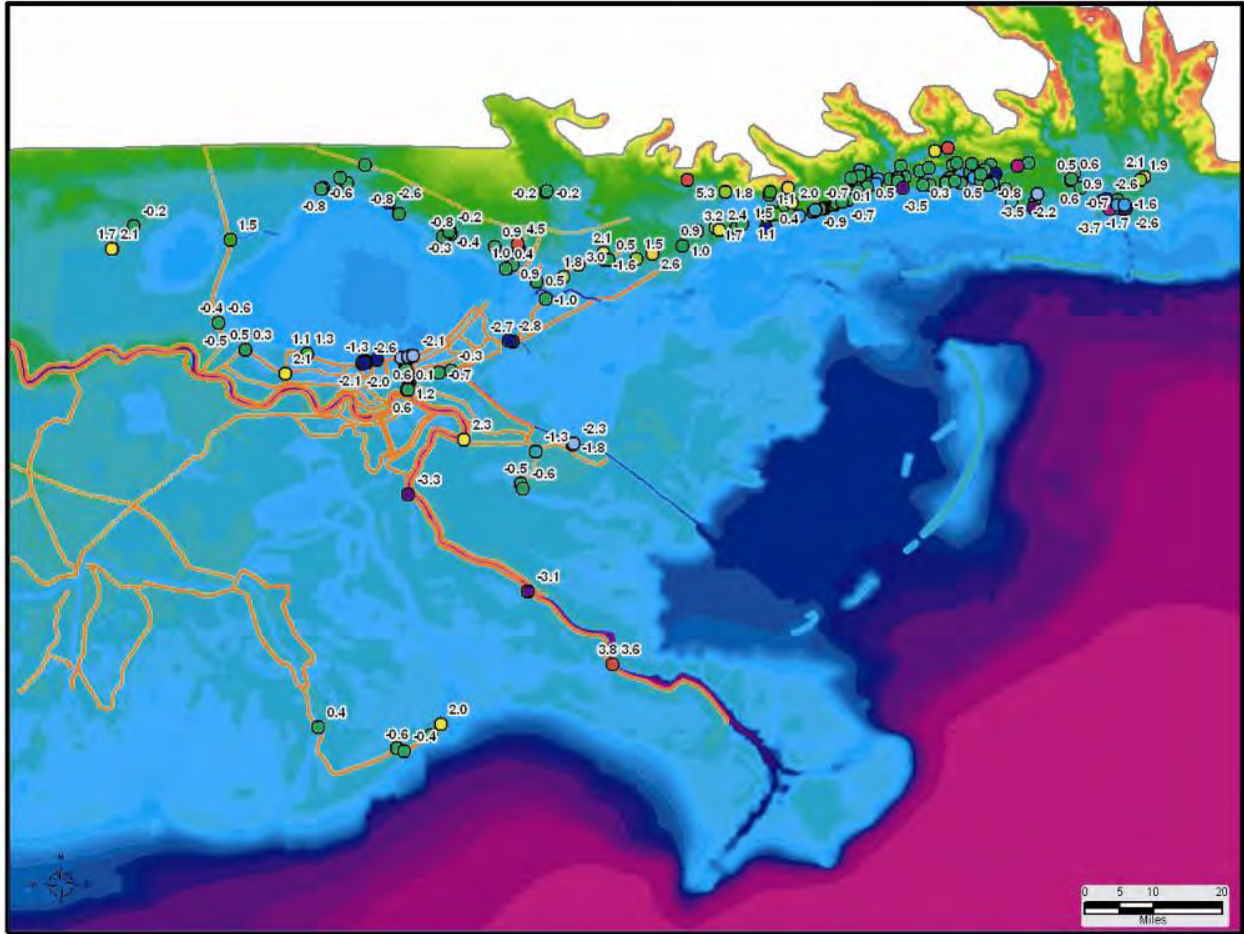


Figure 5-13a. Topographic contours (ft) and HWM elevation errors (ft) with the error value (ft) in Southern Louisiana and Mississippi

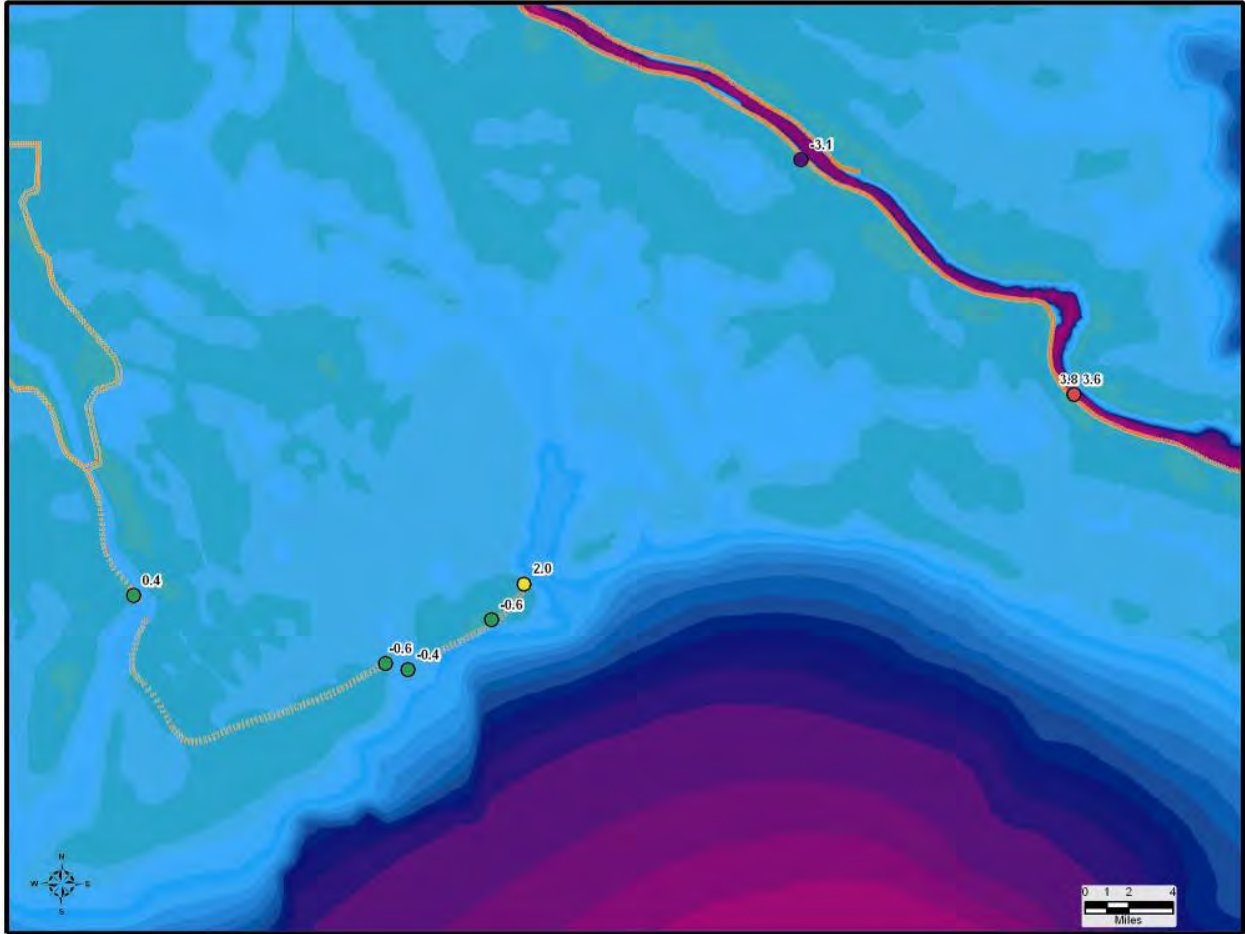


Figure 5-13b. Topographic contours (ft) and HWM elevation errors (ft) with the error value (ft). Detail between Grande Isle and western Plaquemines Parish



Figure 5-13c. Topographic contours (ft) and HWM elevation errors (ft) with the error value (ft). Detail in the vicinity of metropolitan New Orleans



Figure 5-13d. Topographic contours (ft) and HWM elevation errors (ft) with the error value (ft). Detail in the vicinity of the GIWW and IHNC





Figure 5-13e. Topographic contours (ft) and HWM elevation errors (ft) with the error value (ft). Detail of Orleans Parish and southern shore of Lake Pontchartrain





Figure 5-13f. Topographic contours (ft) and HWM elevation errors (ft) with the error value (ft). Detail of Lake Pontchartrain



Figure 5-13g. Topographic contours (ft) and HWM elevation errors (ft) with the error value (ft). Detail of Orelans Parish and Slidell, MS

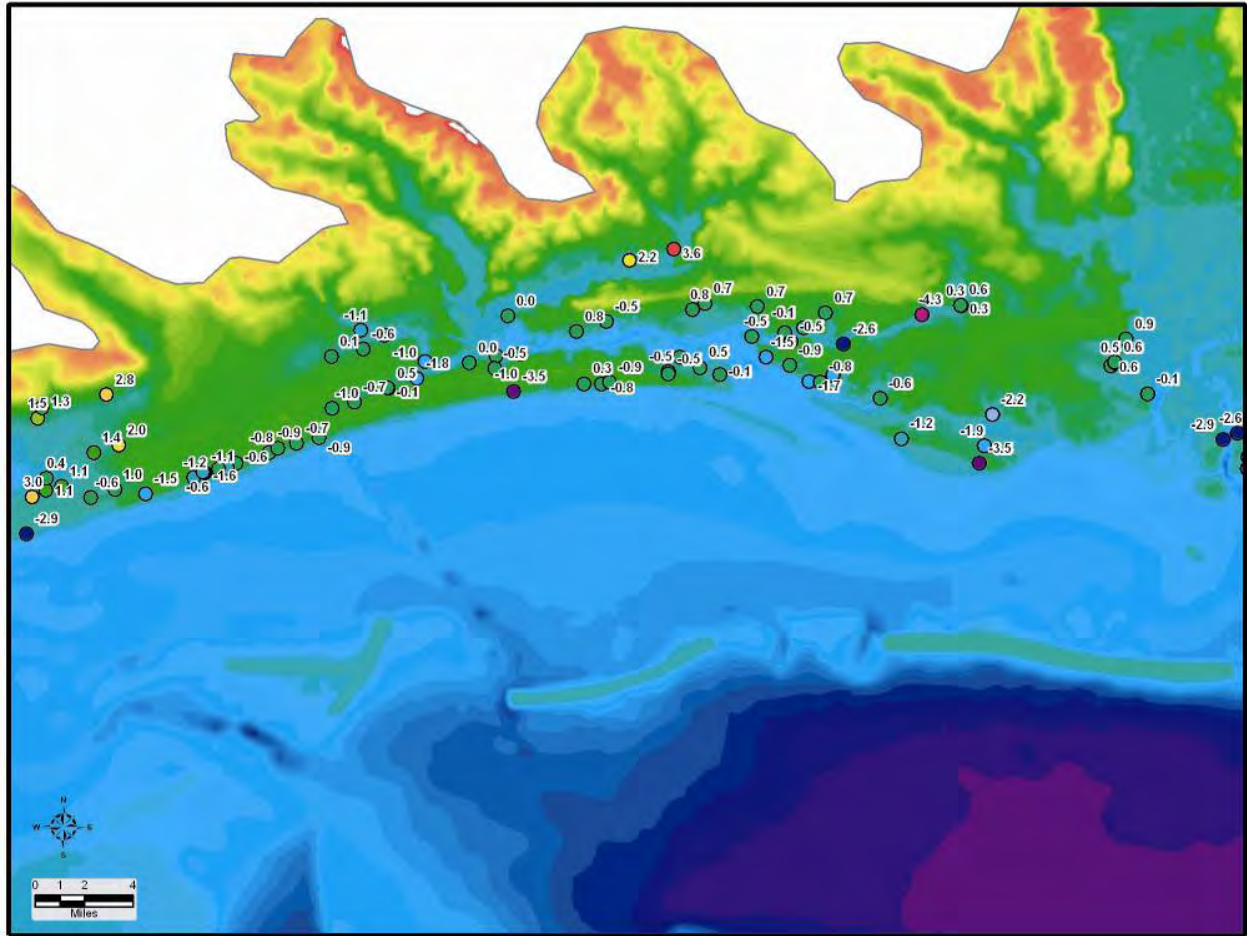


Figure 5-13h. Topographic contours (ft) and HWM elevation errors (ft) with the error value (ft). Detail of Mississippi coast



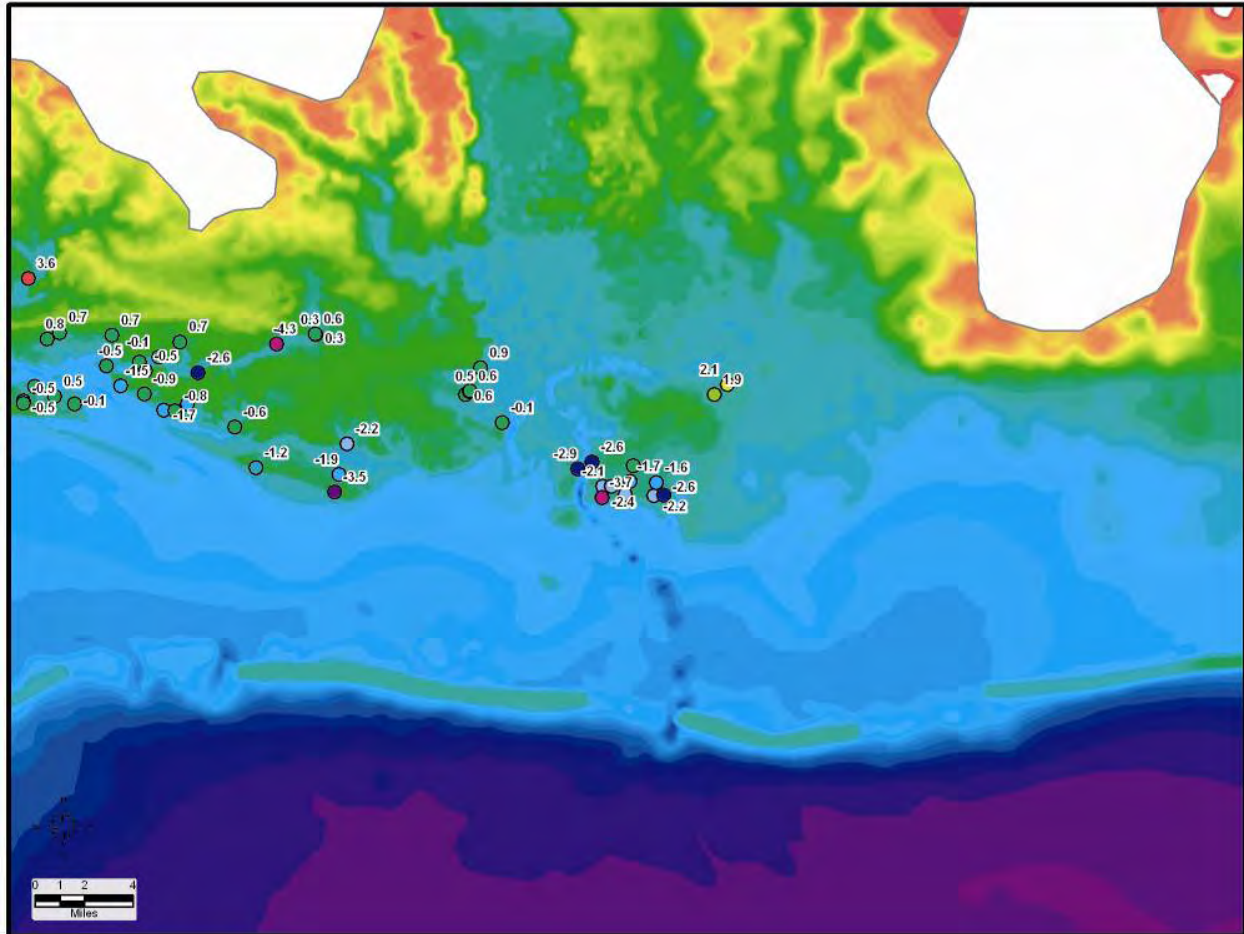


Figure 5-13i. Topographic contours (ft) and HWM elevation errors (ft) with the error value (ft). Detail of Jackson County, MS

## Forcing, Parameter and Feature Sensitivity Studies

The goals of the sensitivity analysis are to 1) evaluate the contributions of various forcing conditions to the resulting peak water level and 2) examine sensitivity of peak surge to a) uncertainty in wind fields and associated parameters, b) bottom friction parameterization, and c) physical features. Sensitivity tests were performed to compare the surge computed by the model for the base condition previously described, to surges calculated when various perturbations were made to the base condition. Table 5-3 summarizes the various cases studied. The base simulation forcing conditions includes tides, river discharge, storm winds and atmospheric pressures, and waves. Table 5-3 indicates that the contributions of these forcing conditions are evaluated (Runs 1 and 2) by repeating the base condition without one forcing condition (waves and tide, respectively). Examination of the sensitivity of predicted peak surge to various perturbations in the wind forcing, bottom friction, and physical features are also made. Sensitivity of peak surge to these perturbations include 1) increasing the wind speed by 5%, 2) decreasing the wind speed by 5%, 3) applying a wind drag cutoff of 0.0025, and 4) applying a different wind stress formulation (Agorocho and DeVries, 1980), 5) applying a spatially-varying

friction field to represent Pre-Katrina vegetation including herbaceous wetland, woody wetland, swamp, scrubland, orchard, grassland, pasture, crops, recreational grass, fallow, sand, gravel, Cypress forest, deciduous forest, evergreen forest, mixed forest, as well as city conditions including low residential, high residential, and commercial areas, 6) applying a spatially-varying friction field to represent Post-Katrina vegetation, 7) deflation of Chandeleur Island to the Post-Katrina condition.

## **Contribution of Forcing Conditions**

The base simulation forcing conditions are tide, river discharge, storm winds and atmospheric pressures, and waves. Evaluating the relative contribution of these forcing conditions is accomplished by repeating the base condition without one forcing condition and comparing the resulting peak surge to the base condition peak surge. Two sensitivity runs were made with one forcing condition eliminated for each simulation. Differences in the resulting peak surge maps indicate the contribution from the missing forcing condition. Figure 5-14 shows that the wave contribution to peak surge is most significant on the bird foot delta, Grand Isle, and shoreward of the Mississippi barrier islands and is approximately 0.5 – 2.5 ft. Figure 5-15 shows that the tidal contribution to peak surge is approximately 1 ft throughout the open water region, 0.2 ft in Lake Pontchartrain, and 0.5 ft in the Plaquemines and St. Bernard Parish regions.

## **Sensitivity to Wind Uncertainty and Parameterization**

In order to examine sensitivity of peak surge to uncertainty in wind fields and associated wind parameters, sensitivity simulations were performed to compare the surge computed by the model for the base condition to surges calculated when various perturbations are made to forcing wind fields. The four sensitivity simulations of peak surge to wind forcing are as follows: a)  $H*Wind/IOKA$  wind speed increased by 5%, b)  $H*Wind/IOKA$  wind speed decreased by 5%, c) applying a wind drag cutoff, and d) applying an alternative (Amorocho and DeVries) wind stress formulation. The standard method for applying surface wind stress within storm surge models, such as ADCIRC, is the quadratic stress law via a surface drag coefficient  $C_d$ . This coefficient is based on regression fits of field measurements, under conditions of moderate to strong wind speed, and has been found to be directly related to wind speed, wave state and atmospheric stability (Garratt, 1977, Large and Pond, 1981 and Trenberth et. al. 1989). Recent research (Powell, 2003) has found that under extreme winds, the linear extrapolation of the drag coefficient provides a clear overestimate of  $C_d$  and that the enforcement of a drag coefficient limit may be appropriate. Sensitivity simulation 5 examines this by specifying a drag coefficient upper limit of 0.0025.

Increasing the wind speed by 5% increases peak surge by 1-3 ft throughout the Hurricane Katrina impacted area, with the greatest increases in water level occurring along the Mississippi coast (Figure 5-16). The maximum surge for the Mississippi coast near Hurricane Katrina landfall is approximately 2.5-3.4 ft greater than maximum surge for the base condition. The peak surge away from the center of the storm is 1.0-2.0 ft higher with the increased wind speed. Peak surge in Lake Pontchartrain is increased by 1.0 ft or less with the increased wind speed. Decreasing the wind speed by 5% has the opposite effect, decreasing water levels 1-5 ft



throughout the Hurricane Katrina impacted area (Figure 5-17). The greatest decreases in water level are along the Mississippi coast.

Applying a wind drag cutoff decreases peak surge of 1-4 ft, with the greatest decreases along the Mississippi coast (Figure 5-18). The decrease in peak surge near St Bernard Parish is 1-2 ft and the decrease near Plaquemines Parish is approximately 2 ft. Applying an alternative wind stress formulations (Amorocho and Devries, 1980) results in a slightly smaller reduction in peak surge than the wind drag cutoff reduction in water level, but the overall pattern is quite similar (Figure 5-19). All changes in the wind forcing cause the greatest change in peak surge along the Mississippi coast, and similar patterns of change in Plaquemines Parish, St Bernard Parish, and Lake Pontchartrain.

### **Variable Friction Field**

As described in the main report, bottom friction parameterization in the base simulation applies a constant value of  $C_f$ . Sensitivity of model predicted peak surge to this parameter was examined by performing two variable friction sensitivity simulations. In the first, the Pre-Katrina friction formulation was changed from a single value of  $C_f$  to a spatially-varying Manning's  $n$  friction field to represent Pre-Katrina vegetation. The purpose of this simulation is to examine sensitivity to a broad (constant value) description of bottom friction versus a detailed representation of bottom friction. In the sensitivity simulation, applying a spatially-varying friction field to represent Pre-Katrina vegetation includes herbaceous wetland, woody wetland, swamp, scrubland, orchard, grassland, pasture, crops, recreational grass, fallow, sand, gravel, Cypress forest, deciduous forest, evergreen forest, mixed forest, as well as city conditions including low residential, high residential, and commercial areas. Manning  $n$  values are based on the USGS land use factors and are summarized in Table 5-4. Open water Manning  $n$  was specified as 0.020. In the second bottom friction sensitivity simulation, changes in the spatial extent of vegetative marshes are simulated to determine the significance of marsh loss to peak surge levels. USGS maps of Pre-Katrina and Post-Katrina vegetation (Figures 5-20 and 5-21) show that there was a decrease in marsh area (increase in open water), particularly in the St. Bernard and Plaquemines Parishes after Hurricane Katrina. Many of the wetland areas appear less solid and more web-like due to the increase in open water. In the second sensitivity simulation, the spatially-varying friction field was adjusted to represent post-Katrina conditions and was compared to the base condition and the Pre-Katrina spatially-varying friction field simulation.

Changing the Pre-Katrina friction formulation from a single value to a spatially-varying friction field to represent Pre-Katrina vegetation, results in an increase in peak water level in deeper water and a decrease in water level in the overland areas (Figure 5-22). This is related to the decrease in bottom friction in open waters with the Manning  $n$  specified equal to 0.020 there and the increase in frictional resistance in due to high Manning  $n$  values inland. Note that the extensive network of connecting channels that occur throughout the marshes, cyprus forests and other regions in Southern Louisiana were not considered in these simulations.

The Post-Katrina spatially-variable friction field results in an increase in peak surge when compared to both the base (single value friction) and the Pre-Katrina variable friction field

(Figures 5-22 and 5-23). Changing the friction formulation from a single value to a spatially-varying friction field to represent Post-Katrina vegetation, results in an increase in peak water level in deeper water and a decrease in water level in the overland areas. The increase in peak surge for Post-Katrina variable friction compared to the Base simulation (Figure 5-23) is greater than the increase in surge for the Pre-Katrina variable friction compared to the Base simulation (Figure 5-22). The comparison of Pre-Katrina and Post-Katrina peak surge (Figure 5-24) shows the reduction in vegetation (increase in open water) results in an increased peak surge of 0.5-1.5 ft.

### Deflation of Chandeleur Island

Deflation of the protective barrier islands along the Mississippi and Louisiana coast may leave these coastal regions more vulnerable to inundation from future storms. This supposition was examined by changing the bathymetric configuration of Chandeleur Island to the post-Katrina condition and repeating the ADCIRC simulation of Hurricane Katrina. A SHOALS survey of the barrier island was collected after Hurricane Katrina (Fall 2005) and shows that approximately half of the barrier island that was previously emergent had submerged after Hurricane Katrina (Figure 5-25). The majority of the loss of emergent area was from the southern end of the island. The post-Katrina configuration of Chandeleur Island was incorporated into the ADCIRC mesh for the sensitivity simulation. The results shown in Figure 5-26 indicate that deflation of Chandeleur Island provided a means for a greater volume of water to pass over the deflated island and increase water levels landward of the island. In general, peak water levels for the Chandeleur Island sensitivity simulation are 0.5 ft greater than the base conditions simulation.

<b>Table 5-3 Summary of forcing function, parameter and feature sensitivity tests</b>	
<b>Run</b>	<b>Description</b>
1	Base simulation without waves
2	Base simulation without tides
3	Increase winds by 5%
4	Decrease winds by 5%
5	Garrat Wind drag cut off of 0.0025
6	Apply Amorocho and DeVries wind drag law
7	Variable Manning n friction field for Pre-Katrina vegetation
8	Variable Manning n friction field for Post-Katrina vegetation
9	Deflation of Chandeleur Island to Post-Katrina condition

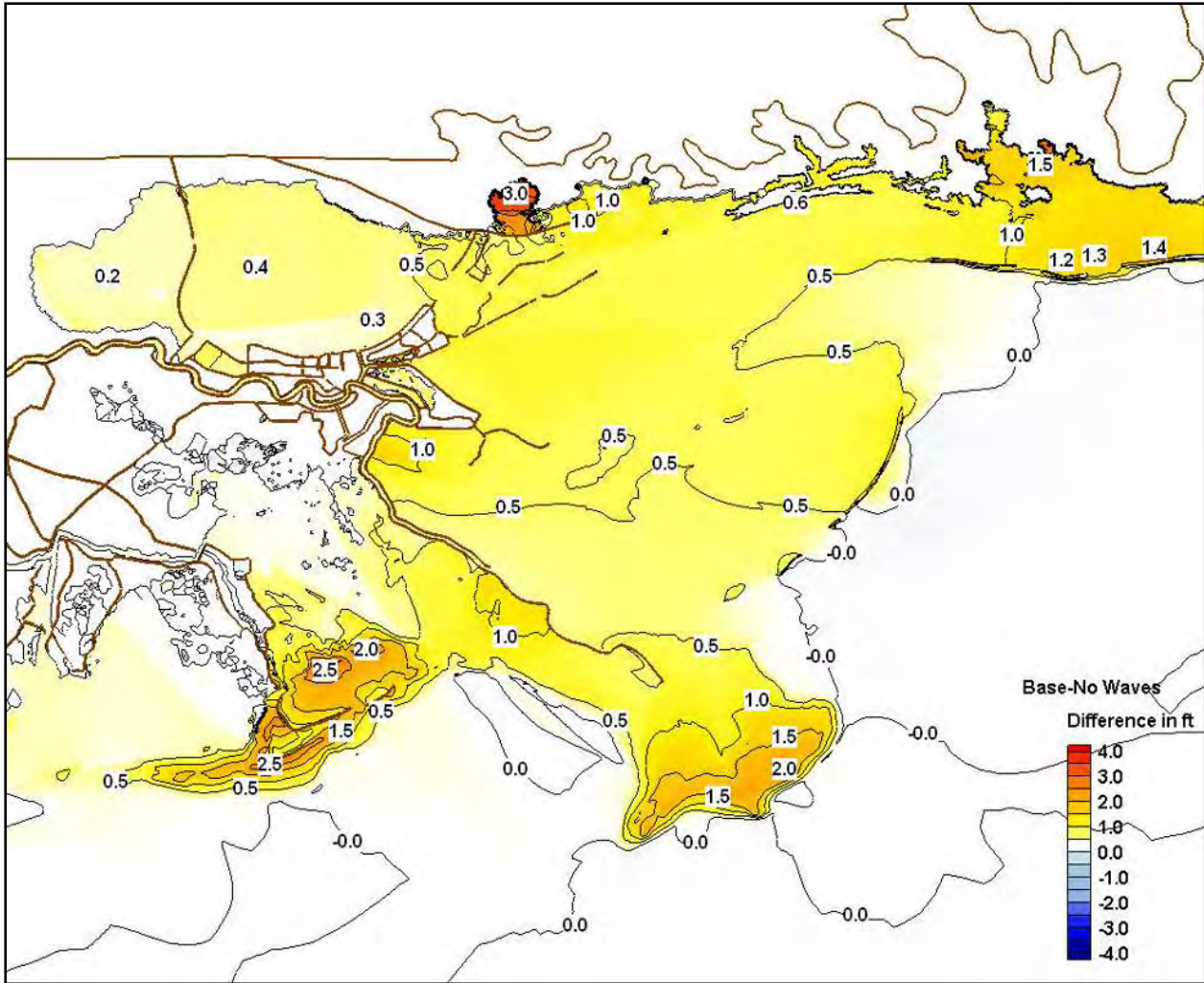


Figure 5-14. Difference in peak surge between the base simulation and the sensitivity simulation without wave forcing

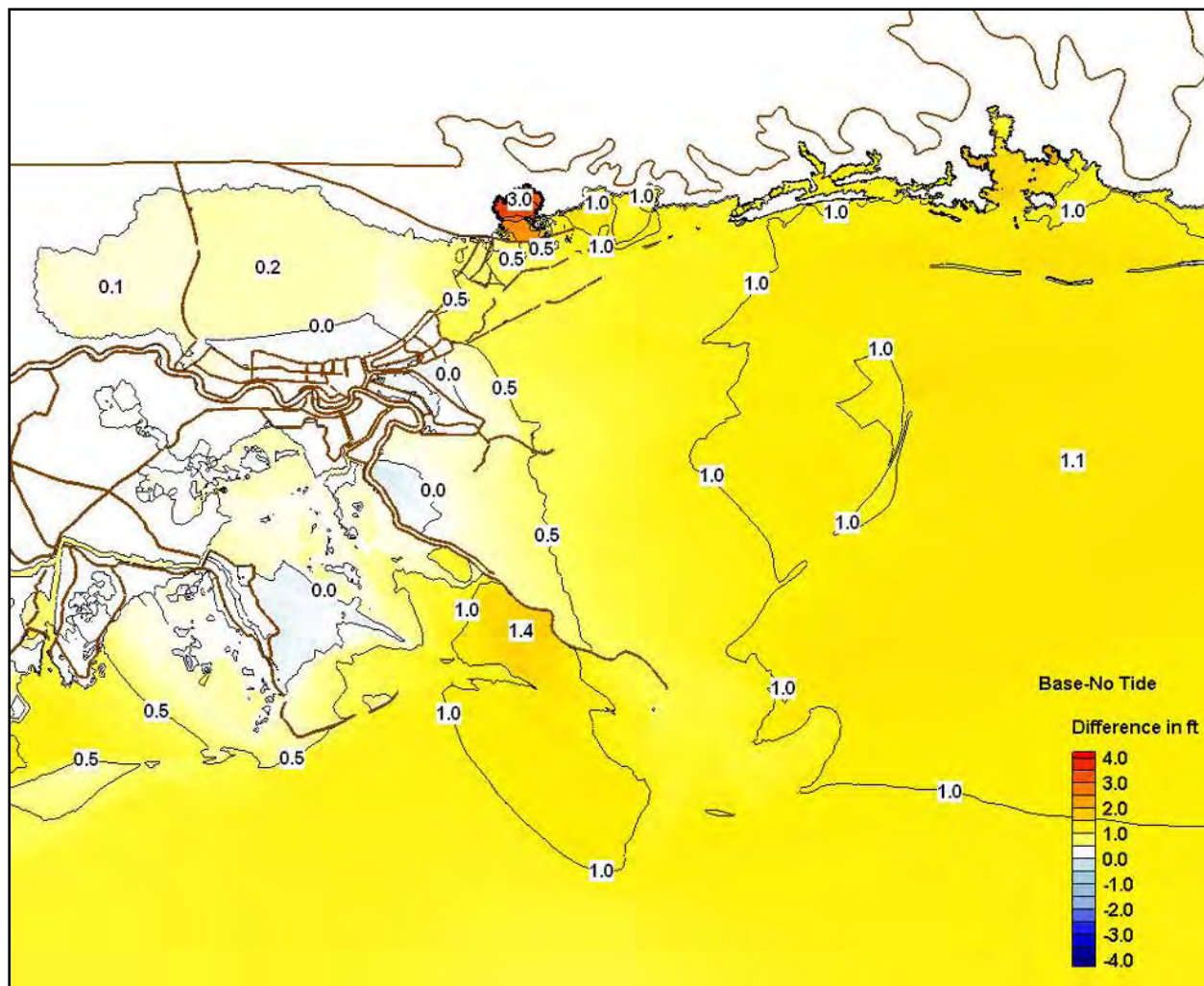


Figure 5-15. Difference in peak surge between the base simulation and the sensitivity simulation without tidal forcing



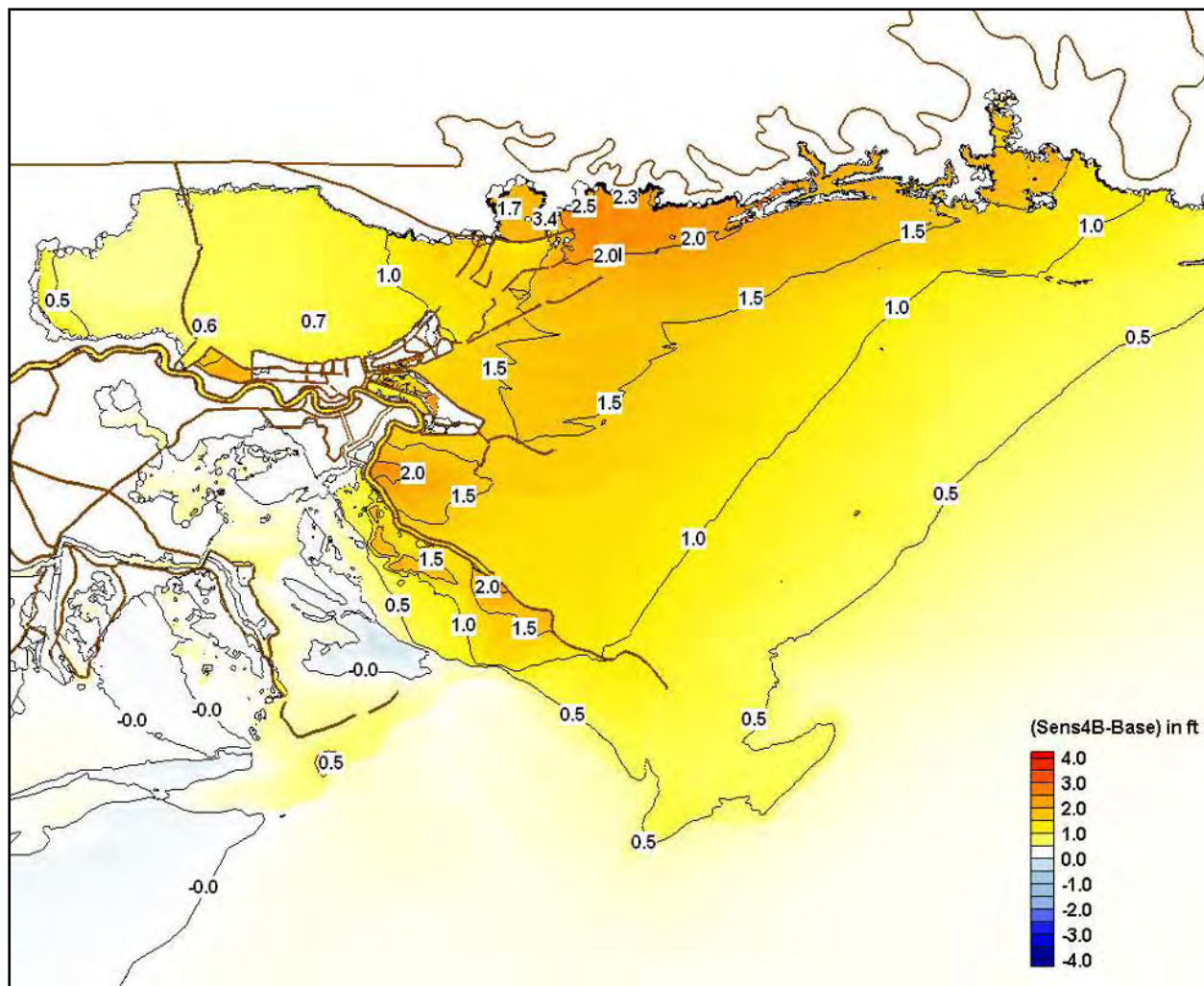


Figure 5-16. Difference in peak surge between sensitivity simulation with 5% increase in wind speed and the base simulation



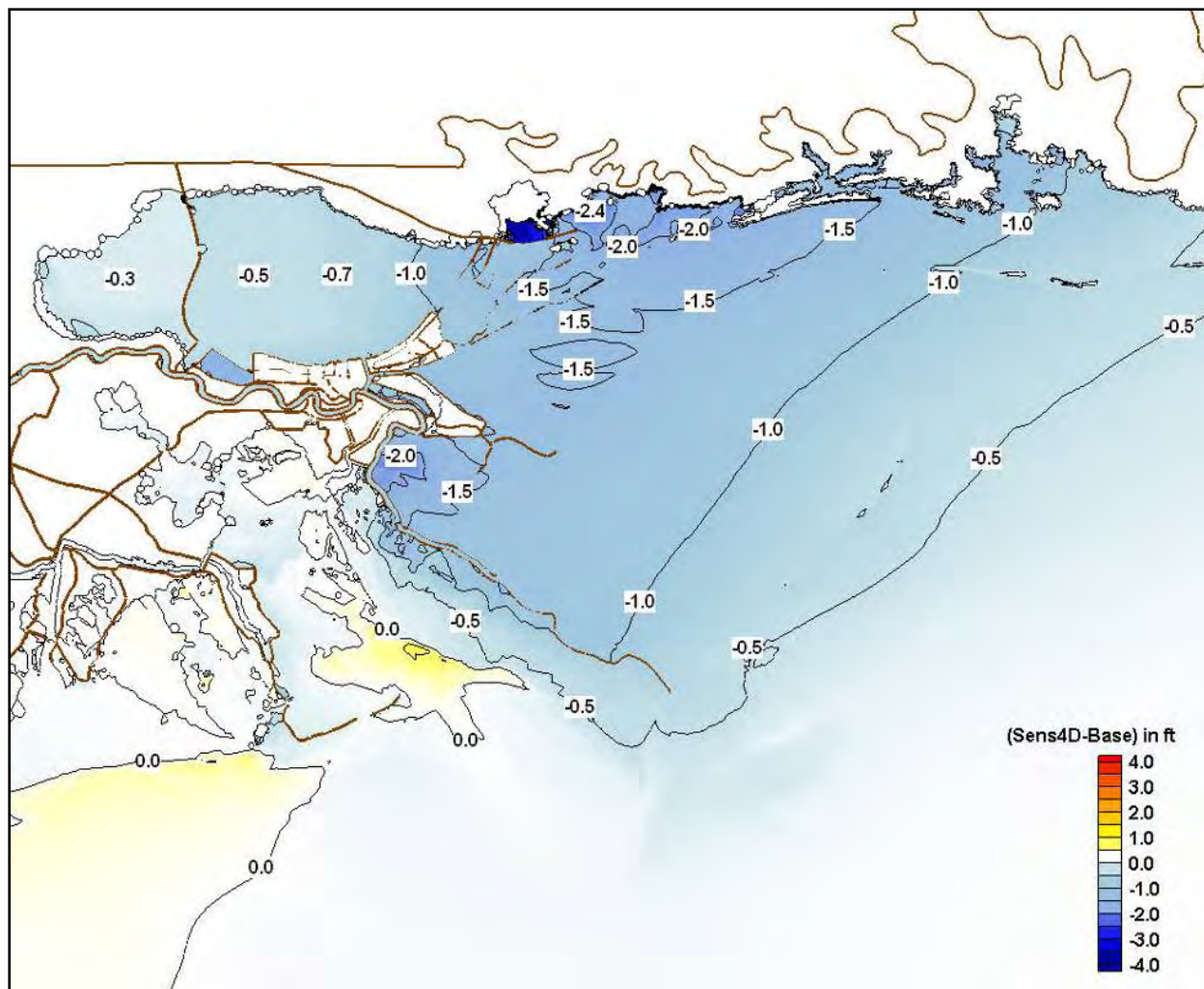


Figure 5-17. Difference in peak surge between sensitivity simulation with 5% decrease in wind speed and the base simulation

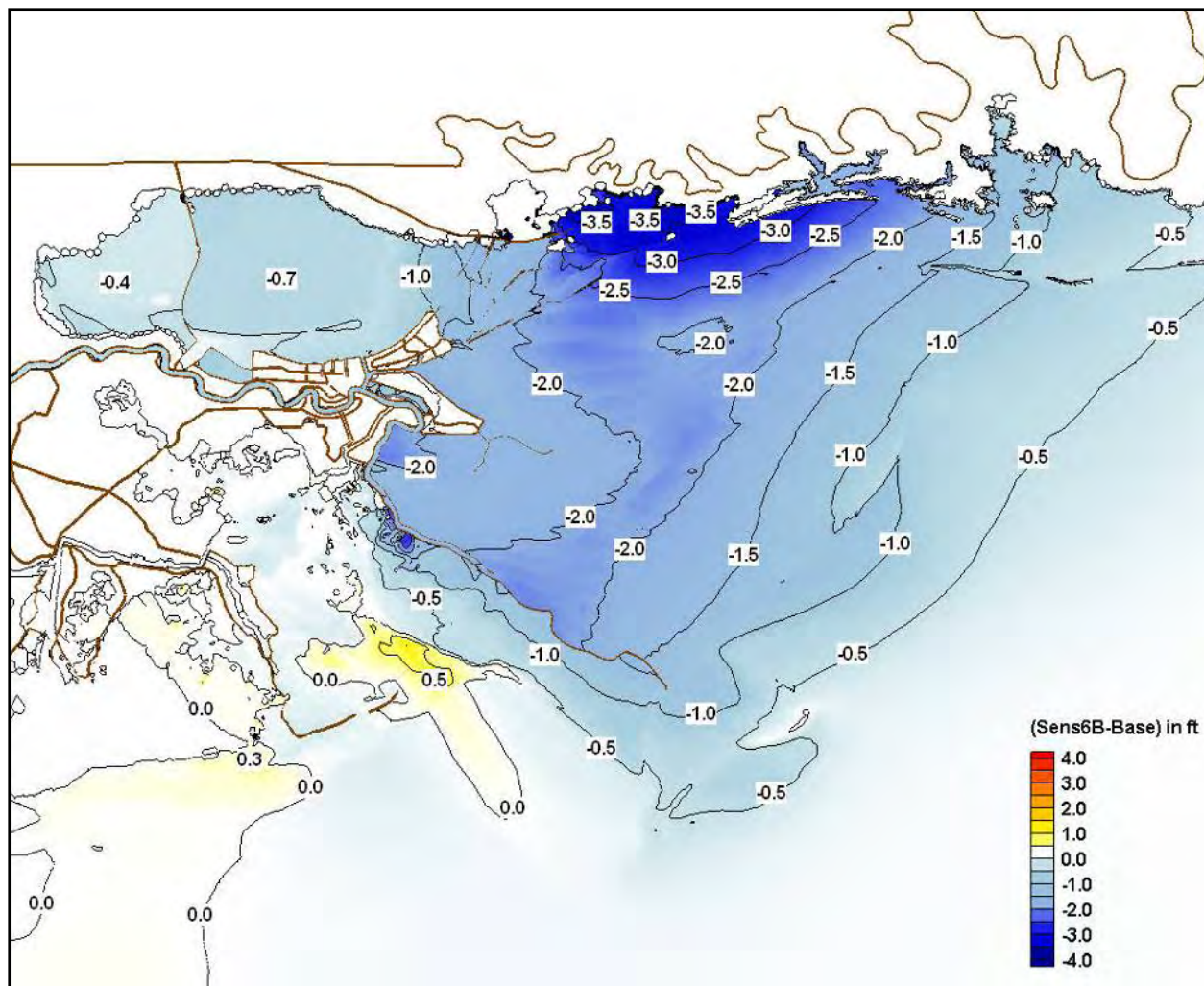


Figure 5-18. Difference in peak surge between sensitivity simulation with wind drag cutoff and the base simulation

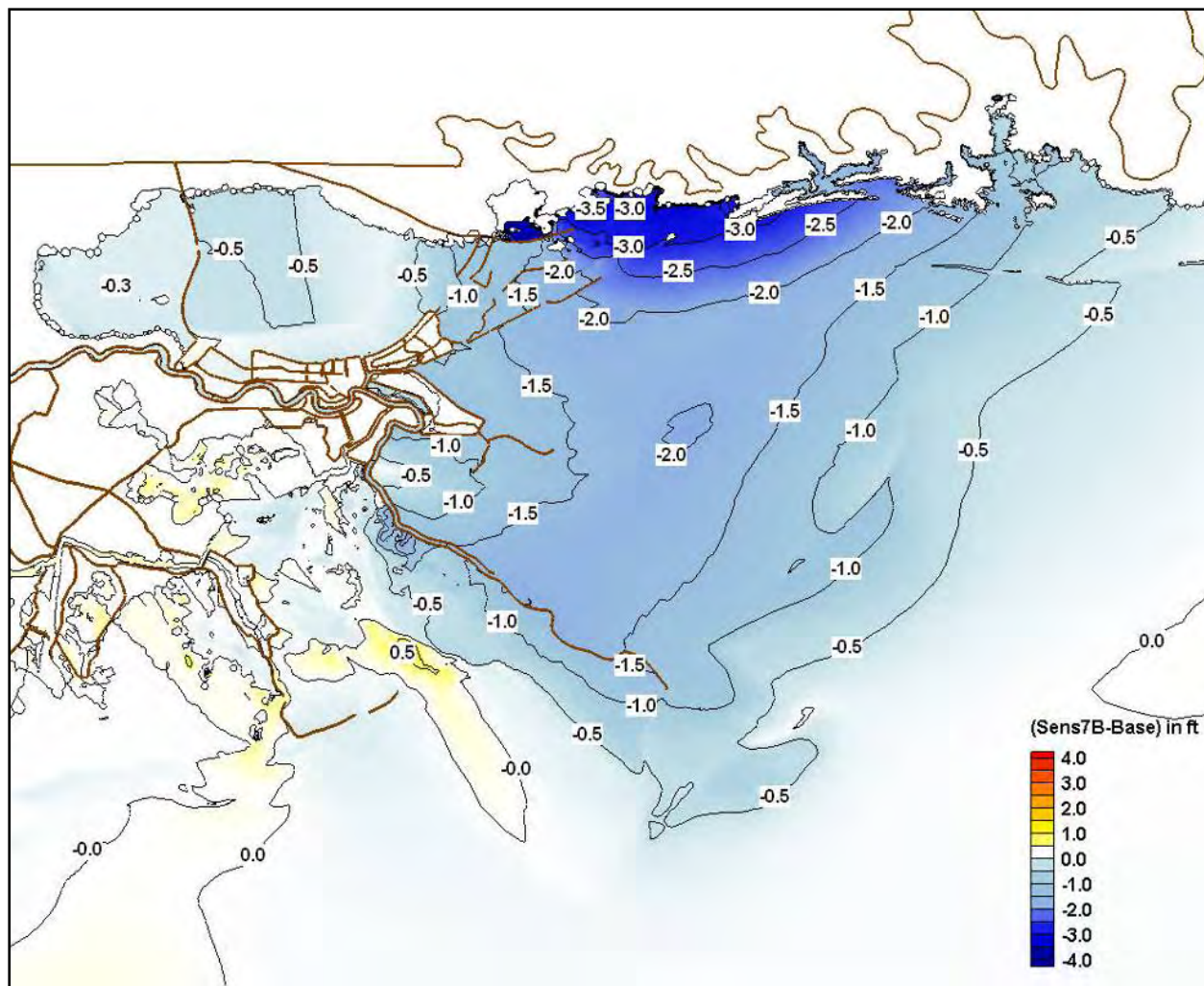


Figure 5-19. Difference in peak surge between Amorocho and DeVries wind stress formulation and the base simulation.

**Table 5-4  
Manning n values for various NLCD classes**

NLCD Class	Description	Manning-n
11	Open Water	0.020
12	Ice/Snow	0.020
21	Low Residential	0.070
22	High Residential	0.140
23	Commercial	0.050
31	Bare Rock/Sand	0.040
32	Gravel Pit	0.060
33	Transitional	0.100
41	Deciduous Forest	0.120
42	Evergreen Forest	0.150
43	Mixed Forest	0.120
51	Shrub Land	0.050
61	Orchard/Vineyard	0.100
71	Grassland	0.034
81	Pasture	0.030
82	Row Crops	0.035
83	Small Grains	0.035
84	Fallow	0.030
85	Recreational Grass	0.025
91	Woody Wetland	0.100
92	Herbaceous Wetland	0.035
95	Cypress Forest	0.100



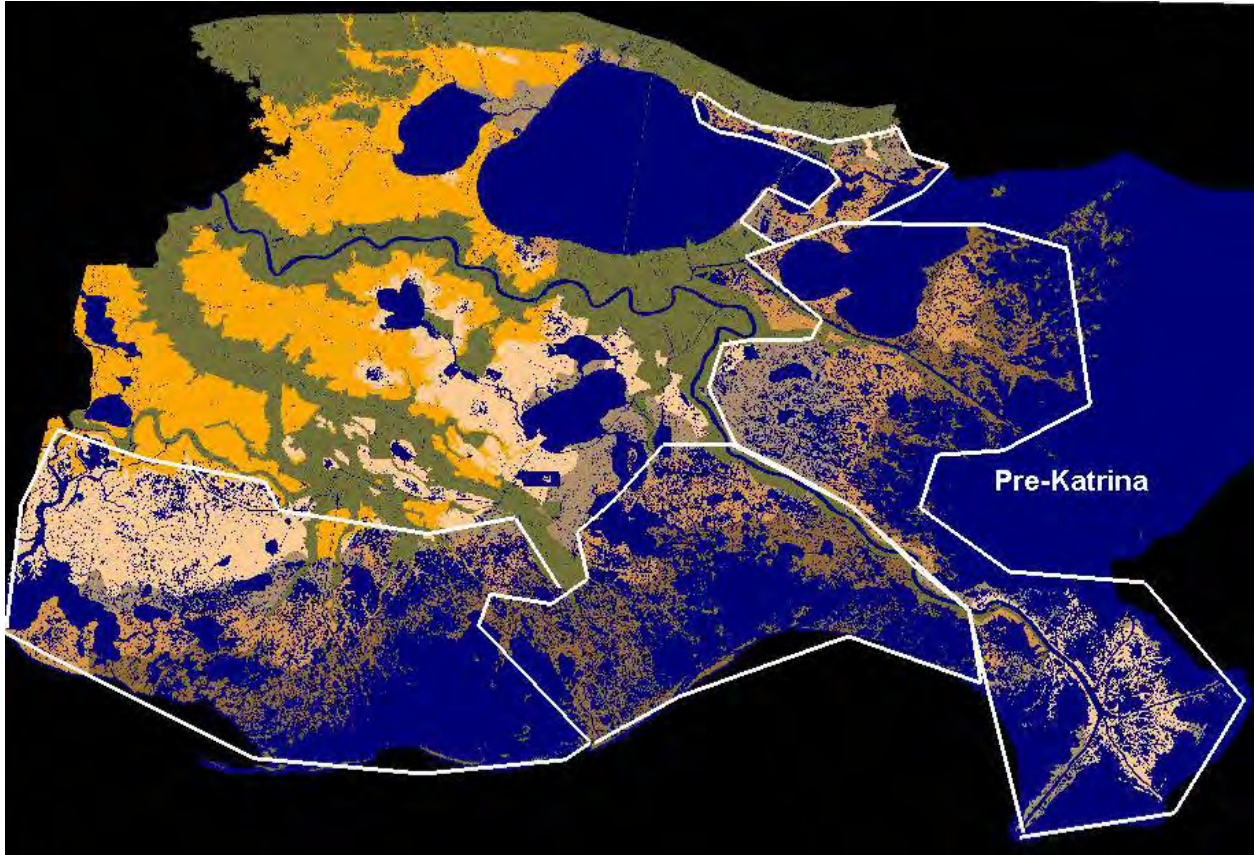


Figure 5-20. Pre-Katrina vegetation coverage (from USGS)



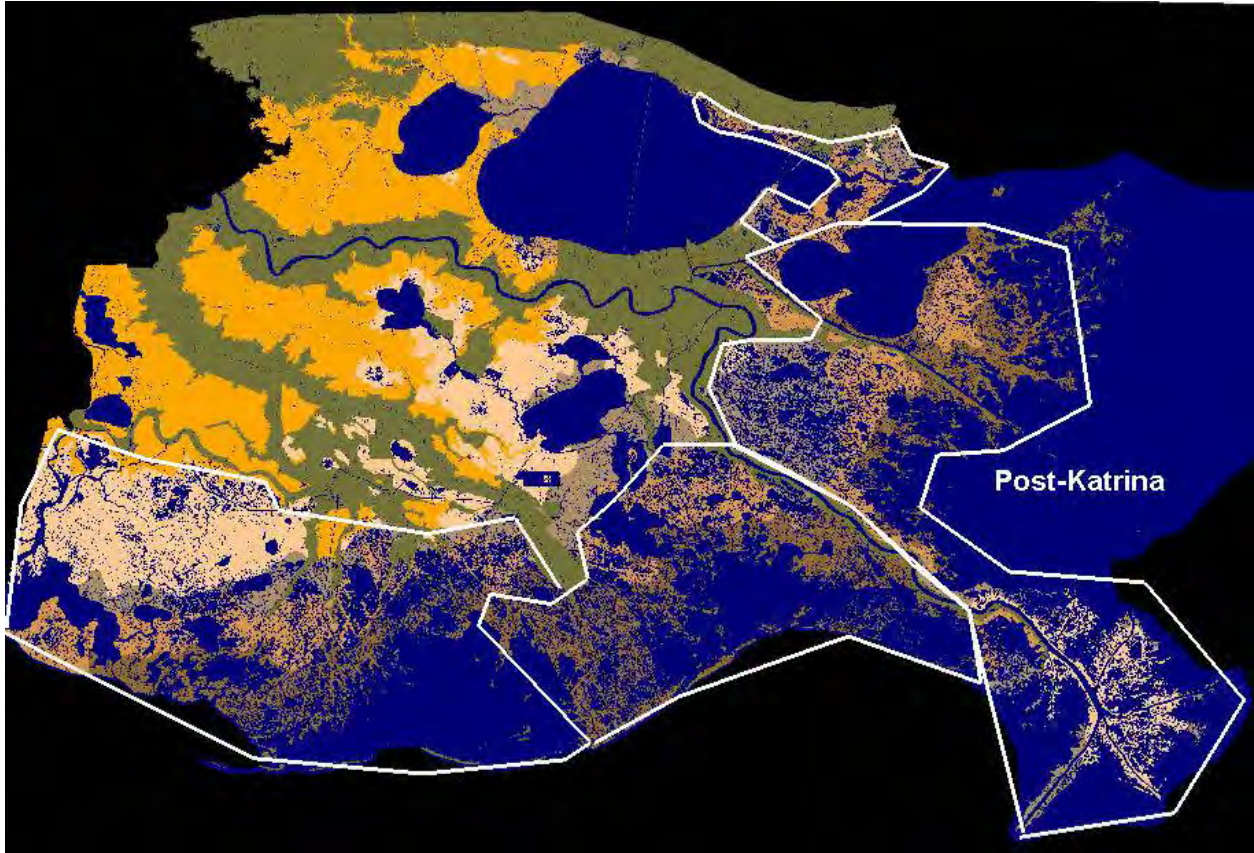


Figure 5-21. Post-Katrina vegetation coverage (from USGS)

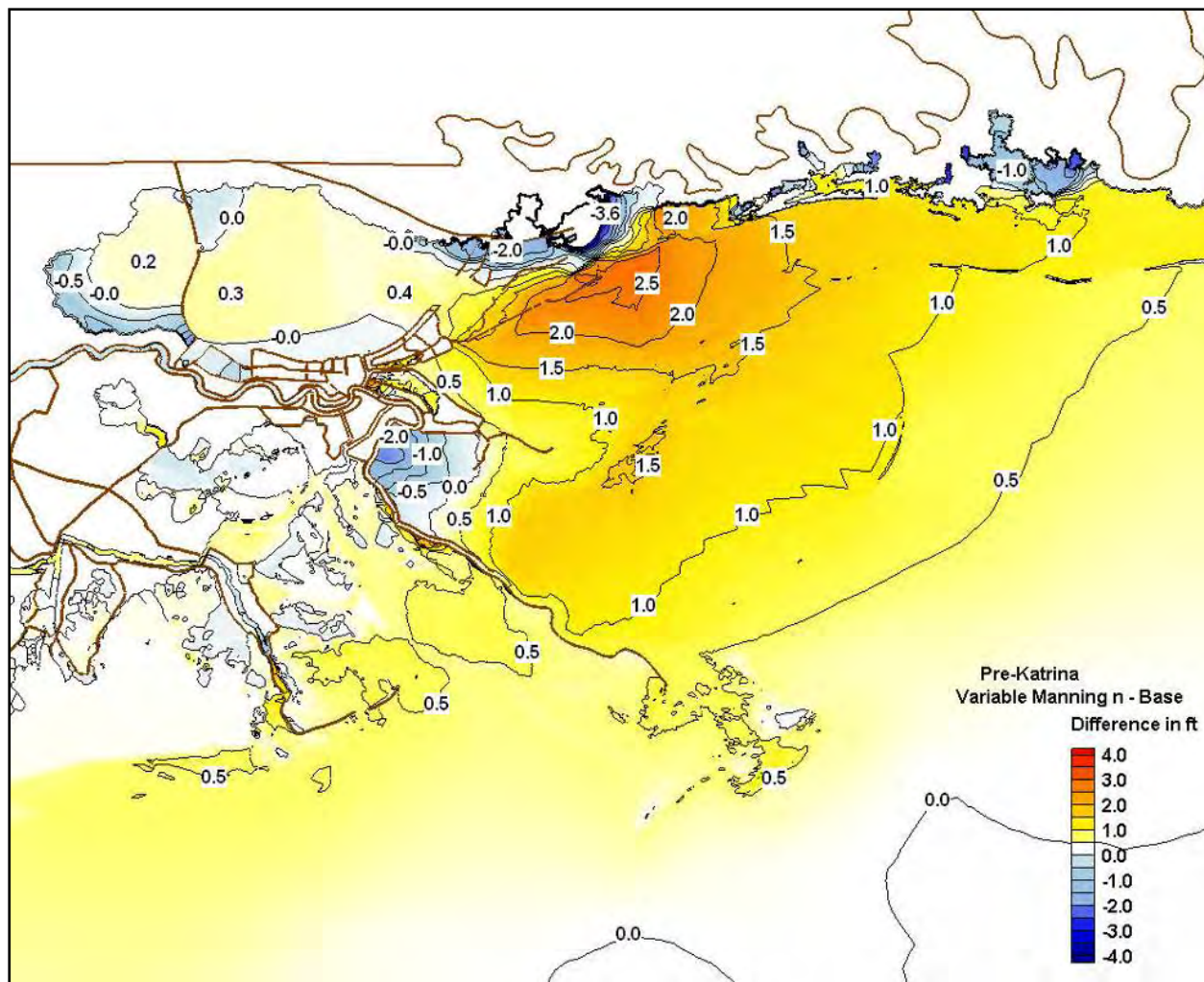


Figure 5-22. Difference in peak surge between sensitivity simulation with Pre-Katrina variable friction and the base simulation



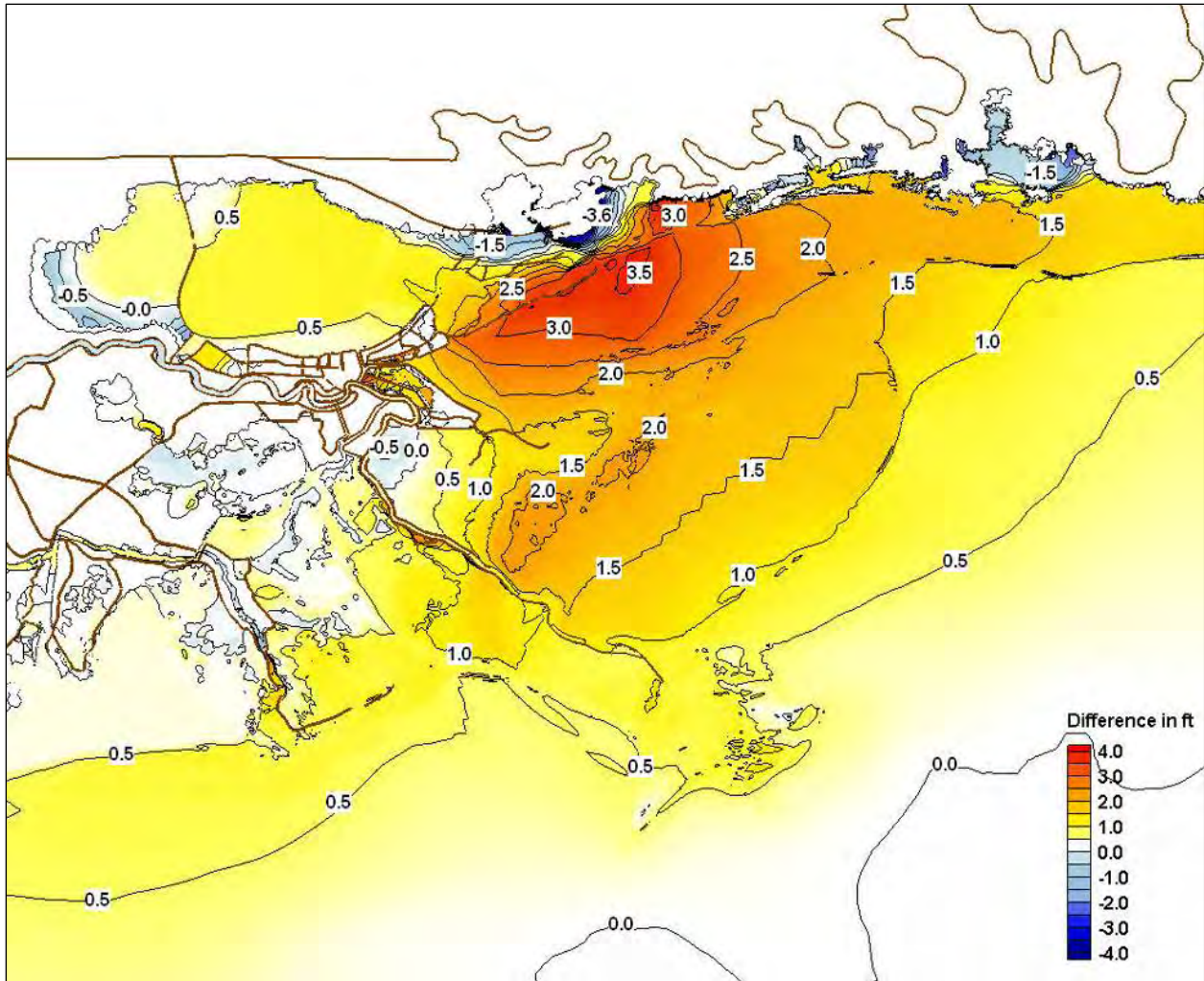


Figure 5-23. Difference in peak surge between sensitivity simulation with Post-Katrina variable friction and the base simulation

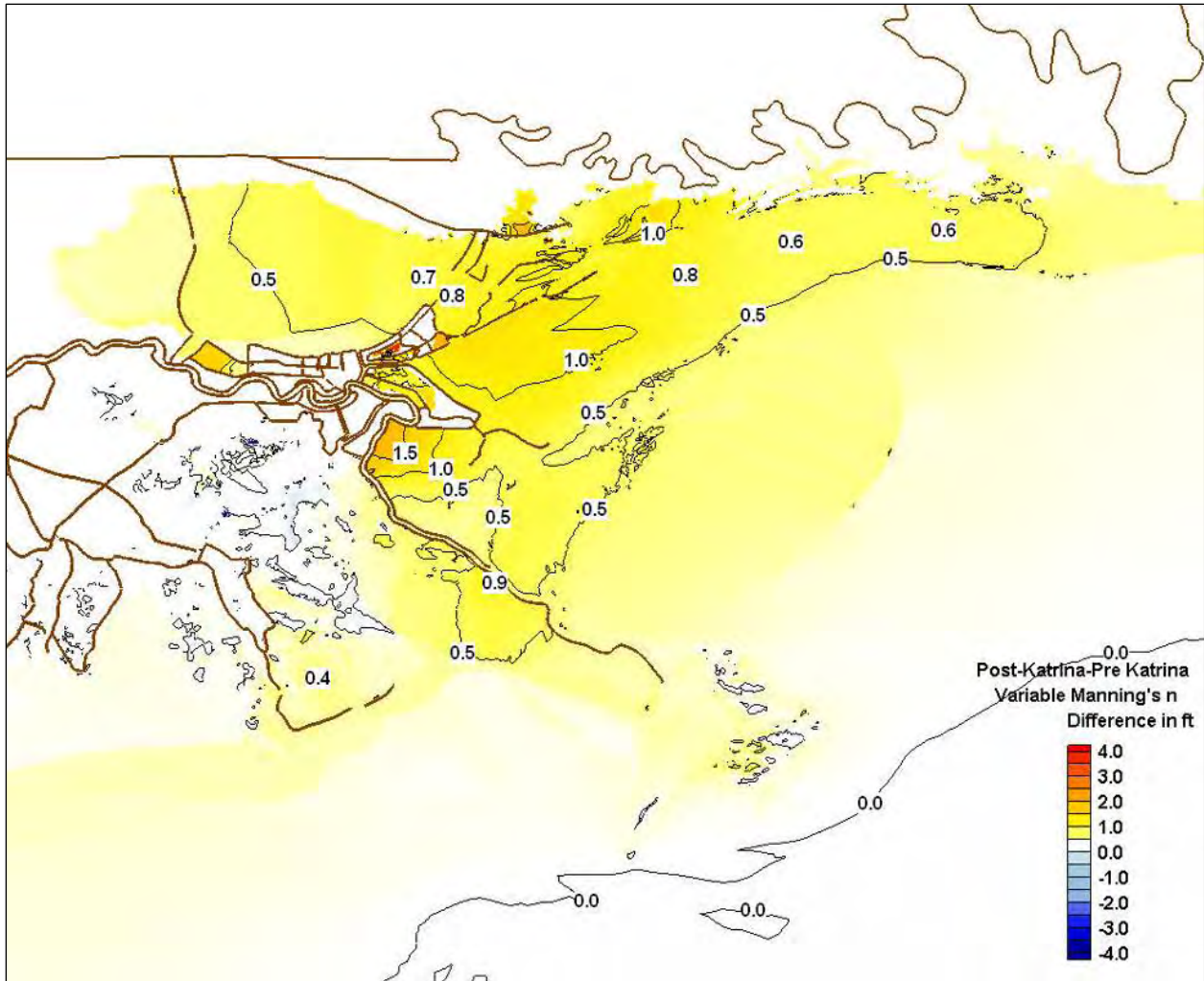


Figure 5-24. Difference in peak surge between sensitivity simulation with Post-Katrina variable friction and Pre-Katrina variable friction

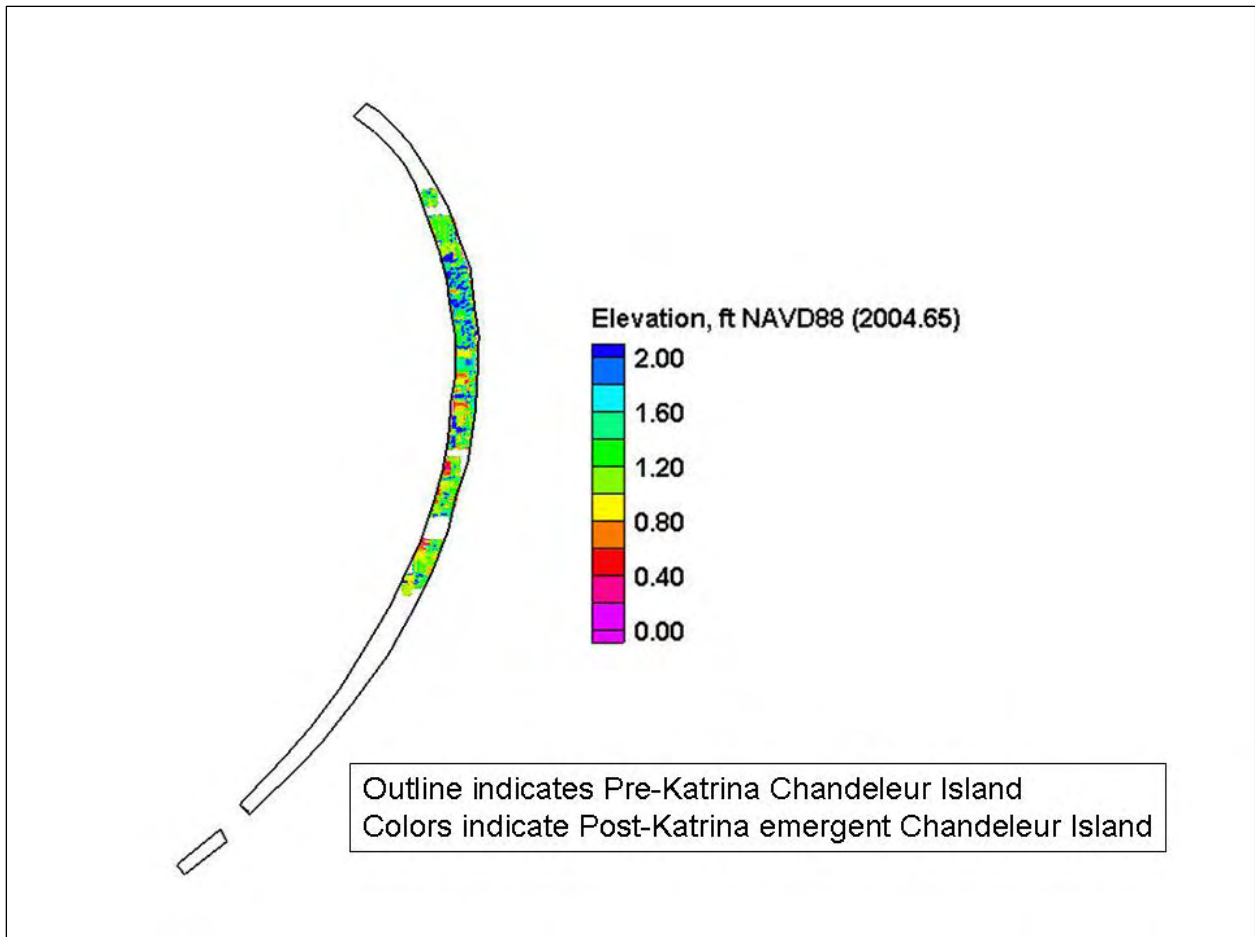


Figure 5-25. Pre-Katrina and Post-Katrina configuration of Chandeleur Island



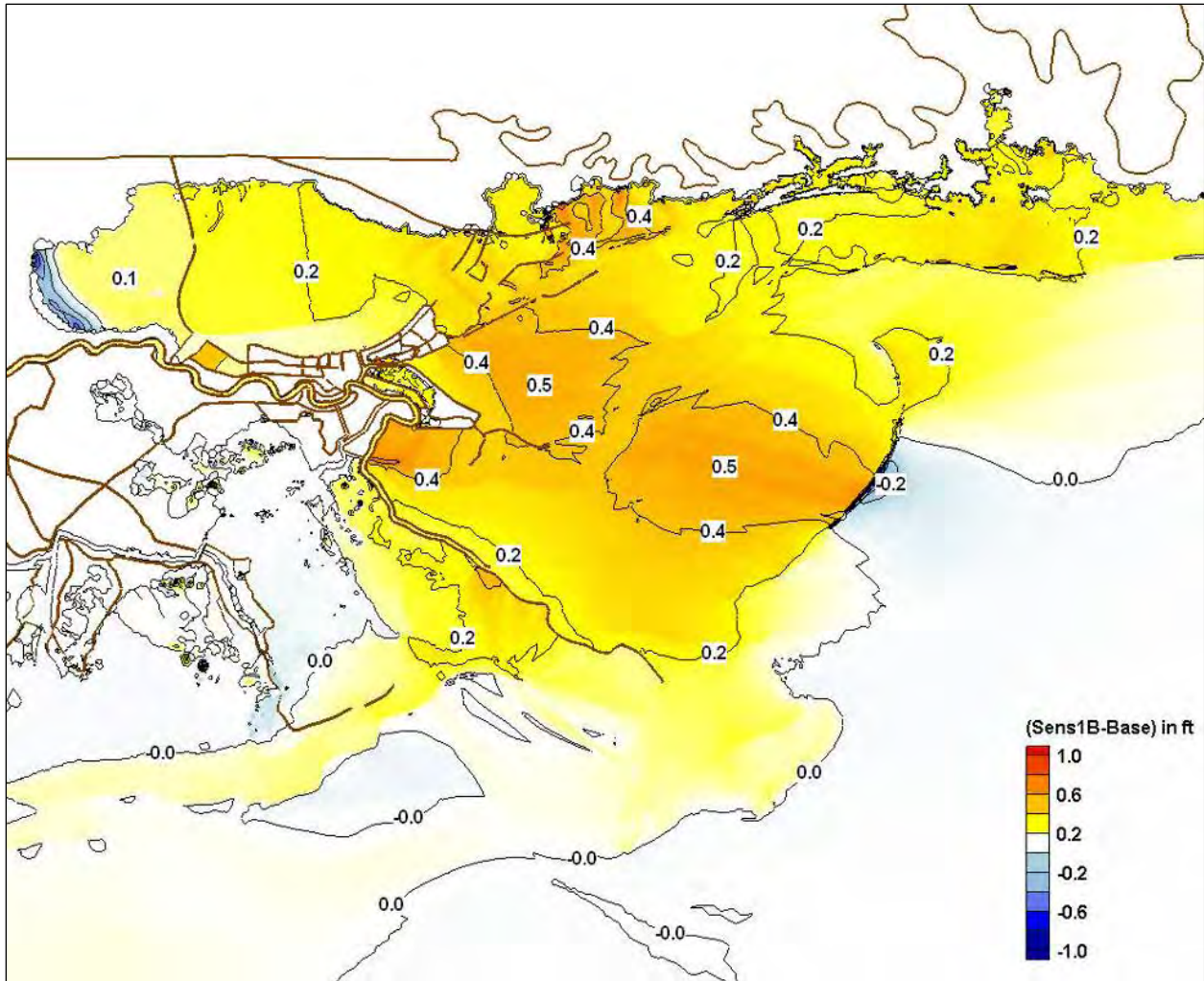


Figure 5-26. Difference in peak surge between sensitivity simulation with Post-Katrina configuration of Chandeleur Island and the base simulation

## References

- Atkinson, J.H., J.J. Westerink and J.M. Hervouet, 2004: Similarities between the wave equation and the quasi-bubble solutions to the shallow water equations. *Int. J. Numer. Methods Fluids*, **45**, 689-714.
- Blain, C.A., J.J. Westerink and R.A. Luettich, 1994: The influence of domain size on the response characteristics of a hurricane storm surge model. *J. Geophys. Res., [Oceans]*, **99** (C9), 18467-18479.
- Blain, C.A., J.J. Westerink and R.A. Luettich, 1998: Grid convergence studies for the prediction of hurricane storm surge. *Int. J. Num. Meth. Fluids*, **26**, 369-401.
- Cardone, V.J., C.V. Greenwood, and J.A. Greenwood, 1992: Unified program for the specification of hurricane boundary layer winds over surfaces of specified roughness. *Contract Report CERC-92-1*, U.S. Army Corps of Engineers. Available at: ERDC Vicksburg (WES), U.S. Army Engineer

Waterways Experiment Station (WES), ATTN: ERDC-ITL-K, 3909 Halls Ferry Road, Vicksburg, MS, 39180-6199.

Cardone, V.J., A.T. Cox, J.A. Greenwood, and E.F. Thompson, 1994: Upgrade of the tropical cyclone surface wind field model. *Miscellaneous Paper CERC-94-14*, U.S. Army Corps of Engineers. Available at: ERDC Vicksburg (WES), U.S. Army Engineer Waterways Experiment Station (WES), ATTN: ERDC-ITL-K, 3909 Halls Ferry Road, Vicksburg, MS, 39180-6199.

Charnock, H., 1955: Wind stress on a water surface. *Quart. J. Royal Met. Soc.*, **81**: 639-640.

Dawson, C., J.J. Westerink, J.C. Feyen, and D. Pothina, 2006: Continuous, discontinuous, and coupled discontinuous-continuous Galerkin finite element methods for the shallow water equations, *Intl. J. Numer. Methods Fluids*, in press.

Dietrich, J.C., R.L. Kolar and J.J. Westerink, 2006: Refinements in continuous Galerkin wetting and drying algorithms. *Estuarine and Coastal Modeling, Proc. of the Ninth Int. Conf.*, M. Spaulding et al., Eds., Charleston, SC, Am. Soc. Civ. Eng., in press.

Federal Emergency Management Association, 2005: HAZUS: Hazard loss estimation methodology. [http://www.fema.gov/hazus/hz\\_index.shtm](http://www.fema.gov/hazus/hz_index.shtm).

Feyen, J.C., J.H. Atkinson and J.J. Westerink, 2000: Issues in hurricane surge computations using a GWCE-based finite element model. Proc., *XIII Conf. on Computational Methods in Water Resources*, Vol. II, L. Bentley, J. Sykes, C. Brebbia, W. Gray and G. Pinder, Eds., 865-872.

Feyen, J. C., J. J. Westerink, J. H. Atkinson, R. A. Luettich, C. N. Dawson, M. D. Powell, J. P. Dunion, H. J. Roberts, E. J. Kubatko, and H. Pourtaheri, 2005: A New Generation Hurricane Storm Surge Model for Southern Louisiana, *Bulletin of the American Meteorological Society*, In Review, 2005.

Galland, J., N. Goutal and J. Hervouet, 1991: A new numerical model for solving the shallow water equations. *Adv. Water Res.*, **14**: 138-148.

Garratt, J.R., 1977: Review of drag coefficients over oceans and continents. *Mon. Wea. Rev.*, **105**, 915-929.

Hanert E., V. Legat and E. Deleersnijder, 2002: "A comparison of three finite elements to solve the linear shallow water equations," *Ocean Modell.*, **5**, 17-35.

Hagen, S.C., J.J. Westerink and R.L. Kolar, 2000: Finite element grids based on a localized truncation error analysis. *Int. J. Num. Meth. Fluids*, **32**, 241-261.

Hagen, S.C., J.J. Westerink, R.L. Kolar and O. Horstmann, 2001: Two dimensional unstructured mesh generation for tidal models. *Int. J. Num. Meth. Fluids*, **35**, 669-686.

Holland, G., 1980: An analytic model of the wind and pressure profiles in hurricanes. *Mon. Wea. Rev.*, **108**, 1212-1218.

Hsu, S. 1988: *Coastal Meteorology*. Academic Press, 260 pp.

Jelesnianski, C. P., and A. D. Taylor, 1973: A Preliminary View of Storm Surges Before and After Storm Modifications, NOAA Technical Memorandum ERL WMPO-3.

- Kinnmark, I., 1986: The shallow water wave equations: formulation, analysis, and application. *Lecture Notes in Engineering*, No. 15, Springer-Verlag, 187 pp.
- Knabb, R. D., J. R. Rhome, and D. P. Brown, 2005: Tropical Cyclone Report, Hurricane Katrina, 23-30 August 2005, National Hurricane Center, NOAA, 20 December, [http://www.nhc.noaa.gov/pdf/TCR-AL122005\\_Katrina.pdf](http://www.nhc.noaa.gov/pdf/TCR-AL122005_Katrina.pdf)
- Kolar, R. and W. Gray 1990: Shallow water modeling in small water bodies. *Computational Methods in Surface Hydrology*, G. Gambolati, A. Rinaldo, C. Brebbia, W. Gray and G. Pinder, Eds., 149-155.
- Kolar, R.L., J.J. Westerink, M.E. Cantekin and C.A. Blain, 1994a: Aspects of nonlinear simulations using shallow water models based on the wave continuity equation. *Comput. Fluids*, **23**, 523-538.
- Kolar, R.L., W.G. Gray, J.J. Westerink and R.A. Luettich, 1994b: Shallow water modeling in spherical coordinates: equation formulation, numerical implementation and application. *J. Hydraul. Res.*, **32**, 3-24.
- Kolar, R.L. and J.J. Westerink, 2000: A look back at 20 years of GWC-based shallow water models. *Proc., XIII Conf. on Computational Methods in Water Resources*, Vol. II, 899-906.
- Komen, G., L. Cavaleri, M. Donelan, K. Hasselmann, S. Hasselmann and P. Jansse, 1994: *Dynamics and Modelling of Ocean Waves*. Cambridge University Press, 532 pp.
- Le Provost, C., F. Lyard, J. Molines, M. Genco and F. Rabilloud, 1998: A hydrodynamic ocean tide model improved by assimilating a satellite altimeter-derived data set. *J. Geophys. Res. [Oceans]*, **103**, 5513-5529.
- Luettich, R.A., J.J. Westerink, and N.W. Scheffner, 1992: ADCIRC: an advanced three-dimensional circulation model for shelves, coasts and estuaries, report 1: theory and methodology of ADCIRC-2DDI and ADCIRC-3DL. *Tech. Rep. DRP-92-6*, U.S. Army Corps of Engineers. Available at: ERDC Vicksburg (WES), U.S. Army Engineer Waterways Experiment Station (WES), ATTN: ERDC-ITL-K, 3909 Halls Ferry Road, Vicksburg, MS, 39180-6199.
- Luettich, R.A. and J.J. Westerink, 1995: Continental shelf scale convergence studies with a barotropic model. *Quantitative Skill Assessment for Coastal Ocean Models, Coastal and Estuarine Studies Series No. 47*, D.R. Lynch and A.M. Davies, Eds., Amer. Geophys. Union, 349-371.
- Luettich, R.A. and J.J. Westerink, 1999: Elemental wetting and drying in the ADCIRC hydrodynamic model: upgrades and documentation for ADCIRC version 34.XX. *Contractors Report*, U.S. Army Corps of Engineers. Available at: ERDC Vicksburg (WES), U.S. Army Engineer Waterways Experiment Station (WES), ATTN: ERDC-ITL-K, 3909 Halls Ferry Road, Vicksburg, MS, 39180-6199.
- Luettich, R.A. and J.J. Westerink, 2003: Combined discharge and radiation boundary condition in the ADCIRC hydrodynamic model: theory and documentation. *Contractors' Report*, U.S. Army Corps of Engineers New Orleans District. Available at: U.S. Army Engineer Corps of Engineers, New Orleans, ATTN: CEMVN-IM-SM Library, P.O. Box 60267, New Orleans, LA, 70160-0267.
- Luettich, R.A. and J.J. Westerink, 2004: Formulation and Numerical Implementation of the 2D/3D ADCIRC Finite Element Model Version 44.XX; Report [http://www.marine.unc.edu/C\\_CATS/adcirc/adcirc\\_theory\\_2004\\_12\\_08.pdf](http://www.marine.unc.edu/C_CATS/adcirc/adcirc_theory_2004_12_08.pdf)

- Luettich, R.A. and J.J. Westerink, 2005: ADCIRC: A parallel advanced circulation model for oceanic, coastal and estuarine waters; user's manual for version 45.08; [http://www.marine.unc.edu/C\\_CATS/adcirc/document/ADCIRC\\_title\\_page.html](http://www.marine.unc.edu/C_CATS/adcirc/document/ADCIRC_title_page.html).
- Lynch, D.R. and W.G. Gray, 1979: A wave equation model for finite element tidal computations. *Comput. Fluids*, **7**, 207-228.
- Lynch, D.R., 1983: Progress in hydrodynamic modeling, review of U.S. Contributions 1979-1982. *Rev. Geophys. Space Phys.*, **21**, 741-754.
- Mukai, A., J.J. Westerink, R. Luettich, Jr. and D. Mark, 2002: Eastcoast 2001: A tidal constituent database for the Western North Atlantic, Gulf of Mexico, and Caribbean Sea. *Tech. Rep. ERDC/CHL TR-02-24*, U.S. Army Corps of Engineers. Available at: ERDC Vicksburg (WES), U.S. Army Engineer Waterways Experiment Station (WES), ATTN: ERDC-ITL-K, 3909 Halls Ferry Road, Vicksburg, MS, 39180-6199.
- National Geophysical Data Center, 1988: *ETOPO5 Technical report*, National Oceanic and Atmospheric Administration, <http://edcsgs9.cr.usgs.gov/glis/hyper/guide/etopo5>.
- National Ocean Service Hydrographic Survey Division, 1997: *Hydrographic Survey Digital Database*, Vol. 1, 3rd ed., National Oceanic and Atmospheric Administration.
- National Wetlands Research Center, Biological Research Division, 2004: Land cover classification for the Louisiana GAP analysis. *Tech. Rep.*, United States Geological Survey, [http://sabdata.cr.usgs.gov/sabnet/pub/pub\\_sab\\_app.aspx?prodid=780](http://sabdata.cr.usgs.gov/sabnet/pub/pub_sab_app.aspx?prodid=780).
- Powell, M., S. Houston and T. Reinhold, 1996: Hurricane Andrew's landfall in South Florida. Part I: Standardizing measurements for documentation of surface windfields. *Wea. Forecasting*, **11**, 304-328.
- Powell, M. and S. Houston, 1996: Hurricane Andrew's landfall in South Florida. Part II: surface wind fields and potential real-time applications. *Wea. Forecasting*, **11**, 329-349.
- Powell, M., S. Houston, L. Amat and N. Morrisseau-Leroy, 1998: The HRD real-time hurricane wind analysis system. *J. Wind Engr. Indust. Aero.*, **77-78**: 53-64.
- Powell, M., P. Vickery and T. Reinhold, 2003: Reduced drag coefficient for high wind speeds in tropical cyclones. *Nature*, **422**, 279-283.
- Reid, R.O., 1990: Tides and storm surges. *Handbook of Coastal and Ocean Engineering*, J. Herbich, Ed., Gulf Publishing, 533-590.
- Reid R.O. and R. Whitaker, 1976: Wind-driven flow of water influenced by a canopy. *J. Waterw., Harbors, Coastal Engr. Div.- Am. Soc. Civ. Eng.*, **102**, WW1, 61-77.
- Simiu, E. and R. Scanlan, 1986: *Wind Effects on Structures*. Wiley Interscience, 604 pp.
- Thompson, E.F., and V.J. Cardone, 1996: Practical modeling of hurricane surface wind fields. *J. Waterw., Port, Coastal Eng.*, **122**, 195-205.

- U.S. Army Engineer District New Orleans, 1965: Report on Hurricane Betsy, 8-11 September 1965 in the U.S. Army Engineer District, New Orleans. *Tech. Rep.*, U.S. Army Corps of Engineers New Orleans District. Available at: U.S. Army Engineer Corps of Engineers, New Orleans, ATTN: CEMVN-IM-SM Library, P.O. Box 60267, New Orleans, LA, 70160-0267.
- Westerink, J.J. and W.G. Gray, 1991: Progress in surface water modeling. *Rev. Geophys.*, **29**, April Supplement, 210-217.
- Westerink, J.J., R.A. Luetlich, A.M. Baptista, N.W. Scheffner and P. Farrar, 1992: Tide and storm surge predictions using a finite element model, *J. Hydraul. Eng.*, **118**, 1373-1390.
- Westerink, J.J., R.A. Luetlich and J.C. Muccino, 1994: Modeling tides in the Western North Atlantic using unstructured graded grids. *Tellus*, **46A**, 178-199.
- Westerink, J.J., R.A. Luetlich and A. Militello, 2001: Leaky Internal-Barrier Normal-Flow Boundaries in the ADCIRC Coastal Hydrodynamics Code. *Coastal and Hydraulic Engineering Technical Note IV-XX*, U.S. Army Corps of Engineers. Available at: ERDC Vicksburg (WES), U.S. Army Engineer Waterways Experiment Station (WES), ATTN: ERDC-ITL-K, 3909 Halls Ferry Road, Vicksburg, MS, 39180-6199.
- Westerink, J. J., R. A. Luetlich, J. C. Feyen, J. H. Atkinson, C. Dawson, M. D. Powell, J. P. Dunion, H. J. Roberts, E. J. Kubatko, and H. Pourtaheri, 2005: A Basin to Channel Scale Unstructured Grid Hurricane Storm Surge Model for Southern Louisiana , *Monthly Weather Review*, In Preparation.



# Appendix 6

## Note on the Influence of the Mississippi River Gulf Outlet on Hurricane Induced Storm Surge in New Orleans and Vicinity

---

Joannes Westerink  
Department of Civil Engineering and Geological Sciences  
University of Notre Dame, Notre Dame IN 46556

Bruce Ebersole  
Coastal and Hydraulics Laboratory  
U.S. Army Engineer Research and Development Center  
Vicksburg, MS 39180

Harley Winer  
New Orleans District, U.S. Army Corps of Engineers  
New Orleans, LA 70160

February 21, 2006

Concerns have been raised regarding the role of the Mississippi River Gulf Outlet (MRGO) on storm surge propagation into metropolitan New Orleans and vicinity. This note discusses hydrodynamic model simulations that evaluate the influence of the MRGO on flooding during major hurricane events. This note (whitepaper) is not intended as a final expression of the findings or conclusions of the United States Army Corps of Engineers, nor has it been adopted by the Corps as such. Rather, this note is a preliminary report summarizing data and interim conclusions compiled to date. As a preliminary report, this document and the information contained therein are subject to revisions and changes as additional information is obtained.

The physical system here is very complex, one comprised of a network of estuaries, lakes, rivers, channels, and low lying wetlands, with topographic major relief defined by river banks and an extensive system of levees and raised roads. Water surface elevation response is driven by storm surge, tides, and wind-waves. Both storm surge and tides are characterized as forced very long wavelength inertial gravity waves, while wind-waves are gravity waves defined by their short period. All three types of waves propagate and experience various levels of local

forcing which can further build amplitudes. In metropolitan New Orleans and vicinity, the amplitude of the tides is small; the maximum tide range is on the order of one half foot in Lake Pontchartrain and two feet in Chandeleur Sound. The amplitude of a storm surge can be much higher; for Hurricane Katrina, the peak storm surge along the MRGO adjacent to the St. Bernard Parish/Chalmette hurricane protection levee was computed to be as much as 18 ft. This note focuses on the relevant long period motion that dominates the circulation patterns in the area. In particular, the impact of the MRGO on large scale catastrophic storm surge development and propagation is examined.

The MRGO is a dredged channel that extends southeast to northwest from the Gulf of Mexico to a point where it first merges with the Gulf Intracoastal Waterway (GIWW), and then continues westward until it intersects the Inner Harbor Navigation Canal (IHNC) as shown in Figure 1. The first 9 miles, the bar channel, are in the open Gulf. The next 23 miles of the channel lie in the shallow open waters of Breton Sound. From there, the inland cut extends 14 miles to the northwest with open marsh on the northeast and a 4,000-ft wide dredged material placement bank on the southwest side. At this point the channel cuts across the ridge of a relict distributary of the Mississippi River, Bayou La Loutre. For nearly the next 24 miles, there is a hurricane protection levee atop a dredged material placement bank on the southwest side of the channel and Lake Borgne and open marsh lie to the northeast. A portion of the levee protecting St. Bernard Parish/Chalmette and the portion of the hurricane protection levee along the south side of Orleans East Parish, north of the GIWW, form the “funnel” that is often referenced. The point where the MRGO and GIWW channels merge is just to the east of the Paris Road Bridge (see Figure 1). From this point, the merged GIWW/MRGO channel continues west for about 6 miles to the point where it intersects the IHNC; this portion has hurricane protection levees on both banks. The IHNC extends from Lake Pontchartrain, to the north, to the Mississippi River to the south. The IHNC has levees or floodwalls along both banks. The IHNC Lock, which connects the IHNC to the Mississippi River, is located at the southern limit of the IHNC. The MRGO bar channel authorized depth is 38 ft; the authorized bottom width is 600 ft. The remainder of the channel has an authorized depth of 36 ft and an authorized bottom width of 400 or 450 ft, depending on location.

It is important to distinguish between two sections of the MRGO and the role each plays in tide and storm surge propagation. One is the east-west oriented section that runs between the IHNC and the confluence of the GIWW/MRGO near the Paris Road Bridge, labeled as the GIWW/MRGO in Figure 1, and hereafter referred to as Reach 1. The other is the much longer southeast-northwest section designated as the MRGO in Figure 1, and hereafter referred to as the Reach 2.

The critical section of the MRGO is Reach 1, the combined GIWW/MRGO. It is through this section of channel that Lake Pontchartrain and Lake Borgne are hydraulically connected to one another via the IHNC. Reach 1 existed as the GIWW prior to the construction of the MRGO, although the maintained depth was lower. Because of this connectivity, the local storm surge and astronomical tide in the IHNC and in the section designated GIWW/MRGO is influenced by the tide and storm surge in both Lake Pontchartrain and Lake Borgne. The two Lakes are also connected to each other via the Rigolets and Chef Menteur Pass; the IHNC is the smallest of the three connections. The Reach 1 GIWW/MRGO section of channel is very important in

determining the magnitude of storm surge that reaches the IHNC from Lake Borgne and Breton Sound. If the hydraulic connectivity between Lake Pontchartrain and Lake Borgne is eliminated at a point within this section of channel, tide or surge to the west of this point will become primarily influenced by conditions at the IHNC entrance to Lake Pontchartrain; and tide or storm surge to the east of this point will become primarily influenced by conditions in Lake Borgne.

Much concern seems to be focused on MRGO/Reach 2 that runs from the GIWW/MRGO confluence, just east of the Paris Road Bridge, to the southeast. Past work, McAnally and Berger (1997), Carillo et al. (2001), and Tate et al. (2002) for example, has shown that this section of the MRGO channel, along with the critical section, the GIWW/MRGO/Reach 1, plays an important role in the propagation of the astronomical tide wave and in the flux of more saline water from Lake Borgne/Breton Sound into Lake Pontchartrain via the IHNC. The significant role of the MRGO in the propagation of the low-amplitude tide has been established.

Three previous studies have been performed to examine the influence of MRGO/Reach 2 on flooding in New Orleans and vicinity. The first of these studies, Bretschneider and Collins (1966), was performed for the U.S. Army Corps of Engineers, New Orleans District (USACE-MVN). The primary objective of the study was to determine the effects of the MRGO channel, and dredged material placement banks, and associated works, on the hurricane surge environment of an area to the east of the Mississippi River from the southern end of the MRGO to the IHNC. The study looked at Hurricane Betsy and six synthetic storms. Based on simplified one-dimensional numerical computations and estimates of channel conveyance effects, the report concluded that Betsy would have produced essentially the same surge elevations with or without the MRGO.

The second study was also commissioned by the USACE-MVN and involved “closing” the MRGO/Reach 2 with a barrier placed across the MRGO extending out from state road 624 and the La Loutre Ridge (U.S. Army Corps of Engineers, New Orleans District, 2003). That closure was located just to the southeast of Shell Beach in Figure 1. The study examined 9 synthetic storms with a track to the west of the Mississippi River running parallel to the MRGO with input strengths varying from 65 to 124 knots and forward speeds ranging from 5 to 20 knots. In addition, Hurricane Betsy input winds were examined. Each of the 10 storms was simulated with and without the MRGO closure along the La Loutre Ridge. The study applied the S08 high resolution unstructured finite element grid with detailed refinement of the MRGO, GIWW, IHNC, the Rigolets Inlet and Chef Menteur Pass (Feyen et al. 2005, Westerink et al. 2006). Resolution and domain definition requirements have been verified for the S08 grid and the resulting model has been validated (Blain et al. 1994, Blain et al. 1998, Westerink et al. 2000, Feyen et al. 2002, Feyen et al. 2005, Westerink et al. 2006). The S08 grid applies a larger approximation for the width of the MRGO/Reach 2 channel, thus leading to conservative estimates of the influence of the channel. A two dimensional depth integrated version of the ADCIRC model (Luettich et al. 1992, Luettich and Westerink 2004, Luettich and Westerink, 2005, Westerink et al. 2006), a finite element based shallow water equation code that is accurate, stable and robust, was used to perform the computations.

Results from this study showed that for low-amplitude storm surges (peak surge having a magnitude of 4 feet or less), the presence of MRGO/Reach 2 increased the storm surge by up to

the following amounts: 0.5 ft at Shell Beach and Bayou Dupre, and 0.3 ft at Paris Road Bridge and the IHNC Lock. For nearly all situations that were examined (results for all ten storms at the four locations shown in Figure 1), the presence of the MRGO/Reach 2 either did not cause a significant change or the increase was less than 0.3 ft. In a few situations, notably a slow moving weak storm, the presence of the MRGO/Reach 2 channel actually led to a very small decrease in peak surge level at the four locations. For higher amplitude storm surges, peak surges on the order of 7 to 12 feet (which included Hurricane Betsy), changes induced by MRGO/Reach 2 were 0.3 ft or less for all situations. The MRGO did however considerably enhance drainage from Lake Pontchartrain through the IHNC/GIWW out to Breton Sound following passage of the storms.

A follow up study was commissioned by the State of Louisiana, Department of Natural Resources and implemented by URS Corporation (2006). This study applied the same unstructured S08 grid but filled in the MRGO/Reach 2 channel to surrounding topographic/bathymetric levels. This study also applied the ADCIRC code and the results were similar to the USACE-MVN study. Reach 2 of the MRGO had a very limited impact on increasing storm surge for large storms, including Hurricanes Betsy and Katrina. All changes were less than 0.6 ft and most changes were less than 0.3 ft, in the vicinity of New Orleans. Results also indicated that the MRGO enhanced post storm drainage from portions of the system.

In general, the studies cited above reached consistent conclusions. The change in storm surge induced by MRGO/Reach 2 (computed as a percentage of the peak surge magnitude) is greatest when the amplitude of the storm surge is low, on the order of a few feet or less. In these situations, changes induced by the MRGO are rather small, 0.5 ft or less, but this amount is as much as 25% of the peak surge amplitude. When the long wave amplitude is very low, the surge is more limited to propagation via the channels. Once the surge amplitude increases to the point where the wetlands become inundated, this section of the MRGO plays a diminishing role in influencing the amplitude of storm surge that reaches the vicinity of metropolitan New Orleans. For storm surges of the magnitude produced by Hurricanes Betsy and Katrina, which overwhelmed the wetland system, the influence of MRGO/Reach 2 on storm surge propagation is rather small. When the expansive wetland is inundated, the storm surge propagates primarily through the water column over this much larger flooded area, and the channels become a much smaller contributor to water conveyance.

The results of these studies can be readily understood by considering in more detail the evolution of storm surge for critical hurricane tracks passing to the west of the Mississippi River. These storms blow wind across the region first from the northeast, then from the east, then from the southeast and south and finally from the west. The sustained northeasterly and especially easterly winds push water onto the wide and shallow Mississippi-Alabama Shelf into Breton and Chandeleur Sounds, and Lake Borgne. These winds build surge up regionally on the shelf and in particular against the Mississippi River and hurricane protection levees in Plaquemines Parish, against the St. Bernard Parish/Chalmette hurricane protection levee system and into the so called funnel defined by the levees protecting St. Bernard Parish/Chalmette and New Orleans East along the confluence of the GIWW/MRGO. As winds become southerly, the significant surge that has built up along the Mississippi River levees in southern Plaquemines Parish starts to propagate north as a constrained wave up the Mississippi River and as an unconstrained wave

through Breton Sound, both influenced by the strength and direction of the winds. Finally, westerly winds blow surge away from these levees.

We note that the surge driven by the sustained northeasterly and easterly winds is not influenced by the MRGO, since the direction of water movement is from east to west across Breton and Chandeleur Sounds and Lake Borgne. The brief southeasterly and southerly winds do guide the substantial surge wave that has built up in Plaquemines Parish north across Breton Sound. In the case of Hurricane Betsy, the surge propagated in a northerly direction along the Mississippi River levees and was stopped by river levees at English Turn. In the case of Hurricane Katrina, the surge propagated in a northeasterly direction perpendicular to the MRGO towards Gulfport, Mississippi. In either case, the northerly movement of water is not significantly influenced by the MRGO since the size of the surge is substantially larger than the increased cross sectional area for flow, or conveyance, offered by the MRGO. Furthermore the alignment of the MRGO does not coincide with the direction of propagation of the massive surge as it heads north and only briefly coincides with southeasterly winds which locally force flow.

We have simulated Hurricane Katrina both with the MRGO/Reach 2 in place as well as with the MRGO/Reach 2 filled to surrounding bathymetric and topographic levels. The hydrodynamic computations were performed with the TF01 ADCIRC model of Southern Louisiana which is a refinement of the earlier S08 model with added details and resolution for the coastal floodplains of the north shore of Lake Pontchartrain, Mississippi and Alabama (Interagency Performance Evaluation Task Force, 2006). We applied identical wind and pressure fields derived from a Planetary Boundary Layer (PBL) model to simulate the atmospheric forcing functions during the Katrina event (Thompson and Cardone, 1996). A sequence of hourly snapshots of water surface elevations with super-imposed winds (Figure 2) shows the evolution of storm surge with the MRGO in place. More detailed elevation values are given in corresponding labeled water elevation contour plots in Figure 3. Surge buildup starts with easterly winds blowing water from east to west against the Mississippi River levees in Plaquemines Parish as well against the hurricane protection levees of St. Bernard Parish/Chalmette in addition to driving water into the funnel defined by the levees protecting St. Bernard Parish/Chalmette and New Orleans East. When winds become southerly, the massive surge that has built up in Breton Sound propagates north. We note that the northeasterly propagating storm surge has a crown of more than 16 ft above NGVD 29 extending out more than 12 miles and water levels in the entire Mississippi-Alabama Shelf exceed 10 ft above NGVD 29.

The simulation without the MRGO/Reach 2 results in very similar water levels in most of the domain for the Katrina event. Differences in the maximum Katrina event water levels with and without the MRGO in place are shown in Figures 4a and 4b. Notable differences with the MRGO Reach 2 channel in place are as follows: there is a reduction of water level of up to 0.2 ft at the entrance to the MRGO's inland cut; there is an increase of 0.3 to 0.4 ft in the marshes west of the MRGO in the region delineated by Pointe a la Hache, Carlisle, Stella, Caernarvon and Verret; a maximum increase of approximately 1.1 ft locally east of English Turn; in Lake Borgne along the MRGO there is a 0.1 to 0.2 ft increase; there is a 0.1 to 0.2 ft decrease along the St. Bernard Parish/Chalmette protection levee; and finally there is a 0.1 to 0.2 ft increase in a portion of the GIWW/MRGO/Reach 1. In all other regions, including in the IHNC, differences are less than 0.1 ft. In addition, the New Orleans and vicinity protection system is not impacted



more than 0.2 ft. These results coincide with those from the earlier studies. We note that the small increases in surge due to the presence of MRGO/Reach 2 can be traced to the alignment of the local southeasterly winds that briefly occur later in the storm and that do in fact drive more water up the MRGO/Reach 2. These waters then feed into the northward-propagating surge wave and spread laterally relative to the propagation direction. However due to fact that the alignment between the wind and the MRGO/Reach 2 is brief and in light of the shelf-wide high water levels at this stage of the storm, the impact on channel conveyance is small. The largest difference and its associated pattern seen at English Turn is related to this mechanism as well as small differences in the northward propagating waves' phasing properties coupled with the winds turning at this point as the eye of the storm moves across this area. The small decreases in maximum water elevations occur due to a small reduction in the local resistance to water being pushed by local winds in a northwesterly direction at the entrance to the MRGO/Reach 2 inland cut and due to increased water depths reducing local set-up against the St. Bernard Parish/ Chalmette protection levee (local wind driven set-up is inversely proportional to the depth of the water).

The reasons for the very limited influence of the MRGO/Reach 2 in the vicinity of New Orleans for strong storm events are clear. First, the MRGO does not influence the important preliminary east–west movement of water that drives the significant build up of surge in the early parts of the storm. Second, the northerly propagation of surge during the later stages of the storm are only minimally influenced by the MRGO because the increased hydraulic conveyance associated with the channel is very limited for large storms due to the large surge magnitude and especially due to the very large lateral extent of the high waters on the Mississippi-Alabama shelf that build up early on from the east. In addition, the propagation direction of this surge wave does not typically align with the MRGO and furthermore the southeasterly winds which align with the MRGO occur only very briefly.

The fact that all studies show a larger proportional influence of the presence of the MRGO/Reach 2 for low intensity (low peak surge magnitude) events is related to the fact that the proportional increase in conveyance due to Reach 2 is greater when the surge is small and the water levels in Breton Sound and Lake Borgne are generally low. This also explains why we see a more rapid drop in post-storm Lake Pontchartrain levels for large-scale events with the MRGO in place. Waters typically withdraw relatively rapidly from Breton Sound and Lake Borgne due to the direct connection to open waters. The total combined conveyance of the Rigolets, Chef Menteur Pass and the IHNC/GIWW/MRGO system is increased with the MRGO in place under the lower post-storm levels on the Mississippi-Alabama shelf.

While the simulations clearly show that Reach 2 of the MRGO does not significantly influence the development of storm surge in the region for large storm events, Reach 1 (the combined GIWW/MRGO section) and the IHNC, together, provide a hydraulic connection between Lake Borgne and Lake Pontchartrain. As a result of this connection, the storm surge experienced within the IHNC and Reach 1 (GIWW/MRGO) is a function of storm surge in both Lakes; a water level gradient is established within the IHNC and Reach 1 that is dictated by the surge levels in the two lakes. This is true for both low and high storm surge conditions. To prevent storm surge in Lake Borgne from reaching the IHNC or GIWW/MRGO sections of waterway, flow through the Reach 1 channel must be dramatically reduced or eliminated, either

by a permanent closure or some type of structure that temporarily serves to eliminate this hydraulic connectivity. The presence of an open channel is the key factor.

The hurricane protection levees along the south side of Orleans Parish and the eastern side of St. Bernard Parish along the MRGO, which together are referred to as a funnel, can locally collect and focus storm surge in this vicinity depending on wind speed and direction. This localized focusing effect can lead to a small local increase in surge amplitude. Strong winds from the east tend to maximize the local funneling effect.

## References

- Blain, C.A., J.J. Westerink and R.A. Luettich, 1994: The Influence of Domain Size on the Response Characteristics of a Hurricane Storm Surge Model. *Journal of Geophysical Research - Oceans*, **99**, C9, 18467-18479.
- Blain, C.A., J.J. Westerink and R.A. Luettich, 1998: Grid Convergence Studies for the Prediction of Hurricane Storm Surge. *International Journal for Numerical Methods in Fluids*, **26**, 369-401.
- Bretschneider, C. L., and J.I. Collins, 1966: Storm Surge Effects of the Mississippi River-Gulf Outlet, Study A. NESCO Report SN-326-A, National Engineering Science Company, Pasadena, CA.
- Carillo, A. R., R.C. Berger, M.S. Sarruff, and B.J. Thibodeaux, 2001: Salinity Changes in Pontchartrain Basin Estuary, Louisiana, Resulting from Mississippi River-Gulf Outlet Partial Closure Plans. ERDC/CHL TR-01-04, U.S. Army Corps of Engineers, Engineer Research and Development Center, Vicksburg, MS.
- Feyen, J.C., J.H. Atkinson and J.J. Westerink, 2002: GWCE-Based Shallow Water Equation Simulations of the Lake Pontchartrain - Lake Borgne Tidal System. *Computational Methods in Water Resources XIV*, S.M. Hassanizadeh et al. Eds., Volume 2, Developments in Water Science, 47, Elsevier, Amsterdam, 1581-1588.
- Feyen, J.C., J.J. Westerink, R.A. Luettich, J.H. Atkinson, C.N. Dawson, M.D. Powell, J.P. Dunion, H.J. Roberts, E. J. Kubatko, H. Pourtaheri, 2005: A New Generation Hurricane Storm Surge Model for Southern Louisiana. *Bulletin of the American Meteorological Society*, In Review.
- Interagency Performance Evaluation Task Force, 2006: Performance Evaluation Plan and Interim Status, Report 1 of a Series; Performance Evaluation of the New Orleans and Southeast Louisiana Hurricane Protection System. Report MMTF 00038-06, U.S. Army Corps of Engineers, Washington D.C.
- Luettich, R.A., J.J. Westerink, and N.W. Scheffner, 1992: ADCIRC: An Advanced Three-Dimensional Circulation Model for Shelves, Coasts and Estuaries, Report 1: Theory and Methodology of ADCIRC-2DDI and ADCIRC-3DL. *Technical Report DRP-92-6*, Department of the Army, U.S. Army Corps of Engineers, Washington D.C.
- Luettich, R.A. and J.J. Westerink, 2004: Formulation and Numerical Implementation of the 2D/3D ADCIRC Finite Element Model Version 44.XX.  
[http://www.marine.unc.edu/C\\_CATS/adcirc/adcirc\\_theory\\_2004\\_12\\_08.pdf](http://www.marine.unc.edu/C_CATS/adcirc/adcirc_theory_2004_12_08.pdf)

- Luettich, R.A. and J.J. Westerink, 2005: ADCIRC: A Parallel Advanced Circulation Model for Oceanic, Coastal and Estuarine Waters; Users Manual for Version 45.08.  
[http://www.marine.unc.edu/CATS/adcirc/document/ADCIRC\\_title\\_page.html](http://www.marine.unc.edu/CATS/adcirc/document/ADCIRC_title_page.html)
- McAnally, W. H., and R.C. Berger, 1997: Salinity Changes in Pontchartrain Basin Estuary Resulting from Bonnet Carre Freshwater Diversion. Technical Report CHL-97-2, U.S. Army Engineer Waterways Experiment Station, Vicksburg, MS.
- Tate, J. N., A.R. Carillo, R.C. Berger, and B.J. Thibodeaux, 2002: Salinity Changes in Pontchartrain Estuary, Louisiana, Resulting from Mississippi River-Gulf Outlet Partial Closure Plans and Width Reduction. ERDC/CHL TR-02-12, U.S. Army Corps of Engineers, Engineer Research and Development Center, Vicksburg, MS.
- Thompson, E.F., and V.J. Cardone, 1996: Practical Modeling of Hurricane Surface Wind Fields. *Journal of Waterway, Port, and Coastal Engineering.*, **122**, 4, 195-205.
- U.S. Army Corps of Engineers, New Orleans District, 2003: Numerical Modeling of Storm Surge Effect of MRGO Closure. New Orleans, LA.
- URS Corporation, 2006: The Direct Impact of the Mississippi River Gulf Outlet on Hurricane Storm Surge. Performed under contract 2503-05-39, Prepared for State of Louisiana Department of Natural Resources, Baton Rouge, LA.
- Westerink, J.J., R.A. Luettich, H. Pourtaheri, 2000: Preliminary Sensitivity Studies of Tidal Response in the Lake Ponchartrain-Lake Borgne System. Contractors report prepared for the U.S. Army Corps of Engineers, New Orleans District, New Orleans, LA.
- Westerink, J.J., R.A. Luettich, J.C. Feyen, J.H. Atkinson, C. Dawson, M.D. Powell, J.P. Dunion, H.J. Roberts, E. J. Kubatko, H. Pourtaheri, 2006: A Basin to Channel Scale Unstructured Grid Hurricane Storm Surge Model for Southern Louisiana. *Monthly Weather Review*, To be submitted.

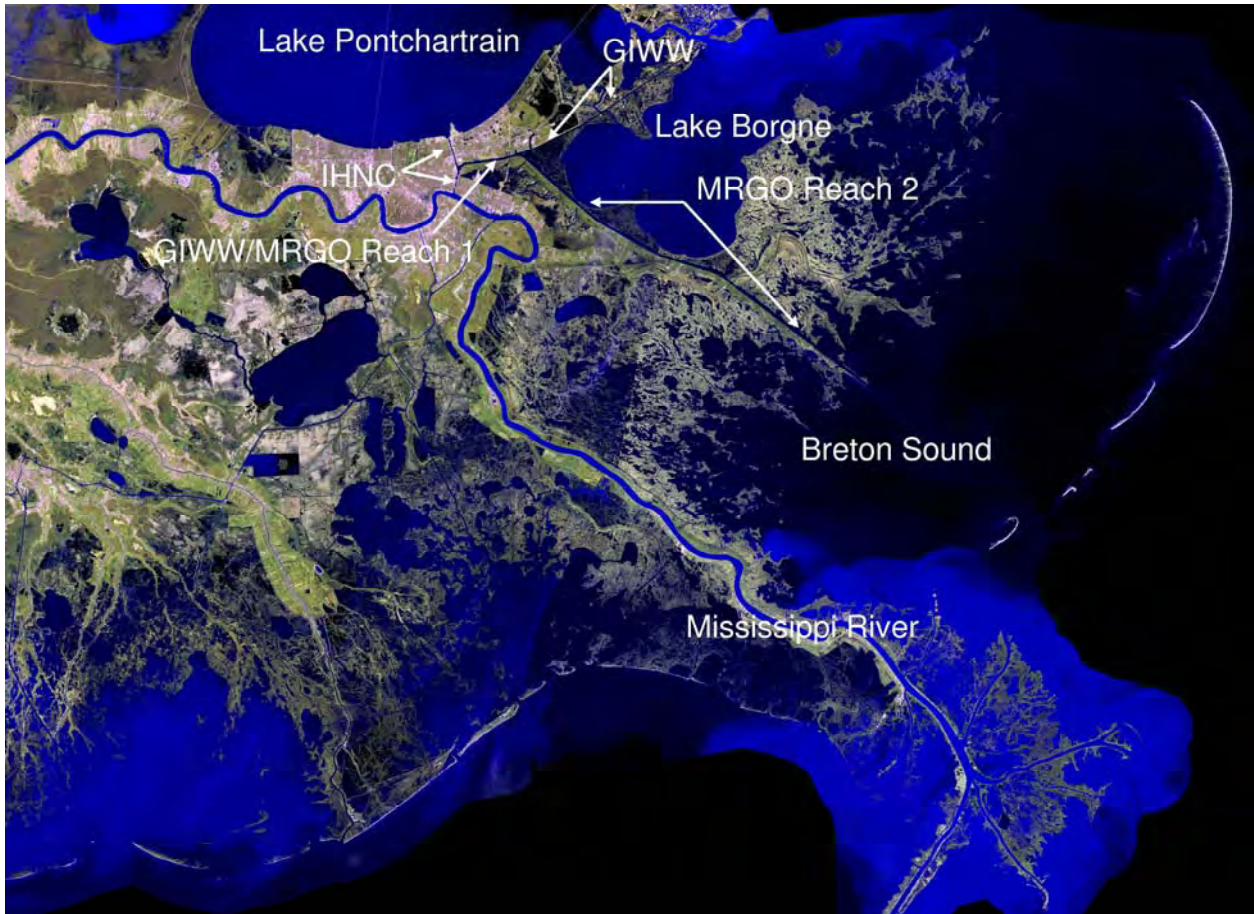


Figure 1a. Satellite image of Southeastern Louisiana





Figure 1b. Satellite image of metropolitan New Orleans and vicinity



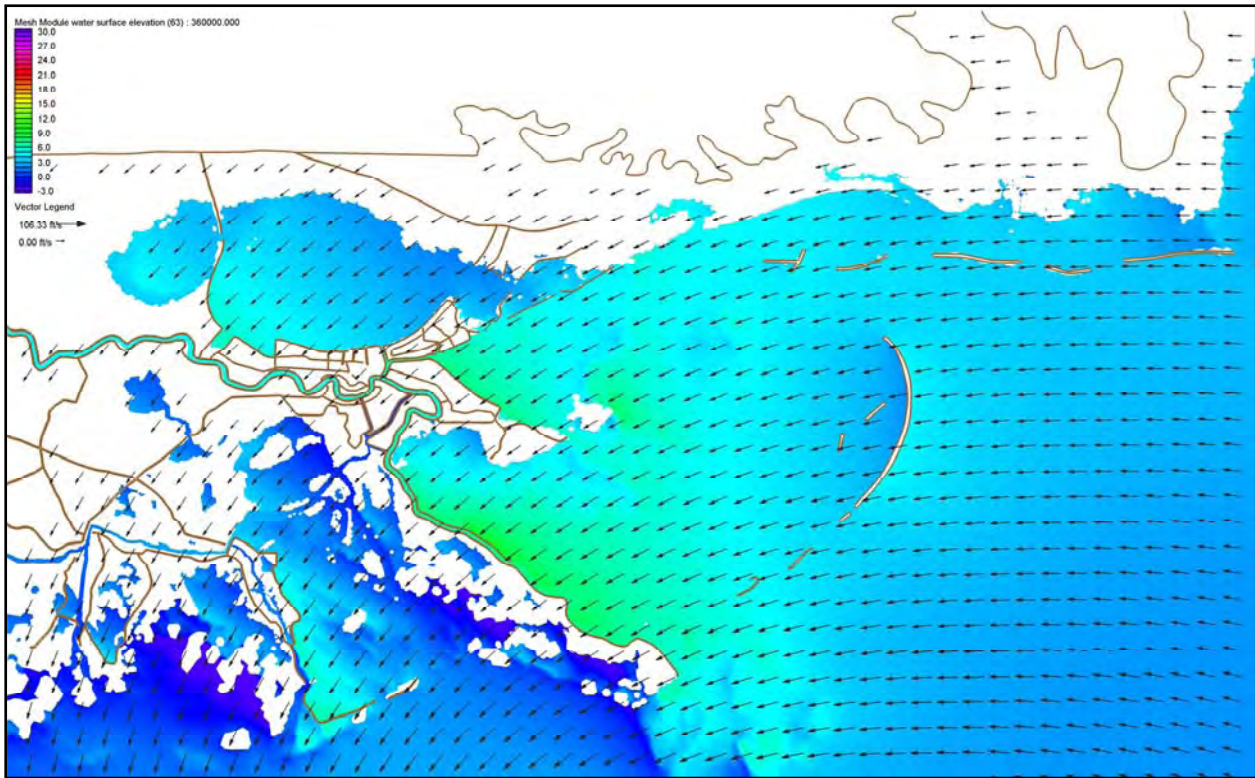


Figure 2a. Water surface elevation with respect to the NGVD29 (ft) with boundary layer adjusted wind velocity vectors (knots) during Hurricane Katrina on August 29, 2005 at 0700UTC

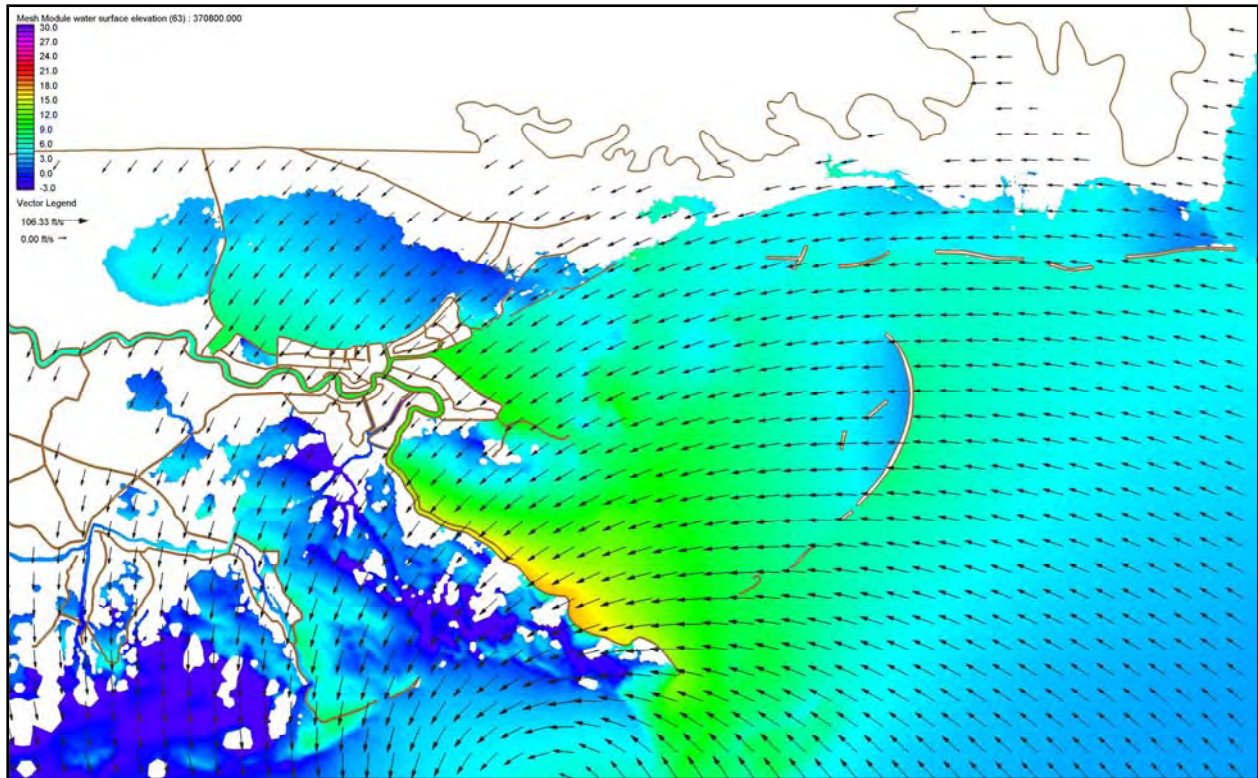


Figure 2b. Water surface elevation with respect to the NGVD 29 (ft) with boundary layer adjusted wind velocity vectors (knots) during Hurricane Katrina on August 29, 2005 at 1000UTC

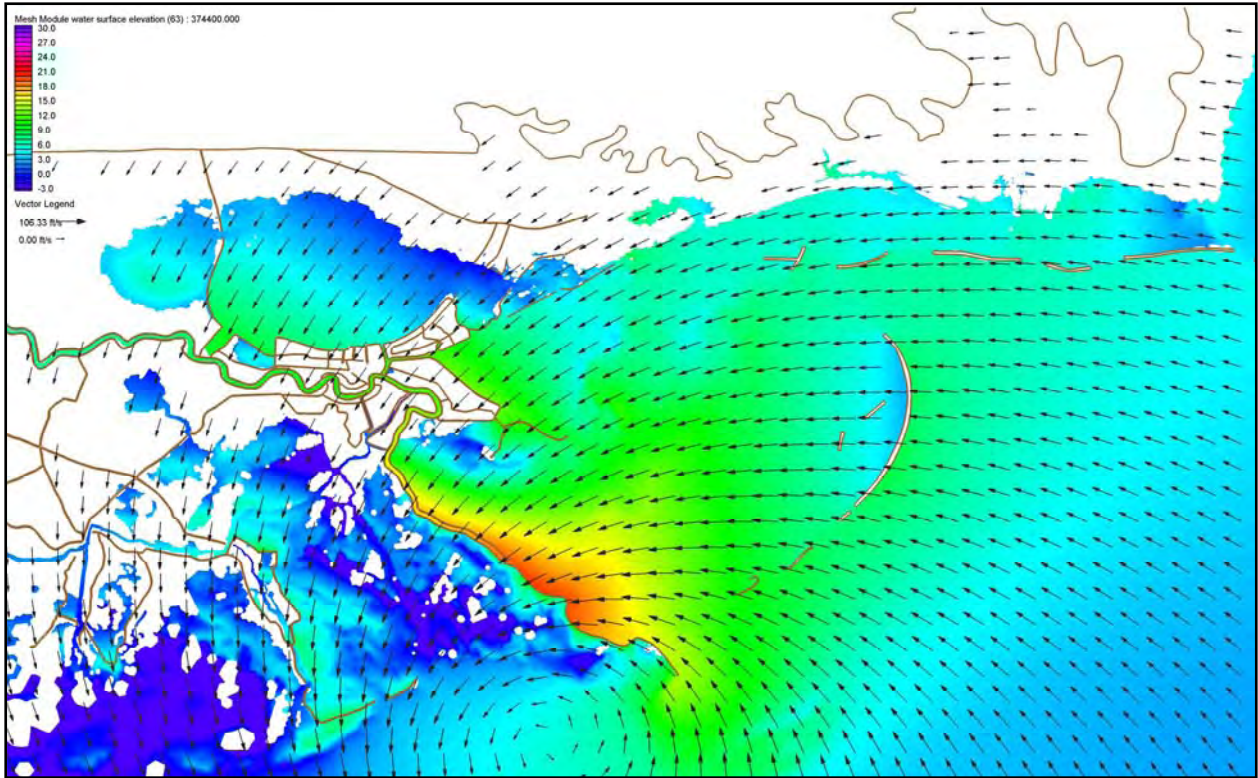


Figure 2c. Water surface elevation with respect to the NGVD 29 (ft) with boundary layer adjusted wind velocity vectors (knots) during Hurricane Katrina on August 29, 2005 at 1100UTC



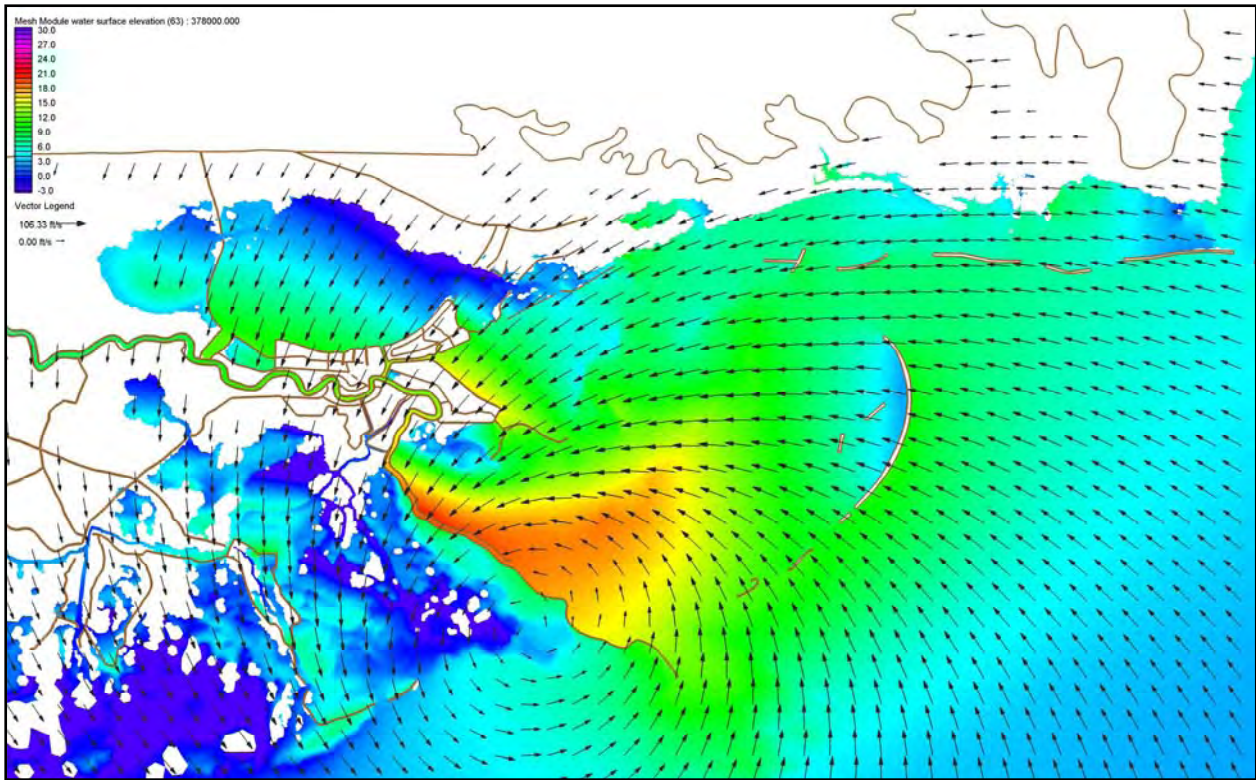


Figure 2d. Water surface elevation with respect to the NGVD 29 (ft) with boundary layer adjusted wind velocity vectors (knots) during Hurricane Katrina on August 29, 2005 at 1200UTC

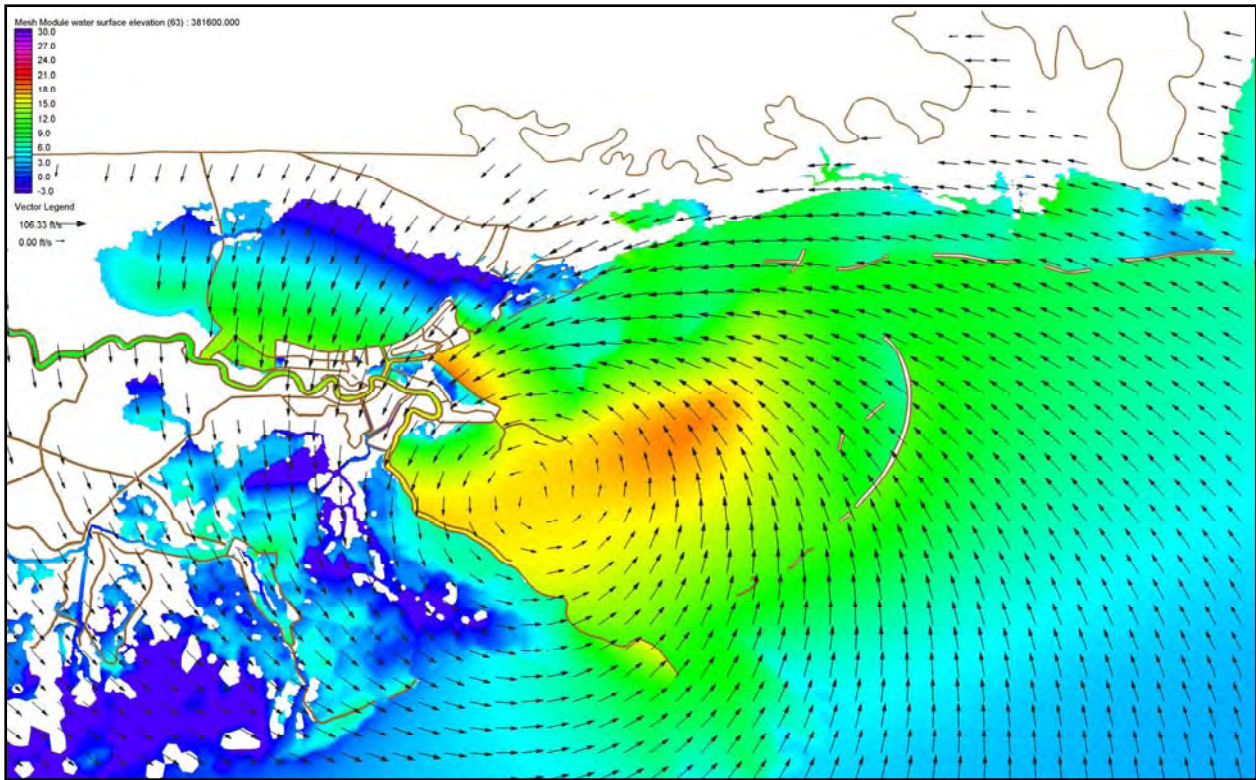


Figure 2e. Water surface elevation with respect to the NGVD 29 (ft) with boundary layer adjusted wind velocity vectors (knots) during Hurricane Katrina on August 29, 2005 at 1300UTC



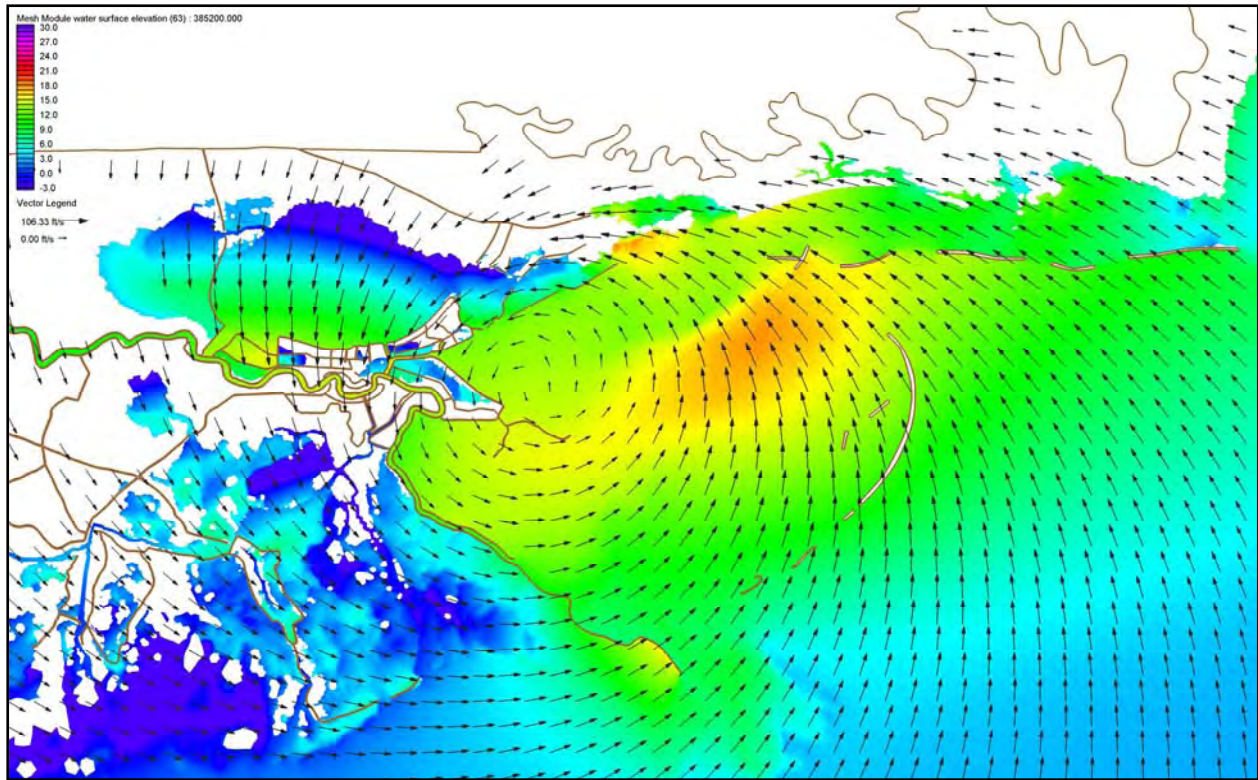


Figure 2f. Water surface elevation with respect to the NGVD 29 (ft) with boundary layer adjusted wind velocity vectors (knots) during Hurricane Katrina on August 29, 2005 at 1400UTC

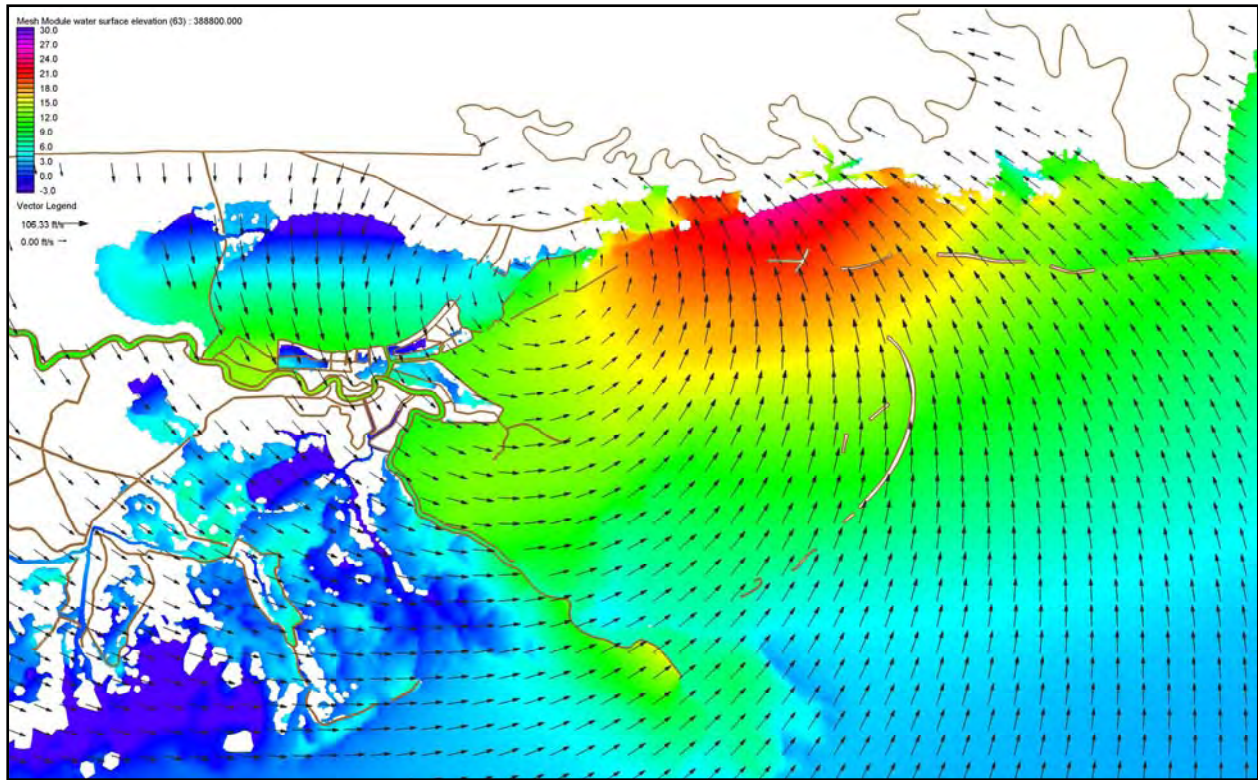


Figure 2g. Water surface elevation with respect to the NGVD 29 (ft) with boundary layer adjusted wind velocity vectors (knots) during Hurricane Katrina on August 29, 2005 at 1500UTC



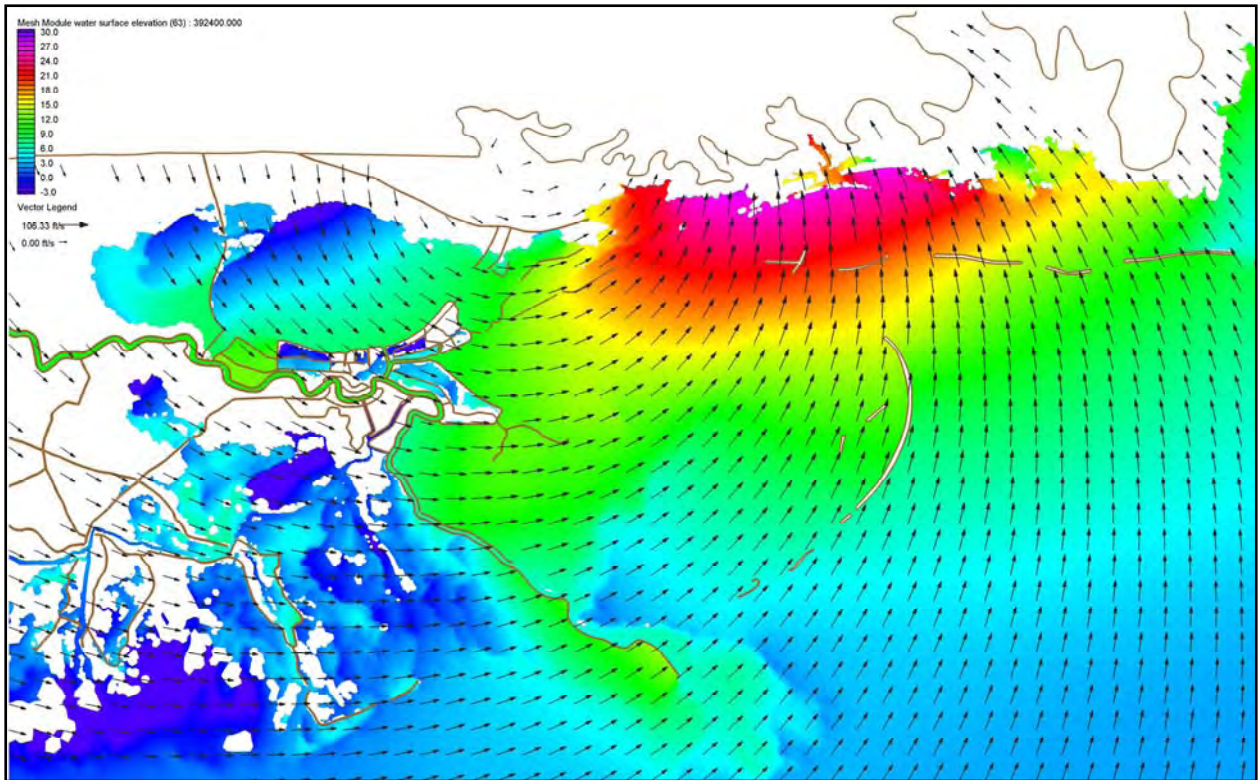


Figure 2h. Water surface elevation with respect to the NGVD 29 (ft) with boundary layer adjusted wind velocity vectors (knots) during Hurricane Katrina on August 29, 2005 at 1600UTC

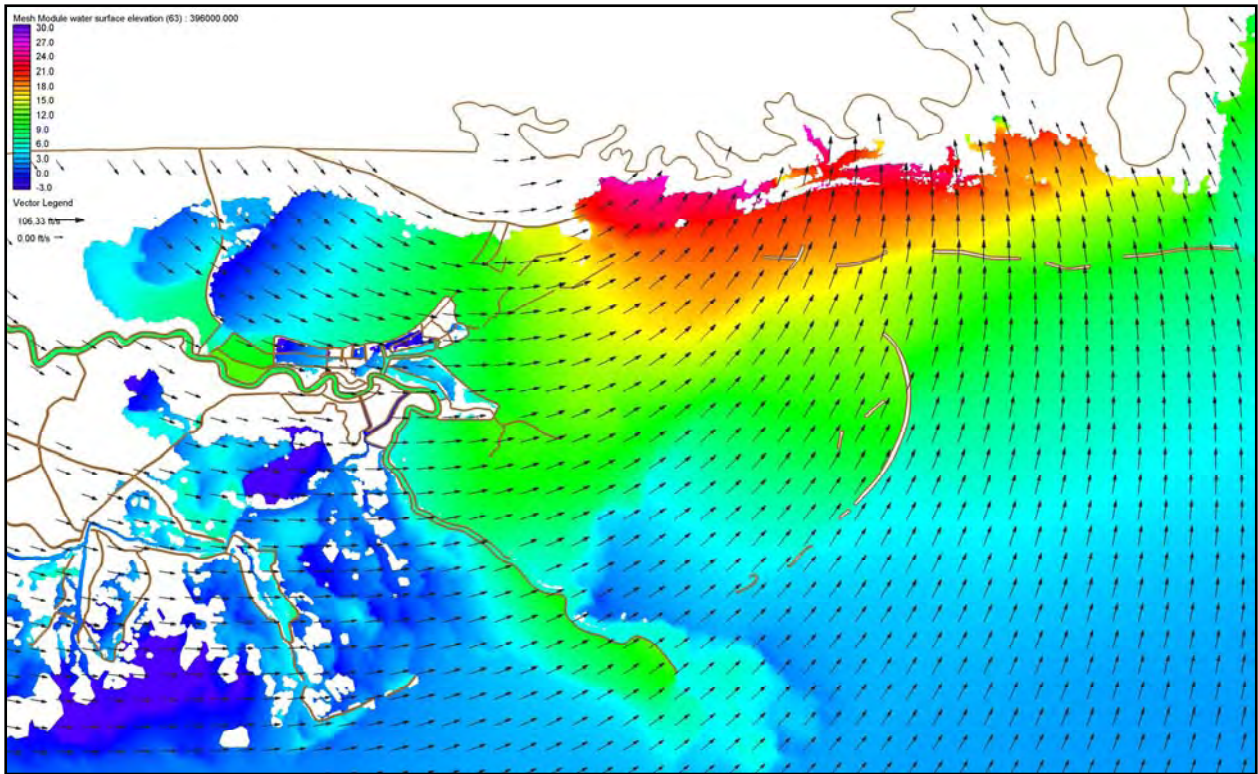


Figure 2i. Water surface elevation with respect to the NGVD 29 (ft) with boundary layer adjusted wind velocity vectors (knots) during Hurricane Katrina on August 29, 2005 at 1700UTC

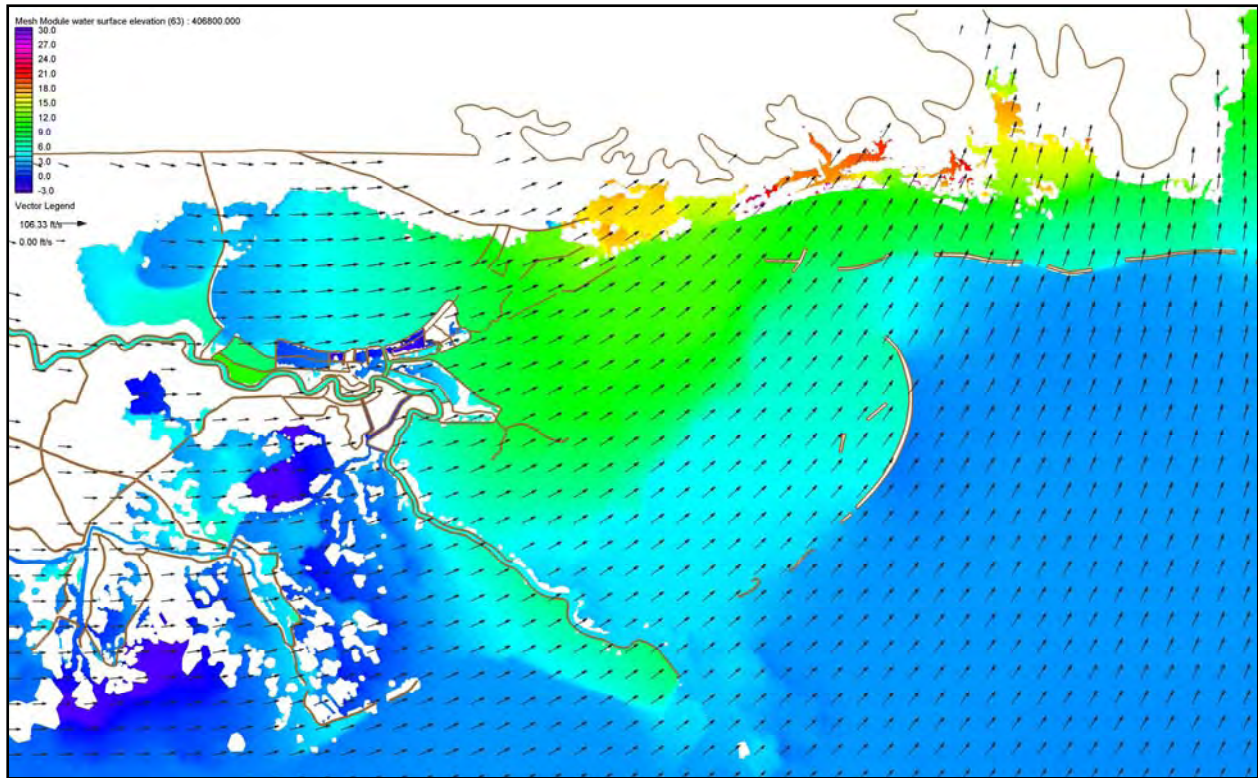


Figure 2j. Water surface elevation with respect to the NGVD 29 (ft) with boundary layer adjusted wind velocity vectors (knots) during Hurricane Katrina on August 29, 2005 at 2000UTC



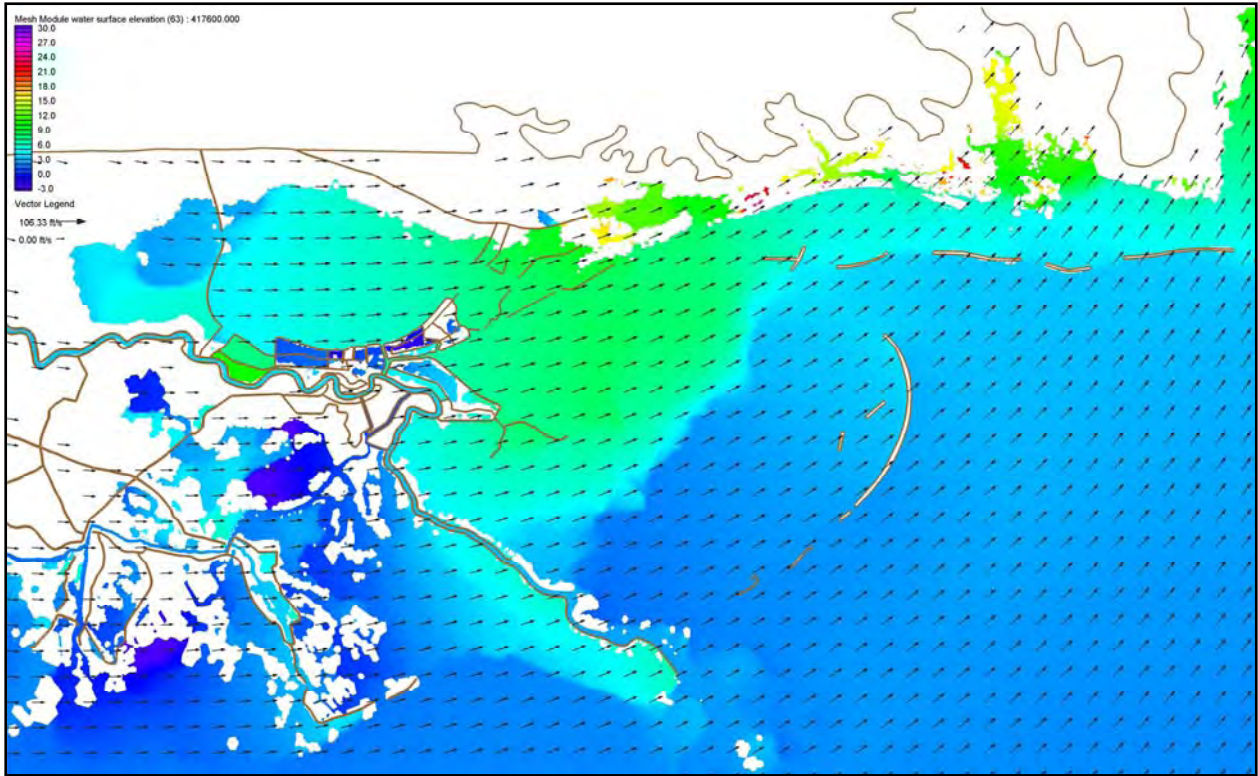


Figure 2k. Water surface elevation with respect to the NGVD 29 (ft) with boundary layer adjusted wind velocity vectors (knots) during Hurricane Katrina on August 29, 2005 at 2300UTC

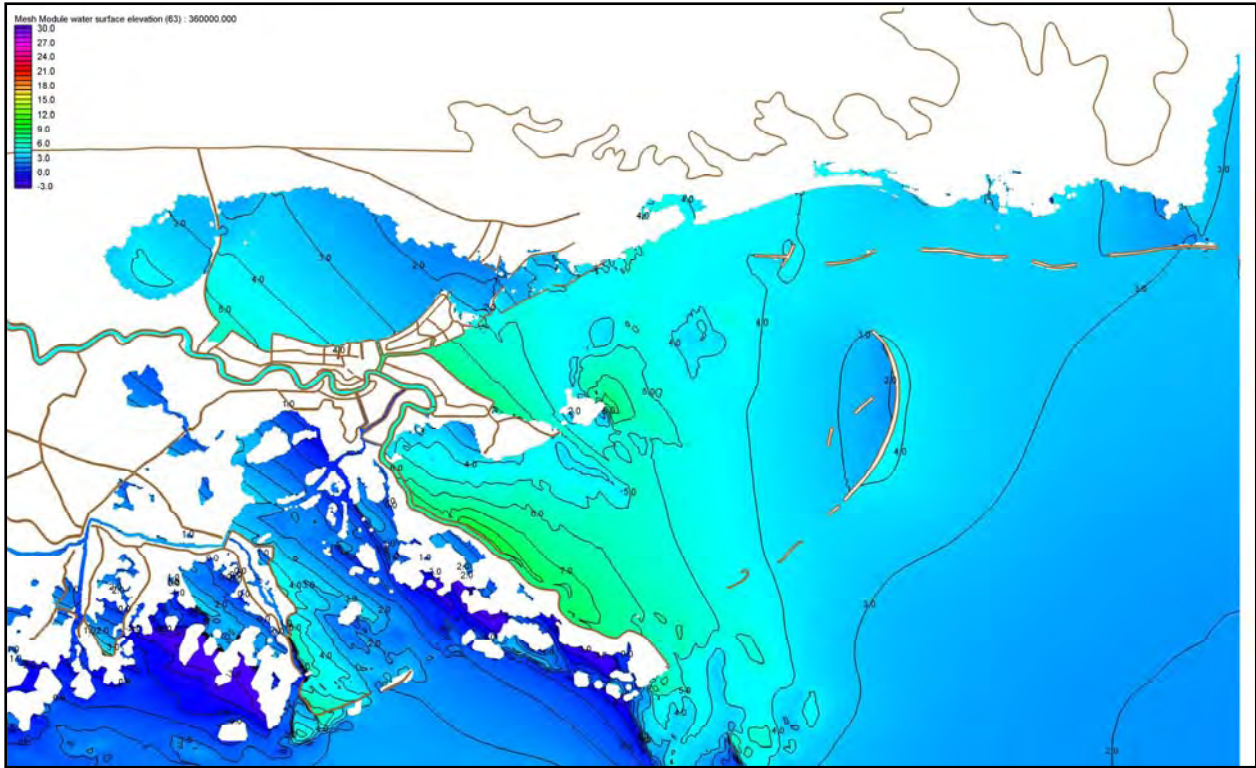


Figure 3a. Water surface elevation with respect to the NGVD 29 (ft) with labeled contours during Hurricane Katrina on August 29, 2005 at 0700UTC

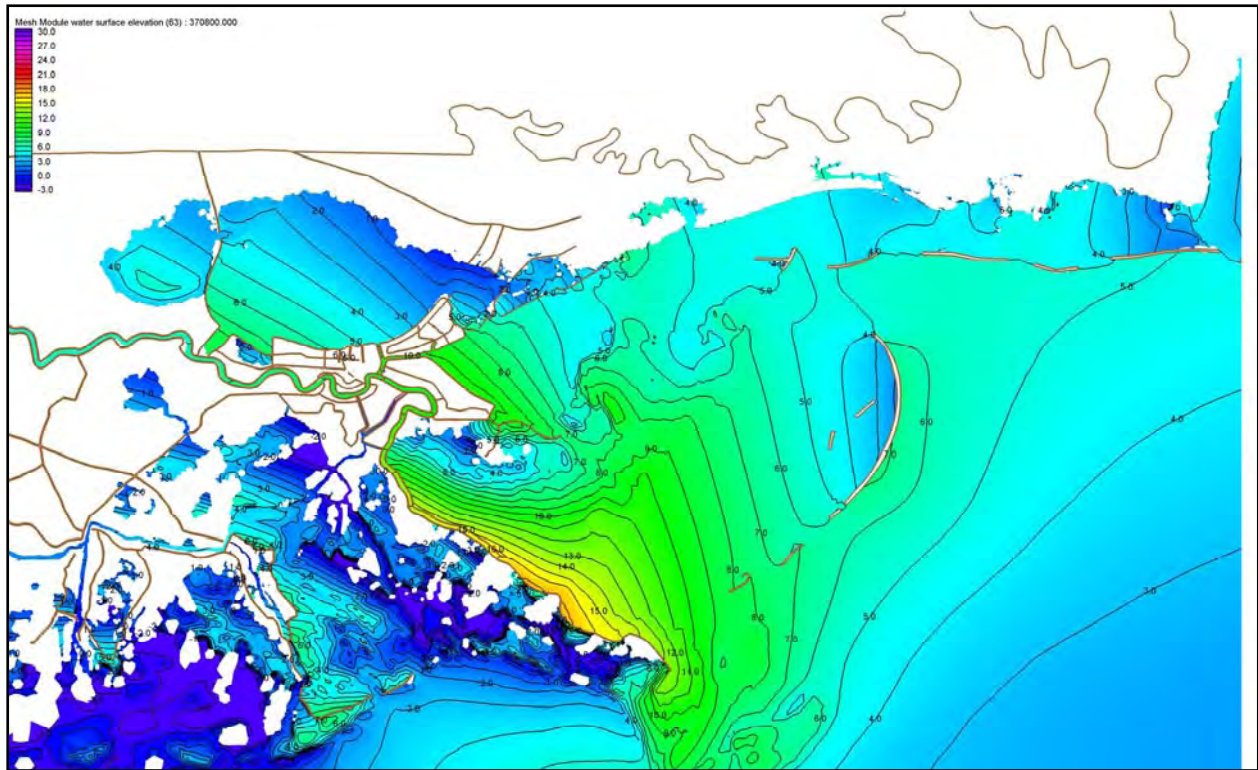


Figure 3b. Water surface elevation with respect to the NGVD 29 (ft) with labeled contours during Hurricane Katrina on August 29, 2005 at 1000UTC



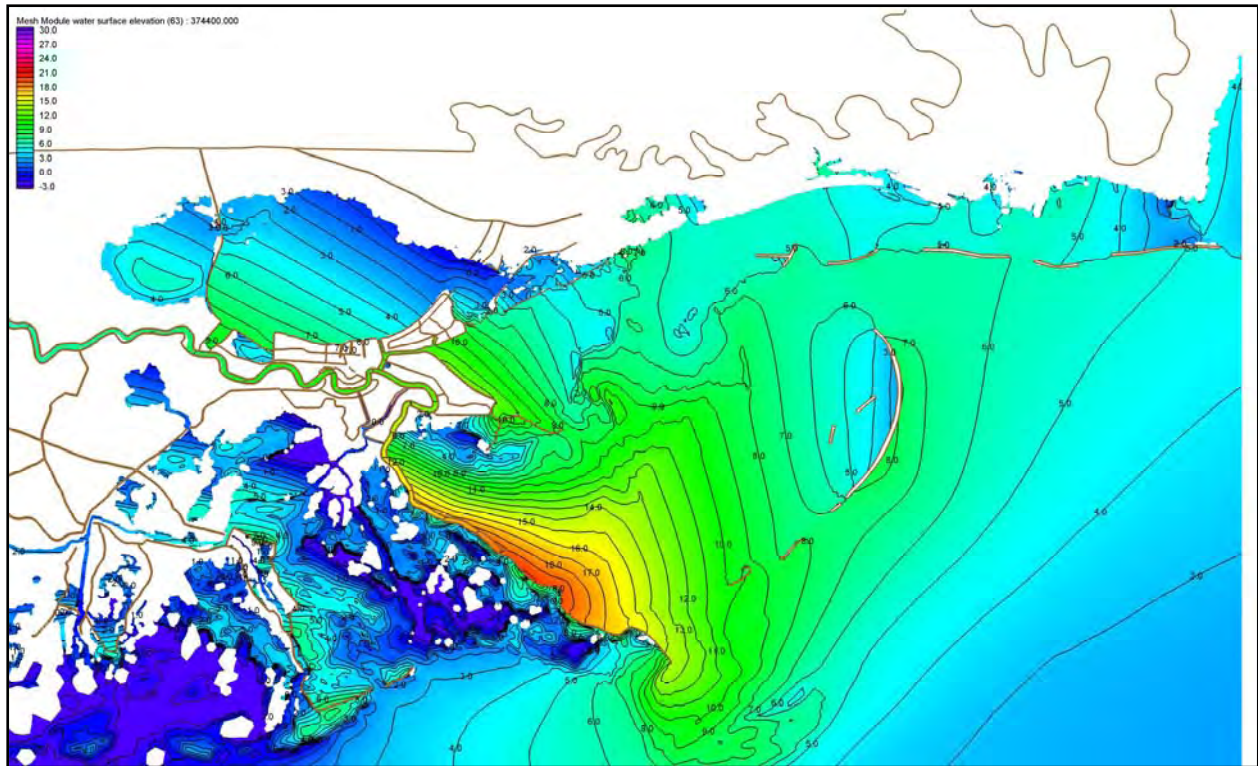


Figure 3c. Water surface elevation with respect to the NGVD 29 (ft) with labeled contours during Hurricane Katrina on August 29, 2005 at 1100UTC

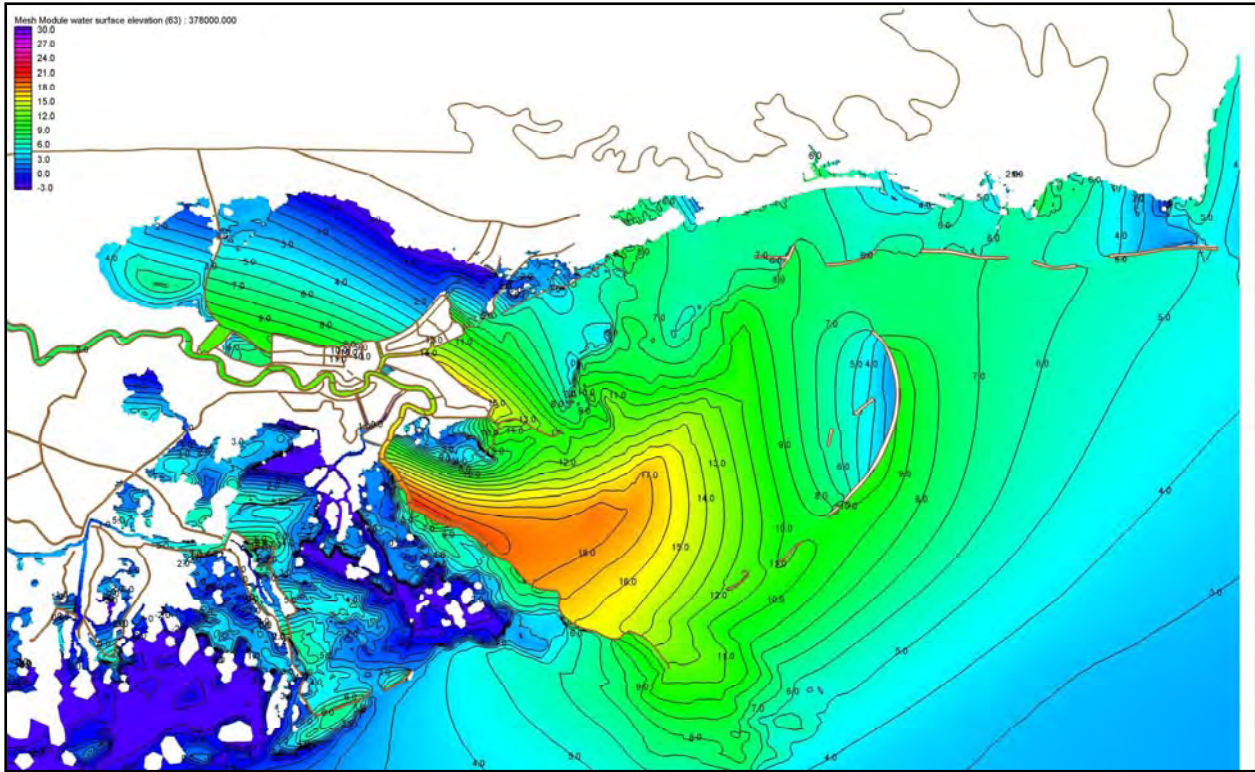


Figure 3d. Water surface elevation with respect to the NGVD 29 (ft) with labeled contours during Hurricane Katrina on August 29, 2005 at 1200UTC



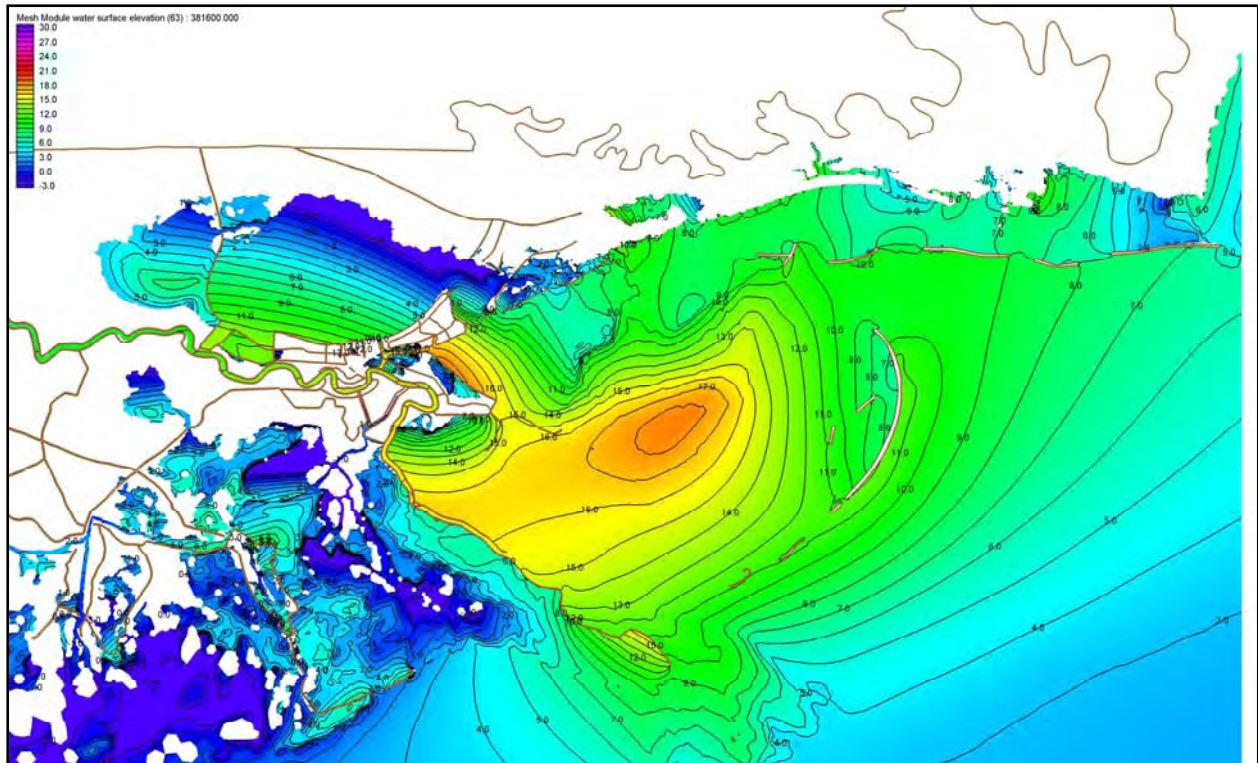


Figure 3e. Water surface elevation with respect to the NGVD 29 (ft) with labeled contours during Hurricane Katrina on August 29, 2005 at 1300UTC

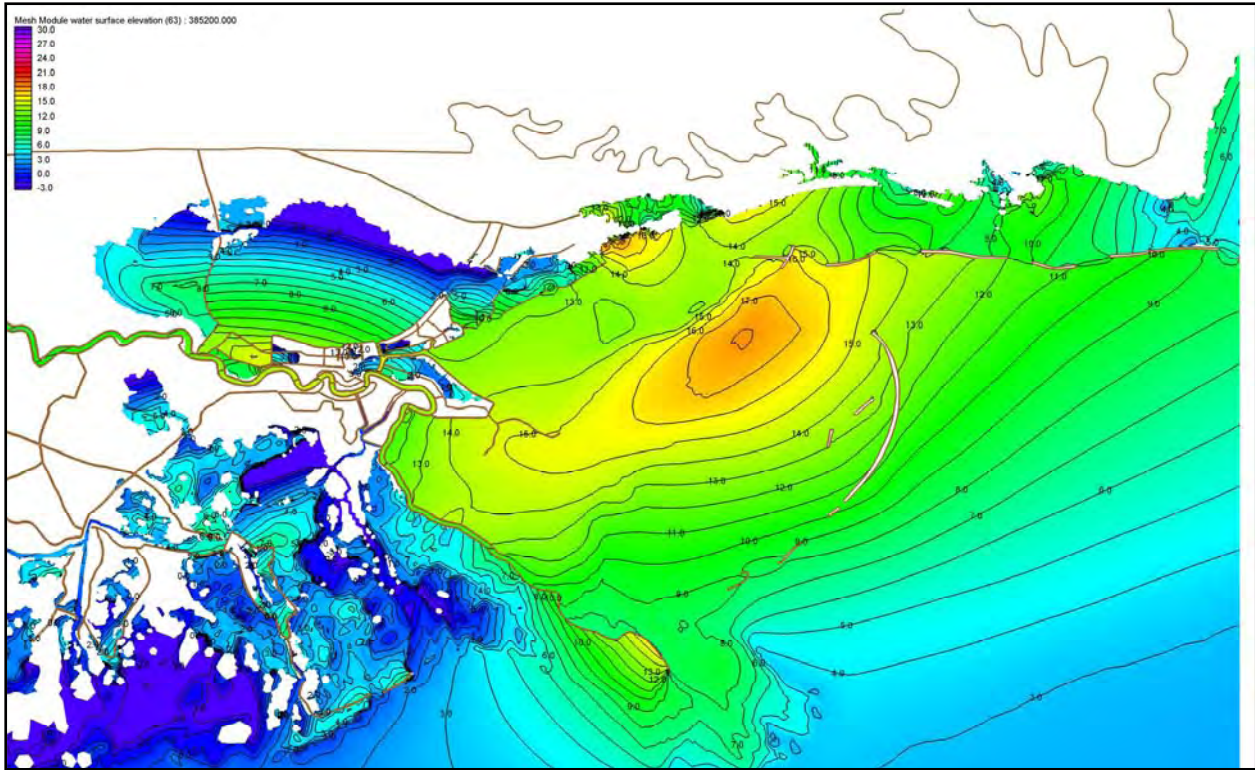


Figure 3f. Water surface elevation with respect to the NGVD 29 (ft) with labeled contours during Hurricane Katrina on August 29, 2005 at 1400UTC

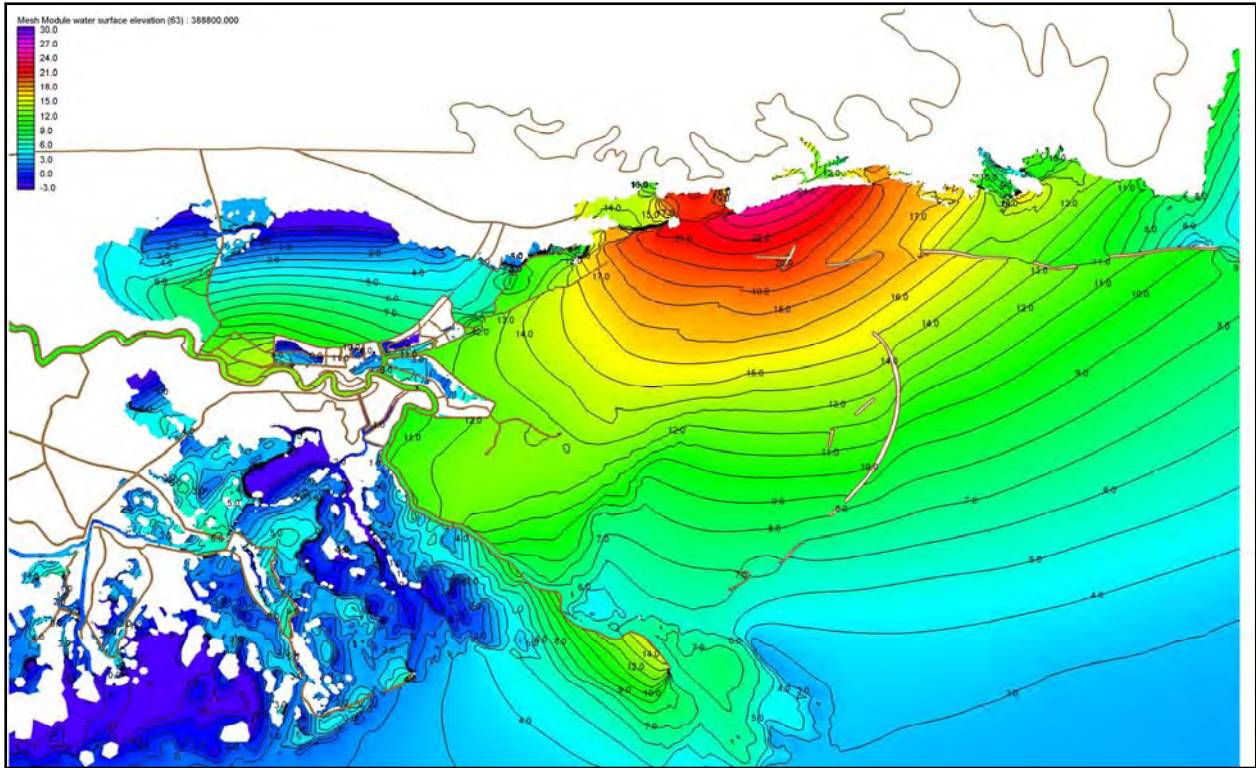


Figure 3g. Water surface elevation with respect to the NGVD 29 (ft) with labeled contours during Hurricane Katrina on August 29, 2005 at 1500UTC



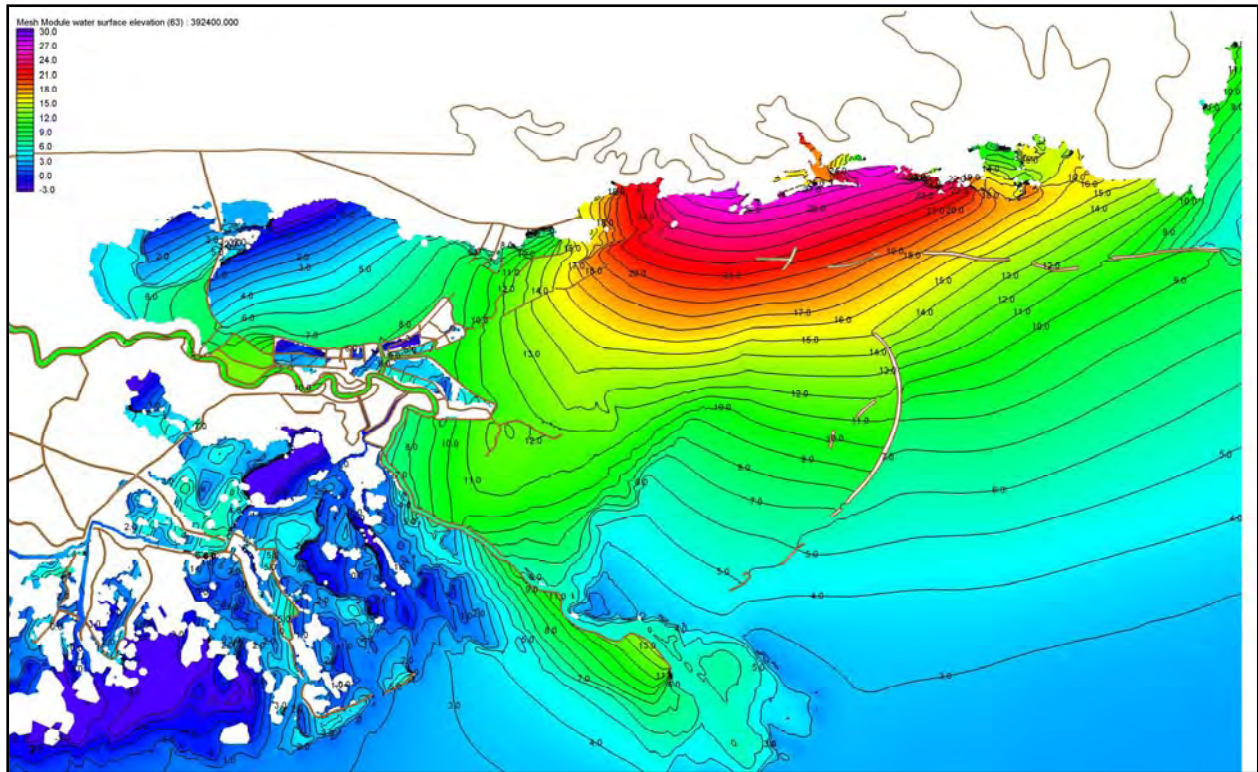


Figure 3h. Water surface elevation with respect to the NGVD 29 (ft) with labeled contours during Hurricane Katrina on August 29, 2005 at 1600UTC

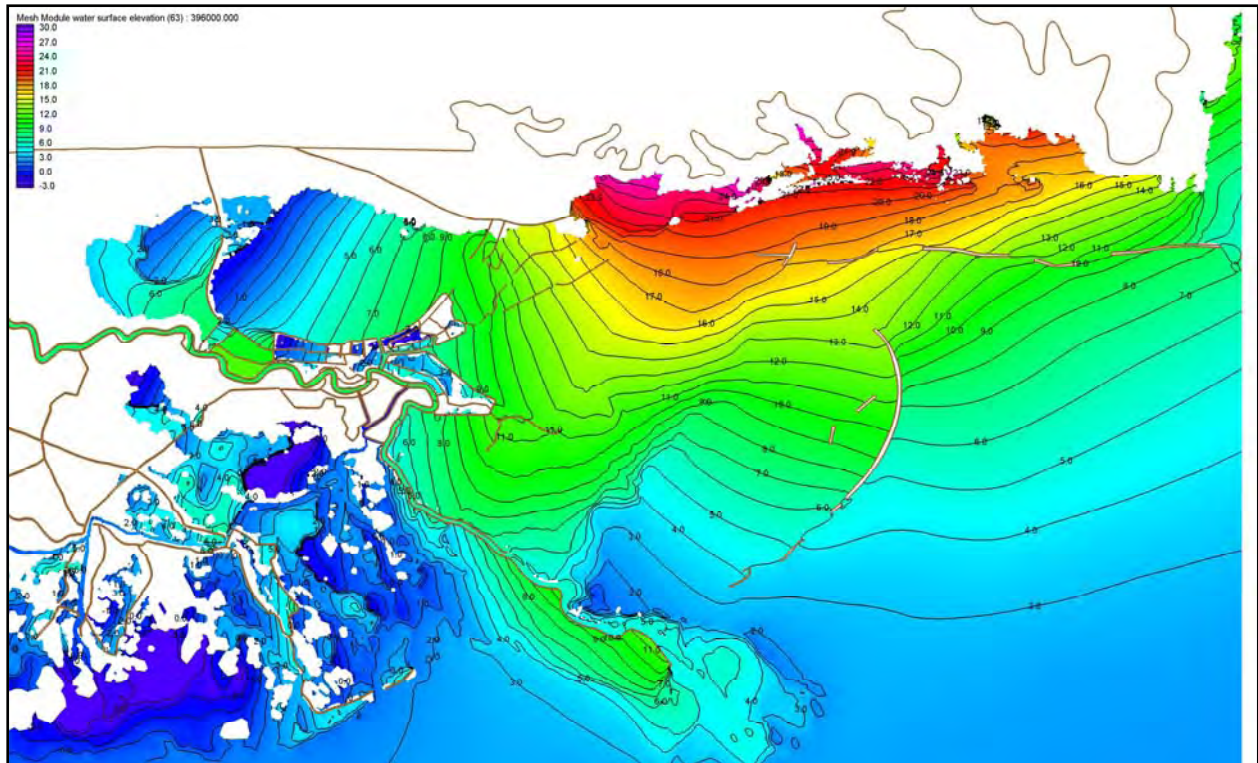


Figure 3i. Water surface elevation with respect to the NGVD 29 (ft) with labeled contours during Hurricane Katrina on August 29, 2005 at 1700UTC



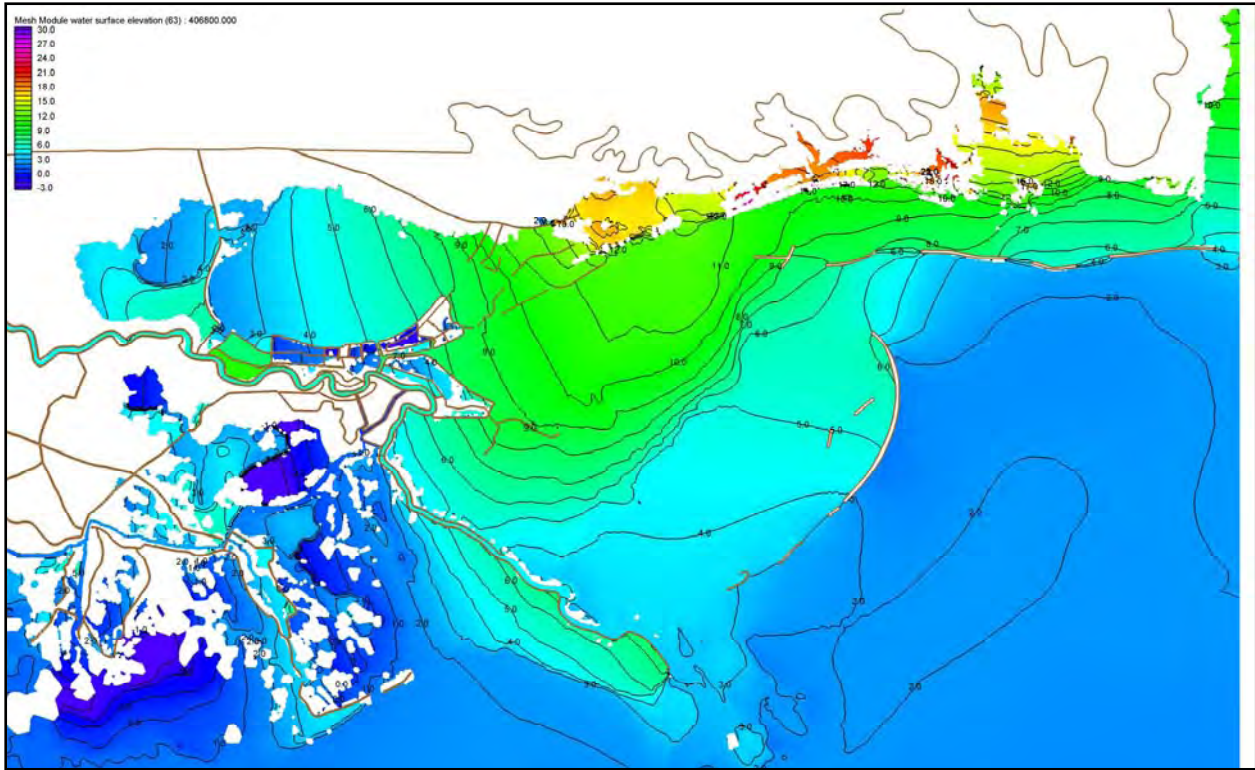


Figure 3j. Water surface elevation with respect to the NGVD 29 (ft) with labeled contours during Hurricane Katrina on August 29, 2005 at 2000UTC

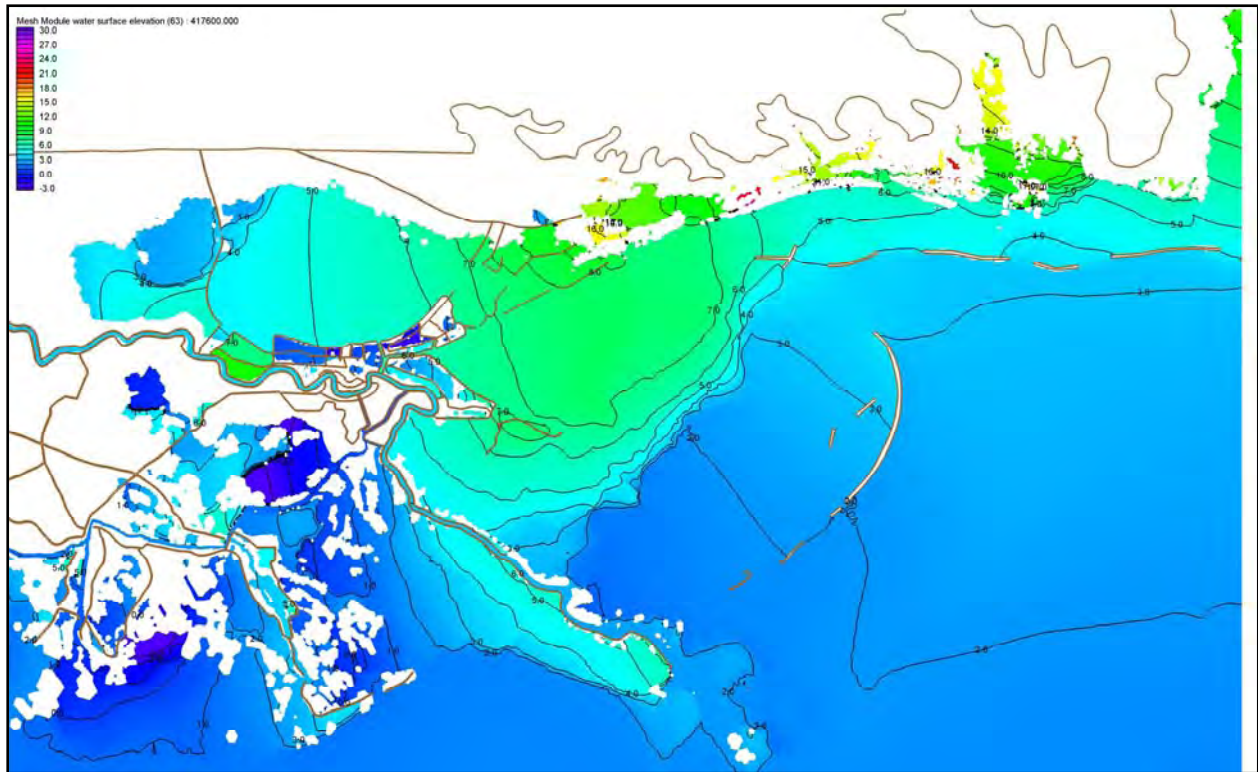


Figure 3k. Water surface elevation with respect to the NGVD 29 (ft) with labeled contours during Hurricane Katrina on August 29, 2005 at 2300UTC

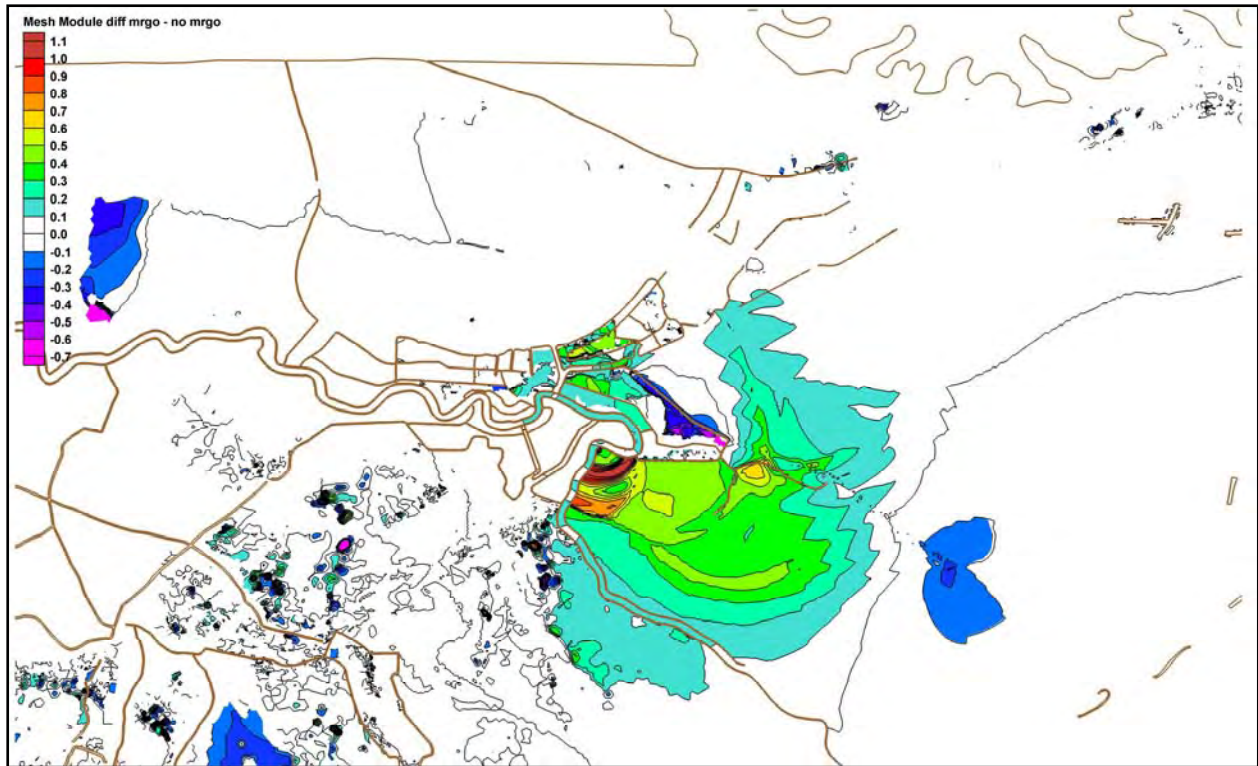


Figure 4a. Maximum Hurricane Katrina event differences in ft, for simulations with and without the MRGO in place. Positive differences indicate increased elevations with the MRGO in place while negative differences indicate decreased water levels with the MRGO in place

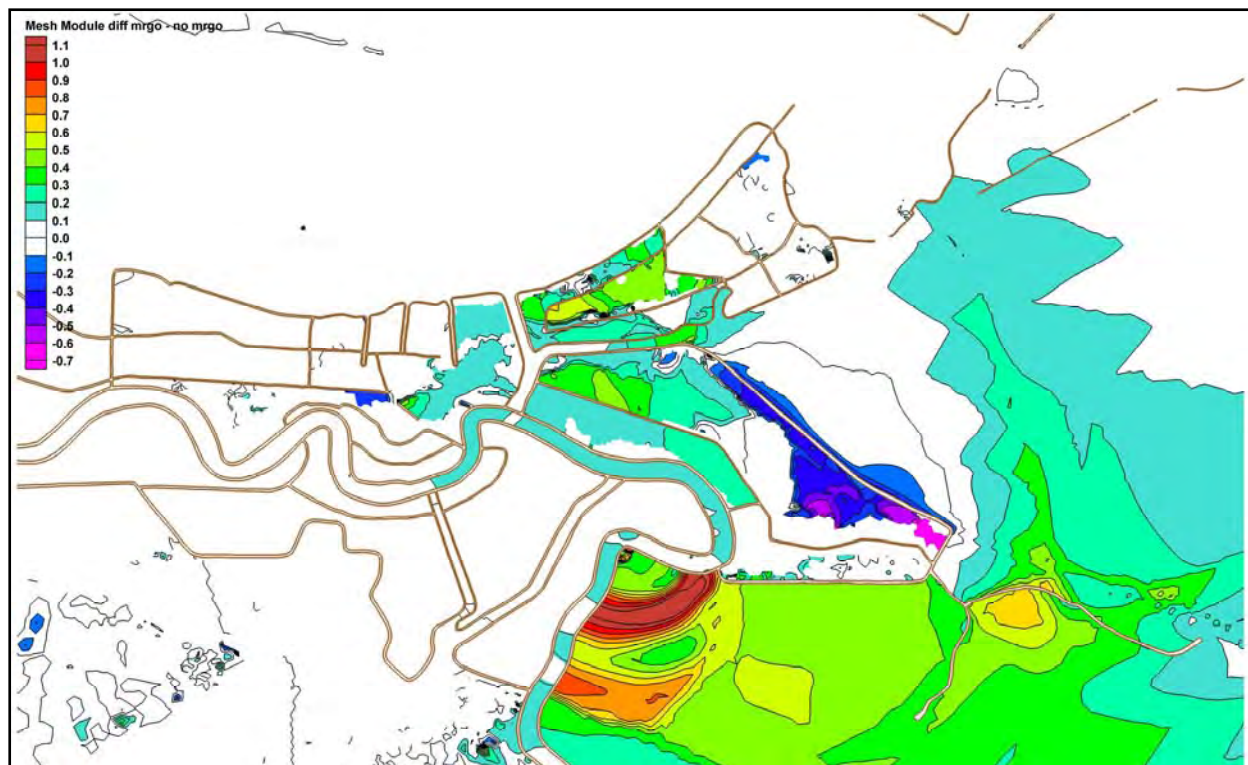


Figure 4b. Maximum Hurricane Katrina event differences in ft in metropolitan New Orleans and vicinity, for simulations with and without the MRGO in place. Positive differences indicate increased elevations with the MRGO in place while negative differences indicate decreased water levels with the MRGO in place



# Appendix 7

## Eyewitness Accounts of Flooding Caused by Hurricane Katrina

---

### Introduction

As part of the IPET field data collection task, Corps employees assigned to IPET interviewed survivors of Hurricane Katrina to record first-hand observations of flooding that occurred during and after the hurricane. The interviewers focused on collecting information about the timing of events, rate of water level rise, source of floodwaters, and direction of flow. Where feasible, interviews were conducted in person at the site of the observations. These eyewitness accounts, with identifying information removed, are presented in this appendix. The approximate location of the reported observations in UTM NAD 1983 Zone 15 coordinates (meters) is noted for each interview.

It is important to note that while some groups of interviews are remarkably consistent or can be confirmed by data from other sources, other interviews provide unique information that can not be confirmed by other available data. Also, in some cases, all or part of an interview may conflict with other interviews in nearby locations or with data from other sources.



## 17th Street Canal

779,100

3,321,500

The following information is from a recorded cell phone message. Resident reported that a neighbor called and left messages concerning water levels. Each message was time tagged. Begin phone messages: 0649-So far, your house is fine, 6 inches of water in the street out front. 0725-The water climbed about 4 inches more, barely over our bottom step. 0841-Shed door blew open and water on Toyota but not over seats yet. Water will need to come up 2 more feet before house is threatened. 1207-Worst seems to be over. Water got high but never got in house. 1338-House is flooding! 1617-We have 2 ft of water inside. I imagine you do too. Toyota submerged. Next message at unknown time: Sorry, I've been out of touch. I left the house at 8:30 (2030 hrs) last night when we had 48 inches (of water) inside. End of recorded phone messages.

779,100

3,321,500

Eyewitness confirmed leaving phone messages described in previous interview. Water level at 7:25 a.m. was much higher than observed during normal rainfall. Water moved south and west around house following railroad embankment towards Canal Street. Water was rising about 1 inch every 5 minutes once water entered the house. The eyewitness marked the water level marked on the living room door 10.5 inches above floor at 2:25 p.m.. About 8:30 to 8:45 p.m., eyewitness walked out along the railroad track under clear skies and crossed Canal Blvd. Water was flowing north to south on Canal Blvd at about 10 mph. The water level was a least up to the low chord of the railroad bridge.

779,000

3,321,600

On Monday morning at 7 am, the eyewitness was in her home and water started coming into her home. It was coming in fast and in a very short time, in a matter of minutes, it was well above her ankles in her den -- about 3-4" deep. The water did not slow down, and by 11am, it was in her kitchen 1 ½ ft deep, about ½ way up her cabinets. Using the steps in her house, she said the water was rising about 8" every hour. It continued to rise like that all day and into the night; she got to her second story and stayed there the night, next to the window in case she had to get to the roof. On Tuesday morning at 9 am, she got a boat to stop, by they were full, and said they would come back for her. The water was then was flowing over her 9 ft concrete fence in her yard. She said the water was 10 ft deep, and that even then it still had a current and was flowing north to south—from the Lake. The water was deep enough that the boat that came back for her at 12 on Tuesday had a motor on it and was driving in the water like it was a lake.

779,400  
3,321,900

On Monday morning about 7:30 am, the worst of the storm had passed, and he went to the yard to clean up. There was no water in the street at that time. At 8 am, he noticed water pilling up in the street, but it was not a rush at all, but a slow steady rise. It got closer and closer to his home, and he was able to put most of what he wanted up and into the attic. It rose all day until about 4 pm, stopping about 5 ft in his house; his home is about 2 ft off the ground. They stayed the night in the attic and left on Tuesday morning at 8:30 am. The water had not fallen any at that time.

778,700  
3,324,200

He reported hearing a loud boom and rumbling like thunder. 20 to 30 minutes after boom he saw a wave of black water at bottom of house; this was about 0930 to 1030 time frame. Every 10 to 20 minutes it went up another ½ foot. By 1200 to 1400 hrs water was up to ceiling. He thinks he has 12-foot ceilings, but not sure. He found a battery-operated clock that he knew was functioning before the flood, which showed 1240 hrs. This clock was at about chest level.

778,400  
3,321,500

On early Monday the 29<sup>th</sup>, the storm came in, and there was a lot of rain and wind. They had moved their cars to high ground in front of the home and were waiting it out. About 11 am to 12, the wind was still blowing, but not nearly as badly, and all seemed to be okay. There was water from the storm all in the street. At 12:30 pm, she looked out and noticed water in the street and getting higher; she thought the pumping station would come on, but it never did. She said the water was rising quickly and was coming from the north, flowing south; by 3:00 pm, the water was over the cars, which she said was about 4-5 ft deep in the street. Her brother was at the home with her, and he got in a boat to look for people. She said the current was strong, but he could paddle around in it. He was out in the water until just before dark, about 6:30 pm, and by then the current had increased to the point he was not sure if he could get back to the home, but he did make it, and it was still coming from the north. At 6 pm, the water was 2” from the second story porch they were on, and that story is 12 ft from the ground. By 6 am Tuesday, the water had risen the 2” and was lapping onto the porch, but did not come up more from there.

778,700  
3,324,200

On Monday morning the rainwater was in the street about 18” deep and the water was clear, and was ½ way up the lawn but not close to the slab of the home. About 10 am, the water turned brown and there was a flow in the water, about 5 knots the witness said, flowing west to the east. The water was rising 6” to 1 ft every hour after 10 am. By about 3 pm, the water had finished rising and was just under the gutters of the home. He thought the pumps would pump the water down, but they did not come on. Tuesday morning, it had risen about 6” and he left at 7 pm on Tuesday, and by then it had settled.

Hammond Bridge  
17th Street Canal

The witness was called about a breach at 17th Street canal around noon on Monday, August 29. He arrived at the breach site at 12:46 pm. At that time, he reported that the Bellaire area was already flooded and water was pouring through the breach

779,300  
3,323,700

On Monday about 9 am, the worst of the storm had passed and there was about 8 to 12” of water in the street with the drains stopped up, so he went to his garage to get a rake to clean the drains. When he came back to the front of his yard, water was creeping up his driveway. At 9:32 am, he looked at his watch, and the water was rapidly rising. He got inside and moved a few things to the second floor, but by 9:45 am there was 6 ft of water in his home. The water rose until it was 6” from the ceiling. It stayed at that elevation and did not rise or fall until 4:30 pm on Tuesday when he left. The floor of his home is about 3-½ ft off the ground and about 4-½ ft above the street elevation.

777,700  
3,323,700

At about 5 am on Monday the 29<sup>th</sup>, the wind from the hurricane shifted but still blew until about 9-9:30 am. From his second floor apartment, the eyewitness could see water was in the street (Bellaire) about 2 ft and moving down from the north like a rapid. The water flowed like this until about 10:30-11:00 am. Suddenly the water rose fast and was in his carport in front of his house about 3 ft deep, which because of the difference in elevation was about 6 ft in the street. The water came up about 3 ft in 15 minutes. It looked as if the water had stopped rising, so he lay down to get some sleep. His wife woke him in about 30 minutes to tell him the water was rising again, and he looked out to see and could tell she was right. The water was now about 5 ft in his carport and in a matter of minutes was at the landing of the steps leading to his apartment. He measured the rise all along, and the water was rising 4" an hour from 3 pm Monday to 7 pm Monday afternoon, and cresting at about 9 pm, where he drew a water line on his wall. He said the water was flowing, moving differently later; it was not a push or a surge like earlier, but a slow steady rise. From 9 pm Monday night to 9 am Tuesday morning, the water rose slightly, maybe ½' at the most. They were out on a boat on Tuesday about 9 am.

778,100  
3,324,700

The eyewitness was on the 8<sup>th</sup> floor of Lake Marina Tower, and had a telescope, watching the area. He said that just as dawn broke, about 6:20 am, he was looking at the levee wall and saw what he thought was just 1 section of the levee gone. He said it might have bent over from the pressure of the water, but he could not see it. He said the water was flowing through the opening at that time, and it eroded the earth below the rest of the sections and as the day went on, more and more of the sections failed, like dominos. He said he never saw the water overtopping the levee. The water flowed south first, and then started flooding to the north to the Hammond Highway area then to the Marina Drive area. He watched the water rise all day, and in the late afternoon, the water was at its highest point. The subject was called back on April 18, 2006, to find out more information. According to his report, he did not see any wave action in the canal beside wind blow water disturbance. He said there was not what he would classify as wave action in the canal. He said the water elevation was what he estimated was 1 1/2 ft below the top of the levee wall on the west side of the canal, when he first looked into the canal. He emphasize he was a long distance from the area, and he was looking through a telescope, but he said that depth seemed correct. He said the debris in the canal below the Bridge was nothing more than should be expected...some trash and small limbs, etc., that there was a massive back-up of debris on the north side of the bridge, and this was holding up most of the trash.

Various locations

The eyewitness is a New Orleans police officer that lives close to the breach but was not there at the time of the hurricane, but was on duty. On Monday morning the 29<sup>th</sup>, the wind from the hurricane started to shift. At the time, he was at 650 Poydras with his unit. At that location, there was wind and rain, but there was no flooding. At 11 am on Monday, the wind shifted, and he and some other officers went to the street level and looked around. He heard on the radio about the 17th Street breach. The eyewitness, along with two fellow officers left 650 Poydras, to look at damage in the area. They drove down Carrollton Street, and saw no measurable water in the streets beyond rainwater. They drove to Wisner to 1700 Moss Street, where Special operations center was located. The whole area there, and at the Center, was high and dry. They then drove to Lakefront, where one of the men had a home on Lake Vista. All the way there, and the area when they got there was flood free. He estimates it was about 12-12:30 pm. They then drove up Robert E. Lee to I-10 West, where water was about 3 ft deep. It was 1:00 pm at the time; that was as close as they got to 39<sup>th</sup> Street and his home. They drove back to Poydras, and he knew his home was under. They left 650 Poydras, and drove to Orleans Street, which had 2-3 ft of water. At 5-6 pm on Monday, they went to the Dome, which was dry at the time; then to the interstate at Carrollton, which was completely under water. The police moved the base to Serio's restaurant. At 3 am on Tuesday, they moved to Harrah's.

777,800

3,324,400

The eyewitness rode out Hurricane Katrina in his home on Kenison Street. His house is located a couple of blocks from the 17th Street Canal breach. Between 8:00 and 9:00 am on Monday, August 29, he saw some rain water in the street but none in his yard. His house is raised, sitting 5 to 6 feet off the ground. By 9:00 am, he had some water in his carport. He saw a 5 to 8 foot wave coming down the street from the south. He climbed onto a neighbor's shed and then climbed onto his roof about 9:15 am. By 2:00 to 3:00 pm, the water was to the top of the door jams in his house. He was rescued at about 5:00 pm by firemen in a boat and taken to Old Hammond Highway Bridge. From the bridge, he could see 2 floodwall panels were pushed out but not gone.

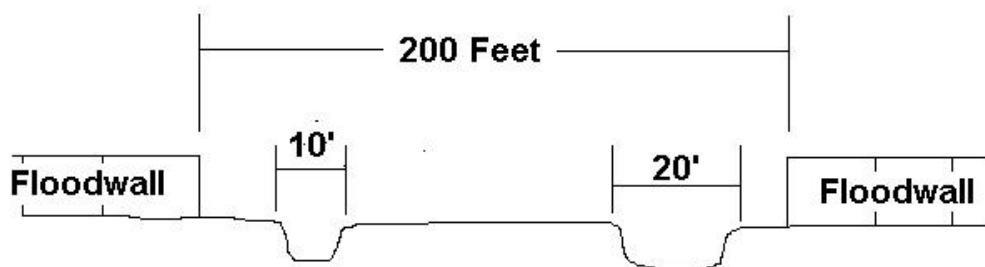


777,500  
3,320,300

On Monday, he had no flooding at all. He drove to the Animal Hospital on Metairie, and it was all dry there. On Tuesday morning about 10 a.m., the water started rising and it was in the street, but not over the curb. At 2 pm, there was 6” of water in the street and from 2 to 6 pm it rose several feet, and by 6 pm the water was over the fire hydrant in the street. The water was flowing very fast and you could hear the water rushing under the house like a waterfall, flowing to the canal from east to west. About 2 am on Wednesday, the water flow suddenly stopped and the water went calm, and stagnant. The water held there for two days till Friday and it dropped about 3” then. He left in a boat Wednesday about noon.

778,100  
3,324,700

This eyewitness rode out Hurricane Katrina on the 18th floor of the Lake Marina Tower. They were on the balcony on the protected side of the building from the wind. The balcony faces west toward the 17th Street Canal breach. The wind then shifted from the east to the northwest. The eyewitnesses noticed the breach around 11:30 am on Monday, August 29. The gentleman believes the breach occurred between 10:00 and 11:30 am with his best guess around 11:00 am. He did not see anything hit the wall. Another eyewitness in the complex, a New Orleans fireman who lives close to the breach and a retired civil engineer witness in the high rise both said that the work barges that were in the canal were removed prior to Hurricane Katrina. The fireman has reported seepage under the levee in the past. The eyewitness said that the water level in the canal was several feet below the top of the floodwall. In fact, he described the water level as being at the berm elevation below the top of the floodwall. He studied the breach with binoculars and reported that the flow was concentrated in 2 deeper sections with shallow flow over the higher middle section as shown in the furnished sketch. He was ordered to watch the breach the rest of the day and to continue to report on the conditions.



778,400  
3,323,800

This eyewitness rode out Hurricane Katrina in his home. He reported that his house is located 600 feet as the crow flies from the 17th Street breach. He first noticed water in his yard at 3:15 pm on Monday, August 29. By 4:30 pm the water was 5 feet deep.

778,800  
3,322,900

On Monday morning the eyewitness was on the second floor of her house; there was a lot of wind and she did have some wind damage, but she was okay. About 9:30 am she looked out and there was still wind, but in her back yard, there was about 1 ft of water, but she said maybe was rainwater. She thought that was more water for the amount of rain than they had had. She heard on her radio there had been a break on the levee, and the water in the back yard was lower than in the front, and she said that might be water from the break, so she thought about moving things upstairs. At 9:45 am, water started coming through her floor furnace into her home. In 10-15 minutes there was 6" of water in her house, and she went upstairs. Within 1 hour, she had 5 ft of water in her house. About 12:30 pm, she said water was still rising, and it rose all day, until there was 10 ft of water in her yard, and about 7-8 ft in her house. On Tuesday, the water was about the same. She said on 6:15 pm on Tuesday she said the Mayor said the levee had broken at 17th, and the pumps were cut off, so she knew she had to leave. She left at the end of the week.

778,000  
3,323,700

The eyewitness rode out Hurricane Katrina in his home. He was very fuzzy on times. He had no clock and no watch. After the storm passed, the wind changed direction and started coming out of the west. He heard rushing water at his door sometime between 11:00 am and 1:00 am on Monday, August 29. He looked out and saw 2½ feet of water against the door. He grabbed his cat and put the cat in a pet carrier, and a small shovel and jumped out of the window on the east side of his house. The water was rushing down the street and to stay out of the current, he broke out the window of his neighbor's house with the shovel. The neighbor has an elevated patio so he looked for the stairs. When he realized that the stairs were outside, he got out of a window beside the stairs. He put his cat on the stairs as high as he could reach and swam up to the second story patio. He grabbed the gutter and pulled himself up onto the patio. At that time the water level was approximately 7+ feet deep. The eyewitness estimated that it took him no longer than 5 to 10 minutes from the time he heard the rushing water at his door until he got on the neighbor's patio. Once on the patio, he said that the water was rising on his neighbor's house at a rate of approximately 1 brick every 10 minutes. He stayed on the patio until he was rescued by boat at approximately 3:30pm.

777,700

3,324,200

The eyewitness evacuated during Hurricane Katrina but had observed and reported possible seepage under the 17th Street Canal floodwall prior to Katrina. She first notices water in her front yard in November 2004. She thought that she had a waterline leak so reported it to the New Orleans Sewerage and Water Board. They sent a contractor to investigate. He probed and told her the water was not from the water line but was “levee water”. The Sewerage and Water Board did come out in January 2005 and made a repair under her neighbor’s driveway. She still had a soggy back yard throughout the summer of 2005 that she believes was due to seepage under the floodwall.

777,600  
3,324,200

This eyewitness lives on the west side of the canal in Jefferson Parish. Early in the morning, about 1 hour before sunrise, there was about 4" of water right outside his door, and deeper in the street. He thought it was rainwater, but he got a boat he had and got a pallet from his truck, and rowed to the west side of the 17th Street Levee behind his apt, and looked over. One of the wall sections was leaning over at about a 30-degree angle and water was flowing out of the canal into the street. He could see well, and there was just the one section leaning. The flow was moving very fast in the canal. The bridge, north of the break, kept trash and boats from getting to the break. He went back to his apartment and came back about 2 hours later and then there were a number of sections all the way down or gone – they were under the flow if they were still there. He said it was about 75-100 ft of opening. Between the first and second look, he heard there had been a break. He said at the first look, the water was about 1 ft from the top of the wall. He said the water was high all day, and he could not see a difference in the water surface upstream of the bridge to his north. There were no waves in the canal at any time that he saw.

The eyewitness was called again on April, 19, 2006 to verify information.

Verified that first trip out was around daybreak. The power was out and he was unsure of the exact time. It was light enough to see clearly. The weather was not bad at that time – windy with occasional sprinkles; he didn't even wear his raingear.

During his second trip out, it was windy with light rain. I described the heavy weather seen in the Lake Marina Tower video, but he couldn't relate what he had seen to the timing of the heavy weather. He confirmed that he heard a radio announcement, possibly on WWL, regarding a breach at 17th St Canal before he went out the second time.

He made other trips out to look later in the day including a trip up to the bridge.

The water level in the canal was high (about a foot below the top of the wall) when he went out the first time. He was unsure about water levels on the second trip out. He was certain the water was lower later in the day.

He verified that a small section, perhaps a single 30 ft panel, had been pushed back and was leaning over, the first time he went out. That section was located almost directly across from Ash St (near south end of breach at Spencer Ave). Water was flowing over the top and around the edges of that wall section. He didn't see any waves in the canal, but there was a current coming in from the lake.

On a later trip, he went out to the bridge and observed a lot of debris piled against the bridge. There was still a north to south current thru the bridge.

#### Pump Station 6

The eyewitness rode out Hurricane Katrina at Pump Station 6. He reported that on Monday, August 29, the station lost power and couldn't pump. Around 5:00 or 6:00 pm, he saw a wall of water coming down the canal. He got out in a car on the Metairie side on Thursday, September 1.

778,100  
3,324,700

The eyewitness is a retired civil engineer and was on the 14th floor of the Lake Marina Tower during Hurricane Katrina. At 11:00 am on Monday, August 29, he noticed a house on fire. He went down to the 2nd floor to report the house fire to firemen in the building. He returned to the 14th floor and noticed the floodwall break shortly after 11:00 am. It appeared to the witness that the floodwall had lain over but did not overtop. He had witnessed the work barges in the 17th Street Canal be removed from the canal at least 2 days prior to Hurricane Katrina. He says that the barges were lifted out of the canal by a crane and placed on trucks. The barges were off loaded in the work yard located adjacent to the floodwall on the New Orleans side.

- 778,500  
3,322,700
- Basement has flooded 4 times in 10 years, prepared by moving stuff out of basement.
  - Observed minor street flooding during the early morning.
  - Talked to brother by phone about 9 a.m. (major flooding occurred later).
  - Water entered house through floor furnace about 10 a.m., Monday, 29 Aug 05.
  - Water rose 5 to 6 ft in first 30 minutes.
  - Water flowing in from both west and north.
  - During night water rose about ½ inch/hour all night.
  - Water stopped rising about 9 a.m. Tuesday.
  - At peak, house had 18” of water on second floor, didn’t stay long.
  - Clock on top of refrigerator stopped at 2:20 p.m. when refrigerator fell over.
  - Left on Tuesday about 1-2 p.m.

- 778,600  
3,323,900
- Water flowing from north to south.
  - Initial rise was ankle to waist deep in 10-15 minutes.
  - House flooded to above windows but not to ceiling.
  - Water rose steadily all afternoon until it reached roof of house on NE corner.
  - Water peaked Tuesday morning.

779,000  
3,323,800

The eyewitness said she had a call from ADT that morning at 9:03 am that her glass break sensors were going off. The only broken window we had after the storm was from where the guard came in. All of the seals on the downstairs thermal windows DID fail though from water pressure.



	779,600
	3,323,300
<ul style="list-style-type: none"> <li>• High winds started around 2 a.m., Monday, 29 Aug 05; checked conditions every 15 minutes.</li> <li>• Winds died down significantly at first light.</li> <li>• Water in streets was moving south to north, normal direction for rainfall induced street flooding.</li> <li>• Flow of water in street changed directions between 8 and 9 a.m. (closer to 9 a.m.).</li> <li>• Slow rise occurring at 9 a.m. followed by rapid rise of about 4 ft in an hour (fairly certain of level, because he was waiting to float boat out of the garage).</li> <li>• Rate of rise steadily decreased throughout the day.</li> <li>• Level may have reached 5 to 6 ft by mid-day (noon to 1 p.m.)</li> <li>• Boated out to Harrison Ave about 5 p.m.</li> <li>• Returned to boat Tuesday morning to assist with rescue efforts; water still rising.</li> <li>• Strong currents (north to south) under I-10 between Pump Station I-10 and the 17th Street Canal.</li> <li>• Did not observe currents in the canal and did not travel as far south as the RR embankment.</li> <li>• Fish finder recorded depths of 8 to 12 ft in Lakeview late Tuesday.</li> </ul>	

	777,500
	3,320,400
<p>Monday, 29 Aug 05, 11:30 p.m. – water rushing under house from (east to west) into canal (suction side of Pump Station 6)</p> <p>Debris accumulation in back yard supports this description</p>	

	777,400
	3,322,900
<p>Telephone interview with the eyewitness on the west side of 17th Street Canal. The eyewitness stayed during the storm but did not get out early. She stated that later in the day she went out to walk along the levee, and she observed fish that had presumably come over the floodwall.</p>	

777,400  
3,322,900

Sometime between 0500 and 0700 hrs, the eyewitness noticed water coming over the west wall of the 17th Street Canal. Appeared to be driven by the wind as waves. His apartment is located adjacent to the wall and has a large sliding glass door that faces the canal. The view of the wall from this window is clear and unobstructed. He was looking out of this window as he noticed the water and wood debris coming over the wall. He was not sure of the exact time when he first noticed this, but stated the approximate times mentioned above. Sometime between 0800 and 0900 he noticed that water was no longer coming over the wall. He assumed that that is when the breach occurred. He seems sure that after 0900 he did not see any more waves. He also has photos of helicopters dropping sandbags into breach several days later. Some of these show all or parts of the breach.

777,400  
3,322,900

The eyewitness called the IPET hotline, and asked to be called back about what he saw. When I called him, he said he had not stayed in New Orleans during Katrina, but had left on Sunday about 2 pm., but he did want us to be aware that when he left his home on Maryland Drive about 2 pm Sunday, he drove north along the 17th Street Canal. He said he drove over the Hammond Street Bridge at 2 pm and he said he stopped and looked south into the canal. He said the water in the canal was higher than he had ever seen it before – that it was to the base of the concrete wall, but not onto the concrete yet. He said at that time the wind was coming from the northeast, but later when he looked at the weather, it was from the northwest. Northeast wind was blowing water away from the canal entrance, but the change would have pushed water from the lake into the canal. He also said he had owned a boat that was at the Municipal Yacht harbor, but had sold it, but he had friend that had boats there that were destroyed. He said the Municipal was father north than the Orleans Marina, which is across North Breakwater Drive and between North and South Breakwater Drive. He said some people would have had water gages that would have tracked the water depths there.

778,000  
3,324,100

Veteran, mechanical engineering student

Wears Timex wrist-watch all the time, very confident of timeline and time of breach

Location is 7 houses east of the floodwall (less than a football field away)

Was awake at 3 a.m. watching the weather from 2<sup>nd</sup> floor apartment – windy

Power went out about 4:30 a.m. – house got hot

Talked to his sister by phone around 6:30 a.m.

Went downstairs about 8:30 a.m. to check on music studio; planned to move instruments & equipment if threatened by flooding. Observed clear water at or just over curb level; was more concerned about observed ceiling leak.

Was listening to description of damage in Plaquemines Parish on Big 870 radio at 8:55 a.m. (radio announcer noted time).

Heard loud noises (things crashing to floor) at 9 a.m.; took off headphones and observed black water (filled with garbage) pouring into house.

House (1<sup>st</sup> floor) was full of water (floating sofa hit 8 ft ceiling) in less than 10 minutes – estimated water depth in house of 6½ ft (very rough estimate of depth – water reached/covered last step in stairwell but didn't reach 2<sup>nd</sup> floor – water got to 7<sup>th</sup> step on outside balcony).

Water was flowing from west to east with tremendous force; knocked oak trees in front yard down; his truck floated through a fence; heavy furniture thrown through exterior doors.

Pulled neighbor out of tree in back yard. Noted that they were on the 2<sup>nd</sup> floor talking at 9:40 a.m.

Mid-afternoon: observed strong, river like current with undertows directed SE or SSE

Observed helicopters performing S&R missions around 6 p.m.

Left by boat just before dark; strong SE/SSE currents still present; went to Orleans Canal levee/floodwall at Marconi & Fillmore

Walked out along east side of Orleans Canal to RR embankment at end of canal (pump station operators were camped out under bridge at 5 a.m.), turned west and walked RR to Uptown, which was not flooded Tuesday morning.

777,600  
3,323,100

The eyewitness lives in an apartment immediately next to the west side of the 17th Street Canal. His apartment is north of Veterans, and about 1 mile south of the Hammond Bridge. The floodwall north of Veterans on the west side has an elevation of about 12.3 ft. He stayed during the storm and said he was the only person who stayed in his building. He stated the power went off around 5:00 am and he turned on his battery-powered radio/TV and heard that there was some flooding reported. At around 8:00 am he went outside where he said the wind was high and reported seeing water from waves coming over the 17th Street Floodwall. Waves were moving in the canal from north to south. He stated that the waves could have been occurring before 8:00 am but it only became light enough to see at 8:00. He said the amount of water coming over the wall was not great because his patio did not flood. He took a picture (Figure 1) that shows the splash and a wave crest behind the tree limb. He stated the picture was a case of unfortunate timing but the wave crests were clearly visible and up to 1 ft above the wall. He said this continued until around 10:00 am. I asked him how far north and south the water was coming over the wall. He stated that his field of view width was limited to about 50 yards but water was coming over that entire width. At 10:00 am, he walked to the wall and looked over the wall and observed the water level in the canal at about 2 ft below the top of the floodwall and moving rapidly toward the lake. He went to the Hammond bridge on Monday afternoon and took pictures at 2:00 and 3:00 pm (Figures 2 and 3). Based on the brown part of the floodwall being 65” high and the top of floodwall at elevation 12.5 ft, the water level at 2-3:00 pm was at elevation 4.0 ft. In the interview, the witness described this as a high tide level.

### West London Canal

780,600  
3,324,600

The eyewitness works as a contractor for the USDA Southern Regional Research Center. He rode out Hurricane Katrina at the Research Center on Robert E. Lee Blvd. He reported that at 6:00 pm on Monday, August 29, the winds died down and they only had rainwater ponded in low areas. Between 7:00 and 8:00 pm, they noticed some water in the parking lot but he described it as “very little”. At 10:00 pm, he went to bed. Just after midnight, they noticed some water in the basement. At 2:00 am on Tuesday, August 30, the water was 2 to 3 feet deep in the parking lot and they began to notice some water on the 1<sup>st</sup> floor. They measured the water depth in the basement some time between 2:00 and 5:00 am at 53 inches. After the sun came up, they noticed the water level in the parking lot was at the bottom of a Do Not Enter sign. The sign is located on Agriculture Drive on the southwest side of the building entrance. He reported that the water didn’t rise any higher than the bottom of the sign. The gentleman left the Research Center on Thursday, September 1

782,600  
3,322,000

On Monday morning, the 29<sup>th</sup> the storm had passed but there was still some wind, but not bad. He went outside to check his house and yard. He thought he was okay and was picking up limbs in the yard at about 11 am to 12. He saw water down the street on Paris Street (the northwest), and it seemed to be coming toward him as it rose. He also noticed the water coming from behind his home, through the undergrowth, from the east where the London Canal is located. The two waters met about 12:00. He and his wife went to the deck on the back of the home and sat on the rails there a while, then climbed onto the roof of the home when the water did not stop rising. The water rose fast and steady until about 5 pm on Monday when they were in their attic. By 5 the current that was there before had stopped and was just a rise. It got to about 4- 4-½ ft in the home. The water held there the next day, and was there when they left on Tuesday afternoon.

782,500  
3,324,000

The eyewitness lives on the west side of the London Avenue canal just north of Mirabeau Drive. He said that the electricity went off between 3:00 or 4:00 am on Monday, August 29 because he heard his generator kick on. At 6:00 am, Monday the streets were dry. He remembers this because they were outside looking at a tree that had fallen across the road in front yard. Shortly after 6:00 am, he began to see water in the street. His house is elevated. By 4:00 pm, water started to get into his house. The neighbors close by came and got them in a boat. They spent the night in a home close to the breach.

782,600  
3,323,500

The eyewitness rode out Hurricane Katrina at his home. At 5:51 am on Monday, August 29 the electricity went off. Between 7:15 and 7:20 am the water started rising in the street. At that time, it was raining but not very hard. By 7:30 am, the water had risen high enough to start coming into his house. By 8:30 am, the water was waist deep in his house. The water was initially rising fast, then slowed but continued to rise. He got to the neighbor's deckhouse a few houses away between 11:30 am to 12:00 noon. He stayed at the deckhouse until a helicopter rescued him on Wednesday between 11:20 and 11:30 am.

781,500  
3,324,700

I was in a building at the corner of Robert E. Lee and Wisner (on the City Park side) and we had water coming up over the curbs at around midnight Monday night after the storm had passed. Not sure if it was from the London or 17th Street canal, because this location is somewhere in the middle of those two waterways.



782,000  
3,324,900

This couple and their daughter and her boyfriend stayed in their home during Hurricane Katrina. The witness said that they had no boards covering their windows and the wind was no worse than during Hurricane Betsy. By Monday, noon (August 29), the winds and rain died down and the only damage was minor shingle losses and a downed fence. He picked up several sections of fence and started to pick up debris in the street to clear the drains, after which the street was dry on both Bertha and Frankfort. He walked down Frankfort to the London Avenue Canal levee sometime after noon where he saw the water was at least 6 feet below the top of the levee. About 3:00 pm on Monday, the water started to rise on Frankfort, coming from the west and reached his house about 6:00 pm Monday. The water was 6 inches deep in his house Monday night and reached 12 inches deep by Tuesday evening. At that time, they left by canoe to his mother's house in Lake Vista (about ½ mile due west). They stayed in Lake Vista Tuesday night and walked out along the lakefront on Wednesday morning.

782,000  
3,323,100

- Water was just over curb right after storm (wind died off around noon – little rain)
- Water reached first expansion joint in driveway about an hour later
- At 2-story house across street (4600 St Bernard), water covered an additional step between house and sidewalk roughly every hour (0.6 ft/hr). He stayed here after his house flooded.
- Water observed coming in from back (east to west) after he started moving furniture to keep it out of the water
- Water rose at steady rate until it reached bottom of street signs, then slowed
- About 5 p.m., water reached level of door bell on his house (5.7 ft above expansion joint in driveway; 1.1 to 1.4 ft/hr)
- Tuesday morning – water level was stable

782,200  
3,322,100

The storm started in on Sunday night and on Monday morning was blowing hard. Whenever there is a storm she goes across the street to her friend's home in the projects and stays with her on the second story that faces her home, so she can watch her home. Monday morning at 5:00 the power and phones went off. Monday was the worse, and then the winds died down. About 2 pm on Monday she was sitting on the balcony with her friend and saw water rising in the street, but it was coming up slow, but steady. She saw the water in her yard and by night it was up to her second step leading to her home. They could not see after that and went to sleep that night. Tuesday morning, the water had risen and was in her home then. It was up to half way of her window, which she said was about 5 ft deep. She saw people walking in the water, and knew it was about 5 ft. She could not tell any direction, it was not flowing fast, but was steady coming up. She stayed in her friend's home until Wednesday when she was made to leave. She said the water started to recede a little on Wednesday, but just a little bit. When she left, the water was still to her window in her home.

781,300  
3,323,600

On Monday the 29<sup>th</sup>, there was no water except from the rain in the street, but he lost power about 5:30 that morning, and the phone went off at 1 pm. On Tuesday morning, about 7 am, he first notices the water in the street in front of his home, and it is more that normal. The water behind his home from Bayou St. John was lower and in the street the water was coming up faster and was moving faster. Slowly though Tuesday morning, the water rose and reached its peak and leveled off about 12 to 1 pm on Tuesday. The water from the street and from the Bayou met about 3 pm and was about 2 ½ ft in his home, making it about 6-7 ft in the street. The rise to that point was a steady rise, but he did not know a direction, but was a rise. On Wednesday it raised maybe an inch more. By Friday, the water had dropped a few inches, but it was real slow in dropping. He stayed upstairs in the home.

781,700  
3,323,900

On Monday the 29<sup>th</sup>, the weather started clearing after the storm passed and about 12 - 1 pm, there was a ray of light now and then. There was some water in the street in front of the home, but just rainwater, but about 11:30 am to 12, the water in the street started to rise. Using the fire hydrant in front of the home as a gage, the water was about 3 ft. It rose very quickly from half way of the hydrant to over it, then to about 5 ft using a stop sign in front of the home. At about 1 pm, a friend walked to their house, and the water was to his neck in the street and he is 5'10", the water seemed to rise more based on the water at their driveway. By 2 pm, it was 6 ft and by 3-3:30 pm, the water was 8-10 ft in the street. It rose all during the night, and by morning, it had come into their home and was about 2" deep in the home. On Tuesday morning, the water was at it highest, and after that it slowly started dropping. On Wednesday, 10 days later, the water down to about 3 ft in the street. They said they know their slab is 4 ft above sea level.

781,800  
3,322,500

On Monday about 7 am to 1 pm, he watched the storm. A friend of his came to his home and asked his to come to a store at 3610 Jumonville, about a block south of him, where a lot of people were, so he got in his car and drove that way. Halfway there, the water in the street got a little deeper—about 18", but at his house it was only a few inches deep. He only stayed there about 45 minutes and drove back to his home about 2 pm, in the same spot as before where it was 18", not it was about 3' and he had to drive on the curb to get out of the water. The water was slow and steady in the rise. By 4-5 pm on Monday the water was 3 ft deep in his home and he had gotten to a boat he had in the yard. He used the boat over the next days to save people. The water stopped rising about 6 pm on Monday and did not drop.

782,500  
3,322,200

No water in 1965. Water started coming up Tuesday morning. Left by boat Wednesday after water stopped rising.

782,400  
3,323,700

On Monday the 29<sup>th</sup>, at 9:20 am, he was there and talking to his sister on his cell phone. He said he heard an explosion, but not like a bomb, and told his sister he thought the levee close to him had broken. He went outside to see, and at that time there was about 4" of water in the street, which was normal for the rain they were getting. He said that water then was rainwater. He walked two blocks both north and south, checking the levee and did not see a break at that time. He went back to his home and was going to watch the news, but before he did, he heard something and got up to see what it was. He said 20 minutes had passed from the first noise he heard, and the water was 2 ft in the street and it was rising. He went outside and walked in water to his knees, and walked to his left, toward Filmore to check the levee there. It was dry at the bridge on Filmore at that time. He went back to his home, and was going to pack to leave, and while he was inside, water came up and into his home. He went to the back of the home and water was in the yard there. Water was about 1 ft in his home and about 2 ½ to 3 ft in the street. He climbed onto his roof to escape the water. He said the water that was coming from the west... that is from the Paris road area. The water was rising faster in the front of his home than in the back. He said he was on his roof at 10:15 am on Monday, and at that time the water was still rising. It rose all day and into the night. He used the house next door as a gage, and at 2 am on Tuesday, the water seemed to quit rising and settled out. He estimated it was 12 ft deep at that time. At 5 am, he swam away from the home and was able to get to UNO where it was dry and he was rescued from there.

782,200  
3,322,700

At 7:00 am on Monday the 29<sup>th</sup>, there was wind and rain from the storm, with it getting worse at 8 am. The eyewitness called his wife in Dallas at 8:15 and said he was good. At 8:30 he looked outside and water was 6-8" in the street, but was just rainwater. The wind got worst and blew part of his roof off, but by 11:30 am, it seemed to have passed. At 11:30, he saw brown water backing up into his bathtub, and said that worried him. He looked outside again and saw brown water about 18" deep in the street, flowing from Duplessis to Paris – west to east. The water was rising, and it was still raining and the drains were not able to handle the water. By 2:30 pm, the water backing up in his tub started to overflow into his home, and the water outside was about 3½ ft deep in his yard. By 3 pm, the water was 5½ ft in the yard. His is a one-story home, so he had to get out, seeing it was still rising. He walked in the water to his sister home at Duplessis and Harrison, and water there was to her front door, but rising to. He said the walk there took him about 30 minutes. He kept going and walked about two miles to Broad and St. Bernard where he was picked up by firemen in a boat rescuing people and carried to Fairgrounds.

782,100  
3,322,100

Had 3-4 ft of water Monday evening (3-4 p.m.). Rose to 5 ft of water Tuesday morning, then 6-7 ft later Tuesday. Water generally came from the north. Used his boat to pick up about 30 people. Paris Ave only had 3 ft of water Tuesday and Wednesday. Evacuated Wednesday.

781,600  
3,324,600

On Monday, at 7:30 am, the eyewitness was in touch with his daughter on the phone, and all was okay he said. There was a lot of wind and some rain, but not really bad. He stayed at the windows and watched what was going on from there. About 9:30 – 10 am, there was water in the street, but nothing more than a hard rain. But at 10 am, he noticed the water was starting to rise, and it was rising real fast. He used his truck as a gage, and at 10 am he called his daughter the last time to say the water was about 8” deep in the street, the he lost the use of his phone. By 12:30 pm, he thought he might have to leave because the water was about 3-½ ft deep in the street then. He said the water was rising about 2” every hour. The direction seemed to be east to west. He left his apartment, and went to the one next door, which is 2 stories, and he thought he would be good there. He stayed there Monday evening and night, and by 11 am on Tuesday the water had slowed and had crested he thought. He was using the bricks as a gage. He was rescued on Tuesday evening and by then the water had settled.

782,300  
3,322,400

On Monday morning the 29<sup>th</sup>, the wind and storm were mostly over, but the wind was still blowing, but not real bad. On Tuesday morning the 30<sup>th</sup>, the water started rising about 7 am, and the witness thought it would be slow and would taper off, but at that time, it was 3 ft in the street at her home. The water rose all day, not a rush, but a steady rise. By 2 pm on Tuesday, the water was over her head in the street and she is 5’2”. At 4 pm on Tuesday, she got in a boat with her son, and she said the water was about 9 ft deep at that time. They boated to Pratt Drive to check on her mother, and at the stop sign there, the water was over her son’s head and he is 5’10”. They boated back to the projects just below their house on Sybil, and were there until rescued.

782,600  
3,324,400

No water in street Tuesday morning. (Area is called Pilot-land, early part of the city built on relatively high ground, usually doesn’t flood.) Rapid, sudden rise (3 ft in 20 minutes) occurred 10 a.m. Tuesday morning. Water came up to front porch but didn’t get in house. The eyewitness stated that elevation drops about 4 ft proceeding down Mirabeau towards the lake. He thinks water filled low areas towards lake, and then backed up in Pilot Land.

782,400  
3,322,500

The eyewitness is an elderly lady who says that she had just put a meatloaf in the oven, and the rain had stopped when she heard a loud boom, and then saw water rising. She was very fuzzy on times – Monday or Tuesday, or the exact time of day. She says that water came rushing in through her floor furnace, and her grandson had to help her out of the house and she said the water was neck high.

782,000  
3,322,600

On Monday about 7:30 am he woke up, and the looked out and there was water in the street, but windblown water from the storm and normal. He went back and about 9 am laid down to take a nap. At 11 am he woke up and looked out, and there was water in the street and it was rising, so he got his son to help him and they went to the backyard and started filling sandbags to block the door. About 30 minutes, by the time they got the bags filled, the water had risen and was about 4” in his home. It was a slow steady rise of the water. He could hear the water coming through the bricks in his home. By that afternoon about 4:30 pm the water was 4-½ ft in the house and was still coming up, so he decided to knock a hole in the ceiling and in the roof, and climb out onto the roof of the home. He was on the roof by 5:30 pm, and using the brick on the home next door, he could tell the water was rising about 1” every hour. He could tell from his neighbor’s home, that the water was about 7 ft deep in the street. He stayed on the home until 10:30 pm Monday when they were rescued.

782,400  
3,324,600

House is located right at the northern breach site of the London Canal. Canal breached to the west at this location. The witness had a clock in the house that stopped at 7:10. Was not at location during event. He has pictures taken after he returned. These pictures show a child's clubhouse near floor level of the home in the back yard facing the I-wall. In a second photo the same clubhouse is shown after the event. In this photo the clubhouse is raised 4 to 5 (looks more like 6 to 10 feet in the picture) feet above the original ground level. It indicates massive upward movement of the levee bank or foundation. The clubhouse was not inundated nor the interior contents disturbed at all. The eyewitness believes that the clubhouse was raised to that height by heaving soil as the floodwall was pushed up and out.

782,700  
3,321,800

The eyewitness woke up on Monday, August 29 and saw no water in the street. By 10:00 am, the water started slowly rising. He estimated the water was rising at a rate of approximately 1 inch per hour. By 10:30 am the water jumped to its peak of about 3 feet deep in the street (up to top of steps of his front porch). The water stayed at that level until he left on Thursday, September 1. The water flowed from the west to the east.



782,700  
3,321,800

These two eyewitnesses rode out Hurricane Katrina in their house. They were sitting in their kitchen during the early afternoon on Monday, August 29. They noticed the water beginning to rise. In 1 hour between 2:00 and 3:00 pm, the water rose from knee deep to 5 to 6 feet deep in the street. The water got to 3 feet deep in their house and stayed in the house for about 5 days. They left the house after 7 days.

782,700  
3,323,000

We were informed a witness had photos of London Avenue Canal east floodwall breach. He was called and got his voice mail. A message was left for him to call, but we haven't heard from him. We later learned all pictures were lost in the water.

This eyewitness said that on Monday, August 29 between 6:00 and 7:00 am, her back yard began gradually filling with water. By 11:00 am, there was 3 to 4 feet of water in the street. She said that on Monday, August 29 between 7:00 and 8:00 pm, they noticed water flowing through the London Avenue Canal east side breach which they could see from the 2<sup>nd</sup> floor of their house (see over the west floodwall). Between 8:30 and 9:00 pm, they could hear the water flowing through the breach – sounded like a waterfall. She could hear a kid screaming on the roof between 9:00 and 10:00 pm.

782,500  
3,323,800

Sunday the rain started and wind was blowing late and into the morning on Monday. The power went off about 5 am and she got up at 6 am, and all was okay then. There was no water in the street and her neighbor called her to check on her, and he came over for breakfast. When he came in about 7, there was water splashing under the door, and she thought it was from the gutters. He tasted the water and it was salty. He and she started moving things up high, and the water kept rising. At about 10 am, the water was rising still so he got a boat she had in the back yard to get out, but when they got into it, it sunk, and they got to the roof; the water was 5ft deep then. About an hour before it got dark, she could see water flowing over the 6ft fence in her yard. They were rescued on Tuesday, and the water was to the roof of all the homes.

781,900  
3,323,300

About 5 am on Monday the power went off. There was a lot of wind and rain, but there was no flooding in the streets. At 9:30 am the run off water was clear and clean, but at 10 am the water started running and it was black and dirty water then. The water was coming west to east from St Bernard toward Paris. The home has two steps to the yard and by 10:30 it was 2 ft in the house, they got to the second floor and by 12 there was 4 ft in the home. It rose all day and by 5 pm, the water was about 7 ft based on the steps to the second floor. At 6 am on Tuesday, the water was up about 1 ft, but at mid morning, the water dropped about 6" and was flowing now toward St. Bernard – east to west. But that lasted only about 1 hour, and then it settled again at that elevation till they were rescued at 11:30 am on Wednesday.

782,800  
3,321,900

These two eyewitnesses live on Gentilly Blvd adjacent to the London Avenue Canal west side flood wall. They evacuated during Hurricane Katrina but one said he had noticed seepage along the floodwall in the past. He said that sometime after the wall was finished (1996 – 2000) he noticed leaking under the floodwall at seams during a “normal” storm. He reported the leaking to the Levee Board. The Levee Board people came out and sandbagged along the floodwall. Once the storm passed and the water went down, the Levee Board came back and removed the sandbags and “pushed cement into the seams”. Since that time, he hasn’t noticed any leaking

782,300  
3,321,800

The eyewitness rode out Hurricane Katrina in her house on Paris Avenue. She reported that after the storm had passed, on Monday, August 29, she was outside cleaning out the storm water drains in the afternoon, maybe around 12:30 to 1:00 pm. She went inside the house and when she came back out, the water was rising quickly. The water got to 4 feet deep in the street but didn’t get into her house because her house is elevated. She reported that the water was coming from “all directions”. She stayed until Wednesday, August 31. At that time, the water was still up.

### East London Canal

783,300  
3,324,100

The eyewitness rode out Hurricane Katrina at his home. He reported that at 7:30 am on Monday, August 29, there was only rainwater in the streets. Between 7:30 and 9:00 am, the water rose quickly. By 10:00 am water was chest deep in his house. His house sits 2 feet off the ground. Between 10:00 and 11:00 am, he swam to higher ground at the University of New Orleans. When he left, the water was still rising, and he estimates that it peaked at least 2 feet higher.

	783,500
	3,323,600
This eyewitness reported the water peaked at the porch level and didn't get into their house.	

Pump Station 4	782,700
	3,324,200
The eyewitness rode out Hurricane Katrina at Pump Station 4. He is a pump station operator. He reported that at 9:45 am on Monday, the water reached the pump house and they lost water pressure and shut down the pumps. By 5:00 pm, water was in the pump station office. He slept in the back of a truck at the station on Monday night. The water level peaked at ½ of the office wall height. He was rescued by boat on Tuesday.	

	782,800
	3,323,800
The eyewitness rode out Hurricane Katrina at his home. On Monday, August 29, he noticed rainwater in the street between 5:30 and 6:00 am, but he was not sure if this was just rainwater. By 9:00 am, the water had risen to about 2 feet deep in the street. By 10:00 the water depth in the street was 4 feet. By 11:00 am, the water had risen to over the gentleman's head, approximately 6 feet deep. He described the water as swift flowing, too swift to paddle, needed a motor for a boat. The water continued to rise but at a slower rate until about 2:00 pm. He said that waves were pushing through with the water flowing from the south to the north, and without a motor on a boat, you could not paddle through it. The water didn't rise any higher after Tuesday evening. He left around 10:00 am on Thursday, September 1. At that time, the water level hadn't dropped. I observed a distinct watermark on the outside of his house at approximately 6 ½ feet above the ground.	

	783,300
	3,322,200
The eyewitness rode out Hurricane Katrina at his house. He reported that by noon on Monday, August 29, the rainwater had disappeared. He lay down to sleep around noon and woke up at 3:00 pm to water coming in his house. The water continued to rise and was up another 3 feet by 6:00 pm.	

783,300  
3,324,600

This eyewitness and 16 others rode out Hurricane Katrina at Our Lady of Lavang Catholic Church located at the intersection of Robert E. Lee Blvd and Vermillion Blvd. He reported that on Sunday, August 28 the power went off at 11:00 pm. At that time the wind was blowing. By 7:30 am on Monday, August 29, the wind was calm and no water other than rainwater. At 8:00 am, the water started to rise very fast. By 8:30 am, the water was knee deep in the church. The water was coming from the west. Between 9:00 to 10:00 am, water was chest deep in the church. The people staying there got out to the 2<sup>nd</sup> floor by 10:00 am. During the day on Monday the water rose to 8 feet deep and kept rising to about 12 feet by Tuesday. On Wednesday, August 31, the water level dropped 1-½ feet. He stayed at the church until Sunday, September 4 at which time he left by helicopter after Sunday mass.

783,100  
3,322,900

The eyewitness rode out Hurricane Katrina at his brother's house. He reported that the water began to gradually rise between 9:30 and 10:00 am on Monday, August 29. The water was coming from the north and west. By 10:30 am the water was approximately 2 ½ feet deep (porch level). At that time, he got into a boat and left.

782,700  
3,324,000

This eyewitness's name was given by a neighbor. The neighbor evacuated during Katrina but reported that the eyewitness called him twice on August 29. Once at 1:00 am and told him there was 3 feet of water in the street. The neighbor said that the witness called again at around 4:00 am and told him that the water was so high that he had to climb out onto his roof. The eyewitness got up early Monday morning (August 29) and still had electricity. He lost electricity and the water was rising (didn't know time). Around 1:00 pm (fuzzy on time) he had approximately 3 feet of water in his house. Water continued to rise to 5 ½ feet of water in his house. He got on roof while it was still daylight. Slept on roof Monday (August 29) night. Around noon on Tuesday, August 30, he swam across the street to the pump station. They got a boat and picked up people in the neighborhood and took them to the pumping station. All total, 27 people were staying at the pump station. They paddled the boat to UNO several times until all the people at the pump station were at UNO. Stayed at UNO Tuesday night (August 30) and Wednesday night (August 31).

783,300  
3,324,900

The eyewitness is a New Orleans Police Officer who rode out Hurricane Katrina in his home. He also recorded a written timeline during the storm. He reported that at 5:45 am on Monday, August 29, there was no water in the street. By 9:00 am, the water started to rise steadily. Between noon and 1:00 pm, the water was still rising so he called for a police boat for rescue. He was ordered to stay. By 3:00 pm, water started entering his house. His house is elevated so the water had to be 4 ½ feet deep to get into his house. The house is a 2 story duplex, and he has the bottom floor. The house has a mid entry to upstairs so he cut a hole through the wall into the stairwell. He grabbed his bag and went upstairs to the neighbors. The water continued to rise and peaked at 10 to 11 feet deep. He marked various water levels in the stairwell. He stayed until 2:00 to 3:00 pm on Tuesday.

782,800  
3,323,300

Lived at this residence. Claimed to have been at house during breach. He said water came about 0700 to 0800. Reluctant to say more at this interview. Nov 3rd. we were able to reconfirmed that this witness' house is right at the breach on London canal at Mirabeau.

782,900  
3,323,100

On Monday the storm passed and things were okay, no big damage. He was in the house, going to sleep, at 1:30 pm when he said he heard a loud explosion. He looked out the window and saw nothing. At 1:45 pm, he heard water running, and there was 1 ft in his house at 1:45 and coming in very fast. He got to his roof from outside, and by 2:30, the water was to the gutters; about 10-11 ft in the street. He was there 3 days and the water never fell.



782,700  
3,323,600

On Monday morning August 29th 200, the eyewitness was up around 0730 hrs and looked out front (facing east toward Warrington St.) window. There was not much water in the street so he laid down to rest. Before he could get to sleep he heard a sound like a dog quickly lapping water. As he stepped out of bed his foot touched water. Startled, he jumped up and ran to the front window where he saw fast moving dirty and black water in the street going toward the lake (Pontchartrain, north). The water was nearly up to the window ledge and gurgling into the house under the doors. He and a friend thought to go up in the attic but realized that they would have no way to get out, so they busted out a back (window/door?) and ran to the highest ground, which was the berm (levee) on which the I-wall was built. There was much more water in front of the house than on the backside, which is why they went out the back. They got the neighbor from the north house and the three of them ran up the levee. Once up on high ground they ran toward Mirabeau intending to cross the bridge and get to Gregory Jr. High School which was high ground and on the west side of the canal. They had to make their way through blown down trees, and at this time there was plenty of light to see where they were going. En route, they stopped to lift one of them up to see over the top of the wall. He reported water about a foot below the top, and could touch the water with his hand. As they moved south they heard a loud cracking boom type sound and at the same instant the wall burst open in front of them. Water gushed out like 'twenty fire hydrants'. They did not stop to observe any more, but immediately turned and ran as fast as they could to the Filmore St bridge. They crossed the bridge to the west toward Paris St, but noticed that water on this side of the canal was moving to the south. Ran half the way to Paris St and then had to swim some to get to the Beacon Light Church in that vicinity. They stayed there for 1 1/2 days.

On 21 Mar 06, interviewed a neighbor across the street from this witness, and asked if there was a clock in his house? His wife affirmed that it was running and the elevation above the floor was 5.0 ft. Pictures of the clock are available showing its exact position after the flood. A high water mark was found in the house of 8 feet above the floor.

783,400  
3,323,800

The eyewitness rode out Hurricane Katrina with his sister at his. He reported that by mid morning (not sure of specific time) on Monday, August 29 the storm was over and the wind had slowed down. At that time, his sister told him that water was coming into the house. He opened the back door and found water knee deep against the door. He got his sister into the attic. In 20 minutes, the water was waist in the house. They spent 2 nights in the attic. They got out of the attic onto the roof through a roof vent hole. They were rescued on Wednesday, August 31 by boat.

782,700  
3,323,600

The eyewitness said the storm did very little damage to the area, but the levees breaking caused the flooding. He said he was asleep about 6:30 – 7: 00 am on Monday, when a friend in the house woke him saying they were getting water in the house. He said the water was coming up very fast and through the toilets and sink. He said by the time he got up and got pants on, and to the window, the water was knee deep in the house and in the yard it was to his waist. He said that by the time he was in the yard it was no more than 15 minutes, so about 7:15 am. He said it was raining and the wind was blowing, but it was not raining hard, nor was the wind excessive. He did not notice that the wind got worse, but in the next hour or so, it did rain a little harder, but it was never a downpour. They go west to the levee, and then walk on the high ground at the base of the levee south toward Gregory Francis Elem. School at 1700 Pratt Dr, which is where people go when it is high water. He and his friends walk the levee until they get to Mirabeau. He said the walk from his house on Warrington to the breach at Mirabeau took about 12-15 minutes, and he was with two friends the entire time, one who was also interviewed independently. He said he did not look over the levee wall at Mirabeau, but the water was gushing through the break in front of them and the flow was over his head and he is 5'9". The witness said the water was gushing like a river through the break, and was flooding the streets below. He said it had not just broken because there was way to much water in the streets to have just broken. They walked the levee back to Filmore, and there both he and his friend climbed a ladder that was in place, and looked over into the canal. He said the water was about a foot or a little more from the top of the levee. The water was flowing fast enough to move a crane and was rushing toward the break south of them. As they moved away from the levee at Filmore, and went west toward Paris Ave., they were in water that was about a foot deep, but they soon had to swim in the water. He remembers his foot getting tangled on a bench, and they used it as a ladder at a church they went to that was on higher ground. He estimated the journey from the break near Mirabeau to the church taking about an hour. He remembers a clock on the wall that has 8:48 on it, but he was not sure if it was running or not. They were there 3-4 days on the roof.

783,300  
3,323,000

The eyewitness rode out Hurricane Katrina at his home. He reported that at 9:00 am on Monday, August 29, the water was 1 foot deep in his yard. Shortly after 9:00 am, he heard a loud noise. He noticed water flowing from the west down Sumpter but at that time, the water was not yet into his house. Within a few hours (noon), water was coming into his house. In another 3 hours (3:00 pm) waster was chest deep. As the water was rising, he got into his attic. Before dark, he decided he needed to get out of the attic. He came down into the house and swam outside. He climbed a ladder onto his roof. The witness spent 2 nights on his roof. On Wednesday, August 31, he swam from his house west on Sumpter to St. Anthony where he was picked up in a boat. The boat brought him back to his house to get some clothes and then took him to higher ground on Gentilly.

783,400  
3,322,900

The eyewitness and his wife reported that the storm had passed with the only damage being a few trees down. Between 8:30 and 9:00 am on Monday, August 29, they notice water started to enter their yard. The water rose to about 1 foot deep in the yard and stayed at that level for one hour. The water started rising again between 9:30 and 10:00 am. The water was flowing from the northwest. Within minutes the water was knee deep. The gentleman got his wife and dogs into the attic. Within about 2 hours, he said the water was chest deep. They stayed in the attic for 2 days. He finally pushed the vent out and got on the roof. A friend in a boat rescued them on Wednesday, August 31. When rescued, the water level had not dropped.

784,000  
3,324,200

The eyewitness rode out Hurricane Katrina at his home on St. Roch Avenue. At 10:00 am on Monday, August 29, he noticed water started coming into his house. He estimated that the water was rising at a rate of approximately 1 foot per hour. Between noon and 1:00 pm, the water was waist deep. The water was coming from the west and flowing like a white water rapid. The witness got out of his house and into his boat. He climbed on his roof. By Monday night, the water was 8 feet deep in his back yard. He spent Monday night in his neighbors 2<sup>nd</sup> story. The water kept rising to 10 feet deep (above the ground) on Tuesday morning. He got out in his boat Tuesday morning about 7:00 am.

783,600  
3,324,800

This is a second-hand interview with a son of the eyewitness who was not present at the time of the interview. The son informed that the father stayed 7 days at the residence. He said water came into his home early about 7:30 –8:30 am Monday, and in 30 minutes was 3 ft in his home. He got in a boat and left right away, and the water was still rising...did not know the direction of the water or the depth for sure.

783,300  
3,323,300

Very strong winds about 0300. Water came up to the curb sometime around 0600-0700. Around 0800 water came up really fast, and then continued to rise throughout the day. Observed a car floating down the road from west to east on Mirabeau at maybe 5 mph. Water reached its peak when it covered the Mirabeau Street sign on the SW corner of Mirabeau and Pauger. The eyewitness was in the 2<sup>nd</sup> story and viewed out this window. He used the street signs as a gage to see how high the water was and if and when it was receding. He noticed that at its highest point it covered the Mirabeau Street sign, but not the Pauger Street sign, which was just above the Mirabeau sign. Estimates that it leveled out sometime later in the day and peaked sometime Monday afternoon or evening, but not exactly sure about the time. A wall clock in the witness' den is about 5.5 feet above the floor. This floor is the same elevation as the garage floor. Clock has a battery, was functioning before flood, and stopped at 7:18.

783,700  
3,322,600

The location of this account is on Elysian Fields and north of Gentilly Blvd. The eyewitness rode out Hurricane Katrina at his store. At the store, they lost power a little after 6:00 am on Monday, August 29. He called his wife in Dallas at 11:00 AM to report limited damage. Around 12:30 pm, he noticed the water start to rise in the street. Between 2:00 and 2:30 pm, the neutral ground (median) on Elysian Fields started to go under water. Later in the day on Monday, the water level reached the ground between the 2<sup>nd</sup> and 3<sup>rd</sup> posts from the street in his parking lot. The water was flowing from the south to the north. Around 5:00 pm, he noticed the flow reversed and was flowing from the north to the south. He attributed this to his belief that the city got the Florida Avenue pumps running. Later, he noticed that the flow reversed back, coming from the south to the north. On Tuesday, the water rose in the parking lot to the bottom of the 4<sup>th</sup> post from the street and peaked at that level. Since the store is on Gentilly Ridge (higher ground), people started coming there. His son pulled people off rooftops Tuesday and part of the day Wednesday. Wednesday night there were 55 people staying at his store ranging in age from 3 months to 93 years. He stayed until Labor Day.

784,500  
3,322,800

This eyewitness lives on Franklin Ave just north of Gentilly. He filmed water coming down the Franklin Ave (south to north) from Gentilly Ridge. Est. times: 1200-1300 walked on ridge near house and water was up to sidewalk. 1500-1700 water had reached Max level. This was at the top of the concrete steps at his house.

783,000  
3,324,200

The eyewitness said on Monday the 29<sup>th</sup>, about 10 am, they noticed water in the street about 1 ft deep, and they said they thought it was from the Lake. They watched the water and said it was rising about 6” per hour, and that it was coming from the northeast. The water kept rising and they have a diesel tank in the yard, and used it as a gage of the depth, and it was quickly over the tank, about 3 ½ to 4’ of water then. At 7 pm on Monday night, the water was about 12 ft, and that was the maximum depth. The next morning, Tuesday, the water had not risen or fallen, and they were rescued on a boat on Tuesday afternoon.

783,700  
3,324,800

According to the eyewitness, on Monday the rain was very hard and there was a lot of water in the street from that. He said the water was about 3 ft in his yard at noon, and that is had leveled out, and he said it was rainwater. About 4:30 pm on Monday he heard a boom and in 30 minutes the water was up to his ceiling in his home.

784,500  
3,323,900

The eyewitness lives in a 2-story building. He rode out the hurricane with his son, and another gentleman.

At 5:12 am on Monday, August 29 the power went out. At 6:15 am the roof blew off the house while the witness was on the phone with a reporter from Baton Rouge. By 8:30 – 9:00 am, water was flowing down Franklin Avenue approximately 2 feet deep. He assumed that the water was coming from Lake Pontchartrain since the flow was from north to south. The water started to build up and by 10:00 am the water was approximately knee deep on the 1<sup>st</sup> floor. At about 10:30 am, he noticed that water flowing down Franklin from the lake and water flowing across Franklin from the levee break. The water stop rising but then started up again and peaked at around 11:30 am – 12:00pm. The witness estimated the water was approximately 10 feet deep in the street. He has 17 steps to his second floor. Water got to 5<sup>th</sup> step from the top. He got out to UNO on Tuesday night (August 30), left UNO on a helicopter on Wednesday (August 31).

The eyewitness was contacted again and asked about the water direction in his location. His description differed from that of one of the other gentleman at the store with the witness, so clarification was needed. What we have in his account is wrong --- he said, and the son was also interviewed separately, the water was flowing south to north, from the city to the Lake. This eyewitness interview matches the other interview.



	783,300
	3,323,100

On Monday the 29<sup>th</sup>, he said there was little water – not a lot of rain – but a lot of wind, and he said the little bit of water in the street was from the rain. He thought the storm had passed and was on the couch in his home; he said some people were outside looking around at that time. At about 9:30- to 10 am on Monday, he heard people talking loud, and he looked out and could see water coming from the west in waves through the streets and into homes. In 3-4 minutes he said the water rose and came into his home and was 4 ft in his house. The water kept rising all day, but it was not the rush like at the beginning, but a steady rise of the water. By the middle of the afternoon, about 2:30 pm, the water was 8 ft in the street. The water was clean, not dirty water.

			782,800
			3,323,800

This interview was given through an interpreter. On Monday the 29<sup>th</sup>, at 10 am, the storm seemed to have passed and the weather was getting better. There was a light wind at the time, but not bad. He saw water coming down the street from the south flowing to the north, from the Filmore Street area toward Robert E Lee. The water was flowing fast, but it was not a rush of water, but a continual flow. His home sits about 3-4 feet off the street level, and within less than an hour, but 11 am, he estimated the water was in his home about 3 ft deep, and was about 6-7 ft in the street. The water was coming in so fast, he was worried he might drown, so he got a life vest on and left the home swimming toward a friend’s home.

	783,300
	3,322,200

On Monday the 29<sup>th</sup>, the winds had passed and about 2 pm, and the eyewitness went to the front door and opened to look out. He walked to the back of the home and looked and there was water coming up from the south, from the Gentilly Blvd area. He said the water was coming like a river; so fast you could not walk in it, and was rising fast. His home sits on the highest point in that area, so when the water came, he said it flooded the homes around him, but it slowed quickly as it came to his home. By 3 pm on Monday, the water had risen to the bottom on his first step to his home or about 6 – 8”. His home never flooded. That afternoon, about 4:30 pm, he walked from his home to Gentilly Blvd., and then to the west to the London Canal and the water was 2 ½ ft deep there, but it was deeper on the west side of the 610 crossover. He was in the home till Wednesday when he lost water and gas.

784,000  
3,323,200

According to this eyewitness, on Monday the 29<sup>th</sup>, at 5:30 am, the electricity went out in the area. The rain and all was coming down, and there was some water in the street, but just from the storm. At about 12, the storm was about over, and he looked out to see water on the sidewalk in front of his home and by 2 pm the water had risen to his front door. The water was coming south to north on Spain and west to east on Mirabeau, and was flowing very fast and hard. About 5 pm, before it got dark, he put a canoe in the water, and went around looking some, and there was still current then, but nearly as strong. The water seemed to settle out about 8 pm on Monday and was about 7 ft in the middle of the street and 4 - 4½ ft in front of his home and 2-3 ft in his home. He spent the night in his home and got out on his boat, going to UNO on Tuesday.

783,800  
3,323,800

Monday the storm had passed and the house was in good shape without any damage that he could notice. The eyewitness' wife, who had left, called to check on him and he told her he was okay and that the house seemed to have come trough it okay. About 3-4 pm on Monday the 29<sup>th</sup>, he noticed water on Mandeville and that it was rising. He looked at the parked car across the street and used it as a gage or the water elevation, and it was steadily rising on the car. At about 5:30 pm, he thought the water was not going to stop, so he climbed onto the roof of his home and felt he was safe there. By the time he had gotten onto his roof, the water was about 9ft deep in his yard. The water settled there, and he spent the night on the roof alone. He was picked up by a boat on Tuesday about 11 am and taken to a school on Elysian Fields. He stayed there the night, then left when a Guard unit picked him up.

783,300  
3,323,300

On Monday morning the 29<sup>th</sup>, the eyewitness was in this location with his wife, daughter and nephew. The storm passed and they had received very little damage and thought the worst was over. The house faces the south and the winds were behind them, so they were on the porch and watched the rain and wind from there, until it seemed to calm. They had rainwater in the street, which did not surprise them at all, but there was no water in the yard. About 12:00, it seemed to be all over, and they were relaxed and calm with the storm passed. Then just about noon, he could see water coming from the west down Mirabeau, heading to the east; in about 5 minutes, the water rose from the street to his yard and then on to the top of his porch, which took about 15 minutes, and is about 2 ½ to 3 ft in elevation. The water was traveling very fast and was rising quickly. He could see cars floating by and trees caught in the water rush. By 1:00 pm, he had 3 ft of water in his home and they had moved to the second story of the home. The water rose slow and steadies, but the rush of water was over. By 8 pm on Monday, he had 5ft of water in his house and by the next morning, Tuesday; it had risen only about another ½ ft and was settled. They were able to get a boat and left the house that way on Tuesday afternoon.

783,000  
3,323,200

This eyewitness had spent the night Sunday-Monday at her work to monitor the hurricane, and when the storm seemed to have subsided, she went home to her house on Annette Street. The weather was trying to improve and she could see some sunlight in some places. She got to her home about 9 am on the 29<sup>th</sup>, and looked around her home and saw neither major damage, nor any unusual water in the street. About 9:30 am on Monday, she saw water on Annette moving quickly and rising fast. She used the hydrant on the corner as a gage, and in a matter of minutes it rose from ½ way of the hydrant to over the top of it. In about 2-3 hours, the water was about 3 ft high in her home. From street level to 3 ft in her home she said took about 2 ½ to 3 hours. The home is a two story brick home, and she climbed to her roof when the water started rising so fast, and she was rescued from her roof on Tuesday.

783,500  
3,322,700

Monday at 5-6 am, this witness reported he heard 2 explosions, and very quickly saw a rush of water coming down the street, from the north toward the south. He said it was a wall of water. He was on the second floor of his apartment and watched the water flow and fills and then rises up steadily. By 12 pm, the water had stopped the rush, but it rose until about an hour before dark; at about 7pm, it stopped and never fell from that point. He said the water was 10-12 ft in the street when it was at its peak. He was there 3 days then went to the cemetery, and stayed there 4 days.

782,800  
3,322,700

This couple stayed at this address during the hurricane, and on Monday the 29<sup>th</sup>, and witnessed early in the morning, after daylight, the wind and rain was bad and the house was shaking, but by noon, it seemed the worst of the weather had passed, and they felt their house was okay and had survived with little damage. About 3 pm, they saw water in the street in front of the house, and could see that the water was coming from behind their house and from behind the homes next to their house. The water was coming from the back yards to the front, and flowing into the streets. There was too much water for the drains to handle and it began to rise in the street. The water rose into his yard, onto his steps, but was he was not aware of an accurate time, but he said he though it was about an hour and a half from the time it started until the time his home had 4 ft of water in it. That night, just before it got to dark to see, he said estimated by things he knew in the yard, there was 7 ft of water in the street. They were in the house until Wednesday evening.

783,800  
3,323,400

On Monday the 29<sup>th</sup>, about 11am, the storm seemed to have passed and the worst was over. The eyewitness called family and said all was okay with little damage. She was on the couch about 2 pm when she looked out and saw water on the 3<sup>rd</sup> step in front of their home. She and husband discuss leaving, but in 30 minutes the water was in the home, and was about a foot deep in the house. She said her home is about 3 ft above street level, so it was about 4 ft in the street. The water kept rising and they got on the dinning room table with their dogs, and at 2 – 2:30 pm, it kept coming up, so they got chairs and set them on the table and sat in them. By the time it was just getting dark, about 7:30 pm the water at her calves as she sat on the table, at least 4 ft in her home, and maybe more. She estimates that at about 9 pm it had risen another 6-8”, and then it stopped. Tuesday morning, it was the same, and they left by a friends boat on Tuesday at 4 pm, and it was the same depth. She was not sure of the direction, but maybe moving northward.

784,600  
3,322,900

On Monday, the eyewitness said the power went off at 6:30 am and the storm was bad, but by noon it seemed to have passed. He was out in his yard and was cleaning up limbs and such, when he noticed water coming into the streets, which had dried from the storm by that time. About 2-3 pm, the water was flowing by the curb, then over the curb and onto the sidewalk, and then up into his yard. He said the water was flowing very fast and running like a river from Gentilly toward the Lake -- south to north, which he had never seen before. By 4 pm, the water was 3 ft from his home, which is terraced to the street, and he said the street water was about 3-4 ft deep. He said the water pooled there and does not rise any more. Thursday, he said the water receded some, but held in the street for days after.

783,900  
3,324,600

The eyewitness looked outside Monday morning after storm passed and saw normal accumulation of rainwater in yard. Took a brief nap, and when he woke, he looked outside and water was higher. There was a dump truck across street that wasn't flooded but went under water in 4-5 hours. Took refuge in blockhouse adjacent to railroad track that night, then walked out along Simon, then to levee commission office on Lake Shore. Water crested about 2 ft below tracks and Simon Road embankment. His truck parked facing uphill on embankment had water on rear wheels (didn't flood). Had to wade occasionally (knee deep water). Sav-a-Center parking lot at Franklin Ave was flooded. Road to Lake Shore was dry.

784,500  
3,323,900

About 4:30 am on Monday, the eyewitness woke and there was bad wind and rain. At 4:40 am he heard an explosion and immediately the power went off. At 6:30 am the storm got real bad, and at 7 am the roof was blown off and at 8 am they went downstairs. About 9:30-10 am, he saw water rushing down Franklin toward the lake, south to north. At 11am they rescued a family from the water and it was 18 to 24” deep in the street then. They went upstairs at 12:15 pm, and it was about 3 ft in the street then. At 2pm, he was looking out the back of the building and the water was 2 ft below the windows of the homes and rising 3 weatherboards every 30 minutes. At 3 pm, it was still rising. He was rescued at 4 pm on Monday and when he left, the water was still coming up.

**IHNC West**

783,000  
3,320,400

The eyewitness said he was in house during flood. He first saw water in street sometime in the morning. At peak, the water was over full-size Pick-up truck parked on the high ground on AP Tureaud Blvd. center strip. This was sometime morning to mid morning Monday Aug 29.

783,200  
3,320,000

The eyewitness rode out storm in his home. 0830 saw water in street. About 0900 water was 1 ft high in street. 15 to 20 minutes later it was rising fast, to about 4-½ ft more. He walked in street in water up to neck. Managed to get back in house and up onto roof where he lived for the next two weeks. During the time it rose rapidly, the strongest part of the storm had passed, not very windy; the last of the squalls was coming through.

783,600  
3,321,500

The eyewitness is a plumber who rode out Hurricane Katrina at his home. He said that at 8:45 am on Monday, August 29, there was approximately 1 foot of water in the street. Between 9:00 and 10:00 am, the water started rising. He said that he tasted the water and it was salty. He knew that the water was coming from Lake Pontchartrain, and he told his son that they were in trouble. By 10:30 am, the water was 3 feet deep in the street. By 11:00 am the water was 6 feet deep in the street. His house is elevated so he stayed in the house for 7 days after the hurricane hit.



782,500  
3,320,000

Note: On October 14, we measured depth from low spot on street (bottom of curb) to HWM on house to be 3.5 feet

The eyewitness said that the water started rising between 8:00 am and 10:00 am on Monday, August 29. By mid afternoon (between 2:00 and 4:00 pm) the water was 4 to 5 feet deep. The water didn't get any deeper. The water got on the steps leading up to his house but didn't get onto his porch. He stayed in the house until Sunday, September 4.

783,900  
3,321,300

The eyewitness rode out Hurricane Katrina at her sister's house. The witness reported that on Monday, August 29 between 9:00 and 9:30 am, water began rising, approximately 1 foot deep in the yard. She heard a loud boom and then the water started quickly rising. The water was coming from the west. Within minutes, water was waist deep in the house. She got out the back door, climbed over the back fence, and got into the neighbor's 2-story house. She stayed on the 2<sup>nd</sup> floor of the neighbor's house Monday night. On Tuesday morning between 10:00 and 11:00. She was picked up in a boat.

784,400  
3,320,200

These two eyewitnesses rode out Hurricane Katrina at their house. They reported that between 10:30 pm and 12:00 am on Sunday, August 28, the water was rising and was at the tip of tires of vehicles parked on the street. Around 3:00 on Monday, August 29, the electricity went off. By 4:00 am, the water had risen to the bottom of the mirror on their truck. By 10:00 am, the water was 8 feet deep and was over the vehicles parked on the street. The water level held at that level. By 2:30 pm the skies had cleared. They stayed until Wednesday, August 31.

785,900  
3,321,100

This eyewitness said a neighbor across the street from his home saw water rush through street. He called his neighbor while he was on the roof at about 0730-0800 hrs.

784,700  
3,322,800

The witness reported very early in morning when still windy and rainy, called 911. They could not help. Water at this time was up to sidewalk. After unknown time packed suitcase and went to gate to observe. Water was about 2-3 feet in roadway and running very fast from north to south

784,700  
3,322,000

This eyewitness reported the storm was 5 am to 9:30 am Monday. At 9:45 am, the water rolled down the alley and street very fast from north to south. By 10:00 am, there was 7 ft of water in the street. He is on the second floor with a balcony. The water stopped rising about 2 pm on Monday; stayed there until Wednesday when it rose 2 ft, and they all were rescued on Thursday.

784,500  
3,320,200

The eyewitness was at this address during the storm, and said on Sunday, the 28<sup>th</sup>, the wind started, but got worst in the middle of the night – Monday morning. Monday morning about daybreak, he said there was a little water in the street, but he thought that was from the rain from the storm. In about an hour or so, the water started rising in the street, but it was not a rush of water, but a steady rise. The gentleman went to move his car to a safe location, and then the water came in fast. In a matter of minutes it was to his knees in the street and rose really fast to about 6-½ ft in the street, and was flowing like a river.

782,300  
3,320,700

The eyewitness stayed at this location which is his Mom’s house. He said water rose from wheels to hood of pickup truck in 45 around mid-day to mid-afternoon Monday. House is 2 ft off the ground. Water was coming in through floor furnace. Water stopped rising Monday evening with about 2 ft of water in the house. Left Tuesday.

783,400  
3,320,800

According to this eyewitness, this 100+-year-old house didn’t flood in 1965. She watched TV news Sunday night. Water started rising Monday morning before daylight. (She opened closet and thought she saw a rat; was going to beat it with a stick; realized that it was water.) Water rose very fast. She had just enough time to grab her purse before climbing ladder to attic to get out of water. Water was about 5 ft deep in house when she left by boat Monday morning.

781,000  
3,319,300

This eyewitness stated that about one hour after the storm at about 1700-1800, on Monday, he left and went to Morris Jefferson Scholl near St Peters and Lopez. He was very fuzzy on times, and water heights.

784,100  
3,322,400

This eyewitness was awakened at 4:30-5:00 am when the power went off, and the storm came in between 6 and 8 am on Monday morning. The hurricane lasted a few hours until 10-11 am on Monday with strong winds and blowing a lot, but it eased about noon. About 1:30 pm, he was outside in front of his home, and looked toward Franklin, the east, and saw water coming from there. He said the water was coming straight down Franklin. He had a battery-operated radio, and he said the radio said there was a major breach in the 9<sup>th</sup> and he expected the water to be coming from the west, but it was coming from the east. The water rose all that day at a slow steady rise, until it was about 2- 2 ½ ft deep at about 7 pm that night, just about when it was to dark to see well. On Tuesday morning at 7 am, he had 3½ ft of water in his home and it was about 5 ft in the yard. His radio said the 17th had broken that afternoon, and the London break was on the radio on Wednesday. The eyewitness said the water seem to go down some on Tuesday, and by Friday it was down a great deal to the point he could walk in the yard.

783,900  
3,322,300

On Monday the 29<sup>th</sup>, after the power went off, and the eyewitness went outside to check for damage to his home. At about 9 –9:30 am, he noticed water in the street, but it was very little and next to the curb, and he thought it was rainwater, but it was moving pretty fast. He watched the water, and within 10 minutes the water was over the curb, in 15 minutes more it was over the sidewalks, and 10 minutes more, it was to his knees in his carport. The water was rising very fast and was flowing swiftly. It was flowing from Gentilly –coming north to south. His home is about 1 ft above the street elevation and by 10:30, he had 3 ft of water in his home and there were 4 ft in the street. The water leveled out about 12 and later that afternoon, just as it was getting dark, he said the water had dropped about 6”. The next morning, Tuesday, it had dropped another 6” and Wednesday morning another 6”, but when he left Wednesday afternoon, the water had settled and had dropped no more.

783,600  
3,322,200

The eyewitness reported the really hard rain started about 4:30 am on Monday the 29<sup>th</sup>, and continued until about 6 am, and the power went off about 6 am. He went outside after the storm and was cleaning up some around his apartment. At 8 am, there was about a foot of water in the street, but he said that was normal rainwater from the storm. He was up all night, and went to sleep but he was awoke up at 9:45, and at that time there was 3 ft of water in the parking lot in front of the home, and about 4 in the street. The water was coming up from the sewer drains and you could see water pushed into the air. In the courtyard of the apt., he saw water coming out the drain covers and into the courtyard, which was flooding then. Over the next hour, he saw it rise about another foot, and only about another 2” from then until when he left on Wednesday morning.

784,600  
3,319,900

The eyewitness was at this address with another lady at the home with her. They went to sleep Sunday night, the 28<sup>th</sup> of August, and they knew the storm was coming, but they were fine. Her friend woke up before her on Monday morning and awoke her saying there was water in the house. The power was off at that time. She said at 7-8 am on Monday when they awoke, the water was about 9" deep in her house at that time and that it was rising, but very slowly. She walked in the water some, and used that as a gage to the depth of the water. About 2 pm on Monday, the water had risen in her home and was about 1 foot deep in the house. She remained on her bed and watched the water from there. She said they felt they were okay, because the water was not coming up fast at all. By Monday night, about dark, the water had come up just a small amount, and they slept in the house that night. Tuesday morning, when she woke about 6 am, she walked in the water and said it had come up to about 18" in her home. When she was rescued in a boat at 3 pm on Tuesday, she said she had noticed the water coming up any more. Her home had 3 steps leading to a porch on the front. And the porch is a forth step, so she estimated the water in the street to be about 4 1/2' deep.

782,700  
3,320,600

The eyewitness said at 10 am on Monday the 29<sup>th</sup>, she was in the address with her family. One of her daughters looked out the window and told her father to come look, because there was water in the street. He said not to worry, it was just rainwater, but she said it was rising fast. Her husband then looked out, and the water was at their first step, and coming up very fast. By 10:15 am, the water was 4 ft deep in the street and beginning to come into the home. Her husband went to the garage to get an ax so they could get into the attic, but by then the refrigerator was floating and blocking the door into the garage. They decided to go to her sister' home on the opposite corner. She is 5'7" and the water was over her head in the street. She said the water was coming with a lot of force, with white caps, from the A. P. Tureaud area, which is east of her home. They made it to her sister's home by about 11 am and the water was still rising, but not nearly as fast as at the start. They could see across the street to a home there and used slats on that home as a gage to see how high the water was going. She said the water rose and then settled about 1 pm, and by 4 pm had dropped 2 slats. But at dark, her husband used a flashlight to look at the slats, and it was back up again. They decided to leave the home and went to St. Augustine school. The water was still rising when she left her sisters for the school at 2600 A. P. Tureaud Ave. On Tuesday morning, she said the water in the area had settled and she heard on the radio the levees had broken. On Tuesday morning, the water was about 7 ft at the school. They spent two days there.

786,300  
3,319,900

According to the eyewitness account, around dawn Monday morning water came into street. At unknown time in day left to take family to Tulane St business where he works. Mantel clock about 4.5 feet above driveway and battery operated stopped at 7:46, clock was functional. Water was chest level in den before leaving for Tulane St. Returned Tues., water had risen to max level and receded.

784,200  
3,320,300

According to the eyewitness, on Monday at 4:30-5 am, there was a lot of wind and rain and the power went off about 6 am. About 7 am there was about 4 ft of water in the street and about to the front step of the home. The water was coming from west to the east and was flowing strong with a lot of current. About 9 am, the water is about 3 ft in his home, which is about 5 ft off the street level. About 11:30 to 12 pm, the water stops rising and he thinks he will have to raft away from his home. He climbs to the roof, but it gets cold, so he gets back into the attic about 2 pm on Monday. He looks out and can see the water is about 3" from going over the top of the stop sign by the house. The water never falls, and he is rescued about 7:30 on Monday night.

784,900  
3,322,000

This couple sat down to breakfast on Monday morning at 0600. The eyewitnesses say that at 0605 the water began to gush in the house. She said that water was spewing out of the floor furnace. By 0645, he said the water had peaked and was 6-7 feet high on the house. He also said that the water was coming directly from the east (Peoples Canal area) and was flowing very fast (6-7 knots). He had to swim upstream to the house next door to check on his mother-in-law. He is an experienced swimmer and kayaker. He said that the water stayed up for long time, and recession was slow.

783,200  
3,321,600

The eyewitness said on Monday there was wind and rain, but it was not as much as he thought they would get, and about 10-11 am on Monday they were on his porch looking at the damage. The water in the streets was clean and was draining out and he could see a lot of the crown of the street. He looked to the south toward Humanity Street, and saw a wave of water flowing west to east. The water would fill a low area and then move to another street and fill there. It filled the street at his home from the south to north. He went out and saw water passing over Gentilly at the 610, and flowing into Humanity. He said the water rose at his home a few inches an hour and by 7 pm on Monday, the water had stopped rising, and had not gotten into his home.

786,100  
3,321,600

The eyewitness said that at approximately 0700 Monday August 29<sup>th</sup> water came in 'like a mighty rushing wind, took with it everything, cars, trucks pieces of houses'. After some time it receded for a while, then went back up. Water levels undulated throughout the day. Photos show water above the eaves of houses across the street in the first wave. Wind and rain are visible in this picture. Pictures in which the same reference points are visible and without the rain and wind, show already lower water levels. This lady's house (strong two story house) rocked and moved as the water rushed by.



INHC Lock

This eyewitness is the IHNC Lock Master. He rode out Hurricane Katrina at the lock. He furnished us their canal gage at the lock readings for August 28 and 29. He contents that the breach occurred between 9:00 and 10:00 am on Monday, August 29 when the gage readings began to fall. That could be the case or that could be when the storm passed and the surge began to recede. The permanent canal gage extends only to 8 feet. The lock crew added a second, higher gage by reading the permanent gage and setting the new gage to the same reading. Furnished below are the Canal gage readings for August 29.

Time Gage Reading (feet) Time Gage Reading (feet)

0:01 7 8:00 14.5  
1:00 7.8 9:00 15  
2:00 8 10:00 13  
3:00 8.8 11:00 12.4  
4:00 10 12:00 12.1  
5:00 11 13:00 10.8  
6:00 12 14:00 10  
7:00 13 15:00 8.1

Pump Station 19

According to an eyewitness at the station, floodwater came early morning, not sure when. No one in the pump house was sure of timing. Logbooks were not helpful.

785,500  
3,321,400

The eyewitness was asleep in her home on the morning of the 29<sup>th</sup>, when he awoke about 2 a.m., hearing water running. He went to the window, looking out to see water on in front of the house. He woke her and told her about the water, and when she went to look, she said there was water about 3 ft deep in the street at that time – it was to the side mirror of her X-Terra. She said there was a thin sheet of water in her house, and she started to mop it up, but her boyfriend told her that was not going to work, that the water was rising. She said the water was coming from the east to the west. She and her boyfriend got into the attic, and the water steadily rose for about 2-3 hours; by daylight, the water was to the lights switch plates in the house. The water held there with no noticeable changes that she could tell, and they were in the attic for 2 days. When they left, they went to Press and north, then west to Almonaster, south to Florida. She said the deepest water seem to be at Florida and Almonaster, and looked higher to the east.

785,600  
3,320,200

The eyewitness said water entered the house sometime after 0600 at floor level, early Monday morning Aug 29<sup>th</sup>. Water entered house in a big wave. In a very short time it was up to her neck in the house. The floor of the house is maybe 4 to 5 feet above the road level. She is over 70 years old and is an early riser. Always gets up and has coffee at about 0600 to 0630. At this time called her friend. Shortly after that is when the water wave entered her house. Estimates the wave of water between 0630 and 0730.

786,100  
3,319,100

This eyewitness was interviewed while he was working at a location near Franklin and Abundance St. He says that he lives in the Ninth Ward and that he rode the storm out in his house. He said that he first started seeing water between 0400 and 0500 on Monday morning. He said that it was about 1 foot deep then and continued to rise gradually until about 1800 that evening when it was 10-11 feet high

785,800  
3,321,400

The eyewitness says water started to come into his house in a rush at 0630 on Monday morning. It was rising so fast that he and his brother cut a hole in the ceiling and put his mother in the attic. He said that when he first went into the attic the water was around his ankles. When he came back down after getting his mother settled, it was already up to his waist. They spent four days in the attic.

786,100  
3,321,600

The eyewitness reported on early Monday morning, he was in the house and the winds were making the home shake and rattle a lot. On Monday morning, about daylight, the water was up to the steps on his home. The water elevation seemed to go up and down some, but he said the water was from the north to the south.

785,800  
3,321,100

The eyewitness said on Monday there was a lot of wind and rain, but not any water to speak of at all beyond normal rainwater. About 1 pm on Monday the water started coming from the north to the south, and was sure –not from Seal Land area. He pointed out two trees in the back yard that he said were pushed over by the water on Monday, and they were leaning north to south. He went upstairs and looked out from there, and the water was about 3 ft in the street in an hour's time, at about 2 pm. By 2:30 pm, the water had risen and it was 5ft in his home at that time. He slept that night upstairs, and in the morning on Tuesday, the water had not risen any more. He was rescued at about 12 on Tuesday, and the water was the same elevation, but not flowing in any direction then. He said the water in the street was about 10-11 feet deep.

785,500  
3,321,200

In a telephone Interview on 24 March 06, the eyewitness reported :

- Her house is on relatively high ground (*DEM indicates ground above sea-level*).
- Stayed in her 2-story house. House is on high ground above street level.
- Was watching the storm come in from her doorway with her granddaughter at 6:45 a.m., Monday, 29 Aug 05 (storm wasn't bad yet, light rain falling, power off).
- Left doorway to put a pot of water on the stove; granddaughter came in a couple of minutes later telling her to come look at the water.
- Water was running rapidly from east to west down Abundance and rising. (Her description implied an uphill slope from Felencia to St Ferdinand St., which appears to agree with the DEM.)
- She woke up other family members so they could save the generator and begin moving things upstairs.
- Water was coming into the house by 7 a.m.
- Water was waist deep by 7:15 a.m.
- House suffered significant wind damage later in the morning: collapsed ceilings and wall blown in (possible tornado?)
- Water stopped rising Monday after the hurricane passed, fell some and came back up.

785,900  
3,319,000

The witness said on Monday morning before daylight the power went off. At 7:30 to 8 am on Monday, the water rushed into the house very fast and with a lot of force. They were able to get into the loft (attic) of the home and to safety there. They were there a few hours, and could look back into the house. Right after lunchtime, the water had gone and there was just water ankle deep in the house and they walked around in it like that that day. Outside the water was over the truck in the street, but only lapping onto the porch of the home. The water never rose or fell until they were rescued on Thursday. She could not tell a direction of the water. It rose very fast and then left by noon on Monday – the bathtub was full of water from the rising.

786,300  
3,320,200

The eyewitness said at about 3-4 am on Monday the 29<sup>th</sup>, water was flowing in front of his home from the north down Alvar and from the east. The two flows seemed to converge at his home on the corner, building up in that location, but flowing no more in either direction. Two houses were caught in the water flowing down Alvar, and lodged for a while directly in front of his home. He could see the water rising and coming into is yard. Around 5:30 – 6 am on Monday, the water was raising so fast he thought it might come into his house as fast as it was rising, so he lowered the steps from his attic, and climbed into the attic with his two dogs. The witness' daughter, who was at the site when we talked to the gentleman, said she called her father at 6 am, just before she was leaving for work, and said he was in the attic at that time, with an ax and his life jacket. When the witness lowered the ladder to climb into the attic, he said the water was about a foot deep in his home, and rising steadily. When he got into the attic, he watched the rise on the rungs of the ladder and used that as a gage of the depth. When his daughter called at 6 am, he said the water was about 2 ft in the home, which she said was what he had said. Within an hour, by about 7:30 am, the water was 6 ft based on the ladder, and had just about stopped rising any more. He realized then that he had no water in the attic with him, so he climbed down the steps and retrieved a plastic container of water he had filled to get into the attic with him. He walked through the house with the container, and said he was on his tiptoes and the water was at his chin – he said he was 6'1" tall. The water did not rise after 12 pm on Monday. He was in the attic for 3 days. He could tell from the street signs that the water seemed to drop some on Monday, but Tuesday evening just before dark, he said the water started to rise again, and was not stable until Wednesday. His neighbor on the southwest corner was also in his attic, and they were able to talk to each other across the way. The eyewitness left Wednesday morning by a boat. A battery operated clock, 5-½ ft up the wall in the house stopped at 8:02.

### Bartholomew Golf Course

785,500  
3,324,000

According to the eyewitness, on Monday the 29<sup>th</sup> the wind and storm were bad, but there was little damage to the house or yard. About 10:00 am, she saw water in the street that she said was rainwater and it was about 18" deep on the tires of the car. She thought the storm had passed, so she went upstairs to her room and went to sleep. When she woke about 6 pm, she went to the stairs, and there was water on the first floor of the home, and she is 4'11" and it was too deep for her to walk in. She said the water was at least 5' in the home at 6 pm Monday. She called her Dad and brother and told them the water was in the home and stayed upstairs until Thursday. She said on Wednesday morning, the water rose, using a stop sign as a gage, from the bottom of STOP on the sign to covering the sign totally by Wednesday afternoon. The Coast Guard rescued her on Thursday.

785,000  
3,324,900

According to the eyewitness, the storm had passed and they were okay, and had slept the night there at the home. She was with her 2 sons, 2 sisters and her niece. They woke up and felt they were safe and had done well. About 2- 2:30 pm on Monday the 29<sup>th</sup>, they were in the house and were not aware of water in the street or in the neighborhood until water started to come into the house. She could not give a direction from which it was coming, but she said it was dirty water, not rainwater. The water was coming in fast and was rising quickly. By 5-5:30, it was about chest deep in her house, she said about 4 ft. – she is 5’6” tall. They were walking around in the house in the water, placing the young children on the tops of things higher up, thinking the water would stop rising, and that they would be safe on top of things. She said the water was coming up at a steady rise, but not a flood rush. About 6 pm the water seemed to slow down in the rise, but it was still coming up. They could see the water was still rising, so they got to the back of the home and got a wood picnic table in the back, and used it as a float, placing the children on it and got outside onto the car roof, and then onto the roof of the home. This was Monday evening about 7 –7:30 pm. Her sister is a bigger lady, so she could not climb onto the roof, so she stayed on the roof of the car in the driveway. They spent the night on the roof, awake all night and watching the water, which she said slowed down some in the rising, but still came up. They were there all night using flashlights to try to signal helicopters overhead, but they were not rescued until Tuesday about 3:30 pm. The sister, who stayed on the car roof, said she was sitting on the roof of the car when they were rescued, and they could see the water was to her neck. The eyewitness said the water was about 7-8 ft deep in the street at that time. She did not ever notice the water going down at all.

785,000  
3,324,100

On Monday the storm had passed and the weather was improving. There was some water in the street, but it was no more than they normally get from a hard rain. At mid morning – she thought about 10 to 11 am, they noticed water in the street and that it was rushing by them, running from the south to the north, toward the lake, not away from it. In a matter of 10 minutes, they had water in the house about 4” deep and they knew they were in trouble. It rose about 1 foot every hour until they went outside to the van in the yard and climbed onto the top of it. The water kept coming up, and by 2:00 pm, it was 5 ft deep in the yard. Some were able to climb from the van roof to the house roof, but she did not. The water kept coming up, and at 6:30 pm, a neighbor came and got them in a boat and took them south to the New Orleans Baptist Seminary. They stayed in a friends home that night, Monday, and on Tuesday, that house started getting water, so they left it in the boat, to a bridge and were rescued from there.



785,600  
3,323,200

The eyewitness reported the power went off at 9 am on Monday the 29<sup>th</sup> and the winds were strong and blowing most of the morning. There were trees down in the yard and next door, one punching a hole in the roof in the den, but the home had survived. About 3:30 – 4:00 pm (first said at 10 pm, but sister said this time) on Monday he heard a noise and went to the front of the house and had water on the floor, he thought from the hole in the roof, but he saw water coming in under the door. He said by 4:30 the water was waist deep in the house. He looked out and saw more water in the street and it seemed to be rising so he went next door to get his neighbor. He said the water then was about 5 ft deep in the street. They left the home and went to an abandoned movie theater at Gentilly Woods Shopping Center. He said the water seemed to be coming from Louisa toward Press – in a westward direction. Some at the theater went to the corner of Louisa and Stephen Girard, two blocks eastward, and the water there was at least 6 ft deep. Tuesday morning the water still seemed to have some current, but not a lot, but by Wednesday, the water was stagnant, and was rising and falling with the tide. They stayed Saturday morning, and the water did not fall for weeks.

785,000  
3,324,100

Sky was overcast with faint sun occasionally peaking through after storm passed. Water came in Monday evening (4-5 p.m.). Water was coming up out of sewer (storm drains). Water was clean (like rainwater) at first but turned black on Tuesday. 7-8 ft of water in street by Monday night by 8 p.m. 8-9 ft by Tuesday morning. Water peaked on Wednesday. Watermark just above front door (photo). (Bottom of door ~ 1-2 ft above street.) Railroad track (behind houses across street) was never overtopped. Business establishment also flooded.

785,600  
3,324,300

The eyewitness lives on a two-story home that is about 1 ½ ft above street level. On Monday about 5:30 am the power went off and he started listening to the radio. He said he had about 1 ft of water in his home as the sun came up on Monday and he expected the water to stop, but it did not and it rose all day long, and by dark, he had about 3-4 ft of water in his home. On Tuesday and Wednesday, the water continued to rise and was rising faster on Tuesday than on Monday. By Wednesday night at dark, he had about 5 ft of water in his home on the first floor. When he was rescued on Thursday evening, he has about 10 ft of water in his home. He could not tell direction on any of the days, and thought the water was just rising; not a rushing flow, but a steady rise of water.

786,300  
3,323,500

The eyewitness said on Monday the 29<sup>th</sup>, about 2 am the wind and rain was in the area and it lasted most of the day until about 3:15 pm. There was water in the street about 1 ½ to 2 ft, and about 8” in his home at that time. He was in his attic during the worst of it all. After the storm passed, he came out of his home to look around, and walked up and down the street. At 4 pm, he was back at his home, and the water was ankle deep in the street then, and seemed to be draining. He took a bath at about 6 pm, and then looked out after that at 7 pm., and saw the water was rising. It was coming down Congress from the west toward his home on Stephen Girard at a slow rate. He went to slept that night in the bedroom downstairs, and 6am on Tuesday, he went outside, and the water was in his garage, and right at his step down into his driveway – about 6” deep. In 20 minutes, it rose about 6” and was coming into his house. In 45 minutes, it was 2-½ ft in his home, and 3 ft in his back yard. He has a 9 ft concrete fence in his back yard and he climbed over that to go toward Chef Highway, and there was no water on the other side to the south side — the ground was dry at 8 am. He went to a friend’s at Chef Highway and Congress, and the water was 6” deep in the driveway and about 3 ½ ft deep in the street. About 9 am, he went back to his home and got his truck, and drove it down Congress that was 4 ft deep with water and to his friends where he stayed all day Tuesday. 9am Tuesday till 9 pm Tuesday, the water rose about 1 ft. The water was coming down Congress at a slow steady rise all that time. At 9 pm Tuesday, he went to the old New Orleans Federal Bldg. across the street, and spelt the night. At 5 am on Wednesday, the water had come up and was about 4 ft deep in the street at Congress and Chef.

785,700  
3,325,200

The eyewitness reported the storm let up about 0700-0800 on Monday morning, and then started again about 1000 and stopped at 1430. At that time he said that the water was up to the tires on his van in driveway. At 1600, he said water started coming into his house. Between 1700-1800, it was rising very fast. At 1800 he went onto his roof. He said that while he was on the roof he did not see water coming over the IHNC floodwall. He said the water was coming from the west. He was picked up from his rood by a helicopter on Tuesday at 1500.

786,300  
3,323,300

The eyewitness said on Monday, he was looking out at 7-8 am and saw no water beyond rainwater in the streets, and none at all in his building. He went out and looked up Congress to the north and saw water in the street in the distance, and said it was about 4-5 ft deep at the north end of Pauline. He heard the 17th had broken and also the London. On Tuesday, he started getting water about mid-day, and he could see water across Chef to the southeast and saw water rushing through breaks in the curbing walls there. He said the water in that direction came from the south to the north and when it got to an opening it was rushing like a fire hydrant. He said the water filled the west side across the highway, and he saw a lot of cars floating in that area.

785,800  
3,325,500

At 8:30 am on Monday, he saw water coming in his back yard and into his home. The water was being blown over the levee wall, and into his backyard, but it flowed from the back of his home to the front and out, and did not pool up. By 9:30 am on Monday, the water had passed out of his home, and it was starting to dry up. About 11 am, he is in his home and sees water at the base of his picture window in his living room, and it is about 1 ½ ft there and about 3 ft in the street. He looks out back at the levee, and the water is coming in the street, north to south in direction, and it is not coming over the Levee wall now. The water rises very fast, and is 18” inside his home in an hour. The water rises about 1” to 2” every hour, and is a slow steady rise. By 5 pm on Monday the water is 4 ft deep in his home. The weather has cleared, and by 6 pm it is getting dark, and has risen more, so he goes into his attic. He uses a tape measure to measure the rise, and can see it still coming up. 7 pm to 9:30 pm, it is still coming up, At 9:30 pm, he decided to get onto the roof of his home, and has to go down into the house to do so, and he said the water was chest high in his home at that time. By 10:15 pm he was on his roof, and it was 5 ft in his home then. He stayed on his roof from 10:30 pm Monday to 1:30 pm Tuesday, and that whole time, the water was creeping up, and he decided at 1:30 to swim away. He can see the levee wall, and it is dry, so he swims to it, and climbs onto the wall and walks the wall north to the Bridge where he is picked up. He said as far as he could see to the south, the water was not coming over the levee wall to the south, and it did not after about 8:30 am on Monday. The water at 1:00 pm on Tuesday did not seem to have direction, but he saw debris got south, and in a while would float back north, then south again. The water behind his house, between his home and the levee, was dry the last 3-½ ft toward the levee. He saw no water coming out of any of the relief wells. He also said the wall at the north end of the wall where it turns east was closed.

786,000  
3,324,500

On Monday the storm had passed and it was clearing. He lay on the couch and went to sleep. At about 11 am, he woke and there were a few inches of water in the house and coming in under the door. The water rose all day and he went to the roof just at dark, and the water was to the ceiling in his home at that time. He said the water was coming from the north to the south – Leon Simon area by the lake, toward Chef. He stayed there the night with his 4 dogs, and then he decided to leave since it was not falling. He swam to the levee at French Road, and walked it to Chef Highway. There was not water over it at that time, but some boats were against it on the east side -- the canal side.

785,600  
3,325,200

On Monday morning about 7:30 am, the eyewitness had eaten breakfast in his kitchen and walked toward the front of the home, and noticed water about 1/2” in the hallway. He looked in the bathroom and the toilet was bubbling and water was coming out, and he thought it was from that. But as he got closer to the front, the water was a little deeper and he could tell it was coming into the home from outside. He climbed a ladder to some furniture that was high, and sat there. By then the water was about 2-3” in the home and was rising slowly, and when he went to sleep Monday night, it was about ½ way up to the first rung on the ladder. By Tuesday morning when he woke at about 9 am, the water was about 4 ft in his home and by 11:30 am it was about 5 1/2 ft deep. In the house the water was to his chin. He went out the back door and down two steps and the water was over his head there... he is 5’9”. He made his way onto his truck and about 11am, the water rose quickly, and was still rising. He got to the top of his carport and was rescued from there at 2 pm on Tuesday. The water by then was onto his roof, over the gutters. He estimated it was 12 ft deep then. When he got to the roof, he could see the water was coming from Press toward Congress – west to east.

786,300  
3,323,800

According to the eyewitness account, on Monday morning, water was at the top of the canal side of the floodwall with some water splashing over. There was water in the street and it reached the back patio. They didn’t have sandbags and stuffed towels around back door to keep water out of the house. Hurricane left early afternoon, about 1-2 p.m., and water was receding. Water started coming back up late afternoon about 5:30 – 6 p.m. and rose steadily. 5 ft of water in house by noon Tuesday. They left Wednesday morning; they helped some neighbors get out, and camped out next to floodwall. By Wednesday morning, water was higher in sub-division than on canal side.

**Lower Ninth Ward and St. Bernard Parish**

789,300  
3,319,500

The eyewitness said on Monday way before dark, he had 3ft of water in his home on the second floor, about 12 ft deep he said. On Tuesday about 4 pm, the water seemed to pick up his home and turn it around. He said the water was coming from St. Bernard parish west into Orleans on the second floor, he sat on a heater and the water was to his waist. He said the water ended about 20 ft in the street.

788,500  
3,319,600

At 4:30 am on Monday, he saw water in the street in front of his home. He said his driveway is about 40ft, and in a matter of 5-10 minutes his freezer was floating in his home. He lives in a two-story home and it was on the first floor. By 5 am, he said the water was at the top of the first floor, but it seemed to have stopped rising. He said the water was from the Industrial Canal and flowed down Galvez Street, west to east. He said at the maximum, the water was 25 ft deep in the street. On Tuesday morning about 10 am, the water stopped rising because the pumps were cut on, but in 10 minutes they shut them off and it rose back to where it was before. About 12 pm on Tuesday, the water rose another 4 ft. They were rescued on Wednesday, and the water had not risen any more.

788,600  
3,317,900

The eyewitness said on Monday, August 29, she went to her front door at 7:30 am and saw some water in the street. By the time she walked from her front door to her dining room, water was shooting up through her floor furnace. In 15 minutes, the water was 9 feet deep in her house. The witness said that the water was flowing down North Rampart Street from west to east. At that time, she went upstairs and the water stopped rising. She stayed in her house until Wednesday, August 31 when firemen in a boat rescued her. At the time she was rescued, the water had receded on a few inches.

788,500  
3,317,400

After 0700 hrs there was a change of shifts at the facility. He and others were in a causeway between two buildings looking west. They observed very strong winds and it was still raining. Probable time bracket was 0700 to 0800. Wind was from the north. At first there was typical rainwater in the street. Sometime around 0800 to 0900 they noticed significant water, much more than normal rainfall. Estimated the time to rise from wheels to top of cab of large military transport trucks was about 1-1/2 hrs max. He took many still photos. Date on these photos shows Aug 28, but he is certain that they were taken on Monday Aug 29 in the morning. Thinks times are close to actual clock time, but not sure if they were adjusted to day-light-savings-time. Later analysis of photos showed that the camera clock was 12 hours behind actual time. His photos were used to produce a hydrograph at this location.



788,900  
3,319,200

According to the eyewitness account:

- Tupelo Street (actually a blvd) is a covered canal.
- About 0530, Monday, 29 Aug 05, he saw water flowing down Tupelo St (SSW) towards the Mississippi River with a slight angle to the east. Storm wasn't bad at this time, drizzle with some wind, still dark outside.
- He and his wife took refuge in a 2-story house next door. Water quickly rose to level of light switch plates (3 to 4 ft above floor) on 2nd floor. They moved to the attic.
- Placed a 911 call at or before 0630 Monday from his cell phone while in the attic. Believes 911 services will be able to verify cell phone location - he has proper equipment for location service. Placed multiple 911 calls. Heard helicopters flying overhead but couldn't get their attention (removed turbine vent from roof, but could only wave through it).
- Strongest winds occurred about 0800 Monday morning.
- Water started to recede Tuesday morning falling to level on 2nd floor balcony. They were picked by a Wildlife & Fisheries boat at 1030 Tuesday and carried to the St Claude Ave Bridge.
- Noted that levees were modified when Florida Ave Bridge was replaced. Levee to the south of bridge was restored to its proper height. Section of levee between old and new bridge locations was never completed and was lower than adjacent levee.

788,500  
3,317,400

Eyewitness provided several photos, which he stated were corrected to day-light-savings-time and show the water just as it is coming up on the General's private auto. At 0813 the water is already up to the wheels of this vehicle. Another photo taken at 0746 shows soldiers standing and looking at the wind and rainwater in the street. i.e. the flood waters had not yet arrived at 0746.

788,500  
3,317,400

The eyewitness verified information provided by others at this site and added several useful bits of information. The clock in the Bks Museum had stopped at 9:35 and was about 9-10 feet above the floor of the building, which was at about ground level. Also, he had called his wife on the cell phone as the water was coming up the street in front of the HQ Bldg and rising quickly. In a later conversation he verified that time as 08:01 Monday morning. Also ID'd a HW mark across the street.

Pump Station 5

This individual is an operator at Pump Station 5 who stayed during the storm. The logbook entry in the information gathered by Task 8 of IPET shows an entry for Pump Station 5 at 5:30 on 8/29/05 that power was turned off to the station for safety due to high water levels. In a telephone interview, the operator was asked about his observations during the storm. He confirmed that the 5:30 entry was Monday morning. He confirmed that the logbook entry was correct regarding shutdown at 5:30 AM. He stated that by 4:30 AM, water was halfway up a chain link fence at the station and that by 5:30 AM the fence was completely underwater. He stated all this was happening while it was still dark. He said water was coming into the station by 5:30 AM but not certain where it was coming from. He stated they had to swim to pumps A and B. He stated the people at PS#5 were not aware of the floodwall breach near Pump Station 5 until Tuesday morning. Four other operators stayed during the storm also, but were not able to be contacted. The drainage station supervisor also did not know how to contact them. One operator is now at Pump Station 19 and he was contacted on 5/4/06 about his observations. He stated he was the operator on duty and he was the person who would have written in the logbook the 5:30 AM entry although he did not have a specific recollection of making that entry. He stated from 3:00 AM to 5:00 AM and in the next sentence from 4:00 AM to 6:00 AM they were battling electrical feed problems. He remembered that at 6:10 AM, “water was filling up the yard”.

**Chalmette**

795,300  
3,316,800

This eyewitness best estimate of water coming up the street was about 0830. Water first ran about 1 ft deep in street carrying with it grass islands. Cars also began floating away. Made marks on upstairs wall of water elevation and times. Also, stated that clock in kitchen stopped at about 9:10. The witness' son later stated that it stopped at exactly 9:20. It was 6.96 feet above the floor. This was the surveyed elevation. Floor elevation was 1.3, and HW mark was measured to be 9.65 feet.

795,100  
3,316,700

This eyewitness reported that power went out about 0500 on Monday morning Aug 29th 2005. She saw rainwater in the street, but no floodwater at about 0800. Sometime shortly thereafter the floodwaters came and in about 15 minutes they were up to the ceiling in the lower floor. They stayed at that level for about 10 days. The wind abated about 1600 hrs, which is approx when they could get a boat to rescue her and her husband and son. She stated that they have 10-foot ceilings in the house. She has videos and will share when she is able to get them copied. All clocks in the house stopped around 9:05, being about 8 feet above the floor. The water was black in appearance.

Various

The eyewitness was at the County Courthouse the morning of the flood. According to his account, first reports of floodwaters came from a Sheriff sub station near Jackson Bks. reporting a foot of water in the streets. At the courthouse they saw water coming from the north and within 3 hours the water was 8 feet deep in the courthouse offices. He also informed that he made a survey of levee damage by helicopter shortly after the hurricane (2-3 days later). Videos of it are with unknown staff member who took them. In days after Katrina he noticed tremendous amounts of dark sediment and parta spatins grass in streets and up against and in houses south and west of Forty Arpent Canal. He is convinced that these masses of vegetation and sediment came from the N. E. and were easily carried over the + 8 foot levee of that canal by the storm surge. He has a house near the MRGO, which he states had water marks (grass) at about elevation 19 feet. Stated that the elevation of this house is accurately surveyed.

### East New Orleans

788,200  
3,324,600

The eyewitness said power in house went off on off for good sometime between 0400-0600. At this time water was in the yard. Went back and lied down to sleep but was up within ½ to 1 hour due to noise etc. Water started coming in house. Within about 45 minutes, water entered the house and it was up to the ceiling joists and then some. Managed to get into attic and cut his way out onto roof. From that viewpoint he observed ice chests, debris and whitecap waves coming from the north going south. By about noon the water receded approx 3.5 feet to the visible dark watermarks on the house. Brother came in boat at evening. Boat could float well over 4-foot high chain link fence. Evidence in this neighborhood does indicate strong flow from north to south as shown by moved houses, displaced entry lamps, damage on N side of buildings, and bent over trees and poles.

787,800  
3,322,000

According to research, a large transport from Holland named Ariake (maybe Ariate) Star was moored next to the large warehouse during the storm. Personnel at the site were given copies of these photos taken during the storm. The photos are very good and seem to cover early morning hours and the rising waters. Noteworthy is a small portable building on the west side of the warehouse that is missing in later frames; however the timing could not be verified.

795,300  
3,323,600

According to eyewitness at the Entergy plant who stayed during storm, they were taking on water about 0600 to 0630. Shortly after, white caps came over the floodwall.

786,800  
3,326,800

At 0630 the eyewitness was on the bottom floor of the airport terminal building and saw sheet flow coming from the NE across the tarmac. Tried to wake up other employees. By 0645 to 0700 hrs a flood wave had entered the building and broke out the large glass windows on the bottom floor. This wave came from the NE. Water stayed at elevated levels for several hours, and then the wave went out to the NE. He took pictures looking north and we can find them at 'Orleanslevee.com'. Some of these pictures are possibly time tagged. Also, personal observations on south side of airport between it and the RR track show that the levee was overtopped and that a large wave must have moved from approx N to S as evidenced by scour on south of levee wall and by aircraft carried over fences and deposited on the other side without damaging the fences.

788,100  
3,324,500

On Monday morning about 7:30-8:00, he woke up and went to the kitchen to get coffee and as he did he looked out front into the street and saw water in the street about 18" deep, based on his truck tires, but did not think much of it, thinking it was rainwater. He made coffee and got some for his wife and was going back to the bedroom when he walked by the front room and saw water coming in under the door. He went to the bedroom and got his wife up, and she dressed while he untied a boat he had next to the house and ran a rope into a raised-room window. He said about 30 minutes from when he first woke, the water was waist deep on his wife – about 8:30 am. By 9:00, the water was 5 ft deep in his home, and his home is on pilings about 3 feet off the street. They moved to the raised area in the home, and when the water was 7 ft the rest of the house, it was 2-3 ft in that area. The water rose to about 7 ft in his home – he had 8 ft ceilings – and then it fell to about 3-4 ft in the home late that night and the next morning, and stayed there for about 3 weeks. He left on Wednesday with his son who came by boat and got them.

787,300  
3,324,100

Owners stated much evidence that water moved from south to north along this road.

789,800  
3,326,300

This eyewitness says about 0845 water entered house. Came from north. Got up to about 7 to 8 feet high in the house. In about 15 to 30 minutes it filled the house, maybe less.

789,500  
3,323,900

During observation by our team, we had noticed on Old Gentilly Rd east of Industrial Canal, clear evidence that flow had gone from S to N. Fence, trees and debris all lean northward. The eyewitness got into an upstairs apartment. From that location he observed the following. Water sneaked in, and then rose up fast. It came rushing through and around the railroad tracks from the south to the north, gushing down Wilson, crossing Chef Menteur to the north. Happened around 0630-0700. Depth of the water was above the chain link fence behind the building. (~5-7 feet?). Not much rain, but lots of wind, which came from the north. He reported that water rushed over and around and under the railroad cars and locomotives.

789,600  
3,325,300

At same location also interviewed a second eyewitness who said the storm had passed about 0530. Then about 1/2 hour later there was a big boom and water rushed into the house. Got up to chest height in less than 15 minutes. Water went from southwest to northwest. Stayed in house for 3 1/2 days. Floated out on door via Werner Drive to Chef Menteur.

788,500  
3,326,300

These eyewitnesses stated early morning of Monday 29 Aug 05, were in garage holding garage door to keep it from blowing open so that garage roof wouldn't blow off. About 0900 hrs water began rushing up driveway and into the garage. Within minutes it had surrounded the house and blew in the front door, knocking one of the witnesses to the floor. The son and wife struggled to 2nd floor. They saw water going down the street north to south. Between 0930 and noon the water reached a peak height. This was at the 'gutter can' on the houses across the street. Water reached the third step from the second floor landing in his house. He stated that he kept looking at his watch as events happened, and thus felt fairly certain about the times he reported.



794,000  
3,325,100

The storm came in on Monday, and they were okay with that with little damage. About 2-3 p.m. on Monday, he first noticed water coming toward his home. It was rising very slowly at first, but was steady. The water was coming from the Chef Highway – the south. By nightfall on Monday, he had 2½ ft of water in his house, and it seemed to settle there. It was about the same in the morning. There was about 5-½ to 6 ft of water in the street in front of his home. On Tuesday morning the water had not gone only about ½”, and he heard the levees had broken, so he left the house.

793,600  
3,325,100

Houses on high ground along Wright Road did not flood.

790,700  
3,325,200

On Monday about 10 am the wind and rain was very bad, and water was in the street from the rain. He son looked out about 11:15, and there was water rising and it was to her door at that time. They started moving things up, but as they did the water kept coming in and rising, so they started getting into the attic, about 12. The wind was still blowing hard and they could see the water in the house to the ceilings, about 8 ft deep. Just about 12:30, the wind stopped and the water quit rising. They stayed in the attic and the next day, Tuesday, at 2:30 pm, that water had dropped and was about 4 ft in the house and 6-7 ft in the street. She said the water was coming from the south, the Chef Highway area and flowing north toward the lake.

786,900  
3,325,500

The eyewitness said on Monday the 29<sup>th</sup> about 9:30 to 10:00 am, the storm was dying down and they were on the sofa in the house, with the window open. They heard a noise, and went to the door and looked out to see what it was. The water was swirling and filling in front of their home like in a swimming pool. It was so fast; you could not swim against it if you had to. The pressure was breaking window pains in the home. The water was on Cornwall and coming from Gentilly – from the south, not from Haynes Street area – the north. Suddenly, the water started coming in the door, and they tried to move things higher, but it was coming up to fast. They went upstairs to escape the water; this was a matter of about 15 minutes. They were able to look back to the first floor and the water was about 5 ft deep in the home. By 10:45 am, the water seemed to settle out and quit rising; at 11 am., her husband went down into the water to get some water for them to have upstairs. She said just after 11 am they thought the water went down a little, but she was not sure. He looked out the back of the home and it seemed to be higher in the front than in the back. They stayed there for 4 days, and the water did not drop any as she could tell. When they thought more water might come and drown them, they were able to get help and get out of the home.

789,900  
3,324,400

On Monday about 9:40 am, he was eating breakfast, and he stopped when he saw a tree limb pass in front on his home. He went to the door as another passed and could tell the water was rising fast. He put two chairs on a table for he and his wife to sit on, but by that time the water was in his home about 1 foot deep, and that would be about 3 ft deep outside. He knew it was coming in to fast, so they got into the attic at 10 am. The water rose to within 3” of the opening, and he said that was almost 10 ft deep, when it seemed to stop rising. About 2:45 pm on Monday it went down about 3” and by 3:30 pm down another 2”. They slept in the attic on Monday night, and Tuesday morning at 10:30 am, the water had dropped to doorknobs in the house. Later Tuesday afternoon, about 4 pm, he said the water rose about 1 foot in the house and was about 5 ft outside – to his chest and he is 5’11”. He was sure the water was from the southeast to the north.

789,700  
3,325,600

The eyewitness rode out Katrina at his apartment in East New Orleans. The apartment is located on the I-10 Service Road off of Crowder Blvd. On the morning of Monday, August 29, the gentleman heard bubbling by his apartment door. At that time the electricity was still on. Between 8:00 am and 8:30 am, the force of the water broke down his door. The water was rising quickly and was chest deep. Between 9:30 am and 10:00 am he went upstairs. The water continued to rise. Since he can’t swim, he took the mattress from the baby bed and floated on the mattress to the apartment building roof. He stayed on the roof for 2 days and was rescued on Wednesday, August 31 around 2:00.

787,300  
3,325,800

The eyewitness interview says on Monday morning at 8:15, it was raining hard and water was swirling in the street in front of the home that faces the Lake area, from the hard rain, but not flooding. At 8:30 am her son went to the back of the house and opened the door and the water flooded into the home. Water was coming through and around the home, into the street and filling it. It rushed in so fast they only had time to get to their attic. While they were getting into the attic, she said it was about 3 ft and by the time she was into the attic, at 9:00 am, (she said she kept checking the time) it was 5 ft. The water was coming from the Morrison Road area, from the south to the north. It rained hard while they were up there, and the water held at about 5-6 ft until 5:30 pm Monday, when it started to drop. Just at dark, about 7 pm, they climbed into the house and it was 3 ft deep in the home then. She said there is about 2 ft difference from her home to the street elevation. On Tuesday about 8 am, the water began to slowly rise again, and by Wednesday morning it was 5 ft deep in the home again. They were rescued Wednesday about 2:30 pm.

793,500  
3,325,200

House on high ground on Nottingham Road did not flood.

791,000  
3,324,900

The wind was blowing hard from the northeast. About 9:30-10 a.m., she saw a surge of water coming from the north on Knight Dr., but was not sure how big. The water settled in the street at about 3-½ ft. On Tuesday morning, the water goes down to about 2 ft, but about mid-day, it the water color turns from a dirty grey to almost black, as it rose again to about 3 ft in the street. It stayed like that for 2-3 days.

797,100  
3,327,200

Monday morning about 2 a.m. the storm started and was blowing hard from 4 a.m. until about noon. There was a lot of wind and rain with the storm. It started dropping off about 11 a.m. The eyewitness said he had rainwater flowing through the Church grounds, but it was normal rainwater. About 5 p.m., the water started rising, and was until Wednesday morning. The water was flowing west to east. From 5 p.m. on Monday until 5 p.m. on Tuesday, the water rose very fast, about 1 ½” per hour, but after that until Wednesday morning, the rise was slow, but steady. The water at its highest was about 18” to 2 ft deep in the area. The priest and the people at the Church left on Wednesday afternoon.

791,600  
3,327,300

During Hurricane Katrina, the eyewitness stayed with his elderly parents in their home. The home is located in the Warwick East Subdivision on the north side of I-10 near Read Road. The eyewitness stated that the power went off during the night on Sunday. On Monday morning (August 29) he got up during daylight. Around 8:00 am he noticed rainwater in the street. Between 9:30 am and 10:30 am a little water started coming in the house. He was mopping the water up with a towel when heard a loud pop. The sound was the force of the water popping open the locked door. The water was 4 feet deep in a matter of seconds. He is a 6 feet tall. He said that by 10:45 am to 11:00 am that the water was a little over waist deep. His parent’s house is on a slab at ground level. He went to the bedroom and picked up his invalid father. They were trapped in the house for 2 days. During the day on Tuesday, the water level gradually increased to chest deep. They were rescued on Wednesday around 5:00 pm by a neighbor in a boat.

793,800  
3,325,600

About 6:30 a.m. on Monday he was okay and was sending emails out to his friends. The storm got bad, and he got a lot of wind and rain. At that time, there was no standing water in the streets, but within 1½ hour, there was water in the streets. He said he saw a flounder in the water. At 10:15 a.m., the water was at his sidewalk in front of his home, and by 11:45, it was in his home, and was 2-½ to 3 ft in his home. The water kept rising for about 4 ½ hours and reached its peak then. The water was flowing from the west to the east. After Monday about dark, there was no more rise or fall for the next few days, and he stayed for two weeks. He said the stop sign in front of his house is at a +13 elevation.

792,400  
3,325,600

Sunday night there was some wind and the storm was coming. He went to sleep in the upstairs bedroom, and Monday morning he woke to find water about 24” in his home. The water rose all day and by Monday night, he had about 4 ½ ft in his house. Tuesday morning, it was 5-½ ft deep in his home. The water peaked on Wednesday morning at about 6 ft in his house. The water seemed to be coming from the east to the west.

792,200  
3,325,200

He stayed at home during the storm Early in the morning on the 29<sup>th</sup>, he noticed heavy rainwater in street. He tasted it and it was fresh water. About 1030, the water started coming up quickly. The water got up to chest high by mid afternoon. It continued to rise slowly and came up about another 1 foot later in the evening, before sunset. Tasted the water later in the day and it was salty, so he knew that it came from something other than the rain.

Pump Station 20

788,200

3,322,500

Eyewitness was at Pump Station 20 during the hurricane. His eyewitness account said the water was over the whole levee at the Intracoastal Waterway. He said the station was 13 ft high, and the water was clearing the levee by at least 2 ft from 6 a.m. on Monday until 11 a.m. on Monday, and then after that it was just waves topping the levee. By 1 p.m. the overflowing had stopped totally. All he could see on the north side of the levee was flooded. At 8 a.m., he called Station 16, and asked if they had water there; the operator said he was dry at the time, and the witness said he would get it very soon. The witness talked to the operator at 16 about 3 weeks later about Katrina, and said he was flooded by 8:30 a.m. and the water came from the south to the north. He said he saw no flooding over the levee at Haynes, but just some water wash over. He said the pump station operator at 14 stayed for 22 days at his pump, but it was down a lot of that time.

I talked with the witness at Pump Station 20 again on April 18, 2006, and tried to clarify some information. The station is located north of the Intracoastal Waterway and east of Inner Harbor Navigation Cannel, just south of Almonaster. He said from as early as he could see in the morning, about 6:20, he looked to the south toward St. Bernard Parish, and water was flowing over the levee like a waterfall. The witness stated that lasted about 1 ½ hrs or until right about 8 a.m., and then there was not a waterfall look, but the water just covered the entire area like a lake -- he told me it was like looking at the Gulf. He said the water from the Intracoastal was flowing over the north side levee wall, filling the area north of the Waterway, and also over the south side levee wall, flooding into the swampy area south of the Intracoastal Waterway. He said about 8 am, south of the Waterway, all he could see were treetops. He could not see back toward New Orleans, to the north as he described it. He shut down his pump at 6:45 am, as instructed, because water was filling the basement of the Station where the diesel reserve that ran the pump was located; if not the water in the diesel would ruin the pump. He said the station is about 20 ft high, and the wall is about 13 feet, and the water around the station got to about 7-8 feet deep.

798,300

3,327,100

Monday morning about 4 a.m. the storm started blowing hard. There was no water in the streets at that time. As the sun came up, the rain was harder, and the wind was blowing more. The water started pilling up in the street, and was about 1 ft in the street by about 8 a.m. By 10 a.m., the water was about 2 ft in the street. Her husband went out to clean the drains, and it started to run out then; she said he did this every hour or so, but soon it was not draining. By dark, the water was 4 ft deep in the streets. She said the water seemed to be rising all over, and she could not tell a direction. She said when she went to sleep on Monday night, and the water was about 3 ft in her downstairs. On Tuesday morning, the water had risen a little, but early it went down a little. Later in the morning, the water started to rise again, and they left by boat mid-day Tuesday.



795,300  
3,323,600

The Entergy Michoud Generating Plant is located on Paris Road on the southeast side of the I-510 and Gentilly Road intersection. During Hurricane Katrina, the Entergy employees took video and pictures. We have acquired a copy of their video and pictures. The pictures show the earthen levee under the I-510 Bridge overtopping and the waves splashing over the concrete floodwall. The Entergy employees reported that water started coming into the plant basement around 6:15 am on Monday, August 29 and continued to come in until about 10:20 am. The water filled the Entergy property to a depth of about 5 to 5 ½ feet. By the end of the day on August 29, the water on the property had dropped to about 3 feet deep. The property was basically dry 3 days later.

793,300  
3,325,100

According to the eyewitness account, the eye of the storm came in about 10 a.m. on Monday, and for about 10-15 minutes it was total calm and quite. That is when he saw water coming into the area. About 10:10 a.m. the water started to rise, and it rose very quickly. In less than an hour, the water was in his home about 18" deep. The water kept a slow, steady rise until Wednesday morning when the water was at its peak at about 2-½ ft in his house, and about 4 ft in the street. The water started to drop after that. He could not tell if there was a current to the water, but thought not. By the following Monday, a week later, there was about 1 ft in his home.

792,500  
3,325,400

Monday morning about 11 a.m. there was a lot of wind and rain. He noticed water in the street, and did not worry too much until he could tell it was rising, fast. He said he saw water spraying like a fountain, which seems to be street drains backing up, and the water forced out the openings. When the water rose into his driveway and seemed to still be coming up, he went up into his attic. By 11:30 a.m., the water was at his front door. By 12:30 p.m., it was 18-24" in his house, but it never rose more than that 24". He was in the attic for 24 hours. He left the house on Tuesday afternoon, and when he got to Reed and Pressburg, the water was about 6-½ ft deep in the street at the intersection.

793,000  
3,325,100

The eyewitness said on Monday morning the power was on and there was no water in the street beside normal rainwater. About noon, he started seeing water, and it was rising in the streets. It was still raining some, but this was more than rainwater. The water was rising rather fast in the street, coming from Pressburg St and Prentiss Av. -- north to south. The water was in the street about 18" then in a couple of hours it was 2 ft deep. The water rose to within a few feet of his house, but never got into his home. The water rose just a little more each day until Thursday when it stopped rising. He left his home on Thursday afternoon, and it had not risen since the morning. He said there was current to the water from the north to the south, but by late Wednesday, that had stopped.

791,300  
3,327,900

The power went off early on Monday morning. About 10:30 a.m. on Monday, she sees water coming, and she started moving things to higher spots in the apartment. The water rose very fast between 10:30 and 11 a.m., so she went to friend's apartment on the second floor. The water continued to rise all day, and about nightfall it was 3 ft deep in her apartment. The water rose overnight about another foot and then seemed to hold there. Her home faces the south, and she said it was deeper on the south side of the home than the north, so when they left, they went north toward Haynes. They walked from Curran toward Haynes, and the walked the levee west to Downman, and said there were no breaks in the levee at all.

791,000  
3,324,500

Water in the yard, but not in home on high ground along Charlene Drive. The water came from east to west.

790,400  
3,327,400

Early in the morning, the eyewitness went outside and saw things flying around, then the wind stopped and it got real quite. He looked north to the levee, and could see water overtopping it in waves, but it was not a break. The wind picked up again, and the water from the lake was being pushed over the levee. There was water in the street about 4 ft deep on Monday. He got water in his home overnight, but it drained out by mid-day Tuesday. About 4 hours later, the water started flowing back into his home, and he left. The second rise was from the south to the north. He left toward Haynes, and it was totally dry on Haynes to about 1 block south of Haynes.

	792,000
	3,328,600
<p>Monday at mid-morning, the weather was great with sunny skies and the eyewitness and her husband drove east to Paris Road on Haynes to see what it looked like, and they could see water was over the railroad tracks by the lake, and some small erosion by the lights, but the levee was in great shape. They were working in the yard about 2-3 p.m., when her husband noticed water in the street, coming from the south. They thought it was over, but the water kept coming and rose all night. By Tuesday morning, they had about 2" of water in their den, which is a step-down add-on to their home, so the water was not in the rest of the home. That is where it stopped, and it was about 2-½ ft in the street. They had a boat, and used it to look around, and went toward Paris St. to check on a hunting camp they had south of there. The water stayed that deep 3-4 days until the pump started again. On Tuesday, the 30<sup>th</sup>, they drove the levee road from Unity southward to Paris, and there was no washout at all on the levee. He husband drove from Unity northward all the way to Downman, and again there was not washout that way. The further he went east, the more the water was away from Haynes.</p>	

**New Orleans Downtown**

	779,300
	3,316,800
<p>The eyewitness' location is near canal that drains into 17th Street Canal (west of Superdome). He said water backed up through pumping station, knee high in 15 minutes, 3 ft deep in 3 hours, 4.5-5 ft deep in 6 hours (Tuesday about 4 p.m.). By 6 p.m. Tuesday, water was 6 ft deep. Rise slowed; water was 7-8 ft deep by next morning. Heard that levee broke about 9-9:15 a.m. Tuesday. Lives in 2-story house that sheltered 11 people Wednesday night.</p>	

	780,400
	3,319,300
<p>This eyewitness rode out Hurricane Katrina in the clinic behind Mercy Hospital (Lindy Boggs Medical Center) on Bienville Avenue. The eyewitness reported that he spent the night on Monday, August 29 in the clinic. When he went to bed Monday night, he saw no water. At 6:00 am on Tuesday, August 30, he woke to find 2 feet of water in the lobby of the clinic. By 11:00 am, the water in the lobby was 4 feet deep. By noon, at the time they evacuated, the water was 4 ½ feet deep in the lobby.</p>	

	782,100
	3,317,900
<p>The eyewitness was at a Hotel at the corner of Canal and Claiborne. She checked out of hotel around 1130-1230 on Monday with the intent to drive back to her house. At that time she said that there was only about 1"-2" of water in the street. However by the time she got to the corner of Canal and Broad, she said that the water was up on the stop signs.</p>	

779,100  
3,316,000,

The eyewitness has photographs taken in the Broadmoor neighborhood on August 29, there was street flooding in the morning, which receded in the afternoon of the 29<sup>th</sup>, and by Monday night, the streets in the area were dry. Late Tuesday morning, the water came back and it rose all that day and into Wednesday morning. He also has photographs taken on Monday afternoon, near the Superdome, in the mid-city from the South Jeff Davis overpass, Pump Station 1, the Washington Avenue canal and the Carrollton/ I-10 interchange.

779,200  
3,319,800

The eyewitness said between 3:30 and 7:00 pm on Monday the 29<sup>th</sup>, after the storm had passed, he noticed flooding on Canal Street in front of the church, and that it was passable still, but he did not notice any direction to the flow. A little after 7 pm, on the 29<sup>th</sup>, there was no floodwater observed on the church or school property. A little later, it was reported that there was water in the basement of the Rectory, north of the church. The laundry room, which is in the northwest corner of the Rectory, and lower than the rest of the floor level had about 3 ft of water there. He thought a water main had broken and the sewer/water department was called, but the lines were too bust to get through. At 8 pm, there appeared to be no reason for alarm, and they thought the water was as a result of common flash flood rain or perhaps seepage into the basement. At 3 am on Tuesday, the witness awoke and shined a flashlight from the third floor in the Rectory, and saw the grounds covered with water. Wednesday the 31<sup>st</sup>, the floodwaters were still rising and reached maximum level at about 5 pm. The Rectory and school buildings had flooded, but water had stopped at the top step of the church. The witness left the church by boat about 5 pm on Wednesday.

- 782,700  
3,317,700
- Some water accumulated in Rampart Street during the hurricane, but they didn't consider that unusual (with heavy rain) or significant.
  - Went out Monday evening after hurricane had passed, walked several blocks down Canal St. towards the river, didn't see any flooding
  - 6 a.m. Tuesday morning, observed water covering sidewalk along Rampart St.
  - By 8:30 to 9:00 a.m. Tuesday, water was a foot to 1.5 ft deep in lobby, which is perhaps 0.5 ft (1 step) above sidewalk. The Rampart Street median strip was not completely submerged at this time. They walked out along the median strip.
  - 2nd hand account places onset of flooding in this area at 3-4 a.m. Tuesday.

# Appendix 8

## Dynamic Forces and Moments on Flood Walls

---

### Introduction

Dynamic forces and moments on flood walls due to waves can be large in comparison with their static counterparts and therefore of significance in design and performance. This appendix presents the results of very simple calculations which compare the ratios of the dynamic forces and moments to static forces and moments for waves traveling along the floodwall. These results apply to outfall canals where the waves generally traveled along the canal. These results do not apply to floodwalls along the Lake Pontchartrain lakefront where the highest forces are from waves traveling perpendicular to the wall (head-on). The calculations are based on linear shallow water wave theory. Figure 8-1 provides a definition sketch.

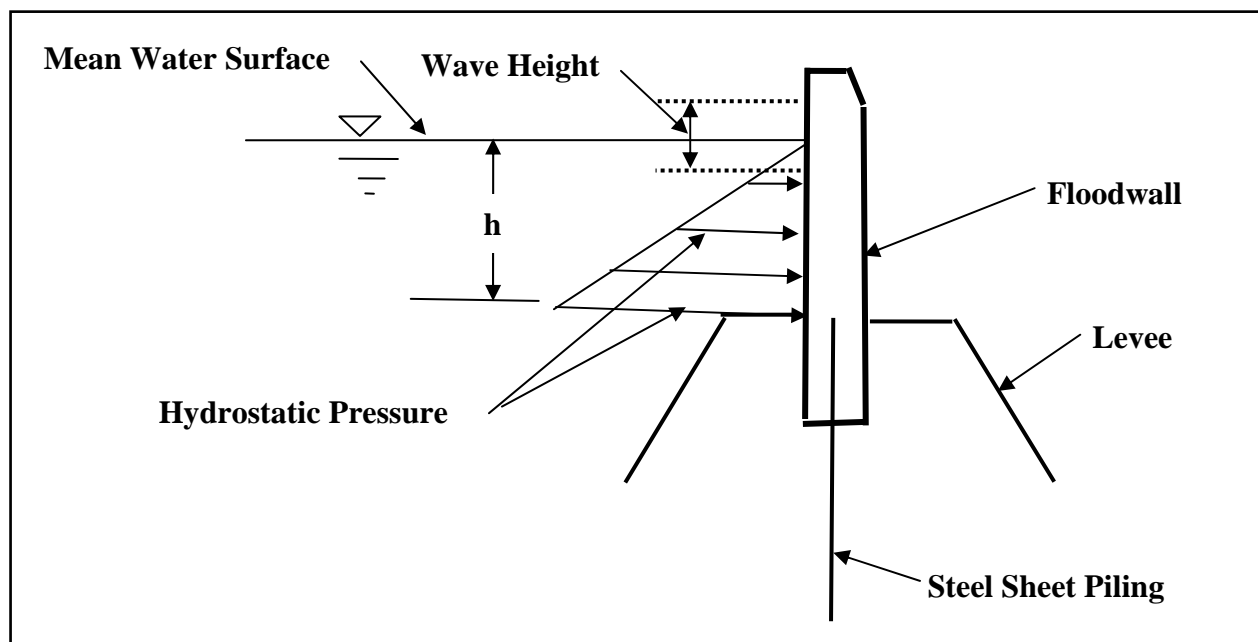


Figure 8-1. Definition Sketch of Hydrostatic Forces Acting on a Floodwall and the Wave Height Superposed on the Mean Water Surface, assuming wave is traveling along floodwall



## Forces and Moments

### Forces

The static force,  $F_s$  per unit length, acting on the floodwall due to a water level,  $h$ , is

$$F_s = \frac{\rho g}{2} h^2$$

The total maximum force,  $F_T$ , including the effect of a wave of height  $H$  (assuming crest and trough are equidistant from the mean water surface) is

$$F_T = \frac{\rho g}{2} \left( h + \frac{H}{2} \right)^2$$

Thus, the ratio of the dynamic force contribution to the static force,  $R_F$ , is

$$R_F = \frac{F_T - F_s}{F_s} = \frac{H}{h} + \frac{1}{4} \left( \frac{H}{h} \right)^2$$

The ratio  $R_F$  is only a function of the ratio  $H/h$ , and so the ratio of dynamic to static force components is a constant if  $H/h$  is constant. It is noted that the ratio  $H/h$  has a maximum which will be taken as 0.78 herein.

Figure 8-2 presents the ratio of dynamic to static forces versus water depth and wave height. The stable shallow water wave height limit of  $H/h = 0.78$  is also shown. The range of wave heights from 1 ft to 1.5 ft is highlighted as the approximate wave height range determined to occur at the 17th Street and London Avenue floodwalls during Katrina. It is seen that for a water depth against the floodwall of, say, 4 ft, and a wave height of 1 ft to 1.5 ft, the *total force* ranges between approximately 128% and 140 % of the static force component.

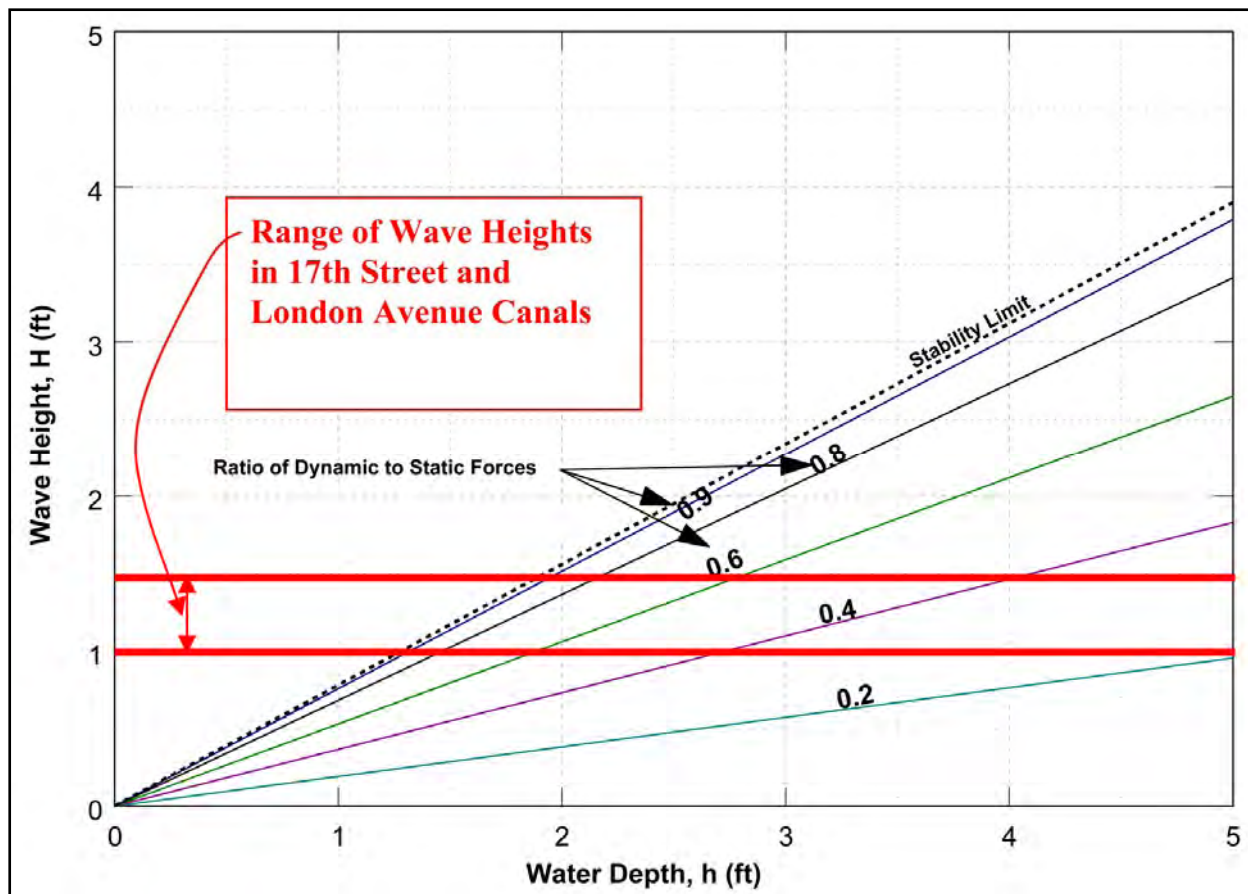


Figure 8-2. Isolines of Constant Values of the Ratio of Dynamic to Static Force Components,  $R_F$  versus water depth,  $h$ , and wave height,  $H$

## Moments

The same general procedure as applied above for forces is applied for moments. The static moment about the base is

$$M_s = \frac{\rho g}{6} h^3$$

and the total moment including the effect of waves is

$$M_T = \frac{\rho g}{6} \left( h + \frac{H}{2} \right)^3$$

Thus the ratio of dynamic to static moment components,  $R_M$  is

$$R_M = \frac{M_T - M_S}{M_S} = \frac{3}{2} \left( \frac{H}{h} \right) + \frac{3}{4} \left( \frac{H}{h} \right)^2 + \frac{1}{8} \left( \frac{H}{h} \right)^3$$

Figure 8-3 presents the ratio of dynamic to static moments versus water depth and wave height. The stability limit of  $H/h = 0.78$  is also shown. It is seen that the ratios of dynamic to static moment components are larger than their force counterparts (Figure 8-2). Again for a water depth against the floodwall of 4 ft, and a wave height range of 1 ft to 1.5 ft, the corresponding range of *total moments* would be approximately 145% to 165% of the static moment component.

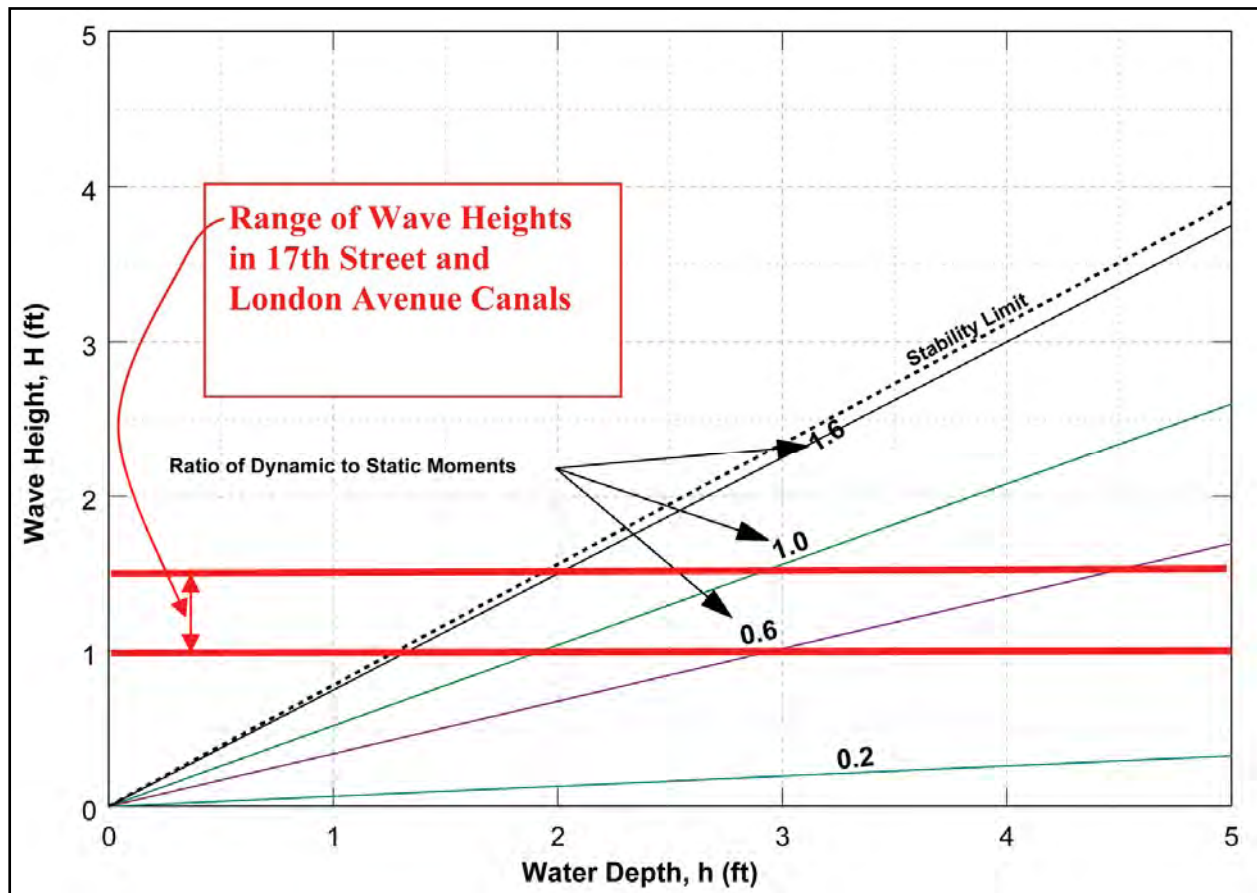


Figure 8-3. Isolines of the ratio of dynamic to static moment components,  $R_M$  versus water depth,  $h$  and wave height,  $H$

To put the information in Figure 8-3 into some context, Figures 8-4 – 8-7 contain the sill elevations and floodwall elevations for the three outfall canals and navigation canal.

## Summary

For both wave-induced forces and moments acting on a floodwall, results have been presented for the ratios of dynamic to static components for waves traveling along the floodwall.

The magnitudes of these ratios are such that the dynamic forces and moments associated with the presence of waves should be taken into account in floodwall design and analysis.

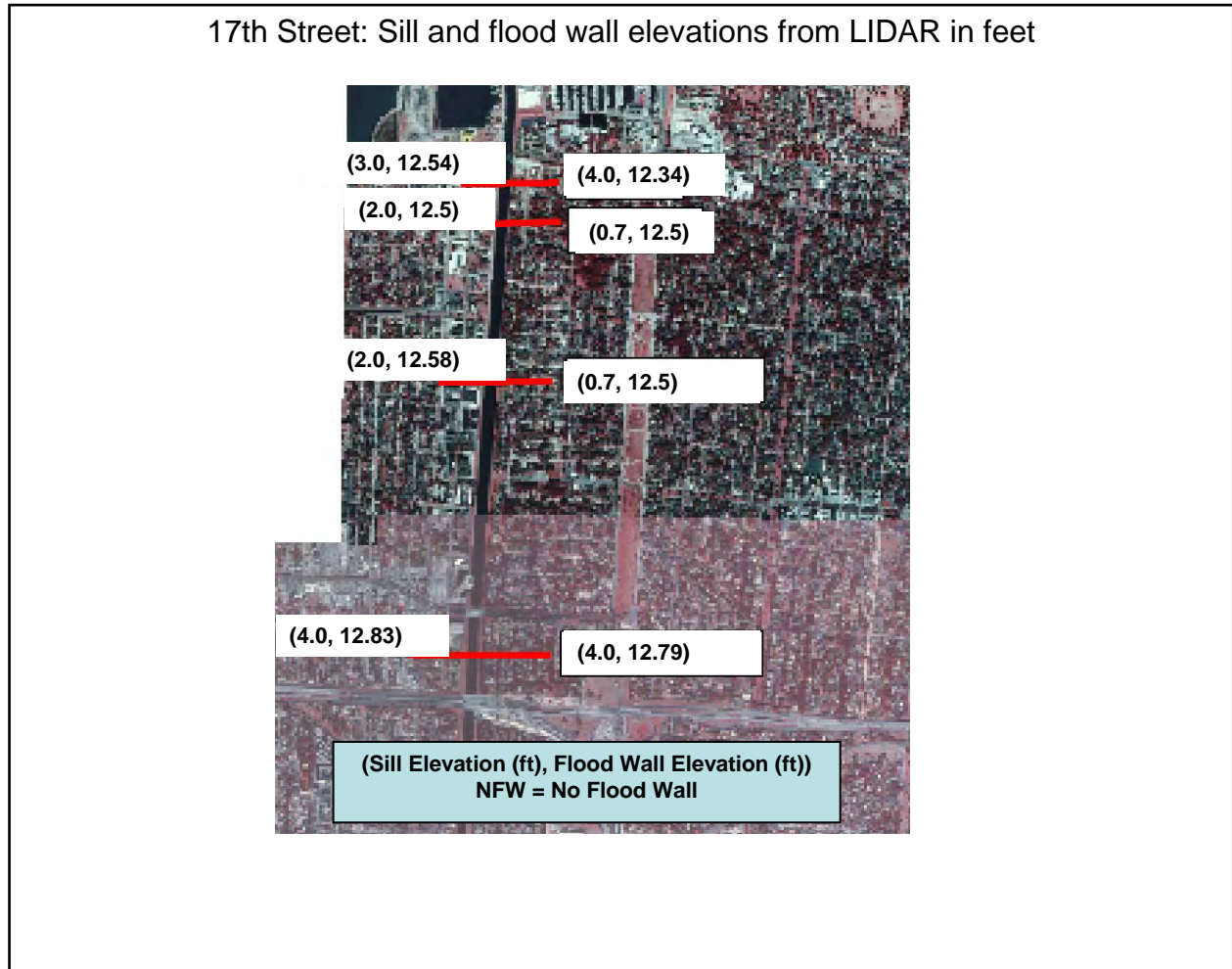


Figure 8-4. Aerial photograph of 17th Street Canal showing sill and floodwall elevations

London Avenue: Sill and flood wall elevations from LIDAR in feet

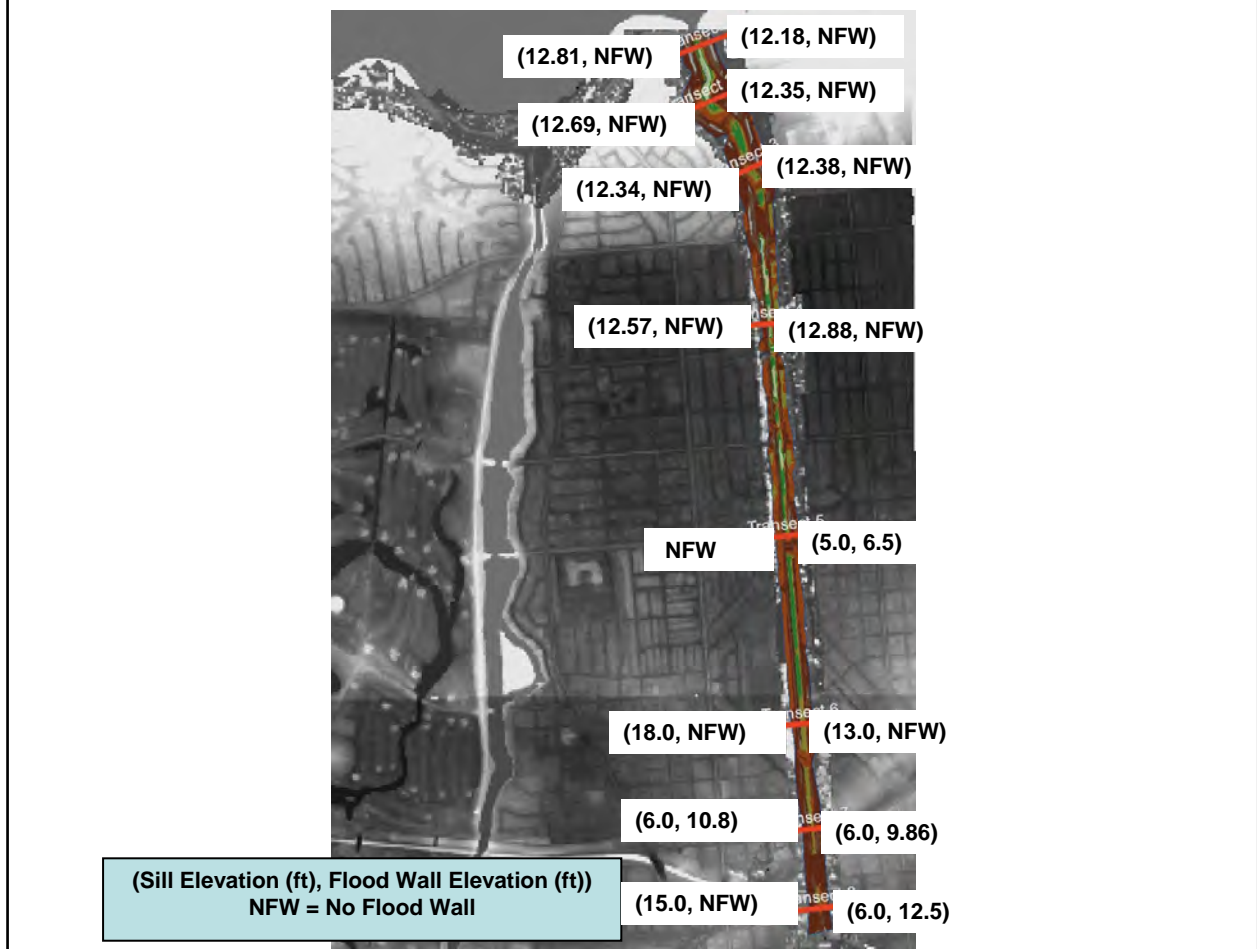


Figure 8-5. Aerial photograph of London Avenue Canal showing sill and floodwall elevations



Orleans: Sill and flood wall elevations from LIDAR in feet

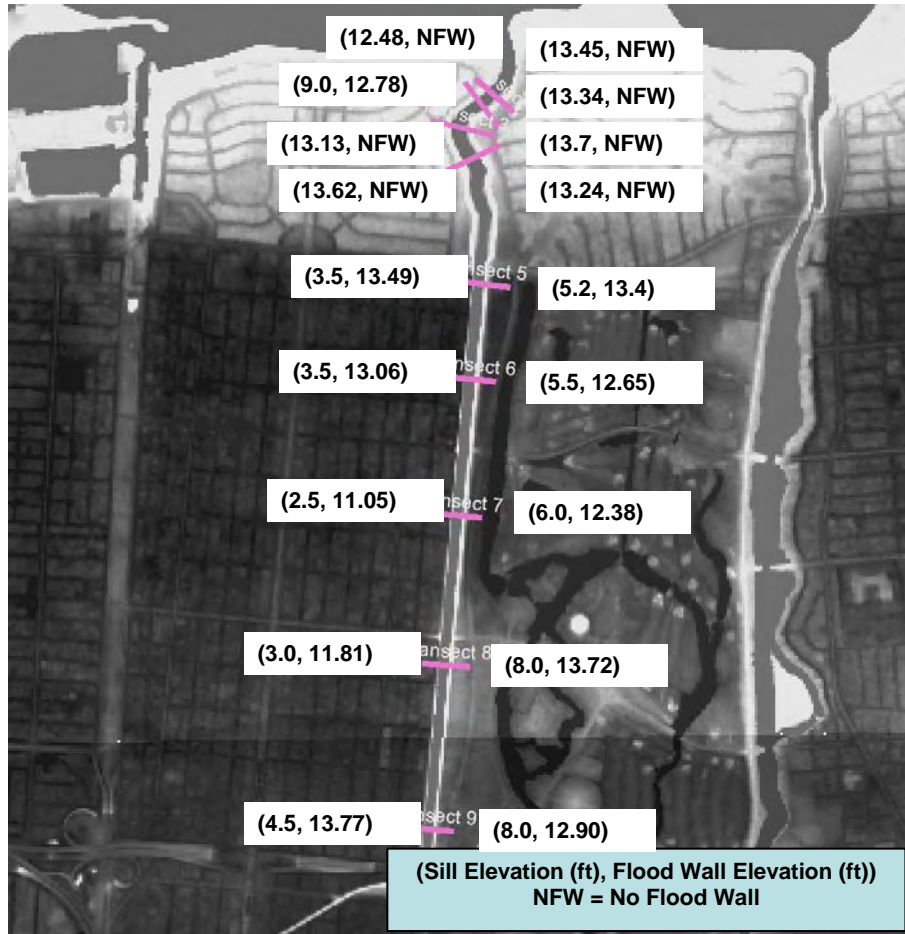


Figure 8-6. Aerial photograph of Orleans Avenue Canal showing sill and floodwall elevations

IHNC: Sill and flood wall elevations from LIDAR in feet

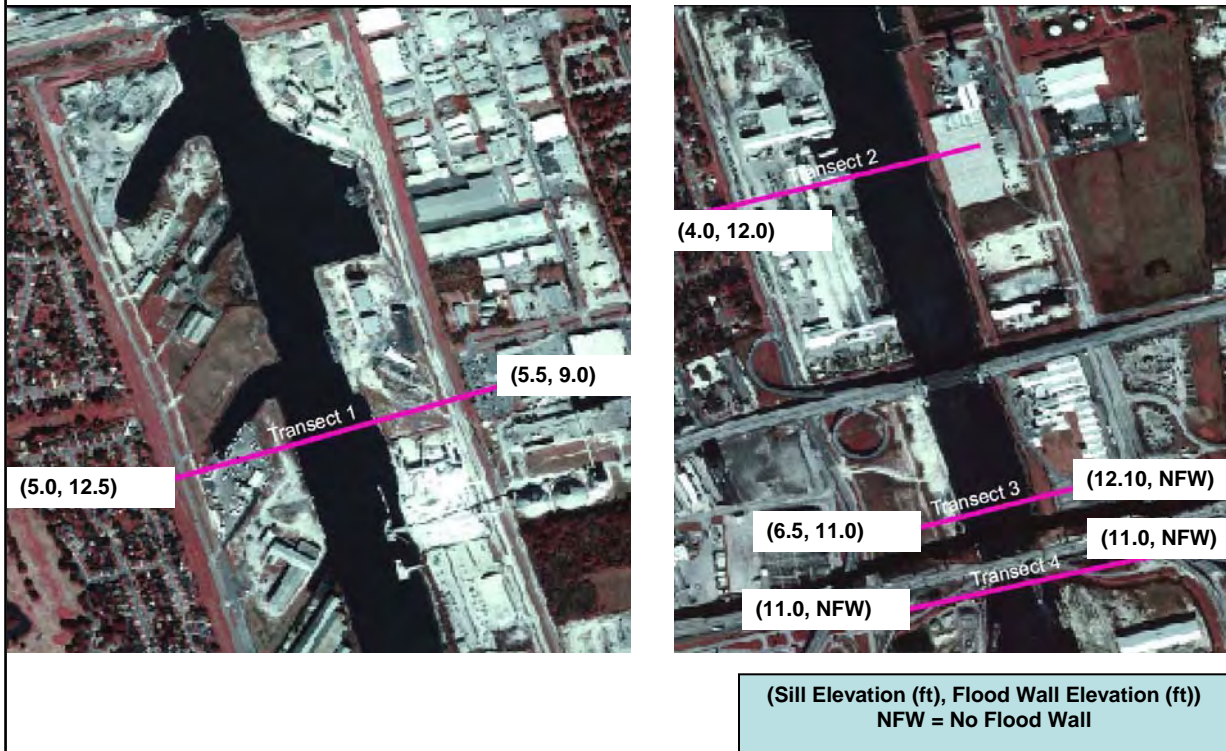


Figure 8-7. Aerial photograph of IHNC showing sill and floodwall elevations

# Appendix 9

## Basic Engineering Analyses

---

### Background

Levee damage observed after Hurricane Katrina suggests several primary hydrodynamic phenomena were contributors. These include:

1. Waves entering the canals.
2. Wave and hydrostatic forces on canal floodwalls.
3. Wave and steady flow overtopping of floodwalls.
4. Wave breaking and runup on earthen levees.
5. Wave overtopping of earthen levees.
6. Combined wave and steady flow overtopping of earthen levees.
7. Lakefront revetment armor damage.

The objective of this appendix is to discuss typical engineering design methods that would be used to approximate the detailed hydrodynamics. In some situations, these results can provide bracketing solutions for the more detailed numerical and physical model studies described in subsequent appendices. However, for most of the failures, traditional engineering solutions are not adequate to investigate the detailed hydrodynamics and resulting response of the levee systems.

### Water level variation in Canals

The water level variation in the canals using standard analytical techniques is described in detail in Appendix 10.

### Wave Transmission into Canals under Canal Bridges

If the outfall canals had relatively simple entrances, then simple analytical tools could be used to determine wave energy propagating into the canals. However, the low and complex topography near the canal entrances results in complex wave dissipation and reflection that significantly reduced the wave energy entering the canal, as shown by the physical model results in Appendix 12. Even approximate solutions to this problem require physical modeling or highly

detailed and complex numerical hydrodynamic models. Thus no attempt is made in this section to determine wave energy propagating into the canals from the lake.

Wave energy is reduced at the canal bridges due to two primary mechanisms: 1) drag and entrance losses through the bridge piles and the narrow, rock-armored channel beneath the bridge, and 2) wave interaction with the bridge deck. Some canal bridges also have a rock sill under the bridge that further reduces wave energy through increased drag and reflection.

In regard to the Hammond Highway Bridge on the 17th Street Canal, wave height reduction due to losses along the rough side walls and drag and reflection from the bridge piles was determined using data from the physical model study. Early in the morning of the hurricane, when the water levels were below the bridge deck, the physical model showed a transmission coefficient of 82 percent at 5 am and 57 percent at 6 am.

The interaction of wind waves and a bridge deck is very complicated due to wave overtopping and air entrapment between beams, as depicted in Figure 9-1. However, the wave transmission coefficient  $K_t$  may not be very sensitive to the detailed wave mechanics in the vicinity of the bridge deck. As a first approximation, the bridge deck may be approximated as a rectangular box and linear wave theory may be applied by neglecting energy dissipation and wave energy transmission over the bridge.

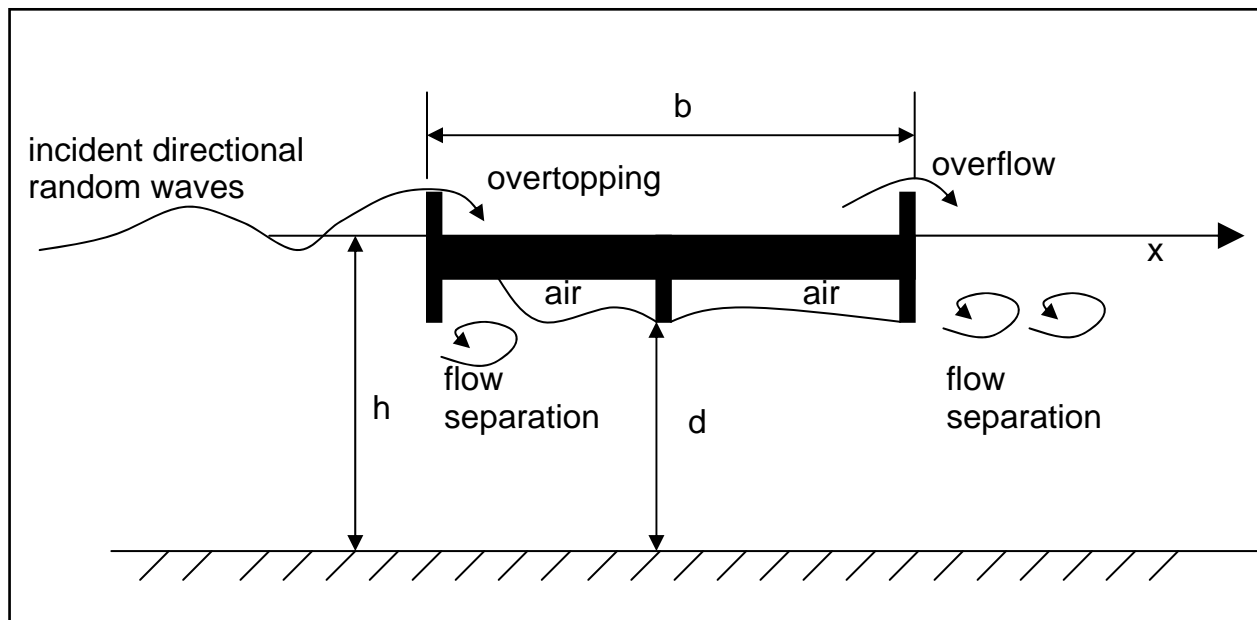


Figure 9-1. Conceptual sketch of wave interaction with bridge deck

An analytical solution of the boundary value problem for the wave interaction with the bridge deck yields the following relations for reflection and transmission past the bridge deck.

#### Reflection

$$K_{Rb}^2 = \frac{\left(kb \frac{h}{d}\right)^2}{4 + \left(kb \frac{h}{d}\right)^2} \quad (1)$$

Transmission

$$K_{Tb}^2 = \frac{4}{4 + \left(kb \frac{h}{d}\right)^2} \quad (2)$$

where  $k = 2\pi/L =$  wave number;  $L$  is the wave length,  $b =$  bridge deck width;  $d =$  water depth below the bridge deck; and  $h =$  water depth in canal. The water depth below the bridge deck is variable. In this case we have assumed an average deck elevation of  $d = 26.8$  ft NAVD88 (2004.65) and have used an equivalent width of  $b = 40$  ft. In addition, we have assumed a mean low water elevation of 20 ft.

Equation 1 indicates that the component wave transmission coefficient  $K_{tb}$  depends mainly on the ratio between the deck width  $b$  and the wavelength  $L$ .

The total transmitted wave height through the bridge can be computed by a simple energy balance. The resulting equation is given as

$$K_T^2 = 1 - K_{Rp}^2 - K_{Rb}^2 - K_{Dp}^2 \quad (3)$$

where  $K_{Rp} =$  reflection from the piles and  $K_{Dp} =$  drag and entrance losses under bridge. Table 9-1 shows the parameters used to compute the transmission coefficient in Equation 3.

<b>Table 9-1 Parameters for Computing Transmission Coefficient</b>							
Time, am CDT	Mean Period, sec	Surge, ft	Total Depth, $h$ , ft	Wave Height $H_i$ , ft	Wave Length, $L_m$ , ft	Bridge Width, $b$ , ft	Bridge height, $d$ , ft
5	4.7	4.9	24.9	0.17	145	40	26.8
6	4.7	5.9	25.9	0.37	151	40	26.8
7	4.7	8.4	28.4	0.96	165	40	26.8
8	5.3	10.7	30.7	1.90	194	40	26.8
9	5.3	11.3	31.3	2.20	198	40	26.8
10	5.3	9.4	29.4	1.41	186	40	26.8
11	5.3	7.2	27.2	0.69	172	40	26.8



The resulting total estimated transmission coefficient compared to that measured in the physical model is plotted in Figure 9-2 for the 17th street canal. Figure 9-2 indicates that the estimation methods work reasonably well and could be extended to other bridges.

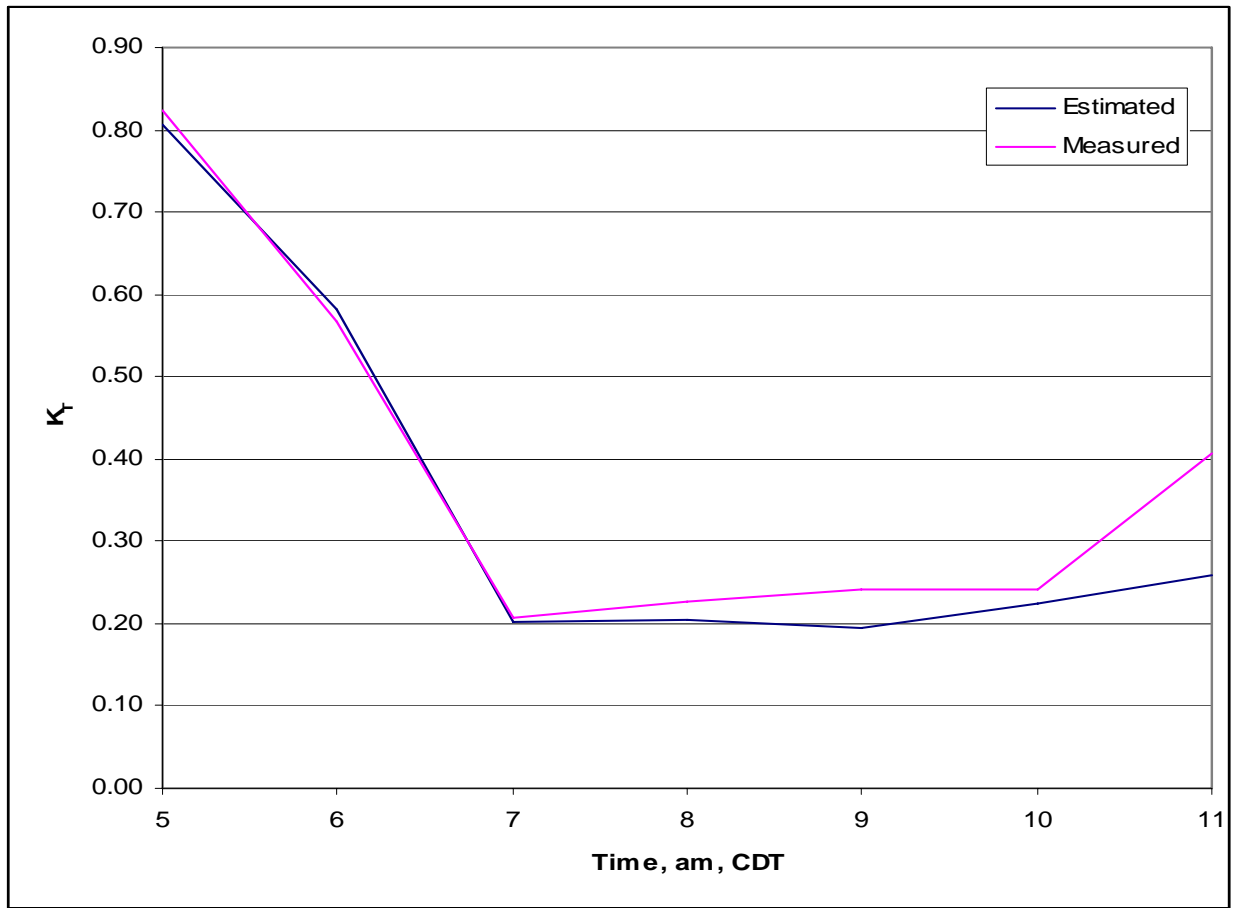


Figure 9-2. Estimated transmission coefficient for 17th Street Canal Hammond Highway Bridge resulting from drag and wave interaction with the bridge deck, for time-varying water depth

The disturbance of the wave field caused by the bridge deck is likely to generate waves with small wave periods. The flow separation depicted in Figure 9-1 is likely to dissipate waves with long wave periods more because the eddy formation increases with the decrease of  $b/L$  (e.g. wave diffraction around a large body versus a drag force around a small body).

Since the bridge decks appear to have been undamaged by Hurricane Katrina, it might be possible to estimate the upper limit of the wave height which would not cause any damage to the reinforced concrete deck. According to the Japanese manual for port facility design (Japan Port Association 1999), the impulsive lift pressure can be as large as  $P_l = 8\rho gh$  with  $\rho =$  fluid density. However, this very large pressure does not act on the entire deck simultaneously. For the design of a pier, the impulsive lift pressure of  $P_l = 2\rho gh$  is recommended where this pressure is assumed to act on the entire deck simultaneously. The lift force would be roughly  $F_l = 2 - 4$  kips for the range of depths in the canals.

## Overflow at Floodwall

Water overflowing the floodwalls along the Inner Harbor Navigation Canal caused extensive scour and erosion in some locations. In particular, overtopping was observed 1) on the west side just inside the canal entrance, 2) along the terminal walls near the confluence of GIWW and IHNC, and 3) at the floodwall between Florida Avenue and the lock in the Lower Ninth Ward. A simple model for estimating the overflow characteristics based on elementary fluid mechanics is depicted in Figure 9-3 where  $\eta$  = free surface elevation above the top of the floodwall;  $H_w$  = floodwall height above the horizontal ground,  $x$  and  $y$  are the horizontal and vertical coordinates,  $h$  is the local depth,  $v_o$  is the velocity at the crest of the wall and  $v_s$  is the velocity of the nappe-ground intersection. The most simple model assumes that the overflow is critical and its horizontal velocity  $v_o$  is  $v_o = (g\eta)^{1/2}$ . However, a slightly more complex analysis will provide improved estimates. The steady overflow for a sharp-crested weir is commonly given as

$$q = C_d \frac{2}{3} \sqrt{2g} \eta^{3/2} \quad (4)$$

where the empirical value of  $C_d$  is given by

$$C_d = 0.611 + 0.08 \left( \frac{\eta}{h} \right) \quad (5)$$

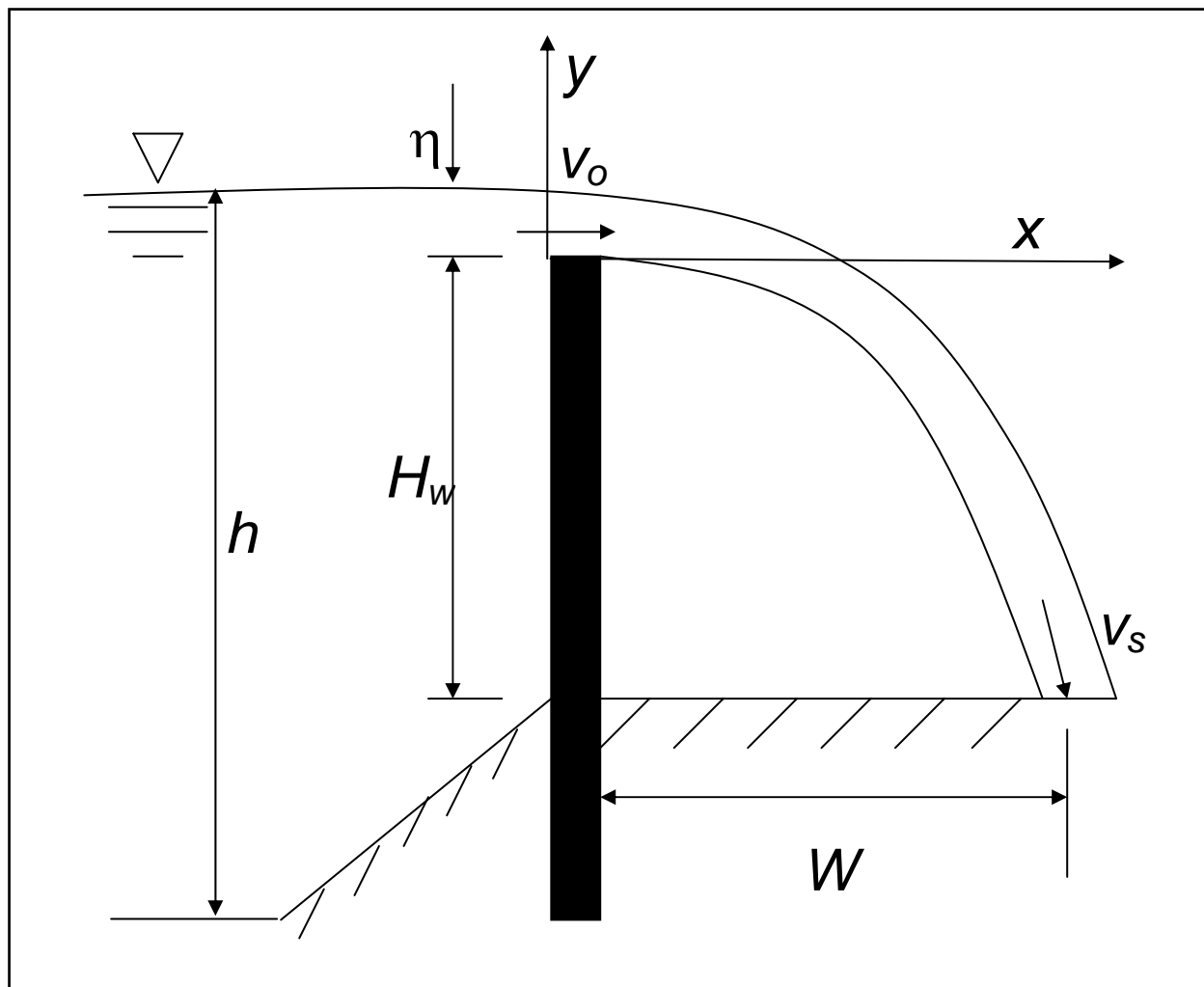


Figure 9-3. Definition sketch for overflow of floodwall

Equations 4 and 5 were used to compute overflow along the IHNC. No theory exists to predict simultaneous wave and steady overtopping discharge. Generally, the waves will be running mostly along the canal so the portion of the wave in the crest above the wall height will contribute to overtopping while the portion in the trough above the wall will decrease overtopping. For shallow water waves, more of the wave height is above the still water level (roughly 70 percent) and the trough is long and flat. If the surge height is below the wall crest, only the wave crests will spill over the wall. However if the surge height is, say, 1 ft over the wall, then a 1-ft-high wave would not contribute much to surge because the additional overtopping from the wave crest would be roughly balanced by the decrease in overtopping from the trough. It is also likely that the larger waves would contribute more to overtopping than the smaller waves. Therefore, the appropriate wave height statistic to use is not clear. Finally, the distribution of wave heights in the canal is unknown and the effect of these details is dependent on the surge height over the wall crest and on the wave direction.

In this effort, a crude estimate of the water surface elevation was assumed as simply the surge height. The water levels were used to determine overtopping at the Lake Pontchartrain

entrance floodwall, the Lower Ninth Ward floodwall, and the port floodwall. For this simplistic analysis, the overtopping at the canal entrance was taken as  $q = 0$ , contrary to eyewitness accounts. Therefore, a more sophisticated analysis of this location is necessary using physical, Boussinesq or Navier-Stokes nearshore wave models. Figures 9-4 and 9-5 show floodwall elevations at the entrance and at the Lower Ninth Ward, respectively. Figure 9-6 shows overflow rate and the overflow elevation at the Lower Ninth Ward.



Figure 9-4. Floodwall elevations at the IHNC entrance to Lake Pontchartrain





Figure 9-5. Floodwall elevations at the IHNC



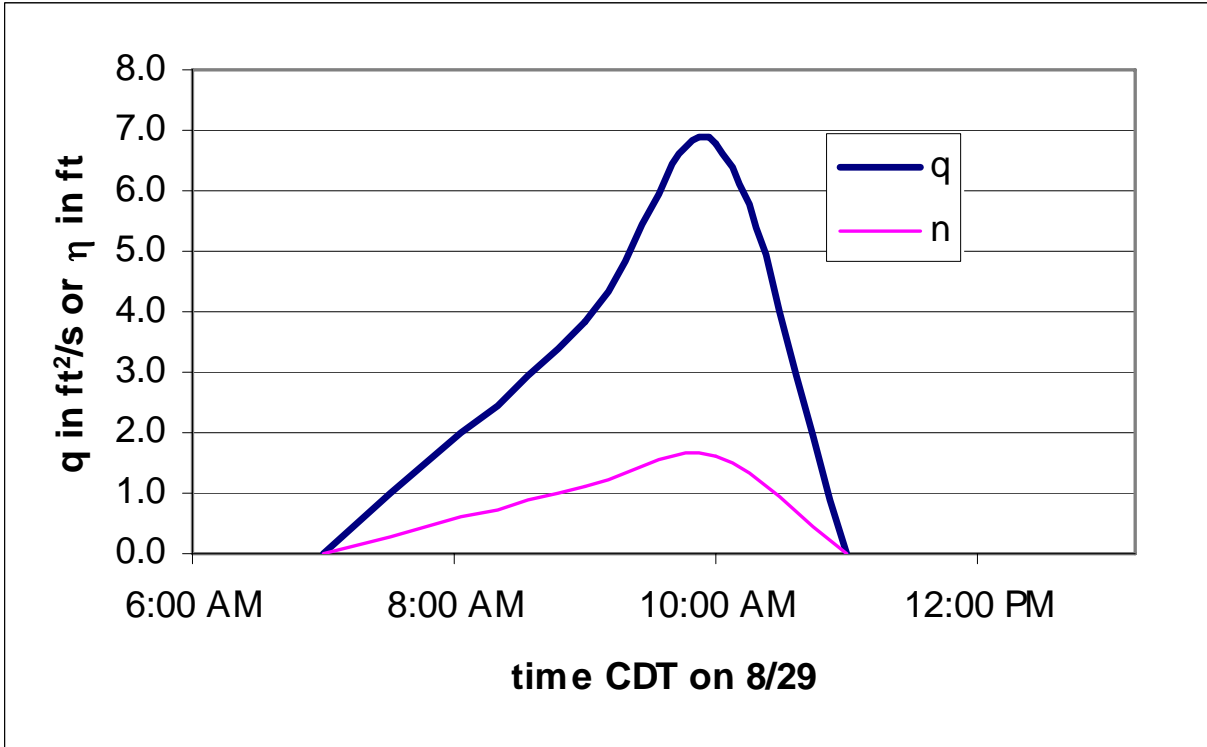


Figure 9-6. Overtopping flowrate at floodwall along IHNC at Lower Ninth Ward during Hurricane Katrina using Equations 4 and 5. Floodwall height used was 12.6 ft.

Hughes, et al. (2006) summarized the shape, trajectory and impact velocity of the nappe. The trajectories of the upper and lower nappes are given by

$$\frac{y}{H} = A \left( \frac{x}{H} \right)^2 + B \left( \frac{x}{H} \right) + C \quad (\text{lower nappe}) \quad (6)$$

$$\frac{y}{H} = A \left( \frac{x}{H} \right)^2 + B \left( \frac{x}{H} \right) + C + D \quad (\text{upper nappe}) \quad (7)$$

where  $H = \eta + \frac{v^2}{2g}$  and  $A = -0.425 + 0.25 G$ . The coefficients in Equations 6 and 7 are given by

$$B = 0.411 - 1.603 G - \sqrt{1.568 G^2 - 0.892 G + 0.127} \quad (8)$$

$$C = 0.150 - 0.45 G \quad (9)$$

$$D = 0.57 - 0.02 [10 (G - 0.208)]^2 \exp [10 (G - 0.208)] \quad (10)$$

$$G = \frac{v^2}{2gH} \quad (11)$$

An approximation of  $H \approx \eta$  reduces these equations to

$$\frac{y}{\eta} = A \left( \frac{x}{\eta} \right)^2 + B \left( \frac{x}{\eta} \right) + C \quad (12)$$

$$\frac{y}{\eta} = A \left( \frac{x}{\eta} \right)^2 + B \left( \frac{x}{\eta} \right) + C + D \quad (13)$$

where  $A = -0.425$ ,  $B = 0.055$ ,  $C = 0.150$ , and  $D = 0.559$ . Solving Equations 12 and 13 yields

$$\frac{x_L}{\eta} = \frac{-B - \sqrt{B^2 - 4A(C - y/\eta)}}{2A} \quad (\text{lower nappe}) \quad (14)$$

$$\frac{x_U}{\eta} = \frac{-B - \sqrt{B^2 - 4A(C + D - y/\eta)}}{2A} \quad (\text{upper nappe}) \quad (15)$$

Substituting the height of the floodwall  $y = H_w$  into 14 and 15 yields the nappe impact location and the width of the nappe at ground level. For the Lower Ninth Ward floodwall on the IHNC,  $H_w = 12.6 - 6.6 = 6$  ft. In addition,  $0 \leq \eta \leq 1.6$  ft. So  $x_L \leq 5.0$  ft and  $x_U \leq 5.3$  ft at the ground. The jet entry angles are given by

$$\theta_L = \tan^{-1} \left( \frac{2Ax_L}{\eta} + B \right) \quad (16)$$

$$\theta_U = \tan^{-1} \left( \frac{2Ax_U}{\eta} + B \right) \quad (17)$$

$$\theta_C = \frac{(\theta_L + \theta_U)}{2} \quad (18)$$

For the Lower Ninth Ward floodwall, these angles are  $\theta_L = -90$  to  $-68$  deg,  $\theta_U = -90$  to  $-70$  deg and  $\theta_C = -90$  to  $-69$  deg for  $\eta = 0$  to 1.6 ft. Finally, the velocity at impact is given by

$$v_C = \frac{q}{(x_U(y = -H_w) - x_L(y = -H_w)) \sin(-\theta_C)} \quad (19)$$

For overtopping of the Lower Ninth Ward floodwall, this velocity ranges from 0 to 22 ft/s. This indicates that the jet impacts over a relatively small footprint with a high velocity. Seiffert and Philipse (1990) showed experimentally that water velocities of 13 ft/s, running essentially parallel to the grass mats on the Dutch dikes, would cause erosion. Also, as the total head increases, the obliquity of the impacting jet to the ground increases. This results in a wider area of damage. Finally, as the jet impacts the ground it spreads and creates a wide area of damage on the lee side of the floodwall.

### **Flow through Breaches at IHNC**

Once the IHNC floodwalls along the Lower Ninth Ward were breached, the flow into the area increased significantly. The breach sill heights appeared to be at elevation of roughly +1 ft. The flow through the breaches at the IHNC can be approximated.

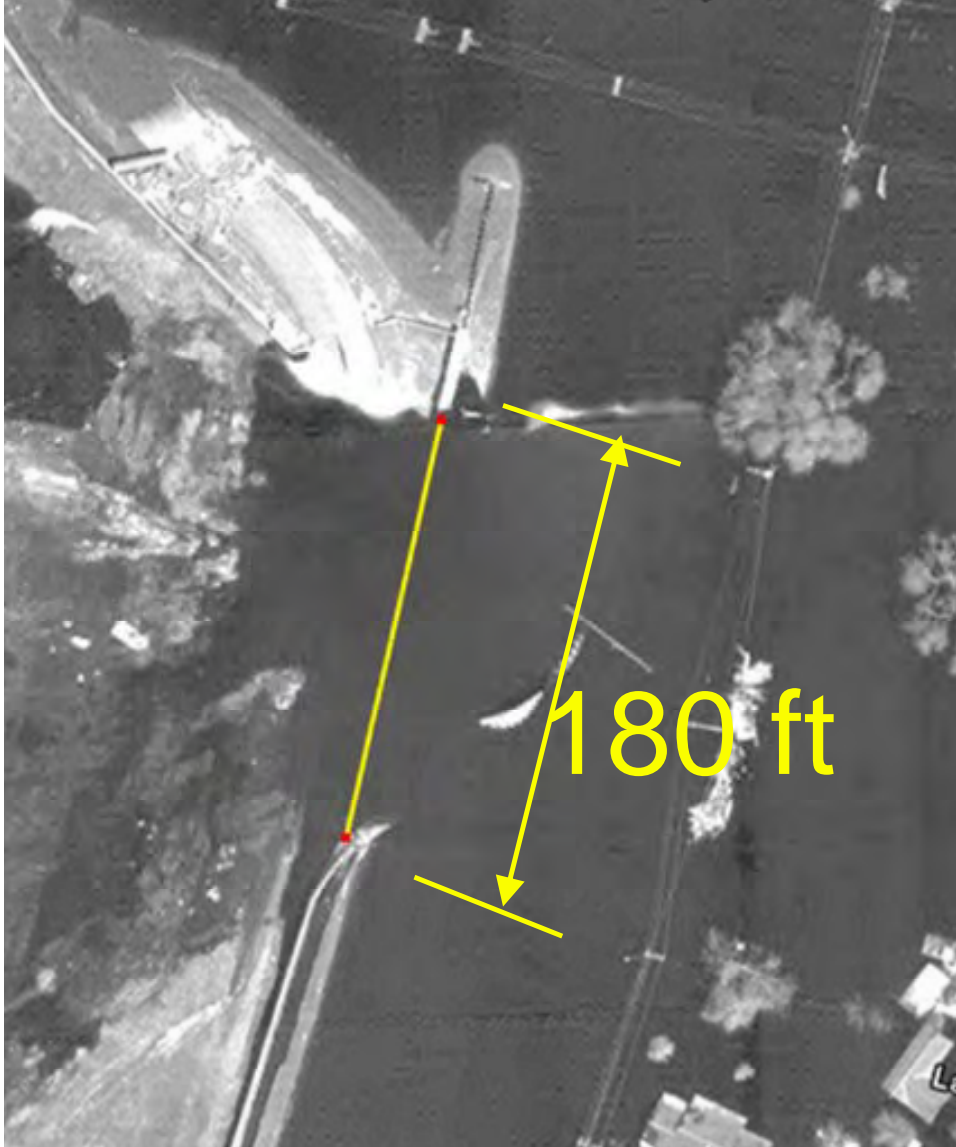


Figure 9-7. North breach on IHNC at Lower Ninth Ward

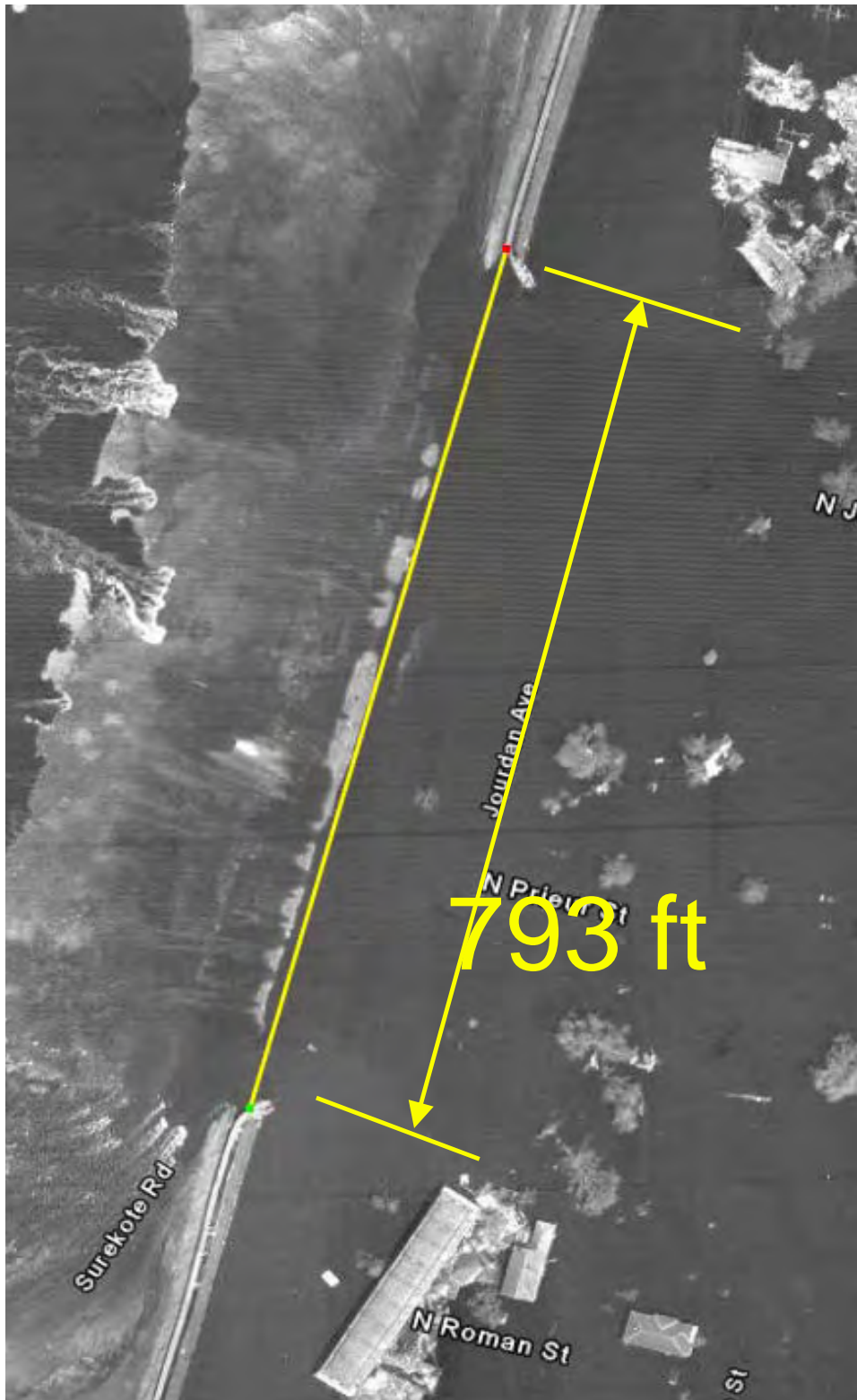


Figure 9-8. South breach on IHNC at Lower Ninth Ward



## Hydrodynamic Forces on Floodwalls

For the analysis of seepage flow and geotechnical stability of a floodwall, the pressure distribution on the floodwall (only on the segment exposed to water directly) and the canal bottom is essential information. In the absence of wind waves, the pressure may be assumed to be hydrostatic below the still water level (SWL) associated with the time-varying storm surge. The hydrostatic bottom pressure  $P_s$  is hence given by  $P_s = \rho gh$  with  $h$  = local water depth below SWL. The major unresolved issue is in regard to the wave-induced pressure, which varies rapidly with time, and its contribution to slow seepage flow and geotechnical stability. Moreover, it is not clear whether the repeated cycling of wave-induced pressure reduces the geotechnical strength of the foundation.

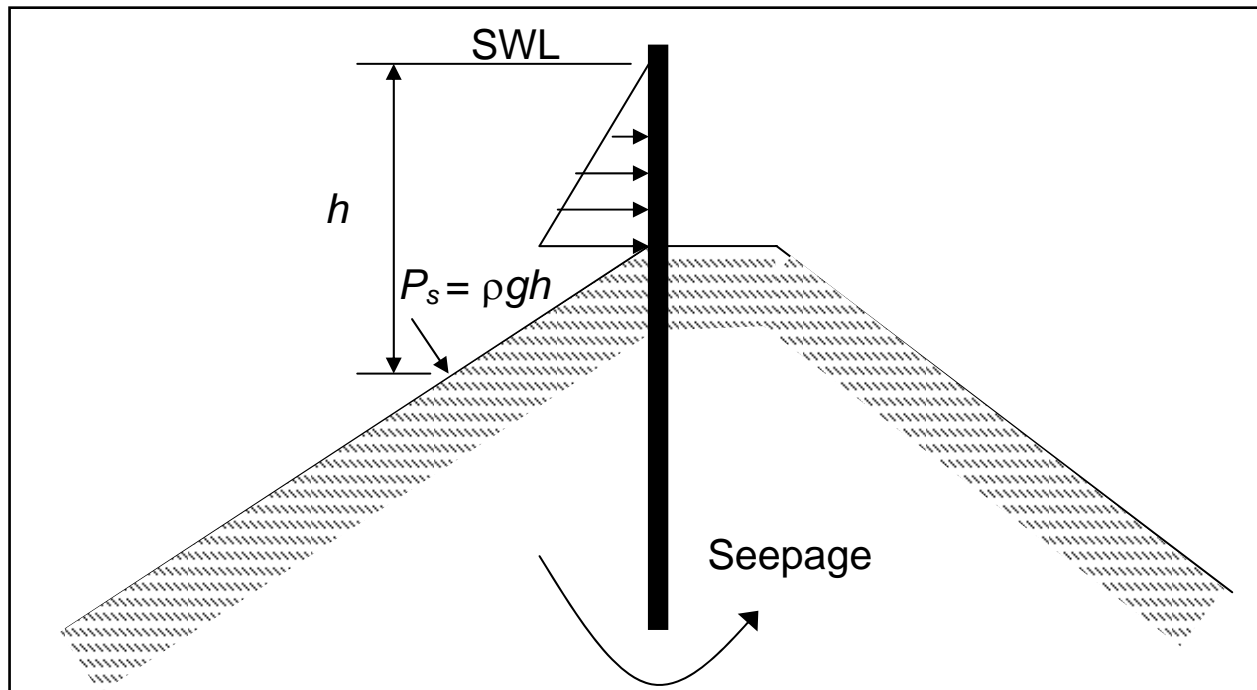


Figure 9-9. Definition sketch for forces on floodwall

Formulas for the wave-induced pressure, such as that of Goda (1985), were developed for vertical breakwaters that respond to individual waves. The formulas also assume that the maximum wave force acts simultaneously along a vertical wall. This assumption results in significant overestimation of the instantaneous wave force on the floodwall, as the real waves are multi-directional in the canal. The formula of Goda (1985) predicts the wave-induced pressure  $P_w$  of the order of

$$P_w \approx 1.5\rho gH \quad (20)$$

which was proposed by Hiroi (1919) according to Goda (1985). The design wave height  $H$  for a vertical breakwater on a rubble mound is normally taken as the maximum wave height  $H_{max} \approx 1.8H_{mo}$ . It appears reasonable to use  $H \approx H_{mo}$  for the geotechnical stability analysis.

# Wave Runup and Overtopping of Earthen Levees and Revetments

## Wave Runup on Levees and Revetments

In order to evaluate the performance of the Mississippi River-Gulf Outlet Levees and Mississippi River Levees, an analysis of wave runup and wave-and-steady-flow overtopping is required. As discussed in the Coastal Engineering Manual (CEM 2002), the modern form for empirical prediction of irregular wave runup on coastal structures was given by Battjes in 1974. De Wall and Van der Meer (1992) and Van der Meer and Janssen (1995) extended these results for various types of structures and incident wave conditions. The equations given for the 2-percent exceedance value of irregular wave runup on a slope are

$$\frac{R_{2\%}}{H_s} = 1.5 \xi_{op} \gamma_r \gamma_b \gamma_h \gamma_\beta \quad 0.5 < \xi_{op} \leq 2.0 \quad (21)$$

$$\frac{R_{2\%}}{H_s} = 3.0 \gamma_r \gamma_b \gamma_h \gamma_\beta \quad 2.0 < \xi_{op} < 3 - 4 \quad (22)$$

$$\xi_{op} = \frac{\tan \alpha}{\sqrt{s_{op}}} \quad s_{op} = \frac{H_s}{L_{op}} \quad L_{op} = \frac{gT_p^2}{2\pi} \quad (23)$$

where

$R_{2\%}$  = wave runup height on the structure with 2 percent probability of exceedance

$H_s$  = significant wave height,  $H_{mo}$  in this case, where  $H_{mo} = 4(m_o)^{1/2}$  and  $m_o$  is the zero moment of the incident wave spectrum

$\gamma_r$  = slope roughness correction, 1.0 for smooth slope

$\gamma_b$  = berm influence factor, 1.0 for non-bermed slope

$\gamma_h$  = depth-limited wave correction, 1.0 for Rayleigh distributed waves

$\gamma_\beta$  = wave direction and directional spreading correction, 1.0 for head-on waves

$\xi_{op}$  = Iribarren parameter based on the peak period

$L_{op}$  = Airy wave length based on the peak period

$s_{op}$  = wave steepness based on the local wave height, deep water wave length, and peak period

$\alpha$  = structure seaward slope

$T_p$  = wave period corresponding to spectral peak

$g$  = acceleration of gravity

The runup reduction formula for depth-limited waves is the Raleigh relationship between the 2 percent exceedance value of wave height and the spectral significant wave height, or

$$\gamma_h = \frac{H_{2\%}}{1.4H_s} \quad (24)$$

This relation requires measurement of  $H_{2\%}$ . The physical model may be used to determine this value. The correction for slope roughness is given as

$$\begin{aligned} \gamma_r &= 0.9 - 1.0 \text{ for grass slope} \\ \gamma_r &= 0.50 - 0.60 \text{ for stone armor} \end{aligned}$$

The correction for wave direction is given by:

$$\begin{aligned} \text{Long-crested waves: } \gamma_\beta &= \begin{aligned} &= 1.0 \text{ for } 0^\circ \leq \beta \leq 10^\circ \\ &= \cos(\beta - 10^\circ) \text{ for } 10^\circ < \beta \leq 63^\circ \\ &= 0.6 \text{ for } \beta > 63^\circ \end{aligned} \end{aligned} \quad (25)$$

$$\text{Short-crested waves: } \gamma_\beta = 1 - 0.0022\beta \quad (26)$$

For rock-armored slopes, appropriate for lakefront revetments, the CEM gives similar equations for runoff. Also, De Waal and van der Meer (1992) provided similar equations for determining irregular wave runoff on a compound slope. These relations can be used to determine the extent of the wave runoff on the slopes of structures.

## Wave Overtopping of Levees

For impermeable rough slopes, the volume rate of irregular wave overtopping per unit length of structure  $q$  is given by van der Meer and Janssen (1995) as

$$\frac{q}{\sqrt{gH_s^3}} \sqrt{\frac{s_{op}}{\tan \alpha}} = 0.06 \exp \left( -5.2 \frac{R_c}{H_s} \frac{\sqrt{s_{op}}}{\tan \alpha} \frac{1}{\gamma_r \gamma_b \gamma_h \gamma_\beta} \right) \quad (27)$$

$$\text{for } \xi_{op} < 2 \text{ and } 0.3 < \frac{R_c}{H_s} \sqrt{\frac{s_{op}}{\tan \alpha}} \frac{1}{\gamma_r \gamma_b \gamma_h \gamma_\beta} < 2 \quad (28)$$

and

$$\frac{q}{\sqrt{gH_s^3}} = 0.2 \exp\left(-2.6 \frac{R_c}{H_s} \frac{1}{\gamma_r \gamma_b \gamma_h \gamma_\beta}\right) \quad (29)$$

for  $\xi_{op} > 2$

These equations, and similar equations for impermeable smooth and permeable rough slopes, can be used to evaluate the degree of wave overtopping on structures where there was no steady flow overtopping.

### Flood Overtopping of Levees

Steady flow over levees was described clearly by Powledge et al. (1989). As shown in Figure 9-10, flow is subcritical on the seaward side of the levee and supercritical on the leeward side. Flow in zone 1 will not be erosive for steady flow unless the crest materials are highly erodible. In Erosion zone 2, the flow transitions to critical and then supercritical. Materials can erode in this region depending on the flow velocity and the erodibility of the materials. The leeside crest corner is particularly susceptible to erosion if the material is erodible. In zone 3, the flow accelerates to fully developed supercritical and proceeds downslope until it reaches the base of the slope or the leeside pool where a hydraulic jump develops. Erosion can occur due to high velocities on the lee side and due to turbulence under the hydraulic jump. The toe of the slope is the most common location for initiation of erosion. The erosion typically progresses upslope as a headcut develops.

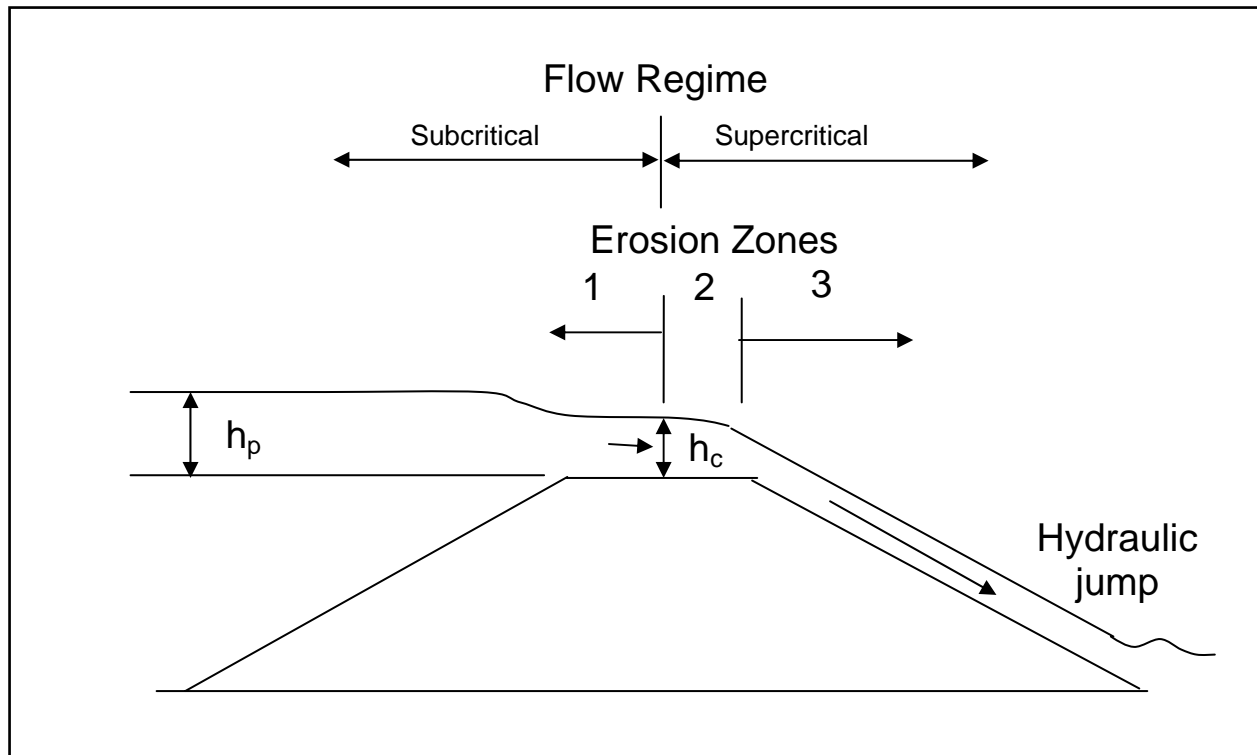


Figure 9-10. Flow regimes and erosion zones for steady flow over earthen levee, after Powledge et al. (1989)

Steady-flow overtopping of levees is similar to overtopping of a broad-crested weir, which is covered in hydraulics textbooks. An evaluation of the energy balance across the weir yields the relation for discharge per running length.

$$q = 0.54\sqrt{g}h_p^{3/2} \quad (30)$$

where  $h_p$  is the pool water level elevation above the structure crest and  $g$  is the acceleration of gravity. For this study, the pool elevation is the difference between the storm surge height and the structure crest height. Equation 30 is commonly applied to levee overtopping discharge. Grass on levees produces some reduction in overtopping flow; however, this reduction is often neglected for conservative design. For critical flow on the crest, the velocity is usually written as

$$v_c = \sqrt{gh_c} = \sqrt{gh_p 2/3} \quad (31)$$

In zone 3, the flow is supercritical and the velocity is given by Manning's equation as

$$v_3 = \left[ \frac{1.49\sqrt{\sin \theta}}{n} \right]^{3/5} q^{2/5} \quad (32)$$



Mannings  $n$  for grass covered slopes is given as  $n = 0.044$  in FHWA (1987).

## References

- CEM (2002). *Coastal Engineering Manual*. US Army Engineer Research and Development Center, Vicksburg, MS.
- De Wall, J.P. and Van der Meer, J.W. (1992). "Wave run-up and overtopping on coastal structures," Proc. 23rd Intl Conf on Coast Eng., ASCE, Reston, VA, 1758-1771.
- Goda, Y. (1985). *Random Seas and Design of Maritime Structures*. Univ. of Tokyo Press, Tokyo, Japan.
- Seiffert, J.W., and Philipse, L. (1990). "Resistance of grassmat to wave attack," Proc. 22nd Coast. Eng. Conf. ASCE, Reston, VA, 1662-1674.
- Van der Meer, J.W., and Janssen, W. (1995). "Wave run-up and wave overtopping at dikes," In *Wave Forces on Inclined and Vertical Wall Structures*, Kobayashi and Demirbilek, eds., ASCE, Reston, VA, 1-27.

# Appendix 10

## Hydraulic Flows Through the 17th Street Canal Breach

---

### Introduction

This report addresses the general issue of flows through the breach on the east side of the 17th Street Canal during the morning of August 29, 2005. This report first presents the governing equations and the solution method followed by the timing considered for the flood wall failure. Finally, results are provided including sensitivity tests of the results to the friction factors considered and various degrees of flow blockage by the debris against the lake side of the Hammond Highway Bridge. A final scenario is for a different early breach evolution.

Figure 10-1 shows an oblique view of the canal, the breach and the debris impounded on the lake side of the Hammond Highway Bridge. Figure 10-2 presents an idealization of the canal as analyzed here.



Figure 10-1. 17th Street Canal August 29, 2005. Looking south showing breach and debris impounded against Hammond Highway Bridge

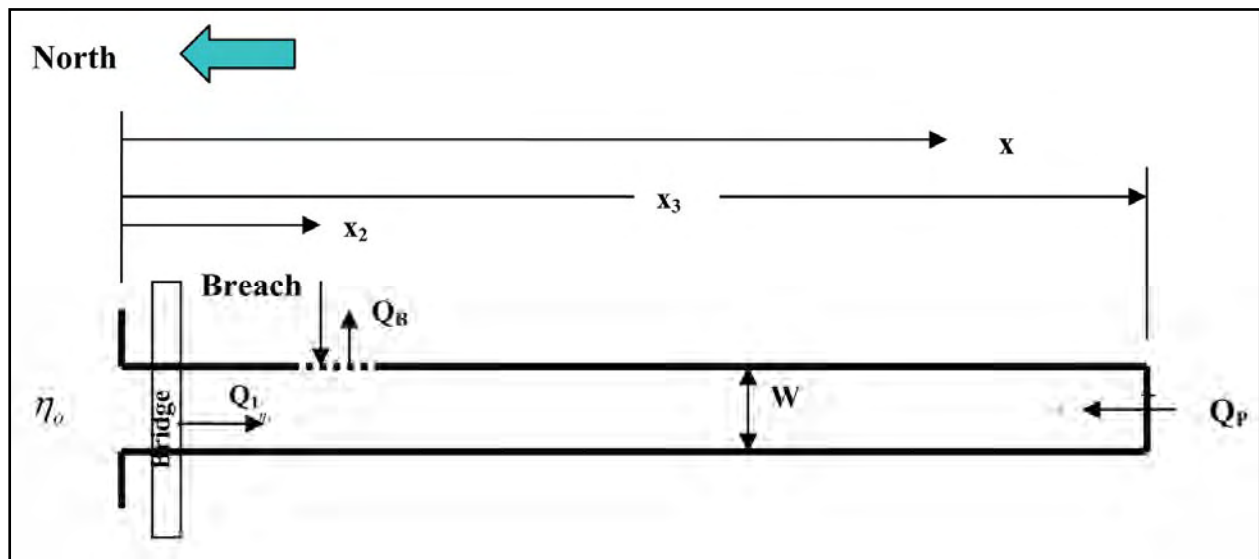


Figure 10-2. Idealized planview of 17th Street Canal

# Governing Equations and Their Solution

## Governing Equations

The canal is represented as cells, each 50 ft in length. Considering a typical section of the canal and designating the index of a typical cell as  $i$ , the basic steady state equation representing the hydraulics in the canal is:

$$H_{i+1} = H_i + \Delta H_{i,i+1} \quad (1)$$

where  $H_{i+1}$  is the total head at the  $i+1^{\text{th}}$  cell and  $\Delta H_{i,i+1}$  represents the head loss between the  $i^{\text{th}}$  cell and the  $i+1^{\text{th}}$  cell.

This equation can also be written as

$$\eta_i + \frac{Q_i^2}{2gA_i^2} = \eta_{i+1} + \frac{Q_{i+1}^2}{2gA_{i+1}^2} + \frac{f \Delta x_{i,i+1} Q_i^2}{4R_{i,i+1} \overline{A_{i,i+1}^2} 2g} + \text{Minor Head Losses} \quad (2)$$

in which  $\eta_i$  is the water surface displacement at the  $i^{\text{th}}$  cell,  $Q_i$  is the discharge in the  $i^{\text{th}}$  cell,  $\overline{A_{i,i+1}}$ , is the average flow cross-sectional area between the  $i^{\text{th}}$  and  $i+1^{\text{th}}$  cell,  $\overline{R_{i,i+1}}$  is the average hydraulic radius for the  $i^{\text{th}}$  and  $i+1^{\text{th}}$  cells,  $\Delta x_{i,i+1}$  is the canal length between the  $i^{\text{th}}$  and  $i+1^{\text{th}}$  cell and  $f$  and  $g$  are the Weisbach-Darcy friction factor and the gravitational constant, respectively. The terminology “Minor Head Losses” does not imply that these losses are smaller than the friction losses shown explicitly in Eq. (2). Rather, they are more properly considered as “abrupt” rather than distributed. The losses due to the bridge fall into this “Minor Loss” category.

The bridge (minor) losses include the effects of constriction, the drag on the support piling and, when present, the effects of the debris blockage. Additionally, as discussed in greater detail later, the water levels can exceed the lower elevation of the bridge and thus transform the bridge from an open channel to a closed conduit flow.

The channel width at the bridge is 150 feet wide compared to the normal channel width of 200 feet. The expansion loss,  $\Delta H_E$  is described by

$$\Delta H_E = \frac{V_B^2}{2g} - \frac{V_C^2}{2g} \quad (3)$$

in which  $V_B$  is the average velocity under the bridge and  $V_C$  is the average velocity in the channel. The losses due to the pilings are represented as an effective friction factor,  $f_p$  by

equating the drag forces on the piling to the shear force associated with the effective friction factor, resulting in

$$\rho f_p \frac{V^2}{8} W_B \Delta x_B = N_p C_D \frac{\rho D}{2} (h + \eta) \frac{V^2}{2g} \quad (4)$$

in which  $\rho$  is the mass density of water,  $W_B$  is the channel width under the bridge (150 ft),  $\Delta x_B$  is the length of the channel under the bridge (50 ft),  $N_p$  is the number of pilings,  $h$  is the water depth,  $\eta$  is the water surface elevation relative to some fixed elevation datum and  $C_D$  is the drag coefficient (here taken as 2.2, see Munson, et al, Page 536 (2006)). Eq. (4) can be simplified to

$$f_p = \frac{2N_p C_D D (h + \eta)}{W_B \Delta x_B} \quad (5)$$

There are 40 square piling, each 2 ft on a side supporting the bridge, the bridge dimension in the flow direction is approximately 50 ft and a representative depth  $(h + \eta) = 20$  ft, an approximate value of  $f_p \approx 0.47$  which is 5.9 times greater than the usual value of the friction coefficient. A value of  $f_p = 0.5$  was utilized in the calculations.

Critical flow is considered to occur through the breach resulting in

$$q_B = \sqrt{g} \left[ \frac{2}{3} (H_i - z_{s,i}) \right]^{3/2} \quad (6)$$

where  $q_B$  = is the discharge per unit width through the breach,  $H_i$  is the total head at the breach location, and  $z_{s,i}$  is the “sill” elevation at the breach location.

Standard hydraulic equations are employed for the head losses at the Hammond Street Bridge to account for the increase in wetted perimeter when the water level reaches the underside of the bridge, limiting the cross-sectional flow area.

### **Solution of Governing Equations**

At any time, the quantities that are considered known are: 1) The lake level,  $\eta_o$ , 2) The pump discharge at the south end of the canal,  $Q_p$ , 3) The breach width, and 4) The sill elevation at the breach.



## Solution Procedure

The solution is determined by an iterative procedure with the following steps.

- (1) A discharge from Lake Pontchartrain into 17th Street,  $Q_o$  is assumed.
- (2) Equation (2) is applied (by iteration) to determine the water surface elevation at the first grid at the entrance to the canal.
- (3) This procedure of applying Eq. (2) is continued cell by cell (the cells are 50 ft in length) until the breach is reached.
- (4) At the breach, Eq. (6) is applied and the discharge through the breach deducted from the canal discharge.
- (5) Continue this process to the south end of the canal.
- (6) After the hydraulic calculations described in Steps (1) to (5) are completed, calculate the error in continuity,  $\varepsilon_Q$

$$\varepsilon_Q = Q_o - \sum Q_B + Q_P \quad (4)$$

A revised estimate of  $Q_o$  is made based on the error and the calculations repeated until the error,  $\varepsilon_Q$  is acceptably small.

## The Failure Characteristics

Several unknowns exist relative to the actual failures of the 17th Street Canal floodwalls and levees. These unknowns include the timing of the progressive nature of the failure and the degree of blocking of the Hammond Highway Bridge by floating debris and its hydraulic effect (see Figure 10-1). For these reasons, several scenarios were examined in an attempt to bracket the breach discharge quantities and to obtain a better understanding of the sensitivity to hydraulic factors incorporated into the solution.

Table 10-1 presents the characteristics of the four scenarios for which runs were conducted.

**Table 10-1  
Characteristics of Scenarios Considered**

Scenario	Description	Plots Presented
1	Base Conditions	Breach Discharge, Water Surface Profiles Along Canal
2	Sensitivity to Friction Factors of $\pm 50\%$ Variation	Breach Discharge for Various Friction Factors
3	Sensitivity to Debris Blockage of Flow by Reductions of 25% and 50%	Breach Discharge, Water Surface Profiles Along Canal
4	Reduced Initial Breach Width	Water Surface Profiles at Lake and Breach

Where appropriate, additional details will be provided describing the characteristics of the individual scenario runs.

## Results

### General

The canal length is 13,800 ft long and the individual computational cells comprising the canal were each 80 ft long. The base Weisbach-Darcy friction coefficient,  $f$  is 0.08. The lake elevations for all runs are as shown in Figure 10-3 and the pump discharge at the south end of the canal is shown in Figure 10-4. The breach sill elevations were taken as -1.0 ft based on surveys conducted on August 30, 2005.

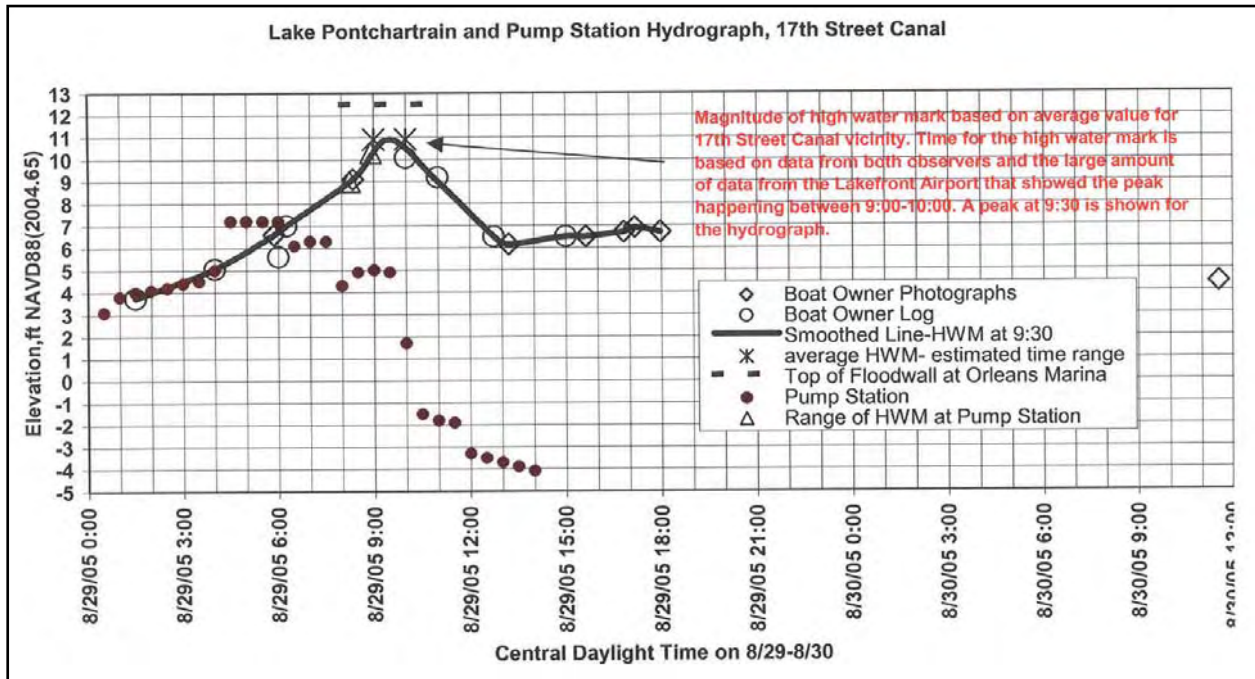


Figure 10-3. Estimated water levels in Lake Pontchartrain near north end of 17th Street Canal. The solid line is used for calculation purposes here

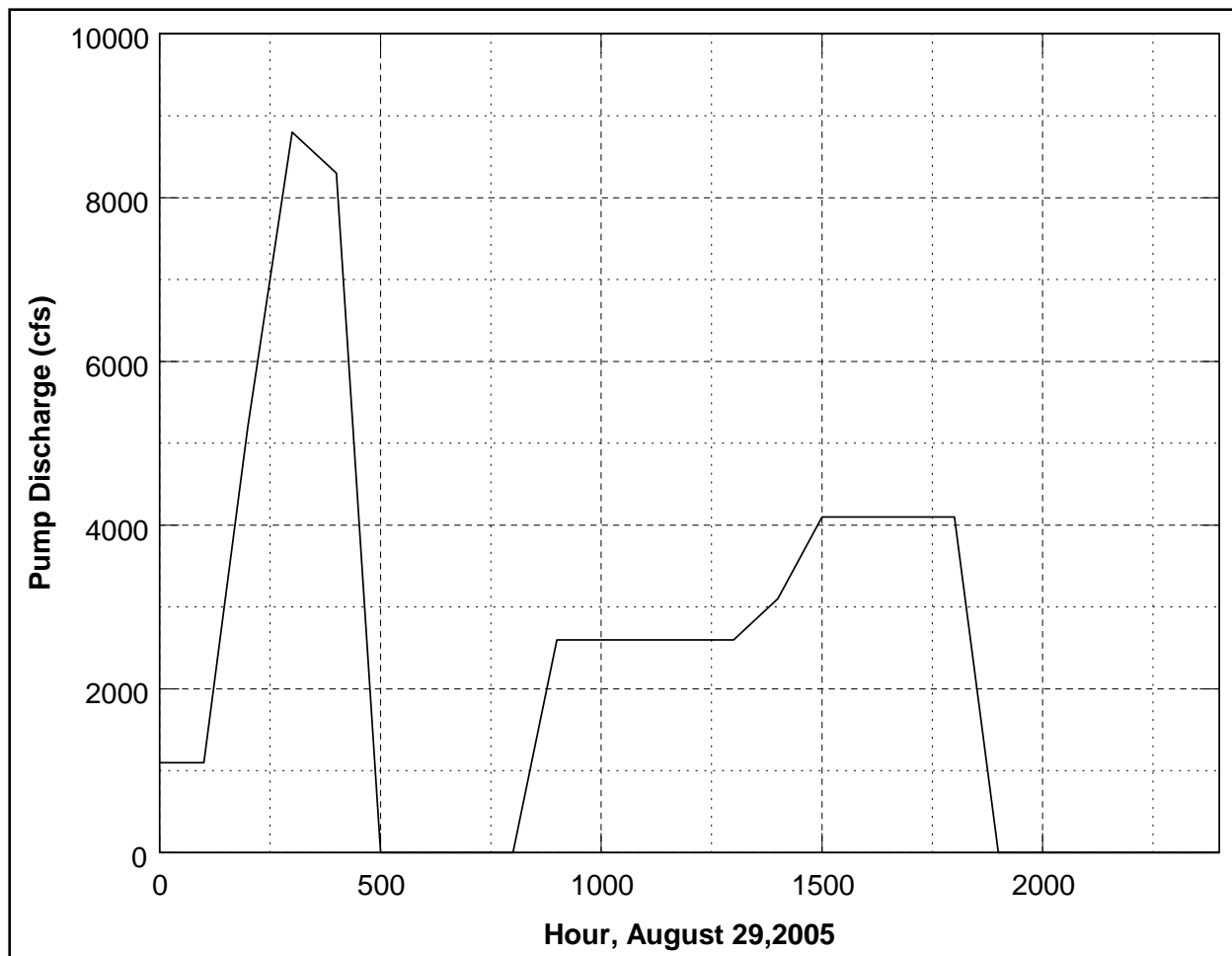


Figure 10-4. Pump discharge into south end of 17th Street Canal

### Scenario 1: Base Conditions

The failure sequence considered in this scenario is that by 0600, the breach width was 200 ft. and that between 0900 and 1000, the breach had increased to its final width of 450 ft. As discussed, the Hammond Highway Bridge is represented as a restriction to the flow and for sufficiently high lake water levels, the underside of the bridge acts as a “lid” to the flow causing a flow reduction; however, no debris effects are included in Scenario 1.

### Breach Discharge

Figure 10-5 presents the breach discharge and the discharges from the lake and the pump for this case. It is seen that the peak breach discharge is slightly less than 29,000 cubic feet per second (cfs).

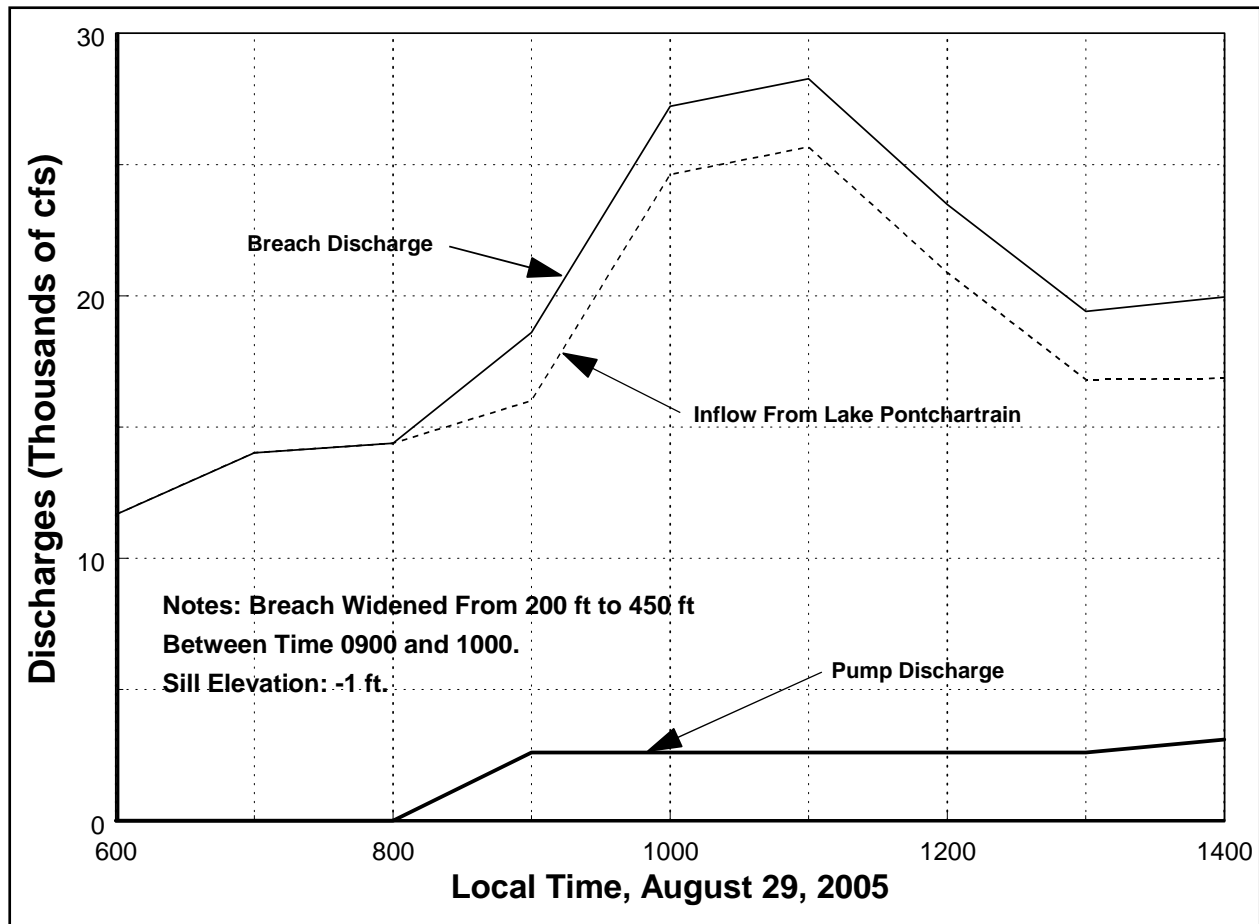


Figure 10-5. Time history for breach discharge. Scenario 1

## Water Levels Along 17th Street Canal

Figure 10-6 presents the distribution of water levels along the 17th Street Canal for various times for Scenario 1.

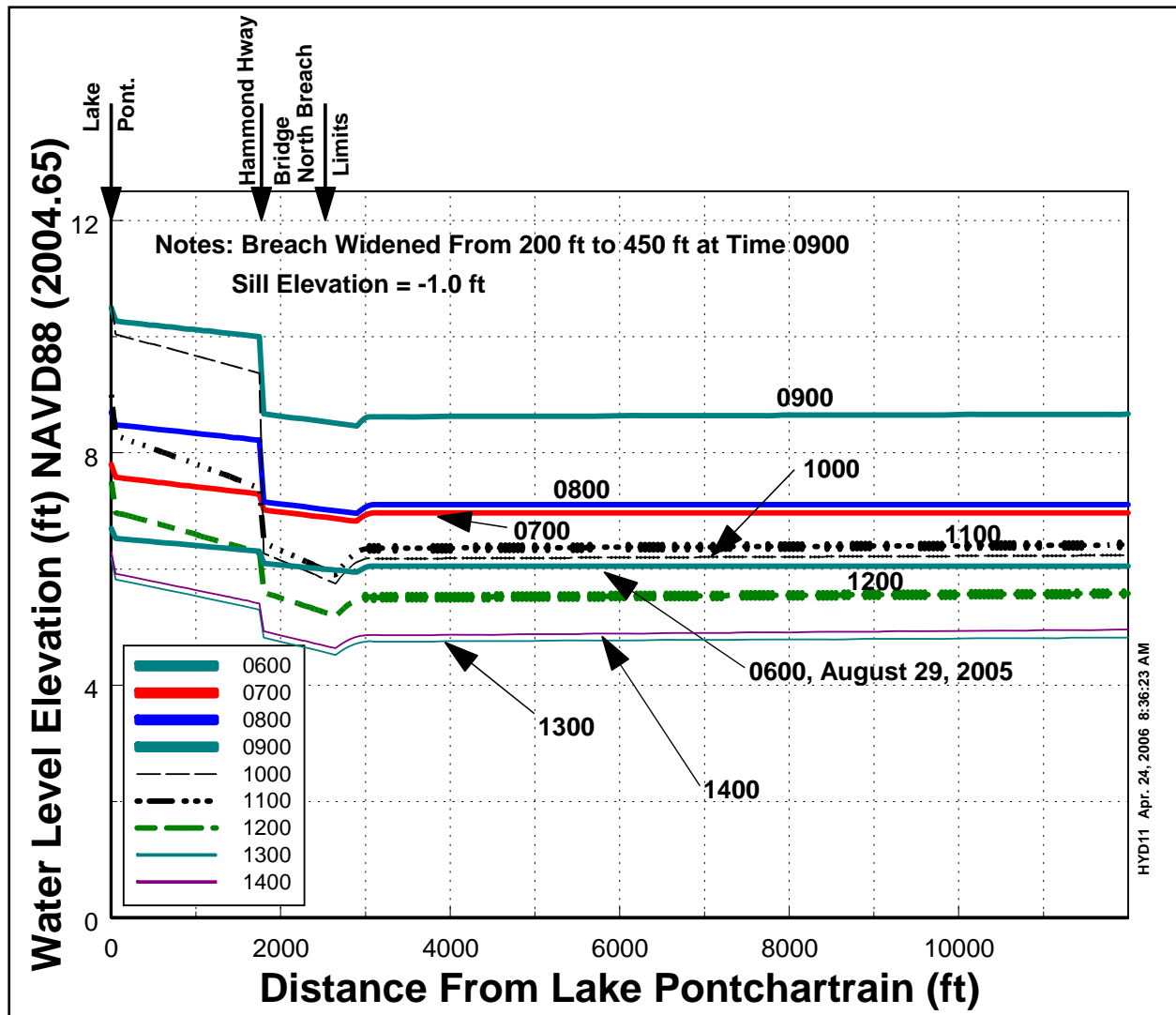


Figure 10-6. Water levels along 17th Street Canal. Scenario 1

### Scenario 2: Breach Discharge Sensitivity to Weisbach-Darcy Friction Factor

Scenario 2 evaluates the sensitivity of the breach discharge characteristics to the value of the Weisbach-Darcy friction factor.

#### Breach Discharges

Figure 10-7 presents the breach discharges for the reference value of the Weisbach-Darcy friction coefficient,  $f = 0.08$  and values of this coefficient of 0.04 and 0.12. The response of the breach discharge to this  $\pm 50\%$  change in  $f$  are changes of -8% and +4%. Thus, the breach discharges are not overly sensitive to the values of the Weisbach-Darcy friction coefficient. The explanation for the unexpected lower discharge shown in Figure 10-7 at time 1100 for the smaller Weisbach-Darcy coefficient is an unusual interaction of the flow with the Hammond Highway Bridge wherein the lower friction coefficient causes a smaller reduction in water level



north of the bridge resulting in the bridge behaving as a closed conduit rather than an open conduit and causing a somewhat smaller discharge.

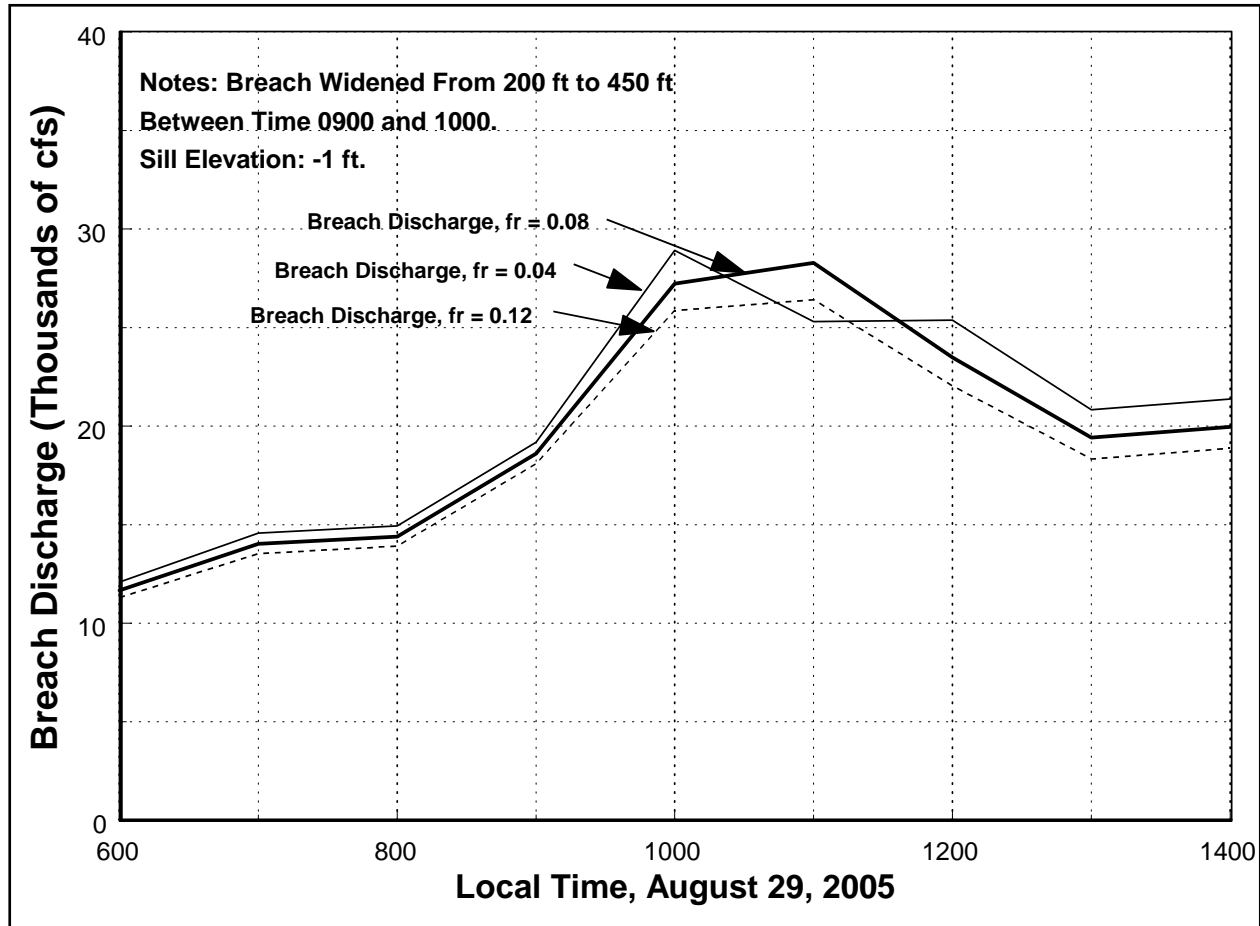


Figure 10-7. Sensitivity of breach discharge to Weisbach-Darcy friction coefficient

### Water Levels In Lake and Vicinity of Breach

Figure 10-8 presents the time histories of the lake level and the water levels slightly south of the breach in the 17th Street Canal for the three friction factors. As for the discharges, with the exception of the effects of the bridge at 1100 (and for the water levels, at 1200), the effects are as expected and fairly minimal.

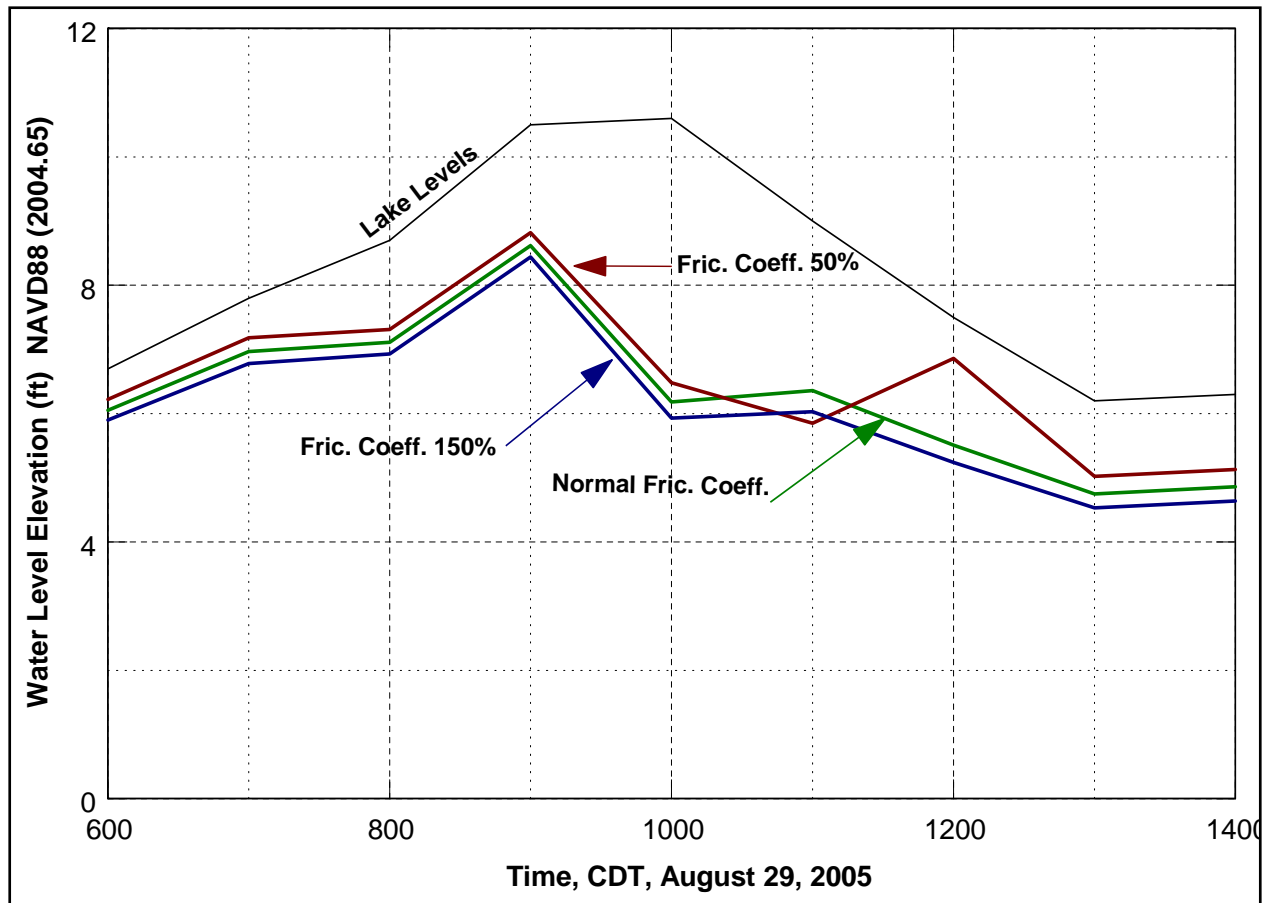


Figure 10-8. Sensitivity of water levels in vicinity of breach to Weisbach-Darcy friction coefficient

### Scenario 3: Sensitivity to Hammond Highway Bridge Flow Area Blockage by Debris

Scenario 3 is the same as Scenario 1 except debris blockages of 25% and 50% of the Hammond Highway Bridge flow area are considered. These results are pertinent to uncertainty of some photographs and eyewitness reports indicating that the water levels south of the breach were on the order of 4 feet at 1100 on August 29, 2005.

### Breach Discharge Characteristics

Figure 10-9 presents the breach discharges for the percent blockages noted.

### Water Level Distributions at 0900 and 1100 in the Canal

Figure 10-10 presents the water surface distributions along the 17th Street Canal at 0900 CDT, August 29, 2005 for flow blockage areas of 0%, 25% and 50%. Figure 10-10 presents the same information for 1100 CDT. At these times, the breach is considered to have widened to 450 ft. For these cases, the blockages have a substantial influence on the water surface elevations.

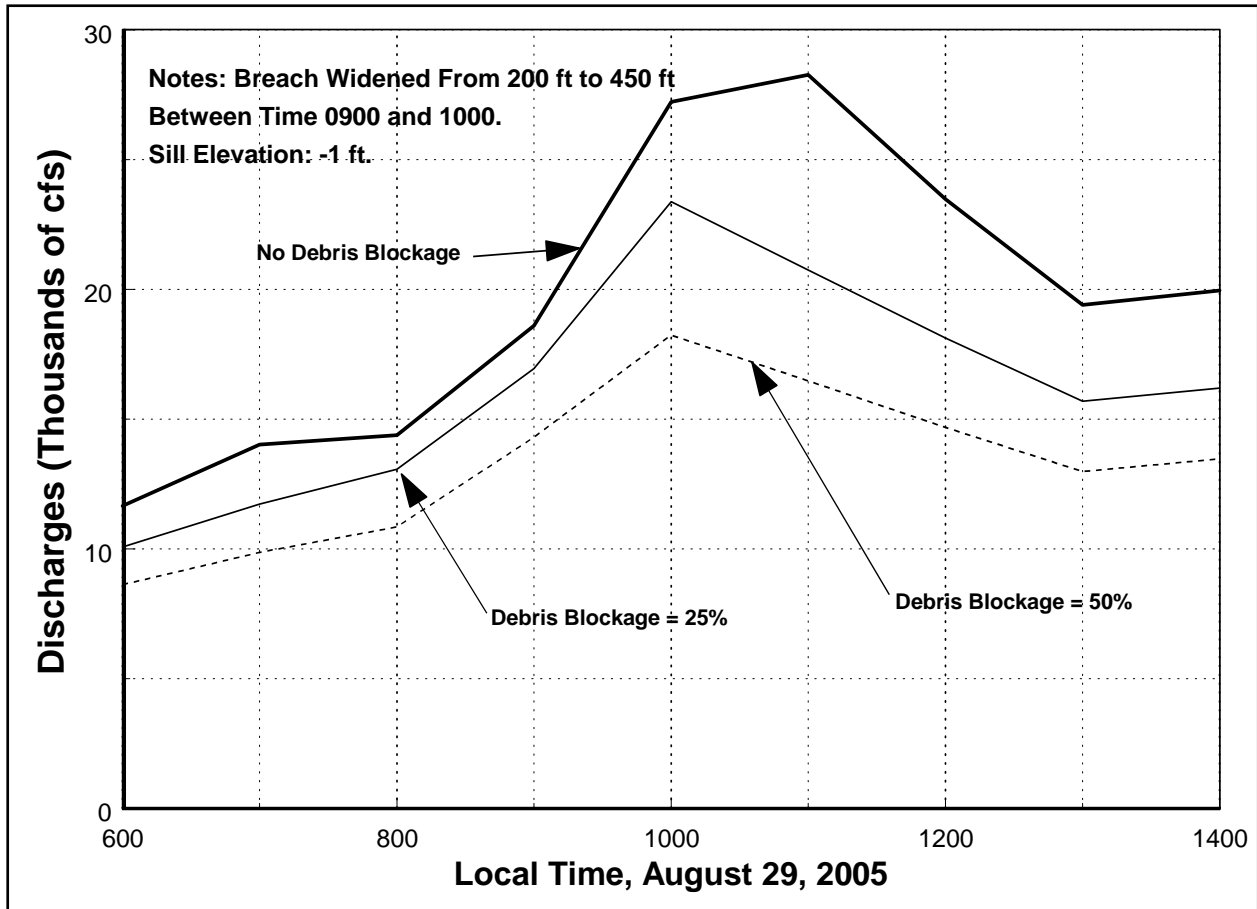


Figure 10-9. Breach discharges as a function of blockage of Hammond Street Bridge flow area

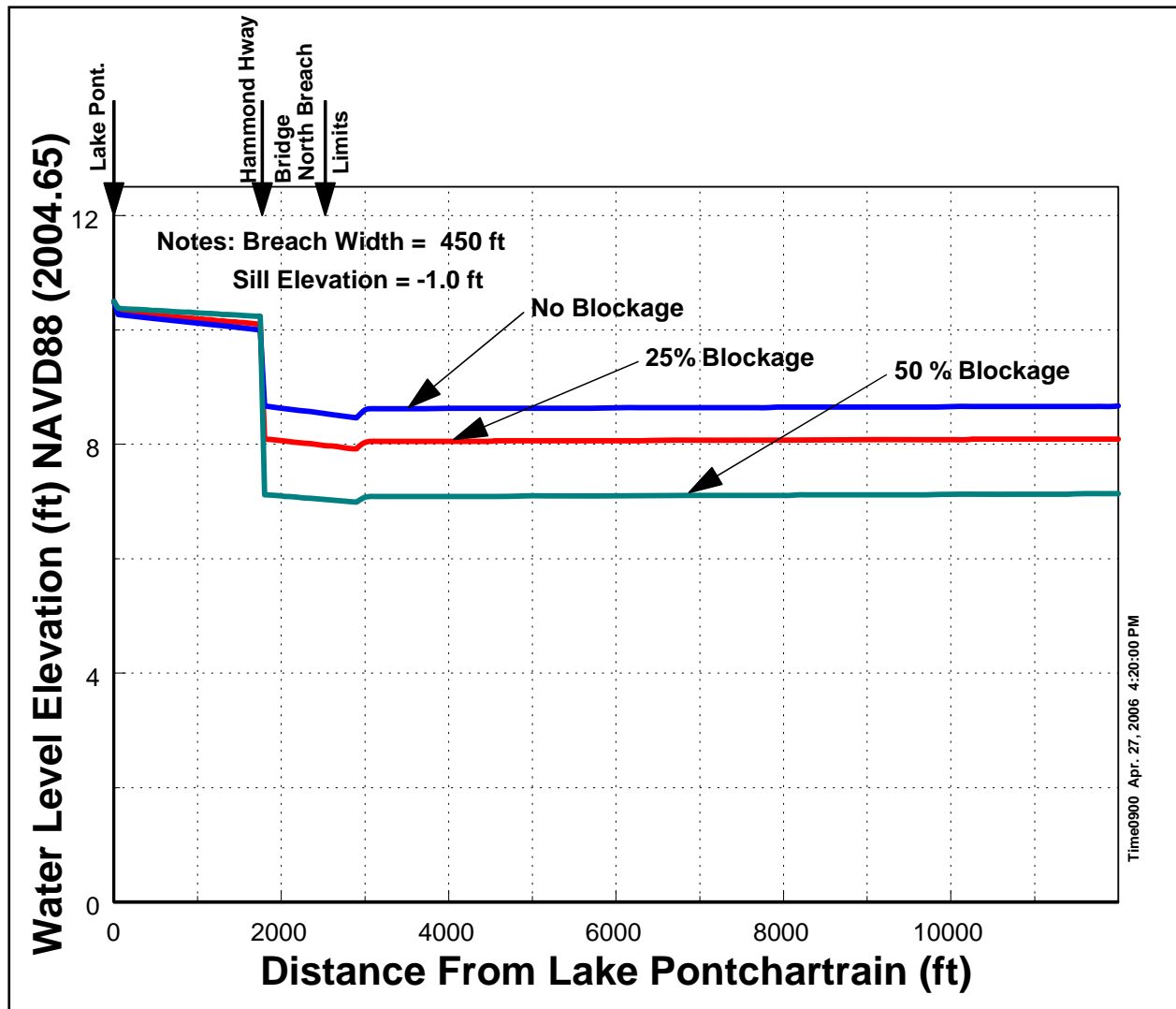


Figure 10-10. Water level distributions along 17th Street Canal for three flow blockages. Time: 0900 August 29, 2005

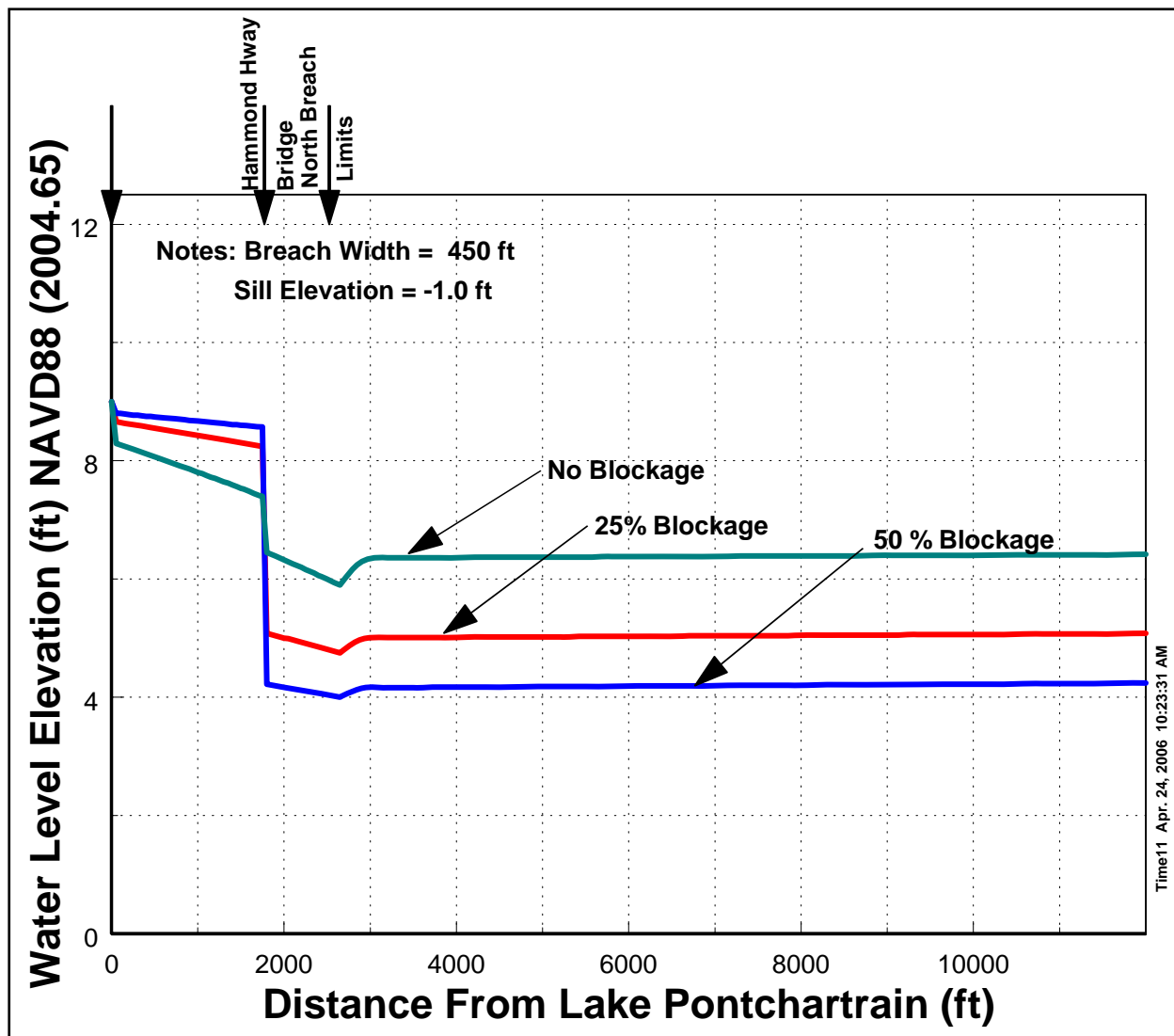


Figure 10-11. Water level distributions along 17th Street Canal for three debris flow blockages. Time: 1100 August 29, 2005

### Water Levels In Lake and Vicinity of Breach

Figure 10-12 presents the time histories of the lake level and the water levels slightly south of the breach in the 17th Street Canal for the case of normal blockage and for 25% and 50% flow blockage by the bridge. As for the discharges, with the exception of the effects of the bridge at 1100 (and for the water levels, at 1200), the effects are as expected and fairly minimal.



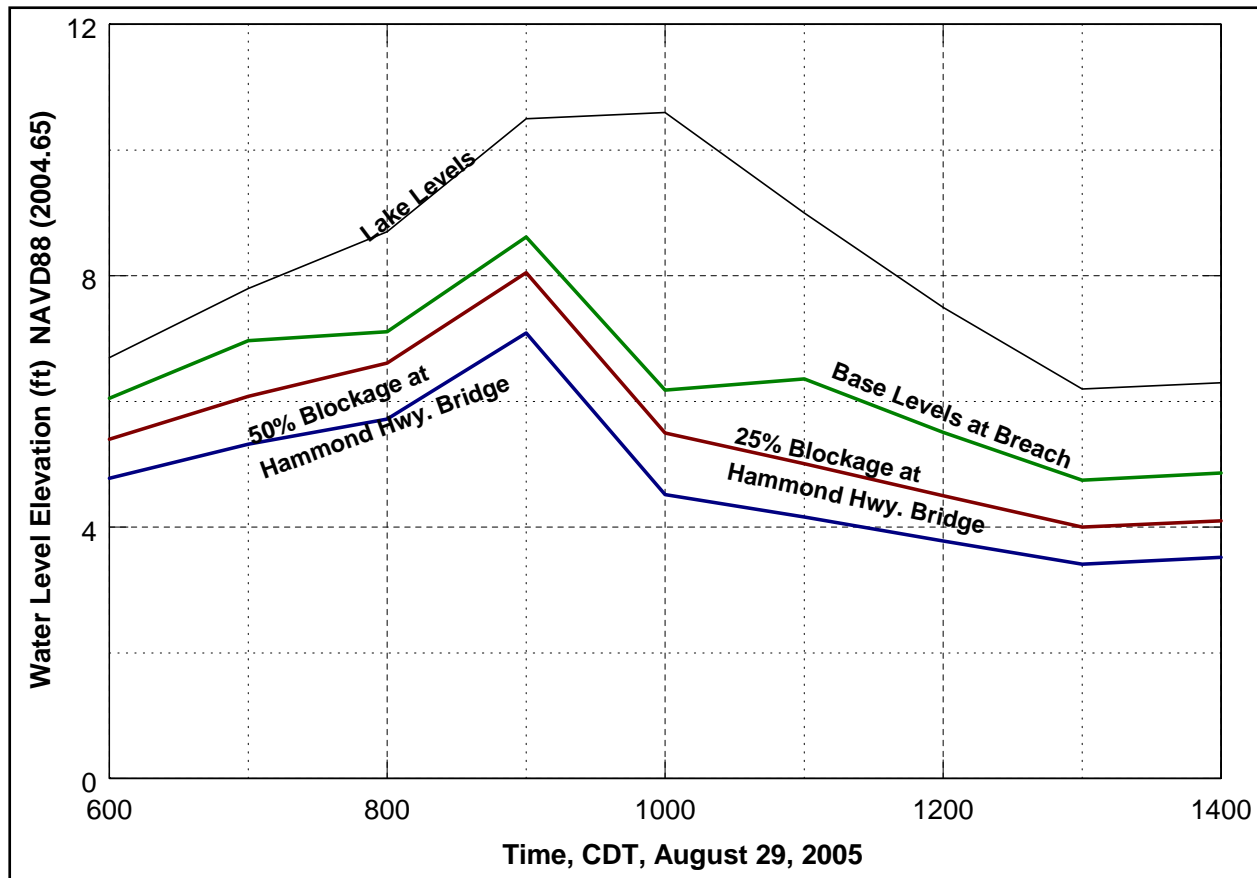


Figure 10-12. Sensitivity of water levels in vicinity of breach to flow blockages of Hammond Highway Bridge

#### Scenario 4: Reduced Initial Width Opening

This scenario examines a smaller initial breach width. Some eyewitness reports indicate that the initial breach comprised the failure of only one floodwall panel. Thus, the conditions of this scenario are the same as for Scenario 1 except the breach width for 0600, 0700 and 0800 is 30 ft which is the length of a single floodwall panel.

#### Water Levels in Lake and in Vicinity of Breach

Figure 10-13 presents the water levels in Lake Pontchartrain and in the vicinity of the breach for Scenarios 1 and 4. With only one floodwall panel failed, the water levels in the canal are very nearly the same as those in the lake.

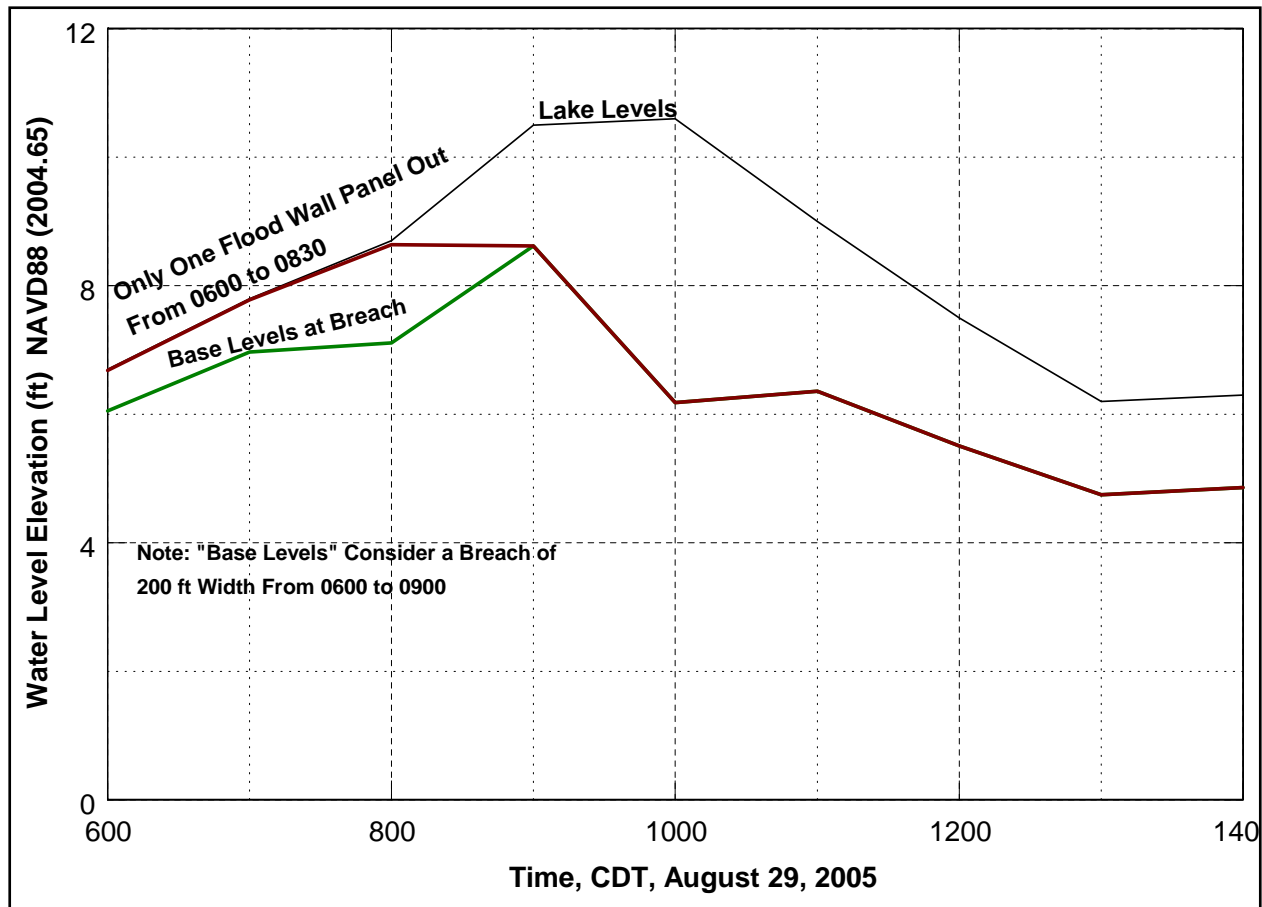


Figure 10-13. Calculated water levels in Lake Pontchartrain and in vicinity of breach for Scenario 4

## Discussion

The breach discharge characteristics and water surface profiles along the 17th Street Canal have been investigated using a steady state formulation of the governing hydraulic equations. Sensitivities of the breach discharges to Weisbach-Darcy friction coefficients have been evaluated. Additionally, the effect of flow blockage by debris on the lake side of the Hammond Highway Bridge on breach discharges and water surface profiles in the canal have been examined. Finally an initial breach width of only one floodwall panel length was considered.

It was found that the breach discharges were relatively insensitive to the Weisbach-Darcy friction coefficients. However, blockage by debris of the flow area under the Hammond Highway Bridge caused both a substantial reduction in the breach discharges and the water surface profile elevations along the 17th Street Canal. For the range of conditions examined with and without the flow blockage, the peak breach discharge ranged from approximately 18,000 cfs to 29,000 cfs. The scenario of a breach of one floodwall panel length indicates that the water surface gradients in the canal are very small resulting in the water surface elevation at the breach being approximately the same as in Lake Pontchartrain.

## Reference

Munson, B. R., D. F. Young and T. H. Okiishi (2006) "Fundamentals of Fluid Mechanics", Fifth Edition, John Wiley and Sons, Inc., Hoboken, NJ, 769 pages.

# Appendix 11

## Breach Flow London Avenue

---

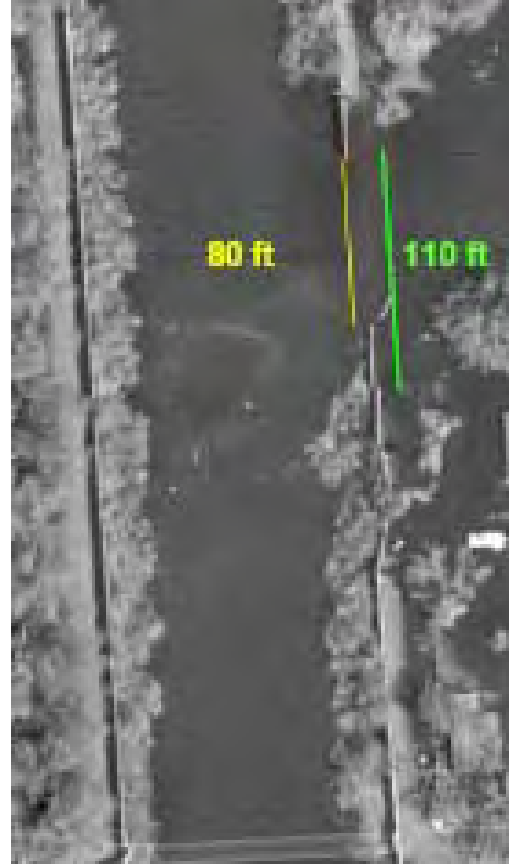
### Introduction

This appendix addresses flows through the north and south breaches that occurred in the London Avenue Canal on August 29, 2005, as well as the water levels in the canal. The methodology used in this analysis is the same as described in Appendix 10 for flows through the breach in the 17th Street Canal, and will not be repeated here.

Figures 11-1a and 11-1b show plan views of the canal in the vicinity of the breaches. Figure 11-2 presents an idealization of the canal as analyzed here.



(a) North breach near Robert E. Lee Bridge  
 Figure 11-1. London Avenue Canal breaches



(b) South breach at Mirabeau Avenue

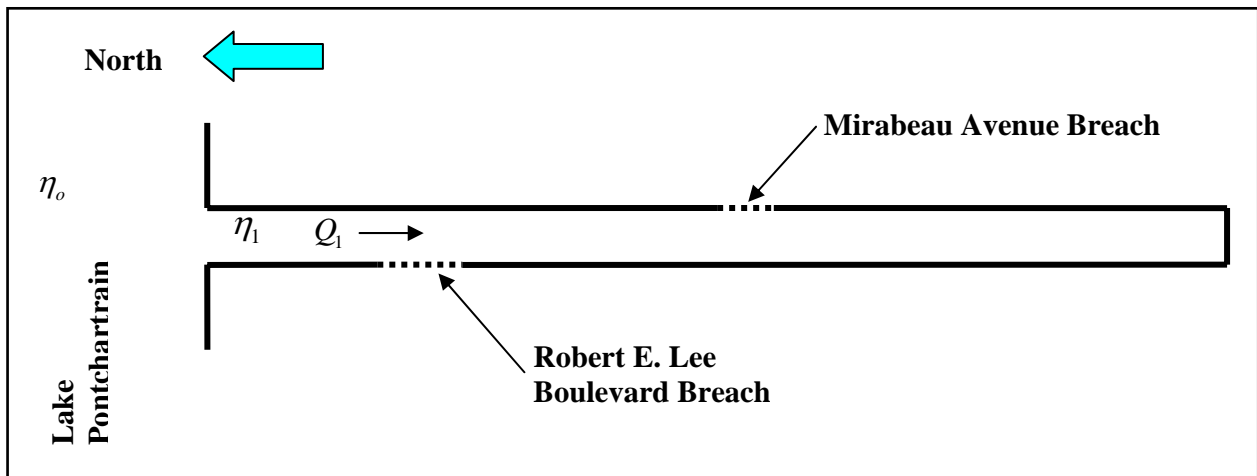


Figure 11-2. Schematic of London Avenue Canal



## The Failure Characteristics

The failure characteristics for the London Avenue Canal floodwalls are not as well established as for the 17th Street Canal. The estimates of pertinent variables used in the analysis reported herein are presented below.

### North Breach at Robert E. Lee Boulevard:

- Breach occurred between 0700 and 0730, August 29, 2005
- Breach “sill” unknown, but here estimated at + 4.0 ft.
- Breach Length = 300 ft.
- North end of breach = 4,200 ft. from Lake Pontchartrain.

### South Breach at Mirabeau Avenue

- Breach occurred between 0700 and 0800, August 29, 2005
- Breach “sill” unknown, but here estimated at - 1.0 ft.
- Breach Length = 80 ft.
- North end of breach = 8,380 ft. from Lake Pontchartrain.

The limited pump discharge information at Pump OP#7 at the south end of the canal is shown in Figure 11-3. Note that the pump discharge was reported to have completely ceased at 0820. The estimated hydraulic effects of the seven bridges are considered in the analysis.

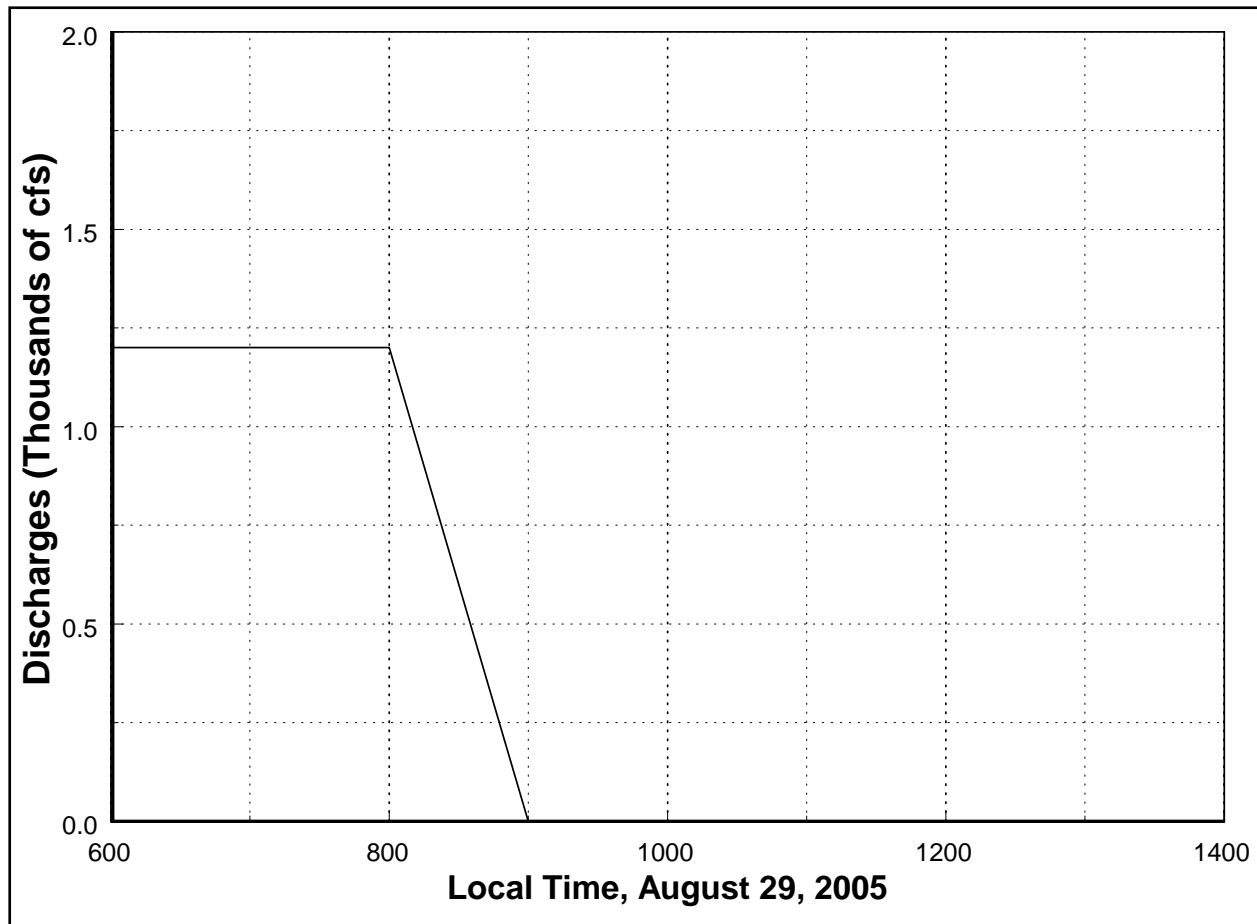


Figure 11-3. Pump discharges into the south end of the London Avenue Canal from pump OP#7

## Results

### General

The canal is 15,400 ft long and the individual computational cells representing the canal were each 50 ft long. The Weisbach-Darcy friction coefficient  $f$  was taken as 0.08 and the breach sill elevations were those provided above. The lake elevations are shown in Figure 11-4. Only one scenario has been considered for the London Avenue Canal.



Figure 11-4. Estimated water levels in Lake Pontchartrain near north end of London Avenue Canal

### Breach Discharges

Figure 11-5 presents the discharges from the breach and from the lake. It is seen that the maximum total peak discharge through the breach is approximately 22,000 cubic feet per second (cfs). The peak discharges through the north and south breaches are (coincidentally) approximately the same. Recalling that the north breach was wider than the south breach however, the sill elevation was higher at the north breach. Initially before breaching occurs (at 0600 and 0700), the flow is out of the canal into Lake Pontchartrain in accord with the pump discharge into the canal at the south end.

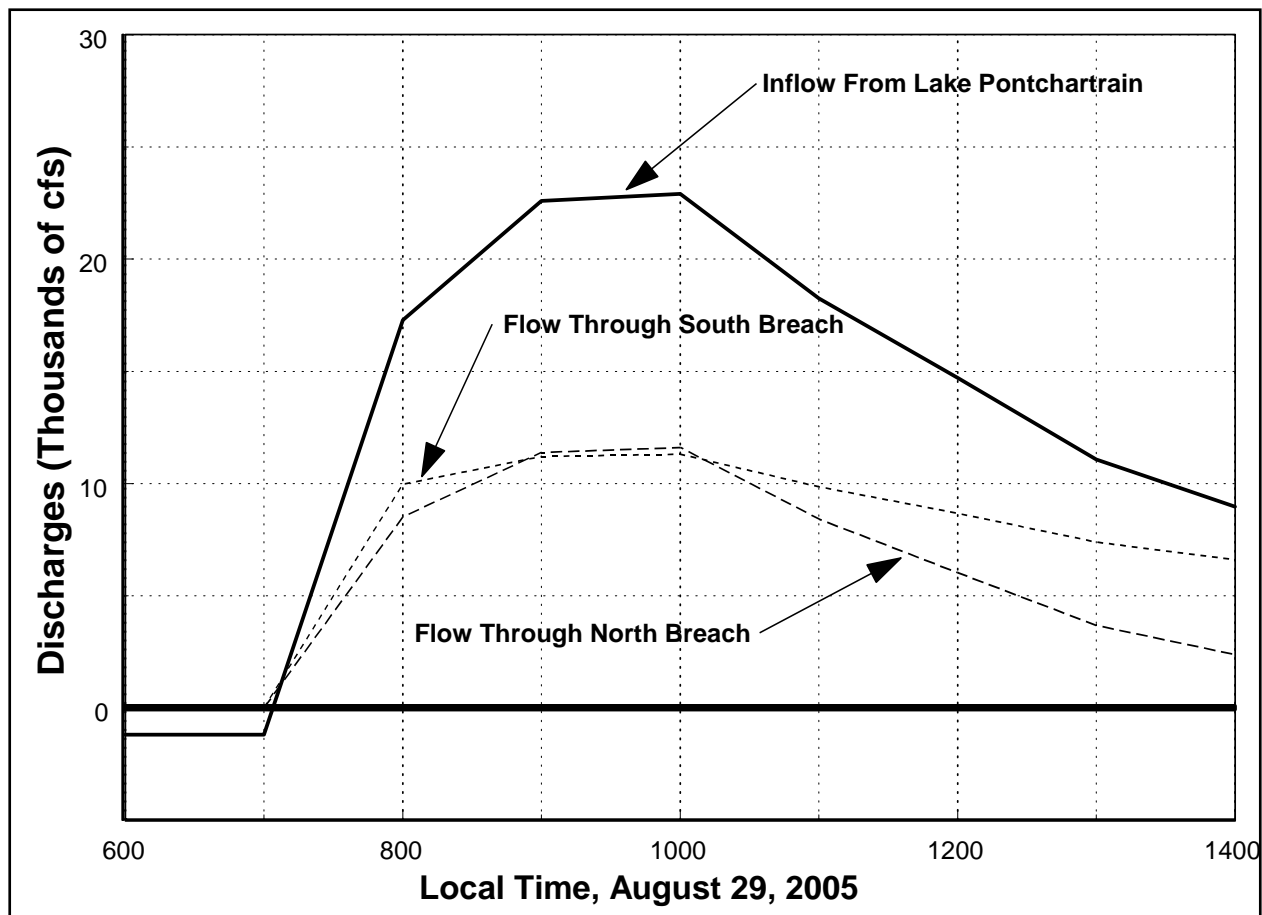


Figure 11-5. Time history of breach and lake discharges

### Water Levels Along 17th Street Canal

Figure 11-6 presents the distribution of water levels along the London Avenue Canal for times from 0600 to 1400 on August 29, 2005. The water levels at 0600 and 0700 prior to breach occurrence are nearly horizontal with the water surface sloping downward toward the lake in response to the pump discharge at the southern end.

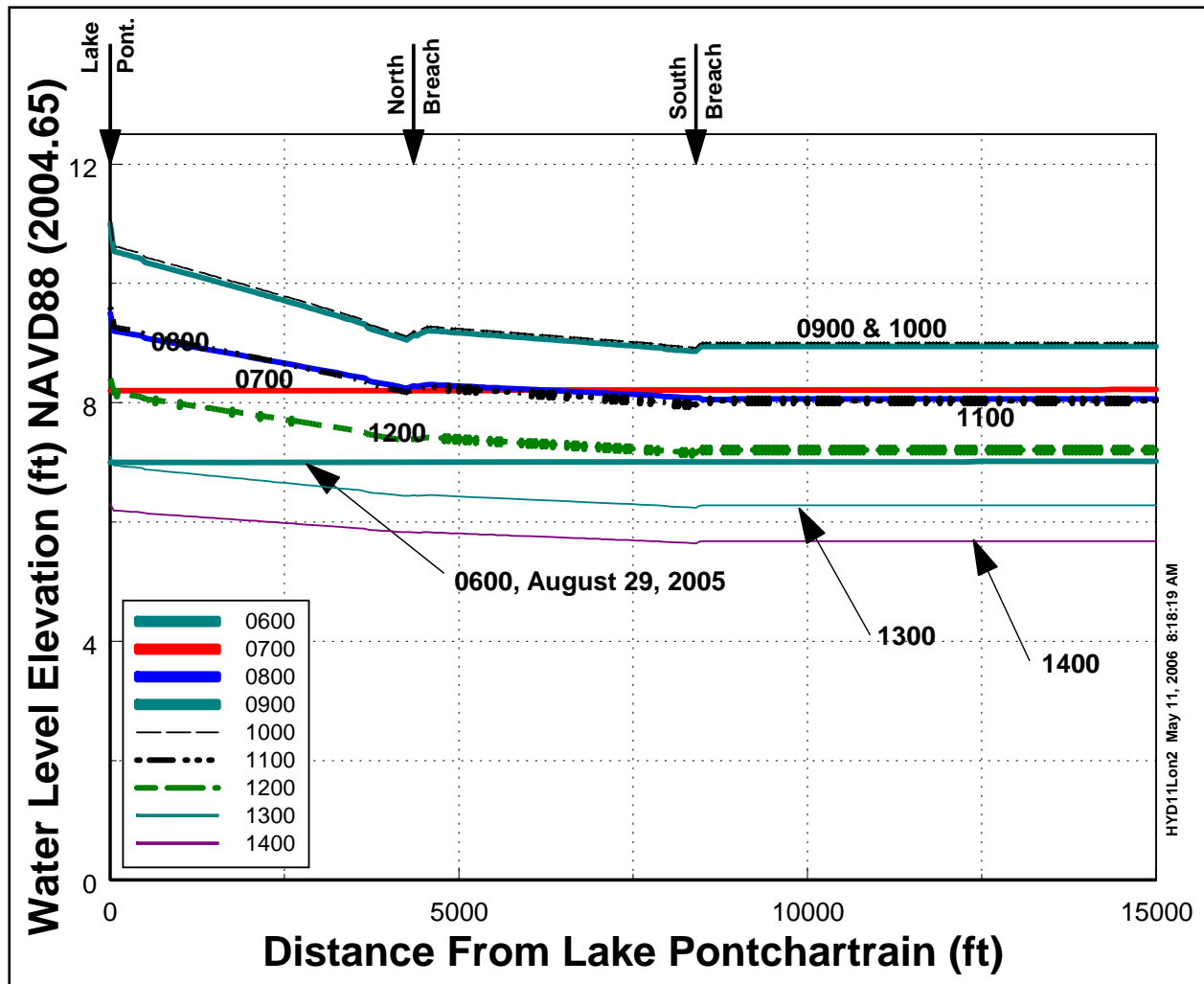


Figure 11-6. Water Levels along London Avenue Canal for various times

## Discussion

The breach discharge characteristics and water surface profiles along the London Avenue Canal have been investigated using a steady state formulation of the governing hydraulic equations. Discharges through the north and south breaches have been modeled from 0600 to 1400 on August 29, 2005. The maximum peak total breach discharge is approximately 22,000 cfs at time 1000. The water level variations along the canal are consistent with expectations.



# Appendix 12

## Physical Model of 17th Street Canal

---

### Purpose

Although numerical models were the backbone of the Hurricane Katrina analysis, a physical model was also developed for the northern portion of the 17th Street Canal for use in studying its behavior. A physical model was deemed necessary primarily in order to quantify the effect that the Hammond Highway Bridge had on wave transmission and flow toward the breach (see Figure 12-1) – issues that were beyond the capabilities of modern numerical models. Physical model studies were also needed to supply calibration information required by the numerical models, and to supply measurements for checking numerical results for detailed currents in the breach area. These currents were due to both waves and pump station operation.

### Model Design and Construction

Figure 12-2 shows the 1:50 scale physical model layout. The region covered by the model was required to provide all controlling bathymetry and topography that would significantly affect the representation of wave transmission toward the breach. Since the high water level during the storm would submerge the Coast Guard Harbor to the west, and the Municipal Harbor to the east, waves could propagate toward the canal from almost all lakeside directions and could potentially contribute wave energy in the vicinity of the breach. The physical model included, in accurate detail, a region of up to about 1200 ft beyond the southern end of the breach. The remainder of the canal is idealized as a basin region. This portion of the model provides storage for wave-induced setup and provides an input region for flow induced to simulate the drainage canal pumping system.

Bathymetric and topographic data were collected from several sources. NOAA navigation charts provided much of the Lake Pontchartrain bathymetric information. ERDC personnel surveyed the region north of the canal entrance, and New Orleans District survey information provided the remainder of the bathymetric information. Topographic information was obtained from a Louisiana State University LIDAR survey performed in 1999. The bathymetric and topographic data were converted to a common datum, NGVD29 (Vertcon 1994) using Corpscon 6.0.1. This datum is 0.69 ft lower than the NAVD88 (2004.65) datum.

The 14,500 sq ft physical model was accurately molded from concrete grout, representing 1.2 sq miles in the prototype. Vertical aluminum templates were placed throughout the constructed region at spacing of either two feet or four feet, dependent on complexity of bathymetry. Vertical accuracy of the model was  $\pm 0.2$  ft in the prototype. The model represented one mile of the Lake Pontchartrain shoreline. Construction was performed in 6 weeks, for a model area that would typically require 4 months to construct. Figure 12-3 shows the model during the final stages of construction. Figure 12-4 shows the fully constructed model.



Figure 12-1. 17th Street Canal entrance region, Hammond Highway Bridge, and breach location

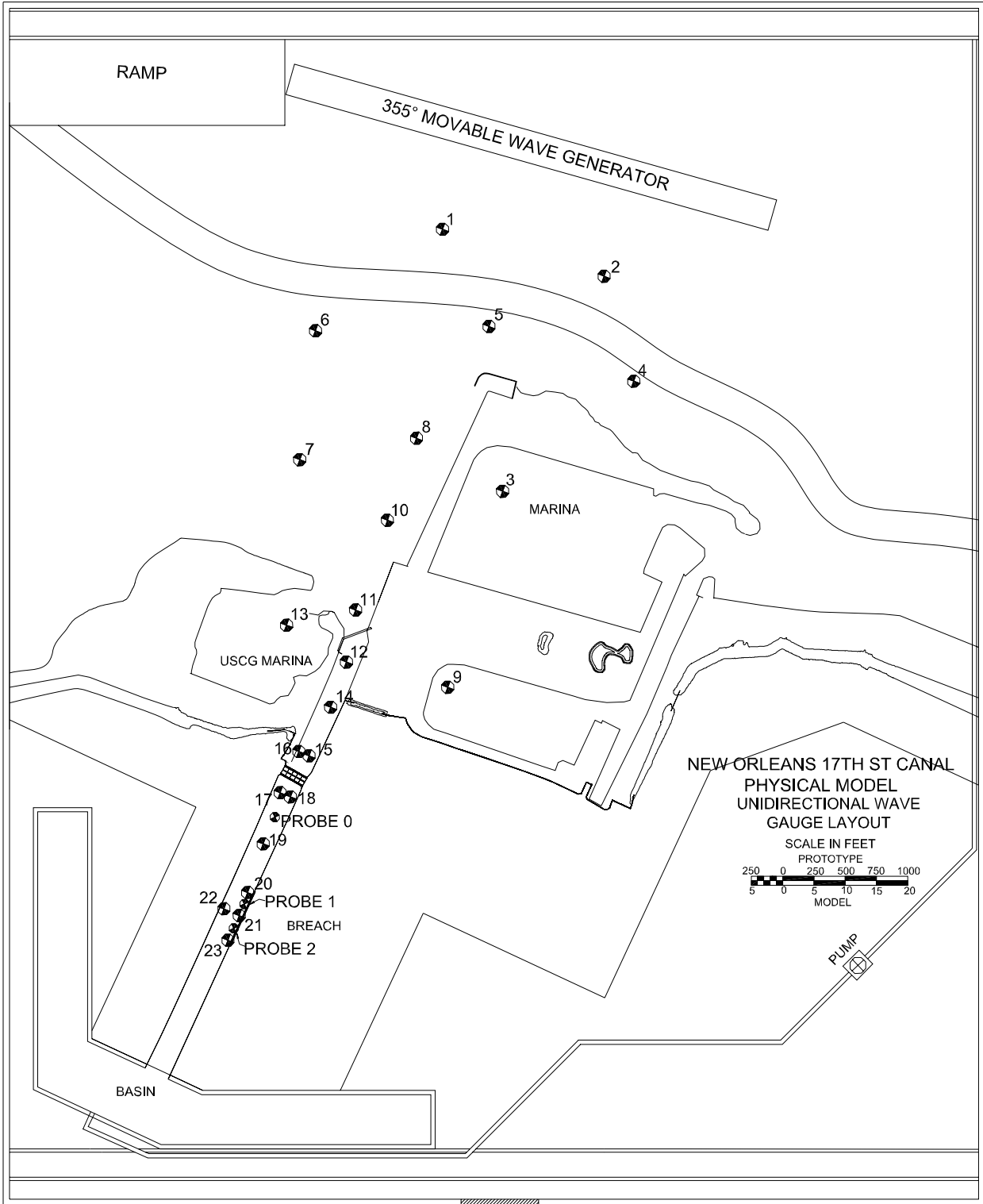


Figure 12-2. Model layout showing gauge locations and wave generator location for initial testing of bridge influence on waves





Figure 12-3. Physical model during construction; left photo showing overall view, and right view looking southward down the 17th Street Canal



Figure 12-4. 1:50 scale model of 17th St Canal and vicinity. The directional spectral wave generator used for part of the testing is shown on the right side of the photo



## Model Test Conditions

Input for reproduction of waves and water levels in the physical model was received from Tasks 4 and 5A. Figure 12-5 shows the surge height, wave height, period and direction as the storm progressed through time near the 17th St Canal. Wave information, in the form of a time series of directional wave spectra, was provided by Tasks 4 & 5a at four evenly spaced locations along the one mile of lakefront that the physical model reproduced. The data for the four locations plotted nearly on top of one another, indicating uniformity in wave height, period and direction for the 17th St region of lakefront.

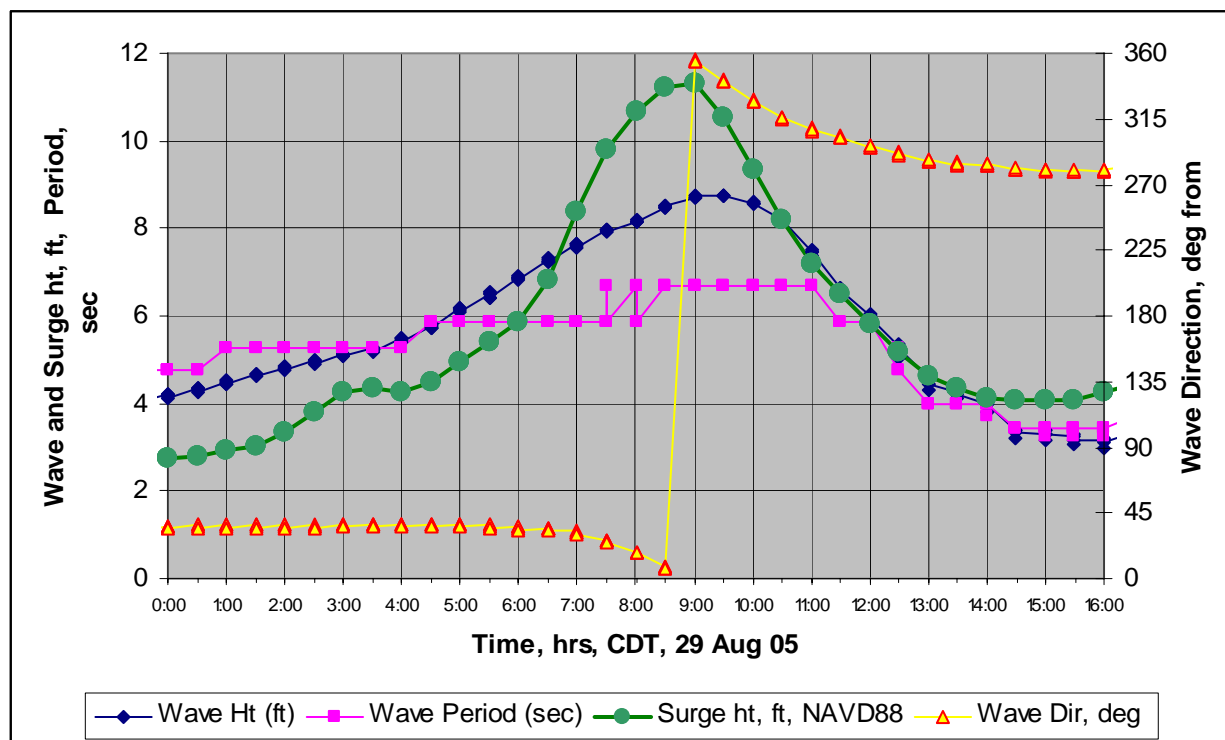


Figure 12-5. Wave height, wave period, and surge height determined from numerical models

The input data were used in physical model operation in the following manner. A test condition consisted of setting a particular water level and reproducing a particular wave spectrum for a certain time during the storm. In addition, when simulating the pump-station induced flow, water was introduced into the south end basin at a controlled rate, also determined for a given time during the storm.

Referring to Figure 12-5, wave height and velocity data were collected at hours, 0500, 0600, 0700, 0800 (rising surge level), at hour 0900 (peak surge level) and at hours 1000 and 1100 (falling surge level), CDT. Focus was on times of rising and at peak surge levels, as failure of the floodwall likely occurred during this time frame. For each one-hour interval, repeat tests were run. The water level was varied based on the numerical surge prediction between 0500 and 1100 hrs, and wave height varied based on the numerical wave model prediction for the same time interval.

## Model Equipment and Instrumentation

Two wave generators were used in the study. A Directional Spectral Wave Generator (DSWG) was used during the main testing period, during which data were collected for all wave directions during 0500 to 1100 hrs, CDT. While awaiting the move of the DSWG from another test basin to the 17th St Canal model, a two-dimensional, plunger-type wave generator was utilized. The data generated from these runs were used to provide initial numerical model calibration data, particularly at the Hammond Highway Bridge. Waves were run essentially straight into the canal entrance (wave generator set for 355 deg wave approach) with the unidirectional generator. Once the DSWG was installed, multidirectional waves could be run. Figure 12-6 shows two examples of three-dimensional wave spectra used for the DSWG-driven testing.

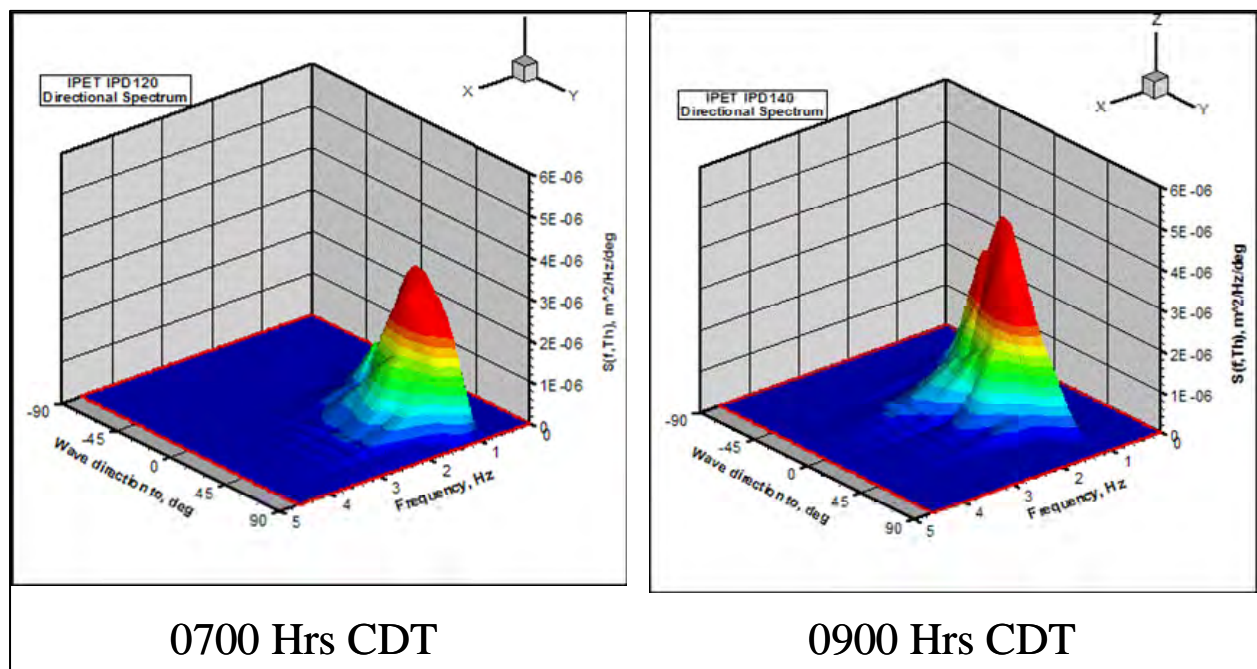


Figure 12-6. Wave spectra used by the directional spectra wave generator

Wave height and velocity data were collected in the canal region and at various locations approaching the canal. Waves could be measured at twenty-six locations simultaneously, using electrical capacitance wave gauges (Figure 12-4). The gauges were calibrated daily with a computer-controlled procedure that incorporates a least square fit of measurements at 11 steps of gauge elevation. This averaging technique, using 21 voltage samples per gauge, minimizes the errors from slack in the gear drives and any hysteresis in the sensors. Typical calibration errors are less than 1 percent of full scale for the capacitance wave gauges, resulting in measurements accurate to 0.05 ft. in the prototype. Wave signal generation and data acquisition were controlled by personal computer.

Velocity data were collected with SonTek 2D Acoustic Doppler Velocimeters (ADV) with a side-looking probe that is oriented to collect x-y horizontal velocity information in a horizontal

plane. Samples were collected at 20 Hz for ten minutes (i.e. 12,000 data points). Accuracy is 0.5 percent of the measured velocity, with resolution of 0.1 mm/s and threshold of 0.1 cm/sec. The probe samples a  $0.25\text{cm}^3$  volume located 5 cm from the sensor heads.

## Model Scaling

Based on Froude's model law and the linear scale of 1:50, the model-prototype relations in Table 12-1 can be derived. Dimensions are in terms of length ( $\ell$ ) and time ( $t$ ).

<b>Table 12-1 Model-Prototype Scale Relations at 1:50 Undistorted Scale</b>		
<b>Characteristic</b>	<b>Dimension</b>	<b>Model-Prototype Scale Relation</b>
Length	$\ell$	$\ell_r = 1:50$
Area	$\ell^2$	$A_r = \ell_r^2 = 1:2,500$
Volume	$\ell^3$	$V_r = \ell_r^3 = 1:125,000$
Time	$t$	$t_r = \sqrt{\ell_r} = 1:7.07$
Velocity	$\ell/t$	$U_r = \ell_r/t_r = 1:7.07$
Discharge	$\ell^3/t$	$Q_r = \ell_r^3/t_r = 1:17,678$

## Data Analysis

Wave data were analyzed by spectral analysis using an FFT. FFT or single-channel frequency domain analysis was performed over the entire 12,000 data points of each record ( $\Delta t = 0.05$  sec). Wave height is reported as  $H_{m0}$ , which is four times the square root of the integral of the variance in the wave spectrum. This is typically equivalent to significant wave height, or the average of the highest one-third of the measured wave heights.

## Initial Testing: Bridge Effect on Wave Transmission

The uni-directional plunger-type wave generator was set so as to produce a wave crest from 355-deg, creating a refracted wave that was approaching directly into the canal. The purpose of these tests was to provide data for calibration of the numerical model. Especially important was the effect of the Hammond Highway Bridge on waves that would transmit into the breach region, about 900 feet south of the bridge. Figure 12-2 shows the generator location and wave gauge arrangement for these tests. All test waves were from the 355-deg direction, whereas water level and wave height varied according to Table 12-2.

**Table 12-2  
Conditions for Uni-directional Wave Generator Tests**

Test Name	Wave Ht, ft	Period, sec	Dir from	Surge Level, Ft, NAVD 88 (2004.65) Datum ( )=NGVD29(Vertcon 1994)
Level 1_uni	6.2	5.9	355	4.9 (5.6)
Level 2_uni	6.9	5.9	355	5.9 (6.6)
Level 3_uni	7.6	5.9	355	8.4 (9.1)
Level 4_uni	8.2	6.7	355	10.7 (11.4)
Level 5_uni	8.7	6.7	355	11.3 (12.0)
Level 6_uni	8.6	6.7	355	9.3 (10.0)
Level 7_uni	7.4	6.7	355	7.2 (7.9)

Figure 12-7 shows the wave height data on the northern side of the bridge, as well as the ratio of wave height reduction after waves travel under the bridge for the conditions shown in Table 12-2. This initial information was provided for use in calibrating numerical wave models.

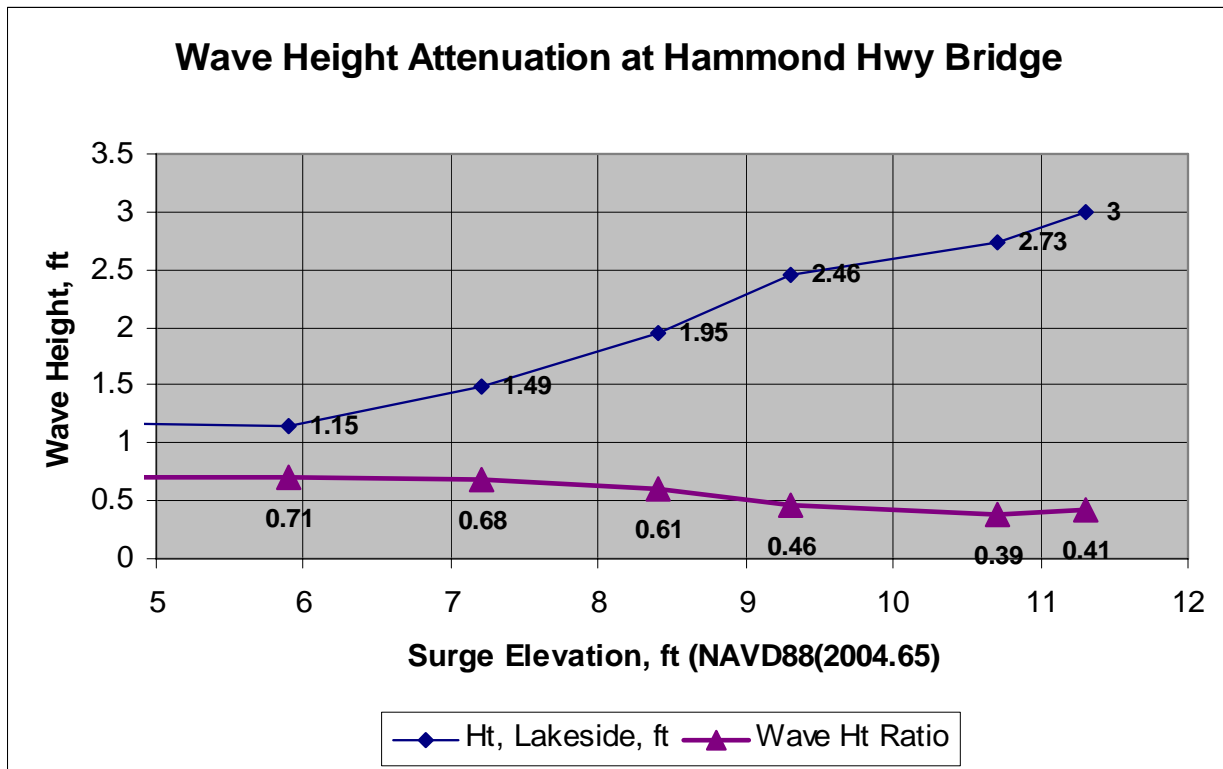


Figure 12-7. Preliminary Data on effect of bridge on wave height in the breach region

## Wave Tests Using Directional Spectral Wave Generator

Once the directional spectral wave generator (DSWG) was available and installed in the model basin, detailed wave transformation and current measurements were performed for the conditions presented in Table 12-3. At each model time the surge water level was established in

the model, and the DSWG programmed with the appropriate directional wave spectrum. Hydrodynamic data were collected at the locations shown in Figure 12-8, as described below.

<b>Table 12-3 Test Conditions for Directional Spectral Wave Generator Tests</b>					
<b>Test Name</b>	<b>Time 29 Aug, Hrs, CDT</b>	<b>Wave Ht, ft</b>	<b>Period, sec</b>	<b>Dir from</b>	<b>Surge Level, ft NAVD 88 (2004.65) Datum</b>
Level 1_dswg	0500	6.2	5.9	37	4.9
Level 2_dswg	0600	6.9	5.9	35	5.9
Level 3_dswg	0700	7.6	5.9	32	8.4
Level 4_dswg	0800	8.2	6.7	18	10.7
Level 5_dswg	0900	8.7	6.7	355	11.3
Level 6_dswg	1000	8.6	6.7	326	9.3
Level 7_dswg	1100	7.4	6.7	308	7.2

### Wave Data

Figure 12-9a shows a photograph of the 17th Street Canal model under conditions at 0900 hrs CDT. Hmo results from each instrument are plotted in Figure 12-9b, progressing from the lake into the canal. All of the wave height results for the conditions of Table 12-3 are presented in the plot. There is an initial drop in wave height between gauge 5 and gauge 8, and another significant drop between Gauges 11 and 12, as waves enter the canal. Wave heights at 0900 hrs, CDT, have a reduction in height from about 6 ft to 3.5 ft between Gauges 11 and 12. Wave height stays at about 2.5 ft until the bridge is reached. At this point an additional reduction is observed between the gauges straddling the bridge, i.e. Gauge 26 and Gauges 17 & 18. Wave heights approaching the breach zone are less than 0.5 ft. The processes responsible for wave height reduction include: 1) refraction of wave energy over the shallower submerged land areas around the harbor, 2) reflection of energy off vertical walls in the region between the entrance to the canal near the Coast Guard Harbor and the Hammond bridge; and 3) interaction of the waves with the bridge, including reflection, which will be discussed in detail later in this appendix.

### Velocity Measurements

Figure 12-8 shows the location of Probe 0, Probe 1 and Probe 2. Probe 1 data are presented in Figure 12-10 and are representative of the maximum velocities that occurred at each hour, and are associated with the propagating waves. The x component velocity is directed along the canal and the y-component is perpendicular to the canal wall. Along-canal current maximums were usually in the 0.6 to 0.7 ft/sec range (4.2 to 5 ft/sec prototype). Cross-canal current maximum values were in the 0.1 to 0.3 ft/sec range (0.7 to 2.1 ft/sec prototype).



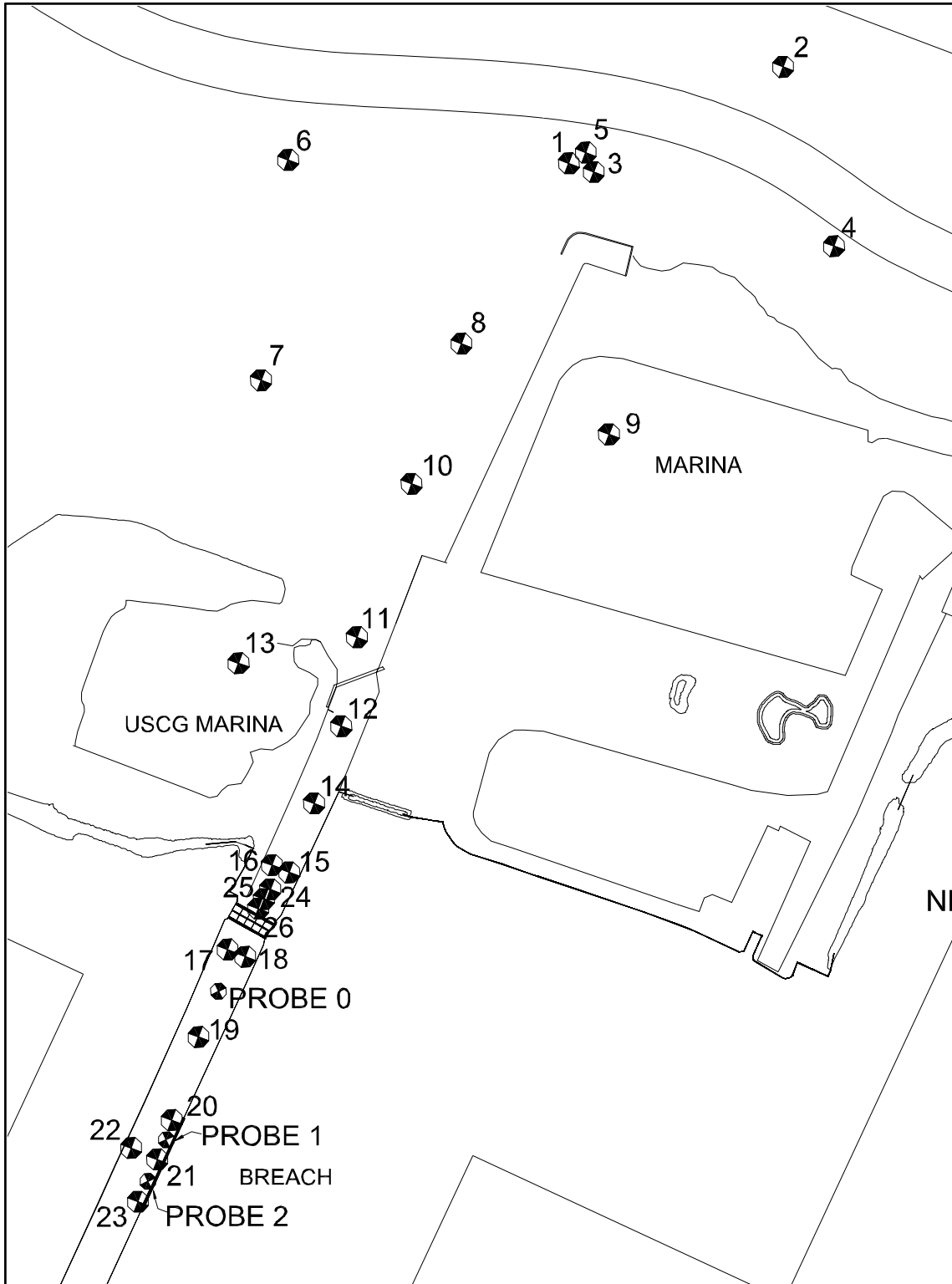


Figure 12-8. Instrument locations for DSWG tests. Wave gauges are labeled 1-23. 'Probe' locations are where currents were measured. Probes 1 and 2 are along the (intact) floodwall at the location where the breach ultimately occurred



Figure 12-9a. Waves approaching 17th St Canal, 0900 hrs, CDT

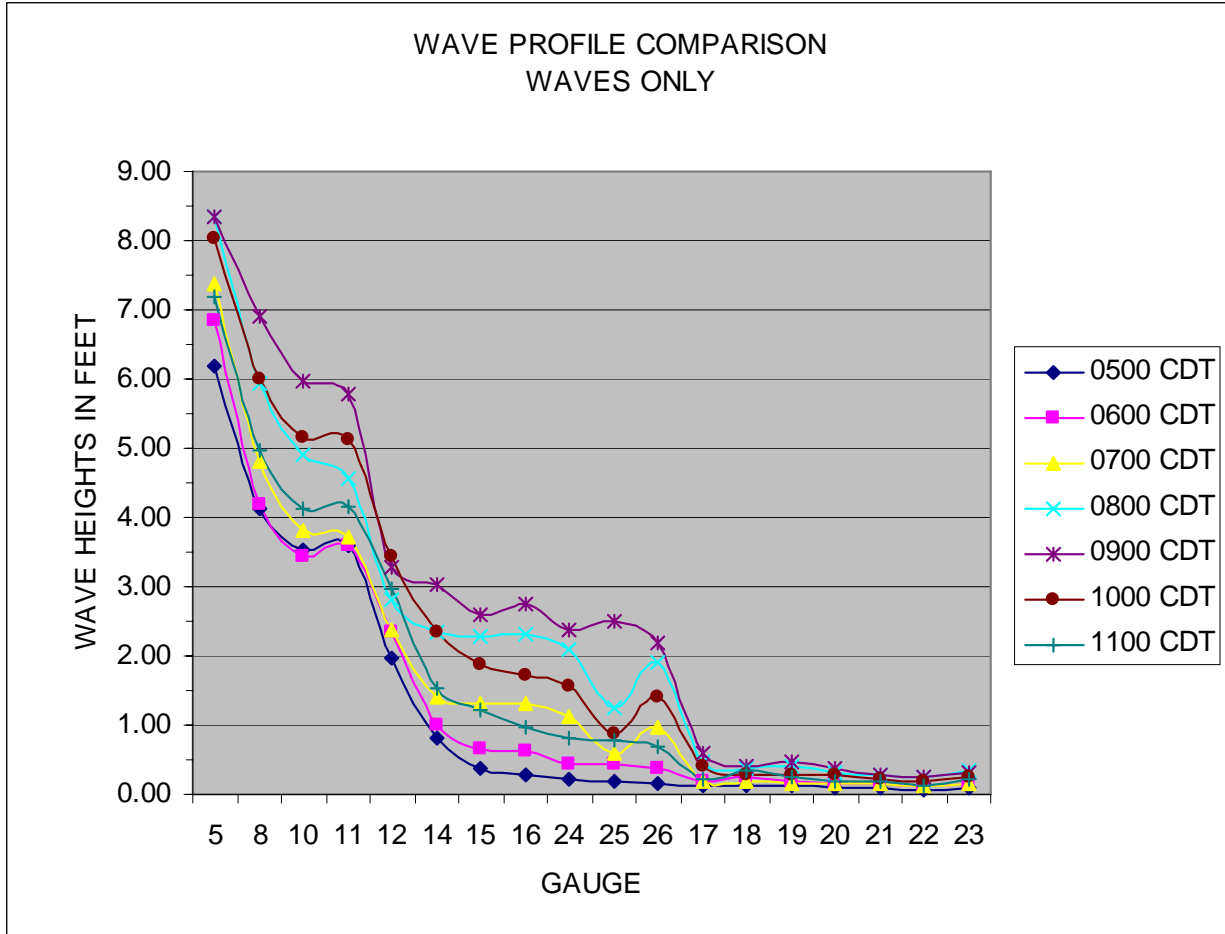


Figure 12-9b. Wave heights progressing from the lake into the canal

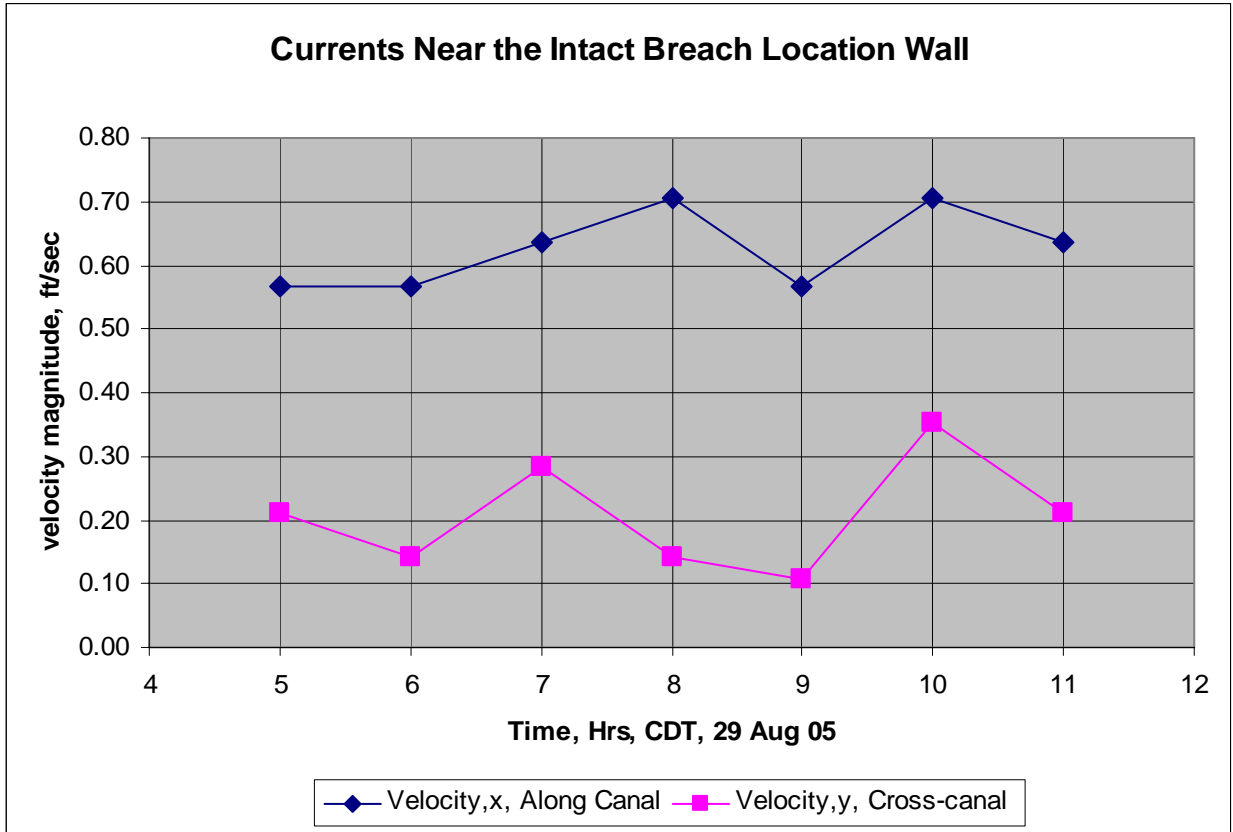


Figure 12-10. Currents near the (intact) floodwall at the location of the breach in prototype scale)

## Detailed Wave Measurements Near the Bridge

Figure 12-11 shows a cross-section of the Hammond Highway bridge. Since the canal is not intended to be a navigable waterway, the bridge is relatively close to the water surface. Consequently, as the storm surge elevation approached 6 to 7 ft, the bridge facing began to interact with waves. This phenomenon is not well-represented by numerical models, hence the impetus for a physical model. Gauges 24, 25 and 26 (see Figure 12-8) were situated so that an analysis of the waves reflected back by the bridge could be performed, and reflection coefficients determined. A high-water line is indicated in Figure 12-11.

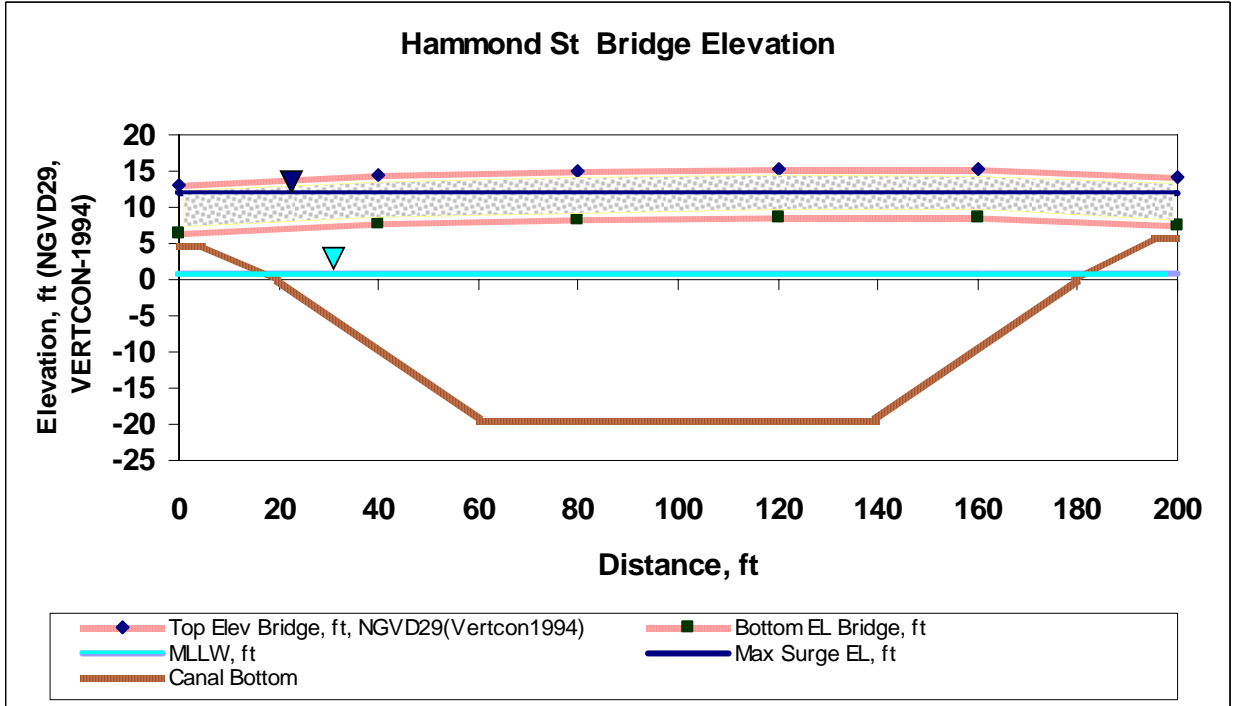


Figure 12-11. Schematic profile of the Hammond Highway Bridge

Figure 12-12 presents a photograph of the model in the region straddling the bridge. The rough water surface on the right-hand (north) side is indicative of reflected wave energy, whereas the left side is relatively quiescent. The results of reflection analyses, shown in Figure 12-13, indicate that as the hurricane surge rises, the reflection coefficient jumps from about 10 percent to nearly 35 percent. Figure 12-14 shows the change in wave behavior across the bridge as a function of time during the Katrina simulation.



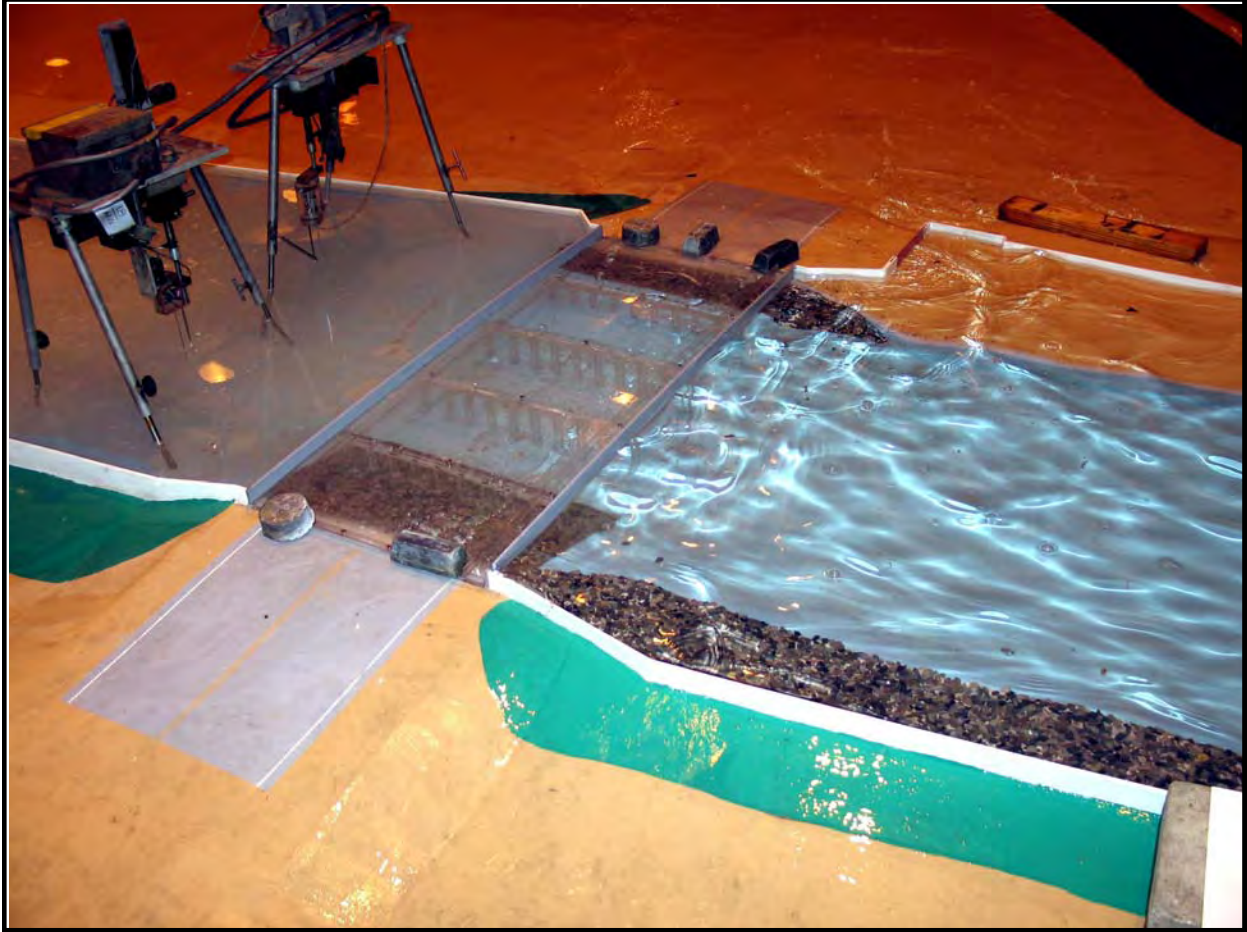


Figure 12-12. Wave reflection at the Hammond Highway Bridge. Region to right of bridge is lake-side (north side)

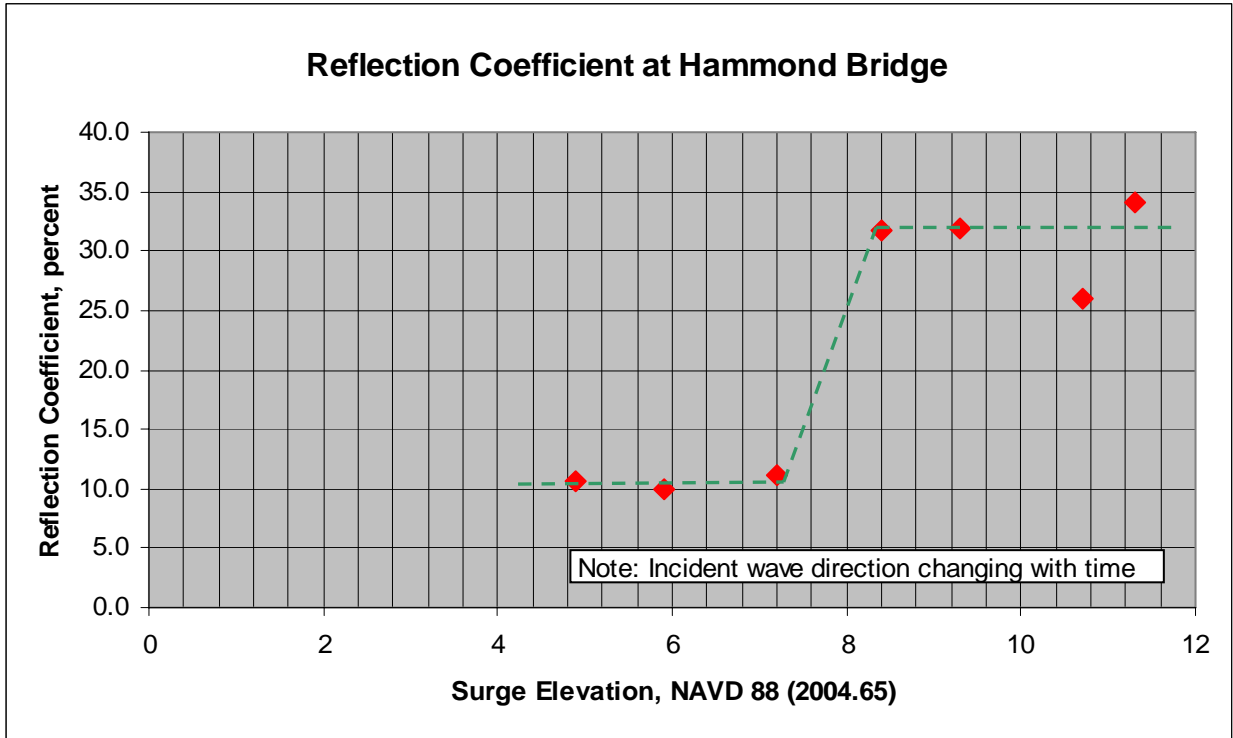


Figure 12-13. Wave reflection coefficient for Hammond Bridge as a function of surge elevation

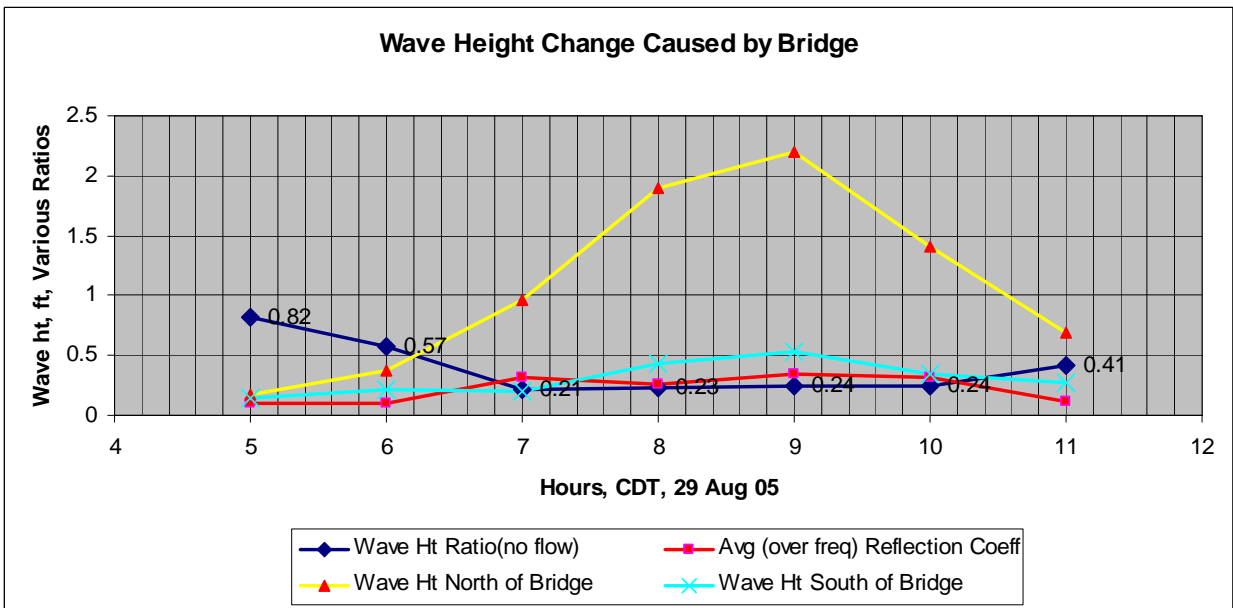


Figure 12-14. Wave height behavior at Hammond Bridge during Katrina's landfall

## Examination of Pump Station Flow Effects on Waves and Currents

Mid-way through the physical model study, IPET field interviewers were able to obtain the pumping records of Pump Station 6 during the hurricane. Table 12-4 presents these actual pumped flow rates as a function of time, including the period between 0500 and 0800 when power was off and the pumps were not operating. The scaled flows adopted in the physical model are provided in the right-hand column. Note that pumped flows were included in the testing that were probably not actually occurring at hours 0600 and 0700. Non-zero rates were used during these times to provide artificial continuity to the data set so that trends in wave-current interaction might be identified.

Figure 12-15 provides wave height measurements taken during the pumping schedule from Table 12-4. Figure 12-16 presents the difference between waves only (see Figure 12-9a) and waves-with-pumped-flow (no-pumping minus with-pumping). The difference plot indicates that there is a slight increase when flow from the pump station interacts with the incoming waves, especially in the region north of the bridge. This is a typical result when waves meet an adverse current. A closer examination of wave height change at the bridge is shown in Figure 12-17. The smaller wave heights south of the bridge were not impacted by the flow.

Velocity measurements in the canal along the (intact) wall section where the breach ultimately occurred were at their maximum when the pump station was at its maximum output (Figure 12-18). With 8,300 cfs flowing north through the canal, along-canal velocities next to the breach area wall were 3.25 ft/sec. The cross-canal velocity was 0.5 ft/sec. When pump station operation dropped to 2,600 cfs, along-canal velocity dropped to just below 1.5 ft/sec and cross-canal velocity was about 0.25 ft/sec.

**Table 12-4  
Pump Station 6 Flow Rates**

Time, Hrs, CDT	Prototype Flow, cfs	Modeled Flow, cfs (prototype)
0000	1100	--
0100	1100	--
0200	5200	--
0300	8800	--
0400	8300	--
0500	0	8300*
0600	0	2600*
0700	0	2600*
0800	0	2600*
0900	2600	2600
1000	2600	2600
1100	2600	2600
1200	2600	--
1300	2600	--
1400	3100	--
1500	4100	--
1600	4100	--
1700	4100	--
1800	4100	--
1900	0	--

\*Note: These flows were tested in model to provide continuity to data collection and possibly flows could be occurring near 0500 and 0800 hrs, CDT

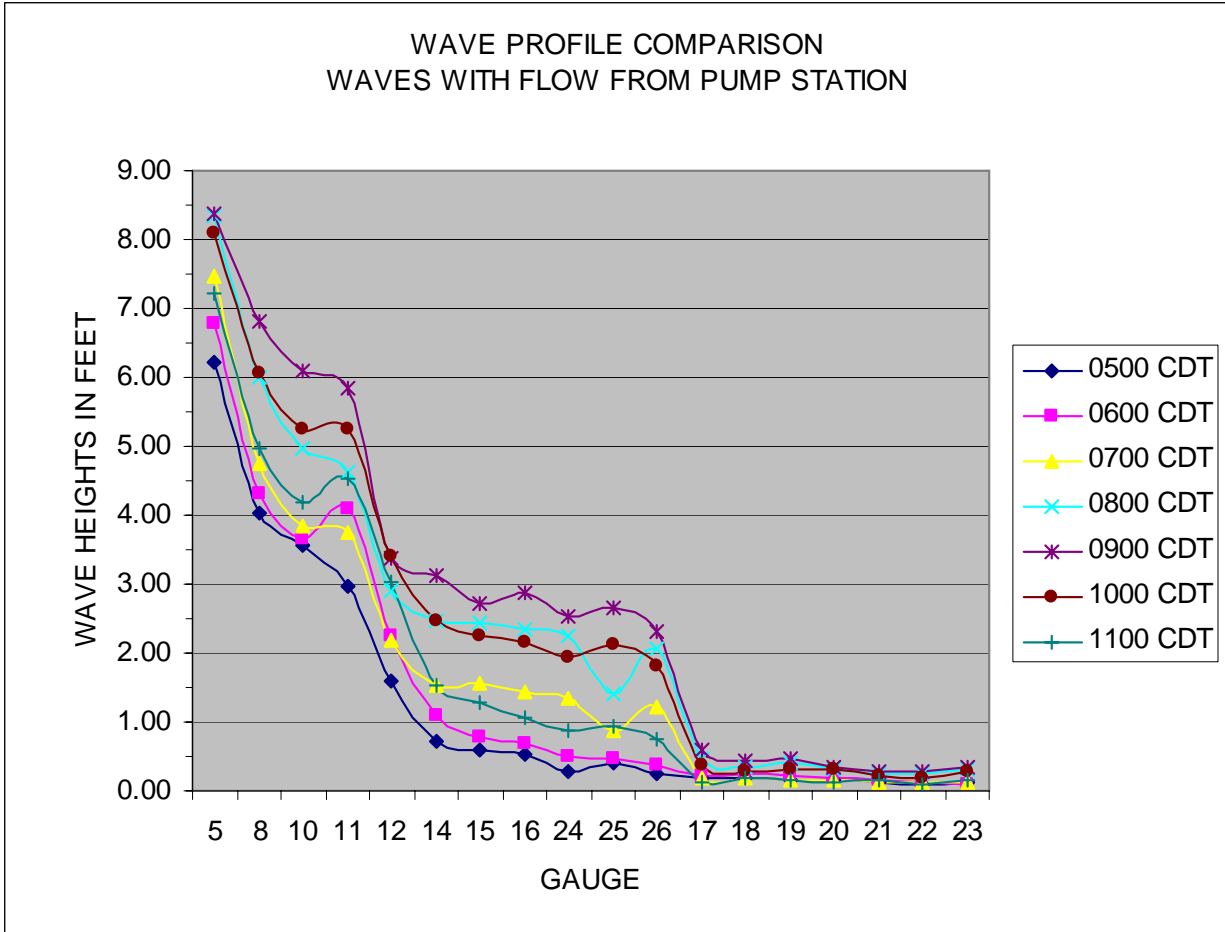


Figure 12-15. Wave heights for hrs 0500 to 1100 with pump station operational



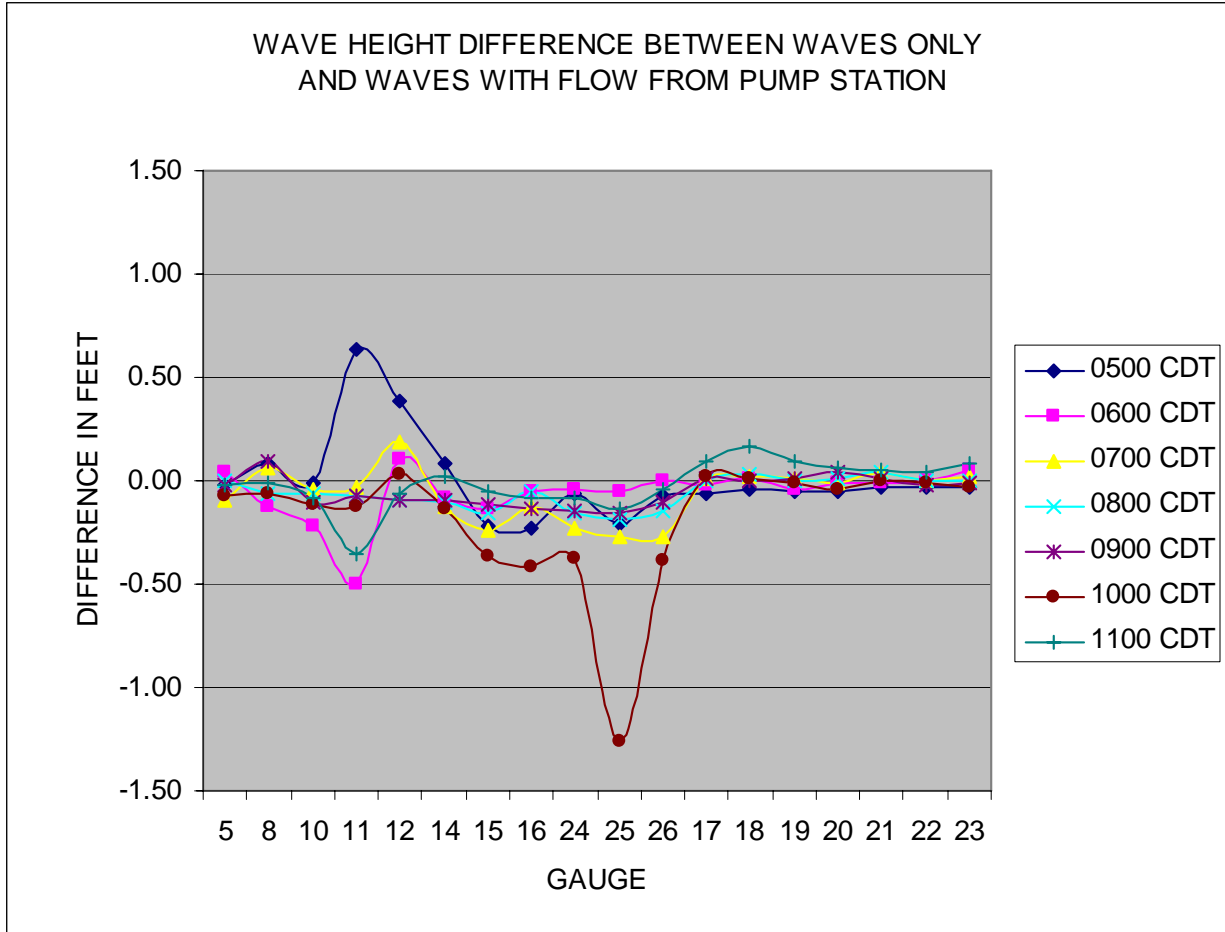


Figure 12-16. Wave height difference for waves-only and waves-with-pump-station operation for hrs 0500 to 1100

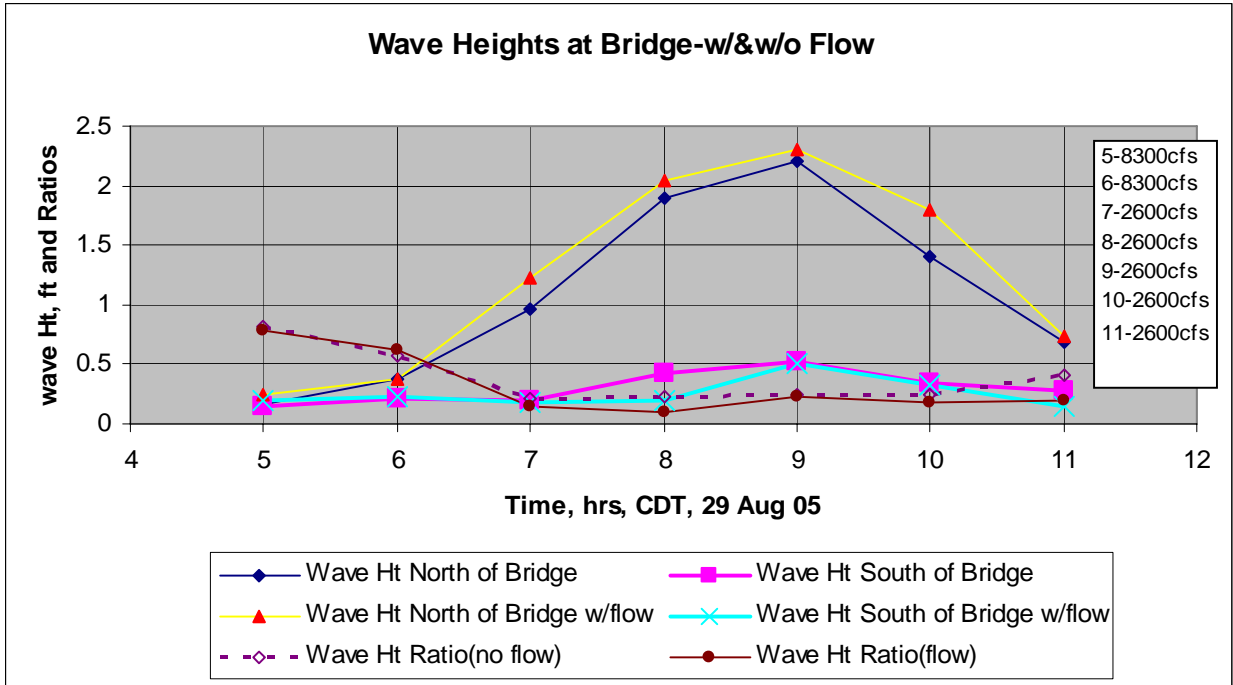


Figure 12-17. Wave heights at bridge with and without Pump Station 6 operating

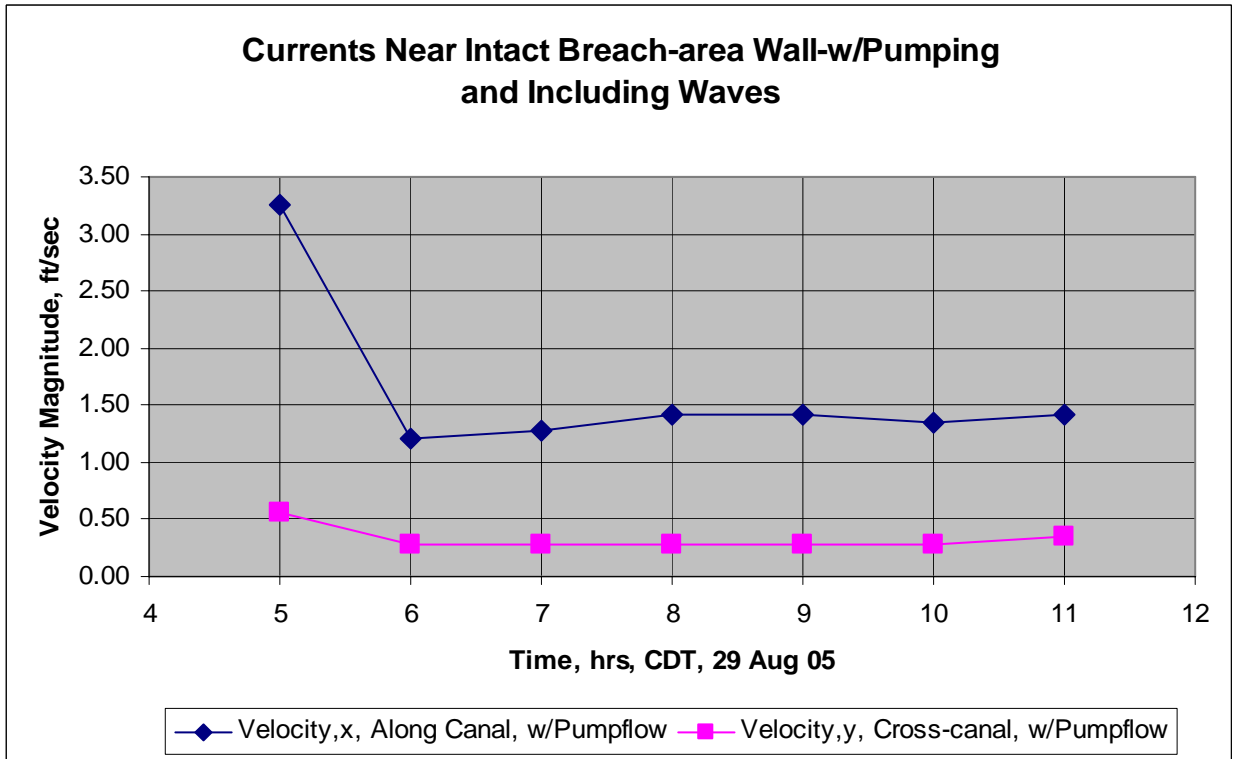


Figure 12-18. Velocities near intact wall with Pump Station 6 operational

## **Examination of Debris Field at Bridge: Influence on Waves and Flow**

Post-storm aerial photos showed a large debris field jammed against the lake side of the Hammond Highway Bridge (see Figure 12-19). It reasonable to conclude that a major portion of the debris material was derived from structures that were on piles just north of the canal entrance, and that most likely debris started gathering at the bridge when flow through the breach was strong enough to draw water from Lake Pontchartrain. Initial tests of the physical model were conducted to determine the effect of the debris plug on wave transmission. Because it was unknown exactly when the material was deposited at the bridge, model data were collected from 0500 to 1100 hrs for two idealized debris conditions.



Figure 12-19. Post-storm debris at Hammond Highway Bridge. The triangular wedge is about 200 ft across at bridge

The debris field was simulated in the physical model using a bound fiber mesh material, cut to represent the planform geometry of the plug shown in Figure 12-19. The plug was studied in two configurations: 1) a two-inch thick sheet (Configuration 1), and 2) a four-inch thick sheet (Configuration 2). Figure 12-20 shows the material and its placement in the model. The material was attached to a foam sheet for consistent elevation of flotation.



Figure 12-20. Debris field simulation using fiber mesh material

## Debris Effect on Waves

The same wave and water level conditions were run with the two different debris thicknesses. The wave height results and difference from the initial wave runs are shown in Figures 21-24. Differences that are positive indicate wave height reduction and differences that are negative indicate wave height increase. Wave height reductions south of the debris field are about 0.05 to 0.25 ft. Some small increases (negative difference) in the lakeside gauges are due to reflection from the debris. Debris Configuration 2 impacts the wave field to a slightly greater degree than Configuration 1.



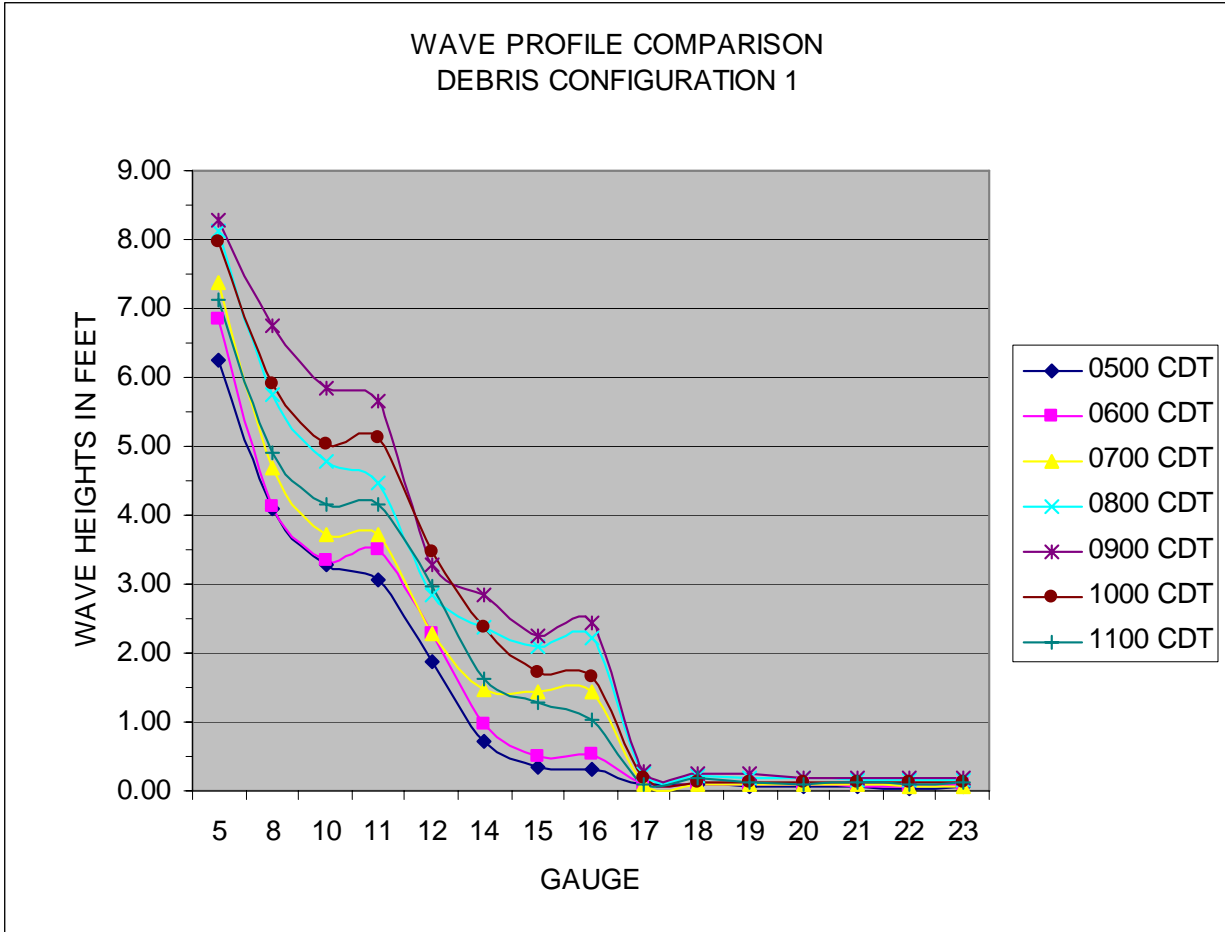


Figure 12-21. Wave height results for Debris Configuration 1 in place

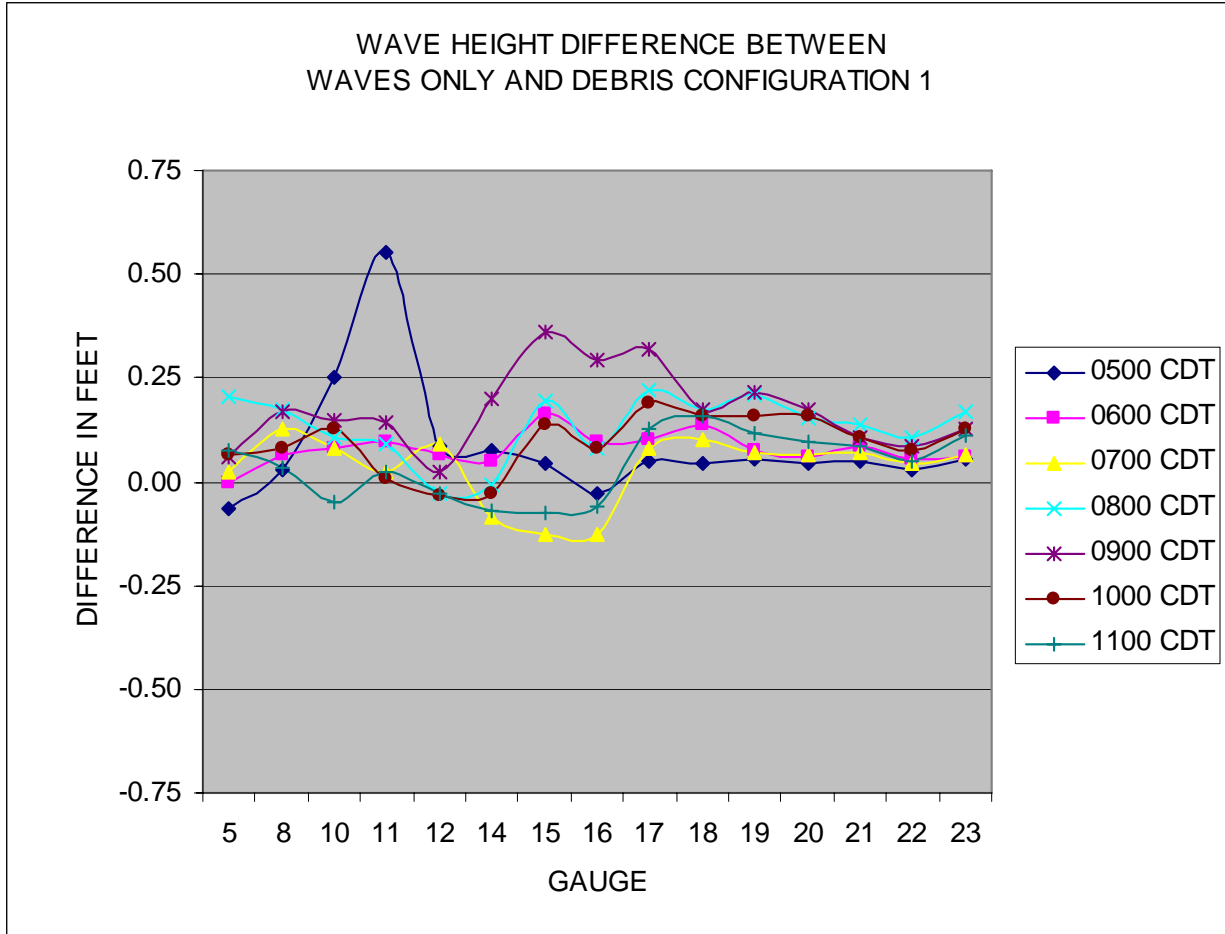


Figure 12-22. Differences in wave height between no-debris (Figure 12-9b) and Debris Configuration 1

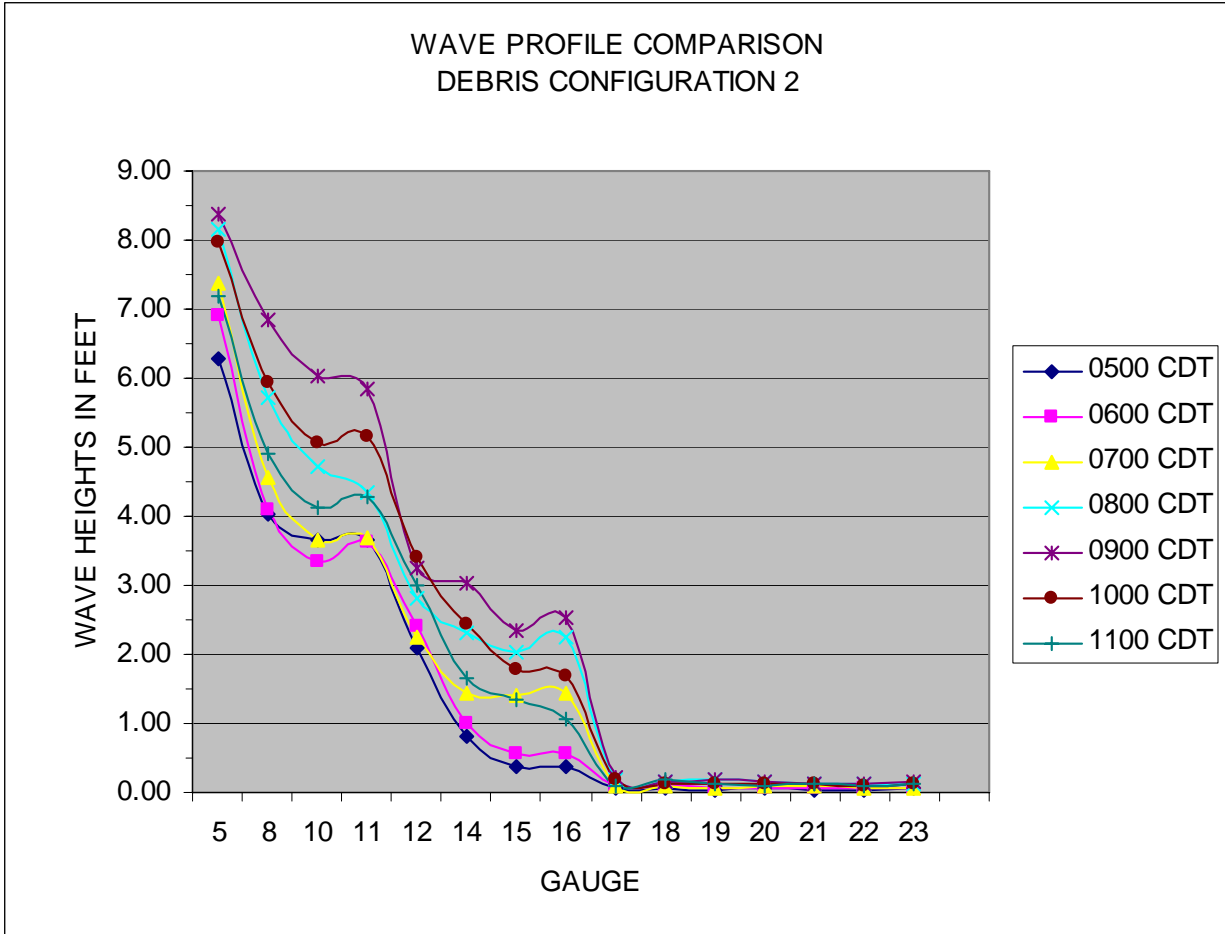


Figure 12-23. Wave heights with Debris Configuration 2 in place

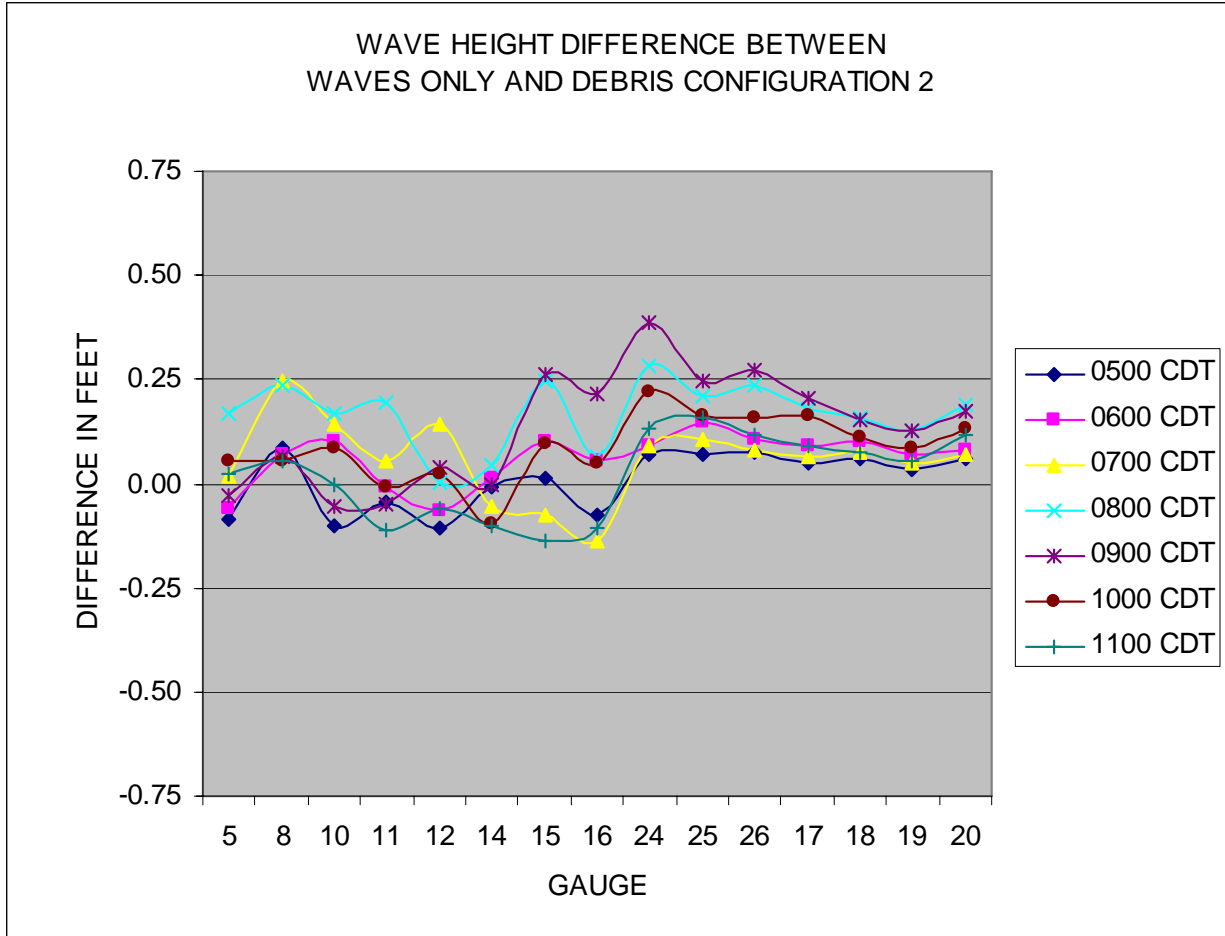


Figure 12-24. Differences in wave height between no-debris (Figure 12-9b) and with Debris Configuration 2

## Effect of Debris on Flow along the Canal

Maximum velocities along the breached zone (but without replicating breaching itself) were recorded with the debris fields discussed above and are presented in Figure 12-25. This figure may be compared to Figure 12-10 for the fully open canal. The debris-induced reductions are on the order of 0.1-0.2 ft/sec, except for the x-component with the heavier debris field 2, which causes significant blockage at the lower water levels.

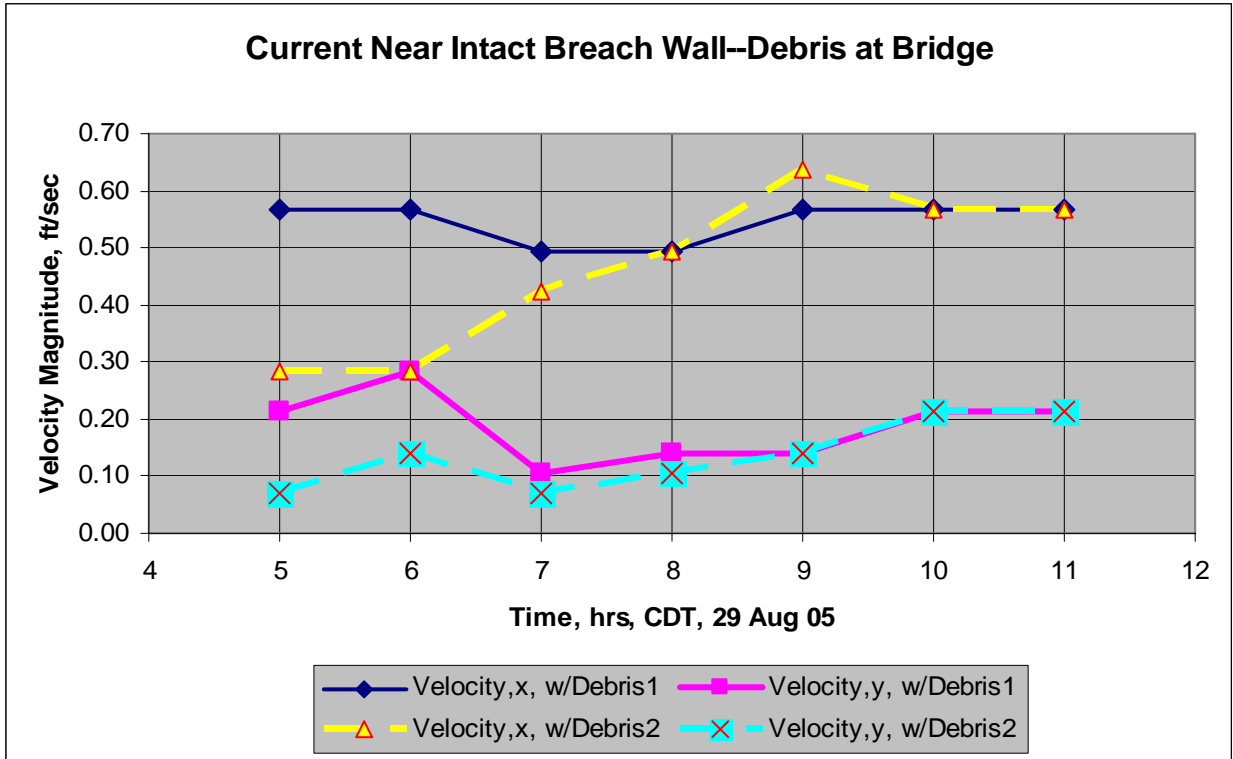


Figure 12-25. Effects of debris field at bridge on canal current near intact breach zone

## Debris Effect on Head Loss at Bridge

In order to more precisely quantify the blockage by Debris Configurations 1 and 2, tests were conducted during which the channel on the lakeside of the Hammond Highway Bridge was blocked a specified amount, and head losses measured. With measurements of head losses across the two debris configurations also measured, their representative areas could be determined from the plot in Figure 12-26. The discharges that were modeled were in a range of estimated discharges flowing through the breach. Flows of 2,953, 15,000, 22,000 and 29,000 cfs were simulated. The flows were created by maintaining a constant Lake Pontchartrain elevation at + 9.3 ft, NAVD88 (2004.65). A breach was not created, but the flow was drained from the basin at the end of the canal (see Figure 12-2) through a pipe and control valve. Discharge was monitored with a Doppler ultrasonic flow meter attached to the discharge pipe. The cross-sectional area changes were created by blocking off the upper portion of the water column with plywood. Flow would be forced to pass along the bottom of the canal as if flowing under the debris field.



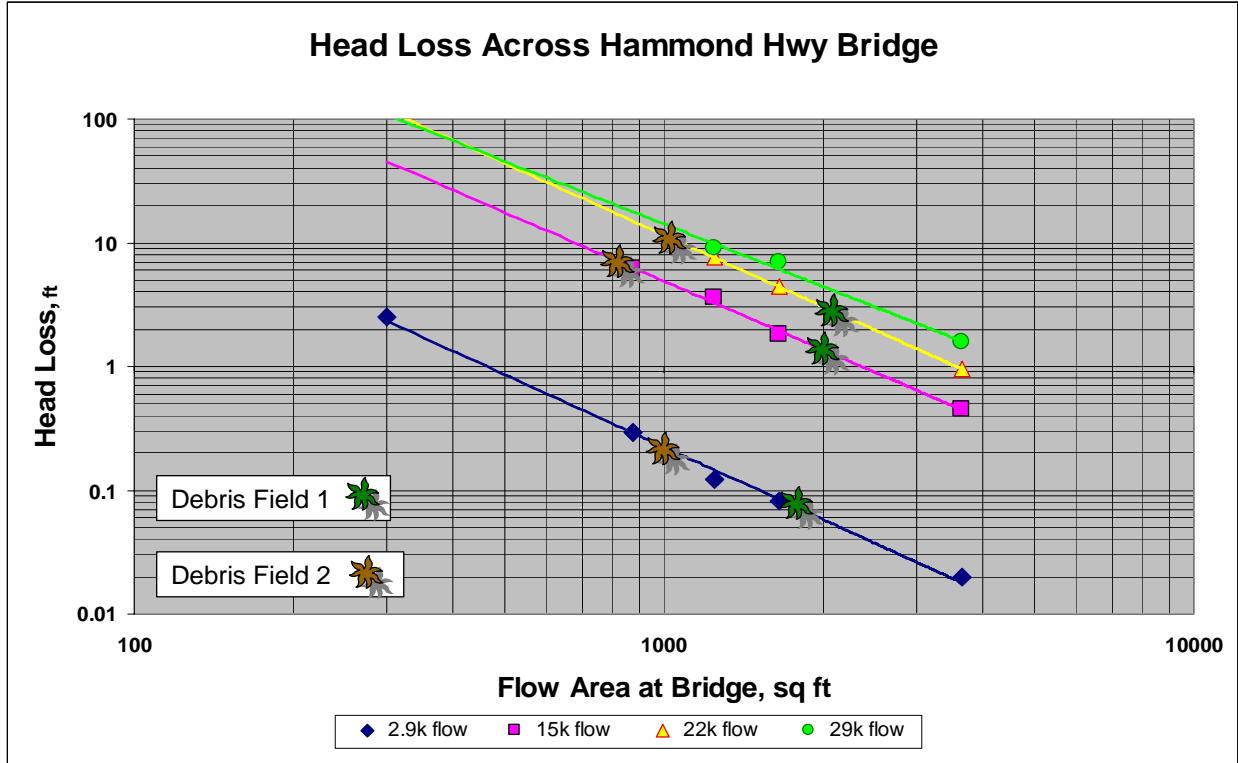


Figure 12-26. Head loss measured between north side and south side of Hammond Hwy Bridge for various canal discharges (lake level at +9.3 ft)

From Figure 12-26, the equivalent flow area of Debris Configuration 1 and 2 were found by finding the flow area on the chart for the measured head loss for the debris fields. Debris Configuration 1 had a flow cross-sectional area in the canal in the range of 1800 to 2000 sq ft. Debris Configuration 2 represented reduced cross-sectional flow area in the range of 850 to 1000 sq ft. Considering the total cross-sectional area under the bridge of 3651 sq ft at the surge level of 9.3 ft, Debris Configuration 1 represented a blockage of about 48 percent of the canal cross-section. Debris Configuration 2 represented about 75 percent blockage.

Based on a photograph taken at 1100 CDT looking through the actual breach into the canal, a graph may be created to estimate the blockage that occurred during the storm. From the photograph, the water elevation in the canal is estimated to be at approximately +3.0 ft. At 1100, Lake Pontchartrain was at elevation +7.2 ft, indicating a head difference of 4.2 ft. Re-plotting the data from Figure 12-26 in the manner shown in Figure 12-27, and assuming a flow range of 15,000 to 29,000 cfs through the breach (this range is representative of breach flow conditions based on analytical work performed in this task area and discussed in Appendix 10. Figure 12-27 shows the flow area blockage by the debris would be in the range of 40 to 70 percent.

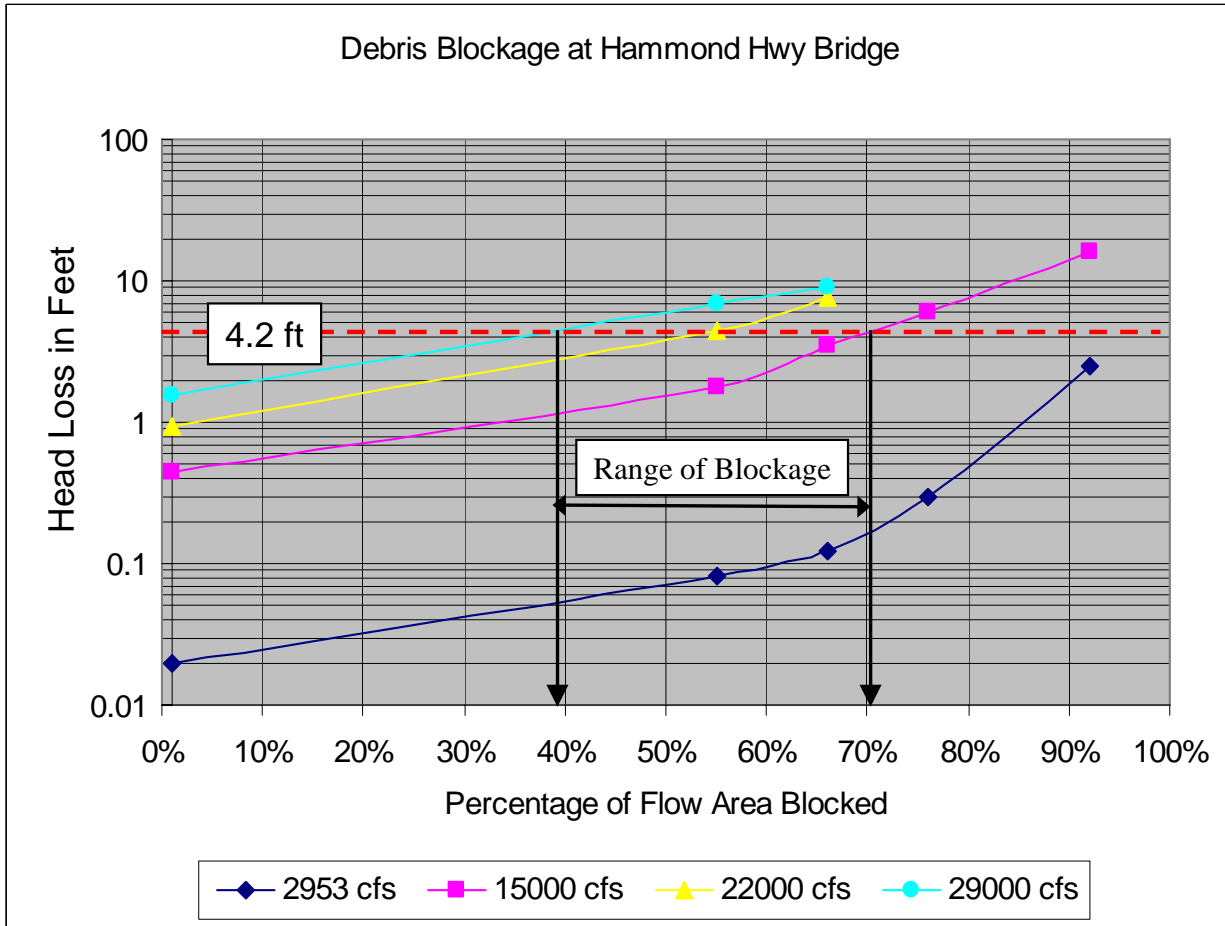


Figure 12-27. Estimated blockage of 17th St Canal by debris at the Hammond Highway Bridge

## Examination of Flow in Canal under Breached Conditions

While making the head-difference measurements discussed above, velocity data were collected at the six locations shown in Figure 12-28. Only data collected at Probes 0, 1 and 2 are discussed here, as these locations would be somewhat representative of actual breach conditions. In this simulation flow is removed from the basin at the end of the canal to create the flow field discussed above, and so the measurements from Probes 3, 4, and 5 would not be indicative of conditions during the breach.

Table 12-5 shows a compilation of the average velocities measured at Probes 0, 1 and 2. Probe 1 was in the center of the canal, south of the bridge. Probe 1 was placed close to the bottom of the canal, near the floodwall, just before the breach zone is reached. Probe 2 was adjacent to the floodwall and near the surface. Canal velocities were measured as high as 11.4 ft/sec (prototype). The flow-restricted areas also created higher velocities approaching the breach zone than for a completely open canal, due to the jetting effect of flow through a smaller area.

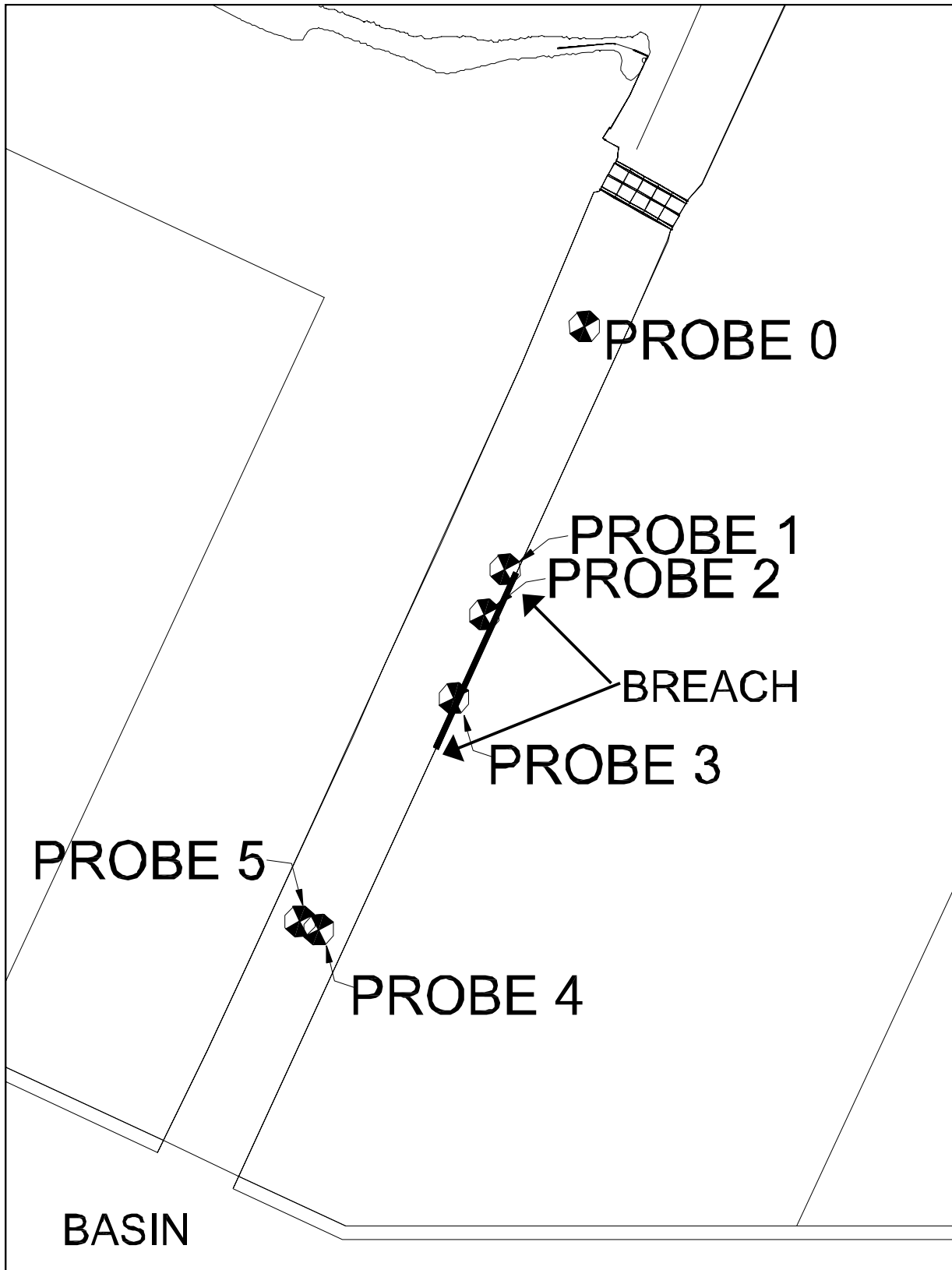


Figure 12-28. Location of velocity probes for breach magnitude flow measurements

**Table 12-5  
Breach Simulation Velocities for Lake Level of 9.3 ft**

Q, cfs	Flow Area, ft <sup>2</sup> at Bridge	Probe 0			Probe 1			Probe 2		
		Vx	Vy	Mag V-Avg	Vx	Vy	Mag V-Avg	Vx	Vy	Mag V-Avg
15,000	3734 (no restriction)	-4.0	0.2	4.0	-3.6	0.1	3.6	-3.7	0.1	3.7
	1650	-4.2	0.3	4.2	-4.3	0.2	4.3	-4.5	0.1	4.5
	1245	-5.1	0.2	5.1	-4.3	0.2	4.3	-4.3	0.3	4.4
	875	-5.6	0.2	5.6	-4.6	0.1	4.6	--	--	--
	300	-7.8	0.9	7.8	--	--	--	--	--	--
	Debris Configuration 1	-5.4	0.1	5.4	-3.8	0.1	3.8	-4.2	0.1	4.2
	Debris Configuration 2	-7.9	1.4	8.0	-4.8	0.0	4.8	--	--	--
22,000	3734 (no restriction)	-6.3	0.5	6.3	-5.6	0.1	5.6	-5.8	0.1	5.8
	1650	-6.9	0.3	6.9	-6.9	0.2	6.9	-6.3	0.2	6.3
	1245	-7.4	0.3	7.4	-8.5	0.3	8.5	-7.6	0.6	7.7
	Debris Configuration 1	-7.7	0.4	7.7	-6.1	0.2	6.1	-6.5	0.0	6.5
	Debris Configuration 2	-11.3	1.3	11.4	-7.4	0.3	7.4	-3.8	0.3	3.9
	3734 (no restriction)	-7.5	0.6	7.6	-6.7	0.2	6.7	-7.3	0.2	7.4
29,000	1650	-11.4	-0.1	11.4	-9.0	0.3	9.0	-9.4	0.6	9.4
	1245	-9.0	0.4	9.0	-10.5	0.4	10.5	-8.4	0.7	8.4

## Summary and Conclusions

A 1:50 scale physical model was designed and constructed for the 17th Street Canal region, New Orleans, on the southern coast of Lake Pontchartrain. The purpose of the model was to aid in establishing wave and current conditions in the 17th St Canal during the time period leading up to the breaching of the floodwall within the canal. The 14,500 sq ft model represented about 1.3 sq miles of the local area in and around the Canal. The ability of a physical model to accurately represent the complex wave interaction with submerged harbors and with the Hammond Highway Bridge justified the study, also providing calibration information for numerical wave models.

Wave and water level conditions from 0500 through 1100 hrs, CDT, on 29 Aug 05 were obtained from numerical studies to provide the boundary forcing conditions for the physical model. Modeling work focused on this time frame in providing wave heights and velocity information throughout the immediate Lake Pontchartrain and Canal region. State of the art equipment, including a directional spectral wave generator, was used in creating the hydrodynamic conditions and making measurements of wave height and velocity.

Physical wave height measurements and photographic observations indicated a number of processes occurring as waves approached the location of the breach. The processes involved in wave height reduction include: 1) refraction of wave energy over the shallower submerged land areas surrounding the harbor away from the canal; 2) reflection of energy off vertical walls in the region between the entrance to the canal near the Coast Guard Harbor and the bridge; and 3) interaction of the wave with the Hammond Highway bridge, most notably reflection. Wave heights near the lakeside of the bridge were 1 to 3 ft in height, reduced from the 6 to 9 ft wave

heights in the open lake. Waves on the south side of the bridge were further reduced to heights below 1 ft.

Velocity measurements due to waves, in the vicinity of the intact floodwall in the region of the breach, were in the range of 0.5 to 0.7 ft/sec along-canal and 0.1 to 0.3 ft/sec cross-canal, i.e., perpendicular to the floodwall.

The Hammond Highway Bridge became an effective reflector of wave energy as water levels rose. Once the surge level reached 8 ft, the wave reflection coefficient increased from 10 percent to nearly 35 percent.

Pump station flow was simulated also, with maximum canal currents reaching 3.2 ft/sec along the canal and 0.5 ft/sec cross-canal in the region of the breach. The flow field from the pumps had minor effect on waves.

The debris field was simulated in the physical model. It most likely was not fully formed until the breach occurred, drawing debris to the bridge due to the strong drawdown of flow from the lake towards the breach. Once the debris was in position, it could reduce both mean flow and wave penetration south of the bridge. The areas represented by the model debris fields were determined by a calibration procedure of measuring head loss due to varying cross-sectional areas at the bridge. Calibration curves from these tests were used to estimate that at potential flow magnitudes through the breach, the debris blocked from 40 to 70 percent of the channel area at the Hammond Highway Bridge.



# Appendix 13

## ADCIRC Numerical Modeling

---

A series of ADCIRC (Luettich and Westerink, 2004) model tests was performed to examine the variation of water surface elevation and maximum current speeds in the 17th Street, Orleans, and London Avenue Canals. Additionally, ADCIRC simulations were performed to examine the variation of water surface elevation in the Inner Harbor Navigation Canal (IHNC). The following provides details on the numerical model setup and results of these tests.

### Grid Development

Individual high-resolution ADCIRC grids were developed for model tests in the 17th Street, Orleans, and London Avenue Canals (Figure 13-1). The grid domains used for these three canals encompasses a portion of Lake Pontchartrain, and spans the entire length of each respective canal, from the lake to its southern pump station. Grid resolution within the canals is on the order of 10 m. Grid bathymetry for all three of these individual grids was developed from the bathymetric data compiled by IPET Task 1.

An examination of the ADCIRC grid used in the Task 4 analysis of Hurricane Katrina suggested that the IHNC and the Mississippi River Gulf Outlet (MRGO) were reasonably well-resolved spatially (on the order of 100m). Comparisons between the more recent bathymetric data compiled by IPET Task 1 and that used originally to develop the large-domain IPET Task 4 grid suggested there were sufficient differences to warrant updating the bathymetry and repeating the Katrina simulation. Therefore, IHNC model tests for this investigation were performed using the large-domain ADCIRC grid used in IPET Task 4 with updated bathymetry.

### Lake Pontchartrain Boundary Conditions

Test simulations using the three individual grids forced along the offshore model boundary in Lake Pontchartrain using water surface elevation (WSE) time series were constructed from observations compiled by IPET Task 1. For the 17th Street model, the observed WSE time history compiled by IPET Task 1 was used directly (Figure 13-2a). For the London Avenue and Orleans models, WSE time histories were estimated by scaling the observed time history for the 17th Street model by the ratio between the observed peak WSE at either London Avenue or

Orleans and the observed peak WSE at 17th Street (Figures 2b and 2c). Because the WSE time series used for these three canals are based on observations, they inherently include the contributions of local and far-field surge generation by wind, barometric pressure, astronomical tide, and wave setup. Lateral boundary conditions within Lake Pontchartrain were defined as radiation boundaries. Sensitivity tests of lateral boundary conditions were performed and findings are summarized in the Sub-Appendix.

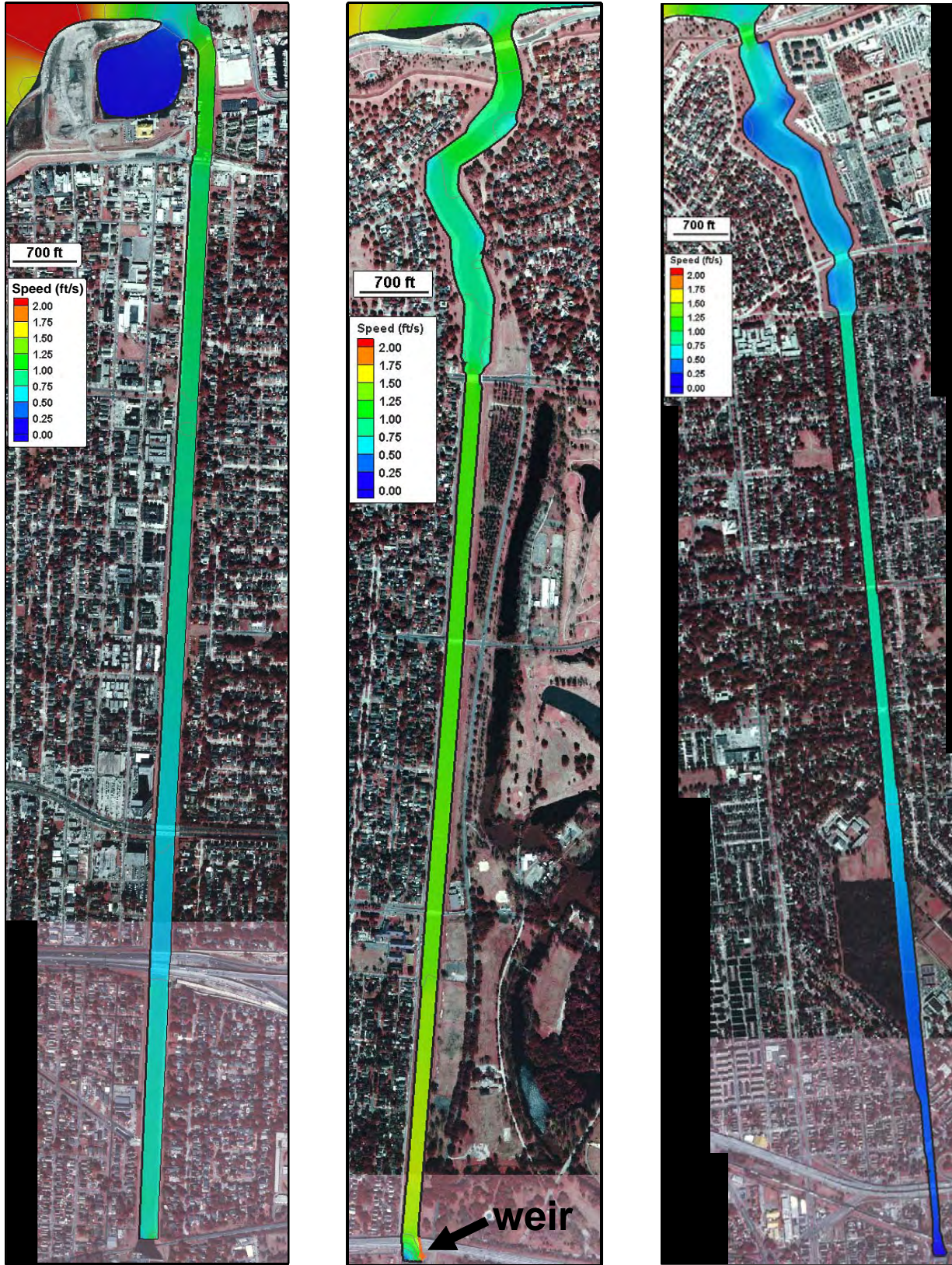


Figure 13-1. 17th Street (left), Orleans (center) and London Avenue (right) Canals grid domains and maximum current speeds without breaches



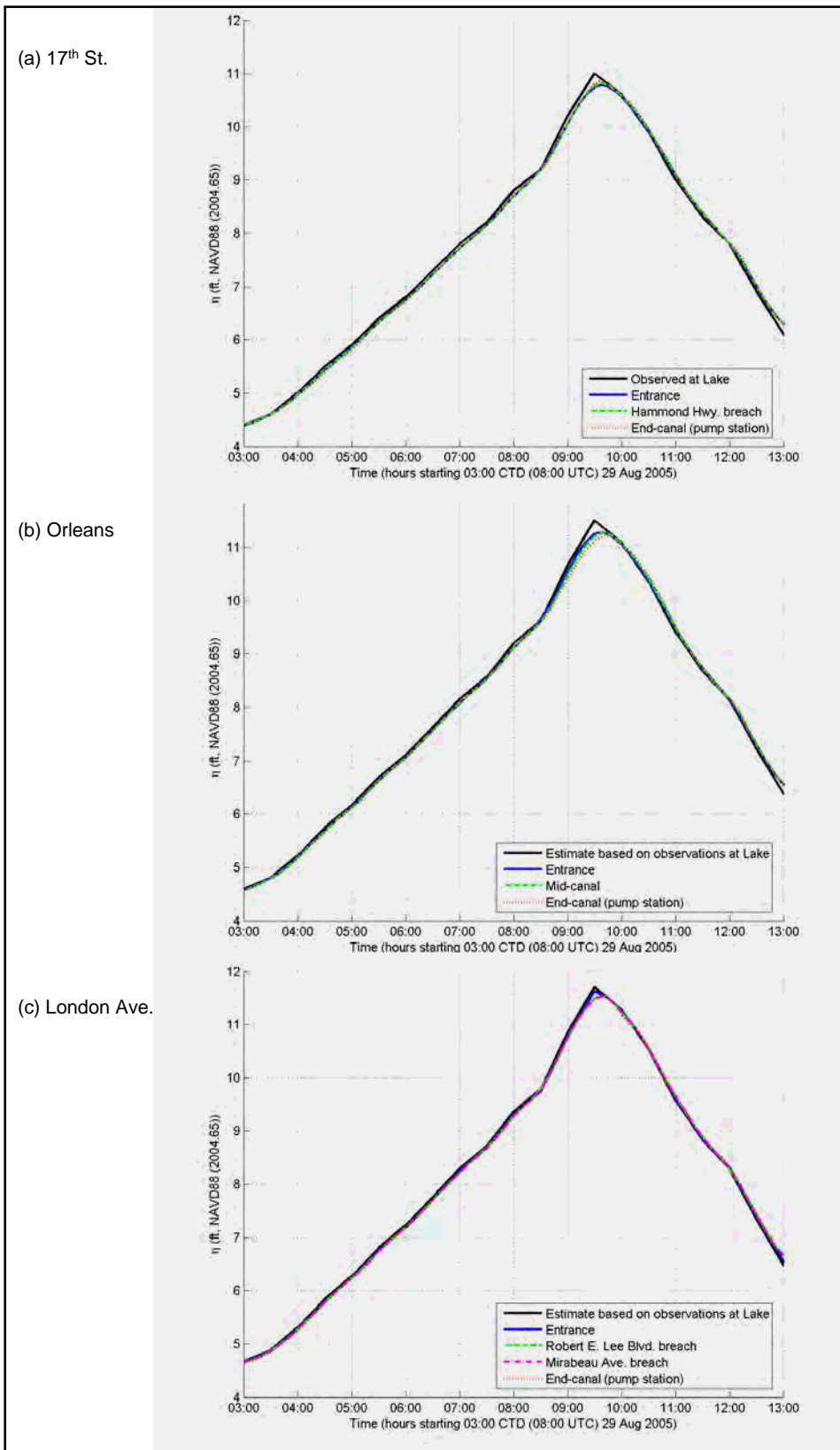


Figure 13-2. Time series of the canals' water surface elevation along the 17th Street, Orleans and London Avenue Canals compared with lake forcing time series

Because simulations in the IHNC were performed using the large-domain grid, water surface elevation at the boundaries of the IHNC were simulated within the ADCIRC model by wind forcing throughout the domain and wave forcing in nearshore domain areas, as performed for IPET Task 4.

## Canal Conditions

In all canals, the side-wall boundary was defined using a slip condition, representing an idealized flow along the canal walls. Additionally, in Orleans canal a sharp-crested weir boundary condition was specified in the vicinity of the existing weir at the pump station (Figure 13-1, center). The ADCIRC input that describes the weir characteristics was modified to accommodate the standard weir formula:

$$q = C \sqrt{g} \left[ \frac{2}{3} H \right]^{3/2} \quad (1)$$

in which,  $q$  is the flow per unit width,  $H$  is head above the weir crest and  $C$  is the discharge coefficient. A reasonable range for the discharge coefficient, based on measurements, is 1.12 to 1.76 (Brater et. al. 1996).

Based on information compiled by IPET Task 1, the Orleans weir's sill elevation was set to 9.7 ft NAVD88 (2004.65), and the discharge coefficient was taken as 1.76 to maximize the influence of this weir on flow and water level in Orleans Canal.

Bottom friction was defined throughout the model domains using a quadratic friction law with the dimensionless friction factor held constant at 0.003<sup>1</sup>. Tests conducted to determine sensitivity to both side-wall boundary conditions and to bottom friction are summarized in the Sub-Appendix.

## No-Breaching Simulation Results

Initial simulations were performed without allowing the canals to breach. In all three of the small scale grid tests maximum velocity magnitudes during the storm, in the absence of a breach, were small. Maximum current speed within the three canals is presented in Figure 13-1. Current speeds were the largest in Orleans Canal, where the influence of the weir at the pump station resulted in maximum current magnitudes around 1.2 fps throughout the southernmost two thirds of the canal.

Figure 13-2 presents simulated WSE time series, with no breaching, for the three canals at the canal entrance, at the breach location(s) or mid-canal, and at the pump station. As the figure

---

<sup>1</sup> In ADCIRC, the friction factor is defined as:  $C_f = \frac{g n^2}{h^{1/3}}$  where  $n$  is Manning's  $n$ .



demonstrates, the WSE time series throughout the three canals varied little, less than 0.2 ft, from the input forcing hydrograph at the Lake Pontchartrain boundary. The simulation results show a slight phase lag of about 15 minutes in the peak surge as the surge wave propagates through the three canals.

Figure 13-3 presents WSE time series simulated in the IHNC using updated bathymetry. The figure shows WSE to the north of the confluence of the IHNC and MRGO, at the confluence of the IHNC and MRGO and adjacent to the Lower 9th Ward breach location. Simulated peak WSE in the IHNC varies from 11.3 ft north of the MRGO confluence to 12.8 ft adjacent to the Lower 9th Ward breach location. Figure 13-3 also presents the simulated time series produced by Task 4 with the original bathymetry. The bathymetric changes made to the ADCIRC grid in the IHNC result in differences in peak water surface of about 0.5 ft and differences in the time of the peak on the order of an hour or two.

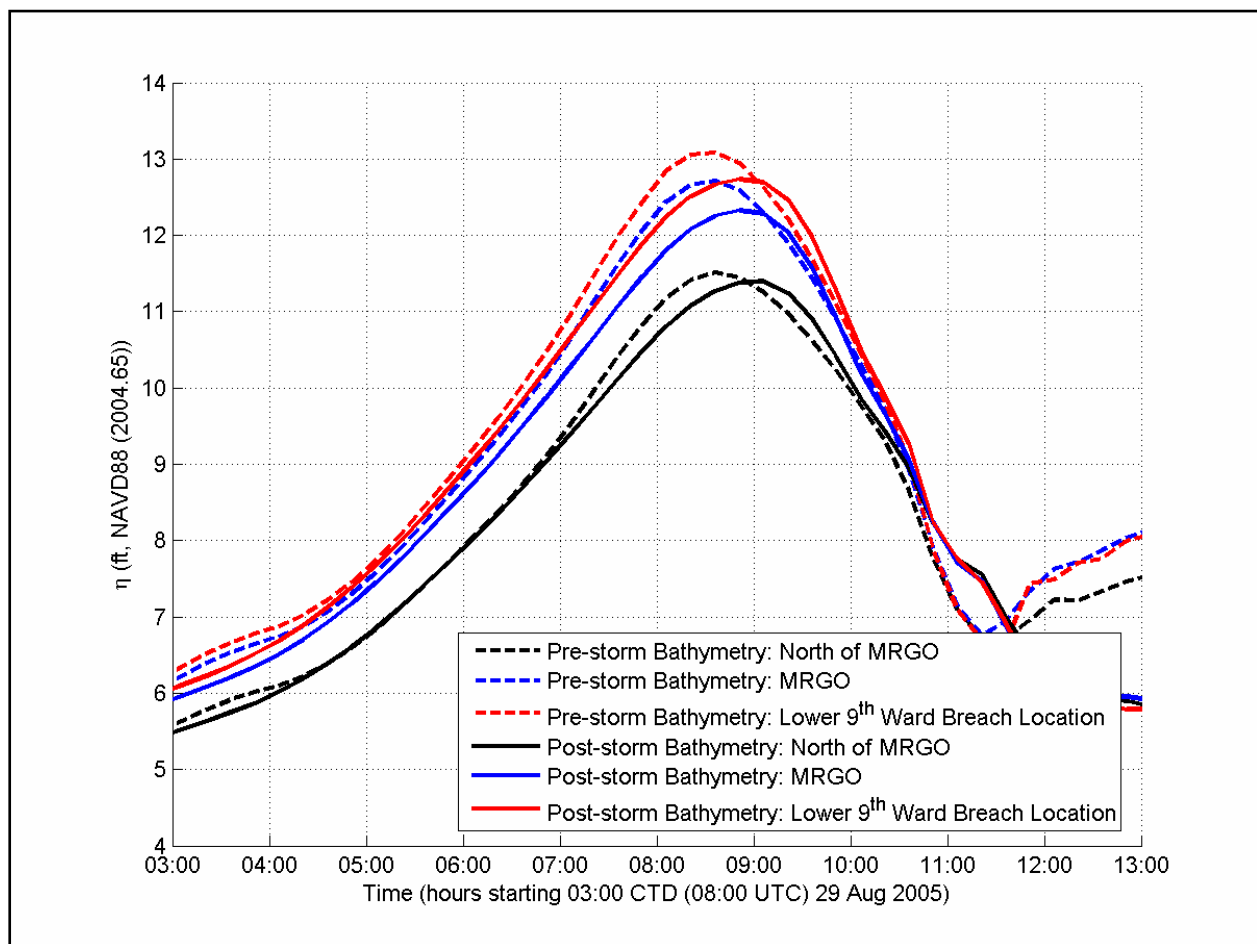


Figure 13-3. Simulated water surface elevations made with updated bathymetry within the IHNC and comparisons with simulations made by IPET Task 4 with original bathymetry

## 17th Street Canal – Detailed Investigation

Additional testing was performed focusing on the 17th Street Canal breach to investigate the influence of pump station operation, bridge piers, and the breach itself on flow and water levels.

### Pump Station Operation

Based on operator interviews and logs at the 17th Street pump station, a time series of pump operations was constructed by IPET Task 1. Figure 13-4 presents the time series of pump operations (top) as synchronized in time with the observed water level (bottom) at the lakefront. Due to 60 and 25 Hz power failures, respectively, Figure 13-4 shows that the pump operation was irregular and not to the station capacity.

The effect of the 17th Street canal pump operation during the storm was initially investigated by disabling the lake WSE forcing to isolate the currents in the vicinity of the breach, without the breach in place. Due to power outages, the pumps performed at capacity for only a brief period of time, and consequently contributed little to the current speed and WSE prior to breaching. As seen in Figure 13-5, the maximum WSE, with pump operation as the only model forcing, was less than 0.4 ft, which is small in comparison to the predicted peak surge. For this same simulation, the maximum outflow current speeds near the breach during peak pump flow (03:00 CDT) were small, between 0.50 fps to 0.65 fps.

With pump operation and the lake WSE boundary enabled, the maximum currents speeds near the breach location decreased to 0.35 fps to 0.50 fps. At the breach location, simulated WSE time series for this simulation (Figure 13-5) is nearly identical to that simulated without pump operation but with the lake WSE forcing (Figure 13-2a). Peak WSE at the breach location for this simulation is 10.8 ft.

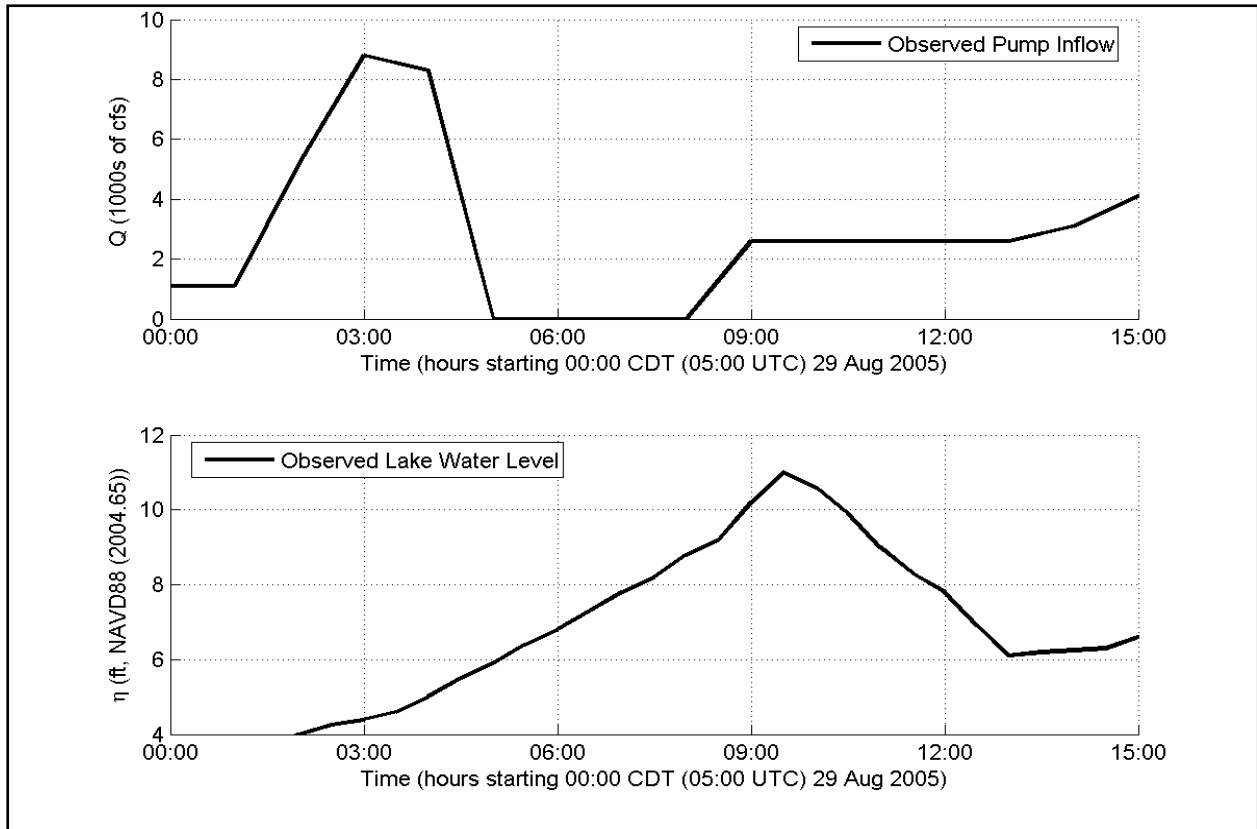


Figure 13-4. Synchronized time series of the 17th Street pump station flows and the observed water levels at the lakefront

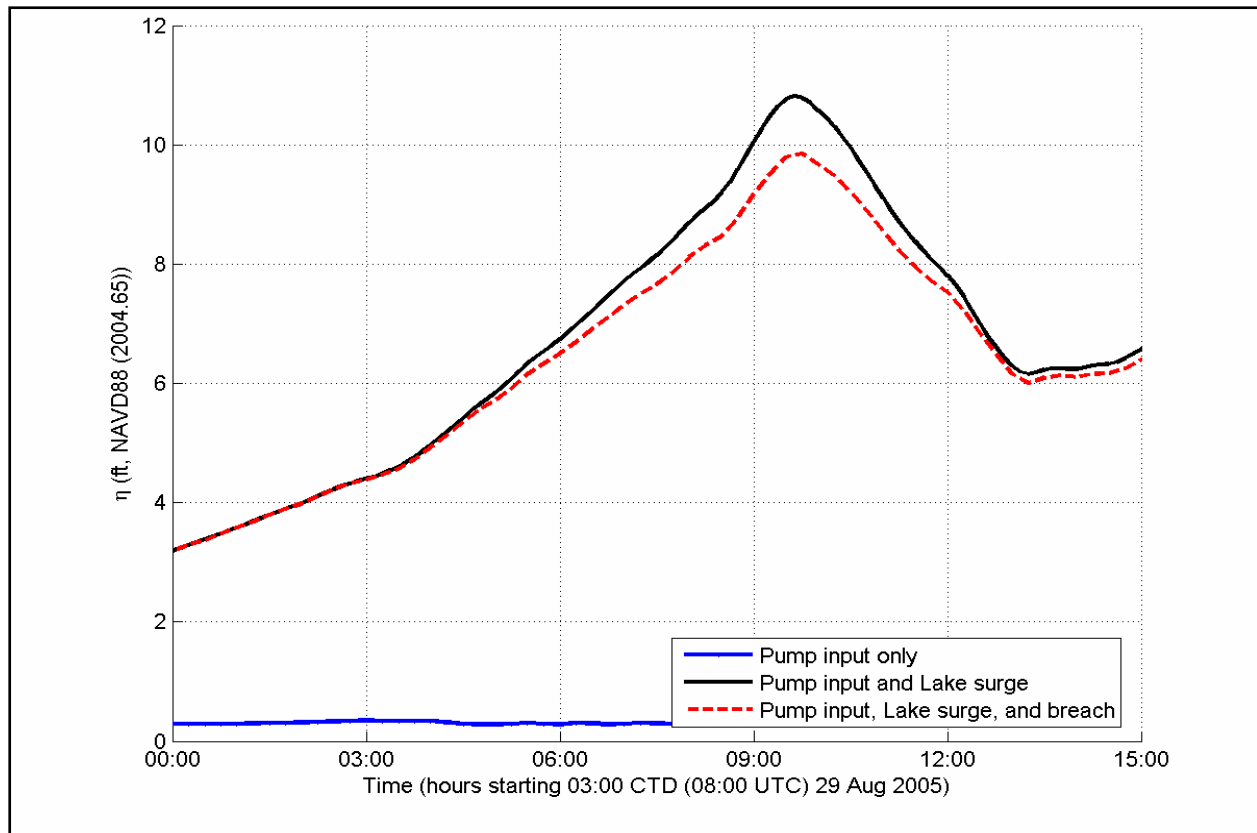


Figure 13-5. Time series comparing predicted water surface elevation change due to the pump, lake surge, and breach

## Bridges

To account for friction losses due to the Hammond Highway Bridge, the ADCIRC bridge pier feature was employed. Although the flow beneath the Hammond Bridge was ultimately obstructed by debris subsequent to the breach, sensitivity tests using varying degrees of bridge pier friction and the ratio of pile projected area to flow area showed little effect on current speeds and water surface elevation simulated with ADCIRC at the breach location.

### Breach South of Hammond Highway Bridge

Model simulations with the breach south of the Hammond Highway Bridge in place were performed by using a sharp-crested weir boundary condition to define the breach. A range of sharp-crested weir coefficients, sill elevations, and breach widths were tested. Sill elevation and breach widths were based on the information regarding the breach timing and breach dimensions gathered by IPET Task 1. Initially, two breach geometries were tested. Breach Geometry 1 is defined by a sill height of 7 ft NAVD88 (2004.65) and breach width of 225 ft to represent the initial but small breach that occurred around 06:00 CDT. Breach Geometry 2 is defined by a sill height of 4 ft NAVD88 (2004.65) and breach width of 450 ft to represent the wider and deeper

breach that occurred after 09:30 CDT. Three simulation configurations were tested using these geometries:

- Breach Geometry 1 throughout the simulation duration.
- Breach Geometry 2 throughout the simulation duration.
- Breach Geometry 1 from the start of the simulation to 09:30 CDT and Breach Geometry 2 from 09:30 CDT to the end of the simulation.

Each of these geometric configurations was simulated with ADCIRC twice, first setting the weir discharge coefficient to 1.12 (lower limit) and then setting the weir coefficient to 1.76 (upper limit) to bracket the range of discharge expected through the breach opening.

As expected, there were measurable differences between the peak discharge through the breach for configurations A and B. However, differences between the peak discharge through the breach for configurations B and C were comparable. There were some differences in the simulated discharge time series between 06:00 CDT and 09:00 CDT between configurations B and C. The remainder of the discussion herein will focus on configuration C, as it appears to reasonably represent the breach within ADCIRC, particularly during peak flows at the time of final levee wall failure.

Figure 13-6 presents simulated WSE time series for selected locations within the 17th Street canal for the upper (top) and lower (bottom) values of the discharge coefficient. The figure shows that the lower value of discharge coefficient results in a larger peak surge at the breach and pump station. Simulated peak WSE at the breach is about 10.3 ft and 9.8 ft, NAVD88 (2004.65) with the lower and upper discharge coefficients, respectively.

Figure 13-7 presents a comparison of contour snapshots of peak current speed as a function of discharge coefficient. The contour plots show that the upper and lower values of the discharge coefficient result in currents speeds that are on the order of 10 and 7 fps, respectively. Figure 13-8 presents snapshots of the current field near the breach at various times in the simulation for the upper discharge coefficient case. For this case, maximum current speeds in the canal ranged from 4 fps to 6 fps during the initial outflow of the breach (06:00 CDT) to 8 fps to 10 fps at the storm peak (09:30 CDT), respectively.

Figure 13-9 presents the total breach discharge time series as simulated with ADCIRC using the lower and upper values for discharge coefficient and compares them with a basic hydraulic-formula solution for 17th Street provided in Appendix 12. Although there is a difference in the time of the peak outflow, the magnitudes of the predictions bracket the basic-formula solution well.

## Summary

In summary, the ADCIRC model tests demonstrated that, in the absence of breaching, current speeds within the canals are small, on the order of 1 fps. In the absence of breaching, WSE nearly matches lake WSE throughout the 17th Street, Orleans, and London Avenue Canals. Conversely, WSE in the IHNC does vary from the Lake WSE by more than 1.5 ft.



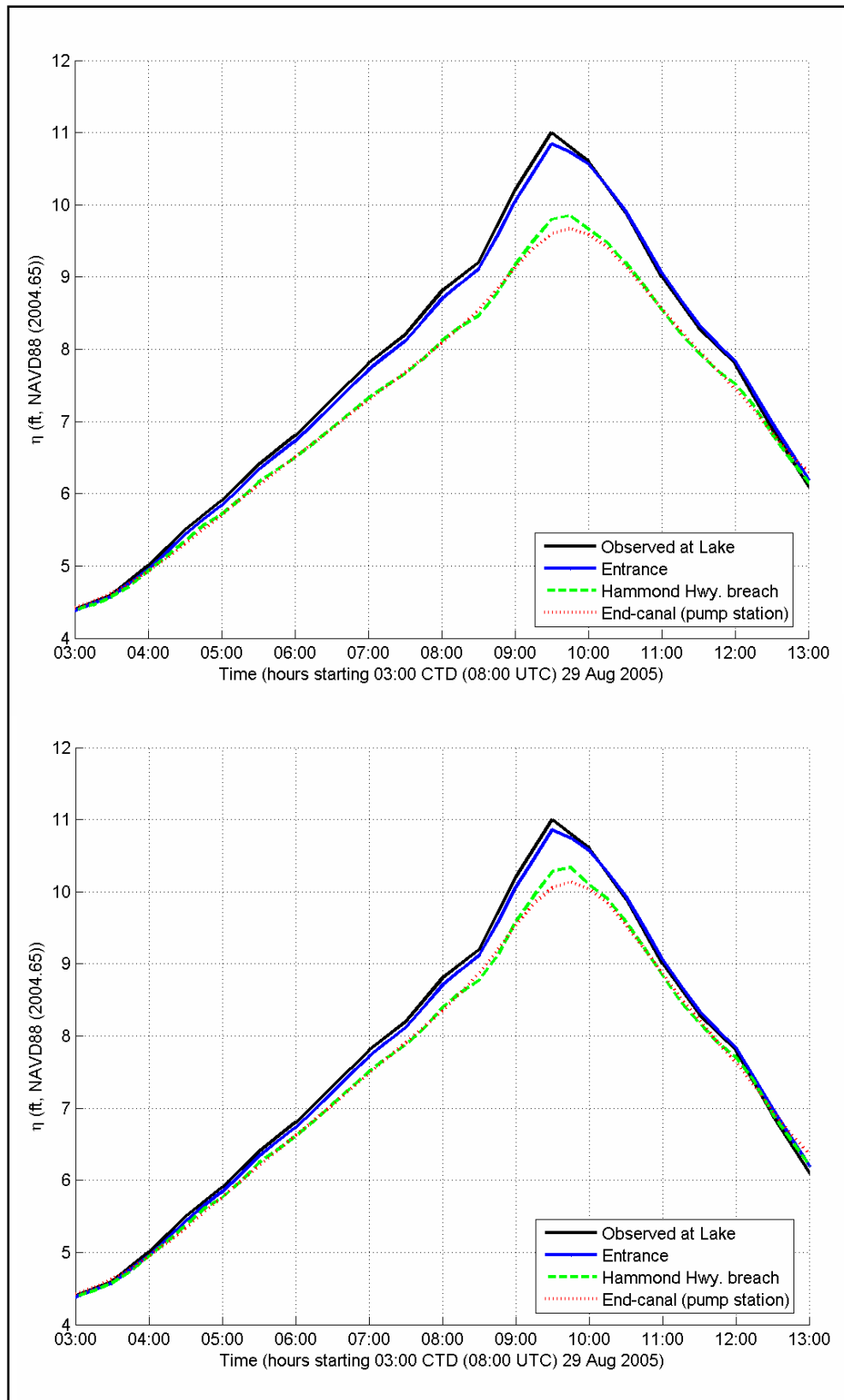


Figure 13-6. Comparison of water surface time series throughout the 17th Street Canal for bracketing values of the discharge coefficient: 1.76 (top panel) and 1.12 (bottom panel)

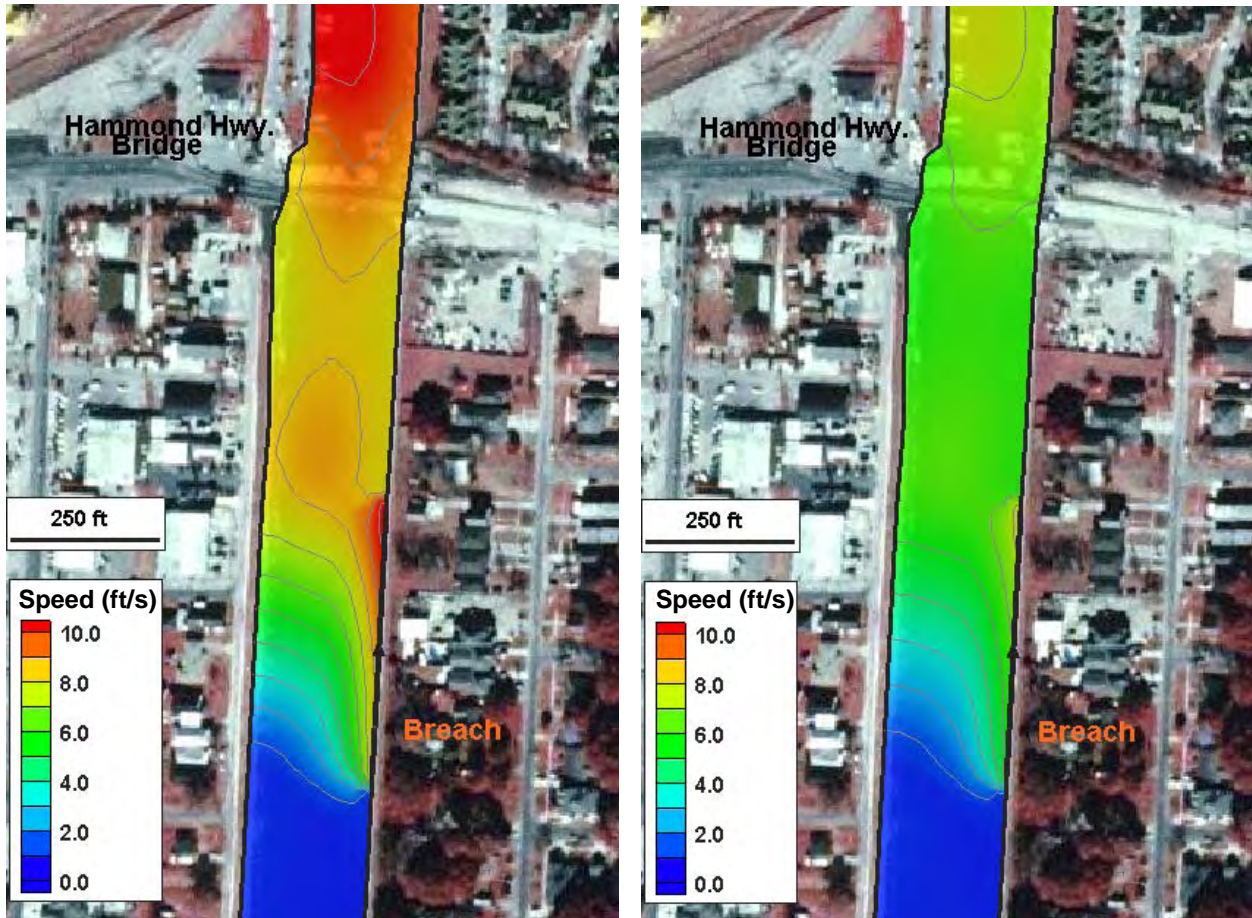


Figure 13-7. Maximum current speed with breach discharge for simulations with the upper (left) and lower (right) discharge coefficients

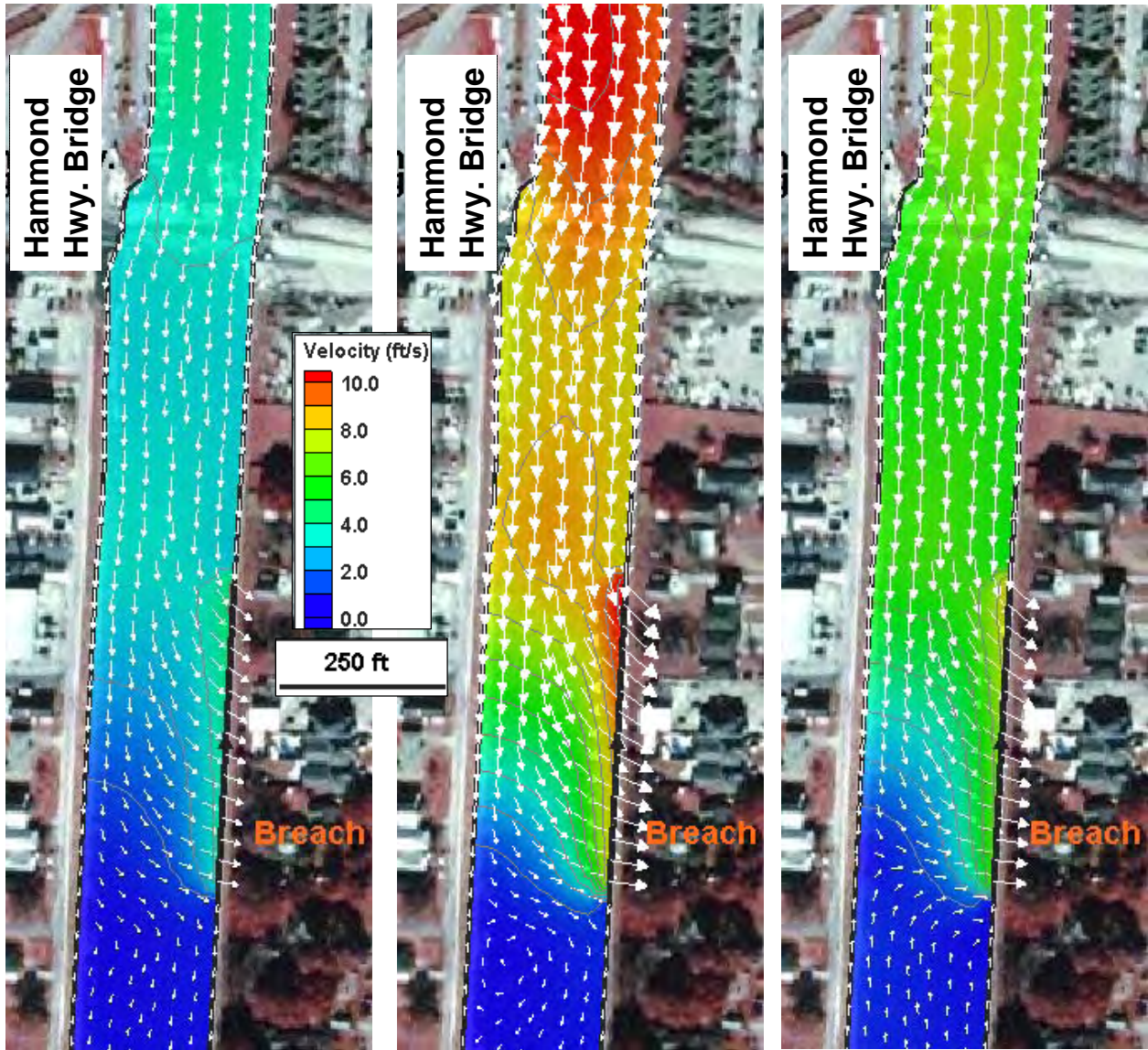


Figure 13-8. Snapshots of simulated current field during 17th Street breach event at 0600 CDT (left), 0930 CDT (center), and 1100 CDT (right)



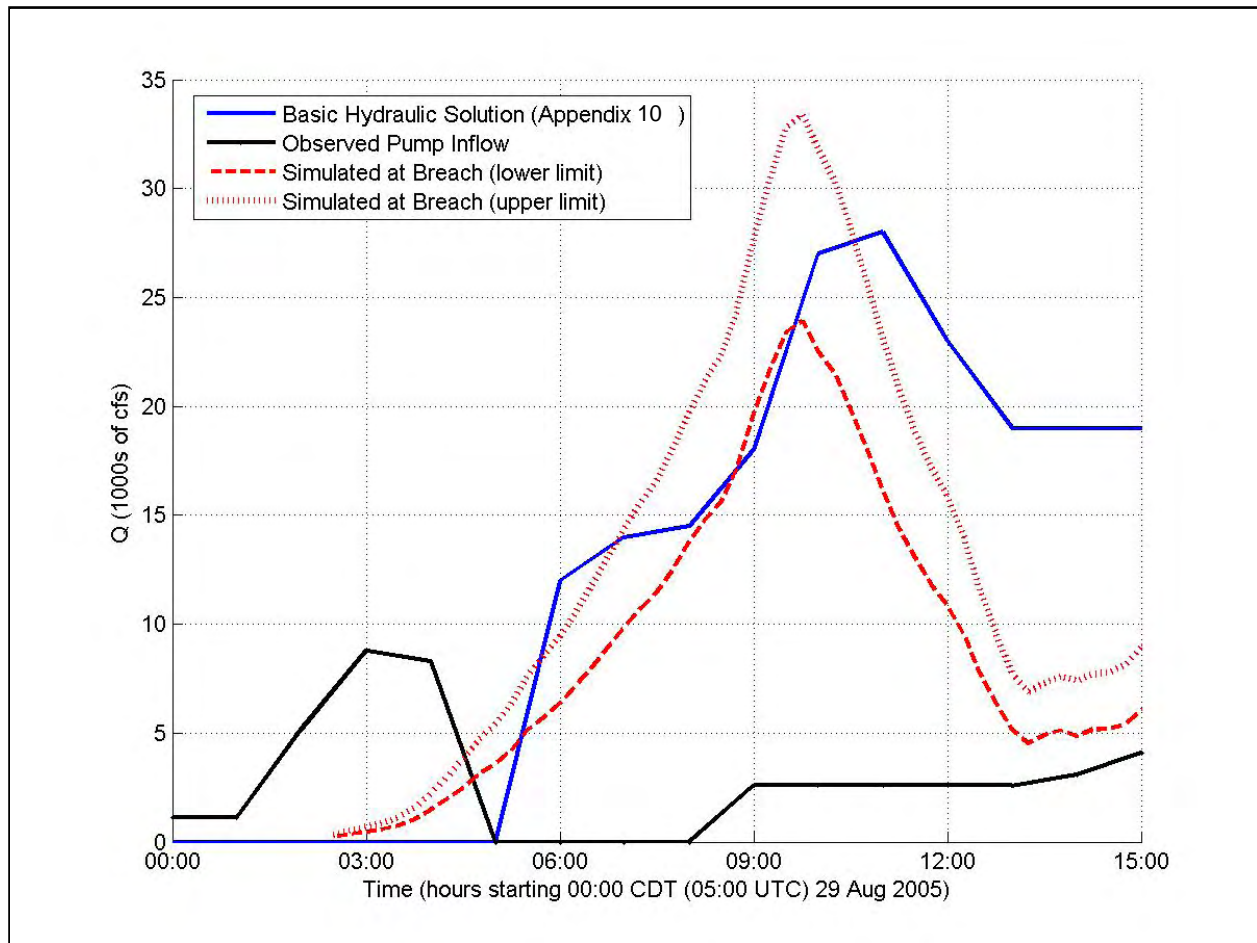


Figure 13-9. Simulated breach discharge for specified discharge coefficients as compared with Dean's solution

In the 17th Street canal, model tests indicate that pump operations had negligible impacts on the flow field and WSE within the canal. With a breach open south of the Hammond Highway Bridge, flow conditions change dramatically, with peak currents as high as 10 fps, while peak WSE drops by almost 1.5 ft relative to the peak lake WSE.

## Sub-Appendix

The effect of the specification of the open water lateral boundary conditions was investigated via a series of test simulations on the 17th Street model. The offshore lake boundary condition is a time series of WSE from the Katrina ADCIRC output provided by IPET Task 4. The lateral boundaries are specified as combinations of radiation and slip wall. In all of the test cases of the lateral boundary conditions the WSE variations at the breach are essentially the same regardless of the boundary condition specified, with the exception that the case where no radiation boundary was specified, a small amplitude numerical reflected wave occurred.

A series of tests was conducted to investigate the canal side-wall boundary condition using the London Avenue canal model. Two boundary conditions were tested: 1) a slip condition, representing an idealized flow at the canal walls and 2) a no-slip condition, representing the effects of viscosity on the flow at the canal walls. While there are some differences in the velocity fields between the slip and no-slip cases, differences in water level within the canal are imperceptible. Furthermore, these differences in water level are well within the uncertainty of the water level hydrograph input and numerical model error.

To determine the relative impact of friction on the velocity fields and water levels within the canals, sensitivity tests were conducted using the London Avenue Canal model. Bottom friction was defined throughout the model domain using a quadratic friction law, with the dimensionless friction factor,  $C_f$ , held constant. Two values of the dimensionless friction factor were assessed: 0.003, representing a smoother bottom, and 0.005, representing a rougher bottom. These values were selected to represent a reasonable range within the canals and follow the recommended values presented in Chow (1959). As with the side-wall boundary condition investigations, bottom friction impacts to water levels within the canal were imperceptible. In addition, the differences in velocity fields were small, with the largest differences occurring at the canal entrance during rising surge. Here, the largest difference was 0.03 ft/s, or 3%.

## References

Brater, E. F., King, H. W., Lindell, J. E. and C. Y. Wei. 1996. Handbook of Hydraulics, 7th Edition, McGraw-Hill Inc., New York.

Chow, V. T. 1959. Open Channel Flow. McGraw-Hill Book Co., New York.

Luetlich, R. and J, Westerink. 2004. A (Parallel) **AD**vanced **CIRC**ulation Model for Oceanic, Coastal and Estuarine Waters: ADCIRC Formulation Version 44.19.

[http://www.marine.unc.edu/C\\_CATS/adcirc/document/ADCIRC\\_main\\_frame.html](http://www.marine.unc.edu/C_CATS/adcirc/document/ADCIRC_main_frame.html)



# Appendix 14

## Detailed-Scale STWAVE Modeling

---

### Introduction

This appendix contains a description of the general STWAVE model used in this study. In this appendix we shall only treat some modifications to the general model to allow its application to key situations within the scope of this study and to describe the model applications.

### Modifications to STWAVE

In the form of STWAVE distributed for general use, only two types of side boundary conditions are allowed:

1. Fully-absorptive boundaries where all energy is absorbed; and
2. Radiative boundaries where all energy is assumed to pass through the side without any reflection.

Neither of these conditions is appropriate for wave propagation within a steep-sided or walled canal. Consequently, the model was adapted for use here via the incorporation of reflective points that were aligned along the sides of the canal. Once these points were identified, and energy was propagated into them, the waves were reflected using the “mirror-angle” assumption with no diffraction, i.e.

$$\alpha_r = \theta_m - \alpha_i$$

where

$\alpha_i$  is the incident angle

$\alpha_r$  is the reflected angle, and

$\theta_m$  is the angle of the mirror

The present wave generation equations included within STWAVE are based on wave growth within an infinitely wide fetch. Recent publications (Kahma and Pettersson, 1994; Pettersson, 2004) have presented evidence suggesting that the wave generation process can be significantly affected by fetch width. The primary equation within STWAVE governing wave growth is its representation of the evolution of peak spectral frequency as a function of propagation time between two adjacent columns in the computational grid. Pettersson's work suggests that the rate of change of peak frequency at short fetches is reduced by about a factor of 40%. This adjustment was made to the growth equation in the standard version of the model.

Studies have shown that, even in situations with complex bathymetry, diffraction in most wave spectra can be modeled via a phase-averaged diffusion operator; however, such an approximation may not be very good in the vicinity of a hard, surface-piercing structure. As part of an ongoing effort to update the STWAVE code, a new method for representing diffraction in spectral models has been formulated. This form preserves solution accuracy in both the near field and far field of the domain, even for the case of very narrow spectra near structures.

A single spectral component (or its monochromatic counterpart) will have a velocity potential of the form

$$\phi = \frac{g}{\omega} \frac{\cosh[k(h+z)]}{\cosh(kh)} a e^{-i\omega t}$$

where  $g$  is gravity,  $h$  is the water depth,  $z$  is the vertical coordinate with zero at the water surface,  $a$  is the topography of the free surface at time = 0 (basically an amplitude function in  $x$  and  $y$ ),  $\omega$  is radial frequency,  $k$  is wave number and  $t$  is time. Since the velocity potential is irrotational, we must have

$$\frac{\partial^2 a}{\partial x^2} + \frac{\partial^2 a}{\partial y^2} + k^2 a = 0$$

If we consider a second function such that

$$\varphi = \frac{\cosh[k(h+z)]}{\cosh(kh)} D_0(kr) e^{-i\omega t}$$

it can be shown that  $\varphi$  also satisfies the Laplace equation, and we have

$$\frac{\partial^2 D_0}{\partial x^2} + \frac{\partial^2 D_0}{\partial y^2} + k^2 D_0 = 0.$$

Using Green's theorem and noting that the form of  $D_0$  can be written in terms of Bessel functions of order zero, Lacombe shows that the complex amplitude of a wave inside a bounded

region can be written as an integral around the boundary (similar to the derivation of wave diffraction in the Huyghens-Kirchoff integral used in optics),

$$a_p = \oint_S \frac{a(s) \cos(\theta) + \cos(\alpha)}{\sqrt{r}} \frac{1}{2} e^{-i(\rho_0(s) + kr - \pi/4)} ds$$

where  $a(s)$  is the amplitude at point “s” along the boundary S,  $\rho_0(s)$  is the phase of the complex amplitude at s, r is the distance from the boundary to point “p”,  $\theta$  is the direction from “s” to “p”, and  $\alpha$  is the wave propagation angle at “s.” For the case of a straight-line boundary (ignoring 180° reflections) and normalizing r by the wavelength, this can be written as

$$a_p = \int_Y \frac{a(y) \cos(\theta) + \cos(\alpha)}{\sqrt{y}} \frac{1}{2} e^{-i[2\pi(y \sin \alpha + r) - \pi/4]} dy$$

where the integral proceeds along y over the line segment “Y.” This form for diffraction allows for a variation in wave height along Y rather than requiring a constant wave height as in a Fresnel integral form for diffraction but is otherwise quite similar to that representation, with the added stipulation that a near-field solution form can be used in the representation shown here in place of the  $\sqrt{r}$  denominator.

Berkoff (1973) showed that the combined effects of refraction and diffraction could be solved via the “mild-slope approximation”

$$\frac{1}{a} \left\{ \Delta a + \frac{1}{c c_g} \nabla a \cdot \nabla (c c_g) \right\} + k^2 - \nabla \rho \cdot \nabla \rho = 0$$

and

$$\nabla \cdot (a^2 c c_g \nabla \rho) = 0$$

where c is the wave phase velocity  $c_g$  is the wave group velocity, and  $\rho$  is wave phase along the ray. The first equation is the eikonal equation for the refracted-diffracted ray and the second is the condition for energy conservation along the ray. The second term within the curly brackets is the combined refraction-diffraction coupling term. Accurate solution of this equation requires a resolution in x and y such that the grid increment is smaller than L/8 where L is wavelength.

A singularity in the amplitude function exists at the boundary of a surface-piercing structure. The sharp interference patterns in monochromatic waves passing by such a structure are created by the superposition of the diffracted wave from this singularity and the geometric wave passing by it. Near a singularity, we have

$$\frac{\frac{\partial a}{\partial y}}{\frac{\partial^2 a}{\partial y^2}} \rightarrow 0$$

as  $y \rightarrow 0$ . This suggests that the diffraction pattern will depend primarily on the first term in the curly brackets near a structure, with a secondary (relatively slow) dependence on refraction and other processes. In such cases, it is possible to adapt a series solution for this problem, i.e.

$$\bar{\Gamma}_p = \bar{\Gamma}_p^{(0)} + \bar{\Gamma}_p^{(1)} + \dots$$

where  $\bar{\Gamma}_p$  is the energy flux vector at “p” and the superscripts “(0)” and “(1)” refer to the order of magnitude of the terms. In this case, we allow the diffraction solution to represent order zero and add the effects of refraction as a second step to the solution.

The solution for diffraction is very accurate provided that the resolution along y is sufficiently small, say on the order of  $L/20$ . However, its solution is quite slow numerically on such a scale; hence direct solution of the Huyghens-Kirchoff form for diffraction is too cumbersome for most wave modeling purposes. Thus, instead of the exact form, we substitute a pre-solved, discretized complex operator D, defined as

$$\{R[D(\delta y, \delta x, \alpha), I(\delta y, \delta x, \alpha)]\}$$

where R is the real part of the H-K integral and I is the imaginary part of the H-K integral for an incident wave of unit amplitude. The terms inside the parentheses denote the resolution in y and x for fixed values of  $\alpha$ , respectively. After sensitivity testing, these have been set in the current version of the code to  $\delta y = L/400$ , and  $\delta x = L/10$ . Inside STWAVE diffraction then becomes represented as a simple inner product with amplitude

$$|a_p| = \left[ \sum_{k=1}^M a_k R_k(\delta x, \delta y, \alpha) \right]^2 + \left[ \sum_{k=1}^M a_k I_k(\delta x, \delta y, \alpha) \right]^2 + R_B + I_B$$

where M is taken to cover a sufficient range in y to provide an accurate approximation to the total integral. The phase of the wave at “p” is given by

$$\rho_p = \tan^{-1} \left( \frac{\sum I}{\sum R} \right)$$

where  $\Sigma_I$  and  $\Sigma_R$  are the sum of the imaginary and real contributions to the H-K integral, respectively. The energy flux angle at “p” is found from

$$\alpha_I = \sin^{-1} \left( \frac{k \partial \rho_p}{\partial y} \right)$$

By shifting the discretized elements of the operator  $\pm n$  positions along  $y$ , a simple estimate of the angle can be obtained that is not directly dependent on the scale of the grid resolution.

Treating the diffraction-only solution in terms of a field equation for the rays, we can represent the effects of refraction on path (flux angle and displacement) and amplitude as

$$y_I^{(1)} = y^{(0)} + \sum_{i=I_0+1}^I \delta y_i(x, y)^{(0)}$$

$$\alpha_I^{(1)} = \alpha^{(0)} + \sum_{i=I_0+1}^I \delta \alpha_i(x, y)^{(0)}$$

$$a_I^{(1)} = a^{(0)} \prod_{i=I_0+1}^I S_{r_i}(x, y)^{(0)}$$

where  $I_0$  references the  $x$ -location of the boundary and  $I$  references the location of the point at “p.” The term  $S_{r_i}$  references the effective change in amplitude along the ray due to refraction at the  $I^{\text{th}}$  column of the grid. To implement additional source terms such as wave breaking, this is modified to the form

$$a_I^{(2)} = a^{(0)}(x_0, y_0) \prod_{i=I_0+1}^I S_{r_i}(x, y) S_{e_i} [a^{(1)}(x, y)^{(1)}]$$

where the term  $S_{e_i}$  represents the sum of all additional source terms considered at the  $I^{\text{th}}$  column of the grid.

The same bathymetries generated for the ADCIRC grids were adapted to a rectangular basis and used for all simulations in the outfall canals (17th Street, London Avenue, and Orleans Avenue) and in the navigation canal (Inner Harbor Navigation Canal, IHNC). In all three of the outfall canals, dissipation due to entrance losses was similar to those observed in both the physical model and the Boussinesq model. Energy losses due to bridges were simulated by an empirical loss function that simply removed the same proportion of energy from the waves passing under the bridge as measured in the physical model study, rather than simulating the energy loss via equivalent frictional loss process.

The results of the STWAVE simulations showed that waves in the outfall canals were essentially damped to less than 1 foot by the time they reached the “hurricane proof” bridges at



the 17th Street Canal and the London Avenue Canal. These runs also showed that waves in the Orleans Avenue Canal were almost entirely blocked by the extremely curved entrance to this canal. In all areas in the outfall canals, waves were continually reduced due to side losses and interactions with bridges and at all sites along these canals waves did not exceed 1½ feet, including local wind wave generation.

In the IHNC, runs with the “narrow-fetch” version of STWAVE were used to estimate wave conditions along the canal. Figure 14-1 shows the line of maximum wave height along the MRGO/GIWW entrance to the IHNC from the east; and Figure 14-2 shows the line of maximum wave height along the northern portion of the IHNC down to its southern end. In both cases, two patterns are evident: a rapid damping of longer period waves that are entering the canals from the Gulf on the east and Lake Pontchartrain on the north and a growth of waves due to local wind generation along the canals. As seen in Figure 14-2, estimates of the latter process appear to be consistent with photographic evidence at the southern end of the IHNC.

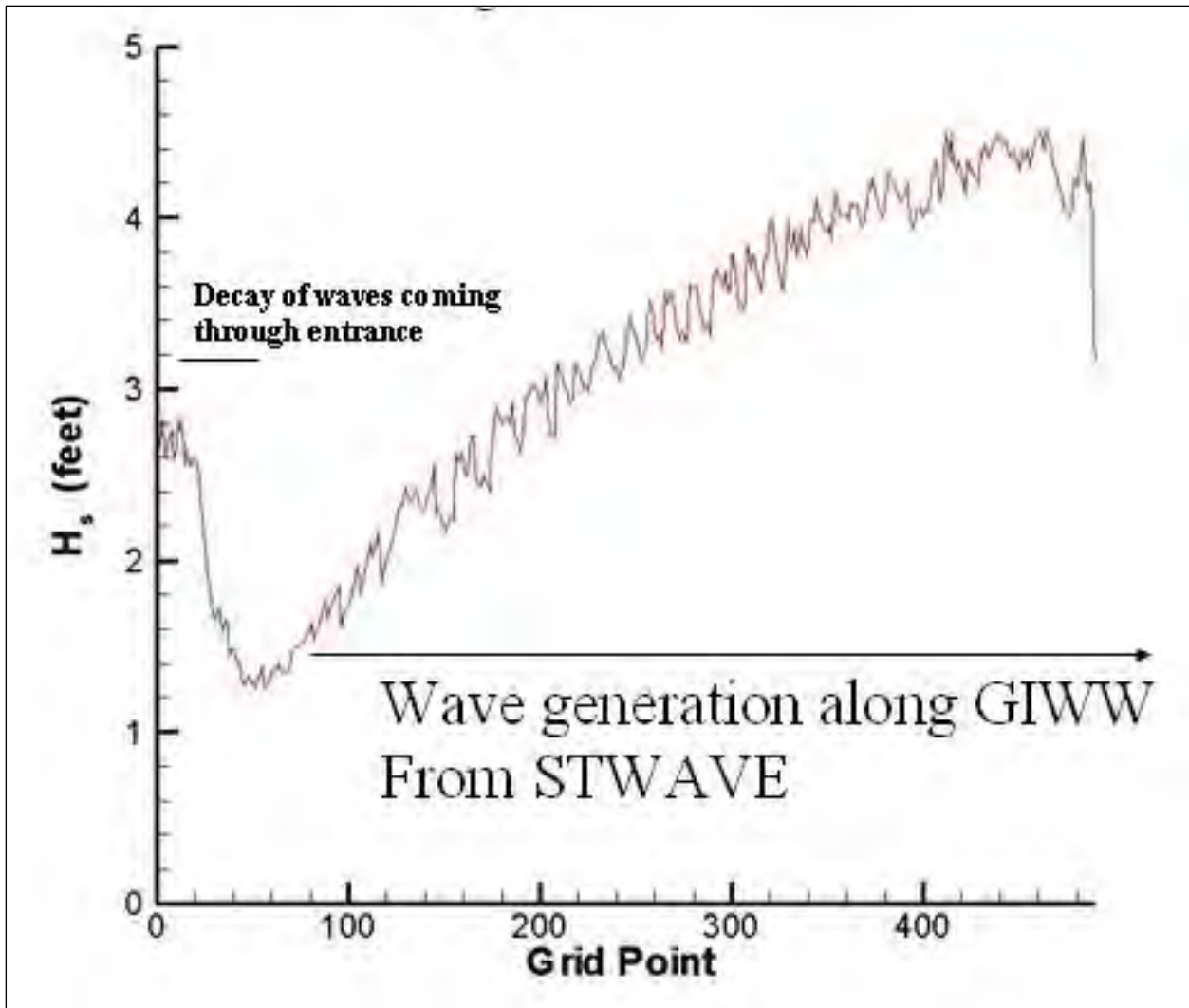


Figure 14-1. Line of maximum wave heights within the MRGO/GIWW entrance to the IHNC showing decay of waves coming in through the entrance and local generation of waves within the canal. Grid spacing is 20 meters

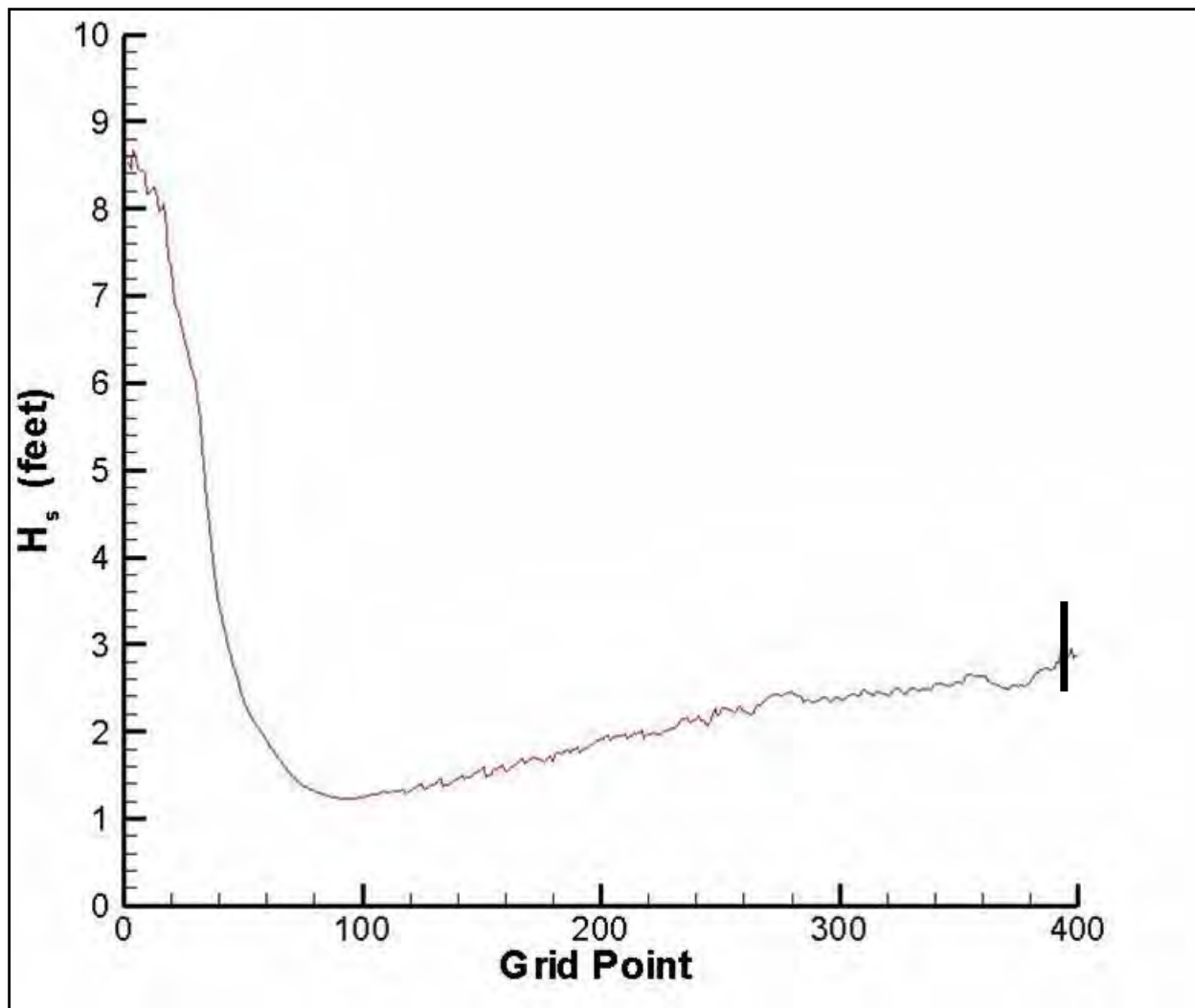


Figure 14-2. Line of maximum wave heights along the IHNC for waves entering from Lake Pontchartrain. This shows the decay of waves coming in through the entrance and local generation of waves within the canal. Grid spacing is 20 meters. Vertical Line around grid point 400 represents estimates of wave height near this point made from photographs

As a final exercise of STWAVE, a run was made to examine the potential wave heights along the sites of levee breaches along the Lower Ninth Ward using the phase-resolving modification discussed in this Appendix. Not surprisingly, these results show that the major source of waves propagating onto these floodwalls early in the storm, at about the time of their overtopping/breaching, came from waves reflecting back from the west side of the IHNC. This raises the problem that the coefficient of reflection for waves incident on that side is a relative unknown. Sensitivity tests showed that for a range of energy reflection coefficients from 0.5 to 0.8, significant wave heights arriving at the site of the northern breach into the Lower Ninth Ward were in the range of 2 to 3 feet at the time shown in Figure 14-1.

## References

Kahma, K.K. and H.Pettersson,1994: Wave growth in a narrow fetch geometry, *The Global Atmosphere and Ocean System*, **4**, pp. 253-263.

Pettersson, H., 2004: Wave growth in a narrow bay. Finnish Institute of Marine Research, Contribution 9, 105 p.

# Appendix 15

## Boussinesq Modeling

---

### Organization of Appendix

This appendix contains information on the Boussinesq model (COULWAVE) used in simulations for this report along with descriptions of the applications and development of force estimates. The sections are given below:

- Basic Boussinesq Model Information: COULWAVE
- Description of Method used to Determine Force along Canal Walls
- Details on Wave Simulation near and inside the 17th Street Canal
- Details on Wave Simulation near and inside the London Canal
- Details on Wave Simulation near and inside the Orleans Canal
- Details on Wave Simulation near and inside the Inner NHC
- Details on Wave Simulation along MRGO Levees
- Details on Wave Simulation along New Orleans East Levees
- Details on Wave Simulation along Mississippi River Levees in Plaquemines Parish

### Basic Boussinesq Model Information: COULWAVE

COULWAVE (Cornell University Long and Intermediate Wave Model) was developed by Patrick Lynett (Texas A&M) and Phil Liu (Cornell) at Cornell during the late 90's. The target applications of the model are nearshore wind wave prediction, landslide-generated waves, and tsunamis, with a particular focus on capturing the movement of the shoreline, i.e. runup and inundation.

COULWAVE has the capability of solving a number of wave propagation models, however the applications for this project use the Boussinesq-type equations. To derive the Boussinesq-type model, one starts with the primitive equations of fluid motion, the Navier-Stokes equations, which govern the conservation of momentum and mass. The fundamental assumption of the Boussinesq equations is that the wavelength to water depth ratio is large; thus the model is meant to study shallow water waves. This fundamental assumption yields additional physical limitations, such as the vertical variation of the flow must be small, and turbulence must be



parameterized – physics such as wave overturning and interaction, and overtopping of vertical structures are, theoretically speaking, beyond the application bounds of the model.

Applications for which COULWAVE has proven very accurate include wave evolution from intermediate depths to the shoreline, including parameterized models for wave breaking and bottom friction. A number of examples comparisons are described below.

## **Wave Propagation**

COULWAVE is based on the Boussinesq-type equations, which are known to be accurate for in viscid wave propagation from fairly deep water (wavelength/depth about 2) all the way to the shoreline (Wei *et al*, 1995). To accommodate frictional effects, viscous submodels are integrated into COULWAVE.

## **Wave Breaking**

The wave breaking model has received much attention and has undergone numerous validation exercises. The wave breaking model is based on the “eddy-viscosity” scheme, where energy dissipation is added to the momentum equation when the wave slope exceeds some threshold value, and continues to dissipate until the wave slope reaches some minimum value when the dissipation is turned off.

One set of comparisons is shown in Figure 15-1 for a number of regular waves breaking and running up a slope. As can be seen, COULWAVE captures the mean values of height and water level to a high degree of accuracy. While these comparisons show that the model is capable of capturing a simplified, laboratory setup, it is also necessary to gauge the accuracy against real, field conditions. COULWAVE has been compared with data from a number of field sites; one such comparison is given in Figure 15-2. As can be seen, the model captures the spectral transformation of random waves through the surf zone. Note that the breaking model uses a single set of parameters for all trials, so there is no individual case optimization.

The horizontal velocity profile under breaking waves is a necessary component to capture accurately for transport-related physics. Using a process of superposition of velocity profiles (Lynett, 2006), instantaneous and mean profiles under breaking waves are predicted well (see Figure 15-3.)

## **Wave Runup and Inundation**

The moving shoreline condition has been shown to capture shoreline motion due to a wide range of wave frequencies, wave heights, and beach slopes. The shoreline algorithm was originally developed to simulate the important motion of tsunami runup (Lynett *et al*, 2002). Recently (Korycansky & Lynett, 2005), extensive comparisons have been made with empirical runup laws and existing experimental data for runup due to regular waves. Figure 15-4 shows

how COULWAVE compares with the so-called Iribarren scaling for runup, an established coastal engineering relation based on deep water properties of the waves.

## Current and Vorticity

To include wave interaction with currents, it is necessary to first be able to include the dynamic effects of horizontal-plane vorticity due to, for example, strong currents passing a bridge pier or other obstacle. With the inclusion of a sub-grid mixing model, COULWAVE has been shown to be capable of modeling this vortex-shedding phenomenon. Figure 15-5 shows COULWAVE results for currents passing by a submerged obstacle, with experiment and numerical velocity fields given. COULWAVE is also an excellent predictor of wave-current interaction, on par with full potential flow numerical models (Ryu *et al.*, 2003).

## Large-Scale Simulation

Using the Boussinesq-type equations requires significant computational resources, with mid-sized domains, on the order of  $1 \text{ km}^2$ , often requiring days of computer time to complete just an hour of physical simulation time. To alleviate this burden, COULWAVE has been parallelized for use on distributed-memory, cluster-type computing facilities (Sittanggang & Lynett, 2005). With the parallel implementation, the size of the domain becomes limited only by the number of computers available, and has been applied to study domains larger than  $400 \text{ km}^2$  on modest (about 25 computers) clusters (see Figure 15-6). The parallel capabilities of COULWAVE allow for simulation of waves throughout the entire lengths of canals.

It is remarked that the total CPU-clock hours used for the simulations presented here exceeded 3.0 years (meaning it would have taken 3.0 years to complete these simulations on a single processor). 90% of this time was used in the last three weeks of the project period, after the near final waves and surges were provided. Simulations were performed on the 24-CPU cluster maintained by Dr. Lynett and the 256-CPU “Tensor” cluster maintained by Texas A&M University.

## References cited above

1. Korycansky, D. G. and Lynett, P., “Offshore Breaking of Impact Tsunami: the Van Dorn Effect Re-Visited,” *Geophysical Research Letters*, v. 32, No. 10, 10.1029/2004GL021918. 2005
2. Lynett, P., Wu, T.-R., and Liu, P. L.-F., “Modeling Wave Runup with Depth-Integrated Equations,” *Coastal Engineering*, v. 46(2), p. 89-107. 2002
3. Ryu, S., Kim, M.H., and Lynett, P., “Fully Nonlinear Wave-Current Interactions and Kinematics by a BEM-based Numerical Wave Tank,” *Computational Mechanics*, v. 32, p. 336-346. 2003.
4. Sittanggang, K. and Lynett, P., “Parallel Computation of a Highly Nonlinear Boussinesq Equation Model through Domain Decomposition” *International Journal for Numerical Methods in Fluids*, doi: 10.1002/flid.985. 2005

5. Wei, G., Kirby, J. T., Grilli, S. T. and Subramanya, R., 1995. "A fully nonlinear Boussinesq model for surface waves. I. Highly nonlinear, unsteady waves", *Journal of Fluid Mechanics*, 294, 71-92.

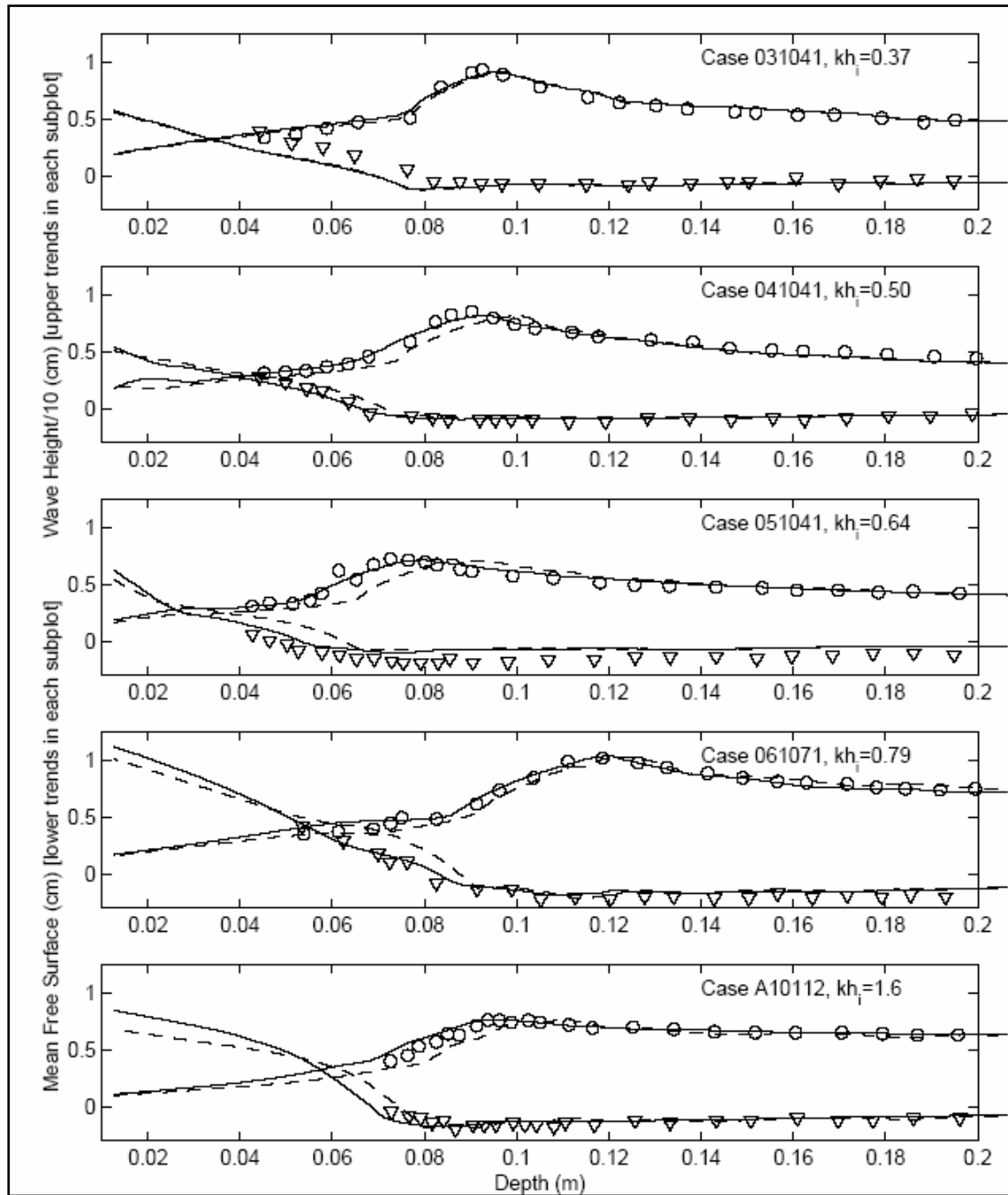


Figure 15-1. Wave height and mean free surface measurements from the experiments of Hansen and Svenson (1978) (symbols), from the traditional Boussinesq model (dashed-line), and from COULWAVE (solid line). Trials are for monochromatic waves breaking on a planar 1/20 slope

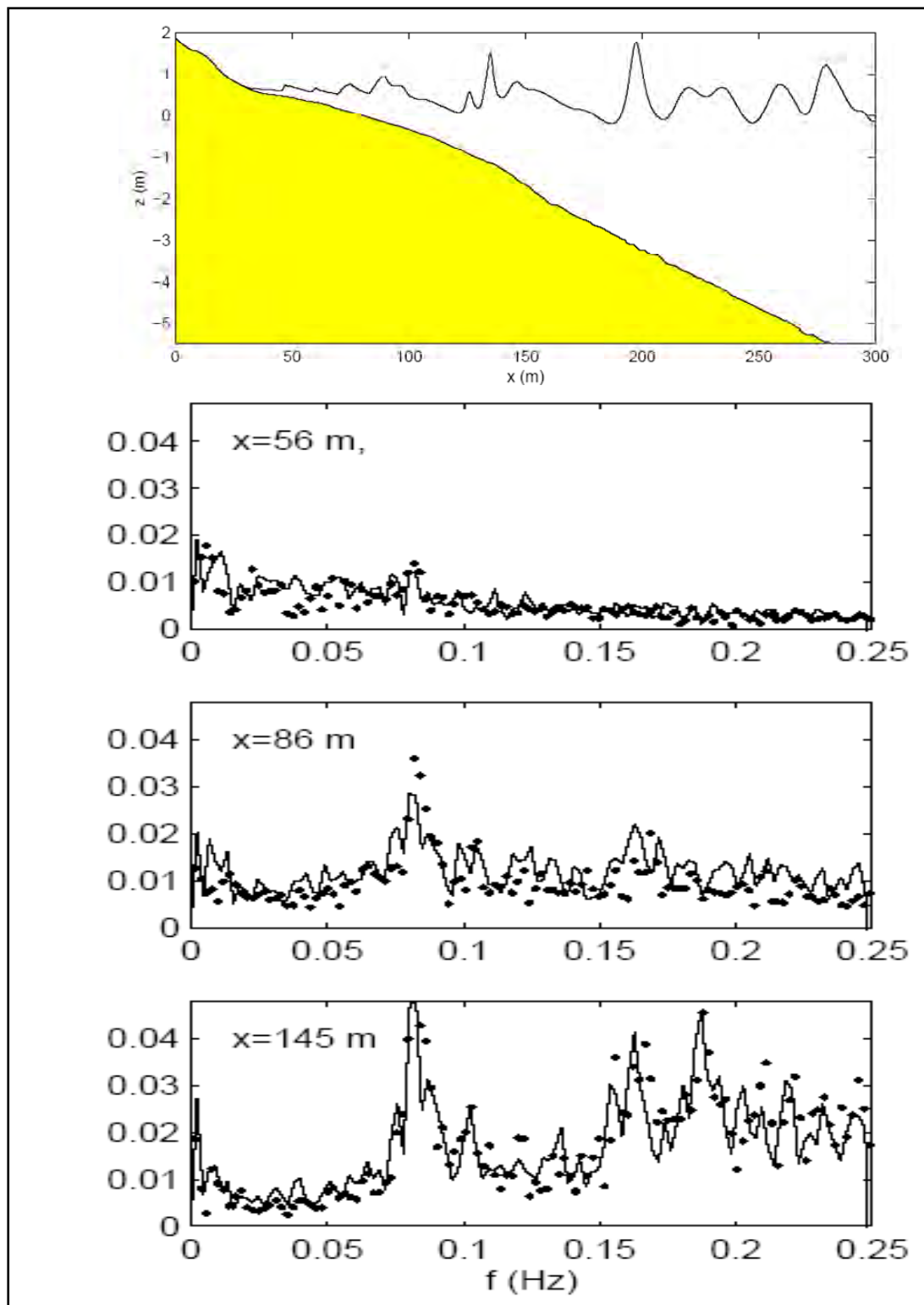


Figure 15-2. COULWAVE comparison with random-wave field data. The lower subplots show the spectrum comparisons at three different locations, where the dots are the field data from Raubenheimer (2002), and the solid lines are the COULWAVE results

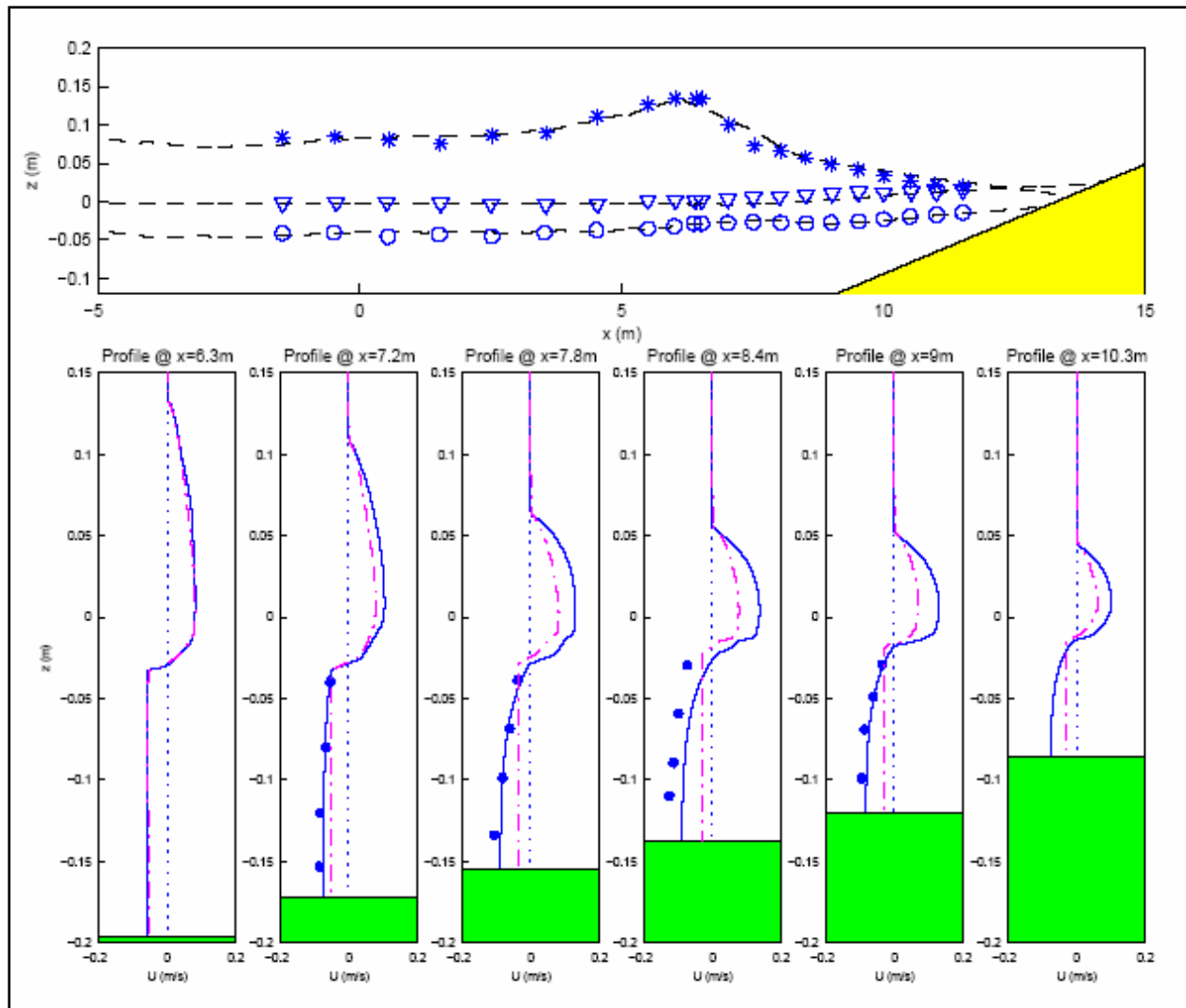


Figure 15-3. Comparison with the data of Ting and Kirby (1995) for a spilling breaker. The top plot shows the mean crest level (stars), mean water level (triangles), and mean trough level (circles) for the experiment as well as the numerical simulation. The lower subplots are the time-averaged horizontal velocities, where the experimental values are shown with the dots, COULWAVE results by the solid line, and the standard Boussinesq results by the dashed-dotted line



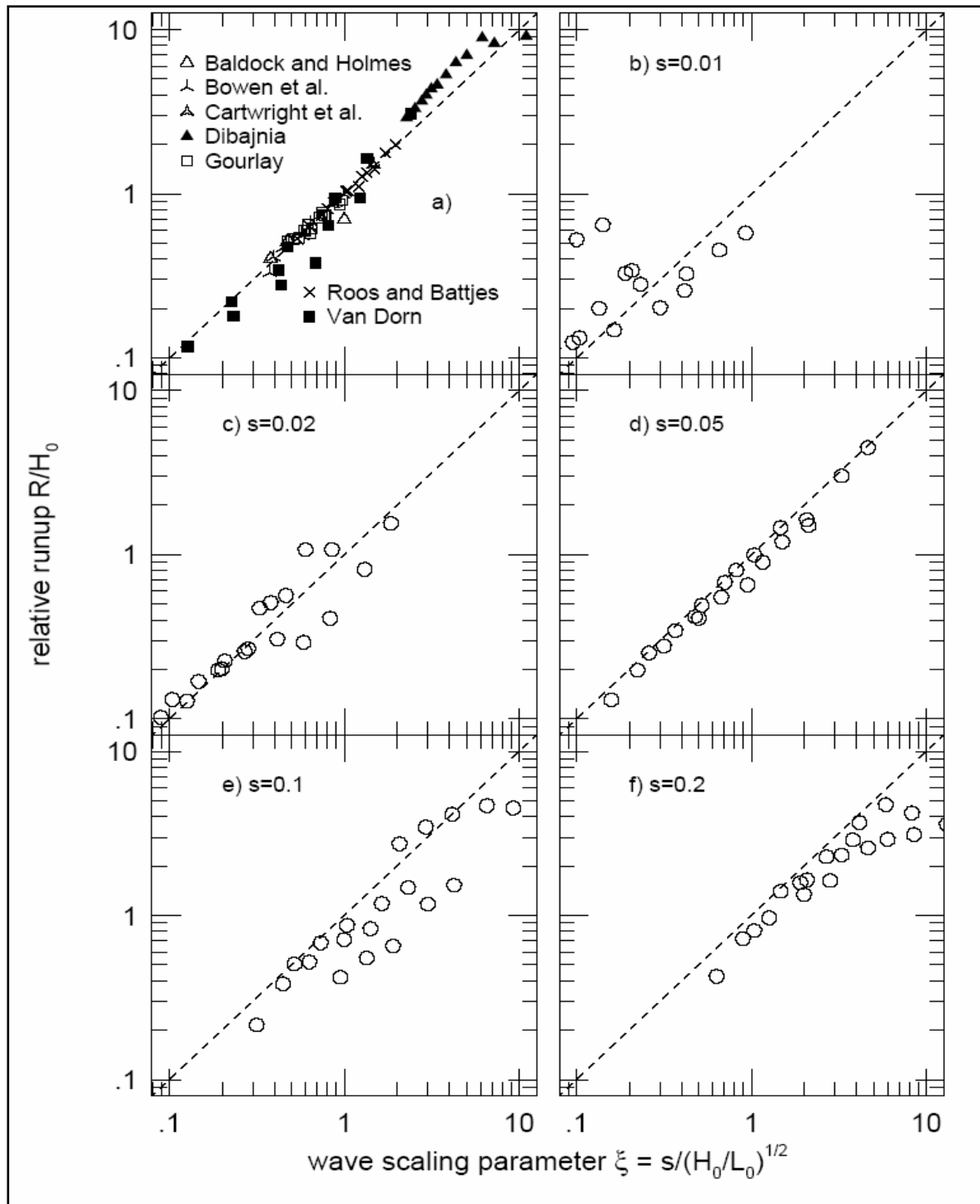


Figure 15-4. Wavetank experimental measurements of runup from the literature (Bowen *et al.*, 1968; Roos and Battjes, 1976; Van Dorn, 1976, 1978; Gourlay, 1992; Baldock and Holmes, 1999; Gourlay, 1992; Djabnia, 2002) and COULWAVE runup results (open circles). The relative runup  $R/H_0$  is plotted vs. the wave scaling parameter  $\xi = s(H_0/L_0)^{1/2}$ . Panel a) Experiments; b) COULWAVE runs with  $s=0.01$  c) COULWAVE runs with  $s=0.02$  d) COULWAVE runs with  $s=0.05$  e) COULWAVE runs with  $s=0.1$  f) COULWAVE runs with  $s=0.2$

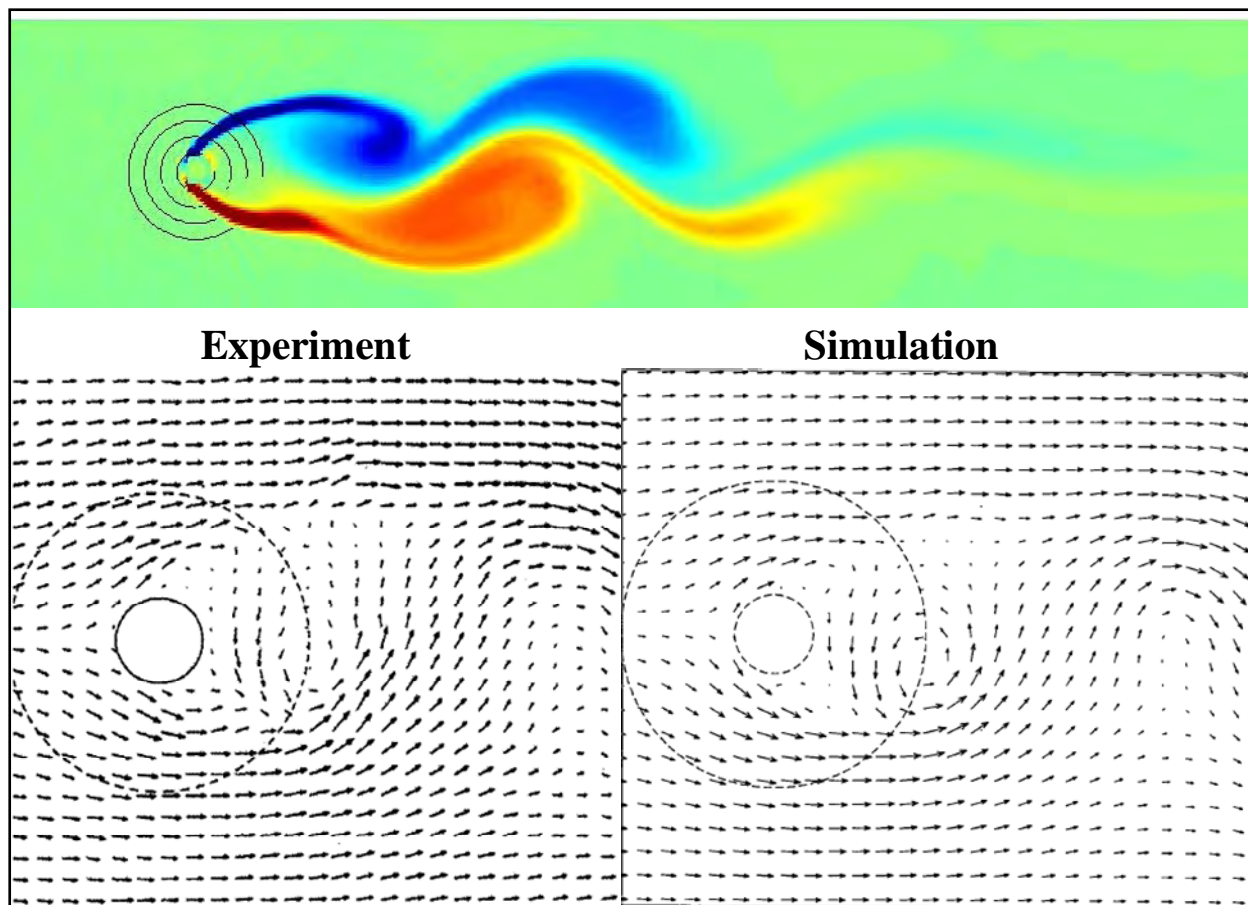


Figure 15-5. COULWAVE comparisons with experimental data for current passing a submerged conical island. The top plot is a snapshot of vorticity as predicted by COULWAVE. The bottom plots are instantaneous snapshots of the horizontal velocity field from experiment and COULWAVE

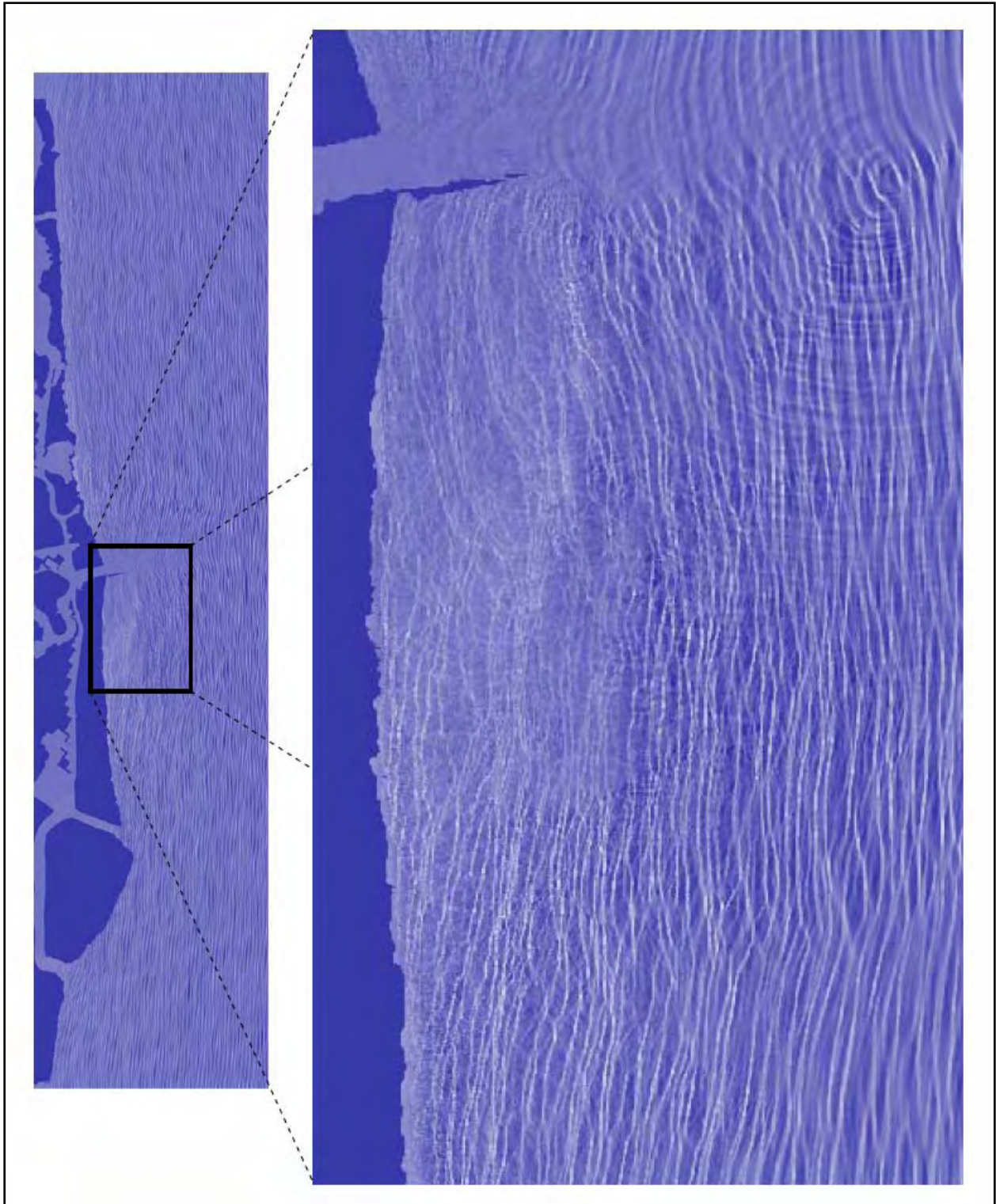


Figure 15-6. Parallel COULWAVE simulations along the coast of Texas. The simulation is centered on the inlet of Freeport, with a domain size of 10 km by 40 km. The grid size used by the model is 5 m, equating to roughly 16 million grid points

## Description of Method used to Determine Force along Canal Walls

The nonlinear and dispersive physics contained in the Boussinesq model allow for the numerically predicted vertical pressure distribution to include dynamic effects due to waves and currents. These vertical distributions can then be integrated to provide forces and lines of action. For the most part, this integration is performed inside the code and vertical distributions are not written to file. The output is a time series of force per unit length and line of action at locations along the canal walls. To provide a statistical measure of the force along a single wall panel, three time series are written to file; two on the lateral extents of the wall and one in the middle. An example of such a time series is shown in Figure 15-7. This particular time series corresponds to the London Avenue Canal just south of the Robert E Lee Bridge near the time of failure, 0700 local time.

To provide a statistical force measure, a peak force distribution is created. This is done by parsing through the time series, delineating “distinct” oscillations due to waves with zero-crossing analysis, recording the peak force during each distinct wave oscillation, and finally sorting the peaks to create a cumulative distribution function (CDF). An example of a CDF is given in Figure 15-7. With this CDF it is possible to specify a force with any arbitrary exceedance probability. For this analysis,  $F_{2\%}$ , the force which is exceeded by only two percent of the waves, was selected to represent the maximum force related to waves.

For a single panel,  $F_{2\%}$ , given in units of lb/ft, is derived from the time series written in the middle of the panel. It is also of interest to quantify the variation of the force along a single panel. This variation, for example a larger force (due to a higher water surface elevation) acting on one end, leads to a moment about a vertical axis through the center of the panel. This variation,  $\Delta F$ , is calculated through the two force time series written at the ends of a panel. An example of two such time series is given in Figure 15-8; this data is taken from simulations of the 17th Street Canal near the failure time, 0600 local time. The two time series are subtracted from one another, and the procedure used to find  $F_{2\%}$  is repeated. An example of a  $\Delta F$  CDF is shown in Figure 15-8. Thus  $\Delta F$  is also a 2 percent exceedance value.

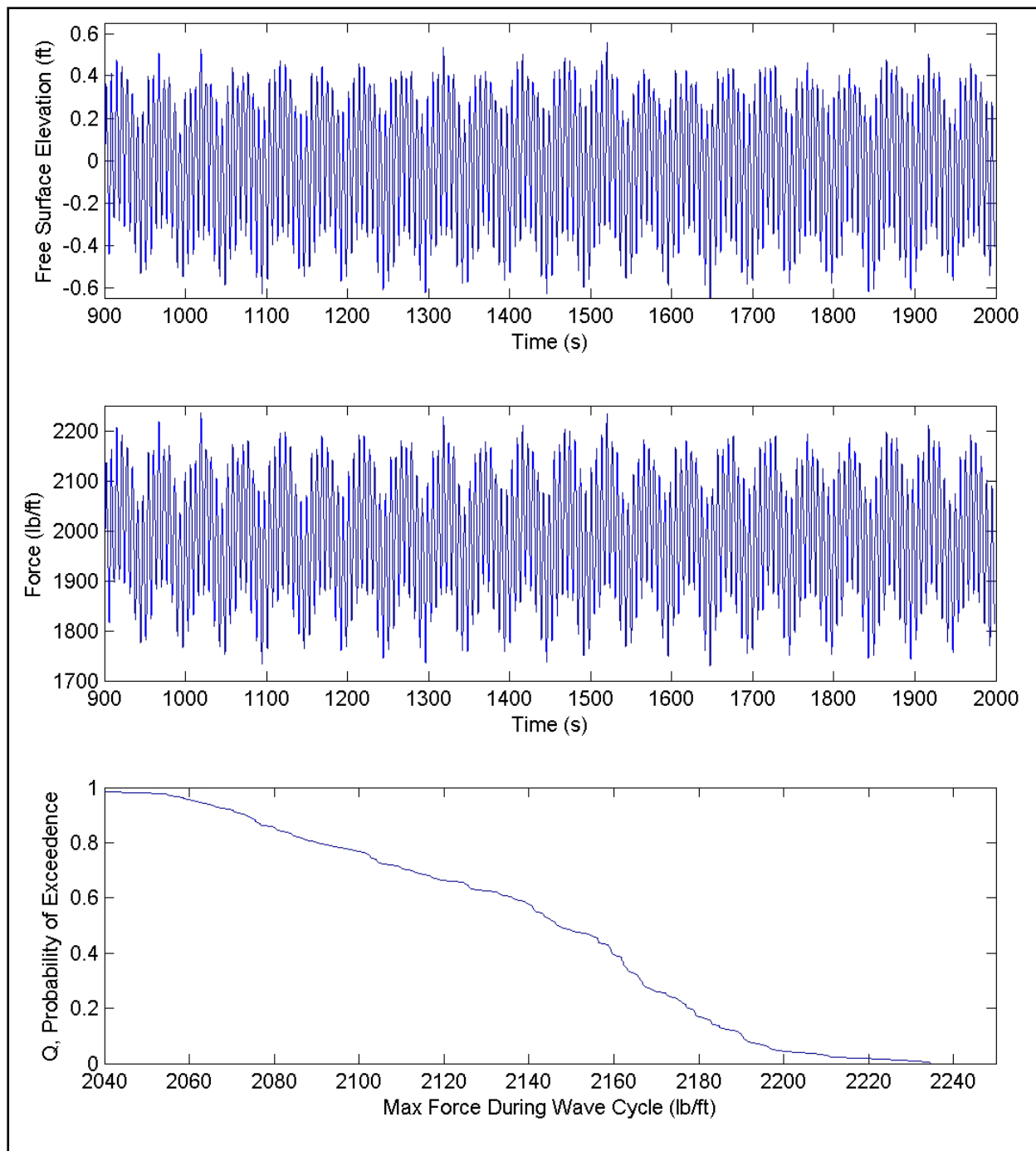


Figure 15-7. Input and output data required for calculation of  $F_{2\%}$ . The top plot is a time series of free surface displacement at the center of a panel, the middle plot is a time series of force (lb/ft) at the center of a panel, and the lower plot is the CDF resulting from a zero-crossing, peak force analysis of the force time series



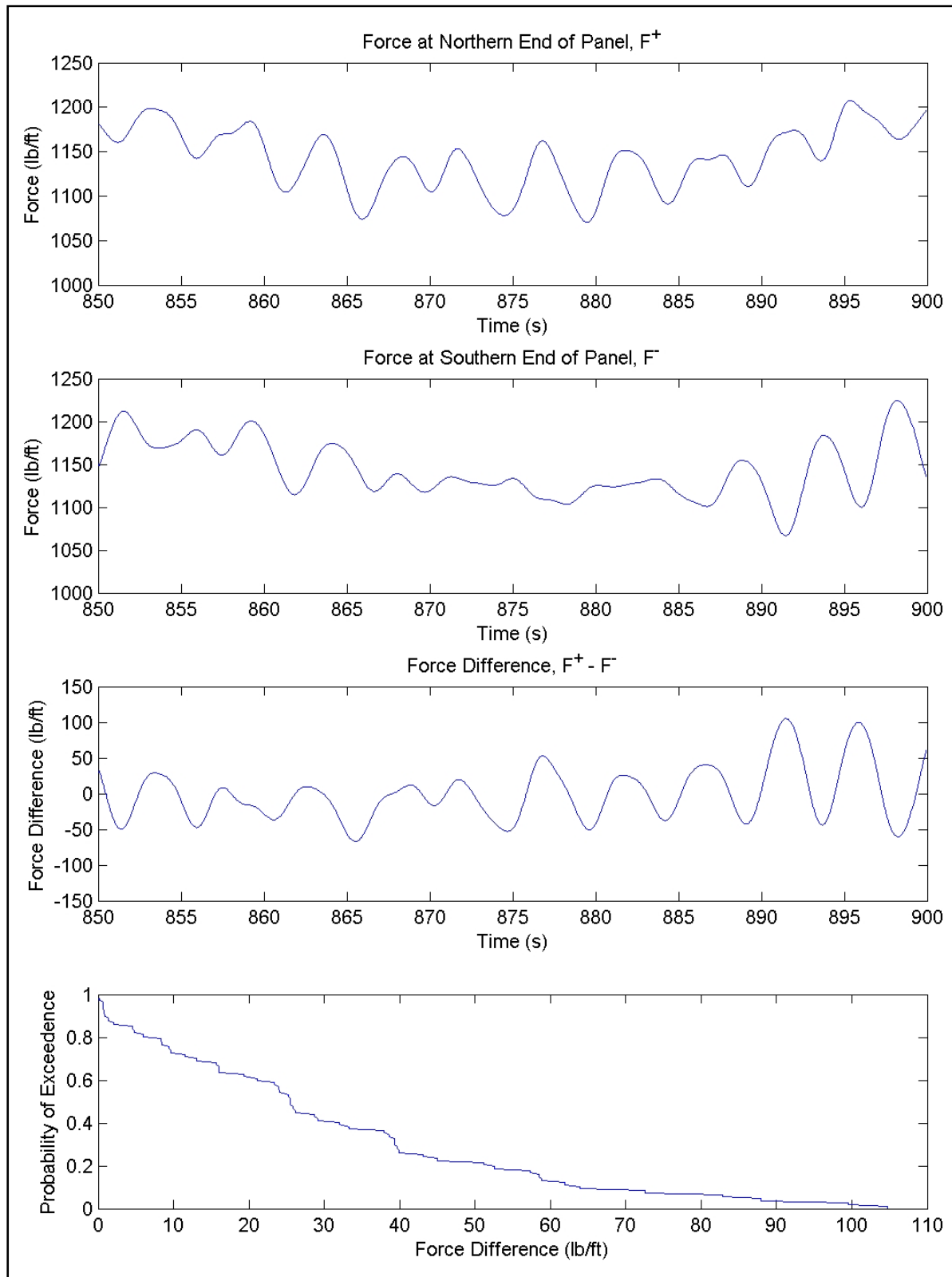


Figure 15-8. Input and output data required for calculation of  $\Delta F$ . The two top plots are time series of force (lb/ft) at the panel ends, the third plot is the difference, and the lower plot is the CDF resulting from a zero-crossing, peak analysis of the force difference time series

# Details on Wave Simulation near and inside the 17th Street Canal

## Calibration with Physical Model Data

Before application of the Boussinesq model for wave propagation into the New Orleans canals, a calibration and validation process must be undertaken. This process will use the experimental data created by the physical model of the 17th Street Canal. The first step will be creation and validation of a model approximating the bridge dissipation and transmission. The bridge effect will be modeled through a drag-type formulation, added to the conservation of momentum equation:

$$\mathbf{U}_t + \mathbf{U} \cdot \nabla \mathbf{U} + \dots + R_{BRIDGE} = 0$$

where

$$R_{BRIDGE} = \frac{1}{2} f_{BRIDGE} \frac{\mathbf{U}|\mathbf{U}|}{H},$$

$\mathbf{U}$  is the horizontal velocity vector,  $H$  is the total water depth, and  $f_{BRIDGE}$  is a bridge-related friction factor or drag coefficient. It is anticipated that  $f_{BRIDGE}$  is in-between 0.1 and 2, which are the high Reynolds number drag coefficients for a flat plate parallel to the flow and normal to the flow, respectively. In reality,  $f_{BRIDGE}$  will not be a constant, but a function of the surge, as the wave impact with the deck becomes increasingly important as the surge approaches the deck level. To determine how  $f_{BRIDGE}$  varies with the surge, comparisons are made with the physical model time series immediately in front of and behind the bridge. The frictional coefficient is tuned until the numerical wave heights match the experimental. The results of the bridge frictional calibration are shown in Figure 15-9;  $f_{BRIDGE}$  ranges from 0.45 during low surge levels to 1.4 for high surge. A numerical snapshot of how the bridge changes the wave form is given in Figure 15-10. The bridge is very effective at damping out the high frequency energy, an observation made in the physical model as well.

Next, the numerical model is validated for wave entrance into the canal. The area near the canal entrance is characterized by complex and rapidly varying bathymetry and topography. Six individual comparisons are made with the experimental data. These comparisons are for uni-directional incident wave spectra, with incident directions aligned parallel to the canal. The six conditions represent a range of low to high waves and surge. Wave height is compared from offshore, into the canal entrance, and past the bridge. Three of the comparisons are given in Figure 15-11. The calibrated numerical model appears to perform well in predicting the wave heights throughout the domain.

## Simulation Setup

The height increases from 4.5ft to 8.2ft, and surge elevation increases from 3.5ft to 10.5ft. The bathymetric grid utilized here is a combination of the ADCIRC grid covering the length of the canal, and the high-resolution physical model grid. The ADCIRC grid is down-interpolated using an inverse distance-weighted algorithm with care taken to eliminate coarse grid artifacts such as stepped bathymetry profiles. The total Boussinesq numerical grid is 2 square miles, using a 4-ft grid step in both horizontal directions. A single bridge is included in this domain, the Hammond Hwy Bridge.

Incident wave conditions are taken from the percent STWAVE output. STWAVE recording locations are just offshore of the area. Two-dimensional spectra are used to drive the Boussinesq runs. Simulations are performed for four different times, 0100, 0500, 0700, and 0900 CTD on the 29<sup>th</sup>. Dominant wave direction varies significantly across this time span, from nearly out of the east at 0100 CDT to a northern approach at 0830. Between 0100 and 0900, model output includes wave to be presented includes wave height profiles throughout the canal, forces and lines of action on a panel near the failure location, and vertical distributions of pressure at select times. Note that the Boussinesq simulations do not include any local generation due to wind.

## Simulation Results: Wave Heights and Periods

Numerical results will be discussed in a time-ordered manner. A plan view snapshot of the wave field at 0100 CDT is given in Figure 15-12. Waves approach from an ENE direction. At this time, the marina area to the northeast of the canal entrance is not yet inundated by the surge. The marina acts as an effective wave shield for the canal, as demonstrated by the wave shadow zone leeward of the marina. There is little wave energy in the canal at this time, with wave heights on the order of 0.6ft as shown in Figure 15-13. However, the predicted peak period in the canal is 50 seconds. This dominant period inside the canal appears to be due to a high frequency filtering at the canal entrance, and an additional high frequency energy reduction at the bridge. While not shown, wave-induced water level changes throughout the canal are minimal, on the order of a fraction of an inch.

By 0500 CDT, the marina area is inundated, as shown in Figure 15-14, and the wave direction is from the NE. However, predicted wave heights and periods inside the canal are still similar to those at 0600, as shown in Figure 15-13, despite increased offshore energy. Significant refraction near the marina, and increased bridge dissipation are possible explanations. Wave heights in the canal at 0700 CDT are again small, on the order of 1ft. By 0900 CTD, the wave approach is almost normal to the lakefront as shown in Figure 15-15; this condition should represent the time of largest wave energy entering the canal. Looking again at Figure 15-13, it is clear that there is significant wave energy entering the canal as evidenced by the 2ft waves north of the bridge. However, at this time, surge is maximum and the bridge dissipation is greatest; wave heights south of the bridge are 1ft or less. Thus, a general conclusion is that wave heights south of the bridge were likely on the order of 1ft over the entire duration of the storm. Again, this statement does not take into account local wave generation, although this should not be important in the immediate vicinity of the bridge.

## Simulation Results: Wave Forces

Calculation of the water forces is described in the “Description of Method used to Determine Force along Canal Walls” section. The 17th Street Canal wall cross section is shown in Figure 15-16, where  $h$  is the still water depth measured from the soil base of the vertical wall, and  $z_r$  is the line of action of the water force, also measured from the soil base of the wall. Before summarizing the forces on the walls at the various times, an example pressure distribution is provided. This pressure distribution, taken at the simulated time of 0700 CTD, is given in Figure 15-17. Note that the distribution is linear to a high degree of approximation. This implies that the pressure distribution is essentially hydrostatic with the addition of the wave water surface displacement. This hydrostatic approximation was checked inside the code for all pressure distributions at all times, and was found to have a maximum deviation at any time of 4 percent on the total force (mean deviation <0.1 percent). Thus a linearly increasing pressure distribution, starting from the instantaneous free surface, provides an excellent approximation of the pressure distribution, and the resulting force and line of action.

Water forces and lines of action are summarized in the table below. In the table, the force,  $F_{nw}$ , is the force that would result from a static water column of height,  $h$ . Note that even though significant wave heights are about 1ft or less, the additional force due to the 2 percent wave can be significant. Also, the 2 percent exceedance forces correspond to crest elevations that are approximately 80-90 percent of the local significant wave height.

Time (CDT)	Surge (ft)	$h$ (ft)	$F_{nw}$ (lb/ft)	$z_r$ w/ $F_{nw}$ (ft)	$F_{2\%}$ (lb/ft)	$z_r$ w/ $F_{2\%}$ (ft)	$\Delta F$ (lb/ft)
0100	3.5	2.8	245	0.93	262	0.97	16
0500	5	4.3	577	1.4	781	1.7	217
0700	6.6	5.9	1,086	2.0	1435	2.3	267
0900	10.5	9.8	2,996	3.3	3580	3.6	358

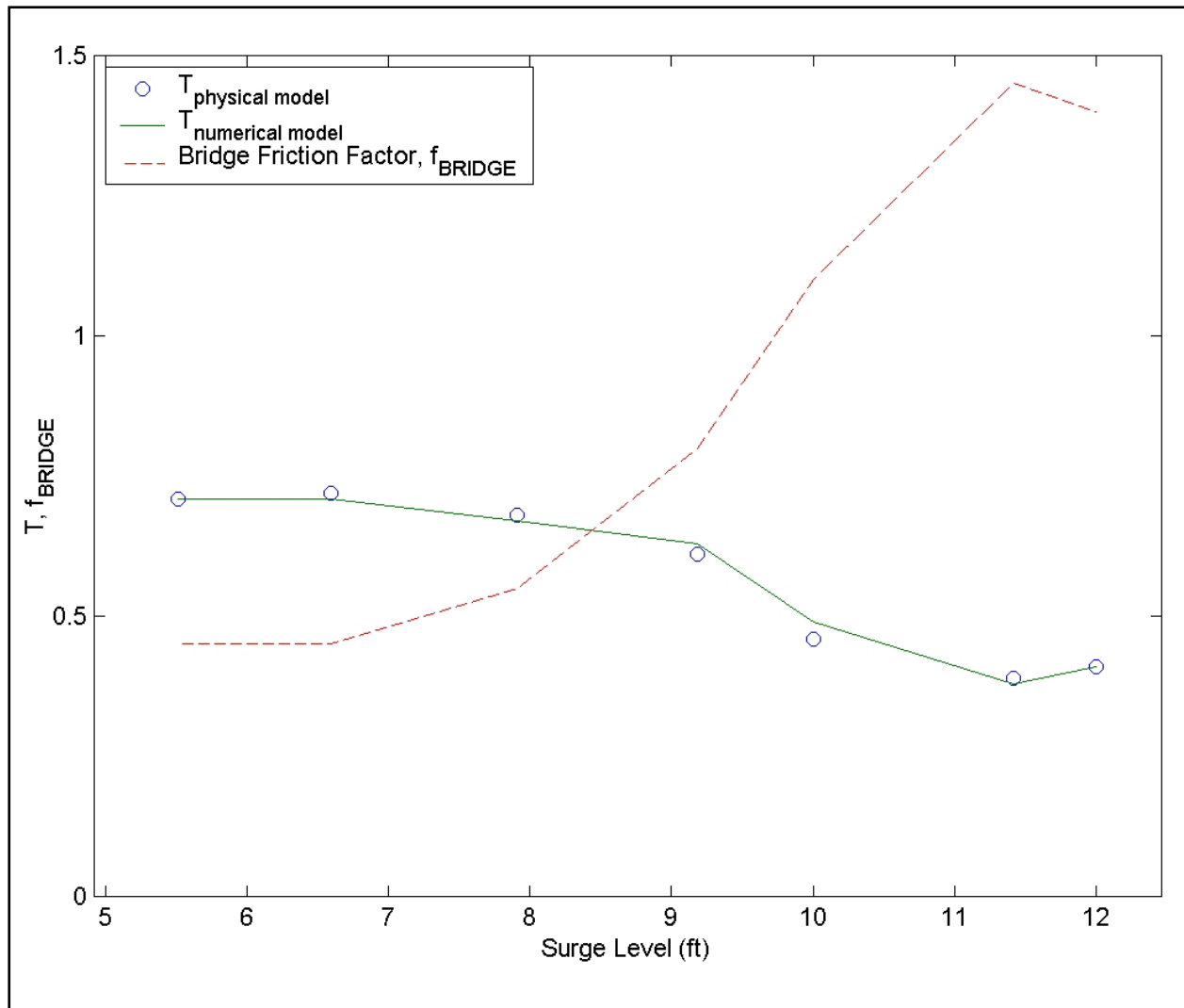


Figure 15-9. Results of the bridge model calibration, where  $T$  is that transmission coefficient, and  $f_{BRIDGE}$  is the bridge friction factor used in the numerical model. The circles are physical model data, and the lines are from the numerics



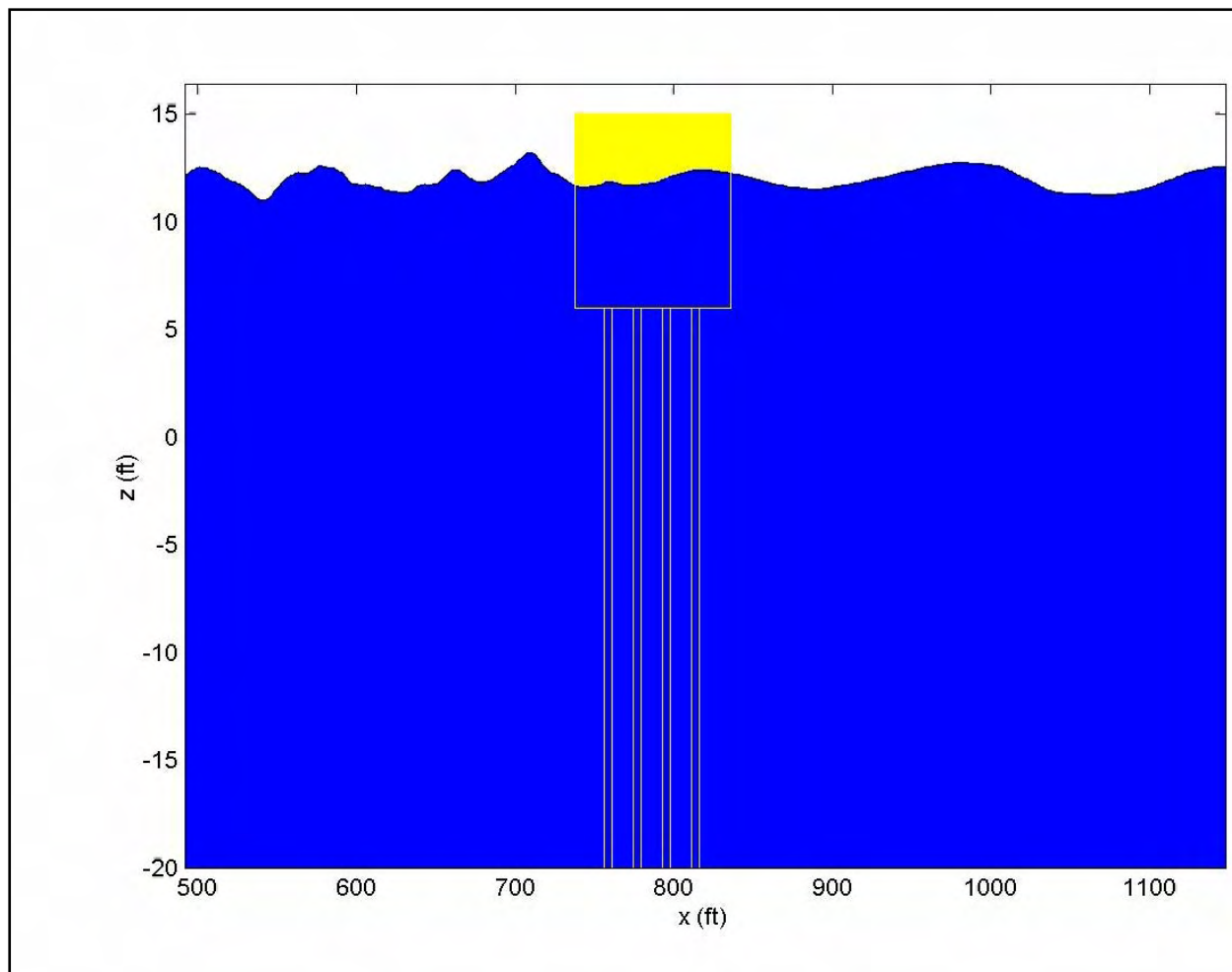


Figure 15-10. Example of the numerical bridge effect. Waves approach the bridge from the left (north)

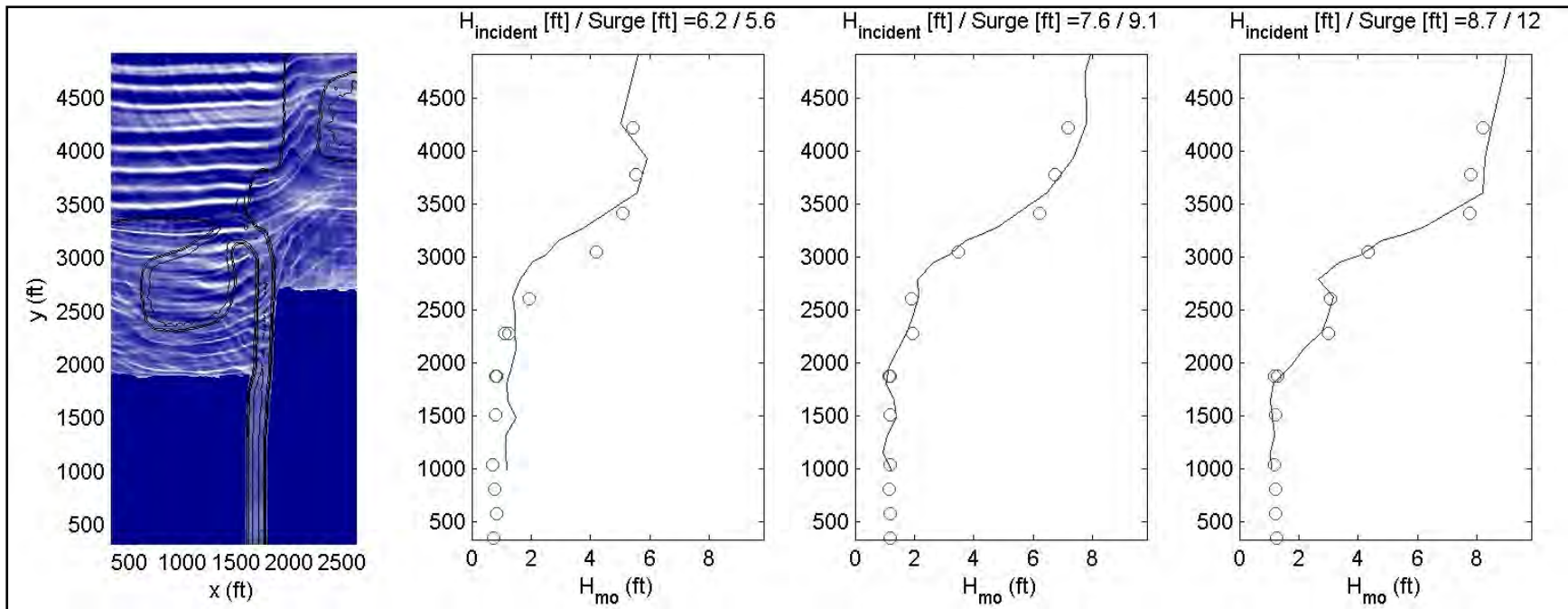


Figure 15-11. Numerical-experimental comparison of wave height through the canal, for three different wave and surge conditions. The circles are the physical model data, and the lines are from the Boussinesq model

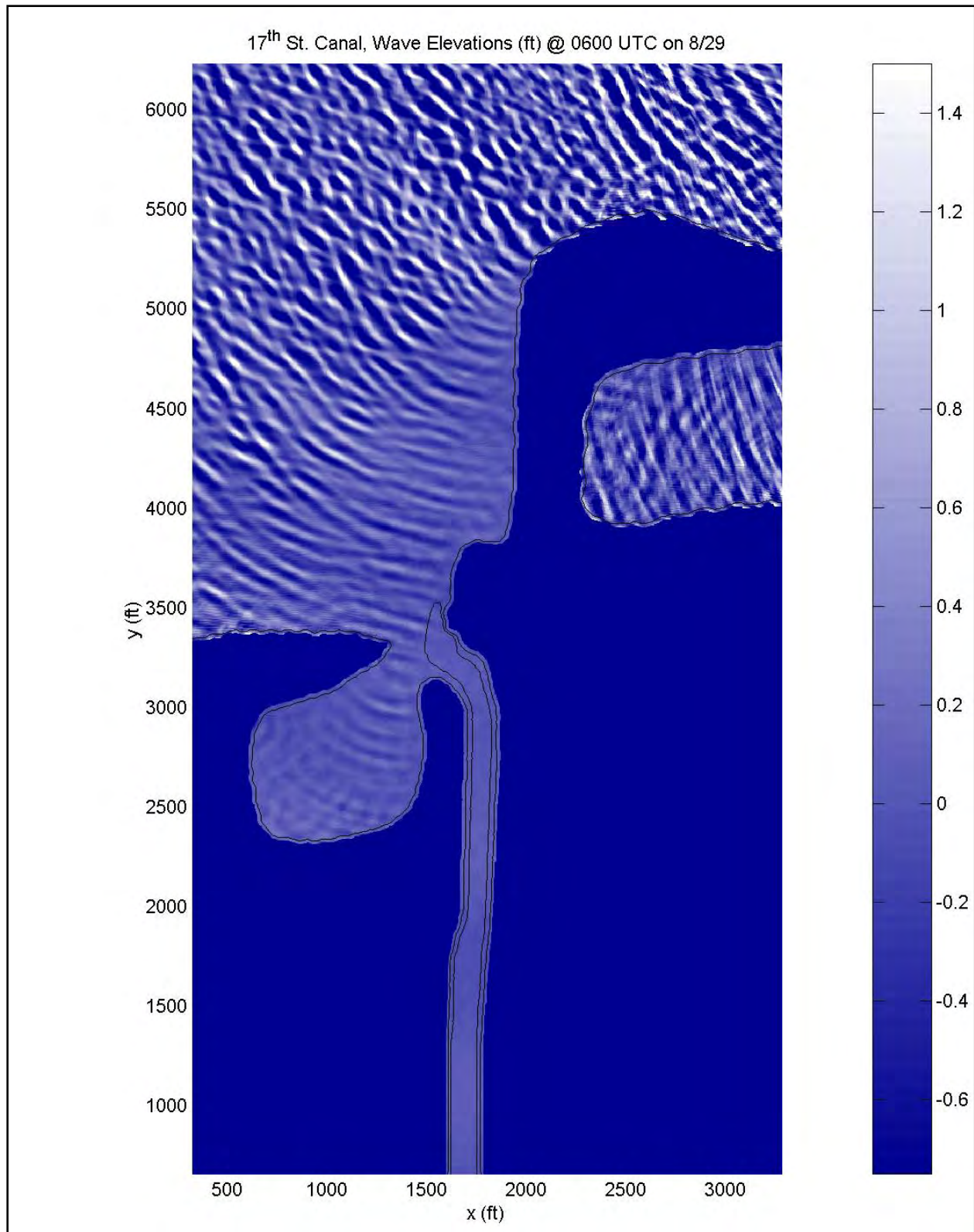


Figure 15-12. Simulated wave field for 17th Street Canal at 0100 CDT

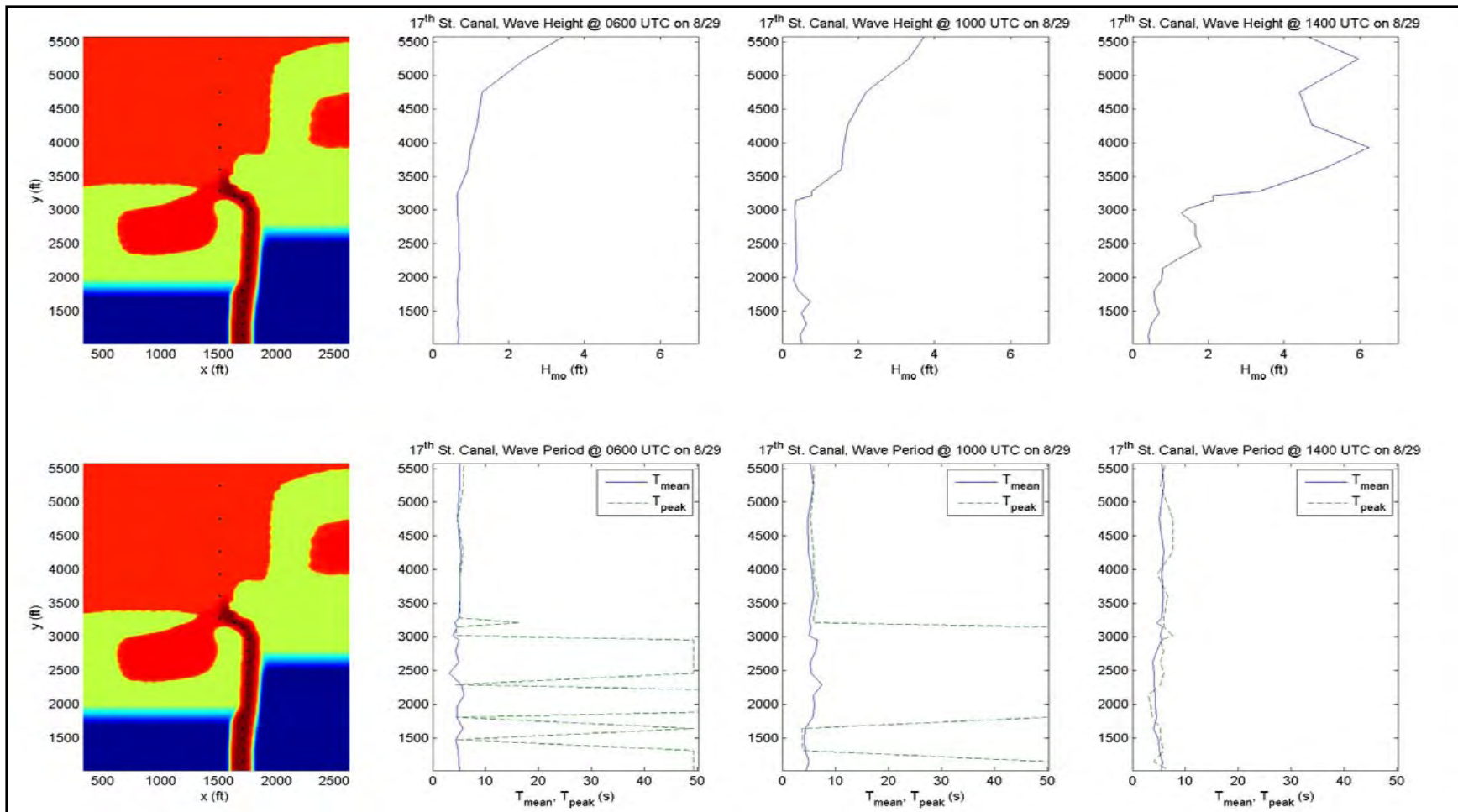


Figure 15-13. Profiles of significant wave height and period through 17th Street Canal at three times. Wave heights are given in the top row and periods in the bottom. Both peak (from spectral analysis) and mean (from zero-crossing) periods are shown, to provide a measure of the periods of dominant wave energy. The first plot on the left gives the domain and the recording points, given by the black dots



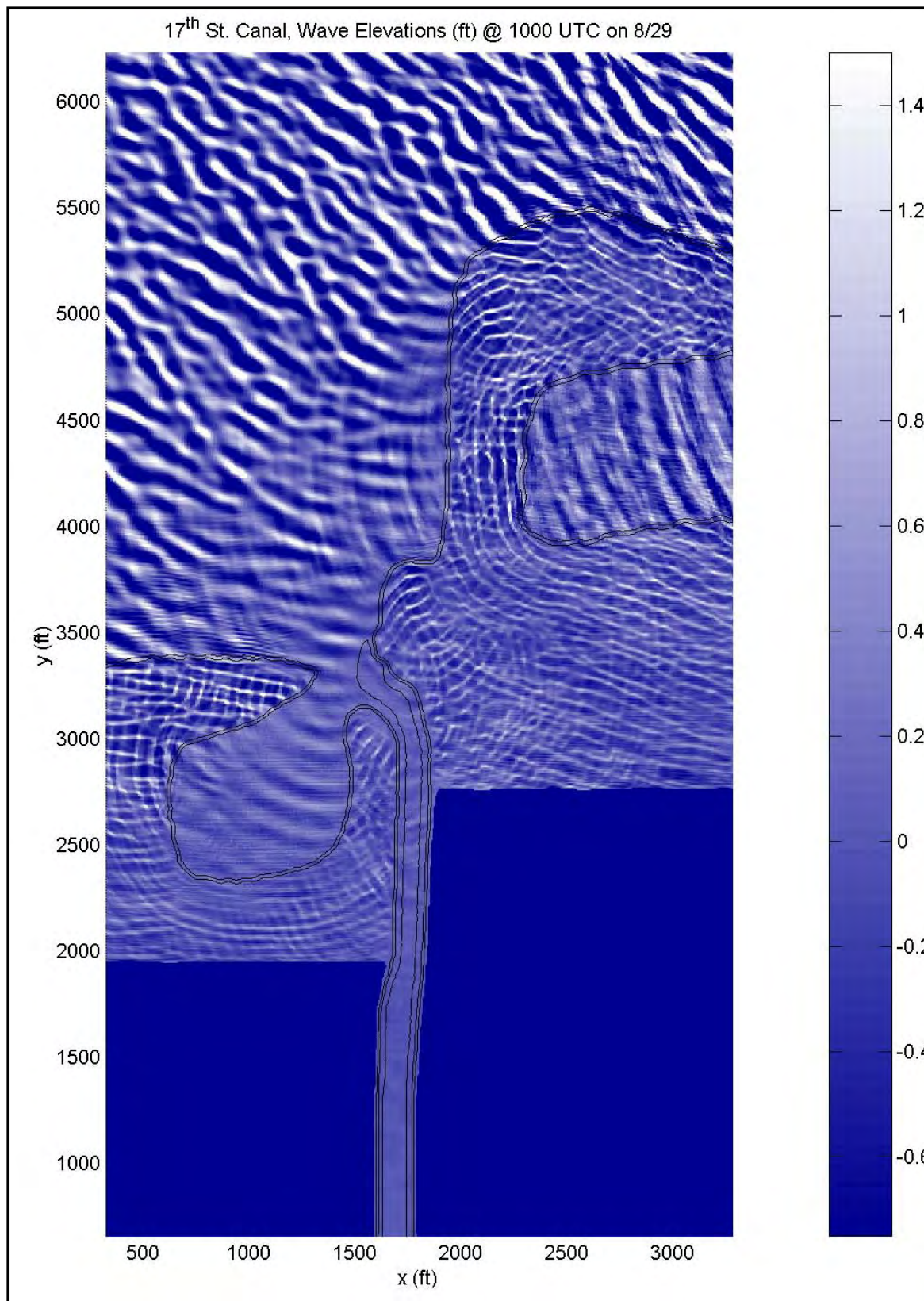


Figure 15-14. Simulated wave field for 17th Street Canal at 0500 CDT



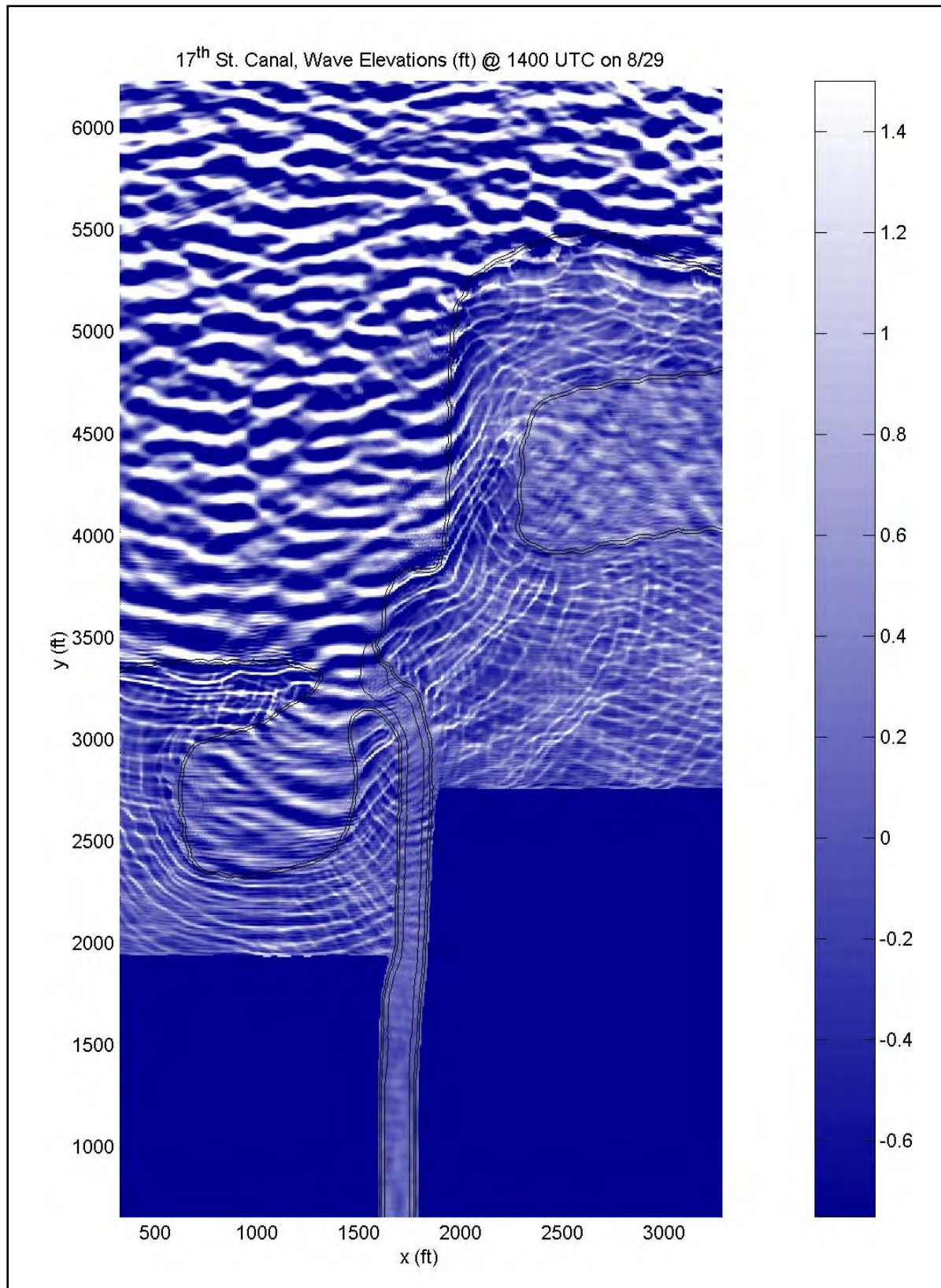


Figure 15-15. Simulated wave field for 17th Street Canal at 0900 CDT

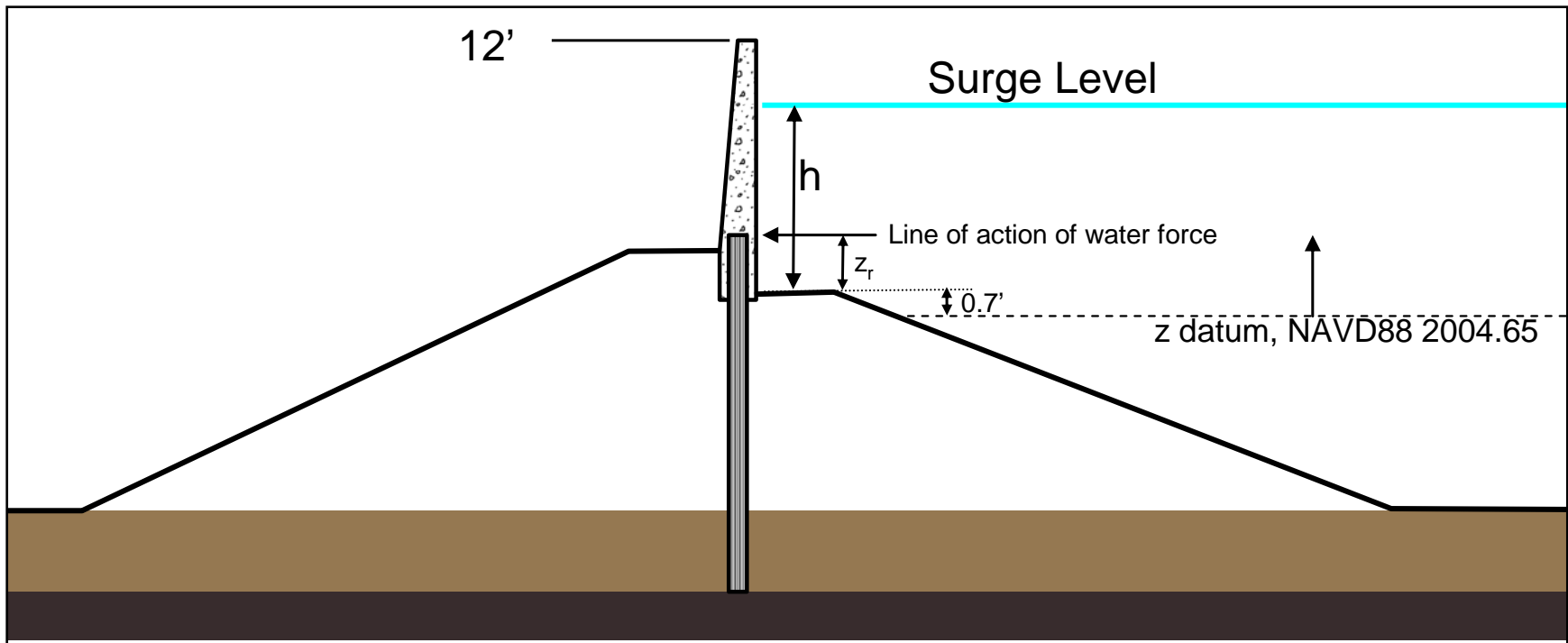


Figure 15-16. Cross-sectional schematic for 17th Street Canal walls near failure location

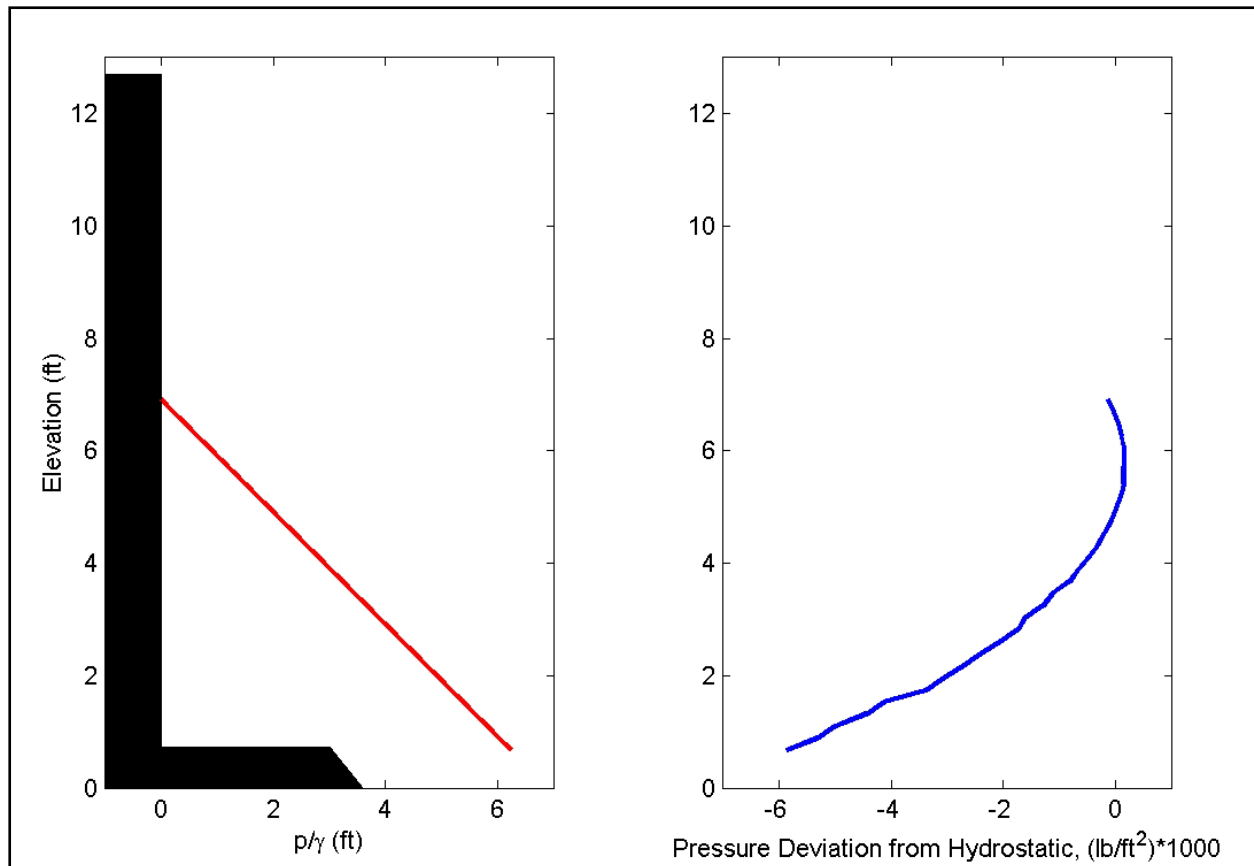


Figure 15-17. Example of numerically predicted vertical distribution of pressure under a wave crest near 17th Street Canal failure location at 0700 CDT. The red line in the left plot shows the distribution, while the plot on the right gives the deviation from hydrostatic pressure based on the instantaneous water surface elevation. Note that the units on the right plot are pounds per square foot\*1000, thus the deviation is very small

## Details on Wave Simulation near and inside the London Avenue Canal

### Simulation Setup

The bathymetric grid utilized here is from the ADCIRC grid. The ADCIRC grid is down-interpolated using an inverse distance weighted algorithm with care taken to eliminate coarse grid artifacts such as stepped bathymetry profiles. The total Boussinesq numerical grid is 1.5 square miles, using a 4 ft grid step in both horizontal directions. Three bridges cross the canal in this domain: the Lakeshore Drive Bridge near the canal entrance, the Lean C. Simon Bridge, and the Robert E. Lee Bridge. Note that this analysis focuses specifically on only the failure near the Robert E Lee Bridge. However, the hydrodynamic conditions at the failure near the Mirabeau Avenue Bridge will likely be very similar, although local generation may have increased the wave height when the winds come from the north. Local generation is not replicated by the Boussinesq model.

Incident wave conditions are taken from the 95 percent STWAVE output. STWAVE recording locations are just offshore of the area. Two-dimensional spectra are used to drive the Boussinesq runs. Simulations are performed for four different times, 0600, 1000, 1200, and 1400 UTC on the 29<sup>th</sup>. Dominant wave direction varies significantly across this time span, from nearly out of the east at 0600 to a northern approach at 1400. Between 0600 and 1400, wave height increased from 3.9ft to 8.2 ft, and surge elevation increased from 3.7ft to 11ft. The model output to be presented includes wave height transects along the canal, forces and lines of action on a panel near the failure location, and vertical distributions of pressure at select times.

## Simulation Results: Wave Heights and Periods

Numerical results will be discussed in a time-ordered manner. A plan view snapshot of the wave field at 0600 UTC is given in Figure 15-18. Waves approach from an ENE direction. Little wave energy enters the canal at this time, with wave heights inside the canal less than half a foot, as shown in Figure 15-19. As with the 17th Street Canal, wave-induced water level changes throughout the canal are minimal, on the order of an inch.

By 1000 UTC, the offshore wave height has increased to 5.4ft and the wave direction is from the NE. However, due to the approach angle, there is still very little wave energy in the canal; again on the order of 0.5ft as shown in Figure 15-19. When the waves begin to approach directly into the canal, wave energy enters in larger fractions, as shown in the wave snapshot at 1400 UTC (Figure 15-20). At 1400, wave heights near and south of the Robert E Lee Bridge are about 1ft. At this location, significant wave energy is present in both the peak incident period, 6 s, and a long period carrier frequency of roughly 50 s.

## Simulation Results: Wave Forces

Calculation of the water forces is described in the “Description of Method used to Determine Force along Canal Walls” section. The London Avenue Canal wall cross section is shown in Figure 15-21, where  $h$  is the still water depth measured from the soil base of the vertical wall, and  $z_r$  is the line of action of the water force, also measured from the soil base of the wall. Before summarizing the forces on the walls at the various times, an example pressure distribution is provided. This pressure distribution, taken at the simulated time of 1200 UTC, is given in Figure 15-22. As noted with the 17th Street Canal simulations, the pressure distribution is linear to a high degree of approximation. Water forces and lines of action are summarized in the table below. In the table, the force,  $F_{nw}$ , is the force that would result from a static water column of height,  $h$ .

Time (UTC)	Surge (ft)	h (ft)	$F_{nw}$ (lb/ft)	$z_r$ w/ $F_{nw}$ (ft)	$F_{2\%}$ (lb/ft)	$z_r$ w/ $F_{2\%}$ (ft)	$\Delta F$ (lb/ft)
0600	3.7	3	281	1.0	328	1.1	12
1000	5.8	5.1	812	1.7	906	1.8	256
1200	8	7.3	1,663	2.4	2105	2.7	331
1400	11	10.3	3,310	3.4	3910	3.7	394

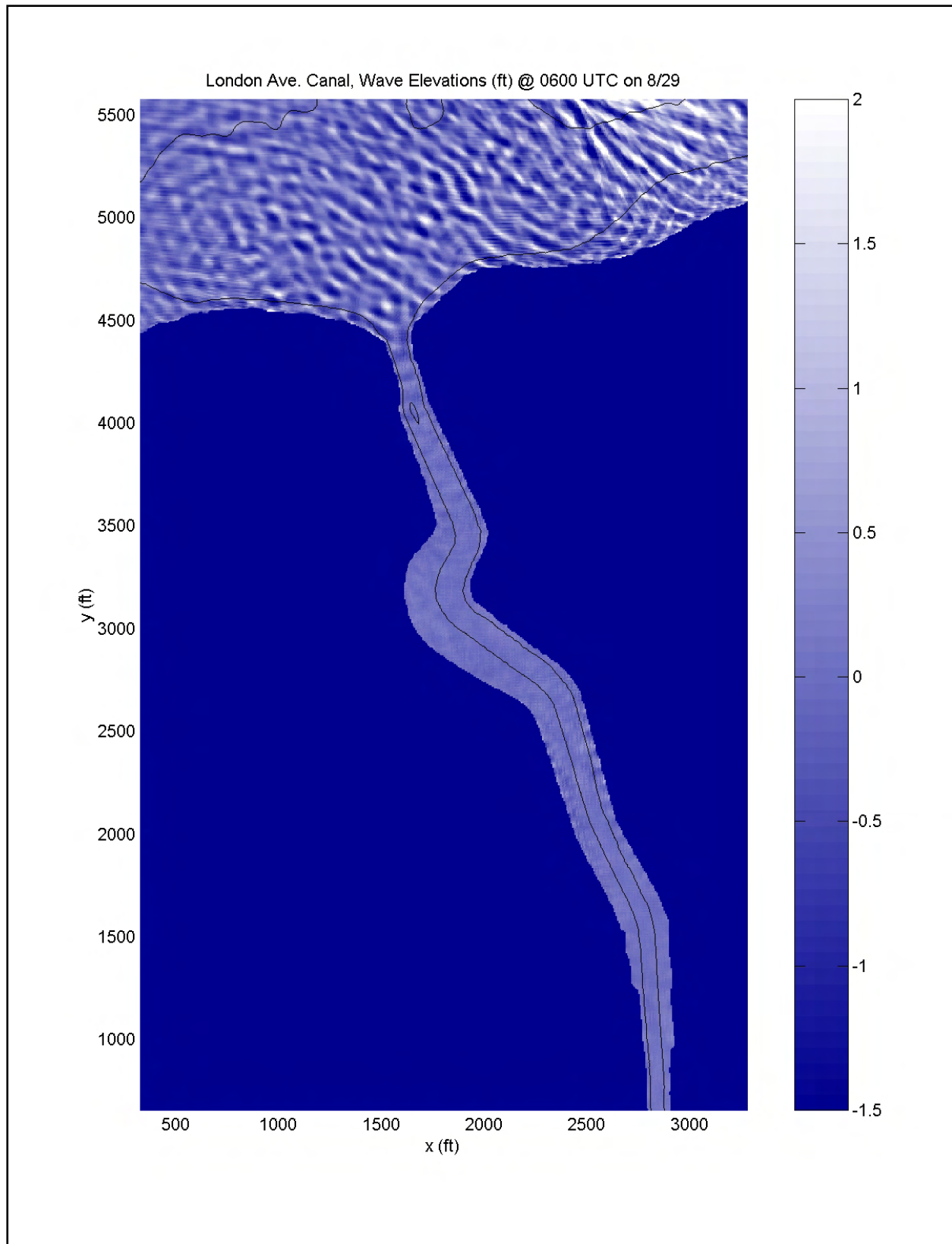


Figure 15-18. Simulated wave field for London Avenue Canal at 0600 UTC



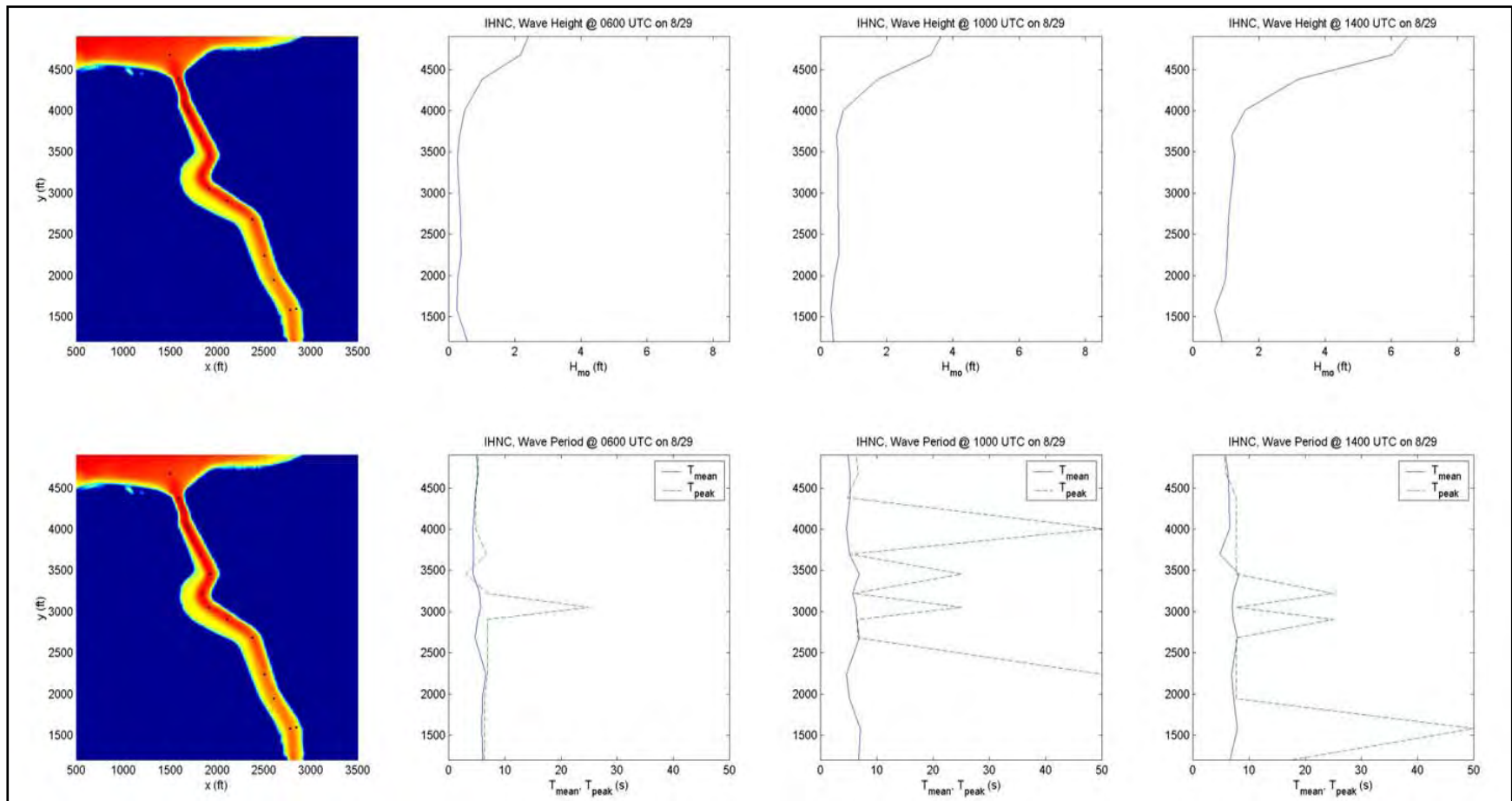


Figure 15-19. Transects of significant wave height and period along the London Avenue Canal at three times. Wave heights are given in the top row and periods in the bottom. Both peak (from spectral analysis) and mean (from zero-crossing) periods are shown, to provide a measure of the periods of dominant wave energy. The first plot on the left shows the domain and the recording points, given by the black dots

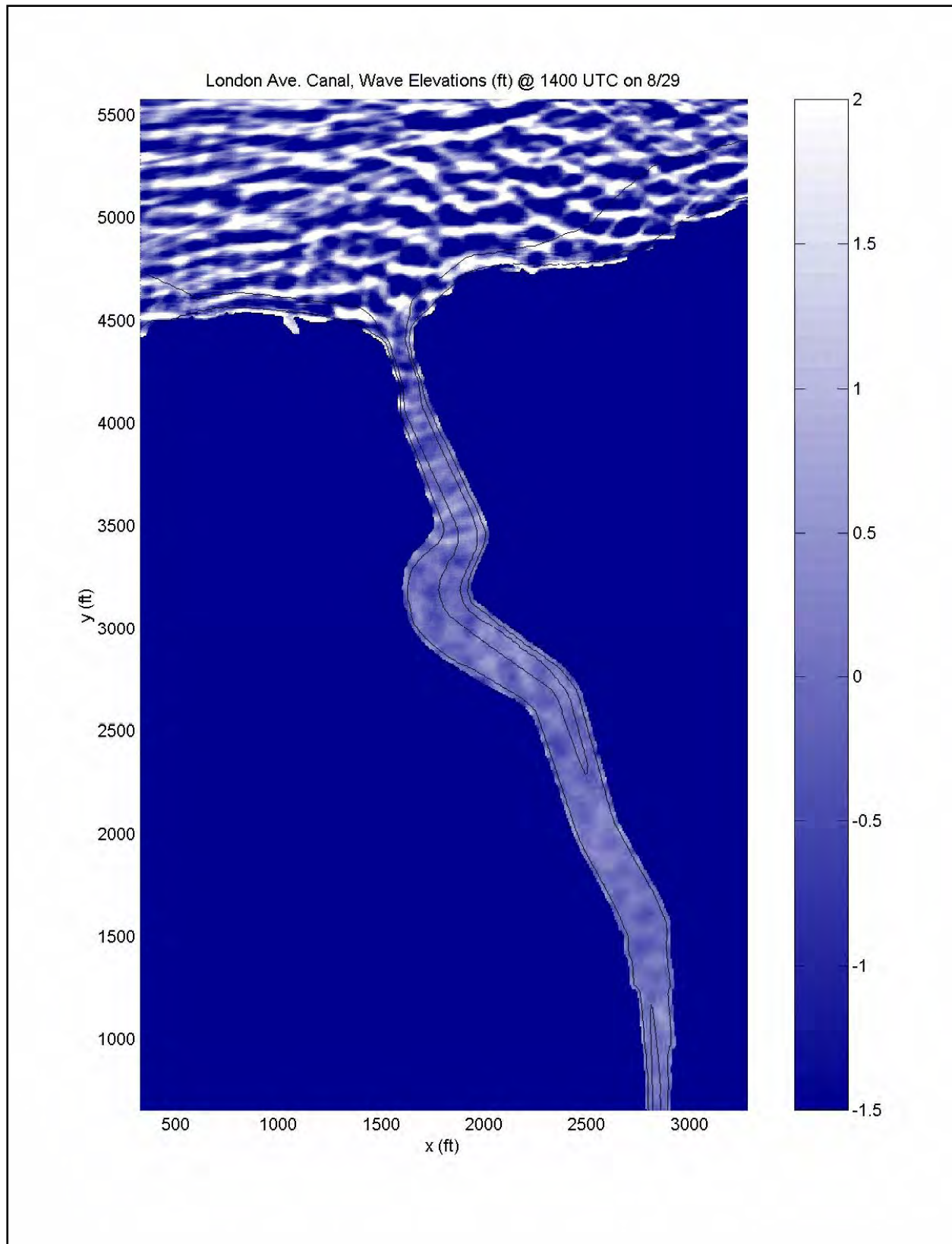


Figure 15-20. Simulated wave field for London Avenue Canal at 1400 UTC

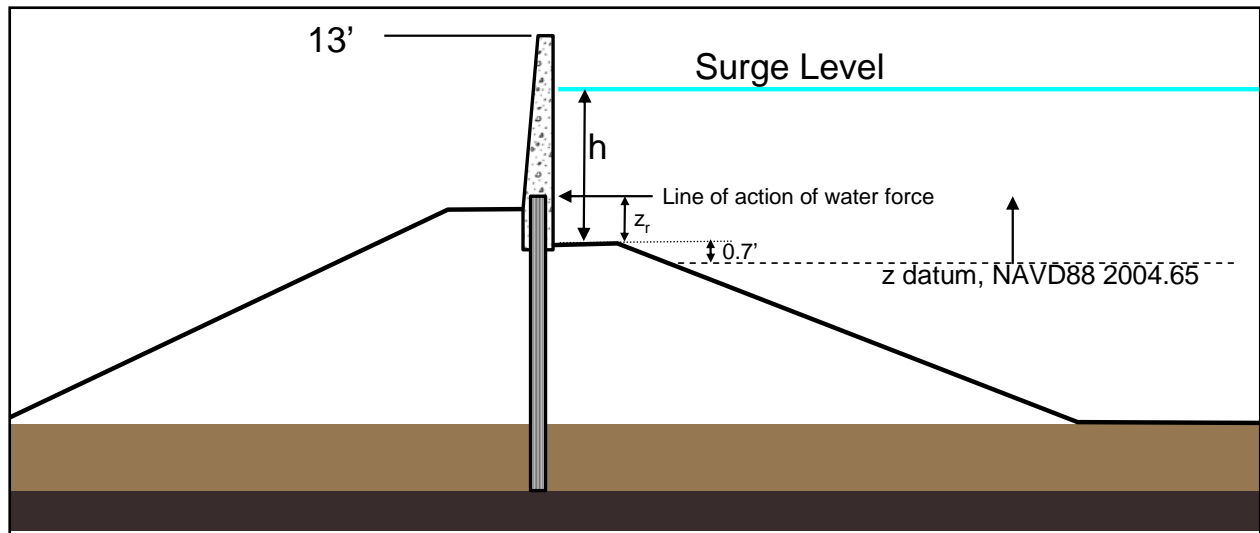


Figure 15-21. Cross-sectional schematic for London Avenue Canal walls near failure location just south of Robert E. Lee Bridge

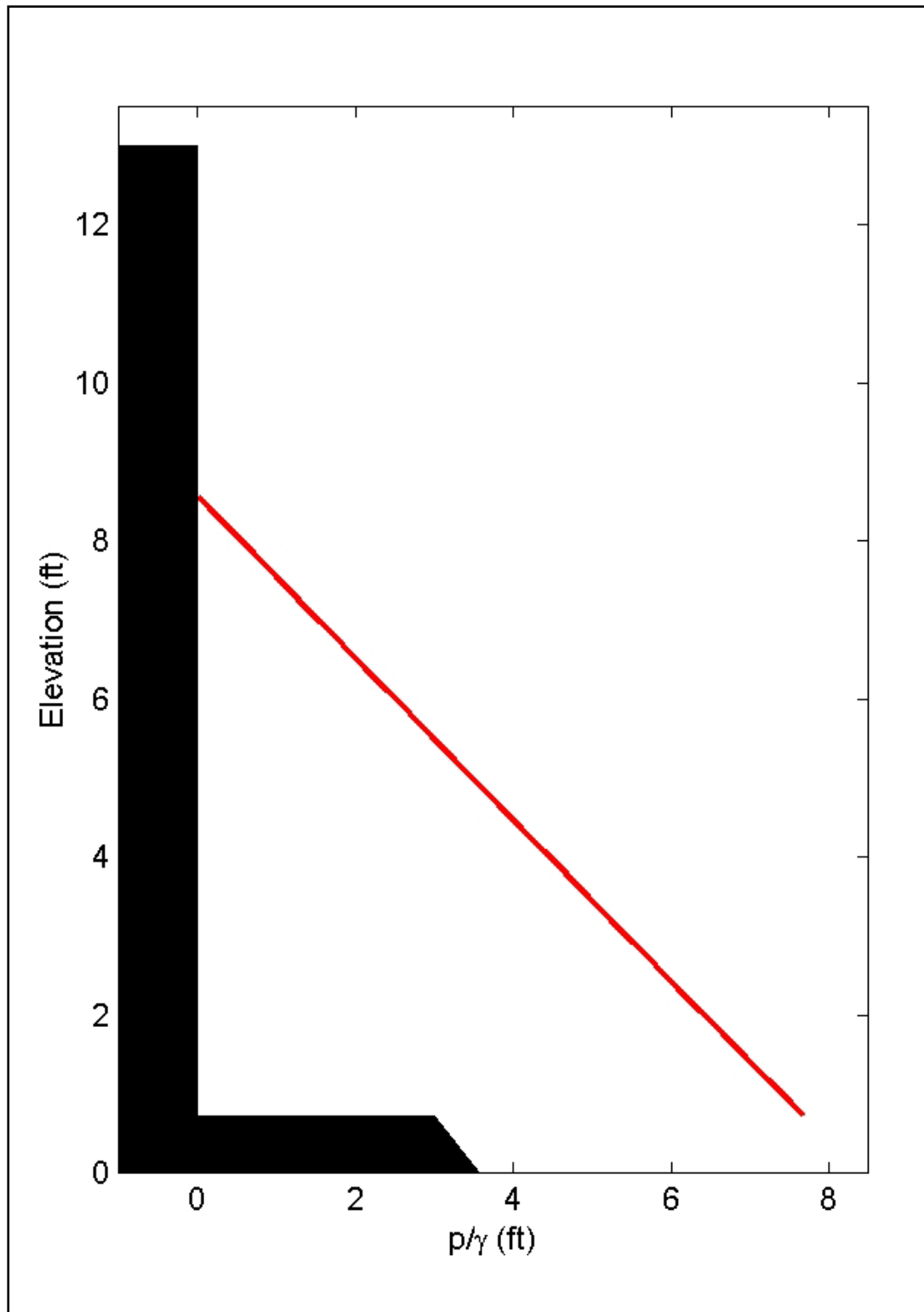


Figure 15-22. Example of numerically predicted vertical distribution of pressure under a wave crest near the London Avenue Canal failure location just south of Robert E. Lee Bridge at 1200 UTC. The black shape represents the floodwall and the red line is the distribution

# Details on Wave Simulation near and inside the Orleans Avenue Canal

## Simulation Setup

The bathymetric grid utilized here is from the ADCIRC grid. The ADCIRC grid is down-interpolated using an inverse distance weighted algorithm with care taken to eliminate coarse grid artifacts such as stepped bathymetry profiles. The total Boussinesq numerical grid is 0.5 square miles, using a 4 ft grid step in both horizontal directions. Two bridges cross the canal in this domain: the Lakeshore Drive Bridge near the canal entrance and the Robert E Lee Bridge farther to the south.

Incident wave conditions are taken from the 95 percent STWAVE output. STWAVE recording locations are just offshore of the area. 2D spectra are used to drive the Boussinesq runs. Simulations are performed for a single time, 1400 UTC on the 29<sup>th</sup>, which is expected to be the condition with the largest waves and water force on the canal walls. Dominant wave direction at this time is out of the north. Wave height and surge are 8.2ft and 11ft, respectively. The model output to be presented includes a wave height transect along the canal, and forces and lines of action on a panel south of the Robert E Lee Bridge.

## Simulation Results: Wave Heights and Periods

A plan view snapshot of the wave field at 1400 UTC is given in Figure 15-23. Waves approach the canal from the north, and waves are large for the first few hundred feet into the canal. The first major bend in the canal appears to restrict the wave energy entering the remainder of the canal, as can be seen in the wave height profile in Figure 15-24. This bend has the effect of reducing the high frequency energy, evident from the jump in peak wave period. In addition, bottom friction, driven by the relatively shallow banks of the canal in the northern section, damp out much of the high frequency energy. Peak wave periods through the majority of the canal are near 50 s. At the Robert E Lee Bridge, the wave height has been reduced to 1.3ft. As with the 17th Street Canal, wave-induced water level changes throughout the canal are minimal - on the order of a couple of inches.

It is noteworthy to mention the simulations indicate that, among the 17th, Orleans, and London Canals, the Orleans Avenue Canal experienced the largest wave-related hydrodynamic loadings. This is likely due to the fact the canal entrance is simple and un-obstructed (unlike 17th Street Canal) and this canal is relatively straight (unlike London Avenue Canal), thereby allowing the largest fraction of wave energy to enter and propagate through the canal. Again, local wave generation by wind blowing across the canal is not taken into account here.

## Simulation Results: Wave Forces

Calculation of the water forces is described in the “Description of Method used to Determine Force along Canal Walls” section. The Orleans Avenue Canal wall cross section is shown in



Figure 15-25. The location of the water force described here is immediately south of the Robert E Lee Bridge. Water forces and lines of action are summarized in the table below. In the table, the force,  $F_{nw}$ , is the force that would result from a static water column of height,  $h$ .

Time (UTC)	Surge (ft)	$h$ (ft)	$F_{nw}$ (lb/ft)	$z_r$ w/ $F_{nw}$ (ft)	$F_{2\%}$ (lb/ft)	$z_r$ w/ $F_{2\%}$ (ft)	$\Delta F$ (lb/ft)
1400	11	10.3	3,310	3.4	3964	3.8	422

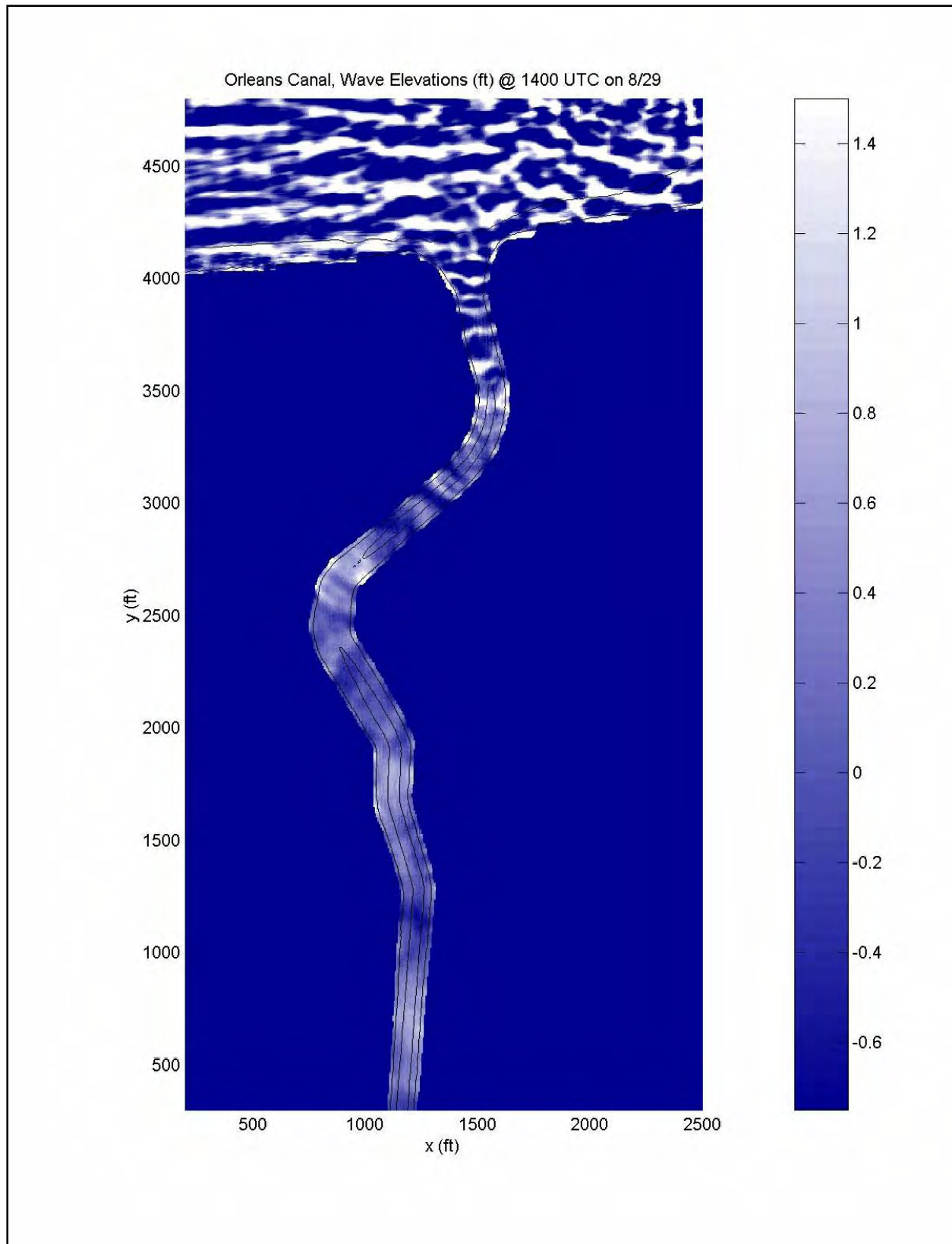


Figure 15-23. Simulated wave field for Orleans Avenue Canal at 1400 UTC

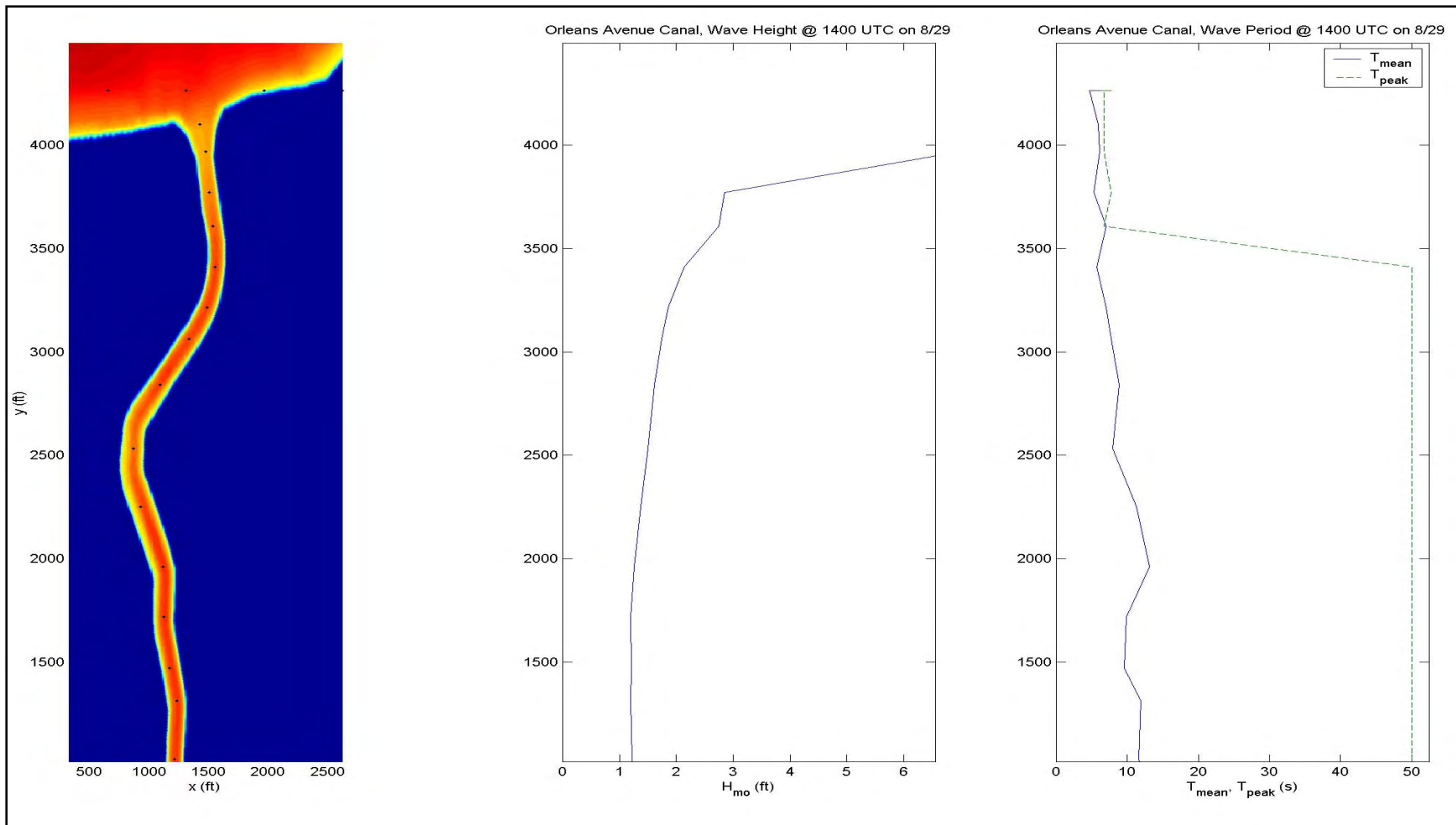


Figure 15-24. Transects of significant wave height and period along the Orleans Avenue Canal at 1400 UTC. Both peak (from spectral analysis) and mean (from zero-crossing) periods are shown, to provide a measure of the periods of dominant wave energy. The first plot on the left provides the domain and the recording points, denoted by the black dots

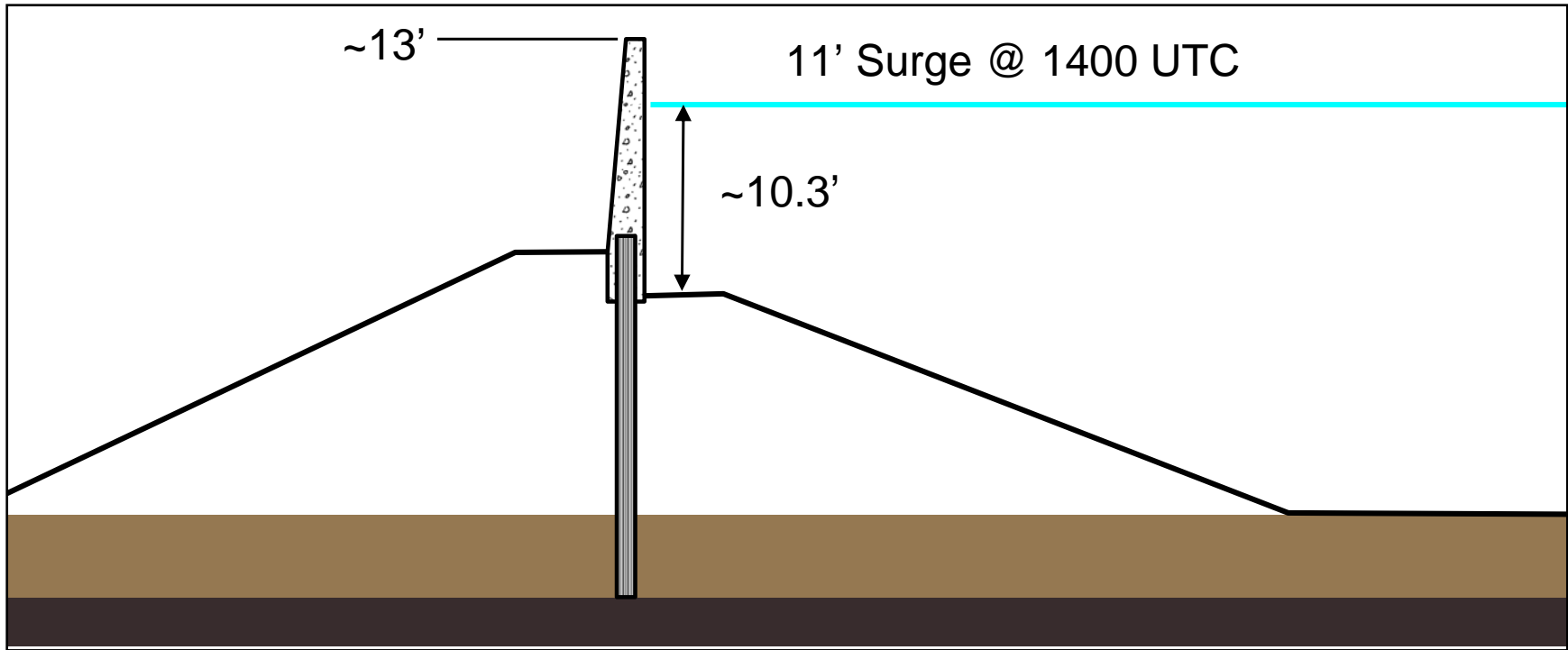


Figure 15-25. Cross-sectional schematic for Orleans Avenue Canal south of the Robert E Lee Bridge

## Details on Wave Simulation near and inside the IHNC

### Simulation Setup

The bathymetric grid utilized here is from the ADCIRC grid. The ADCIRC grid is down-interpolated using an inverse distance weighted algorithm with care taken to eliminate coarse grid artifacts such as stepped bathymetry profiles. Manual modifications are made to the wall locations to better represent the canal boundaries. The total Boussinesq numerical grid is 3.5 square miles, using a 4 ft grid step in both horizontal directions. Two bridges cross the canal in this domain: the Florida Avenue Bridge and the North Claiborne Avenue Bridge.

Incident wave conditions are taken from the STWAVE simulations of wave evolution through the GIWW including local wave generation. The STWAVE output location is near the connection of the IHNC and the GIWW. Two-dimensional spectra are used to drive the Boussinesq runs. Simulations are performed for three times, 0630, 0930 and 1030 UTC on the 29<sup>th</sup>. Due to the early morning times of these simulations, only the waves coming through the GIWW will be used to force the Boussinesq; waves coming down the northern section of the IHNC are assumed short and small, and are ignored. Waves enter the IHNC from the GIWW at an angle nearly perpendicular to the IHNC. The model output to be presented includes wave height transect along the canal, forces, and the vertical distribution of pressure on a panel near the failure locations.

### Simulation Results: Wave Heights and Periods

A plan view snapshot of the wave field at 0630 UTC is given in Figure 15-26. At this time, the significant wave height at the end of the GIWW is 2.4ft. Due to the nearly perpendicular angle of entry into the IHNC, little wave energy makes it south to near the Lock. The wave height transect along the IHNC is shown in Figure 15-27. Wave heights at the Florida Avenue Bridge are about a quarter of a foot. At 0930 UTC, the wave height in the GIWW is near 3.4ft, and wave heights near the Florida Avenue Bridge are close to 0.6ft. By 1030 UTC, the significant wave height at the end of the GIWW has grown to 4.1ft. A snapshot of the waves at this time is shown in Figure 15-28. Here, more wave energy is able to turn into the southern reach of the IHNC, such that the significant wave height near the Florida Avenue Bridge is 1ft. Wave properties through the IHNC at 1030 are also shown in Figure 15-27.

### Simulation Results: Wave Forces

Use of the Boussinesq model to provide estimates of wave force on the IHNC walls near the failure locations is undesirable. The reason for this is that there was wave and surge overtopping, and the Boussinesq model is not capable of simulating overtopping of vertical structures such as canal walls. To address this deficiency, a Navier-Stokes hydrodynamic model is employed. The model used is called COBRAS, developed principally by Prof. Phil Liu at Cornell University. This numerical model is able to accurately simulate wave overturning, 2D(V) turbulence and vorticity and, important to this investigation, overtopping of vertical structures.



The general IHNC canal wall profile is taken from design memoranda. As the actual wall height is highly variable in the area of the failures, the simulations are reduced to a simple set where the surge is +1ft above the wall crest. Specifically, the surge is set as 13.5ft and the top of the wall at 12.5ft. Two simulations are run; one with no waves, and another with 1ft waves with a period of 5 seconds. Pressure distributions and fluid speeds are presented for both cases. Figure 15-29 shows the values for the no-wave case and Figure 15-30 for the wave case. What is evident here, as with all other canal simulations, is that the pressure is nearly hydrostatic, i.e. linearly varying from the instantaneous free surface elevation. The resulting force for the no-waves case is 1940 lb/ft, and 2260 lb/ft under the mean wave crest for the waves case. Note that this force is a mean value, not a 2 percent exceedence. The computational requirements of the Navier-Stokes simulations prohibit the long duration runs with input spectra required to derive statistical relations. Maximum fluid speeds on the backsides of the walls are close to free-fall speeds, near to 16 ft/s for both cases.

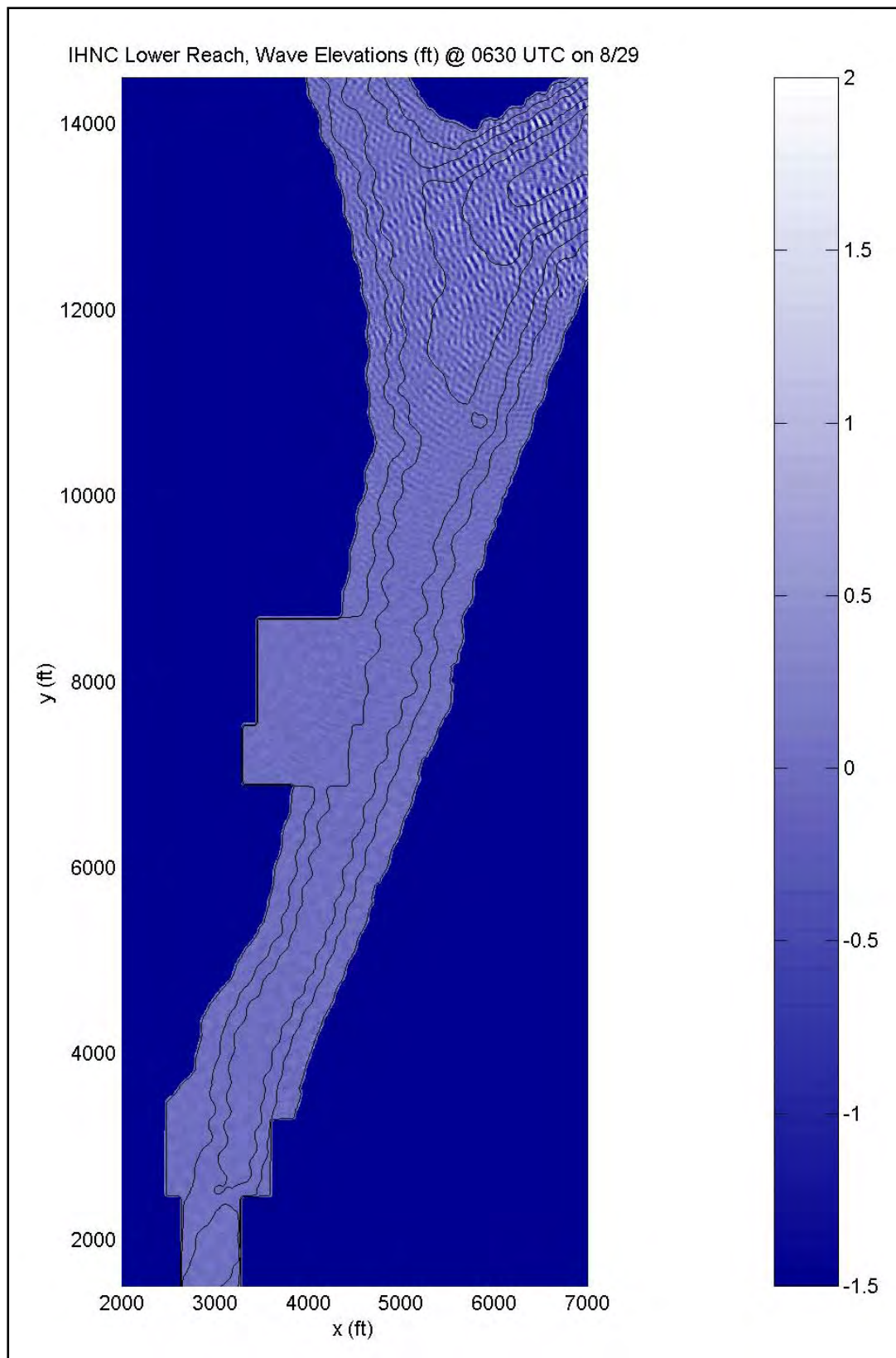


Figure 15-26. Simulated wave field for the lower IHNC at 0630 UTC

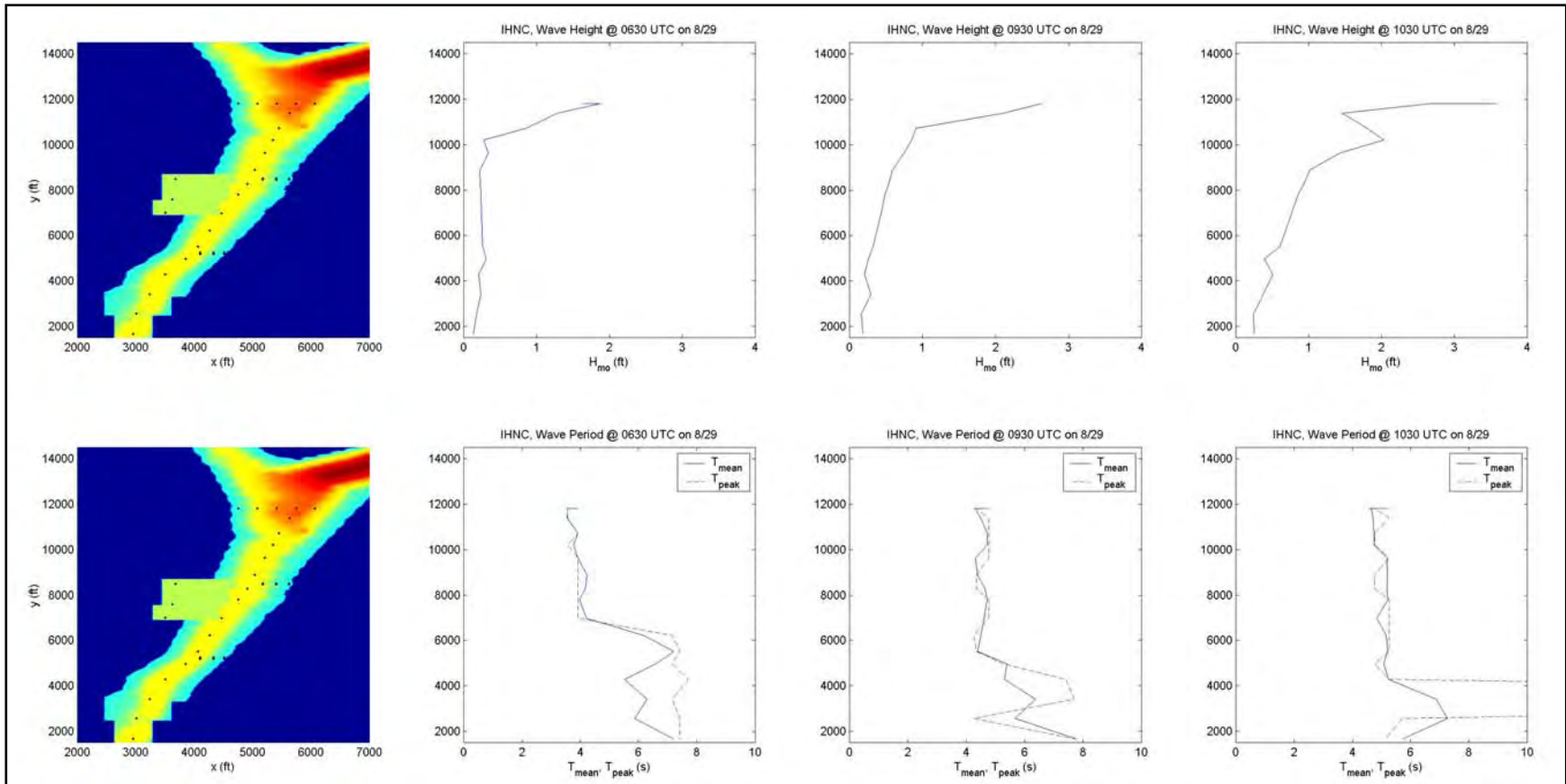


Figure 15-27. Transects of significant wave height and period along the lower IHNC at the three times. Wave heights are given in the top row and periods in the bottom. Both peak (from spectral analysis) and mean (from zero-crossing) periods are shown, to provide a measure of the periods of dominant wave energy. The first plot on the left gives the domain and the recording points, given by the black dots

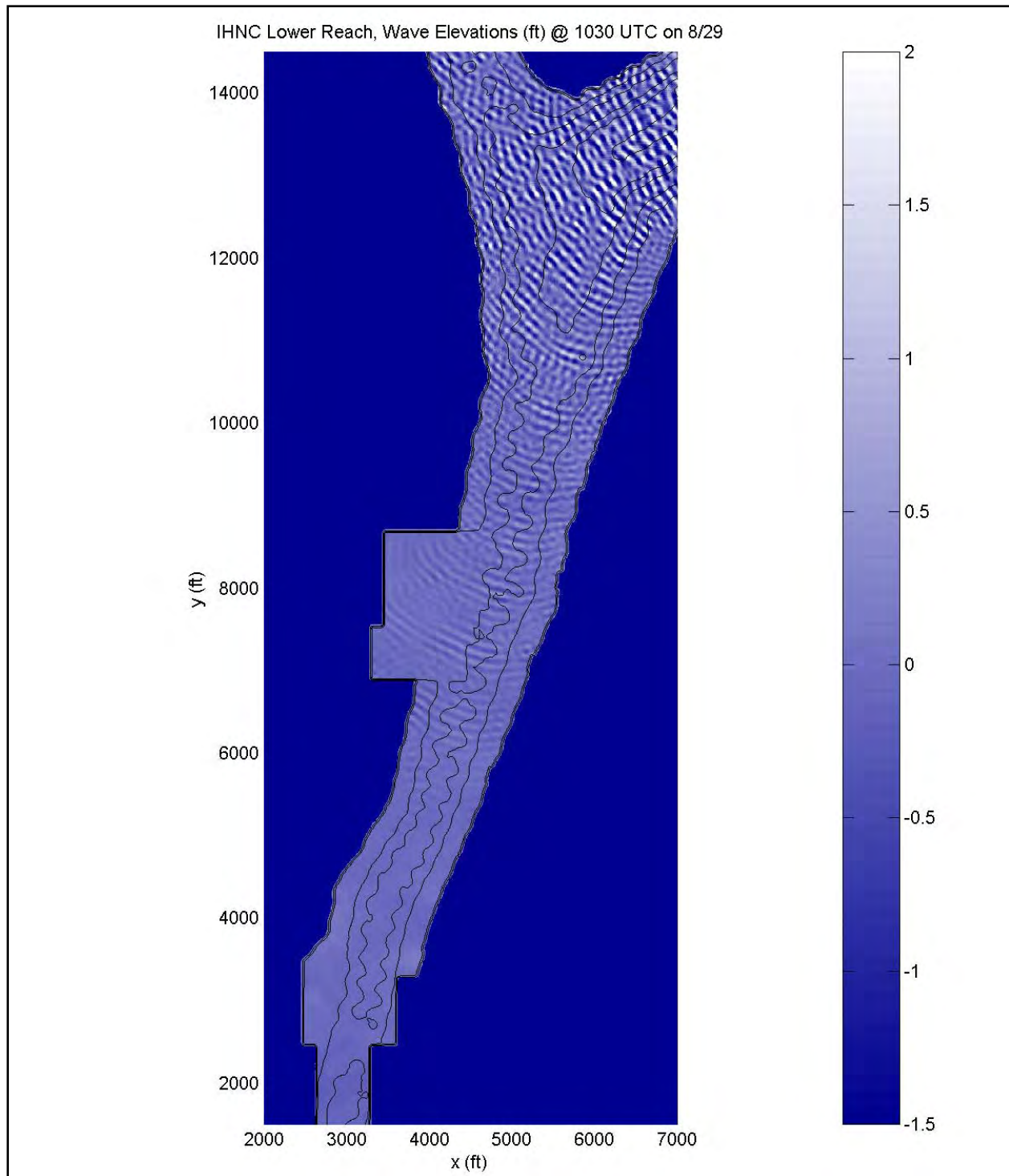


Figure 15-28. Simulated wave field for the lower IHNC at 1030 UTC

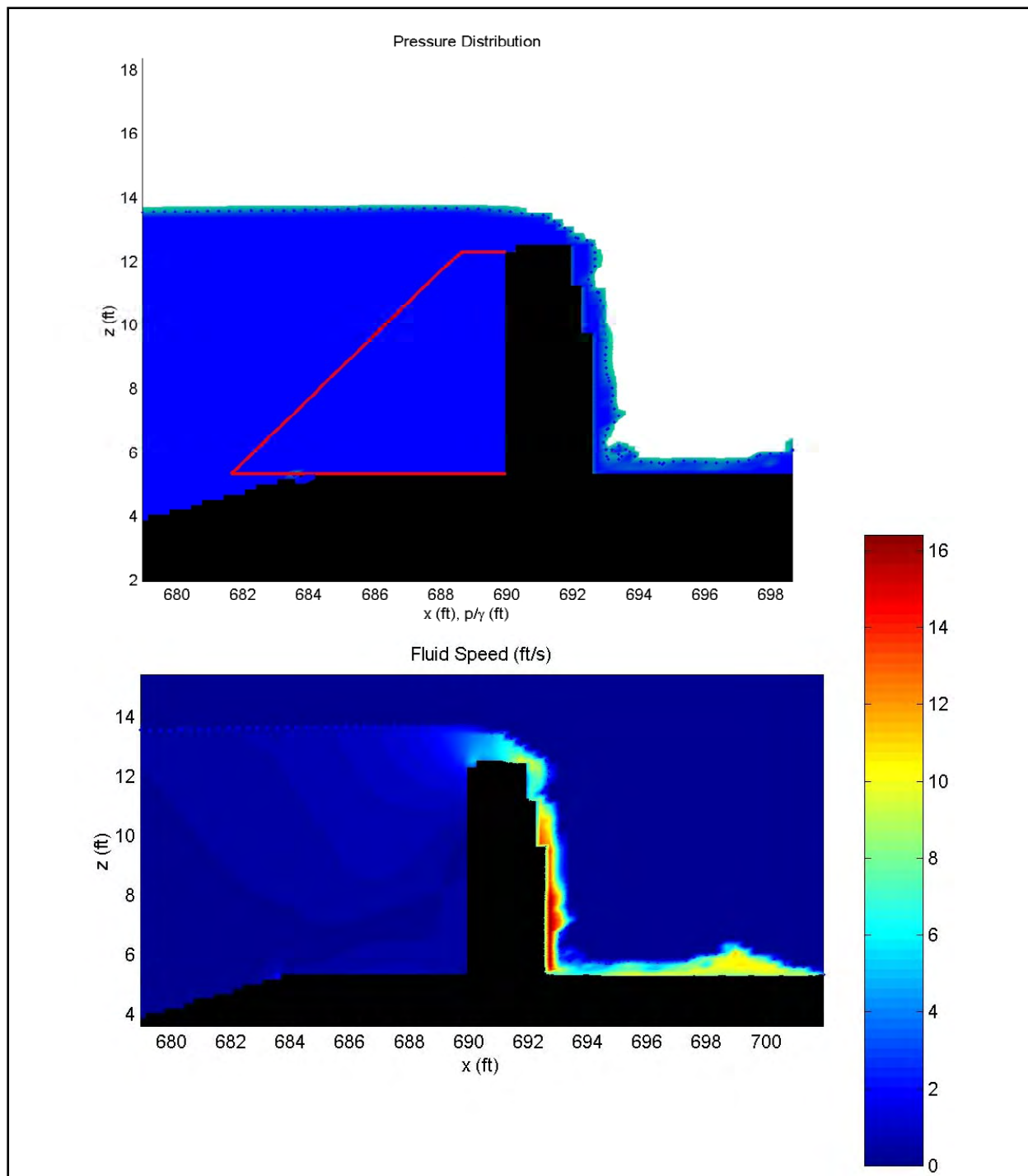


Figure 15-29. Surge overtopping an IHNC wall with no waves. The wall elevation is specified as 1ft below the surge. The top plot gives the water surface and pressure distribution, the lower plot gives the fluid speed field



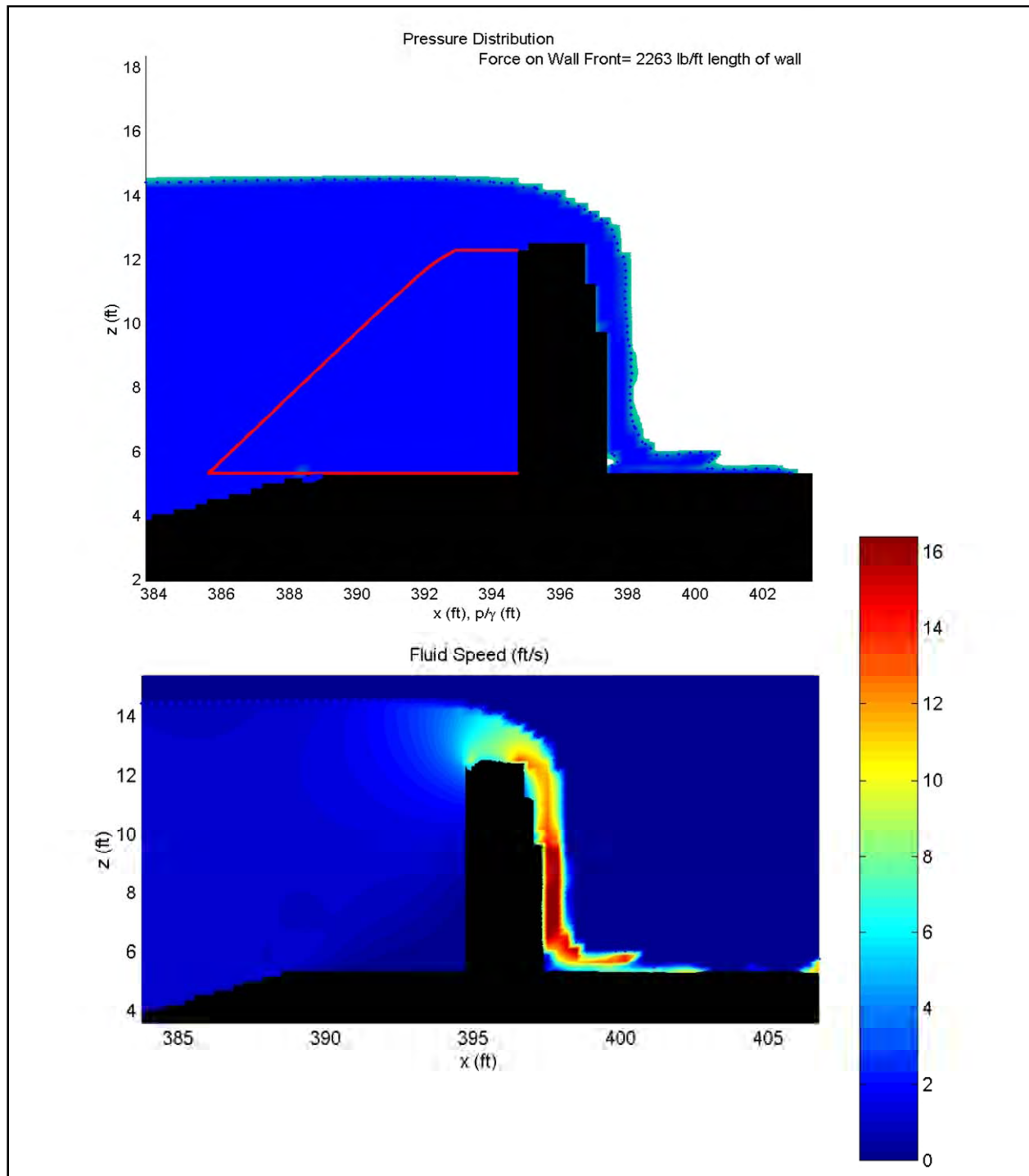


Figure 15-30. Surge overtopping an IHNC wall with 1 foot, 5 second waves. The wall elevation is specified as 1ft below the surge. The top plot gives the water surface and pressure distribution, the lower plot gives the fluid speed field.

# Details on Wave Simulation along MRGO Levees

## Simulation Setup

Wave impacts on levees along MRGO are simulated at four specific transects, as shown in Figure 15-31. These four locations cover the length of the leveed section of the MRGO, and represent the range of conditions experienced along the MRGO. The levee profiles are taken from the “Lake Pontchartrain, LA and Vicinity Design Memorandum No. 3”, dated November 1966. Following this document, the locations examined here correspond to station numbers, starting from the north, #430 (point 1 in Figure 15-31), #540 (point 2), #670 (point 3), and #880 (point 4). The levee profiles from the design memorandum are shifted vertically such that the levee crest elevation matches data from pre-Katrina lidar surveys. Levee crest elevation varies widely along the MRGO, from elevations approaching 19ft (NAVD88 2004.65) near the MRGO-GIWW confluence to values as low as 13.5ft in a region of high spatial variability of crest elevation near the Lake Borgne outlet.

Incident wave conditions are provided by the 95 percent STWAVE results recorded just offshore of the levees in the MRGO. Wave conditions are taken at chosen times throughout the storm from 0630-1500 UTC on the 29<sup>th</sup>, and the quasi-steady conditions at these times are simulated (i.e. for a single simulation, at for example 1230 UTC, the incident wave condition is constant). To estimate the worst case hydrodynamics, the 2D spectra provided by STWAVE are reduced to 1D spectra, and the numerical simulations are performed on a 2D(V) cross-section of the levee. This approach is justified by the observation that the primary wave direction is normal to the MRGO levees, and so predicted 2D(V) hydrodynamics will be a reasonable representation of the full 3D problem. It is noted that while there is little available data to determine the correlation between levee (or seawall) overtopping/runup and peak incident angle for multi-directional spectra, there are indications that the incident angle is not strongly correlated to overtopping rates for incident angles less than 30°, with maximum overtopping occurring at small, but off-normal angles (Owen, 1980).

Hurricane surge levels are taken from a combination of the ADCIRC-provided surge time series and measured watermark elevations. In general, the ADCIRC predictions are about 2.6ft low during the peak of the storm along the MRGO. This is an average value used for the entire length of the MRGO, and is based on interpretation of the few high-confidence water marks found in this area. This 2.6ft is added to the ADCIRC time series at the peak of the storm, with a linearly reduced addition to the time series 2 hours before and after the peak. Outside of this four-hour window, when the surge levels are relatively low, the ADCIRC time series is utilized unmodified.

## Simulation Results

An example of the detail provided by these simulations is given in Figure 15-32. This figure is a single snapshot (i.e. just one of about 30,000 time steps) at location point 2. The physical time corresponding to this condition is 1230 UTC. For the four locations, 24 times are simulated, with a range of 0630-1500 UTC, in 30 minute increments. The simulations provide

“instantaneous” information, predicting variations on the order of the time step of the numerical model, approximately 1/10 of a second. A wealth of information is provided by each simulation. To distill this information for engineering use, time series of free surface elevation, bottom velocity, depth-averaged velocity, and volume flux is written at a few characteristic locations: along the front face of the levee, at the levee crest, and along the backface of the levee. From these time series, time-averaged values and mean maximum values (mean values under the wave crest) are calculated along the levee profile.

For all locations along the length of the MRGO, there is some overtopping from 1130-1430 UTC. The maximum overtopping flux takes place between 1230-1300, and occurs at the time of peak surge for all cases. Time-averaged overtopping rates range from 0.2-20 ft<sup>3</sup>/s/ft. Values on the low end of this range are due to wave overtopping with a surge less than the levee crest elevation, whereas values on the high end arise from surge elevations about 3.5ft above the levee crest, and likely represent the worst conditions experienced along the entire MRGO. Along the backface of the levees, time-averaged, near-bottom flow speeds range from 2.5-15 ft/s during peak conditions, while mean maximum speeds fall between 7-20 ft/s. Wave setup does not play a significant role during the peak conditions. This is due to small waves at the time (2-3ft), and the observation that the waves typically initiate breaking ¼-½ of a wavelength before overtopping the levee, and thus the wave momentum is carried over the levee, rather than through a dissipative surf zone. Later during the day, near 1500 UTC, the wave height reaches 5-6ft, and there is wave setup on the levee front face on the order of 1-2ft. At this time, however, overtopping is minimal. The levee profile geometry appears to play a strong role in setup. To estimate the wave-induced, longshore current, a single 3D simulation was run for point 2 during peak surge-induced currents (1230 UTC). A plan view snapshot of the wave field is given in Figure 15-33. The longshore current prediction is near 0.1 ft/s, and is dwarfed by both the surge-induced current (about 4.5 ft/s) and the cross-shore velocities on the levee front face (about 5 ft/s). The reason for the weak longshore current during peak surge conditions follows that for the small wave setup.

A complete summary of the numerical results for the four MRGO locations is provided in Figures 15-34 to 15-37. The time series of overtopping flux, crest velocity, and backface velocity are very closely correlated to the time series of surge. The peak in wave height, occurring 2.5 hours after the surge peak leads to a temporal extension of the overtopping, where some of the levees experience overtopping until 1600 UTC. Mean maximum values, due to the wave crest, are 1.5-8 times larger than the time-averaged values.

## References

Owen, M. 1980. Design of seawalls allowing for wave overtopping. Tech. Rep. EX 924. Hydraulics Research Wallingford.

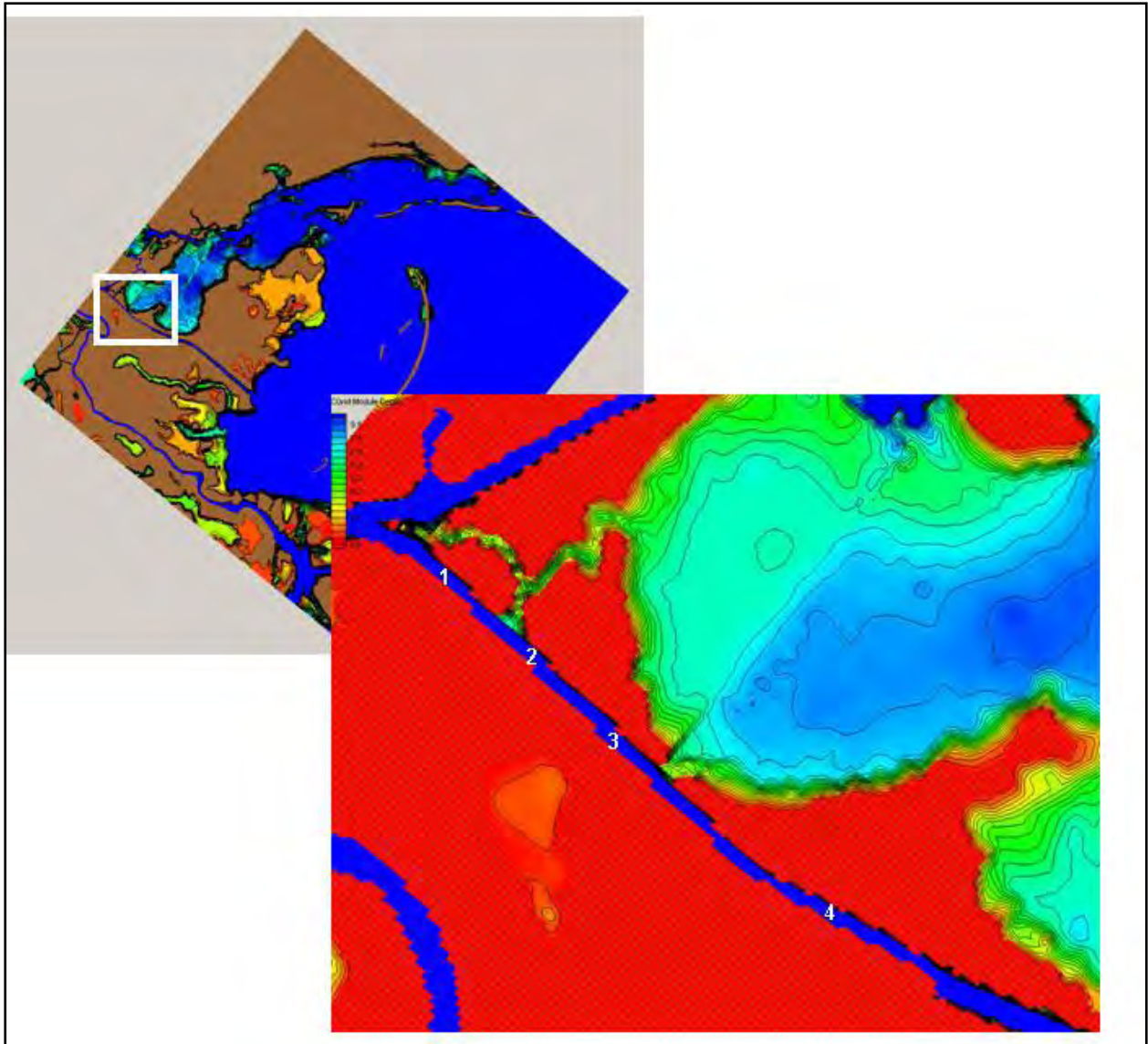


Figure 15-31. Location of MRGO transects for simulation

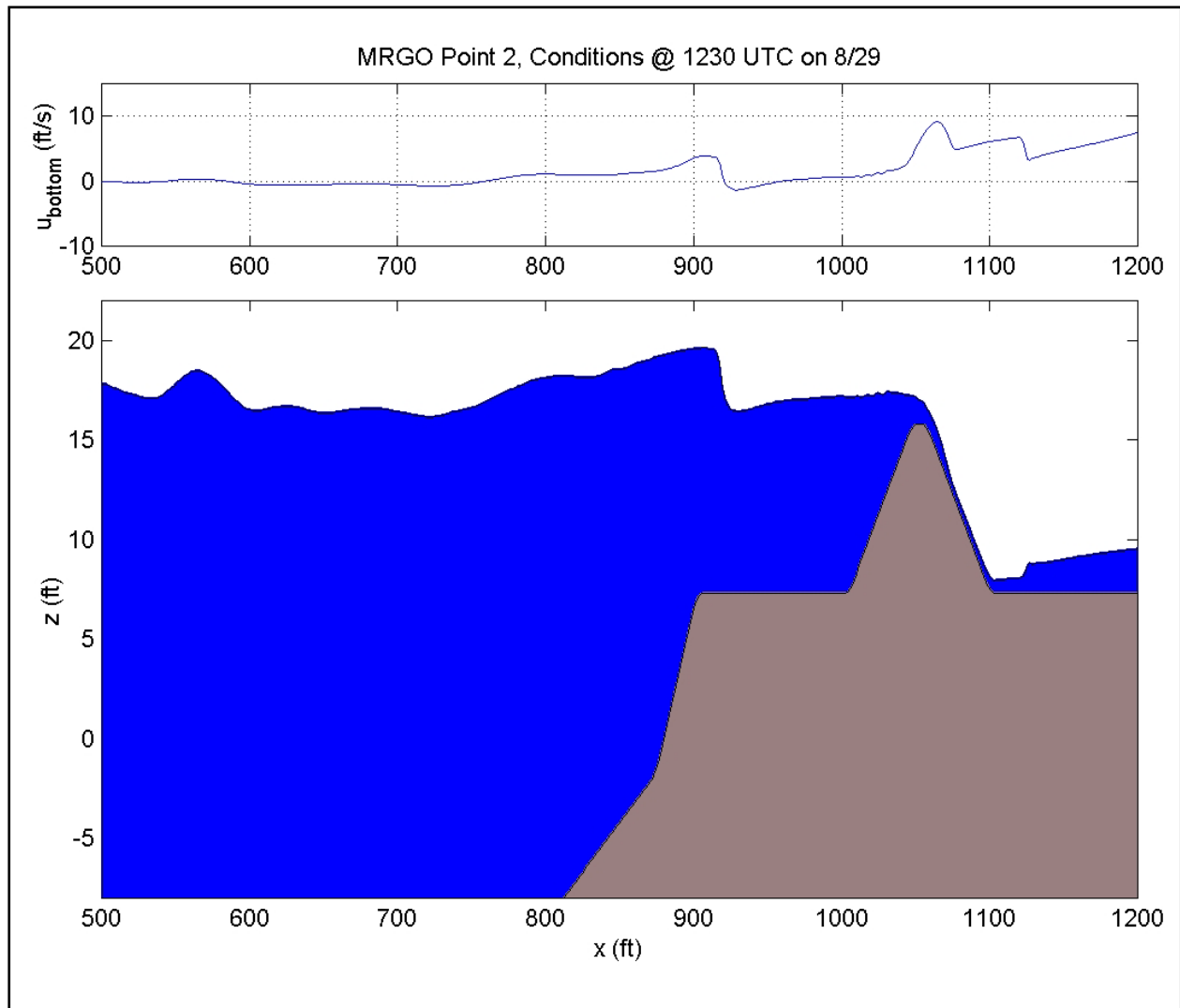


Figure 15-32. Simulation snapshot for MRGO point 2 @ 1230 UTC, where  $H_{mo}=3.2\text{ft}$ , surge elevation=17.4ft, and levee crest elevation=15.8ft. Top plot shows the spatial profile of the near bottom velocity



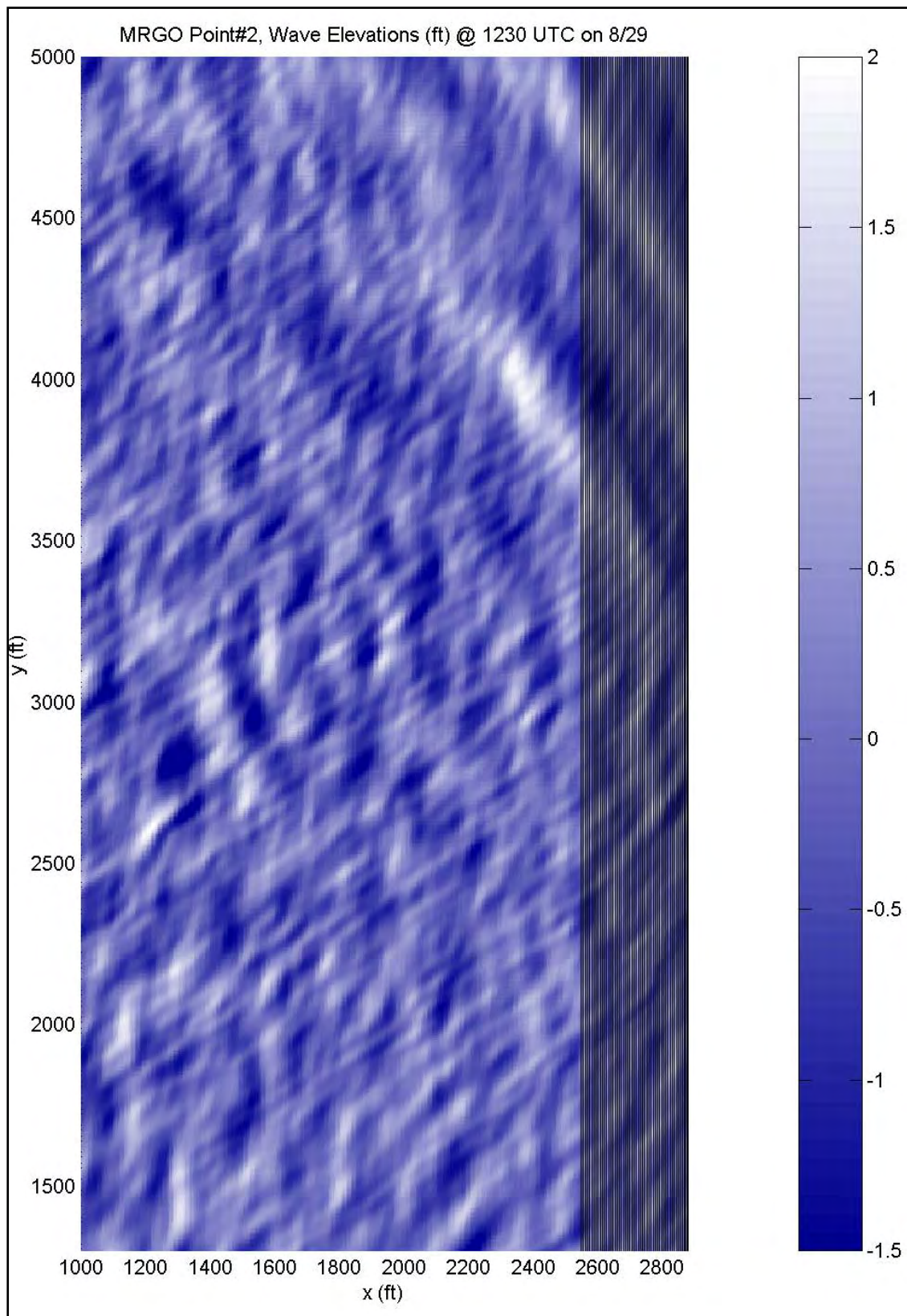


Figure 15-33. Plan view snapshot for 3D simulation at MRGO point 2 @ 1230 UTC, where  $H_{mo}=3.2\text{ft}$ , surge elevation=17.4ft. The levee front face is given by the dense black contours on the right

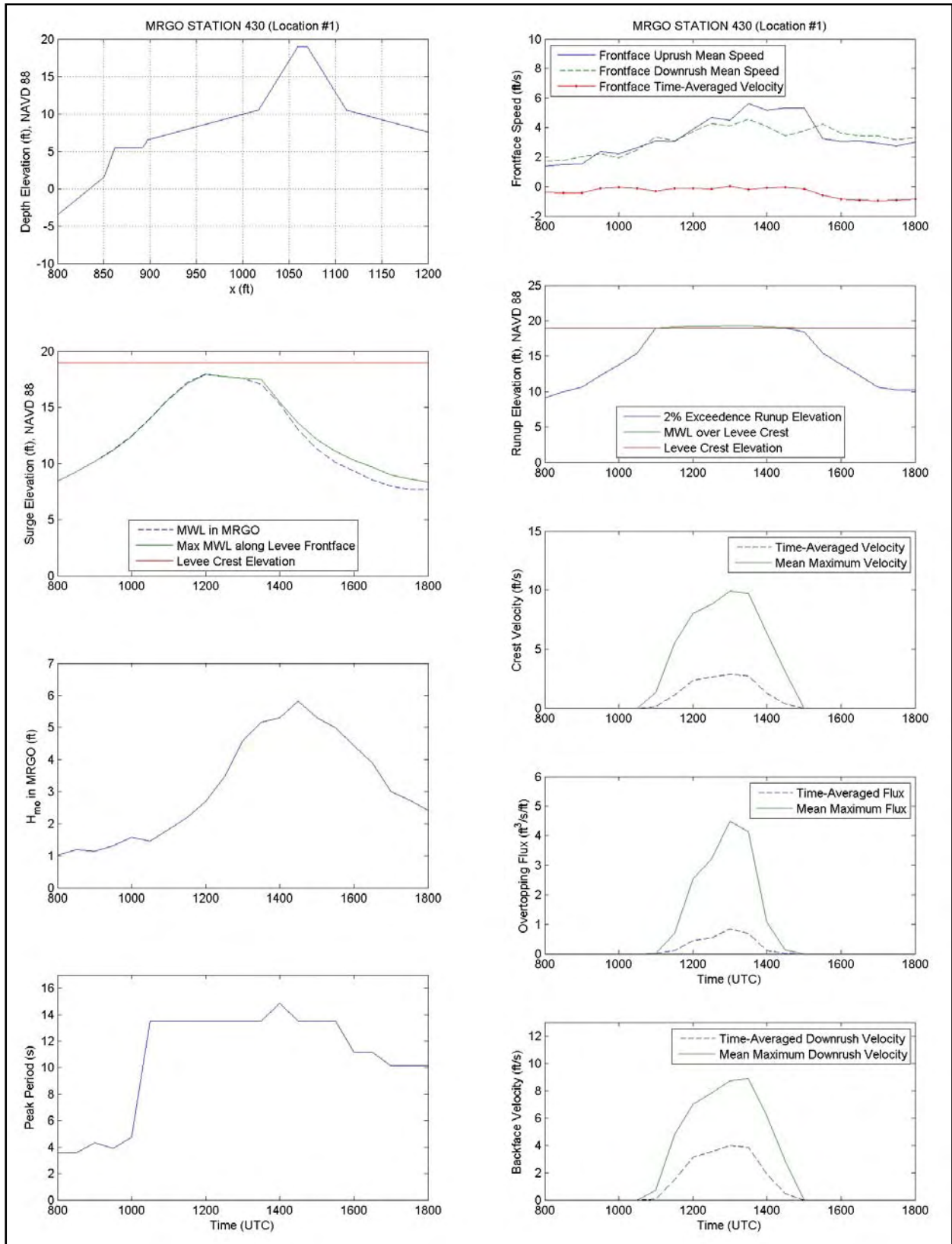


Figure 15-34. Simulation output summary for MRGO point #1

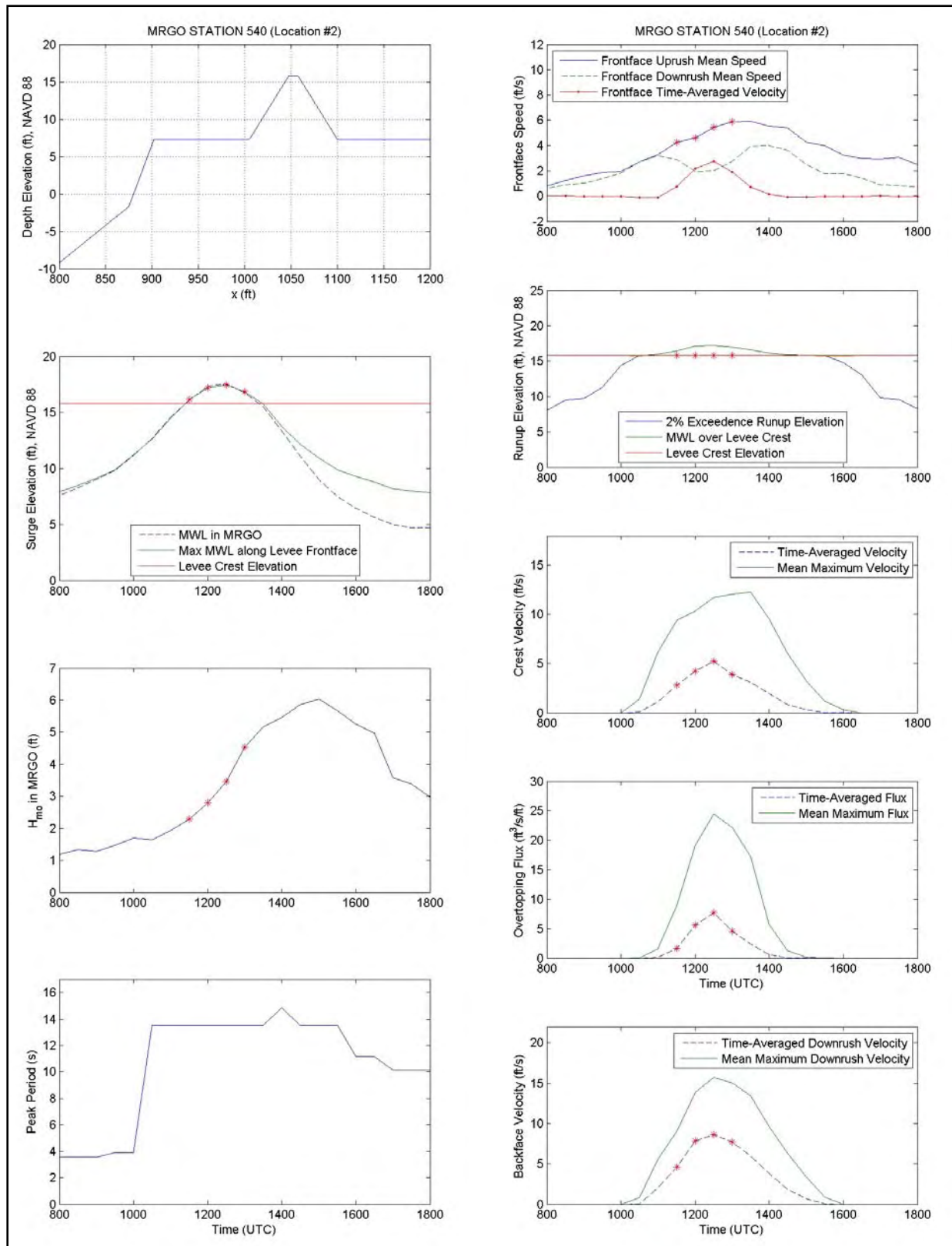


Figure 15-35. Simulation output summary for MRGO point #2. Red stars indicate time of continuous overtopping



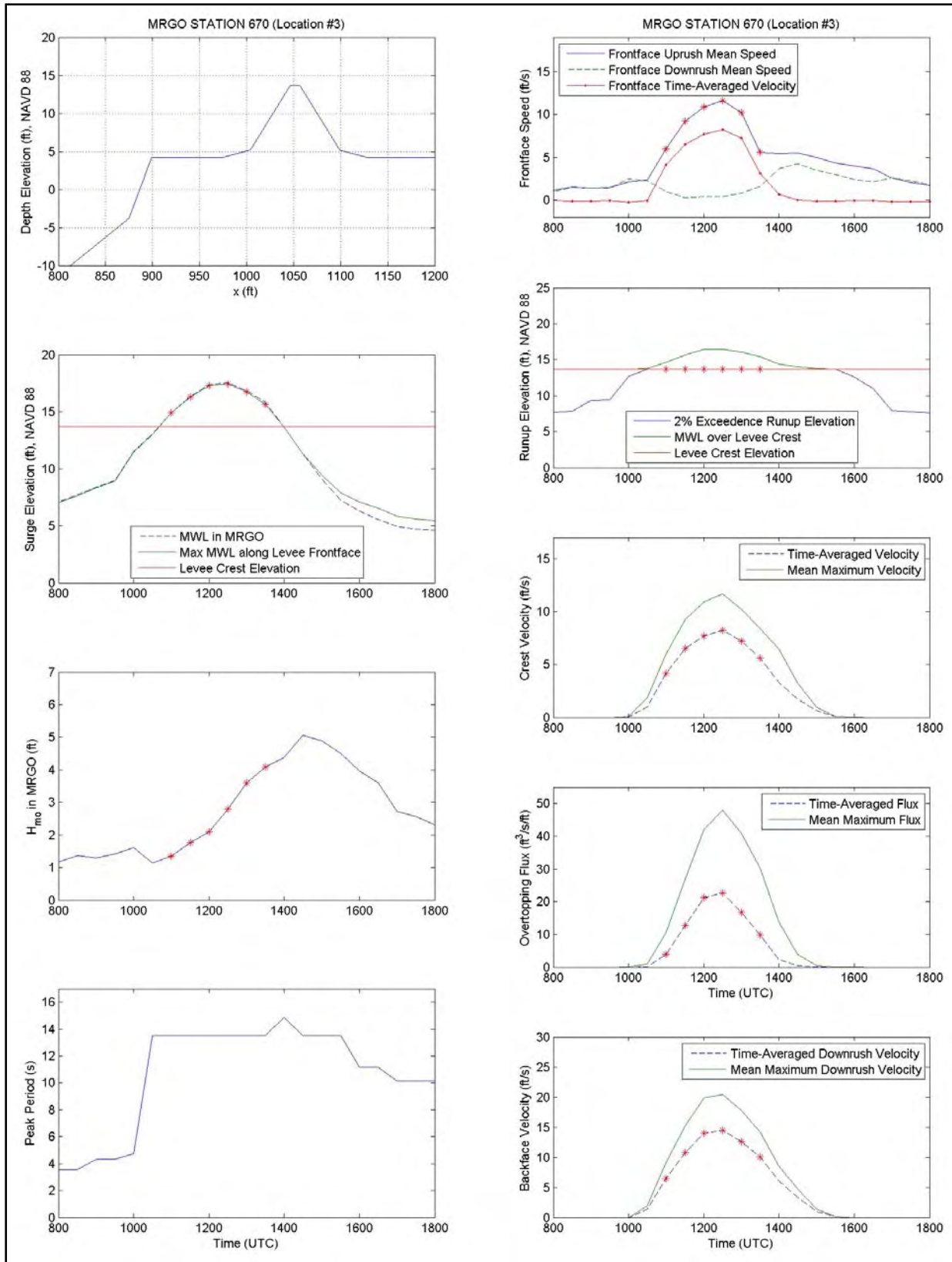


Figure 15-36. Simulation output summary for MRGO point #3. Red stars indicate time of continuous overtopping

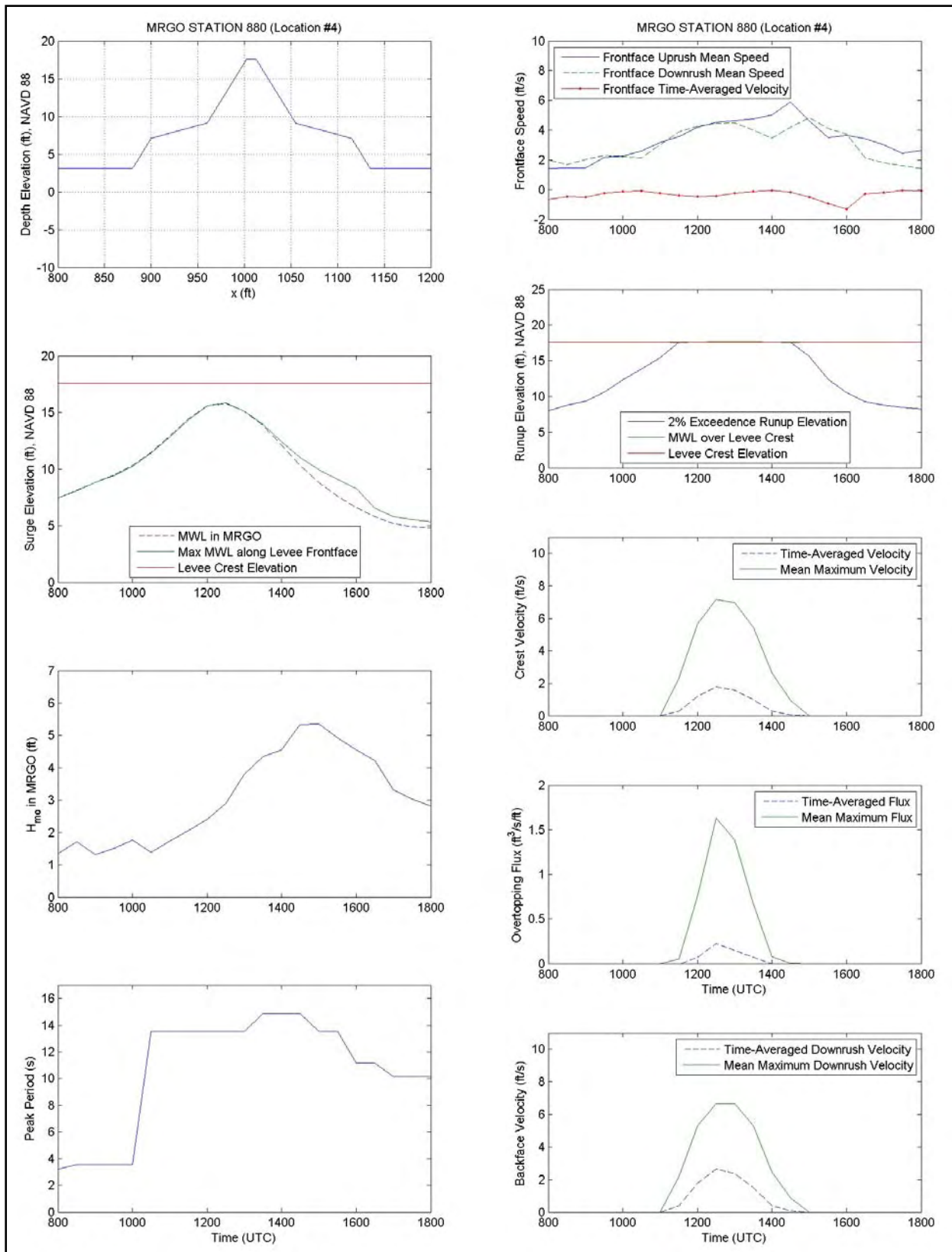


Figure 15-37. Simulation output summary for MRGO point #4



# Details on Wave Simulation along New Orleans East Levees

## Simulation Setup

In New Orleans East the two locations along the GIWW, and shown in Figure 15-38, are examined. The first, at the far east extension of the levees along the GIWW, will utilize 2D(V) simulations similar to those performed along the MRGO. However, only the conditions at the surge peak will be simulated. The levee profile is taken from the design memoranda, and the profile is shifted vertically to match pre-Katrina lidar survey data. The levee crest elevation is 15.5' (NAVD88 2004.65). A difference in the levees near this location is a small seadike, with elevation 4', seaward of the main levee. The second location is near the Paris Road Bridge, on the north side of the GIWW, where the well-circulated photograph of overtopping was taken (see Figure 15-39). The levee profile is again taken from the design memoranda, and shifted vertically to match the pre-Katrina crest elevation of 13.6'.

Incident wave conditions are provided by the 95 percent STWAVE results developed near the levee locations. As with the MRGO simulations, for the 2D(V) simulation, the 2D spectrum is reduced to a 1D spectrum with all energy placed into the shore normal direction. For the 3D simulation near the Paris Road Bridge, the 2D directional spectrum is used to force the simulation.

Since only the conditions at the peak surge are being simulated at the eastern location, the water level provided by measured high water marks is used. High water marks near this levee are 15.7'. At the Paris Road Bridge, simulated conditions are meant to recreate those shown in the photograph (Fig. 2), such that simulation numbers may be approximately associated with the energetics shown in the photo. It is postulated that in this photo, waves are dominating the overtopping, as hinted at by the apparent low overtopping flux region (wave trough) adjacent to the high flux region (wave crest). These regions are denoted in Figure 15-39. In addition, while the time of the photograph is not known, judging from the natural light in the photo, the time is estimated as 0700-0800 local time. In accordance with this time, it can be estimated that the surge is about 1' less than the peak surge of 15'. Thus it is expected that the surge elevation is near the levee crest elevation, and will be set 0.5' above the levee crest.

## Simulation Results

Firstly, the simulation at the far eastern levee along the GIWW is discussed. A snapshot of the numerical simulation is given in Figure 15-40. For this peak condition, the surge elevation is 15.7', the wave height is 4.2', and the peak wave period is 14 seconds. Time-averaged values of overtopping flux, crest velocity, and backface velocity are 1.0 ft<sup>3</sup>/s/ft, 2.0 ft/s, and 6.0 ft/s, respectively. The mean maximum values, associated with the wave crest, are 8.7 ft<sup>3</sup>/s/ft, 8.5 ft/s, and 12.5 ft/s, respectively

Second, output from the 3D simulation near the Paris Road Bridge is presented. An elevated side-view image from the simulation is given in Figure 15-41. Here wave height is 4.0', the peak wave period is 13.5 seconds, and the dominant wave direction is parallel to the GIWW. As the

waves propagate through the GIWW, large-angle refraction along the channel side levee face causes a local decrease in the wave height. This refraction can be seen in Figure 15-41 by the bending of the wave crests before overtopping the levee. Of primary interest are the fluid velocities along the backface of the levee. Figure 15-42 gives a plan view snapshot of the fluid speed, taken at the same time as Figure 15-41. The numerical model predicts maximum velocities (under the wave crests) near 8 ft/s, while overtopping velocities under the troughs are much lower, near 3-5 ft/s. In fact, the levee crest will occasionally go “dry” along a wave trough, when the water elevation dips below the levee crest elevation. One such instance is shown in Figure 15-41. Time-averaging the backface velocity gives values near 4.5 ft/s along the levee crest, with little variation. The overtopping energy shown in this simulation, while significant, is on par with peak conditions predicted at “point 1” of the MRGO simulations. Near this MRGO location, there was only minor overtopping damage/erosion. Thus, while the overtopping shown in Figure 15-39 certainly appears impressive, it was likely not at the level required to cause serious levee damage. This may partially explain why there was only minor levee erosion in this area. It must also be noted again that the time of the photo in Figure 15-39 was probably an hour or so after the surge peak, and thus conditions may have been considerably worse before this photo was taken.

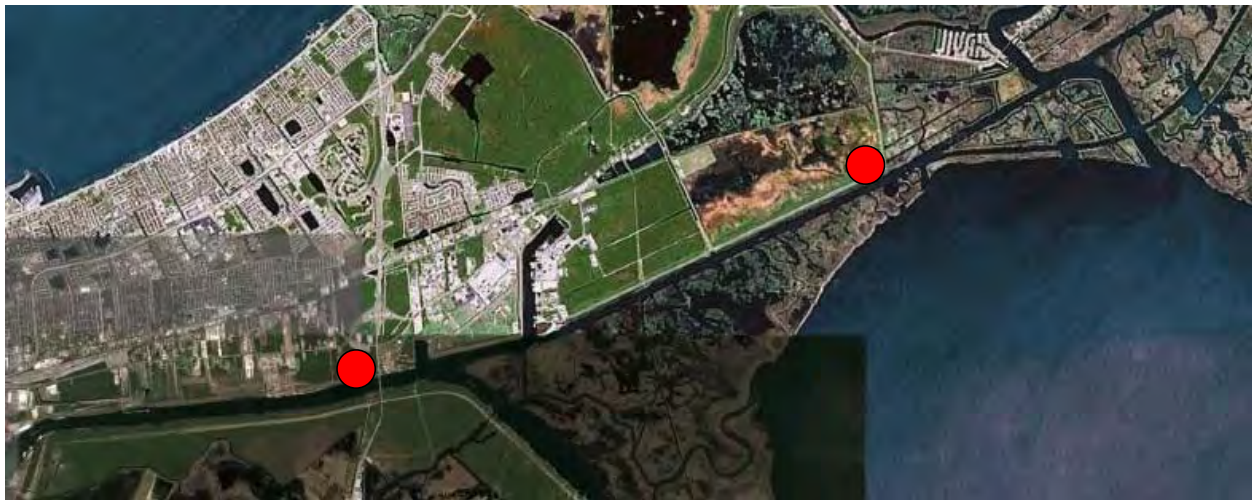


Figure 15-38. Map showing eastern (right) and Paris Road Bridge (left) locations for levee simulations along New Orleans East

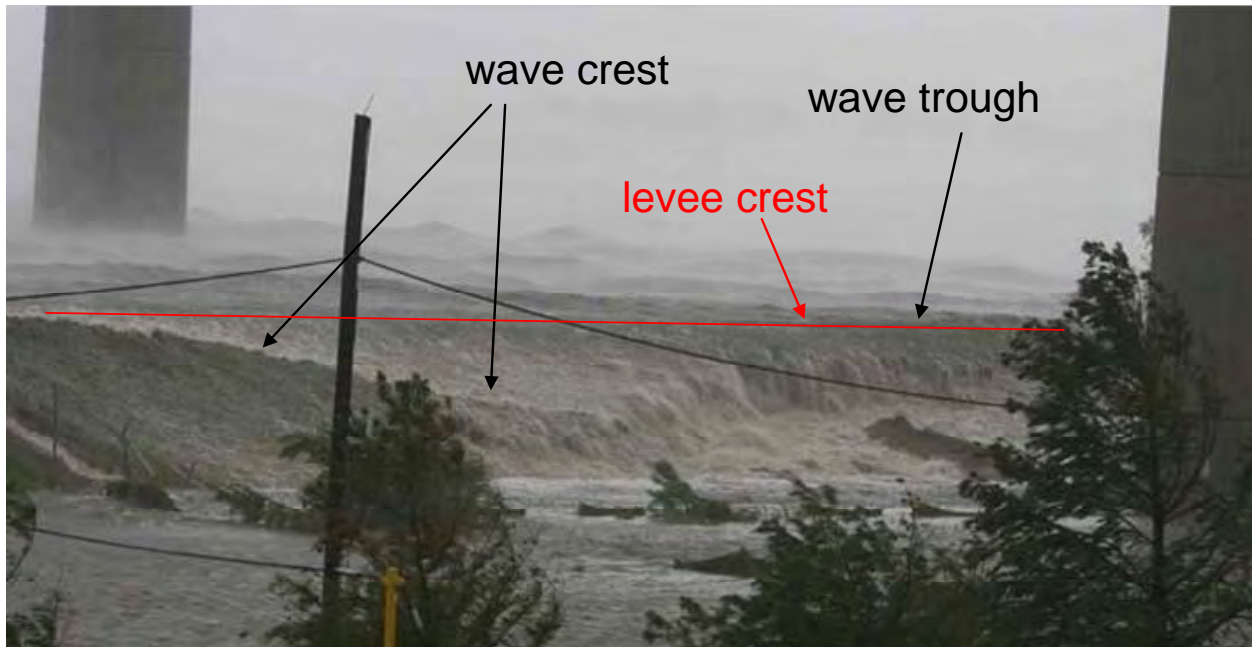


Figure 15-39. Photograph showing overtopping of levee under the Paris Road Bridge. Time of the photo is not known with certainty. View is from the north side of the levee, looking towards the southwest. Waves are traveling from the east (left side of photo) towards the IHNC

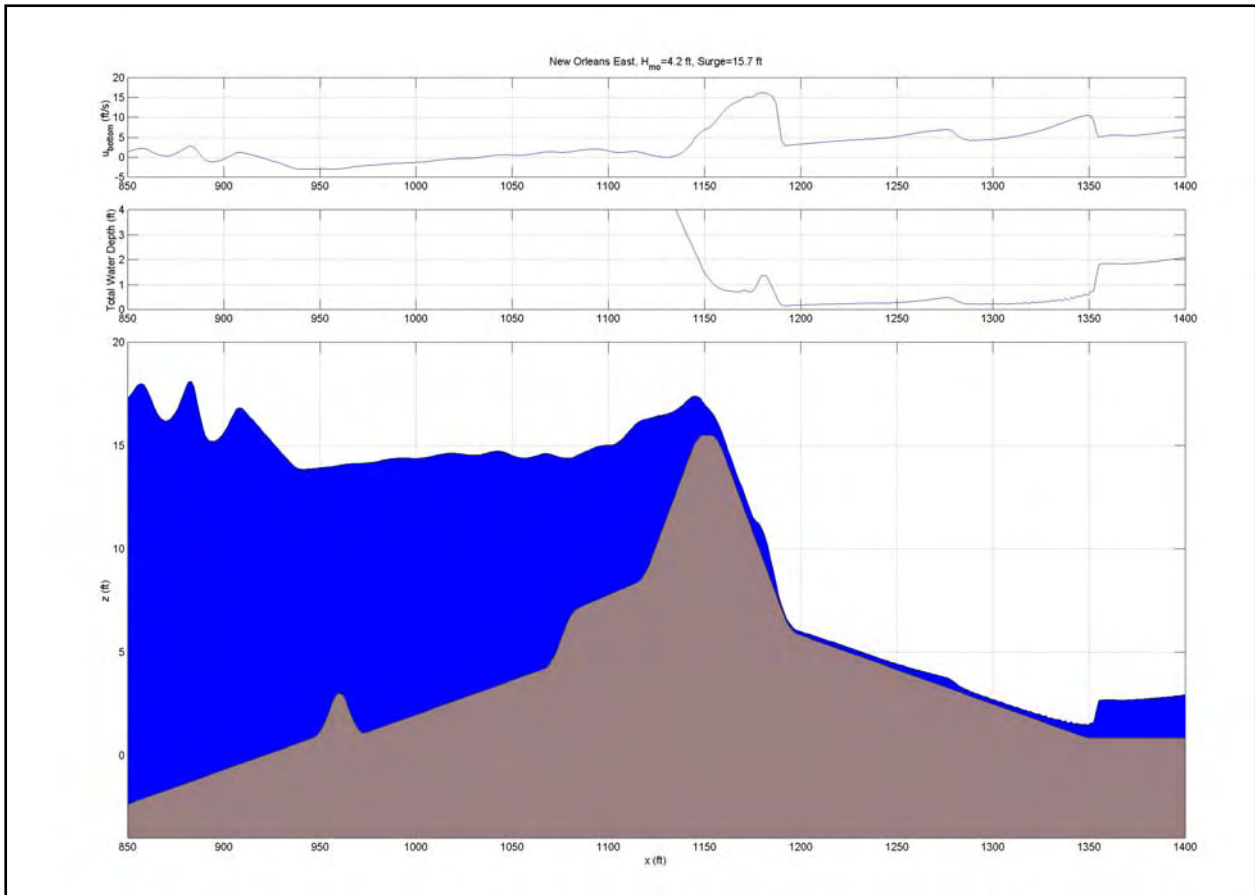


Figure 15-40. Snapshot from the numerical simulation of overtopping the far eastern GIWW levees. Conditions correspond to 1230 UTC on the 29<sup>th</sup>, with  $H_{mo}=4.2'$  and surge=15.7'. Spatial transects of near bottom velocity and total water depth are given in the top two subplots

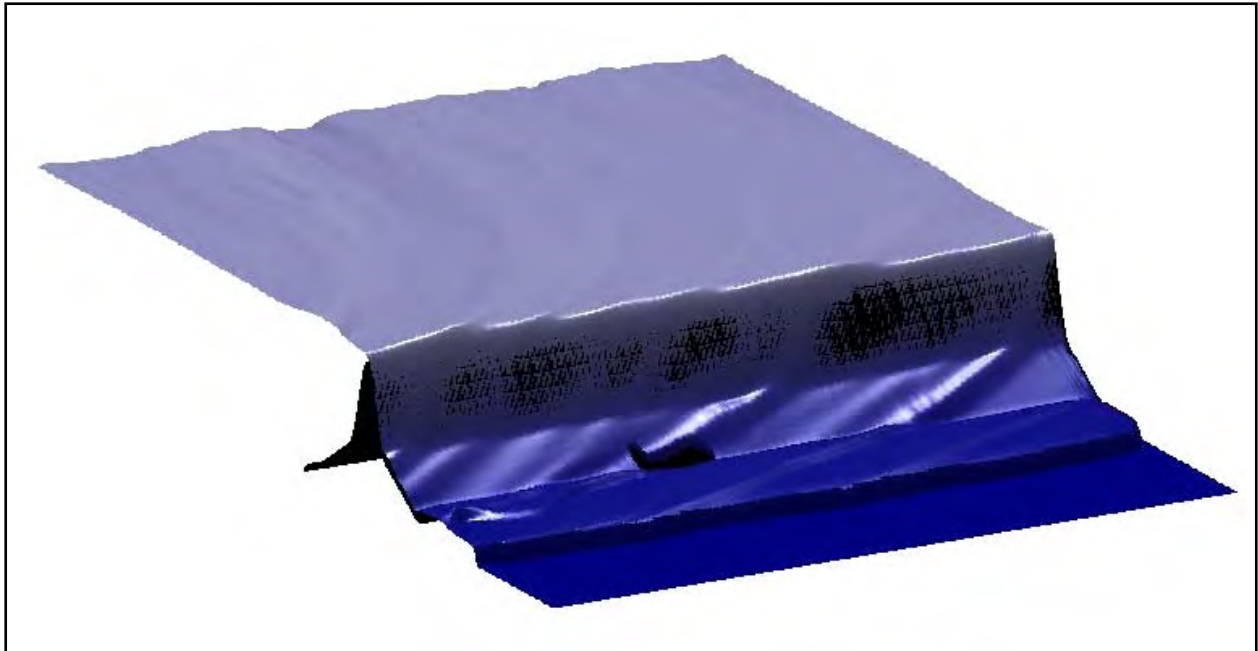


Figure 15-41. Side angle view of numerical waves overtopping the levee near the Paris Road Bridge. The levee is shown as the submerged black shape. View is looking towards the southwest; waves are from the east (left side of image)



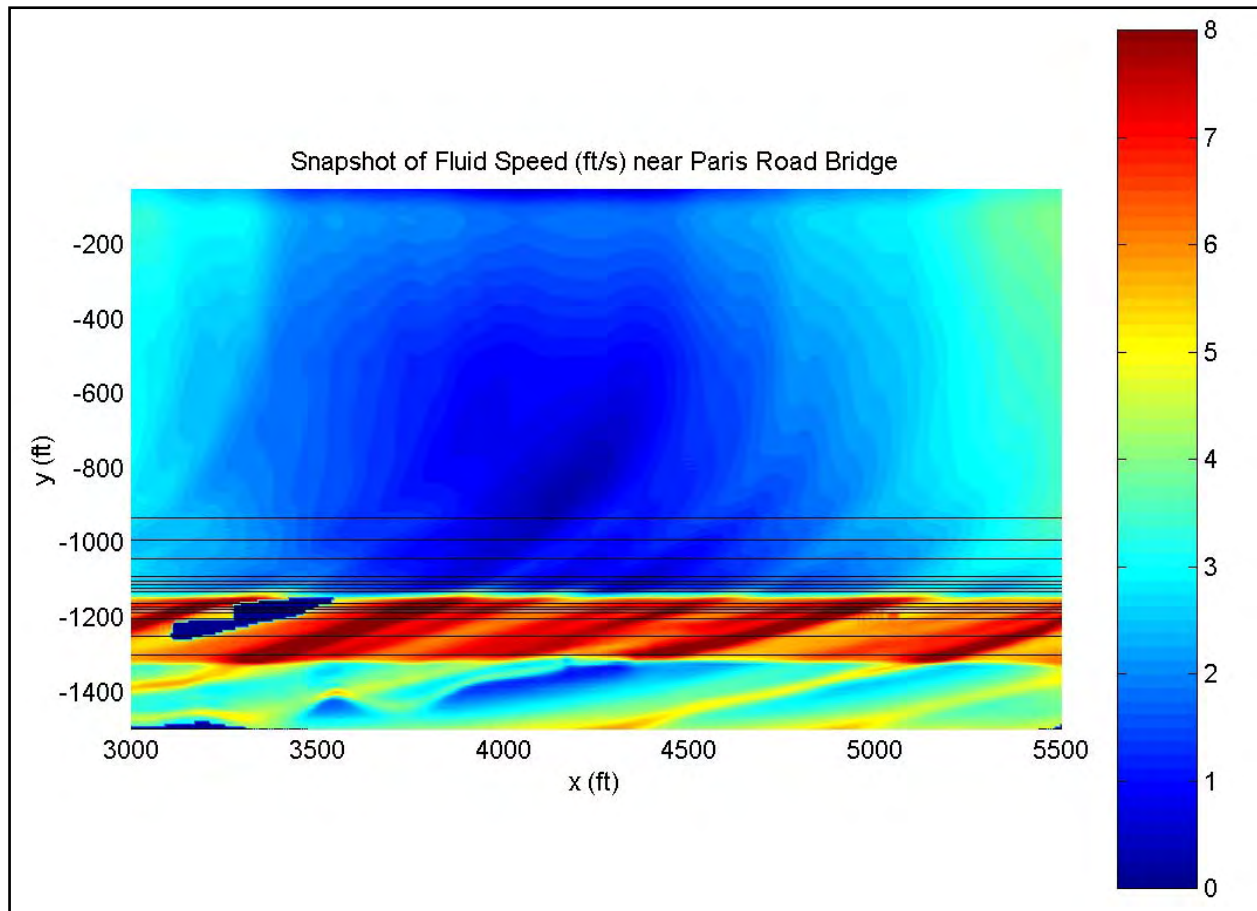


Figure 15-42. Plan view of near-bottom fluid speed. Time corresponds to that shown in Figure 15-41. The levee location is given by the solid black contour lines along the top of the plot (levee crest near  $y=1150$  ft). View is looking from above at the north side levee; the center of the channel is near the top of the image, and waves are from the east (left side of image)

## Details on Wave Simulation along Mississippi River Levees in Plaquemines Parish

### Simulation Setup

Herein, wave and surge impact are investigated at a single location along the Mississippi River in Plaquemines Parish. The location is near Davant, shown in Figure 15-43. The structure profile here is taken as a T-wall on an earthen levee. The T-wall extends above ground from +10' to +17' elevation. The surge is set as 20'. Wave conditions are taken from STWAVE at the time of the surge peak. These conditions are  $H_{mo}=5.4'$  and  $T_{peak}=15$  s.

### Simulation Results: Wave Forces

As for the IHNC analysis, the Boussinesq model is not capable of simulating overtopping of vertical structures, and the Navier-Stokes model is used here. Figure 15-44 summarizes the

results of the simulation. Shown is the pressure distribution and speed field at the time of maximum (crest) and minimum (trough) force. Here, the dynamic impact can be seen in the pressure distribution under the wave crest, as the vertical distribution is not linear. Under the trough, however, the distribution is linear. This is an expected result with large amplitude waves. The force under the crest is 3930 lb/ft, and 2960 lb/ft under the wave trough. These forces are mean values, not a 2 percent exceedence. The computational requirements of the Navier-Stokes simulations prohibit the long duration runs with input spectrums required to derive statistical relations. Note that the dynamic effect under the crest adds approximately 6 percent to the total force acting on the wall; the hydrostatic load on this wall with a 23' instantaneous water surface elevation is 3710 lb/ft. Maximum fluid speeds on the backsides of the walls are extreme when the crest impacts the wall, near to 25 ft/s. Under the wave crest, there is sufficient horizontal velocity under the wave to create a jet which hits the soil 5-10' past the back of the T-wall. Overtopping flux under the wave crest is 67 ft<sup>3</sup>/s/ft; under the trough this dips to 9 ft<sup>3</sup>/s/ft. The wave-averaged value of overtopping flux is 22 ft<sup>3</sup>/s/ft, which is a value much closer to the trough due to the wave asymmetry.



Figure 15-43. Photograph showing the location of the simulation conducted in Plaquemines Parish

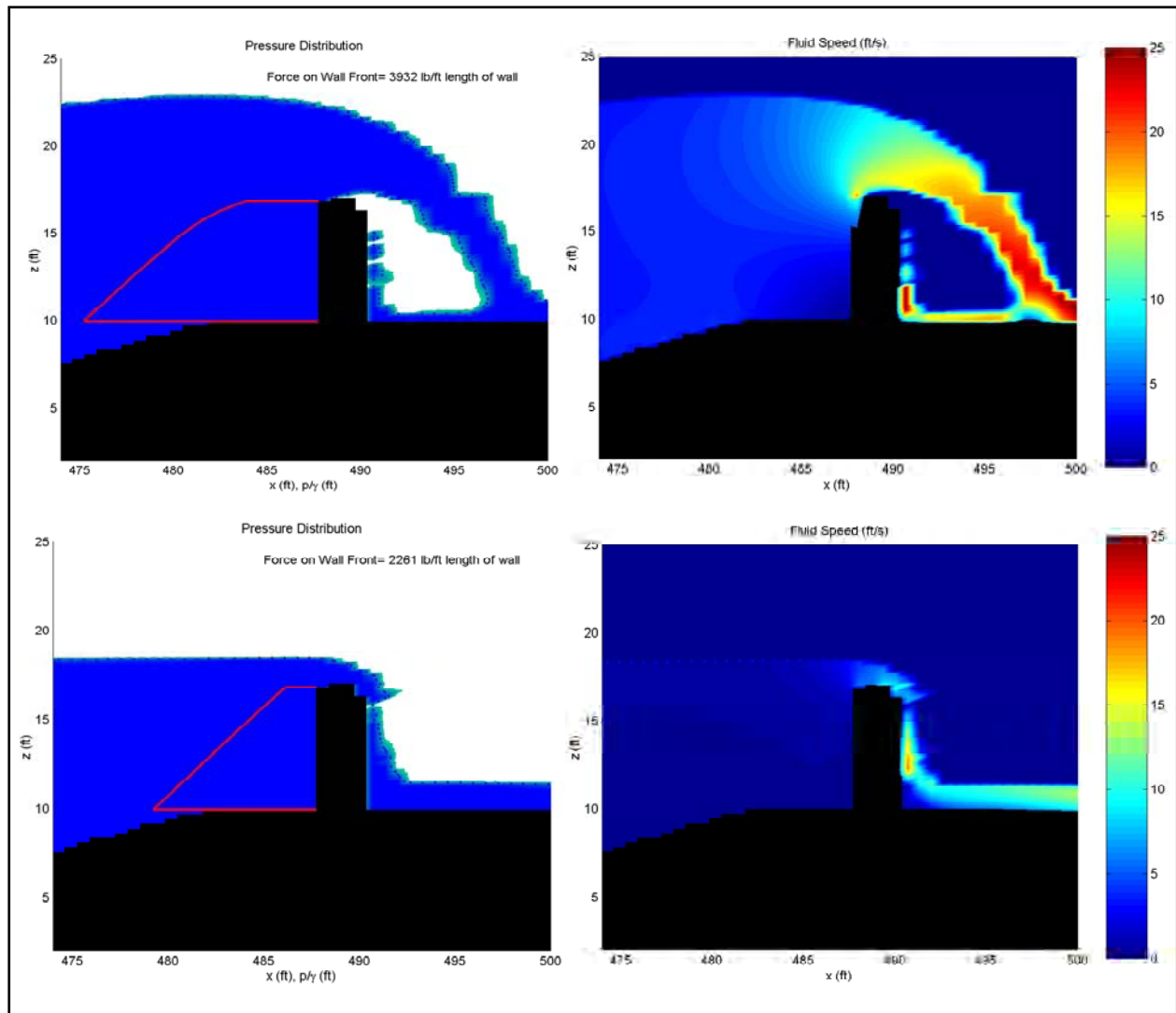


Figure 15-44. Pressure distribution (left) and speed field (right) under the wave crest (top) and wave trough (bottom) for wave overtopping the levee wall

# Appendix 16

## Assessment of Changes of the Mississippi River Gulf Outlet (MRGO) Levees Determined from Pre- and Post-Katrina LIDAR Surveys

---

Airborne LIDAR surveys were performed on the MRGO levee system in the year 2000, and repeated after Hurricane Katrina in 2005. These two surveys are compared in Figures 16-1 to 16-9, which present both line plots of levee crest elevations, as well as 3D renditions (note that the along-levee scales are not consistent among the figures). Also presented is a line denoting the typical levee design crest-elevation of 16.5 ft NAVD2004.65, and a band denoting the range of maximum storm surge elevations, determined from a combination of high water marks and numerical modeling results (17.5-18.5 ft) as described in other appendices of this report. Although there is an obvious, but as yet unresolved, ubiquitous offset between the two crest elevation surveys, heavily damaged sections are clearly identified.

In many locations the MRGO levee is topped by sheet pile floodwall, in order to bring an otherwise low levee up to the design crest-elevation. However, these slender structures are not captured clearly with the resolution of the LIDAR. An attempt has been made to label these areas of floodwall. It is noted that floodwall zones generally are manifest in the crest-elevation plots in those locations where the 2000 survey fell well below the design height, but did not appear to suffer any damage from the storm.

Referring to Figure 16-1, it appears that levee damage began just to the south of the floodwall-topped section that ends at Station 2,250, with the damage becoming catastrophic between 3,500 and 4,500. Although short sections survived, the heavy damage persists southward (Figures 16-2 to 16-3) until around Station 25,000 (Figure 16-4), where damage then abates for about 9,000 ft (Figures 16-4 and 16-5) until Station 34,000. Heavy damage then returns for the next 10,000 ft (Figure 16-6), before finally abating throughout the remainder of the surveyed levee – a distance of about 20,000 ft (Figures 16-7 to 16-9) to Station 64,000.



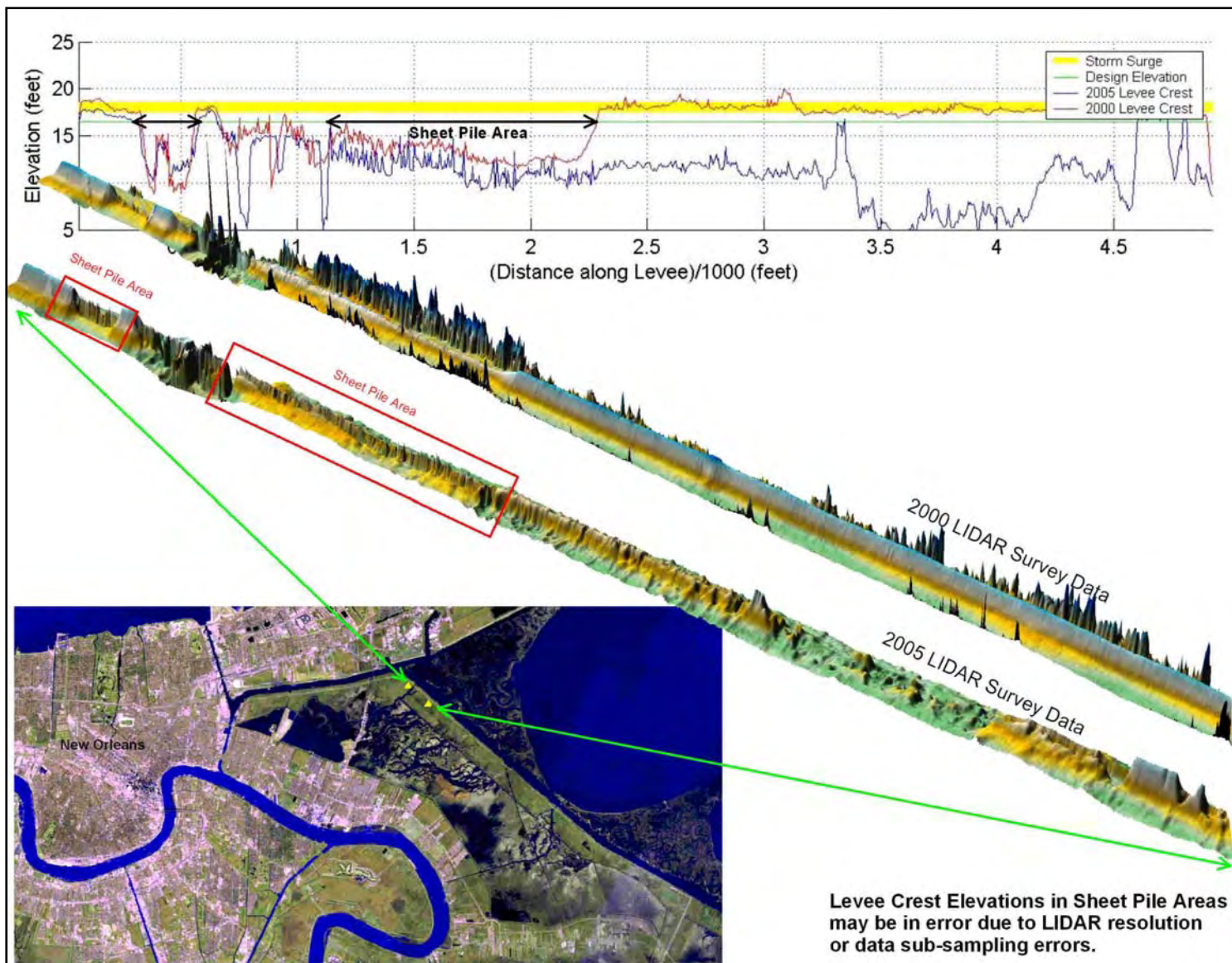


Figure 16-1. MRGO levee damage determined from LIDAR surveys; Station 0 to 4,500 ft



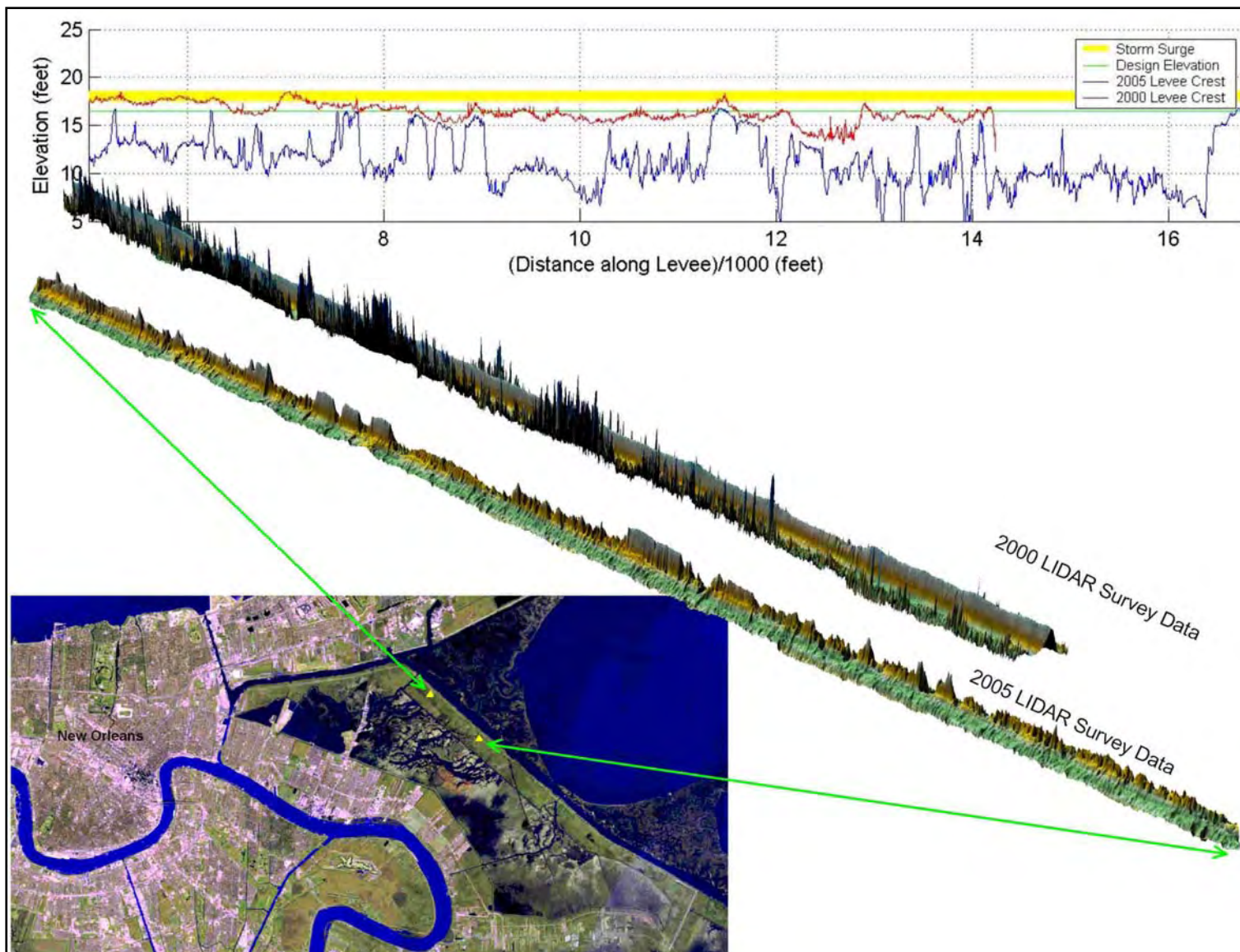


Figure 16-2. MRGO levee damage determined from LIDAR surveys; Station 6,000 to 16,000 ft

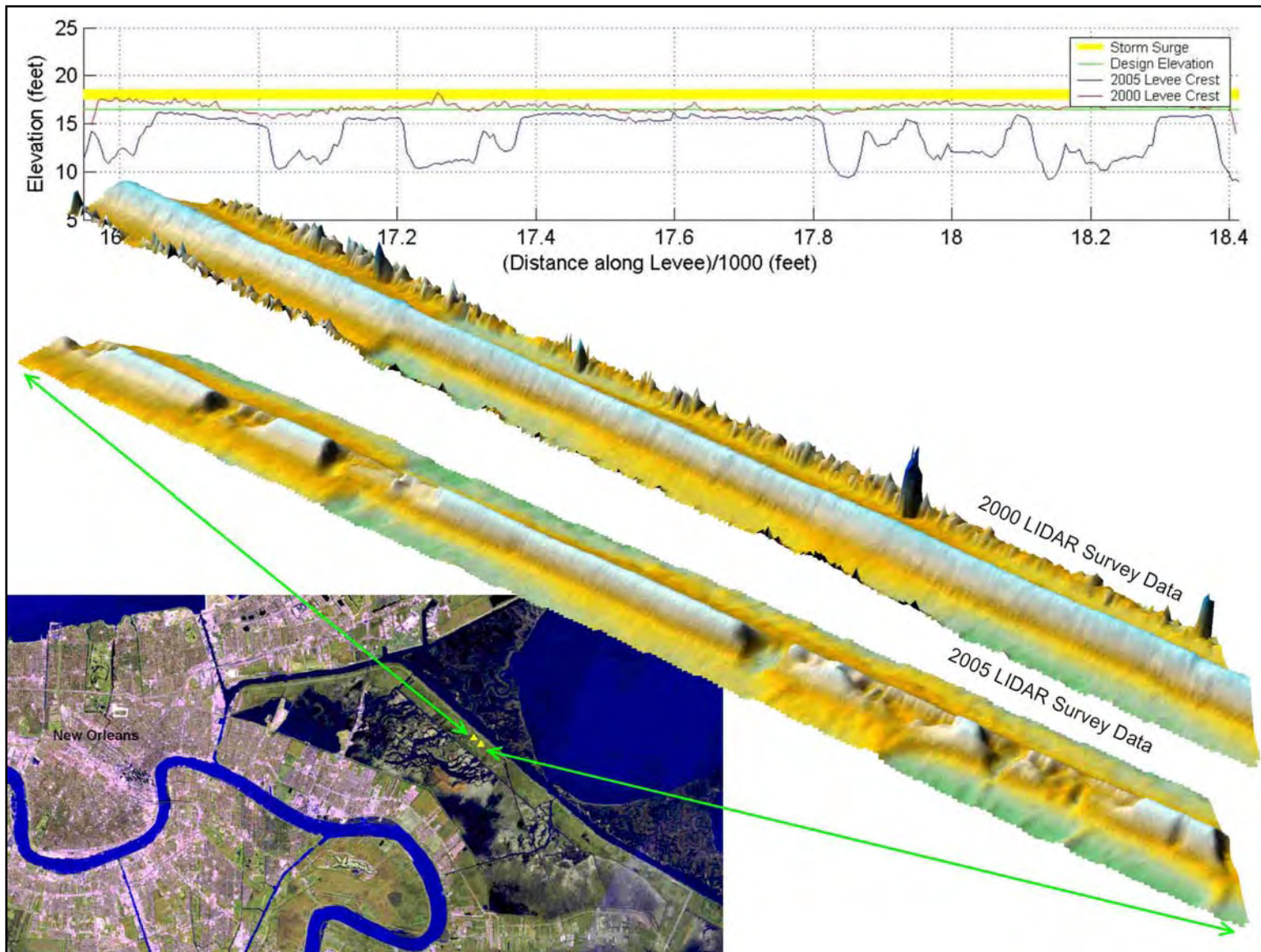


Figure 16-3. MRGO levee damage determined from LIDAR surveys; Station 16,800 to 18,400 ft



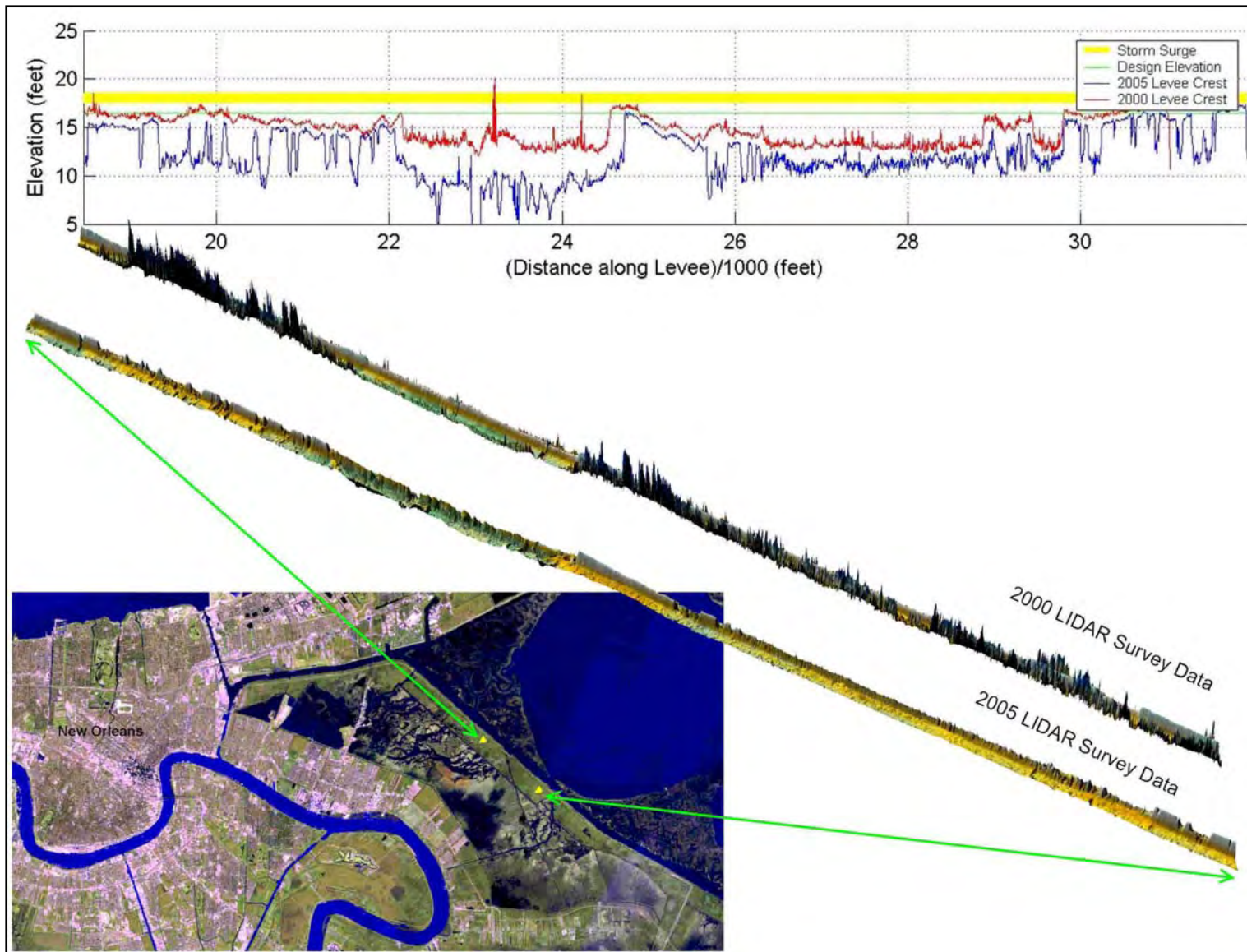


Figure 16-4. MRGO levee damage determined from LIDAR surveys; Station 20,000 to 30,000 ft

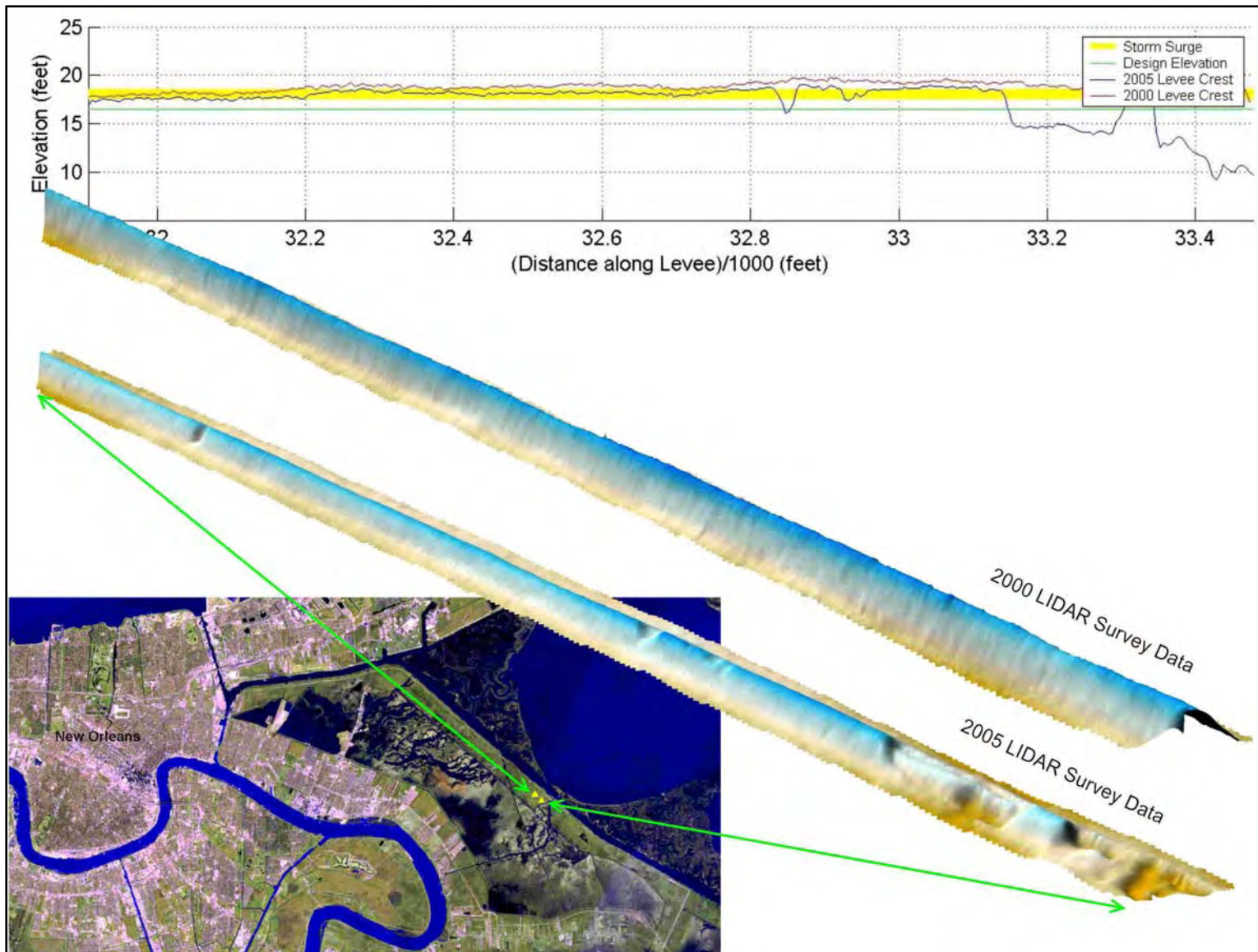


Figure 16-5. MRGO levee damage determined from LIDAR surveys; Station 32,000 to 33,400 ft



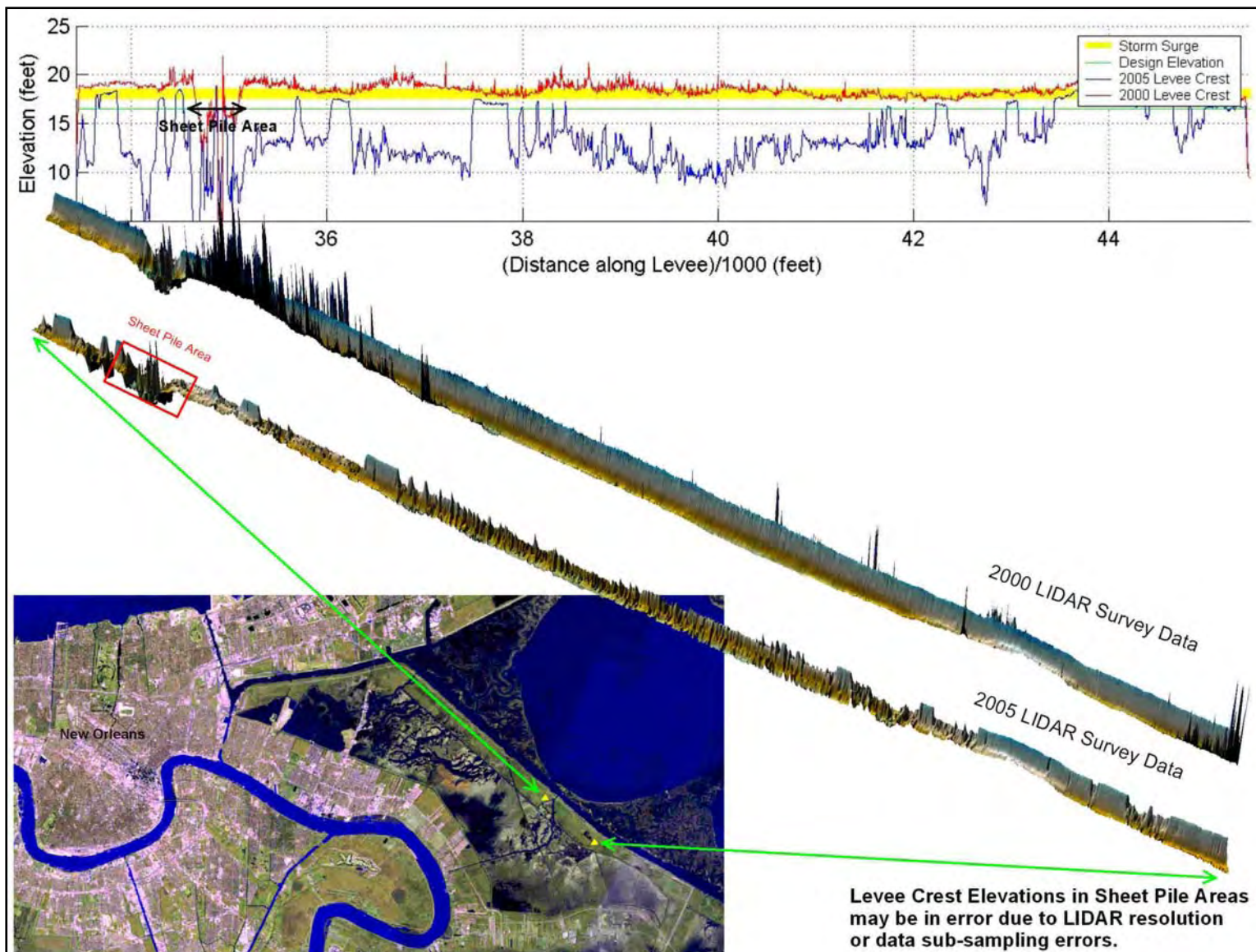


Figure 16-6. MRGO levee damage determined from LIDAR surveys; Station 34,000 to 44,000 ft



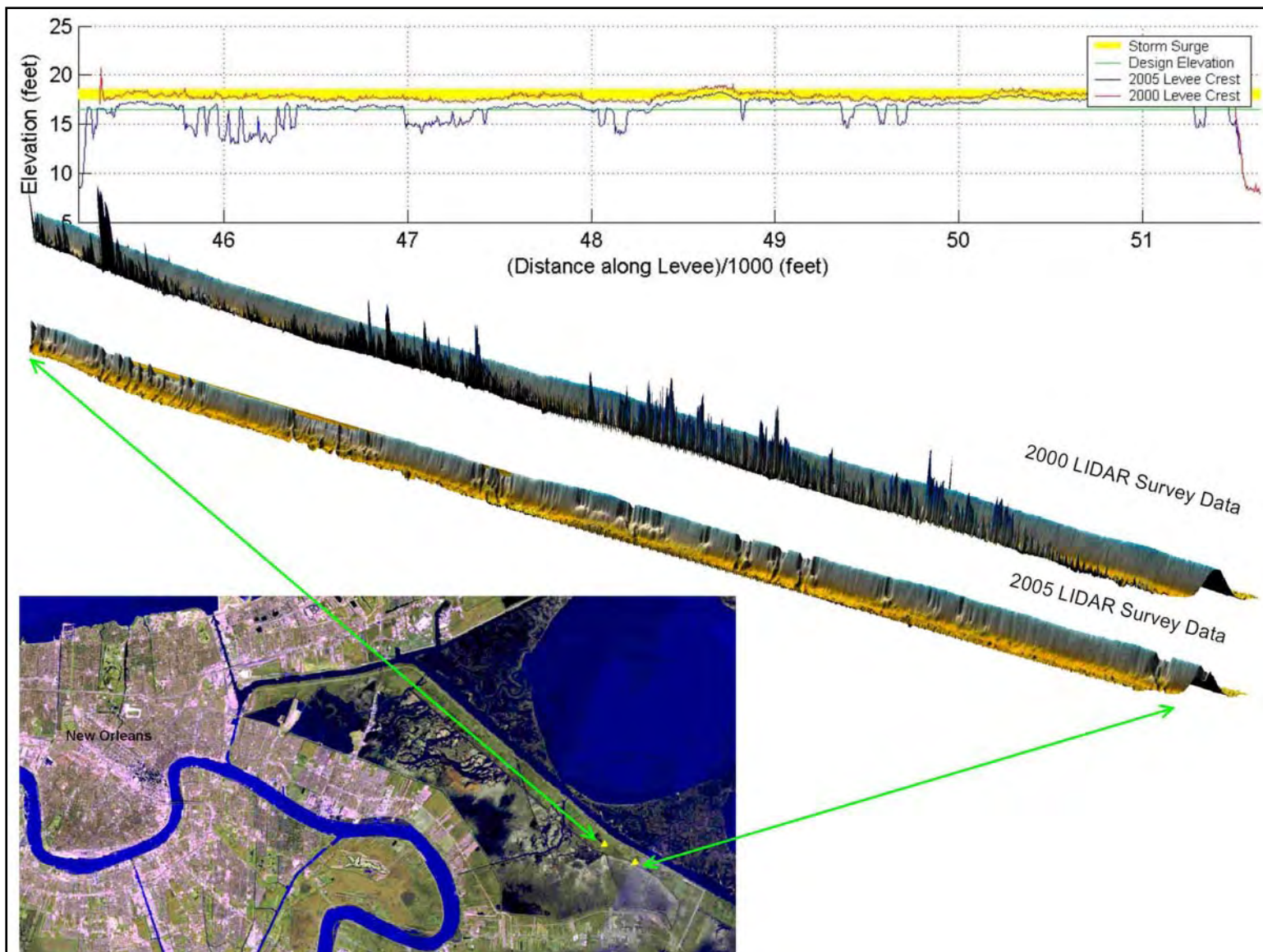


Figure 16-7. MRGO levee damage determined from LIDAR surveys; Station 46,000 to 51,000 ft

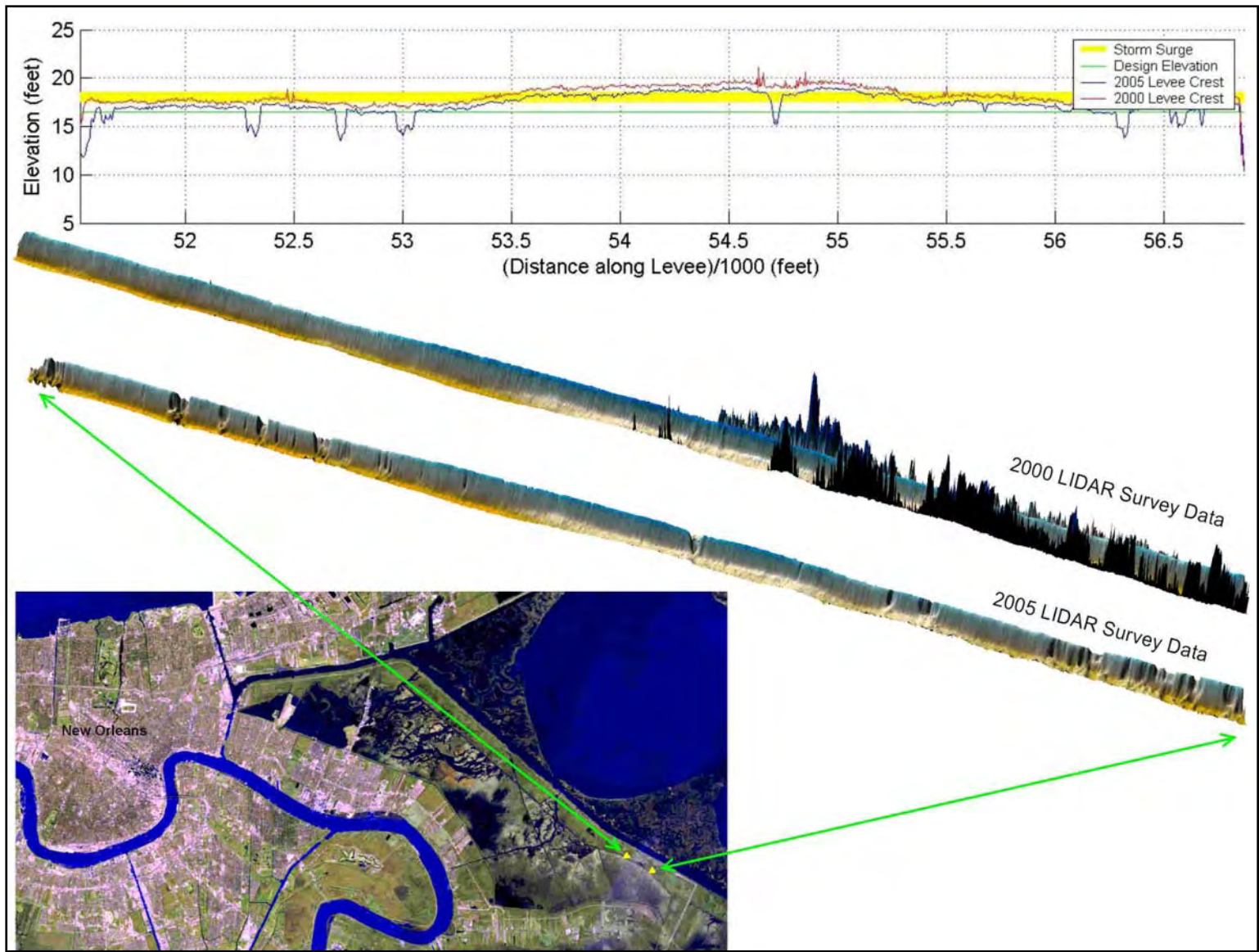


Figure 16-8. MRGO levee damage determined from LIDAR surveys; Station 52,000 to 56,500 ft



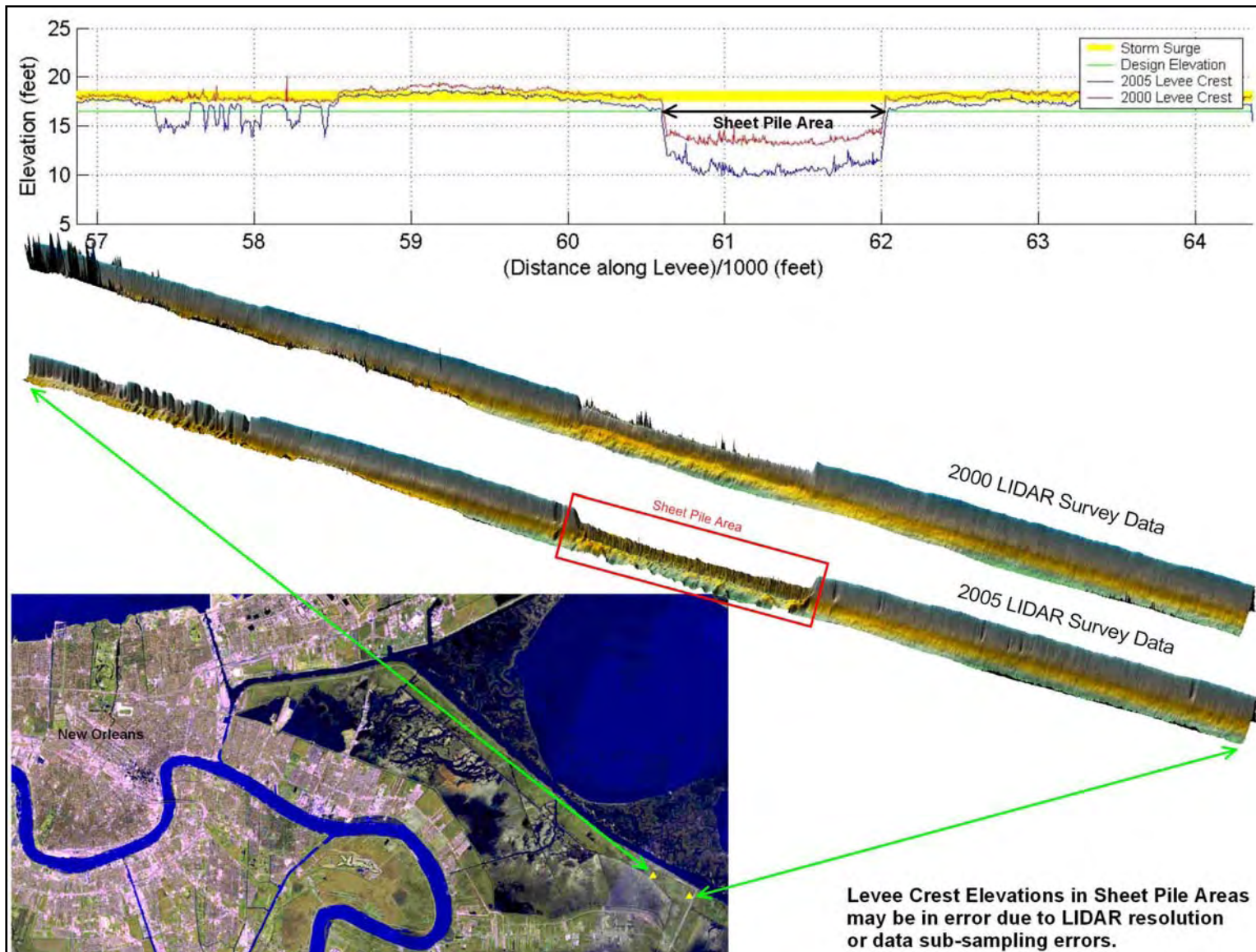


Figure 16-9. MRGO levee damage determined from LIDAR surveys; Station 57,000 to 64,000 ft

# Appendix 17

## Consideration of Wind-Induced Barge Motions and Associated Forces in the Inner Harbor Navigation Canal

---

### Introduction

This appendix addresses the issue of whether the barge that traversed from the Inner Harbor Navigation Canal (IHNC) through the flood wall to the Lower Ninth Ward could have been a cause of the levee failure in this area or whether the barge was simply transported through the levee subsequent to its failure. The analysis presented below develops a method for calculating forces acting on the wall due to a freely floating barge. However, uncertainty remains due to lack of requisite necessary information. Thus, the contribution here may be useful as more details become available.

This brief report examines the wind forces exerted on the barge and the associated velocity, momentum and energy of the barge as it traverses a path across or diagonally along the canal to the location of levee failure. This analysis considers the situation prior to levee failure and no water current or wave forces are considered. Following development of the velocity and trajectory equations, examples are presented to illustrate application of the methodology.

This report is organized as follows. The next section describes, to the extent possible, the characteristics of the barge that was located outside the IHNC after the levee failed. Estimates are developed of the winds and wind forces on a barge immersed within the wind boundary layer. These wind forces on a static barge are compared with the static hydrodynamic forces which existed immediately prior to levee overtopping. This is followed by an examination of the dynamics of the barge for various drafts and provides a basis for quantifying the barge trajectory and momentum and energy upon impact with the east floodwall. Examples are presented illustrating application of the methodology developed. Recommendations and a summary and conclusions are presented in the final section.

The main focus of this report is to provide a method for quantifying the barge kinematic and dynamic characteristics relative to its possible role in failure of the IHNC east flood wall. The detailed calculations employing this methodology will require improved estimates of the barge

and other characteristics associated with the methodology. Figure 17-1 shows a plan view of the barge in the IHNC and the winds that were directed on the barge.

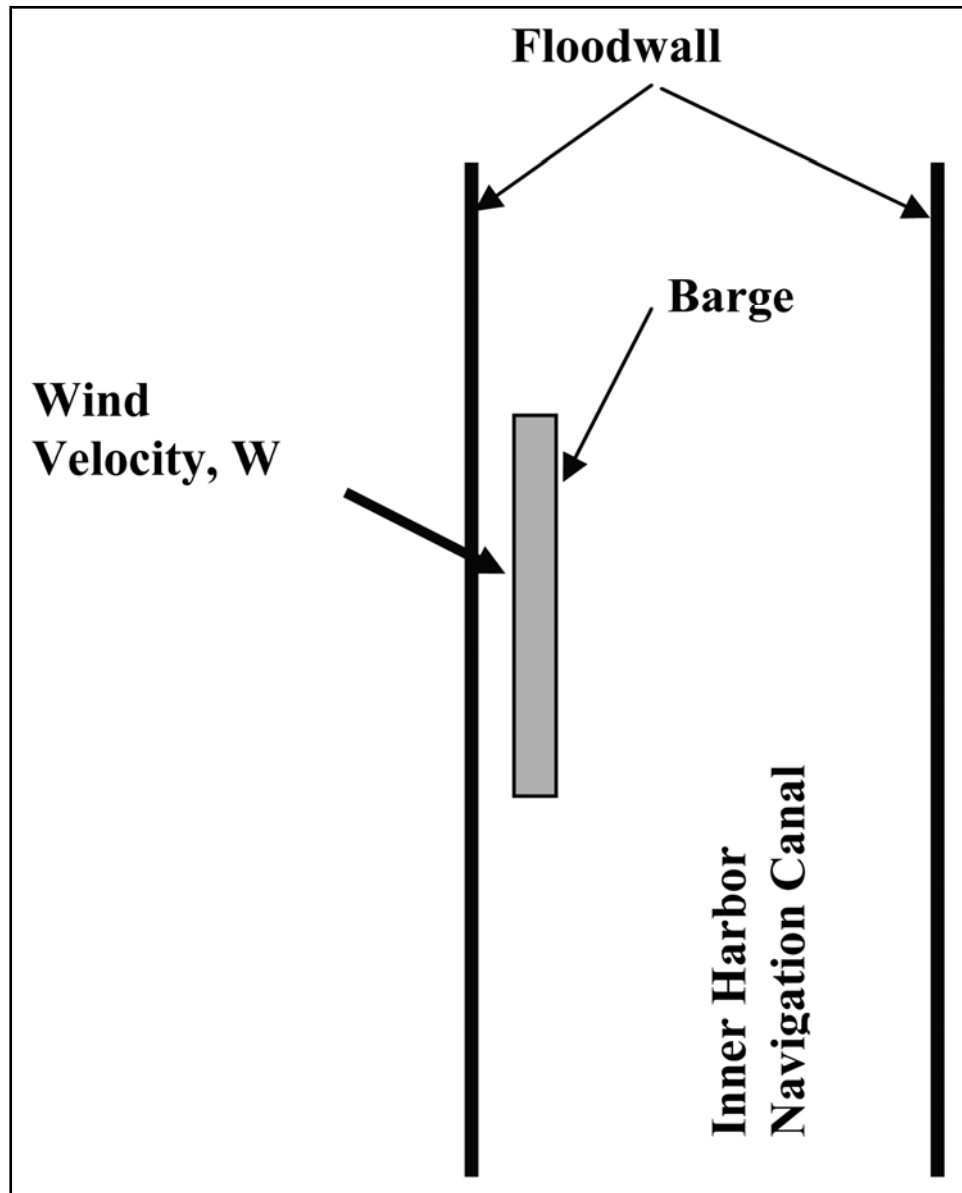


Figure 17-1. Definition sketch of Inner Harbor Navigation Canal and wind blowing on the barge

## Barge Characteristics

During a site visit on December 22, 2005, the dimensions of the barge identified as “**ING 4727**” were estimated as:

- Hull Depth = 12 feet
- Superstructure Height Including Covers for Contents = 11 feet
- Barge Length = 200 feet



- Barge Width = 35 feet

Figure 17-2 presents these barge dimensions.

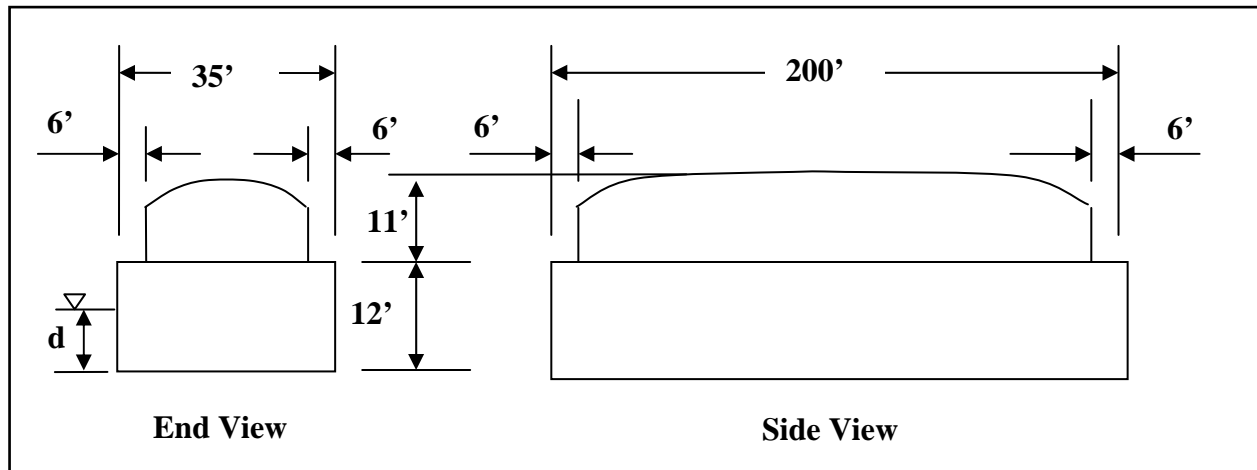


Figure 17-2. Estimated dimensions of barge observed on site visit to Lower Ninth Ward

## Wind Loading and Comparison with Hydraulic Forces on East Flood Wall

### Wind Profile and Effective Wind Speed, $W_{eff}$

The relevant wind speed is that which is exerted on the barge. For a drag force relationship, this is the root-mean-square of the wind speed over the vertical dimension of the above water portion of the barge. For purposes here, the following simple relationship for the vertical distribution of wind speed is considered

$$W(z) = W(30) \left( \frac{z}{30} \right)^{1/7} \quad (1)$$

in which  $z$  is the elevation above the water surface in feet and  $W(30)$  is the reference wind speed at 30 feet above the water surface. The draft of the barge will be denoted as  $d$ . Thus the vertical dimension of the barge exposed to the wind is  $(23-d)$  feet. The effective wind speed,  $W_{eff}$  for drag force computations is therefore

$$W_{eff} = \sqrt{\frac{\int_0^{23-d} W^2(z) \ell(z) dz}{\int_0^{23-d} \ell(z) dz}} \quad (2)$$

in which  $\ell(z)$  is the length of a barge element at elevation  $z$  and  $23-d$  is the height of the barge above the water level. Although the length of a barge element does vary somewhat with elevation as shown in the previous section, this variation is reasonably small and for purposes here we will consider that  $\ell(z)$  is uniform over the height,  $23-d$ . This results in the effective velocity,  $W_{eff}$

$$W_{eff} = 0.882 \left( \frac{23-d}{30} \right)^{1/7} W(30) \quad (3)$$

### Wind Drag Forces on Barge

The drag force,  $F_{D,a}$  exerted by the wind on the barge is given by

$$F_{D,a} = \frac{\rho_a C_{D,a} A_a W_{eff}^2}{2} \quad (4)$$

in which  $\rho_a$  is the mass density of air,  $C_{D,a}$  is the so-called “drag coefficient” of the barge to winds and  $A_a$  is the “projected area” of the barge perpendicular to the wind velocity vector.

For purposes of examples presented in this report, we will consider the wind to be directed broadside to the barge, a wind mass density,  $\rho_a = 0.002$  slugs/ft<sup>3</sup> and a barge length = 200 feet. Thus, the relevant area in Eq. (4) is

$$A_a = 200(23-d) \quad (5)$$

### Static Hydraulic Forces and Moments on Flood Wall Immediately Before Overtopping

Figure 17-3 depicts a typical section of the flood wall at an imminent overtopping condition. The hydrostatic force,  $F_{HS}$  on the floodwall per unit floodwall length for the imminent overtopping condition shown in Figure 17-3 is

$$F_{HS} = \rho_w g \frac{h^2}{2} \quad (6)$$

in which  $\rho_w$  is the mass density of water taken here as 1.94 slugs/ft<sup>3</sup> and  $g$  is the acceleration of gravity.

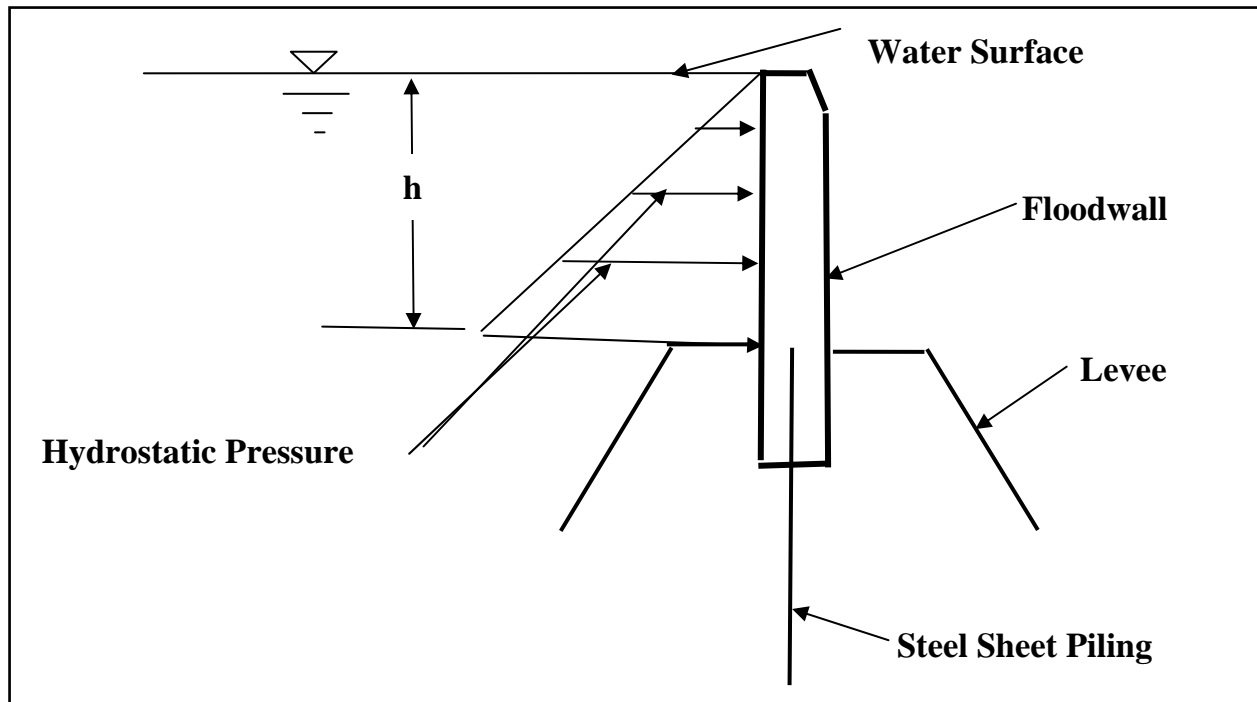


Figure 17-3. Definition sketch for east floodwall at imminent overtopping condition

The hydrostatic moment,  $M_{HS}$  about the base of the floodwall per unit length of flood wall is given by

$$M_{HS} = \rho_w g \frac{h^3}{6} \quad (7)$$

## Comparison of Hydrostatic Forces and Moments with Static Wind forces and Moments

To calculate wind forces, we need to select a reference wind speed,  $W(30)$  as shown in Eq. (1). For most of the examples presented in this report, a reference wind speed of 100 miles per hour<sup>1</sup> (146.7 ft/sec) and a wind drag coefficient,  $C_{D,a} = 0.5$ <sup>2</sup> have been selected for illustration purposes. To illustrate the maximum wind force, a lightly loaded barge condition is selected with

<sup>1</sup> The actual wind speeds were less than 100 mph, the value used here for illustration purposes.

<sup>2</sup> See, for example, Schlichting (1955, Page 16) for a plot of drag coefficient vs Reynolds Number for a smooth circular cylinder. The Reynolds number for this case is approximately  $5 \times 10^6$  which is post-critical resulting in a smooth cylinder drag coefficient on the order of 0.2. Drag coefficients for rough cylinders have a minimum drag coefficient of approximately 0.5. Also note that the finite length of the barge would result in a reduced drag coefficient relative to the infinitely long case. Finally, the air and water drag coefficients should be approximately the same and any errors in their individual values will tend to cancel.

a barge draft,  $d = 4$  feet. Applying Eq. (3), the reference wind speed,  $W_{eff} = 121.2$  ft/sec. The wind drag force per unit barge length  $f_{HS}$ , is then

$$f_{D,a} = \frac{\rho_a C_{D,a} (23-d) W_{eff}^2}{2} = 139.5 \text{ pounds/foot} \quad (8)$$

This value is compared to the hydrostatic force per unit length of 1,999 pounds/foot based on a floodwall height = 8 feet. Thus, the static wind force is equal to approximately 7% of the hydrostatic force. However this result is based on a uniform transfer of the wind load on the barge to the floodwall. If this transfer is concentrated, the local wind related loads acting on the floodwall per unit length could be much greater than those calculated above.

The wind related moments about the bottom of the floodwall are considered to result from application of the wind related forces at the mid-elevation of the barge draft, i.e. 2 feet below the crest of the floodwall. In this case, the moment due to the wind is 837 foot pounds per foot compared to the hydrostatic moment of 5,331 foot pounds per foot, i.e. the wind moment is approximately 16% of the hydrostatic moment. However, the same comment applies to moments as was presented for forces regarding the consideration that the wind forces were applied uniformly along the wall.

The following section examines the kinematics and dynamics of the floating barge.

## Barge Dynamics Under the Action of Wind Forces

### Equation of Motion and Solution

The equation of motion of the barge is:

$$m_T \frac{dV}{dt} = K_1 W_{eff}^2 - K_2 V^2 \quad (9)$$

in which  $m_T$  is the total effective mass of the floating barge and is the sum of the physical mass and the added mass,  $V$  is the barge velocity,  $t$  is time after the barge starts to float free, and  $W_{eff}$  is the effective wind speed acting on the barge as described earlier. The factor,  $K_1$  has been defined earlier as

$$K_1 = \frac{\rho_a C_{D,a} A_a}{2} \quad (10)$$

The factor  $K_2$  is defined as

$$K_2 = \frac{\rho_w C_{D,w} A_w}{2} \quad (11)$$

in which  $\rho_w$  has been defined as the mass density of water,  $C_{D,w}$  is the so-called “drag coefficient” of the barge to the water motion and  $A_w$  is the “projected area” of the barge perpendicular to the water velocity vector. In subsequent calculations, the following values of drag coefficients will be applied:  $C_{D,a} = C_{D,w} = 0.5$ . The dimensions of both  $K_1$  and  $K_2$  are “force/velocity squared”. The complete barge dimensions were presented in an earlier section.

## Estimation of $K_1$ and $K_2$ Factors and Steady State Velocities

From Eq. (9), it is seen that the steady state (or terminal) velocity of the barge,  $V(\infty)$  is given by

$$V(\infty) = \sqrt{\frac{K_1}{K_2}} W_{eff} \quad (12)$$

The values of  $K_1$  and  $K_2$  will be estimated for the case of the barge fully loaded, and loaded very lightly. The barge is considered broadside to the wind. The results of these estimates are presented in Table 17-1. The values of the dimensionless terminal barge velocity,  $V(\infty)/W_{eff}$ , are also presented in Table 17-1. Note that the length of the barge acted upon by winds has been taken as 188 feet.

Case	Description	$K_1$ (Pounds-sec <sup>2</sup> /ft <sup>2</sup> )	$K_2$ (Pounds-sec <sup>2</sup> /ft <sup>2</sup> )	$V(\infty)/W_{eff}$
1	Fully Loaded, Draft $d = 9$ feet	1.32	873	0.039
2	Lightly Loaded, Draft $d = 4$ feet	1.79	388	0.068

## Non-Dimensionalization and Solutions of the Equation of Motion

It is useful to cast the equation of motion in non-dimensional form as:

$$\frac{m_T}{K_1 W_{eff}^2} \frac{dV}{dt} = 1 - \frac{K_2}{K_1} \frac{V^2}{W_{eff}^2} \quad (13)$$



from which the solution can be shown to be:

$$V(t) = V(\infty) \tanh\left(\frac{\sqrt{K_1 K_2}}{m_T} W_{eff} t\right) \quad (14)$$

The non-dimensional time,  $t_*$ , is defined as

$$t_* = \frac{m_T}{\sqrt{K_1 K_2} W_{eff}} \quad (15)$$

and is the time at which the barge velocity is 76.2% of its terminal velocity. Choosing the non-dimensional velocity as the terminal velocity,  $V(\infty)$ , and denoting non-dimensional quantities by primes (e.g.  $t' = t/t_*$ , the solution for the non-dimensional velocity,  $V'(t')$  is

$$V'(t') = \tanh(t') \quad (16)$$

The non-dimensional barge displacement,  $x'(t') = x(t)/x_*$ , can be shown to be

$$x'(t') = \ln[\cosh(t')] \quad (17)$$

where

$$x_* = \frac{m_T}{K_2} \quad (18)$$

The advantages of the non-dimensional solutions presented is that they depend on only one variable,  $t'$ .

Figure 17-4 presents the non-dimensional solutions for the range  $0 < t' < 5$  which will be shown to provide adequate information to analyze the case of the barge motions and forces in the IHNC canal.

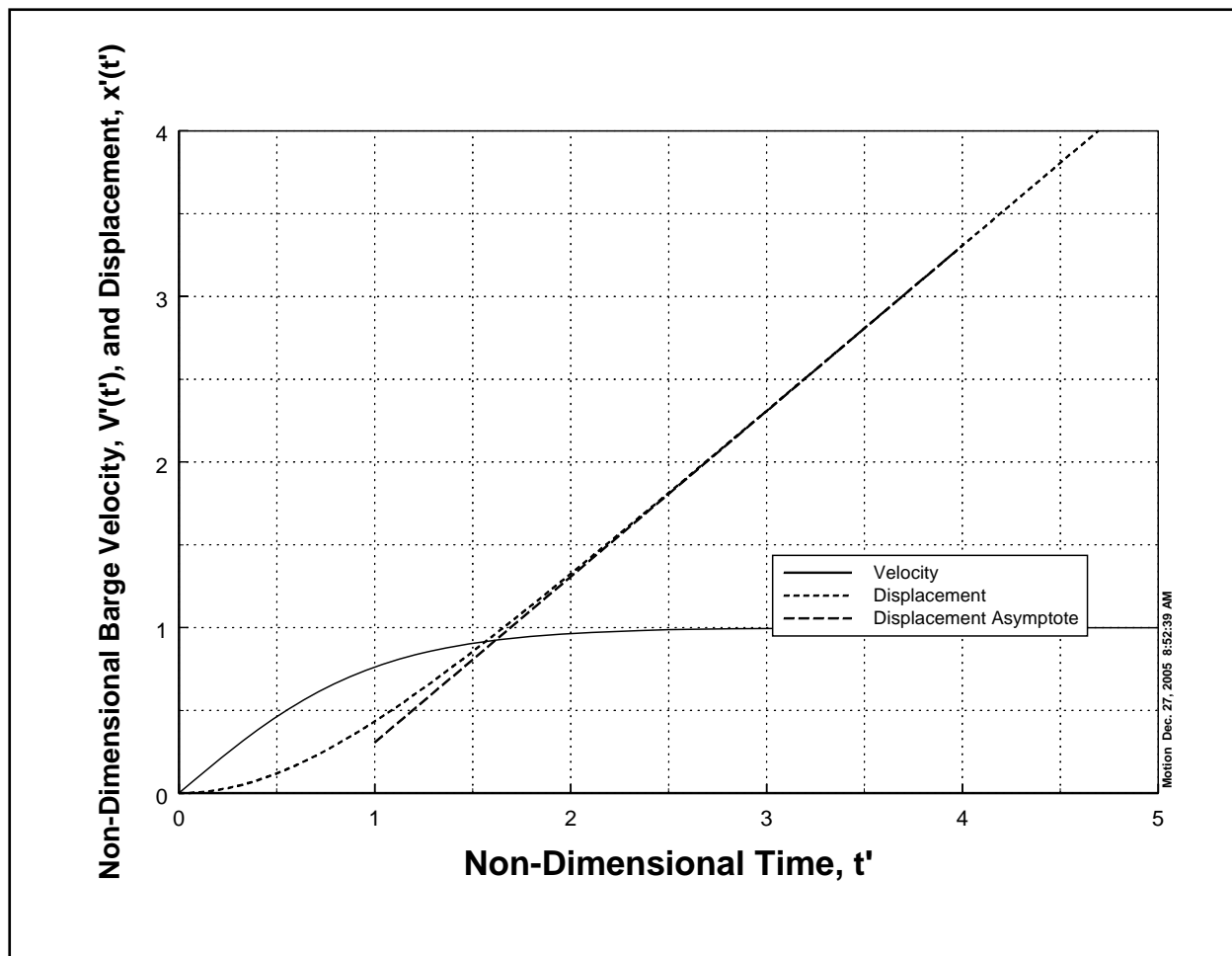


Figure 17-4. Non-dimensional barge velocity and displacement

The non-dimensional relationships are plotted in a different manner in Figure 17-5, which has advantages for our particular application. Figure 17-5 presents the non-dimensional barge velocity,  $V'(t')$  as a function of the non-dimensional barge displacement,  $x'(t')$ . In application, the quantity  $x$  is the path of the barge from its starting point to its ending point where it would impact the east flood wall of the IHNC canal. This quantity is based on barge and other conditions and is the non-dimensional distance,  $x'$ . Entering Figure 17-5 with this  $x'$  quantity on the abscissa, the non-dimensional velocity,  $V'$  is determined. The dimensional velocity,  $V$  is then quantified. Finally the momentum and energy of the barge upon impact are determined as:

$$\text{Momentum} = m_T V \quad (19)$$

$$\text{Energy} = \frac{m_T V^2}{2} \quad (20)$$

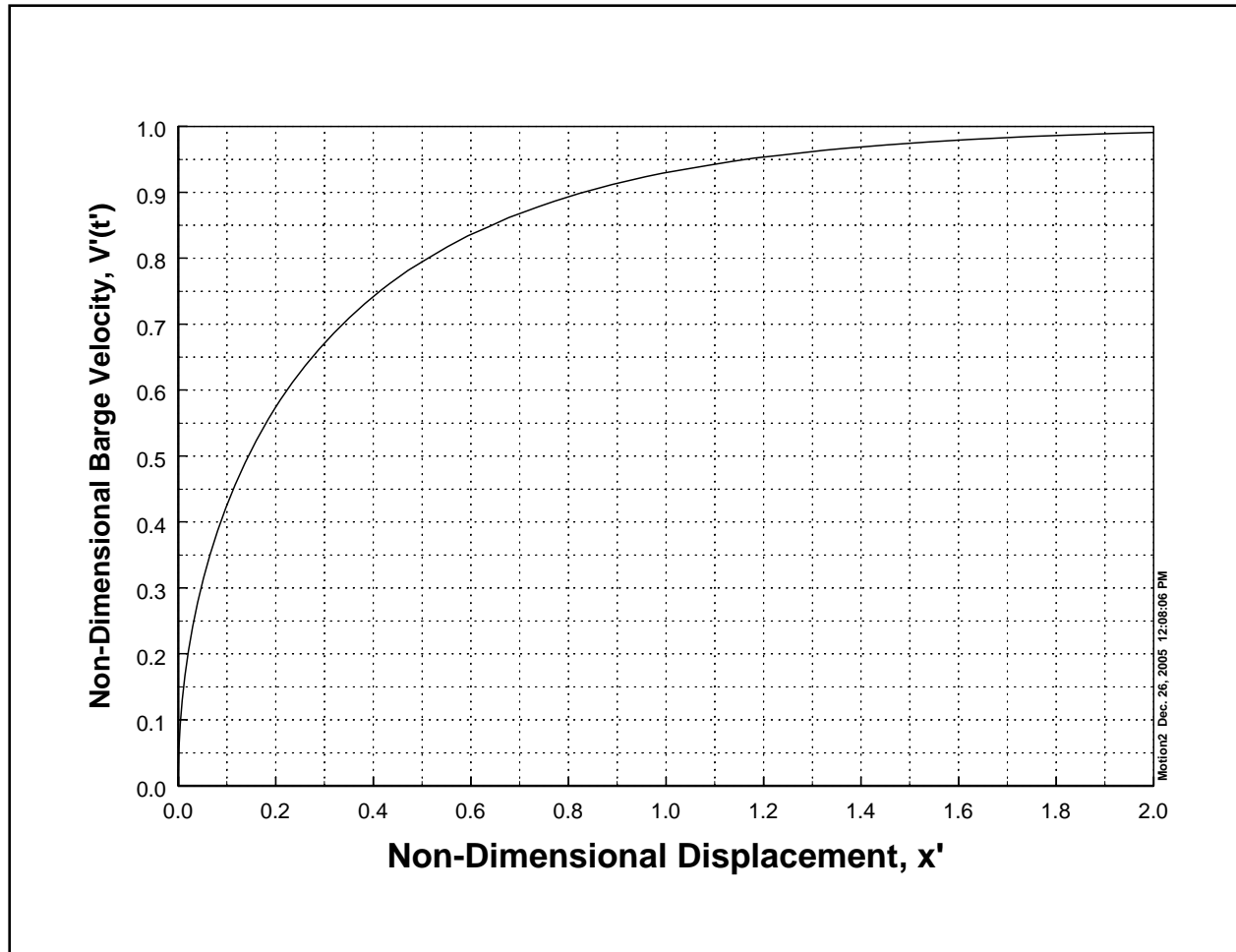


Figure 17-5. Relationship between non-dimensional barge velocity,  $V'(t')$  and non-dimensional displacement,  $x'(t')$

The barge displacement,  $x$ , should increase linearly with time after the barge has reached its terminal velocity,  $V(\infty)$  and this appears to be the case from Figure 17-4 but is not so apparent from Eq. (17). However, from Eq. (17), for large  $t'$ ,

$$x'(t') = t' - \ell \ln(2) \quad (21)$$

which is plotted as the asymptote in Figure 17-4. Expressing Eq. (21) in dimensional form, this equation becomes

$$x(t) = V(\infty)t - \frac{m_T}{K_2} \ell \ln(2) \quad (22)$$

which demonstrates the expected linearity of the relationship for large time. The second term on the right hand side of the above equation accounts for the acceleration phase of the barge

response, as can be appreciated by the role of the total mass,  $m_T$ , such that a larger mass tends to prolong the acceleration phase and thus reduce the displacement at any particular time. The procedure for calculating barge motion characteristics will be illustrated with examples in the following section of this report.

## Examples Illustrating Application of the Methodology

Consistent with the results in Table 17-1, two cases are considered: Case 1 in which the barge is fully loaded with a draft of 9 feet and Case 2 for which the barge draft is 4 feet. It is noted that the examples presented here are for illustrative purposes of the methodology application. With the detailed characteristics of the barge more fully established, the motion and force characteristics can be refined.

### Case 1. Barge Fully Loaded

For Case 1, the total mass,  $m_T$  is the sum of the physical mass,  $m_p$  and the added mass,  $m_A$ . The physical mass is equal to the mass of the displaced water or 122,220 slugs. Assuming an added mass coefficient of 0.2, the total mass,  $m_T = 144,664$  slugs.

For a barge exposure above water of 14 feet ( $d = 9$  feet), based on Eq. (3), the reference wind velocity,  $W_{eff}$  is  $0.791 \times W(30)$ . Considering, as an example,  $W(30) = 100$  mph = 146.7 ft/sec,  $W_{eff} = 116.0$  ft/sec. The  $K_1$  and  $K_2$  values are 1.32 pound-sec<sup>2</sup>/ft<sup>2</sup> and 873 pound-sec<sup>2</sup>/ft<sup>2</sup>, respectively as given in Table 17-1. The non-dimensional quantities are  $t_* = 36.7$  sec,  $V(\infty)$ , the barge terminal velocity = 4.52 ft/sec, and  $x_* = 165.7$  ft.

The distance across the IHNC from the western floodwall to the eastern floodwall is approximately 1,100 feet. Considering that this is the trajectory of the barge, the translation distance is 1,065 feet (the width of IHNC minus the barge width). Thus the value of  $x'$  is 6.42. Referring to Figure 17-5, it is clear that the barge would have achieved its terminal velocity,  $V(\infty)$  of 4.52 ft/sec. Thus the momentum and energy upon impacting the wall are:

- Impact Momentum = 653,900 pound sec.
- Impact Energy = 1.48 million foot pounds.

This example is provided as an illustration of the application/interpretation of the impact momentum. Consider this momentum to be transferred in, say 10 seconds allowing for barge deformation. If the form of the transfer is triangular, that is the force starts at zero, rises to twice the average value, then decreases to zero force in 10 seconds, then the maximum force acting on the flood wall would be 130,780 pounds. This is compared to the hydrostatic force of 399,000 pounds over the barge length of 200 feet. Thus, for this impact time of 10 seconds, the maximum impact force is 33% of the hydrostatic force. It is cautioned that: (1) The actual impact time would require a careful analysis of the barge and floodwall deformation characteristics and

consideration of various barge orientations upon impact. Shorter impact times will result in greater maximum impact forces, and (2) the impact forces may be localized thus resulting in greater impact forces per unit length of the floodwall.

## Case 2. Barge Lightly Loaded

The draft for this case is 4 feet as shown in Table 17-1. As for Case 1, the total mass,  $m_T$  is the sum of the physical mass,  $m_p$  and the added mass,  $m_A$ . The physical mass is equal to the mass of the displaced water or 54,320 slugs. Again assuming an added mass coefficient of 0.2, the total mass,  $m_T = 65,184$  slugs.

For a barge exposure above water of 19 feet ( $d = 4$  feet), based on Eq. (3), the reference wind velocity,  $W_{eff}$  is  $0.826 \cdot W(30)$ . Considering  $W(30) = 100$  mph = 146.7 ft/sec,  $W_{eff} = 121.2$  ft/sec. Considering  $C_{D,a} = C_{D,w} = 0.5$ , the  $K_1$  and  $K_2$  values are 1.79 pound-sec<sup>2</sup>/ft<sup>2</sup> and 388 pound-sec<sup>2</sup>/ft<sup>2</sup>, respectively as given in Table 17-1. The non-dimensionalizing quantities are  $t_* = 20.4$  sec,  $V(\infty)$ , the barge terminal velocity = 8.24 ft/sec, and  $x_* = 168.0$  ft.

Considering the same barge trajectory as for Case 1, the value of  $x'$  is 6.34. As for Case 1, referring to Figure 17-5 it is clear that the barge would have achieved its terminal velocity,  $V(\infty)$  of 8.24 ft/sec. Thus the momentum and energy upon impacting the wall are:

- Impact Momentum = 537,120 pound sec.
- Impact Energy = 2.21 million foot pounds.

## General Case of Arbitrary Draft

It has been demonstrated that for a reference wind speed of 100 miles per hour, the barge will reach its terminal velocity regardless of the draft and with a minimum distance of the IHNC width translation distance (minus the barge width). Thus, it is possible to develop the following simple equations for impact momentum and energy for the barge of interest.

### Impact Momentum

For the barge of interest and considering that the barge had reached its terminal velocity at impact, the equation for the terminal momentum can be written as

$$\text{Terminal Momentum} = 283.9\sqrt{d}(23-d)^{9/14}W(30) \text{ (in pound sec)}$$

Note that consistent units must be used in these equations. Thus  $W(30)$  is in ft/sec.



## Impact Energy

For the same considerations as above for terminal momentum, the terminal energy can be shown to be

$$\text{Terminal Energy} = 2.47(23 - d)^{9/7} (W(30))^2 \text{ (in foot pounds)}$$

Figure 17-6 presents non-dimensional plots of terminal momentum and energy versus barge draft. For purposes here, the non-dimensional terminal momentum and velocity have been defined as the ratio of these quantities to the values for a 9 foot barge draft and for a wind speed,  $W(30) = 144.67$  ft/sec (100 miles per hour).

Thus the terminal momentum for any draft and wind speed is determined by multiplying the value for 9 feet (653,900 pound sec) by the appropriate value in Figure 17-6 and the ratio of the wind speed of interest,  $W(30)$  to 146.7 (all in feet/sec).

Similarly, the terminal energy is determined by multiplying the terminal energy for a draft of 9 feet (1.48 million foot pounds) by the appropriate value in Figure 17-6 and the ratio of the square of the wind speed of interest, i.e.  $W^2(30)$  to  $(146.7)^2$  where all wind speeds are in ft/sec.

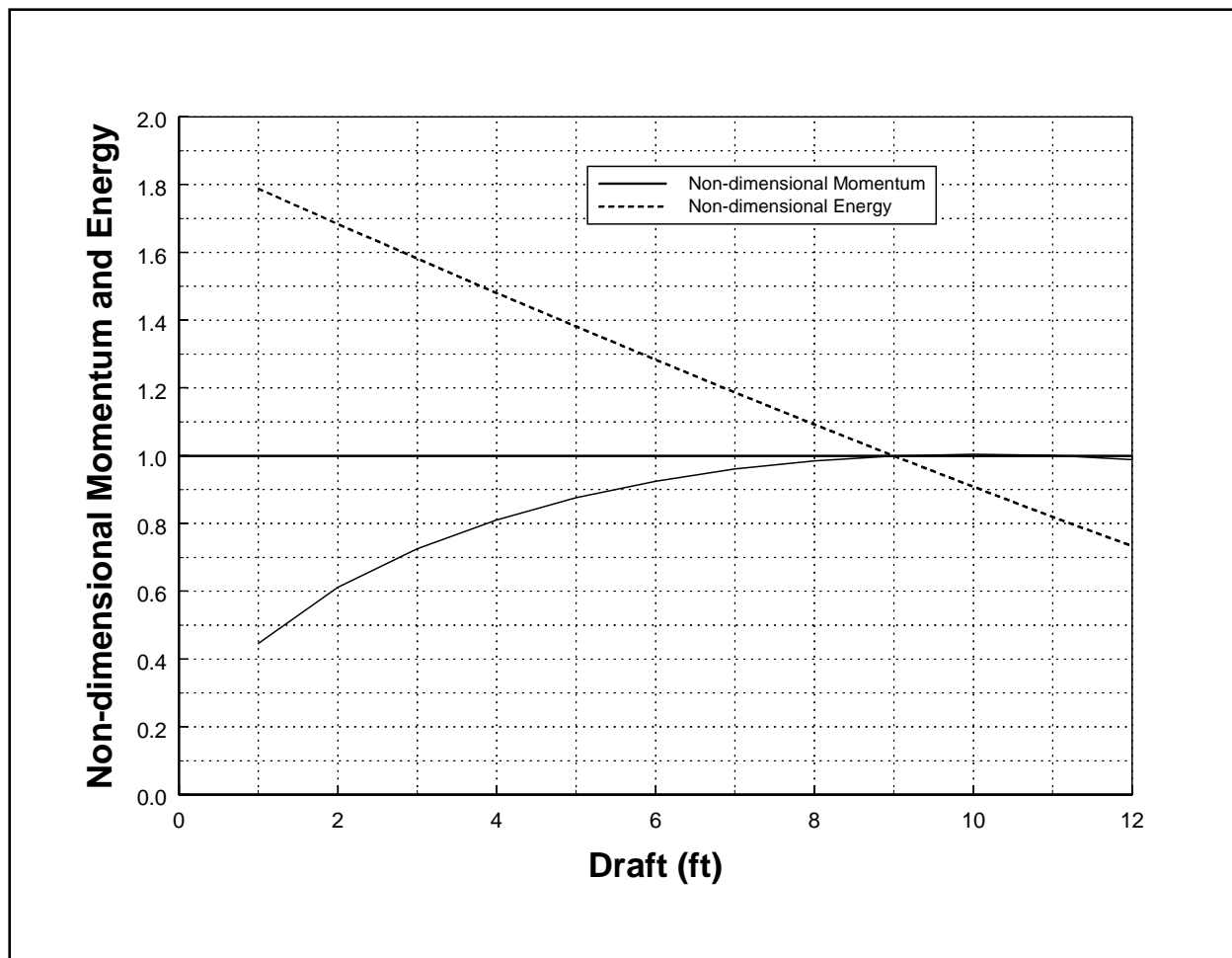


Figure 17-6. Non-dimensional barge terminal momentum and energy vs barge draft

## Recommendations

Although it has been demonstrated that the barge terminal momentum and energy could have been considerable and thus possible contributors to the levee failure at the Lower Ninth Ward, this is not evidence that the barge did contribute to the failure. Thus it is recommended that other types of forensic evidence be sought, including 1) indications of whether the barge shows evidence of substantial impact with the flood walls, and 2) information as to the mooring arrangement and conditions of the mooring lines after levee failure. Other types of forensic evidence may also be available.

## Summary and Conclusions

The equations governing the effective wind speed acting on a barge present in the wind boundary layer have been examined and an effective wind speed defined for drag force calculations. Static wind forces and moments acting on a lightly loaded barge and then

transferred to the east IHNC floodwall due to a wind speed of 100 miles per hour have been examined and found to represent a reasonably small fraction of the hydrostatic forces and moments exerted directly on the floodwall. These forces and moments have been expressed as averages per unit length on the floodwall although the barge-related forces would likely be transferred in a concentrated manner rather than uniformly.

The equation of motion of a freely floating barge has been developed and cast in non-dimensional form for easy application. The equations include development of the terminal velocity of the barge. The equation is solved for the non-dimensional velocity and displacement.

It is found that the terminal velocity of the barge is achieved rather quickly for the wind speed examined (100 miles per hour) and that for barge conditions in the IHNC, the momentum and energy impact on the east flood wall depend primarily on the draft of the barge during the event. Simplified equations have been presented for terminal momentum and energy for use by others in evaluating whether the barge was a contributor to the failure of the IHNC flood wall in the Lower Ninth Ward area.

It is emphasized that, although the methodology presented here provides a basis for calculating the actual motions and force characteristics associated with a freely floating barge acting under the action of wind, the examples presented are for illustration only and have purposely avoided attempting to utilize actual wind characteristics.

## Reference

Schlichting, H. (1955) "Boundary Layer Theory", McGraw-Hill Book Company, Inc., New York, NY.

# Appendix 18

## Brief Documentation of Unknowns

---

### Hydraulics of Canals

The main unknowns associated with the hydraulic analyses of the 17th Street Canal and London Avenue Canal are associated with the time histories of the breach geometries and the clogging characteristics of the Hammond Highway Bridge by debris.

#### 17th Street Canal

The eyewitness accounts of the breach occurrences in the 17th Street Canal suggest that at approximately 0630 on August 29, 2005, an initial breach had occurred. By 0930, the breach had widened to its full width of 450 feet. Photographic evidence documents that at approximately 1100, the water level in the vicinity of the breach was approximately 4 ft which is considerably less than the value of 9 ft in Lake Pontchartrain suggesting that the debris blockage at the bridge was constricting the flows in the vicinity of the breach. Sensitivity studies confirm that approximately 50% blockage at this time would be required to conform to these water level observations.

#### London Avenue Canal

The eyewitness and other accounts in the vicinities of the two London Avenue Canal breaches support that the northern breach was initiated between approximately 0700 and 0730 and the southern breach occurred between 0700 and 0800 on August 29, 2005. As for the case at 17th Street Canal, the evolution of the geometries of these breaches over time is poorly known. The sill depths at the two breaches are particularly poorly known. Additionally, at present the flow restrictions associated with the five bridges along London Avenue Canal are not as well established as at Hammond Highway Bridge over the 17th Street Canal.

## **Barge Motions and Dynamics**

The intent of the report describing the response of a barge under the action of wind is to provide a basis for calculations and to provide insight into the behavior of the barge. The unknowns are related to the particular draft of the barge and the specific related characteristics including the wind and water drag coefficients, attitude of the barge as it drifted under the action of wind, etc. The application is aided through presentation of the equations in non-dimensional form. The example applications are not intended as necessarily characteristic of the actual barge conditions. Rather, they were selected to be reasonably representative. Thus, there are no inherent unknowns in the equations in the relevant appendix that are provided for future applications.

## **Dynamic Forces and Motions on Flood Walls**

Similar to the case of the barge treatment, the results presented for dynamic forces and moments on a flood wall provide a basis for calculation and the examples provided are not necessarily intended to be representative of the actual conditions. Linear shallow water wave theory was considered in the applications; however, the associated results should be within  $\pm 20\%$ . Thus, in application of this methodology, the unknowns would occur in establishing the water levels and wave heights to be used as input to the equations and graphs. In particular, in some cases, the vegetation along the interior of the flood walls could reduce the wave heights considerably.